CERTIFICATION TESTING OF UNITED STATES DEPARTMENT OF ENERGY ATLAS AND BUFFER RAILCARS–PHASE 4 REPORT

for the United States Department of Energy

Prepared by Chris Pinney, David Cackovic, and Russell Walker

Certification Report

P-22-012

January 18, 2023

Revised July 21, 2023



MxV Rail

A subsidiary of the Association of American Railroads

Pueblo, Colorado USA

www.mxvrail.com

DISCLAIMER:

Disclaimer: This report was prepared by Transportation Technology Center, Inc. (MxV Rail) of Pueblo, Colorado, a subsidiary of the Association of American Railroads (AAR). Investigations and/or tests reported herein were authorized by the AAR and conducted in accordance with the appropriate AAR standard(s). This report is provided for consideration by the appropriate AAR technical committee and does not constitute in any way approval or disapproval of the product(s) tested. The contents of this report imply no endorsements whatsoever by MxV Rail or AAR of products, services, or procedures, nor are they intended to suggest the applicability of the test results under circumstances other than those described in this report. MxV Rail is not a source of information with respect to these tests, nor is it a source of copies of this report. MXV RAIL MAKES NO REPRESENTATION OR WARRANTIES, EITHER EXPRESSED OR IMPLIED, WITH RESPECT TO THIS REPORT OR ITS CONTENTS. MXV RAIL ASSUMES NO LIABILITY FOR SPECIAL, COLLATERAL, EXEMPLARY, INDIRECT, INCIDENTAL, CONSEQUENTIAL, OR ANY OTHER KIND OF DAMAGES RESULTING FROM THE USE OR APPLICATION OF THIS REPORT OR ITS CONTENTS.

Executive Summary

As part of the United States Department of Energy (DOE) Atlas Railcar Project, the Atlas and Buffer railcars were developed to meet the need for future large-scale rail transport of spent nuclear fuel and high-level radioactive waste. MxV Rail (formerly Transportation Technology Center, Inc.), a subsidiary of the Association of American Railroads (AAR), performed single-car certification testing and modeling on these railcars.

Testing and modeling were performed according to the certification requirements in the AAR *Manual of Standards and Recommended Practices* (MSRP), Standard S-2043, "Performance Specification for Trains Used to Carry High-Level Radioactive Material (HLRM)."[1] This report provides a summary of testing and modeling results in accordance with S-2043 requirements for the Single-Car Test (Paragraph 5.0) and Post-Test Analysis (Paragraph 8.0). The work was performed as part of Phase 4 under DOE Contract 89243218CNE000004/P00022.

In summary, Phase 4 covered the following Standard S-2043 test criteria for the Atlas and Buffer Railcars.

Standard S-2043 Test Criteria covered in Phase 4

S-2043 Paragraph		
5.2 Nonstructural Static Tests	5.2.1	Truck Twist Equalization
	5.2.2	Carbody Twist Equalization
	5.2.3	Static Curve Stability
	5.2.4	Horizontal Curve Negotiation
5.4 Structural Tests	5.4.2	Squeeze (Compressive End) Load
	5.4.3	Coupler Vertical Loads
	5.4.4	Jacking
	5.4.5	Twist
	5.4.6	Impact
	5.4.7	Securement System Analysis
5.5 Dynamic Tests	5.5.7	Hunting
	5.5.8	Twist and Roll
	5.5.9	Yaw and Sway
	5.5.10	Dynamic Curving
	5.5.11	Pitch and Bounce (Chapter 11)
	5.5.12	Pitch and Bounce (Special)
	5.5.13	Single Bump Test
	5.5.14	Curve Entry/Exit
	5.5.15	Curving with Single Rail Perturbation
	5.5.16	Standard Chapter 11 Constant Curving
	5.5.17	Special Trackwork
	5.5.18	Ride Quality (N/A for Atlas and Buffer)

Notes:

- Paragraph 5.3, Static Brake Tests, not listed in the table above, were performed at Kasgro Rail prior to shipment to the Transportation Technology Center (TTC).
- Paragraph 5.4.7, Securement System Analysis, was satisfied through analysis rather than test as allowed in the paragraph.

The Atlas railcar met most of the AAR S-2043 criteria. However, when the Atlas railcar test included a minimum test load and the AAR Standard KR wheel profile (i.e., worn) wheelsets and operated at high speed (above 65 mph), it did not meet the single-car dynamic test requirement for hunting (S-2043, Paragraph 5.5.7). All three of these conditions were necessary simultaneously to create poor hunting performance. Based on the test results, it was determined that DOE could adjust any one of three conditions to meet the test requirement for hunting. The adjustment options included:

- For shipments with a very light shipping cask, the DOE could add ballast weight to the load.
- The DOE could replace the wheelsets on a regular schedule before they become significantly worn.
- Operate the train in accordance with the 50-mph speed limit of S-2043, which references AAR Circular No. OT-55 "Recommended Railroad Operating Practices for Transportation of Hazardous Materials." Given the 50-mph speed limit for actual train operations, the train's speed should never approach 65 mph as required during testing.

It should be noted that during Phase 5 testing of the Atlas train, which was underway as this Phase 4 report was being prepared, the Atlas Railcar Project discovered that all the railcars exhibited better curving performance with 2A wheel profiles. In order to achieve acceptable curving performance, the Project, with agreement from the AAR, had to change all the wheels from the 1B profile to the new 2A profile. The 1B wheel profile is being phased out across the freight rail industry. The 2A profile is similar to the KR (i.e., worn) profile and will likely produce hunting performance similar to the KR. Therefore, DOE will not be able to choose the second option above to prevent hunting. Nevertheless, the first and third options above are still operative. The Atlas railcar will have acceptable hunting performance as long as DOE operates the trains with heavy loads and/or in strict accordance with the 50-mph speed limit.

The Atlas railcar testing and modeling results were presented to AAR's Equipment Engineering Committee (EEC) for approval with the exceptions not met under the hunting (S-2043, Paragraph 5.5.7) requirements. Based on the compromise of hunting performance versus curving performance, and because OT-55 restricts loaded Atlas railcar operations to speeds well below the hunting speed of 65 mph, the EEC granted approval for single-car testing of the Atlas railcar under S-2043. The summary results for the Atlas railcar can be referenced in Table 6 of this report.

The Buffer car met all S-2043 single-car structural and dynamic testing requirements of Phase 4. Under specific modeling cases, the S-2043 criteria were not met. The unmet criteria do not affect approval but are included as information regarding the railcar's overall performance. The summary results for the Buffer railcar can be referenced in Table 7 of the report.

The AAR EEC approval letters for the Atlas and Buffer railcars for Phase 4 testing and modeling are included in Appendix A, Appendix B, and Appendix C for reference. With the AAR EEC approval of the single-car tests of Atlas and Buffer railcars in 2021 and 2022, the next testing phase began. This is Phase 5, which is ongoing and includes Multiple-Car Tests (S-2043, Paragraph 6.0). During Phase 5, the Atlas and Buffer railcars, along with the new Rail Escort

Vehicle (REV), are being tested as a complete train on test tracks and on selected revenue services routes.

The first three completed design and fabrication phases of this project, governed by DOE Contract Number DE-NE0008390 (Reference: EIR-3021970 – Design and Prototype Fabrication of Railcars for Transport of High-Level Radioactive Material; Phase 3 – Prototype Fabrication and Delivery), as well as the current completed phase (4) and the next phase (5) of testing and modeling, are summarized below.

1. Phase 1 Mobilization and Conceptual Design (completed) included:
   a. The mobilization and conceptual design of an Atlas railcar and its associated Buffer railcar.
   b. The conceptual design of cask cradles for securement of HLRM casks on the Atlas railcar.
   c. General Loading Procedures for cask-to-cradle-to-railcar.
   d. The railcar's functional, design, operational, and maintenance requirements.
2. Phase 2 Preliminary Design (completed) entailed:
   a. The submission of the preliminary design packages of the Atlas and Buffer railcars designed to meet the AAR Standard S-2043 guidelines.
   b. The delivery of the preliminary design data package and dynamic modeling input and output data files to the DOE.
   c. The subsequent receipt from the AAR EEC of a notice to "proceed with the test phase," which allows the prototype railcars to be built in accordance with Paragraph 3.2.1 of S-2043.
3. Phase 3 Fabrication and Delivery (completed) comprised:
   a. The fabrication and delivery of one Atlas and two Buffer prototype railcars,
   b. The delivery of an as-built design package including drawings, inspection reports, and Bill of Materials (BOM) for both the Atlas and Buffer railcars.
   c. Operation and maintenance manuals, including maintenance intervals for both the Atlas and Buffer railcars.
   d. Final design information necessary for the fabrication of test loads, cradles, and end stops necessary for testing of the Atlas railcar.
4. Phase 4 Single-Car Tests (completed) involved:
   a. Fabrication of test loads, cradles, and end stops necessary for future testing of the Atlas railcar.
   b. S-2043 (Paragraph 5.0) Static, structural, and dynamic testing and modeling.
   c. S-2043 (Paragraph 8.0) Post-Test Analysis modeling.
   d. Approval from the AAR EEC of the single-car tests on the Atlas and Buffer railcars.
5. Phase 5 Multiple-Car Tests (ongoing) will include Atlas and Buffer railcars tested together with an REV under the requirements of S-2043:
   a. Dynamic tests at the controlled test site.
   b. System monitoring tests.
   c. Revenue service tests.

d. Demonstration Test Run.
e. Approval from the AAR EEC of the final tests including the Atlas, Buffer, and REV railcars as a complete train.

Table of Contents

1.0 Introduction 1
2.0 Objective 1
3.0 AAR Standard S-2043 1
4.0 Atlas and Buffer Railcar description 3
4.1 Atlas Railcar Description 3
4.1.1 Variations in Components During Testing 5
4.2 Buffer Railcar Description 6
5.0 Summary Results 8
5.1 Atlas Railcar Summary Results 9
5.2 Derailment Incident and Investigation during Atlas Testing 13
5.3 Buffer Railcar Summary Results 15
5.4 Weld Cracks on the Atlas Railcar 17
5.4.1 Design Change as a Result of Cracking Issue 20
5.5 Dunnage Blocks – Lateral Movement 22
6.0 Overview of Reports for Atlas and Buffer Railcars 24
6.1 Atlas Railcar Reports With S-2043 References 24
6.1.1 S-2043 Certification Tests of U.S. DOE Atlas Railcar Design Project 12-Axle Cask Car (Single-Car Test Report P-21-037) 24
6.1.2 Atlas Car Post-Test Analysis (Report P-21-049 [formerly Report P-21-042]) 26
6.2 Buffer Railcar Reports 27
6.2.1 AAR Standard S-2043 Single-Car Certification Tests of U.S. DOE Atlas Railcar Design Project Buffer Railcar (Report P-20-032) 27
6.2.2 Buffer Car Post-Test Analysis (Report P-21-013) 28
7.0 Conclusions 29
Attachments 1
Kasgro Report 1 Metallurgical Report 2
Kasgro Report 2 Tri-span Inspection Report 20
Kasgro Report 3 Metals Investigation Report 23
Appendix A EEC Approval Letters for Atlas Railcar (Single-Car Test and Post-Test Analysis A-1
Appendix B EEC Approval Letters for Buffer Railcar (Single-Car Test) B-1
Appendix C EEC Approval Letter for Buffer Railcar (Post-Test Analysis) C-1
Appendix D P-21-037 S-2043 Certification Tests of United States Department of Energy Atlas Railcar Design Project 12-Axle Cask Car D-1
Appendix E P-21-049 Atlas Car Post Test Analysis Report (formerly P-21-042) E-1

Appendix F P-20-032 AAR Standard S-2043 Single-Car Certification Tests of U.S. Department of Energy Buffer Railcar F-1
Appendix G P-21-013 Buffer Car Post Test Analysis Report G-1

List of Figures

Figure 1. Simulation and Test Results on L/V ratios 2
Figure 2. IDOX 010001 during Testing with Minimum Test Load 3
Figure 3. Exploded view of Swing Motion® truck 4
Figure 4. Primary Suspension (or Bearing Adapter) Pad 4
Figure 5. Axle and side naming convention 5
Figure 6. Buffer railcar IDOX 020001 during static testing 7
Figure 7. Buffer railcar IDOX 020001 arrangement drawing 7
Figure 8. Derailed Axle 6 in final position outside of the curve 13
Figure 9. Atlas Railcar – Crack is on Left Side of Centerplate, B-Truck 18
Figure 10. Atlas Railcar – Close-up of Crack on Left Side of Centerplate, B-Truck 18
Figure 11. Cracks in B-end tri-span bolster, C-truck centerplate 19
Figure 12. Cracking in tri-span bolster with new B truck centerplate 19
Figure 13. Magnified image of cracks in tri-span bolster 19
Figure 14. 12-bolt centerplate mounted to replacement Atlas tri-span bolster 21
Figure 15. Atlas BL-end centerplate after removal 21
Figure 16. Tri-span section sent for NDE testing 22
Figure 17. Dunnage problem: block on right side has slipped downward 23
Figure 18. Solution of the dunnage movement problem 23

List of Tables

Table 1. Standard S-2043 Test Criteria 2
Table 2. Atlas Railcar Dimensions 4
Table 3. Atlas Railcar Configuration 5
Table 4. Buffer Railcar dimensions 7
Table 5. Buffer railcar truck configuration 8
Table 6. Atlas Railcar Summary Analysis and Test Results 10
Table 7. Buffer Railcar Summary Test Results 16

Table 8. Atlas Railcar Single-Car Tests Report Reference Table 24
Table 9. Atlas Railcar Post-Test Analysis Report Reference Table 26
Table 10. Buffer Railcar Single-Car Tests Report Reference Table 27
Table 11. Buffer Railcar Post-Test Analysis Report Reference Table 29

1.0 INTRODUCTION

The Atlas and Buffer railcars were developed and are being tested as part of the U.S. Department of Energy (DOE) Atlas Railcar Project to meet the need for future large-scale rail transport of spent nuclear fuel and high-level radioactive waste. Transportation Technology Center, Inc. (MxV Rail), a subsidiary of the Association of American Railroads (AAR), performed single-car certification testing and modeling on the DOE twelve-axle Atlas cask-carrying railcar and the four-axle Buffer railcar.

The testing and modeling were performed to determine whether the Atlas and Buffer railcars meet the requirements of the AAR *Manual of Standards and Recommended Practices* (MSRP), Standard S-2043, "Performance Specification for Trains Used to Carry High-Level Radioactive Material," revised 2017.[1] This report provides a summary of the testing and modeling results for the Single-Car Test (Paragraph 5.0) and Post-Test Analysis (Paragraph 8.0) phase of certification for the Atlas and Buffer railcars.

The Atlas and Buffer railcar testing and analysis was conducted primarily by MxV Rail at the Transportation Technology Center (TTC) in Pueblo, Colorado. The work reported was performed during Phase 4 under DOE Contract 89243218CNE000004/P00022.

2.0 OBJECTIVE

The objective of this report is to provide a summary of testing and modeling results for Single-Car Test (Paragraph 5.0) and Post-Test Analysis (Paragraph 8.0) for Phase 4 certification activities.

3.0 AAR STANDARD S-2043

In North America, freight rail is relied upon for the safe movement of all types of commodities, including hazardous materials. The AAR Safety and Operations (S&O) Department is responsible for the rules and standards for rail vehicles used on North American railroads. These rules and standards are developed and maintained by the voting members of the various S&O technical committees and published by the AAR. Each railroad is required to sign and abide by an interchange agreement before it can interchange rolling stock with other common carrier railroads. The common carrier obligation refers to the statutory duty of railroads to provide transportation or service on reasonable request.

There are more than 600 AAR standards and specifications that cover a wide variety of components and sub-systems used in the North American market. The AAR introduced the term "High-Level Radioactive Material (HLRM)" to include high-level radioactive waste and spent nuclear fuel. The DOE has accepted this term for the purpose of rail transport. To ensure the safety of transport of HLRM, AAR created Standard S-2043, "Performance Specification for Trains Used to Carry High-Level Radioactive Material." It is the most robust of all AAR standards. For example, AAR Specification M-1001, Chapter 11, "Service-Worthiness Tests and Analyses for New Freight Cars," presents guidelines for testing and analysis to ascertain the worthiness of the interchange-service and the safety of new freight car designs. Standard S-2043 applies to all railcars used in trains that transport HLRM, including spent nuclear fuel cask-carrying railcars and non-HLRM equipment, and requires the use of the same vehicle

performance regimes for testing and analysis as AAR Specification M-1001, Chapter 11. However, S-2043 requires higher levels of performance than those already considered sufficient to ensure an adequate margin of safety for railcars as indicated in M-1001, Chapter 11.

Atlas railcar dynamic curving test results and simulation predictions are shown in Figure 1 The simulations and tests showed lateral/vertical (L/V) ratios below the Chapter 11 requirement of 1.0 and the more stringent S-2043 requirement of 0.8.

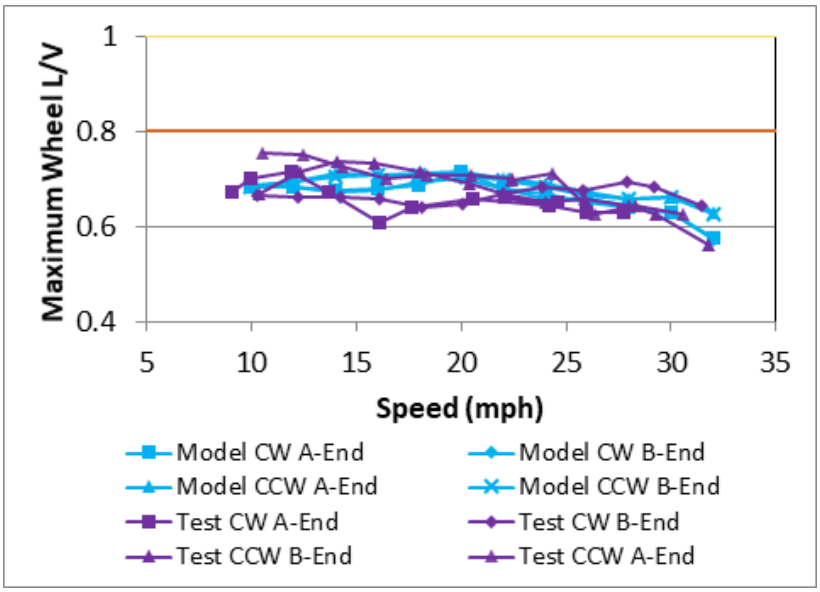


Figure 1. Simulation and test results on L/V ratios

In summary, Phase 4 covered the following test criteria of Standard S-2043 for both the Atlas railcar and the Buffer railcar (see Table 1).

Table 1. Standard S-2043 test criteria

S-2043 Paragraph		
5.2 Nonstructural Static Tests	5.2.1	Truck Twist Equalization
	5.2.2	Carbody Twist Equalization
	5.2.3	Static Curve Stability
	5.2.4	Horizontal Curve Negotiation
5.4 Structural Tests	5.4.2	Squeeze (Compressive End) Load
	5.4.3	Coupler Vertical Loads
	5.4.4	Jacking
	5.4.5	Twist
	5.4.6	Impact
	5.4.7	Securement System Analysis
5.5 Dynamic Tests	5.5.7	Hunting
	5.5.8	Twist and Roll
	5.5.9	Yaw and Sway
	5.5.10	Dynamic Curving
	5.5.11	Pitch and Bounce (Chapter 11)

S-2043 Paragraph		
	5.5.12	Pitch and Bounce (Special)
	5.5.13	Single Bump Test
	5.5.14	Curve Entry/Exit
	5.5.15	Curving with Single Rail Perturbation
	5.5.16	Standard Chapter 11 Constant Curving
	5.5.17	Special Trackwork
	5.5.18	Ride Quality (N/A for Atlas and Buffer railcars)

Notes:

- Paragraph 5.3 Static Brake Tests, not listed in the table above, were performed at Kasgro Rail prior to shipment to the TTC.
- Paragraph 5.4.7 was satisfied through analysis rather than testing as allowed in the paragraph.

4.0 ATLAS AND BUFFER RAILCAR DESCRIPTION

In 2018, Kasgro manufactured the Atlas railcar in addition to two prototype Buffer railcars. The Atlas railcar delivered for testing was numbered IDOX 010001. The Atlas (12-axle) and Buffer (four-axle) cars are designed to be operated as a railcar transport system propelled by a locomotive and accompanied by a Rail Escort Vehicle (REV).

4.1 Atlas Railcar Description

The Atlas railcar is a 12-axle span bolster railcar with fittings to accommodate cradles and end stops designed to allow the railcar to carry various casks used for the transportation of spent nuclear fuel and high-level radioactive waste. The railcar deck is supported on two span bolsters. Each span bolster rests on three two-axle trucks. Figure 2 shows the railcar with a test load installed. Table 2 lists the railcar dimensions.



Figure 2. IDOX 010001 during testing with minimum test load

Table 2. Atlas railcar dimensions

Dimension	Value
Length over pulling faces	78 feet 1 1/4 inches
Length over strikers	73 feet 5 1/4 inches
Span bolster spacing	38 feet 6 inches
Axle spacing on trucks	72 inches
Distance between adjacent trucks	10 feet 6 inches

The railcar uses six Amsted Swing Motion® trucks (Figure 3). Each truck uses two wheelsets with AAR Class K-axles and AAR-1B narrow flange wheels. These wheels are specified for this railcar because the increased gage clearance allows more lateral movement for better performance. The trucks are designed to use a primary suspension polymer pad between the bearing adapter and the side frame. The suspension polymer pad gives the truck an improved passive steering capability. Figure 4 shows the primary suspension polymer pad (also called a bearing adapter pad).

Table 3 shows the truck configuration used for testing. The secondary suspension is made up of springs in a non-AAR-standard configuration.

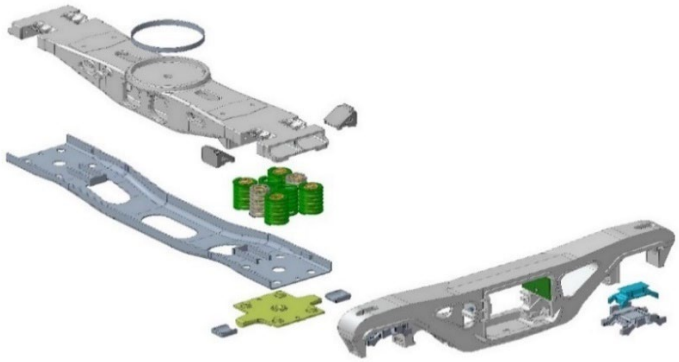


Figure 3. Exploded view of Swing Motion® truck



Figure 4. Primary suspension (or bearing adapter) pad

Table 3. Atlas railcar configuration

Component	Description	
Secondary Suspension Springs at End Trucks (A,B,D,E)	(2) 1-94, (2) 1-95, (2) 1-96, (4) 1-97, (4) 1-92, (4) 1-99	
Secondary Suspension Springs at Middle Trucks (C,F)	(2) 1-88, (2) 1-89, (2) 1-90, (4) 1-91, (4) 1-92, (2) 1-93, (4) 1-99	
Primary suspension	12A Adapter Plus pads, ASF-Keystone part number 10523A	
Side Frames	F9N-10FH-UB	
Bolsters	B9N-71 EJFZ on A, F, and C-trucks B9N-71 HN-FX on B, D, and E-trucks	
Side Bearings	Miner TCC-III 60LT	
Friction Wedge, composition faced (four per truck)	ASF-Keystone Part number 48446	
Bearings and Adapters	AAR Class K 6 1/2 × 9 bearings with 6 1/2 × 9 Special Adapter ASF-Keystone Part number 10523A	
Center Bowl Plate	Metal Horizontal Liner	
	End Truck Average	Middle Truck Average
Minimum Test Load Spring Nest Height	8.97 inches	9.13 inches
Maximum Test Load Spring Nest Height	8.20 inches	8.17 inches
	Actual Weight on Rail Used During Testing	
Scale Weight Empty Test Load	222,050 (lbs.)	
Scale Weight Minimum Test Load	421,050 (lbs.)	
Scale Weight Maximum Test Load	709,050 (lbs.)	

The convention for wheel and truck identification is shown in Figure 5. The B-end of a railroad freight car is normally the end with the handbrake, but because the Atlas railcar has two handbrakes, the railcar manufacturer designated and stenciled the B-end. The right and left sides of the railcar are designated from the perspective of standing at the B-end of the railcar and looking toward the A-end of the car. Axles are numbered starting from the B-end. For axle numbers greater than nine, the locations are stenciled with letters descending from Z.

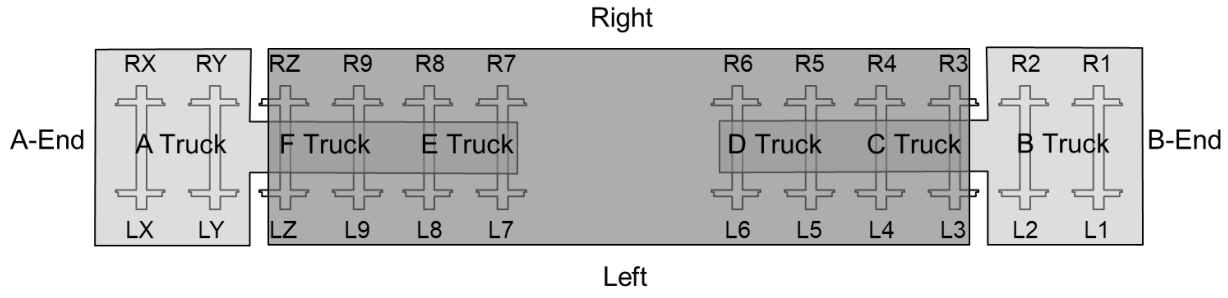


Figure 5. Axle and side naming convention

4.1.1 Variations in Components During Testing

During the initial tests, the Atlas railcar, loaded with the minimum test load, showed some hunting instability at speeds above 65 mph. The Atlas railcar was stable up to 75 mph when

loaded with the maximum test load. MxV Rail tested different side bearings, centerplate liners, and primary pads to address the hunting instability with the minimum test load. The stiffer primary pads (prototype chlorosulfonated polyethylene or CSM 70 pads) were the only change that improved the hunting performance. After the change to stiffer pads resulted in improved hunting stability performance, all Standard S-2043 prescribed dynamic test regimes were completed with CSM 70 pads. However, using these stiffer pads, railcar performance did not meet Standard S-2043 criteria in Dynamic Curving or Curve with Single Rail Perturbation regimes, despite the improved hunting stability performance.

On October 15, 2020, MxV Rail reviewed the results with the AAR Equipment Engineering Committee (EEC). The EEC directed MxV Rail to re-test the railcar with softer primary pads with a minimum test load in the Dynamic Curving regime. Because the railcar would be limited to less than 50 mph by OT-55 when in high-level radioactive material (HLRM) service, the EEC noted that curving performance was more important than high speed stability performance.

During the testing program, MxV Rail tested the railcar with a total of four primary suspension pad models. The pads are made from CSM and are categorized by the Shore D durometer hardness value with higher numbers indicating a harder pad. The railcar arrived with CSM 58 production pads. MxV Rail also tested the railcar with prototype pad types CSM 70, CSM 68, and CSM 65.

The hunting regime was tested with CSM 58 pads in both the minimum and maximum test load conditions. The dynamic curving regime was tested with CSM 58 pads in the minimum test load condition. All other dynamic tests were completed with CSM 70 pads. Considering the results of curving and hunting tests, when compared to the tested alternative pad materials, the production CSM 58 pads provided the best performance overall.

Recorded test data regimes using CSM 70 pads were modeled with these pads to demonstrate the model was validated. These regimes were modeled again with CSM 58 pads to show the change in performance with the final pad.

4.2 Buffer Railcar Description

The Buffer railcar is a four-axle flatcar with a permanently attached ballast load (Figure 6). In 2018, Kasgro manufactured IDOX 020001 and IDOX 020002, two prototype Buffer cars that were delivered to the TTC. The tests described in this report were conducted on IDOX 020001. Figure 7 shows the general arrangement drawing of the car. Table 4 shows the railcar dimensions.



Figure 6. Buffer railcar IDOX 020001 during static testing

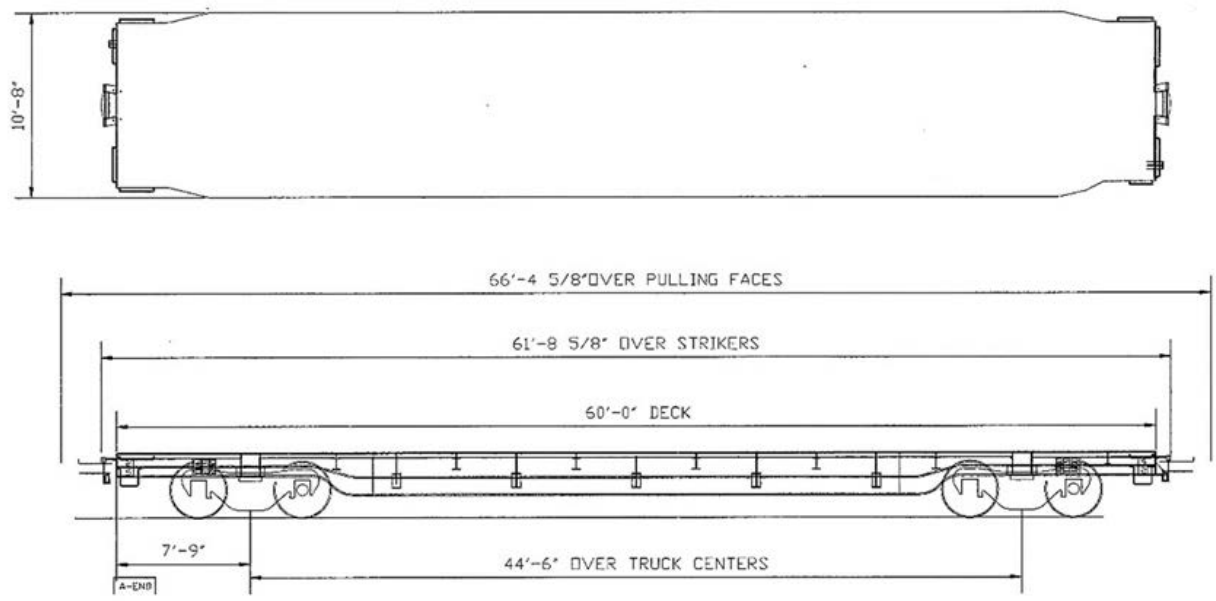


Figure 7. Buffer railcar IDOX 020001 arrangement drawing

Table 4. Buffer railcar dimensions

Dimension	Value
Length over pulling faces	66 feet, 4 5/8 inches
Length over strikers	61 feet, 8 5/8 inches
Truck center spacing	44 feet 6 inches
Axle spacing on trucks	72 inches

The computer vehicle dynamic simulations required for Standard S-2043 showed that an empty Buffer railcar would not meet the requirements in the buff and draft curving regime

(S-2043, Paragraph 4.3.13). A ballast weight of 196,000 pounds—included as permanently installed steel plates—was added to resolve this issue.

The steel plates were welded to the railcar during the manufacturing process, resulting in a railcar with a permanent gross rail load of 263,000 pounds. Because the railcar was not rated to carry any additional load, 263,000 pounds was the only load condition that was tested.

The railcar uses two Swing Motion® trucks supplied by Amsted Rail. Each truck uses two wheelsets with K-axles and AAR-1B[1] narrow flange wheels. These wheels were specified for use with this railcar because the increased gage clearance allowed more lateral movement for better performance. The trucks were specially designed to use a polymer pad between the bearing adapter and side frame to give each truck a passive steering capability. The Buffer railcar bearing adapter pad is the same as the Atlas railcar's pad shown in Figure 4. The truck uses two KONI 04A 2032 vertical dampers to control the vertical motion of the railcar suspension. The dampers are needed on the Buffer railcar and not on the Atlas railcar because track geometry deviations have more input on the four-axle railcar than on a twelve-axle railcar so additional damping is required. The Buffer railcar truck configuration is shown in Table 5.

Table 5. Buffer railcar truck configuration

Part	Description	
Secondary suspension	Five D7 outer coils, five D6 inner coils, five D6A inner-inner coils, two 49427-1, two 49427-2	
Primary suspension	Adapter Plus pads, ASF part number 10523A	
Side bearings	Miner TCC-III 60LT	
Friction wedge	Amsted part number 1-9249	
Bearings and adapters	K class 6 1/2 x 9 bearings with 6 1/2 x 9 special adapter ASF Part number 10523A	
Center bowl plate	Metal horizontal liner	
Vertical hydraulic dampers	KONI damper 04a 2032	
Side frames	F9N-10FH-UB	
Bolsters	B9N-714N-FS	
	A-end truck average	B-end truck average
Spring nest height	7.75 inches	7.78 inches
Scale weight	131,200 pounds	131,975 pounds

5.0 SUMMARY RESULTS

The summary testing and modeling results for the Single-Car Test and Post-Test Analysis are presented in Section 5.1 for the Atlas railcar and Section 5.3 for the Buffer railcar. Section 5.2 is a brief discussion of the Atlas derailment that occurred during testing. Section 5.4 is a brief

[1] The AAR-1B wheel profile was subsequently changed to the AAR-2A wheel profile. See Section 5.1.

discussion of the Atlas weld cracks that occurred during testing. Section 5.5 is a brief discussion of a design change necessary to keep the dunnage blocks secured on Atlas.

5.1 Atlas Railcar Summary Results

The Atlas railcar testing and modeling results shown in Table 6 were presented and approved by the AAR's EEC. The letter of approval from EEC is presented in Appendix A.

During the Post-Test Analysis (S-2043, Paragraph 8.0), results from the finite element analysis (FEA) structural simulations and structural test strain measurements listed in Table 6 (S-2043, Paragraph 5.4.2–5.4.6) were evaluated to determine if stresses were less than 75 percent of the allowable stress for all load cases. The results indicate that stresses were less than 75 percent of the allowable stress, thereby eliminating the requirement for "Refining the FEA" (S-2043, Paragraph 8.1).

The Atlas railcar met most AAR S-2043 non-structural static and dynamic criteria. However, the Atlas railcar equipped with CSM 58 primary suspension pads 1) with a minimum test load, 2) with AAR Standard KR wheel profile (i.e., worn) wheelsets, and 3) while operating at a high speed (above 65 mph) did not meet the single-car dynamic test requirement for hunting (S-2043, Paragraph 5.5.7) referenced in Table 1. Additional testing with an alternative pad (CSM 70) was part of the testing regime. The stiffer CSM 70 pad met the hunting performance criteria but did not meet curving performance criteria under the single-car dynamic test (S-2043, Paragraph 5.5.10) parameters. After much testing, modeling, and analysis, the Project decided to go back to using CSM 58 pads in order to meet the curving performance criteria.

With the CSM 58 pads, however, the Project still had a problem with hunting performance. When the test included all three of the other conditions listed above simultaneously, the railcar failed to meet the hunting test requirement. Therefore, DOE had three remaining options for meeting the hunting test requirement:

- Adding ballast weight to the load for shipments with a very light shipping cask
- Replacing the 1B-profiled wheelsets on a regular schedule before they become significantly worn.
- Operating the train strictly in accordance with the OT-55 speed limit of 50 mph.

It should be noted that during Phase 5 testing of the Atlas train, which was underway as this Phase 4 report was being prepared, the Atlas Railcar Project discovered that all the railcars exhibited better curving performance with 2A wheel profiles. In order to achieve acceptable curving performance, the Project, in consultation with the AAR, had to change all the wheels from the 1B profile to the new 2A profile. The 1B wheel profile is being phased out across the freight rail industry. The 2A profile is similar to the KR (i.e., worn) profile and will likely produce hunting performance similar to the KR. Therefore, DOE will not be able to choose the second option above to prevent hunting. Nevertheless, the first and third options above are still operative. The Atlas Railcar will have acceptable hunting performance as long as DOE operates the trains with heavy loads and/or in strict accordance with the 50-mph speed limit.

The testing and vehicle dynamic modeling results of the Atlas railcar equipped with CSM 58 pads were presented to AAR's EEC for approval, with the exception of the criteria for hunting (S-2043, Paragraph 5.5.7). Based on the compromise of hunting performance versus curving performance described in Appendix D, and because OT-55 restricts Atlas railcar operations to speeds well below the hunting speed of 65 mph, the EEC granted approval for single-car testing of the Atlas railcar under S-2043. The summary results for the Atlas railcar are in Table 6.

The preliminary vehicle dynamic simulations were performed according to Standard S-2043, Paragraph 4.3 (Dynamic Analysis) as part of the railcar design phase before the prototype railcar was built. The results of the preliminary simulation were submitted to the AAR as part of the preliminary design review package. Following the vehicle characterization and the dynamic tests, the models of the vehicles were revised to better represent the vehicles. The test results were compared to the preliminary dynamic analysis predictions and revised model predictions to verify that modeling accurately represents the vehicle as required in Standard S-2043, Paragraph 8 (Post-Test Analysis).

As part of the design criteria, static brake testing was conducted at the manufacturer's facility per relevant requirements of AAR Standards S-401 and S-486 (Paragraph 4.0). The Atlas and Buffer railcars Single Car Testing (Paragraph 5.0) was conducted primarily by MxV Rail at the TTC.

Table 6. Atlas railcar summary analysis and test results

Standard S-2043 Paragraph	Atlas Railcar Met/Not Met	
	Revised Simulations CSM 58 pads	Test Result and Details if Not Met
4.2 Nonstructural Static Analysis/5.2 Nonstructural Static Tests		
4.2.1/5.2.1 Truck Twist Equalization	Not Simulated	Not Met with CSM 58 pads EEC Comment: "Most cases of this very severe requirement were met. EEC understands why the center truck of a tri-span bolster would have difficulty meeting the requirement. Values found were 10-17 percentage points less than allowed by S-2043. A minimum of 24% of the static load was still carried, which is reasonable. This is a stationary test, and the EEC accepts the results based on the more important dynamic aspects of proper equalization were shown to be acceptable by performance in 5.5.15 Curving with single perturbation, 5.5.10 Dynamic curving, and 5.5.14 Limiting spiral"
4.2.2/5.2.2 Carbody Twist Equalization	Not Simulated	Met with CSM 58 pads

Standard S-2043 Paragraph	Atlas Railcar Met/Not Met	
	Revised Simulations CSM 58 pads	**Test Result and Details if Not Met**
4.2.3/5.2.3 Static Curve Stability	Not Simulated	Met with CSM 58 pads
4.2.4/5.2.4 Horizontal Curve Negotiation	Not Simulated	Met with CSM 58 pads
5.4.2 Squeeze (Compressive End) Load	Not Simulated	Met with CSM 58 pads
5.4.3 Coupler Vertical Loads	Not Simulated	Met with CSM 58 pads
5.4.4 Jacking	Not Simulated	Met with CSM 58 pads
5.4.5 Twist	Not Simulated	Met with CSM 58 pads
5.4.6 Impact	Not Simulated	Met with CSM 58 pads
4.3.11.3/5.5.7 Hunting	Not Met	Not Met with CSM 58 pads (At Minimum Test Load: Railcar did not meet the carbody lateral acceleration standard deviation criteria of 0.13 at speeds greater than 65 mph) EEC Comment: “The hunting measured with the CSM 58 adapter pad was mild and does not present safety concerns. Additionally, the conditions that the railcar hunted in test will not be encountered in service (i.e., operating at speeds above 65, use of wide flange worn wheelsets with a conicity prone to hunting). The operating plan must include a maximum speed to avoid the speeds at which hunting was encountered.”
4.3.9.6/5.5.8 Twist and Roll	Met	Not tested with CSM 58 pads – Met with CSM 70 pads
5.5.9 Yaw and Sway	Met	Not tested with CSM 58 pads – Met with CSM 70 pads
5.5.10 Dynamic Curving	Met	Met with CSM 58 pads
4.3.9.7/5.5.11 Pitch and Bounce (Chapter 11)	Met	Not tested with CSM 58 pads – Met with CSM 70 pads
4.3.9.7/5.5.12 Pitch and Bounce (Special)	Met in preliminary simulations	Not tested because the truck center spacing is close to Chapter 11 wavelength (EEC approved)
4.3.10.1/5.5.13 Single Bump Test	Met	Not tested with CSM 58 pads – Met with CSM 70 pads
4.3.11.6/5.5.14 Curve Entry/Exit	Met	Not tested with CSM 58 pads – Met with CSM 70 pads

Standard S-2043 Paragraph	Atlas Railcar Met/Not Met	
	Revised Simulations CSM 58 pads	**Test Result and Details if Not Met**
4.3.10.25.5.15 Curving with Single Rail Perturbation	Not met	Minimum Test Load: Not met with CSM 70 pads: EEC Comment: “Testing did not meet criteria using the CSM 70 and CSM 65 pads. However, modeling with the CSM 58 pad produced successful results for wheel/rail forces. The EEC considers the wheel/rail force requirements to be met. The carbody roll angle that does not meet in modeling with a 3-inch perturbation is simply an effect of local track geometry that cannot be addressed realistically. The EEC accepts the roll angle results as they are.”
4.3.11.4/5.5.16 Standard Chapter 11 Constant Curving	Met	Not tested with CSM 58 pads – Not Met with CSM 70 pads: EEC Comment: “Test results were produced using the CSM 70 adapter pads. The CSM 58 pads provide better curving as shown by modeling results. The EEC considers this requirement to be met by use of the CSM 58 pads.”
4.3.11.7/5.5.17 Special Trackwork, No. 7 (analysis) No. 10 (test) Crossovers	Met	Not tested on No. 7 with CSM 58 pads – Tests met with CSM 70 pads on a No. 10 crossover
4.3.11.5 Curving with Various Lubrication Conditions	Not Met in following cases Min Test Load with new profiles, case 4 Min Test Load with worn profiles, cases 1, 2 and 4 Max Test Load with worn profiles, cases 1, 2, and 4	Testing not required EEC Comment in response to these results: The EEC agrees with the expert review recommendations that during multiple car testing the Atlas railcar be stopped in the TTC WRM 12 degree curve, the local depot activity 10 degree curve, and the BNSF Alps N.M. horseshoe 10 degree curve (if possible), and the car slowly pulled through the exit spiral of the curve while gage spreading and gage spreading forces are monitored.
4.3.12 Ride Quality	Met in preliminary simulations	Testing not required for non-passenger-carrying railcars
4.3.13 Buff and Draft Curving	Met	Single car testing not required
4.3.14 Braking Effects on Steering	Met in preliminary simulations	Testing not required

Standard S-2043 Paragraph	Atlas Railcar Met/Not Met	
	Revised Simulations CSM 58 pads	Test Result and Details if Not Met
4.3.15 Worn Component Simulations	Not Met for: Hunting stability, maximum lateral acceleration standard deviation	Testing not required EEC Comment: "The hunting measured with the CSM 58 adapter pad was mild and does not present safety concerns. Additionally, the conditions that the car hunted in test will not be encountered in service (i.e., operating at speeds above 65, use of wide flange worn wheelsets with a conicity prone to hunting). The operating plan must include a maximum speed to avoid the speeds at which hunting was encountered."

5.2 Derailment Incident and Investigation during Atlas Testing

At 1:00 p.m. (MDT) on July 8, 2020, one axle of the DOE Atlas railcar test train derailed during testing on the Urban Rail Building (URB) north wye track at the TTC. No one was injured. The leading axle of the trailing (B-end) span bolster of Atlas railcar IDOX 010001, climbed the gage face of the outside (high) rail, then traveled about 19 feet with the flange on the top of the rail before dropping to the field side. The derailment occurred when MxV Rail personnel were testing the Atlas railcar in the Curving with Single Rail Perturbation (CWSRP) test zone specified in AAR Standard S-2043.[1]



Figure 8. Derailed Axle 6 in final position outside of the curve

The point of derailment (POD) was in the body of a 12-degree left-hand (LH) curve with no superelevation. The POD was within the 2-inch-high rail dip of the CWSRP, resulting in a reverse cross level of 1.88 inches. At the POD, the gage was 56.72 inches, and the curvature was 12.5 degrees. The alignment deviation of a 62-foot chord from average curvature (155-foot average) was 3.7 inches at the POD. At the time of the derailment, the railcar was being shoved at 6 mph. The subject railcar was at the lead end of the movement with the instrumentation railcar and locomotive trailing.

At the time of the derailment, all six axles of the B-end (trailing) span bolster were instrumented wheelsets (IWS) that had been installed for testing. The railcar was tested with a simulated load (without any hazardous material).

MxV Rail noted damage to 1) two of the IWS, 2) the B-end span bolster, and 3) the left-side frame of the D-truck. The IWS were inspected, tested, and returned to service. The span bolster damage was repaired per the railcar builder's instructions, and the damaged left-side frame was replaced.

A three-dimensional wheel-rail contact analysis was also conducted to estimate how the angle of attack of the wheelset to the rail would affect the contact conditions. The results showed that the angle of attack of the wheelset to the rail changes the contact condition, causing the maximum contact angle to reduce by approximately 1 degree for the likely values of the angle of attack. The reduced contact angle, combined with high friction measured at the derailment point, may have contributed to the derailment occurring at a lower L/V than expected.

While it includes cross level and gage definitions for this test zone, AAR Standard S-2043 is silent on curvature and alignment tolerances. The post-derailment track geometry test zone measurements showed variations in curvature and alignment, resulting in a test zone that was more challenging than intended. Simulations conducted as part of the derailment investigation showed that improvements in the curvature and alignment variation with other test zone parameters held constant resulted in a railcar performance that would meet AAR Standard S-2043 criteria.

MxV Rail proposed revisions to AAR Standard S-2043 that would add tolerances for curvature and alignment and adjust the track to meet the proposed requirements and retest with no modifications to the railcar other than the necessary repairs. The AAR EEC accepted the proposed revisions and agreed that the CWSRP test needed to be repeated. MxV Rail adjusted the test zone and repeated the test on August 26 and August 27, 2020. The results from the retest met AAR Standard S-2043 criteria.

The primary cause of the derailment was a 3.7-inch variation in high rail alignment over a 47-foot test zone that resulted in a test zone that was more challenging than intended. A revision to AAR Standard S-2043 that will include additional requirements for curvature and alignment in the test zone is in progress.

5.3 Buffer Railcar Summary Results

The Buffer railcar results were presented and approved by AAR's EEC based on the testing and modeling results shown in Table 7. The letters of approval from the EEC are presented in Appendix B and Appendix C.

The Buffer railcar met all S-2043 single-car structural and dynamic testing requirements for approval of the next phase of testing. The results in Table 7 also provide the S-2043 criteria not met under specific modeling conditions. The EEC considered the performance sufficient to ensure an adequate margin of safety and granted approval for S-2043 requirements under Phase 4 testing and modeling. With EEC approval of the Buffer railcar for the Design (S-2043, Paragraph 4.0), Single Car-Testing (S-2043, Paragraph 5.0), and Post-Test Analysis (S-2043, Paragraph 8.0) results under Phase 4, the next testing and modeling phase based on S-2043 requirements is Multiple-Car Testing (S-2043, Paragraph 6.0).

The Post-Test Analysis (S-2043, Paragraph 8.0) using FEA simulations and structural test strain measurements showed that stresses were less than 75 percent of the allowable stress for all load cases listed under S-2043, Paragraph 5.4 Structural Tests in Table 7, eliminating the requirement for FEA to be refined per Paragraph 8.1 of Standard S-2043.

The revised Buffer railcar vehicle dynamics model did not meet the criteria for peak-to-peak carbody lateral acceleration for the 39-foot wavelength inputs (1.38g, limit = 1.3g) or the 44.5-foot wavelength inputs (1.31g, limit = 1.3g) in yaw and sway simulations. In contrast, the Buffer railcar met the test requirements for yaw and sway, indicating that the model is conservative. The yaw and sway test was only performed with 39-foot wavelength inputs. The EEC chose to approve the Buffer railcar in this regime based on the test result.

The revised vehicle dynamics modeling predictions did not meet the S-2043 criteria for truck side L/V ratio (0.52, limit = 0.5) in the Curving with Various Lubrication Conditions regime (S-2043, Paragraph 4.3.11.5). This exception occurred for counterclockwise runs with Case 2 lubrication and the worn wheel profile at 12 and 24 mph. The Case 2 lubrication condition was a 0.5 coefficient of friction on the top of both rails and a 0.2 coefficient of friction on the gage face of the high rail. The simulations met S-2043 criteria for curving with various lubrication conditions during clockwise runs for this lubrication and profile case and for all runs with other lubrication and profile combinations. The EEC chose to approve the Buffer railcar in this regime based on the near pass.

Because there were only small changes to the design of the Buffer railcar since the original dynamic predictions were performed, only a small subset of the regimes was run with the revised dynamic model. These regimes were chosen because they allowed comparison with the test data or because the original dynamic predictions for the regime were close to or did not meet the criteria.

As part of the railcar design phase, preliminary simulations were performed according to the Dynamic Analysis (S-2043, Paragraph 4.3) before the prototype railcar was built. The results of the preliminary simulation were submitted to the AAR as part of the preliminary design review package. These test results were used to compare the preliminary dynamic analysis predictions

and the revised model predictions to verify that modeling accurately represents the vehicle as required in Post-Test Analysis (S-2043, Paragraph 8.0).

As part of the design criteria (S-2043, Paragraph 4.0), static brake testing was conducted at the manufacturer's facility per the relevant requirements of AAR Standards S-401 and S-486.

Table 7 shows a summary of the test results and the model predictions for the Buffer railcar.

Table 7. Buffer Railcar Summary Test Results

S-2043 Paragraph	Met/Not Met	
	Revised Simulations	**Test Result**
5.2 Nonstructural Static Tests		
4.2.1/5.2.1 Truck Twist Equalization	Simulated with the Original Model Only*	Met
4.2.2/5.2.2 Carbody Twist Equalization	Simulated with the Original Model Only*	Met
4.2.3/5.2.3 Static Curve Stability	Simulated with the Original Model Only*	Met
4.2.4/5.2.4 Horizontal Curve Negotiation	Simulated with the Original Model Only*	Met
5.4 Structural Tests		
5.4.2 Squeeze (Compressive End) Load	Simulated with the Original Model Only**	Met
5.4.3 Coupler Vertical Loads	Simulated with the Original Model Only**	Met
5.4.4 Jacking	Simulated with the Original Model Only**	Met
5.4.5 Twist	Simulated with the Original Model Only**	Met
5.4.6 Impact	Not Required per S-2043	Met
5.5 Dynamic Tests		
4.3.11.3/5.5.7 Hunting	Met	Met
4.3.9.6/5.5.8 Twist and Roll	Met	Met
5.5.9 Yaw and Sway	Not Met P-P Lat Accel 1.38 Limit=1.3 EEC chose to approve due to the test result.	Met
5.5.10 Dynamic Curving	Met	Met
4.3.9.7/5.5.11 Pitch and Bounce (Chapter 11)	Met	Met
4.3.9.7/5.5.12 Pitch and Bounce (Special)	Met	Met
4.3.10.1/5.5.13 Single Bump Test	Simulated with the Original Model Only*	Met
4.3.11.6/5.5.14 Curve Entry/Exit	Simulated with the Original Model Only*	Met
4.3.10.25.5.15 Curving with Single Rail Perturbation	Met	Met
4.3.11.4/5.5.16 Standard Chapter 11 Constant Curving	Simulated with the Original Model Only*	Met

S-2043 Paragraph	Met/Not Met	
4.3.11.7/5.5.17 Special Trackwork	Simulated with the Original Model Only*	Met
4.3.11.5 Curving with Various Lubrication Conditions	Not Met Truck Side L/V 0.52, Limit=0.50 EEC chose to approve due to the near pass.	Testing not required
4.3.12 Ride Quality	Simulated with the Original Model Only*	Testing not required for non passenger-carrying railcars
4.3.13 Buff and Draft Curving	Met	Single car testing not required
4.3.14 Braking Effects on Steering	Simulated with the Original Model Only*	Testing not required
4.3.15 Worn Component Simulations	Simulated with the Original Model Only*	Testing not required
*Because the revised model showed little change compared to the original model, and because the original dynamic analysis showed a margin of safety with respect to the criteria for these regimes, these regimes were not simulated with the revised model. **Revised FEA predictions were not required per standard S-2043 paragraph 8.1 because no measured stress exceeded 75% of the allowable stress.		

5.4 Weld Cracks on the Atlas Railcar

In December 2020, cracked tri-span bolster center plate welds were found during track performance testing. In January 2021, Kasgro sent welders to the TTC to remove the defects and reweld the center plates. After all weld repairs, MxV Rail personnel performed a non-destructive examination (NDE) of the repair welds, which were found to be acceptable with no cracks.

In June 2022, MxV Rail's Rail Vehicle Maintenance (RVM) department inspected the Atlas railcar, the Buffer railcars, and the REV. One crack was found in the B-truck centerplate on left side of the Atlas railcar, parallel to the rail.

The crack was discussed with the DOE and Kasgro and was to be repaired in July while the consist was parked for installation of IWS. Figure 9 and Figure 10 show the crack defect.



Figure 9. Atlas Railcar – Crack is on Left Side of Centerplate, B-Truck



Figure 10. Atlas Railcar – Close-up of Crack on Left Side of Centerplate, B-Truck

During Kasgro repairs to the weld cracks discovered in June, more serious defects were found in the tri-span bolster base material. It was agreed that both tri-span bolsters be shipped back to Kasgro to be repaired and to begin studies to determine whether the cracks were the result of an engineering/design issue, a manufacturing process or repair process problem, or a material/metallurgical issue. The Atlas railcar cracking discovery progression can be outlined as follows:

- Cracking Type 1 (B-end tri-span bolster, B-truck centerplate) – Reported to DOE in June 2022 – cracks parallel to the weld beads in Figure 9 and Figure 10 as shown above.

- Cracking Type 2 (B-end tri-span bolster, C-truck centerplate) – Discovered Monday, July 25, 2022. Figure 11 shows vertical cracks that have the potential to migrate to the base tri-span bolster material. Kasgro determined that these cracks were in the centerplate.



Figure 11. Cracks in B-end tri-span bolster, C-truck centerplate

- Cracking Type 3 (B-span bolster, newly replaced B-truck centerplate). Cracks found after Kasgro's repair of Cracking Type 1, shown in Figure 12 and Figure 13. The cracks were in the tri-span bolster, above and perpendicular to the top weld bead. These cracks were significantly more concerning as they were in the tri-span bolster.



Figure 12. Cracking in tri-span bolster with new B truck centerplate



Figure 13. Magnified image of cracks in tri-span bolster

The DOE, Kasgro, and MxV Rail agreed that both tri-span bolsters be shipped back to Kasgro for repairs or replacement. The tri-span bolsters were shipped by MxV Rail to Kasgro at the end of the first week of August 2022, and replacements were received back at the TTC on August 29, 2022. When received, MxV Rail installed the replacement tri-span bolsters to continue testing.

5.4.1 Design Change as a Result of Cracking Issue

To avoid future cracking issues, Kasgro changed the attachment method for the six centerplates to the two Atlas railcar tri-span bolsters. The former method, from the original build drawings, is to bolt and weld them in place.

The revised method, which will be used for further dynamic tests regarding the Atlas railcar, will use a standard AAR bolting arrangement plus a tack weld to the bolt heads so the bolts cannot back out.

Kasgro has revised the Atlas fabrication drawings and is awaiting documentation and analysis requirements from the EEC. The AAR EEC is developing those requirements as of the writing of this report. In addition, Kasgro has provided information from the tests performed to determine the root cause of the cracking issues. When weld cracks were again found in June 2022 in the tri-span bolster center welds, Kasgro sent a repair welder to MxV Rail to do on-site repairs. The repairs to the B-end of the tri-span bolster center plate consisted of removing the original bolted and welded center plate before installing a new center plate of the same configuration. After rewelding the center plate, MxV Rail personnel performed an NDE on the B-end tri-span center plate repair welds and the adjacent tri-span bolster base metal (Figure 13 and Figure 14). The repair welds did not have any indications or cracks, but it was noted that there were now transverse surface cracks along the center plate weld heat affected zone (HAZ) of the B-end tri-span bolster base metal that had not been previously noted.

The decision to return the tri-span bolsters to Kasgro shop was made so that all required repairs could be handled at the Kasgro facility in a controlled shop environment, allowing Kasgro to correctly repair and return the tri-span bolsters to MxV Rail as soon as possible. The most practical way to repair these defective welds and the cracks in tri-span bolster base metal was discussed by Kasgro Engineering and fabrication personnel. Kasgro decided that making additional weld repairs to tri-span bolster center plate welds and the tri-span bolsters base metal cracks along the HAZ was not the best path forward.

The Atlas tri-span bolsters were delivered to the Kasgro Rail shop for repairs on August 11, 2022. All components and attachments to the original tri-span bolsters were removed, and Kasgro used two new tri-span bolsters to replace the original tri-span bolsters. In addition, the attachment design for center plates to tri-span bolster was changed from a bolt and welded design to a 12-bolt design center plate design (Figure 14).



Figure 14. 12-bolt centerplate mounted to replacement Atlas tri-span bolster

Kasgro had the 12-bolt design center plates in stock. Because Kasgro could not confirm what was causing the weld cracks, the all-bolt design was chosen to avoid any additional weld cracking issues with the Atlas tri-span bolster center plates for the remainder of the S-2043 Atlas railcar testing. All AAR requirements for use of bolted center plates were followed.

All repairs and modifications were completed, and the two (2) tri-span bolster assemblies were shipped back to MxV Rail and delivered at the end of August.

Kasgro sent the original center plate (Figure 15) removed from the B-end, left side of the Atlas railcar to an independent metallurgical test lab to determine if there were any issues with material properties of center plates. The metallurgical test lab concluded the center plate mechanical and chemical properties were in the acceptable range, and it was likely the cracks developed in the welds initially and then propagated into the center plate (see Kasgro Report 1).



Figure 15. Atlas BL-end centerplate after removal

Kasgro also sent a section of the original B-end tri-span bolster back to the steel mill that originally made the steel (Figure 16). The steel mill metallurgical lab investigated the surface indications located in the HAZ (Figure 12 and Figure 13) using a liquid dye penetrant NDE along the welds and determined that the originally noted surface indications were most probably

a result of the welding process and not material related. Kasgro's opinion is that the indications were most likely caused by the arc gouging removal of cracked welds and subsequent repair welding. The steel mill test lab did use NDE and ultrasonic testing to find two crack indications, that extended 5 inches and 6 inches in length but did not appear to encroach on the exterior edges of the test sample (see Kasgro Report 2).



Figure 16. Tri-span section sent for NDE testing

The steel mill lab conclusions indicated both the chemical composition and mechanical tests results obtained from the sample received for investigation meet the ASTM A572-15 GR. 60 steel requirements. These results were consistent with MTR (Material Test Reports) of the possible plate serials, and they match the chemistry of the plates sent to Kasgro (see Kasgro Report 3).

Based on the results from the sample received from the investigation, both testing laboratories concluded there was no evidence that points out issues related to the material. The multiple cracks that were observed are probably related to welding practices used during the fabrication of the part.

5.5 Dunnage Blocks – Lateral Movement

Whenever the Atlas railcar is carrying a load that requires end stops, dunnage is required as padding between the load and the end stops. This dunnage is in the form of heavy wooden blocks. Movement of one of the dunnage blocks on the Atlas Cask railcar was exhibited during testing at the TTC (Figure 17). A design modification was required to prevent the heavy wooden blocks from wiggling free and falling off the side of the railcar.



Figure 17. Dunnage problem: block on right side has slipped downward

The solution to this issue is welding pieces of angle iron to the Atlas railcar's end stops. This will prevent lateral movement of the dunnage blocks as the railcar experiences many miles of bumps and turns on the nation's rail lines. Orano, DOE's contractor for the cask securement system design and manufacture, approved MxV Rail's proposal to weld 2- to 4-inch, 72-inch-long angles to the end stops on each side of the dunnage blocks. The angles would be installed 1 to 2 inches outside the dunnage block. The angle flat edge will be on the block side. Slot welds will be used and ground smooth on the block side to eliminate the possibility of restricting block movement. The angle top edge will be welded to hinder water entry from above, while the bottom edge will not be welded to encourage moisture to drain.

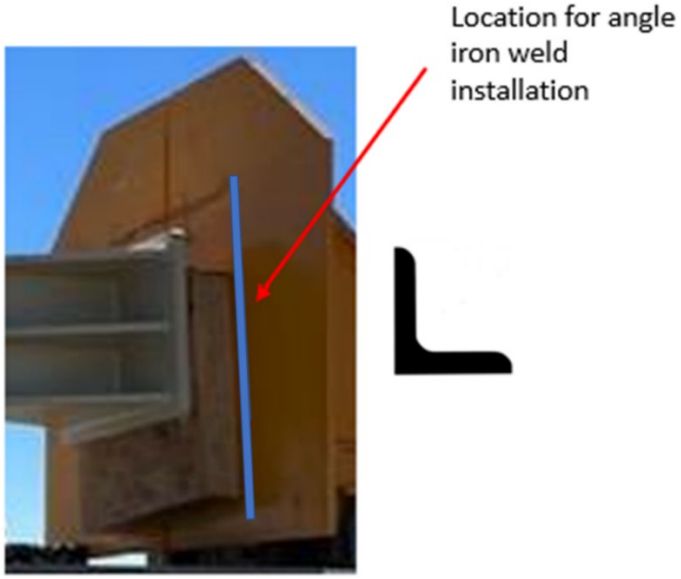


Figure 18. Solution of the dunnage movement problem

6.0 OVERVIEW OF REPORTS FOR ATLAS AND BUFFER RAILCARS

This section provides a general overview and reference tables for the four full reports developed under Phase 4 certification activities for the Atlas and Buffer railcars. Each of these two railcars has a Test Report and a Post-Test Analysis report. The tables are designed to provide a specific reference for testing and modeling report sections with corresponding references to AAR S-2043 paragraph certification requirements. Each of the four full reports is provided as an appendix in this Phase 4 Report (Appendix D through Appendix G).

6.1 Atlas Railcar Reports With S-2043 References

Atlas Single-Car Test and Post-Test Analysis testing and modeling report sections with S-2043 reference paragraphs are provided in Sections 6.1.1 and 6.1.2 of this summary report.

6.1.1 S-2043 Certification Tests of U.S. DOE Atlas Railcar Design Project 12-Axle Cask Car (Single-Car Test Report P-21-037)

Single-car testing is performed to verify that the railcar performs as designed throughout the static and dynamic testing of the railcar. The Single-Car Test report sections with S-2043 paragraphs can be referenced in Table 8. Appendix D provides the full Atlas railcar Single-Car Test report that corresponds with Table 8.

Table 8. Atlas railcar single-car tests report reference table

Atlas Railcar Test Report P-21-037: Reference			S-2043 Reference(s)
Report Section	Description	Page	Paragraph
8	Results	8	5.0
8.1	Vehicle Characterization Tests	9	5.1
8.1.1	Component Characterization Tests	9	5.1.3
8.1.2	Vertical Suspension Stiffness and Damping	16	5.1.4.3
8.1.3	Lateral Suspension Stiffness and Damping	22	5.1.4.4
8.1.4	Truck Rotation Stiffness and Breakaway Moment	28	5.1.4.5
8.1.5	Interaxle Longitudinal Stiffness	32	5.1.4.6
8.1.6	Modal Characterization	35	5.1.4.7
8.2	Nonstructural Static Tests	39	5.2
8.2.1	Truck Twist Equalization	39	5.2.1
8.2.2	Carbody Twist Equalization	42	5.2.2
8.2.3	Static Curve Stability	44	5.2.3
8.2.4	Horizontal Curve Negotiation	45	5.2.4
8.3	Static Brake Tests	45	5.3
8.4	Structural Tests	45	5.4
8.4.1	Preliminary and Post Test Inspection	49	5.4.1.1
8.4.2	Measured Stress from Test Loads	49	5.4.1.2
8.4.3	Squeeze (Compressive End) Load	51	5.4.2
8.4.4	Coupler Vertical Loads	61	5.4.3

Atlas Railcar Test Report P-21-037: Reference			S-2043 Reference(s)
Report Section	Description	Page	Paragraph
8.4.5	Jacking	67	5.4.4
8.4.6	Twist	71	5.4.5
8.4.7	Impact	79	5.4.6
8.4.8	Securement System Analysis	84	5.4.7
8.4.8.1	Dimensional Inspection	84	5.4.7
8.4.8.2	Force Calculations	86	5.4.7
8.4.8.3	Stress Analysis	88	5.4.7
8.4.8.4	Allowable Stresses, Acceptance Criteria, and Margin of Safety	89	5.4.7
8.4.8.5	Component Stress Analysis	90	5.4.7
8.4.8.6	Weld Analysis	103	5.4.7
8.5	Dynamic Tests	105	5.5
8.5.1	Primary Suspension Pad Configuration Changes	108	7.2
8.5.2	Minimum Load Hunting	110	5.5.7
8.5.3	Maximum Load Hunting	112	5.5.7
8.5.4	Minimum Test Load Twist and Roll	114	5.5.8
8.5.5	Maximum Test Load Twist and Roll	115	5.5.8
8.5.6	Yaw and Sway	116	5.5.9
8.5.7	Minimum Load Dynamic Curving	117	5.5.10
8.5.8	Maximum Load Dynamic Curving	118	5.5.10
8.5.9	Pitch and Bounce (Chapter 11)	121	5.5.11
8.5.10	Pitch and Bounce (Special)	122	5.5.12
8.5.11	Minimum Load Single Bump Test	122	5.5.13
8.5.12	Maximum Load Single Bump Test	123	5.5.13
8.5.13	Minimum Test Load Curve Entry/Exit	124	5.5.14
8.5.13.1	Minimum Load Limiting Spiral Negotiation	124	5.5.14.1
8.5.13.2	Minimum Load Normal Spiral Negotiation	126	5.5.14.2
8.5.14	Maximum Load Curve Entry/Exit	127	5.5.14
8.5.14.1	Maximum Load Limiting Spiral Negotiation	128	5.5.14.1
8.5.14.2	Maximum Load Normal Spiral Negotiation	129	5.5.14.2
8.5.15	Minimum Load Curving with Single Rail Perturbation	130	5.5.15
8.5.16	Maximum Load Curving with Single Rail Perturbation	134	5.5.15
8.5.17	Minimum Load Standard Chapter 11 Constant Curving	137	5.5.16
8.5.18	Maximum Load Standard Chapter 11 Constant Curving	139	5.5.16
8.5.19	Minimum Test Load Special Trackwork	141	5.5.17
8.5.20	Maximum Test Load Special Trackwork	145	5.5.17
8.6	Ride Quality	148	5.5.18

6.1.2 Atlas Car Post-Test Analysis (Report P-21-049 [formerly Report P-21-042])

The Post-Test Analysis report shows comparisons of pre-test FEA structural simulations and the vehicle dynamic modeling predictions with test data for the Atlas railcar from the Single-Car Test. If necessary, models are revised to represent the vehicle more accurately, and revised predictions are also presented in the post test analysis report. The Post-Test Analysis testing and modeling report sections with S-2043 paragraphs can be referenced in Table 9. Appendix E provides the full Atlas Post-Test Analysis report that corresponds with Table 9.

Table 9. Atlas railcar post-test analysis report reference table

Atlas Railcar Post-Test Analysis Report P-21-049 (formerly P-21-042)			**AAR S-2043 Report Reference: Paragraph(s)**		
Report Section	Description	Page	4.0 DESIGN	5.0 SINGLE-CAR TEST	8.0 POST-TEST ANALYSIS
4	Refining the FEA	5			8.1
4.1	Loading Conditions for Structural Tests	6	4.1.5.2		
4.1.1	Test Loads	6	4.1.5.2		
4.1.2	Measured Stresses from Test Loads	6	4.1.5.2		
4.2	Squeeze (Compressive End) Load	9	4.1.5.7	5.4.2	
4.3	Coupler Vertical Loads	12	4.1.5.3	5.4.3	
4.4	Jacking	14	4.1.5.4	5.4.4	
4.5	Twist	16	4.1.5.5	5.4.5	
4.5.1	Suspension Twist	16	4.1.5.5	5.4.5.1	
4.5.2	Carbody Twist	19		5.4.5.2	
4.6	Impact	21	4.1.5.8	5.4.6	
5.0	New FEA Predictions	23			8.2
6.0	Refining the Dynamic Model	23			8.3
7.0	New Dynamic Predictions	27			8.4
7.1	Twist and Roll	29	4.3.9.6	5.5.8	
7.2	Pitch and Bounce (Chapter 11)	32	4.3.9.7	5.5.11	
7.3	Yaw and Sway	35	4.3.9.8	5.5.9	
7.4	Dynamic Curving	37	4.3.9.9	5.5.10	
7.5	Single Bump Test	43	4.3.10.1	5.5.13	
7.6	Curving with Single Rail Perturbation	47	4.3.10.2	5.5.15	
7.7	Hunting	53	4.3.11.3	5.5.7	
7.8	Constant Curving	57	4.3.11.4	5.5.16	
7.9	Curving with Various Lubrication Conditions	61	4.3.11.5		
7.10	Limiting Spiral Negotiation	71	4.3.11.6	5.5.14.1	
7.11	Special Trackwork: Turnouts and Crossovers (S-2043, Paragraph 4.3.11.7)	74	4.3.11.7	5.5.17	

Atlas Railcar Post-Test Analysis Report P-21-049 (formerly P-21-042)			AAR S-2043 Report Reference: Paragraph(s)		
Report Section	Description	Page	4.0 DESIGN	5.0 SINGLE-CAR TEST	8.0 POST-TEST ANALYSIS
7.12	Buff and Draft Curving	77	4.3.13		
7.13	Worn Component Simulations	79	4.3.15		
7.13.1	Worn Constant Contact Side Bearings	80	4.3.15		
7.13.2	Centerplate	82	4.3.15		
7.13.3	Primary Pad	84	4.3.15		
7.13.4	Friction Wedges	86	4.3.15		
7.13.5	Broken Spring	88	4.3.15		

6.2 Buffer Railcar Reports

Buffer Single-Car Test and Post-Test Analysis testing and modeling report sections with S-2043 reference paragraphs are provided in Section 6.2.1 and 6.2.2.

6.2.1 AAR Standard S-2043 Single-Car Certification Tests of U.S. DOE Atlas Railcar Design Project Buffer Railcar (Report P-20-032)

The single-car test is performed to verify that the Buffer railcar performs as designed through static and dynamic testing of the railcar. The Single-Car Test report sections with S-2043 paragraphs can be referenced in Table 10. Appendix G provides the full Buffer railcar Single-Car Test report that corresponds with Table 10.

Table 10. Buffer railcar single-car tests report reference table

Buffer Railcar Test Report P-20-032: Reference			S-2043 Reference(s)
Section	Description	Page	Paragraph (s)
5	Results	4	5.0
5.1	Vehicle Characterization	4	5.1
5.1.1	Component Characterization Tests	4	5.1.3
5.1.2	Vertical Suspension Stiffness and Damping	10	5.1.4.3
5.1.3	Lateral Suspension Stiffness and Damping	16	5.1.4.4
5.1.4	Truck Rotation Stiffness and Breakaway Moment	21	5.1.4.5
5.1.5	Interaxle Longitudinal Stiffness	23	5.1.4.6
5.1.6	Modal Characterization	25	5.1.4.7
5.2	Nonstructural Static Tests	28	5.2
5.2.1	Truck Twist Equalization	28	5.2.1
5.2.2	Carbody Twist Equalization	29	5.2.2
5.2.3	Static Curve Stability	31	5.2.3
5.2.4	Horizontal Curve Negotiation	31	5.2.4

Buffer Railcar Test Report P-20-032: Reference			S-2043 Reference(s)
5.3	Static Brake Tests	32	5.3
5.4	Structural Tests	32	5.4
5.4.1	Preliminary and Post Test Inspection	35	5.4.1.1
5.4.2	Squeeze (Compressive End) Load	35	5.4.2
5.4.3	Coupler Vertical Loads	36	5.4.3
5.4.4	Jacking	37	5.4.4
5.4.5	Twist	38	5.4.5
5.4.6	Impact	41	5.4.6
5.4.7	Securement System	41	5.4.7
5.5	Dynamic Tests	42	5.5
5.5.1	Hunting	44	5.5.7
5.5.2	Twist and Roll	46	5.5.8
5.5.3	Yaw and Sway	46	5.5.9
5.5.4	Dynamic Curving	47	5.5.10
5.5.5	Pitch and Bounce (Chapter 11)	48	5.5.11
5.5.6	Special Pitch and Bounce	49	5.5.12
5.5.7	Single Bump Test	50	5.5.13
5.5.8	Limiting Spiral Negotiation	51	5.5.14.1
5.5.9	Normal Spiral Negotiation	52	5.5.14.2
5.5.10	Curving with Single Rail Perturbation	54	5.5.15
5.5.11	Standard Chapter 11 Constant Curving	56	5.5.16
5.5.12	Special Trackwork	57	5.5.17
5.6	Ride Quality	61	6.5.18

6.2.2 Buffer Car Post-Test Analysis (Report P-21-013)

The post-test analysis report shows comparisons of pre-test FEA structural simulations and the vehicle dynamic modeling predictions with test data for the Buffer railcar from the single-car test results. MxV Rail revised the model to reflect the vehicle more accurately and performed simulations to 1) demonstrate the model performance compared to test data and 2) check the performance in regimes where the original dynamic analysis was close to or did not meet the criteria. Section 7 of the Post-Test Analysis report describes the regimes that were not included in new dynamic predictions. The Post-Test Analysis, testing, and modeling report sections with S-2043 paragraphs can be referenced in Table 11. Appendix F provides the full Buffer railcar Post-Test Analysis report that corresponds with Table 11.

Table 11. Buffer railcar post-test analysis report reference table

Buffer Car Post-Test Analysis Report P-21-013			S-2043 Report Reference(s): Paragraph(s)		
Section	Description	Page	4.0 DESIGN	5.0 SINGLE-CAR TEST	8.0 POST-TEST ANALYSIS
4	Refining the Finite Element Analysis (FEA)	4			8.1
4.1	Squeeze (Compressive End) Load	4	4.1.5.7	5.4.2	
4.2	Coupler Vertical Loads	5	4.1.5.3	5.4.3	
4.3	Jacking	6	4.1.5.4	5.4.4	
4.4	Twist	7	4.1.5.5	5.4.5	
4.4.1	Suspension Twist	7	4.1.5.5	5.4.5.1	
4.4.2	Carbody Twist	8		5.4.5.2	
4.5	Impact Test	9	4.1.5.8	5.4.6	
5	New Finite Element Analysis Predictions	10			8.2
6	Refining the Dynamic Model	10			8.3
7	New Dynamic Predictions	14			8.4
7.1	Twist and Roll	15	4.3.9.6	5.5.8	
7.2	Pitch and Bounce	17	4.3.9.7	5.5.11	
7.3	Special Pitch and Bounce (44.5-foot wavelength)	18	4.3.9.7	5.5.12	
7.4	Yaw and Sway	20	4.3.9.8	5.5.9	
7.5	Dynamic Curving	22	4.3.9.9	5.5.10	
7.6	Curving with a Single-rail Perturbation	24	4.3.10.2	5.5.15	
7.7	Hunting	26	4.3.11.3	5.5.7	
7.8	Curving with Various Lubrication Conditions	27	4.3.11.5		
7.9	Turnouts and Crossovers	29	4.3.11.7	5.5.17	
7.10	Buff and Draft Curving	30	4.3.13		

7.0 CONCLUSIONS

Both the Atlas and Buffer railcars received EEC approval of Single-Car Testing in accordance with AAR S-2043. Both of these railcars have since moved into the Multicar Testing (Paragraph 6.0) phase of AAR S-2043 certification.

On behalf of the DOE, MxV Rail requested exceptions from the AAR EEC to approve the Atlas railcar because the post-test simulations with the production CSM 58 pads did not meet some of the criteria for hunting, curving with single rail perturbation, and curving with various lubrication conditions. The onset of the hunting regime occurred at speeds above 65 mph—beyond the 50-mph limit recommended in OT-55 for cars in HLRM service. Although the performance

simulated for curving with a single rail perturbation and curving with various lubrication conditions did not meet Standard S-2043 criteria, it did meet Chapter 11 criteria.

The results from the Single Car-Test (Paragraph 5.0) for the Atlas railcar, specifically the FEA simulations and structural test strain measurements, both showed that stresses were less than 75 percent of the allowable stress, thereby eliminating the requirement in Standard S-2043, Paragraph 8.1 for the FEA to be refined.

The Buffer railcar met all S-2043 single-car structural and dynamic test requirements. The FEA simulations and structural test strain measurements both showed that stresses were less than 75 percent of the allowable stress, thereby eliminating the requirement for the FEA to be refined (S-2043, Paragraph 8.1).

The revised vehicle dynamics model simulation predicted the Buffer railcar would not meet the criterion for peak-to-peak carbody lateral acceleration for the 39-foot wavelength inputs (1.38g, limit=1.3g) or the 44.5-foot wavelength inputs (1.31g, limit=1.3g) in yaw and sway tests. In contrast, the Buffer railcar met test requirements for yaw and sway tests. The yaw and sway test is only performed with 39-foot wavelength inputs.

The revised vehicle dynamic modeling predictions for the Atlas railcar did not meet criteria for truck side L/V ratio (0.52, limit=0.5) in the curving with various lubrication conditions regime. This exception occurred for counterclockwise runs with Case 2 lubrication and the worn wheel profile at 12 and 24 mph. The Case 2 lubrication condition is a 0.5 coefficient of friction on the top of both rails and a 0.2 coefficient of friction on the gage face of the high rail. Simulations meet S-2043 criteria for curving with various lubrication conditions during clockwise runs for this lubrication and profile case and for all runs with other lubrication and profile combinations.

References

1. AAR *Manual of Standards and Recommended Practices*, Car Construction Fundamentals and Details, Performance Specification for Trains Used to Carry High-Level Radioactive Material, Standard S-2043, Effective: 2003; Last Revised: 2017, Association of American Railroads, Washington, D.C.

2. Electronic Code of Federal Regulations, Title 49, Subtitle B, Chapter II, Part 213—Track Safety Standards. Downloaded from https://www.ecfr.gov/cgibin/retrieveECFR?gp=&SID=5dd8cd0b6dd88207ddc99c4bbc9527e0&mc=true&r=PART&n=pt49.4.214.

3. Wu, H., and Elkins, J. "Investigation of Wheel Flange Climb Derailment Criteria." Research Report R-931. Association of American Railroads, Pueblo, CO. 1999.

4. Elkins, J., and Wu, H. "New Criteria for Flange Climb Derailment." IEEE/ASME Joint Railroad Conference paper. Newark, New Jersey. April 4-6, 2000.

5. 2020 Field Manual of The AAR Interchange Rules, adopted by The Association of American Railroads, Safety and Operations, Rules and Standards, Effective January 1, 2020, Association of American Railroads, Washington, D.C.

6. AAR Manual of Standards and Recommended Practices Section C – Part II, "Design, Fabrication and Construction of Freight Cars." Appendix C Specification for Instrumented Wheelsets, Association of American Railroads, Washington D.C., 2003; implemented November 2015.

7. EEC Docket 209.240. "Kasgro DOE HLRM Cask and Buffer Car." TTCI Document Number CR-20-002. TTCI local area network < Q:\Business Services\Tech Docs\DOE Controlled Document Folder\CR-Correspondence>, January 2016, revised August 20, 2020.

ATTACHMENTS

KASGRO REPORT 1
METALLURGICAL REPORT

Miller, Bret A. 2022. Metallurgical Evaluation of a Welded Steel Plate. Report No. 20221788. IMR Test Labs, Louisville, KY. Proprietary Report.

KASGRO REPORT 2
TRI-SPAN INSPECTION REPORT

CLIFFS

Atlas Project Trispan Test Piece

Inspectors: Inspection completed by B Wowianko III and J Carrier I

Date: September 2, 2022

Equipment: Epoch 650 7809, 2.25 MHz 1"x0.5" Transducer, with 45 deg Wedge

During the inspection of the sample two (2) cracks indications were found on the BR side of the sample. The two crack indications in question extend 5" and 6" in length. These indications do not appear to encroach to the exterior edges of the test sample.



Figure 1: Image of Trispan Test Piece showing two (2) crack indications on the BR side of the sample

CLIFFS

Atlas Project Trispan Test Piece

Inspectors: Inspection completed by B Wowianko III and J Carrier I

Date: September 2, 2022

Equipment: Epoch 650 7809, 2.25 MHz 1"x0.5" Transducer, with 45 deg Wedge

During the inspection of the sample two (2) cracks indications were found on the BR side of the sample. The two crack indications in question extend 5" and 6" in length. These indications do not appear to encroach to the exterior edges of the test sample.



Figure 1: Image of Trispan Test Piece showing two (2) crack indications on the BR side of the sample



Figure 2: Image showing the crack indication that is 5" in length



Figure 3: Image showing the crack indication that is 6" in length

Brock Wowianko III

Brock Wowianko Level III, Jason Carrier Level I

KASGRO REPORT 3
METALS INVESTIGATION REPORT

September 15, 2022

To: Eric Beach
General Manager Plate
Triad Metal International
Pittsburgh, PA

From: S. Smith, B. Wowianko and T. Ros
Cleveland-Cliffs
Burns Harbor Plate Quality Assurance

Customer Claim - Triad Metals Investigation

Background

Triad Metals submitted a specimen to the Burns Harbor Plate Mill Metallurgical Laboratory for evaluation due to cracking near the weld of the fabricated sample. The plate grade is ASTM A572-15 GR 60 with two possible serials H023195 or J020022 shown in table 1. Both possible serials were rolled and shipped from Burns Harbor in early 2018.

The provided plate was torch cut in two locations as seen in Figure 1. The specimens extracted from the two locations were given the following I.D.s "BI" (SS00001) and "BR" (SS00002). Samples from both locations were prepared for chemical analysis, tensile and V-Notch Charpy impacts tests. The results of these tests are found in tables 2, 3, and 4.

Dye penetrant and ultrasonic evaluation was conducted on the BR side of the sample to determine the presence of cracks or any other imperfection in the material and the weld.

Table 1. Possible serial numbers of the provided plate.

SM Grade	Serial Number	Heat Number	Ship Manifest	Ship Date
A257	H023195	812z36570	803-29091	01/26/2018
A257	J020022	812z36480	803-29364	02/09/2018



Figure 1. Cut procedure on the provided plate with labeled I.D.s.

Non-Destructive Testing

Dye penetrant testing was performed on the BR side of the sample. Multiple small crack indications were found along the weld in the Heat Affected Zone (HAZ). Refer to the arrows in Figure 2 and Figure 3.

An Ultrasonic evaluation was conducted on the sample, two ultrasonic indications were found on the BR side of the sample. These indications were found roughly one inch into the sample and did not propagate to the surface or edge of the material. These indications lined up with the location of the support beams on the bottom of the part, as shown in Figure 3.

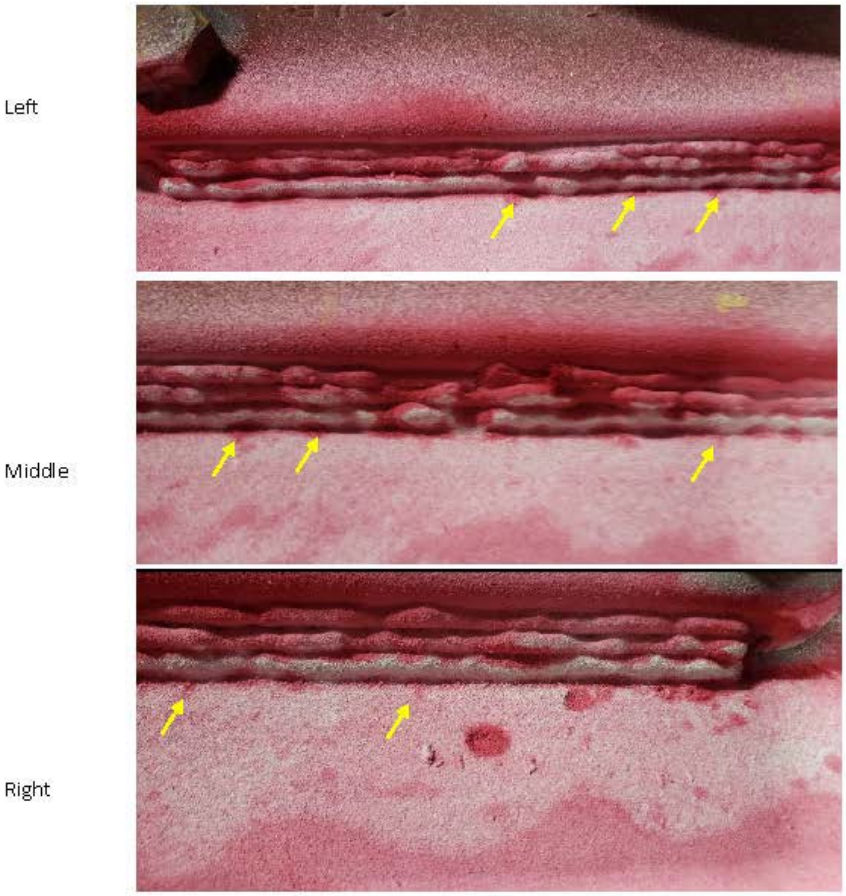


Figure 2. Multiple small cracks in the HAZ detected by Dye Penetrant inspection in the BR side of the sample received for investigation.

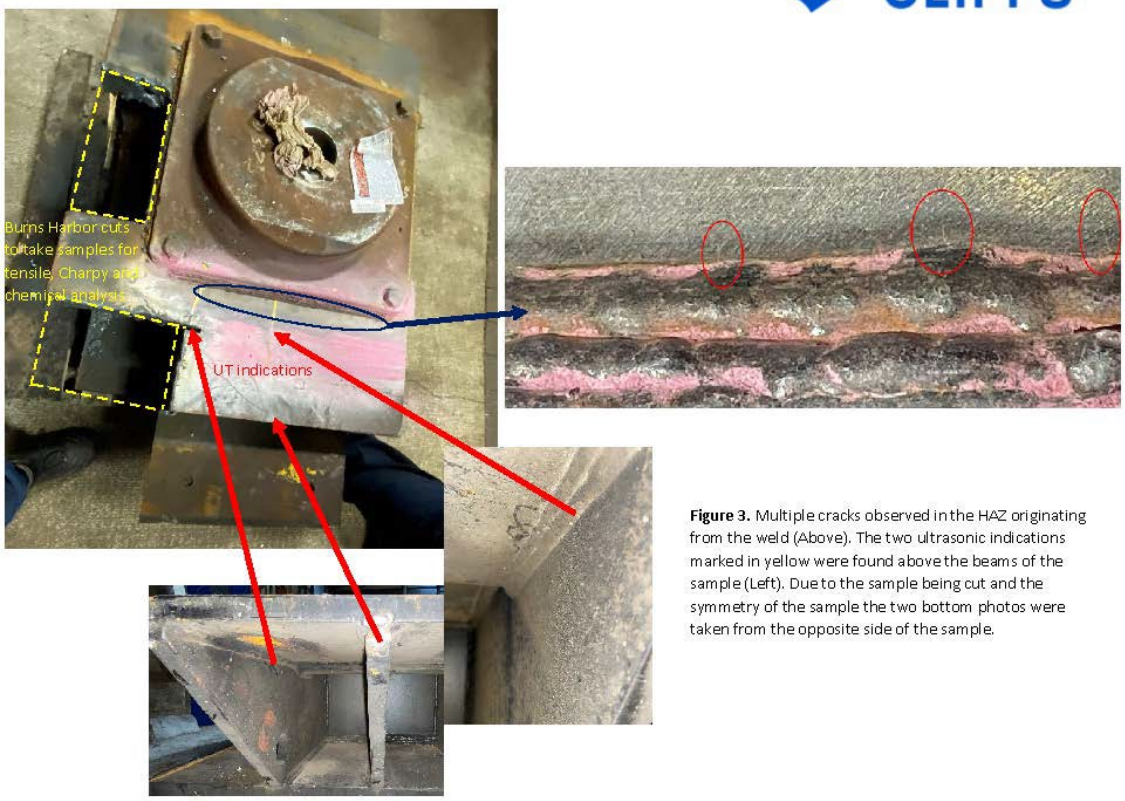


Figure 3. Multiple cracks observed in the HAZ originating from the weld (Above). The two ultrasonic indications marked in yellow were found above the beams of the sample (Left). Due to the sample being cut and the symmetry of the sample the two bottom photos were taken from the opposite side of the sample.

Tensile Tests Results

Tensile properties were found to be acceptable and consistent with the properties reported in the Plate Material Test Results (MTR).

Table 2. Tensile results

I.D. Number	Sample	Location	Yield (ksi)	Tensile (ksi)	Elongation (%)
SS00001	BI	Top	78.3	94.6	25
SS00001	BI	Bottom	78.3	94.6	25
SS00002	BR	Top	78.6	94.4	27
SS00002	BR	Bottom	78.6	94.4	27
H023195^	-	-	76	94.1	28
J020022^	-	-	80.8	96.6	34

^ indicates certified test results from shipped plate

Charpy V-Notch Impact Tests Results

Charpy tests were conducted at 0°F. All impact tests results met specifications and are consistent with the properties reported in the MTR.

Table 3. Impact results

I.D. Number	Sample	Energy (FT.LBS)			Average (FT.LBS)
SS00001	BI	83	107	129	106
SS00002	BR	106	91	106	101
H023195^	-	107	63	87	86
J020022^	-	89	80	74	81

^ indicates certified test results from shipped plate

Chemical Composition Results

The chemical analysis conducted on the sample returned from the customer is consistent with the heat analysis as reported on MTR.

Table 4. Chemical composition results

Element Symbol	Composition		
	BR (wt%)	H023195 (wt%)^	J020022 (wt%)^
C	0.171	0.17	0.18
Mn	1.24	1.18	1.19
P	0.011	0.011	0.012
S	0.003	0.003	0.004
Si	0.281	0.265	0.275
Cu	0.017	0.018	0.021
Ni	0.01	0.01	0.01
Cr	0.03	0.03	0.03
Sn	0.002	0.002	0.002
Mo	0.005	0.003	0.007
V	0.089	0.083	0.088
Al	0.35	0.033	0.03
Cb	0.002	0.002	0.002
B	0.0003	0.0002	0.0002
Ti	0.002	0.002	0.002
Ca	0.0022	0.0024	0.0023

^ indicates certified test results from shipped plate

Conclusions

The chemical composition and mechanical tests results obtained from the sample received for investigation meet the requirements of the ASTM A572-15 GR 60.

These results are consistent with MTR of the possible Plate Serials and match the chemistry of the plates sent to the customer.

Based on the results from the sample received from the investigation there is no evidence that point out issues related to the material. The multiple cracks that were observed are most probably related to the welding practice used during the fabrication of the part.

APPENDIX A
EEC APPROVAL LETTERS FOR ATLAS RAILCAR (SINGLE-CAR TEST AND POST-TEST ANALYSIS

Ron Hynes
Assistant Vice President
Technical Services
rhynes@aar.org

ASSOCIATION OF AMERICAN RAILROADS

Nichole Fimple
AVP Business Services / Executive
Director Rules and Standards
nfimple@aar.org

Transmitted via email

April 29, 2022
File 209.240

Dr. Patrick Schwab
Nuclear Engineer
U.S. Department of Energy, Office of Nuclear Energy
19901 Germantown Road
Germantown, MD 20874

Subject: AAR Standard S-2043 Approval of DOE Atlas Railcar Single Car Tests

Dear Dr. Schwab,

The AAR Equipment Engineering Committee (EEC) has completed their review of the following S-2043 Reports:

- S-2043 Certification Tests of the United States Department of Energy Atlas Railcar Design Project 12-Axle Cask Car submitted in TTCI Report P-21-037
- Atlas Car Post Test Analysis Report submitted in TTCI Report P-21-042
- The expert reviews of the same reports conducted by Objective Engineers, Inc.

The EEC hereby approves the results which demonstrate that the requirements of the following sections of Standard S-2043 have been met:

1. Paragraph 5.1 Vehicle Characterization
2. Paragraph 5.2 Nonstructural Static Tests
3. Paragraph 5.3 Static Brake Tests
4. Paragraph 5.4 Structural Tests
5. Paragraph 5.5 Dynamic Tests

EEC's acceptance of specific test results and guidance (as necessary) follow, organized by the relative section of Standard S-2043:

- Paragraph 5.5.7 Hunting
  The hunting measured with the CSM 58 adapter pad was mild and does not present safety concerns. Additionally, the conditions that the car hunted in test will not be encountered in service (i.e. operating at speeds above 65, use of wide flange worn wheelsets with a conicity prone to hunting). The operating plan must include a maximum speed to avoid the speeds at which hunting was encountered.

- Standard Chapter 11 Constant Curving
  Test results were produced using the CSM 70 adapter pads. The CSM 58 pads provide better curving as shown by modeling results. The EEC considers this requirement to be met by use of the CSM 58 pads.

- 5.2.1 Truck Twist Equalization
  Most cases of this very severe requirement were met. EEC understands why the center truck of a tri-span bolster would have difficulty meeting the requirement. Values found were 10-17 percentage points less than allowed by S-2043. A minimum of 24% of the static load was still carried, which is reasonable. This is a stationary test, and the EEC accepts the results based on the more important dynamic aspects of proper equalization were shown to be acceptable by performance in:
  1. 5.5.15 Curving with single perturbation
  2. 5.5.10 Dynamic curving, and
  3. 5.5.14 Limiting spiral

- 5.5.15 Curving with Single Rail Perturbation
  Testing did not meet criteria using the CSM 70 and CSM 65 pads. However, modeling with the CSM 58 pad produced successful results for wheel/rail forces. The EEC considers the wheel/rail force requirements to be met. The car body roll angle that does not meet in modeling with a 3-inch perturbation is simply an effect of local track geometry that cannot be addressed realistically. The EEC accepts the roll angle results as they are.

The Atlas Railcar test results and models are considered by the EEC as satisfactory, and the latest dynamic models are approved to use for project analysis going forward.

The Atlas Railcar is now approved to proceed to the Multiple-Car Test phase of Standard S-2043. The EEC agrees with the expert review recommendations that during multiple car testing the Atlas car be stopped in the TTC WRM 12 degree curve, the local depot activity 10 degree curve, and the BNSF Alps N.M. horseshoe 10 degree curve (if possible), and the car slowly pulled through the exit spiral of the curve while gage spreading and gage spreading forces are monitored.

If you have any questions, please contact Mr. Jon Hannafious of our MxV Rail subsidiary at (719) 251-6571.

Sincerely,

Nichole Fimple

Nichole Fimple

NF/jsh

cc: Karen Carriere, MxV Rail
David Cackovic, MxV Rail
Equipment Engineering Committee

APPENDIX B
EEC APPROVAL LETTERS FOR BUFFER RAILCAR (SINGLE-CAR TEST)

Ron Hynes
Assistant Vice President
Technical Services

Nichole Fimple
Executive Director
Rules and Standards

ASSOCIATION OF AMERICAN RAILROADS
Transmitted via email

August 30, 2021
File 209.240

Subject: AAR Standard S-2043 Single Car Test Approval of DOE Atlas Railcar Design Project Buffer Car

Patrick Schwab
Nuclear Engineer
U.S. Department of Energy, Office of Nuclear Energy
19901 Germantown Road
Germantown, MD 20874

Dear Mr. Schwab:

The AAR Equipment Engineering Committee (EEC) has completed their review of the Single Car Test results of the DOE Atlas Railcar Design Project Buffer Car submitted in TTCI Certification Report P-20-032, and of the Expert Review of the same report conducted by Objective Engineers, Inc. The EEC hereby approves the Buffer Car Single Car Test results based on satisfactory completion/results of the following sections of S-2043:

1. Paragraph 5.1 Vehicle Characterization
2. Paragraph 5.2 Nonstructural Static Tests
3. Paragraph 5.3 Static Brake Tests
4. Paragraph 5.4 Structural Tests
5. Paragraph 5.5 Dynamic Tests

The buffer car is now approved to proceed to the Multiple-Car Test phase of Standard S-2043.

If you have any questions please contact Mr. Jon Hannafious of our Transportation Technology Center, Inc., subsidiary at (719) 584-0682.

Sincerely,

Nichole Fimple

NF/jsh

cc: Equipment Engineering Committee
MaryClara Jones, TTCI

APPENDIX C
EEC APPROVAL LETTER FOR BUFFER RAILCAR (POST-TEST ANALYSIS)

Ron Hynes
Assistant Vice President
Technical Services

Nichole Fimple
Executive Director
Rules and Standards

ASSOCIATION OF AMERICAN RAILROADS
Transmitted via email

August 30, 2021
File 209.240

Subject: AAR Standard S-2043 Approval of DOE Atlas Railcar Design Project Buffer Car Post Test Analysis (Single Car Test)

Patrick Schwab
Nuclear Engineer
U.S. Department of Energy, Office of Nuclear Energy
19901 Germantown Road
Germantown, MD 20874

Dear Mr. Schwab:

The AAR Equipment Engineering Committee (EEC) has completed their review of the Post Test Analysis (of Single Car Test) of the DOE Atlas Railcar Design Project Buffer Car submitted in TTCI Report P-21-013, and of the expert review of the same report conducted by Objective Engineers, Inc. The EEC hereby approves the Post Test Analysis based on satisfactory modeling results that show the intent of the following sections of S-2043 have been met:

1. Paragraph 8.1 Refining the FEA - Was not necessary.
2. Paragraph 8.2 New FEA Predictions - Were not necessary.
3. Paragraph 8.3 Refining the Dynamic Model – Model improved to better match test results.
4. Paragraph 8.4 New Dynamic Predictions – New simulations conducted based on effect of changes made in the model.

The buffer car simulation results and models are considered by the EEC as satisfactory, and the revised dynamic models approved to use for project analysis going forward.

If you have any questions please contact Mr. Jon Hannafious of our Transportation Technology Center, Inc., subsidiary at (719) 584-0682.

Sincerely,

Nichole Fimple

NF/jsh
cc: Equipment Engineering Committee
MaryClara Jones, TTCI

APPENDIX D
P-21-037 S-2043 CERTIFICATION TESTS OF UNITED STATES DEPARTMENT OF ENERGY ATLAS RAILCAR DESIGN PROJECT 12-AXLE CASK CAR

S-2043 CERTIFICATION TESTS OF UNITED STATES DEPARTMENT OF ENERGY ATLAS RAILCAR DESIGN PROJECT 12-AXLE CASK CAR

Certification report for Prepared for U.S. Department of Energy

Report P-21-037

April 1, 2022

Prepared by Russell Walker, MaryClara Jones, Juan Carlos Valdes-Salazar, Richard Joy, Mitch Miller, and Brent Whitsitt

TRANSPORTATION TECHNOLOGY CENTER, INC.

Pueblo, Colorado 81001 USA
www.ttci.tech

TTCI is a wholly owned subsidiary of the Association of American Railroads.

Disclaimer: This report was prepared by Transportation Technology Center, Inc. (TTCI) of Pueblo, Colorado, a subsidiary of the Association of American Railroads (AAR). Investigations and/or tests reported herein were authorized by the AAR and conducted in accordance with the appropriate AAR standard(s). This report is provided for consideration by the appropriate AAR technical committee and does not constitute in any way approval or disapproval of the product(s) tested. The contents of this report imply no endorsements whatsoever by TTCI or AAR of products, services, or procedures, nor are they intended to suggest the applicability of the test results under circumstances other than those described in this report. TTCI is not a source of information with respect to these tests, nor is it a source of copies of this report. TTCI MAKES NO REPRESENTATION OR WARRANTIES, EITHER EXPRESSED OR IMPLIED, WITH RESPECT TO THIS REPORT OR ITS CONTENTS. TTCI ASSUMES NO LIABILITY FOR SPECIAL, COLLATERAL, EXEMPLARY, INDIRECT, INCIDENTAL, CONSEQUENTIAL, OR ANY OTHER KIND OF DAMAGES RESULTING FROM THE USE OR APPLICATION OF THIS REPORT OR ITS CONTENTS.

Executive Summary

Transportation Technology Center, Inc., a subsidiary of the Association of American Railroads (AAR), performed certification testing on the United States Department of Energy's (DOE's) 12-axle cask car (Atlas car). The Atlas car has been developed as part of the DOE's Atlas railcar Design Project that is intended to meet the need for future large-scale transport of spent nuclear fuel and high-level radioactive waste. Tests were performed according to the AAR's *Manual of Standards and Recommended Practices* (MSRP), Standard S-2043, "Performance Specification for Trains Used to Carry High-Level Radioactive Material," revised 2017.[1] For the purpose of these tests, DOE designed and fabricated a minimum test load and a maximum test load.

Early vehicle testing revealed truck instability at higher speeds when the car was at the minimum test load. TTCI tested different side bearings, centerplate liners, and primary pads to address this behavior. The use of stiffer primary pads (prototype CSM 70 pads) was the only change that improved the hunting performance. All dynamic testing was completed with the CSM 70 pads, though some dynamic test regimes were also completed with different primary pads. On October 15, 2020, TTCI reviewed the results with the AAR Equipment Engineering Committee (EEC). The EEC directed TTCI to re-test the car with softer primary pads and a minimum test load in the dynamic curving regime. The EEC emphasized that curving performance was more important than high speed stability performance because the car would be speed limited to less than 50 mph by AAR circular OT-55 when in high-level radioactive material (HLRM) service.

The chosen primary suspension pads were made from chlorosulfonated polyethylene or CSM and are categorized by the Shore D durometer hardness value. The production CSM 58 pads were chosen based on the balance of curving and high-speed stability performance. The hunting regime was tested with CSM 58 pads in both minimum and maximum test load conditions. The dynamic curving regime was tested with CSM 58 pads in the minimum test load condition. All other dynamic tests were completed with CSM 70 pads. The effect of the pad change on other regimes will be evaluated using modeling and then documented in the post-test analysis report. The table below shows the tests performed, the results of the tests, data where criteria were not met, and the primary pad used during testing. Vehicle characterization tests are not listed because there are no pass-fail criteria in Standard S-2043 for the characterization tests, as the tests are intended to provide input for simulations.

Analysis was also performed on the securement system, and welds were fabricated and inspected as required in AWS D15.1. Detailed analysis shows that pin stresses do not exceed the ultimate stress. Maximum strains are below the ultimate strain levels.

Standard S-2043 Section	Pad Type	Met / Not Met	Test Measurement (if S-2043 Criteria was Not Met)	Performance requirement
5.2 Nonstructural Static Tests				
5.2.1 Truck Twist Equalization	CSM 58	Not Met	**Minimum Test Load:** Wheel load at 50% during 2" drop condition. Wheel load at 24% during 3" drop condition. **Maximum Test Load:** Wheel load at 43% during 2" drop condition. Wheel load at 29% during 3" drop condition.	60% minimum wheel load at 2" drop. 40% minimum wheel load at 3" drop. 60% minimum wheel load at 2" drop. 40% minimum wheel load at 3" drop.
5.2.2 Carbody Twist Equalization	CSM 58	Met		
5.2.3 Static Curve Stability	CSM 58	Met		
5.2.4 Horizontal Curve Negotiation	CSM 58	Met		
5.4 Structural Tests				
5.4.2 Squeeze (Compressive End) Load	CSM 58	Met		
5.4.3 Coupler Vertical Loads	CSM 58	Met		
5.4.4 Jacking	CSM 58	Met		
5.4.5 Twist	CSM 58	Met		
5.4.6 Impact	CSM 58	Met		
5.4.7 Securement System Test	CSM 58	Met		
5.5 Dynamic Tests				
5.5.7 Hunting	CSM 58	Not Met	**Minimum Test Load:** Car unstable at speeds greater than 65 mph with KR wheel profiles	Truck hunting may not be observed at speeds of 70mph or less.
	CSM 70	Met		
5.5.8 Twist and Roll	CSM 70	Met		
5.5.9 Yaw and Sway	CSM 70	Met		
5.5.10 Dynamic Curving	CSM 58	Met		
	CSM 70	Not Met	**Maximum Test Load:** Wheel L/V ratio = 0.81	0.80 maximum wheel L/V ratio.
5.5.11 Pitch and Bounce (Chapter XI)	CSM 70	Met		
5.5.12 Pitch and Bounce (Special)	CSM 70	Met		
5.5.13 Single Bump Test	CSM 70	Met		
5.5.14 Curve Entry/Exit	CSM 70	Met		
5.5.15 Curving with Single Rail Perturbation	CSM 65	Not Met	**Minimum Test Load:** Wheel L/V ratio = 0.84	0.80 max wheel L/V
	CSM 70	Not Met	**Minimum Test Load:** Wheel L/V ratio = 0.88 Truck L/V ratio = 0.50	0.80 max wheel L/V 0.50 max truck L/V
5.5.16 Standard Chapter XI Constant Curving	CSM 70	Not Met	**Minimum Test Load:** Wheel L/V ratio = 0.86 95% Wheel L/V ratio = 0.66 **Maximum Test Load:** 95% Wheel L/V ratio = 0.63	0.80 max wheel L/V 0.60 max wheel L/V 0.60 max wheel L/V
5.5.17 Special Trackwork	CSM 70	Met		

Table of Contents

1. Introduction 1
2. Atlas RailCar Description 1
3. Variations in components during testing 4
4. Empty Car Configuration 5
5. Test Loads / Test Configurations 6
6. Test Overview 8
7. Objective 8
8. Results 8
   - 8.1 Characterization Tests 9
     - 8.1.1 Component Characterization Tests 9
     - 8.1.2 Vertical Suspension Stiffness and Damping 16
     - 8.1.3 Lateral Suspension Stiffness and Damping 22
     - 8.1.4 Truck Rotation Stiffness and Breakaway Moment 28
     - 8.1.5 Interaxle Longitudinal Stiffness 32
     - 8.1.6 Modal Characterization 35
   - 8.2 Nonstructural Static Tests 39
     - 8.2.1 Truck Twist Equalization 39
     - 8.2.2 Car Body Twist Equalization 42
     - 8.2.3 Static Curve Stability 44
     - 8.2.4 Horizontal Curve Negotiation 45
   - 8.3 Static Brake Tests 45
   - 8.4 Structural Tests 45
     - 8.4.1 Preliminary and Post Test Inspection 49
     - 8.4.2 Measured Stress from Test Loads 49
     - 8.4.3 Squeeze (Compressive End) Load 51
     - 8.4.4 Coupler Vertical Loads 61
     - 8.4.5 Jacking 67
     - 8.4.6 Twist 71
     - 8.4.7 Impact 79
     - 8.4.8 Securement System Analysis 84
       - 8.4.8.1 Dimensional Inspection 84
       - 8.4.8.2 Force Calculations 86
       - 8.4.8.3 Stress Analysis 88

8.4.8.4 Allowable Stresses, Acceptance Criteria, and Margin of Safety 89
8.4.8.5 Component Stress Analysis 90
8.4.8.6 Weld Analysis 103
8.5 Dynamic Tests 105
8.5.1 Primary Suspension Pad Configuration Changes 108
8.5.2 Minimum Load Hunting 110
8.5.3 Maximum Load Hunting 112
8.5.4 Minimum Test Load Twist and Roll 114
8.5.5 Maximum Test Load Twist and Roll 115
8.5.6 Yaw and Sway 116
8.5.7 Minimum Load Dynamic Curving 117
8.5.8 Maximum Load Dynamic Curving 118
8.5.9 Pitch and Bounce (Chapter 11) 121
8.5.10 Pitch and Bounce (Special) 122
8.5.11 Minimum Load Single Bump Test 122
8.5.12 Maximum Load Single Bump Test 123
8.5.13 Minimum Test Load Curve Entry/Exit 124
8.5.13.1 Minimum Load Limiting Spiral Negotiation 124
8.5.13.2 Minimum Load Normal Spiral Negotiation 126
8.5.14 Maximum Load Curve Entry/Exit 127
8.5.14.1 Maximum Load Limiting Spiral Negotiation 128
8.5.14.2 Maximum Load Normal Spiral Negotiation 129
8.5.15 Minimum Load Curving with Single Rail Perturbation 130
8.5.16 Maximum Load Curving with Single Rail Perturbation 134
8.5.17 Minimum Load Standard Chapter 11 Constant Curving 137
8.5.18 Maximum Load Standard Chapter 11 Constant Curving 139
8.5.19 Minimum Test Load Special Trackwork 141
8.5.20 Maximum Test Load Special Trackwork 145
8.6 Ride Quality 148
9. Additional Tests 148
10. Conclusions 148
References 151
Appendix A. EEC Letter – Empty Atlas Railcar 1
Appendix B. Atlas Car Test Plan 1

Appendix C. Static Brake Force Testing Documentation 1
Appendix D. Atlas Car Strain Gage Information 1
Appendix E. Critical Buckling Load 1
Appendix F. Compression Test 1
Appendix G. Vertical Coupler Force Test Results 1
Appendix H. Jacking Results 1
Appendix I. Twist Test 1
Appendix J. Impact Test 1
Appendix K. Atlas 12 Axle Flat Car Attachment to Deck Weldment 1
Appendix L. Test Zone Compliance for Dynamic Test Regimes 1

List of Tables

Table 1. Car Dimensions 2
Table 2. Car Configuration 3
Table 3. Adapter Pads used during Testing 5
Table 4. Weight Conditions used in Testing 6
Table 5. Spring Characteristics from the Manufacturer 11
Table 6. Spring Characteristic from Testing* 12
Table 7. Comparison of the Spring Characteristic from Testing to the Manufacturer Specification 13
Table 8. Comparison of the Tested Springs vs the Manufacturer Specifications and Acceptance Tolerances 14
Table 9. Spring rate equivalency at nominal load for the entire spring nest, based on the individual spring rates 14
Table 10. Vertical Test Results on End Truck with Wedges Installed and Minimum Load Spring Height 19
Table 11. Vertical Test Results on End Truck with Wedges Installed and Maximum Load Spring Height 19
Table 12. Vertical Test Results on End Truck with Wedges Removed and Maximum Load Spring Height 19
Table 13. Vertical Test Results on Middle Truck with Wedges Installed and Minimum Load Spring Height 20
Table 14. Vertical Test Results on Middle Truck with Wedges Installed and Maximum Load Spring Height 20
Table 15. Vertical Test Results on Middle Truck with Wedges Removed and Maximum Load Spring Height 20
Table 16. Lateral Suspension Test for End Truck (Wedges Installed and Minimum Load Condition) 25
Table 17. Lateral Suspension Test for End Truck (Wedges Installed and Maximum Load Condition) 25
Table 18. Lateral Suspension Test for End Truck (Wedges Removed and Maximum Load Condition) 25
Table 19. Lateral Suspension Test for Middle Truck (Wedges Installed and Minimum Load Condition) 26
Table 20. Lateral Suspension Test for Middle Truck (Wedges Installed and Maximum Load Condition) 26
Table 21. Lateral Suspension Test for Middle Truck (Wedges Removed and Maximum Load Condition) 27

Table 22. Truck Rotation and Break Away Moment Matrix 29
Table 23. Loads on Trucks and Span Bolster, Nominal Loads from Truck Load Equalization Test 32
Table 24. Truck Rotation Moments and Estimates of the Associated Friction Coefficients 32
Table 25. Side Frame to Axle Stiffness Data per Pad 34
Table 26. Modal Characterization Results (Hz) 37
Table 27. Truck Twist Equalization Results 40
Table 28. Truck Loads with and without 3/8" Shim 42
Table 29. Car Body Twist Equalization Results 43
Table 30. Summary of structural tests and load condition 47
Table 31. Survey Measurements 49
Table 32. Highest Measured Stresses for Atlas Car Loaded to Maximum Test Load Condition with no Additional Applied Forces 50
Table 33. Highest Measured Stresses for Atlas Car Loaded to Minimum Test Load Condition with no Additional Applied Forces 51
Table 34. Locations with Highest Total Tension and Compression Stress under Maximum Load Condition 56
Table 35. Locations with Highest Stress from Applied Load under Maximum Load Conditions 56
Table 36. Locations with Highest Total Tension and Compression Stresses under Minimum Load Condition 60
Table 37. Locations with Highest Stress from Applied Load under Minimum Load Condition 60
Table 38. Vertical Coupler Force Test Locations with Total Tensile and Compressive Stresses 65
Table 39. Vertical Coupler Force Test Locations with Highest Stresses from Aplied Loads 66
Table 40. Jacking Test Locations with Highest Total Tensile and Compressive Stresses 70
Table 41. Jacking Test Locations with the Highest Stresses from Applied Loads 70
Table 42. Highest Total Tensile and Compression Stresses from Suspension Twist Test 74
Table 43. Highest Stresses from Applied Load during Suspension Twist Test 74
Table 44. Highest Total Tensile and Compression Stresses from Carbody Twist Test 78

Table 45. Highest Total Tensile and Compression Stresses from Applied Loads during Carbody Twist Test 78
Table 46. Atlas Car Impact Test Results 80
Table 47. Highest Total Tensile and Compression Stresses from 6-mph Impact Test .. 83
Table 48. Highest Stresses from Applied Load during 6-mph Impact Test 83
Table 49. Family 1 (HI-STAR 190 XL) Force Calculation Results, Including 1.1 Load Factor 87
Table 50. Family 2 (MAGNATRAN) Force Calculation Results 88
Table 51. Bounding Loads 88
Table 52. Material Properties 89
Table 53. Central Block Under Vertical Load 90
Table 54. Central Block Under Lateral Load 90
Table 55. Shear Block Under Longitudinal Load 90
Table 56. Outer Block Under Longitudinal Load 90
Table 57. Pins Stress Analysis Results (Hand Calculations) 93
Table 58. Pin Stress Results Comparison 93
Table 59. Material Properties 95
Table 60. Securement System Results Summary 103
Table 61. Loading Factors for Weld Calculations 103
Table 62. Weld Analysis Results Summary 104
Table 63. Standard S-2043 Dynamic Testing Performance Criteria 107
Table 64. Minimum Load Hunting Test Dates and Rail Friction Data 110
Table 65. Minimum Load Hunting Test Results 111
Table 66. Maximum Load Hunting Test Dates and Rail Friction Data 113
Table 67. Maximum Load Hunting Test Results 113
Table 68. Minimum Test Load Twist and Roll Test Results 114
Table 69. Maximum Test Load Twist and Roll Test Results 115
Table 70. Yaw and Sway Test Results to 70 mph 116
Table 71. Minimum Load Dynamic Curving Test Dates and Rail Friction Data 117
Table 72. Minimum Load Dynamic Curving Test Results 118
Table 73. Maximum Load Dynamic Curving Test Dates and Rail Friction Data 119
Table 74. Maximum Load Dynamic Curving Test Results 119
Table 75. Summary of Pitch and Bounce (Chapter 11) Results 121

Table 76. Summary of Test Results for the Minimum Load Single Bump Test 123
Table 77. Summary of Test Results for the Maximum Load Single Bump Test 124
Table 78. Minimum Load Limiting Spiral Test Date and Rail Friction Data..... 125
Table 79. Minimum Load Limiting Spiral Summary Test Results 125
Table 80. Minimum Load Normal Spiral Negotiation Test Dates and Rail Friction Data 126
Table 81. Minimum Load Normal Spiral Summary of Test Results 127
Table 82. Maximum Load Limiting Spiral Test Dates and Rail Friction Data..... 128
Table 83. Maximum Load Limiting Spiral Summary Test Results 128
Table 84. Maximum Load Normal Spiral Negotiation Test Dates and Rail Friction Data 129
Table 85. Maximum Load Normal Spiral Negotiation Summary of Test Results Without 12-Degree North Spiral 130
Table 86. Minimum Load Curving with Single Rail Perturbation Test Dates and Rail Friction Data..... 131
Table 87. Minimum Load Curving with Single Rail Perturbation Summary of Test Results 131
Table 88. Maximum Load Curving with Single Rail Perturbation Test Dates and Rail Friction Data..... 135
Table 89. Maximum Load Curving with Single Rail Perturbation Summary of Test Results 135
Table 90. Minimum Load Constant Curving Test Dates and Rail Friction Data..... 137
Table 91. Minimum Load Constant Curving Summary of Test Results 138
Table 92. Maximum Load Constant Curving Test Dates and Rail Friction Data..... 139
Table 93. Maximum Load Constant Curving Summary of Test Results 140
Table 94. Special Track Work Components 143
Table 95. Minimum Load Special Trackwork Test Dates and Rail Friction Data 143
Table 96. Minimum Load Turnout Summary of Test Results 144
Table 97. Minimum Load Crossover Summary of Test Results 145
Table 98. Maximum Load Special Trackwork Test Dates and Rail Friction Data 146
Table 99. Maximum Load Turnout Summary of Test Results 146
Table 100. Maximum Load Crossover Summary of Test Results 147
Table 101. Summary of Test Results 150

List of Figures

Figure 1. IDOX 010001 during Testing with Minimum Test Load 1
Figure 2. Exploded view of Swing Motion® truck. 2
Figure 3. Roller Bearing Adapter Pad..... 3
Figure 4. Axle and side naming convention..... 4
Figure 5. Central Beam Assembly Being Mounted on Minimum Test Load Cradle..... 7
Figure 6. Minimum Test Load Assembly Mounted on Atlas Railcar 7
Figure 7. Maximum Test Load Assembly with End Stops Mounted on Atlas Railcar 8
Figure 8. Spring Group General Arrangement 10
Figure 9. Miner TCC-III 60LT CCSB..... 15
Figure 10. B-Truck Right Side CCSB Force-Displacement Data..... 15
Figure 11. C-Truck Left Side CCSB Force-Displacement Data..... 16
Figure 12. String Potentiometer for Measuring Spring Vertical Displacement..... 17
Figure 13. Load Bar for Measuring Vertical Force..... 18
Figure 14. Truck total vertical wheel load plotted against average secondary suspension displacement, wedges installed, end truck, maximum test load, 0.1Hz. 21
Figure 15. Truck total vertical wheel load plotted against average secondary suspension displacement, wedges installed, middle truck, maximum test load condition, 0.1Hz..... 21
Figure 16. Truck total vertical wheel load versus average primary suspension displacement, end truck, maximum test load, at 0.1 Hz input..... 22
Figure 17. Flat Car Connected to the MSU during Lateral Characterization Tests..... 23
Figure 18. Load Cell for Lateral Force Measurements 24
Figure 19. Instrumentation Setup to Measure Lateral Movements of Pads..... 24
Figure 20. Truck lateral load plotted against lateral secondary suspension displacement. End truck with wedges, minimum test load, 0.1 Hz. 27
Figure 21. Truck lateral load plotted against lateral secondary suspension displacement. End truck with wedges, minimum test load, transom restrained, 0.1 Hz..... 28
Figure 22. Primary suspension with wedges, middle truck, maximum test load, 0.1 Hz 28
Figure 23. Truck Rotation Setup with Truck Floating on Air Table and One Lateral Actuator 29
Figure 24. Test Setup for the Span Bolster Test Showing Connected Air Tables 30
Figure 25. String Potentiometers Used for Truck Rotation Measurement 30
Figure 26. Example of Air Table Data for a D-truck of Atlas Car with Maximum Load .. 32

Figure 27. Configuration and Measurements for Interaxle Longitudinal Stiffness Tests 34
Figure 28. Example Data for Longitudinal Axle Stiffness Tests Showing the Force and Displacement Across one Primary Pad 35
Figure 29. Actuator Attached to Carbody during Modal Testing with Lateral Input..... 36
Figure 30. Distribution of Accelerometers during the Atlas Railcar Modal Test..... 36
Figure 31. Frequency Response Function Sample 38
Figure 32. Bending Mode Shape at 8.49 Hz. (Minimum Load)..... 38
Figure 33. Atlas car with maximum test load in the RDL. Note the central beam assembly contacts the end stops..... 39
Figure 34. L4 Truck Twist Result for All Increments (Minimum Test Load) 41
Figure 35. R9 Truck Twist Result for All Increments (Maximum Test Load)..... 41
Figure 36. L4 Truck Twist Result for All Increments (Maximum Test Load) 42
Figure 37. Atlas Railcar with Minimum Test Load during Carbody Twist Equalization Test 43
Figure 38. Car Body Twist for Minimum Test Load Condition (BR) - Results for All Wheels 44
Figure 39. Car Body Twist for Maximum Test Load Condition (BR) - Results for All Wheels 44
Figure 40. Atlas Railcar during the Static Curve Stability Test 45
Figure 41. Location of Strain Measurements Monitored during Structural Testing..... 48
Figure 42. Results of Level Loop around the Car Deck..... 49
Figure 43. Measurement with Highest Measured Stress from Test Loads Only..... 51
Figure 44. Maximum Test Load Compressive End Load Test..... 52
Figure 45. Summary of Atlas Railcar Squeeze Test Results – Maximum Test Load Condition with 1,000 Kips Applied Compressive Load (1 of 2)..... 54
Figure 46. Summary of Atlas Railcar Squeeze Test Results – Maximum Test Load Condition with 1,000 Kips Applied Compressive Load (2 of 2)..... 55
Figure 47. Summary of Atlas Railcar Squeeze Test Results – Minimum Test Load Condition with 1,000 Kips Applied Compressive Load (1 of 2)..... 58
Figure 48. Summary of Atlas Railcar Squeeze Test Results – Minimum Test Load Condition with 1,000 Kips Applied Compressive Load (2 of 2)..... 59
Figure 49. Locations with Highest Measured Stress during Squeeze (Compressive End) Load Test 61
Figure 50. Coupler Carrier Plate after the Coupler Vertical Load Test 62
Figure 51. Stress from Downward Coupler Vertical Load Test (1 of 2) 63
Figure 52. Stress from Downward Coupler Vertical Load Test (2 of 2) 64

Figure 53. Stress from Jacking Test with Maximum Test Load (1 of 2) 68
Figure 54. Stress from Jacking Test with maximum Test Load (2 of 2) 69
Figure 55. Jacking Test Locations with Highest Stresses from Applied Loads 71
Figure 56. Stress from Suspension Twist Test, A-End LH Side (1 of 2) 72
Figure 57. Stress from Suspension Twist Test, A-End LH Side (2 of 2) 73
Figure 58. Maximum Stressed Gauges during Suspension Twist Test (Maximum Load Condition) 75
Figure 59. Stress from Carbody Twist Test, B-End RH Side (1 of 2) 76
Figure 60. Stress from Carbody Twist Test, B-End RH Side (2 of 2) 77
Figure 61. Stress Location with Highest Measured Strain during Carbody Twist Test 79
Figure 62. Atlas Car Impact Test Setup 79
Figure 63. Stress from Impact Test, 6 mph run (1 of 2) 81
Figure 64. Stress from Impact Test, 6 mph run (2 of 2) 82
Figure 65. Securement System Layout 84
Figure 66. Cask installation in securement mounts 85
Figure 67. Typical alignment of cask and securement mounts, shown with and without retainment pin. 86
Figure 68. Pin Designations 87
Figure 69. General Pin Loading Assumption 91
Figure 70. Central Pin (Pins 1-4) Loading Schematic 92
Figure 71. Outer Pin (Pins 5-20) Loading Schematic. Note that 3" dimension shown here was updated to 3.25" for subsequent analysis, based on as-built dimensions of the tested car, IDOX 010001. 92
Figure 72: Tensile Test Results for Pin Material 94
Figure 73. Tensile Test Results for Block Material 94
Figure 75. Outer Location Cross Section 96
Figure 76. Central Location Model 96
Figure 77. Central Location Cross Section 97
Figure 78. Loading Condition (Outer Pin) 97
Figure 79. Loading Condition (Center Pin) 98
Figure 80. Outer Pin Total Strain (in/in) 98
Figure 81. Outer Pin Plastic Strain (in/in) 99
Figure 82. Outer Pin Plastic Strain Depth 99

Figure 83. Outer Block Total Strain (in/in) 100
Figure 84. Outer Block Plastic Strain (in/in)..... 100
Figure 85. Central Pin Total Strain (in/in) 101
Figure 86. Central Pin Plastic Strain (in/in)..... 101
Figure 87. Central Blocks Total Strain (in/in)..... 102
Figure 88. Central Blocks Plastic Strain (in/in) 102
Figure 89. Example securement system welds and measurements 105
Figure 90. Location of IWS during Dynamic Tests 108
Figure 91. Hunting Results with Different Primary Suspension Pads (Minimum Test Load Condition), Worst Case of A or B-end Standard Deviation of Lateral Carbody Acceleration over 2000-feet, CSM 58 pads Selected..... 109
Figure 92. Dynamic Curving Test Results with Different Primary Suspension Pads (Minimum Test Load) , CSM 58 pads Selected 110
Figure 93. 2000-foot Standard Deviation of Lateral Acceleration for Minimum Load Hunting Tests 112
Figure 94. Minimum Load Hunting Standard Deviation of Lateral Carbody Acceleration, B-End (Lead End), KR Wheel Profiles, 68 mph..... 112
Figure 95. 2,000-foot Standard Deviation of Lateral Acceleration for Maximum Load Hunting Tests 114
Figure 96. Minimum Test Load Twist and Roll Test, Maximum Carbody Roll versus Speed 115
Figure 97. Maximum Test Load Twist and Roll Test, Maximum Carbody Roll versus Speed 116
Figure 98. Maximum Test Load Yaw and Sway Test, Peak-to-Peak Lateral Acceleration versus Speed..... 117
Figure 99. Minimum Load Dynamic Curving L/V Results versus Speed 118
Figure 100. Maximum Load Dynamic Curve Wheel L/V Results versus Speed 120
Figure 101. Axle 6 Right Wheel L/V Ratio during A-end Leading Maximum Load CCW Dynamic Curving at 14 mph 121
Figure 102. Maximum Test Load Pitch and Bounce, Maximum Vertical Acceleration versus Speed..... 122
Figure 103. Maximum Vertical Acceleration versus Speed for Minimum Load Single Bump Test 123
Figure 104. Maximum Vertical Acceleration versus Speed for Maximum Load Single Bump Test 124
Figure 105. Minimum Load Limiting Spiral Results 126

Figure 106. Minimum Load Normal Spiral B-End CW Summary 127
Figure 107. Maximum Load Limiting Spiral Results 129
Figure 108. Maximum Load Normal Spiral B-End CW Summary 130
Figure 109. Wheel L/V vs Speed for CSM 70 Primary pads Through the Single Rail Dip 132
Figure 110. Right Side Axle 6 Single Wheel L/V Ratio and Right Side D Truck Side L/V Ratio with CSM 70 Primary Pads, Minimum Load, Single Rail Dip at 14 mph. 133
Figure 111. Wheel L/V vs Speed for CSM 65 Primary pads Through the Single Rail Dip 134
Figure 112. CSM 65 Primary pads Minimum Load Single Rail Dip 50ms Max L/V Axle 6 Right Wheel 134
Figure 113. Maximum Load Curving with Single Rail Bump Perturbation Plot of Vertical Wheel Load versus Speed 136
Figure 114. Maximum Load Curving with Single Rail Dip Perturbation Plot of Vertical Wheel Load versus Speed 136
Figure 115. Minimum Load Constant Curving 95 Percent Wheel L/V versus Speed 138
Figure 116. Minimum Load Constant Curving 12-degree curve CCW A-End Leading Axle 6 Left Wheel at 15 MPH Wheel L/V 139
Figure 117. Maximum Load Constant Curving 95 Percent Wheel L/V versus Speed . 140
Figure 118. 95 Percent Wheel L/V Maximum Load Left Axles 3 and 5, 12-degree Constant Curving 141
Figure 119. Pre-test Survey Alignment Measurements for Turnout Test Zone 142
Figure 120. Pre-test Survey Alignment Measurements for Crossover Test Zone 142
Figure 121. Minimum Load Turnout Special Trackwork Wheel L/V Ratio versus Speed 144
Figure 122. Minimum Load Crossover Special Trackwork Wheel L/V Ratio versus Speed 145
Figure 123. Maximum Load Turnout Special Trackwork Wheel L/V Ratio versus Speed 147
Figure 124. Maximum Load Crossover Special Trackwork Wheel L/V Ratio versus Speed 148

Definitions/Acronyms

A vs B-end	As designated by AAR standards, defining the directionality of a car
AAR	Association of American Railroads
AAR observer	A designated employee responsible for documenting that test operating procedures are followed
AAR-1B	Wheel profile as specified by AAR
Buffer car	A car that is part of a test train consist that is needed for overall train make-up (axle count, car type, etc)
CCSB	Constant contact side bearings
CCW	Counter-clockwise
CG	Center of Gravity
Chapter 11	MSRP Section C-Part II, M-1001, Chapter 11
Crossover	On track, an arrangement of two switches such that a train may change tracks where two or more parallel tracks are present
Curvature	The measurement of the tightness of a curve (high degree curvature = small radius of curvature)
CW	Clockwise
DOE	U.S. Department of Energy
EEC	AAR Equipment Engineering Committee
FRA	Federal Railroad Administration
Gage	The distance between rails, nominally 56.5" for standard gage
Grade crossing	Where a surface street crosses a railroad, on grade
HLRM	High-level Radioactive Material
Hunting	Lateral oscillating instability in the trucks, typically occurring at higher test speeds
Hz	Hertz (frequency measurement in cycles per second)
IWS	Instrumented wheelset
Kasgro	Atlas cask car manufacturer
KR wheel profile	Wheel profile specified by Chapter 11 for high-speed stability tests
L/V ratio	Ratio of the lateral load vs the vertical load on a wheel or combination of wheels
LVDT	Linear variable differential transducer
MSRP	Manual of Standards and Recommended Practices
MSU	Mini-Shaker Unit

RDL	Rail Dynamics Laboratory
Standard S-2043	MSRP governing the performance requirements of cars designed for HLRM
Special trackwork	Track that consists of switches or other track construction components that are not found in open track
Spiral	Transition between tangent track and a constant curvature
Superelevation (cant)	Relative height between rails within a curve (where the "outside," outermost rail is higher
Tangent track	Straight track
TTC	Transportation Technology Center. FRA facility northeast of Pueblo CO
TTCI	Transportation Technology Center, Inc. (A subsidiary of the Association of American Railroads)
URB	Urban Rail Building
URB Wye	Track wye in close proximity to the Urban Rail Building
WRM	Wheel Rail Mechanisms Loop

1. INTRODUCTION

The United States Department of Energy (DOE) contracted with Transportation Technology Center, Inc. (TTCI) to perform certification testing on its Atlas railcar. The Atlas railcar has been developed as part of DOE's Atlas railcar Design Project that is intended to meet the needs for future large-scale transport of high-level radioactive material (HLRM) as defined in AAR Standard S-2043 that includes spent nuclear fuel and high-level waste.

All tests were performed according to the Association of American Railroads' (AAR) *Manual of Standards and Recommended Practices* (MSRP), Standard S-2043, "Performance Specification for Trains Used to Carry High-Level Radioactive Material," Section 5.0 – Single Car Tests.[1] Single car testing of the Atlas railcar was conducted primarily at the United States Department of Transportation's Transportation Technology Center (TTC) near Pueblo, CO between April 2019 and August 2021. Static brake testing was conducted per relevant requirements of AAR Standards S-401 and S-486 at the manufacturer's facility prior to delivery.

2. ATLAS RAILCAR DESCRIPTION

The Atlas railcar was a 12-axle span bolster car with fittings to accommodate various cradles and end stops designed so the car can carry various casks used for transportation of spent nuclear fuel and/or high-level waste. The car deck was supported on two span bolsters. Each span bolster rested on three 2-axle trucks. Figure 1 shows the car with a test load installed. Table 1 shows the car dimensions.

Kasgro Rail Corporation (Kasgro) manufactured the Atlas railcar along with two prototype buffer railcars in 2018. The car delivered for testing was numbered IDOX 010001.



Figure 1. IDOX 010001 during Testing with Minimum Test Load

Table 1. Car Dimensions

Dimension	Value
Length over pulling faces	78 feet 1-1/4 inches
Length over strikers	73 feet 5-1/4 inches
Span bolster spacing	38 feet 6 inches
Axle spacing on trucks	72 inches
Distance between adjacent truck centers	10 feet 6 inches

The car used six Swing Motion® trucks (Figure 2). Each truck used two wheelsets with AAR Class K-axles and AAR1B narrow flange wheels. Narrow flange wheels were specified for this car because the increased gage clearance allowed more lateral movement for better performance. The trucks were specially designed to use a polymer element between the bearing adapter and side frame. This gave the truck a passive steering capability. Figure 3 shows the bearing adapter pad. Table 2 shows the truck configuration used for testing. The secondary suspension was made up of non-AAR-standard springs. A detailed description of these springs is given in Section 7.1.1.

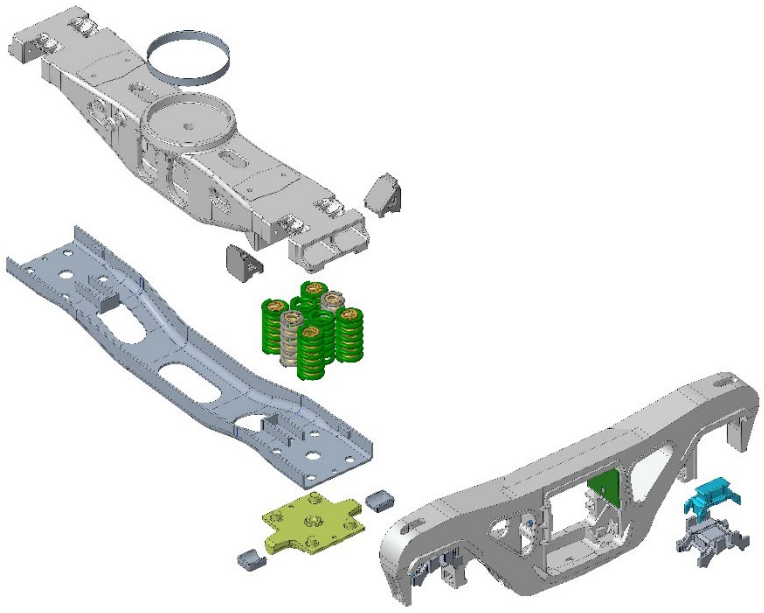


Figure 2. Exploded view of Swing Motion® truck.



Figure 3. Roller Bearing Adapter Pad

Table 2. Car Configuration

Component	Description	
Secondary Suspension End Truck (A,B,D,E)	(2) 1-94, (2) 1-95, (2) 1-96, (4) 1-97, (4) 1-92, (4) 1-99	
Secondary Suspension Middle Truck (C,F)	(2) 1-88, (2) 1-89, (2) 1-90, (4) 1-91, (4) 1-92, (2) 1-93, (4) 1-99	
Primary suspension	12A Adapter Plus pads, ASF-Keystone part number 10522A	
Side Frames	F9N-10FH-UB	
Bolsters	B9N-71 EJFZ on A, F, and C-trucks B9N-71 HN-FX on B, D, and E-trucks	
Side Bearings	Miner TCC-III 60LT	
Friction Wedge, composition faced (four per truck)	ASF-Keystone Part number 48446	
Bearings and Adapters	AAR Class K 6 1/2 x 9 bearings with 6 1/2x9 Special Adapter ASF-Keystone Part number 10523A	
Center Bowl Plate	Metal Horizontal Liner	
	End Truck Average	Middle Truck Average
Minimum Test Load Spring Nest Height	8.97 inches	9.13 inches
Maximum Test Load Spring Nest Height	8.20 inches	8.17 inches

The convention for wheel and truck identification is shown in Figure 4. The B-end of a railroad freight car is normally the end with the handbrake, but because the Atlas car had two handbrakes, the car manufacturer designated and stenciled the B-end. The right and left sides of the car are designated when standing at the B-end of the car and looking toward the A-end of the car. Axles are numbered starting from the B-end. For axle numbers greater than 9 the locations are stenciled with letters descending from Z.

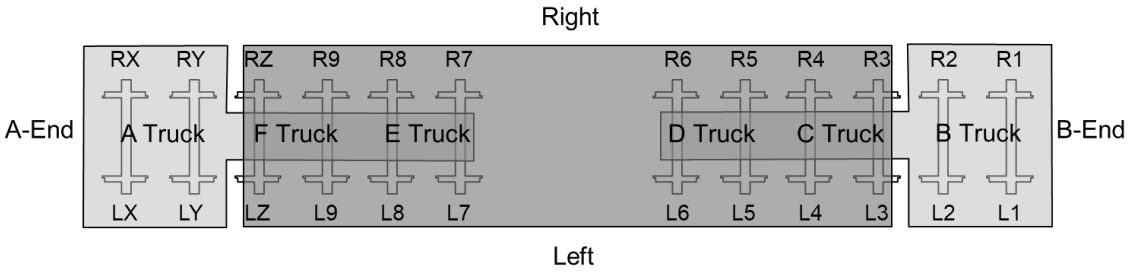


Figure 4. Axle and side naming convention.

3. VARIATIONS IN COMPONENTS DURING TESTING

During initial tests the Atlas car loaded with the minimum test load showed some hunting instability at speeds above 65 mph. TTCI tested different side bearings, centerplate liners, and primary pads to solve the problem. Stiffer primary pads (prototype chlorosulfonated polyethylene or CSM 70 pads) were the only change that improved the hunting performance. After the change to stiffer pads resulted in improved hunting stability performance, all Standard S-2043 prescribed dynamic test regimes were completed with the CSM 70 pads. However, using these stiffer pads, car performance did not meet Standard S-2043 criteria in dynamic curving or curve with single rail perturbation regimes.

On October 15, 2020, TTCI reviewed the results with the AAR EEC. The EEC directed TTCI to re-test the car with softer primary pads with minimum test load in the dynamic curving regime. because the car would be limited to less than 50 mph by AAR circular OT-55 when in HLRM service the EEC noted that curving performance was more important than high speed stability performance.

During the testing program, TTCI tested the car with a total of four models of primary suspension pad. The pads are made from chlorosulfonated polyethylene (CSM) and are categorized by the Shore D durometer hardness value. The production pads the car arrived with were CSM 58. TTCI also tested the car with prototype pad types CSM 70, CSM 68, and CSM 65. CSM 58 pads are designated for their minimum hardness value, while the CSM 70 pads are designated for their target hardness value.

The hunting regime was tested with CSM 58 pads in both the minimum and maximum test load conditions. The dynamic curving regime was tested with CSM 58 pads in the minimum test load condition. All other dynamic tests were completed with CSM 70 pads. Considering the results of curving and hunting tests, the production CSM 58 pads provide improved performance overall, when compared to the alternative pad materials that were tested. The effect of the pad change on other regimes will be evaluated using modeling and documented in the post-test analysis report. Table 3 displays the tests completed and the adapter pad type that was tested.

The production CSM 58 pads were chosen for use in service based on the balance of curving and high-speed stability performance.

Table 3. Adapter Pads used during Testing

Standard S-2043 Section	Component Type Tested
5.2 Nonstructural Static Tests	
5.2.1 Truck Twist Equalization	CSM 58
5.2.2 Carbody Twist Equalization	CSM 58
5.2.3 Static Curve Stability	CSM 58
5.2.4 Horizontal Curve Negotiation	CSM 58
5.4 Structural Tests	
5.4.2 Squeeze (Compressive End) Load	CSM 58
5.4.3 Coupler Vertical Loads	CSM 58
5.4.4 Jacking	CSM 58
5.4.5 Twist	CSM 58
5.4.6 Impact	CSM 58
5.5 Dynamic Tests	
5.5.7 Hunting	CSM 58, CSM 65, CSM 68, CSM 70
5.5.8 Twist and Roll	CSM 70
5.5.9 Yaw and Sway	CSM 70
5.5.10 Dynamic Curving	CSM 58, CSM 65, CSM 68, CSM 70
5.5.11 Pitch and Bounce (Chapter XI)	CSM 70
5.5.13 Single Bump Test	CSM 70
5.5.14 Curve Entry/Exit	CSM 70
5.5.15 Curving with Single Rail Perturbation	CSM 70
5.5.16 Standard Chapter XI Constant Curving	CSM 70
5.5.17 Special Trackwork	CSM 70

4. EMPTY CAR CONFIGURATION

The Standard S-2043 covers trains and equipment carrying HLRM. The DOE does not plan to put any empty Atlas railcars in trains carrying HLRM. Rather. the intention is to move the empty cars as freight. For this reason, the EEC listed the following actions in a letter dated March 19, 2019 (Appendix A):

- The EEC confirmed that the lightest Atlas railcar to operate in HLRM trains, loaded with an empty cask, be approved under Standard S-2043 rather than an empty car as described in Standard S-2043.

- The EEC confirmed that approving the empty Atlas railcar under M-1001 is the proper approach. Note that approval can only be made under Chapter 12 for Controlled Interchange.

- The EEC approved the DOE's request to classify the Atlas railcar as category D based on its similarities with the empty Navy M-290 HLRM car which has been approved under M-1001 and confirmed that Chapter 11 testing need not be conducted. Category D is for cars with insignificant differences from previously approved cars.

5. TEST LOADS / TEST CONFIGURATIONS

Orano Federal Services (the prime contractor to the DOE for the design and fabrication of the prototype railcar being tested) developed detailed designs for the test loads to simulate the minimum and maximum condition HLRM cask/cradle combinations (packages) the Atlas railcar was designed to transport[2]. The minimum test load assembly was designed to simulate the lightest package (MP197), and the maximum test load assembly was designed to simulate the heaviest package (HI-STAR 190XL).

A single modular test load design that can meet both the minimum and maximum test load conditions was developed. The modular test load assembly consists of a central beam assembly with three weight bundle assemblies that are welded to the frame. Each weight bundle assembly consists of steel plates that are permanently tensioned together with tie rods. Two cradle assemblies are designed to support the central assembly on top of the DOE Atlas railcar. The minimum test load cradle uses a central shear key to support longitudinal loading, while the maximum test load cradle uses end stop assemblies for longitudinal support. The minimum and maximum test load assemblies are completed by bolting on additional weight bundle assemblies. These weight bundles are also composed of steel plates tensioned with tie rods.

Figure 5 shows the central beam assembly being mounted on the minimum test load cradle. Figure 6 shows the minimum test load assembly and its cradle mounted on the Atlas railcar. Figure 7 shows the maximum test load with cradle and end stops.

Table 4 shows the car loading conditions. As explained above, the first condition (empty car) was not tested to Standard S-2043, while the other two conditions were tested. The weights are summed using the measurements made on the TTC track scale.

Table 4. Weight Conditions used in Testing

Condition	Cask/Cradle Description	Load (pounds)	Combined CG Height (in)*	Weight on Rail (pounds)**
Empty Atlas Railcar	None	0	40	222,050
Minimum Test Load	Empty MP-197	199,000	75	421,050
Maximum Test Load	Loaded HI-Star 190 XL	487,000	95	709,050

*CG Heights estimated not including deck or spring deflection
**Actual TTCI scale measurements



Figure 5. Central Beam Assembly Being Mounted on Minimum Test Load Cradle



Figure 6. Minimum Test Load Assembly Mounted on Atlas Railcar



Figure 7. Maximum Test Load Assembly with End Stops Mounted on Atlas Railcar

6. TEST OVERVIEW

Standard S-2043 requires testing to be conducted in two phases, single car tests and multiple car tests. Each railcar type that will eventually be included in a Standard S-2043 compliant train must first undergo a series of single car tests as described in Standard S-2043 paragraph 5.0. These tests are broken down into several groups: Vehicle Characterization, Nonstructural Static Tests, Static Brake Tests, Structural Tests, and Dynamic Tests. The Static Brake Tests were conducted by Kasgro before the railcar left its facility.

The single car tests are followed by a series of multiple car tests as described in Standard S-2043 Paragraph 6.0. Multiple-car tests are designed to verify that the individual railcars do not adversely affect the performance of adjacent railcars. The multiple-car test train consist must match the anticipated HLRM train as closely as possible, with a minimum of one of each type of railcar to be used.

This report provides single car test results only for the Atlas railcar. Single car test results for other railcar types will be reported separately.

7. OBJECTIVE

The objective of the testing reported here was to determine if the DOE's Atlas railcar met the single car test requirements of AAR Standard S-2043, in preparation for inclusion in an AAR Standard S-2043 compliant train. If the AAR EEC provides conditional approval based on this report (and test reports for additional cars being prepared in parallel), the DOE plans to move forward with multiple car tests. The consist for multiple car testing is expected to include an Atlas cask car, two buffer cars, and a rail escort vehicle.

8. RESULTS

This section provides descriptions and results of each of the tests conducted at TTC under the AAR Standard S-2043 as well as the static brake tests conducted at the Kasgro facility. Any

variances from the specification will be noted. Each section contains a brief description of the test conduct. The test plan, included in Appendix B, contains additional test description information.

8.1 Characterization Tests

Characterization tests were conducted to verify that the car and its components were constructed as designed. The vehicle characterization tests include the following:

- Component characterization
- Vertical suspension stiffness and damping
- Lateral suspension stiffness and damping
- Truck rotation stiffness and breakaway moment
- Interaxle longitudinal stiffness
- Modal characterization

Standard S-2043 requires that measured suspension values be compared to the values used in the original model as required by Standard S-2043, Paragraph 4.3 and that the model be adjusted if the values are measurably different from those used in the original model. Detailed comparisons of characterization results and the model inputs will be provided in the "Post-Test Analysis Report" described in Standard S-2043, Paragraph 8.5. Where possible, preliminary comparisons are provided in the test descriptions below. Characterization test results are provided in Sections 8.1.1 to 8.1.6 of the current report.

8.1.1 Component Characterization Tests

TTCI tested the secondary springs and constant contact side bearings (CCSB). Component characterization tests were carried out on a 50,000-pound MTS load frame. TTCI performed component characterization tests on May 20, 2019 and May 21, 2019. Adam Klopp, TTCI Principal Investigator I, witnessed the component characterization tests as the AAR Observer, per Standard S-2043 requirements.

Because it was determined that a component test could not adequately capture the performance, primary pads were not tested as a separate component. Instead, the properties of the primary pads were measured during the system characterization tests.

The Atlas railcar uses different spring group arrangements for the middle and end trucks of each span bolster, as shown in Figure 8. Two samples of each spring type were selected from the car and characterized in a load frame. The following measurements were recorded:

- Unloaded free height
- Stiffness
- Solid height
- Wire diameter

Table 5 shows the spring characteristics from the manufacturer and Figure 8 shows the layout of the spring nests. More details on these secondary suspension coil springs can be found in "S-

2043 Certification: Preliminary Simulations of Kasgro-Atlas 12-Axle Cask Car" (P-17-021)[3] and "Spring Test Requirements and Tolerances Procedure #12 Rev. 4"[4]. Table 6, Table 7, and Table 8 show the test results of each spring type vs the various spring specifications and the acceptance tolerances.

Springs 1-99 on the end-truck were not characterized with the 1-99 mid-truck springs. Data shown for the 1-99 end-truck springs was collected on April 20, 2021, outside of the regular characterization effort. These tests were conducted by Dennis Rule and Juan Carlos Valdez-Salazar but were not witnessed by an official observer. However, the spring rates of these springs were within 1% difference of those tested during the regular characterization effort.

All springs tested fell within the acceptable rate range for an individual spring. It should be noted that three spring types (1-93, 1-95, and 1-99) tested outside of the acceptable spring rate range for a given spring population. For example, the 1-93 springs are specified for 2,219 lb/in rate, but tested at 2,431 lb/in (9% higher than the spec) which is within the acceptance range of an individual spring (but fell outside acceptable range for a spring population), as shown in Table 8. However, the overall equivalent spring rate for the spring nests tested were within 4.5% of the specifications, as shown in Table 9.

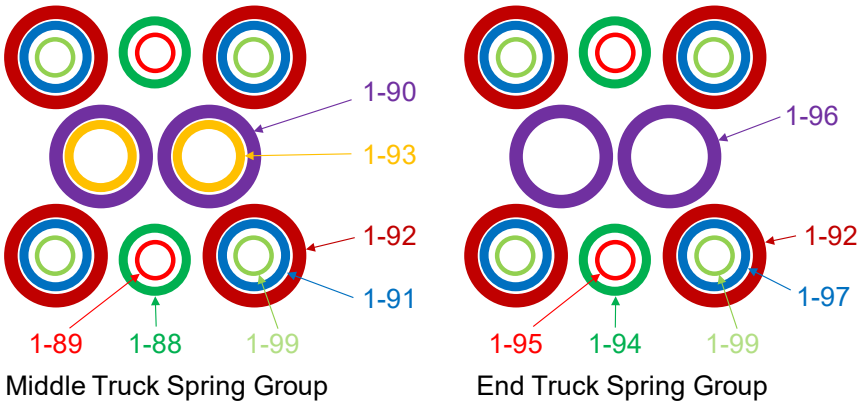


Figure 8. Spring Group General Arrangement

Table 5. Spring Characteristics from the Manufacturer

Spring Group	Type	Description	Bar Diameter (inch)	Free Height (inch)	Solid Height (inch)	Spring Rate (lb/inch)
Mid Truck	1-88	Control Coil Outer	25/32	11 23/32	6 11/16	1,161
	1-89	Control Coil Inner	1/2	11 23/32	6 11/16	500
	1-90	Empty Coil Outer	27/32	13	6 11/16	1,074
	1-91	Empty Coil Inner	1/2	13	6 11/16	348
	1-92	Load Coil Outer	1 1/16	9 1/4	6 11/16	4,183
	1-93	Load Coil Inner	11/16	9 1/4	6 11/16	2,219
	1-99	Load Coil Inner Inner	3/8	7 1/2	5 3/8	550
End Truck	1-94	Control Coil Outer	13/16	11 3/32	6 11/16	1,328
	1-95	Control Coil Inner	17/32	11 3/32	6 11/16	656
	1-96	Empty Coil Outer	31/32	11	6 11/16	2,409
	1-97	Empty Coil Inner	19/32	11	6 11/16	934
	1-92	Load Coil	1 1/16	9 1/4	6 11/16	4,183
	1-99	Load Coil Inner Inner	3/8	7 1/2	5 3/8	550

Table 6. Spring Characteristic from Testing*

Spring Group	Spring Type	Description	Bar Diameter (inch)	Free Height (inch)	Solid Height (inch)	Spring Rate (lb/inch)
Mid Truck	1-88	Control Coil Outer	0.500	11.81	6.46	1,158
	1-88	Control Coil Outer	0.500	11.75	6.36	1,155
	1-89	Control Coil Inner	0.776	11.81	6.57	514
	1-89	Control Coil Inner	0.773	11.75	6.34	528
	1-90	Empty Coil Outer	0.823	13.13	6.57	1,044
	1-90	Empty Coil Outer	0.825	13.13	6.46	1,055
	1-91	Empty Coil Inner	0.500	13.19	6.80	360
	1-91	Empty Coil Inner	0.498	13.13	6.78	354
	1-92	Load Coil Outer	1.063	9.25	6.52	4,329
	1-92	Load Coil Outer	1.066	9.44	6.77	4,356
	1-93	Load Coil Inner	0.684	9.31	6.35	2,385
	1-93	Load Coil Inner	0.689	9.19	6.21	2,477
	1-99	Load Coil Inner Inner	0.375	7.50	5.24	596
	1-99	Load Coil Inner Inner	0.375	7.50	5.37	605
End Truck	1-94	Control Coil Outer	0.800	11.19	6.49	1293
	1-94	Control Coil Outer	0.802	11.19	6.59	1337
	1-95	Control Coil Inner	0.535	11.06	6.31	713
	1-95	Control Coil Inner	0.532	11.06	6.29	708
	1-96	Empty Coil Outer	0.959	11.00	6.51	2434
	1-96	Empty Coil Outer	0.957	11.13	6.30	2351
	1-97	Empty Coil Inner	0.586	11.13	6.38	888
	1-97	Empty Coil Inner	0.597	11.06	6.38	945
	1-92	Load Coil	1.067	9.25	6.52	4399
	1-92	Load Coil	1.064	9.19	6.49	4385
	1-99	Load Coil Inner Inner	0.375	7.72	5.60	594
	1-99	Load Coil Inner Inner	0.375	7.71	5.62	598

*Data includes two springs of each type, quantity 26 of the 224 springs in the railcar

Table 7. Comparison of the Spring Characteristic from Testing to the Manufacturer Specification

Spring Group	Spring Type	Description	Bar Diameter (percent difference from spec)	Free Height (percent difference from spec)	Solid Height (percent difference from spec)	Spring Rate (percent difference from spec)
Mid Truck	1-88	Control Coil Outer	0%	1%	-3%	0%
	1-88	Control Coil Outer	0%	0%	-5%	0%
	1-89	Control Coil Inner	-1%	1%	-2%	3%
	1-89	Control Coil Inner	-1%	0%	-5%	6%
	1-90	Empty Coil Outer	-2%	1%	-2%	-3%
	1-90	Empty Coil Outer	-2%	1%	-3%	-2%
	1-91	Empty Coil Inner	0%	1%	2%	4%
	1-91	Empty Coil Inner	0%	1%	1%	2%
	1-92	Load Coil Outer	0%	0%	-3%	3%
	1-92	Load Coil Outer	0%	2%	1%	4%
	1-93	Load Coil Inner	-1%	1%	-5%	7%
	1-93	Load Coil Inner	0%	-1%	-7%	12%
	1-99	Load Coil Inner Inner	0%	0%	-3%	8%
	1-99	Load Coil Inner Inner	0%	0%	0%	10%
End Truck	1-94	Control Coil Outer	-2%	1%	-3%	-3%
	1-94	Control Coil Outer	-1%	1%	-1%	1%
	1-95	Control Coil Inner	1%	0%	-6%	9%
	1-95	Control Coil Inner	0%	0%	-6%	8%
	1-96	Empty Coil Outer	-1%	0%	-3%	1%
	1-96	Empty Coil Outer	-1%	1%	-6%	-2%
	1-97	Empty Coil Inner	-1%	1%	-5%	-5%
	1-97	Empty Coil Inner	1%	1%	-5%	1%
	1-92	Load Coil	0%	0%	-2%	5%
	1-92	Load Coil	0%	-1%	-3%	5%
	1-99	Load Coil Inner Inner	0%	3%	4%	8%
	1-99	Load Coil Inner Inner	0%	3%	4%	9%

Table 8. Comparison of the Tested Springs vs the Manufacturer Specifications and Acceptance Tolerances

			Design Data		Test Data	Spring Rate, Population Avg			Spring Rate, Individual		
Spring Group	Type	Description	Qty	Spring Rate (lb/in)	Spring Rate (lb/in)	Min (lb/in)	Max (lb/in)	Within req'd range	Min (lb/in)	Max (lb/in)	Within req'd range
Mid Truck	1-88	Control Coil Outer	2	1,161	1,157	1,075	1,248	True	902	1,421	True
	1-89	Control Coil Inner	2	500	521	463	537	True	389	612	True
	1-90	Empty Coil Outer	2	1,074	1,050	974	1,175	True	773	1,376	True
	1-91	Empty Coil Inner	4	348	357	316	381	True	251	446	True
	1-92	Load Coil Outer	4	4,183	4,367	3,830	4,545	True	3,115	5,259	True
	1-93	Load Coil Inner	2	2,219	2,431	2,032	2,410	False*	1,652	2,790	True
	1-99	Load Coil Inner Inner	4	550	598.25	516	595	False*	437	673	True
End Truck	1-94	Control Coil Outer	2	1,328	1,315	1,242	1,416	True	1,069	1,589	True
	1-95	Control Coil Inner	2	656	710.5	614	700	False*	529	786	True
	1-96	Empty Coil Outer	2	2,409	2,393	2,256	2,564	True	1,949	2,872	True
	1-97	Empty Coil Inner	4	934	916.5	875	994	True	756	1,113	True
	1-92	Load Coil	4	4,183	4,367	3,830	4,545	True	3,115	5,259	True
	1-99	Load Coil Inner Inner	4	550	598.25	516	595	False*	437	673	True

*The small number of samples tested does not reflect the population average. The rate still falls within the criteria for a single spring. The car manufacturer's (Kasgro's) procedure is to have the manufacturer test every spring.

Table 9. Spring rate equivalency at nominal load for the entire spring nest, based on the individual spring rates

Spring Rate Equivalency, Complete Nest		
	Mid Truck	End Truck
Specification (lb/in)	30,232	31,454
Tested (lb/in)	31,606	32,364
Percent Diff (%)	4.5%	2.9%

The car is equipped with Miner TCC-III 60LT CCSB between each truck and the span bolsters. Figure 9 shows the side bearings. The setup height of each CCSB is 5 1/16 inches. Two samples were installed in a load frame so the force and displacement characteristics of the samples could be measured. The side bearings were tested in near new condition before any dynamic testing was performed. The side bearings, including the steel cages, were tested as complete components. The loads were applied using constant velocity inputs at a rate of about 0.28 inches per second. Figure 10 shows the test result from an end truck (B-truck) right side bearing and Figure 11 shows the test result from a middle truck (C-truck) left side bearing.



Figure 9. Miner TCC-III 60LT CCSB

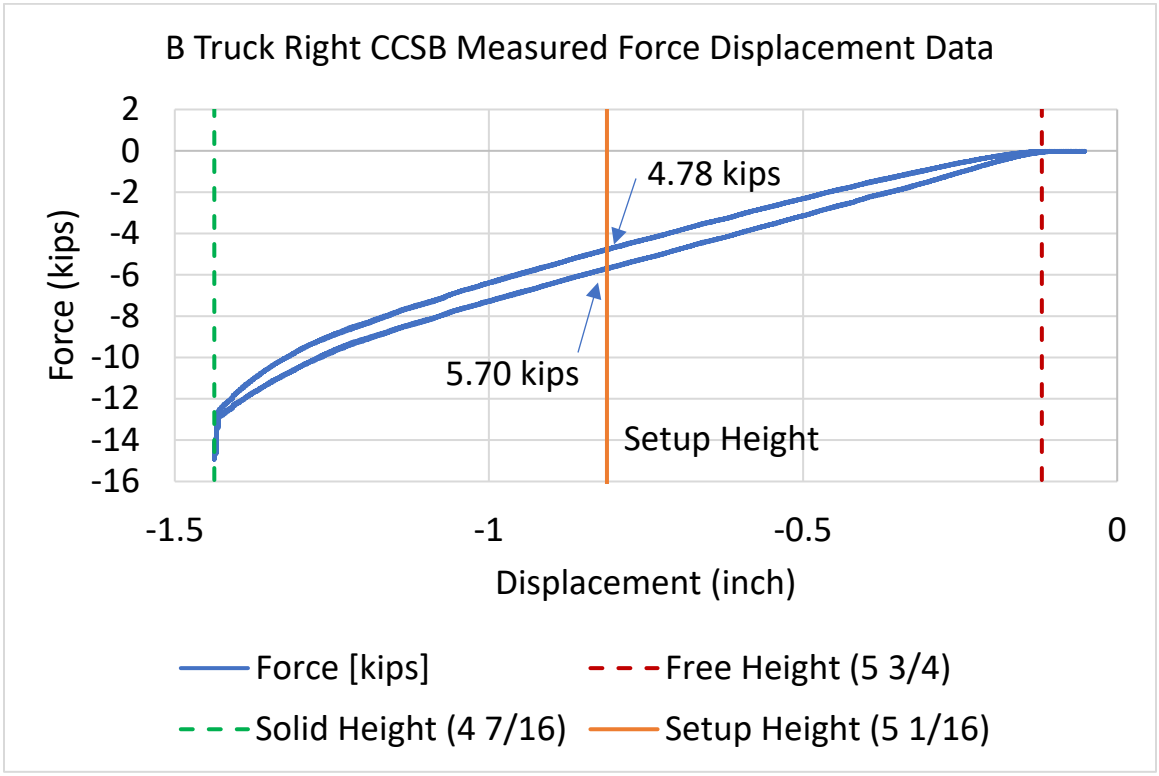


Figure 10. B-Truck Right Side CCSB Force-Displacement Data

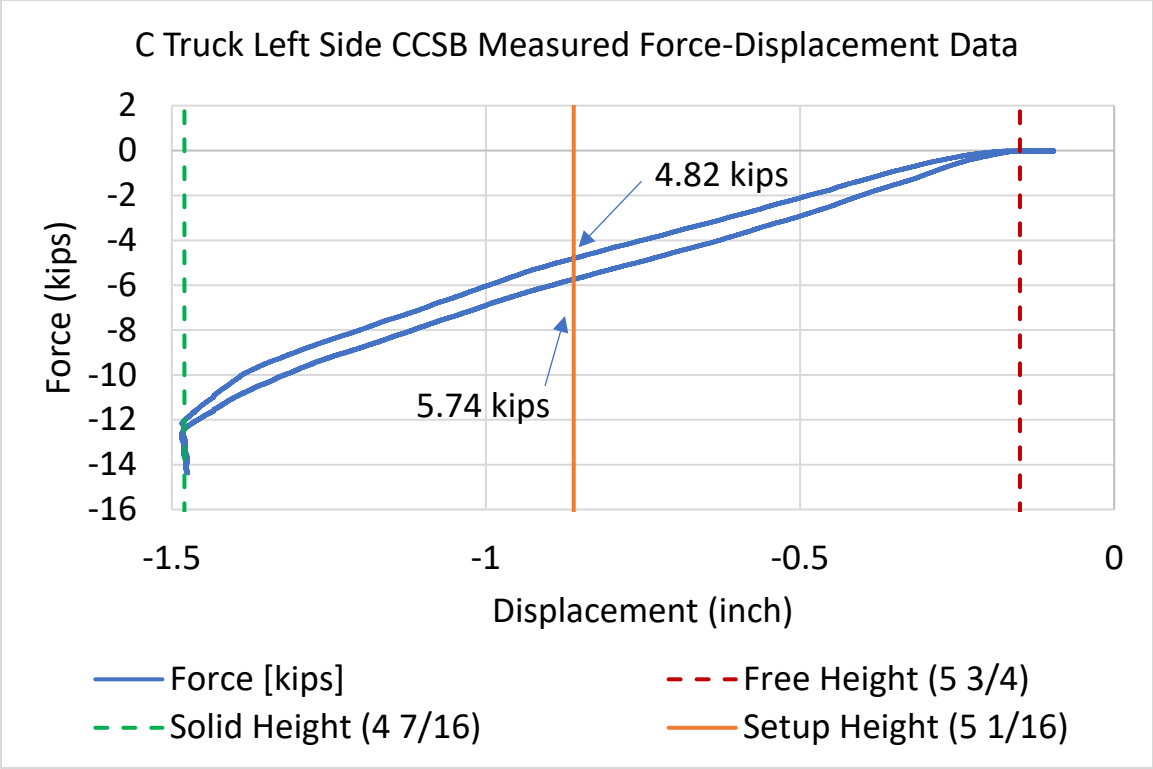


Figure 11. C-Truck Left Side CCSB Force-Displacement Data

8.1.2 Vertical Suspension Stiffness and Damping

The vertical suspension stiffness of the assembled truck was measured on the Mini-Shaker Unit (MSU). One end truck and one middle truck were tested. Each truck tested was installed in a special flat car that had connections for the vertical and lateral MSU actuators.

Displacements were measured across the primary and secondary suspension during vertical characterization tests. Tests were performed in the minimum and maximum loaded conditions. Vertical suspension stiffness and damping tests were performed on June 11, 2019, June 13, 2019, June 25, 2019, and June 26, 2019. Although the trucks were broken-in on load frames at Amsted and during the 1,400-mile journey from Kasgro's facility to TTC, there was no noticeable wear. Adam Klopp and Xinggao Shu, TTCI's Principal Investigators, witnessed the vertical suspension and damping tests as the AAR Observer, per Standard S-2043 requirements.

Tests were performed at loads equivalent to minimum and maximum test load condition with the wedges installed. Tests were performed at maximum test load condition with wedges removed. The purpose for wedges removed tests was to verify the solid height and to document wedge damping. With wedges removed TTCI was able to move the suspension over a wide enough range to observe the stiffness and damping at both the minimum and maximum test load spring nest height when the test car was loaded with the equivalent of maximum test load.

Each configuration was run at 0.1 Hz, 0.5 Hz, and 2 Hz, except for the vertical test with wedges removed. This test was run at 0.1 Hz only to prevent exciting the undamped rigid body modes. The input forces and displacements were adjusted for each run to achieve the desired input range within the capability of the MSU hydraulic and control systems. At a low frequency (0.1 Hz), the suspension was pushed to the stops where possible, but lower amplitude inputs were used at higher frequencies.

The force supplied by the hydraulic actuators was measured by the load cells installed between the actuators and the specially welded brackets where the vertical forces were applied. Vertical forces were also measured under each wheel of the truck using loadbars (load cells used in place of rails). The displacements across the secondary suspension were recorded using string potentiometers. Part of the instrumentation is shown in Figure 12 and Figure 13.



Figure 12. String Potentiometer for Measuring Spring Vertical Displacement

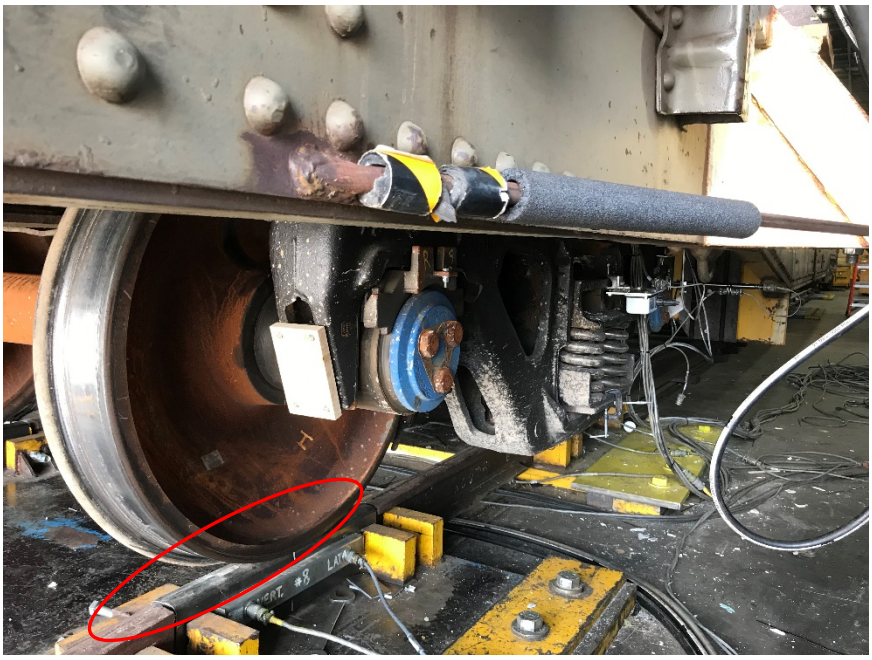


Figure 13. Load Bar for Measuring Vertical Force

The motion between the left and right-side frame and one axle's bearing adapters was measured using six Linear Variable Differential Transformers (LVDTs) on each side. The LVDTs were positioned to allow for the calculation of the relative motion between the side frame and the bearing adapter in the longitudinal, lateral, vertical, roll, pitch, and yaw directions.

The data analysis consisted of preparing force versus displacement plots from the measured wheel/rail forces and displacements across the suspension components. These cross-plots were used to obtain suspension stiffness and damping values.

The results are reported on a truck-by-truck basis by using the total weight on rail of the four wheels, and the average displacement of the two spring sets. The averages of the slopes from the top (loading) and bottom (unloading) regression lines are reported as the stiffness, and the difference in y-values (forces) at displacement corresponding to the dead weight are reported as the damping. For example, when the initial spring displacement was set to zero under dead weight, the difference in the loading vs. unloading force y-intercept values is reported as damping.

Table 10, Table 11, Table 12, Table 13, Table 14, and Table 15 show the results for the vertical tests performed on the Atlas railcar. The listed values are the average values per truck set, rather than the individual values per spring nest or primary pad.

Table 10. Vertical Test Results on End Truck with Wedges Installed and Minimum Load Spring Height

Frequency (Hz)	Aggregate of Whole Truck, Two Spring Nests or Four Primary Pads			
	Secondary Spring Stiffness (kips/inch)	Primary Pad Stiffness (kips/inch)	Secondary Spring Hysteresis Band Width (kips)	Primary Pad Hysteresis Band Width (kips)
0.1	70	775	9	29
0.5	68	805	8	36
2	67	945	10	26

Table 11. Vertical Test Results on End Truck with Wedges Installed and Maximum Load Spring Height

Frequency (Hz)	Aggregate of Whole Truck, Two Spring Nests or Four Primary Pads			
	Secondary Spring Stiffness (kips/inch)	Primary Pad Stiffness (kips/inch)	Secondary Spring Hysteresis Band Width (kips)	Primary Pad Hysteresis Band Width (kips)
0.1	70	850	12	42
0.5	70	1137	13	30
2	71	1,267	14	24

Table 12. Vertical Test Results on End Truck with Wedges Removed and Maximum Load Spring Height

Frequency (Hz)	Aggregate of Whole Truck, Two Spring Nests or Four Primary Pads			
	Secondary Spring Stiffness (kips/inch)	Primary Pad Stiffness (kips/inch)	Secondary Spring Hysteresis Band Width (kips)	Primary Pad Hysteresis Band Width (kips)
0.1	62	1004	4	42

Table 13. Vertical Test Results on Middle Truck with Wedges Installed and Minimum Load Spring Height

Frequency (Hz)	Aggregate of Whole Truck, Two Spring Nests or Four Primary Pads			
	Secondary Spring Stiffness (kips/inch)	Primary Pad Stiffness (kips/inch)	Secondary Spring Hysteresis Band Width (kips)	Primary Pad Hysteresis Band Width (kips)
0.1	69	921	14	28
0.5	67	1,064	14	22
2	64	1,152	13	16

Table 14. Vertical Test Results on Middle Truck with Wedges Installed and Maximum Load Spring Height

Frequency (Hz)	Aggregate of Whole Truck, Two Spring Nests or Four Primary Pads			
	Secondary Spring Stiffness (kips/inch)	Primary Pad Stiffness (kips/inch)	Secondary Spring Hysteresis Band Width (kips)	Primary Pad Hysteresis Band Width (kips)
0.1	68	916	13	37
0.5	68	1,190	17	20
2	68	2,040	19	25

Table 15. Vertical Test Results on Middle Truck with Wedges Removed and Maximum Load Spring Height

Frequency (Hz)	Aggregate of Whole Truck, Two Spring Nests or Four Primary Pads			
	Secondary Spring Stiffness (kips/inch)	Primary Pad Stiffness (kips/inch)	Secondary Spring Hysteresis Band Width (kips)	Primary Pad Hysteresis Band Width (kips)
0.1	61	1,797	1	51

Figure 14 and Figure 15 show examples of the data for the secondary suspension of the end truck and middle truck respectively. The sharp change in slope on the left side of the graph indicates where the springs become solid. The change in slope on the right side of the series indicates where the bolster loses contact with the load coils and is in contact only with the empty coils. Figure 16 shows an example of the data for the primary suspension. Negative displacements indicate compression and positive displacements indicate extension.

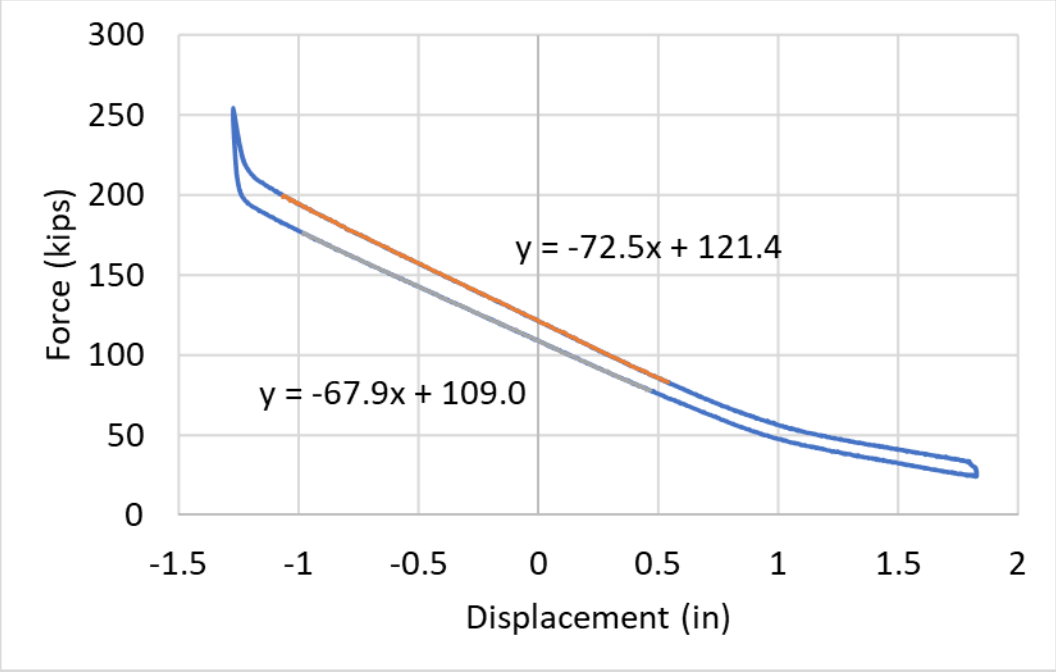


Figure 14. Truck total vertical wheel load plotted against average secondary suspension displacement, wedges installed, end truck, maximum test load, 0.1Hz.

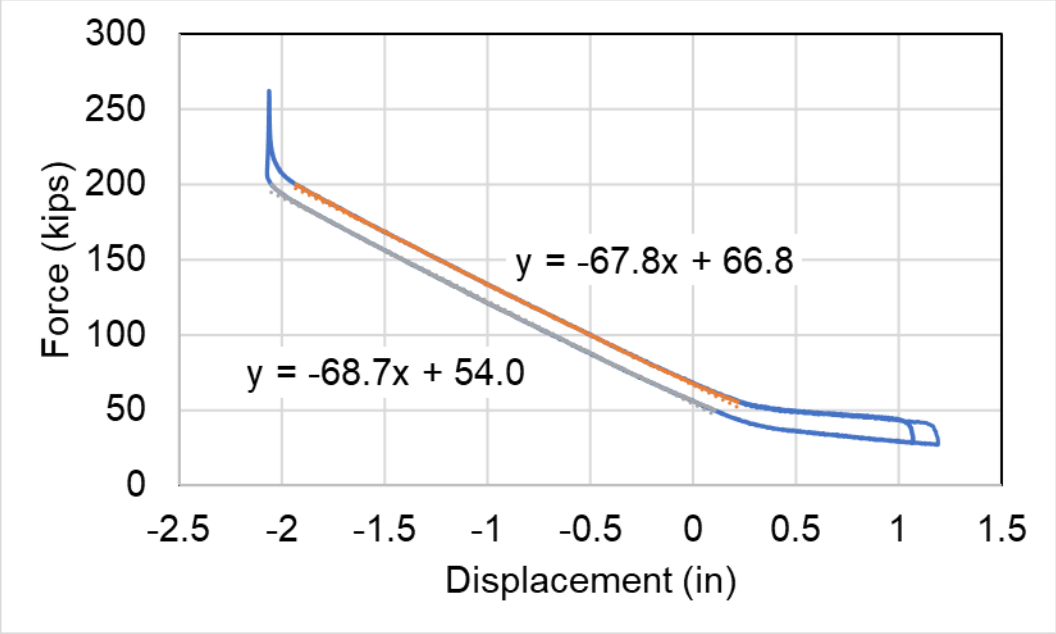


Figure 15. Truck total vertical wheel load plotted against average secondary suspension displacement, wedges installed, middle truck, maximum test load condition, 0.1Hz

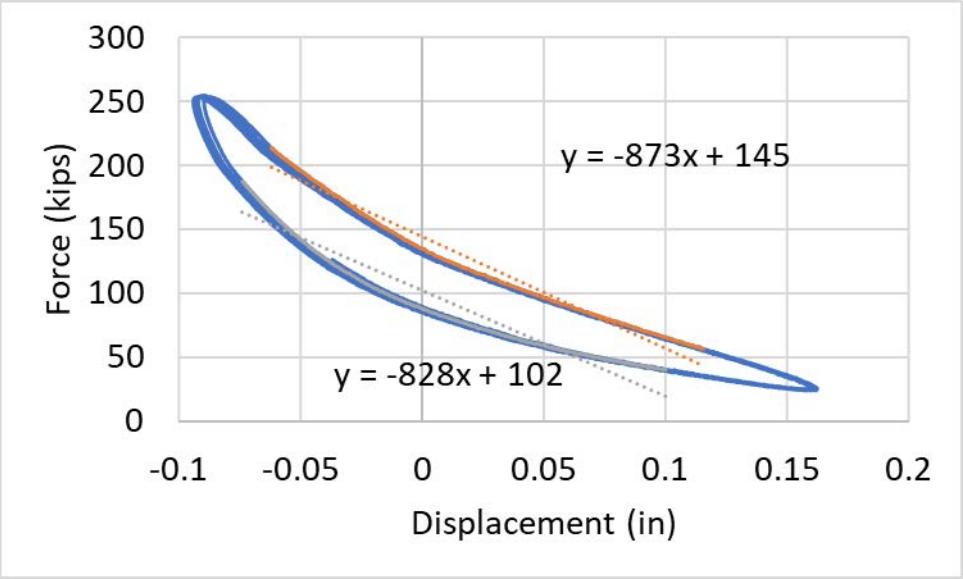


Figure 16. Truck total vertical wheel load versus average primary suspension displacement, end truck, maximum test load, at 0.1 Hz input

8.1.3 Lateral Suspension Stiffness and Damping

Lateral characterization tests were performed by connecting one actuator between the MSU reaction mass and the carbody. One end truck and one middle truck were tested. The trucks were tested in the minimum and maximum loaded cask conditions. Loads were applied at several frequencies: 0.1 Hz, 0.5 Hz and 2.0 Hz, but the most consistent results were found at the lowest frequencies. Input forces and displacements were adjusted for each run to achieve the desired input range within the capability of the MSU hydraulic and control systems. At low frequencies such as 0.1 Hz, the suspension was pushed to the stops where possible, but lower amplitude inputs were used at higher frequencies. Figure 17 shows the MSU configured for lateral characterization testing.

TTCI performed lateral suspension stiffness and damping tests on July 3, 2019, July 8, 2019, July 9, 2019. July 11, 2019, and July 12, 2019. Although the trucks were broken-in on load frames at Amsted and during the 1,400-mile journey from Kasgro's facility to TTC, there was no noticeable wear. Adam Klopp and Xinggao Shu, TTCI Principal Investigators, witnessed the lateral suspension and damping tests as the AAR Observer, per Standard S-2043 requirements.

Tests were performed at loads equivalent to minimum and maximum test load condition with the wedges installed. Tests were performed at maximum test load condition with wedges removed. The purpose for wedges removed tests was to verify the total lateral clearance and to document wedge damping. TTCI believes documenting this condition in the load condition equivalent to the maximum test load is adequate to document these parameters.

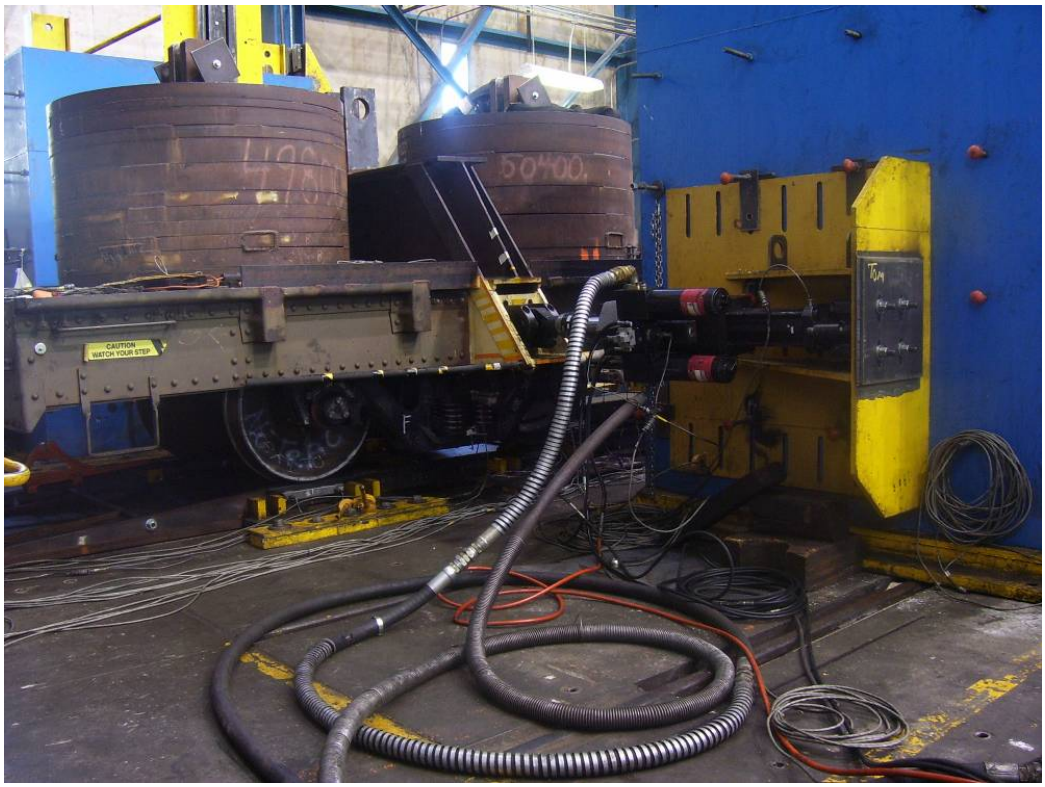


Figure 17. Flat Car Connected to the MSU during Lateral Characterization Tests

The Swing Motion® truck design allows the side frames to roll slightly about the side frame to bearing adapter connections to a greater extent than possible in a typical freight car truck. This allows for additional lateral transom and truck bolster displacement. The displacement between the bolster and transom was measured to determine the shear stiffness of the spring nests. Additional tests were run while restraining the transom lateral displacement by connecting a rigid bar laterally between the transom and the MSU reaction mass.

The lateral tests were run at 0.1Hz, 0.5Hz, and 2Hz with wedges installed and at 0.1Hz with wedges removed. The tests with the restrained transom were run at 0.1 Hz only.

The force supplied by the hydraulic actuator was measured by a load cell installed between the actuator and the specially welded bracket where the lateral force was applied. The lateral displacements were recorded by laser transducers and a series of LVDTs. The setup and part of the instrumentation are shown in Figure 18 and Figure 19.

These trucks also include a primary pad as shown in Figure 3. This pad allows some lateral movement between the side frames and the axles that works in series with the effect of side frame roll. The motion between the left- and right-side frame and the axle 2 bearing adapters was measured using six LVDTs on each side. The LVDTs were positioned to allow the calculation of the relative motion between the side frame and the bearing adapter in the longitudinal, lateral, vertical, roll, pitch, and yaw directions. Because the two primary suspension

pads work in parallel in the lateral direction, only the combined (or average) stiffness and damping can be measured. The lateral stiffness reported is relative to the lateral movement between the side frame and axle at a vertical position equal to the top of the bearing adapter.

Table 16, thru Table 21 show the results from the lateral suspension and damping tests.

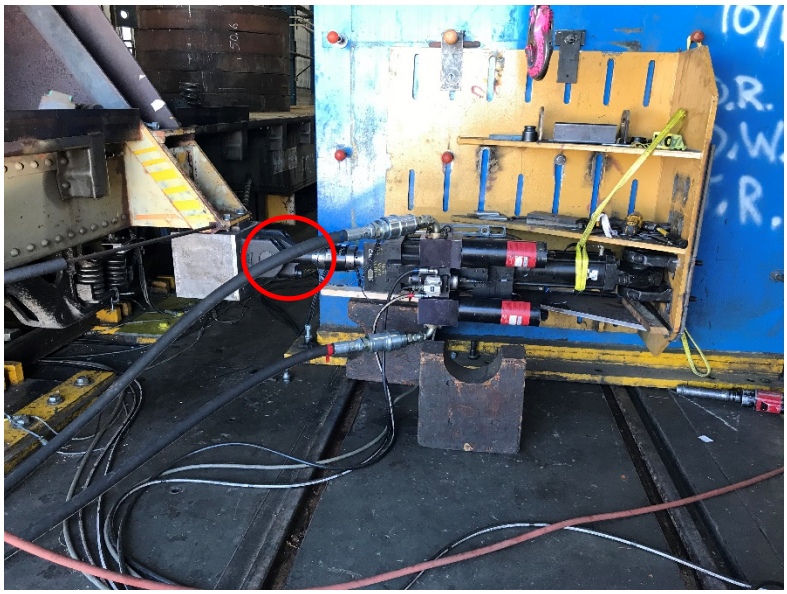


Figure 18. Load Cell for Lateral Force Measurements



Figure 19. Instrumentation Setup to Measure Lateral Movements of Pads

Table 16. Lateral Suspension Test for End Truck (Wedges Installed and Minimum Load Condition)

Frequency (Hz)	Aggregate of Whole Truck, Two Spring Nests or Four Primary Pads			
	Spring Stiffness (kips/inch)	Pad Stiffness (kips/inch)	Spring Hysteresis Band Width (kips)	Pad Hysteresis Band Width (kips)
0.1	8	132	10	10
0.5	8	137	9	7
2	23	220	10	6
0.1 Transom Restrained	15	NA	12	NA

Table 17. Lateral Suspension Test for End Truck (Wedges Installed and Maximum Load Condition)

Frequency (Hz)	Aggregate of Whole Truck, Two Spring Nests or Four Primary Pads			
	Spring Stiffness (kips/inch)	Pad Stiffness (kips/inch)	Spring Hysteresis Band Width (kips)	Pad Hysteresis Band Width (kips)
0.1	14	233	13	9
0.5	14	265	12	11
2	19	329	13	10
0.1 Transom Restrained	23	NA	13	NA

Table 18. Lateral Suspension Test for End Truck (Wedges Removed and Maximum Load Condition)

Frequency (Hz)	Aggregate of Whole Truck, Two Spring Nests or Four Primary Pads			
	Spring Stiffness (kips/inch)	Pad Stiffness (kips/inch)	Spring Hysteresis Band Width (kips)	Pad Hysteresis Band Width (kips)
0.1	16	389	5	7
0.1 Transom Restrained	26	NA	3	NA

Table 19. Lateral Suspension Test for Middle Truck (Wedges Installed and Minimum Load Condition)

Frequency (Hz)	Aggregate of Whole Truck, Two Spring Nests or Four Primary Pads			
	Spring Stiffness (kips/inch)	Pad Stiffness (kips/inch)	Spring Hysteresis Band Width (kips)	Pad Hysteresis Band Width (kips)
0.1	6	110	11	10
0.5	6	108	10	8
2	10	133	12	8
0.1 Transom Restrained	9	NA	9	NA

Table 20. Lateral Suspension Test for Middle Truck (Wedges Installed and Maximum Load Condition)

Frequency (Hz)	Aggregate of Whole Truck, Two Spring Nests or Four Primary Pads			
	Spring Stiffness (kips/inch)	Pad Stiffness (kips/inch)	Spring Hysteresis Band Width (kips)	Pad Hysteresis Band Width (kips)
0.1	13	301	16	14
0.5	13	327	15	12
2	19	427	16	10
0.1 Transom Restrained	19	NA	14	NA

Table 21. Lateral Suspension Test for Middle Truck (Wedges Removed and Maximum Load Condition)

Frequency (Hz)	Aggregate of Whole Truck, Two Spring Nests or Four Primary Pads			
	Spring Stiffness (kips/inch)	Pad Stiffness (kips/inch)	Spring Hysteresis Band Width (kips)	Pad Hysteresis Band Width (kips)
0.1	14	340	7	8
0.1 Transom Restrained	23	NA	9	NA

Figure 20 and Figure 21 show examples of the Lateral Suspension Stiffness and Damping Test results for the end truck at the minimum test load. The side frames were allowed to swing for the test results shown in Figure 20 but the transom was restrained to prevent the side frames from swinging for the test result shown in Figure 21. When the transom is free to swing the total clearance is over three inches, and when the transom is restrained, the total clearance is under two inches.

Figure 22 shows primary suspension lateral displacement plotted against lateral force for the middle truck at the maximum test load.

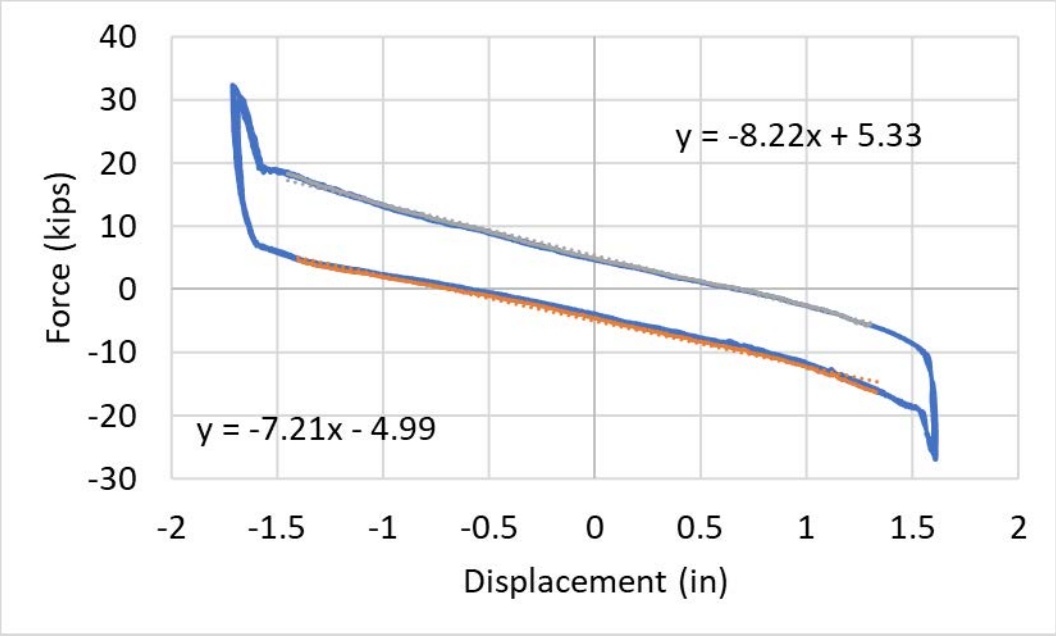


Figure 20. Truck lateral load plotted against lateral secondary suspension displacement. End truck with wedges, minimum test load, 0.1 Hz.

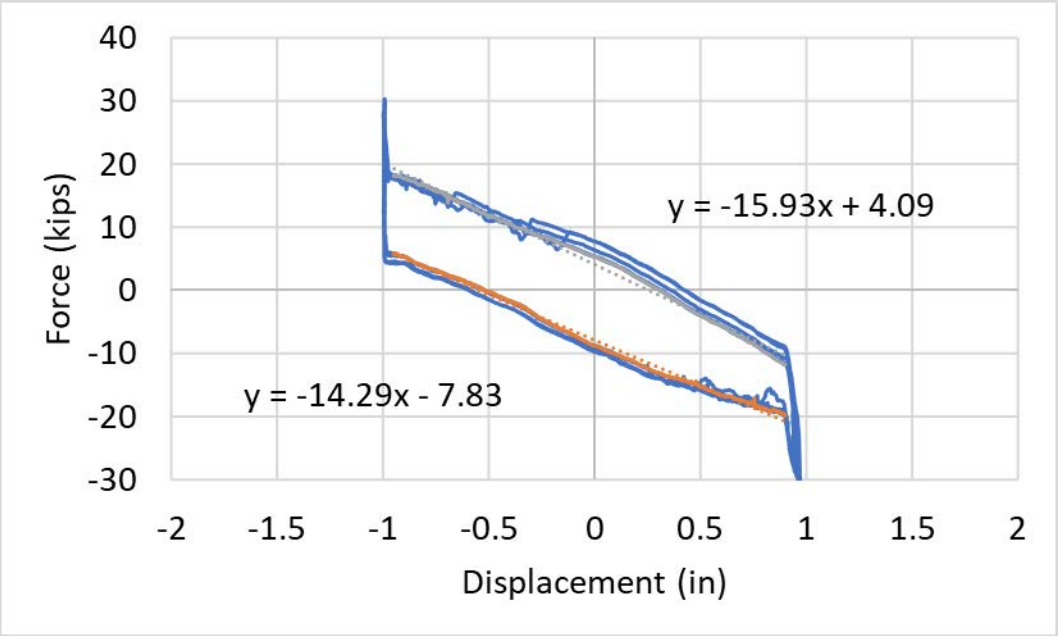


Figure 21. Truck lateral load plotted against lateral secondary suspension displacement. End truck with wedges, minimum test load, transom restrained, 0.1 Hz.

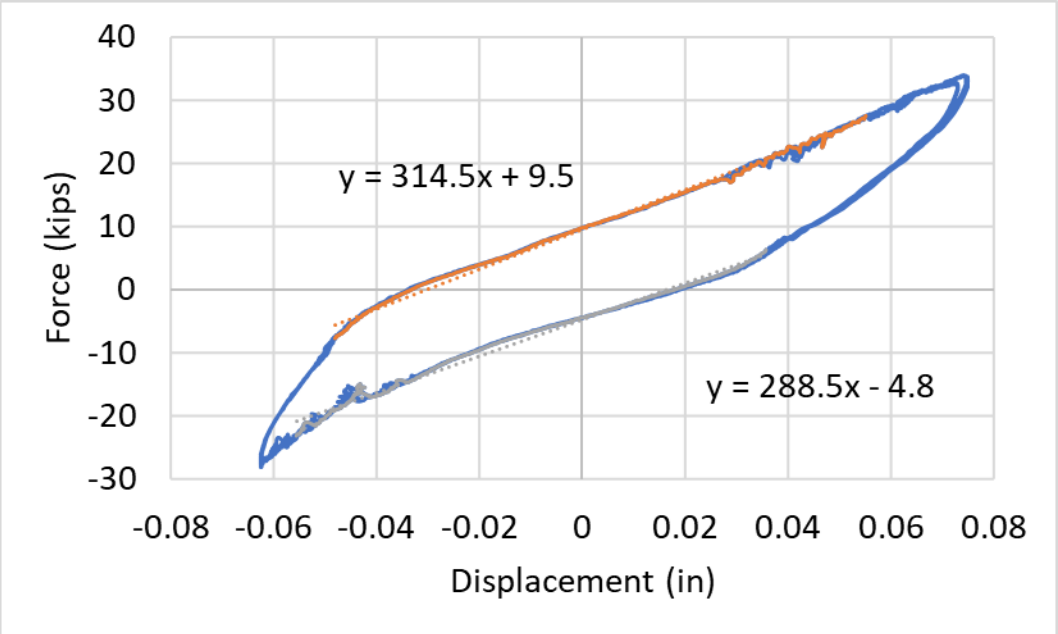


Figure 22. Primary suspension with wedges, middle truck, maximum test load, 0.1 Hz

8.1.4 Truck Rotation Stiffness and Breakaway Moment

Truck rotation stiffness and breakaway moments were measured by suspending one end of the car on air tables and measuring the force required to rotate the trucks relative to the span bolster and the span bolster relative to the carbody. The opposite end of the car was raised up to ensure that the car was leveled when the air tables were inflated. Hydraulic actuators were used to rotate

the tables. To ensure that an equal load was applied on each side of the truck, and to minimize lateral motion and skewing of the air tables, the actuators faced in opposite directions during these tests. These tests were performed at a very low rotational frequency and were considered static tests. These tests occurred between August 21, 2019 and September 5, 2019.

During these tests the centerplates were lubricated with a lubrication disk (Pennsylvania Railcar Part Number D073243) and the CCSB were installed during the test. Adam Klopp, Xinggao Shu, and Abe Meddah, TTCI Principal Investigators, witnessed the truck rotation stiffness and breakaway tests as the AAR Observers per Standard S-2043 requirements. The tests performed are shown in Table 22. Figure 23, Figure 24, and Figure 25 show the experimental set up for these tests.

Table 22. Truck Rotation and Break Away Moment Matrix

Truck Position	Loading Condition	Loading Condition
B	Minimum	Maximum
C	Minimum	Maximum
D	Minimum	Maximum
Span Bolster	Minimum	Maximum



Figure 23. Truck Rotation Setup with Truck Floating on Air Table and One Lateral Actuator



Figure 24. Test Setup for the Span Bolster Test Showing Connected Air Tables

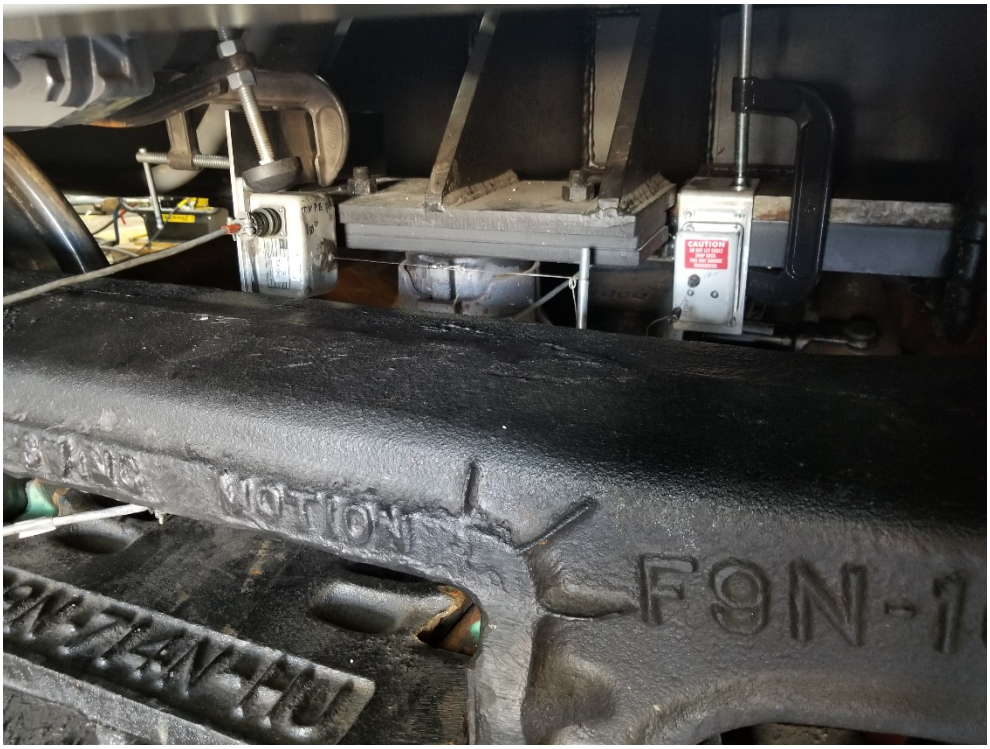


Figure 25. String Potentiometers Used for Truck Rotation Measurement

Table 24 shows the measured friction moments for each condition tested. The coefficient of friction in the centerplate was estimated using the following equation:

$$\mu = \frac{3\,(Torque - 2SBld \times SBdst \times \mu_{sb})(\mathrm{CPrad}^2 - \mathrm{Hrad}^2)}{2\,(\mathrm{Tld} - 2 \times \mathrm{SBld})(\mathrm{Cprad}^3 - \mathrm{Hrad}^3)}$$

Where:

- Torque is the average turning torque measured in the test
- SBld is the CCSB preload measured during side bearing component characterization
- SBdst is the distance from the canter of rotation to the CCSB mounting locations, 25-inches
- μ_{sb} is the assumed coefficient of friction between the CCSB and the body
- Cprad is the centerplate radius
- Hrad is the centerplate hole radius
- Tld is the load carried by the truck center plate and side bearings

Side bearing preload was taken at the middle of the hysteresis loop at setup height shown in Figure 10, 5,240 pounds. The truck rotation test was performed shortly after the car was built. When the side bearings were installed on the new car, a light coat of lubricant was applied to help with break-in. This lubricant had not worn off at the time of the test, so TTCI estimated the coefficient of friction between the truck side bearings and side bearing wear plate was 0.2. The span bolster side bearings were gap type side bearings and therefore contributed no resistance to the span bolster turning moment.

The truck loads were obtained from the nominal load bar readings during the equalization test, shown in Table 23. The span bolster weight (25,200 pounds), truck weight (11,000 pounds), and side bearing preload (5,240 pounds) were subtracted from the weight on rail shown in Table 23 to calculate the load on the span bolster and truck center plates. Figure 26 shows a plot of the data for the run showing the highest aggregate centerplate friction coefficient (0.30) on one of the D-truck maximum load test runs.

Table 23. Loads on Trucks and Span Bolster, Nominal Loads from Truck Load Equalization Test

Truck	Maximum Test Load Condition*	Minimum Test Load Condition*
Gross car Weight (pounds)	714,000	425,000
B-Truck (pounds)	135,000	86,000
C-Truck (pounds)	111,000	54,000
D-Truck (pounds)	130,000	76,000
Span Bolster (pounds)	376,000	216,000

* Values summed from inidividual wheel loads measured with load bars. Due to limits of measurement accuracy these values may not match scale weights.

Table 24. Truck Rotation Moments and Estimates of the Associated Friction Coefficients

Truck	Maximum Load Condition		Minimum Load Condition	
	Mean Torque 1,000 inch-pound	Center Plate Friction Coefficient (μ)	Mean Torque 1,000 inch-pound	Center Plate Friction Coefficient (μ)
B-Truck	150	0.14	140	0.19
C-Truck	220	0.28	120	0.23
D-Truck	260	0.30	117	0.16
Span Bolster	450	0.18	225	0.16

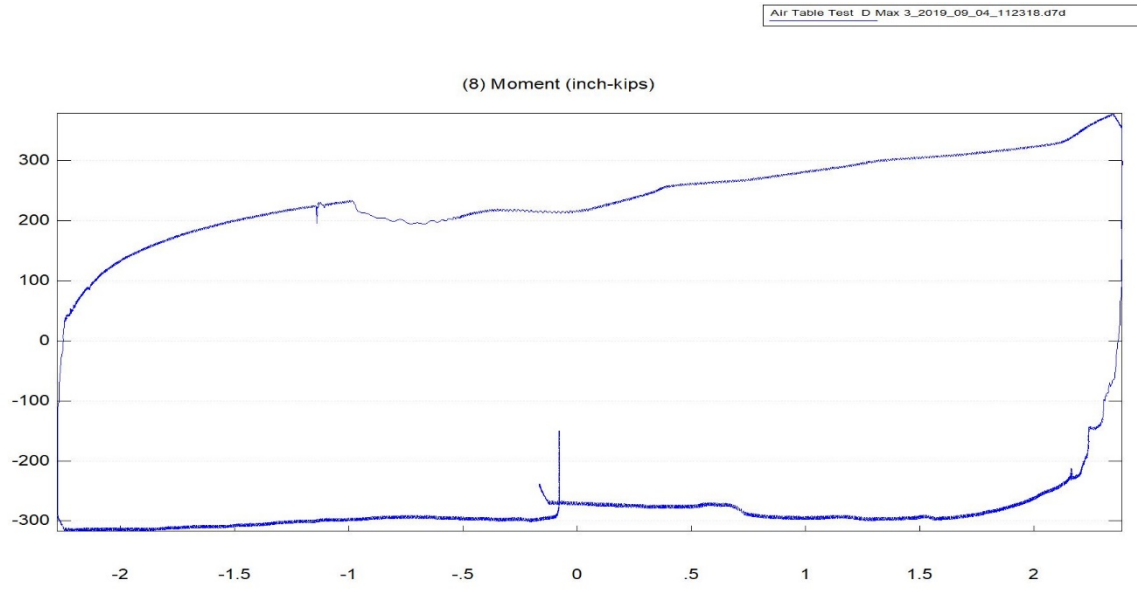


Figure 26. Example of Air Table Data for a D-truck of Atlas Car with Maximum Load

8.1.5 Interaxle Longitudinal Stiffness

The longitudinal stiffness of the axle to side frame connection is critical to vehicle performance in curving and high-speed stability regimes. The interaxle longitudinal stiffness is measured by:

- Installing independently rotating wheels with spindles at the bearing endcaps in the truck
- Mounting actuators and load cells between the spindles on each side of the truck
- Forcing the axles apart and pulling them together while measuring the force and displacement (Figure 27).

Runs were performed while pushing and pulling in phase on each side of the truck and separately while pushing on one side of the truck and pulling on the other side. TTCI performed the interaxle longitudinal stiffness test on July 17, 2019. Adam Klopp, TTCI Principal Investigator I, witnessed the interaxle longitudinal stiffness tests as the AAR Observer, per Standard S-2043 requirements.

The motion between the left and right side frame and the bearing adapters of one axle was measured using six LVDTs on each side. The LVDTs were positioned to allow the calculation of the relative motion between the side frame and the bearing adapter in the longitudinal, lateral, vertical, roll, pitch, and yaw directions.

The applied force at the axle centerline was vertically offset from the level of the axle to side frame connection. This caused the bearing adapters to pitch and shear longitudinally. The shear stiffness data in Table 25are based on longitudinal displacements at the level of the top of the bearing adapter. Pitch stiffness data are based on a rotation of the bearing adapter around the bearing. Axle centerline stiffness data are based on the longitudinal motion of the axle at its axis of rotation. Figure 28 shows example data for longitudinal axle stiffness tests.

Axle yaw stiffness data were determined during push-pull runs, and this data can be expressed as two longitudinal stiffnesses separated by the bearing centerline distance. The effective longitudinal stiffness was calculated from the axle yaw stiffness by this method for comparison with the direct measurements of primary longitudinal stiffness. Given the large variation in the direct measurement of axle centerline longitudinal stiffness, the values derived from axle yaw stiffness agree to within 15% of the average values from the direct measurements.

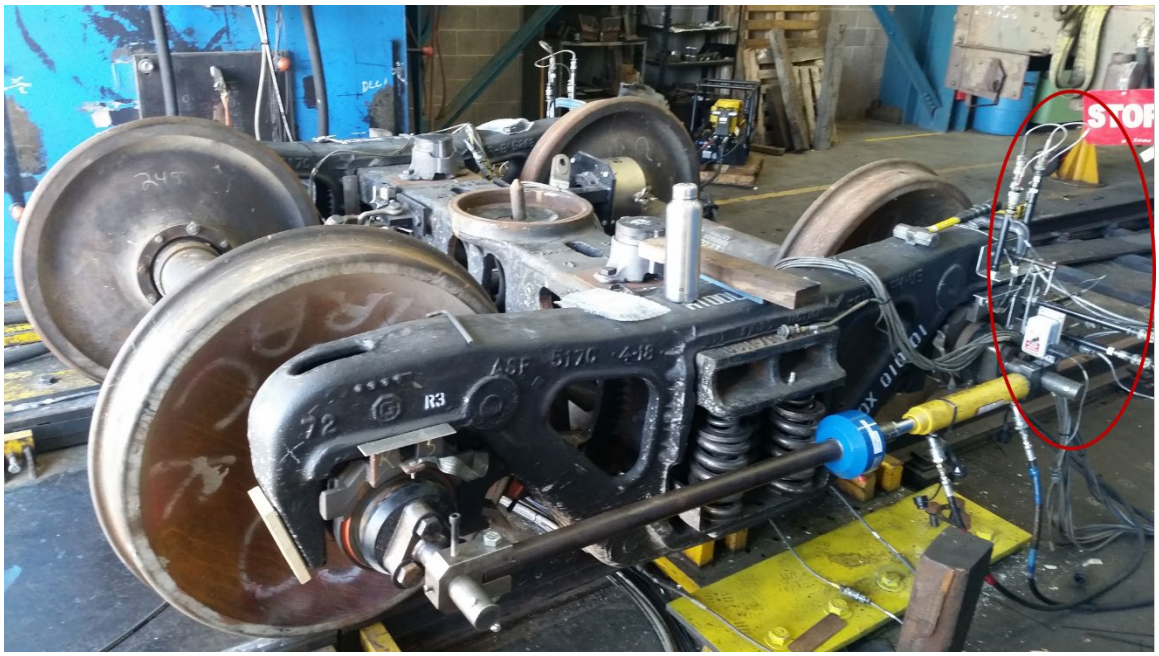


Figure 27. Configuration and Measurements for Interaxle Longitudinal Stiffness Tests

Table 25. Side Frame to Axle Stiffness Data per Pad

Property		Minimum Loading	Maximum Loading
		End Truck	End Truck
Shear Stiffness (1,000-pounds/inch)	Avg	38	39
	Min	16	18
	Max	60	64
Pitch Stiffness (1,000 inch-pounds/rad)	Avg	334	396
	Min	159	213
	Max	447	571
Axle Centerline Longitudinal Stiffness (1,000-pounds/inch, axle motion excited here is longitudinal without any yaw)	Avg	8	9
	Min	3	5
	Max	10	14
Axle Yaw Stiffness (1,000 inch-pounds/rad)	Avg	22,353	24,544
	Min	18,924	24,476
	Max	25,782	24,611
Axle Centerline Longitudinal Stiffness Derived from Axle Yaw (1,000-pounds/inch)	Avg	7.2	7.9

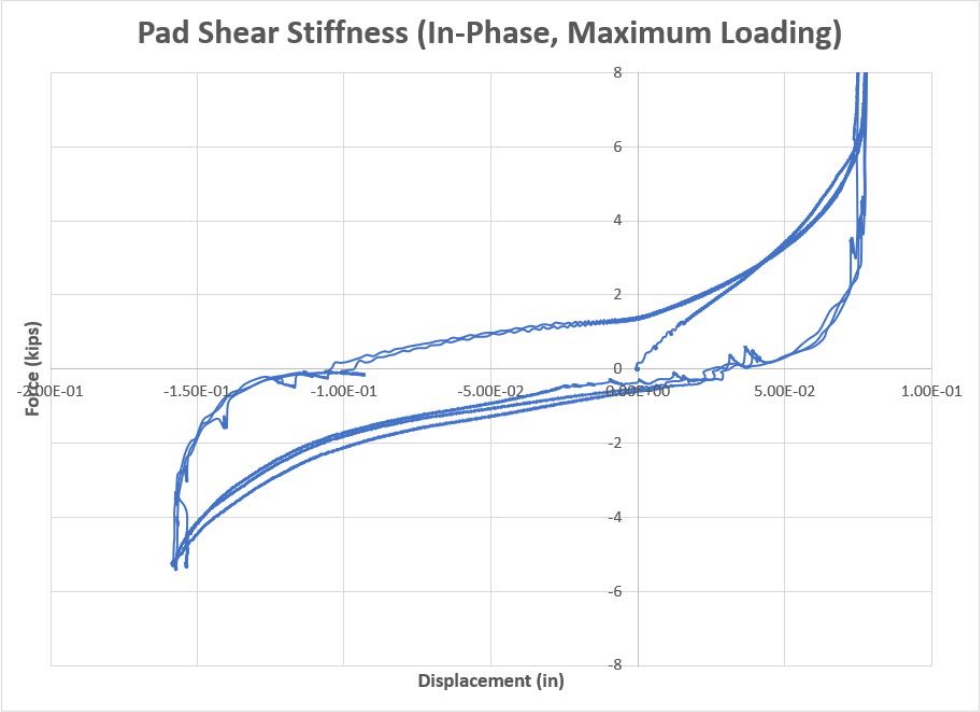


Figure 28. Example Data for Longitudinal Axle Stiffness Tests Showing the Force and Displacement Across one Primary Pad

8.1.6 Modal Characterization

Modal characterization was performed to identify the rigid and flexible body modes of vibration for the vehicle. The Atlas car has a 48-foot deck, but the majority of the load is carried on a short cradle in the center of the car. The concentrated load has large mass and rotational inertias fixed over a short span in the center of the deck that causes the flexible body modes to be coupled with what are normally rigid body modes.

The Atlas car was excited through actuators attached at the B-end jacking locations. Figure 29 shows the car setup for lateral inputs. The car was tested in minimum and maximum load configurations, and wedges were removed for all tests. TTCI performed modal characterization tests between July 07, 2021, and August 06, 2021. Adam Klopp, TTCI Principal Investigator I, witnessed the modal characterization tests as the AAR Observer, per Standard S-2043 requirements.

Actuators were operated in force control at lower frequencies (0.2-10 Hz) and in displacement control for constant acceleration input at higher frequencies (3-30 Hz). In practice, the displacement control inputs were intended to be constant displacement but were limited by the actuator response and displacement amplitude reduced as frequency increased. Frequency was increased linearly with time for the frequency sweeps. The inputs included:

- Lateral excitation with one actuator
- Vertical excitation with one actuator

- Vertical excitation with two actuators operating in phase
- Vertical excitation with two actuators operating 180 degrees out of phase

The Atlas car deck was instrumented with five vertical accelerometers on the right edge, five vertical accelerometers along the left edge, and five lateral accelerometers along the right edge. Figure 30 shows the distribution of the accelerometers used during the modal test. The input forces and displacements were also recorded.



Figure 29. Actuator Attached to Carbody during Modal Testing with Lateral Input

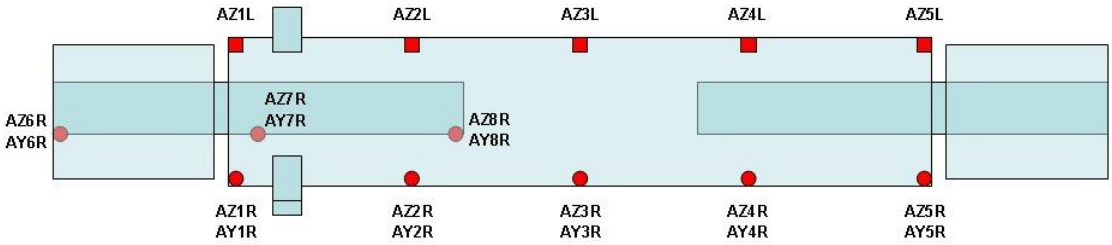


Figure 30. Distribution of Accelerometers during the Atlas Railcar Modal Test

The test was performed according to the following sequence:

1. Vertical rigid body test runs (force control). Minimum load
2. Roll rigid body test runs (force control). Minimum load
3. Vertical flexible body test runs (displacement control). Minimum load
4. Twist flexible body test runs (displacement control). Minimum load

5. Vertical rigid body test runs. Maximum load
6. Roll rigid body test runs. Maximum load
7. Vertical flexible body test runs. Maximum load
8. Twist flexible body test runs. Maximum load
9. Lateral rigid body test runs (force control). Maximum load
10. Lateral flexible body test runs (displacement control). Maximum load
11. Lateral rigid body test runs. Minimum load
12. Lateral flexible body test runs. Minimum load

The accelerometer and force outputs were used to create Operational Deflection Shapes (ODS) and Frequency Response Functions (FRFs). The analysis of the ODS together with the frequency rate used for each test allows for the determination of the corresponding natural frequencies. Table 26 shows the results of the modal characterization tests. The bending mode on the maximum load condition could not be excited during these tests, most likely due to the additional stiffness created by the load distribution as described at the end of this section. This case is marked as Not Observed. Figure 31 shows an example of the FRFs determination. Each one of the peaks was evaluated and further refinements were made as necessary. Figure 32 shows the vertical bending mode at 8.49 Hz.

Table 26. Modal Characterization Results (Hz)

Mode Type	Mode	Minimum Test Load	Maximum Test Load
RIGID BODY	Bounce	2.22	2.04
	Pitch	3.82	3.75
	Upper Center Roll	2.63	2.30
	Lower Center Roll	0.80	0.78
	Yaw	1.62	1.56
FLEXIBLE BODY	Twist	15.5	6.85
	Vertical Bending	8.49	Not Observed
	Lateral Bending	18.9	18.1

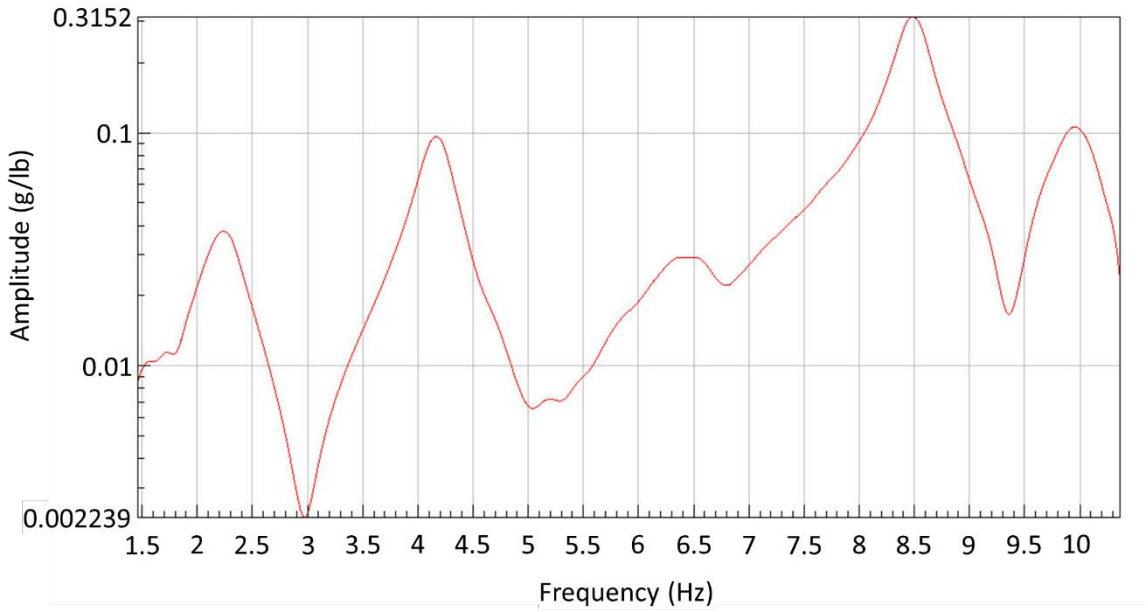


Figure 31. Frequency Response Function Sample

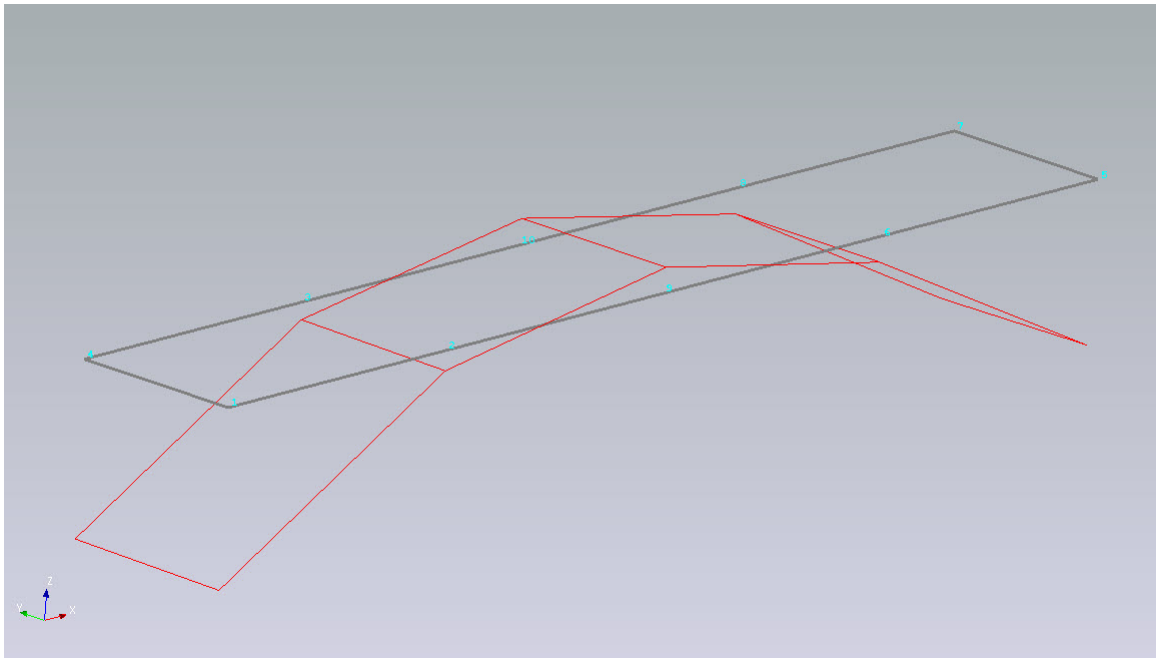


Figure 32. Bending Mode Shape at 8.49 Hz. (Minimum Load)

Figure 33 shows a photo of the Atlas car loaded with the maximum test load in the Rail Dynamics Laboratory (RDL) during modal testing. The end stops restrain the maximum test load longitudinally, and specially cut wooden blocks are wedged in between the end stop and the end of the central beam assembly at each end of the assembly to take up the clearance. The end stops, blocks, and central beam assembly form a longitudinal connection from one end of the car to the other, at a height several feet above the deck surface. The effect of this connection is a significant

stiffening of the car in vertical bending that is believed to have increased the frequency of the vertical bending mode so that it was not observed in the maximum test load condition.



Figure 33. Atlas car with maximum test load in the RDL. Note the central beam assembly contacts the end stops.

8.2 Nonstructural Static Tests

Nonstructural static tests were performed to ensure the vehicle would equalize its load properly under common conditions. Test results are provided in Sections 8.2.1 to 8.2.4. The nonstructural static tests included:

- Truck twist equalization
- Carbody twist equalization
- Static curve stability
- Horizontal curve negotiation

8.2.1 Truck Twist Equalization

The truck twist equalization requirement ensures adequate truck load equalization while negotiating track twist due to low joints or other track geometry conditions. With the Atlas car on level track, vertical wheel loads were measured while raising and lowering one wheel from 0.0 inch to 3.0 inches in increments of 0.5 inch. At 2.0 inches of deflection, the vertical load at any wheel may not fall below 60 percent of the nominal static load. At 3.0 inches of deflection,

the vertical load at any wheel may not fall below 40 percent of the nominal static load. One wheel of each truck in the car was raised and lowered to test this condition (Right Axle 1, Left Axle 4, Right Axle 5, Right Axle 8, Right Axle 9, and Left Axle 12).

The truck twist equalization tests were completed on September 26, 2019, September 30, 2019, October 9, 2019, and October 10, 2019. Adam Klopp, Abe Meddah, and Xinggao Shu, TTCI Principal Investigators, witnessed the truck twist equalization tests as the AAR Observers per Standard S-2043 requirements. The car did not meet the Standard S-2043 requirements. Therefore, on behalf of the DOE, TTCI is requesting an exception from the AAR EEC. Table 27 shows the worst-case truck twist equalization results. Figure 34 displays the wheel load result for all wheels during the lifting and lowering of the L4 wheel with the minimum test load. Figure 35 and Figure 36 display the wheel load results for all wheels during the lifting and lowering of the R9 and L4 wheels, respectively.

In May 2020, 0.375-inch shims were placed between the center plates for the middle trucks (1 each, trucks C and F) and the span bolster. This shim placement was done to improve the load equalization among the three trucks of each span bolster and may improve the performance of the middle trucks in this regime. Table 28 shows the load distribution for trucks under the B-span bolster before and after the shims were installed. Only data from the B-span bolster in shown because the best data from after the shims were installed for comparison to previous load bar data was from instrumented wheel sets (IWS), and IWS were only installed in axles 1-6, under the B-span bolster. The data shows that although the B and D trucks still carry more load than the C truck, the load on the C truck increased by 6 kips or more when the 3/8-inch shim was installed.

The issue of these test results not meeting specification was discussed with EEC October 15, 2020. The EEC did not advise TTCI to repeat these tests at that time.

Table 27. Truck Twist Equalization Results

Condition	Minimum Test Load		Maximum Test Load	
	Percent Load Result	Wheel Raised or Lowered	Percent Load Result	Wheel Raised or Lowered
2-inch Drop	50% at L4 Wheel	L4 Lowered	43% at R9 Wheel	R9 Lowered
3-inch Drop	24% at L4 Wheel	L4 Lowered	29% at L4 Wheel	L4 Lowered

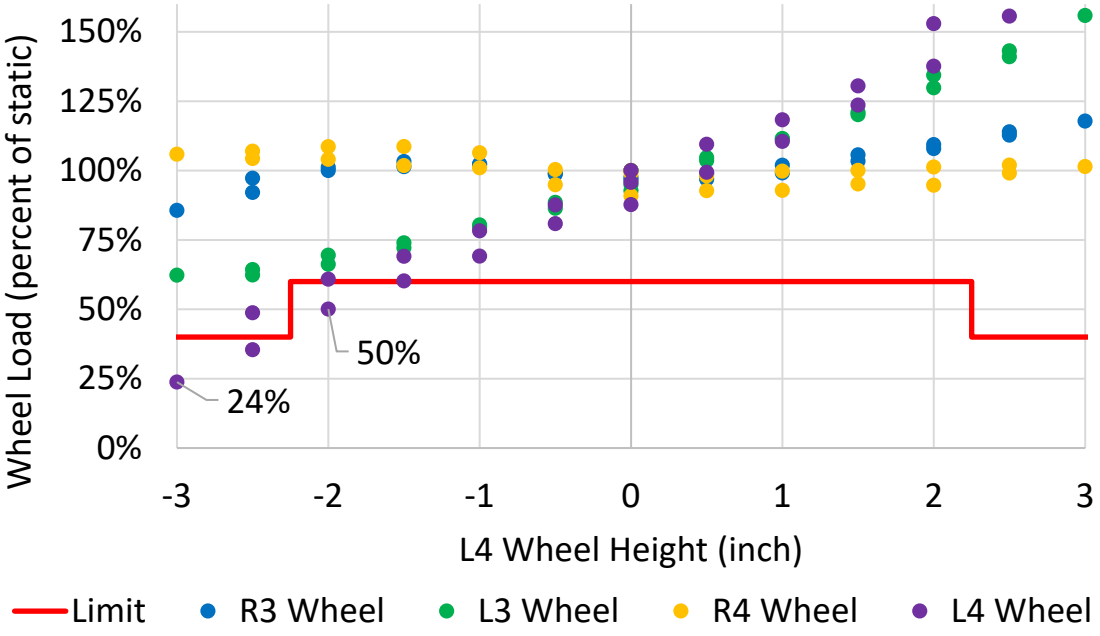


Figure 34. L4 Truck Twist Result for All Increments (Minimum Test Load)

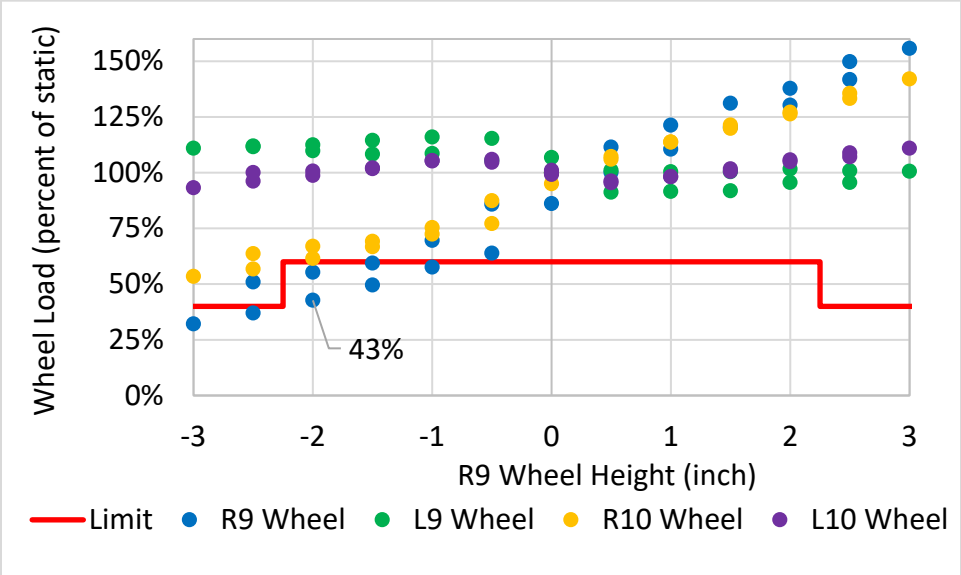


Figure 35. R9 Truck Twist Result for All Increments (Maximum Test Load)

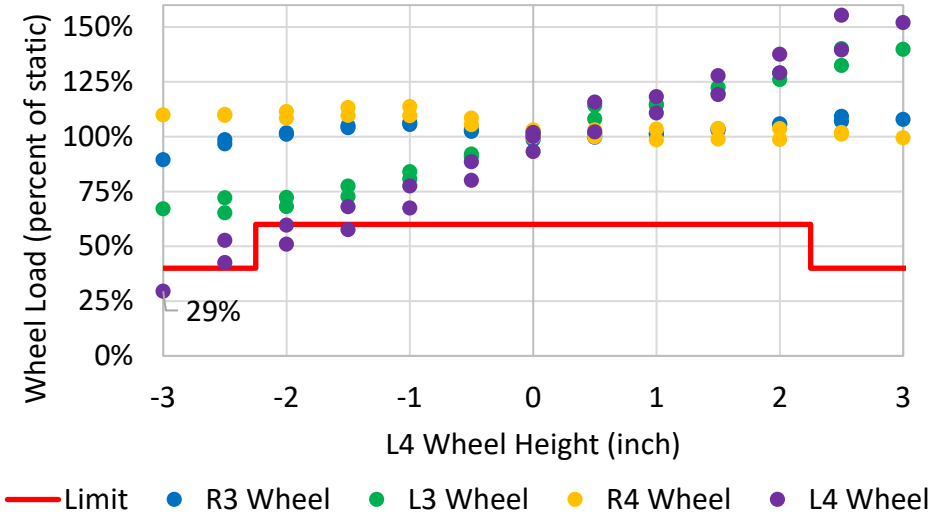


Figure 36. L4 Truck Twist Result for All Increments (Maximum Test Load)

Table 28. Truck Loads with and without 3/8" Shim

Truck Location	Minimum Test Load		Maximum Test Load	
	Load Bar Data without 3/8" Shim in C Truck	IWS Data with 3/8" Shim in C Truck	Load Bar Data without 3/8" Shim in C Truck	IWS Data with 3/8" Shim in C Truck
B Truck Load (kips)	86	80	135	128
C Truck Load (kips)	54	60	111	118
D Truck Load (kips)	76	69	130	121

8.2.2 Car Body Twist Equalization

The carbody twist equalization requirement is the documentation of wheel unloading under carbody twist, i.e., during spiral negotiation. With the Atlas car on level track, vertical wheel loads were measured while consecutively raising and lowering six wheels from 0.0 inch to 3.0 inches in increments of 0.5 inch. At 2.0 inches of deflection, vertical load at any wheel may not fall below 60 percent of the nominal static load. At 3.0 inches of deflection, no permanent damage should be produced and vertical load at any wheel may not fall below 40 percent of the nominal static load. Figure 37 shows the Atlas railcar with minimum test load during Car Body Twist Equalization test.



Figure 37. Atlas Railcar with Minimum Test Load during Carbody Twist Equalization Test

The carbody twist tests were completed on October 1, 2019, October 9, 2019, and October 10, 2019. Adam Klopp and Abe Meddah, TTCI Principal Investigators, witnessed the carbody twist equalization tests as the AAR Observer, per Standard-2043 requirements. The Atlas car met the criteria for carbody twist equalization. No permanent deformation occurred at 3 inches of carbody twist. Table 29 shows the worst-case test results.

Table 29. Car Body Twist Equalization Results

Condition	Minimum Test Load		Maximum Test Load	
	Percent Load	Wheel	Percent Load	Wheel
2-inch Lift	74%	Axle 7 Left	73%	Axle 10 Right
3-inch Lift	71%	Axle 8 Right	65%	Axle 4 Right

Figure 38 and Figure 39 display the load percentage for all wheels during the test for minimum and maximum test load.

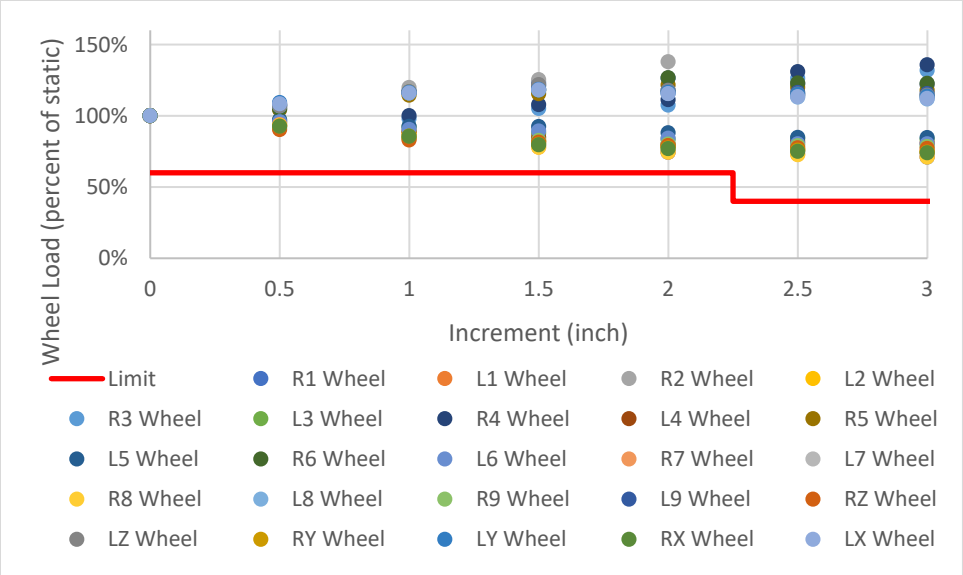


Figure 38. Car Body Twist for Minimum Test Load Condition (BR) - Results for All Wheels

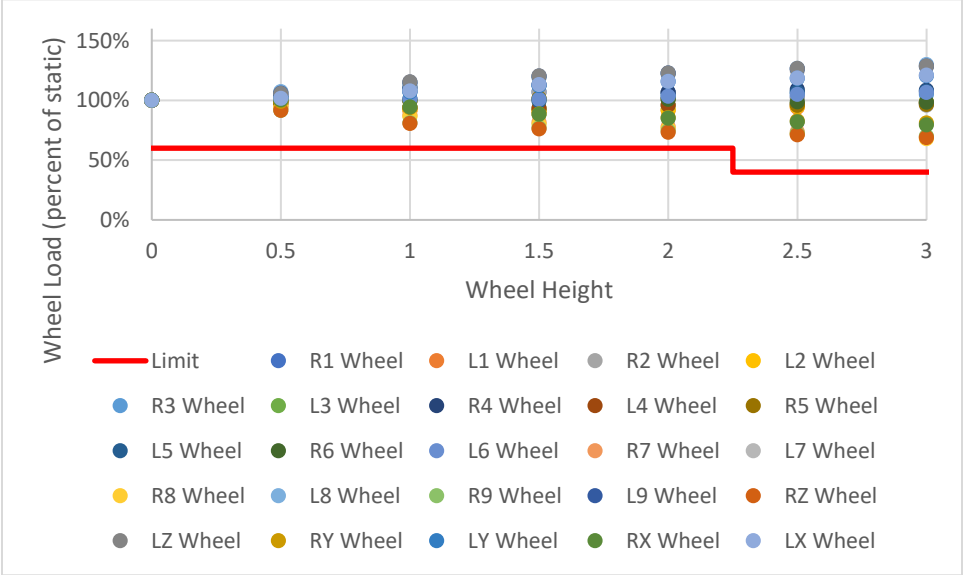


Figure 39. Car Body Twist for Maximum Test Load Condition (BR) - Results for All Wheels

8.2.3 Static Curve Stability

The static curve stability test was performed on the car in the Minimum Test Load condition. Testing was performed on November 4, 2019. Adam Klopp, TTCI Principal Investigator I, witnessed the static curve stability test as the AAR Observer, per Standard S-2043 requirements.

On one end, the Atlas car was coupled to a short base car as defined in AAR MSRP C-II paragraph 2.1.4.2.3[5] and a long car having 90-foot over strikers, 66-foot truck centers, 60-inch

couplers, and conventional draft gear on the other end. The 200,000-pound load was applied and held for more than 20 seconds. The train was chocked in a 10-degree flat curve.

The Atlas railcar must not experience wheel lift or suspension separation during this test. Wheel lift is defined as 1/8-inch lift 2 5/8 inches from the rim face with a feeler gauge. The car met criteria for the static curve stability test.



Figure 40. Atlas Railcar during the Static Curve Stability Test

8.2.4 Horizontal Curve Negotiation

The horizontal curve negotiation test is performed to identify areas of interference in the car suspension, structure, and brake system. The test was performed on the car in the maximum load condition in a 150-foot radius curve on July 7, 2019. Ulrich Spangenberg, TTCI Principal Investigator I, witnessed the horizontal curve negotiation test as the AAR Observer, per Standard S-2043 requirements. No interference was noted; therefore, the Atlas car met the criteria for this test.

8.3 Static Brake Tests

Standard S-2043 requires the static brake force measurements be made per MSRP Section E Standard S-401, and the single-car air brake test must be performed per the AAR MSRP Section E, Standard S-486. These tests were conducted by Kasgro prior to delivery of the Atlas car to the TTC.

The static brake force measurements were conducted on IDOX 010001 A-End and B-End, at the Kasgro Facility in Pennsylvania on February 12, 2019. AAR Standard S-401 testing is documented in a letter from Matt DeGeorge to Jon Hannafious (TTC) dated August 20, 2021. AAR Standard S-486 testing is documented in a letter from Mike Yon to David Cackovic (TTCI) dated March 12, 2019. Both letters are included in Appendix C.

8.4 Structural Tests

Structural tests were conducted to demonstrate the railcar's ability to withstand the rigorous railroad load environment and to verify the accuracy of the structural analysis. Standard S-2043 refers to MSRP Section C Part II, Specification M-1001, paragraph 11.3 (Ref 6) for structural testing details and criteria.

The Standard S-2043 requirement calls for dimensional measurements at the start and conclusion of the structural tests and strain measurements during testing. In addition, visual inspections for damage are required before and after the individual tests. A key criterion from AAR MSRP Chapter 11[6] is that no permanent deformation shall be produced by the testing. This is interpreted as no strain exceeding material yield.

The Atlas railcar was instrumented with 55 strain gauges. The gauges were placed in key locations on the top and bottom of the railcar as specified by the railcar designer The measurements taken by these gauges were used to monitor the strain during each of the structural tests and to verify the FEA. Figure 41 shows the location of strain measurements. A description of each location is included in Appendix B (Table B1). Further detail on the locations, placement, and orientation of the gauges is found in Appendix D.

These gauges were installed on the empty car. A baseline measurement was recorded prior to loading. Additional baselines were recorded for the car loaded to the maximum and minimum test loads. The gauges were zeroed before each test so that test results could be either isolated or combined with the baseline conditions.

Using the following formula, the results have been converted from microstrain (με) to stress (σ, ksi) with a positive value indicating tension and a negative value indicating compression:

$$\sigma = E\mu\varepsilon/1{,}000{,}000$$

Where:

σ = stress (ksi)

E = Young's modulus (29,000 ksi)

με = microstrain (10^{-6} inch/inch)

The MSRP section C-II, Paragraph 4.2.2.4, states "…the allowable design stress shall be the yield or 80 percent of ultimate, whichever is lower, or the critical buckling stress." Kasgro's critical buckling analysis (Appendix E) shows that buckling is not limiting for the Atlas car. With four exceptions, the allowable compressive or tensile stress is yield strength of the material the strain gauges were applied to, 60,000 psi for all the Atlas carbody components, per Kasgro. The exceptions are gauge locations SGBF15, SGBF18, SGBF23 and SGBF26 which are grade 80 plate. For these four locations 80 percent of ultimate is lower than the yield stress and the allowable stress is 72,000 psi.

The structural tests include the following:

- Preliminary and post-test inspection
- Squeeze (compressive end) load
- Coupler vertical loads

- Jacking
- Twist
- Impact

Table 30 shows the structural tests conducted and the associated load condition(s).

Table 30. Summary of structural tests and load condition

Test Name	Maximum	Minimum
Squeeze (compressive end) load	x	X
Coupler vertical loads	x	
Jacking	x	
Twist	x	
Impact	x	

Structural test results are provided in Sections 8.4.1 to 8.4.7.

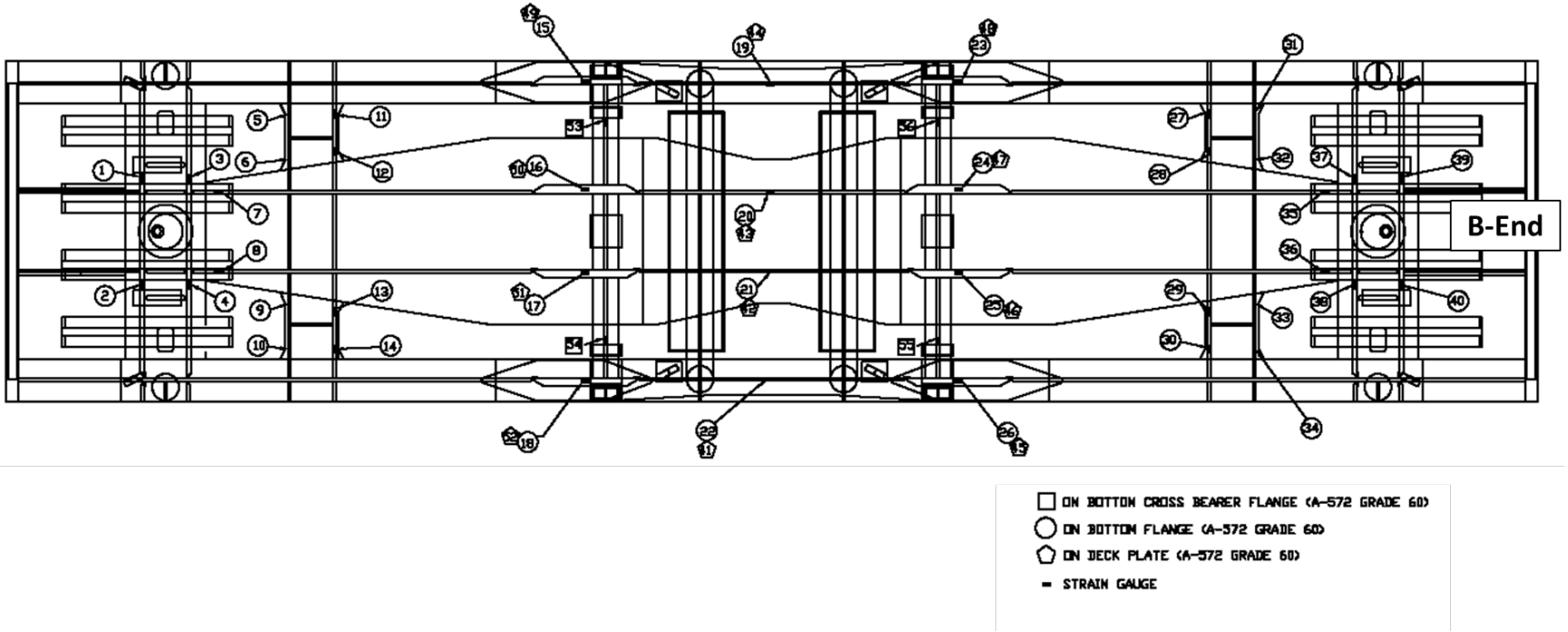


Figure 41. Location of Strain Measurements Monitored during Structural Testing

8.4.1 Preliminary and Post Test Inspection

The Standard S-2043 requirement calls for special measurements during pre- and post-test inspections and strain measurements during testing. These measurements are used to verify the FEA predictions.

The Atlas car length was measured from striker to striker, as well as over the pulling faces. Table 31 shows the results of these measurements before and after the tests were performed. The length over pulling faces increased by 0.875 inch—this amount is considered to be negligible considering the various clearances in the draft system and the measurement accuracy.

A survey total station was used to measure the shape of the railcar deck before and after testing. Figure 42 shows the results of the level measurements before and after structural testing. No significant change in shape of the deck was noted.

Table 31. Survey Measurements

Condition	Striker to Striker	Length over Pulling Faces
Initial Measurement	73 feet 5-1/4 inches	78 feet 1-1/2 inches
Post Squeeze	73 feet 5-1/4 inches	78 feet 2 3/8 inches

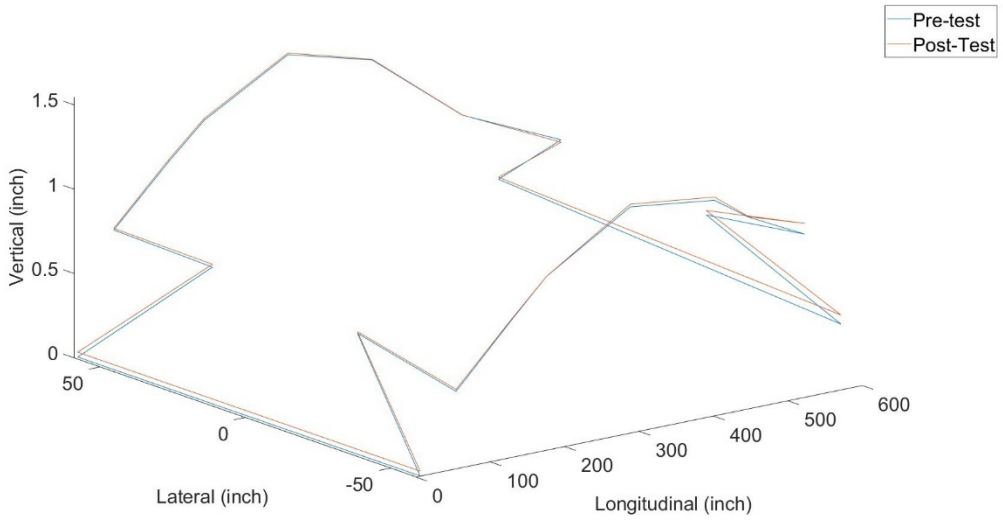


Figure 42. Results of Level Loop around the Car Deck

8.4.2 Measured Stress from Test Loads

Baseline measurements were recorded for the car loaded in both the minimum and maximum test load conditions. There are no Standard S-2043 criteria for the baseline measurements, but it should be noted that no allowable stresses were exceeded.

Table 32 shows a summary of stresses from the baseline measurements of the Atlas car after loading the maximum test load (but without any additional applied load), for the locations with highest measured stress. The maximum measured stress was 27 ksi (38 percent of allowable) in tension measured at SBGF26.This amount of stress was measured at the center of the left-hand side sill bottom flange, approximately 74 1/8 inches from the B-end body bolster toward the center of the car.

Table 33 shows a summary of stresses from the baseline measurements after loading the minimum test load, without any additional applied load for the locations with highest measured stress. The maximum measured stress was 11 ksi (15 percent of allowable) in tension measured at SGBF26.

The locations for the gauges referenced in Table 32 and Table 33 are highlighted in Figure 43.

Table 32. Highest Measured Stresses for Atlas Car Loaded to Maximum Test Load Condition with no Additional Applied Forces

Channel Name	Approximate Location	Measured Stress (ksi)	Allowable Stress (ksi)	Measured Stress as percent of Allowable
SGBF26	Center of LH side sill bottom flange, 74 1/8 inches from B end body bolster toward center of car	27	72	38%
SGDP45	Top of deck plate, above LH side sill web, 66 3/8 inches from line across centermost edges of B-end end stop pin blocks toward center of car	-21	60	35%
SGDP48	Top of deck plate, above RH side sill web, 66 3/8 inches from line across centermost edges of B-end end stop pin blocks toward center of car	-20	60	33%
SGBF15	Center of RH side sill bottom flange, 74 1/8 inches from B end body bolster toward center of car	18	72	25%

Table 33. Highest Measured Stresses for Atlas Car Loaded to Minimum Test Load Condition with no Additional Applied Forces

Channel Name	Approximate Location	Measured Stress (ksi)	Allowable Stress (ksi)	Measured Stress as percent of Allowable
SGBF26	Center of LH side sill bottom flange, 74 1/8 inches from B end body bolster toward center of car	11	72	15%
SGBF15	Center of RH side sill bottom flange, 74 1/8 inches from B end body bolster toward center of car	9.4	72	13%
SGDP52	Top of deck plate, above LH center sill web, 66 3/8 inches from line across centermost edges of A-end stop pin blocks toward center of car	-8.8	60	15%
SGDP45	Top of deck plate, above LH side sill web, 66 3/8 inches from across centermost edges of B-end end stop pin blocks toward center of car	-8.7	60	15%

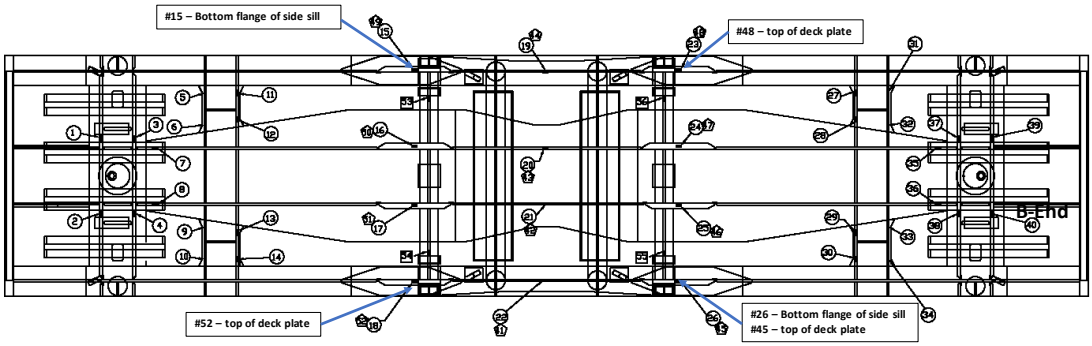


Figure 43. Measurement with Highest Measured Stress from Test Loads Only

8.4.3 Squeeze (Compressive End) Load

The squeeze (compressive end) load test was performed to verify that the Atlas railcar can withstand compressive longitudinal loads. A horizontal compressive static load was applied at the centerline of the draft system of car interface areas using TTCI's squeeze fixture. The load was cycled up to 750,000 pounds three times, and then on the fourth cycle the load was increased to 1,000,000 pounds. The applied load was monitored with a load cell.

The test was performed in the maximum test load configuration on October 22, 2019, to test the worst-case stress condition. The test was also performed in the minimum test load configuration on October 24, 2019, to test the worst-case stability condition. Figure 44 shows the Atlas railcar in the maximum test load car configuration installed in the squeeze fixture just before testing. Adam Klopp, TTCI Principal Investigator I, witnessed

the squeeze (compressive end) load test as the AAR Observer, per Standard S-2043 requirements.

The Atlas railcar met all criteria for the compressive end load test in both the maximum and minimum test load configurations. No permanent deformation or suspension separation was noted.



Figure 44. Maximum Test Load Compressive End Load Test

Maximum Test Load Condition

Figure 45 and Figure 46 show the summary results for the compression test on the Atlas railcar in the maximum test load condition at 1,000 kips of applied compressive end load. Note that the highest total tensile stresses (indicated by positive values in SGBF15 – SGBF26 in Figure 45) are primarily from the maximum test load and are reduced by the applied compressive load. The highest compressive stresses (indicated by negative values in SGDP45 – SGDP52 in Figure 46) are in locations where the stresses from the applied load are relatively low. The highest compressive stresses from the applied compressive end load SGBF7, SGBF8, SGBF35 and SGBF36 are in locations with relatively low tensile stresses from the maximum test load, resulting in relatively low total compressive stresses.

Table 34 shows the locations with the highest total tensile stress (stress from the maximum test load combined with stress from the applied compressive load). The highest total stress was once again at SGBF26. Note that the applied compressive load acted to reduce the tension load from the baseline loading and resulted in a lower total tensile stress of 23 ksi (38 percent of allowable). The highest compressive stress of -21 ksi (35 percent of allowable) is at SGDP45, located on top of the deck plate, above the left-hand

side sill web and approximately 66 3/8 inches from the centermost edges of the B-end end stop pin blocks, toward the center of the car. Table 35 shows the locations with the highest stress from applied load.

In both loading conditions, SGBF26 was the worst location. This location corresponds to the center of the left-hand side sill bottom flange, approximately 2 inches aft of #2 cross bearer. Additional details on the test results are provided in Appendix F.

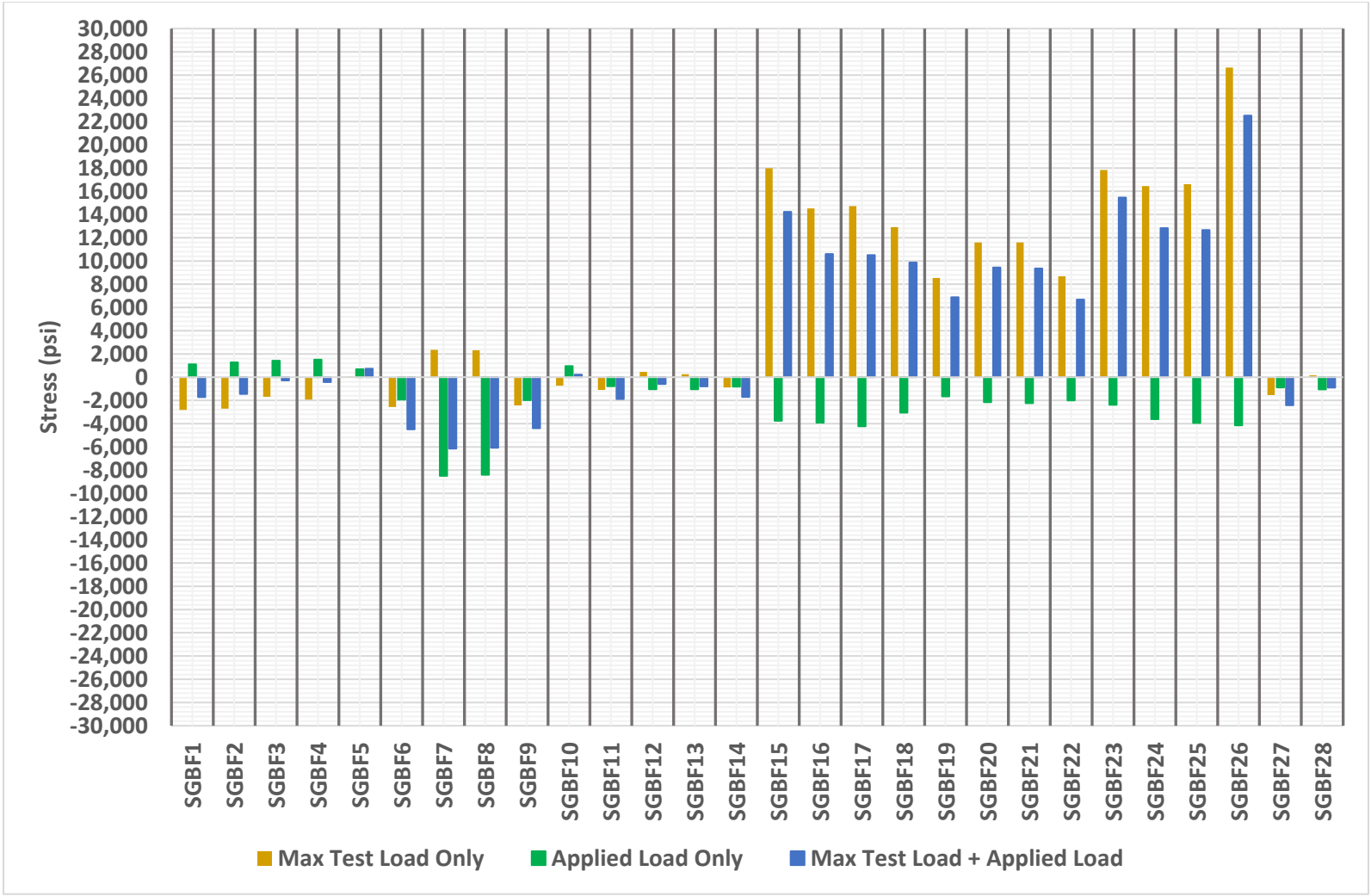


Figure 45. Summary of Atlas Railcar Squeeze Test Results – Maximum Test Load Condition with 1,000 Kips Applied Compressive Load (1 of 2)

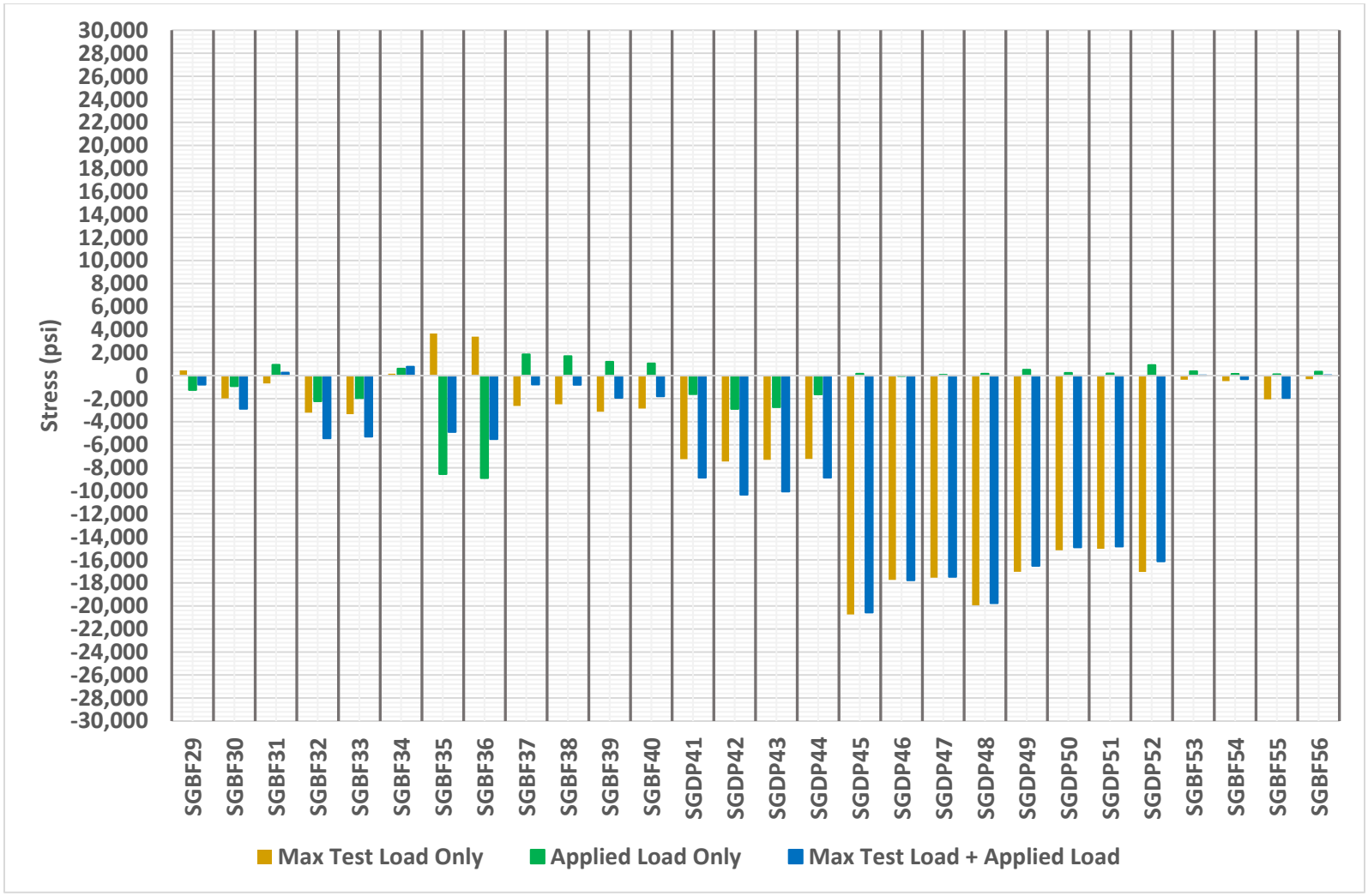


Figure 46. Summary of Atlas Railcar Squeeze Test Results – Maximum Test Load Condition with 1,000 Kips Applied Compressive Load (2 of 2)

Table 34. Locations with Highest Total Tension and Compression Stress under Maximum Load Condition

Channel Name	Approximate Location	Stress from Maximum Test Load (ksi)	Stress from Applied Load (ksi)	Total Stress (ksi)	Allowable Stress (ksi)	Total Stress as percent of Allowable
SGBF26	Center of LH side sill bottom flange, approx. 74 1/8 inches from B end body bolster toward center of car	27	-4.1	23	72	32%
SGDP45	Top of deck plate, above LH side sill web, 66 3/8 inches from line across centermost edges of pin blocks toward center of car (directly above SBGF 26)	-21	0.16	-21	60	35%

Table 35. Locations with Highest Stress from Applied Load under Maximum Load Conditions

Channel Name	Approximate Location	Stress from Maximum test load (ksi)	Stress from Applied Load (ksi)	Total Stress (ksi)	Allowable Stress (ksi)	Measured Stress as percent of Allowable
SGBF36	LH side of bottom flange of center sill - forward of rear body bolster - aligns with center sill web and end stop mount block pin hole	3.4	-8.9	-5.5	60	9%
SGBF35	RH side of bottom flange of center sill - forward of rear body bolster - aligns with center sill web and end stop mount block pin hole	3.6	-8.5	-4.9	60	8%

Minimum Test Load Condition

Figure 47 and Figure 48 show the summary results for the compression test on the Atlas railcar in the minimum test load condition at 1,000 kips of applied compressive end load. As with the maximum test load results, the highest tensile stresses from the minimum test load are reduced by the applied compressive load, resulting in overall tensile stresses below 3 ksi. However, in this case, the highest compressive stresses coincide with the highest compressive stresses from the applied load (SGBF7, SGBF8, SGBF35 and SGBF36).

Table 36 shows the locations with the highest total tensile stress. The highest total stress was once again at SGBF26. The applied compressive load acted to reduce the tension load from the baseline loading and resulted in a lower total tensile stress of 2.9 ksi (only 5 percent of allowable). The highest compressive stress of -9.6 ksi (16 percent of allowable) is at SGDP35, which is on the right-hand side of the bottom flange of the center sill, 5 3/16 inches from the B-end body bolster toward the center of the car. Table 37 shows the locations with the highest stress from applied load.

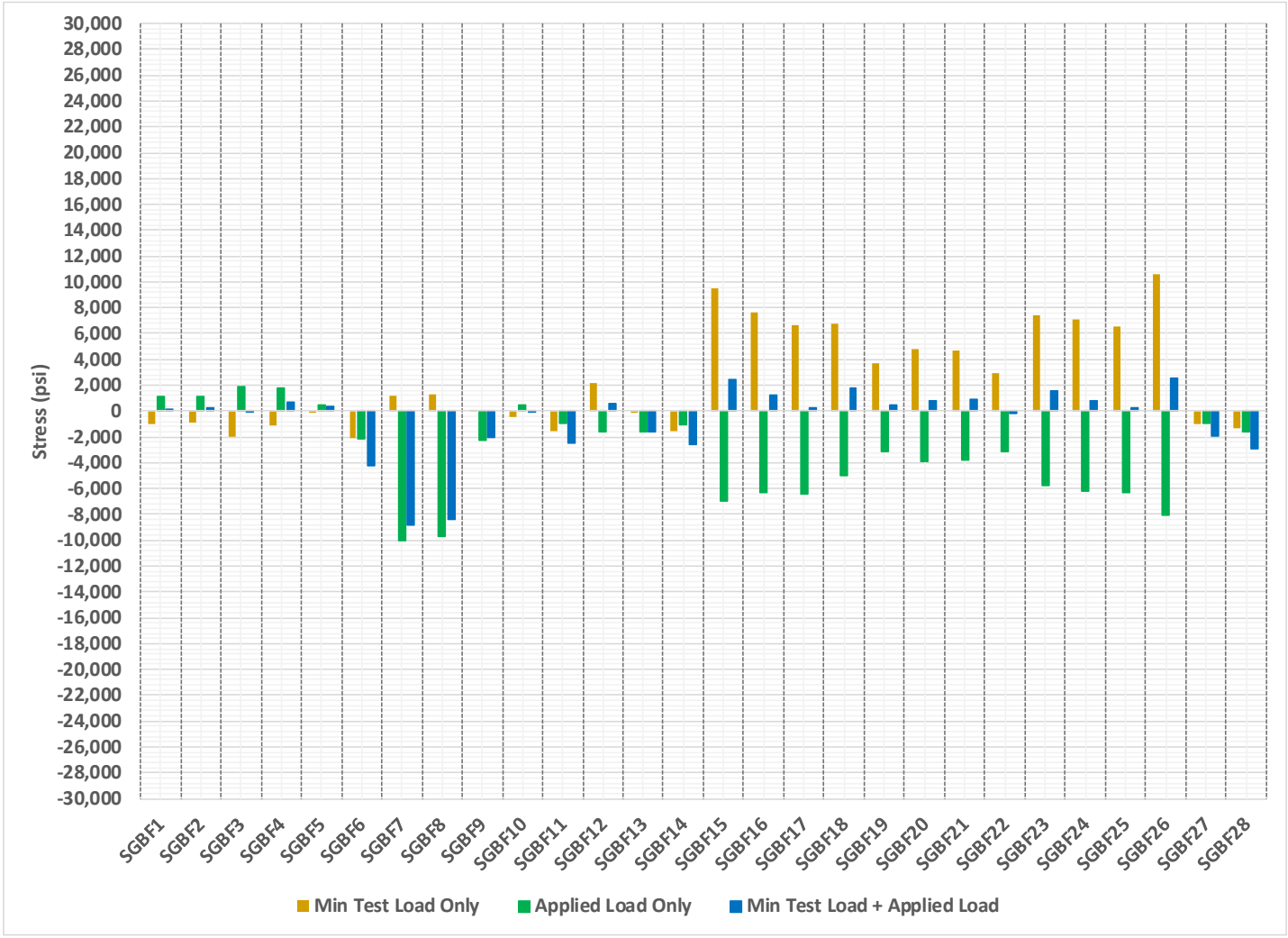


Figure 47. Summary of Atlas Railcar Squeeze Test Results – Minimum Test Load Condition with 1,000 Kips Applied Compressive Load (1 of 2)

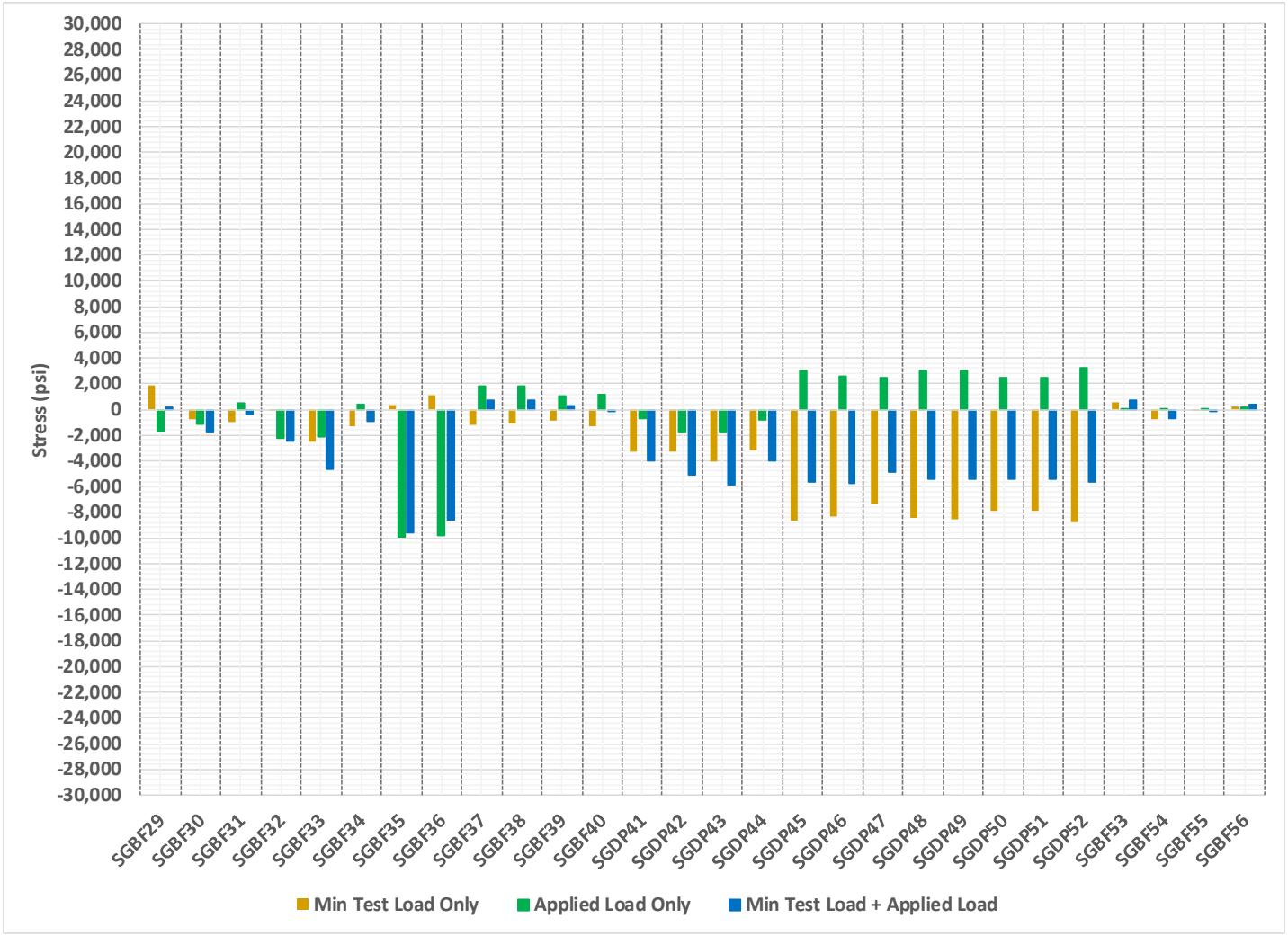


Figure 48. Summary of Atlas Railcar Squeeze Test Results – Minimum Test Load Condition with 1,000 Kips Applied Compressive Load (2 of 2)

Table 36. Locations with Highest Total Tension and Compression Stresses under Minimum Load Condition

Channel Name	Approximate Location	Stress from Minimum test load (ksi)	Stress from Applied Load (ksi)	Total Stress (ksi)	Allowable Stress (ksi)	Measured Stress as percent of Allowable
SGBF26	Center of LH side sill bottom flange, approx. 74 1/8 inches from B end body bolster toward center of car.	11	-0.81	2.9	72	4%
SGBF35	RH side of bottom flange of center sill – 5 3/16 inches from B-end body bolster toward center of car - aligns with center sill web	0.29	-9.9	-9.6	60	16%

Table 37. Locations with Highest Stress from Applied Load under Minimum Load Condition

Channel Name	Approximate Location	Stress from Minimum test load (ksi)	Stress from Applied Load (ksi)	Total Stress (ksi)	Allowable Stress (ksi)	Measured Stress as percent of Allowable
SGBF7	RH side of bottom flange of center sill - 5 3/16 inches from A-end body bolster toward center of car - aligns with center sill web	1.2	-10	-8.8	60	15%
SGBF35	RH side of bottom flange of center sill – 5 3/16 inches from B-end body bolster toward center of car - aligns with center sill web	0.29	-9.9	-9.6	60	16%

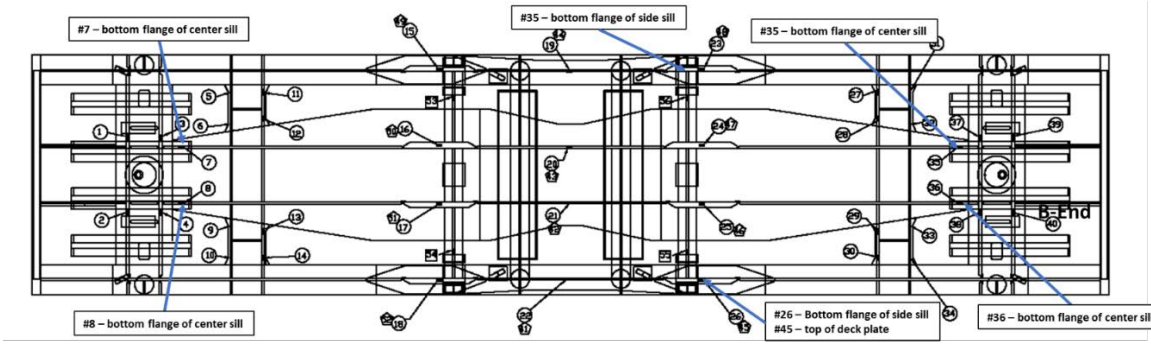


Figure 49. Locations with Highest Measured Stress during Squeeze (Compressive End) Load Test

8.4.4 Coupler Vertical Loads

A load of 50,000-pound was applied in both directions to the coupler knuckle and held for 60 seconds. The test was performed on October 11, 2019, with the maximum condition test load installed. Adam Klopp, TTCI Principal Investigator I, witnessed the coupler vertical load tests as the AAR Observer, per Standard S-2043 requirements.

The car met criteria for the 50,000-pound coupler vertical load test. Figure 50 shows the coupler carrier plate after the coupler vertical load test.

Figure 51 and Figure 52 show results from the downward portion of the test. Results for the upward portion are similar and are included in Appendix G. Note that for the locations measured the applied stresses from the vertical load are small compared to stresses from the maximum test load.

Table 38 shows the locations with highest total tensile and compressive stress. The locations were the same as for the squeeze test, with the highest total tensile stress of 27 ksi (43 percent of allowable) during the upward test at SGBF26. The highest compressive stress of -21 ksi (35 percent of allowable) was at SGDP45, also during the upward test. Table 39 shows the locations with the highest stresses from applied loads. No evidence of gradual zero-shift (plastic deformations) was noted.

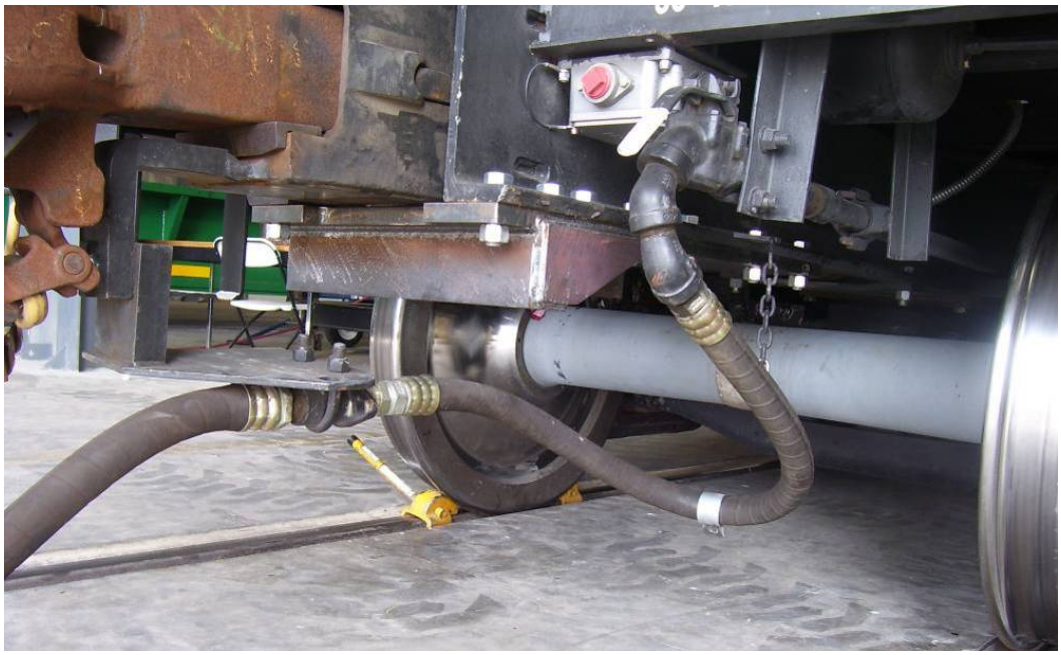


Figure 50. Coupler Carrier Plate after the Coupler Vertical Load Test

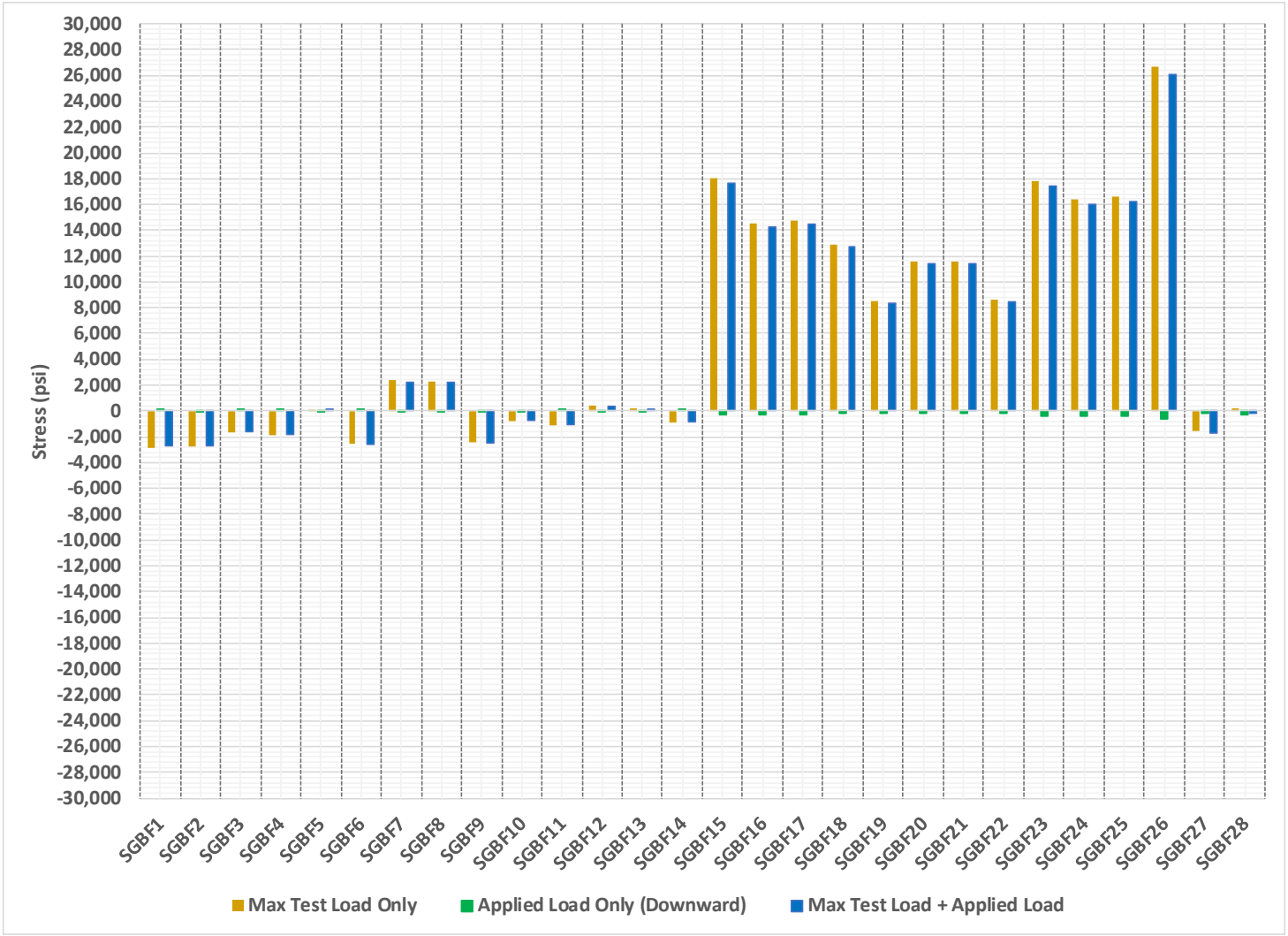


Figure 51. Stress from Downward Coupler Vertical Load Test (1 of 2)

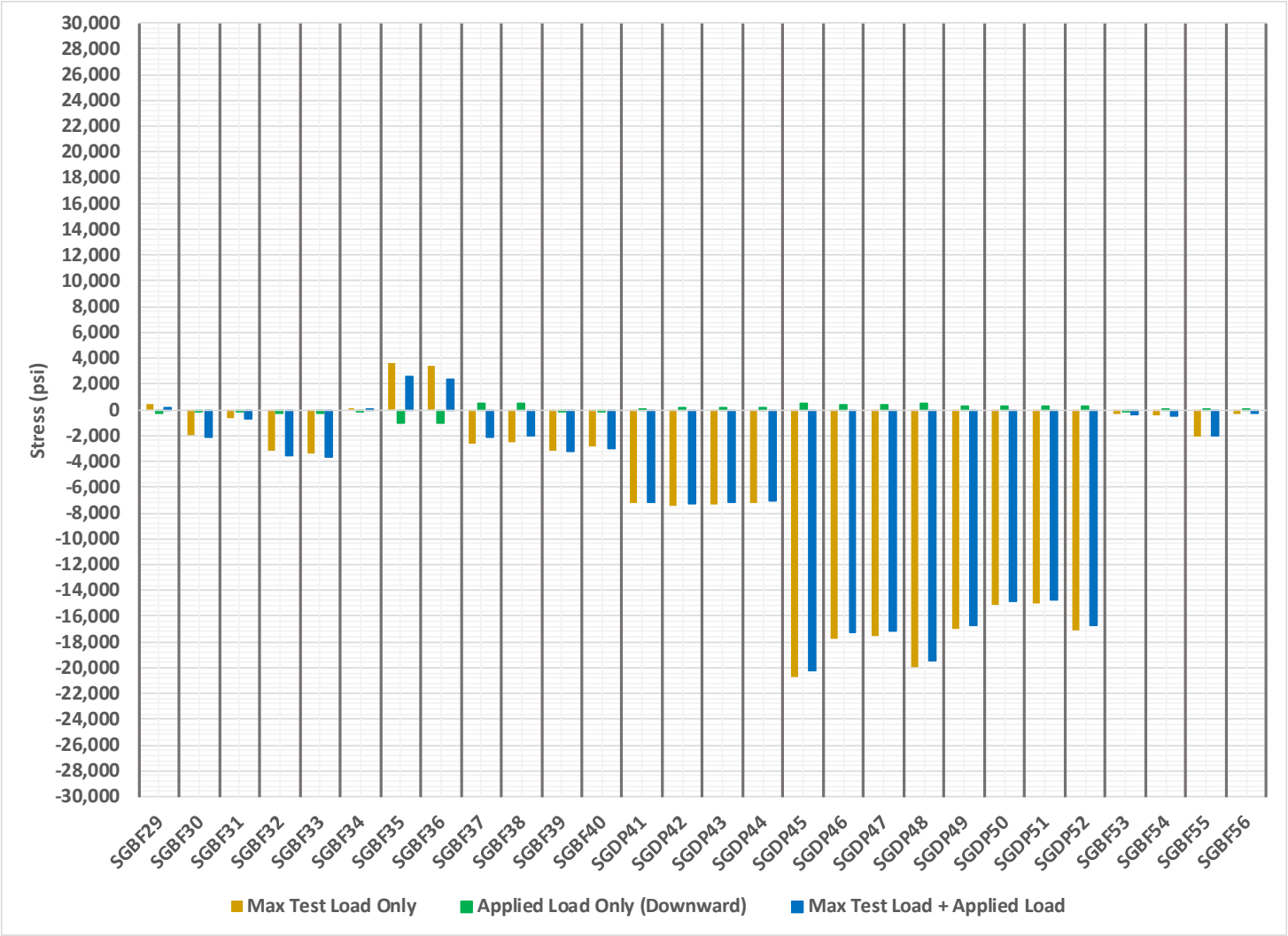


Figure 52. Stress from Downward Coupler Vertical Load Test (2 of 2)

Table 38. Vertical Coupler Force Test Locations with Total Tensile and Compressive Stresses

Channel Name	Approximate Location	Stress from Maximum test load (ksi)	Stress from Applied Load (ksi)	Total Stress (ksi)	Allowable Stress (ksi)	Total Stress as percent of Allowable
Downward Direction						
SGBF26	Center of LH side sill bottom flange, approx. 74 1/8 inches from B end body bolster toward center of car.	27	-0.58	26	72	36%
SGDP45	Top of deck plate, above LH side sill web, 66 3/8 inches from line across centermost edges of pin blocks toward center of car (directly above SBGF 26)	-21	0.47	-20	60	33%
Upward Direction						
SGBF26	Center of LH side sill bottom flange, approx. 74 1/8 inches from B end body bolster toward center of car.	27	0.31	27	72	38%
SGDP45	Top of deck plate, above LH side sill web, 66 3/8 inches from line across centermost edges of pin blocks toward center of car (directly above SBGF 26)	-21	-0.30	-21	60	35%

Table 39. Vertical Coupler Force Test Locations with Highest Stresses from Aplied Loads

Channel Name	Approximate Location	Stress from Maximum test load (ksi)	Stress from Applied Load(ksi)	Total Stress (ksi)	Allowable Stress (ksi)	Total Stress as percent of Allowable
Downward Direction						
SGBF35	RH side of bottom flange of center sill – 5 3/16 inches from B-end body bolster toward center of car - aligns with center sill web	3.7	-1.0	2.6	60	4%
SGBF36	LH side of bottom flange of center sill – 5 3/16 inches from B-end body bolster toward center of car - aligns with center sill web	3.4	-0.98	2.4	60	4%
Upward Direction						
SGBF7	RH side of bottom flange of center sill - 5 3/16 inches from A-end body bolster toward center of car - aligns with center sill web	2.3	0.89	3.2	60	5%
SGBF8	LH side of bottom flange of center sill - 5 3/16 inches from A-end body bolster toward center of car - aligns with center sill web	2.3	0.86	3.2	60	5%

8.4.5 Jacking

The jacking test is performed to verify a fully loaded car can be lifted free of the trucks when supported at the jacking pads. The test was conducted on October 10, 2019. Adam Klopp, TTCI Principal Investigator I, witnessed the jacking test as the AAR Observer, per Standard S-2043 requirements. The Atlas car met criteria for the jacking test. No permanent deformation was noted.

Figure 53 and Figure 54 show results of the jacking test. The highest total tensile stresses (SGBF15 – SGBF26) are primarily from the maximum test load and are slightly modified by the applied load from jacking. Similarly, the highest compressive stresses (SGDP45 – SGDP52) are in locations where the stresses from the applied load are relatively low.

Table 40 shows the jacking test locations with the highest total tensile and compressive stresses. The highest total tensile stress of 28 ksi (47 percent of allowable) was at SBGF26. The highest total compressive stress of -21 ksi (35 percent of allowable) was at SBGF45. No evidence of gradual zero-shift (plastic deformations) was noted.

Table 41 shows the jacking test locations with the highest stresses from applied loads. The highest stresses from the jacking load were seen for gauges SGBF37, SGBF38, SGBF39, and SGBF40. These gauges are located at the front and rear of the B truck, bottom flange of the body bolster near the center sill as shown in Figure 55. Appendix H has further details on the results from all locations.

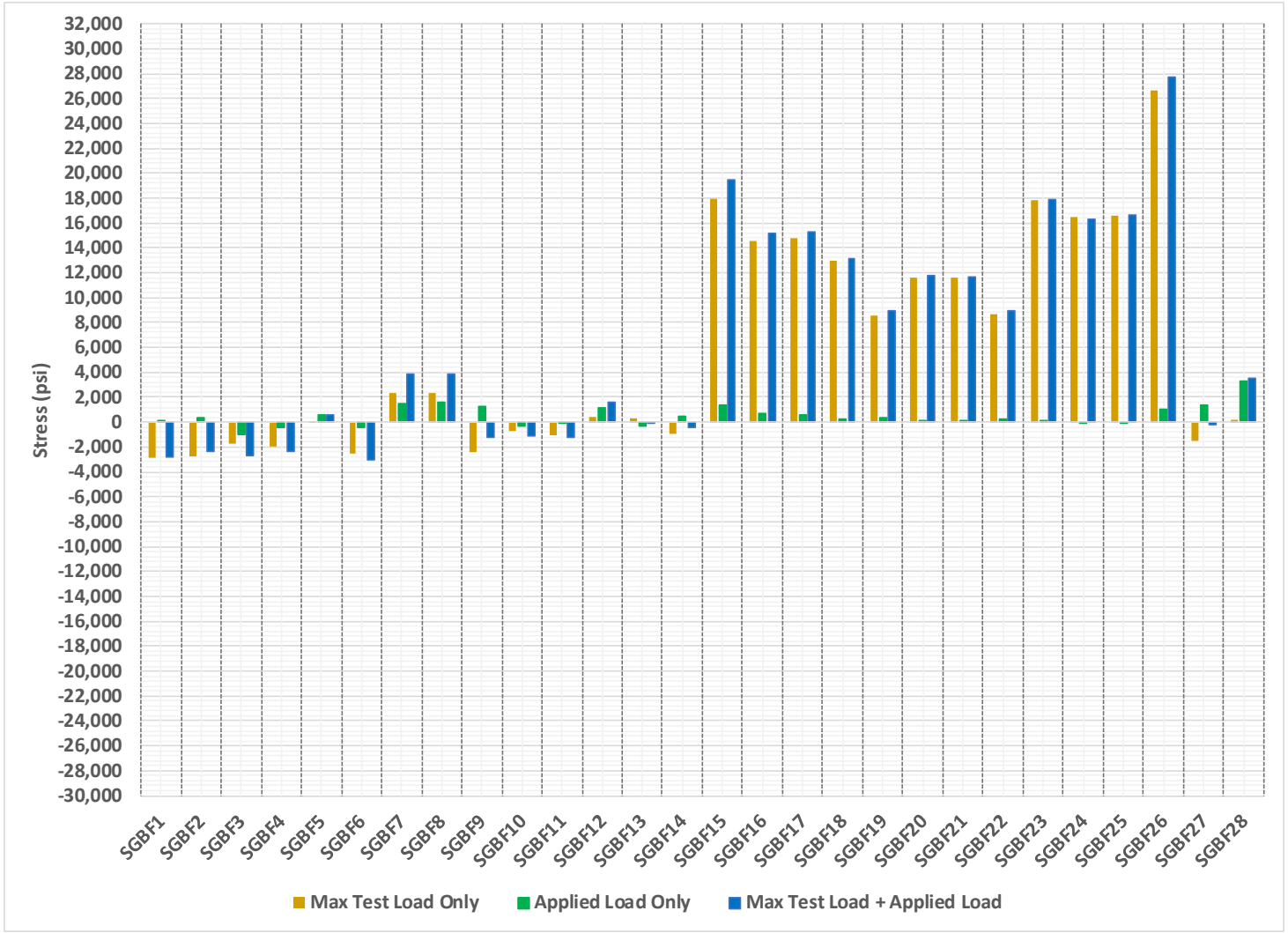


Figure 53. Stress from Jacking Test with Maximum Test Load (1 of 2)

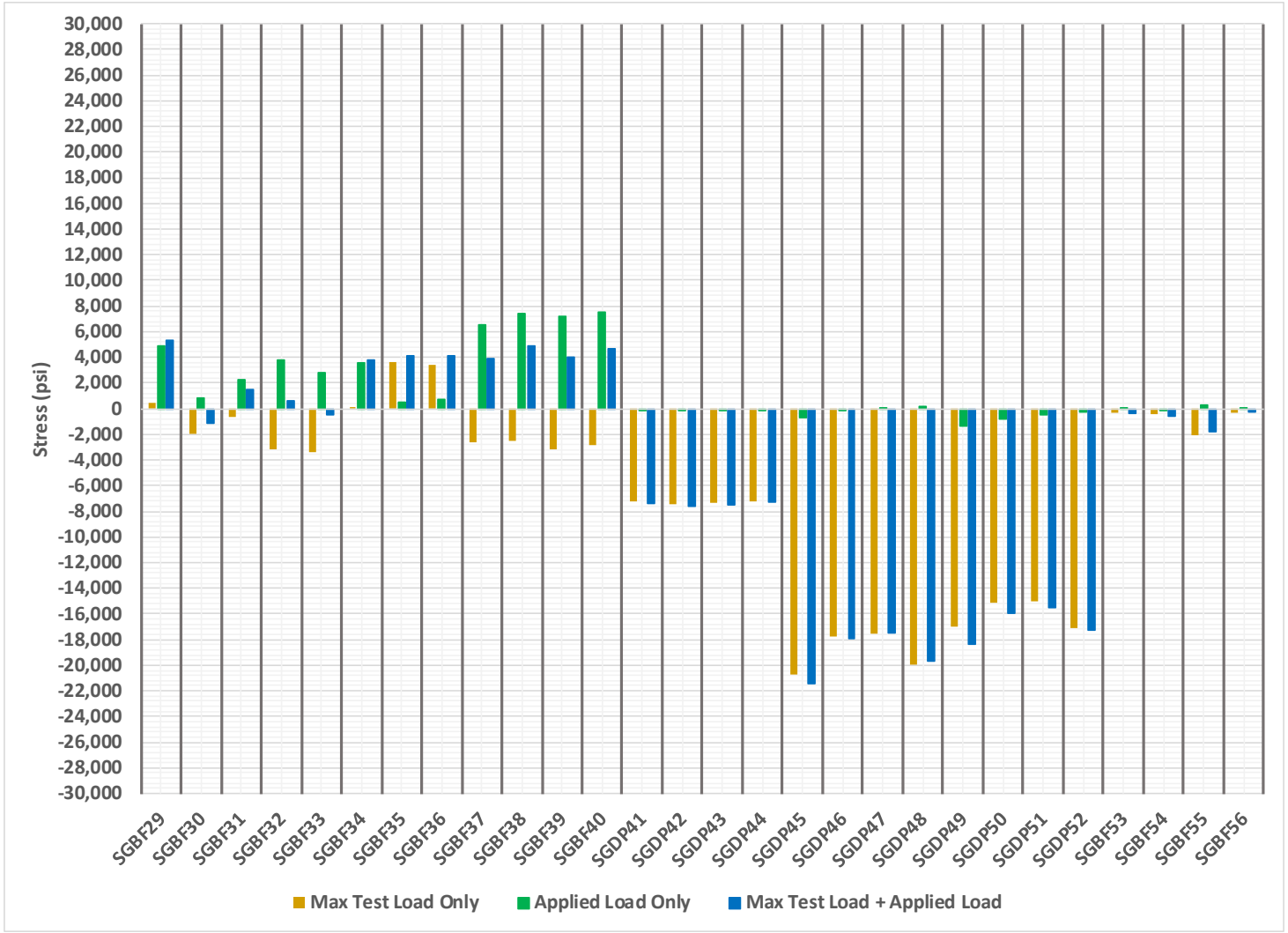


Figure 54. Stress from Jacking Test with maximum Test Load (2 of 2)

Table 40. Jacking Test Locations with Highest Total Tensile and Compressive Stresses

Channel Name	Approximate Location	Stress from Maximum test load (ksi)	Stress from Applied Load (ksi)	Total Stress (ksi)	Allowable Stress (ksi)	Total Stress as percent of Allowable
SGBF26	Center of LH side sill bottom flange, approx. 74 1/8 inches from B end body bolster toward center of car.	27	1.0	28	72	39%
SGDP45	Top of deck plate, above LH side sill web, 66 3/8 inches from line across centermost edges of pin blocks toward center of car (directly above SBGF 26)	-21	0.69	-21	60	35%

Table 41. Jacking Test Locations with the Highest Stresses from Applied Loads

Channel Name	Approximate Location	Stress from Maximum test load (ksi)	Stress from Applied Load (ksi)	Total Stress (ksi)	Allowable Stress (ksi)	Measured Stress as percent of Allowable
SGBF40	Bottom flange of B-end body bolster. On edge nearest B-end. 2 ¼ inches outboard of center sill bottom flange toward LH side of car.	-2.9	7.5	4.6	60	8%
SGBF38	Bottom flange of B-end body bolster. On edge nearest center of car. 2 ¼ inches outboard of center sill bottom flange toward LH side of car.	-2.5	7.4	4.9	60	8%
SGBF39	Bottom flange of B-end body bolster. On edge nearest B-end. 2 ¼ inches outboard of center sill bottom flange toward RH side of car.	-3.1	7.2	4.1	60	7%
SGBF37	Bottom flange of B-end body bolster. On edge nearest center of car. 2 ¼ inches outboard of center sill bottom flange toward RH side of car.	-2.6	6.5	3.9	60	7%

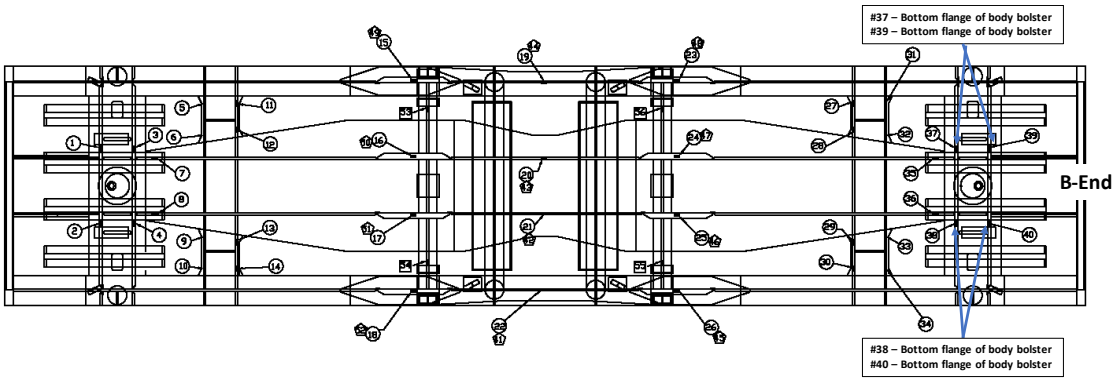


Figure 55. Jacking Test Locations with Highest Stresses from Applied Loads

8.4.6 Twist

The Twist Test consists of two parts. The first part, referred to in this document as the Suspension Twist Test is performed at the same time as the Carbody Twist Equalization Test described in Section 8.2.2. The test procedure is the same, with the additional requirement for the Suspension Twist Test that strain data be measured. It is required in the maximum test load condition only. The test was conducted in the maximum test load condition on October 8, 2019.

The second part is a structural Carbody Twist Test. The carbody is required to be supported at all four jacking pads and one corner will be allowed to drop 3 inches. The Carbody Twist Test was conducted in the maximum test load condition on October 11, 2019. Adam Klopp, Xinggao Shu, and Abe Meddah, TTCI Principal Investigators, witnessed the Suspension Twist Test and Car Body Twist Test as the AAR Observer, per Standard S-2043 requirements.

Standard S-2043 paragraph 4.1.1.5 says that the allowable design stress for twist load shall be 56% of the yield stress. For the grade 80 material this corresponds to 44.8 ksi and for the grade 60 material it corresponds to 33.6 ksi.

Suspension Twist Test

Figure 56 and Figure 57 show results from the Suspension Twist Test with the left-hand corner of the A-end lifted 3 inches. The complete results are provided in Appendix I.

Table 42 shows the highest total tensile and compression stresses from the Suspension Twist Test. The highest total tensile stress was 29 ksi (40 percent of allowable) at SGBF26 with the A-end, right-hand side raised 3 inches. Table 43 shows the highest stresses from the applied load during the Suspension Twist Test. No evidence of gradual zero-shift (plastic deformation) was noted.

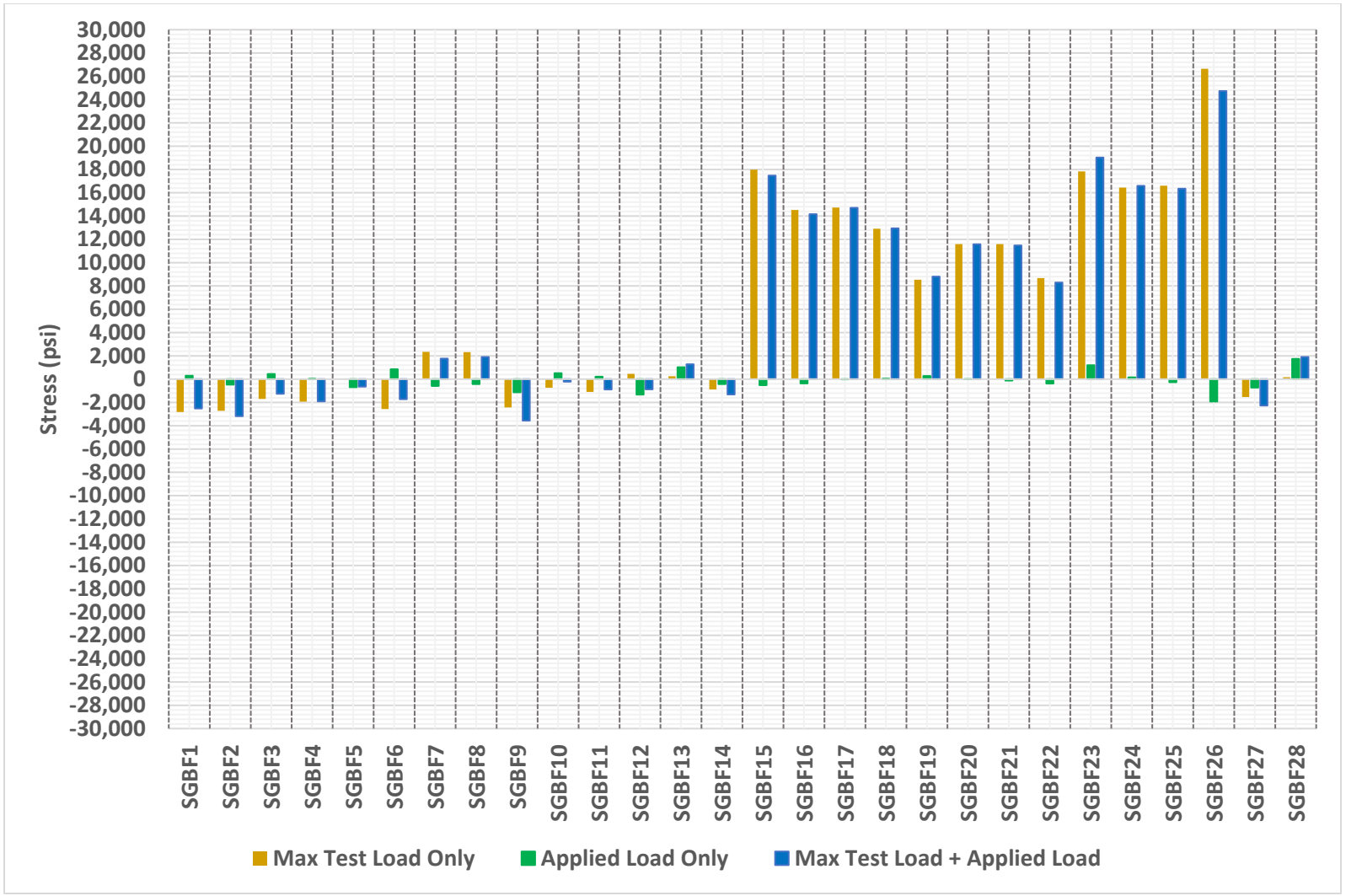


Figure 56. Stress from Suspension Twist Test, A-End LH Side (1 of 2)

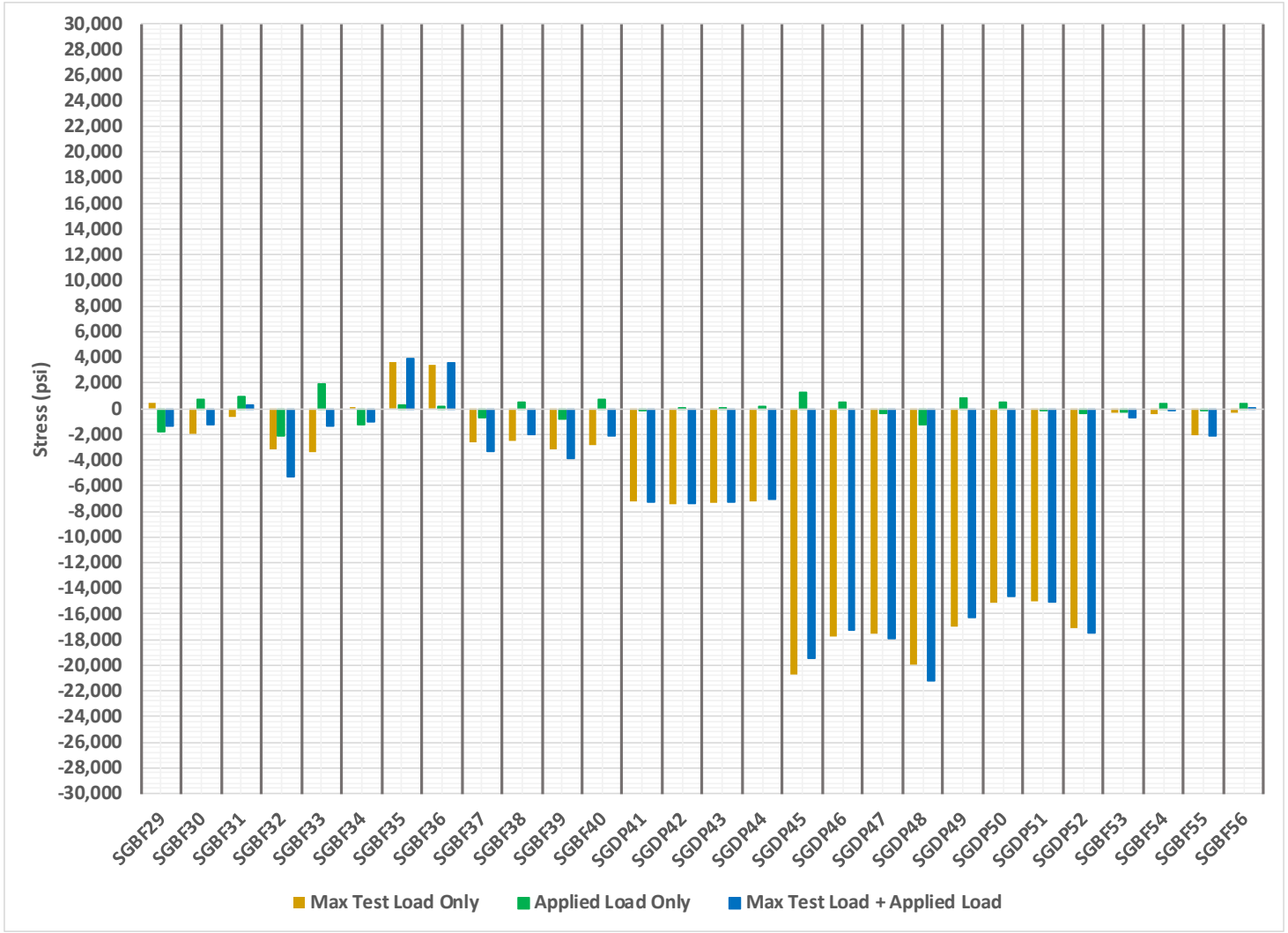


Figure 57. Stress from Suspension Twist Test, A-End LH Side (2 of 2)

Table 42. Highest Total Tensile and Compression Stresses from Suspension Twist Test

Channel Name	Approximate Location	Stress from Maximum test load (ksi)	Stress from Applied Load(ksi)	Total Stress (ksi)	Allowable Stress (56% of Yield, ksi)	Measured Stress as percent of Allowable
SGBF26 (A-end, RH Side)	Center of LH side sill bottom flange, approx. 74 1/8 inches from B end body bolster toward center of car.	27	1.8	29	44.8	65%
SGDP45 (A-End, RH Side)	Top of deck plate, above LH side sill web, 66 3/8 inches from line across centermost edges of pin blocks toward center of car (directly above SBGF 26)	-21	-1.4	-22	33.6	65%

Table 43. Highest Stresses from Applied Load during Suspension Twist Test

Channel Name	Approximate Location	Stress from Maximum test load (ksi)	Stress from Applied Load(ksi)	Total Stress (ksi)	Allowable Stress (56% of Yield, ksi)	Measured Stress as percent of Allowable
SGBF32 (A-End, RH Side)	Rear of bottom flange of cross bearer, 18 1/2 inches from B-end body bolster from center of car. 5 3/4 inches outboard of center sill, toward RH side.	-3.2	2.1	-1.1	33.6	3%
SGBF32 (A-End, LH Side)	Rear of bottom flange of cross bearer, 18 1/2 inches from B-end body bolster from center of car. 5 3/4 inches outboard of center sill, toward RH side.	-3.2	-2.1	-5.3	33.6	16%

Figure 58 shows the locations of the highest stress locations for Part 1 of the Twist Test.

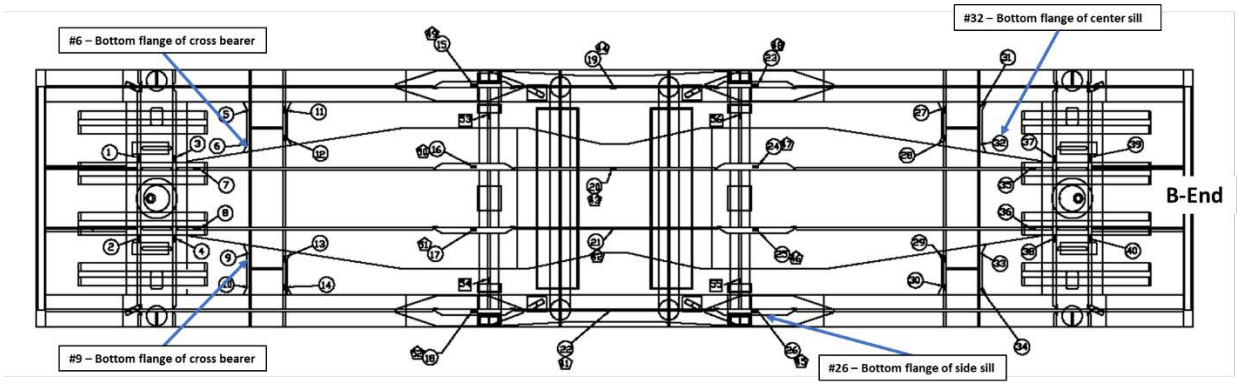


Figure 58. Maximum Stressed Gauges during Suspension Twist Test (Maximum Load Condition)

Carbody Twist Test

The Carbody Twist Test second portion of the Car Body Twist Test requires that the loaded carbody be supported on the four jacking locations. One corner is then lowered 3 inches. Figure 59 and Figure 60 presents the results summary for the Car Body Twist Test. Table 44 shows the highest total tensile and compression stresses from the Carbody Twist Test. The highest total tensile stress was 31 ksi (43 percent of allowable) at SGBF26. Table 45 present the highest stresses from the applied twist condition. No evidence of gradual zero-shift (plastic deformation) was noted.

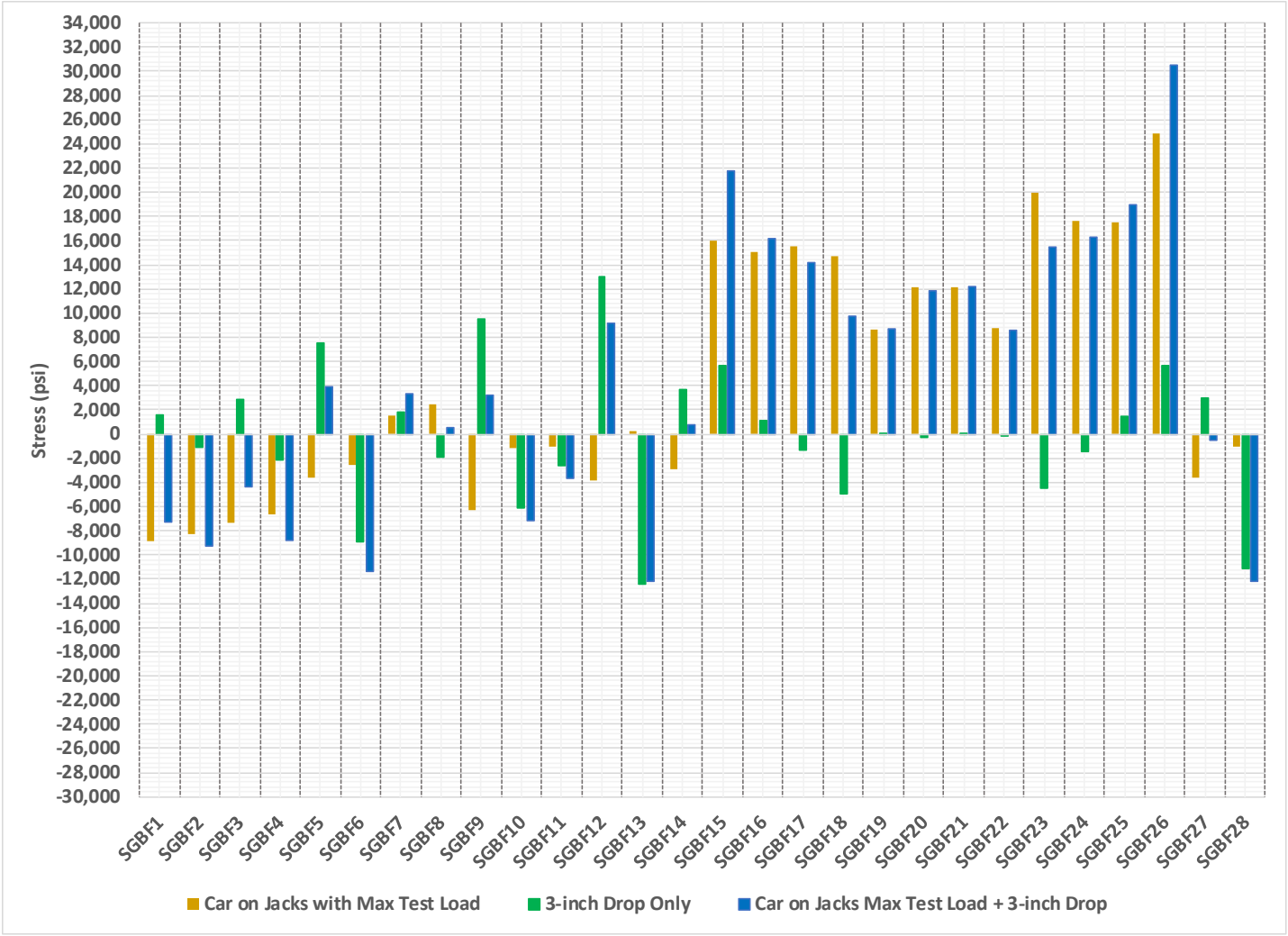


Figure 59. Stress from Carbody Twist Test, B-End RH Side (1 of 2)

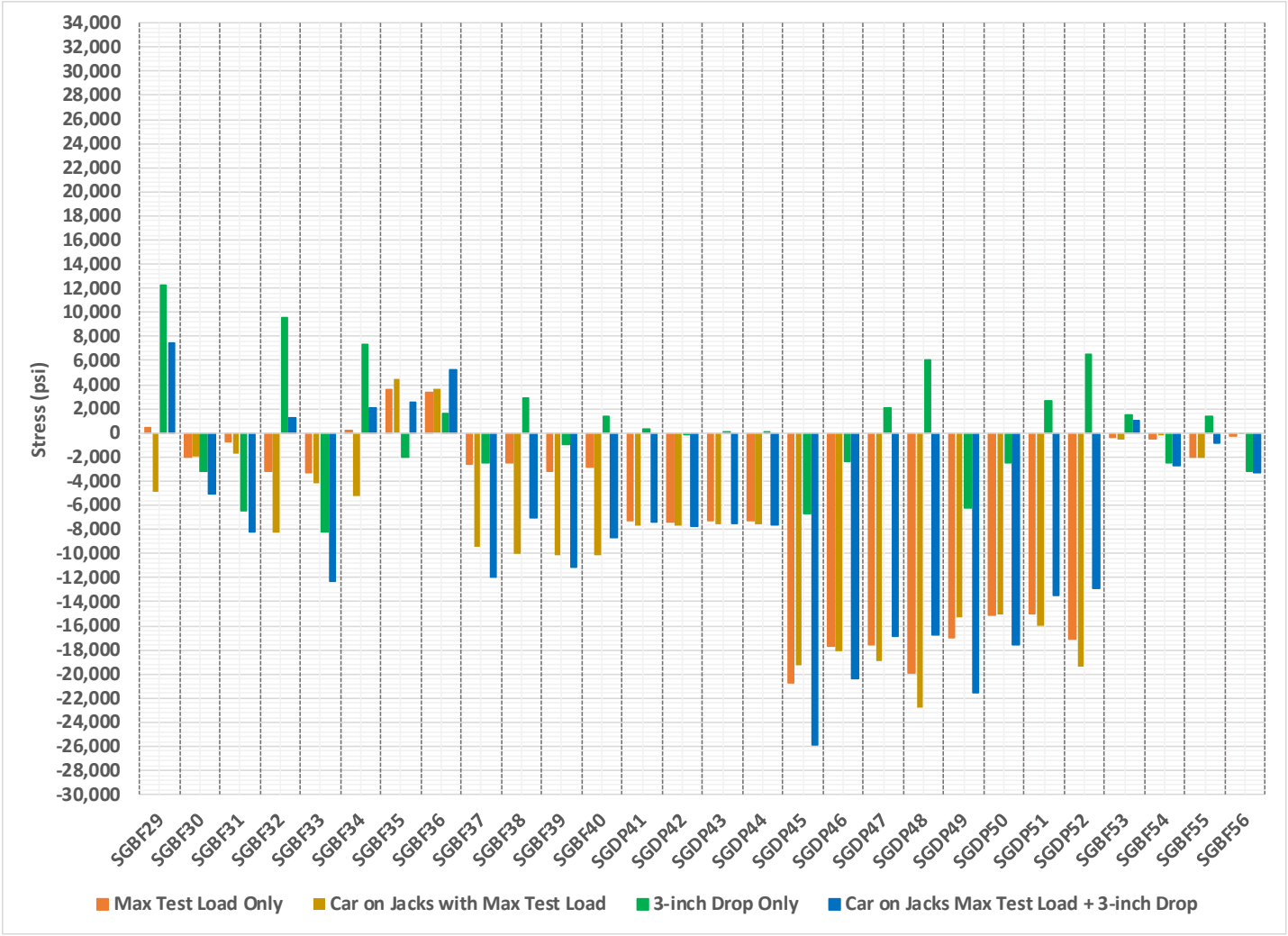


Figure 60. Stress from Carbody Twist Test, B-End RH Side (2 of 2)

Table 44. Highest Total Tensile and Compression Stresses from Carbody Twist Test

Channel Name	Approximate Location	Stress from Maximum test load (ksi)	Measured Stress with car on Jacks (ksi)	Stress from Applied Load(ksi)	Total Stress (ksi)	Allowable Stress (56% of Yield, ksi)	Measured Stress as percent of Allowable
SGBF26	Center of LH side sill bottom flange, approx. 74 1/8 inches from B end body bolster toward center of car.	27	25	5.7	31	44.8	69%
SGDP45	Top of deck plate, above LH side sill web, 66 3/8 inches from line across centermost edges of pin blocks toward center of car (directly above SBGF 26)	-21	-19	-6.7	-26	33.6	77%

Table 45. Highest Total Tensile and Compression Stresses from Applied Loads during Carbody Twist Test

Channel Name	Approximate Location	Stress from Maximum test load (ksi)	Measured Stress with car on Jacks (ksi)	Stress from Applied Load(ksi)	Total Stress (ksi)	Allowable Stress (56% of Yield, ksi)	Measured Stress as percent of Allowable
SGBF12	Rear of bottom flange of #4 cross bearer, RH side between center sill and side sill, near center sill	0.46	-3.8	13	9.2	33.6	27%
SGBF13	Rear of bottom flange of #4 cross bearer, LH side between center sill and side sill, near center sill	0.25	0.21	-12	-12	33.6	36%

Figure 61 shows the locations of the highest stress locations for Part 2 of the Twist Test.

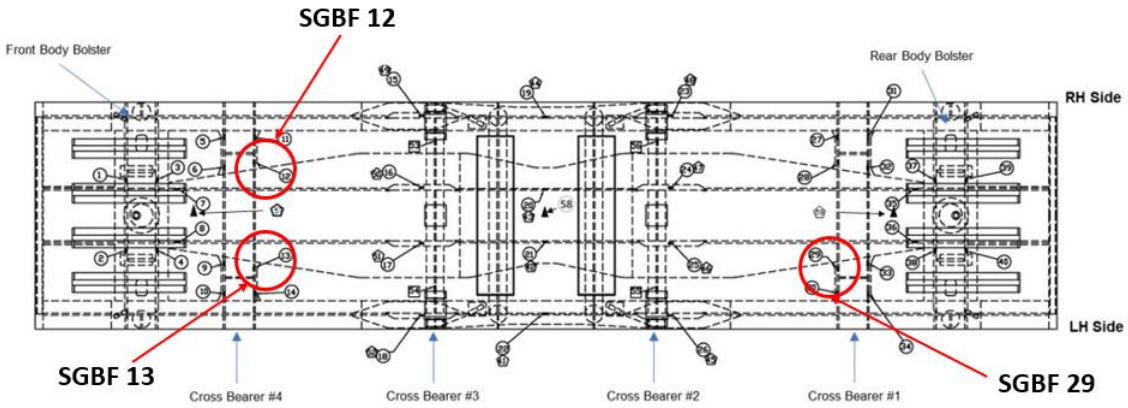


Figure 61. Stress Location with Highest Measured Strain during Carbody Twist Test

8.4.7 Impact

Impact tests were conducted on October 16, 2019. Adam Klopp, TTCI Principal Investigator I, witnessed the impact tests as the AAR Observer, per Standard S-2043 requirements.

The test was conducted by pulling the car up a constant grade a specified distance and allowing it to roll into a standing string of three loaded hopper cars equipped with M-901E draft gear. No brakes except for the handbrake on the last car were applied on the anvil string. There was no free slack between anvil cars, but the draft gears were not compressed. Figure 62 shows a partial view of the setup.



Figure 62. Atlas Car Impact Test Setup

The lead hopper had an instrumented coupler installed to measure the force during coupling. The speed was measured with a tachometer on one axle of the Atlas car. Nominal test speeds were 2 mph, 4 mph, and 6 mph. All strain gauges were monitored and recorded during the tests. The data from all strain gauges are provided in Appendix J. Table 46 shows the measured speed and coupler load for the Atlas Car Maximum Test Load Impact Test. The criteria were met and there was no permanent deformation of the car. The coupling forces did not exceed 1.25 million pounds at speeds of 6 mph or less.

Table 46. Atlas Car Impact Test Results

Run	Speed (mph)	Coupler Load (kips)
1	3.1	175
2	3.9	207
3	5.7	735

Figure 63 and Figure 64 present the results summary for the impact test at 6 mph. Table 47 shows the highest total tensile and compression stresses from the 6-mph impact test. The highest total tensile stress was 20 ksi (28 percent of allowable) at SGBF26. Table 48 presents the highest stresses from the 6-mph impact test. No evidence of zero-shift (plastic deformation) was noted.

Standard S-2043 paragraph 4.1.5.9 Allowable Stresses states “All conditions resulting from live and dead loads in combination with impact loads shall follow the guidelines in MSRP Section C Part II, Specification M-1001, paragraph 4.2.2.6.” Paragraph 4.2.2.6 states that “such loading may develop the ultimate load carrying capacity of the member being investigated.” Because of this TTCI used the ultimate stress as the allowable stress for impact tests.

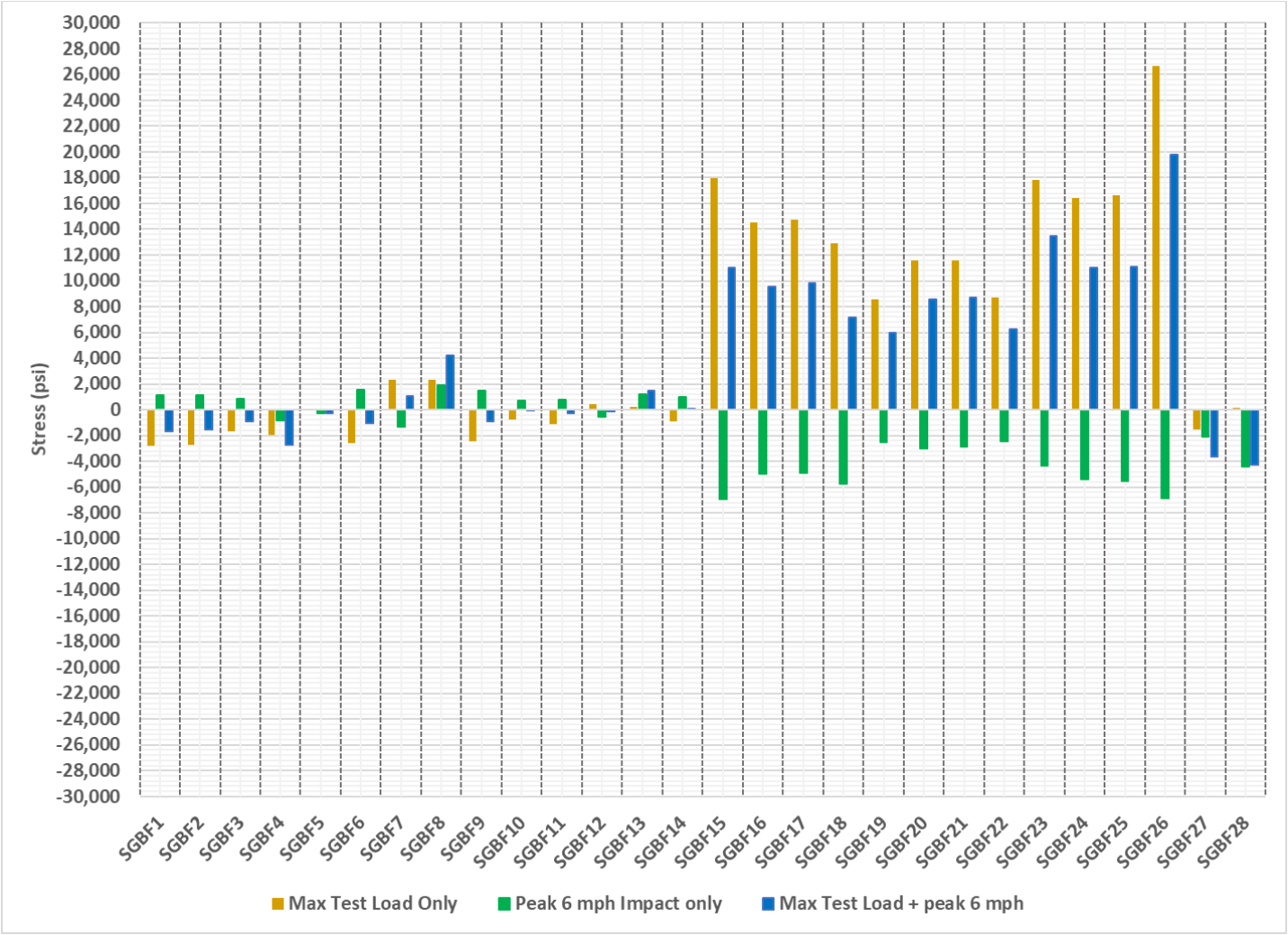


Figure 63. Stress from Impact Test, 6 mph run (1 of 2)

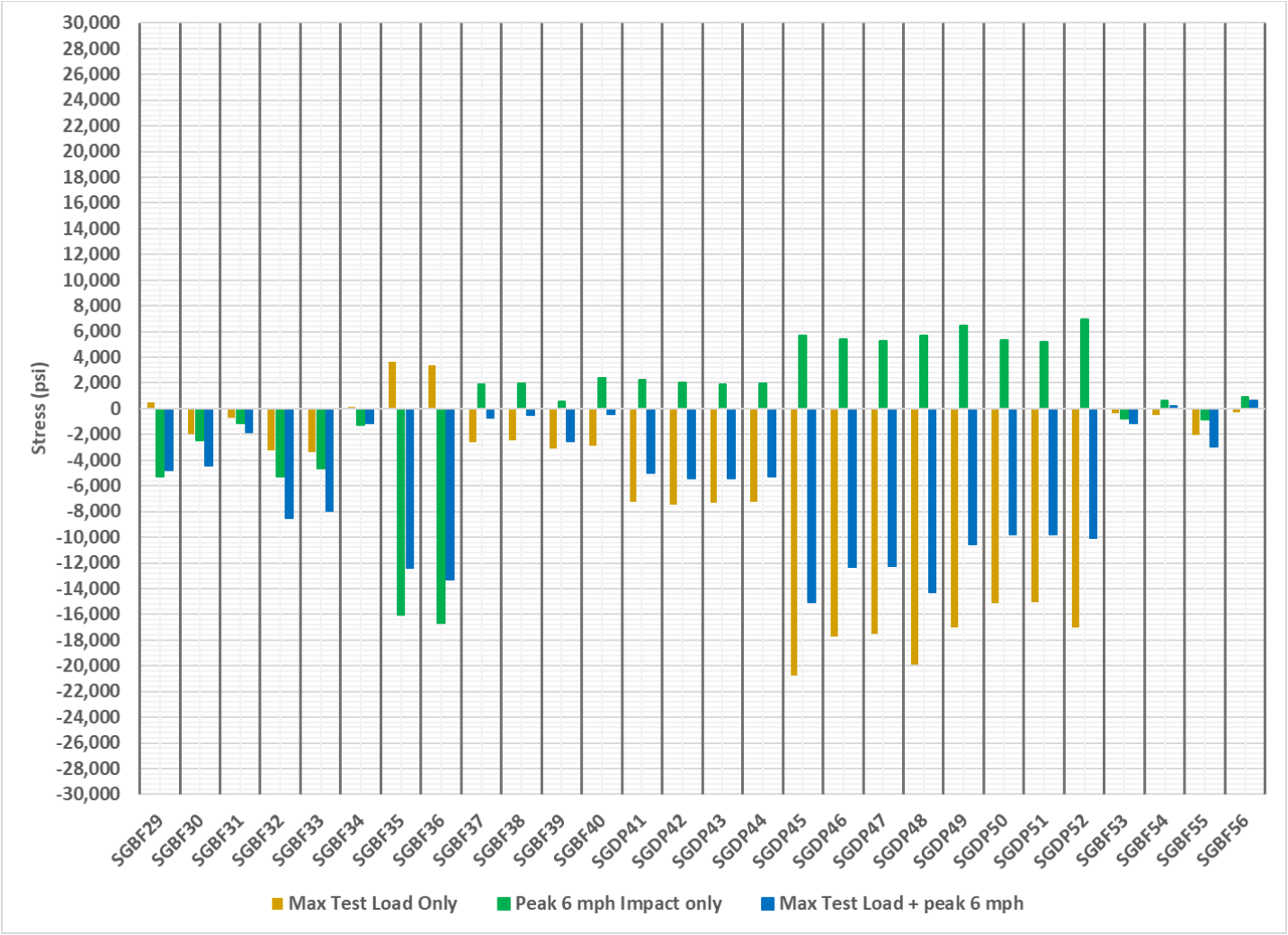


Figure 64. Stress from Impact Test, 6 mph run (2 of 2)

Table 47. Highest Total Tensile and Compression Stresses from 6-mph Impact Test

Channel Name	Approximate Location	Stress from Maximum test load (ksi)	Stress from Applied Load(ksi)	Total Stress (ksi)	Allowable Stress (ksi)	Measured Stress as percent of Allowable
SGBF26 (A-end, RH Side)	Center of LH side sill bottom flange, approx. 74 1/8 inches from B end body bolster toward center of car.	27	-7	20	90	22%
SGDP45 (A-End, RH Side)	Top of deck plate, above LH side sill web, 66 3/8 inches from line across centermost edges of pin blocks toward center of car (directly above SBGF 26)	-21	6	-15	75	20%

Table 48. Highest Stresses from Applied Load during 6-mph Impact Test

Channel Name	Approximate Location	Stress from Maximum test load (ksi)	Stress from Applied Load(ksi)	Total Stress (ksi)	Allowable Stress (ksi)	Measured Stress as percent of Allowable
SGDP52 (A-End, LH Side)	Top of deck plate, above RH center sill web, approx. 2 inches forward of #3 cross bearer	-17	7	10	75	13%
SGBF36 (B-End, LH Side)	LH side of bottom flange of center sill - forward of rear body bolster - aligns with center sill web and end stop mount block pin hole	4	-17	-13	75	17%

8.4.8 Securement System Analysis

Standard S-2043, Paragraph 5.4.7 requires verification of securement system strength. This verification was done by inspection and analysis. For the purpose of these results, the securement system is defined as the cradle attachment fittings (including shear blocks), pins, and welds to the deck of the railcar, as shown in Figure 65. Cradles, end stops, or the deck structure itself are not included within the securement system analysis.

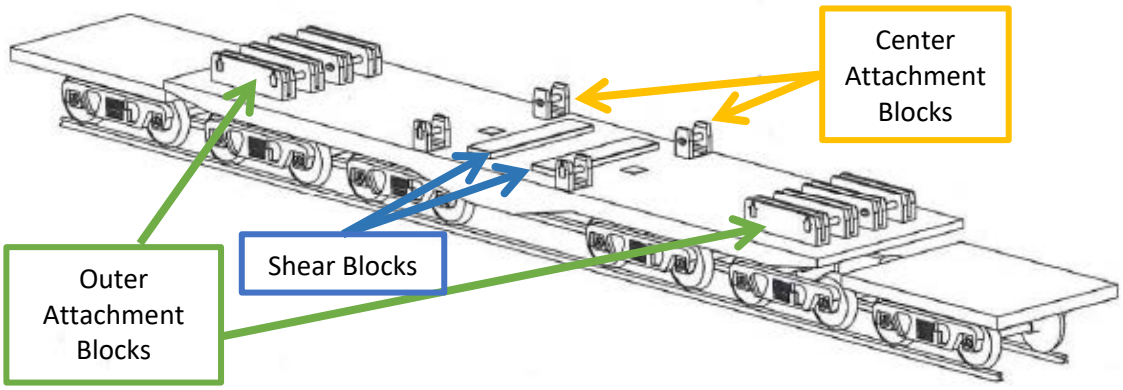


Figure 65. Securement System Layout

8.4.8.1 Dimensional Inspection

The cradle attachment fitting dimensions are of critical importance for the proper mounting of the and function of cask securement. The railcar securement system mounts were measured to determine any variation from the design drawings that could impact the function of the mounting system. The cradle attachment points are fabricated from steel plate and welded to the deck in various locations to allow for the loading of different families of casks, such as what is depicted in Figure 66.



Figure 66. Cask installation in securement mounts

Kasgro supplied TTCI with drawings for the securement system, including the weldments and their overall layout relative to the car deck. TTCI personal performed dimensional checks of the various mounts with standard tape measures, steel rulers, various squares, calipers, etc. These measurements were checked against the manufacturer's drawing dimensions and related tolerances. In many cases, performing the exact measurements listed in the drawings was not possible (such as when the carbody centerline was the reference dimension, and where it was not practicably measured), and several relative measurements had to be combined to make a relevant comparison to the drawing.

TTCI personnel found the dimensions of the Atlas railcar to be more accurate than the construction tolerances of a typical railcar. At no time during the testing of the Atlas railcar did TTCI personnel have difficulty mounting or removing the simulated cask loads due to securement system dimensional accuracy. With few exceptions, the dimensions of the securement system were found to be within the dimensions listed in the drawing, most commonly +/-0.125 inch. The space between the Outer Attachment Block pair faces did fall outside of the expected value (e.g., the design was 3.0 inches and the as-build was 3.25 inches). This change did increase the realized stresses in the retainment pin by increasing the bending moment, and this information is presented in Section 8.4.8.5, Component Stress Analysis.

Overall, however, dimensional relations between the simulated cask (test loads) and the securement system allowed for the proper function, as illustrated in Figure 67.

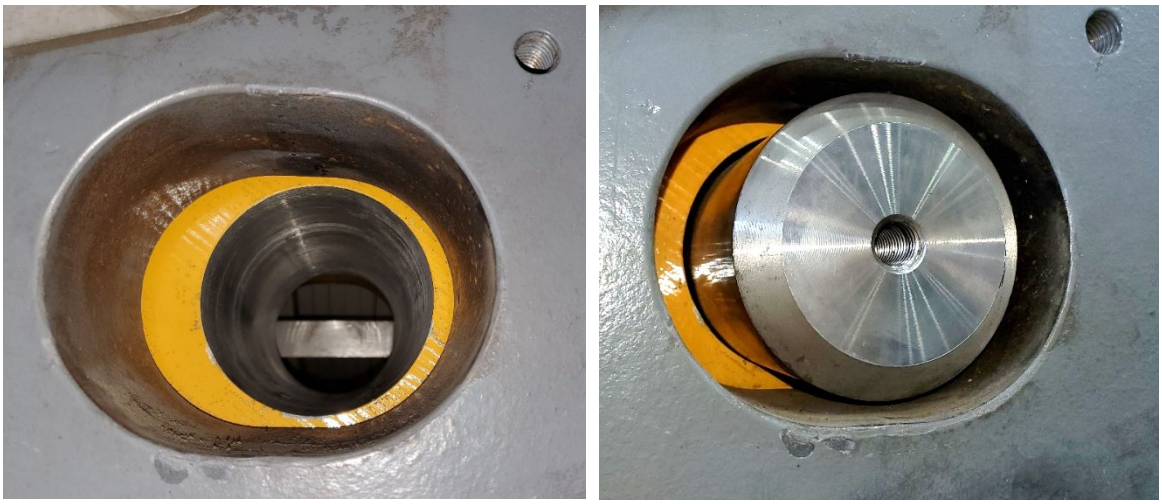


Figure 67. Typical alignment of cask and securement mounts, shown with and without retainment pin.

8.4.8.2 Force Calculations

Load calculations for the securement system were performed for the heaviest cask-cradle in Family 1 (HI-STAR 190 XL), and the heaviest cask-cradle in Families 2, 3, and 4 (MAGNATRAN). The main difference between Family 1 and Families 2, 3, and 4 was the handling of the longitudinal load. Family 1 used end stops to restrain the longitudinal load while Families 2 through 4 used a shear key in the middle of the car.

The securement system is required to support the following dynamic factors per Rule 88:

- Vertical load: 2g
- Lateral load: 2g
- Longitudinal load: 7.5g

Each load is to be applied separately. An additional factor of 1.1 was applied to the result of the force calculations to match Kasgro's and Orano's assumptions. The resulting factored loads were then used for the stress analysis.

Figure 68 shows the pin locations for reference.

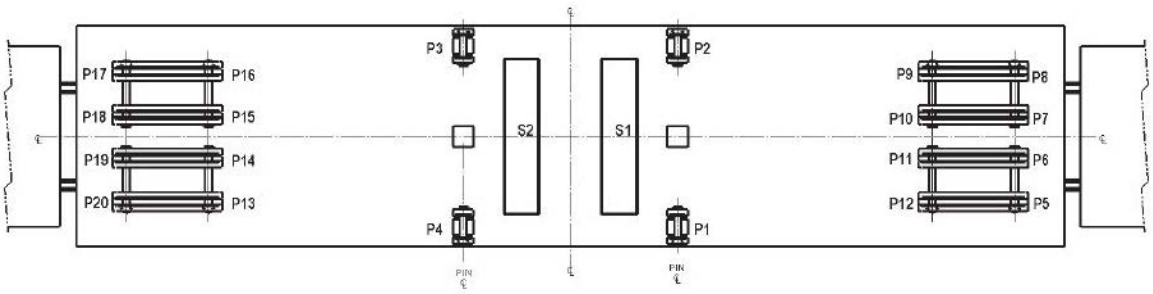


Figure 68. Pin Designations

The following assumptions were made throughout the force calculations:

- For both families, the vertical load is reacted at pins 1 to 4.
- For both families, the lateral load is supported at pins 2 and 3 only.
- For Family 1, the longitudinal load is reacted at the inboard pins of the end stop (pins 9 to 12).
- For Family 2, the longitudinal load is reacted at the shear block S1.
- Because of the offset between the CG location and the reaction forces, both lateral and longitudinal loads create moments that are reacted with vertical forces at the pin blocks.

Table 49 and Table 50 show the results for the load calculations for Families 1 and 2.

Table 49. Family 1 (HI-STAR 190 XL) Force Calculation Results, Including 1.1 Load Factor

Direction	Reaction (Kips)	Location	Accompanying Vertical Reaction	Location of Vertical Reaction
Vertical	174.15	3,4	None	n/a
	305.2	1, 2	None	n/a
Lateral	348.24	3	207.69	3, 4
	610.4	2	364.37	1, 2
Longitudinal	944.15	9-12	1052.14	5-12

Family 2 required additional calculations due to a minimum and maximum axial distance of the combined cask-cradle CG from rear pins 3 and 4.

Table 50. Family 2 (MAGNATRAN) Force Calculation Results

Cask Axial Position	Direction	Reaction (kips)	Location	Vertical Reaction (kips)	Location of Vertical Reaction
Minimum axial CG location	Vertical	177.57	1,2	None	n/a
		211.83	3,4	None	n/a
	Lateral	355.13	2	191.92	1,2
		423.67	3	228.96	3,4
Maximum axial CG location	Vertical	202.49	1,2	None	n/a
		186.91	3,4	None	n/a
	Lateral	404.98	2	218.87	1,2
		373.82	3	202	3,4
Unaffected by Axial position	Longitudinal	2920.5	Shear block	685.62	1-4

An analysis of Table 49 and Table 50 dictates the bounding loads to be used during the stress analysis. Table 51 shows the bounding loads to be used for the stress analysis as well as the values presented by Orano (CALC-3015276, rev 4, page 10). The differences in bounding loads calculated by Orano and TTCI are largely due to rounding differences.

Table 51. Bounding Loads

Component	Load Case Direction	TTCI Calculation (kips)	Orano Calculation (kips)	Percent Difference
Highest Loaded Center Block Pin	Vertical (2 g × 1.1)	686 vertical	730 vertical	6%
	Lateral (2 g × 1.1)	610 lateral on block only 364 vertical	611 lateral on block only 312 vertical	16% on vertical
Shear Block	Longitudinal (7.5 g × 1.1)	2921 longitudinal	2921 longitudinal	0
Highest Loaded Outer Block Pin	Longitudinal (7.5 g × 1.1)	944 longitudinal 1052 vertical	944 longitudinal 1077 vertical	2% on vertical

8.4.8.3 Stress Analysis

The stress analysis considers the following materials and their corresponding properties. The pin blocks are made from ASTM A572, grade 50 steel. The pins are made from ASTM A564, type 630, condition H1025 stainless steel. Table 52 shows the minimum material properties as well as the actual material properties for the materials used on the prototype car from document DW-19-007 Mill Test Reports. The stress analysis uses the minimum material properties as a conservative approach.

Table 52. Material Properties

Material	Yield Strength (ksi)		Ultimate Strength (ksi)	
	Minimum	Mill Test	Minimum	Mill Test
ASTM A572, Grade 50	50	57	65	86
ASTM A564, Type 630, Condition H1025	145	158	155	169

8.4.8.4 Allowable Stresses, Acceptance Criteria, and Margin of Safety

This analysis considers the allowable stress in agreement with MSRP C-II, M-1001, 4.2.2.4 "the allowable design stress shall be the yield or 80% of ultimate, whichever is lower." The allowable stresses considered in this report are as follows:

- ASTM A572, Grade 50
  - Allowable Tensile Stress: 50 Ksi
  - Allowable Shear Stress: 29 Ksi
- ASTM A564, Type 630, Condition H1025
  - Allowable Tensile Stress: 124 Ksi (80% of 155 ksi ultimate stress)
  - Allowable Shear Stress: 83 Ksi (57% of 145 ksi yield stress)

The selected failure theory is the Equivalent von Mises Stress Theory. This theory is used whenever stress components acting simultaneously need to be combined and is preferred over the Tresca failure theory as the von Mises theory has been shown to have a better correlation with experimental data in ductile materials such as steel.[7] Then, the equivalent von Mises Stress is compared against the Yield Strength of the material. The following equation is used to calculate the von Mises Stress:

$$\sigma_{VM} = \sqrt{\sigma_x^2 + 3\tau_{xy}^2}$$

Where:

σ_x is the normal component of stress

τ_{xy} is the shear component of stress, at a single location on the pin

Finally, the Margin of Safety (MS) is calculated as

$$MS = \frac{Allowable\ Stress}{Actual\ Stress} - 1 \geq 0$$

When a stress combination is performed, the Margin of Safety is calculated for the resultant combined stress only.

8.4.8.5 Component Stress Analysis

The stress analysis is performed for the following components under the bounding vertical, lateral, and longitudinal loads shown previously in Table 51.

- Center Attachment Blocks for Pins 1-4
- Shear Blocks, S1 and S2
- Outer Attachment Blocks for Pins 5-20
- Pins

The following tables show the results of the stress analysis for the different components under the different loads they are exposed to. The central, shear, and outer blocks all have a margin of safety greater than zero.

Table 53. Central Block Under Vertical Load

Stress Component	Value (Ksi)	MS
Tensile	14.28	+2.5
Shear Tear-out	12.41	+1.42

Table 54. Central Block Under Lateral Load

Stress Component	Value (Ksi)	MS
Direct Shear	13.2	n/a*
Tensile Stress	3.93	n/a*
Bending Stress	26.3	n/a*
Total Normal Stress	30.23	n/a*
Von Mises Stress	37.9	+0.32

Table 55. Shear Block Under Longitudinal Load

Stress Component	Value (Ksi)	MS
Direct Shear	1.55	+18.34

Table 56. Outer Block Under Longitudinal Load

Stress Component	Value (Ksi)	MS
Normal Vertical Stress	15.99	n/a*
Normal Longitudinal Stress	17.27	n/a*
Total Normal Stress	23.54	+1.13
Shear Tear-out	17.82	+0.63

*Margin of Safety is calculated for the resultant combined stress only.

TTCI performed hand calculations to determine the stress in the Central Block pins and Outer Block pins. These were carried out by assuming the pin is a beam member with a uniform load along the center portion and reaction loads at the end of the pin that are linearly variable distributed loads. Contact stresses were neglected. These assumptions are depicted in Figure 69. The analyzed configurations for both the central and outer pins are shown in Figure 70 and Figure 71.

Table 57 shows the results of the stress calculations for both pin types (Outer Block and Central Block). These analytical calculations showed that the maximum stress in both pin types was well above the allowable amount, where the magnitudes the of maximum bending stress and von Mises stress are equal because they occur within the area of uniform distributed load where the shear load is a minimum. Loading and stress calculations were also performed by Orano, and Table 58 shows the result comparison between the TTCI and Orano calculations.

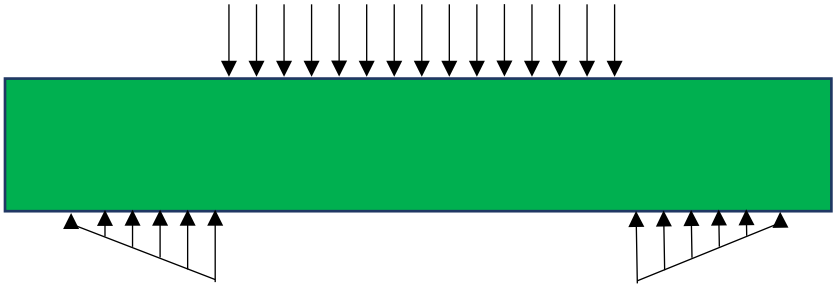


Figure 69. General Pin Loading Assumption

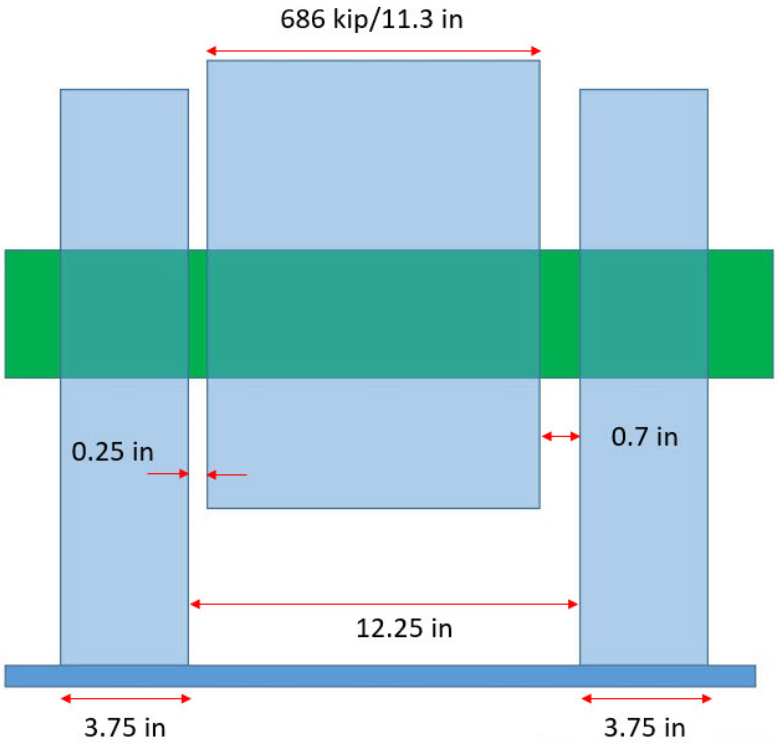


Figure 70. Central Pin (Pins 1-4) Loading Schematic

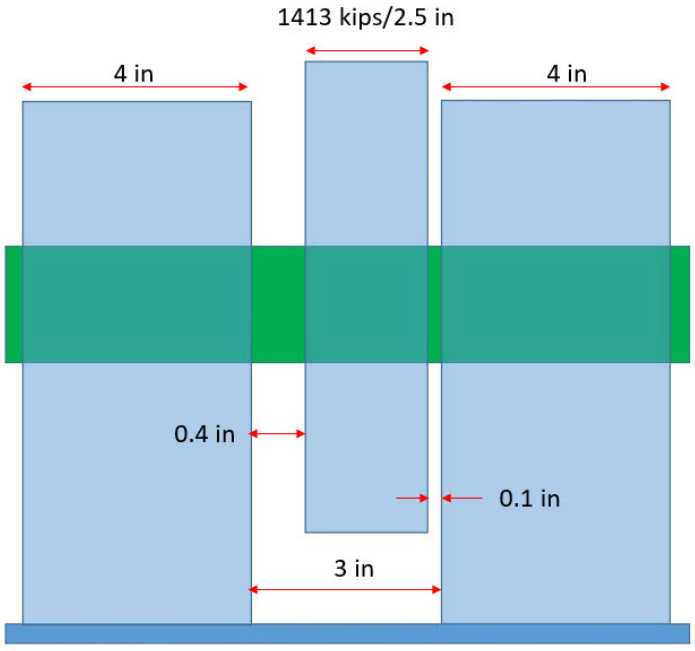


Figure 71. Outer Pin (Pins 5-20) Loading Schematic. Note that 3" dimension shown here was updated to 3.25" for subsequent analysis, based on as-built dimensions of the tested car, IDOX 010001.

Table 57. Pins Stress Analysis Results (Hand Calculations)

Pin Location	Mean Shear Stress (Ksi)	Bending Stress (Ksi)	von Mises Stress (Ksi)	Allowable Stress (Ksi)
Central Block	28.14	248.25	248.25	124
Outer Block	59.24	247	247*	124

* The magnitudes the of maximum bending stress and von Mises stress are equal because they occur within the area of uniform distributed load where the shear load is a minimum. The highest shear stress occurs at a different location.

Table 58. Pin Stress Results Comparison

Pin Location	Shear Stress (Ksi) (TTCI)	Shear Stress (Ksi) (ORANO)	Bending Stress (Ksi) (TTCI)	Bending Stress (Ksi) (ORANO)	von Mises (Ksi) (TTCI)	von Mises (Ksi) (ORANO)	Allowable Stress (Ksi)
Central Block	28.14	30.1	248.25	41	248.25	66.3	124
Outer Block	59.24	70.1	247	66.4	247	138.4	124

The difference in results is a consequence of the loading assumptions. Orano's loading assumption used point loads at the edges of the blocks. TTCI assumed the loads were distributed as described above. Because of concerns that the distributed load assumption was too conservative, TTCI decided to create an FEA model where the loading and reaction assumptions shown above do not play a role in the numerical analysis. The model included actual material properties of both pin and the block components obtained from a series of tensile tests. Figures 72 and 73 show the results from such a test on each material. A bi-linear model was selected for both the pin and the block components leading to a non-linear FEA.

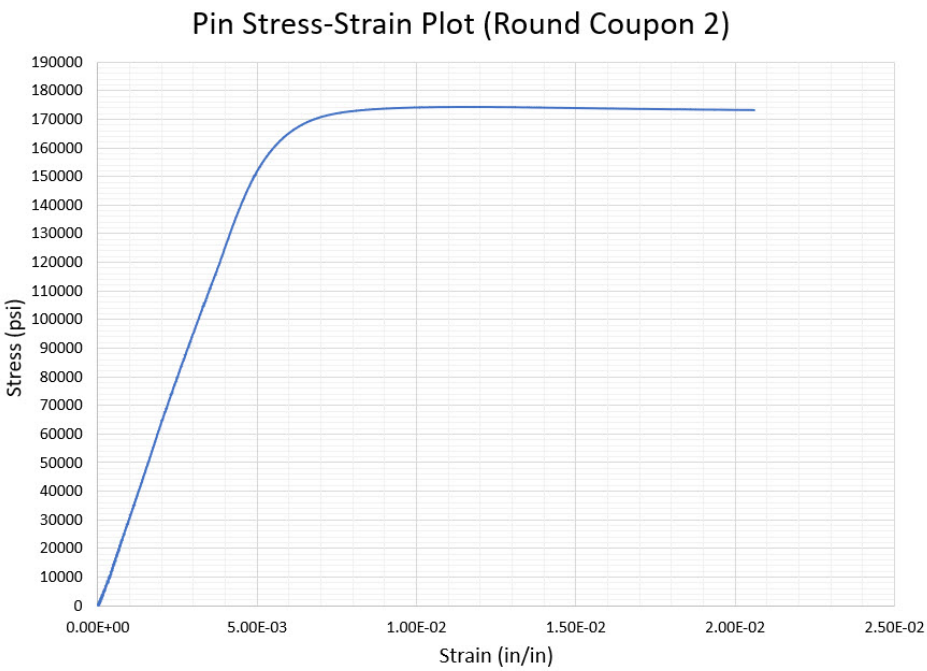


Figure 72: Tensile Test Results for Pin Material

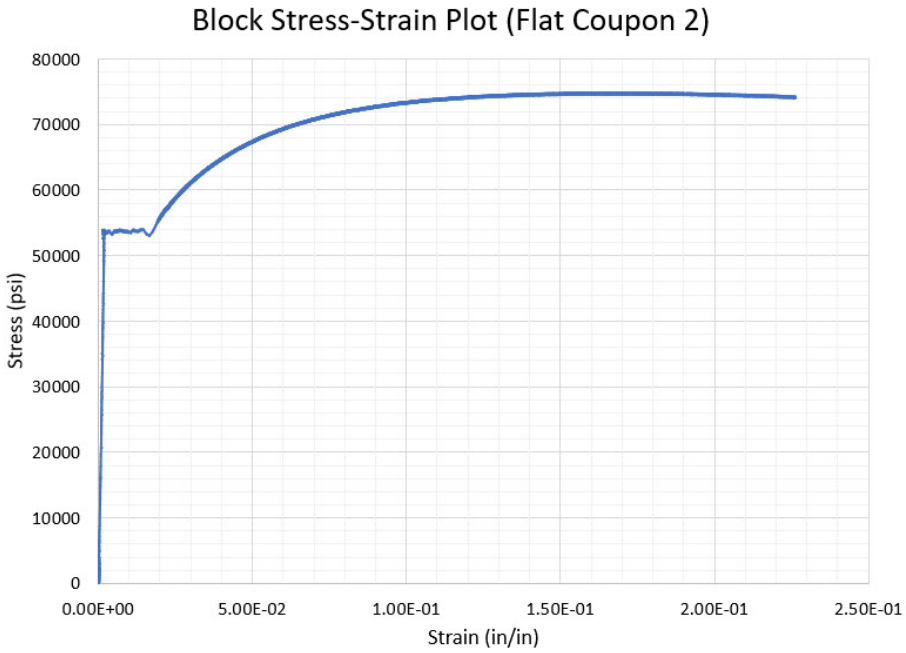


Figure 73. Tensile Test Results for Block Material

Table 60 shows the material properties included in the model

Table 59. Material Properties

Property	Pin	Block
Modulus of Elasticity (psi)	31.8e6	30e6
Yield Stress (ksi)	171.8	54.5
Tangent Modulus (ksi)	61.4	177.2
Ultimate Stress (ksi)	174.56	75.23
Ultimate Strain (%)	2	23

The numerical analysis was carried out for the outer and central positions. Figure 74 through Figure 77 show the model representation for each one of these positions. The model of the outer blocks includes only a short length of the block, long enough to distribute the pin loads to a low stress field where the block is restrained.

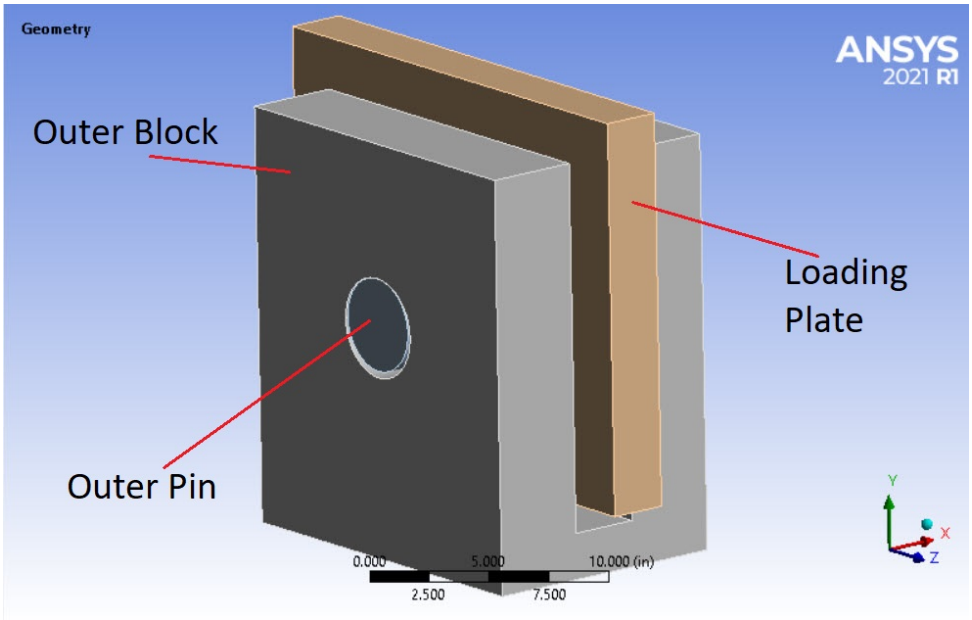


Figure 74. Outer Location Model

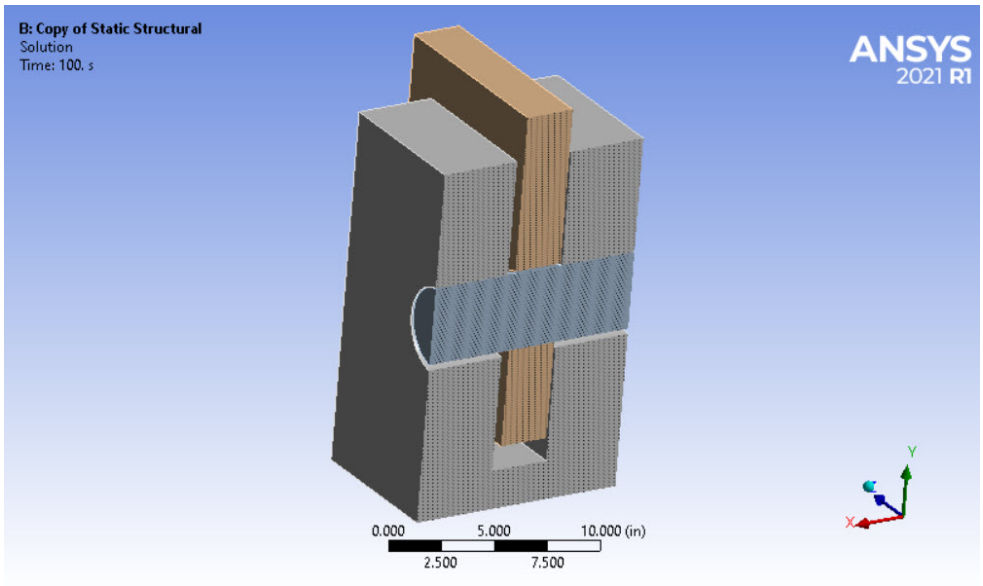


Figure 75. Outer Location Cross Section

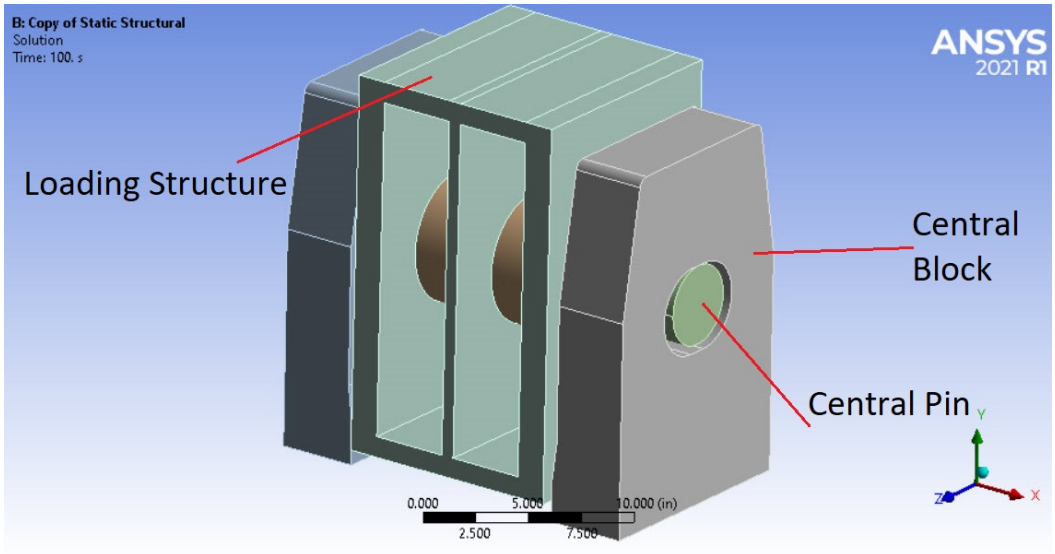


Figure 76. Central Location Model

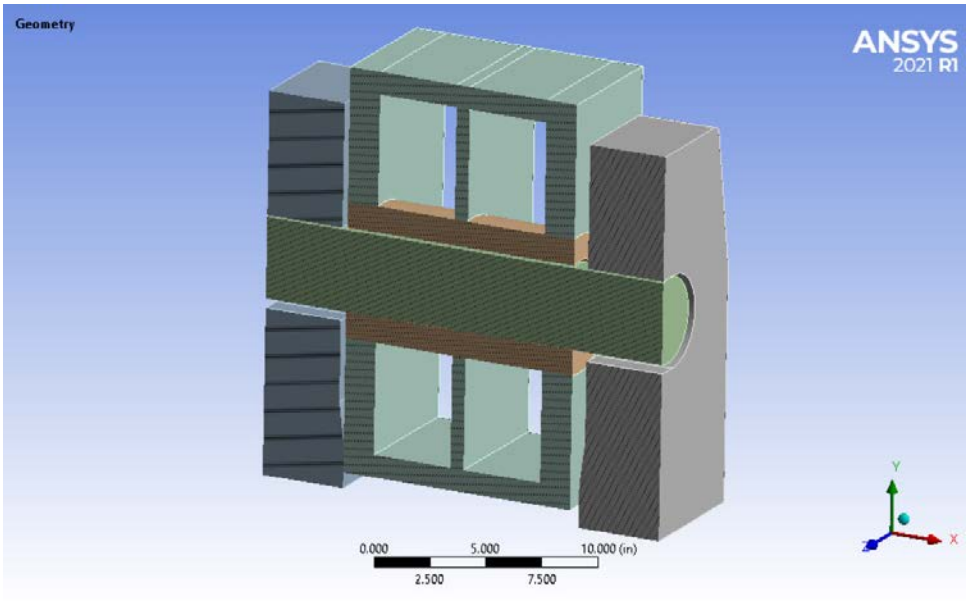


Figure 77. Central Location Cross Section

Figures 78 and 79 show the loading condition for each location

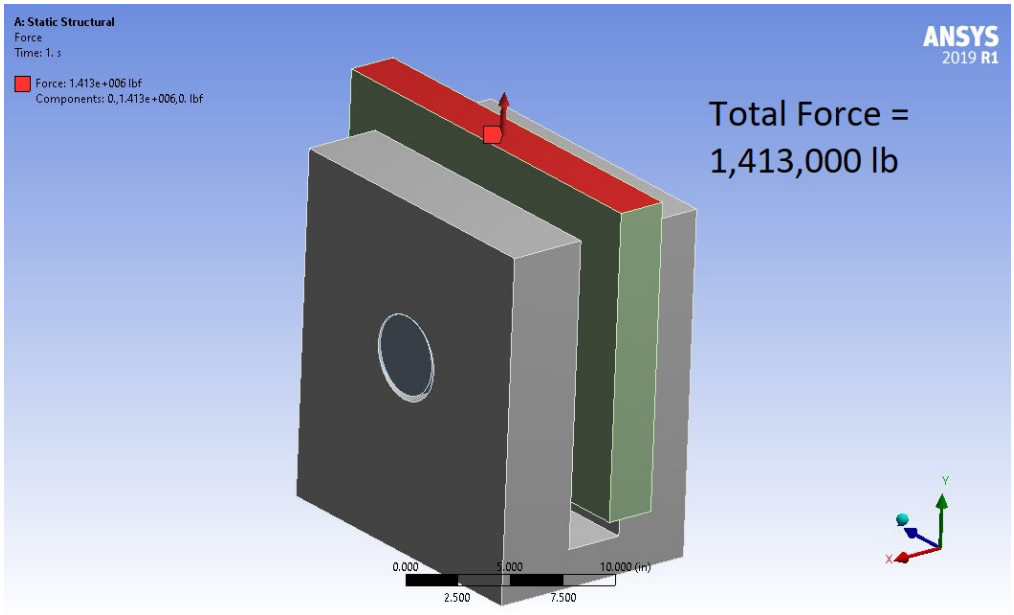


Figure 78. Loading Condition (Outer Pin)

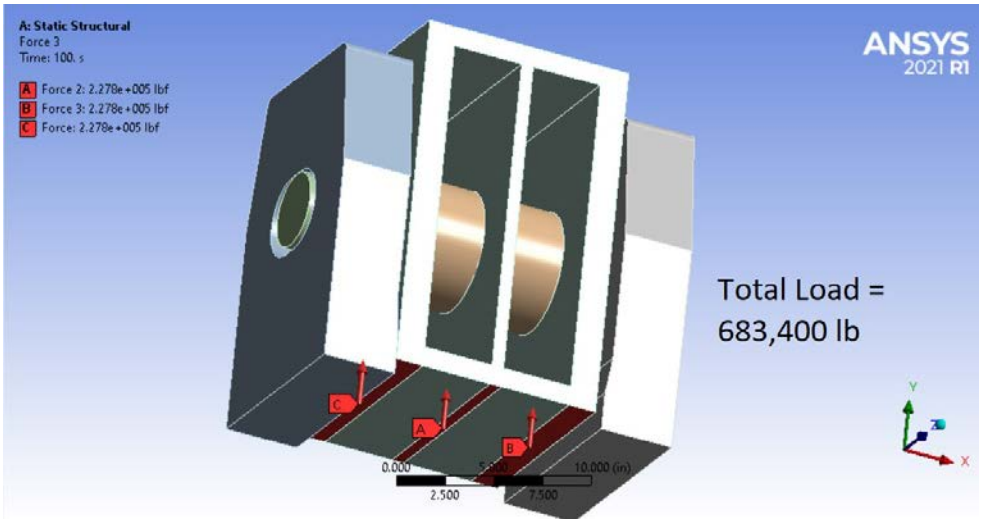


Figure 79. Loading Condition (Center Pin)

The evaluation of the FEA results will be performed in terms of strains which give a better indication of the condition of the part beyond the yield stress. The ultimate strain values are shown on table 58 and are 2% for the pin material and 20% for the block material. Figures 80 through 84 show the results of the analysis for the outer location.

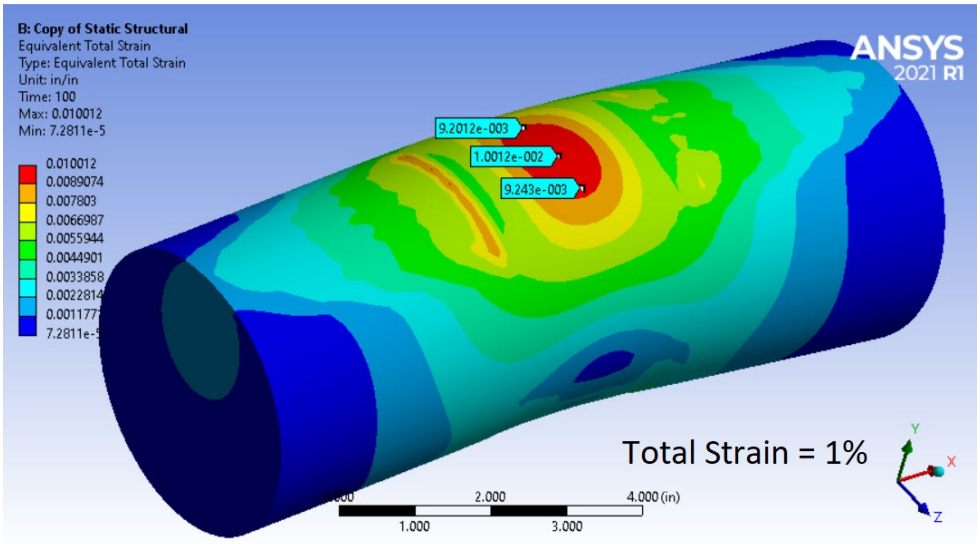


Figure 80. Outer Pin Total Strain (in/in)

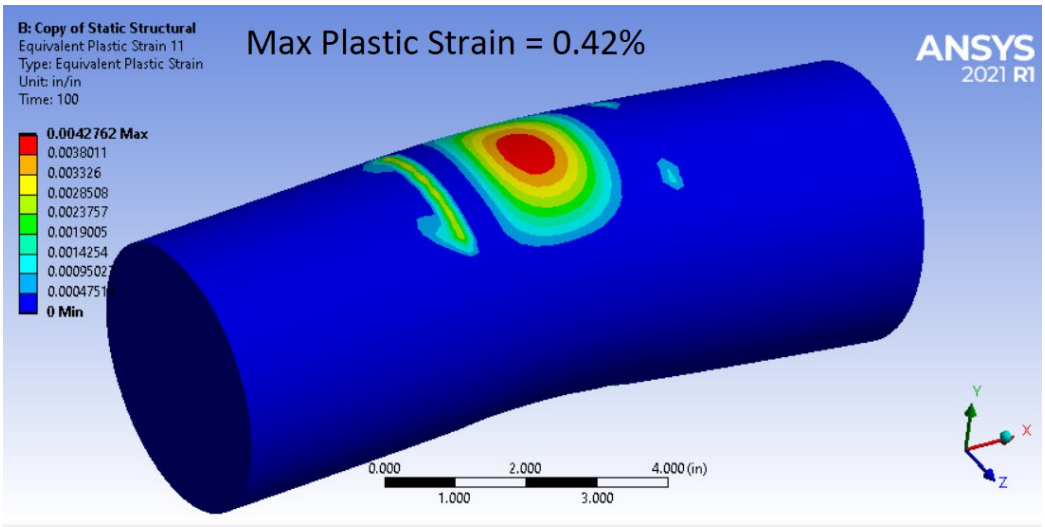


Figure 81. Outer Pin Plastic Strain (in/in)

Figure 82 shows the depth of the plastic strain below the surface. It can be seen that most of the pin cross sectional area remains in the elastic region.

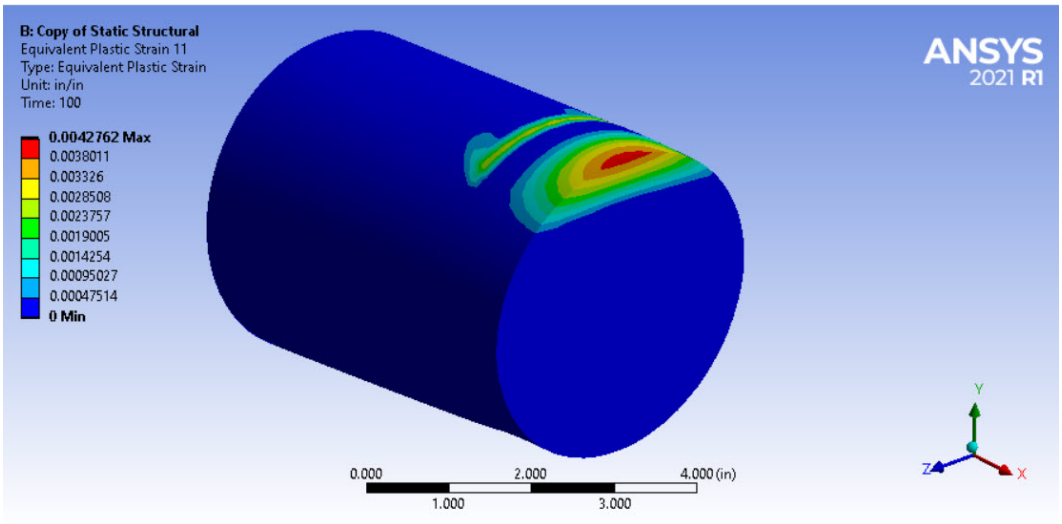


Figure 82. Outer Pin Plastic Strain Depth

The outer block results are shown in Figure 83 and Figure 84

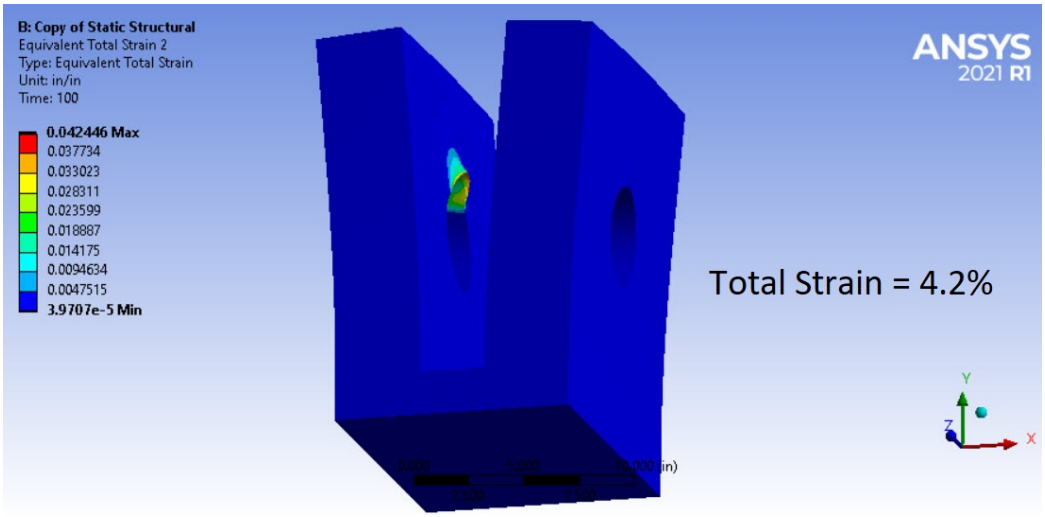


Figure 83. Outer Block Total Strain (in/in)

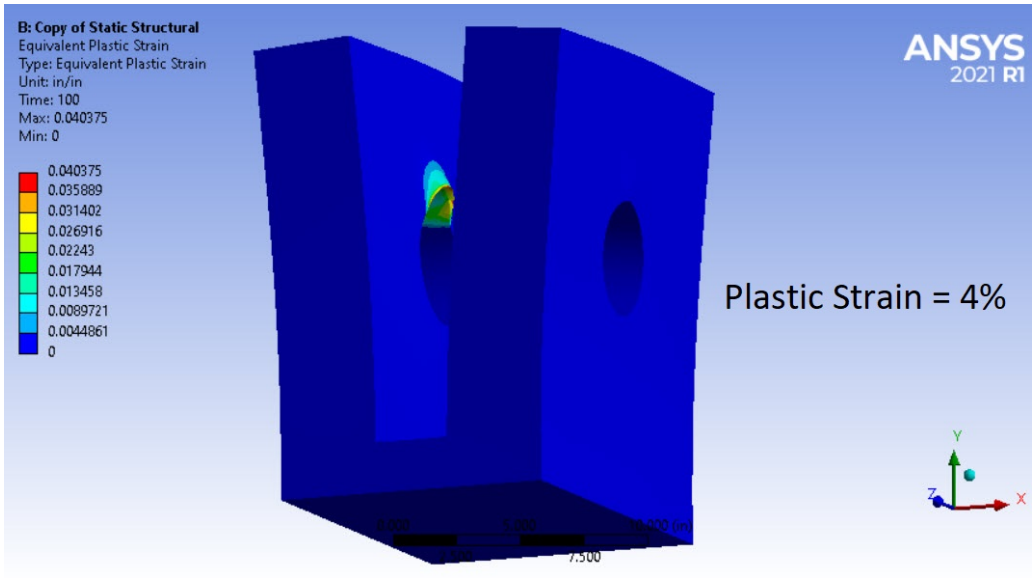


Figure 84. Outer Block Plastic Strain (in/in)

Figures 85 through 89 show the results for the central location

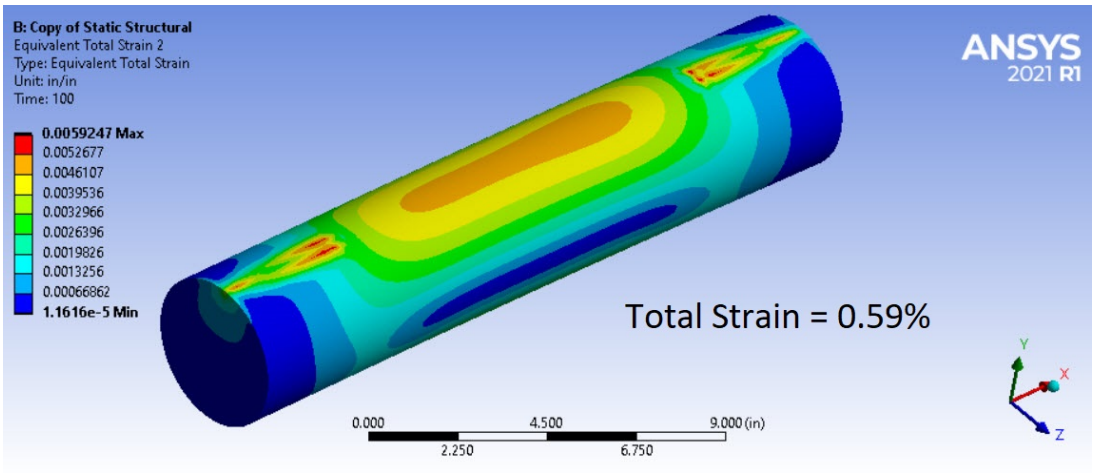


Figure 85. Central Pin Total Strain (in/in)

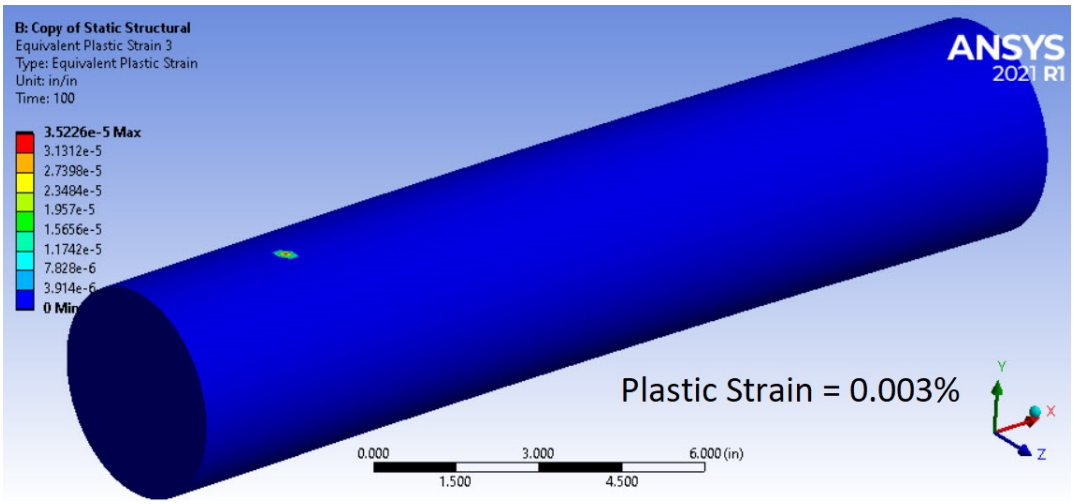


Figure 86. Central Pin Plastic Strain (in/in)

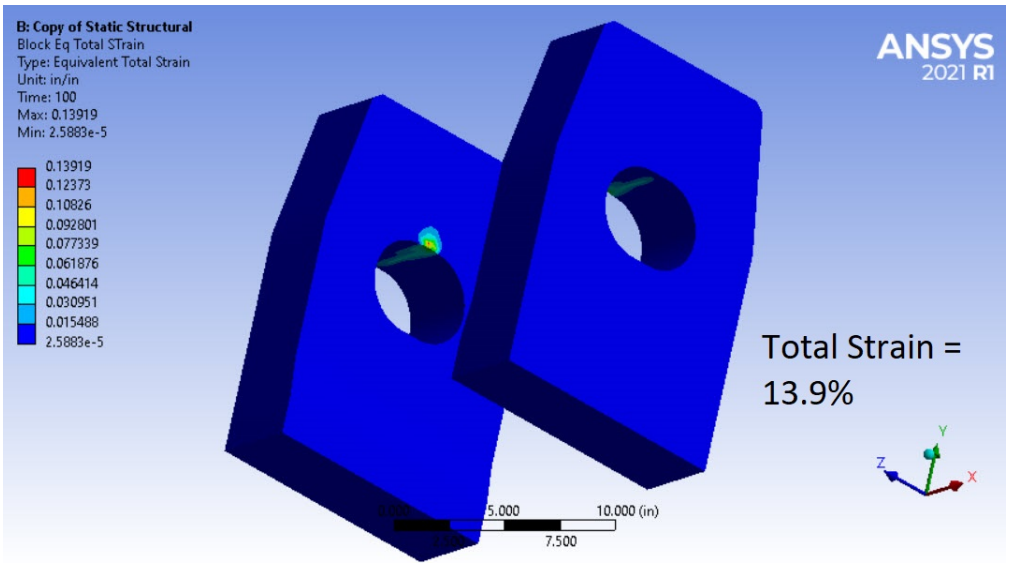


Figure 87. Central Blocks Total Strain (in/in)

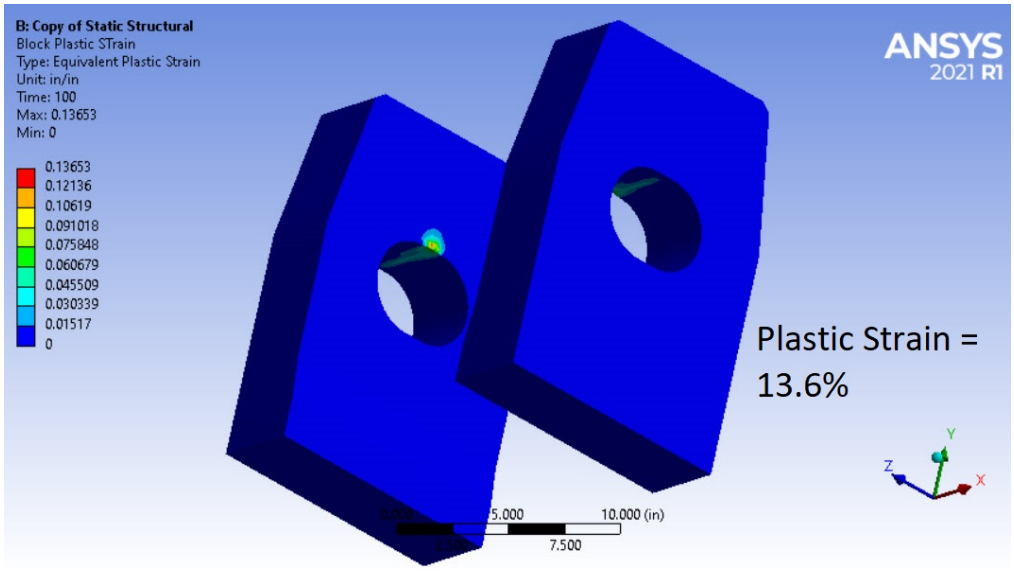


Figure 88. Central Blocks Plastic Strain (in/in)

Table 60 summarizes the FEA structural analysis for the outer and central pins and blocks

Table 60. Securement System Results Summary

Component	Total Strain (%)	Plastic Strain (%)	Ultimate Strain (%)
Outer Pin	1	0.42	2
Outer Block	4.2	4	20
Central Pin	0.59	0.003	2
Central Block	13.9	13.6	20

These results indicate that under the imposed loading conditions, neither pin or block develops its ultimate load carrying capacity.

8.4.8.6 Weld Analysis

The weld analysis was performed for the following elements:

- Center Attachment Block
- Shear Key Block
- Outer Attachment Block

Each weld was analyzed under the requirements of both *10 CFR 71.45* and *Field Manual of the AAR Interchange Rules, Rule 88 A.16.c(3).* These requirements are the bounding criteria for the weld sizing calculations. Table 61 shows the differences in loading factors between these regulations.

Table 61. Loading Factors for Weld Calculations

Loading Factor	Rule 88 A.16.c(3)	10 CFR 71.45
Vertical	2g	2g
Lateral	2g	5g
Longitudinal	7.5g	10g

By using the appropriate load factors, the nominal throat dimension of each of the welds at the central, shear, and outer block may be calculated. For each block type the individual block with the most severe load case was considered. The welds and load cases were analyzed separately as follows:

- **Central Block Weld**
  - Lateral load of 610 kips (including 364 kip vertical reaction)

    - Vertical load of 686 kips
- **Shear Key Block Weld**
    - Longitudinal load of 2921 kips
- **Outer Block Weld**
    - Longitudinal load of 944 kips (including 1052 kip vertical reaction)

The shear resistance of the weld is 33ksi per AAR Section CII, Table 4.3.4.1.3 and AWS D15.1 Table 8.1. Table 62 shows the results summary for the weld calculations. Complete weld design calculations can be found in *Atlas 12 Axle Flat Car Attachment to Deck Weldment* (January 2020), Appendix K.

Table 62. Weld Analysis Results Summary

Weld Location	Required throat size, t (in)	Met/Not Met
Center Attachment Block	100% penetration weld required, for a 3.75 inch wide block	Met
Shear Key Block	$0.41 \leq t \leq 0.55$	Met
Outer Attachment Block	$0.91 \leq t \leq 0.97$	Met

Welds were inspected visually and with magnetic particle inspection (see TUV NDE inspection reports for details, Appendix K). Measurements were made at various locations to verify that the throat sizes met the requirements, and example photos of an Outer Attachment Block and its measurements are shown in Figure 89. Various shims were required during the fit-up of the deck attachment blocks due to the straightness of the deck attachments and camber of the car. Per AWS D15.1, *Railroad Welding Specification for Cars and Locomotives*, the use of shims necessitates increasing the welding fillet size by the shim thickness. For this reason, some portions of the Outer Block weld dimensions are larger than the design fillet when no shims are present.

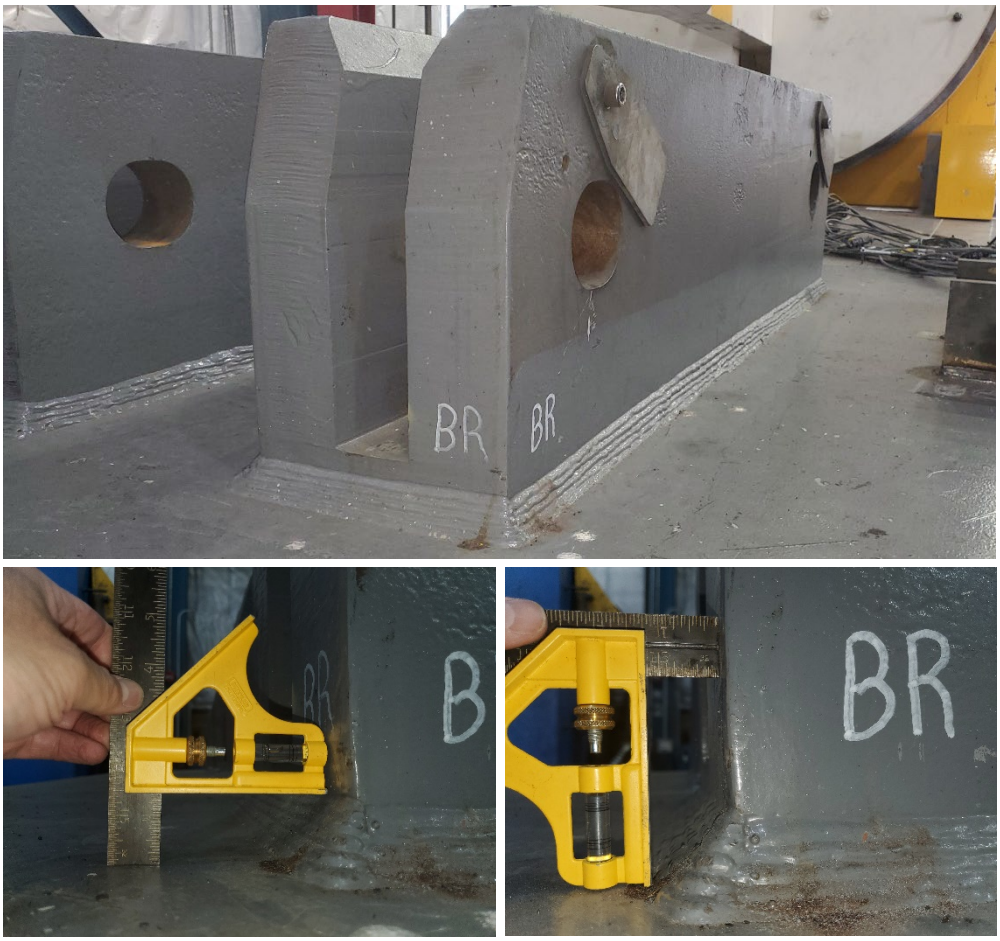


Figure 89. Example securement system welds and measurements

8.5 Dynamic Tests

The dynamic test regimes required by Standard S-2043 include:

- Hunting
- Twist and roll
- Yaw and sway
- Dynamic curving
- Pitch and bounce (Chapter 11)
- Special pitch and bounce
- Single bump test
- Limiting spiral negotiation
- Normal spiral negotiation
- Curving with single rail perturbation
- Standard Chapter 11 constant curving

- Special trackwork
- Ride Quality (not required since not a passenger-carrying car)

Appendix L lists the dates for the test zone compliance for each of the regimes described in this dynamic test section. This appendix also includes the test zone, the date when demonstrated compliance was measured, and date the Atlas railcar test was performed. TTCI's policy established that test zone measurements should be considered valid for 6 months from the last measurement showing compliance.

The dynamic tests were conducted to measure compliance with criteria listed in Table 5.1 of Standard S-2043. That table is reproduced here as Table 63.

Standard S-2043 specifies that non-curving tests be performed up to 75 mph where deemed safe by the test engineer. However, the Standard S-2043 limiting criteria do not apply to test runs at speeds over 70 mph. These tests are done only to further quantify performance and establish trends. The results from tests performed at speeds over 70 mph may be included in worst-case performance statistics depending on the following results:

- If the results of tests executed at speeds over 70 mph meet the test criteria, the results are considered when compiling performance statistics.
- When tests over 70 mph do not meet the criteria, the runs are excluded from consideration for performance statistics, and suitable comments are made in the body of that section.

The Atlas car was pulled from the B-end during most dynamic tests. Instrumented wheelsets (IWS) were placed in Axles 1 through 6 to measure wheel/rail forces (Figure 90). Also, Standard S-2043 requires that curving tests and special track-work tests also be performed with the instrumented span bolster in the trailing position; therefore, these tests were repeated with the A-end leading.

Table 63. Standard S-2043 Dynamic Testing Performance Criteria

Criterion	Limiting Value	Notes
Maximum carbody roll angle (degree)	4	Peak-to-peak
Maximum wheel L/V	0.8	Not to exceed indicated value for a period greater than 50 ms and for a distance greater than 3 feet per instance
95th percentile single wheel L/V (constant curving tests only)	0.6	Not to exceed indicated value. Applies only for constant curving tests.
Maximum truck side L/V	0.5	Not to exceed indicated value for a duration equivalent to 6 feet of track per instance
Minimum vertical wheel load (%)	25	Not to fall below indicated value for a period greater than 50 ms and for a distance greater than 3 feet per instance
Peak to peak carbody lateral acceleration (G)	1.3 0.60	For non-passenger-carrying railcars For passenger-carrying railcars
Maximum carbody lateral acceleration (G)	0.75 0.35	For non-passenger-carrying railcars For passenger-carrying railcars
Carbody lateral acceleration standard deviation (G)	0.13	Calculated over a 2,000-foot sliding window every 10 feet over a tangent track section that is a minimum of 4,000 feet long
Maximum carbody vertical acceleration (G)	0.90 0.60	For non-passenger-carrying railcars For passenger-carrying railcars
Maximum vertical suspension deflection (%)	95	Suspension bottoming not allowed. Maximum compressive spring travel shall not exceed 95% of the spring travel from the empty car height of the outer load coils to solid spring height
Maximum vertical dynamic augment acceleration (G)	0.9	Suspension bottoming not allowed. Vertical dynamic augment accelerations of a loaded car shall not exceed 0.9 G.

According to Sections 5.5.7 through 5.5.16 of Standard S-2043 the above criteria must be met for all tests performed. Some exceptions are:

- The notes for the carbody lateral acceleration standard deviation require it be computed over a 2,000-foot sliding window in a 4,000-foot tangent track section so that value will only be reported for high-speed stability tests.

- L/V and vertical wheel load data is not available for high-speed stability tests with KR wheels (shown as “not measured” on the results tables).

The following sections contain a summary of the data.

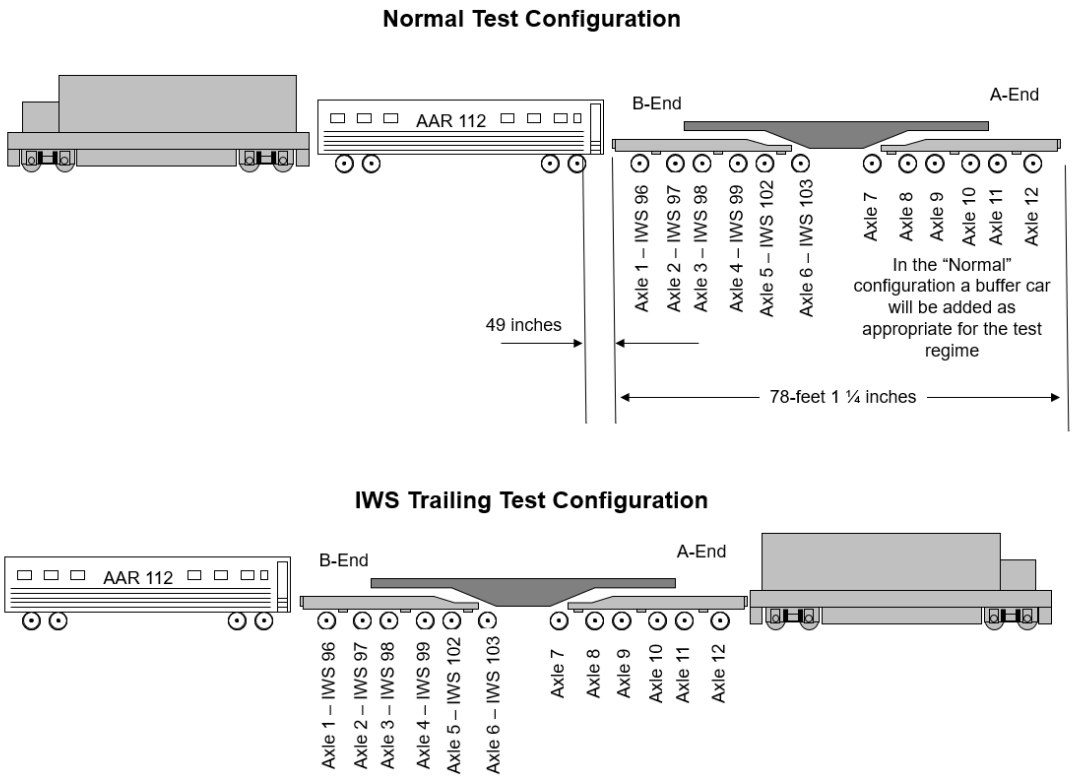


Figure 90. Location of IWS during Dynamic Tests

Figure 90 shows the locomotive coupled directly to the Atlas car for A-end Leading runs. This was the case for special trackwork tests. Constant curving and dynamic curving tests used a buffer car in between the Altas car and the locomotive. The curving buffer car is a loaded 100-ton open top hopper car which is 53 feet over pulling faces with 40 feet 6 inch truck centers. In-train buff and draft forces are generally low during these tests, less than 20,000 pounds based on grade and resistance calculations. This level of force is unlikely to change curving performance regardless of the train makeup.

8.5.1 Primary Suspension Pad Configuration Changes

During the initial tests the Atlas car showed some hunting instability at speeds above 65 mph. Stiffer primary pads (prototype CSM 70 pads) improved the hunting performance. All dynamic testing was completed with the CSM 70 pads. The car performance did not meet the Standard S-2043 criteria in dynamic curving or curve with single rail perturbation regimes with the CSM 70 pads.

On October 15, 2020, TTCI reviewed the results with the AAR EEC. The EEC directed TTCI to re-test the car with softer primary pads with a minimum test load in the dynamic curving regime. The EEC felt that curving performance was more important than high speed stability performance because the car would be limited to less than 50 mph by AAR circular OT-55 when in HLRM service.

During the testing program, TTCI tested the car with a total of four models of primary pad in an attempt to achieve superior performance. The pads are made from chlorosulfonated polyethylene or CSM and are categorized by the Shore D durometer hardness value. The production pads the car arrived with were type CSM 58. TTCI also tested the car with prototype pad types CSM 70, CSM 68, and CSM 65. Figure 91 shows the hunting performance with minimum test load for the four pads tested. Figure 92 shows the dynamic curving performance with minimum test load for the four pads tested. The production CSM 58 pads were chosen based on the balance of curving and high-speed stability performance.

With the CSM 58 pads, the Atlas car meets most of the hunting and dynamic curving requirements of Standard S-2043. The car does not meet the hunting requirements with the minimum test load at speeds over 65 mph, beyond the 50 mph limit recommended in AAR circular OT-55 for cars in high-level radioactive material (HLRM) service. Therefore, on behalf of the DOE, TTCI is requesting an exception from the AAR EEC.

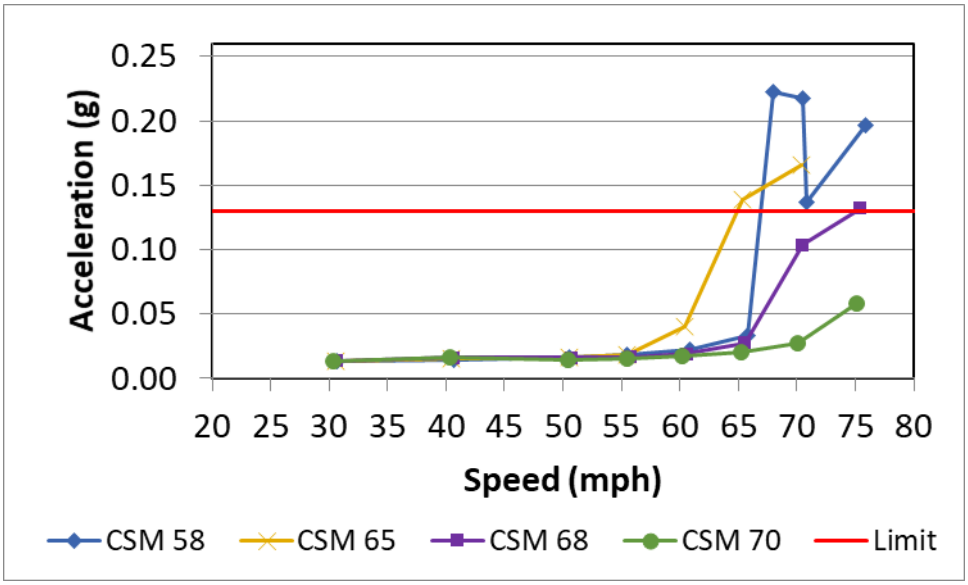


Figure 91. Hunting Results with Different Primary Suspension Pads (Minimum Test Load Condition), Worst Case of A or B-end Standard Deviation of Lateral Carbody Acceleration over 2000-feet, CSM 58 pads Selected

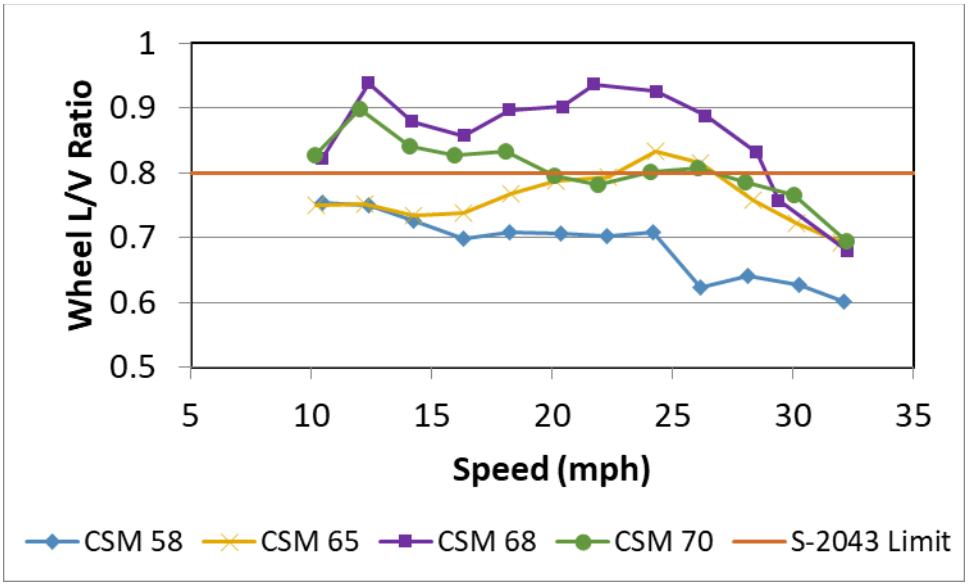


Figure 92. Dynamic Curving Test Results with Different Primary Suspension Pads (Minimum Test Load) , CSM 58 pads Selected

The hunting regime was tested with CSM 58 pads in minimum and maximum test load conditions. The dynamic curving regime was tested with CSM 58 pads in the minimum test load condition. All other dynamic tests were completed with CSM 70 pads. The effect of the pad change on other regimes will be evaluated using modeling and then documented in the post-test analysis report.

8.5.2 Minimum Load Hunting

Standard S-2043 requires that hunting tests be performed with IWS and with wheelsets having KR profiles. If IWS with KR profiles are not available two separate tests may be performed. The minimum load hunting tests were performed with KR wheels using CSM 58 pads, with KR wheels using CSM 70 pads, and with IWS having a new AAR1B narrow flange profiles using CSM 70 pads. Table 64 shows the date each test was conducted and the rail friction measured during each test. The official AAR observers were Xinggao Shu, TTCI Principal Investigator, on November 15, 2019, Adam Klopp, TTCI Principal Investigator, on June 15, 2000, and Ulrich Spangenberg, TTCI Principal Investigator, on October 7, 2020.

Table 64. Minimum Load Hunting Test Dates and Rail Friction Data

Test Condition	Date	Coefficient of Friction	
		Inside Rail	Outside Rail
CSM 58 Pads with KR Profile	11/15/2019	0.54	0.54
CSM 70 Pads with KR Profile	06/15/2020	0.55	0.55
CSM 70 Pads with IWS	10/07/2020	0.53	0.54

The Atlas car did not meet criterion for standard deviation of lateral acceleration over 2000-feet above 65 mph when using CSM 58 primary pads and KR wheel profiles. All other criteria were met. The Atlas car was stable to 75 mph when using CSM 70 primary pads with both KR

wheel profiles and IWS. Note that the AAR circular OT-55 “Recommended Railroad Operating Practices for Transportation of Hazardous Material” restricts trains carrying spent nuclear fuel or HLRM to a maximum speed of 50 mph. Table 65 shows a summary of hunting test results, with the exception shown in red text. Figure 93 shows a plot of the 2,000-foot standard deviation of lateral acceleration versus speed for the minimum load hunting tests and Figure 94 shows a distance plot of the data where criteria was not met.

Table 65. Minimum Load Hunting Test Results

Criterion	Limiting Value	Minimum Load KR Wheel Profile CSM 58 Pad	Minimum Load KR Wheel Profile CSM 70 Pad	IWS with AAR 1B Narrow Flange Wheel Profile CSM 70 Pad
Roll angle (degree)	4	0.7	0.6	0.6
Maximum wheel L/V	0.8	Not Measured	Not Measured	0.13
Maximum truck side L/V	0.5	Not Measured	Not Measured	0.09
Minimum vertical wheel load	25 (% of static)	Not Measured	Not Measured	67%
Lateral peak-to-peak acceleration (g)	1.3	0.80	0.30	0.14
Maximum lateral acceleration (g)	0.75	0.43	0.16	0.07
Lateral acceleration standard deviation	0.13 (g)	**0.22**	0.06	0.02
Maximum vertical acceleration (g)	0.90	0.28	0.30	0.35
Maximum vertical suspension deflection	95 %	10%	7%	7%
Critical Speed	70 mph	>65 mph	> 75 mph	> 75 mph

* L/V and vertical wheel load data is not available for high-speed stability tests with KR wheels (IWS required).

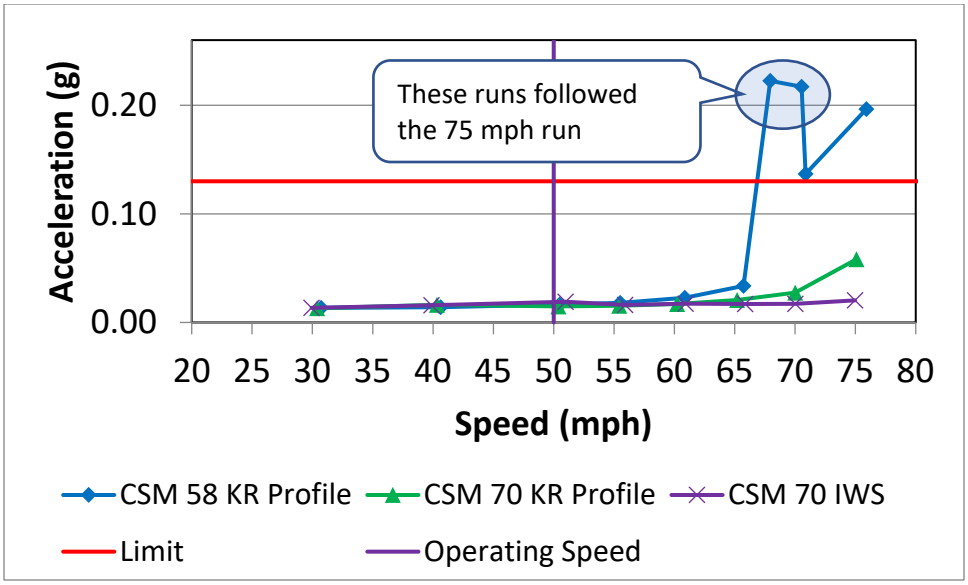


Figure 93. 2000-foot Standard Deviation of Lateral Acceleration for Minimum Load Hunting Tests

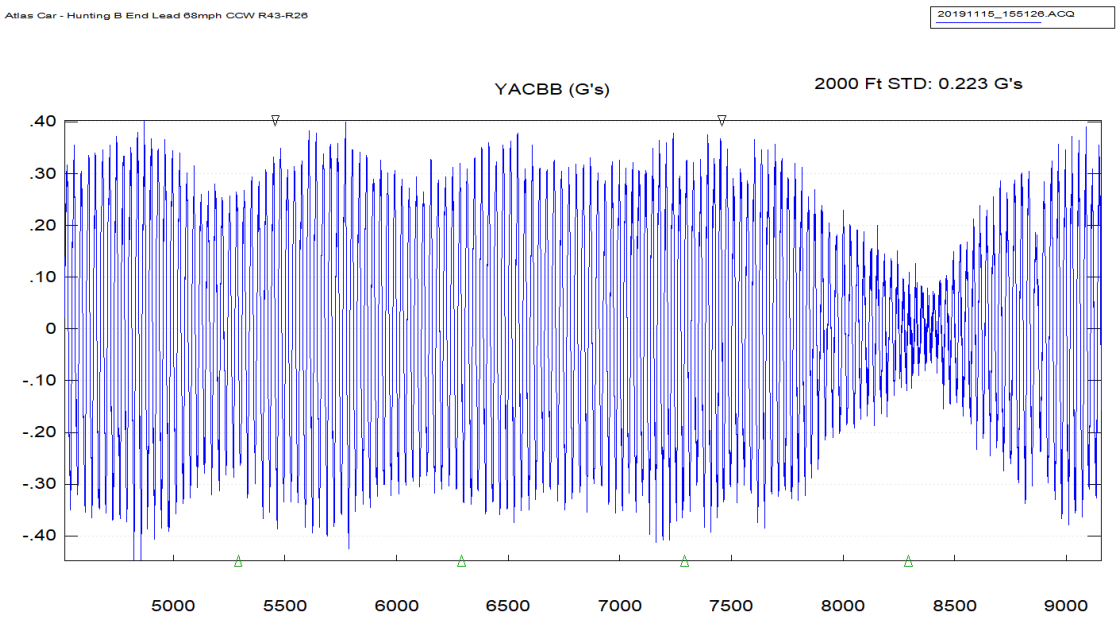


Figure 94. Minimum Load Hunting Standard Deviation of Lateral Carbody Acceleration, B-End (Lead End), KR Wheel Profiles, 68 mph

8.5.3 Maximum Load Hunting

Maximum load hunting tests were performed with KR wheels using CSM 58 pads, with KR wheels using CSM 70 pads, and with IWS having a new AAR1B narrow flange profiles using CSM 70 pads. Table 66 shows the date each test was conducted and the measured rail friction.

The test using CSM 58 pads and KR wheel profiles on December 11, 2019, was originally intended as a troubleshooting test and no AAR official observer was onboard. This test was conducted by Brent Whitsitt, TTCI Senior Engineer. Adam Klopp, TTCI Principal Investigator I witnessed the tests performed on June 18, 2020, and Ulrich Spangenberg, TTCI Principal Investigator I, witnessed the tests on July 6, 2020, as the AAR Observers per Standard S-2043 requirements.

Table 66. Maximum Load Hunting Test Dates and Rail Friction Data

Test Condition	Date	Coefficient of Friction	
		Inside Rail	Outside Rail
CSM 58 Pads with KR Profile	12/11/2019	0.48	0.46
CSM 70 Pads with KR Profile	06/18/2020	0.54	0.55
CSM 70 Pads with IWS	07/06/2020	0.54	0.54

The car was stable with IWS and KR wheel profiles with both CSM 58 and CSM 70 pads. The car met all criteria with both wheel profiles in the maximum load conditions. Table 67 shows a summary of the maximum load hunting test results, and Figure 95 shows a plot of 2,000-foot standard deviation of lateral acceleration versus speed for the configurations tested.

Table 67. Maximum Load Hunting Test Results

Criterion	Limiting Value	Maximum Load KR Wheel Profile CSM 58 Pads	Maximum Load KR Wheel Profile CSM 70 Pads	IWS with AAR 1 B Narrow Flange Wheel Profile CDM 70 Pads
Roll angle (degree)	4	0.6	0.6	0.6
Maximum wheel L/V	0.8	Not Measured	Not Measured	0.10
Maximum truck side L/V	0.5	Not Measured	Not Measured	0.06
Minimum vertical wheel load (%)	25 %	Not Measured	Not Measured	81%
Lateral peak-to-peak acceleration (g)	1.3	0.49	0.31	0.11
Maximum lateral acceleration (g)	0.75	0.30	0.16	0.07
Lateral acceleration standard deviation (g)	0.13	0.11	0.06	0.02
Maximum vertical acceleration (g)	0.90	0.25	0.20	0.16
Maximum vertical suspension deflection	95 %	63%	48%	50%
Critical Speed	70 mph	>75mph	>75mph	>75mph

* L/V and vertical wheel load data is not available for high-speed stability tests with KR wheels (IWS required).

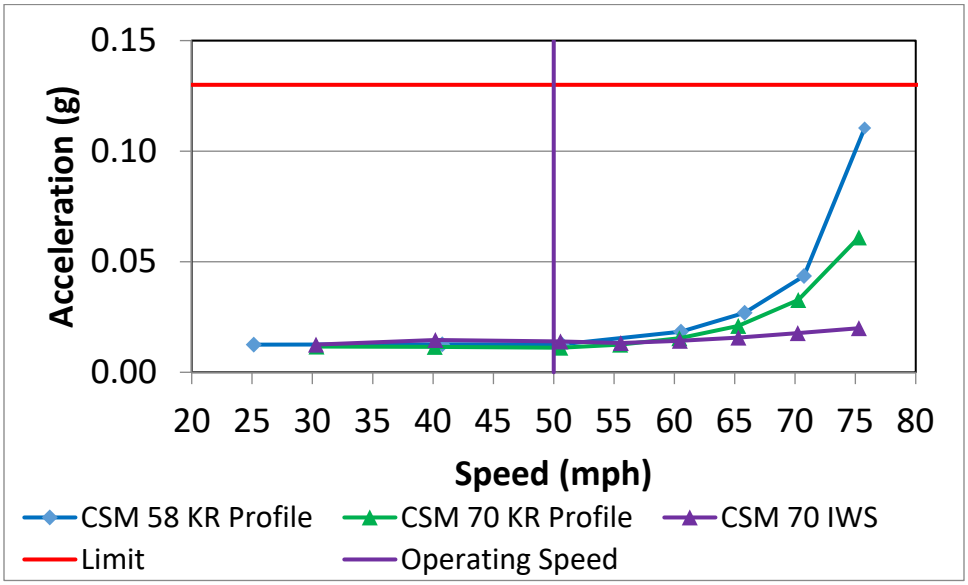


Figure 95. 2,000-foot Standard Deviation of Lateral Acceleration for Maximum Load Hunting Tests

8.5.4 Minimum Test Load Twist and Roll

The twist and roll test in the minimum test load configuration was performed on September 14, 2020. The coefficient of friction was 0.50 on the east rail and 0.50 on the west rail. Adam Klopp, TTCI Principal Investigator I, witnessed the twist and roll test as the AAR Observer, per Standard S-2043 requirements. The car met the criteria for minimum test load over the twist and roll zone. Table 68 contains a summary of the data from the twist and roll tests, and Figure 96 shows a plot of peak-to-peak carbody roll versus speed. The tests presented in this section were done with the prototype CSM 70 suspension pads. The effect of changing pad type from CSM 70 to CSM 58 on performance in this regime will be investigated using modeling and presented in the post test analysis report.

Table 68. Minimum Test Load Twist and Roll Test Results

Criterion	Limiting Value	Minimum Test Load
Roll angle (degree)	4	1.4
Maximum wheel L/V	0.8	0.27
Maximum truck side L/V	0.5	0.19
Minimum vertical wheel load	25 (% of static)	54%
Lateral peak-to-peak acceleration (g)	1.3	0.50
Maximum lateral acceleration (g)	0.75	0.26
Maximum vertical acceleration (g)	0.90	0.36
Maximum vertical suspension deflection	95 %	16%

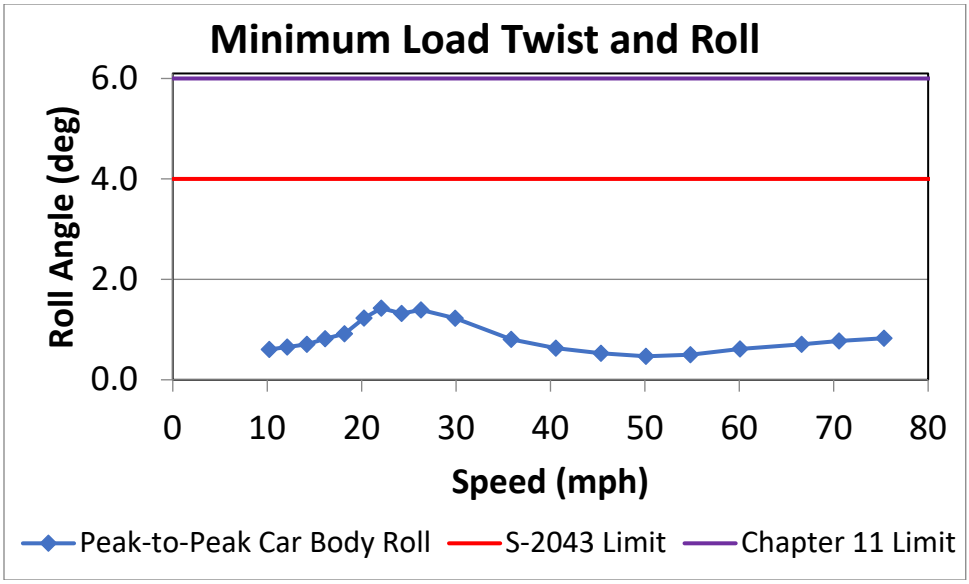


Figure 96. Minimum Test Load Twist and Roll Test, Maximum Carbody Roll versus Speed

8.5.5 Maximum Test Load Twist and Roll

The twist and roll tests were performed in the maximum test load configuration on June 30, 2020, and July 1, 2020. The coefficient of friction was 0.58 on the east rail and 0.59 on the west rail. Abe Meddah, TTCI Principal Investigator I, witnessed the twist and roll test as the AAR Observer, per Standard S-2043 requirements. The car met the criteria for maximum test load twist and roll. Table 69 contains a summary of the data from the twist and roll tests, and Figure 97 shows a plot of peak-to-peak carbody roll versus speed. The tests presented in this section were done with the prototype CSM 70 suspension pads. The effect of changing pad type from CSM 70 to CSM 58 on performance in this regime will be investigated using modeling and presented in the post test analysis report.

Table 69. Maximum Test Load Twist and Roll Test Results

Criterion	Limiting Value	Maximum Test Load
Roll angle (degree)	4	1.3
Maximum wheel L/V	0.8	0.23
Maximum truck side L/V	0.5	0.15
Minimum vertical wheel load	25 (% of static)	64%
Lateral peak-to-peak acceleration (g)	1.3	0.31
Maximum lateral acceleration (g)	0.75	0.17
Maximum vertical acceleration (g)	0.90	0.20
Maximum vertical suspension deflection	95 %	59%

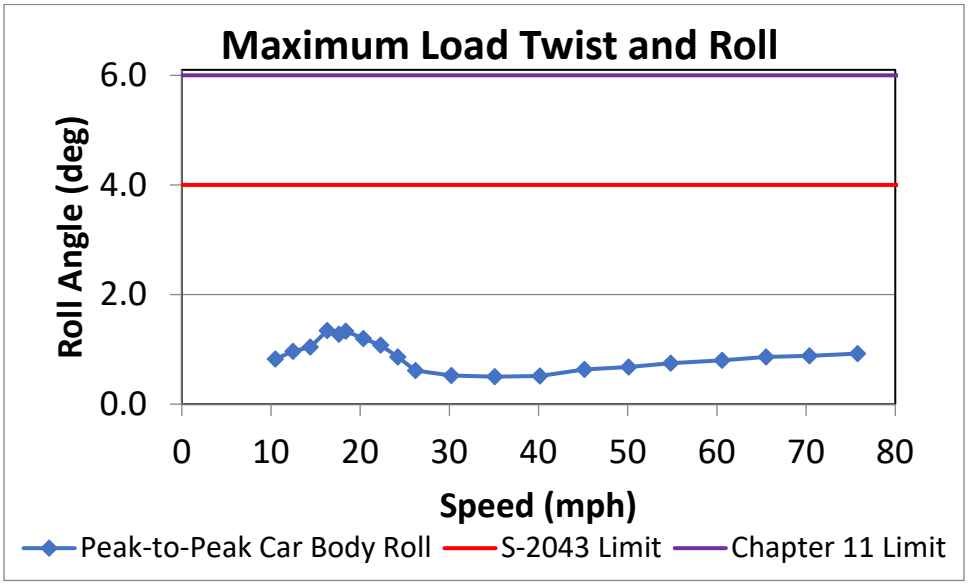


Figure 97. Maximum Test Load Twist and Roll Test, Maximum Carbody Roll versus Speed

8.5.6 Yaw and Sway

Yaw and sway tests were performed in the maximum test load configuration on September 02, 2020, and on September 03, 2020. The coefficient of friction was 0.55 on the east rail and 0.54 on the west rail. Adam Klopp, TTCI Principal Investigator I, witnessed the yaw and sway test as the AAR Observer, per Standard S-2043 requirements. Table 70 shows the results of the tests up to 70 mph and Figure 98 shows plots of the peak-to-peak lateral acceleration versus speed. The car met the criteria for maximum test load yaw and sway. The tests presented in this section were done with the prototype CSM 70 suspension pads. The effect of changing pad type from CSM 70 to CSM 58 on performance in this regime will be investigated using modeling and presented in the post test analysis report.

Table 70. Yaw and Sway Test Results to 70 mph

Criterion	Limiting Value	Loaded Cask
Roll angle (degree)	4	0.7
Maximum wheel L/V	0.8	0.52
Maximum truck side L/V	0.5	0.28
Minimum vertical wheel load	25 (% of static)	71%
Lateral peak-to-peak acceleration (g)	1.3	0.62
Maximum lateral acceleration (g)	0.75	0.36
Maximum vertical acceleration (g)	0.90	0.14
Maximum vertical suspension deflection	95 %	77%

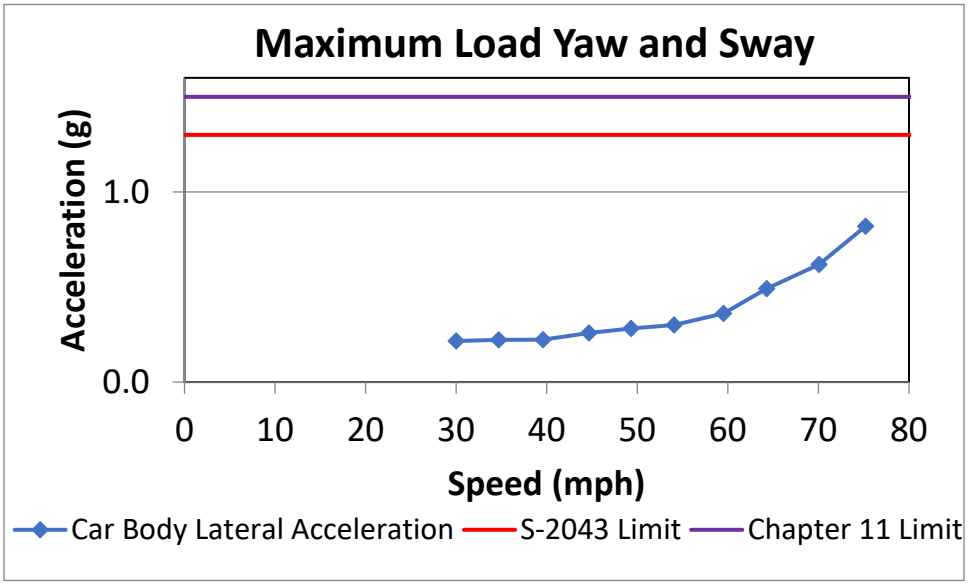


Figure 98. Maximum Test Load Yaw and Sway Test, Peak-to-Peak Lateral Acceleration versus Speed

8.5.7 Minimum Load Dynamic Curving

Dynamic curve testing was conducted, clockwise (CW) and counterclockwise (CCW), with both the A-end leading and B-end leading. The testing dates were June 25, 2021, and June 28, 2021.

Table 71 shows the rail friction data for the different test configurations. When two or more test configurations were done on the same day, the rail friction was only measured once. Ulrich Spangenberg and Adam Klopp, both TTCI Principal Investigator I's, witnessed the minimum load dynamic curving test as the AAR Observer, per Standard S-2043 requirements. The tests presented in this section were done with the CSM 58 production primary suspension pads.

Table 71. Minimum Load Dynamic Curving Test Dates and Rail Friction Data

Test Condition	Date	Coefficient of Friction	
		Inside Rail	Outside Rail
Minimum Load, A-end Leading, CW	06/28/2021	0.51	0.55
Minimum Load, A-end Leading, CCW	06/25/2021	0.49	0.50
Minimum Load, B-end Leading, CW	06/25/2021	0.49	0.50
Minimum Load, B-end Leading, CCW	06/28/2021	0.51	0.55

The car met the criteria for the minimum load dynamic curving tests. Table 72 represents the worst-case scenario test results for each car orientation. Figure 99 shows a plot of single wheel L/V ratios versus speed for each test condition.

Table 72. Minimum Load Dynamic Curving Test Results

Criterion	Limiting Value	A-End CW	A-End CCW	B-End CW	B-End CCW
Roll angle (degree)	4	0.80	0.80	0.80	0.80
Maximum wheel L/V	0.8	0.72	0.75	0.69	0.74
Maximum truck side L/V	0.5	0.38	0.35	0.39	0.38
Minimum vertical wheel load	25 (% of static)	53%	51%	51%	45%
Lateral peak-to-peak acceleration (g)	1.3	0.17	0.20	0.17	0.22
Maximum lateral acceleration (g)	0.75	0.16	0.20	0.15	0.20
Maximum vertical acceleration (g)	0.90	0.12	0.17	0.10	0.16
Maximum vertical suspension deflection	95 %	13%	17%	12%	14%

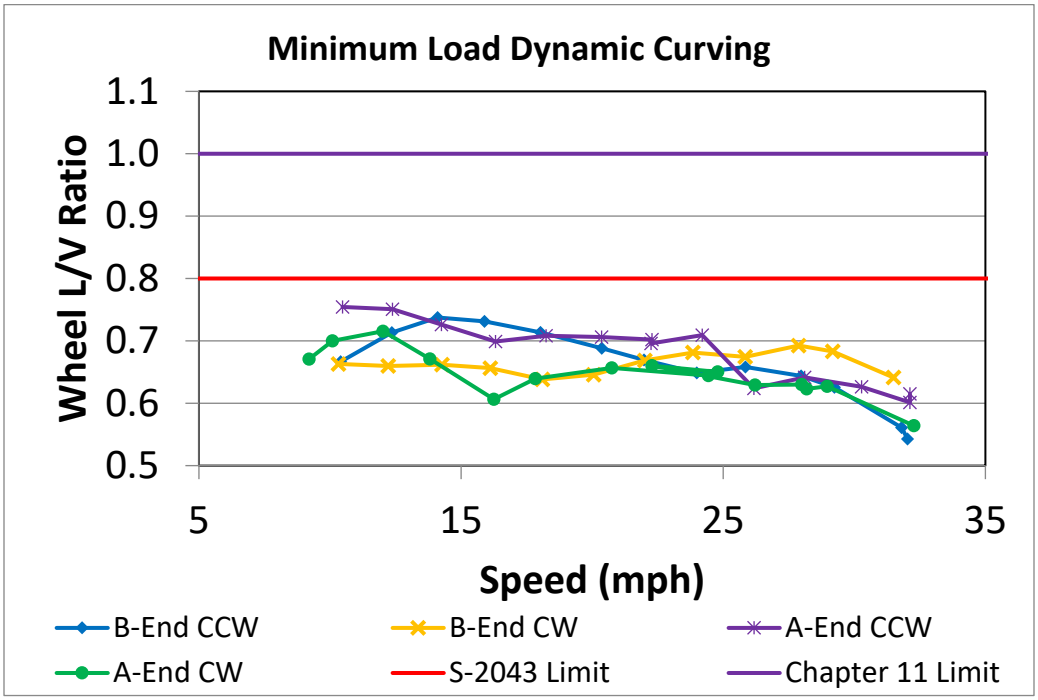


Figure 99. Minimum Load Dynamic Curving L/V Results versus Speed

8.5.8 Maximum Load Dynamic Curving

The maximum load dynamic curve testing was conducted CW and CCW, with both the A-end leading and B-end leading. Table 73 lists the test dates and the rail friction data. When two or more test configurations were done on the same day, friction was only measured once. Abe Meddah, TTCI Principal Investigator I, witnessed the maximum load dynamic curving test as the AAR Observer, per Standard S-2043 requirements.

Table 73. Maximum Load Dynamic Curving Test Dates and Rail Friction Data

Test Condition	Date	Coefficient of Friction	
		Inside Rail	Outside Rail
Maximum Load, A-end Leading, CW	06/30/2020	0.49	0.50
Maximum Load, A-end Leading, CCW	06/25/2020	0.53	0.51
Maximum Load, B-end Leading, CW	06/25/2020	0.53	0.51
Maximum Load, B-end Leading, CCW	06/29/2020	.050	0.50

Tests presented in this section were done with the prototype CSM 70 suspension pads. Table 74 contains a summary of the maximum load dynamic curving test results. Figure 100 shows a plot of maximum wheel L/V versus speed.

Table 74. Maximum Load Dynamic Curving Test Results

Criterion	Limiting Value	A-End CW	A-End CCW	B-End CW	B-End CCW
Roll angle (degree)	4	0.70	0.70	0.70	0.80
Maximum wheel L/V	0.8	0.76	**0.81**	0.72	0.75
Maximum truck side L/V	0.5	0.40	0.39	0.39	0.36
Minimum vertical wheel load	25 (% of static)	50%	45%	47%	51%
Lateral peak-to-peak acceleration (g)	1.3	0.14	0.25	0.17	0.22
Maximum lateral acceleration (g)	0.75	0.14	0.18	0.16	0.19
Maximum vertical acceleration (g)	0.90	0.10	0.08	0.08	0.11
Maximum vertical suspension deflection	95 %	33%	41%	39%	43%

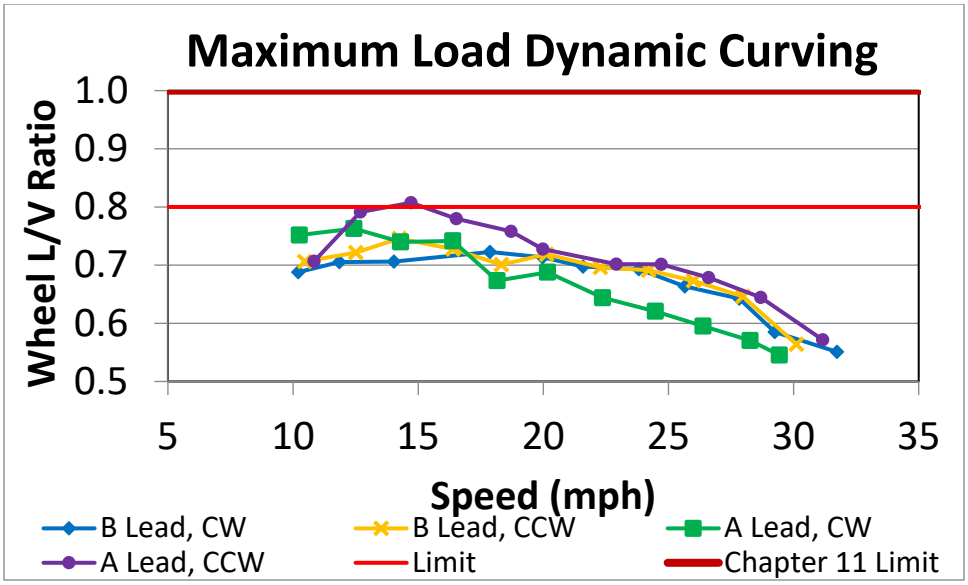


Figure 100. Maximum Load Dynamic Curve Wheel L/V Results versus Speed

In the maximum load condition and with CSM 70 pads, the car did not meet the single wheel L/V criterion at 14 mph when traveling CCW on the dynamic curve zone with the A-end leading. Therefore, on behalf of the DOE, TTCI is requesting an exception from the AAR EEC. Figure 101 shows a plot of the worst-case single wheel L/V that occurs on the right wheel on Axle 6 during a 14-mph run CCW with the A-end leading. The maximum load dynamic curving test runs CCW with the B-end leading, CW with the B-end leading, and CW with the A-end leading all met the criteria.

The effect of changing pad type from CSM 70 to CSM 58 on performance in this regime will be investigated using modeling and presented in the post test analysis report, complete with simulations of the other cask loads.

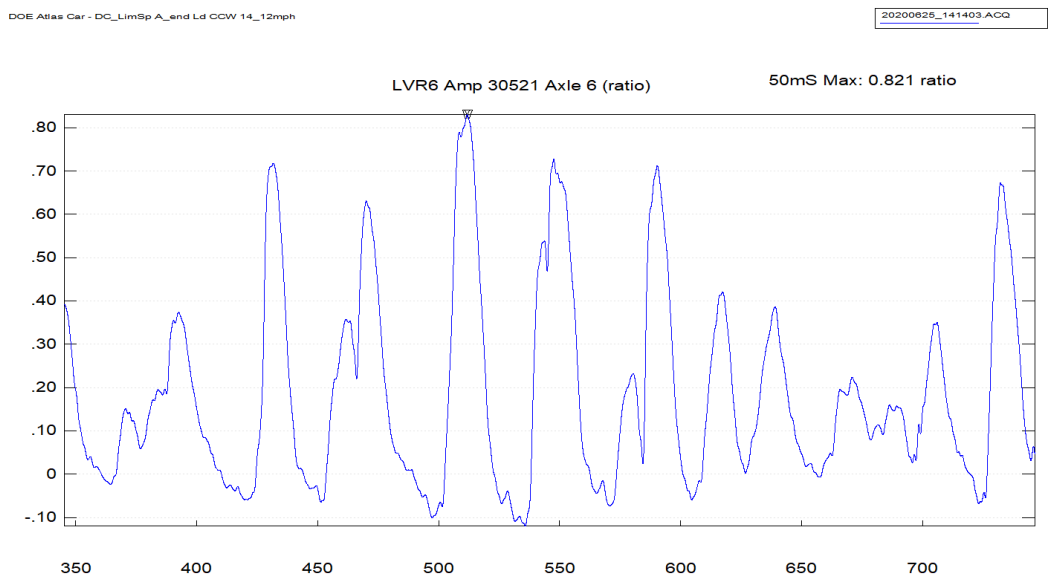


Figure 101. Axle 6 Right Wheel L/V Ratio during A-end Leading Maximum Load CCW Dynamic Curving at 14 mph

8.5.9 Pitch and Bounce (Chapter 11)

Pitch and bounce testing was performed in the maximum load condition only per Standard S-2043. The test was performed on June 30, 2020, and July 1, 2020. The coefficient of friction was 0.53 on the east rail and 0.50 on the west rail. Abe Meddah, TTCI Principal Investigator I, witnessed the pitch and bounce test as the AAR Observer, per Standard S-2043 requirements. The car met criteria for pitch and bounce. Table 75 shows a summary of pitch and bounce test results, and Figure 102 shows a plot of maximum vertical acceleration versus speed. The tests presented in this section were done with the prototype CSM 70 suspension pads. The effect of changing pad type from CSM 70 to CSM 58 on performance in this regime will be investigated using modeling and presented in the post test analysis report.

Table 75. Summary of Pitch and Bounce (Chapter 11) Results

Criterion	Limiting Value	Test Result
Roll angle (degree)	4	0.2
Maximum wheel L/V	0.8	0.09
Maximum truck side L/V	0.5	0.07
Minimum vertical wheel load	25 (% of static)	71%
Lateral peak-to-peak acceleration (g)	1.3	0.09
Maximum lateral acceleration (g)	0.75	0.06
Maximum vertical acceleration (g)	0.90	0.25
Maximum vertical suspension deflection	95 %	56%

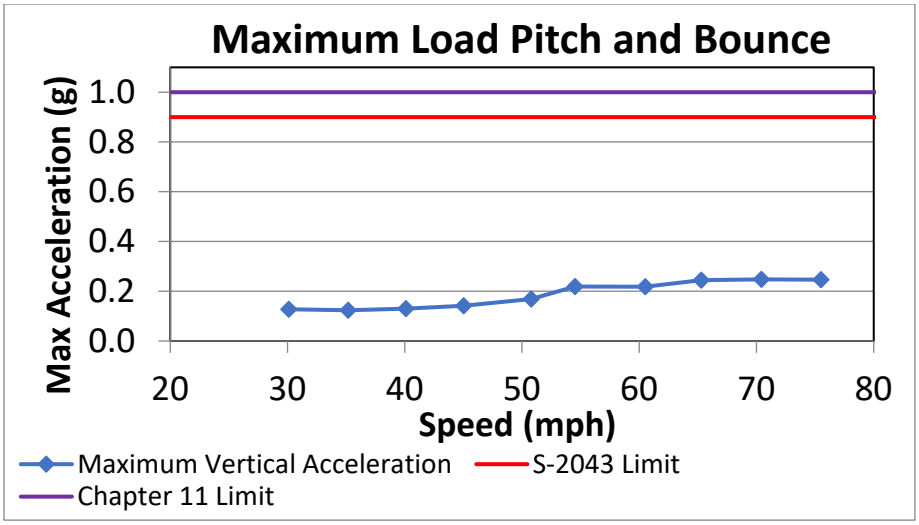


Figure 102. Maximum Test Load Pitch and Bounce, Maximum Vertical Acceleration versus Speed

8.5.10 Pitch and Bounce (Special)

The pitch and bounce (Special) test regime was not tested based on the span bolster center spacing. As described in the test plan (Appendix B) the Atlas car's span bolster center spacing (38.5 feet) is very close to the wavelength of the standard pitch and bounce test section (39 feet).

8.5.11 Minimum Load Single Bump Test

The minimum load single bump test was performed on October 5, 2020. This test is intended to represent a grade crossing and was installed at T15 on the Transit Test Track (TTT) at the TTC. The single bump was a flat-topped ramp with the initial elevation change over 7 feet, a steady elevation over 20 feet, ramping back down over 7 feet. The coefficient of friction on the southeast rail was 0.56 and the coefficient of friction on the northwest rail was 0.54. Adam Klopp, TTCI Principal Investigator I, witnessed the minimum load single bump test as the AAR Observer, per Standard S-2043 requirements. The tests presented in this section were done with the prototype CSM 70 suspension pads. The effect of changing pad type from CSM 70 to CSM 58 on performance in this regime will be investigated using modeling and presented in the post test analysis report.

The car met minimum load single bump criteria. Table 76 shows a summary of test results. Figure 103 shows a plot of maximum vertical acceleration versus speed for the minimum load single bump test.

Table 76. Summary of Test Results for the Minimum Load Single Bump Test

Criterion	Limiting Value	Test Result
Roll angle (degree)	4	0.4
Maximum wheel L/V	0.8	0.13
Maximum truck side L/V	0.5	0.10
Minimum vertical wheel load	25 (% of static)	70%
Lateral peak-to-peak acceleration (g)	1.3	0.17
Maximum lateral acceleration (g)	0.75	0.09
Maximum vertical acceleration (g)	0.90	0.37
Maximum vertical suspension deflection	95 %	15%

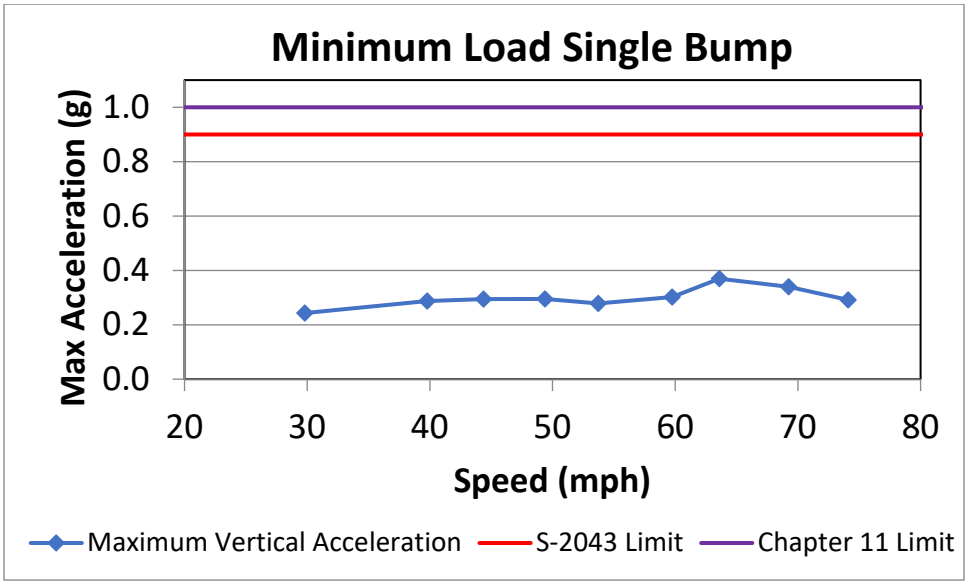


Figure 103. Maximum Vertical Acceleration versus Speed for Minimum Load Single Bump Test

8.5.12 Maximum Load Single Bump Test

The maximum load single bump test was performed on July 6, 2020. The coefficient of friction on the southeast rail was 0.54 and the coefficient of friction on the northwest rail was 0.54. Ulrich Spangenberg, TTCI Principal Investigator I, witnessed the maximum load single bump test as the AAR Observer, per Standard S-2043 requirements. Tests presented in this section were done with the prototype CSM 70 suspension pads. The effect of changing pad type from CSM 70 to CSM 58 on performance in this regime will be investigated using modeling and presented in the post test analysis report.

The car met the maximum load single bump criteria. Table 77 shows a summary of test results. Figure 104 shows a plot of maximum vertical acceleration versus speed for the maximum load single bump test.

Table 77. Summary of Test Results for the Maximum Load Single Bump Test

Criterion	Limiting Value	Test Result
Roll angle (degree)	4	0.3
Maximum wheel L/V	0.8	0.12
Maximum truck side L/V	0.5	0.08
Minimum vertical wheel load	25 (% of static)	74%
Lateral peak-to-peak acceleration (g)	1.3	0.16
Maximum lateral acceleration (g)	0.75	0.08
Maximum vertical acceleration (g)	0.90	0.34
Maximum vertical suspension deflection	95 %	58%

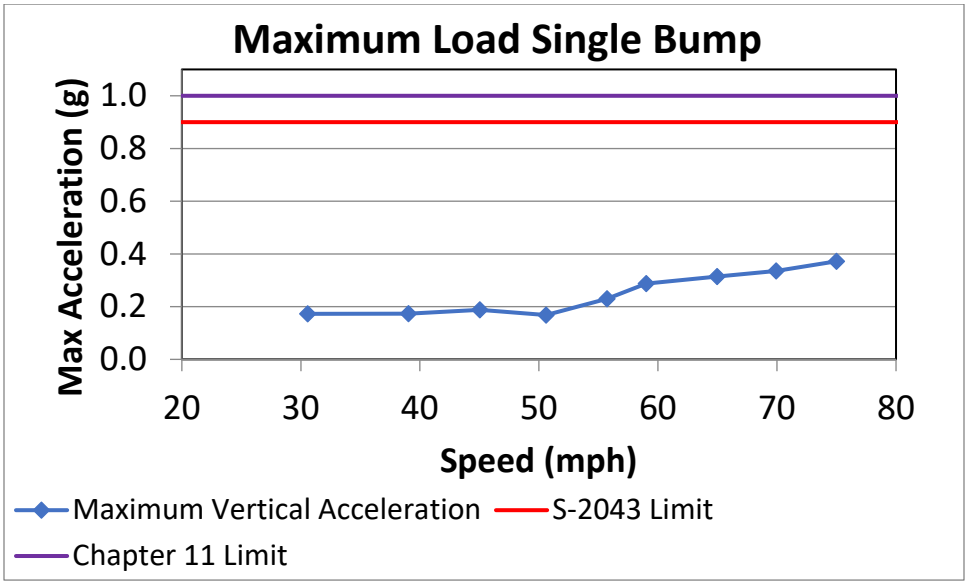


Figure 104. Maximum Vertical Acceleration versus Speed for Maximum Load Single Bump Test

8.5.13 Minimum Test Load Curve Entry/Exit

Spiral negotiation is tested in the limiting spiral test zone. This test zone has a steady change in curvature from 0 to 10 degrees and a steady change in superelevation from 0 to 4 3/8 inches in 89 feet. The limiting spiral test section is located on the same curve as the dynamic curving test section, so those tests were performed at the same time. The data from the normal spirals adjacent to the constant curve sections is also presented in this section. The tests presented in this section were completed with the prototype CSM 70 pads. The effect of changing pad type from CSM 70 to CSM 58 on performance in this regime will be investigated using modeling and presented in the post test analysis report.

8.5.13.1 Minimum Load Limiting Spiral Negotiation

The minimum load limiting spiral negotiation tests were conducted with the minimum load dynamic curving tests on June 25, 2021, and June 28, 2021. Minimum load limiting spiral testing was conducted, CW and CCW, with both the A-end leading and the B-end leading. The CW tests

correspond to the spiral entry and CCW tests correspond to the spiral exit. Table 78 lists the rail friction data for the different test configurations. When two or more test configurations were done on the same day, rail friction was only measured once. Ulrich Spangenberg and Adam Klopp, both TTCI Principal Investigator I's, witnessed the minimum load limiting spiral negotiation test as the AAR Observer, per Standard S-2043 requirements

Table 78. Minimum Load Limiting Spiral Test Date and Rail Friction Data

Test Condition	Date	Coefficient of Friction	
		Inside Rail	Outside Rail
Minimum Load, A-end Leading, CW	06/28/2021	0.55	0.54
Minimum Load, A-end Leading, CCW	06/25/2021	0.50	0.50
Minimum Load, B-end Leading, CW	06/25/2021	0.50	0.50
Minimum Load, B-end Leading, CCW	06/28/2021	0.55	0.54

The car met the criteria for the minimum load limiting spiral tests. Table 79 represents the worst-case test results for each car orientation. Figure 105 is the wheel L/V ratio version speed for each of the maximum test load configurations.

Table 79. Minimum Load Limiting Spiral Summary Test Results

Criterion	Limiting Value	A-End CW	A-End CCW	B-End CW	B-End CCW
Roll angle (degree)	4	0.70	1.60	0.70	1.30
Maximum wheel L/V	0.8	0.62	0.69	0.67	0.61
Maximum truck side L/V	0.5	0.38	0.40	0.42	0.39
Minimum vertical wheel load	25 (% of static)	54%	56%	57%	57%
Lateral peak-to-peak acceleration (g)	1.3	0.17	0.14	0.18	0.17
Maximum lateral acceleration (g)	0.75	0.15	0.14	0.14	0.16
Maximum vertical acceleration (g)	0.90	0.11	0.15	0.16	0.12
Maximum vertical suspension deflection	95 %	17%	20%	17%	20%

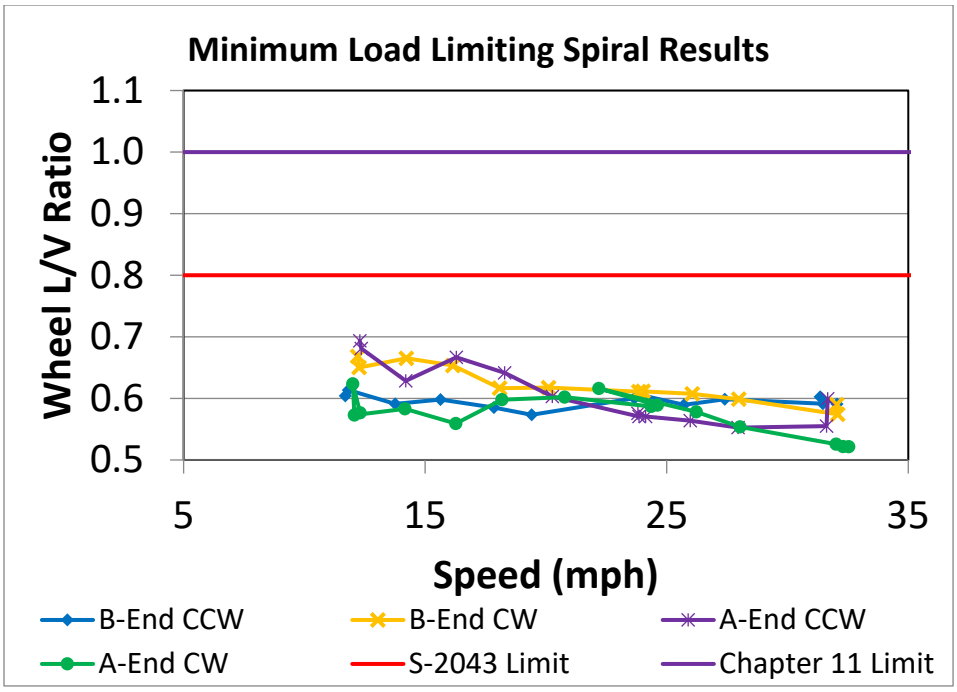


Figure 105. Minimum Load Limiting Spiral Results

8.5.13.2 Minimum Load Normal Spiral Negotiation

Minimum load normal spiral negotiation tests were conducted during minimum load constant curving tests. Minimum load normal spiral testing was conducted, CW and CCW, with both the A-end leading and the B-end leading. Data were summarized from the spirals at each end of each test curves except for the 12-degree north spiral. The 12-degree north spiral is not a normal spiral, because, although the curvature changes steadily over 200 feet, the superelevation change takes place in the middle 100 feet. The AAR does not require tests over this non-typical spiral geometry. Table 80 lists the test dates and the rail friction data for the different test configurations. When two or more test configurations were done on the same day, rail friction was only measured once. Abe Meddah and Adam Klopp, both TTCI Principal Investigator Is, witnessed the minimum load constant curve testing as AAR Observers per Standard S-2043 requirements.

Table 80. Minimum Load Normal Spiral Negotiation Test Dates and Rail Friction Data

Test Condition	Date	Coefficient of Friction					
		7.5-degree		10-degree		12-degree	
		Inside	Outside	Inside	Outside	Inside	Outside
A-end Leading, CW	09/16/2020	0.52	0.53	0.54	0.55	0.53	0.54
A-end Leading, CCW	09/15/2020	0.54	0.55	0.54	0.54	0.55	0.55
B-end Leading, CW	09/15/2020	0.54	0.55	0.54	0.54	0.55	0.55
B-end Leading, CCW	10/01/2020	0.50	0.53	0.53	0.55	0.52	0.54

The car met the criteria for the minimum load normal spiral tests. Table 81 shows a summary of the test results. Figure 106 represents the CW B-end leading for the minimum load normal spiral.

Table 81. Minimum Load Normal Spiral Summary of Test Results

Criterion	Limiting Value	A-End CW	A-End CCW	B-End CW	B-End CCW
Roll angle (degree)	4	0.20	0.30	0.30	0.20
Maximum wheel L/V	0.8	0.62	0.62	0.53	0.56
Maximum truck side L/V	0.5	0.33	0.30	0.34	0.34
Minimum vertical wheel load	25 (% of static)	55%	59%	59%	60%
Lateral peak-to-peak acceleration (g)	1.3	0.14	0.11	0.12	0.12
Maximum lateral acceleration (g)	0.75	0.13	0.10	0.11	0.10
Maximum vertical acceleration (g)	0.90	0.16	0.17	0.14	0.14
Maximum vertical suspension deflection	95 %	17%	17%	13%	14%

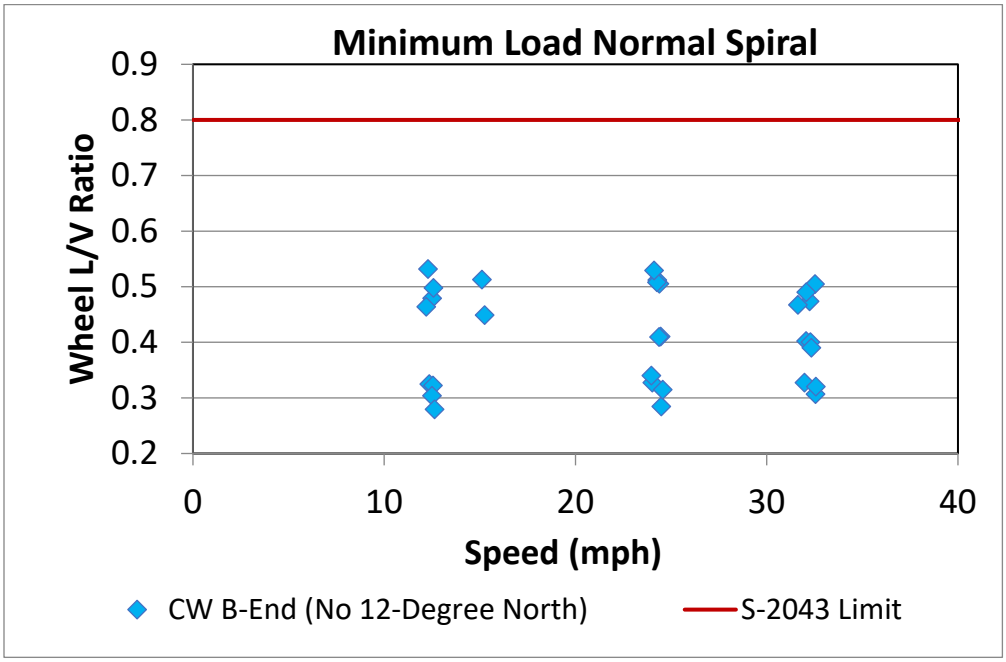


Figure 106. Minimum Load Normal Spiral B-End CW Summary

8.5.14 Maximum Load Curve Entry/Exit

Spiral negotiation is tested in the limiting spiral test zone. This test zone has a steady change in curvature from 0 to 10 degrees and a steady change in superelevation from 0 to 4 3/8 inches in 88 feet. The limiting spiral test section is located on the same curve as dynamic curving, so those tests were performed at the same time. The data from the normal spirals adjacent to the constant

curve sections are also presented in this section. The tests presented in this section were completed with the prototype CSM 70 pads. The effect of changing pad type from CSM 70 to CSM 58 on performance in this regime will be investigated using modeling and presented in the post test analysis report.

8.5.14.1 Maximum Load Limiting Spiral Negotiation

Maximum load limiting spiral testing was conducted CW and CCW, with both the A-end leading and the B-end leading at the same time as the dynamic curving tests (see Section 4.5.8). The CW tests corresponded to spiral entry, and the CCW tests corresponded to spiral exit. Table 82 lists the test dates and the rail friction data. When two or more test configurations were done on the same day, friction was only measured once. Abe Meddah, TTCI Principal Investigator I, witnessed the maximum load limiting spiral negotiation test as the AAR Observer, per Standard S-2043 requirements.

Table 82. Maximum Load Limiting Spiral Test Dates and Rail Friction Data

Test Condition	Date	Coefficient of Friction	
		Inside Rail	Outside Rail
Loaded Cask, A-end Leading, CW	06/30/2020	0.50	0.50
Loaded Cask, A-end Leading, CCW	06/25/2020	0.55	0.55
Loaded Cask, B-end Leading, CW	06/25/2020	0.55	0.55
Loaded Cask, B-end Leading, CCW	06/29/2020	0.50	0.50

The car met the criteria for the maximum load limiting spiral tests. Table 83 represents the worst-case test results for each orientation. Figure 107 shows a plot of the wheel L/V ratios for each car orientation versus the speed.

Table 83. Maximum Load Limiting Spiral Summary Test Results

Criterion	Limiting Value	A-End CW	A-End CCW	B-End CW	B-End CCW
Roll angle (degree)	4	1.00	1.40	0.60	1.30
Maximum wheel L/V	0.8	0.74	0.60	0.71	0.65
Maximum truck side L/V	0.5	0.39	0.36	0.37	0.35
Minimum vertical wheel load	25 (% of static)	30%	29%	45%	52%
Lateral peak-to-peak acceleration (g)	1.3	0.17	0.14	0.11	0.12
Maximum lateral acceleration (g)	0.75	.015	0.14	0.12	0.12
Maximum vertical acceleration (g)	0.90	0.17	0.07	0.06	0.08
Maximum vertical suspension deflection	95 %	56%	64%	64%	66%

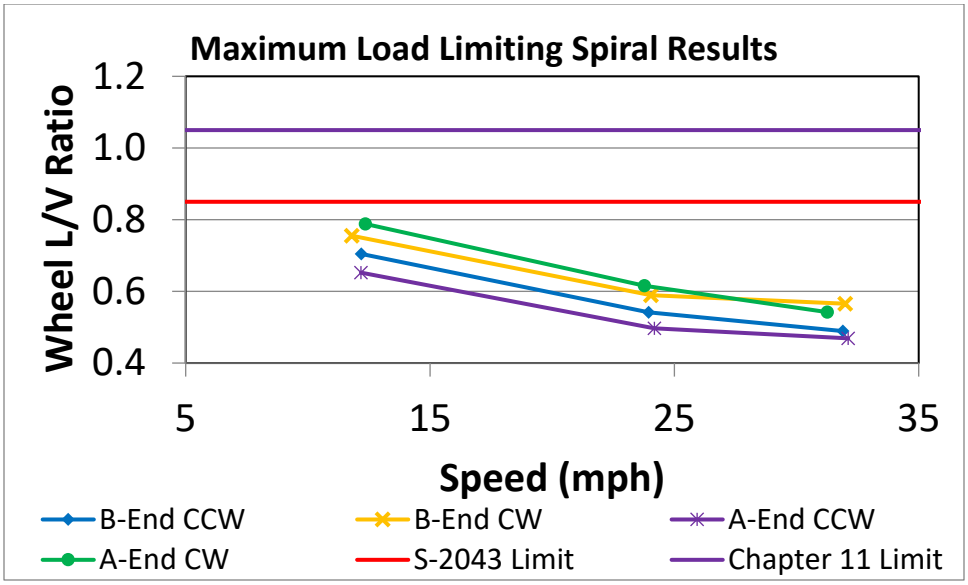


Figure 107. Maximum Load Limiting Spiral Results

8.5.14.2 Maximum Load Normal Spiral Negotiation

Maximum load normal spiral negotiation tests were conducted with the maximum loaded constant curving tests. Maximum load normal spiral testing was conducted CW and CCW, with both the A-end leading and the B-end leading. The data were summarized from the spirals at each end of each test curve except the 12-degree north spiral. The 12-degree north spiral is not a normal spiral, because, although the curvature changes steadily over 200 feet, the superelevation change takes place in the middle 100 feet. The AAR does not require tests over this non-typical spiral geometry. Table 84 shows the test dates and the rail friction data for the different test configurations. When two or more test configurations were done on the same day, the rail friction was only measured once. Abe Meddah, TTCI Principal Investigator I, witnessed the maximum load constant curve testing as the AAR Observer, per Standard S-2043 requirements.

Table 84. Maximum Load Normal Spiral Negotiation Test Dates and Rail Friction Data

Test Condition	Date	Coefficient of Friction					
		7.5-degree		10-degree		12-degree	
		Inside	Outside	Inside	Outside	Inside	Outside
A-end Leading, CW	06/26/2020	0.54	0.55	0.52	0.53	0.53	0.52
A-end Leading, CCW	06/25/2020	0.53	0.54	0.52	0.53	0.54	0.55
B-end Leading, CW	06/25/2020	0.53	0.54	0.52	0.53	0.54	0.55
B-end Leading, CCW	06/29/2020	0.50	0.50	0.50	0.50	0.50	0.50

The car met the criteria for maximum load normal spiral tests. Table 83 shows a summary of the test results. Figure 108 shows the maximum wheel L/V ratios for the CW B-end leading normal spiral runs.

Table 85. Maximum Load Normal Spiral Negotiation Summary of Test Results Without 12-Degree North Spiral

Criterion	Limiting Value	A-End CW	A-End CCW	B-End CW	B-End CCW
Roll angle (degree)	4	0.20	0.20	0.20	0.20
Maximum wheel L/V	0.8	0.54	0.44	0.49	0.56
Maximum truck side L/V	0.5	0.29	0.24	0.30	0.30
Minimum vertical wheel load	25 (% of static)	59%	58%	56%	62%
Lateral peak-to-peak acceleration (g)	1.3	0.12	0.08	0.11	0.10
Maximum lateral acceleration (g)	0.75	0.12	0.13	0.14	0.11
Maximum vertical acceleration (g)	0.90	0.08	0.11	0.09	0.09
Maximum vertical suspension deflection	95 %	31%	38%	36%	35%

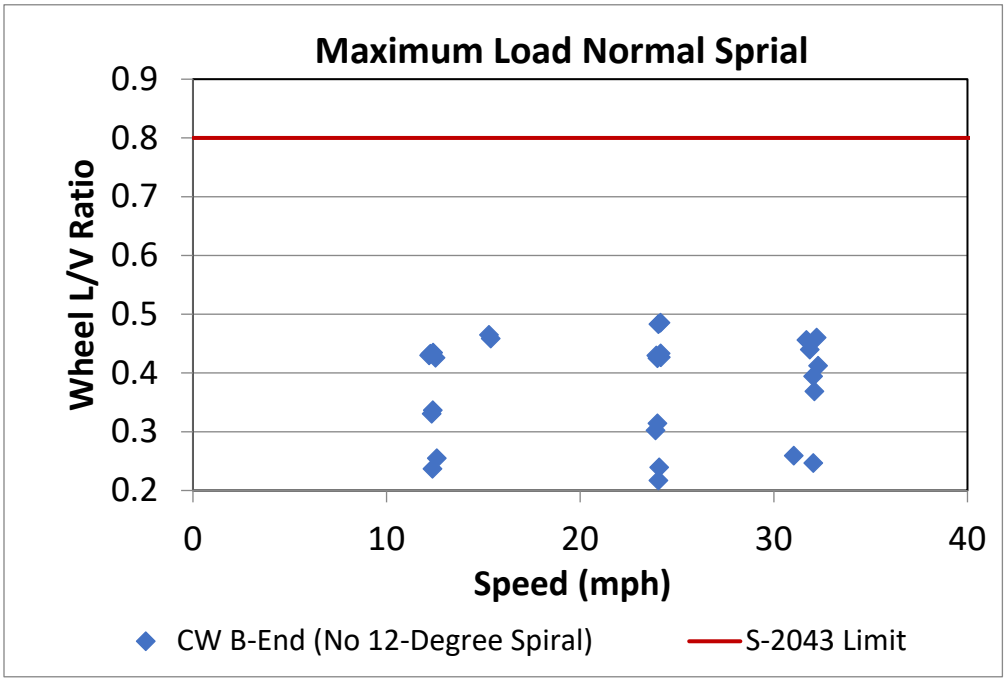


Figure 108. Maximum Load Normal Spiral B-End CW Summary

8.5.15 Minimum Load Curving with Single Rail Perturbation

Minimum load curving with single rail perturbation tests were conducted with the inside rail bump and the outside rail dip about 250 feet apart on the same 12-degree curve. The inside rail bump was a flat-topped ramp with an increase in elevation over 6 feet, a steady elevation over 12 feet, and a decrease in elevation over 6 feet. The outside rail dip was the reverse. The testing was conducted with the A-end leading and the B-end leading in the CW and CCW directions. Adam Klopp, TTCI Principal Investigator I, witnessed the minimum load curving with single rail

perturbation testing, as the AAR Observer, per Standard S-2043 requirements. This set of tests was performed twice, once with CSM 70 pads and then with CSM 65 pads.

Table 86 shows the test dates and the rail friction data for the different test configurations and primary pads. The test presented in this section were completed with the prototype CSM 70 pads and CSM 65 pads. The results show improved performance with the CSM 65 pads, presumably because they are softer. After these tests, a set of even softer pads, CSM 58 production pads, were installed on the Atlas car, but these tests were not repeated. The effect of changing pad type from CSM 70 to CSM 58 on performance in this regime will be investigated using modeling and presented in the post test analysis report.

Table 86. Minimum Load Curving with Single Rail Perturbation Test Dates and Rail Friction Data

Test Zone/Pads	Date	Inside Rail Friction	Outside Rail Friction
CSM 70 Bump	10/05/2020	0.52	0.56
CSM 65 Bump	12/09/2020	0.50	0.50
CSM 70 Dip	10/05/2020	0.51	0.53
CSM 65 Dip	12/09/2020	0.50	0.50

The car did not meet the criteria for minimum load curving with a single rail perturbation. Table 87 shows a summary of the test results for both the CSM 70 and CSM 65 primary pads.

Table 87. Minimum Load Curving with Single Rail Perturbation Summary of Test Results

Criterion	Limiting Value	CSM 70 Pads Bump	CSM 65 Pads Bump	CSM 70 Pads Dip	CSM 65 Pads Dip
Roll angle (degree)	4	1.30	1.08	0.77	0.61
Maximum wheel L/V	0.8	0.77	0.68	**0.88**	**0.84**
Maximum truck side L/V	0.5	0.45	0.36	**0.50**	0.44
Minimum vertical wheel load	25 (% of static)	43%	46%	39%	46%
Lateral peak-to-peak acceleration (g)	1.3	0.24	0.20	0.16	0.18
Maximum lateral acceleration (g)	0.75	0.20	0.16	0.12	0.15
Maximum vertical acceleration (g)	0.90	0.15	0.14	0.28	0.28
Maximum vertical suspension deflection	95 %	34%	34%	20%	17%

With the CSM 70 primary pads the car did not meet the Standard S-2043 criteria for the maximum wheel L/V ratio in the CCW direction with both the A and B ends leading through the dip. Also, the CCW A-end leading's maximum truck side L/V was equal to the Standard S-2043

limit. Figure 109 shows the minimum load single rail dip wheel L/V ratio results for the CSM 70 primary pads. Figure 110 shows the CSM 70 primary pad single rail dip worst-case results that did not meet the Standard S-2043 limit. The top plot in Figure 110 shows the 50 ms maximum L/V ratio for axle 6's right (high rail) wheel. The bottom plot shows the 5ft maximum L/V for D-truck right side (high rail).

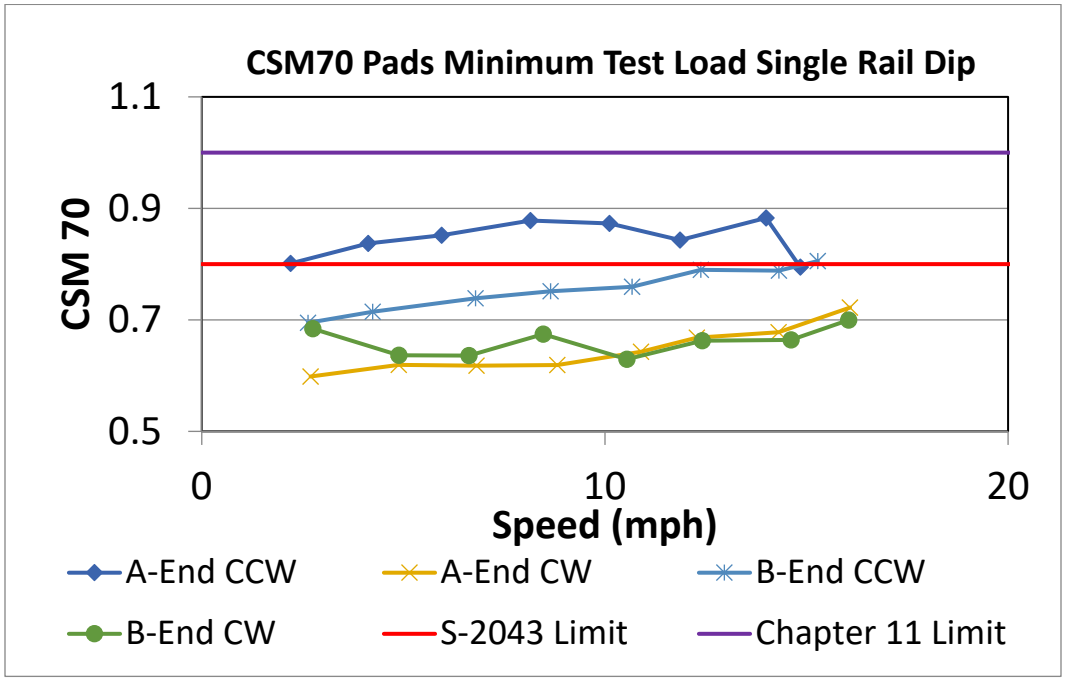


Figure 109. Wheel L/V vs Speed for CSM 70 Primary pads Through the Single Rail Dip

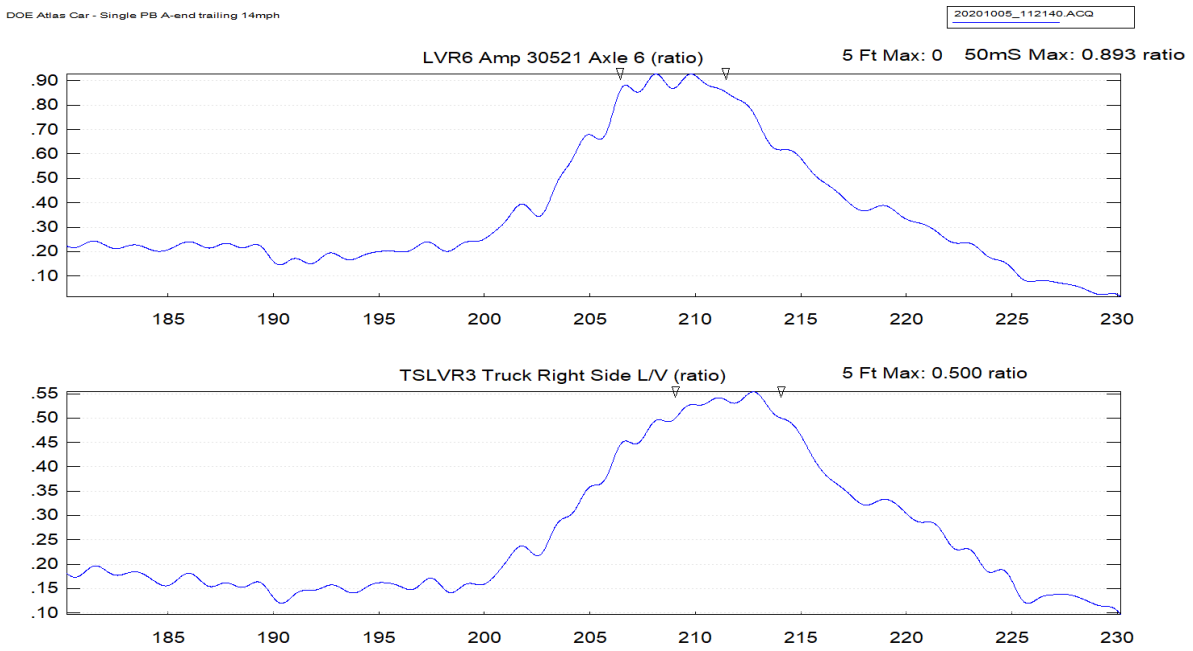


Figure 110. Right Side Axle 6 Single Wheel L/V Ratio and Right Side D Truck Side L/V Ratio with CSM 70 Primary Pads, Minimum Load, Single Rail Dip at 14 mph.

The results of tests conducted with CSM 65 primary pads showed improved performance, but still did not meet the Standard S-2043 limit for maximum wheel L/V in the CCW direction with A-end leading through the dip. Therefore, on behalf of the DOE, TTCI is requesting an exception from the AAR EEC. Figure 111 shows the minimum load single rail dip wheel L/V ratio results for the CSM 65 primary pads. Figure 112 shows the minimum load single rail dip 50 ms max L/V on Axle 6 right (high rail) wheel.

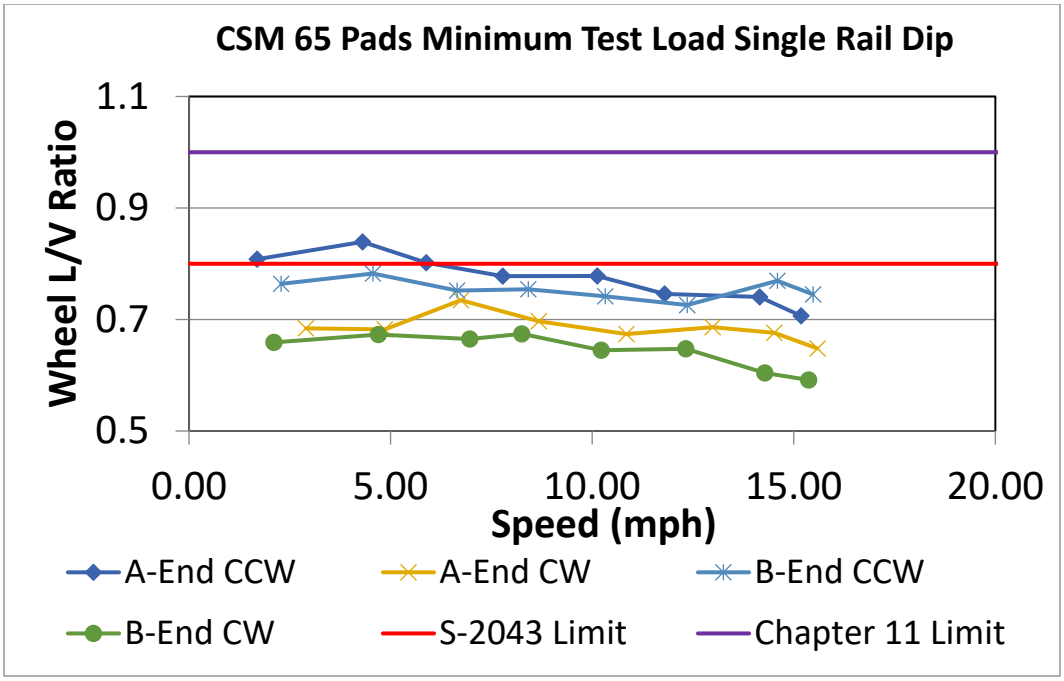


Figure 111. Wheel L/V vs Speed for CSM 65 Primary pads Through the Single Rail Dip

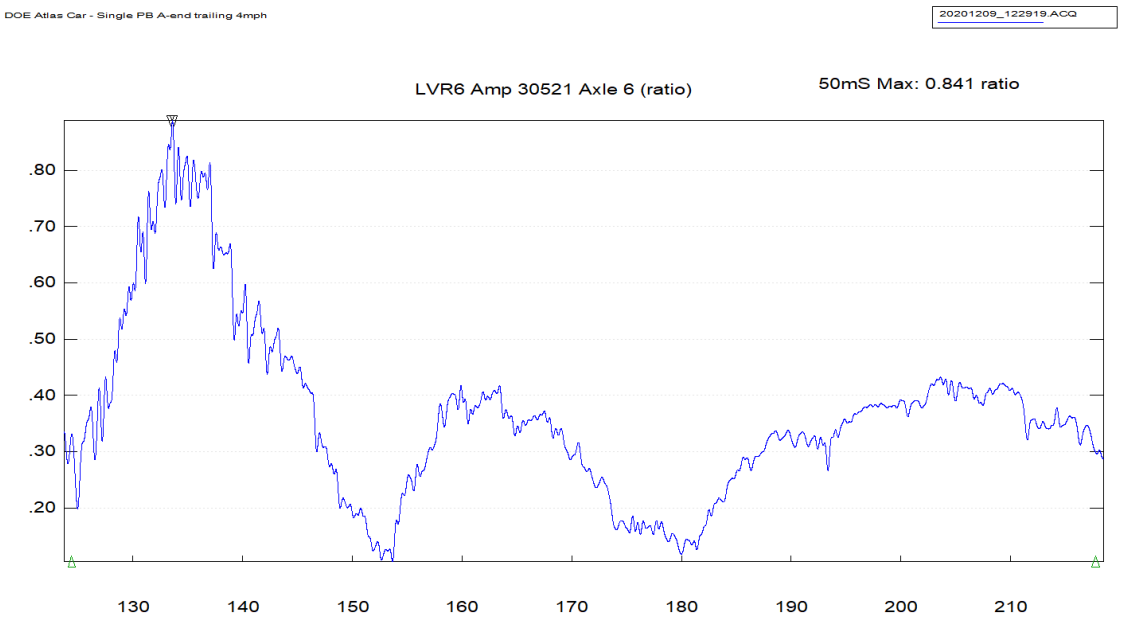


Figure 112. CSM 65 Primary pads Minimum Load Single Rail Dip 50ms Max L/V Axle 6 Right Wheel

8.5.16 Maximum Load Curving with Single Rail Perturbation

Maximum load curving with single rail perturbation tests were conducted with the inside rail bump and the outside rail dip about 250 feet apart on the same 12-degree curve. The inside rail bump was a flat-topped ramp with an increase in elevation over 6 feet, a steady elevation over 12 feet, and a decrease in elevation over 6 feet. The outside rail dip was the reverse. The testing was

conducted with the A-end leading and with the B-end leading in the CW and CCW directions. Adam Klopp, TTCI Principal Investigator I, witnessed the maximum load curving with single rail perturbation testing as the AAR Observer, per Standard S-2043 requirements.

Table 88 shows the test dates and the rail friction data for the different test configurations. The tests presented in this section were completed with the prototype CSM 70 pads. The effect of changing pad type from CSM 70 to CSM 58 on performance in this regime will be investigated using modeling and presented in the post test analysis report.

Table 88. Maximum Load Curving with Single Rail Perturbation Test Dates and Rail Friction Data

Test Zone/Pads	Date	Inside Rail Friction	Outside Rail Friction
CSM 70 Bump	08/26/2020	0.48	0.48
CSM 70 Dip	08/26/2020	0.47	0.47

The car met the criteria for the maximum load curving with a single rail perturbation. Table 89 shows a summary of test results, and Figure 113 and Figure 114 show plots of the vertical wheel load versus speed for the single rail bump and dip perturbations.

Table 89. Maximum Load Curving with Single Rail Perturbation Summary of Test Results

Criterion	Limiting Value	Bump	Dip
Roll angle (degree)	4	2.24	1.59
Maximum wheel L/V	0.8	0.65	0.79
Maximum truck side L/V	0.5	0.38	0.44
Minimum vertical wheel load	25 (% of static)	48%	45%
Lateral peak-to-peak acceleration (g)	1.3	0.20	0.16
Maximum lateral acceleration (g)	0.75	0.14	0.14
Maximum vertical acceleration (g)	0.90	0.10	0.15
Maximum vertical suspension deflection	95 %	59%	59%

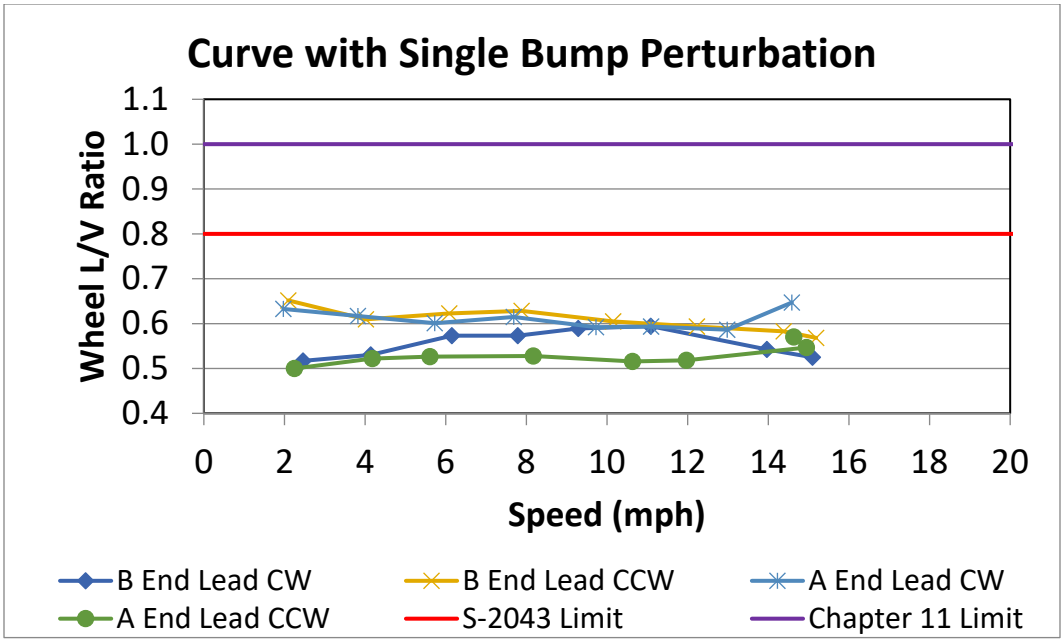


Figure 113. Maximum Load Curving with Single Rail Bump Perturbation Plot of Vertical Wheel Load versus Speed

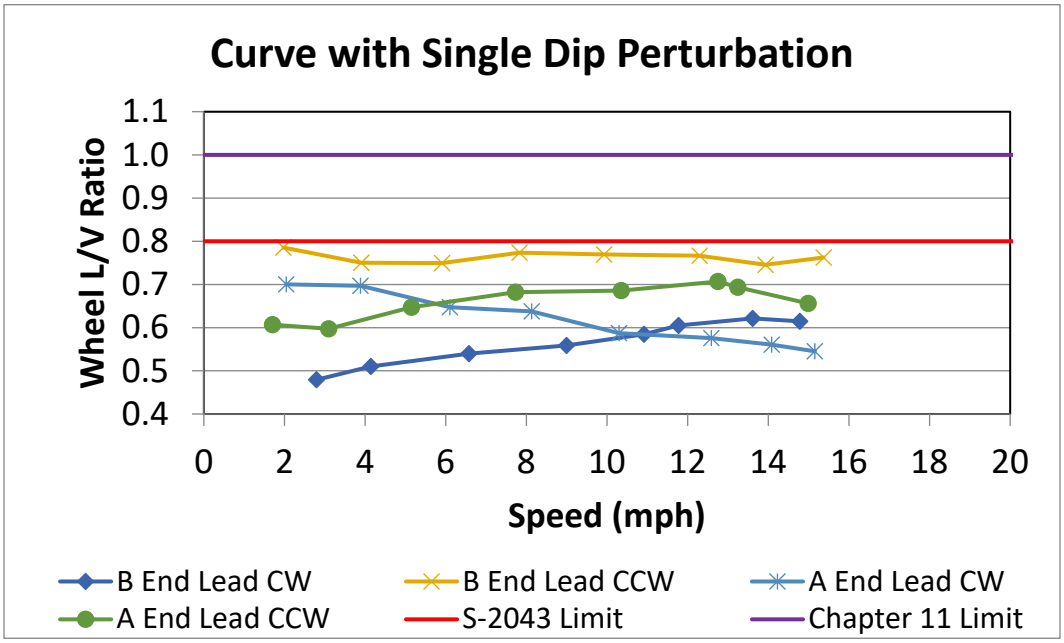


Figure 114. Maximum Load Curving with Single Rail Dip Perturbation Plot of Vertical Wheel Load versus Speed

8.5.17 Minimum Load Standard Chapter 11 Constant Curving

The minimum load constant curving tests were conducted with normal spiral negotiation tests (see Section 4.5.13.2). The minimum load constant curve testing was conducted both CW and CCW, with both the A-end leading and the B-end leading. The data are summarized from the 7.5-, 12-, and 10-degree curves on the Wheel Rail Mechanism (WRM) loop. Table 90 shows the test dates and the rail friction data for the different test configurations. When two or more test configurations were done on the same day, the rail friction was only measured once. Abe Meddah and Adam Klopp, both TTCI Principal Investigator Is, witnessed the minimum load constant curve testing as the AAR Observers, per Standard S-2043 requirements. The tests presented in this section were completed with the prototype CSM 70 pads. The effect of changing pad type from CSM 70 to CSM 58 on performance in this regime will be investigated using modeling and presented in the post test analysis report.

Table 90. Minimum Load Constant Curving Test Dates and Rail Friction Data

Test Condition	Date	Coefficient of Friction					
		7.5-degree		10-degree		12-degree	
		Inside	Outside	Inside	Outside	Inside	Outside
A-end Leading, CW	09/16/2020	0.52	0.53	0.54	0.55	0.53	0.54
A-end Leading, CCW	09/15/2020	0.54	0.55	0.54	0.54	0.55	0.55
B-end Leading, CW	09/15/2020	0.54	0.55	0.54	0.54	0.55	0.55
B-end Leading, CCW	10/01/2020	0.50	0.53	0.53	0.55	0.52	0.54

The car did not meet the maximum single wheel L/V ratio criterion or the 95th percentile single wheel L/V ratio criterion in the 12-degree curve. Therefore, on behalf of the DOE, TTCI is requesting an exception from the AAR EEC. All other criteria were met. Table 91 shows a summary of the test results. The 50 millisecond maximum and 95 percent-wheel L/V ratio results did not meet the criteria in the CCW direction with both the A-end and the B-end leading. The 95 percent-wheel L/V ratio results did not meet the criteria in the CW direction with the B-end leading. Figure 115 shows a plot of the 95th percentile wheel L/V versus speed for the minimum load constant curving tests.

Figure 116 shows the worst-case condition where the data did not meet the maximum wheel L/V criterion. The data in Figure 116 is from the leading axle of the trailing span bolster, high rail side. The L/V ratio was above the 0.8 limit for a distance of 8.3 feet. The maximum contact angle on this wheel (B wheel of IWS 103) was about 72 degrees and the measured friction was 0.55. The NADAL limit is calculated as 0.94.

Table 91. Minimum Load Constant Curving Summary of Test Results

Criterion	Limiting Value	A-End CW	A-End CCW	B-End CW	B-End CCW
Roll angle (degree)	4	0.30	0.30	0.30	0.30
Maximum wheel L/V	0.8	0.63	**0.86**	0.68	**0.82**
95% Wheel L/V	0.6	0.55	**0.66**	**0.63**	**0.62**
Maximum truck side L/V	0.5	0.33	0.47	0.38	0.43
Minimum vertical wheel load	25 (% of static)	56%	55%	54%	54%
Lateral peak-to-peak acceleration (g)	1.3	0.14	0.19	.012	0.16
Maximum lateral acceleration (g)	0.75	0.14	0.17	0.13	0.13
Maximum vertical acceleration (g)	0.90	0.10	0.11	0.09	0.12
Maximum vertical suspension deflection	95 %	17%	18%	14%	14%

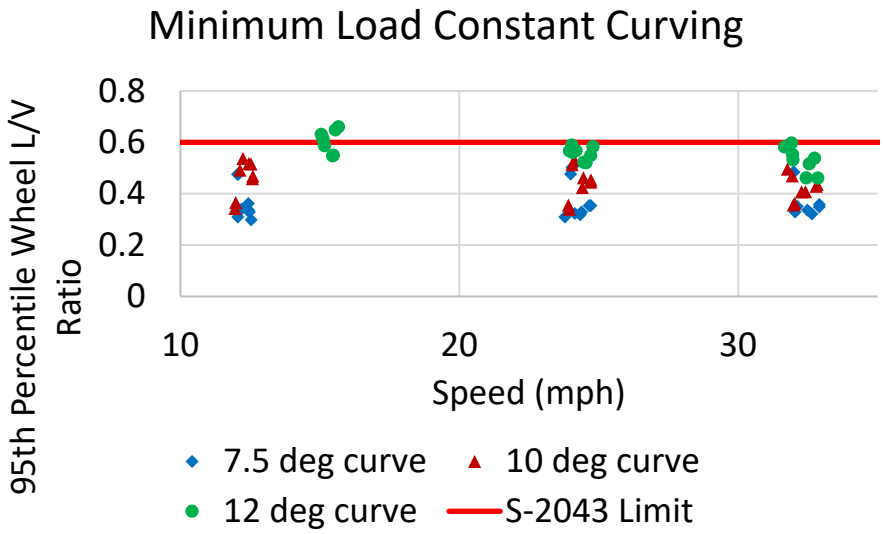


Figure 115. Minimum Load Constant Curving 95 Percent Wheel L/V versus Speed

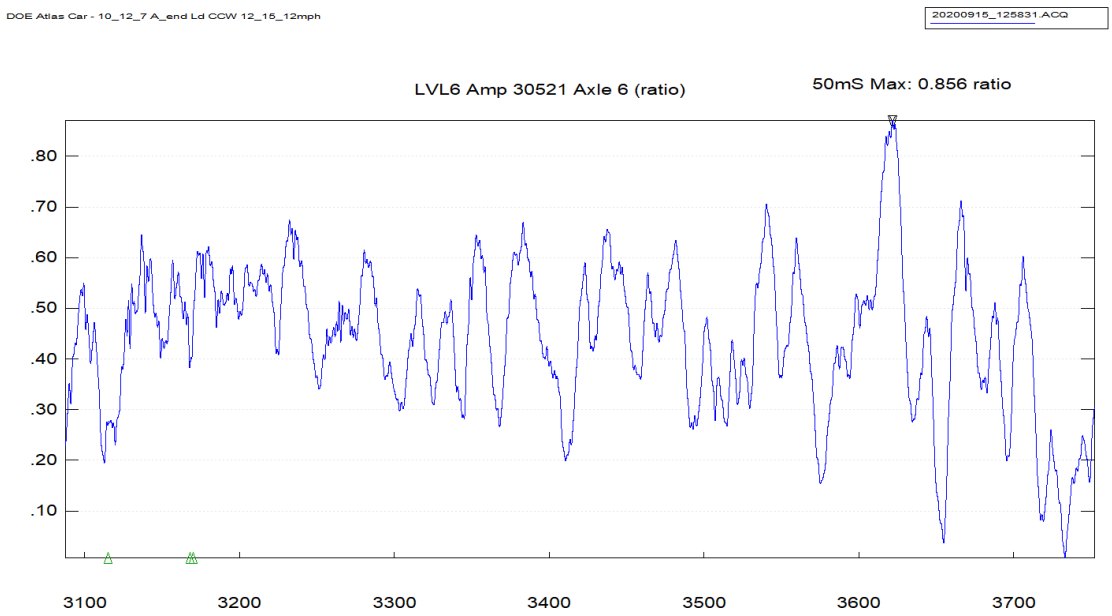


Figure 116. Minimum Load Constant Curving 12-degree curve CCW A-End Leading Axle 6 Left Wheel at 15 MPH Wheel L/V

8.5.18 Maximum Load Standard Chapter 11 Constant Curving

The maximum load constant curving tests were conducted with normal spiral negotiation tests (see section 4.5.14.2). The maximum load constant curve testing was conducted CW and CCW, with both the A-end leading and the B-end leading. Data are summarized from the 7.5-, 12-, and 10-degree curves on the WRM loop. Table 92 shows the test dates and the rail friction data for the different test configurations. When two or more test configurations were done on the same day, the rail friction was only measured once. Abe Meddah, TTCI Principal Investigator I, witnessed the maximum load constant curve testing as the AAR Observer, per Standard S-2043 requirements. The tests presented in this section were completed with the prototype CSM 70 pads. The effect of changing pad type from CSM 70 to CSM 58 on performance in this regime will be investigated using modeling and presented in the post test analysis report.

Table 92. Maximum Load Constant Curving Test Dates and Rail Friction Data

Test Condition	Date	Coefficient of Friction					
		7.5-degree		10-degree		12-degree	
		Inside	Outside	Inside	Outside	Inside	Outside
A-end Leading, CW	06/26/2020	0.54	0.55	0.52	0.53	0.53	0.52
A-end Leading, CCW	06/25/2020	0.53	0.54	0.52	0.53	0.54	0.55
B-end Leading, CW	06/25/2020	0.53	0.54	0.52	0.53	0.54	0.55
B-end Leading, CCW	06/29/2020	0.50	0.50	0.50	0.50	0.50	0.50

The car exceeded the required criteria on the 95 percent-wheel L/V in the CW B-end leading orientation. Therefore, on behalf of the DOE, TTCI is requesting an exception from the AAR EEC. Table 93 shows a summary of the test results. Figure 117 shows a plot of the summary for

the maximum load constant curving 95 percent-wheel L/V results. The loads were consistently over the criteria at 15 mph on the left wheel of Axles 3 and 5 throughout the 12-degree constant curving.

Figure 118 shows the exceeded criteria for the 95 percent wheel L/V for the 12-degree constant curving on the left wheel (high rail) of Axles 3 and 5. Axles 3 and 5 are the leading axles of the middle and trailing truck of the leading span bolster. Of these wheels, the lowest maximum contact angle was about 72 degrees (IWS 102 B wheel) and the measured friction was 0.55 so the NADAL limit is calculated as 0.94.

Table 93. Maximum Load Constant Curving Summary of Test Results

Criterion	Limiting Value	A-End CW	A-End CCW	B-End CW	B-End CCW
Roll angle (degree)	4	0.40	0.50	0.40	0.50
Maximum wheel L/V	0.8	0.64	0.73	0.72	0.70
95% Wheel L/V	0.6	0.55	0.55	**0.63**	0.53
Maximum truck side L/V	0.5	0.34	0.37	0.38	0.37
Minimum vertical wheel load	25 (% of static)	49%	50%	50%	45%
Lateral peak-to-peak acceleration (g)	1.3	0.12	0.11	0.17	0.11
Maximum lateral acceleration (g)	0.75	0.15	0.15	0.17	0.14
Maximum vertical acceleration (g)	0.90	0.08	0.08	0.08	0.09
Maximum vertical suspension deflection	95 %	50%	42%	42%	40%

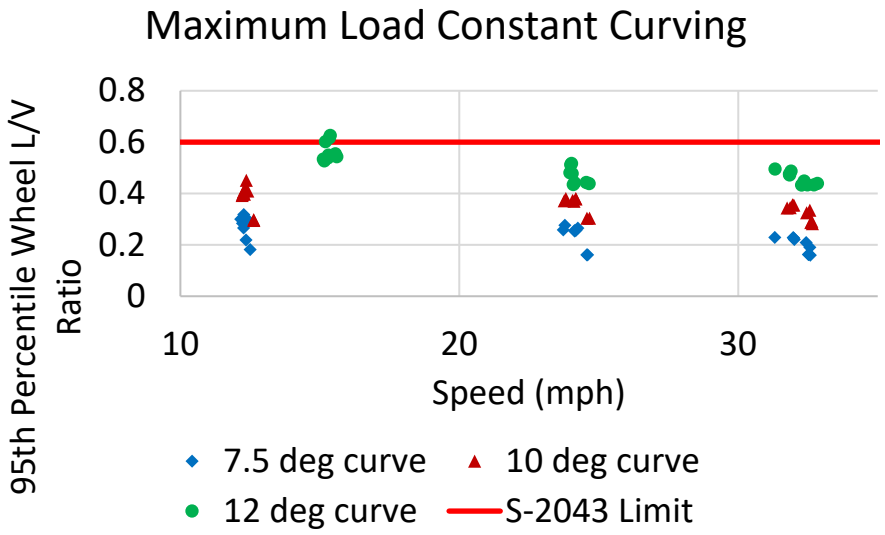


Figure 117. Maximum Load Constant Curving 95 Percent Wheel L/V versus Speed

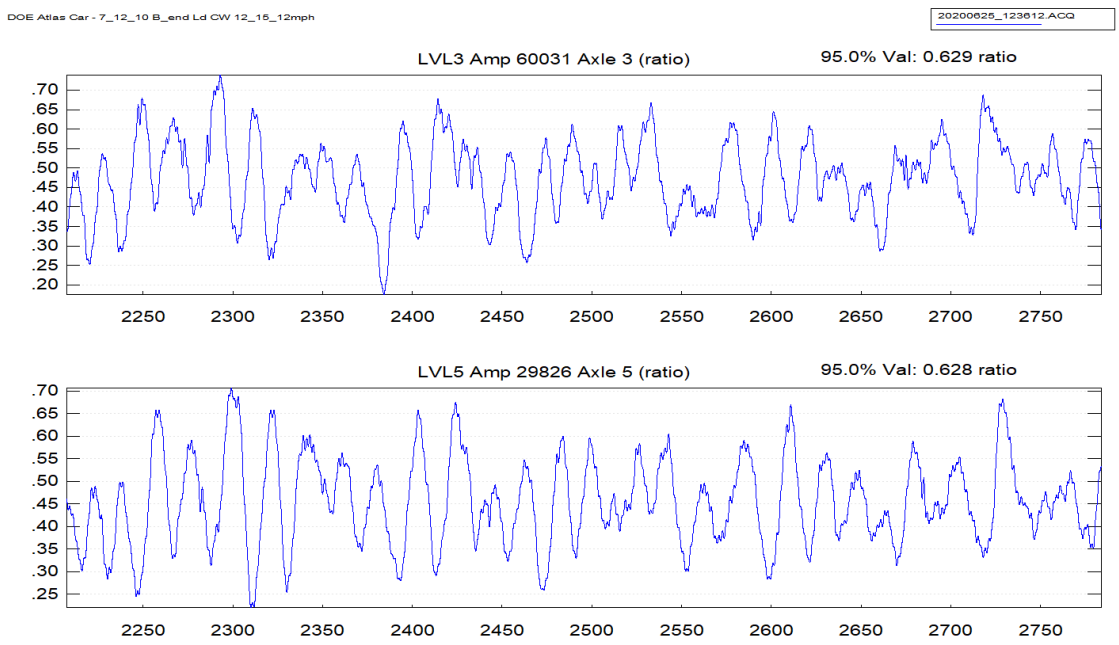


Figure 118. 95 Percent Wheel L/V Maximum Load Left Axles 3 and 5, 12-degree Constant Curving

8.5.19 Minimum Test Load Special Trackwork

Standard S-2043 requires a car be tested through an AREMA straight point turnout with a number 8 or tighter frog angle and also through a crossover with number 10 or tighter turnouts on 15-foot or narrower centers. The turnout test was performed at TTC on the 704 switch between the TTT and the north Urban Rail Building (URB) wye. The crossover test was performed at TTC on the 212 crossover between the Impact Track and the FAST wye.

Standard S-2043 includes specific requirements for track geometry for the special trackwork tests. However, because of the inherent difficulty in defining the turnout alignment specifications, it is acceptable to measure the turnout alignment prior to the commencement of the tests as a baseline and ensure that for subsequent tests on that site alignment is maintained within 1/4 inch of the baseline alignment measurement. The EEC determined that this was not meant to maintain the same geometry in the long run (the last set of tests at the TTC was run approximately 10 years prior).

Standard S-2043 also requires that the alignment measurement be included with the test results. Figure 119 and Figure 120 show the X and Y measurements of the track centerline for the turnout and crossover test zones taken prior to the Atlas railcar tests. These measurements will be used as a baseline for the 1/4-inch alignment tolerance for subsequent tests through these test zones.

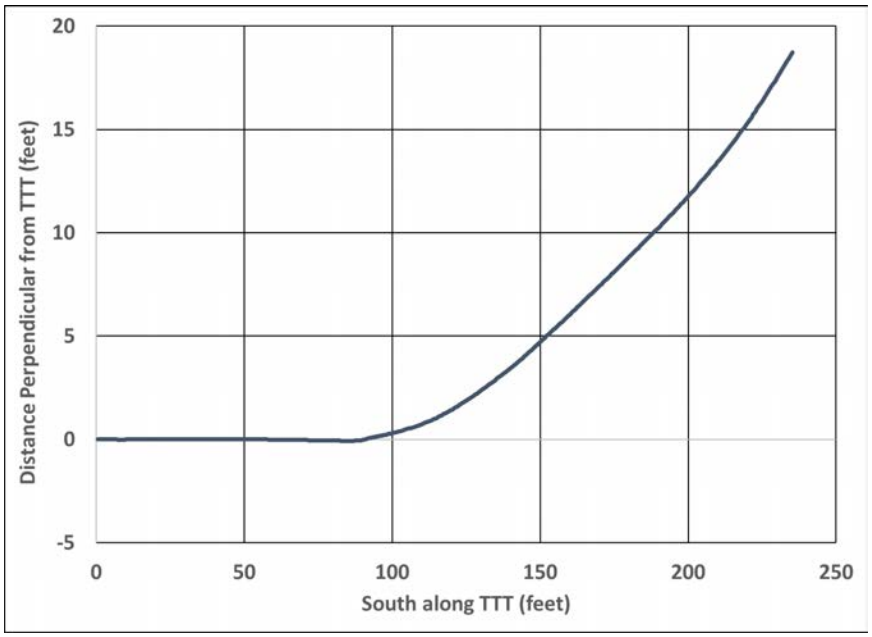


Figure 119. Pre-test Survey Alignment Measurements for Turnout Test Zone

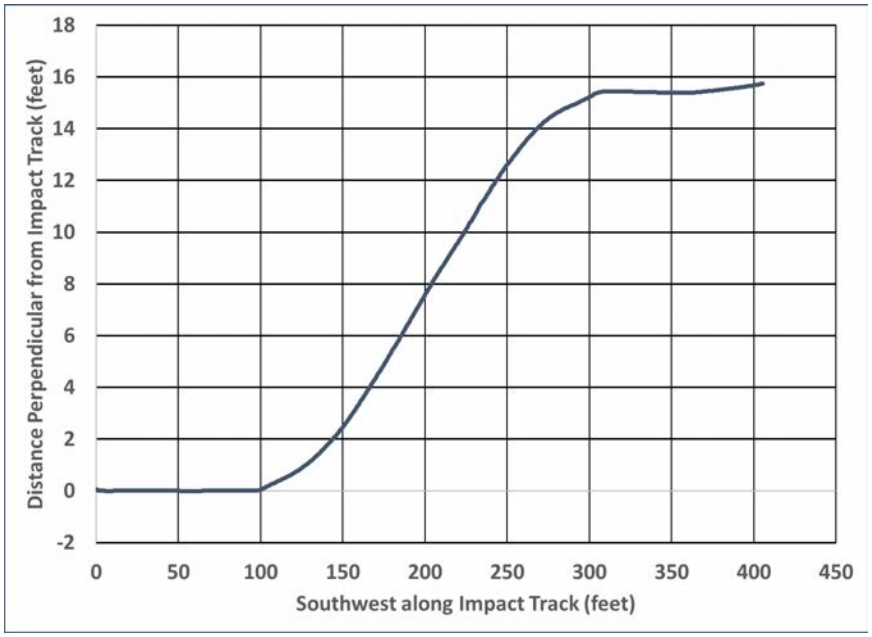


Figure 120. Pre-test Survey Alignment Measurements for Crossover Test Zone

Table 94 shows the description of the track work components contained in the special track work test zones to further document the test conditions.

Table 94. Special Track Work Components

Location	Switch Point		Stock Rail		Frog
	Left	Right	Left	Right	
SW 704	119 pound, 16-foot 6-inch length, standard straight	119 pound, 16-foot 6-inch length, standard straight	119 pound, 39-foot length standard straight	119 pound, 39-foot length standard bent	#8 Rail Bound Manganese
SW 212 A (Impact)	136 pound, 16-foot 6-inch length, samson straight	136 pound, 16-foot 6-inch length, samson straight	136 pound, 39-foot length, samson curved	136 pound, 39-foot length, samson straight	#10 Rail Bound Manganese
SW 212 B (Fast Wye)	136 pound, 16-foot 6-inch length, standard straight	136 pound, 16-foot 6-inch length, standard straight	136 pound, 39-foot length, standard straight	136 pound, 39-foot length, standard bent	#10 Rail Bound Manganese

Table 95 shows the test date and the rail friction data for the minimum load special trackwork tests. Adam Klopp, TTCI Principal Investigator I, witnessed the minimum load special trackwork testing as the AAR Observer, per Standard S-2043 requirements. The tests were performed with both the A-end leading and the B-end leading, passing over the trackwork in both directions. The tests presented in this section were completed with the prototype CSM 70 pads. The effect of changing pad type from CSM 70 to CSM 58 on performance in this regime will be investigated using modeling and presented in the post test analysis report.

Table 95. Minimum Load Special Trackwork Test Dates and Rail Friction Data

Test	Location	Inside Rail Friction	Outside Rail Friction	Date
Crossover Test	SW 212 A	0.53	0.54	10/08/2020
	Crossover	0.54	0.55	10/08/2020
	SW 212 B	0.50	0.51	10/08/2020
Turnout Test	SW 704	0.48	0.51	10/05/2020
	SW 704	0.48	0.51	10/05/2020

The car met the criteria for the minimum load special trackwork turnout tests. Table 96 shows a summary of the test results for the turnout, and Figure 121 shows a plot of the wheel L/V ratios for the special trackwork turnout results.

Table 96. Minimum Load Turnout Summary of Test Results

Criterion	Limiting Value	B-End Lead Facing Point	B-End Lead Trailing Point	A-End Lead Facing Point	A-End Lead Trailing Point
Roll angle (degree)	4	0.57	1.01	0.69	0.54
Maximum wheel L/V	0.8	0.69	0.63	0.62	0.63
Maximum truck side L/V	0.5	0.41	0.35	0.35	0.39
Minimum vertical wheel load	25 (% of static)	62%	57%	63%	62%
Lateral peak-to-peak acceleration (g)	1.3	0.20	0.20	0.21	0.14
Maximum lateral acceleration (g)	0.75	0.14	0.11	0.13	0.09
Maximum vertical acceleration (g)	0.90	0.16	0.15	0.16	0.17
Maximum vertical suspension deflection	95 %	13%	14%	14%	17%

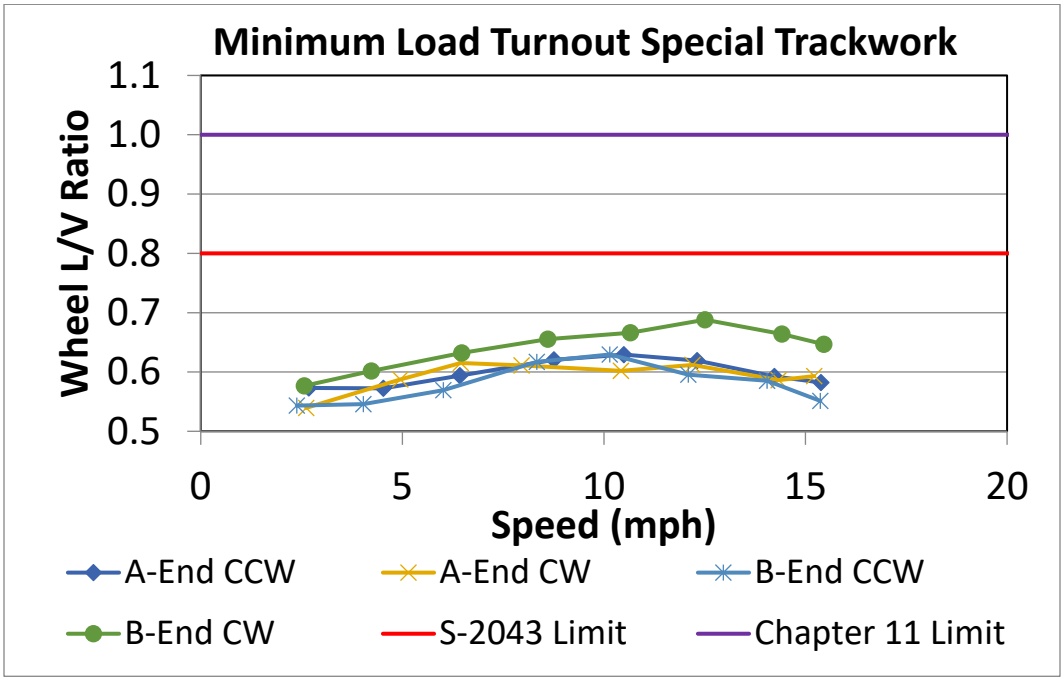


Figure 121. Minimum Load Turnout Special Trackwork Wheel L/V Ratio versus Speed

The car met the criteria for the minimum load special trackwork crossover tests. Table 97 shows a summary of the test results for the crossover, and Figure 122 shows a plot of the wheel L/V ratios for the special trackwork crossover results.

Table 97. Minimum Load Crossover Summary of Test Results

Criterion	Limiting Value	B-End Lead South	B-End Lead North	A-End Lead South	A-End Lead North
Roll angle (degree)	4	0.59	0.80	0.61	0.57
Maximum wheel L/V	0.8	0.54	0.59	0.56	0.53
Maximum truck side L/V	0.5	0.31	0.35	0.35	0.34
Minimum vertical wheel load	25 (% of static)	59%	59%	60%	56%
Lateral peak-to-peak acceleration (g)	1.3	0.19	0.21	0.22	0.22
Maximum lateral acceleration (g)	0.75	0.13	0.12	0.17	0.16
Maximum vertical acceleration (g)	0.90	0.21	0.21	0.22	0.17
Maximum vertical suspension deflection	95 %	10%	11%	11%	10%

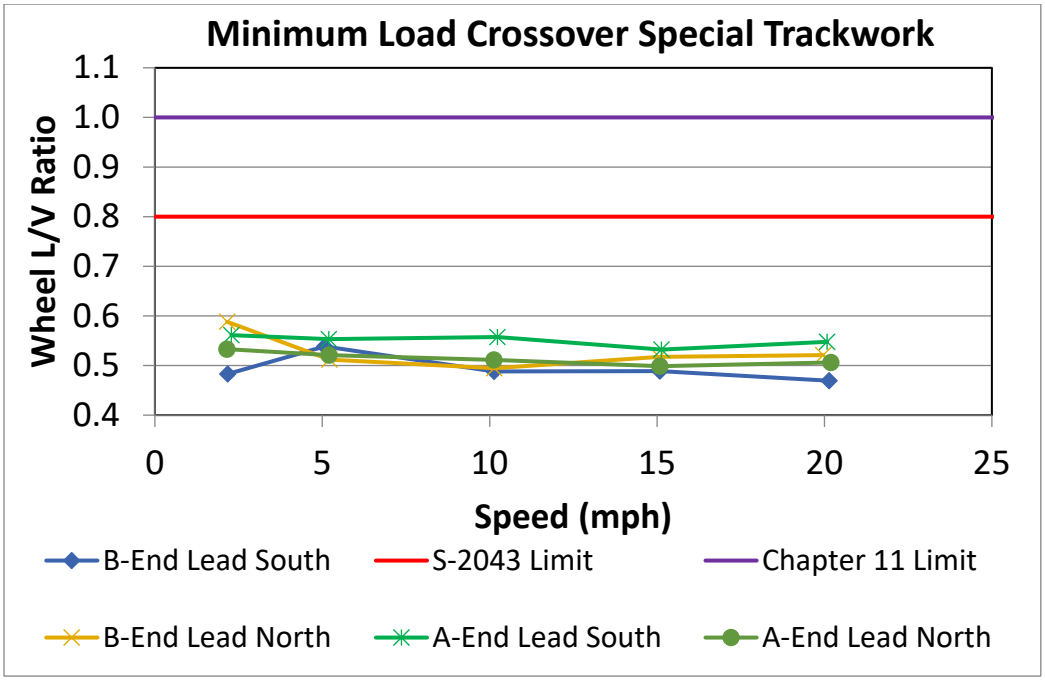


Figure 122. Minimum Load Crossover Special Trackwork Wheel L/V Ratio versus Speed

8.5.20 Maximum Test Load Special Trackwork

The maximum load special trackwork tests were performed in a No. 8 switch and a No. 10 crossover just as the minimum load special trackwork tests were performed. The minimum load special trackwork section (8.5.19) presents the track geometry data and specifications. Table 98 shows the test date and the rail friction data for the different test configurations. Adam Klopp,

TTCI Principal Investigator I, witnessed the maximum load special trackwork testing as the AAR Observer, per Standard S-2043 requirements. The tests were performed with both the A-end leading and the B-end leading and traveling in both directions across the special trackwork. The tests presented in this section were completed with the prototype CSM 70 pads. The effect of changing pad type from CSM 70 to CSM 58 on performance in this regime will be investigated using modeling and presented in the post test analysis report. The car met criteria for maximum test load special trackwork turnout tests. Table 99 shows a summary of the test results for the turnout, and Figure 122 shows a plot of the wheel L/V ratios for the special trackwork turnout results.

Table 98. Maximum Load Special Trackwork Test Dates and Rail Friction Data

Test	Location	Inside Rail Friction	Outside Rail Friction	Date
Crossover Test	SW 212 A	0.52	0.53	08/30/2020
	Crossover	0.50	0.51	08/30/2020
	SW 212 B	0.54	0.54	08/30/2020
Turnout Test	SW 704	0.47	0.48	08/27/2020
	SW 704	0.47	0.48	08/27/2020

Table 99. Maximum Load Turnout Summary of Test Results

Criterion	Limiting Value	B-End Lead Facing Point	B-End Lead Trailing Point	A-End Lead Facing Point	A-End Lead Trailing Point
Roll angle (degree)	4	0.24	0.31	0.28	0.23
Maximum wheel L/V	0.8	0.68	0.60	0.68	0.57
Maximum truck side L/V	0.5	0.40	0.32	0.33	0.35
Minimum vertical wheel load	25 (% of static)	62%	69%	73%	68%
Lateral peak-to-peak acceleration (g)	1.3	0.19	0.11	0.18	0.12
Maximum lateral acceleration (g)	0.75	0.12	0.08	0.12	0.10
Maximum vertical acceleration (g)	0.90	0.13	0.09	0.11	0.10
Maximum vertical suspension deflection	95 %	59%	59%	59%	59%

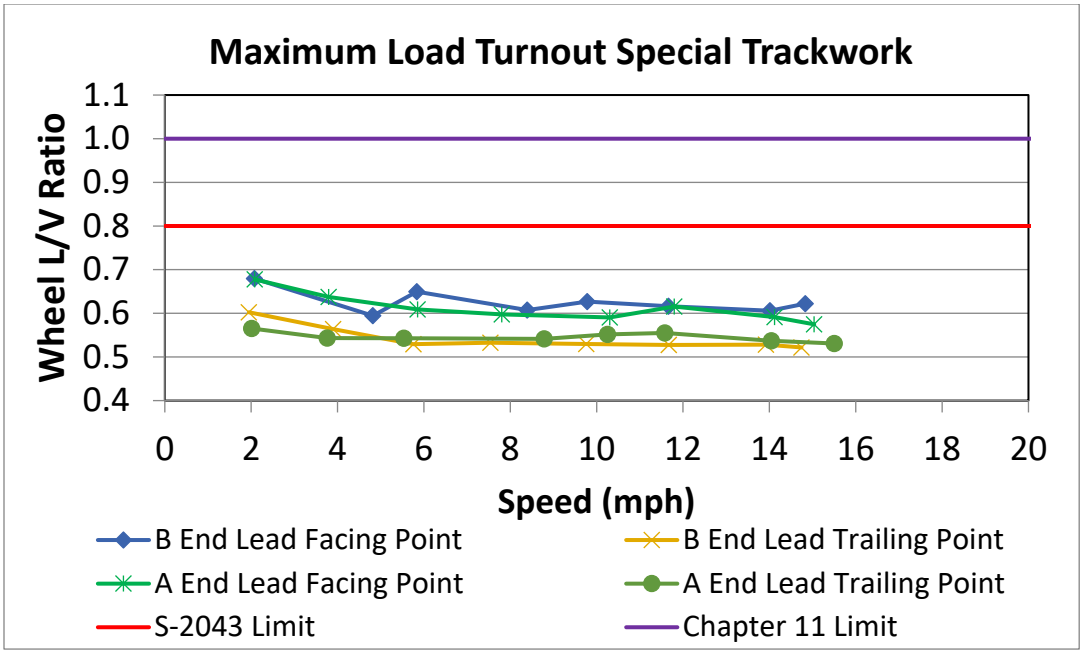


Figure 123. Maximum Load Turnout Special Trackwork Wheel L/V Ratio versus Speed

The car met the criteria for the maximum test load special trackwork crossover tests. Table 100 shows a summary of the test results for the crossover, and Figure 124 shows a plot of the wheel L/V ratios for the special trackwork crossover results.

Table 100. Maximum Load Crossover Summary of Test Results

Criterion	Limiting Value	B-End Lead South	B-End Lead North	A-End Lead South	A-End Lead North
Roll angle (degree)	4	0.21	0.21	0.23	0.25
Maximum wheel L/V	0.8	0.59	0.63	0.58	0.61
Maximum truck side L/V	0.5	0.32	0.33	0.36	0.37
Minimum vertical wheel load	25 (% of static)	69%	67%	65%	66%
Lateral peak-to-peak acceleration (g)	1.3	0.18	0.16	0.22	0.15
Maximum lateral acceleration (g)	0.75	0.13	0.12	0.16	0.12
Maximum vertical acceleration (g)	0.90	0.14	0.11	0.11	0.11
Maximum vertical suspension deflection	95%	56%	52%	55%	54%

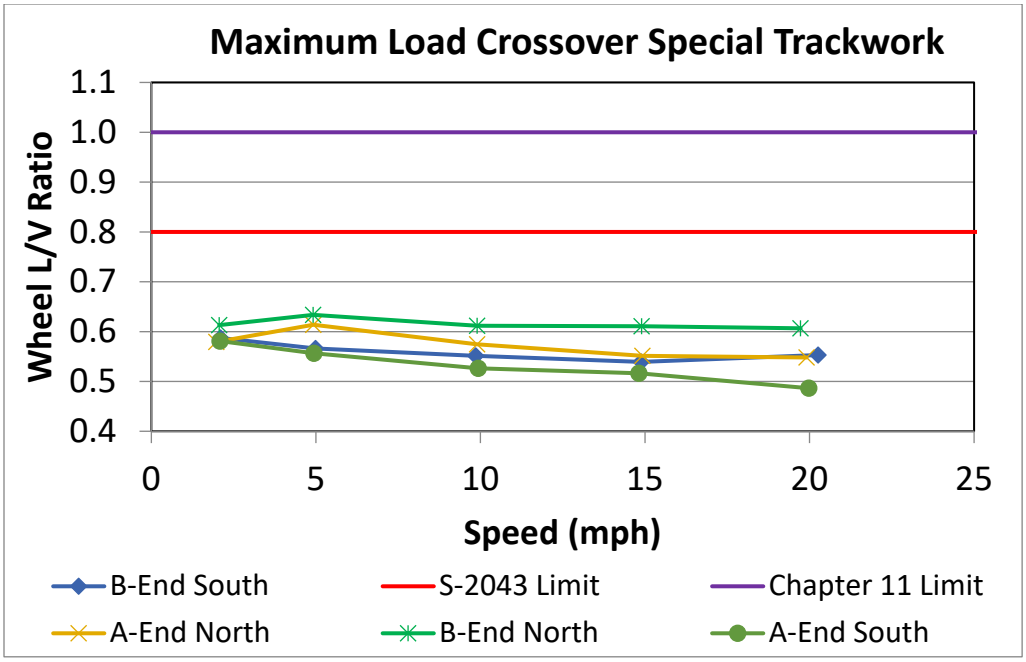


Figure 124. Maximum Load Crossover Special Trackwork Wheel L/V Ratio versus Speed

8.6 Ride Quality

Ride quality testing is not applicable for the Atlas railcar because AAR Standard S-2043 requires ride quality testing only for passenger-carrying railcars.

9. ADDITIONAL TESTS

Paragraph 5.6 of AAR Standard S-2043 includes a provision for the EEC to require additional testing under special conditions. The EEC has specified no additional tests under special conditions for the Atlas railcar. The EEC did request additional dynamic curving tests with softer pads. The additional dynamic curving tests are reported in section 8.5.7.

10. CONCLUSIONS

On behalf of the Department of Energy, TTCI is requesting exceptions from the AAR EEC because the Atlas car has not met some of the criteria for dynamic curving, curving with single rail perturbation, and constant curving test regimes with the CSM 70 primary pads. The car did not meet the criteria for truck twist equalization and high-speed stability with the production CSM 58 pads. The performance in the dynamic curving, curving with single rail perturbation, and constant curving test regimes is expected to improve with the softer, production CSM 58 primary suspension pads. This expectation is based on improved performance measured in minimum load dynamic curving with CSM 58 pads compared to the performance measured with CSM 70 pads. The effect of changing pad type from CSM 70 to CSM 58 on performance in all dynamic testing regimes will be investigated using modeling and presented in the post test analysis report. Criteria for all other test regimes were met. Table 101 contains a summary of the test results.

Analysis was also performed on the securement system, and welds were fabricated and inspected as required in AWS D15.1. Detailed analysis shows that pin stresses do not exceed the ultimate stress. Maximum strains are below the ultimate strain levels.

Table 101. Summary of Test Results

Standard S-2043 Section	Pad Type	Met / Not Met	Test Measurement (if S-2043 Criteria was Not Met)	Performance requirement
5.2 Nonstructural Static Tests				
5.2.1 Truck Twist Equalization	CSM 58	Not Met	**Minimum Test Load:** Wheel load at 50% during 2" drop condition. Wheel load at 24% during 3" drop condition. **Maximum Test Load:** Wheel load at 43% during 2" drop condition. Wheel load at 29% during 3" drop condition.	60% minimum wheel load at 2" drop. 40% minimum wheel load at 3" drop. 60% minimum wheel load at 2" drop. 40% minimum wheel load at 3" drop.
5.2.2 Car Body Twist Equalization	CSM 58	Met		
5.2.3 Static Curve Stability	CSM 58	Met		
5.2.4 Horizontal Curve Negotiation	CSM 58	Met		
5.4 Structural Tests				
5.4.2 Squeeze (Compressive End) Load	CSM 58	Met		
5.4.3 Coupler Vertical Loads	CSM 58	Met		
5.4.4 Jacking	CSM 58	Met		
5.4.5 Twist	CSM 58	Met		
5.4.6 Impact	CSM 58	Met		
5.4.7 Securement System Test	CSM 58	Met		
5.5 Dynamic Tests				
5.5.7 Hunting	CSM 58	Not Met	**Minimum Test Load:** Car unstable at speeds greater than 65 mph with KR wheel profiles	Truck hunting may not be observed at speeds of 70mph or less.
	CSM 70	Met		
5.5.8 Twist and Roll	CSM 70	Met		
5.5.9 Yaw and Sway	CSM 70	Met		
5.5.10 Dynamic Curving	CSM 58	Met		
	CSM 70	Not Met	**Maximum Test Load:** Wheel L/V ratio = 0.81	0.80 maximum wheel L/V ratio.
5.5.11 Pitch and Bounce (Chapter XI)	CSM 70	Met		
5.5.12 Pitch and Bounce (Special)	CSM 70	Met		
5.5.13 Single Bump Test	CSM 70	Met		
5.5.14 Curve Entry/Exit	CSM 70	Met		
5.5.15 Curving with Single Rail Perturbation	CSM 65	Not Met	**Minimum Test Load:** Wheel L/V ratio = 0.84	0.80 max wheel L/V
	CSM 70	Not Met	**Minimum Test Load:** Wheel L/V ratio = 0.88 Truck L/V ratio = 0.50	0.80 max wheel L/V 0.50 max truck L/V
5.5.16 Standard Chapter XI Constant Curving	CSM 70	Not Met	**Minimum Test Load:** Wheel L/V ratio = 0.86 95% Wheel L/V ratio = 0.66 **Maximum Test Load:** 95% Wheel L/V ratio = 0.63	0.80 max wheel L/V 0.60 max wheel L/V 0.60 max wheel L/V
5.5.17 Special Trackwork	CSM 70	Met		

References

1. AAR *Manual of Standards and Recommended Practices*, Car Construction Fundamentals and Details, Performance Specification for Trains Used to Carry High-Level Radioactive Material, Standard S-2043, Effective: 2003; Last Revised: 2017, Association of American Railroads, Washington, D.C.

2. "HLRM Atlas Railcar Test Loads Final Document Package", Prepared by: Orano Federal Services Contract No. TTCI IDIQ 17-1103-007139 Task Order 1, Mod 6. Certificate of conformance signed by D. W. Dalton September 12, 2019.

3. Walker, Russell and Shawn Trevithick, "S-2043 Certification: Preliminary Simulations of Kasgro-Atlas 12-Axle Cask Car". Report No. P-17-021, TTCI Pueblo, CO, December 2017.

4. *Spring Test Requirements and Tolerances Procedure #12 Rev. 4*, Kasgro Rail Corporation, December 2018.

5. AAR Manual of Standards and Recommended Practices, Section C—Part II, Car Construction Fundamentals and Details, Design, Fabrication, and Construction of Freight Cars, paragraph 2.1.4.2.3, Service-Worthiness Tests and Analyses for New Freight Cars, Implemented 09/2017, Association of American Railroads, Washington, DC.

6. AAR Manual of Standards and Recommended Practices, Section C—Part II, Car Construction Fundamentals and Details, Design, Fabrication, and Construction of Freight Cars, Chapter 11, Service-Worthiness Tests and Analyses for New Freight Cars, Implemented 09/2017, Association of American Railroads, Washington, D.C.

7. Norton, R. (1996) *Machine Design*, Prentice Hall, Page 298.

Appendix A. EEC Letter – Empty Atlas Railcar

Ron Hynes
Assistant Vice President
Technical Services

Nichole Fimple
Executive Director
Rules and Standards

ASSOCIATION OF AMERICAN RAILROADS
Transmitted via email

March 19, 2019
File 209.240

Subject: Approval processes for:
1. Empty Atlas Railcar
2. Lightest Atlas Railcar to Operate in HLRM Trains

Patrick Schwab
Nuclear Engineer
U.S. Department of Energy, Office of Nuclear Energy
19901 Germantown Road
Germantown, MD 20874

Dear Mr. Schwab:

The AAR Equipment Engineering Committee (EEC) has considered the requests made in the October 23rd, 2018 letter from Richard Joy of TTCI. The letter included the following requests for the EEC:

1. To consider revising S-2043 to change the requirement that empty cask cars meet S-2043, to instead require the lightest loaded cask car to be operated in HLRM train meet S-2043.
2. To confirm that the lightest Atlas Railcar to operate in HLRM trains, which will be loaded with an empty cask, be approved under S-2043 rather than an empty car as described in S-2043.
3. To confirm that the empty Atlas Railcar not be required to be approved under S-2043, but instead allow approval under M-1001, since the empty car will never operate in HLRM trains.
4. To classify the empty Atlas Railcar as a Category D car as defined in M-1001, paragraph 1.3.2, based on its similarities with the Navy M-290 car.

Respective actions of the EEC follow:

1. The EEC prefers that the specification remain as printed regarding the requirement to test empty cask cars.
2. The EEC confirms that the lightest Atlas Railcar to operate in HLRM trains, loaded with an empty cask, be approved under S-2043 rather than an empty car as described in S-2043.
3. The EEC confirms that approving the empty Atlas Railcar under M-1001 is the proper approach. Note that approval can only be made under Chapter 12 for Controlled Interchange.
4. The request to classify the Atlas Railcar as category D was approved, and Chapter 11 testing need not be conducted.

Association of American Railroads
425 Third Street, SW, Suite 1000, Washington D. C. 20024, (202) 639-2139 FAX No. (202) 639-2179

If you have any questions or need additional information, please contact Mr. Jon Hannafious of our Transportation Technology Center, Inc., subsidiary at jon_hannafious@aar.com or (719) 584-0682.

Sincerely,

Nichole Fimple

Nichole Fimple

NF/jsh

cc: David Cackovic, TTCI
Richard Joy, TTCI
Equipment Engineering Committee

Association of American Railroads
425 Third Street, SW, Suite 1000, Washington D. C. 20024, (202) 639-2139 FAX No. (202) 639-2179

Appendix B. Atlas Car Test Plan

TEST IMPLEMENTATION PLAN

SINGLE CAR TEST OF THE

ATLAS RAILCAR

IN ACCORDANCE WITH

ASSOCIATION OF AMERICAN RAILROADS STANDARD S-2043

For the U.S. Department of Energy (DOE)

Prepared by
Transportation Technology Center, Inc.
A subsidiary of the Association of American Railroads
Pueblo, Colorado USA
January 3, 2019

EXECUTIVE SUMMARY

The intent of this Test Implementation Plan (TIP) is to detail the test procedures that will be used to complete single car testing of the U.S. Department of Energy (DOE) Atlas Railcar as required by the Association of American Railroads (AAR) S-2043 standard titled "Performance Specification for Trains used to Carry High-level Radioactive Material," Section 5.0 – Single Car Tests. A separate test plan will be provided for the associated buffer cars.

This test plan addresses all of the requirements of S-2043 Paragraph 5. However, there are three areas where the test plan differs slightly from S-2043.

- The S-2043 specification covers all railcars used in High Level Radioactive Material (HLRM) trains. DOE does not intend to operate empty cars in HLRM consists. TTCI has requested a change to S-2043 on DOE's behalf to clarify requirements for testing of empty cars. This TIP assumes that where testing empty cars is specified, the lightest load intended to be operated in HLRM service will be used.
- S-2043 requires that Dynamic Curving tests be performed for any likely intermediate load condition. Dynamic modeling predictions show that the different cask loads have very consistent dynamic curve performance. The exception is that the HI-STAR 190XL (Maximum Condition Test Load) performs significantly worse than the other cases. Because of this, TTCI plans to test only the Maximum Condition Test Load to represent the worst-case performance and the Minimum condition test load to represent the typical performance.
- In paragraph 5.5.12 Pitch and Bounce (Special) S-2043 requires that a special section of track with 3/4-inch bumps at a wavelength equal to the span bolster center spacing be built for the car being tested. This distance is 38 feet for the Atlas Cask car. TTCI proposes to only test on the existing standard pitch and bounce section built with 39-foot wavelength bumps and not build the special section of track because it would be very similar to the existing test zone. Dynamic analysis shows that the predicted performance of the car on 38-foot wavelength inputs is very similar to performance of the car on 39-foot wavelength inputs.

TABLE OF CONTENTS

Table of Contents 4
1. INTRODUCTION 7
1.1. Purpose 7
1.2. Car Description 7
1.3. Empty Car Tests 7
1.4. Test Tracks 8
2. Safety 8
3. Test Loads 8
4. Vehicle Characterization 10
4.1. Component Characterization (S-2043, Paragraph 5.1.3) 12
4.1.1. Secondary Suspension Coil Spring 12
4.1.2. Constant Contact Side Bearings 14
4.2. Vertical Suspension Stiffness and Damping (S-2043, Paragraph 5.1.4.3) 14
4.3. Lateral Suspension Stiffness and Damping (S-2043, Paragraph 5.1.4.4) 15
4.4. Truck and Span Bolster Rotation Stiffness and Break Away Moment (S-2043, Paragraph 5.1.4.5) 17
4.5. Inter-Axle Longitudinal and Yaw Stiffness (S-2043, Paragraph 5.1.4.6) 19
4.6. Modal Characterization (S-2043, Paragraph 5.1.4.7) 21
4.6.1. Rigid Body Vertical Procedure 24
4.6.2. Rigid Body Roll Procedure 24
4.6.3. Flexible Body Vertical Procedure 25
4.6.4. Flexible Body Twist Procedure 25
4.6.5. Rigid Body Lateral Procedure 25
4.6.6. Flexible Body Lateral Procedure 25
5. Non-Structural Static Testing 25
5.1. Instrumentation 26
5.2. Truck Twist Equalization (S-2043, Paragraph 5.2.1) 27
5.3. Carbody Twist Equalization (S-2043, Paragraph 5.2.2) 28
5.4. Static Curve Stability (S-2043, Paragraph 5.2.3) 28
5.5. Horizontal Curve Negotiation (S-2043, Paragraph 5.2.4) 28
6. Static Brake Tests 29
6.1. Static Brake Force Measurements 29
6.2. Single-Car Air Brake Test 29
7. Structural Tests 30
7.1. Special Measurements (S-2043, Paragraph 5.4.1) 30

7.2. Instrumentation 30
7.3. Squeeze Load (Compressive End) Load (S-2043, Paragraph 5.4.2) 31
7.4. Coupler Vertical Loads (S-2043, Paragraph 5.4.3) 32
7.5. Jacking (S-2043, Paragraph 5.4.4) 33
7.6. Twist (S-2043, Paragraph 5.4.5) 33
7.7. Impact (S-2043, Paragraph 5.4.6) 33
7.8. Securement System (S-2043, Paragraph 5.4.7) 33
8. Dynamic Tests 34
8.1. Track geometry (S-2043, Paragraph 5.5.6) 36
8.2. Instrumentation 37
8.2.1. Data Acquisition 39
8.2.2. Functional Checks 39
8.3. Hunting (S-2043, Paragraph 5.5.7) 41
8.3.1. Hunting Test Procedure and Test Conditions 41
8.3.2. Hunting Test Instrumentation and Test Conduct 41
8.4. Twist and Roll (S-2043, Paragraph 5.5.8) 42
8.4.1. Twist and Roll Test Procedure and Test Conditions 42
8.4.2. Twist and Roll Instrumentation and Test Conduct 43
8.5. Yaw and Sway (S-2043, Paragraph 5.5.9) 44
8.5.1. Yaw and Sway Test Procedure and Test Conditions 44
8.5.2. Yaw and Sway Instrumentation and Test Conduct 45
8.6. Dynamic Curving (S-2043, Paragraph 5.5.10) 46
8.6.1. Dynamic Curving Test Procedure and Test Conditions 47
8.6.2. Dynamic Curving Instrumentation and Test Conduct 47
8.7. Pitch and Bounce (S-2043, Paragraph 5.5.11) 48
8.7.1. Pitch and Bounce Test Procedure and Test Conditions 49
8.7.2. Pitch and Bounce Instrumentation and Test Conduct 49
8.8. Pitch and Bounce Special (S-2043, Paragraph 5.5.12) 50
8.9. Single Bump Test (S-2043, Paragraph 5.5.13) 50
8.10. Curve Entry/Exit (S-2043, Paragraph 5.5.14) 51
8.10.1. Limiting Spiral Negotiation 51
8.10.2. Spiral Negotiation Test Procedure and Test Conditions 51
8.10.3. Spiral Negotiation Instrumentation and Test Conduct 52
8.11. Curving with Single Rail Perturbation (S-2043, Paragraph 5.5.15) 53
8.12. Standard Chapter 11 Constant Curving (S-2043, Paragraph 5.5.16) 53

8.12.1. Curving Test Procedure and Test Conditions 54
8.12.2. Curving Instrumentation and Test Conduct 54
8.13. Special Trackwork (S-2043, Paragraph 5.5.17) 56
9. Test Schedule 57
10. References 59
Appendix A – Test Track Details 60
Appendix B – Strain Gauge Locations for Structural Tests 65

1. INTRODUCTION

1.1. Purpose

The intent of this Test Implementation Plan (TIP) is to detail the test procedures that will be used to complete single car testing of the U.S. Department of Energy (DOE) Atlas railcar as required by the Association of American Railroads (AAR) Manual of Standards and Recommended Practices (MSRP) standard S-2043 titled "Performance Specification for Trains used to Carry High-level Radioactive Material," Section 5.0 – Single Car Tests.[1] S-2043 refers to MSRP Section C-Part II, M-1001, Chapters 2 and 11 for descriptions of several of the tests.[2, 6] A separate test plan will be provided for the associated buffer cars.

1.2. Car Description

The car to be tested is a 12-axle span bolster car with fittings to accommodate various cradles and end stops designed so the car can carry various casks used for transportation of spent nuclear fuel and/or high-level waste. Some basic car dimensions, used in preparing the test plan are shown in Table 1. The design uses three two axle trucks under a single span bolster to support each end of the car. Figure 1 shows a conceptual design.

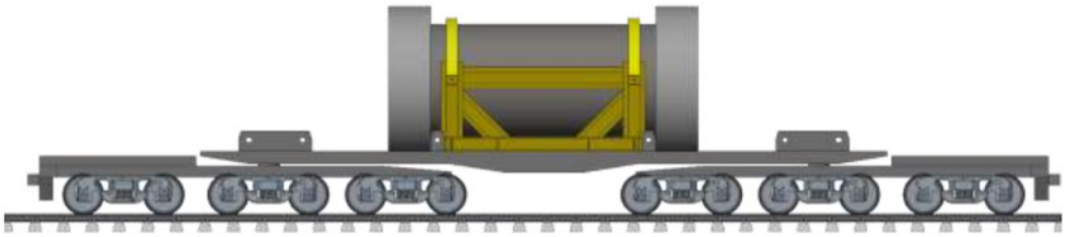


Figure 1. Conceptual Atlas Railcar Design

Table 1. Car Dimensions

Dimension	Value
Length over pulling faces	78′1-1/4″
Length over strikers	73′ 5-1/4″
Spacing of Center Trucks	38′ 6″
Span Bolster Center Plate Spacing	38′
Axle Spacing on trucks	72″
Distance between adjacent trucks	10′ 6″

1.3. Empty Car Tests

The S-2043 specification covers all railcars used in High Level Radioactive Material (HLRM) trains. DOE does not intend to operate empty cars in HLRM consists. TTCI is in the process of requesting a change to S-2043 on DOE's behalf to clarify requirements for testing of empty cars, but this request is still pending. This TIP assumes that where testing empty cars is specified, the lightest load intended to be operated in HLRM service will be used.

1.4. Test Tracks

Testing is planned on various test tracks at the Transportation Technology Center including the Railroad Test Track (RTT), the Wheel Rail Mechanisms (WRM) Loop, the Precision Test Track (PTT), the URB Wye, the Tight Turn Loop (TTL or Screech Loop), and a crossover between the Impact Track and FAST Wye. These tracks are described in Appendix A.

2. SAFETY

Work is to be conducted in accordance with the most current versions of TTCI's Safety Rulebook[4] and Operating Rulebook,[5] which are maintained on TTCI's intranet site.

S-2043 requires that maximum test speeds for all non-curving tests be increased to 75 mph from the standard Chapter 11 maximum of 70 mph where deemed safe by the TTCI test team (see Paragraph 8 of this document). Each applicable test procedures' maximum test speed is listed as 75 mph; however, it is the responsibility of the TTCI test team to determine the maximum safe test speed.

3. TEST LOADS

Based on dynamic modeling results, three potential test load configurations were identified. Orano Federal Services designed the test loads along with associated cradles and end stops for DOE and is currently fabricating them as part of the proposed test program.

A single modular test load design was developed that can meet both the Minimum Condition and Maximum Condition test payloads. An Empty Car Ballast Load was also developed, to be used if testing of the empty car is required. The test loads are described below:

- Minimum Condition Test Load (Figure 2)– simulates empty MP-197 Cask (192,000 pounds including cradle)*
- Maximum Condition Test Load (Figure 3)– simulates loaded HI-STAR 190XL Cask (484,000 pounds including cradle and end stops)
- Empty Atlas railcar Ballast Load (Figure 4) – would likely be required if the empty car was intended to travel in an S-2043 train (200,000 pounds)

* The HI-Star 60 is the lightest cask load, but with the cradle and required end stops, its total weight on the rail car is more than the MP197.

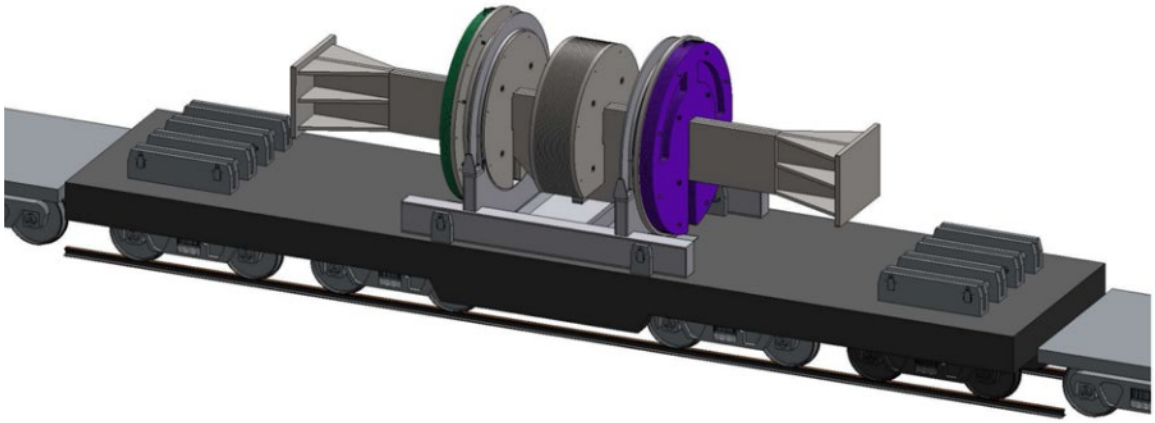


Figure 2. Depiction of MP-197 Minimum Condition Test Load on Atlas Railcar

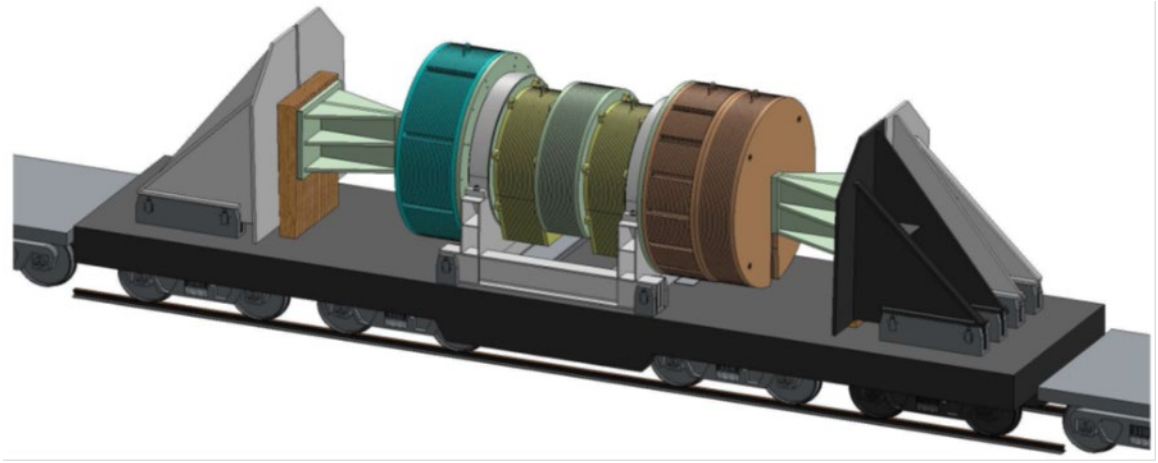


Figure 3. Depiction of HI-Star 190 XL Maximum Condition Test Load on Atlas Railcar

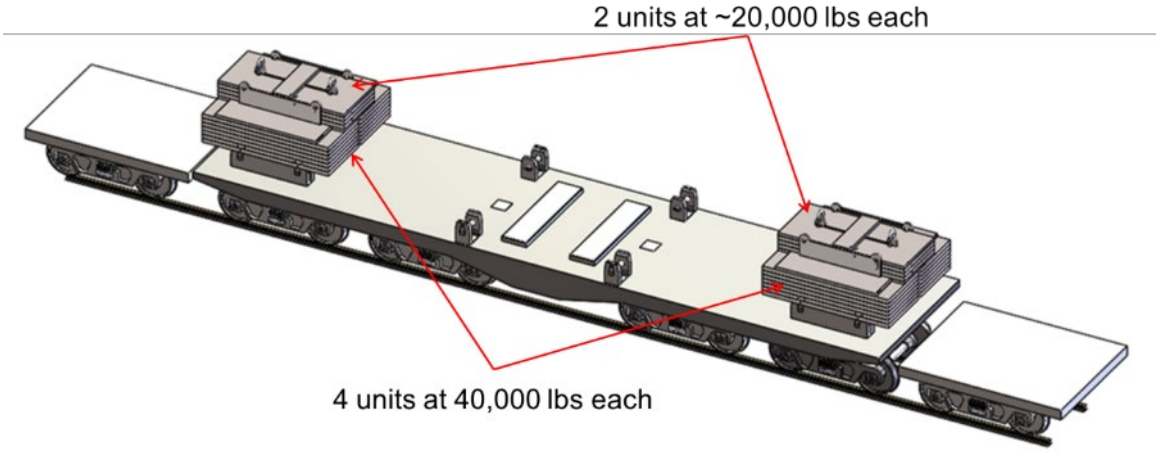


Figure 4. Depiction of Empty Atlas Railcar with Ballast Load

Table 2 provides a summary of the design load conditions. Ranges of weights are given based on Orano's design estimates. The loads will be weighed after fabrication. Based on the ranges given, it is possible that the minimum test load will be lighter than the empty Atlas car ballast load.

Table 2. Summary of Design Load Conditions

Condition	Description	Reference	Load (pounds)	Combined CG Height (in)*	Weight on Rail (pounds)
Empty Atlas Car	Empty Atlas without attachement hardware	Kasgro Drawing 1155 dated 8/16			200,000
Attachment Hardware		Orano CALC-3015276-002	25,498-31,165		225,498 - 231,165
Empty Atlas Car with Ballast Load	Ballast load	Orano Drawing 3020457	190,000-210,000	64	415,498 - 441,165 (includes attacment harware)
Minimum Test Load	Empty MP-197	Orano Drawing 3020458 & 3020459	183,800-199,610	75	409,298 - 430,775 (includes attacment harware)
Maximum Test Load	Loaded HI-Star 190 XL	Orano Drawing 3020460 & 3020461	474,410-494,330	95	699,908 - 725,495 (includes attacment harware)

*CG Heights estimated not including deck or spring deflection

The requirements for single car tests are described in Section 5.0 of the AAR S-2043 specification. The AAR specification requires that all single car tests and subsequent data analysis be witnessed by a qualified AAR observer. TTCI will provide the qualified AAR observer to meet this requirement of the specification.

4. VEHICLE CHARACTERIZATION

Vehicle characterization will be performed to verify that the components and vehicle as a whole were built as designed. Tests will be performed to characterize the properties of the carbody and its suspension in the Rail Dynamics Laboratory (RDL) at TTC. Results of these tests will be used to verify the component and vehicle characteristics used to perform the multi-body dynamic analysis of the vehicle as described in Section 4.3 of the AAR S-2043 specification.

The Mini-Shaker Unit (MSU), a specialized test facility housed in the RDL, will be used extensively to measure vehicle truck suspension system characteristics (see Figure 5). The MSU is comprised of reaction masses and computer controlled hydraulic actuators capable of applying vertical, lateral, or roll input dynamic forces to the vehicle undergoing tests. This unit is especially useful in modal characterization of railcar components and partial rail car systems. The MSU can be configured to perform the rigid and flexible body modal studies of strategic components of the vehicle structure.

The MSU is also used for quantifying the suspension characteristics of assembled suspensions for use in multi-body dynamic models. Measured suspension deflections, reaction forces and wheel/rail forces will be used to determine engineering values for the suspension characteristics.

The MSU is equipped with special instrumented rail sections to measure wheel/rail forces. The use of air bearing tables under the wheels of a vehicle or independently rotating wheels allows for inter-axle shear and yaw stiffness measurements.

Several tests will require trucks to be individually tested in the MSU underneath TTCI's standard truck characterization test flatcar (DOTX 304).

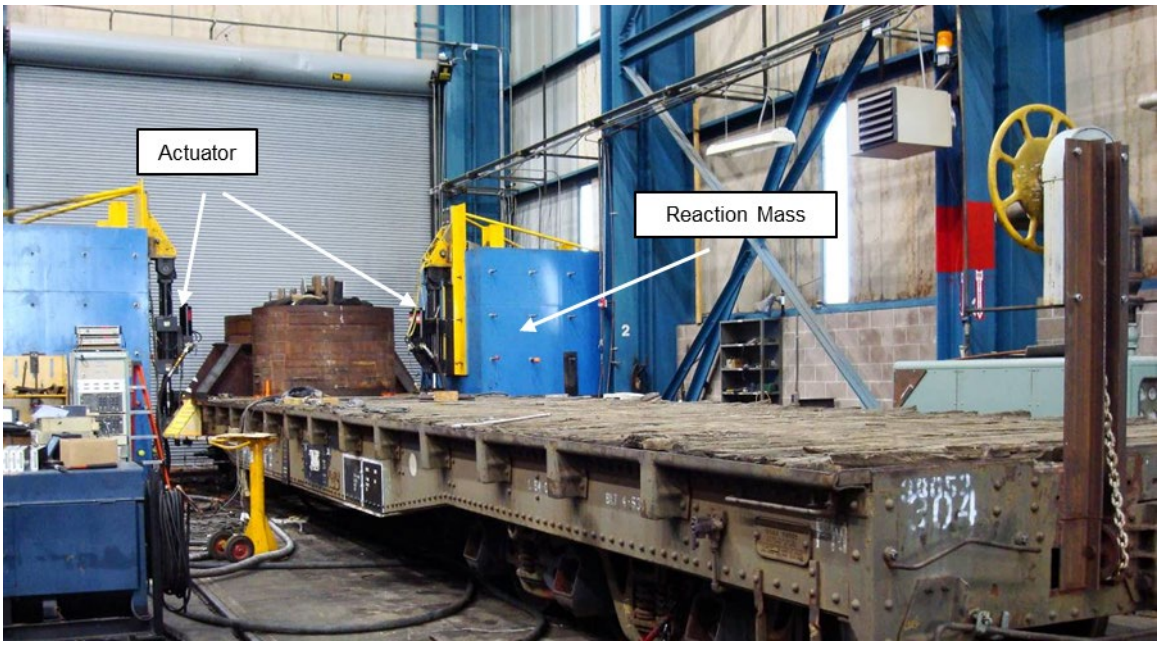


Figure 5. Truck Characterization Test Set-Up in MSU, showing TTCI Standard Test Car and Vertical Actuators attached to Reaction Masses

Characterization tests are summarized in Table 3. A description of each test is provided in the following subsections. The design of each of these tests is based on the vehicle and suspension arrangement described in the comprehensive report on the multi-body dynamic analyses which TTCI compiled for Kasgro.[3]

Table 3. Vehicle Characterization

Test Name	Load Condition	Comments
5.1.3 Component Characterization	NA	2 samples of each type of spring used will be tested. 2 constant contact side bearings will be tested
5.1.4.3 Vertical Suspension Stiffness and Damping	NA	Tests will be performed under DOTX 304. One end truck and one middle truck will be tested
5.1.4.4 Lateral Suspension Stiffness and Damping	NA	Tests will be performed under DOTX 304. One end truck and one middle truck will be tested
5.1.4.5 Truck Rotation Stiffness and Break Away Moment	Equivalent to Minimum Condition Test Load Equivalent to Maximum Condition Test Load	Test three trucks under one span bolster Test one span bolster
5.1.4.6 Inter-Axle Longitudinal Stiffness	Equivalent to Minimum Condition Test Load Equivalent to Maximum Condition Test Load	Tests will be performed under DOTX 304. One end truck and one middle truck will be tested
5.1.4.7 Modal Characterization	Equivalent to Minimum Condition Test Load Equivalent to Maximum Condition Test Load	Actuators will be attached to the Atlas Cask Carbody. Actuators will be operated in force control at lower frequencies (0.2-10 Hz) and in displacement control for constant acceleration input at higher frequencies (3-30 Hz).

4.1. Component Characterization (S-2043, Paragraph 5.1.3)

Tests will be performed to measure the stiffness and damping characteristics of the following individual suspension components, to meet the requirements of S-2043 Section 5.1.3:

- Secondary suspension coil springs
- Constant contact side bearings (between trucks and span bolsters)

4.1.1. Secondary Suspension Coil Spring

The Atlas railcar uses different spring group arrangements for middle and end trucks as shown in Figure 6. Table 4 shows description for all springs.

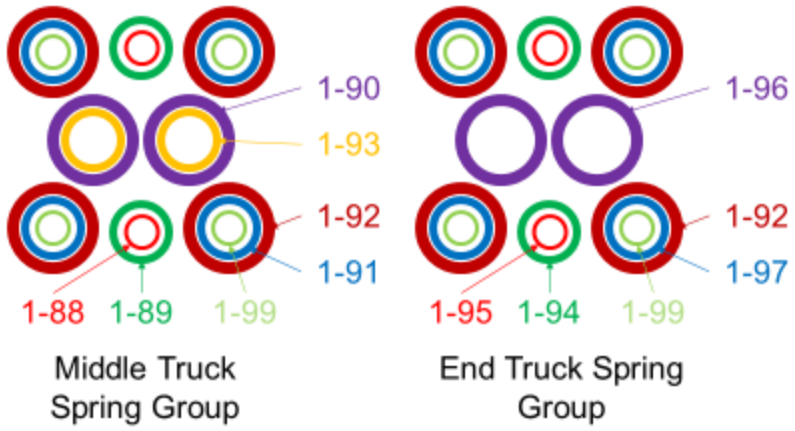


Figure 6. Spring Group General Arrangement

Table 4. Secondary Suspension Spring Types

Spring Group	Type	Description	Quantity per Truck	Bar Diameter (inch)	Free HT (inch)	Solid HT (inch)	Spring Rate (pound/inch)
Middle Truck	1–88	Control Coil Outer	2	0.781	11.72	6.69	1161
	1–89	Control Coil Inner	2	0.500	11.72	6.69	500
	1–90	Empty Coil Outer	2	0.844	13	6.69	1074
	1–91	Empty Coil Inner	4	0.500	13	6.69	348
	1–92	Load Coil Outer	4	1.063	9.25	6.69	4183
	1–93	Load Coil Inner	2	0.688	9.25	6.69	2219
	1–99	Load Coil Inner Inner	4	0.375	7.5	5.38	450
End Truck	1–94	Control Coil Outer	2	0.813	11.09	6.69	1328
	1–95	Control Coil Inner	2	0.531	11.09	6.69	656
	1–96	Empty Coil Outer	2	0.969	11	6.69	2409
	1–97	Empty Coil Inner	4	0.594	11	6.69	934
	1–92	Load Coil	4	1.063	9.25	6.69	4183
	1–99	Load Coil Inner Inner	4	0.375	7.5	5.38	450

Two of each spring type will be selected from the car and tested in a load frame to characterize the stiffness of the springs. The force-displacement characteristics will be measured. The following measurements will also be recorded:

- Unloaded free height
- Solid height
- Wire diameter

4.1.2. Constant Contact Side Bearings

The car is equipped with Miner TCC-III 60LT constant contact side bearings (CCSB) between each truck and the span bolsters. The set-up height of each CCSB will be measured and recorded. Two sample CCSB will be installed in a load frame to measure the force–displacement characteristics.

Output results will include a graph of the force - displacement characteristic, including: Unloaded Free Height, Stiffness, and Fully Compressed Height.

4.2. Vertical Suspension Stiffness and Damping (S-2043, Paragraph 5.1.4.3)

Twist and roll and pitch and bounce performance of a railcar are primarily determined by the characteristics of the vertical suspension. The vertical stiffness and damping characteristics will be measured for the secondary coil spring suspension using the MSU.

For this test, equal measured vertical loads will be applied across the spring groups ranging from zero to 1.5 times the static load if possible, but at least to the static load of the fully loaded car. These tests will be conducted on one middle truck and one end truck. The trucks will be individually tested in the MSU underneath the DOTX 304 flatcar. The flatcar will be ballasted to a load equivalent to the load on the particular truck for the Minimum Condition Test Load. Vertical hydraulic actuators will be attached to each side of the carbody and the MSU reaction masses as shown Figure 5. Vertical deflections across the primary and secondary suspensions of each truck will be measured using displacement transducers and force versus displacement plots will be generated based upon the measured data.

Tests of both trucks will be conducted with the friction wedge control coils installed, and then repeated with the friction wedges and wedge control coils removed. Tests will be conducted for input frequencies of 0.1 Hz, 0.5 Hz and 2.5 Hz. The 0.1 Hz tests will be conducted to move the suspension through its full vertical stroke. The 0.5 and 2.5 Hz tests will be limited in travel due to the limitation of the hydraulic flow rate of the actuators, and to avoid damaging the wear surfaces of the friction wedges.

The test runs required are summarized in Table 5. The data channels to be recorded are listed in Table 6.

Table 5. Run Matrix for Vertical Characterization

	End Truck Empty Cask	End Truck Loaded Cask	Middle Truck Empty Cask	Middle Truck Loaded Cask
Vertical 0.1 Hz (full Stroke)	X	X	X	X
Vertical 0.5 Hz (partial stroke)	X	X	X	X
Vertical 2.0 Hz (partial stroke)	X	X	X	X
Vertical 0.1 Hz (full Stroke) no wedges		X		

Table 6. Measurements for Vertical and Lateral Suspension Characterization

Channel Name	Description	Units	Expected Range
VinpActN	Input signal North actuator	V	±10
VinpActS	Input signal South actuator	V	±10
FZActN	North actuator force	1000-lb	-50 to 77
FZActS	South actuator force	1000-lb	-50 to 77
DZActN	North actuator displacement	in.	±10
DZActS	South actuator displacement	in.	±10
FZRailNE	North East rail vertical force	1,000-lb	0 to 100
FZRailNW	North West rail vertical force	1,000-lb	0 to 100
FZRailSE	South East rail vertical force	1,000-lb	0 to 100
FZRailSW	South West rail vertical force	1,000-lb	0 to 100
FYRailNE	North East rail lateral Force	1,000-lb	-20 to 50
FYRailNW	North West rail lateral force	1,000-lb	-20 to 50
FYRailSE	South East rail lateral force	1,000-lb	-20 to 50
FYRailSW	South West rail lateral force	1,000-lb	-20 to 50
FYRailNE	North East rail lateral Force	1,000-lb	-20 to 50
FYRailNW	North West rail lateral force	1,000-lb	-20 to 50
FYRailSE	South East rail lateral force	1,000-lb	-20 to 50
FYRailSW	South West rail lateral force	1,000-lb	-20 to 50
DZSprN	North vert bolster to sideframe displacement	in.	10
DZSprS	South vert bolster to sideframe displacement	in.	10
DYSprST	Lateral bolster to sideframe displacement – top South	in.	10
DYSprSB	Lateral bolster to sideframe displacement – bot. South	in.	10
DYSprST	Lateral bolster to sideframe displacement – top North	in.	10
DYSprSB	Lateral bolster to sideframe displacement – bot. North	in.	10
DXPadNE1	Longitudinal displacement, NE pad, outside	in.	2
DXPadNE2	Longitudinal displacement, NE pad, inside	in.	2
DYPadNE1	Lateral displacement, NE pad, outside	in.	2
DYPadNE2	Lateral displacement, NE pad, inside	in.	2
DZPadNE1	Vertical displacement, NE pad, outside	in.	2
DZPadNE2	Vertical displacement, NE pad, inside	in.	2
DXPadSE1	Longitudinal displacement, SE pad, outside	in.	2
DXPadSE2	Longitudinal displacement, SE pad, inside	in.	2
DYPadSE1	Lateral displacement, SE pad, outside	in.	2
DYPadSE2	Lateral displacement, SE pad, inside	in.	2
DZPadSE1	Vertical displacement, SE pad, outside	in.	2
DZPadSE2	Vertical displacement, SE pad, inside	in.	2

4.3. Lateral Suspension Stiffness and Damping (S-2043, Paragraph 5.1.4.4)

Twist and roll, yaw and sway, and hunting performance of a railcar are governed by the stiffness and damping characteristics of the lateral suspension. The lateral suspension test will be performed for static vertical loads representing both the Minimum Condition Test Load and the Maximum Condition Test Load. The testing method will ensure that static friction does not limit lateral motion during this test.

These tests will be conducted on one middle truck and one end truck. The trucks will be individually tested in the MSU underneath the DOTX 304 flatcar. The flatcar will be ballasted to a

load equivalent to the load on the particular truck for the Minimum Condition Test Load, and then repeated for the Maximum Condition Test Load. Tests of both trucks will be conducted with the friction wedge control coils installed, and then repeated with the friction wedges and wedge control coils removed.

Lateral deflections across the primary and secondary suspensions of each truck will be measured using displacement transducers and force versus displacement plots will be generated based upon the measured data. A lateral hydraulic actuator will be mounted between the carbody and the MSU reaction mass. Tests will be conducted for lateral input frequencies of 0.1 Hz, 0.5 Hz and 2.5 Hz. The 0.1 Hz tests will be conducted to move the suspension through its full lateral stroke, as determined by the lateral stops between the transoms and the bolsters. The 0.5 and 2.5 Hz tests will probably be limited in travel due to the limitation of the hydraulic flow rate of the actuators, and to avoid damaging the wear surfaces of the friction wedges.

The force will be input at a level above the truck suspension. To minimize carbody roll it may be necessary to use a solid connection (oak blocking or steel shims) between the truck bolster and carbody at the side bearing location.

Lateral deflections across the primary and secondary suspensions of each truck will be measured using displacement transducers. Sufficient displacement transducers will be applied to measure both the lateral and rocking motions of the sideframe and the primary and secondary suspensions.

The test runs required are summarized in Table 7. The channels to be measured are the same as those to be measured during the vertical suspension characterizations as listed in Table 6. Force versus displacement plots will be generated based upon the measured data.

Table 7. Run Matrix Lateral Characterization

Test Run	End Truck Minimum Condition Test Load	End Truck Loaded Cask	Middle Truck Minimum Condition Test Load	Middle Truck Loaded Cask
Lateral 0.1Hz (full Stroke)	X	X	X	X
Lateral 0.5Hz (partial stroke)	X	X	X	X
Lateral 2.0Hz (partial stroke)	X	X	X	X
Lateral 0.1Hz (full Stroke) no wedges		X		
Lateral 0.1Hz (full Stroke) attempt to restrain transom	X	X	X	X
Lateral 0.1Hz (full Stroke) no wedges attempt to restrain transom		X		

4.4. Truck and Span Bolster Rotation Stiffness and Break Away Moment (S-2043, Paragraph 5.1.4.5)

Truck and span bolster rotation stiffnesses and/or break-away moments will also be measured.

For these tests air bearing tables will be used to float the three trucks at one end of the car to ensure the wheels are unrestrained during the test (Figure 7). The opposite end of the car will be raised up to ensure that the car is level when the air tables are inflated. Hydraulic actuators will be used to rotate the tables. To ensure that equal loads are applied on each side of the truck, and to minimize lateral motion and skewing of the air tables the actuators will face in opposite directions during these tests.

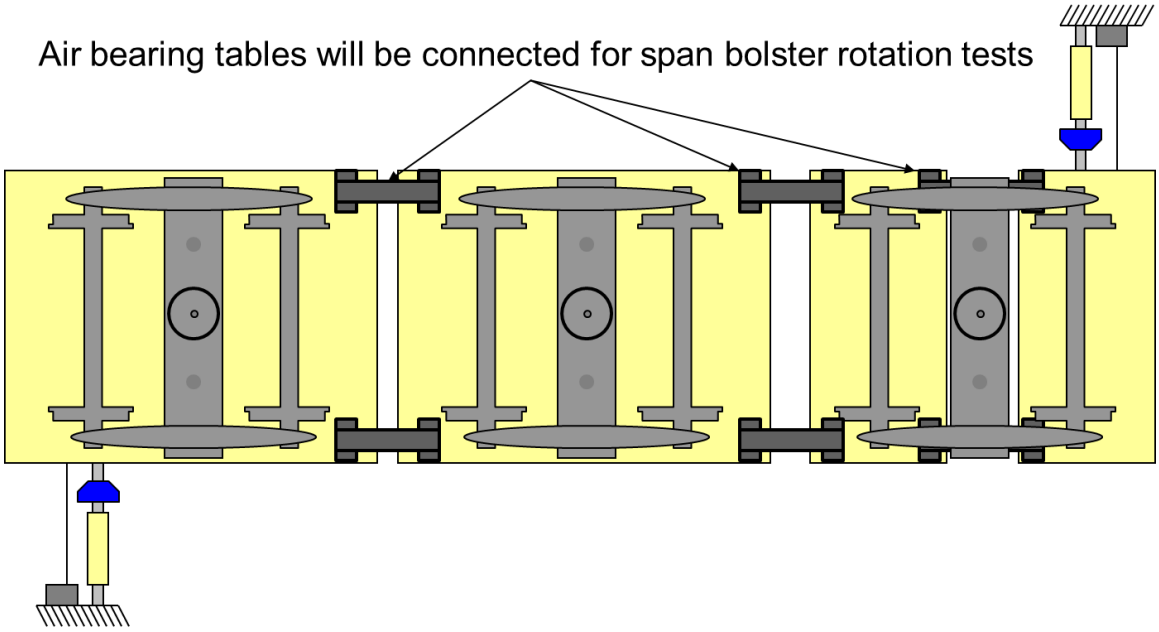


Figure 7. Air Bearing Table Configuration for Span Bolster Rotation Tests

Tests will be performed to measure the rotation of the three trucks under one span bolster truck relative to the span bolster. Actuator force and truck bolster rotation relative to the span bolster will be measured. This test will be performed at a very low rotational frequency and is considered a static test. Both minimum condition test load and maximum condition test load will be tested. Table 8 shows the measurements to be made during truck rotation characterization.

Table 8. Measurements for Truck Rotation Characterization

Channel Name	Description	Units	Expected Range
FYActN	North actuator force	1000-lb	±10
FYActS	South actuator force	1000-lb	±10
DXTBR	Longitudinal displacement span bolster to truck bolster right	In	±5
DXTBL	Longitudinal displacement span bolster to truck bolster left	In	±5
DYTBI	Lateral displacement span bolster to truck bolster inside	In	±5
DYTBO	Lateral displacement span bolster to truck bolster outside	In	±5

Tests will also be performed to measure the rotation of one span bolster relative to the carbody. All the air tables will be fastened together to prevent them from moving relative to each other. Actuator force and span bolster rotation relative to the carbody will be measured. This test will be performed at a very low rotational frequency and is considered a static test. Table 9 shows the measurements to be made during span bolster rotation measurements.

Table 9. Measurements for Span Bolster Rotation Characterization

Channel Name	Description	Units	Expected Range
FYActN	North actuator force	1,000-lb	±10
FYActS	South actuator force	1,000-lb	±10
DXSBR	Longitudinal displacement carbody to span bolster right	in.	±5
DXSBL	Longitudinal displacement carbody to span bolster left	in.	±5
DYSBI	Lateral displacement carbody to span bolster inside	in.	±5
DYSBO	Lateral displacement carbody to span bolster outside	in.	±5

Figure 8 shows a sketch of how the string pots might be placed to measure truck rotation and span bolster rotation. The selection and placement of the string pots must be established so that they are relatively sensitive to translation as well as rotation. The translations of the center plate in the center bowl help the analyst determine if edge contact is occurring, thereby enabling better interpretation of the data. The position of the string pots and load cells relative to the center of rotation must be recorded.

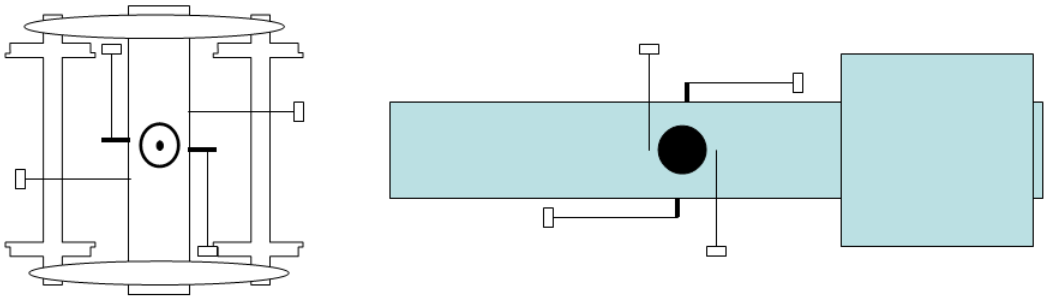


Figure 8. Possible Layout of String Pots for Truck and Span Bolster Rotation Tests

4.5. Inter-Axle Longitudinal and Yaw Stiffness (S-2043, Paragraph 5.1.4.6)

The longitudinal stiffness of the primary suspension system will be determined through two tests. These tests will be conducted in the MSU at the same time as the vertical and lateral truck characterization tests (Sections 4.2 and 4.3) with wheelsets with independently rotating wheels (IRWs) installed to eliminate any effects of wheel rolling resistance and slip resistance. Tests will be conducted for the car ballasted to loads equivalent to the Minimum Condition Test Load and the Maximum Condition Test Load.

The test method uses longitudinal actuators attached between two axles within a truck at each roller bearing end cap, as shown in Figure 9. The actuators will first be operated in phase in both directions. Longitudinal stiffness will be determined by plotting force versus displacement. The actuators will then be operated out of phase to determine axle yaw stiffness. These tests will be performed at a very low frequency and are considered static tests.

During these tests, sufficient displacement transducers will be applied to measure both the longitudinal motions of the axles (bearing adaptors) relative to the sideframe, and the pitching motion of the bearing adaptors relative to the sideframes, as shown in Figure 10. The measurements to be recorded are listed in Table 10.

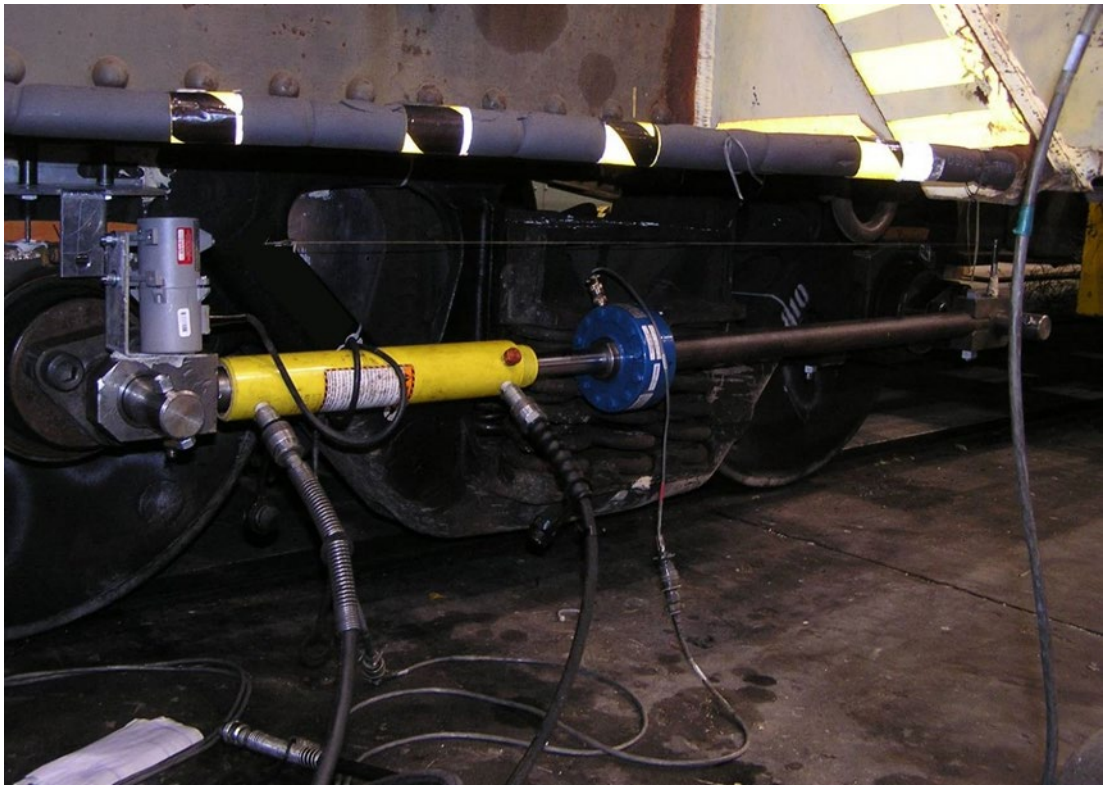


Figure 9. Longitudinal Actuator Installation for Performing Inter-Axle Stiffness Tests

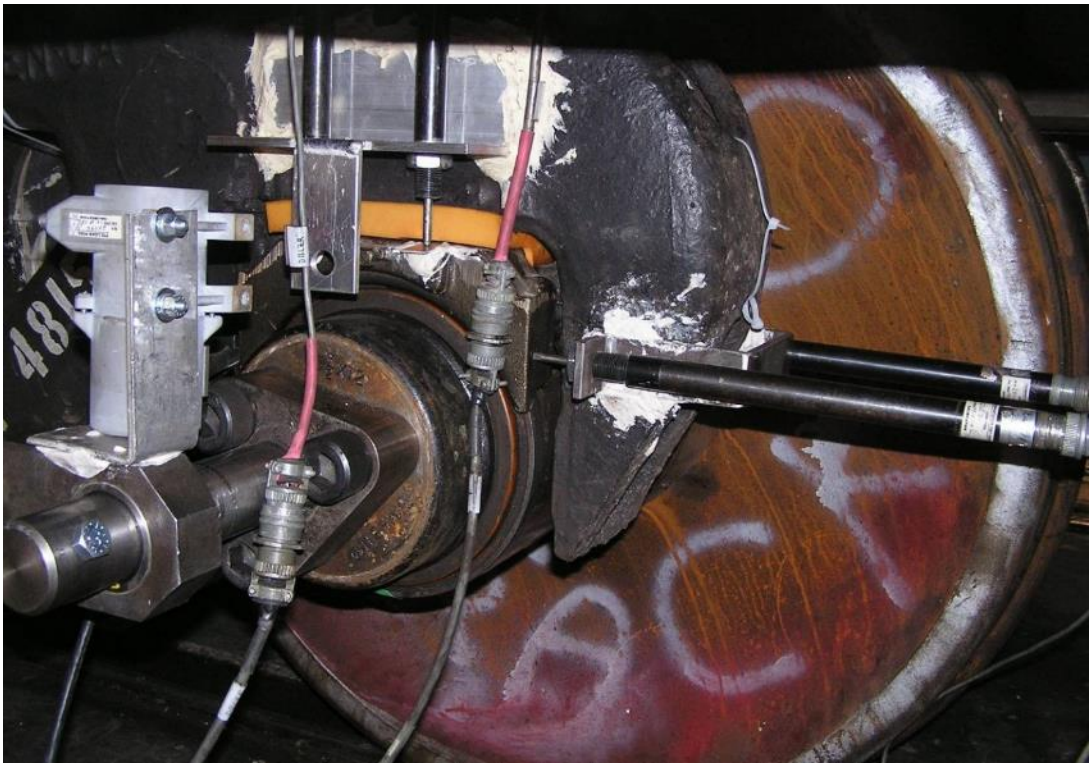


Figure 10. Inter–Axle Stiffness Test Setup Showing LVDTs for Measuring Pitching and Yawing of Bearing Adaptor

Table 10. Measurements for Interaxle Yaw Stiffness Measurements

Channel Name	Description	Units	Expected Range
FXActN	North hydraulic cylinder force	1,000-lb	-10 to 20
FXActS	South hydraulic cylinder force	1,000-lb	-10 to 20
DXActN	North hydraulic cylinder displacement	in.	±10
DXActS	South hydraulic cylinder displacement	in.	±10
DXPadNE1	Longitudinal displacement, NE pad, inside	in.	2
DXPadNE2	Longitudinal displacement, NE pad, outside	in.	2
DYPadNE1	Lateral displacement, NE pad, bottom	in.	2
DYPadNE2	Lateral displacement, NE pad, top	in.	2
DZPadNE1	Vertical displacement, NE pad, outside	in.	2
DZPadNE2	Vertical displacement, NE pad, inside	in.	2
DXPadSE1	Longitudinal displacement, SE pad, inside	in.	2
DXPadSE2	Longitudinal displacement, SE pad, outside	in.	2
DYPadSE1	Lateral displacement, SE pad, bottom	in.	2
DYPadSE2	Lateral displacement, SE pad, top	in.	2
DZPadSE1	Vertical displacement, SE pad, outside	in.	2
DZPadSE2	Vertical displacement, SE pad, inside	in.	2

4.6. Modal Characterization (S-2043, Paragraph 5.1.4.7)

The entire railcar will be characterized to identify critical rigid and flexible body modes. The objective of the test is to identify frequencies for the following modes

Rigid Body

- Bounce
- Pitch
- Yaw
- Lower Center Roll
- Upper Center Roll

Flexible Body

- First mode vertical bending
- First mode twist (torsion)
- First mode lateral bending

The modal tests will be performed on the Atlas cask railcar in the MSU. Brackets will be welded to the carbody at the carbody bolster on the B-end of the car so the actuators can be attached to the car (Figure 11). TTCI will work with Kasgro to develop a bracket arrangement that does not interfere with the trucks or span bolster, and to identify allowable areas for welding the brackets to

the carbody structure. TTCI will remove the bracket at the conclusion of modal characterization testing.



Figure 11. Example of Actuator Attachment Bracket to be Welded to Car

The carbody will be fitted with enough accelerometers to identify bounce, pitch, roll, yaw, sway, vertical bending, lateral bending, and torsion modes of vibration. The railcar will be excited vertically to induce bounce, pitch, and bending modes. Similarly, the railcar will be excited laterally to identify sway, yaw, and bending, and torsionally to identify lower center roll, upper center roll, and torsion modes. In addition to identifying mode shapes with accelerometers, input force and displacement will be measured to help determine damping rates. The data channels to be recorded during modal tests are listed in Table 11. The approximate measurement locations are shown in Figure 12.

Table 11. Measurements for Modal Characterization

Channel Name	Description	Units	Expected Range
VinpActN	Input signal North actuator	V	±10
VinpActS	Input signal South actuator	V	±10
FZActN	North actuator force	1,000-lb	-50 to 77
FZActS	South actuator force	1,000-lb	-50 to 77
DZActN	North actuator displacement	in.	±10
DZActS	South actuator displacement	in.	±10
AZ1R	Vertical accelerometer, B-end, right side	g	±2
AY1R	Lateral accelerometer, B-end, right side	g	±2
AZ1L	Vertical accelerometer, B-end, left side	g	±2
AZ2R	Vertical accel, 1/4 from B-End, right side		±2
AY2R	Lateral accel, 1/4 from B-End, right side	g	±2
AZ2L	Vertical accel, 1/4 from B-End, left side	g	±2
AZ3R	Vertical accelerometer, center, right side	g	±2
AY3R	Lateral accelerometer, center, right side	g	±2
AZ3L	Vertical accelerometer, center, left side	g	±2
AZ4R	Vertical accel, 1/4 from A-End, right side	g	±2
AY4R	Lateral accel, 1/4 from A-End, right side	g	±2
AZ4L	Vertical accel, 1/4 from A-End, left side	g	±2
AZ5R	Vertical accelerometer, A-end, right side	g	±2
AY5R	Lateral accelerometer, A-end, right side	g	±2
AZ5L	Vertical accelerometer, A-end, left side	g	±2
AY6R	Lateral accel on B-end of B span bolster	g	±2
AZ6R	Vertical accel on B-end of B span bolster	g	±2
AY7R	Lateral accel center of B span bolster	g	±2
AZ7R	Vertical accel center of B span bolster	g	±2
AY8R	Lateral accel A-end of B span bolster	g	±2
AZ8R	Vertical accel A-end of B span bolster	g	±2

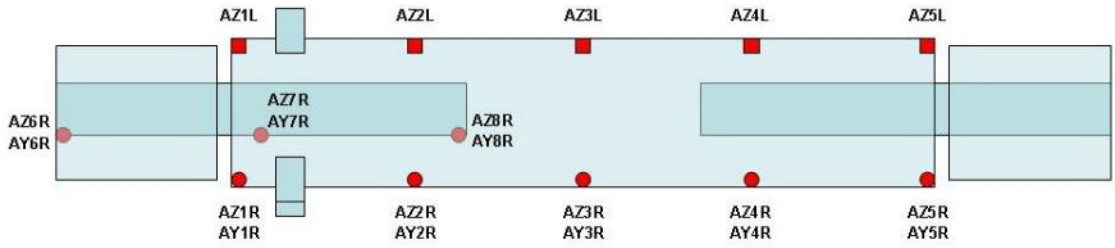


Figure 12. Locations of Modal Accelerometers

Table 12 shows a list of the runs to be performed during modal testing. Rigid body runs will be done using the actuators in force control. Flexible body runs will be done with the actuators in displacement control for constant g runs. The frequency and amplitude values given for each run were based on tests performed of the Kasgro M-290 12-Axle Flat Car.7 Some changes may be made to frequency and amplitudes used for these runs based on test results.

Table 12. Run List for Modal Testing

Run	Description	Actuator Configuration	Control	Frequency (Hz)	Amplitude
Lateral Rigid Body					
1	Lateral Rigid Body	Lateral	Force	0.2 to 10	5 kips
2	Lateral Rigid Body	Lateral	Force	0.2 to 10	10 kips
3	Lateral Rigid Body	Lateral	Force	0.2 to 10	15 kips
Lateral Flexible Body					
4	Lateral Flexible Body	Lateral	Disp.	3 to 30	0.1 g
5	Optional Lat Flex Body	Lateral	Disp.	3 to 30	0.2 g
6	Optional Lat Flex Body	Lateral	Disp.	3 to 30	0.3 g
Vertical Rigid Body					
7	Vertical Rigid Body	Vertical (in phase)	Force	0.2 to 10	5 kips
8	Vertical Rigid Body	Vertical (in phase)	Force	0.2 to 10	10 kips
9	Vertical Rigid Body	Vertical (in phase)	Force	0.2 to 10	15 kips
Vertical Flexible Body					
10	Vertical Flexible Body	Vertical (in phase)	Disp.	3 to 30	0.1 g
11	Optional Lat Flex Body	Vertical (in phase)	Disp.	3 to 30	0.2 g
12	Optional Lat Flex Body	Vertical (in phase)	Disp.	3 to 30	0.3 g
Roll Rigid Body					
13	Roll Rigid Body	Vertical (out of phase)	Force	0.2 to 10	5 kips
14	Roll Rigid Body	Vertical (out of phase)	Force	0.2 to 10	10 kips
15	Roll Rigid Body	Vertical (out of phase)	Force	0.2 to 10	15 kips
Twist Flexible Body					
16	Twist Flexible Body	Vertical (out of phase)	Disp.	3 to 30	0.1 g
17	Optional Twist Flex Body	Vertical (out of phase)	Disp.	3 to 30	0.2 g
18	Optional Twist Flex Body	Vertical (out of phase)	Disp.	3 to 30	0.3 g

4.6.1. Rigid Body Vertical Procedure

The actuators will be cycled in phase. Input frequencies will be increased from 0.2 Hz to 10 Hz. The actuators will be operated in force control with 5, 10, and 15 kip sinusoidal inputs. Pitch and Bounce modes will be determined by the phase relationship between the A and B end accelerometers.

4.6.2. Rigid Body Roll Procedure

The actuators will be cycled 180 degrees out of phase. Input frequencies will be increased from 0.2 Hz to 10 Hz. The actuators will be operated in force control with 5, 10, and 15 kip sinusoidal inputs.

Roll modes will be determined by the phase relationship between the accelerometers mounted at different positions on the car.

4.6.3. Flexible Body Vertical Procedure

The actuators will be cycled in phase. Input frequencies will be increased from 3 Hz to 30 Hz. The actuators will be operated in displacement control and operated to achieve a constant g input.

4.6.4. Flexible Body Twist Procedure

The actuators will be cycled out of phase. Input frequencies will be increased from 3 Hz to 30 Hz. The actuators will be operated in displacement control and operated to achieve a constant g input.

4.6.5. Rigid Body Lateral Procedure

The actuators will be reconfigured so that one actuator is mounted to excite the car laterally. Input frequencies will be increased from 0.2 Hz to 10 Hz. The actuators will be operated in force control with 5, 10, and 15 kip sinusoidal inputs. The Yaw mode will be determined by the phase relationship between the A and B end accelerometers.

4.6.6. Flexible Body Lateral Procedure

This test will be performed while the actuators are in the lateral configuration. Input frequencies will be increased from 3Hz to 30Hz. The actuators will be operated in displacement control and operated to achieve a constant g input.

5. NON-STRUCTURAL STATIC TESTING

Several static tests will be performed to demonstrate the ability of the railcar to maintain adequate vertical wheel loads in extreme load conditions and poor track geometry environments. Tests are required for minimum condition test load and maximum condition test load, depending on the specific test. A summary of the non-structural static tests is presented in Table 13. The data channels to be recorded are presented in Table 14.

Table 13. Nonstructural Static Testing

Test Name	Load Condition	Instrumentation	Comments
5.2.1 Truck Twist Equalization	Minimum Condition Test Load Maximum Condition Test Load	This test will be done using up to 24 load measuring rails. (load bars)	
5.2.2 Carbody Twist Equalization	Minimum Condition Test Load Maximum Condition Test Load	This test will be done using up to 24 load measuring rails (load bars)	
5.2.4 Static Curve Stability	Minimum Condition Test Load	Feeler gages	Currently planning to use the AAR base car and long car (see paragraph 5.4)
5.2.5 Horizontal Curve Negotiation	Maximum Condition Test Load	Visual inspection	Tight Turn Loop (Screech loop)

5.1. Instrumentation

Figure 13 shows load bar installation locations and Table 14 provides additional details of measurements for the Non-Structural Static Tests.

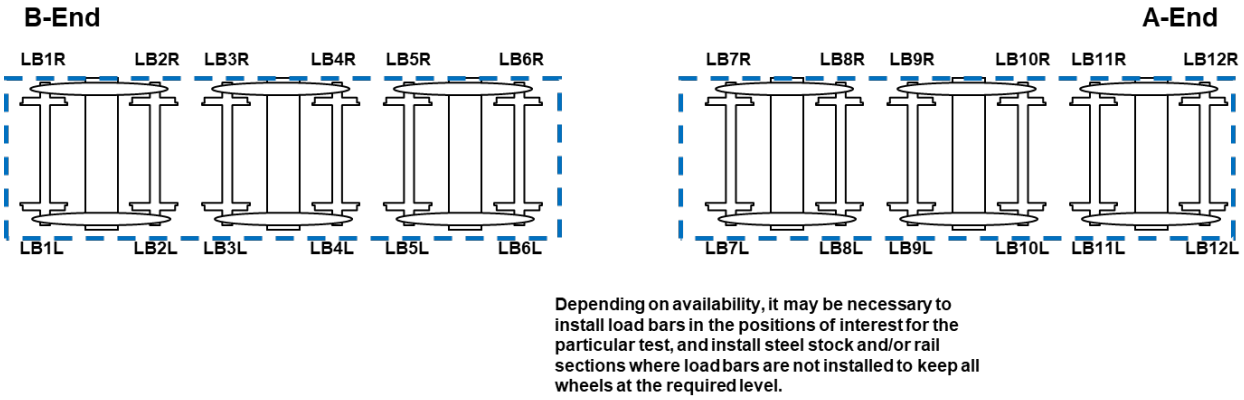


Figure 13. Load Bar Installation Locations

Table 14. Measurements for Non-Structural Static Tests

Channel Name	Description	Units	Expected Range
LB1R	Load bar, axle 1, right wheel	kips	0-70
LB1L	Load bar, axle 1, left wheel	kips	0-70
LB2R	Load bar, axle 2, right wheel	kips	0-70
LB2L	Load bar, axle 2, left wheel	kips	0-70
LB3R	Load bar, axle 3, right wheel	kips	0-70
LB3L	Load bar, axle 3, left wheel	kips	0-70
LB4R	Load bar, axle 4, right wheel	kips	0-70
LB4L	Load bar, axle 4, left wheel	kips	0-70
LB5R	Load bar, axle 5, right wheel	kips	0-70
LB5L	Load bar, axle 5, left wheel	kips	0-70
LB6R	Load bar, axle 6, right wheel	kips	0-70
LB6L	Load bar, axle 6, left wheel	kips	0-70
LB7R	Load bar, axle 7, right wheel	kips	0-70
LB7L	Load bar, axle 7, left wheel	kips	0-70
LB8R	Load bar, axle 8, right wheel	kips	0-70
LB8L	Load bar, axle 8, left wheel	kips	0-70
LB9R	Load bar, axle 9, right wheel	kips	0-70
LB9L	Load bar, axle 9, left wheel	kips	0-70
LB10R	Load bar, axle 10, right wheel	kips	0-70
LB10L	Load bar, axle 10, left wheel	kips	0-70
LB11R	Load bar, axle 11, right wheel	kips	0-70
LB11L	Load bar, axle 11, left wheel	kips	0-70
LB12R	Load bar, axle 12, right wheel	kips	0-70
LB12L	Load bar, axle 12, left wheel	kips	0-70
IC	Instrumented Coupler	kips	±200

5.2. Truck Twist Equalization (S-2043, Paragraph 5.2.1)

This requirement is to ensure adequate truck load equalization. Load bars will be used to measure wheel loads as shown in Figure 13.

- With the car on level track shim each wheel three inches in height. This is the zero condition.
- For one wheel in each truck, measure vertical wheel loads while raising one wheel from 0.0 inch to 3.0 inches, then lowering to -3 inches, then raising back to 0 inches in increments of 0.5 in.
- At 2.0 inches of deflection, vertical load at any wheel may not fall below 60% of the nominal static load.
- At 3.0 inches of deflection, vertical load at any wheel may not fall below 40% of the nominal static load.

Figures 11 and 12 of the dynamic analysis report[3] show that the trucks used in this vehicle are symmetrical front to back and left to right so this test will be performed by raising and lowering just one wheel in every truck.

The test will be performed for a Minimum Condition Test Load and a Maximum Condition Test Load.

5.3. Carbody Twist Equalization (S-2043, Paragraph 5.2.2)

This test will be performed in conjunction with the truck twist test. This requirement is to document wheel unloading under carbody twist, such as during a spiral negotiation. Load bars will be used to measure wheel loads as shown in Figure 13. The railcar shall be jacked by 3.0 in. in 0.5-in. increments from underneath the wheels on one side of all trucks at one end of the car. At 2.0 in. of lift, vertical load at any wheel may not fall below 60% of the nominal static load. At 3.0 in., no permanent damage shall be produced and no static wheel load may fall below 40% of the nominal static wheel load.

This test must be performed by raising and lowering each of the four corners of the railcar individually.

5.4. Static Curve Stability (S-2043, Paragraph 5.2.3)

The curve stability test shall follow the requirements of M-1001 paragraph 11.3.3.3. The test consist will undergo a squeeze and draft load of 200,000 pounds without carbody suspension separation or wheel lift. Load application shall simulate a static load condition and shall be of minimum 20 seconds sustained duration.

For the purpose of this test, wheel lift is defined as a separation of wheel and rail exceeding 1/8-in. when measured 2 5/8-in. from the rim face with a feeler gauge.

The car with the Minimum Test Load will be subjected to squeeze and draft load on a 10-degree curve located at the Urban Rail Building at TTC. The test car will be coupled to a base car as defined in paragraph 2.1.4.2.3 of the AAR M-1001 specification, and a long car having 90-ft over strikers, 66-ft truck centers, 60-in. couplers, and conventional draft gear.

Coupler forces will be measured during the test.

5.5. Horizontal Curve Negotiation (S-2043, Paragraph 5.2.4)

A horizontal curve negotiation test must be performed per M-1001, paragraph 2.1.4. The specification required that this car be able to negotiate a curve of 150-foot radius uncoupled. The test will be performed on the screech loop at TTC which has a radius of 150 feet. The test car will be coupled to three short hopper cars so that the test car can be pushed into the curve without the locomotive entering the curve. The car will be pushed into the curve in stages. At each stage personnel will inspect the car paying special attention to:

- Clearance between wheels and carbody
- Clearance between wheels and span bolster

- Clearance between wheels and brake rigging (including brake cylinder)
- Clearance between truck bolster and brake rigging

6. STATIC BRAKE TESTS

Static brake shoe force tests are to be conducted by Kasgro at their facility. Kasgro has arranged for the assistance of New York Air Brake and an AAR observer. A TTCI engineer will also be present for testing. The TTCI engineer will confirm that the tests are conducted as described below.

6.1. Static Brake Force Measurements

Static brake force measurements will be conducted per *MSRP* Section E, Standard S-401 to demonstrate compliance with S-2043 paragraph 4.4. Braking ratios for freight operation must be verified. Brake shoe force variations must also be within the limits provided in Standard S-401.

6.2. Single-Car Air Brake Test

In addition, a single-car air brake test must be performed per the AAR Manual of Standards and Recommended Practices, Section E, Standard S-486, or other applicable standard.

7. STRUCTURAL TESTS

Structural tests will be conducted to demonstrate the railcar's ability to withstand the rigorous railroad load environment and to verify the accuracy of the structural analysis. The Chapter XI requirement of "no permanent deformation" is interpreted as no stress exceeding material yield for the tests described in the following sections. The structural tests are summarized in Table 15. Measurements for the structural tests are listed in Table 16.

Table 15. Structural Tests

Test Name	Load Condition	Lead End	Instrumentation	Comments
5.4.2 Squeeze (Compressive End) Load	Minimum Condition Test Load (most adverse stability condition) Maximum Condition Test Load (most adverse stress condition)		50-Strain gages, million pound load cell.	
5.4.3 Coupler vertical loads	Minimum or Maximum Condition Test Load (either one is fine, don't need both)		50-Strain gages, 50K load cell.	Apply 50K pounds up and down at pulling face of coupler.
5.4.4 Jacking	Maximum Condition Test Load		50-Strain gages	
5.4.5 Twist	Maximum Condition Test Load		50-Strain gages, 12 load bars	5.4.5.1 performed in conjunction with 5.2.2. 5.4.5.2 performed separately.
5.4.6 Impact	Maximum Condition Test Load	B	50-Strain gages, Instrumented coupler	

7.1. Special Measurements (S-2043, Paragraph 5.4.1)

A survey of the car will be performed before and after all the structural tests have been conducted. The purpose of this survey is to verify the shape and integrity of the car. In addition, a visual inspection of the car will be made after each structural test. The survey will include:

- Measure the length over strikers
- Measure the length over pulling faces
- Using a theodolite, measure a level loop around the car deck to check for a change in camber or twisting of the carbody

7.2. Instrumentation

Strain measurements are to be taken from gauges installed on the railcar under frame and deck surface for each of the tests described in sections 7.3 - 7.7. Strains will be used for post-test comparison to finite-element analysis (FEA) predictions. The car designer has determined the location for the gauges as required by S-2043 paragraph 5.4.1.2, based on design FEA results. In

addition, thermocouples will be installed in 3 locations for temperature compensation of strain measurements.

Table 16 lists the measurements for the structural tests. Strain gauge and thermocouple locations, descriptions, material properties at measurement locations, channel names, measurement units, and expected range are included in Appendix B.

Table 16. Measurements for Structural Tests*

Channel Name	Description	Units	Expected Range
LC1	Load cell for compressive end load	kips	0-1,000
LC2	Load cell for coupler test	kips	0-50
IC	Instrumented Coupler for impact test	kips	0-1250
SPD	Speed Tachometer for impact test	mph	0-15

*See Appendix B for details of strain gauge and thermocouple locations on carbody

Most structural tests are static or quasi-static so filter and sample rates are not critical. Data should be filtered at ≥10-Hz and sampled at a minimum of twice the chosen filter frequency. The exception is the impact test regime, where data will be filtered at a rate ≥100-Hz and < (sample rate/2). The minimum sample rate for impact tests is 1000-Hz. Impact test data will be digitally filtered at 100-Hz during data analysis.

7.3. Squeeze Load (Compressive End) Load (S-2043, Paragraph 5.4.2)

The squeeze test shall follow the requirements of M-1001 paragraph 11.3.3.1. A horizontal compressive static load of 1,000,000 pounds will be applied at the centerline of draft to the draft system of car interface areas using TTCI's squeeze fixture (Figure 14) and sustained for a minimum of 60 seconds. The car tested will simulate an axially loaded beam having rotation- free translation-fixed end restraints. No other restraints, except those provided by the suspension system in its normal running condition, will be permissible. The test will be performed with the car subjected to the most adverse stress condition (Maximum Condition Test Load) and most adverse stability condition (Minimum Condition Test Load).

Prior to testing the squeeze load should be cycled to 750,000 pounds three times to stress relieve the railcar, providing a better correlation between FEA predictions and measured stresses.



Figure 14. 2 1/2 Million Pound Squeeze Test Fixture with Passenger Car Taken to Structural Failure

7.4. Coupler Vertical Loads (S-2043, Paragraph 5.4.3)

The coupler vertical load test shall follow the requirements of M-1001 paragraph 11.3.3.2. A load of 50,000 pounds shall be applied in both directions to the coupler head as near to the pulling face as practicable and held for 60 seconds. This test will utilize a hydraulic cylinder positioned on cribbing to apply the upward force. An A-frame fixture that attaches to the rail and a hydraulic cylinder will be used to apply the downward force (Figure 15).

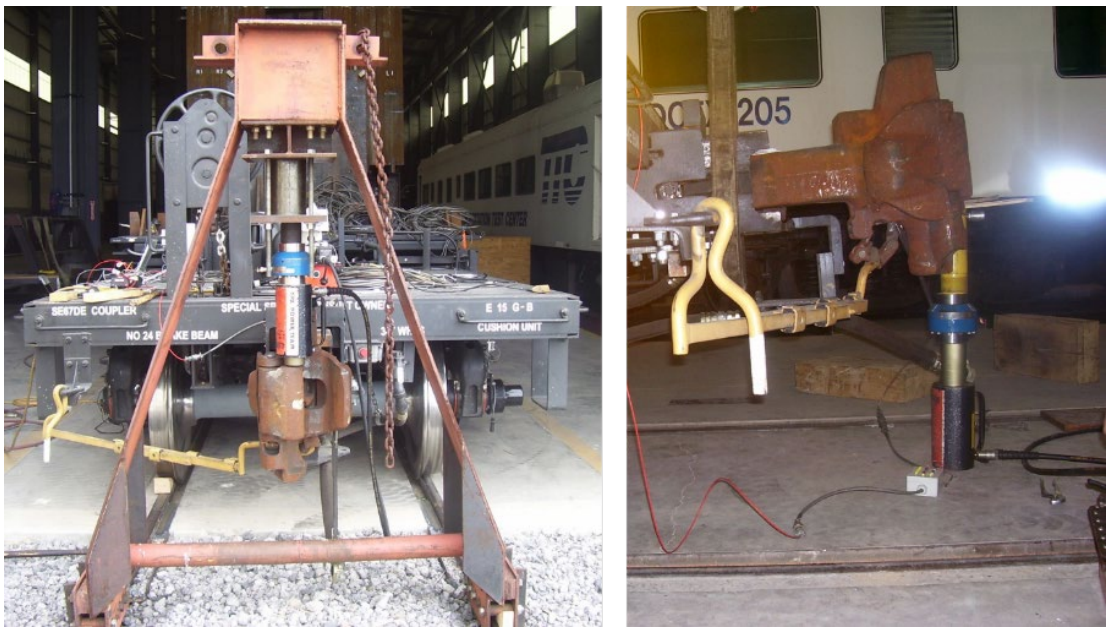


Figure 15. Applying Coupler Vertical Loads

7.5. Jacking (S-2043, Paragraph 5.4.4)

The jacking test shall follow the requirements of M-1001 paragraph 11.3.3.4. Vertical load capable of lifting a fully loaded car will be applied at designated jacking locations sufficient to lift the unit and permit removal of the truck or suspension arrangement nearest to the load application points. Chapter 11 requires that the car withstand the test without permanent deformation of car/unit structure. Strain data will be recorded while the carbody is jacked high enough to permit removal of the span bolster.

7.6. Twist (S-2043, Paragraph 5.4.5)

The twist test shall follow the requirements of M-1001 paragraph 11.3.3.5. The loaded car will be jacked by 3 inches from underneath the wheels on one side of the three trucks at one end of the car. M-1001, Chapter 11 requires that the car withstand the test without permanent deformation of the car structure. This test will be performed in conjunction with the test described in Section 5.3.

In addition, the carbody will be supported at all four jacking pads and one corner will be allowed to drop 3 in.

Strain data will be recorded during these tests.

7.7. Impact (S-2043, Paragraph 5.4.6)

The impact test shall follow the requirements of M-1001 paragraph 11.3.4.1. The loaded candidate car is to be impacted into a string of three standing, fully loaded cars of at least 70-ton capacity. The impact string will be equipped with M-901E draft gear on the struck end and the hand brake will be fully set on the last car (opposite end).

Free slack between cars will be removed; however, draft gears will not be compressed. No restraint other than the hand brake on the last car will be used.

A series of impacts will be made on tangent track section of the Precision Test Track (PTT) at TTC. Successive impacts will be made in increments of 2 mph or less starting at 4 mph or less until the design coupler force of the car (600,000 pounds) as specified in paragraph 4.1.10 or a speed of 14 mph has been reached, whichever occurs first. The coupler force shall not exceed 1,250,000 pounds during any impact with a speed of 6 mph or less.

Strain data, coupler load, and speed will be measured during these tests.

7.8. Securement System (S-2043, Paragraph 5.4.7)

Strength of the securement system will be verified by analysis and inspection. For the purpose of this test, the securement system is defined to be the cradle attachment fittings (including shear blocks), pins, and welds to the deck of the railcar. Cradles, end stops, or deck structure itself are not included. Analysis will include the following:

- Independent calculation of worst-case loads based on 10 CFR 71.45 and Field Manual of the AAR Interchange Rules, Rule 88 A.16.c(3)

- Dimensional inspection of fittings and pins to confirm compliance with design
- Review of Kasgro quality records to confirm materials used and welds comply with design
- Independent calculation of stresses in attachment fittings and pins
- Independent calculation of stresses in welds
- Independent review of design factor of safety based on calculated loads and stresses

8. DYNAMIC TESTS

Dynamic tests include testing as described MSRP Section C Part II, Specification M-1001, Chapter 11, as well as additional requirements. Where Chapter 11 and HLRM criteria differ, the car shall meet both requirements. Table 17 summarizes the required dynamic tests.

Chapter 11 specifies a maximum test speed of 70 mph for all non-curving tests. S-2043 requires the maximum speed be increased to 75 mph where deemed safe by the TTCI test team. Tests at speeds over 70 mph shall be used to quantify performance and limiting criteria will not apply. Table 18 summarizes S-2043 dynamic limiting criteria. Figure 16 illustrates the application of 50 millisecond and 3ft. distance limits for L/V ratio and minimum vertical wheel load.

For cask car tests, instrumented wheelsets (IWS) will be placed in all trucks of a single span bolster. The span bolster with IWS can be placed in either leading or trailing position as required by the particular test.

Table 17. Required Dynamic Tests

Test Name	Load Condition	Lead End	IWS Position	Comments
5.5.7 Hunting	Minimum Condition Test Load Maximum Condition Test Load	B	Axles 1-6	Tests performed with IWS and separately with wheels having the KR tread profile (M-1001 Figure 11.3)
5.5.8 Twist and Roll	Minimum Condition Test Load Maximum Condition Test Load	B	Axles 1-6	
5.5.9 Yaw and Sway	Maximum Condition Test Load	A	Axles 1-6*	
5.5.10 Dynamic Curving	Minimum Condition Test Load Maximum Condition Test Load	B A	Axles 1-6*	
5.5.11 Pitch and Bounce (Ch. 11)	Maximum Condition Test Load	B	Axles 1-6	
5.5.12 Pitch and Bounce Special	Maximum Condition Test Load	B	Axles 1-6	Not required, see 8.8
5.5.13 Single bump test	Minimum Condition Test Load Maximum Condition Test Load	B	Axles 1-6	
5.5.14 Curve Entry/Exit	Minimum Condition Test Load Maximum Condition Test Load	B A	Axles 1-6*	5.5.13.1 Limiting Spiral tests will be done during dynamic curving tests. 5.5.13.2 Spiral Negotiation

Test Name	Load Condition	Lead End	IWS Position	Comments
				tests will be done during Constant Curving tests.
5.5.15 Curving with Single Rail Perturbation	Minimum Condition Test Load Maximum Condition Test Load	B A	Axles 1-6*	Perturbation will be installed on URB North Wye. (Two tests, inside bump and outside bump.)
5.5.16 Standard Chapter XI Constant Curving	Minimum Condition Test Load Maximum Condition Test Load	B A	Axles 1-6*	These tests will be performed on the WRM in the 7.5-, 10-, and 12-degree curves. Testing will be done clockwise and counterclockwise.
5.5.17 Special Trackwork	Minimum Condition Test Load Maximum Condition Test Load	B A	Axles 1-6*	Turnout tests will be carried out on the URB north Y track, possibly in conjunction with 5.5.15 tests. The crossover tests will be conducted on the Impact Track to Fast Wye crossover.

*This means IWS don't move; for B-end leading tests they are in the leading end, for A-end leading tests they are in the trailing end.

Table 18. Dynamic Limiting Criteria

Criterion	Limiting Value	Notes
Maximum carbody roll angle (degree)	4	Peak-to-peak.
Maximum wheel L/V	0.8	Not to exceed indicated value for a period greater than 50 ms. and for a distance greater than 3 ft. per instance*. *Figure 16 illustrates the application of 50 millisecond and 3 ft. distance limits for L/V ratio and minimum vertical wheel load
95th percentile single wheel L/V (constant curving tests only)	0.6	Not to exceed indicated value. Applies only for constant curving tests.
Maximum truck side L/V	0.5	Not to exceed indicated value for a duration equivalent to 6 ft. of track per instance.
Minimum vertical wheel load (%)	25	Not to fall below indicated value for a period greater than 50 ms. and for a distance greater than 3 ft. per instance*.

Criterion	Limiting Value	Notes
Peak-to-peak carbody lateral acceleration (G)	1.3 0.60	For non-passenger-carrying railcars For passenger-carrying railcars
Maximum carbody lateral acceleration (G)	0.75 0.35	For non-passenger-carrying railcars For passenger-carrying railcars
Carbody lateral acceleration standard deviation (G)	0.13	Calculated over a 2000-ft sliding window every 10 ft. over a tangent track section that is a minimum of 4,000 ft. long.
Maximum carbody vertical acceleration (G)	0.90 0.60	For non-passenger-carrying railcars For passenger-carrying railcars
Maximum vertical suspension deflection (%)	95	Suspension bottoming not allowed. Maximum compressive spring travel shall not exceed 95% of the spring travel from the empty car height of the outer load coils to solid spring height.
Maximum vertical dynamic augment acceleration (g)	0.9	Suspension bottoming not allowed. Vertical dynamic augment accelerations of a loaded car shall not exceed 0.9 G.

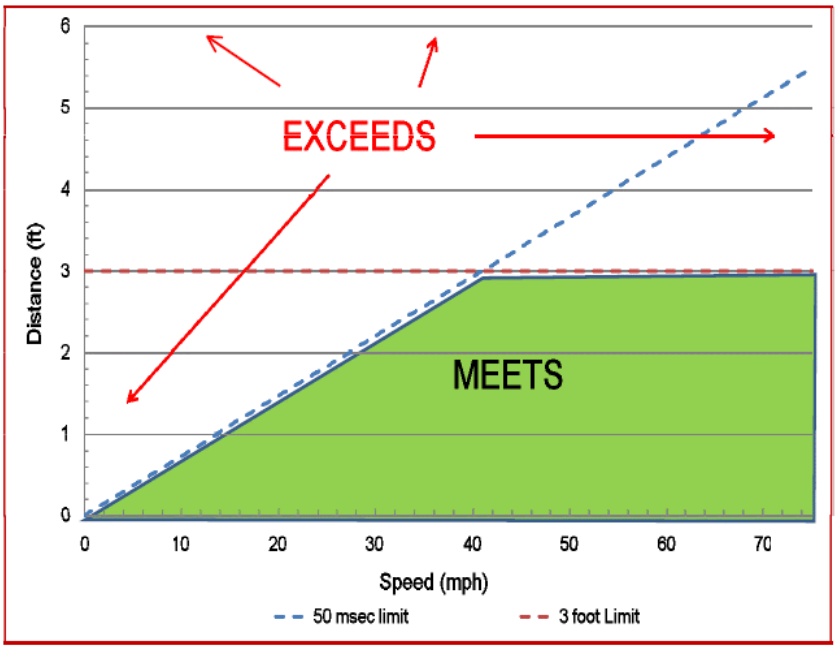


Figure 16. Time and Distance to Climb Limits

8.1. Track geometry (S-2043, Paragraph 5.5.6)

Unless otherwise specified, the track geometry in each test regime must conform to the requirements of *MSRP* Section C Part II, Specification M-1001, paragraph 11.7.2.5, Table 11.2.

8.2. Instrumentation

- The instrumentation / data collection package for these tests will be provided by TTCI and will include all of the necessary transducers for comparison with S-2043 performance measures. Measurements for the dynamic tests are listed in
- Table 19.

To provide precise measurements of wheel/rail forces, six IWS[†] will be installed in all the axles of the one span bolster, which can be placed in either the leading or trailing position as required by the particular test (see Figure 17). The IWS are being fabricated for DOE as part of this project.

Carbody lateral acceleration, carbody roll angle measurements, and spring group vertical displacement will be taken on each end of the vehicle.

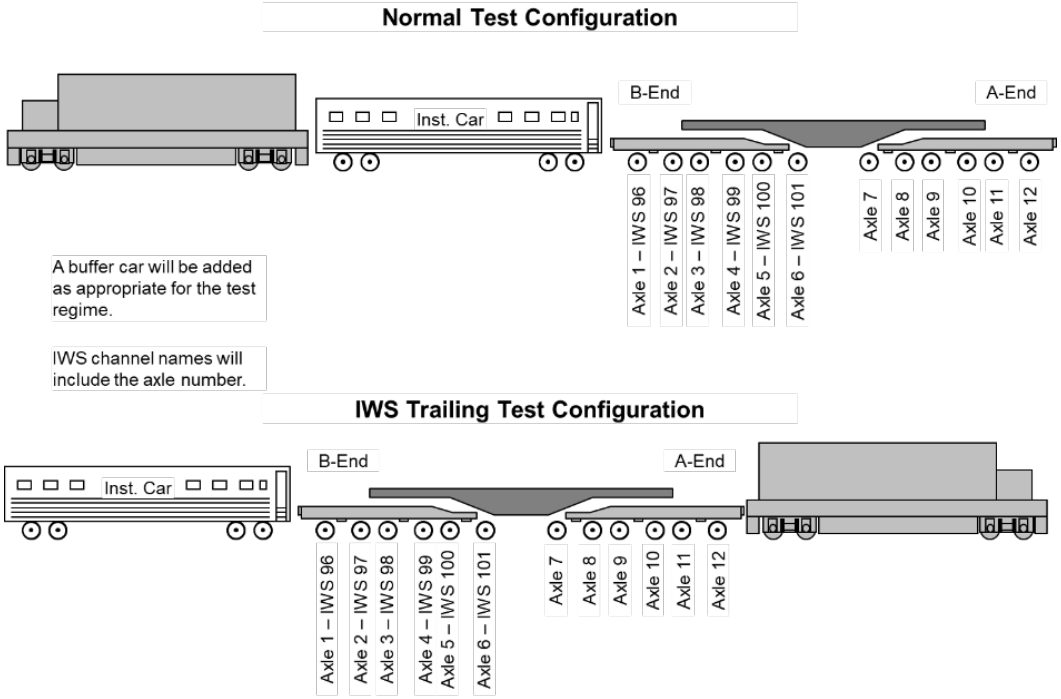


Figure 17. IWS Configuration

Data channels will include:

- 2 each – Roll Gyroscopes
- 2 each – Vertical Accelerometers
- 6 each – Lateral Accelerometers
- 12 each – 10in String Potentiometers
- 6 each – IWS
- 1 each – Speed Tachometer
- 1 each – Automatic Location Device

[††] Instrumented wheelsets must meet requirements of M-1001, Appendix C

Table 19. Measurement List for IWS Testing (1 of 2)

No.	Channel Name	Measurement Description	Expected Range	Measurement Frequency Response	Digital Sample Rate	Estimated Accuracy
1	Speed	Speed	0-80mph	0-1Hz	≥300Hz	better than 1%
2	ALD	Automatic Location Device	0-5V	≥15Hz	≥300Hz	better than 2%
3	VLX VRX LVLX LVRX TSLVLY TSLVRY X=Axle Num. Y=Truck Num.	IWS in Axle 1		≥15Hz	≥300Hz	better than 5%
4		IWS in Axle 2		≥15Hz	≥300Hz	better than 5%
5		IWS in Axle 3		≥15Hz	≥300Hz	better than 5%
6		IWS in Axle 4		≥15Hz	≥300Hz	better than 5%
7		IWS in Axle 5		≥15Hz	≥300Hz	better than 5%
8		IWS in Axle 6		≥15Hz	≥300Hz	better than 5%
9	ZACBB	Lead carbody vertical acceleration*	between ±2g and ±10g	≥15Hz	≥300Hz	better than 1%
10	ZACBA	Trail carbody vertical acceleration*	between ±2g and ±10g	≥15Hz	≥300Hz	better than 1%
11	YACBB	Lead carbody* lateral acceleration	between ±2g and ±10g	≥15Hz	≥300Hz	better than 1%
12	YACBA	Trail carbody lateral acceleration*	between ±2g and ±10g	≥15Hz	≥300Hz	better than 1%
13	YASBA1	Lead span bolster lead lateral acceleration	between ±2g and ±10g	≥15Hz	≥300Hz	better than 1%
14	YASBA2	Lead span bolster trail lateral acceleration	between ±2g and ±10g	≥15Hz	≥300Hz	better than 1%
15	YASBB1	Trail span bolster lead lateral acceleration	between ±2g and ±10g	≥15Hz	≥300Hz	better than 1%
16	YASBB2	Trail span bolster trail lateral acceleration	between ±2g and ±10g	≥15Hz	≥300Hz	better than 1%

*Carbody accelerometers to be placed as closely as possible to the span bolster centers

Table 19. Measurement List for IWS Testing (2 of 2)

No.	Channel Name	Measurement Description	Expected Range	Measurement Frequency Response	Digital Sample Rate	Estimated Accuracy
17	ZDSNBL	Vertical Displacement B truck Left Side >5 inch	>5 inch	≥15Hz	≥300Hz	better than 1%
18	ZDSNBR	Vertical Displacement B truck Right Side	>5 inch	≥15Hz	≥300Hz	better than 1%
19	ZDSNCL	Vertical Displacement C truck Left Side	>5 inch	≥15Hz	≥300Hz	better than 1%
20	ZDSNCR	Vertical Displacement C truck Right Side	>5 inch	≥15Hz	≥300Hz	better than 1%
21	ZDSNDL	Vertical Displacement D truck Left Side	>5 inch	≥15Hz	≥300Hz	better than 1%
22	ZDSNDR	Vertical Displacement D truck Right Side	>5 inch	≥15Hz	≥300Hz	better than 1%
23	ZDSNEL	Vertical Displacement E truck Left Side	>5 inch	≥15Hz	≥300Hz	better than 1%
24	ZDSNER	Vertical Displacement E truck Right Side	>5 inch	≥15Hz	≥300Hz	better than 1%
25	ZDSNFL	Vertical Displacement F truck Left Side	>5 inch	≥15Hz	≥300Hz	better than 1%
26	ZDSNFR	Vertical Displacement F truck Right Side	>5 inch	≥15Hz	≥300Hz	better than 1%
27	ZDSNAL	Vertical Displacement A truck Left Side	>5 inch	≥15Hz	≥300Hz	better than 1%
28	ZDSNAR	Vertical Displacement A truck Right Side	>5 inch	≥15Hz	≥300Hz	better than 1%
29	RDCBB	Carbody roll rotation, B-end	±4deg	≥15Hz	≥300Hz	better than 1%
30	RDCBA	Carbody roll rotation, A-end	±4deg	≥15Hz	≥300Hz	better than 1%
31	GPS	GPS	n/a	≥1Hz	≥1Hz	better than 1%

8.2.1. Data Acquisition

Data will be filtered at a rate ≥ 15 Hz and ≤ (sample rate/2). The minimum sample rate is 300 Hz. Data will be post filtered as required (15 Hz) and analyzed in near-real time using the performance criteria for dynamic testing provided in Table 18.

8.2.2. Functional Checks

Functional checks of the instrumentation should be made to verify that all the measurements are working correctly. These functional checks are not a calibration function but are done to verify the setup.

Common setup errors are faulty transducers, cabling errors, improper gain settings, etc. Perform functional checks to verify that the cables go where they are supposed to and measure about the right value. If a functional check of a transducer shows more than 10% error, look closely at the setup to make sure there are no mistakes.

- Record the functional checks in a data file so you can refer to them later if necessary.
- Perform the functional checks in a specific order and verify that the order matches what you observe in the data file.
- Pay attention to the sign of the output.

The following are typical functional checks for some transducers.

- Roll the accelerometers 90 degrees for a 1g input.
- Pull string pots and verify that extension is positive and that they read 1-inch when pulled one inch.
- Use a block of known size to check LVDTs and bending beams.
- Check speed measurements against GPS speed
- Verify load cells with an Rcal resistor and a breakout box.
- If possible, apply a known force to a loadcell. For example, use the car weight and the track grade from your Operating Rule Book to estimate the average expected force on the appropriate channel for a particular piece of track during resistance testing.

IWS are a special case. The following are suggested for functional tests of IWS. As IWS technology changes the steps might change.

- Verify the cable is connected where you think it is by disconnecting the cable at the wheelset and verifying that the “Disconnected” light comes on at the decoder box where you expect it to.
- Jack all IWS and zero all torque channels through software
- Push the Rcal button on the Decoder box and verify that you see the step change in the correct IWS channels.
- Record sync frequency from decoder boxes and record in the measurement information file (MIF)
- Record data on a portion of tangent track.
    - Vertical loads should match the scale weight to within 5%
    - Lateral loads should be small, resulting in L/V ratios of about 0.05. This may vary depending on truck design and condition.
    - Contact position output should be around zero. This may vary depending on truck design and condition.
    - If the wheelset is equipped with a torque bridge its average should be around zero. This may vary depending on truck design and condition.
- If a truck is fully instrumented with IWS, you can compare the net lateral load to a calculated value for a curve.

8.3. Hunting (S-2043, Paragraph 5.5.7)

The hunting test must conform to the requirements of M-1001 paragraph 11.7.2, with the exception of limiting criteria. High-speed stability (Hunting) testing is conducted to confirm that hunting (lateral oscillating instability in the trucks) does not occur within normal operating speeds of the train. Hunting is inherent in typical railroad freight truck designs when components are allowed to wear beyond normal limits.

The car will be equipped with wheel sets having KR wheel profiles (100,000-mile average worn profile) and will be operated at speeds up to 75 mph on tangent track.

8.3.1. Hunting Test Procedure and Test Conditions

The high-speed stability tests shall be conducted under the following conditions:

- Car will be tested with Minimum Condition and Maximum Condition Test Loads
- The car will be placed at the end of a consist following a stable buffer car (can be the instrumentation car)
- Maximum speed of 70 mph, 75 mph if deemed safe by the TTCI test team
- Track with FRA class 6 or better designation
- Rail profile is AREA 136 lb. or equivalent
- 56 5/16 in. < Track Gauge < 57 in.
- Wheels shall all have KR profile (100,000-mile average worn profile)
- Minimum coefficient of wheel/rail friction of 0.4

Data will be recorded in a short (about 1000-foot) section of the entry and exit spiral at each end of the tangent hunting zone to confirm performance in shallow curves.

8.3.2. Hunting Test Instrumentation and Test Conduct

Because IWS are not available with the KR wheel profile, the hunting tests must be conducted in two configurations:

- Using IWS with the AAR-1B narrow flange profile[8] that is required for all other dynamic tests. During these tests, the wheel sets in positions that are not instrumented must also have the AAR-1B narrow flange wheel profile.
- Using wheel sets (not instrumented) having the KR wheel profile in all positions.
- The test car will be instrumented as described in
- Table 19 with or without IWS as appropriate. Sustained truck hunting shall be determined by measuring the lateral acceleration of the carbody in 2,000-ft windows sliding every 10-ft over a tangent track section that is a minimum of 4,000-ft long. Time histories of the worst-case results that exceed criteria shall be submitted with the report.

Hunting tests will be performed on the RTT between R39 and R33.5. At a minimum data will be recorded from R40 to R33 to observe performance in the entry and exit spiral and curve. If hunting is observed during the test, it must be reported, even if it occurs in the non-tangent test section.

Table 20 shows the run list for each test load condition. Additional speeds may be added by the TTCI test team depending on car performance.

Table 20. Hunting Run List

Filename	Speed (mph)	Comments
	30	Track Conditioning Run
	40	
	50	
	55	
	60	
	65	
	70	
	75	If deemed safe by the TTCI test team

8.4. Twist and Roll (S-2043, Paragraph 5.5.8)

The twist and roll tests must conform to the requirements of M-1001 paragraph 11.8.2, with the exception of limiting criteria. The twist and roll test is conducted to determine the car's ability to negotiate oscillatory crosslevel perturbations. These perturbations are designed to excite the natural twist and roll motions of the car. The twist and roll test will be conducted on the Precision Test Track (PTT), station 1644+10 to 1651+70. Figure 18 provides a description of the Twist and Roll test zone.

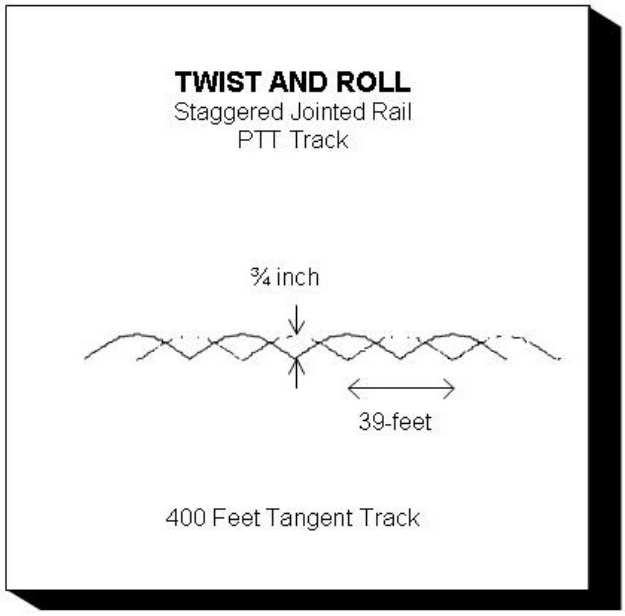


Figure 18. Twist and Roll Test Zone

8.4.1. Twist and Roll Test Procedure and Test Conditions

Twist and roll tests shall be conducted given the following conditions:

- Test car has a stable buffer car at each end (one can be the instrumentation car)
- AAR 1B wheel profiles
- Rail must not have more than 0.25 in. of gauge wear nor have plastic flow on the gauge side greater than 0.25 in.
- Starting test speed is well below predicted resonance and increases in 2 mph increments (or less) until resonance is passed. It is acceptable to approach a resonant condition from a higher speed.
- Minimum coefficient of friction is 0.4
- Tangent track
- Ten staggered perturbations of 39-ft wavelength and 0.75-in. cross-level (see Figure 18)
- Otherwise class 5 or better track

8.4.2. Twist and Roll Instrumentation and Test Conduct

Axles 1-6 will be equipped with IWSs as shown in Figure 17. The test shall be conducted with the B end leading (IWS-equipped span bolster leading). The test car will be instrumented as described in Table 19.

The individual wheel forces and the roll angles at each end of the carbody shall be measured continuously through the test zone. Time histories of the worst-case results that exceed criteria, and the number of exceedances over the various run speeds (as applicable) shall be submitted with the report.

Table 21 shows suggested runs for the twist and roll tests. Runs are performed starting at 10 mph and increasing in 2-mph increments until the lower center roll resonance is passed. Once lower center roll resonance is passed speeds are increased in 5 mph increments until 70 mph is reached. If performance is close to the limits smaller speed increments should be used to assure safety and closely identify the critical speed. If deemed safe by the TTCI test team, a 75-mph run will be performed.

Table 21. Empty Twist and Roll Test Runs

Filename	Speed	Comments
	10 mph	
	12 mph	
	14 mph	
	16 mph	
	18 mph	
	20 mph	
	22 mph	
	24 mph	
	26 mph	Transition from 2-mph increments to 5-mph increments at the discretion of TTCI test team
	30 mph	

Filename	Speed	Comments
	35 mph	
	40 mph	
	45 mph	
	50 mph	
	55 mph	
	60 mph	
	65 mph	
	70 mph	
	75 mph	If deemed safe by the TTCI test team

8.5. Yaw and Sway (S-2043, Paragraph 5.5.9)

The yaw and sway tests must conform to the requirements of M-1001 paragraph 11.8.4, with the exception of limiting criteria. The yaw and sway test is conducted to determine the ability of the car to negotiate laterally misaligned track, which will excite the car in a yaw and sway motion. The speeds at which the resonant dynamic reactions occur will be found if they occur before 75 mph is reached. Station 1921 to 1927 of the PTT is the test site for the Yaw and Sway Test. Figure 19 provides a description of the Yaw and Sway test zone.

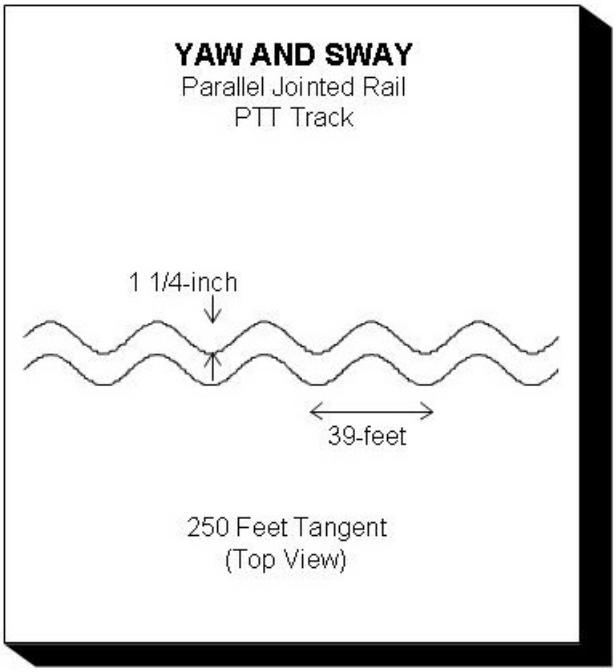


Figure 19. Yaw and Sway Test Zone

8.5.1. Yaw and Sway Test Procedure and Test Conditions

Yaw and sway tests shall be conducted given the following conditions:

- Maximum Test Load Condition only
- Test car has a leading stable buffer with a minimum truck center of 45 ft. (can be the instrumentation car)
- No Trailing buffer car
- Minimum coefficient of friction is 0.4
- AAR 1B wheel profiles
- Rail must not have more than 0.25 in. of gauge wear nor have plastic flow on the gauge side greater than 0.25 in.
- Starting test speed is well below predicted resonance and increases in 5 mph increments (or less) until resonance, an unsafe condition, or 75 mph is reached.
- Tangent track
- Constant wide gauge of 57.5 inch
- Five parallel perturbations of 39-ft wavelength and maximum 1.25-in. lateral amplitude (see Figure 19).
- Track is otherwise class 5 or better

8.5.2. Yaw and Sway Instrumentation and Test Conduct

Axles 1-6 will be equipped with IWSs as shown in Figure 17. Dynamic modeling predictions show that the last truck in the car has truck side L/V ratios that are slightly higher than other locations. Because of this the test shall be conducted with the A end leading (IWS-equipped span bolster trailing). The wheel forces shall be measured continuously through the test zone. Time histories of the worst-case results that exceed criteria shall be submitted with the report.

Table 22 shows suggested runs for the yaw and sway test. Runs are performed starting at 30 mph and increasing in 5 mph increments until 70 mph is reached. If performance is close to the limits smaller speed increments may be used to assure safety and closely identify the critical speed. If deemed safe by the TTCI test team, a 75-mph run will be performed.

Table 22. Loaded Yaw and Sway Test Runs

Filename	Speed	Comments
	30	
	35	
	40	
	45	
	50	
	55	
	60	
	65	
	70	
	75	If deemed safe by the TTCI test team

8.6. Dynamic Curving (S-2043, Paragraph 5.5.10)

The dynamic curving tests must follow the requirements of M-1001 paragraph 11.8.5, with the exception of limiting criteria. The dynamic curving test is designed to determine the ability of the car to negotiate curved track with simultaneous cross level and gage (vertical and lateral) misalignments. The dynamic curving test is conducted on the 10-degree bypass curve of the WRM track. Figure 20 provides a description of the Dynamic Curve Test location.

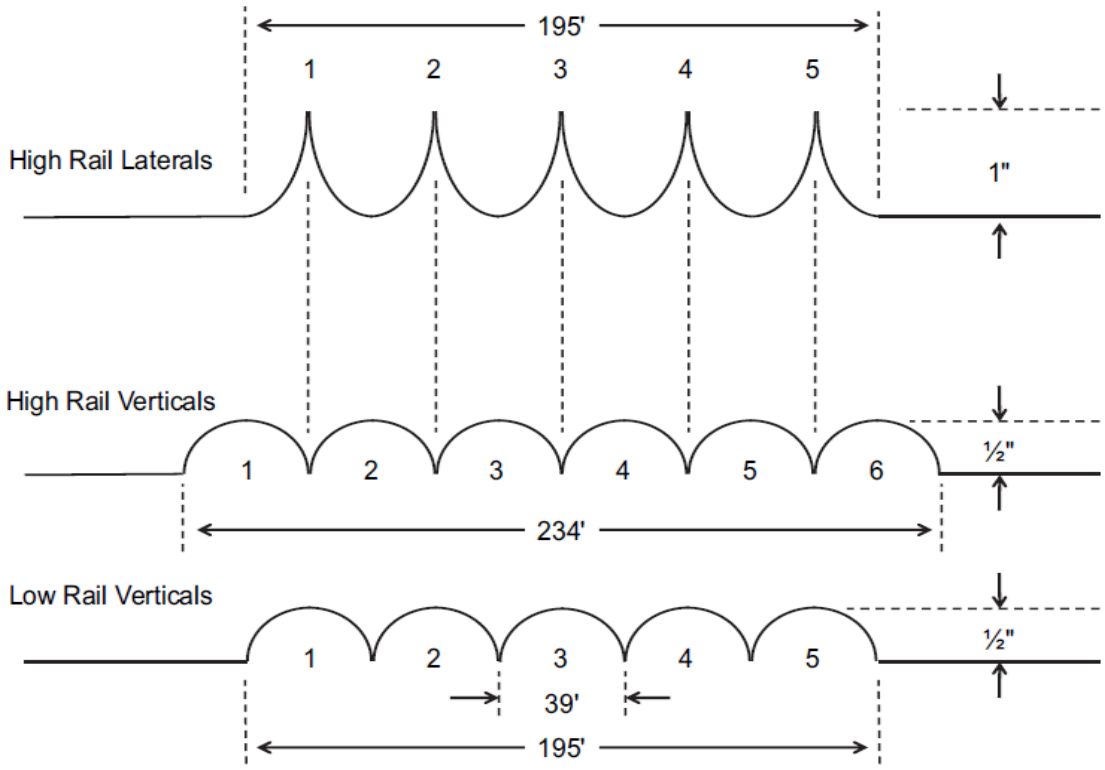


Figure 20. Dynamic Curving Test Zone

S-2043 requires that dynamic curving tests be performed for any likely intermediate load condition. The dynamic modeling prediction report[3] shows in Tables 6, 7, and 8 that the different cask loads have very consistent dynamic curve performance. The exception is that the HI-STAR 190XL (Maximum Condition Test Load) performs significantly worse than the other cases. Because of this, TTCI plans to test only the Maximum condition test load to represent the worst-case performance and the Minimum condition test load to represent the typical performance.

8.6.1. Dynamic Curving Test Procedure and Test Conditions

Dynamic curve tests shall be conducted given the following conditions:

- Minimum Condition and Maximum Condition Test Loads
- Test car between two stable buffers (one can be the instrumentation car)
- Minimum coefficient of friction is 0.4
- AAR 1B wheel profiles
- Rail must not have more than 0.25 in. of gauge wear nor have plastic flow on the gauge side greater than 0.25 in.
- Curvature is between 10° and 15° with a balance speed between 15 and 25 mph.
- Starting test speed is –3 in. under-balance with (but not limited to) 2 mph increments and a maximum of +3 in. over-balance. The resonance point may be approached from a higher speed.
- Five staggered perturbations of 39-ft wavelength and 0.5-in. cross-level (see Figure 20)
- Five alignment cusps having the maximum gauge of 57.5 in. coincident with low points of the outside rail and the 56.5 in. gauge points associated with the inner rail low points (see Figure 20)
- It is recommended that a guard rail be used to prevent unpredicted derailment; however, it must not be in contact with the wheel during normal test running.

8.6.2. Dynamic Curving Instrumentation and Test Conduct

Axles 1-6 will be equipped with IWS as shown in Figure 17. Testing is required with both B and A ends leading (IWS-equipped span bolster leading and trailing). The carbody roll angle shall also be measured at one end of the lead unit. The lateral and vertical wheel forces and the roll angle shall be measured continuously through the test zone. Time histories of the worst-case results that exceed criteria, along with a count of the number of occurrences (as applicable) shall be submitted with the report.

Table 23 shows required runs for the dynamic curving test for each load and leading end condition. Tests are done CW and CCW.

Table 23. Dynamic Curving Test Runs

Filename	Speed	Direction	Comments
	10	CW	
	12	CW	
	14	CW	
	16	CW	
	18	CW	
	20	CW	
	22	CW	
	24	CW	
	26	CW	
	28	CW	
	30	CW	
	32	CW	
	10	CCW	
	12	CCW	
	14	CCW	
	16	CCW	
	18	CCW	
	20	CCW	
	22	CCW	
	24	CCW	
	26	CCW	
	28	CCW	
	30	CCW	
	32	CCW	

8.7. Pitch and Bounce (S-2043, Paragraph 5.5.11)

The pitch and bounce tests must follow the requirements of M-1001 paragraph 11.8.3, with the exception of limiting criteria. The pitch and bounce test is designed to determine the dynamic pitch and bounce response of the car as it is excited by inputs from the track. The pitch and bounce test is conducted on the PTT track, stations 1710 and 1715. Figure 21 provides a description of the Pitch and Bounce test zone.

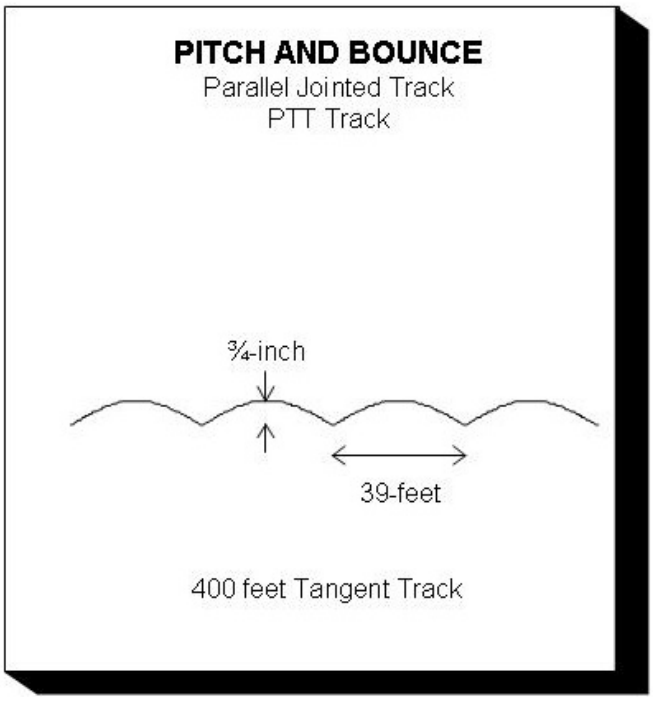


Figure 21. Pitch and Bounce Test Zone

8.7.1. Pitch and Bounce Test Procedure and Test Conditions

Pitch and bounce tests shall be conducted given the following conditions:

- Maximum Condition Test Load
- Test car has a stable buffer car at each end with a minimum 45-ft truck center (one can be the instrumentation car)
- AAR 1B wheel profiles
- Rail must not have more than 0.25 in. of gauge wear nor have plastic flow on the gauge side greater than 0.25 in.
- Starting test speed is well below predicted resonance and increases in 5 mph increments (or less) until resonance, an unsafe condition, or 75 mph is reached. It is acceptable to approach a resonant condition from a higher speed.
- Tangent track
- Ten parallel perturbations of 39-ft wavelength and maximum 0.75-in. vertical amplitude (see Figure 21Figure 21)
- Otherwise class 5 or better track

8.7.2. Pitch and Bounce Instrumentation and Test Conduct

Axles 1-6 will be equipped with IWSs as shown in Figure 17. The test shall be conducted with the B end leading (IWS-equipped span bolster leading). The vertical wheel forces shall be measured continuously through the test zone. Time histories of the worst-case results that exceed criteria shall be submitted with the report.

Table 24 shows suggested runs for the pitch and bounce test. Runs are performed starting at 30 mph and increasing in 5 mph increments until 70 mph is reached. A 75-mph run will be performed if deemed safe by the TTCI test team. If performance is close to the limits smaller speed increments should be used to assure safety and closely identify the critical speed.

Table 24. Pitch and Bounce Test Runs

Filename	Speed	Comments
	30	
	35	
	40	
	45	
	50	
	55	
	60	
	65	
	70	
	75	If deemed safe by the TTCI test team

8.8. Pitch and Bounce Special (S-2043, Paragraph 5.5.12)

S-2043 requires that a special section of track with ¾ inch bumps at a wavelength equal to the truck center spacing be built for the car being tested. For railcars with span bolster suspensions the truck center spacing wavelength should be taken as the spacing of the span bolster center pivots on the railcar body. This distance is 38-feet for the Atlas Cask car.

TTCI proposes to not build a special section of track because it would be very similar to the standard pitch and bounce section built with 39-foot wavelength.

The dynamic analysis report[3] shows in Tables 11 and 12 and Figures 18 and 19 that the predicted performance of the car on 38-foot wavelength inputs is very similar to performance of the car on 39-foot wavelength inputs.

8.9. Single Bump Test (S-2043, Paragraph 5.5.13)

This test is intended to represent a grade crossing. Tests will be performed over a 1.0-in. bump on tangent track. The single bump will be a flat-topped ramp with the initial elevation change over 7 ft., a steady elevation over 20 ft., ramping back down over 7 ft. Track geometry for the single bump test must be maintained to the following tolerances:

- ±1/8-inch amplitude for the bump
- ±1/8-inch cross level
- ±1/4-inch gage

The test zone will be installed on the transit test track at T-15 using rail bent specifically for this purpose.

Table 25 shows suggested runs for the single bump test. Runs are performed starting at 40 mph and increasing in 5 mph increments until 70 mph is reached. A 75-mph run will be performed if deemed safe by the TTCI test team. If performance is close to the limits smaller speed increments should be used to assure safety and closely identify the critical speed. This test will be performed for both Minimum and Maximum Test Load conditions.

Table 25. Single Bump Test Runs

Filename	Speed	Comments
	40	
	45	
	50	
	55	
	60	
	65	
	70	
	75	If deemed safe by the TTCI test team

8.10. Curve Entry/Exit (S-2043, Paragraph 5.5.14)

8.10.1. Limiting Spiral Negotiation

The spiral negotiation tests must conform to the requirements of M-1001 paragraph 11.7.4, with the exception of limiting criteria. Spiral negotiation, or curve entry and curve exit, tests will be performed in conjunction with the dynamic curving tests. A spiral is the transition from a tangent track to a curve that includes constant rates of change in cross level and curvature with distance. The limiting spiral consists of a steady curvature change from 0 degree to 10 degrees and a steady super elevation change of 4 3/8 inches in 89 feet. The purpose of the exaggerated limiting spiral is to twist the trucks and the carbody.

The limiting spiral test zone is located at the beginning of the 10-degree bypass curve of the Wheel/Rail Mechanisms (WRM) track (see Figure 22) during clockwise operation. Tests are done at the same time as the dynamic curving test and in both the clockwise and counter-clockwise directions, with both B and A ends leading (IWS-equipped span bolster leading and trailing). Curve entry and exit performance will also be examined for the 7.5-, 12-, and 10-degree curves (see Figure 22).

8.10.2. Spiral Negotiation Test Procedure and Test Conditions

This test will be carried out concurrently with the curving tests conducted on the WRM track. Curving tests will be performed under the following conditions:

- Speed corresponding to 3 in. of cant (superelevation) deficiency, balance speed, and speed corresponding to 3 in. of cant (superelevation) excess (-3 in., 0 in., and +3 in.)
- Testing in both Minimum and Maximum Test Load conditions
- Use of a leading and trailing buffer car (one of which can be the instrumentation car)
- Test in both directions (turning consist)
- Minimum coefficient of friction is 0.4
- AAR 1B wheel profiles
- Rail must not have more than 0.25 in. of gauge wear nor have plastic flow on the gauge side greater than 0.25 in.
- Minimum curvature is 7° with a balance speed of 20 to 30 mph
- Class 5 track or better
- Spiral geometry shall have a super elevation rate of 3 inches in 62 feet and a minimum length of 89 ft.

8.10.3. Spiral Negotiation Instrumentation and Test Conduct

Axles 1-6 will be equipped with IWS as shown in Figure 17. Testing is required with both B and A ends leading (IWS-equipped span bolster leading and trailing). The lateral and vertical forces and their ratio, L/V, shall be measured continuously through qualified spirals in both directions, and their maxima and minima computed. Time histories of the worst-case results that exceed criteria shall be submitted with the report.

Table 26 shows required runs for the limiting spiral test. Test speeds correspond to 3-inches under balance, balance, and 3-inches over balance. Tests are done in both the CW and CCW directions. Two runs will be done at each speed.

Table 26. Limiting Spiral Test Runs

Filename	Speed	Direction	Comments
	12	CW	
	12	CW	
	24	CW	
	24	CW	
	32	CW	
	32	CW	
	12	CCW	
	12	CCW	
	24	CCW	
	24	CCW	
	32	CCW	
	32	CCW	

8.11. Curving with Single Rail Perturbation (S-2043, Paragraph 5.5.15)

This test is intended to represent a low or high joint in a yard or a poorly maintained lead track. Two test scenarios will be run, one with a 2-inch outside rail dip and the other with a 2-inch inside rail bump. Both tests will be conducted on the URB north wye track, a 12-degree curve with less than 1/2-inch nominal superelevation. The inside rail bump shall be a flat-topped ramp with an elevation change over 6-ft, a steady elevation over 12 ft., ramping back down over 6 ft. The outside rail dip shall be the reverse. Two rails have been bent for these perturbations. The two perturbations will be installed in the URB north wye curve about 250 feet apart. Track geometry for the single bump test must be maintained to the following tolerances:

- ±1/8-inch amplitude for the bump
- ±1/8-inch crosslevel
- ±1/4-inch gage

Table 27 shows required runs for the curving with single rail perturbation test. Tests will be performed in 2-mph increments for 4 mph to 14 mph in both the Minimum and Maximum Test Load conditions. Test runs will be performed traveling south on the Transit test track through the diverging route of the turnout onto the north wye track with B-end of the car leading.

Table 27. Curving with Single Rail Perturbation Test Runs

Filename	Speed	Comments
	4	
	6	
	8	
	10	
	12	
	14	

8.12. Standard Chapter 11 Constant Curving (S-2043, Paragraph 5.5.16)

The constant curving tests must follow the requirements of M-1001 paragraph 11.7.3, with the exception of limiting criteria. Constant curving tests were designed to determine the car's ability to negotiate well-maintained track curves. This test is intended to verify that a car will not experience wheel climb or impart large lateral forces to the rails during curving. Per Table 18, maximum wheel L/V ratio shall not exceed 0.8 for more than 50 ms. and the 95th percentile wheel L/V shall not exceed 0.6.

The train will be operated in the Minimum and Maximum Test Load condition on the 7.5-, 10-, and 12-degree curves of WRM track at speeds corresponding to three inches under balance, balance, and three inches over balance (12, 24, and 32 mph). Tests will be run in both clockwise and counterclockwise directions. Wheel L/V ratios will be monitored to ensure safe test operation. Figure 22 provides a description of the curving test zone.

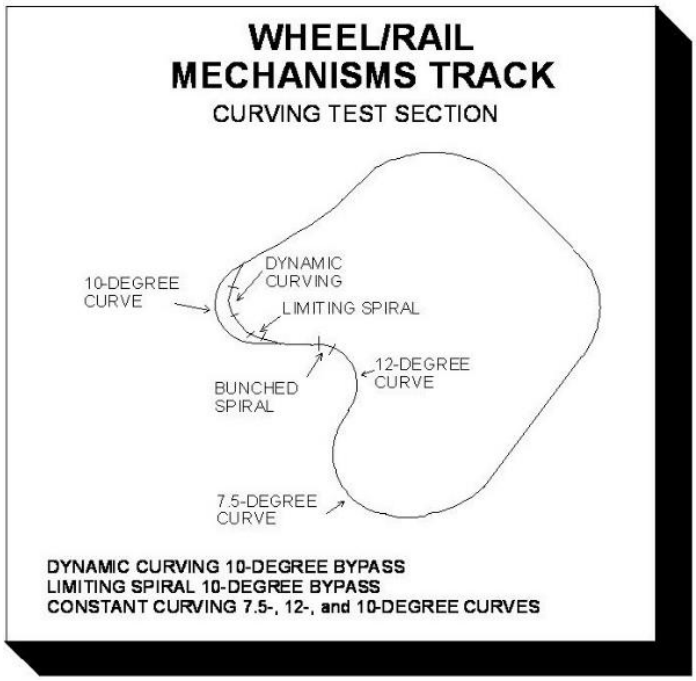


Figure 22. Curving Test Zone

8.12.1. Curving Test Procedure and Test Conditions

Curving tests will be performed under the following conditions:

- Speed corresponding to 3 in. of cant (superelevation) deficiency, balance speed, and speed corresponding to 3 in. of cant (superelevation) excess (-3 in., 0 in., and +3 in.)
- Testing in both Minimum and Maximum Test Load conditions
- Use of a leading and trailing buffer car (one of which can be the instrumentation car)
- Test in both directions (turning consist)
- Minimum coefficient of friction is 0.4
- AAR 1B wheel profiles
- Rail must not have more than 0.25 in. of gauge wear nor have plastic flow on the gauge side greater than 0.25 in.
- Minimum curvature is 7° with a balance speed of 20 to 30 mph
- Class 5 track or better
- Curve length must be a minimum of 500 ft.

8.12.2. Curving Instrumentation and Test Conduct

Axles 1-6 will be equipped with IWS as shown in Figure 17. Testing is required with both B and A ends leading (IWS-equipped span bolster leading and trailing). The lateral and vertical forces and

their ratio, L/V, shall be measured for the length of the body of the curve. A time history of the worst-case results that exceed criteria must be submitted in the report.

Table 28 shows required runs for the steady state curving test for each load and leading end condition. Test speeds correspond to 3-inches under balance, balance, and 3-inches over balance. Tests are done CW and CCW. Repeat each run at least once.

Table 28. Standard Chapter 11 Constant Curving Test Runs

Filename	Speed (mph)	Direction	Comments
	12-15-12	CW	3 in. underbalance speeds for 7.5-, 12-, and 10-degree curves on WRM loop, respectively.
	12-15-12	CW	3 in. underbalance speeds for 7.5-, 12-, and 10-degree curves on WRM loop, respectively.
	24	CW	Approximate balance speed for all curves
	24	CW	Approximate balance speed for all curves
	32	CW	Approximate 3 in. overbalance speed for all curves
	32	CW	Approximate 3 in. overbalance speed for all curves
	12-15-12	CCW	3 in. underbalance speeds for 7.5-, 12-, and 10-degree curves on WRM loop, respectively.
	12-15-12	CCW	3 in. underbalance speeds for 7.5-, 12-, and 10-degree curves on WRM loop, respectively.
	24	CCW	Approximate balance speed for all curves
	24	CCW	Approximate balance speed for all curves
	32	CCW	Approximate 3 in. overbalance speed for all curves
	32	CCW	Approximate 3 in. overbalance speed for all curves

8.13. Special Trackwork (S-2043, Paragraph 5.5.17)

The railcar will be run through various switches, turnouts, and crossovers while measuring wheel/rail forces. The railcar must be run through an AREMA straight point turnout with a number 8 or tighter frog angle. The test will be performed in both directions, at speeds from walking speed to the switch speed limit. Similar tests must be performed through a crossover with number 10 or tighter turnouts on 15-ft or narrower track centers.

The railcar will be tested with the Minimum and Maximum Condition Test Load.

Switch number 704 between the Transit Test Track and the North URB Wye will be used for the turnout tests. Crossover number 212 between the Impact Track and the FAST Wye will be used for crossover tests.

During the walking speed tests, the railcar will be monitored visually to note any binding or interference between the trucks and carbody.

Axles 1-6 will be equipped with IWS as shown in Figure 17. Testing is required with both B and A ends leading (IWS-equipped span bolster leading and trailing). The lateral and vertical forces and their ratio, L/V, shall be measured for the length of the body of the curve. A time history of the worst-case results that exceed criteria must be submitted in the report.

Table 29 shows required runs for the special trackwork turnout test. Test speeds are from walking speed to the turnout speed limit. Tests are done in both directions (switch point leading and trailing) along the diverging route and with B- and A-end leading.

Table 29. Special Trackwork Turnout Test

Filename	Speed	Direction	Comments
	Walking	Facing Point	Check Clearances
	4	Facing Point	
	6	Facing Point	
	8	Facing Point	
	10	Facing Point	
	12	Facing Point	
	14	Facing Point	
	15	Facing Point	
	Walking	Trailing Point	Check Clearances
	4	Trailing Point	
	6	Trailing Point	
	8	Trailing Point	
	10	Trailing Point	
	12	Trailing Point	
	14	Trailing Point	
	15	Trailing Point	

Table 30 shows required runs for the special trackwork crossover test. Test speeds are from walking speed to the crossover speed limit. Tests are done in both directions and with B- and A-end leading.

Table 30. Special Trackwork Crossover Test

Filename	Speed	Direction	Comments
	Walking	Impact-Fast Wye	Check Clearances
	5	Impact-Fast Wye	
	10	Impact-Fast Wye	
	15	Impact-Fast Wye	
	20	Impact-Fast Wye	
	Walking	Fast Wye-Impact	Check Clearances
	5	Fast Wye-Impact	
	10	Fast Wye-Impact	
	15	Fast Wye-Impact	
	20	Fast Wye-Impact	

9. TEST SCHEDULE

Figure 23 provides a preliminary test schedule. Detailed scheduling will be based on resource and facility availability. TTCI is evaluating the potential for accelerating the schedule based on anticipated arrival of the railcar in February 2018.

Single Car Testing	Start	Finish	Qtr3 2018	Qtr4 2018	Qtr1 2019	Qtr2 2019	Qtr3 2019	Qtr4 2019	Qtr1 2020	Qtr2 2020	Qtr3 2020	Qtr4 2020
Buffer Car Tests						* * * * * * * * * * * *						
Instrumentation Preparation	*Apr-19*	*Apr-19*				■						
Characterization Tests	*May-19*	*Jul-19*				■ ■ ■						
Static Tests	*Jul-19*	*Jul-19*				■						
Structural Tests	*Aug-19*	*Aug-19*				■						
Dynamic Tests	*Aug-19*	*Sep-19*				■ ■						
Contingency	*Oct-19*	*Jan-20*				■ ■ ■ ■						
Cask Car Tests						* * * * * * * * * * * *						
Instrumentation Preparation	*Apr-19*	*Apr-19*				■						
Characterization Tests	*May-19*	*Jul-19*				■ ■ ■						
Static Tests	*Aug-19*	*Sep-19*				■ ■						
Structural Tests	*Sep-19*	*Sep-19*				■						
Dynamic Tests	*Oct-19*	*Dec-19*				■ ■ ■						
Contingency	*Jan-20*	*Feb-20*				■ ■						
Reporting / Coordination with EEC									* * * * * * * * *			
Data Analysis and Reporting	*Feb-20*	*Aug-20*							■ ■ ■ ■ ■ ■ ■			
Coordination with EEC	*Apr-20*	*Oct-20*							■ ■ ■ ■ ■ ■ ■			
Approval for Multi-Car Test	*Oct-20*											■

Figure 23. Preliminary Test Schedule

10. REFERENCES

1. *AAR Manual of Standards and Recommended Practices,* Car Construction Fundamentals and Details, Performance Specification for Trains Used to Carry High-Level Radioactive Material, Standard S-2043, Effective: 2003; Last Revised: 2017, Association of American Railroads, Washington, DC

2. *AAR Manual of Standards and Recommended Practices*, Section C—Part II, Car Construction Fundamentals and Details, Design, Fabrication, and Construction of Freight Cars, Chapter 2, General Data, Implemented 11/2017, Association of American Railroads, Washington, DC

3. *AAR Manual of Standards and Recommended Practices,* Section C—Part II, Car Construction Fundamentals and Details, Design, Fabrication, and Construction of Freight Cars, Chapter 11, Service-Worthiness Tests and Analyses for New Freight Cars, Implemented 09/2017, Association of American Railroads, Washington, DC

4. *TTCI Safety Rule Book*, TTCI Intranet, January 2018 or Latest Revision

5. *TTCI Operating Rule Book,* TTCI Intranet, January 2018 or Latest Revision

6. Walker, Russell and Shawn Trevithick, "S-2043 Certification: Preliminary Simulations of Kasgro-Atlas 12-Axle Cask Car". Report No. P-17-021, TTCI Pueblo, CO, December 2017

7. Walker, Russell and Satima Anankitpaiboon. "S-2043 Certification Tests of Kasgro M-290 12-Axle Flat Car". Report No. P-09-044, TTCI, Pueblo, CO, December 2009

8. *Manual of Standards and Recommended Practices* Section G Safety and Operations -- Wheels and Axles, Figure B12, Effective September 2016, Association of American Railroads, Washington, DC,

9. TTCI network: \DOE Controlled Document Folder\DW - Drawings and Specifications\DW-18-002 Kasgro SG Location Cask and Buffer Car .zip\1155-45 REV A Kasgro SG Location Cask Car.dwg

APPENDIX A – TEST TRACK DETAILS

1. INTRODUCTION

Testing is planned on various test tracks at the Transportation Technology Center including the Railroad Test Track (RTT), the Wheel Rail Mechanisms (WRM) Loop, the Precision Test Track (PTT), the URB Wye, the Tight Turn Loop (TTL or Screech Loop), and a crossover between the Impact Track and FAST Wye. Figure A1 shows locations of the various tracks. Sections A2.0 to A6.0 describe the tracks planned to be used for the Atlas and Buffer car testing.

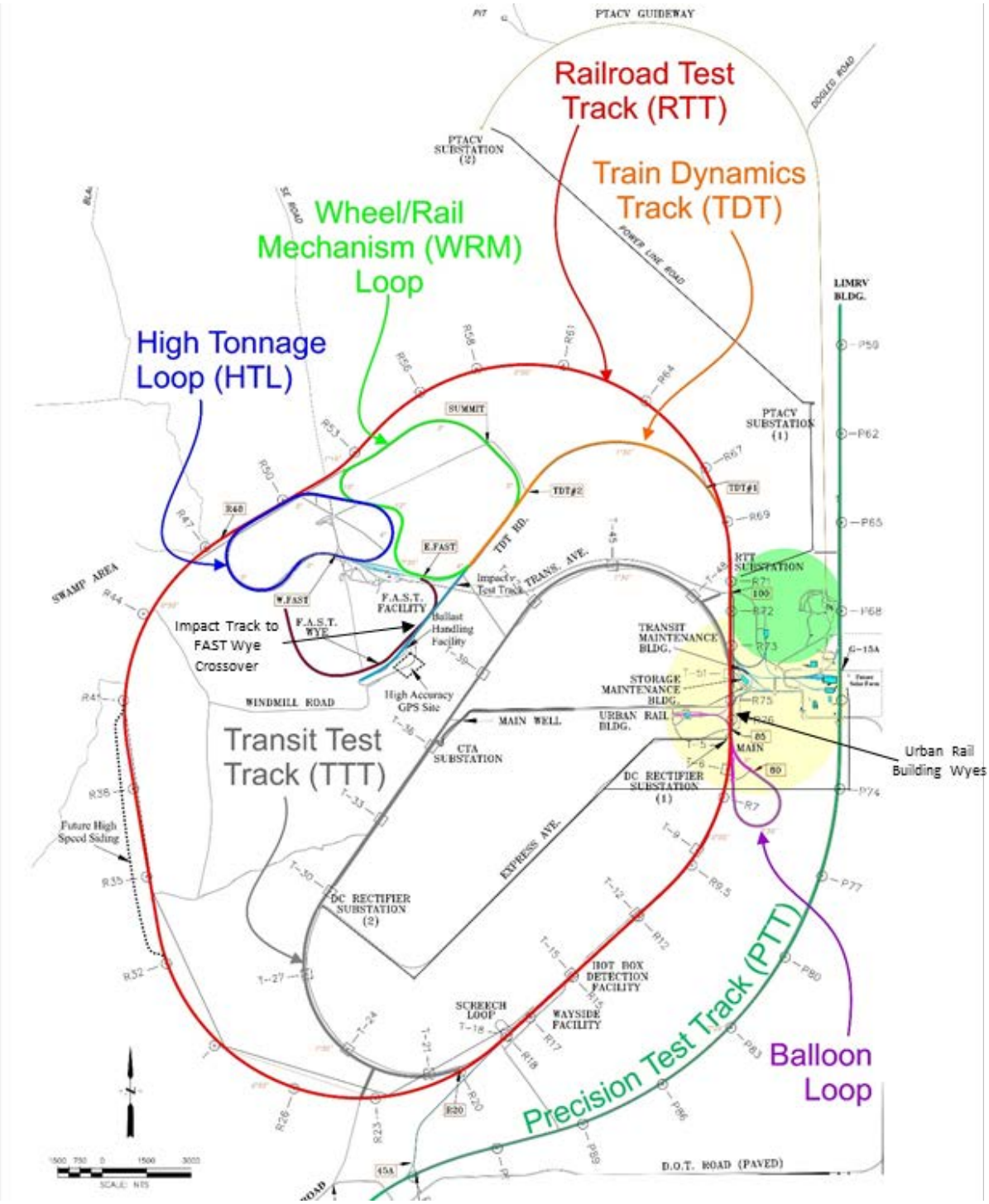


Figure A1 - Test Tracks at TTC

2. RAILROAD TEST TRACK (RTT)

The 13.5-mile Railroad Test Track (RTT) will be used for High Speed Stability (Hunting) testing of the Atlas and buffer cars. The RTT alignment is designed to test passenger vehicles with tilt technology at a maximum running speed of 165 mph. Maximum speed for non-tilting vehicles is typically 124 mph. Freight vehicle testing is limited to 80 mph operating speed, unless qualified for higher speeds.

3. WHEEL / RAIL MECHANISMS (WRM) LOOP

The Wheel / Rail Mechanisms (WRM) Loop incorporates curve variations constructed to meet the curved track test requirements of AAR Specification M-1001, Chapter 11. These variations are also applicable to S-2043 testing and will be used for several tests of the Atlas and buffer cars. The WRM is maintained as a non-lubricated track for test purposes. Strain gages have been installed in some of the curves for measuring Wheel/Rail interaction forces. Figure A2 shows details of track in a siding on the inside of the 10-degree curve that is the location of dynamic curve track perturbations.



Figure A2. Adjustable Tie Plates and Perturbations on the WRM

4. PRECISION TEST TRACK (PTT)

The Precision Test Track (PTT) is a 7.4-mile track section that is used to test for vehicle dynamic response under perturbed track conditions. Three perturbed track test sections have been installed:

- Twist and roll test section in the north tangent section (PTT Stations 1644+10 to 1651+70). Due to the location of these perturbations, and the limited acceleration capability of TTC locomotives, the maximum test speed through this test section is typically about 70 mph, although preparations are being made to achieve 75 mph for this test program.
- Pitch and bounce test section in the south end of the same tangent section (PTT Stations 1710 to 1715).

- Yaw and Sway test section on the south end of the PTT (PTT Approx. Stations 1921 to 1927)

The perturbation sections for twist and roll, and pitch and bounce have been re-built using new ties and adjustable alignment plates with elastic fasteners, screw spikes, and steel shim plates. The adjustable tie plate system is the same that is in place on the WRM Loop.

5. TIGHT TURN LOOP

The Tight Turn Loop (TTL), also called the screech loop, will be used for the Horizontal Curve Negotiation test. It is located at the lower end of the south east tangent section of the Transit Test Track. The TTL layout is as shown on Figure A3. It consists of a 150' radius loop (38.9-degree curve) constructed as a ballasted track with 119-pound continuous welded rail on wood ties. The loop is connected with a short spur track having a 17-⅔ degree curve. The main purpose of the TTL is to provide a facility for the detailed investigation of wheel noise, truck curving behavior, and rail vehicle stability under extreme curvature conditions.

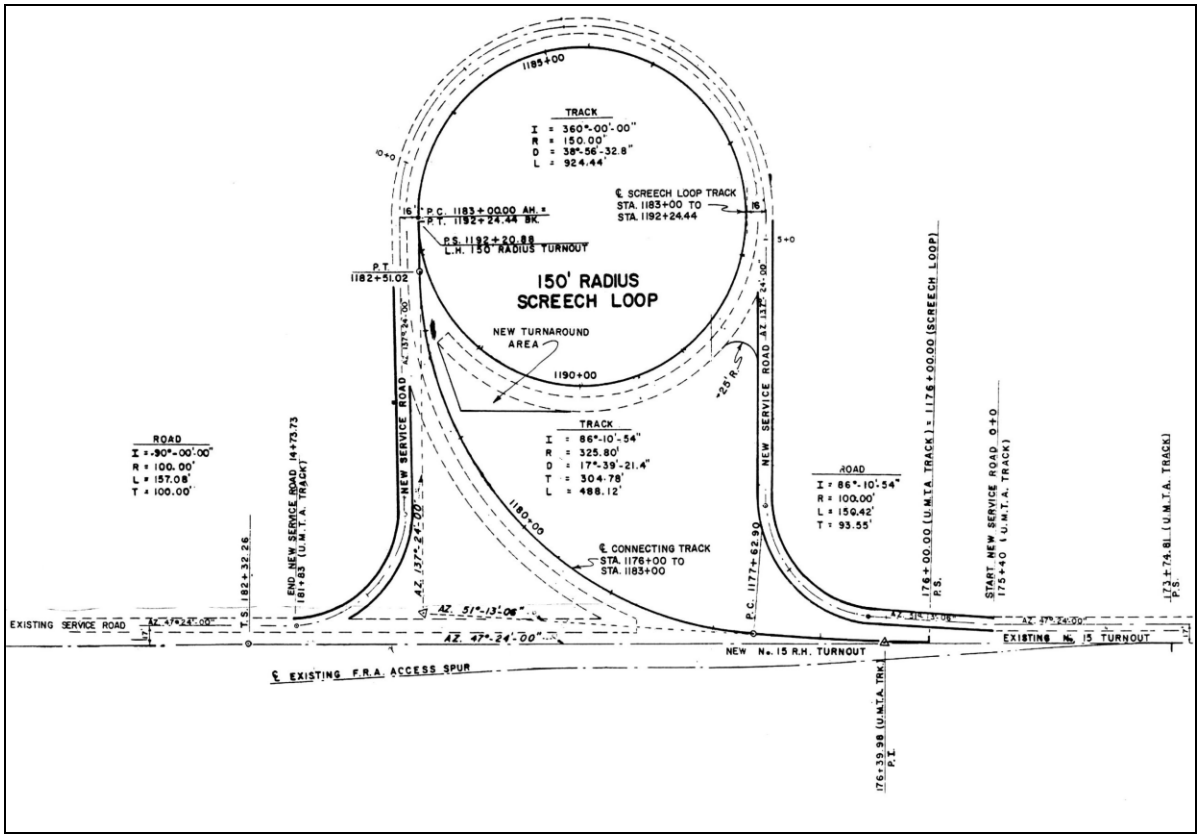


Figure A3 - Tight Turn Loop Layout

6. OTHER LOCATIONS

Testing is also planned on the North URB Wye, which connects the Urban Rail Building access track to the TTT, and on the crossover between the Impact Track and the FAST Wye. See Figure for these locations.

APPENDIX B – STRAIN GAUGE LOCATIONS FOR STRUCTURAL TESTS

Figure B1 provides location details. Table B1 describes the strain gauge channels for structural testing.

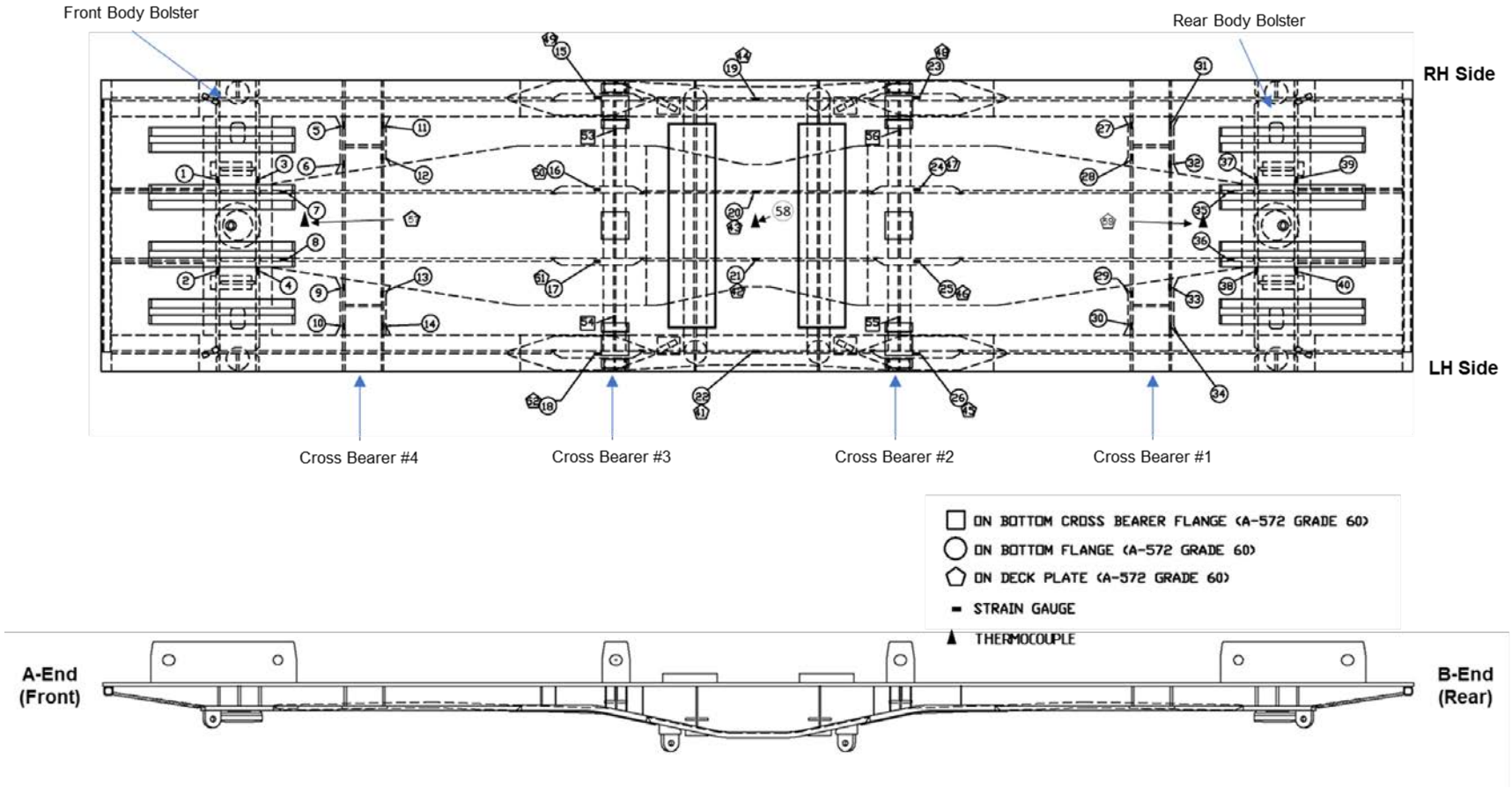


Figure B1. Strain Gauge/Thermocouple Locations

Table B1a. Strain Gauge and Thermocouple Channels (1 of 8)

Figure B1 Ref	Channel Name	Approximate Locations (confirm based on latest version of Kasgro Drawing 1155-45)[9]	Yield Strain at gauge location (μstr)	Modulus of Elasticity at Gauge Location (10^6 ksi)	Units	Expected Range
1	SGBF1	Front of bottom flange of front body bolster near center sill -- RH side	2069	29	μstr	±2500
2	SGBF2	Front of bottom flange of front body bolster near center sill -- LH side	2069	29	μstr	±2500
3	SGBF3	Rear of bottom flange of front body bolster near center sill -- RH side	2069	29	μstr	±2500
4	SGBF4	Rear of bottom flange of front body bolster near center sill -- LH side	2069	29	μstr	±2500
5	SGBF5	Front of bottom flange of #4 cross bearer, RH side between center sill and side sill, near side sill	2069	29	μstr	±2500
6	SGBF6	Front of bottom flange of #4 cross bearer, RH side between center sill and side sill, near center sill	2069	29	μstr	±2500
7	SGBF7	RH side of bottom flange of center sill - aft of front body bolster - aligns with center sill web and end stop mount block pin hole	2069	29	μstr	±2500
8	SGBF8	LH side of bottom flange of center sill - aft of front body bolster - aligns with center sill web and end stop mount block pin hole	2069	29	μstr	±2500

Table B1b. Strain Gauge and Thermocouple Channels (2 of 8)

Figure B1 Ref	Channel Name	Approximate Locations (confirm based on latest version of Kasgro Drawing 1155-45)[9]	Yield Strain at gauge location (μstr)	Modulus of Elasticity at Gauge Location (10^6 ksi)	Units	Expected Range
9	SGBF9	Front of bottom flange of #4 cross bearer, LH side between center sill and side sill, near center sill	2069	29	μstr	±2500
10	SGBF10	Front of bottom flange of #4 cross bearer, LH side between center sill and side sill, near side sill	2069	29	μstr	±2500
11	SGBF11	Rear of bottom flange of #4 cross bearer, RH side between center sill and side sill, near side sill	2069	29	μstr	±2500
12	SGBF12	Rear of bottom flange of #4 cross bearer, RH side between center sill and side sill, near center sill	2069	29	μstr	±2500
13	SGBF13	Rear of bottom flange of #4 cross bearer, LH side between center sill and side sill, near center sill	2069	29	μstr	±2500
14	SGBF14	Rear of bottom flange of #4 cross bearer, LH side between center sill and side sill, near side sill	2069	29	μstr	±2500
15	SGBF15	Center of RH side sill bottom flange, approximately 2 in forward of #3 cross bearer	2069	29	μstr	±2500
16	SGBF16	Center sill bottom flange, aligned with RH center sill web, approximately 2" forward of #3 Cross Bearer	2069	29	μstr	±2500

Table B1c. Strain Gauge and Thermocouple Channels (3 of 8)

Figure B1 Ref	Channel Name	Approximate Locations (confirm based on latest version of Kasgro Drawing 1155-45)[9]	Yield Strain at gauge location (μstr)	Modulus of Elasticity at Gauge Location (10^6 ksi)	Units	Expected Range
17	SGBF17	Center sill bottom flange, aligned with LH center sill web, approximately 2" forward of #3 Cross Bearer	2069	29	μstr	±2500
18	SGBF18	Center of LH side sill bottom flange, approximately 2 in forward of #3 cross bearer	2069	29	μstr	±2500
19	SGBF19	Center of RH side sill bottom flange, at longitudinal center of car	2069	29	μstr	±2500
20	SGBF20	Center sill bottom flange, aligned with RH center sill web, at longitudinal center of car	2069	29	μstr	±2500
21	SGBF21	Center sill bottom flange, aligned with LH center sill web, at longitudinal center of car	2069	29	μstr	±2500
22	SGBF22	Center of LH side sill bottom flange, at longitudinal center of car	2069	29	μstr	±2500
23	SGBF23	Center of RH side sill bottom flange, approx. 2 inches aft of #2 cross bearer	2069	29	μstr	±2500
24	SGBF24	Center sill bottom flange, aligned with RH center sill web, approx. 2" aft of #2 Cross Bearer	2069	29	μstr	±2500

Table B1d. Strain Gauge and Thermocouple Channels (4 of 8)

Figure B1 Ref	Channel Name	Approximate Locations (confirm based on latest version of Kasgro Drawing 1155-45)[9]	Yield Strain at gauge location (μstr)	Modulus of Elasticity at Gauge Location (10^6 ksi)	Units	Expected Range
25	SGBF25	Center sill bottom flange, aligned with LH center sill web, approx. 2 inches aft of #2 Cross Bearer	2069	29	μstr	±2500
26	SGBF26	Center of LH side sill bottom flange, approx. 2 inches aft of #2 cross bearer	2069	29	μstr	±2500
27	SGBF27	Front of bottom flange of #1 cross bearer, RH side between center sill and side sill, near side sill	2069	29	μstr	±2500
28	SGBF28	Front of bottom flange of #1 cross bearer, RH side between center sill and side sill, near center sill	2069	29	μstr	±2500
29	SGBF29	Front of bottom flange of #1 cross bearer, LH side between center sill and side sill, near center sill	2069	29	μstr	±2500
30	SGBF30	Front of bottom flange of #1 cross bearer, LH side between center sill and side sill, near side sill	2069	29	μstr	±2500
31	SGBF31	Rear of bottom flange of #1 cross bearer, RH side between center sill and side sill, near side sill	2069	29	μstr	±2500
32	SGBF32	Rear of bottom flange of #1 cross bearer, RH side between center sill and side sill, near center sill	2069	29	μstr	±2500

Table B1e. Strain Gauge and Thermocouple Channels (5 of 8)

Figure B1 Ref	Channel Name	Approximate Locations (confirm based on latest version of Kasgro Drawing 1155-45)[9]	Yield Strain at gauge location (μstr)	Modulus of Elasticity at Gauge Location (10^6 ksi)	Units	Expected Range
33	SGBF33	Rear of bottom flange of #1 cross bearer, LH side between center sill and side sill, near center sill	2069	29	μstr	±2500
34	SGBF34	Rear of bottom flange of #1 cross bearer, LH side between center sill and side sill, near side sill	2069	29	μstr	±2500
35	SGBF35	RH side of bottom flange of center sill - forward of rear body bolster - aligns with center sill web and end stop mount block pin hole	2069	29	μstr	±2500
36	SGBF36	LH side of bottom flange of center sill - forward of rear body bolster - aligns with center sill web and end stop mount block pin hole	2069	29	μstr	±2500
37	SGBF37	Front of bottom flange of front body bolster near center sill -- RH side	2069	29	μstr	±2500
38	SGBF38	Front of bottom flange of front body bolster near center sill -- LH side	2069	29	μstr	±2500
39	SGBF39	Rear of bottom flange of rear body bolster near center sill -- RH side	2069	29	μstr	±2500
40	SGBF40	Rear of bottom flange of rear body bolster near center sill -- LH side	2069	29	μstr	±2500

Table B1f. Strain Gauge and Thermocouple Channels (6 of 8)

Figure B1 Ref	Channel Name	Approximate Locations (confirm based on latest version of Kasgro Drawing 1155-45)[9]	Yield Strain at gauge location (μstr)	Modulus of Elasticity at Gauge Location (10^6 ksi)	Units	Expected Range
41	SGDP41	Top of deck plate, above LH side sill web, at longitudinal center of car	2069	29	μstr	±2500
42	SGDP42	Top of deck plate, above LH center sill web, at longitudinal center of car	2069	29	μstr	±2500
43	SGDP43	Top of deck plate, above RH center sill web, at longitudinal center of car	2069	29	μstr	±2500
44	SGDP44	Top of deck plate, above RH side sill web, at longitudinal center of car	2069	29	μstr	±2500
45	SGDP45	Top of deck plate, above LH side sill web, approx. 2 inches aft of #2 cross bearer	2069	29	μstr	±2500
46	SGDP46	Top of deck plate, above LH center sill web, approx. 2 inches aft of #2 cross bearer	2069	29	μstr	±2500
47	SGDP47	Top of deck plate, above RH center sill web, approx. 2 inches aft of #2 cross bearer	2069	29	μstr	±2500
48	SGDP48	Top of deck plate, above LH center sill web, approx. 2 in aft of #2 cross bearer	2069	29	μstr	±2500
49	SGDP49	Top of deck plate, above RH side sill web, approx. 2 inches forward of #3 cross bearer	2069	29	μstr	±2500

Table B1g. Strain Gauge and Thermocouple Channels (7 of 8)

Figure B1 Ref	Channel Name	Approximate Locations (confirm based on latest version of Kasgro Drawing 1155-45)[9]	Yield Strain at gauge location (μstr)	Modulus of Elasticity at Gauge Location (10^6 ksi)	Units	Expected Range
50	SGDP50	Top of deck plate, above LH center sill web, approx. 2 inches forward of #3 cross bearer	2069	29	μstr	±2500
51	SGDP51	Top of deck plate, above RH center sill web, approx. 2 inches forward of #3 cross bearer	2069	29	μstr	±2500
52	SGDP52	Top of deck plate, above LH center sill web, approx. 2 inches forward of #3 cross bearer	2069	29	μstr	±2500
53	SGBF53	Center of bottom flange of cross bearer #3, centered in open space between RH side sill bottom flange and center sill bottom flange	2069	29	μstr	±2500
54	SGBF54	Center of bottom flange of cross bearer #3, centered in open space between LH side sill bottom flange and center sill bottom flange	2069	29	μstr	±2500
55	SGBF55	Center of bottom flange of cross bearer #2, centered in open space between LH side sill bottom flange and center sill bottom flange	2069	29	μstr	±2500

Table B1h. Strain Gauge and Thermocouple Channels (8 of 8)

Figure B1 Ref	Channel Name	Approximate Locations (confirm based on latest version of Kasgro Drawing 1155-45)[9]	Yield Strain at gauge location (μstr)	Modulus of Elasticity at Gauge Location (10^6 ksi)	Units	Expected Range
56	SGBF56	Center of bottom flange of cross bearer #2, centered in open space between RH side sill bottom flange and center sill bottom flange	2069	29	μstr	±2500
57	TC1	Thermocouple on center sill bottom flange, centered in open space between front body bolster and cross bearer #4	n/a	n/a	°F	-40 to 150
58	TC2	Thermocouple centered laterally and longitudinally centered on top deck	n/a	n/a	°F	-40 to 150
59	TC3	Thermocouple on center sill bottom flange, centered in open space between rear body bolster and cross bearer #1	n/a	n/a	°F	-40 to 150

Appendix C. Static Brake Force Testing Documentation

TRANSPORTATION TECHNOLOGY CENTER, INC.

Matt DeGeorge
Senior Engineer
Phone: 719-584-0724
Email: matt_degeorge@aar.com

August 20, 2020

Subject: Static Brake Force Test Observations Specification Testing of IDOX 020001, 020002, and IDOX 010001 A-End and B-End

Mr. Jon Hannafious
Senior Manager - Equipment Engineering
Transportation Technology Center, Inc.
Pueblo, CO 81001
Email: Jon_Hannafious@aar.com

Dear Mr. Hannafious,

The static brake force specification testing of the buffer cars (IDOX 020001 and 020002) and the Atlas car (IDOX 010001 A-End and B-End) has been completed. Testing was performed at the Kasgro Rail Corporation facility in New Castle, Pennsylvania on December 4, 2018 (buffer cars) and February 12, 2019 (Atlas car) to comply with Specification S-2043 and S-401.

I was present (test witness) for the required Static Brake Force Tests and can conclude that applicable requirements of AAR Specification S-401 have been satisfactorily addressed.

The details and results of this testing is documented in the attached reports. Should you need any additional information, please do not hesitate to get in contact with me.

Sincerely,

Matt DeGeorge

Atlas Cask Car Brake Testing Report for February 2019

Contract Number: 89243218CNE000004
Author: Matthew DeGeorge
Date: 02/27/2019
Document # RP-19-001

1. TEST OVERVIEW

1.1. Single Car Air Brake Testing of the Buffer Cars

- Testing designed to comply with AAR Standard S-486 (08/2018 Revision)
- Testing repeated on buffer cars to include Cylinder Maintaining Leakage Test (3.5.1)
- Cylinder maintaining retainer test fixture created by Kasgro for testing

1.2. Single Car Air Brake Testing of the Cask Car

- Testing designed to comply with AAR Standard S-486 (08/2018 Revision)
- Cylinder maintaining retainer test fixture created by Kasgro for testing
- Cask car equipped with two braking systems that were tested separately

1.3. Brake Shoe Force Testing of the Cask Car

- Testing designed to comply with AAR Standard S-401 (01/2018 Revision)
- Cask car equipped with two braking systems that were tested separately
- Testing was performed on three trucks at a time using two force measurement systems

1.4. Test Observation and Documentation

- Observation of testing was documented on the attached checklists, which were developed by the TTCI project team and reviewed by the TTCI Project Manager and Quality Specialist

1.5. Test Personnel

- Rick Ford (Kasgro Project Manager)
- Mark Zeigler (Kasgro)
- Mark Baker (Kasgro; performed single car air brake tests)
- Cory Wagner (Kasgro; performed brake shoe force test)
- Tom Sedarski (Amsted Rail; perform brake shoe force test)
- Keith McCabe (Amsted Rail; perform brake shoe force test)
- Mark Denton (Orano)
- Thong Le (Orano)
- Mike Yon (AAR observer)
- Matt DeGeorge (TTCI observer)

1.6. Schedule

- 02/11/19
    - 7:45am – 9:45am: single car air brake testing of buffer car IDOX 020002
    - 10:30am – 11:45am: single car air brake testing of buffer car IDOX 020001
    - 1:15pm – 3:15pm: single car air brake testing of cask car IDOX 010001 A-end
- 02/12/19
    - 6:20 am – 9:00am: single car air brake testing of cask car IDOX 010001 B-end
    - 10:00am – 12:00pm: brake shoe force testing of cask car IDOX 010001 A-end
    - 1:00pm – 2:30pm: brake shoe force testing of cask car IDOX 010001 B-end
- 02/13/19
    - Review of test results
    - Pictures and measurements of buffer and cask cars

2. ISSUES / CONCERNS / COMMENTS

- Daily test performed on Single Car Air Brake Test Device each day before testing
- The piston travel on all cars was initially outside the acceptable range and was adjusted during testing
    - After the pistons were readjusted and several brake reductions were performed to stabilize the system, piston travel in all cars met the criteria
- The cask car has two braking systems and each test was performed on a single system with the other system cut out
- The hand brake portion of the brake shoe force testing was repeated on both sides of the cask car due to an incorrect set force for the Group O hand brake and clearance issues with the smart hook placement
    - The smart hook was placed further back on the hand brake chain to avoid damaging the device during the removal of slack in the chain when setting the hand brake to the proper force
- The brake cylinder leakage test was repeated on the cask car because the Single Car Air Brake Test Device was providing over 90 psi to the brake pipe resulting in higher pressure readings in the brake cylinder after reductions were performed
    - After the device was adjusted the cask car met the criteria in 3.14 of S-486
- An air restriction test was successfully completed on the entire cask car braking system

3. CONCLUSIONS

- Cask car IDOX 010001, buffer car IDOX 020001 and buffer car IDOX 020002 met the criteria put forth in the AAR Standard S-486
- Cask car IDOX 010001 met the criteria put forth in the AAR Standard S-401

4. DOCUMENTATION PHOTOGRAPHS



Figure C1. Atlas Cask Car Isometric View

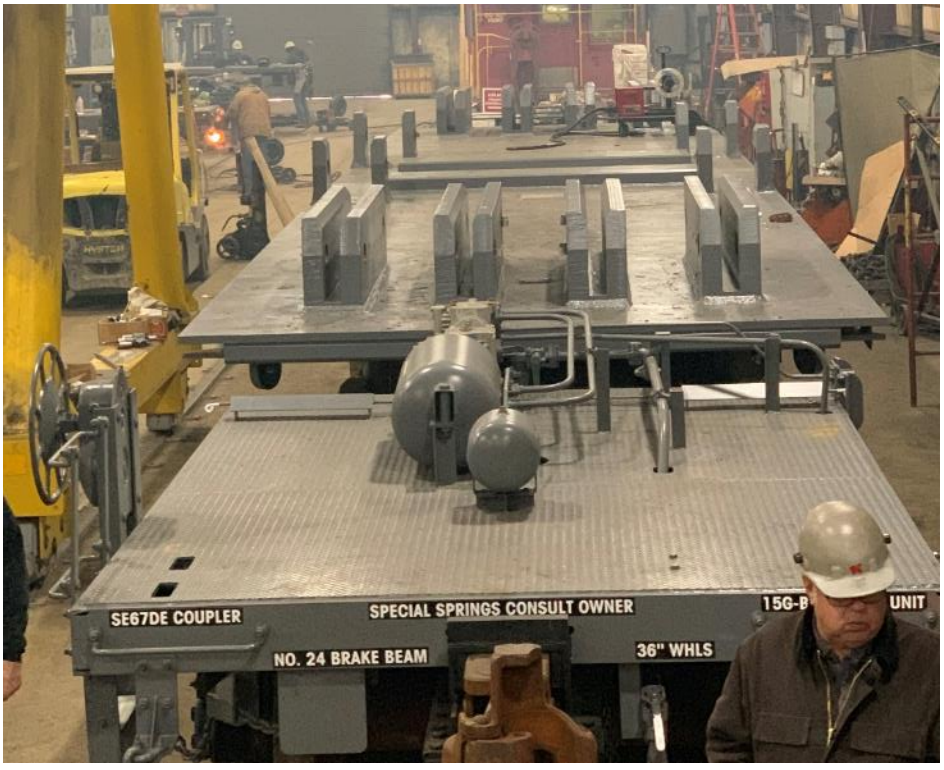


Figure C2. Atlas Cask Car Side View



Figure C3. Cask Car A-End Brake System



Figure C4. Cask Car B-End Brake System



Figure C5. Cask Car Weight Information

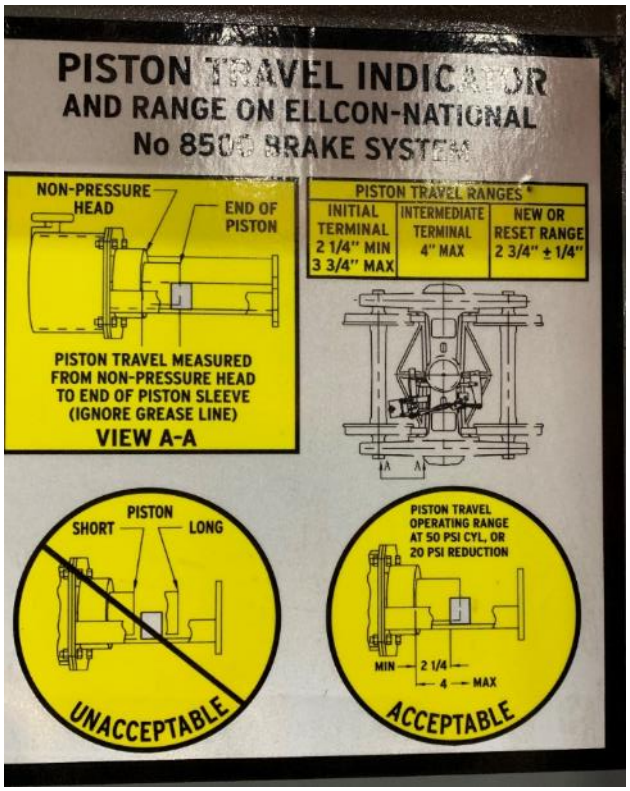


Figure C6. Cask Car Piston Setup Information



Figure C7. Single Car Air Brake Test Device



Figure C8. Single Car Air Brake Test Device Calibration Information



Figure C9. Brake Cylinder Pressure Gauge and Empty/Load Device



Figure C10. Brake Cylinder Pressure Gauge Calibration Information

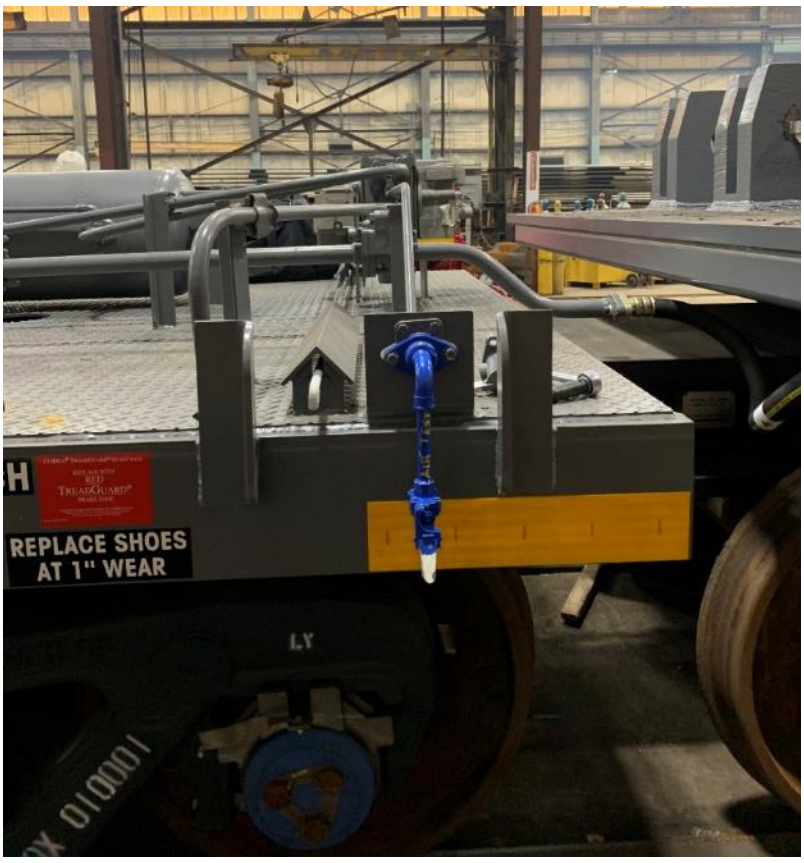


Figure C11. Cylinder Maintaining Retainer Test Fixture

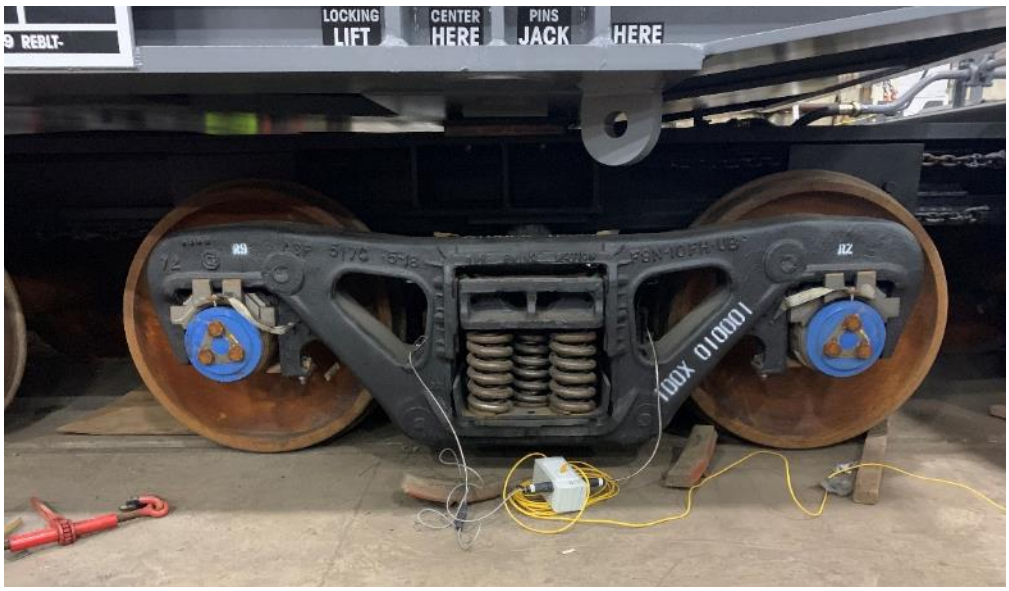


Figure C12. Example Brake Shoe Force Test Sensor Setup



Figure C13. Example Force Sensor



Figure C14. Three Truck Brake Shoe Force Test Setup

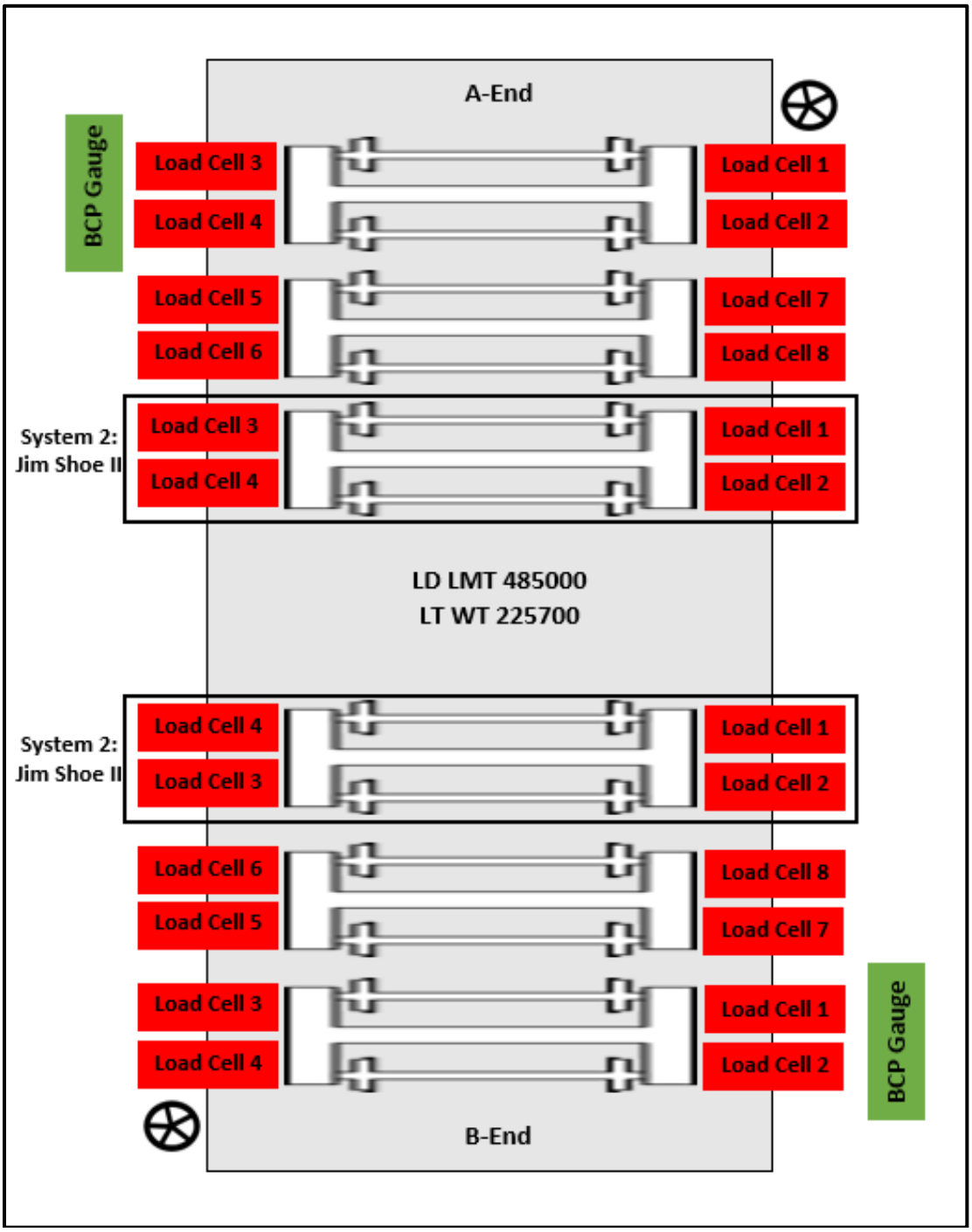
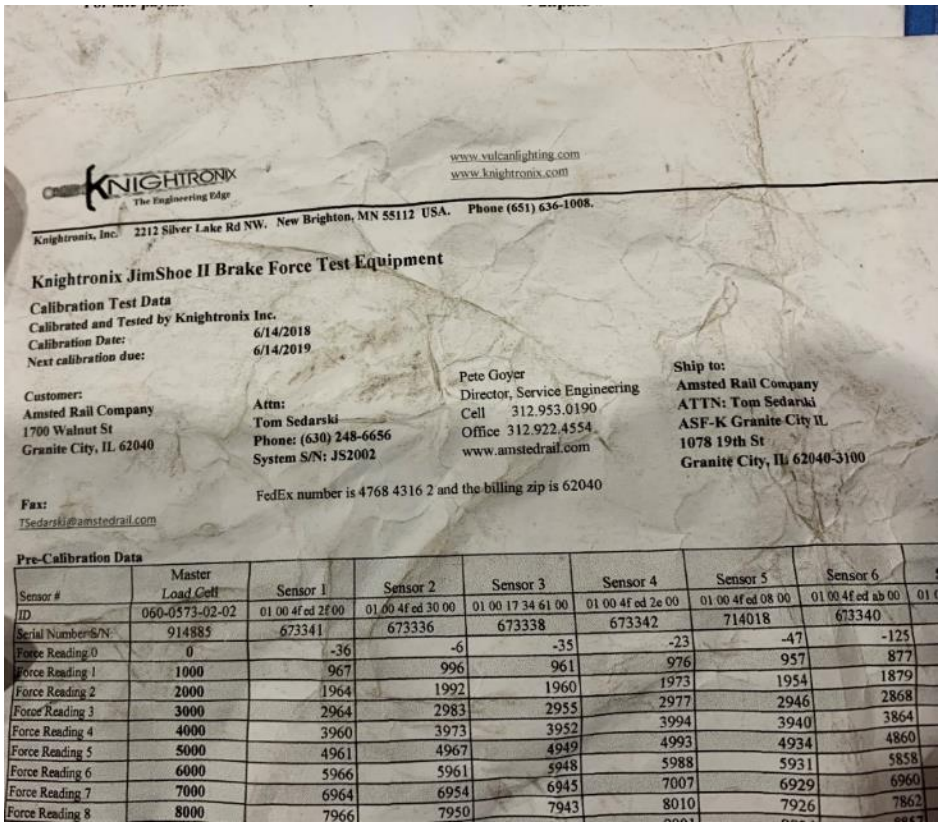


Figure C15. Cask Car Instrumentation Setup Diagram (A-End performed first)



Figure C16. Jim Shoe II Brake Force Measurement System



www.vulcanlighting.com
www.knightronix.com

KNIGHTRONIX
The Engineering Edge

Knightronix, Inc. 2212 Silver Lake Rd NW. New Brighton, MN 55112 USA. Phone (651) 636-1008.

Knightronix JimShoe II Brake Force Test Equipment

Calibration Test Data
Calibrated and Tested by Knightronix Inc.
Calibration Date: 6/14/2018
Next calibration due: 6/14/2019

Customer:
Amsted Rail Company
1700 Walnut St
Granite City, IL 62040

Attn:
Tom Sedarski
Phone: (630) 248-6656
System S/N: JS2002

Pete Goyer
Director, Service Engineering
Cell 312.953.0190
Office 312.922.4554
www.amstedrail.com

Ship to:
Amsted Rail Company
ATTN: Tom Sedarski
ASF-K Granite City IL
1078 19th St
Granite City, IL 62040-3100

Fax:
TSedarski@amstedrail.com

FedEx number is 4768 4316 2 and the billing zip is 62040

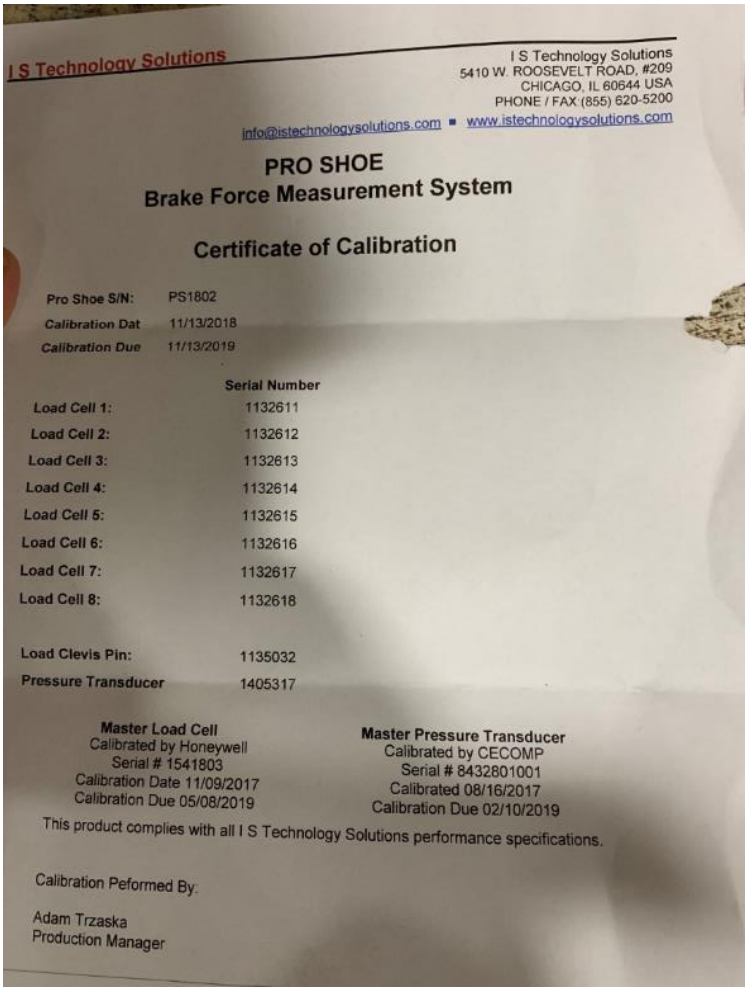
Pre-Calibration Data

Sensor #	Master Load Cell	Sensor 1	Sensor 2	Sensor 3	Sensor 4	Sensor 5	Sensor 6	
ID	060-0573-02-02	01 00 4f ed 2f 00	01 00 4f ed 30 00	01 00 17 34 61 00	01 00 4f ed 2e 00	01 00 4f ed 08 00	01 00 4f ed ab 00	01
Serial Number S/N	914885	673341	673336	673338	673342	714018	673340	
Force Reading 0	0	-36	-6	-35	-23	-47	-125	
Force Reading 1	1000	967	996	961	976	957	877	
Force Reading 2	2000	1964	1992	1960	1973	1954	1879	
Force Reading 3	3000	2964	2983	2955	2977	2946	2868	
Force Reading 4	4000	3960	3973	3952	3994	3940	3864	
Force Reading 5	5000	4961	4967	4949	4993	4934	4860	
Force Reading 6	6000	5966	5961	5948	5988	5931	5858	
Force Reading 7	7000	6964	6954	6945	7007	6929	6960	
Force Reading 8	8000	7966	7950	7943	8010	7926	7862	

Figure C17. Jim Shoe II Calibration Information



Figure C18. Pro Shoe Brake Force Measurement System



I S Technology Solutions

I S Technology Solutions
5410 W. ROOSEVELT ROAD, #209
CHICAGO, IL 60644 USA
PHONE / FAX (855) 620-5200

info@istechnologysolutions.com ▪ www.istechnologysolutions.com

PRO SHOE
Brake Force Measurement System

Certificate of Calibration

Pro Shoe S/N:	PS1802
Calibration Dat	11/13/2018
Calibration Due	11/13/2019

	Serial Number
Load Cell 1:	1132611
Load Cell 2:	1132612
Load Cell 3:	1132613
Load Cell 4:	1132614
Load Cell 5:	1132615
Load Cell 6:	1132616
Load Cell 7:	1132617
Load Cell 8:	1132618
Load Clevis Pin:	1135032
Pressure Transducer	1405317

Master Load Cell
Calibrated by Honeywell
Serial # 1541803
Calibration Date 11/09/2017
Calibration Due 05/08/2019

Master Pressure Transducer
Calibrated by CECOMP
Serial # 8432801001
Calibrated 08/16/2017
Calibration Due 02/10/2019

This product complies with all I S Technology Solutions performance specifications.

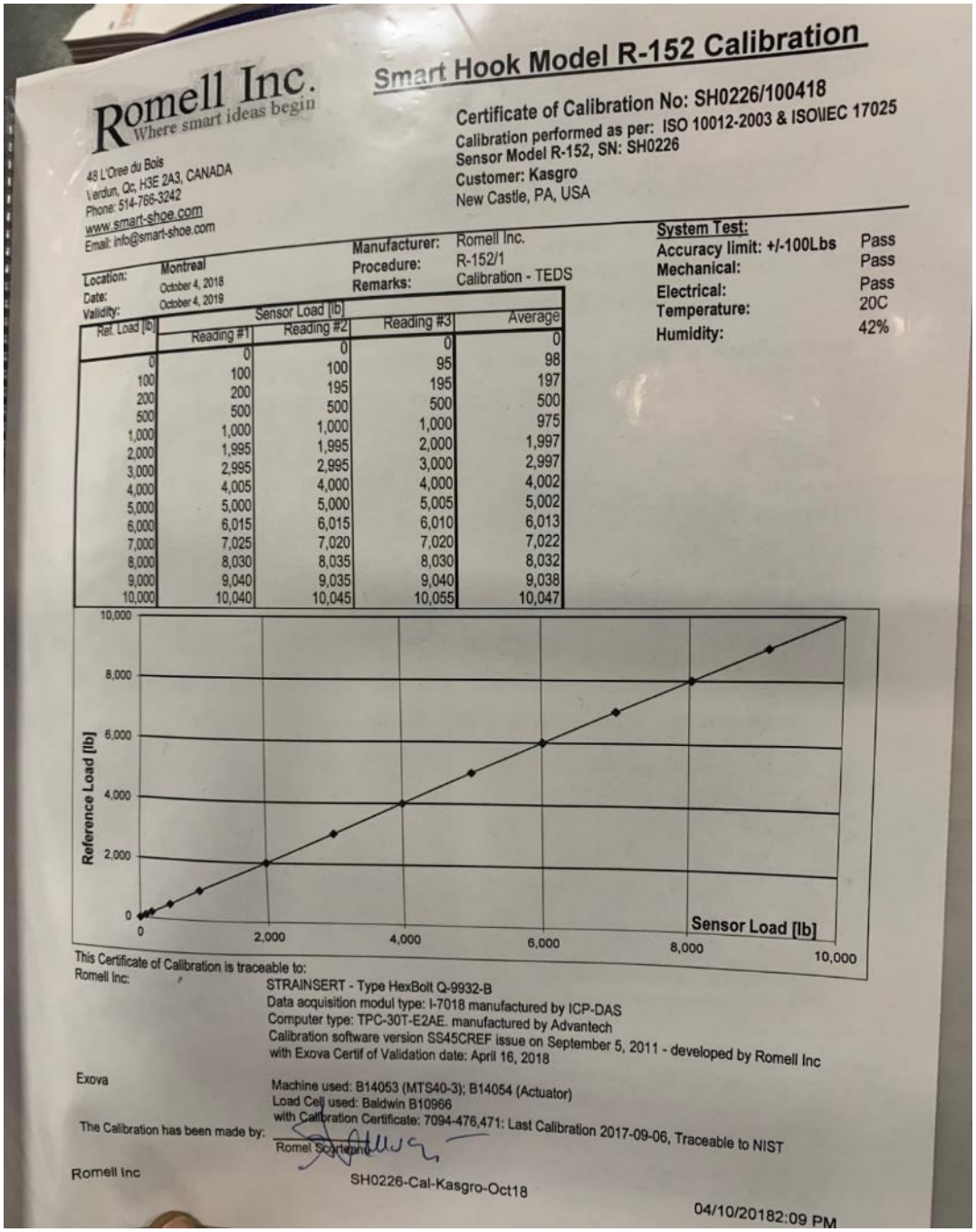
Calibration Peformed By:

Adam Trzaska
Production Manager

Figure C19. Pro Shoe Calibration Information



Figure C20. Smart Hook Force Measurement Device



Romell Inc.
Where smart ideas begin

48 L'Oree du Bois
Verdun, Qc, H3E 2A3, CANADA
Phone: 514-766-3242
www.smart-shoe.com
Email: info@smart-shoe.com

Smart Hook Model R-152 Calibration

Certificate of Calibration No: SH0226/100418
Calibration performed as per: ISO 10012-2003 & ISO\IEC 17025
Sensor Model R-152, SN: SH0226
Customer: Kasgro
New Castle, PA, USA

Location: Montreal
Date: October 4, 2018
Validity: October 4, 2019

Manufacturer: Romell Inc.
Procedure: R-152/1
Remarks: Calibration - TEDS

System Test:

Accuracy limit: +/-100Lbs	Pass
Mechanical:	Pass
Electrical:	Pass
Temperature:	20C
Humidity:	42%

Ref. Load [lb]	Sensor Load [lb] Reading #1	Reading #2	Reading #3	Average
0	0	0	0	0
100	100	100	95	98
200	200	195	195	197
500	500	500	500	500
1,000	1,000	1,000	1,000	975
2,000	1,995	1,995	2,000	1,997
3,000	2,995	2,995	3,000	2,997
4,000	4,005	4,000	4,000	4,002
5,000	5,000	5,000	5,005	5,002
6,000	6,015	6,015	6,010	6,013
7,000	7,025	7,020	7,020	7,022
8,000	8,030	8,035	8,030	8,032
9,000	9,040	9,035	9,040	9,038
10,000	10,040	10,045	10,055	10,047

This Certificate of Calibration is traceable to:
Romell Inc:
STRAINSERT - Type HexBolt Q-9932-B
Data acquisition modul type: I-7018 manufactured by ICP-DAS
Computer type: TPC-30T-E2AE. manufactured by Advantech
Calibration software version SS45CREF issue on September 5, 2011 - developed by Romell Inc
with Exova Certif of Validation date: April 16, 2018

Exova
Machine used: B14053 (MTS40-3); B14054 (Actuator)
Load Cell used: Baldwin B10966
with Calibration Certificate: 7094-476,471: Last Calibration 2017-09-06, Traceable to NIST

The Calibration has been made by:
Romel Sorriano

Romell Inc
SH0226-Cal-Kasgro-Oct18
04/10/20182:09 PM

Figure C21. Smart Hook Calibration Information



Figure C22. Rapping Hammer



Figure C23. Air Restriction Test Device



Figure C24. Air Restriction Test Device Calibration Information

5. COMPLETED TEST CHECKLIST

~7:45 am Start

Single Car Air Brake Test - Atlas Buffer Car (Retest) to include CM feature test

Observer Name: Matt DeGeorge Inspection Date: 02/11/19

Names of Test Personnel: Mike Yon (AAR), Rick Ford, Mark Zeigler, Mark Baker (performed test)

Car and Component Identification

Car Number: IDOX 020002 Brake Pipe Length: 93'

Service Portion Type: DB-10 Emergency Portion Type: DB-20

Type of Single Car Testing Device: Automated | (Manual)

Date of Calibration (within 92 days): 11/20/18

Empty/Load Device (Y) | N (All test procedures must be performed in loaded condition)

Daily Test for Testing the Single Car Testing Device Completed @ 8:00 am

Test 2.3.1: Brake pipe pressure reads 90 PSI (black needle)	(Y)	N
Test 2.3.2: Brake cylinder pressure gauge reads between 77 and 83 PSI	(Y)	N
Test 2.3.3: Leakage is less than 1 PSI over a 1 minute timeframe	(Y)	N
Test 2.3.4: Up to a 1-inch bubble appears in no less than 5 seconds	(Y)	N
Test 2.3.5: Flowrator ball rises & floats in zone b/t condemning line and top of tube	(Y)	N
Test 2.3.6: Leakages do not exceed a 1-inch bubble in 5 seconds	(Y)	N

Single Car Air Brake Test

Initial Car Connection

Test 3.2.2.1: Continuous flow of air through pipe	(Y) / N

Brake Pipe Leakage Test

Test 3.3.1: Top of ball stabilizes below the condemning line	(Y) / N

Continuous Quick Service Valve (If Equipped) No

Test 3.4.1.1: Vent valve does not function and BPP does not reduce to 0 PSI	Y / N
Test 3.4.1.2: Intermittent exhaust at quick-service valve is observed	Y / N

A-1 Reduction Relay Valve (If Equipped) No

B-1 quick service function is nullified	Y / N

Separate Vent Valve Test (If Equipped) Yes

Test 3.4.3.1: Vent valve does not function and BPP does not reduce to 0 PSI	(Y) / N
Test 3.4.3.2: Vent valve functions and immediately vents BPP to 0 PSI	(Y) / N

System Leakage Test

Test 3.5.1: No venting of air from retaining valve and BC piston in release position	(Y) / N
Test 3.5.2: No leakage	(Y) / N
Test 3.5.3: Top of the ball stabilizes below the condemning line	(Y) / N

Cylinder Maintaining Leakage Test (If Equipped) Yes testing device created by Kasgro for the test

Test 3.5.1.1: Brakes apply	(Y)	N
Test 3.5.1.2: Brake cylinder pressure is above 17 PSI	(Y)	N
Test 3.5.1.3: No leakage	(Y)	N
Test 3.5.1.4: Brake cylinder pressure fluctuates by no more than 1 PSI	(Y)	N

BCP initial: X 74psi BCP final: X 74psi remained constant

Hand Brake Inspection (Group U, Ellcon National 35790)

Test 3.6.1: Hand brake in released position; BC piston push rod returned into BC	(Y)	N
Test 3.6.2: Bell crank in normal working range (if equipped)	(Y)	N
Test 3.6.3: All brake shoes applied by hand brake are set firmly against wheels	(Y)	N
Test 3.6.4: Drum chain unwound, bell crank dropped to lower limit, minimal slack	(Y)	N

Slack Adjuster Conditioning (with Blocks)

Conditioning performed	(Y)	N

Service Stability Test

Test 3.8.2.1: Emergency application was not produced	(Y)	N
Test 3.8.2.2: Brake pipe reduction and exhaust at emergency portion stopped	(Y)	N

Piston Travel and Rigging and Brake Cylinder Pressure

Test 3.9.1: Measure and note brake cylinder piston travel: Bend 2 5/8 Aend 2 3/4

Test 3.9.2: Brake levers checked for angularity	(Y)	N
Test 3.9.3: All shoes are applied and firmly set against wheels	(Y)	N
Test 3.9.4: Brake cylinder pressure is greater than 50 PSI	(Y)	N

Test 3.9.5: Note brake cylinder pressure after the BPP has stabilized: 63psi

Emergency Test

Test 3.10.2.1: Control valve emergency application occurred (BBP to 0 PSI)	(Y)	N

Test 3.10.2.2: Brake cylinder pressure is at least 5 PSI greater than 3.9.5: 76psi

Release Test after Emergency

Test 3.11.1: No air exhausting occurred	(Y)	N
Test 3.11.2: The brake pipe pressure continued to rise	(Y)	N

Retaining Valve Test

Test 3.12.1: Brakes remained applied and BCP is >= 12 PSI: ~20psi

Test 3.12.2: Blow of air at retaining valve exhaust	(Y)	N

Minimum Application and Quick-Service Limiting Valve Test

Test 3.13.1: Brakes applied	(Y)	N
Test 3.13.2: Brake pipe reduction and exhaust at emergency portion stopped	(Y)	N

Test 3.13.3: Brake pipe pressure must be >= 80 PSI: ~84psi

Brake Cylinder Leakage Test

Wait 3 minutes after BPP stabilizes at 80 PSI
Test 3.14.1: Note the brake cylinder pressure (must be 12-30 PSI): ~26psi

Wait an additional 1 minute

Test 3.14.2: No more than a 1 PSI fluctuation in brake cylinder pressure	(Y)	N
Test 3.14.3: Top of the flowrator ball is below the condemning line	(Y)	N

Slow-Release Test

Test 3.15.1: Brakes released within specified time: 19 sec

Slack Adjuster Conditioning (without Blocks)

Conditioning performed	(Y)	N

Accelerated Application Valve (AAV) Test

Test 3.17.1: Exhaust from emergency portion while brake pipe reduces	(Y)	N
Test 3.17.2: No emergency application was produced	(Y)	N
Test 3.17.3: Brake pipe reduction stopped	(Y)	N

Recheck of Piston Travel (without Blocks, if Equipped with Automatic Slack Adjusters)

Test 3.18.1: Piston travel falls within +/- ½ inches of 3.9.1 and within nominal range: Bend: 2½ Aend: 2½

Manual Release Valve Test

Test 3.19.1: Brake cylinder piston returned to release position and remained there	(Y)	N
Test 3.19.2: Brake cylinder piston remained in the release position during charging	(Y)	N
Test 3.19.3: Brakes applied	(Y)	N

Car is loaded will not be unloaded (empty)

Empty/Load Test

Test 3.20.1: Brakes applied | Y | N

Test 3.20.2: Brake cylinder pressure at least 17 PSI lower than 3.9.5: _____

Test 3.20.3: No leakage occurred | Y | N

Disconnecting the Single-Car Test Device

Test 3.21.1: No leakage occurred | (Y) | N

Additional Comments: -

CM device created by Kasgro per S-486 spec, Piston travel adjusted and set within acceptable tolerance for test

~9:45am End of Test

~10:30am Start

Single Car Air Brake Test - Atlas Buffer Car (Retest) to include CM feature test

Observer Name: Matt DeGeorge Inspection Date: 02/11/19

Names of Test Personnel: Mike Yon (AAR), Rick Ford, Mark Zeigler, Mark Baker (performed test)

Car and Component Identification

Car Number: IDOX 020001 Brake Pipe Length: 93'

Service Portion Type: DB-10 Emergency Portion Type: DB-20

Type of Single Car Testing Device:	Automated	(Manual)

Date of Calibration (within 92 days): 11/20/18

Empty/Load Device	(Y)	N

(All test procedures must be performed in loaded condition)

Daily Test for Testing the Single Car Testing Device Completed @ start of day in previous test

Test 2.3.1: Brake pipe pressure reads 90 PSI (black needle)	(Y)	N
Test 2.3.2: Brake cylinder pressure gauge reads between 77 and 83 PSI	(Y)	N
Test 2.3.3: Leakage is less than 1 PSI over a 1 minute timeframe	(Y)	N
Test 2.3.4: Up to a 1-inch bubble appears in no less than 5 seconds	(Y)	N
Test 2.3.5: Flowrator ball rises & floats in zone b/t condemning line and top of tube	(Y)	N
Test 2.3.6: Leakages do not exceed a 1-inch bubble in 5 seconds	(Y)	N

Single Car Air Brake Test

Initial Car Connection

Test 3.2.2.1: Continuous flow of air through pipe	(Y) N

Brake Pipe Leakage Test

Test 3.3.1: Top of ball stabilizes below the condemning line	(Y) N

Continuous Quick Service Valve (If Equipped) No

Test 3.4.1.1: Vent valve does not function and BPP does not reduce to 0 PSI	Y N
Test 3.4.1.2: Intermittent exhaust at quick-service valve is observed	Y N

A-1 Reduction Relay Valve (If Equipped) No

B-1 quick service function is nullified	Y N

Separate Vent Valve Test (If Equipped) Yes

Test 3.4.3.1: Vent valve does not function and BPP does not reduce to 0 PSI	(Y) N
Test 3.4.3.2: Vent valve functions and immediately vents BPP to 0 PSI	(Y) N

System Leakage Test

Test 3.5.1: No venting of air from retaining valve and BC piston in release position	(Y) N
Test 3.5.2: No leakage	(Y) N
Test 3.5.3: Top of the ball stabilizes below the condemning line	(Y) N

Cylinder Maintaining Leakage Test (If Equipped) Yes testing device created by Kasgro for the test

Test 3.5.1.1: Brakes apply	(Y)	N
Test 3.5.1.2: Brake cylinder pressure is above 17 PSI	(Y)	N
Test 3.5.1.3: No leakage	(Y)	N
Test 3.5.1.4: Brake cylinder pressure fluctuates by no more than 1 PSI	(Y)	N

BCP initial: ~~24psi~~ BCP final: ~~24psi~~ remained constant

Hand Brake Inspection (Group U, Ellcon National 35740)

Test 3.6.1: Hand brake in released position; BC piston push rod returned into BC	(Y)	N
Test 3.6.2: Bell crank in normal working range (if equipped)	(Y)	N
Test 3.6.3: All brake shoes applied by hand brake are set firmly against wheels	(Y)	N
Test 3.6.4: Drum chain unwound, bell crank dropped to lower limit, minimal slack	(Y)	N

Slack Adjuster Conditioning (with Blocks)

Conditioning performed	(Y)	N

Service Stability Test

Test 3.8.2.1: Emergency application was not produced	(Y)	N
Test 3.8.2.2: Brake pipe reduction and exhaust at emergency portion stopped	(Y)	N

Piston Travel and Rigging and Brake Cylinder Pressure

Test 3.9.1: Measure and note brake cylinder piston travel: Bend 2 7/8 Aend 3

Test 3.9.2: Brake levers checked for angularity	(Y)	N
Test 3.9.3: All shoes are applied and firmly set against wheels	(Y)	N
Test 3.9.4: Brake cylinder pressure is greater than 50 PSI	(Y)	N

Test 3.9.5: Note brake cylinder pressure after the BPP has stabilized: 63psi

Emergency Test

Test 3.10.2.1: Control valve emergency application occurred (BBP to 0 PSI)	(Y)	N

Test 3.10.2.2: Brake cylinder pressure is at least 5 PSI greater than 3.9.5: 76psi

Release Test after Emergency

Test 3.11.1: No air exhausting occurred	(Y)	N
Test 3.11.2: The brake pipe pressure continued to rise	(Y)	N

Retaining Valve Test

Test 3.12.1: Brakes remained applied and BCP is >= 12 PSI: ~22psi

Test 3.12.2: Blow of air at retaining valve exhaust	(Y)	N

Minimum Application and Quick-Service Limiting Valve Test

Test 3.13.1: Brakes applied	(Y)	N
Test 3.13.2: Brake pipe reduction and exhaust at emergency portion stopped	(Y)	N

Test 3.13.3: Brake pipe pressure must be >= 80 PSI: ~82psi

Brake Cylinder Leakage Test

Wait 3 minutes after BPP stabilizes at 80 PSI
Test 3.14.1: Note the brake cylinder pressure (must be 12-30 PSI): ~26psi

Wait an additional 1 minute

Test 3.14.2: No more than a 1 PSI fluctuation in brake cylinder pressure	(Y)	N
Test 3.14.3: Top of the flowrator ball is below the condemning line	(Y)	N

Slow-Release Test

Test 3.15.1: Brakes released within specified time: 19sec

Slack Adjuster Conditioning (without Blocks)

Conditioning performed	(Y)	N

Accelerated Application Valve (AAV) Test

Test 3.17.1: Exhaust from emergency portion while brake pipe reduces	(Y)	N
Test 3.17.2: No emergency application was produced	(Y)	N
Test 3.17.3: Brake pipe reduction stopped	(Y)	N

Recheck of Piston Travel (without Blocks, if Equipped with Automatic Slack Adjusters)

Test 3.18.1: Piston travel falls within +/- ½ inches of 3.9.1 and within nominal range: Bend 2 5/16 Aend 2 5/16

Manual Release Valve Test

Test 3.19.1: Brake cylinder piston returned to release position and remained there	(Y)	N
Test 3.19.2: Brake cylinder piston remained in the release position during charging	(Y)	N
Test 3.19.3: Brakes applied	(Y)	N

car is loaded & will not be unloaded (empty)

Empty/Load Test

Test 3.20.1: Brakes applied — Y / N

Test 3.20.2: Brake cylinder pressure at least 17 PSI lower than 3.9.5: _____

Test 3.20.3: No leakage occurred — Y / N

Disconnecting the Single-Car Test Device

Test 3.21.1: No leakage occurred — (Y) / N

Additional Comments: - CM device created by Kasgro per S-4486 spec. Piston travel adjusted and set within acceptable tolerance for test

~ 11:45am End of test

~1:15pm Start

Single Car Air Brake Test - Atlas Cask Car

Observer Name: Matt DeGeorge Inspection Date: 02/11/19

Names of Test Personnel: Mike Yon (AAR), Rick Ford, Mark Zeigler, Thong Le (Orano), Mark Denton (Orano), Mark Baker (performed test)

Car and Component Identification

Car Number: IDOX 010001 Aend Brake Pipe Length: 48ft

Service Portion Type: DB-10 Emergency Portion Type: DB-20

Type of Single Car Testing Device:	Automated	Manual

Date of Calibration (within 92 days): 11/20/18

Empty/Load Device	Y	N	(All test procedures must be performed in loaded condition)

Daily Test for Testing the Single Car Testing Device Daily performed @ beginning of day for previous testing

Test 2.3.1: Brake pipe pressure reads 90 PSI (black needle)	Y	N
Test 2.3.2: Brake cylinder pressure gauge reads between 77 and 83 PSI	Y	N
Test 2.3.3: Leakage is less than 1 PSI over a 1 minute timeframe	Y	N
Test 2.3.4: Up to a 1-inch bubble appears in no less than 5 seconds	Y	N
Test 2.3.5: Flowrator ball rises & floats in zone b/t condemning line and top of tube	Y	N
Test 2.3.6: Leakages do not exceed a 1-inch bubble in 5 seconds	Y	N

Single Car Air Brake Test

Initial Car Connection

Test 3.2.2.1: Continuous flow of air through pipe	(Y) N

Brake Pipe Leakage Test

Test 3.3.1: Top of ball stabilizes below the condemning line	(Y) N

Continuous Quick Service Valve (If Equipped) No

Test 3.4.1.1: Vent valve does not function and BPP does not reduce to 0 PSI	Y N
Test 3.4.1.2: Intermittent exhaust at quick-service valve is observed	Y N

A-1 Reduction Relay Valve (If Equipped) No

B-1 quick service function is nullified	Y N

Separate Vent Valve Test (If Equipped) Yes

Test 3.4.3.1: Vent valve does not function and BPP does not reduce to 0 PSI	(Y) N
Test 3.4.3.2: Vent valve functions and immediately vents BPP to 0 PSI	(Y) N

System Leakage Test

Test 3.5.1: No venting of air from retaining valve and BC piston in release position	(Y) N
Test 3.5.2: No leakage	(Y) N
Test 3.5.3: Top of the ball stabilizes below the condemning line	(Y) N

Cylinder Maintaining Leakage Test (If Equipped) Yes testing device created by Kasgro

Test 3.5.1.1: Brakes apply	(Y)	N
Test 3.5.1.2: Brake cylinder pressure is above 17 PSI	(Y)	N
Test 3.5.1.3: No leakage	(Y)	N
Test 3.5.1.4: Brake cylinder pressure fluctuates by no more than 1 PSI	(Y)	N

BCP initial: 24psi BCP final: 24psi

Hand Brake Inspection (Group 0)

Test 3.6.1: Hand brake in released position; BC piston push rod returned into BC	(Y)	N
Test 3.6.2: Bell crank in normal working range (if equipped)	(Y)	N
Test 3.6.3: All brake shoes applied by hand brake are set firmly against wheels	(Y)	N
Test 3.6.4: Drum chain unwound, bell crank dropped to lower limit, minimal slack	(Y)	N

Slack Adjuster Conditioning (with Blocks)

Conditioning performed	(Y)	N

Service Stability Test

Test 3.8.2.1: Emergency application was not produced	(Y)	N
Test 3.8.2.2: Brake pipe reduction and exhaust at emergency portion stopped	(Y)	N

Head

7	8	9	Z	Y	X

Piston Travel and Rigging and Brake Cylinder Pressure 78:3 9Z:3

Test 3.9.1: Measure and note brake cylinder piston travel: YX:3

Test 3.9.2: Brake levers checked for angularity	(Y)	N
Test 3.9.3: All shoes are applied and firmly set against wheels	(Y)	N
Test 3.9.4: Brake cylinder pressure is greater than 50 PSI	(Y)	N

Test 3.9.5: Note brake cylinder pressure after the BPP has stabilized: 63to64 psi

Emergency Test

Test 3.10.2.1: Control valve emergency application occurred (BBP to 0 PSI)	(Y)	N

Test 3.10.2.2: Brake cylinder pressure is at least 5 PSI greater than 3.9.5: 76psi

Release Test after Emergency

Test 3.11.1: No air exhausting occurred	(Y)	N
Test 3.11.2: The brake pipe pressure continued to rise	(Y)	N

Retaining Valve Test

Test 3.12.1: Brakes remained applied and BCP is >= 12 PSI: ~77psi

Test 3.12.2: Blow of air at retaining valve exhaust	(Y)	N

Minimum Application and Quick-Service Limiting Valve Test

Test 3.13.1: Brakes applied	(Y)	N
Test 3.13.2: Brake pipe reduction and exhaust at emergency portion stopped	(Y)	N

Test 3.13.3: Brake pipe pressure must be >= 80 PSI: ~82psi

Yes, device created by Kasgro

BPP not stabilized before the start of test (redone)

Brake Cylinder Leakage Test

Wait 3 minutes after BPP stabilizes at 80 PSI

Test 3.14.1: Note the brake cylinder pressure (must be 12-30 PSI): ~~31psi~~ 30psi

Wait an additional 1 minute

Test 3.14.2: No more than a 1 PSI fluctuation in brake cylinder pressure	(Y)	N
Test 3.14.3: Top of the flowrator ball is below the condemning line	(Y)	N

Slow-Release Test

3.11 → 3.15 redone with application cycles to verify 3.15.1 (19sec) + piston travel

Test 3.15.1: Brakes released within specified time: 19sec

Slack Adjuster Conditioning (without Blocks)

Conditioning performed	(Y)	N

Accelerated Application Valve (AAV) Test

Test 3.17.1: Exhaust from emergency portion while brake pipe reduces	(Y)	N
Test 3.17.2: No emergency application was produced	(Y)	N
Test 3.17.3: Brake pipe reduction stopped	(Y)	N

Recheck of Piston Travel (without Blocks, if Equipped with Automatic Slack Adjusters)

Test 3.18.1: Piston travel falls within +/- ½ inches of 3.9.1 and within nominal range: 79 2½ 82 2⅜ XX 2¾

Manual Release Valve Test

Test 3.19.1: Brake cylinder piston returned to release position and remained there	(Y)	N
Test 3.19.2: Brake cylinder piston remained in the release position during charging	(Y)	N
Test 3.19.3: Brakes applied	(Y)	N

Empty/Load Test

Test 3.20.1: Brakes applied	(Y)	N

Test 3.20.2: Brake cylinder pressure at least 17 PSI lower than 3.9.5: 28psi

Test 3.20.3: No leakage occurred	(Y)	N

Disconnecting the Single-Car Test Device

Test 3.21.1: No leakage occurred	(Y)	N

Additional Comments:

Brake application cycling done to correct piston travel and meet acceptable tolerance range. Aend brake system includes 3 trucks 78, 9Z, YX and has a handbrake. Bend brake system cut out to perform Aend testing

3:15pm End of Test

~6:20am Start

Single Car Air Brake Test - Atlas Cask Car

Observer Name: Matt DeGeorge Inspection Date: 02/12/19

Names of Test Personnel: Mike Yon (AAR), Rick Ford, Mark Zgiales, Thong Le (Orano), Mark Denton (Orano), Mark Baker (performed test)

Car and Component Identification

Car Number: IDOX 010001 Bend Brake Pipe Length: 18ft

Service Portion Type: DB-10 Emergency Portion Type: DB-20

Type of Single Car Testing Device: Automated | (Manual)

Date of Calibration (within 92 days): 11/20/18

Empty/Load Device (Y) | N (All test procedures must be performed in loaded condition)

Daily Test for Testing the Single Car Testing Device Daily performed from 6:00 to 6:20am

Test 2.3.1: Brake pipe pressure reads 90 PSI (black needle)	(Y)	N
Test 2.3.2: Brake cylinder pressure gauge reads between 77 and 83 PSI	(Y)	N
Test 2.3.3: Leakage is less than 1 PSI over a 1 minute timeframe	(Y)	N
Test 2.3.4: Up to a 1-inch bubble appears in no less than 5 seconds	(Y)	N
Test 2.3.5: Flowrator ball rises & floats in zone b/t condemning line and top of tube	(Y)	N
Test 2.3.6: Leakages do not exceed a 1-inch bubble in 5 seconds	(Y)	N

Single Car Air Brake Test

Initial Car Connection

Test 3.2.2.1: Continuous flow of air through pipe	(Y) N

Brake Pipe Leakage Test

Test 3.3.1: Top of ball stabilizes below the condemning line	(Y) N

Continuous Quick Service Valve (If Equipped) No

Test 3.4.1.1: Vent valve does not function and BPP does not reduce to 0 PSI	Y N
Test 3.4.1.2: Intermittent exhaust at quick-service valve is observed	Y N

A-1 Reduction Relay Valve (If Equipped) No

B-1 quick service function is nullified	Y N

Separate Vent Valve Test (If Equipped) Yes

Test 3.4.3.1: Vent valve does not function and BPP does not reduce to 0 PSI	(Y) N
Test 3.4.3.2: Vent valve functions and immediately vents BPP to 0 PSI	(Y) N

System Leakage Test

Test 3.5.1: No venting of air from retaining valve and BC piston in release position	(Y) N
Test 3.5.2: No leakage	(Y) N
Test 3.5.3: Top of the ball stabilizes below the condemning line	(Y) N

Cylinder Maintaining Leakage Test (If Equipped) Yes testing device created by Kasgro

Test 3.5.1.1: Brakes apply	(Y)	N
Test 3.5.1.2: Brake cylinder pressure is above 17 PSI	(Y)	N
Test 3.5.1.3: No leakage	(Y)	N
Test 3.5.1.4: Brake cylinder pressure fluctuates by no more than 1 PSI	(Y)	N

BCP initial: 34psi BCP final: 34psi

Hand Brake Inspection (Group 0)

Test 3.6.1: Hand brake in released position; BC piston push rod returned into BC	(Y)	N
Test 3.6.2: Bell crank in normal working range (if equipped)	(Y)	N
Test 3.6.3: All brake shoes applied by hand brake are set firmly against wheels	(Y)	N
Test 3.6.4: Drum chain unwound, bell crank dropped to lower limit, minimal slack	(Y)	N

Slack Adjuster Conditioning (with Blocks)

Conditioning performed	(Y)	N

Service Stability Test

Test 3.8.2.1: Emergency application was not produced	(Y)	N
Test 3.8.2.2: Brake pipe reduction and exhaust at emergency portion stopped	(Y)	N

Bend

1 2	3 4	5 6

Piston Travel and Rigging and Brake Cylinder Pressure

Test 3.9.1: Measure and note brake cylinder piston travel: 12: 2 9/16, 34: 2 3/4, 56: 2 11/16

Test 3.9.2: Brake levers checked for angularity	(Y)	N
Test 3.9.3: All shoes are applied and firmly set against wheels	(Y)	N
Test 3.9.4: Brake cylinder pressure is greater than 50 PSI	(Y)	N

Test 3.9.5: Note brake cylinder pressure after the BPP has stabilized: 64psi

Emergency Test

Test 3.10.2.1: Control valve emergency application occurred (BBP to 0 PSI)	(Y)	N

Test 3.10.2.2: Brake cylinder pressure is at least 5 PSI greater than 3.9.5: 76psi

Release Test after Emergency

Test 3.11.1: No air exhausting occurred	(Y)	N
Test 3.11.2: The brake pipe pressure continued to rise	(Y)	N

Retaining Valve Test

Test 3.12.1: Brakes remained applied and BCP is >= 12 PSI: ~33psi

Test 3.12.2: Blow of air at retaining valve exhaust	(Y)	N

Minimum Application and Quick-Service Limiting Valve Test

Test 3.13.1: Brakes applied	(Y)	N
Test 3.13.2: Brake pipe reduction and exhaust at emergency portion stopped	(Y)	N

Test 3.13.3: Brake pipe pressure must be >= 80 PSI: 81→82psi

Yes, device created by Kasgro

Single car air brake testing device was adjusted so that application caused BPP to decrease to 90 psi. (previously 82 due to over 90 psi supply to brake pipe)

Brake Cylinder Leakage Test

Wait 3 minutes after BPP stabilizes at 80 PSI

Test 3.14.1: Note the brake cylinder pressure (must be 12-30 PSI): ~~32~~ 30 psi 28 psi (cycled through & retested)

Wait an additional 1 minute

Test 3.14.2: No more than a 1 PSI fluctuation in brake cylinder pressure	(Y)	N
Test 3.14.3: Top of the flowrator ball is below the condemning line	(Y)	N

Slow-Release Test

Test 3.15.1: Brakes released within specified time: 22sec

Slack Adjuster Conditioning (without Blocks)

Conditioning performed	(Y)	N

Accelerated Application Valve (AAV) Test

Test 3.17.1: Exhaust from emergency portion while brake pipe reduces	(Y)	N
Test 3.17.2: No emergency application was produced	(Y)	N
Test 3.17.3: Brake pipe reduction stopped	(Y)	N

Recheck of Piston Travel (without Blocks, if Equipped with Automatic Slack Adjusters)

Test 3.18.1: Piston travel falls within +/- ½ inches of 3.9.1 and within nominal range: 5/16 2 1/16 (12 2 5/16, 3/4 2 3/4)

Manual Release Valve Test

Test 3.19.1: Brake cylinder piston returned to release position and remained there	(Y)	N
Test 3.19.2: Brake cylinder piston remained in the release position during charging	(Y)	N
Test 3.19.3: Brakes applied	(Y)	N

Empty/Load Test

Test 3.20.1: Brakes applied	(Y)	N

Test 3.20.2: Brake cylinder pressure at least 17 PSI lower than 3.9.5: 27psi

Test 3.20.3: No leakage occurred	(Y)	N

Disconnecting the Single-Car Test Device

Test 3.21.1: No leakage occurred	(Y)	N

Additional Comments: -

Brake application cycling done to correct piston travel and meet acceptable tolerance range. Bead brake system includes 3 trucks 12, 34, 56 and has a handbrake. Aend brake system cut out to perform Bend testing, Air restriction test performed on entire car brake system

- Brake cylinder leakage test very sensitive to proper reduction to 90 psi. Single car air test device only reduced to 92 psi due to excessive air supply to system (above 90psi). Once corrected the test was successfully performed and computed a value between 17 psi to 30 psi range

~9:00am End of Test

Static Brake Force Test - Atlas Buffer Car

Cask

~10:00am Start

Observer Name: Matt DeGeorge Inspection Date: 02/12/19

Names of Test Personnel: Thong Le (Osmo), Mark Denton (Osmo), Mark Zeigler, Rick Ford, Corey Wagner, Keith McCabe, Tom Sedarski

[Corey, Keith, Tom performed test]

Amsted Rail

Car and Component Identification

Car Number: IDOX 010001 AEnd Brake Pipe Length: 48 ft

Service Portion Type: DB-10 Emergency Portion Type: DB-20

Brake Shoe Force Measurement Device complies with S-4024: (UnSkwill Tom System) (Pro Shoe)	(Y)	N

Date of Calibration: 6/14/2018 11/13/2018

Brake Shoe Force Test

3.2.3: All pins and pin holes free of lubrication	(Y)	N
3.2.4: Reducing valve is used (if Y must perform Equalization Test)	Y	(N)
Equalization Test performed to check piston travel		
3.2.4: BC Pressure equalizes b/t 63.5 and 66.5 psi with min 30 psi reduction	(Y)	N
3.2.5: Rapping done correctly on brake rigging and with acceptable hammer	(Y)	N
3.2.6: No rapping during hand brake force testing	(Y)	N

3.2.7: 6.0 to 7.0 psi BP reduction from 90.0 psi BPP results in all brake shoes forced against wheels Yes

Equalization (Piston Travel)

Acceptable Range: 2 3/4 inch +/- 1/8 inch **Truck** 79 : 2 7/8 in **Truck** 97 : 2 3/4 in **Truck** YX : 2 3/4 in

Min Service Reduction (6-7 psi, Loaded)

Sensor	Wheel Location	Force (lbs)
1	RX	60
2	RY	363
3	LX	264
4	LY	334
5	LZ	272
6	L9	150
7	RZ	154
8	R9	277
Sys II: 1	R8	517
Sys II: 2	R7	518
Sys II: 3	L8	553
Sys II: 4	L7	515

Jim Shoe II System

Average brake shoe force >= 100 lb per wheel: 331.42 lbs

30 psi Reduction (Loaded)

BCP: 63.75 psi

Sensor	Wheel Location	Force initial (lbs)	Force after rapping (lbs)
1	RX	3362	3730
2	RY	4000	4008
3	LX	4032	4330
4	LY	4193	4292
5	LZ	4322	3991
6	L9	3914	4057
7	RZ	3593	3410
8	R9	3692	3829
Sys II: 1	R8	3750	3761
Sys II: 2	R7	3936	4096
Sys II: 3	L8	4390	4383
Sys II: 4	L7	4131	4220

Total Force: 49097 lbs **Average Force per wheel:** 4008 lbs

+/- 12.5% tolerance: 3507 to 4509 lbs

one wheel for each 8 wheels on a car may exceed w/o failure per 5-401 4.2 OK (1 wheel)

4.2: NBR on each wheel is within +/- 12.5% of Average NBR per wheel | Y | (N) |

½ Weight of Loaded Car: 355350 lbs **NET Braking Ratio:** 13.54 % (between 11-14%)

Emergency Application (Loaded)

30 psi reduction BCP: 63.75 psi **Emergency BCP:** 74.25 psi **Percentage:** 116.47 % (15-20%)

test redone b/c improper set force used initially

Hand Brake Test (Loaded) Group D 4027 lb Handbrake force set

Sensor	Wheel Location	Force (lbs)
1	RX	3896
2	RY	5252
3	LX	4740
4	LY	5393
5	LZ	3442
6	LQ	3741
7	RZ	2643
8	RQ	3041
Sys II : 1	RQ	1735
Sys II : 2	R7	3067
Sys II : 3	LQ	2910
Sys II : 4	L7	3225

Total Force: 43,585 lbs **½ Weight of Loaded Car:** 355,350 lbs

Net Braking Ratio: 12.27 % (>10%)

Min Service Reduction (6-7 psi, Empty)

Sensor	Wheel Location	Force (lbs)
1	RX	29
2	RY	310
3	LX	714
4	LY	760
5	LZ	210
6	LQ	98
7	RZ	53
8	RQ	734
Sys II : 1	RQ	376
Sys II : 2	R7	453
Sys II : 3	LQ	475
Sys II : 4	L7	433

Average brake shoe force >= 100 lb per wheel: 262.88 lbs

30 psi Reduction (~~Loaded~~ Empty)

BCP: ~~675~~ 27 psi

Sensor	Wheel Location	Force initial (lbs)	Force after rapping (lbs)
1	RX	595	515
2	RY	1542	1580
3	LX	1445	1371
4	LY	1612	1600
5	LZ	1294	1478
6	L9	1310	1417
7	RZ	820	1099
8	R9	1395	1392
SysII: 1	R8	1131	1350
SysII: 2	R7	1599	1651
SysII: 3	L8	1848	1803
SysII: 4	L7	1678	1675

Total Force: 17,231 lbs **Average Force per wheel:** 1436 lbs

½ Weight of Loaded Car: 112,950 lbs **NET Braking Ratio:** 15.27 % (between 15-32%)

Additional Comments: -

Hand brake test performed twice because incorrect hand brake set force was used. A end system includes 3 trucks 78, 9Z, XY, B end system cut out to perform A end testing

~ 12:00pm End of Test

~1:00pm Start

Static Brake Force Test - Atlas Buffer Car

Cask

Observer Name: Matt DeGeorge Inspection Date: 07/12/19

Names of Test Personnel: Thong Le (Orano), Mark Denton (Orano), Mark Zeigler, Rick Ford, Corey Wagner, Keith McCabe, Tom Sedarski

[Corey, Keith, & Tom performed Test] → Amsted Rail

Car and Component Identification

Car Number: TTAX 010001 B End Brake Pipe Length: 49 ft

Service Portion Type: DB-10 Emergency Portion Type: DB-20

Brake Shoe Force Measurement Device complies with S-4024:	(Y)	N

Jim Shoe II Pro Shoe

Date of Calibration: 6/14/2019 11/13/2018

Brake Shoe Force Test

3.2.3: All pins and pin holes free of lubrication	(Y)	N
3.2.4: Reducing valve is used (if Y must perform Equalization Test)	Y	(N)

Equalization Test performed to check piston travel

3.2.4: BC Pressure equalizes b/t 63.5 and 66.5 psi with min 30 psi reduction	(Y)	N
3.2.5: Rapping done correctly on brake rigging and with acceptable hammer	(Y)	N
3.2.6: No rapping during hand brake force testing	(Y)	N

3.2.7: 6.0 to 7.0 psi BP reduction from 90.0 psi BPP results in all brake shoes forced against wheels 1/5

Equalization (Piston Travel)

Acceptable Range: 2 3/4 inch +/- 1/8 inch **Truck** 12 : 2 5/8 in **Truck** 34 : 2 7/8 in **Truck** 56 : 2 3/4 in

Measured

Min Service Reduction (6-7 psi, Loaded)

Sensor	Wheel Location	Force (lbs)
1	R2	670
2	R1	649
3	L2	813
4	L1	565
5	L3	450
6	L4	490
7	R3	1130
8	R4	950
SYS II: 1	R6	1085
SYS II: 2	R5	935
SYS II: 3	L5	880
SYS II: 4	L6	1110

Average brake shoe force >= 100 lb per wheel: 859.75 lbs

30 psi Reduction (Loaded)

BCP: 63.5 psi

Sensor	Wheel Location	Force initial (lbs)	Force after rapping (lbs)
1	R7	4226	4052
2	R2	4482	4294
3	L2	4137	4020
4	L1	3566	3505
5	L3	3482	3160
6	L4	3986	4065
7	R3	4354	4000
8	R4	3949	3951
SYS II: 1	R6	3752	4417
SYS II: 2	R5	4086	4414
SYS II: 3	L5	3610	3928
SYS II: 4	L6	4020	4032

Total Force: 47,778 lbs **Average Force per wheel:** 3977 lbs

+/- 12.5% tolerance: 3490 to 4475 lbs

One wheel for each 8 wheels on a car may exceed w/o failure per S-401 (OK 1 wheel)

4.2: NBR on each wheel is within +/- 12.5% of Average NBR per wheel | Y | (N) |

½ Weight of Loaded Car: 355,350 lbs **NET Braking Ratio:** 13.43 % (between 11-14%)

Emergency Application (Loaded)

30 psi reduction BCP: 63.5 psi **Emergency BCP:** 73.9 psi **Percentage:** 16.22 % (15-20%)

retested b/c initial force value low (limited by smart hook) clearance

Hand Brake Test (Loaded) (Group 0)

Sensor	Wheel Location	Force (lbs)
1	R2	4976
2	R1	4923
3	L2	5018
4	L1	4176
5	L3	2420
6	L4	3514
7	R3	3408
8	R4	3518
Sys II: 1	R6	3135
Sys II: 2	R5	2777
Sys II: 3	L5	2048
Sys II: 4	L6	3271

Total Force: 47529 lbs **½ Weight of Loaded Car:** 355350 lbs

Net Braking Ratio: 11.97 % (>10%)

Min Service Reduction (6-7 psi, Empty)

Sensor	Wheel Location	Force (lbs)
1	R2	349
2	R1	307
3	L2	505
4	L1	343
5	L3	349
6	L4	653
7	R3	775
8	R4	601
Sys II: 1	R6	679
Sys II: 2	R5	677
Sys II: 3	L5	557
Sys II: 4	L6	690

Average brake shoe force >= 100 lb per wheel: 556.17 lbs

30 psi Reduction (~~Loaded~~ Empty)

BCP: 26 psi

Sensor	Wheel Location	Force initial (lbs)	Force after rapping (lbs)
1	R2	1580	1618
2	R1	1710	1676
3	L2	1590	1634
4	L1	1746	1466
5	L3	1153	1216
6	L4	1515	1505
7	R3	1948	1749
8	R4	1566	1586
Sys II: 1	R6	1601	1680
Sys II: 2	R5	1488	1438
Sys II: 3	L5	1409	1453
Sys II: 4	L6	1596	1675

Total Force: 19,098 lbs **Average Force per wheel:** 1592 lbs

½ Weight of Loaded Car: 117,950 lbs **NET Braking Ratio:** 16.92 % (between 15-32%)

Additional Comments: - Hand brake test performed twice because proper hand brake set force, could not be achieve first try due to smart hook clearance issues. Bend system including 3 trucks 12, 34, 56 + Aend system cut out to perform Bend testing

~2:30pm End of Test

Transportation Technology Center, Inc.

Mike Yon
Field Inspector - MID/QA Auditor
Cell: 814-515-3803
Email: Mike_yon@aar.com

March 12, 2019

File:KAS-NEWCPA-MC06-0219b-MSY

Subject: Single Car Air Brake Test Observations Specification testing of IDOX 010001, Heavy Duty Flat Car

Mr. David L. Cackovic
Chief – Technical Standards & Inspections
Transportation Technology Center, Inc.
P.O. Box 11130
Pueblo, CO 81001
E-mail: David_Cackovic@aar.com

Dear Mr. Cackovic,

Specification testing of IDOX 010001, Heavy Duty Flat Car, specifically the Single Car Air Brake Test and restriction test has been completed. Testing was done at the Kasgro Rail Corporation facility in New Castle, Pennsylvania on February 12, 2019 to comply with Specification S-2043 and S-486.

I was present (test witness) for the required Single Car Air Brake Test and can conclude that applicable requirements of AAR Specification S-486 have been satisfactorily addressed.

Attached information was supplied by the Kasgro Rail Corporation in support of the approval process. Should you need any additional information, please do not hesitate to call.

Sincerely,



Mike Yon

cc: Anna Fox, TTCI
Richard Jones, Kasgro
J. Hannafious, TTCI
Kasgro, mark@kasgro.com

Rev.1

Kasgro Rail Corp

FORM 6-A 2/25/2016

Air Brake Test Report
(X=Tested)

CAR NUMBER ZDXX 010001

Single Car Test, 1Set		Single Car Test, 2 Sets	X
Single Car Test (Includes B.C. Pressrure Test)		Single Car Test (Includes B.C. Pressure Test), 2 Sets	X
Slack Adjuster Test	X	Retainer Valve Test	X
Empty / Load Valve Test	X	Brake Pipe Leakage Test	X
System Leakage Test	X	Equalization Pressure	X
Piston Travel (Unit Brakes)		If Equipped With Load Sensor	X
Piston Travel (Trk MTD Brakes)	X	Equalization Pressure Load Sensor	X
WABCO PAC / NYPCAC Piston Travel Adjustment		Equalization Pressure Loaded	X
(Truck Mounted Brakes with Slack Adjuster		Equalization Pressure Empty	X
#1 #2 #3 #4		Slack Adjuster Rack Measurement	X
Lube Handbrake			

SYSTEM REPAIRS- List repairs, parts replaced, Location, and why made.

Piston Travels B 2⅜, C 2¼, D 2⅛, E 2½, F 2⅛, A 2⅝

EQUALIZATION PRESSURE: B END SER 64, EM 76, EMPTY 22
A END SER 63, EM 76, EMPTY 20

NEW YORK AIR BRAKE ELK-R LOW SENSOR 4076

DB-10E
DB-20 } H+B END

RESTRICTION TEST 46.7 MIN, 50 ACTUAL (S40T BALL OK)

Signature of Tester [illegible] Date 2-12-19

Note: The recording of false, fictitious, or fraudulent statements on this document may be punishable as a felony under federal statues.

Appendix D. Atlas Car Strain Gage Information

This appendix contains details on the location, installation, and shunt calibration of the strain gages used to measure strain on the Atlas Car. All the strain gages used on the Atlas car are of the same type: CEA-06-500UW-350 with the following characteristics:

- Encapsulated constantan alloy (bondable)
- Grid Length: 0.5 in
- Uniaxial type
- 350 ohm
- Gage Factor: 2.155

The gages were installed as ¼ bridge active gages. Installation procedures are followed from the Vishay standard protocols for bondable strain gages.

Figure D1 to Figure D4 show the locations of the strain gages. These drawing show detailed locations for gages on one quadrant of the car. The gages in the other quadrants are symmetrical.

Figure D5 to Figure D60 show photos of the installed strain gages.

Figure D61 shows a photo of one of the installed thermocouples.

Figure D62 to Figure D69 show data recorded during a shunt calibration check just before the one million pound squeeze test. The 175 kΩ shunt resistor was placed across the active arm of the bridge to perform the shunt calibration. Unfortunately, the output signals from these gages was wired incorrectly into the data acquisition system, so these Rcal steps show a positive step rather than a negative one. This error was addressed during data analysis.

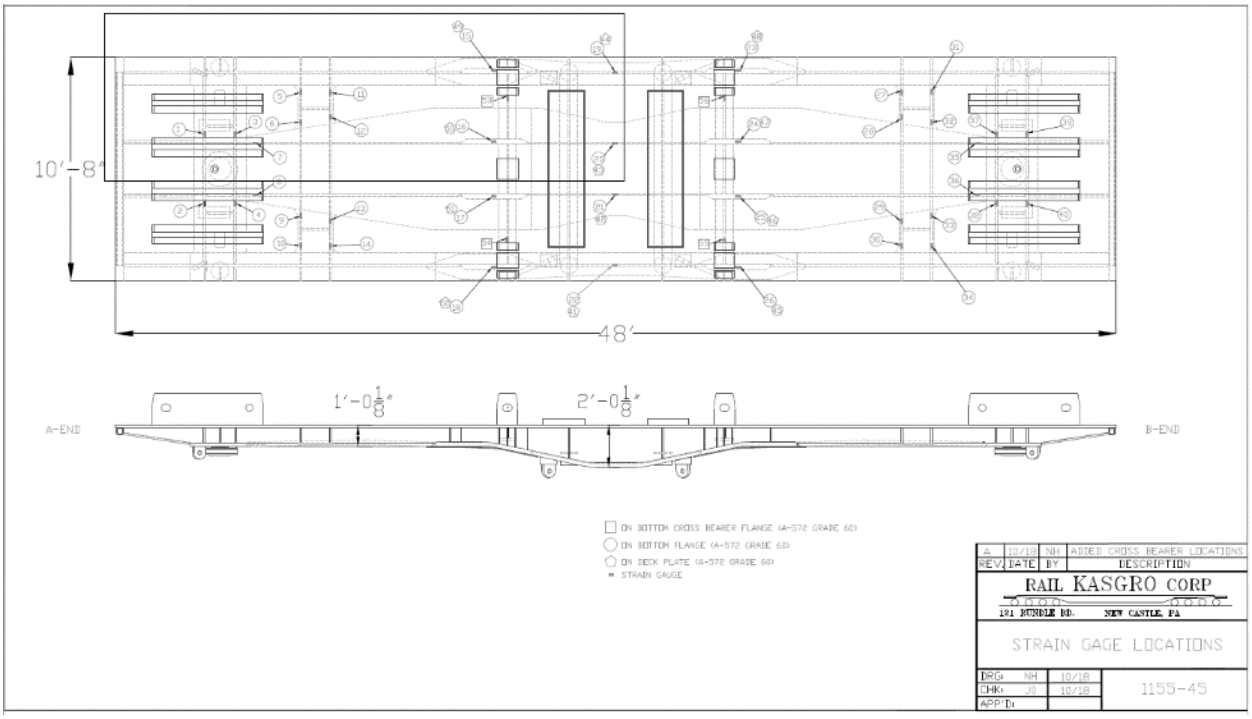


Figure D1. Strain Gage Locations

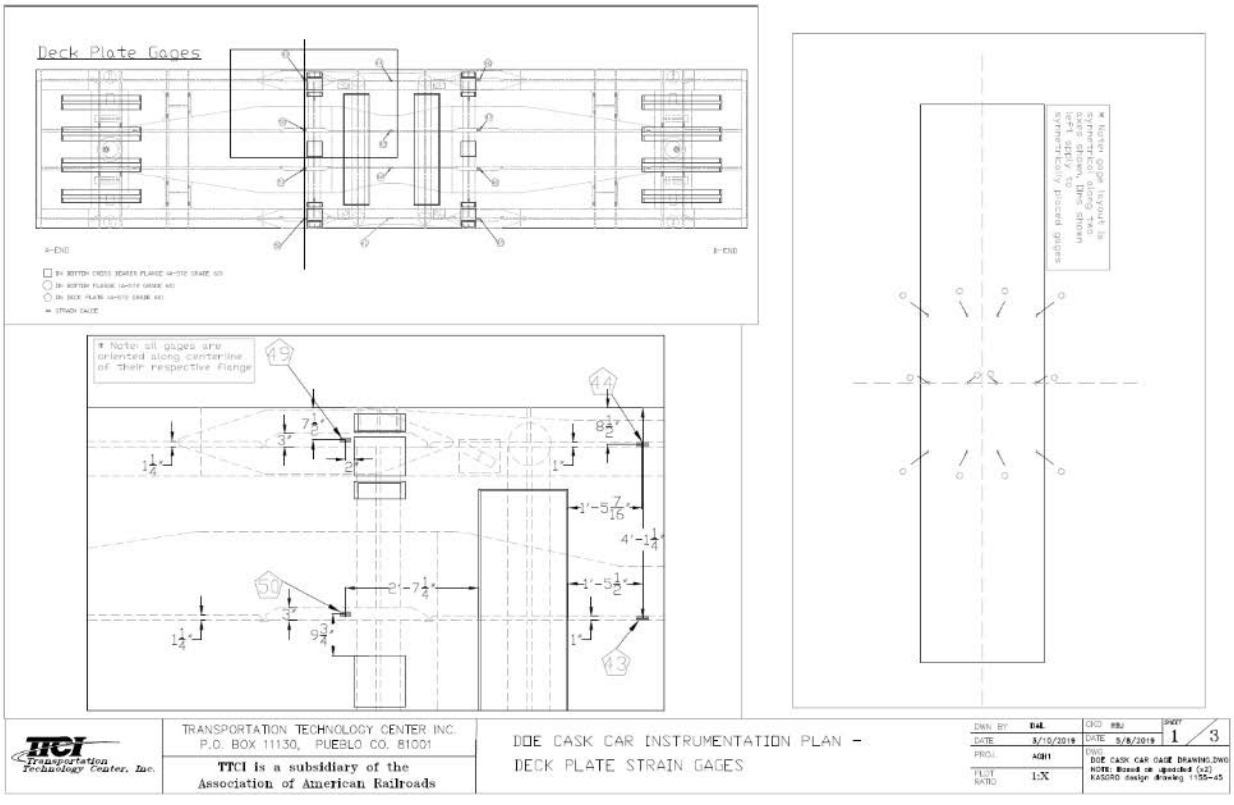


Figure D2. Detailed Strain Gage Locations, on Deck Plate

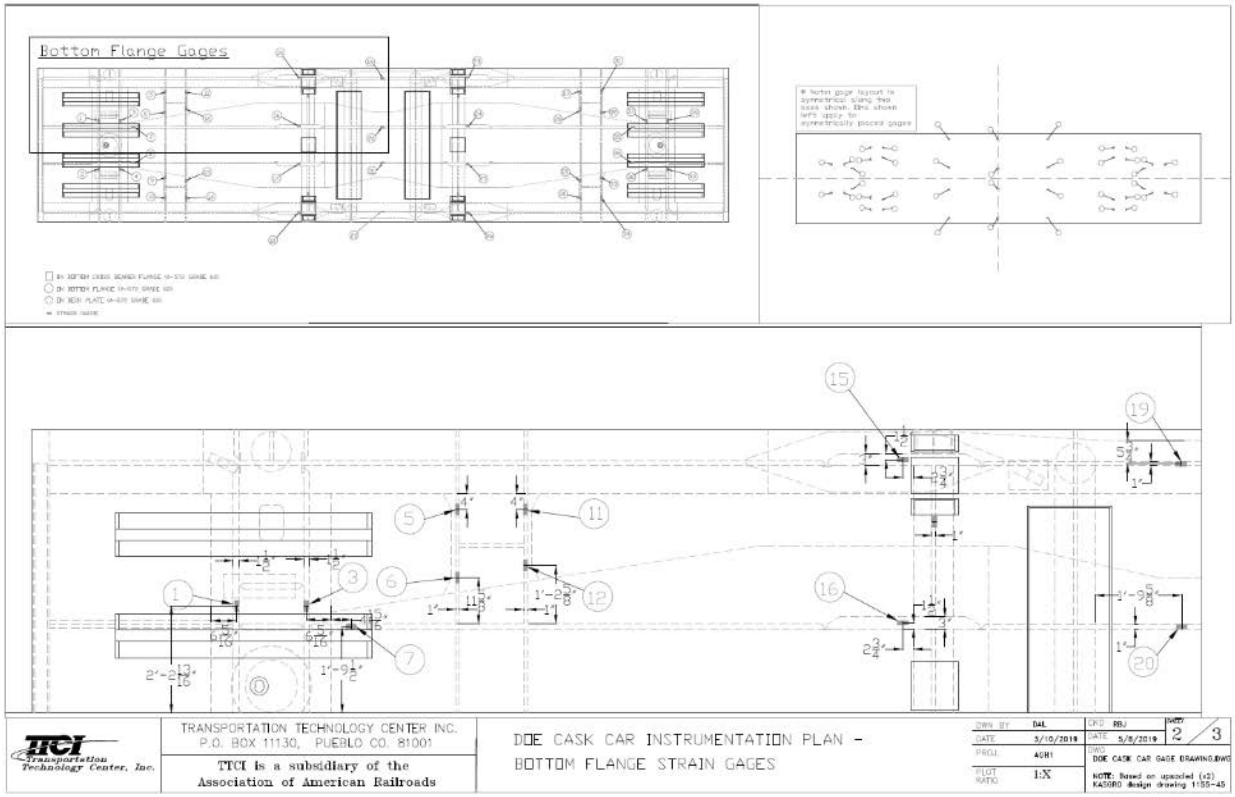


Figure D3. Detailed Strain Gage Locations, on Bottom Flange

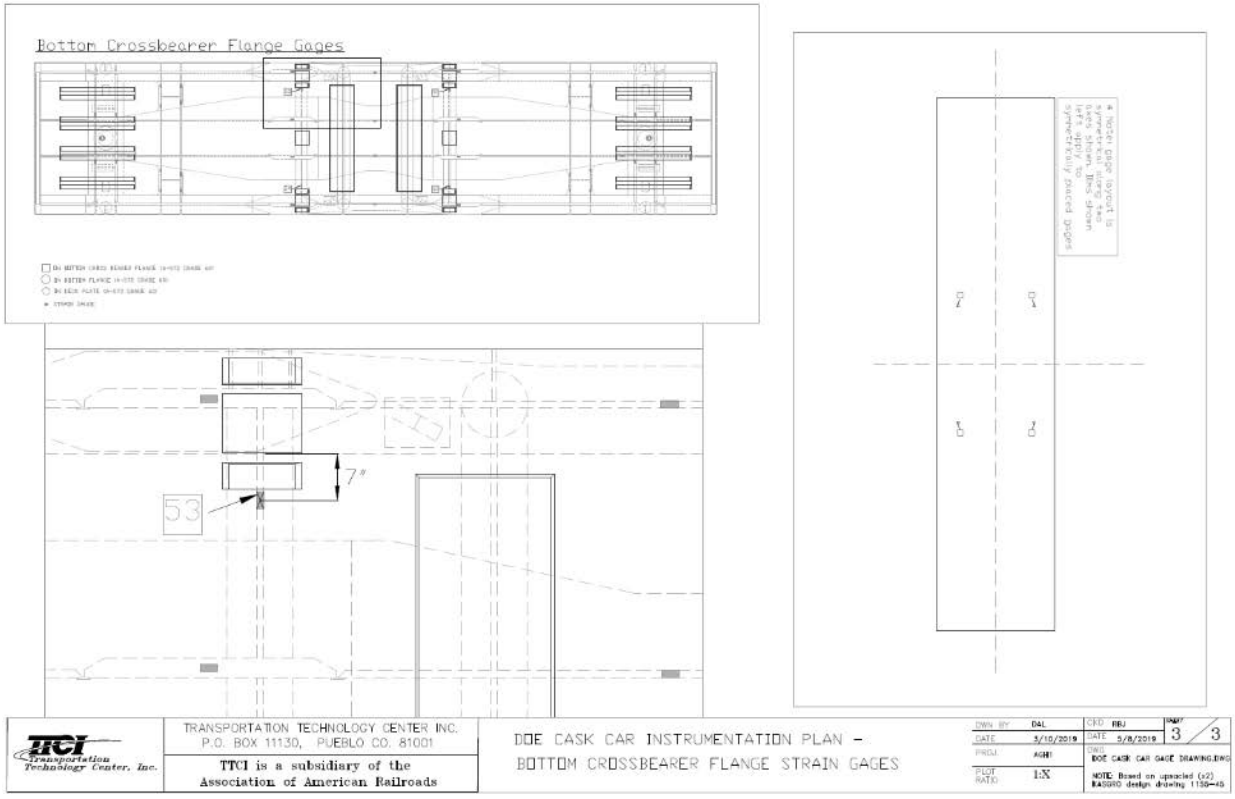


Figure D4. Detailed Strain Gage Location, on Bottom Cross Bearer Flange

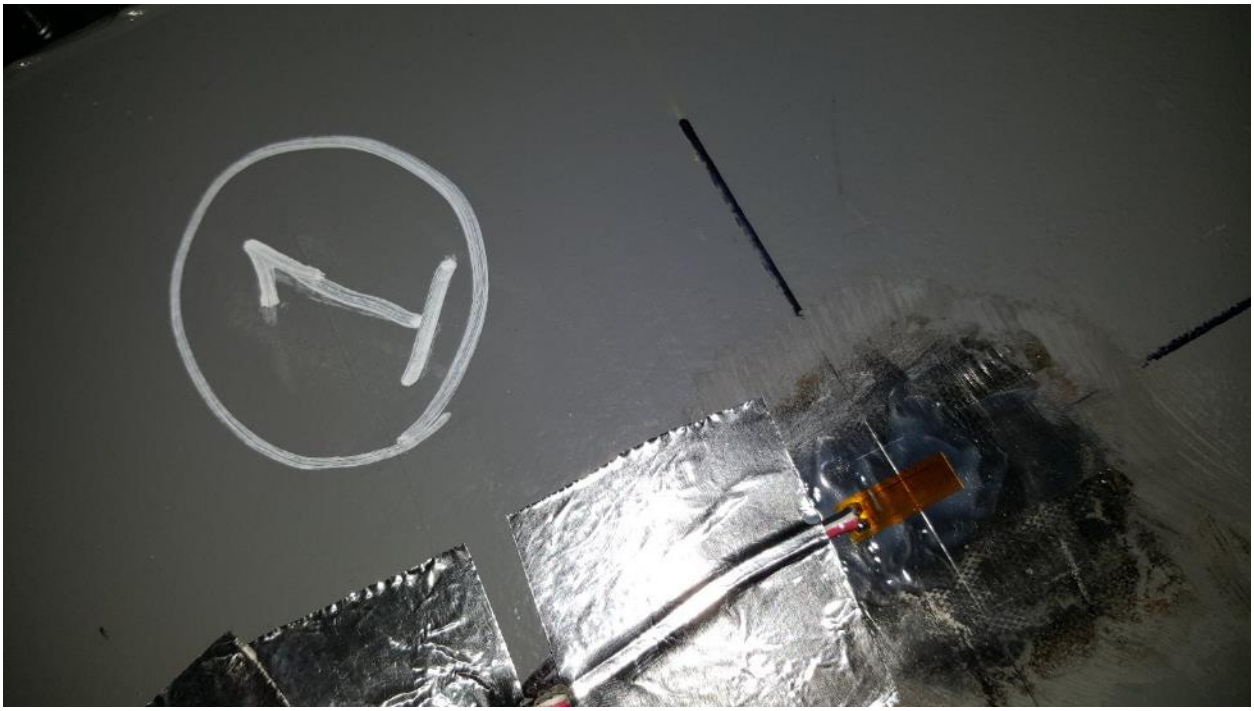


Figure D5. SGBF 1 Front of Bottom Flange of From Body Bolster near Center Sill, RH Side

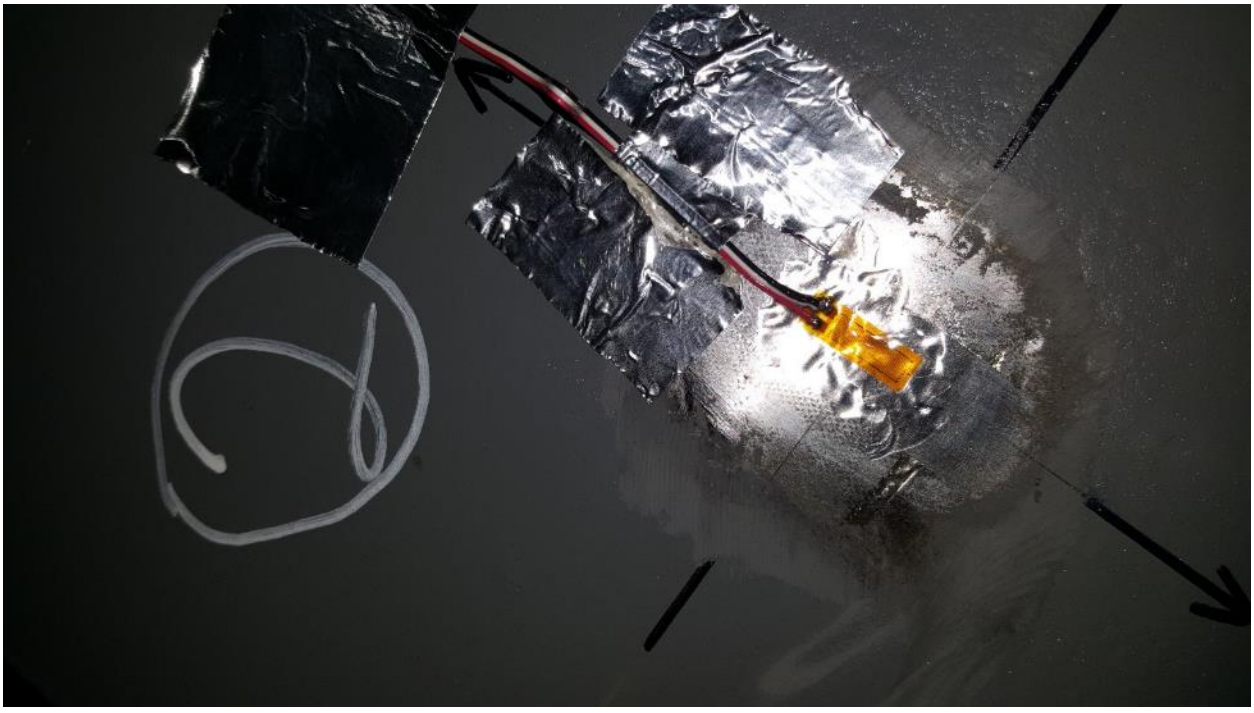


Figure D6. SGBF2 Front of Bottom Flange of Front Body Bolster near Center Sill, LH Side

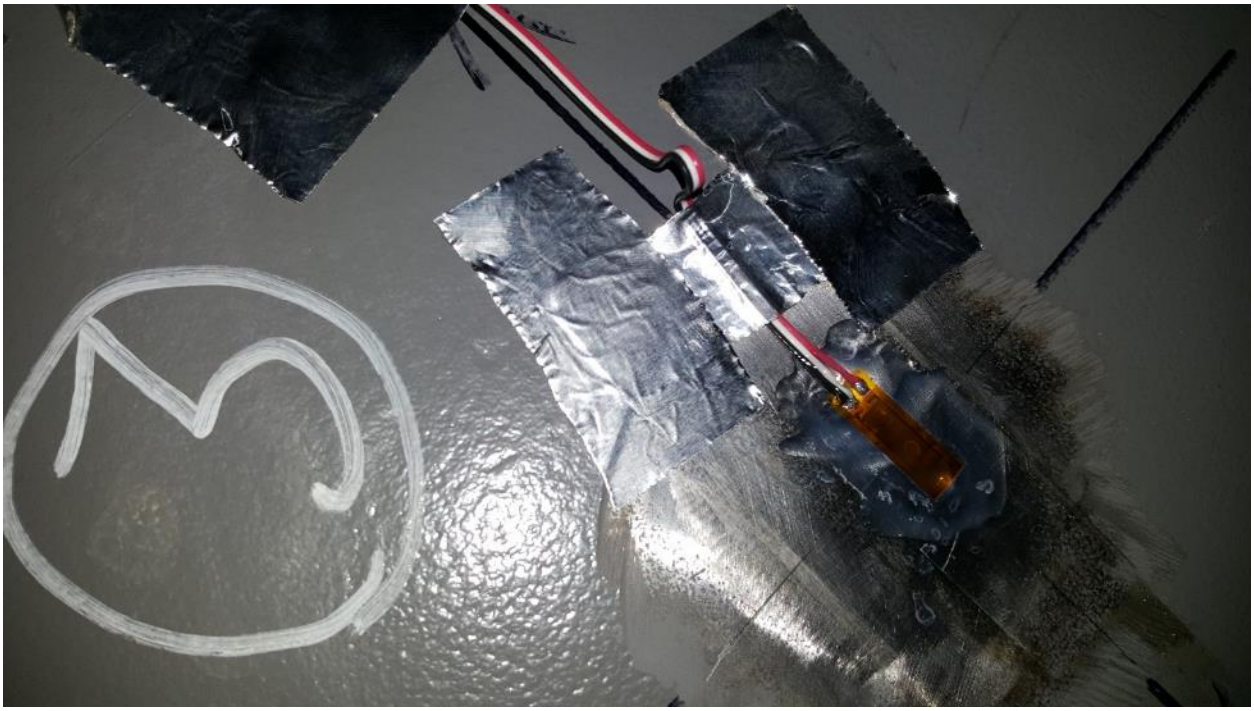


Figure D7. SGBF3 Rear of Bottom Flange of Front Bolster near Center Sill, RH Side

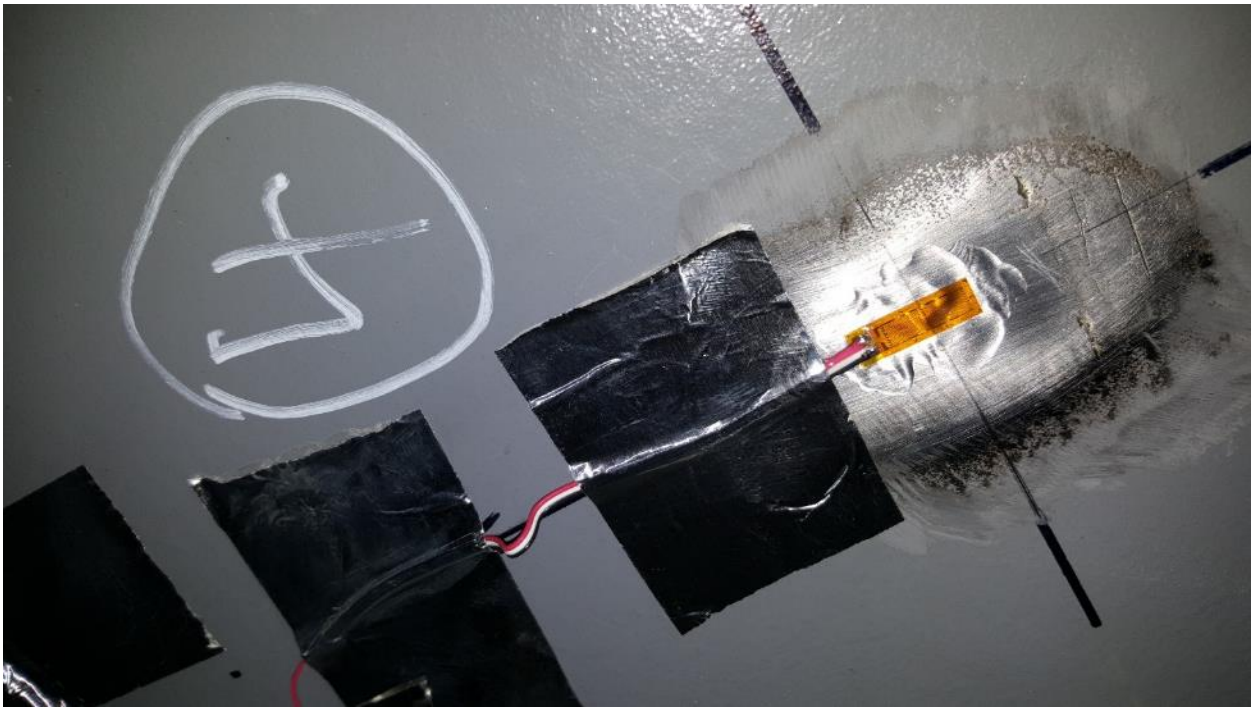


Figure D8. SGBF4 Rear of Bottom Flange of Front Body Bolster near Center Sill, LH Side

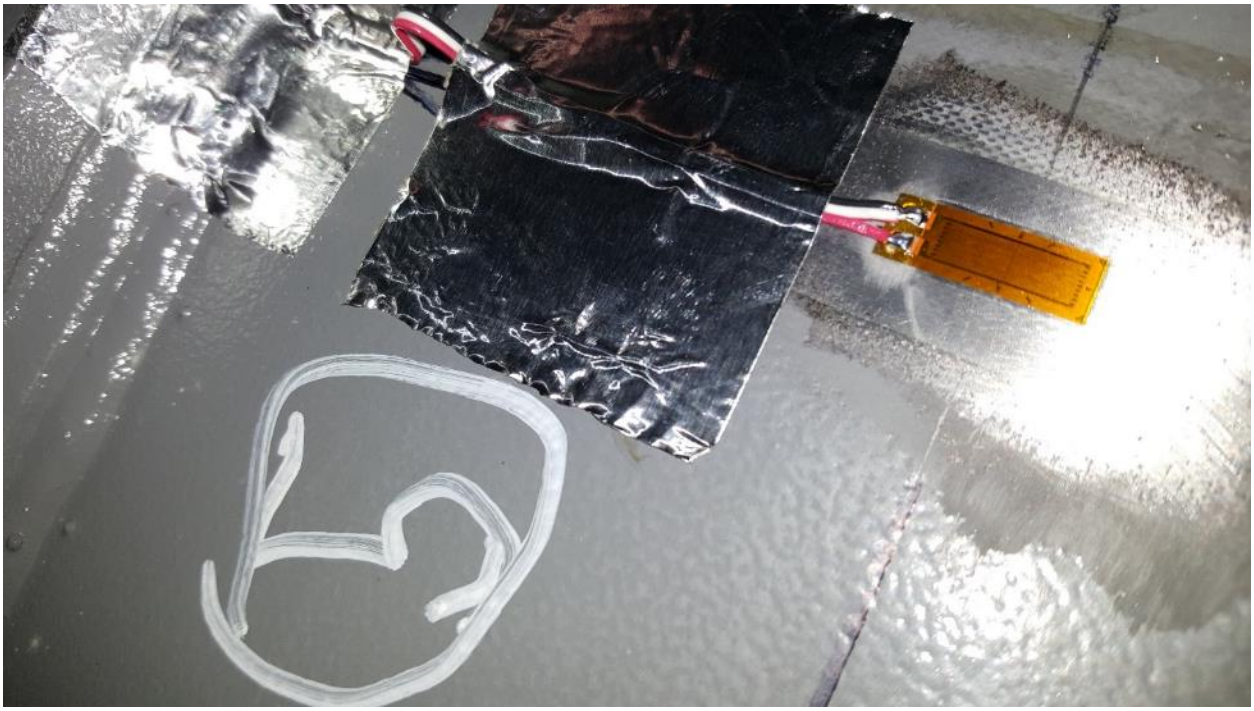


Figure D9.SGBF5 Front of Bottom Flange of #4 Cross Bearer, RH Side between Center Sill and Side Sill, near Side Sill



Figure D10. SGBF6 Front of Bottom Flange of #4 Cross Bearer, LH Side between Center Sill and Side Sill, near Center Sill

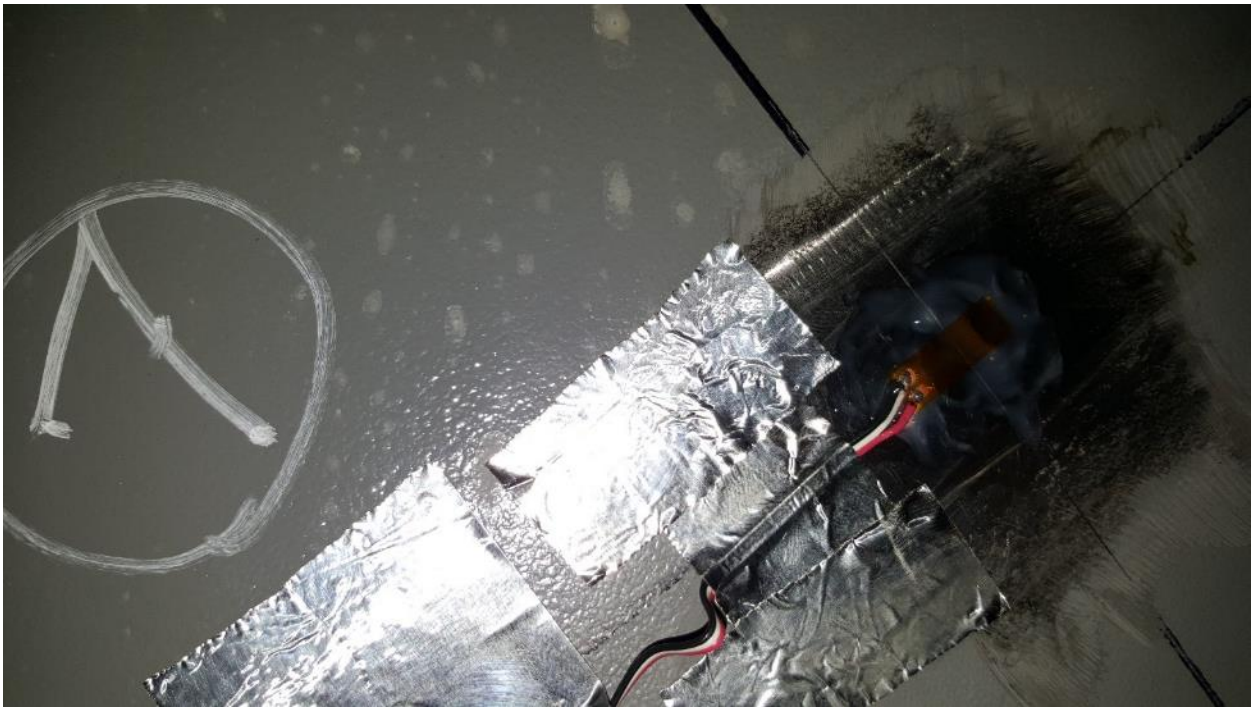


Figure D11. SGBF7 RH Side of Bottom Flange of Center Sill, aft of Front Body Bolster, aligns with Center Sill Web and End Stop Mount Block Pin Hole

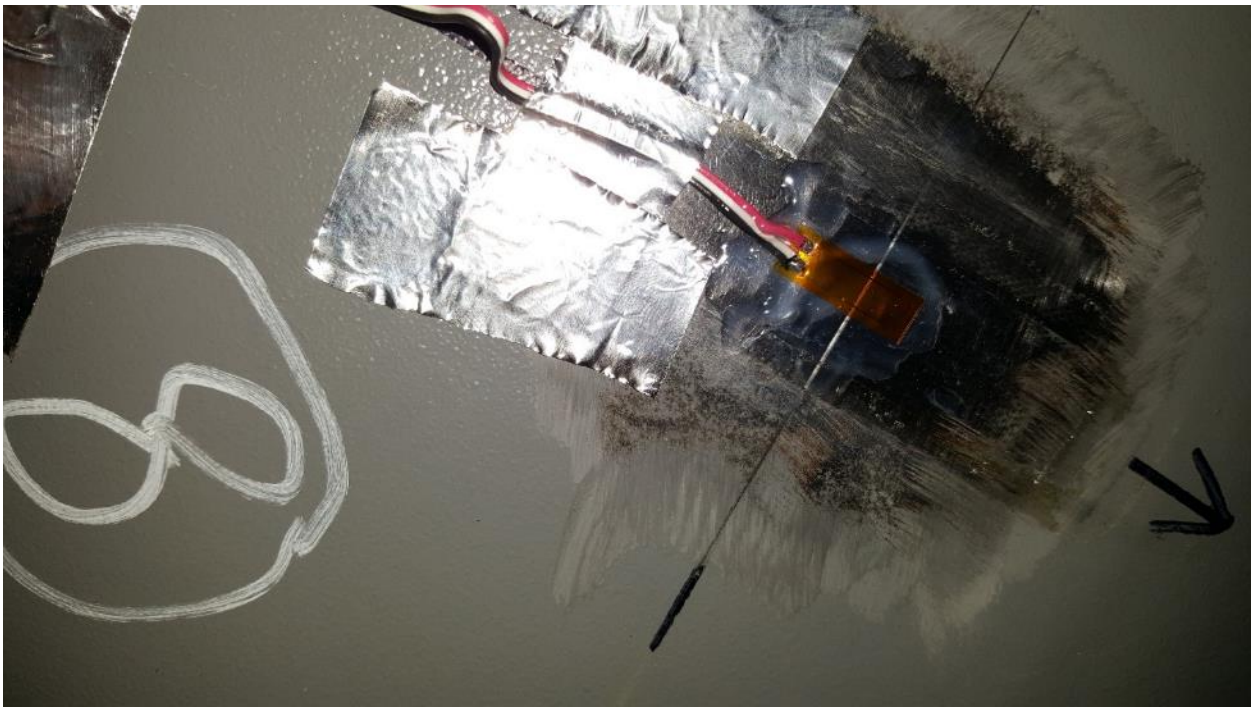


Figure D12. SGBF8 LH side of Bottom Flange of Center Sill, aft of Front Body Bolster, aligns with Center Sill Web and End Stop Mount Block Pin Hole

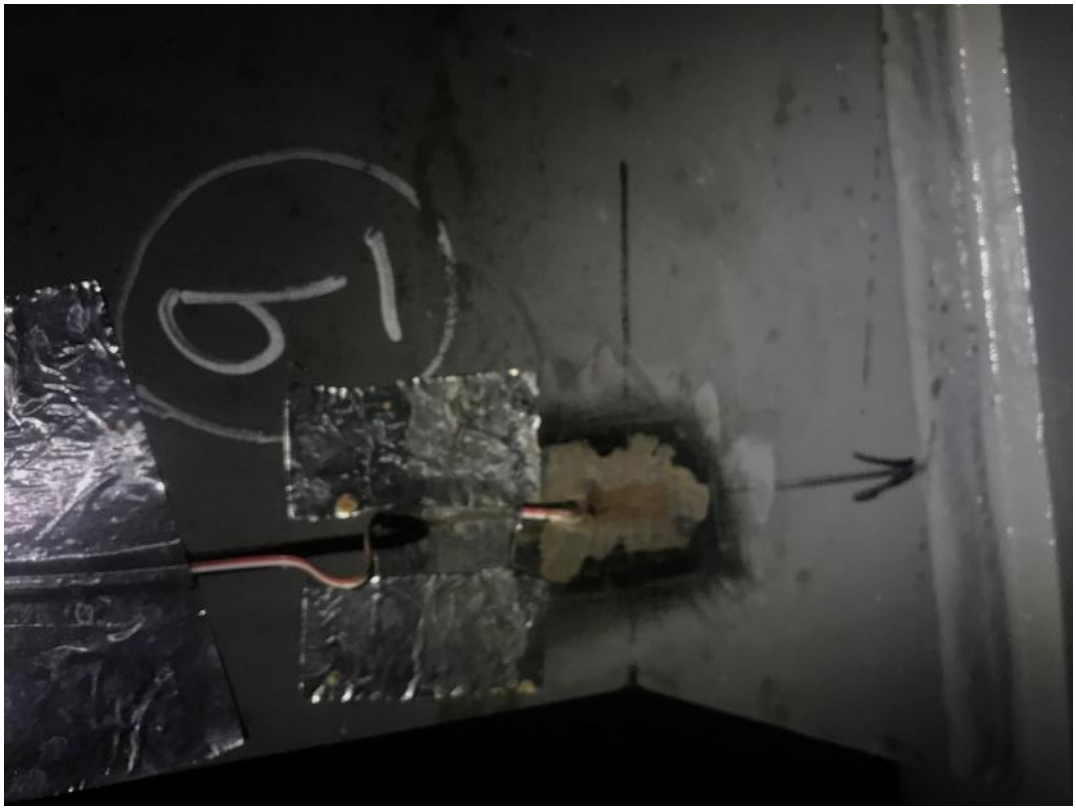


Figure D13. SGBF9 Front of Bottom Flange of #4 Cross Bearer, LH Side between Center Sill and Side Sill, near Center Sill

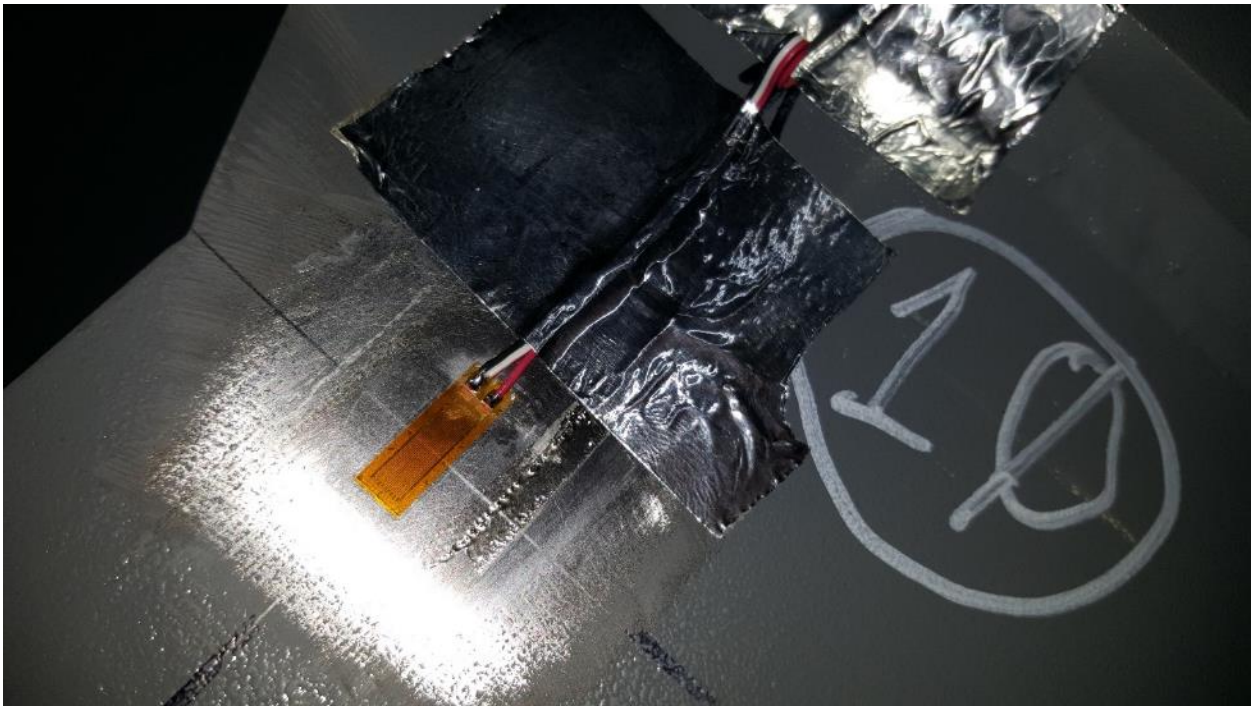


Figure D14. SGBF10 Front of Bottom Flange of #4 Cross Bearer, LH Side between Center Sill and Side Sill, near Side Sill

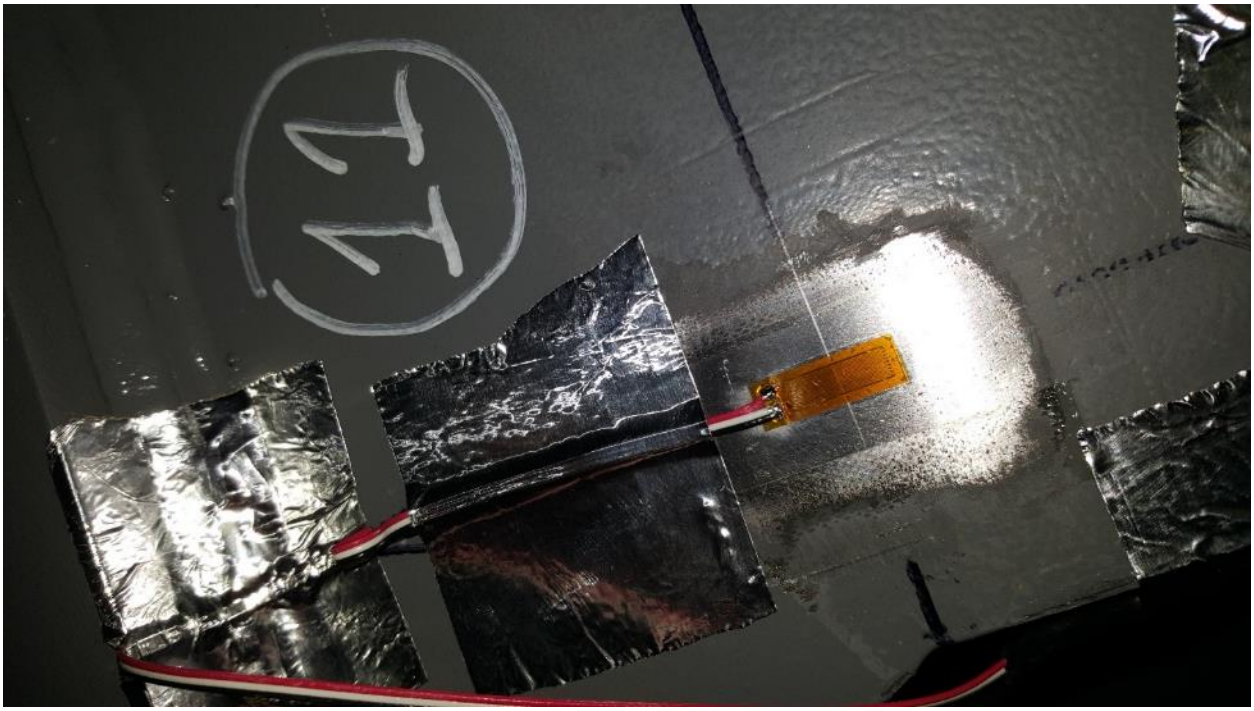


Figure D15. SGBF11 Rear of Bottom Flange of #4 Cross Bearer, RH Side between Center Sill and Side Sill, near Side Sill

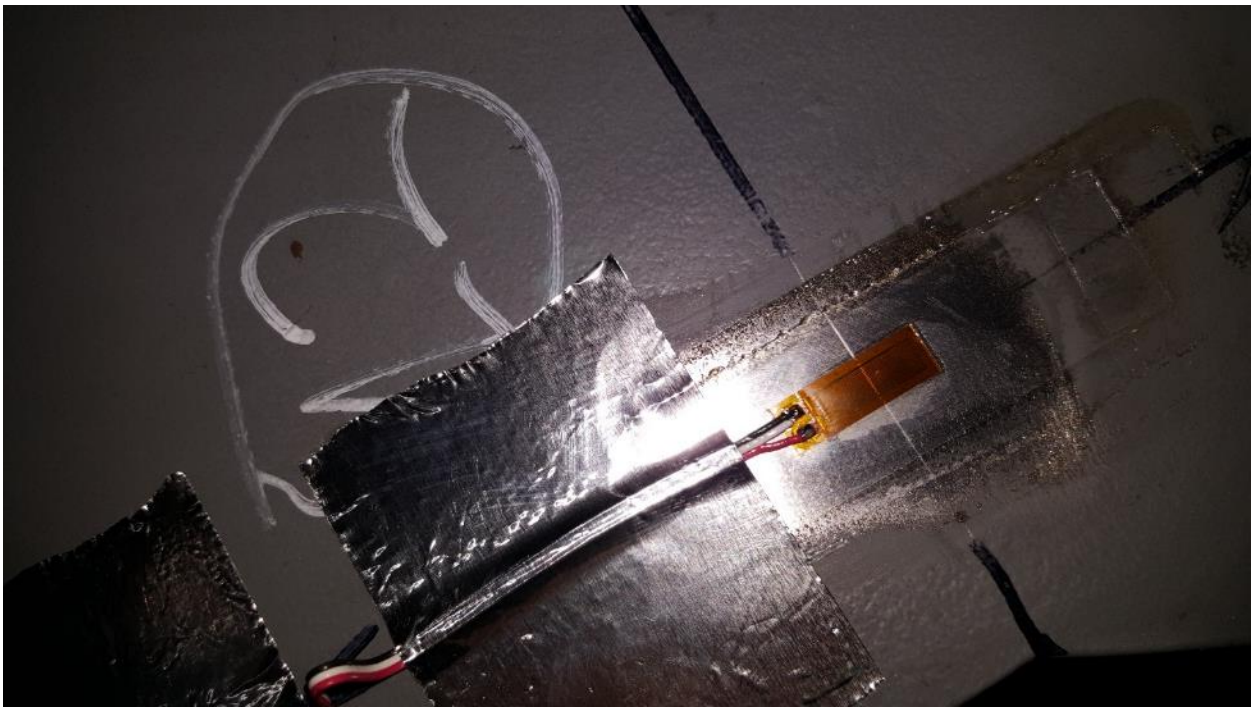


Figure D16. SGBF12 Rear of Bottom Flange #4 Cross Bearer, RH side Between Center Sill and Side Sill, near center Sill

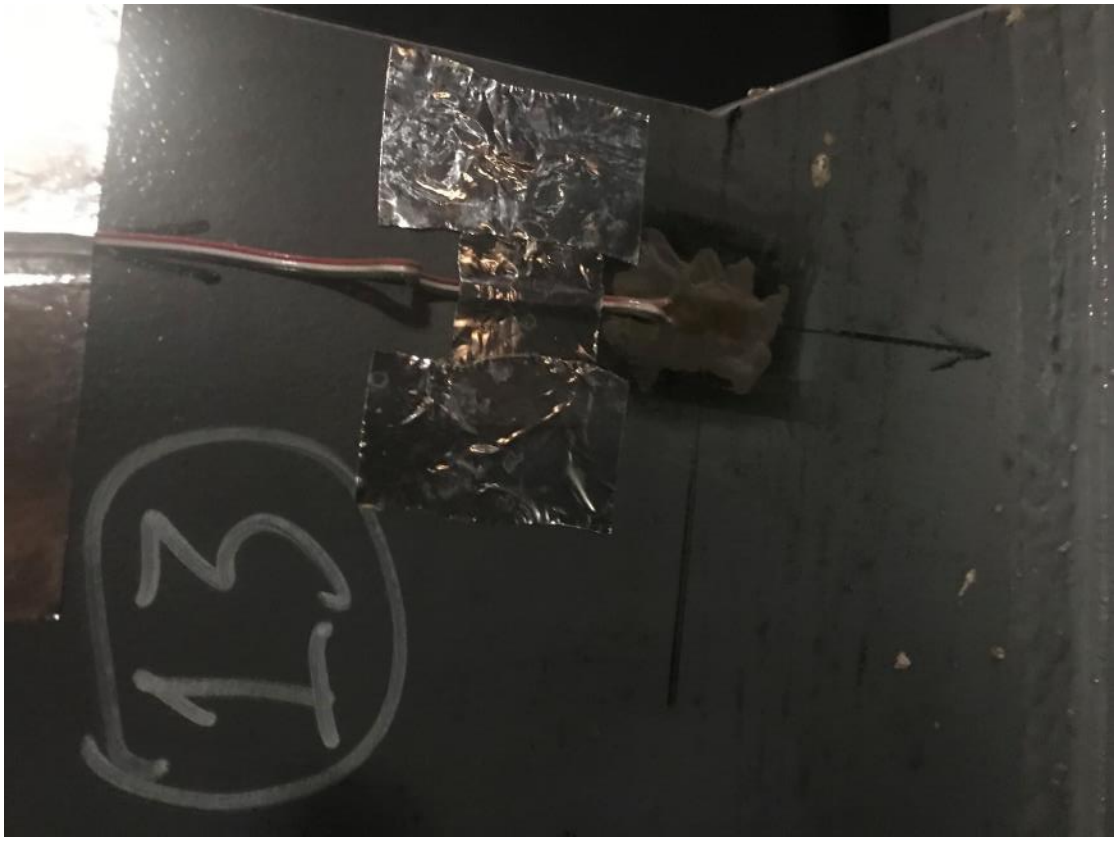


Figure D17. SGBF13 Rear of Bottom Flange of #4 Cross Bearer, LH side between Center Sill and Side Sill, near Center Sill

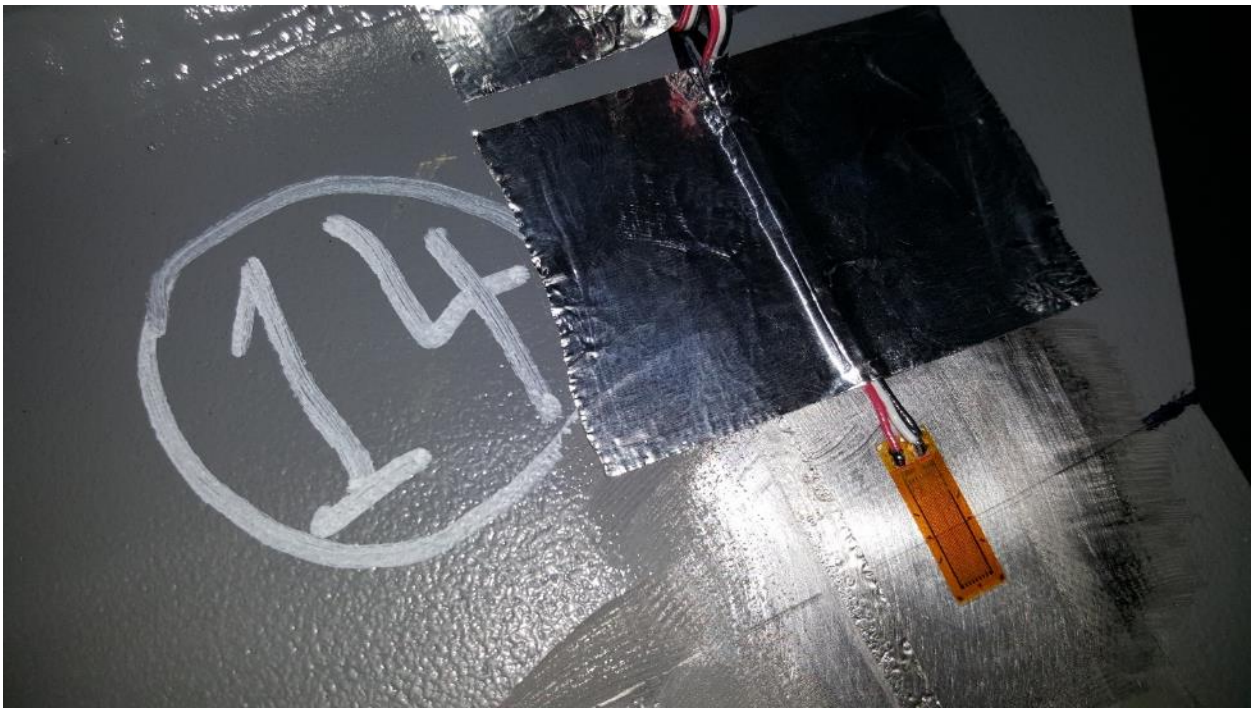


Figure D18. SGBF14 Rear of Bottom Flange of #4 Cross Bearer, LH side between Center Sill and Side Sill, near Side Sill

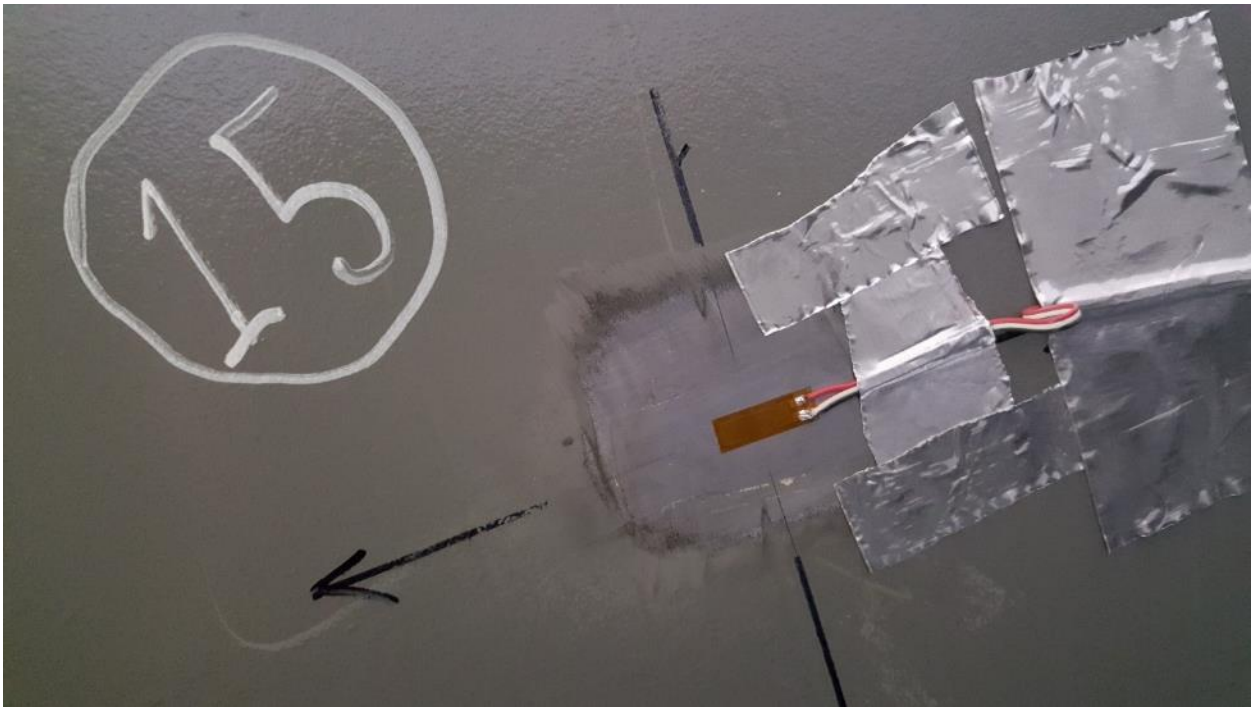


Figure D19. SGBF15 Center of RH Side Sill Bottom Flange, approximately 2" forward of #3 Cross Bearer

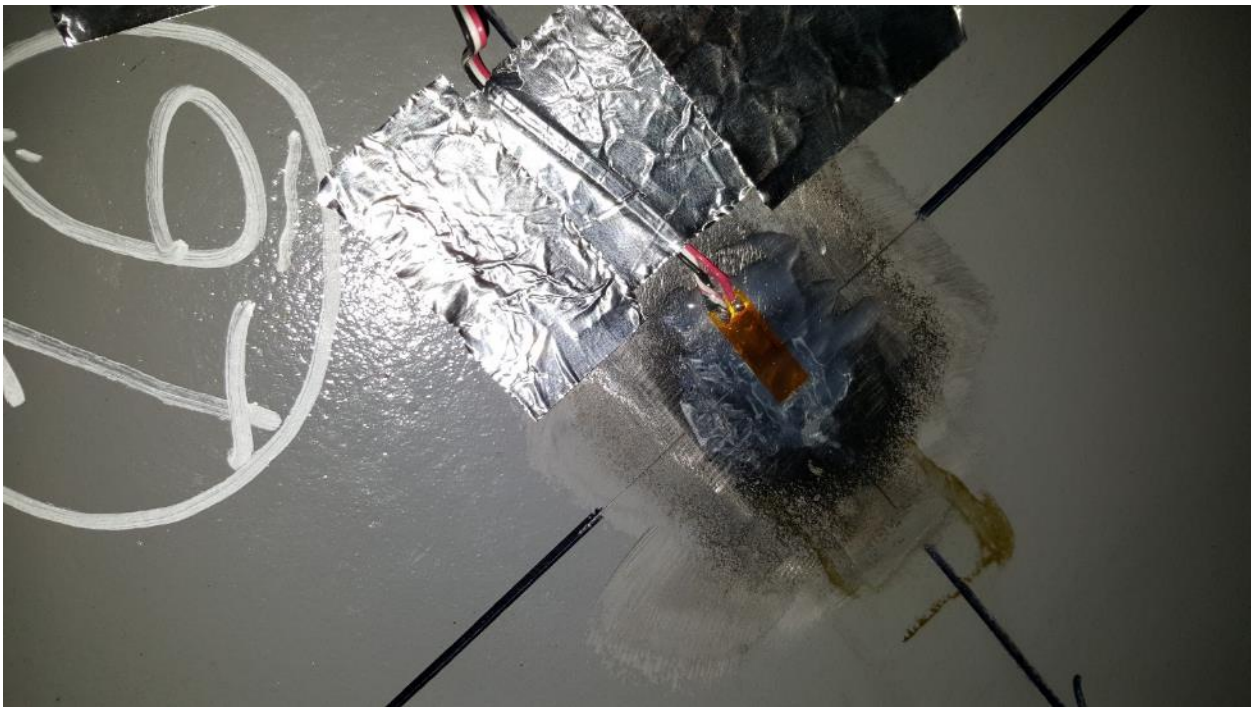


Figure D20. SGBF16 Center Sill Bottom Flange, aligned with RH Center Sill Web, approximately 2" forward of #3 Cross Bearer

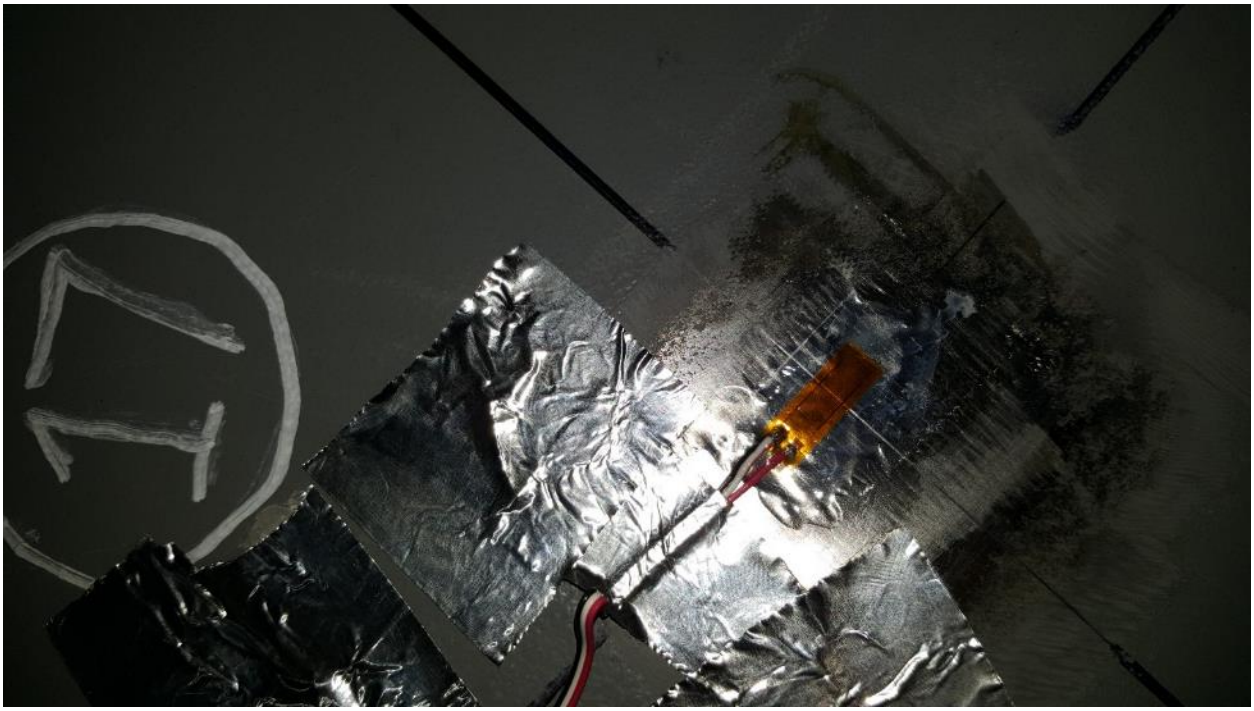


Figure D21. SGBF17 Center Sill Bottom Flange, aligned with LH Center Sill Web, approximately 2" forward of #3 Cross Bearer

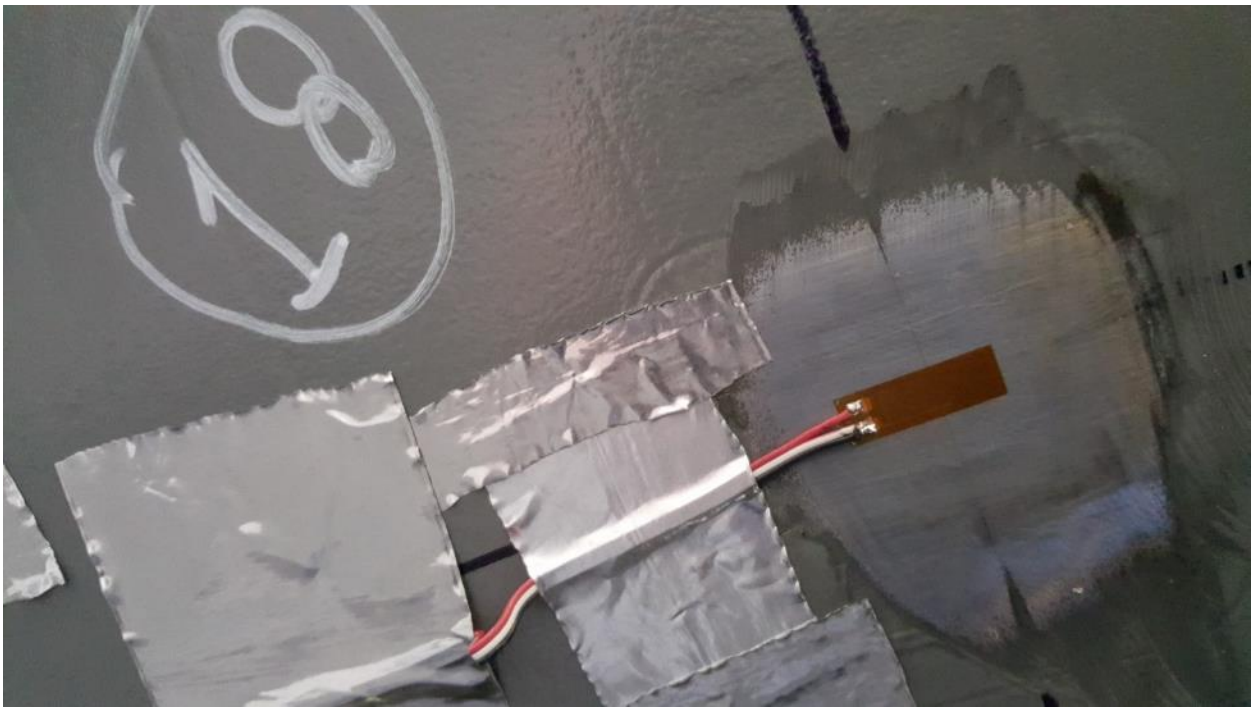


Figure D22. SGBF18 Center of LH Side Sill Bottom Flange, approximately 2" forward of #3 Cross Bearer

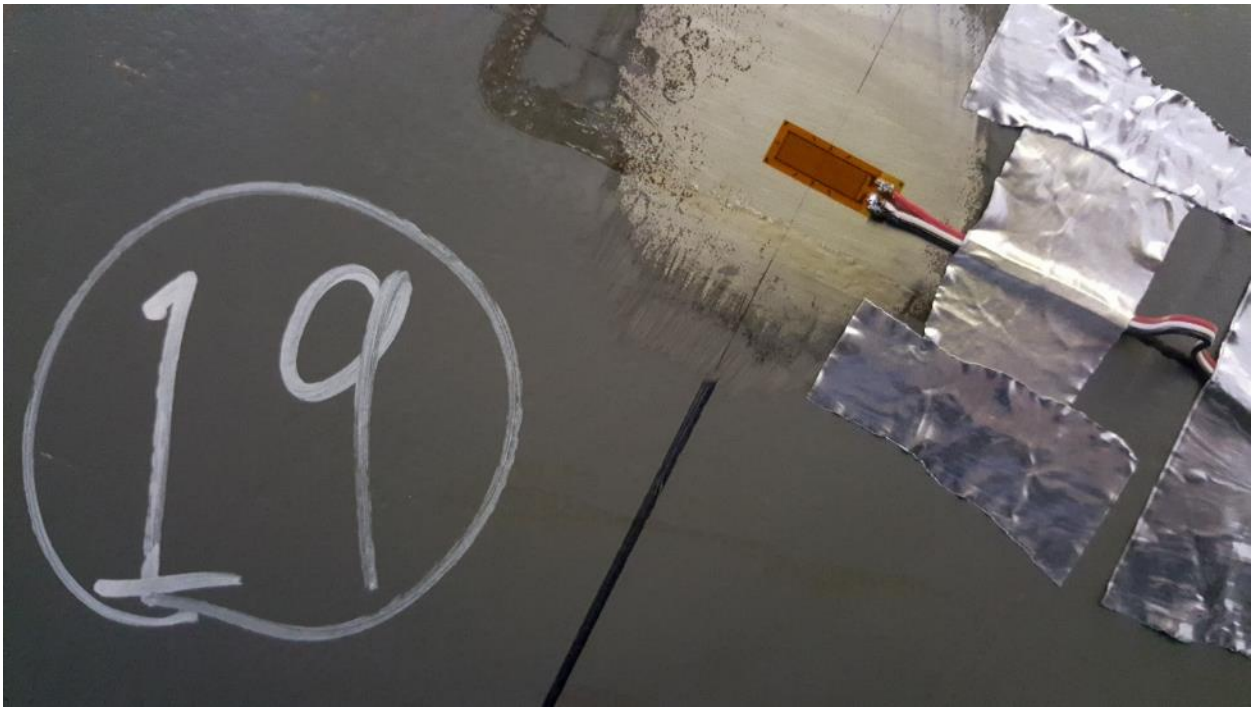


Figure D23. SGBF19 Center of RH Side Sill Bottom Flange, at Longitudinal center of Car

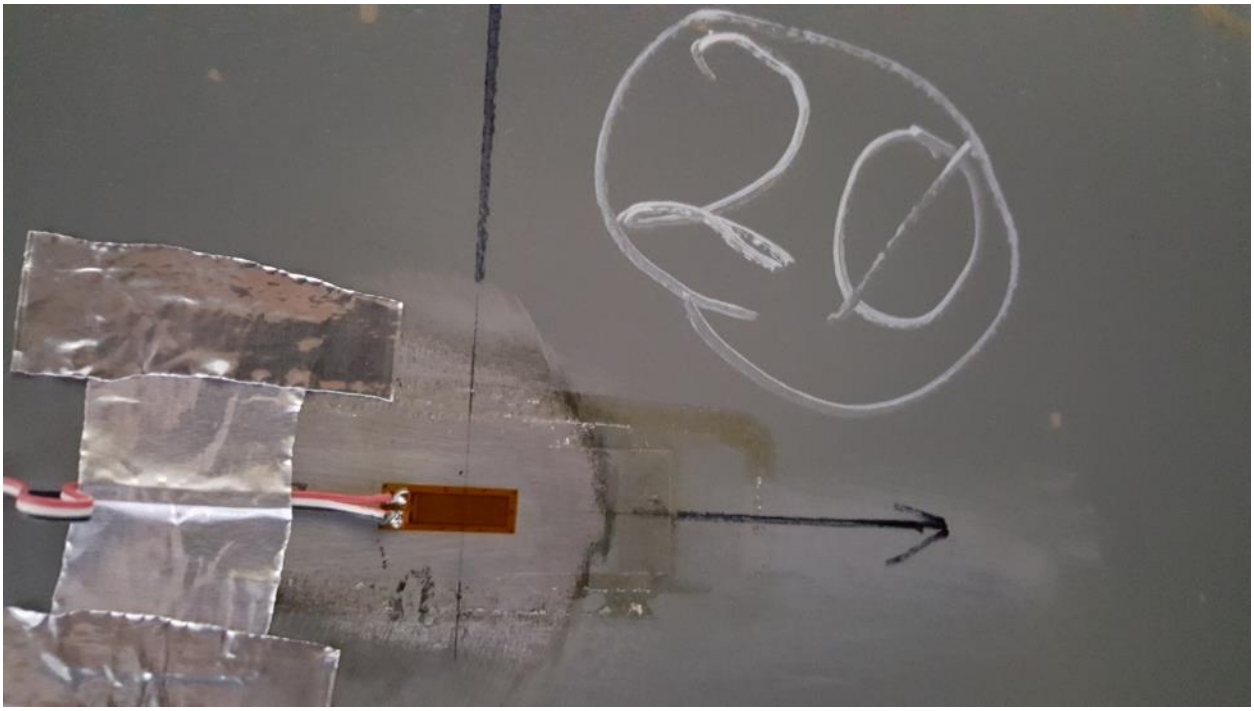


Figure D24. SGBF20 Center Sill Bottom Flange, aligned with RH Center Sill Web, at Longitudinal center of Car



Figure D25. SGBF21 Center Sill Bottom Flange, aligned with LH Center Sill Web, at Longitudinal center of Car



Figure D26. SGBF22 Center of LH Side Sill Bottom Flange, at Longitudinal center of Car



Figure D27. SGBF23 Center of RH Side Sill Bottom Flange, approximately 2” aft of #2 Cross Bearer

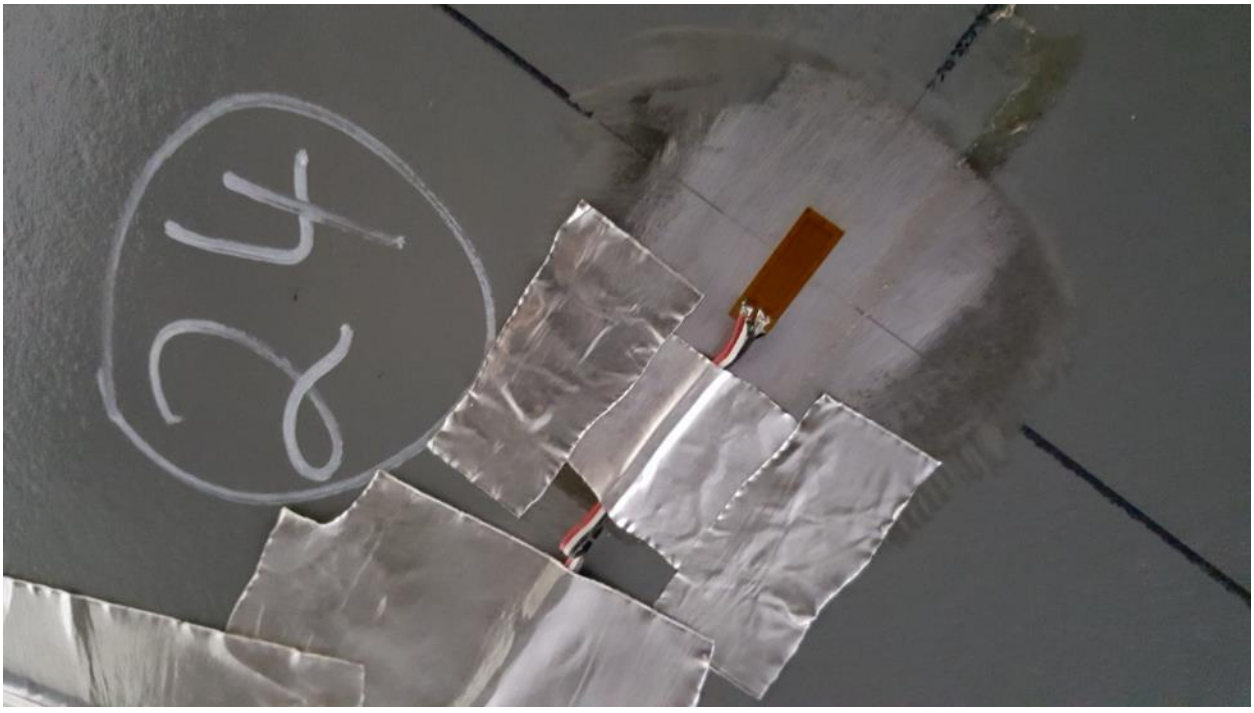


Figure D28. SGBF24 Center Sill Bottom Flange, aligned with RH Center Sill Web, approximately 2” aft of #2 Cross Bearer



Figure D29. SGBF25 Center Sill Bottom Flange, aligned with LH Center Sill Web, approximately 2” aft of #2 Cross Bearer



Figure D30. SGBF26 Center of LH Side Sill Bottom Flange, approximately 2” aft of #2 Cross Bearer

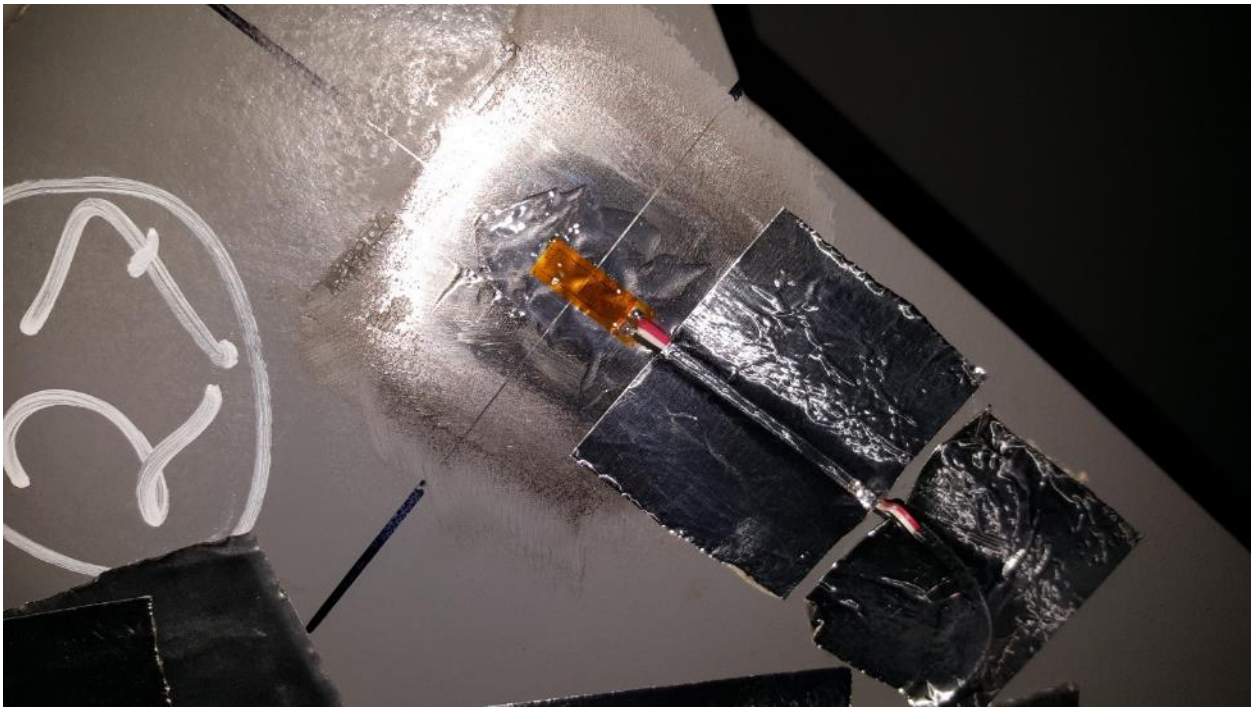


Figure D31. SGBF27 Front of Bottom Flange of #1 Cross Bearer, RH Side between Center Sill and Side Sill, near Side Sill

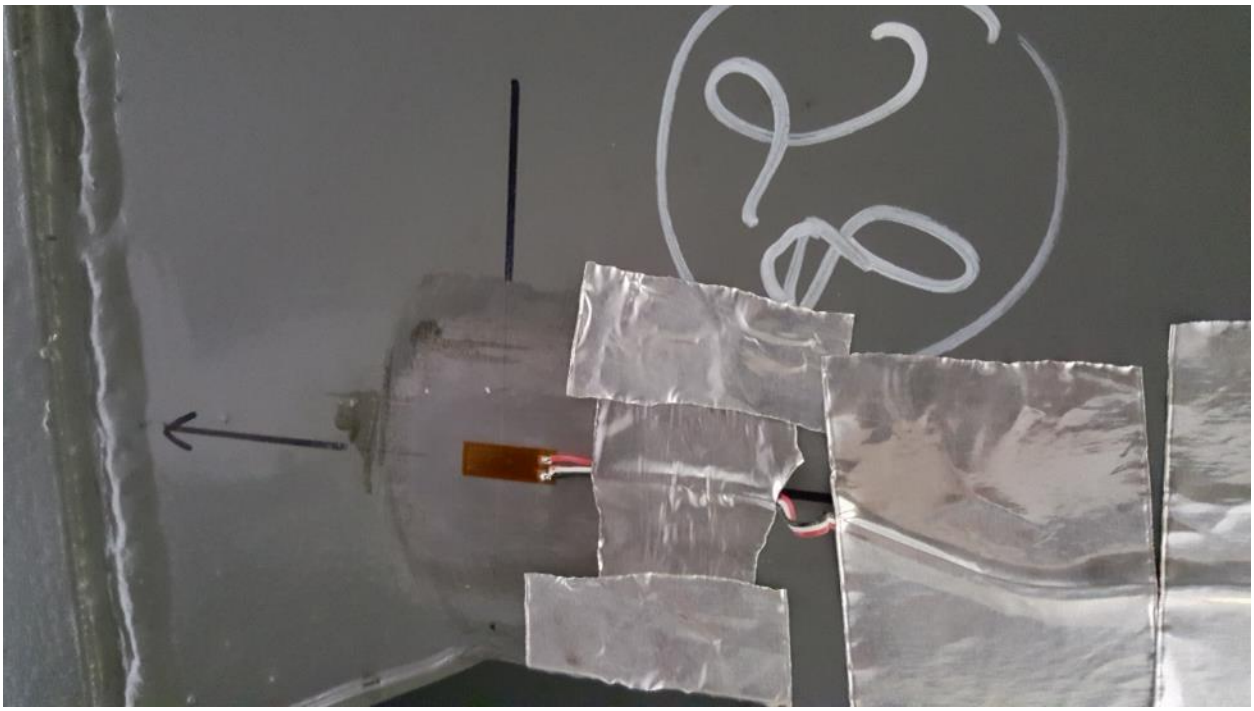


Figure D32. SGBF28 Front of Bottom Flange of #1 Cross Bearer, RH Side between Center Sill and Side Sill, near Center Sill

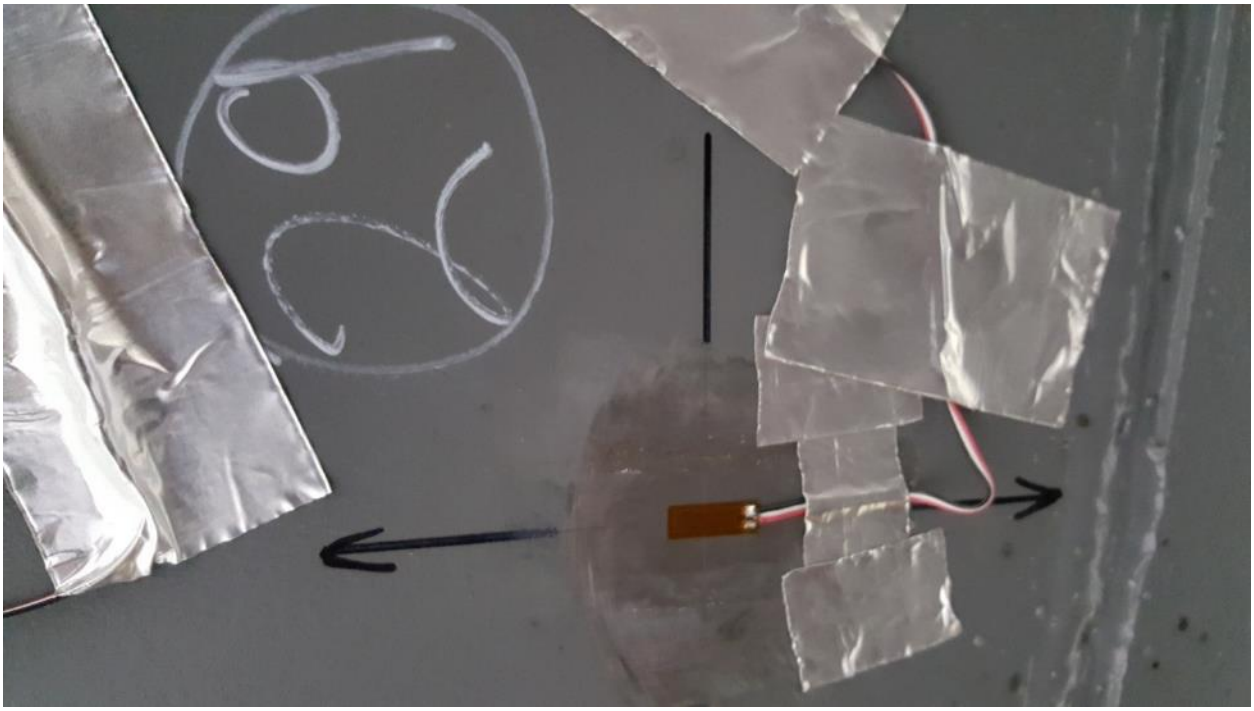


Figure D33. SGBF29 Front of Bottom Flange of #1 Cross Bearer, LH Side between Center Sill and Side Sill, near Center Sill

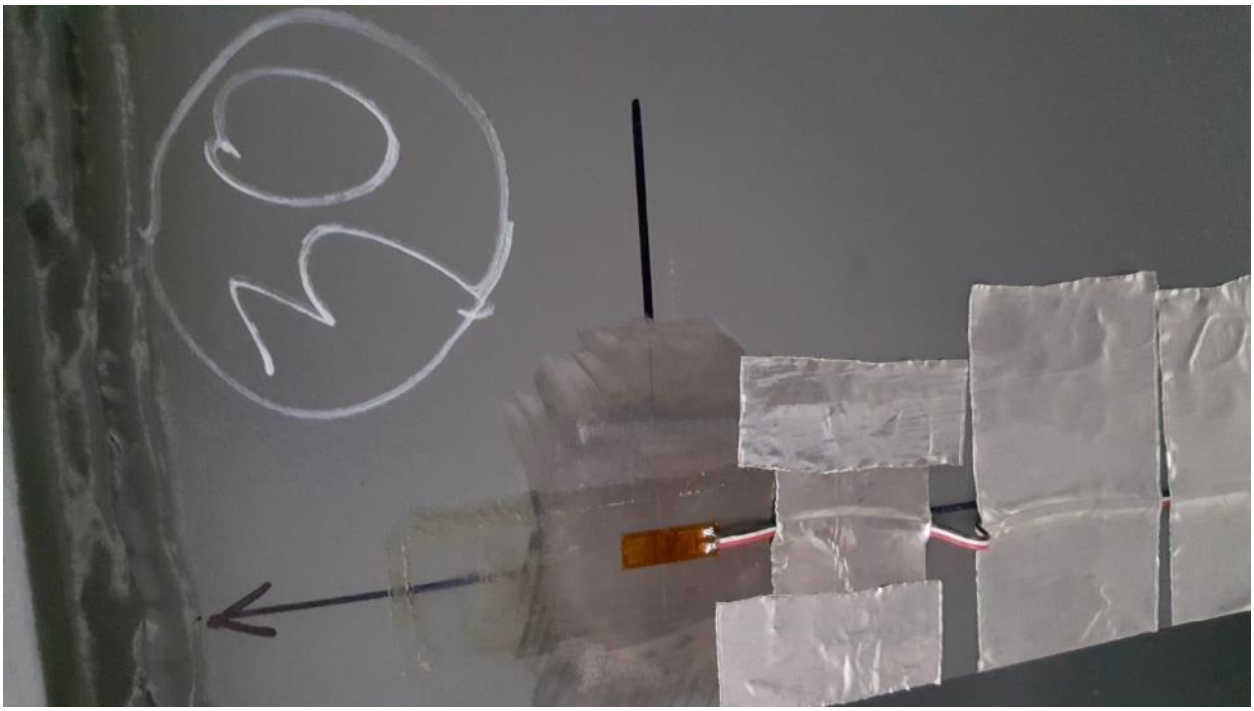


Figure D34. SGBF30 Front of Bottom Flange of #1 Cross Bearer, LH Side between Center Sill and Side Sill, near Side Sill

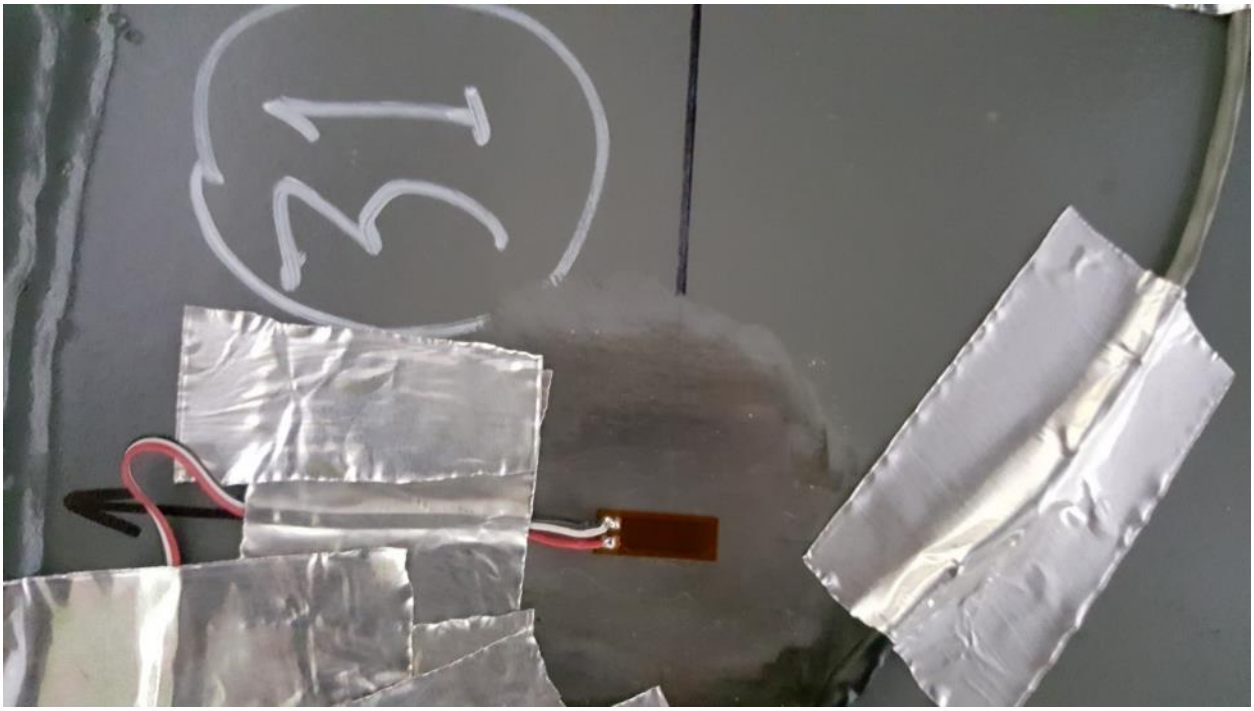


Figure D35. SGBF31 Rear of Bottom Flange of #1 Cross Bearer, RH Side between Center Sill and Side Sill, near Side Sill

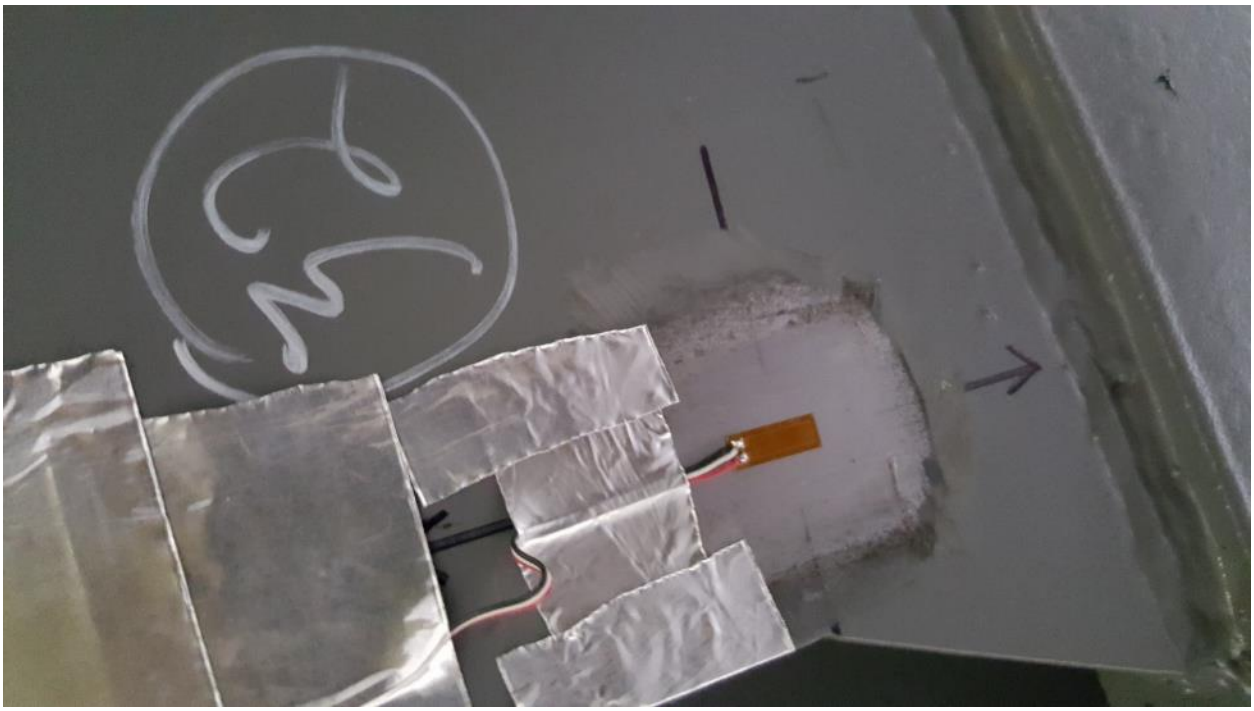


Figure D36. SGBF32 Rear of Bottom Flange of #1 Cross Bearer, RH Side between Center Sill and Side Sill, near Center Sill

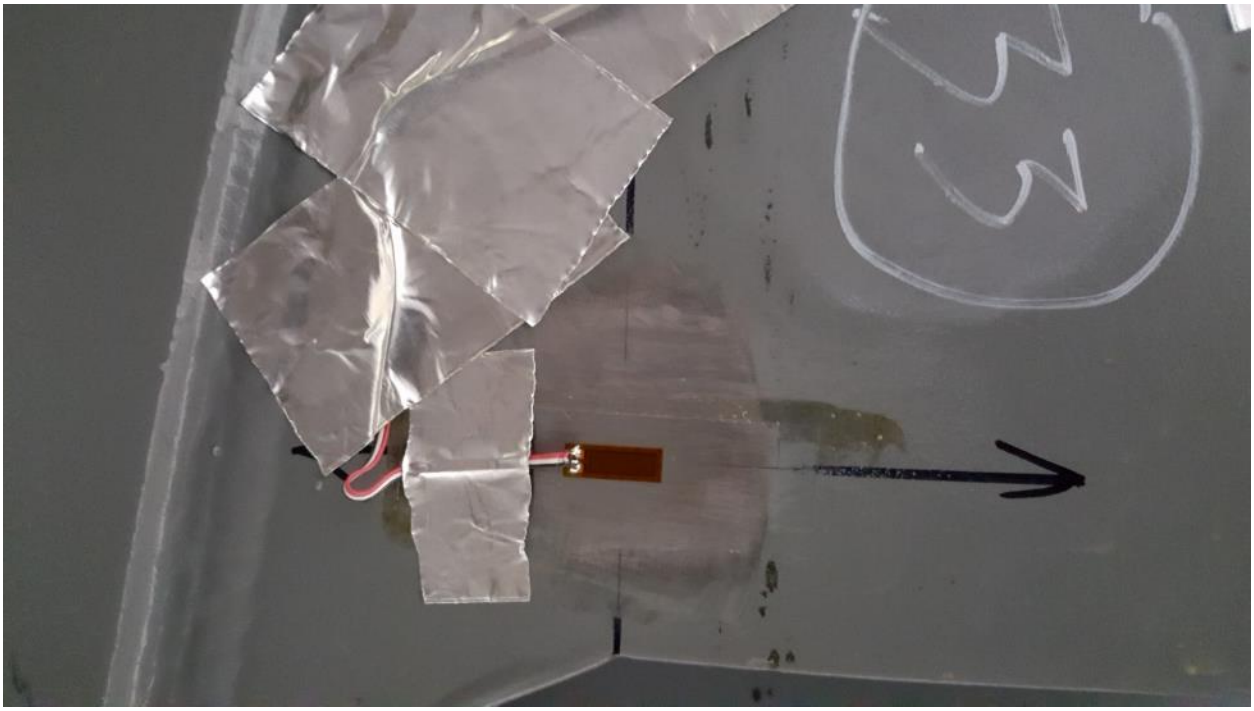


Figure D37. SGBF33 Rear of Bottom Flange of #1 Cross Bearer, LH Side between Center Sill and Side Sill, near Center Sill

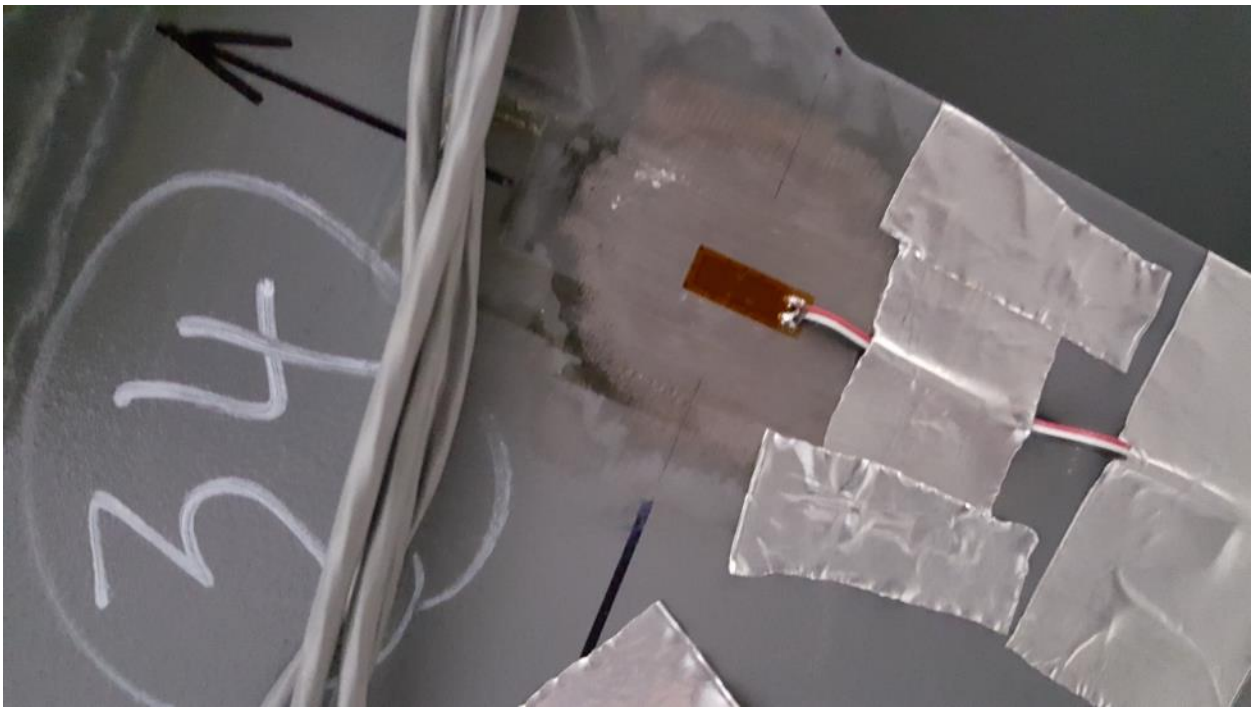


Figure D38. SGBF34 Rear of Bottom Flange of #1 Cross Bearer, LH Side between Center Sill and Side Sill, near Side Sill



Figure D39. SGBF35 RH Side of Bottom Flange of Center Sill, forward of Rear Body Bolster, aligns with Center Sill Web and End Stop Mount Block Pin Hole

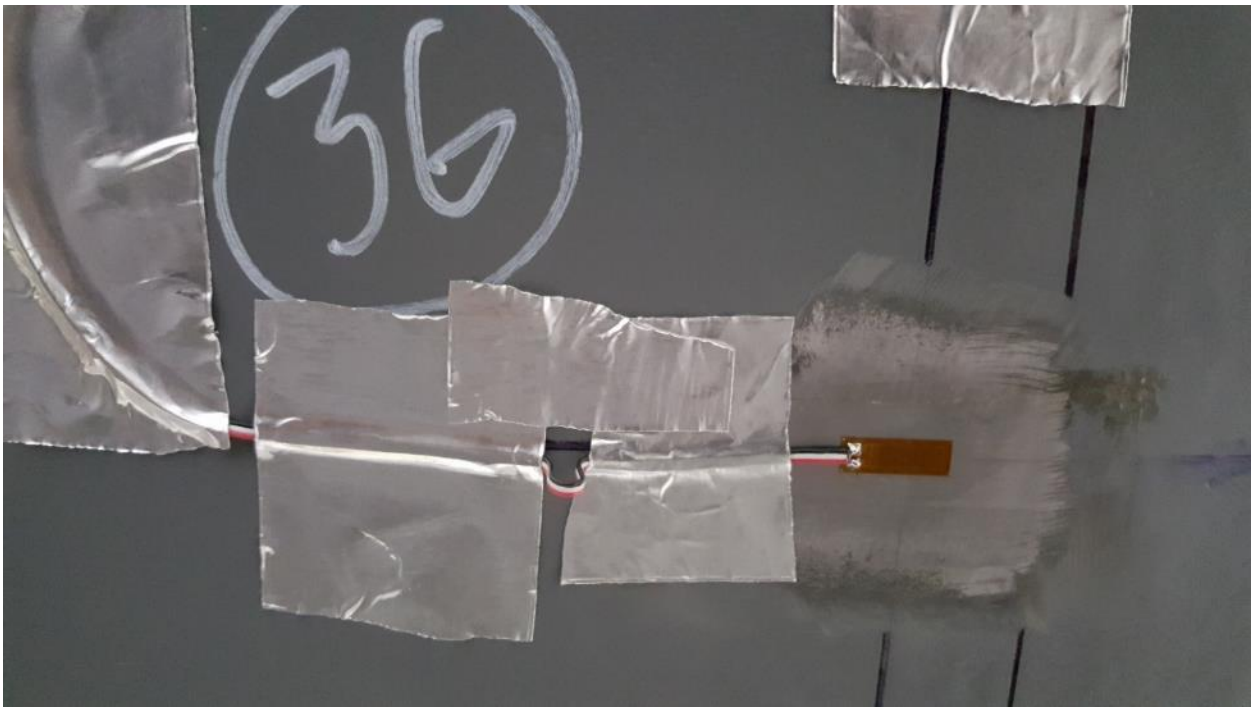


Figure D40. SGBF36 LH Side of Bottom Flange of Center Sill, forward of Rear Body Bolster, aligns with Center Sill Web and End Stop Mount Block Pin Hole



Figure D41. SGBF37 Front of Bottom Flange of Front Body Bolster near Center Sill, RH Side

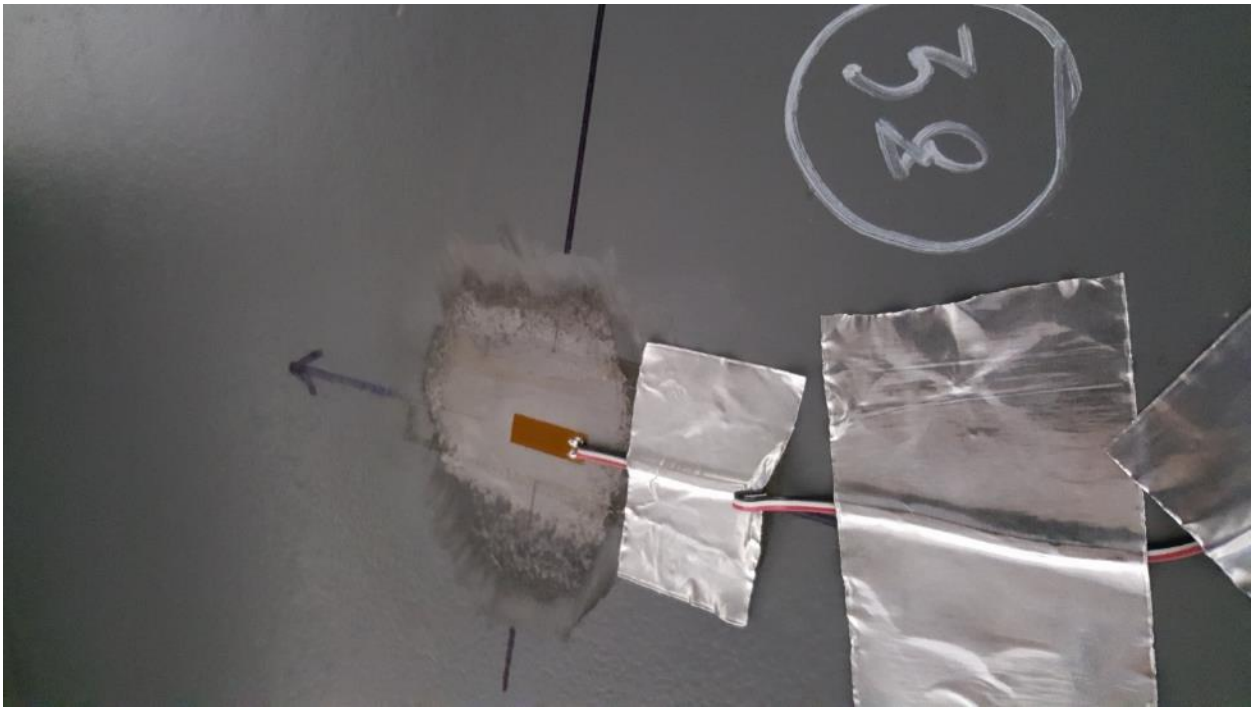


Figure D42. SGBF38 Front of Bottom Flange of Front Body Bolster near Center Sill, LH Side

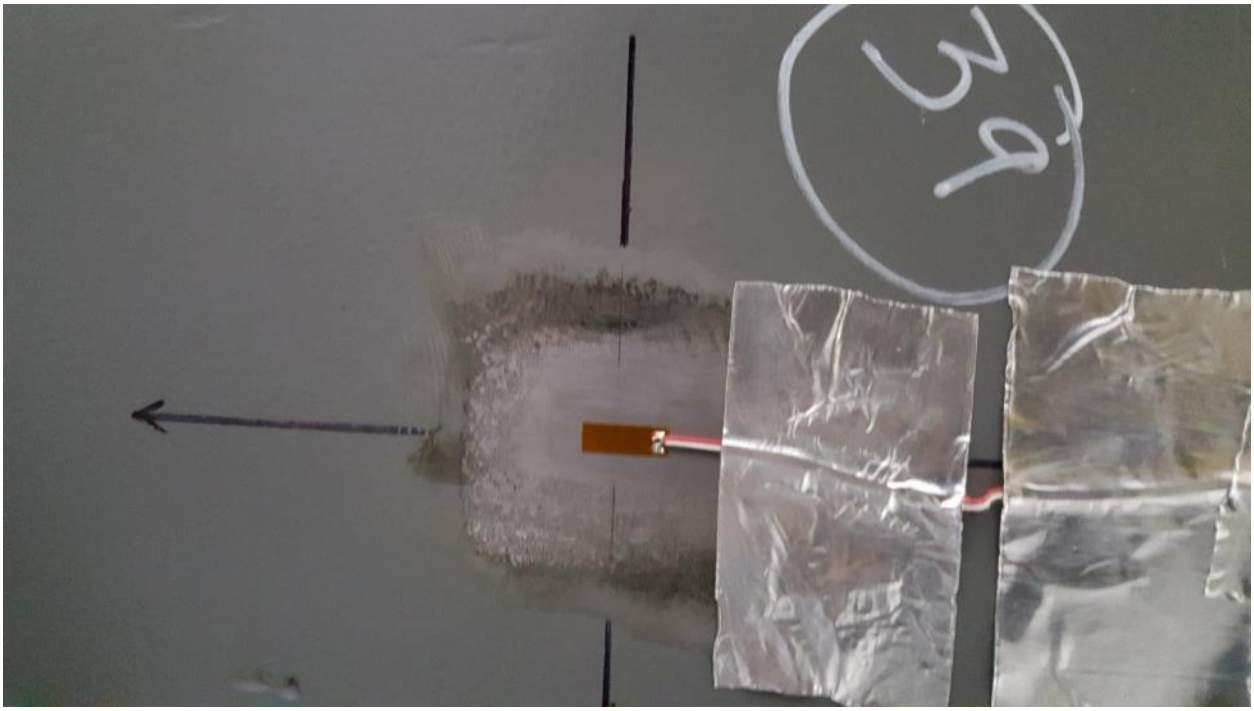


Figure D43. SGBF39 Rear of Bottom Flange of Rear Body Bolster near Center Sill, RH Side



Figure D44. SGBF40 Rear of Bottom Flange of Rear Body Bolster near Center Sill, LH Side

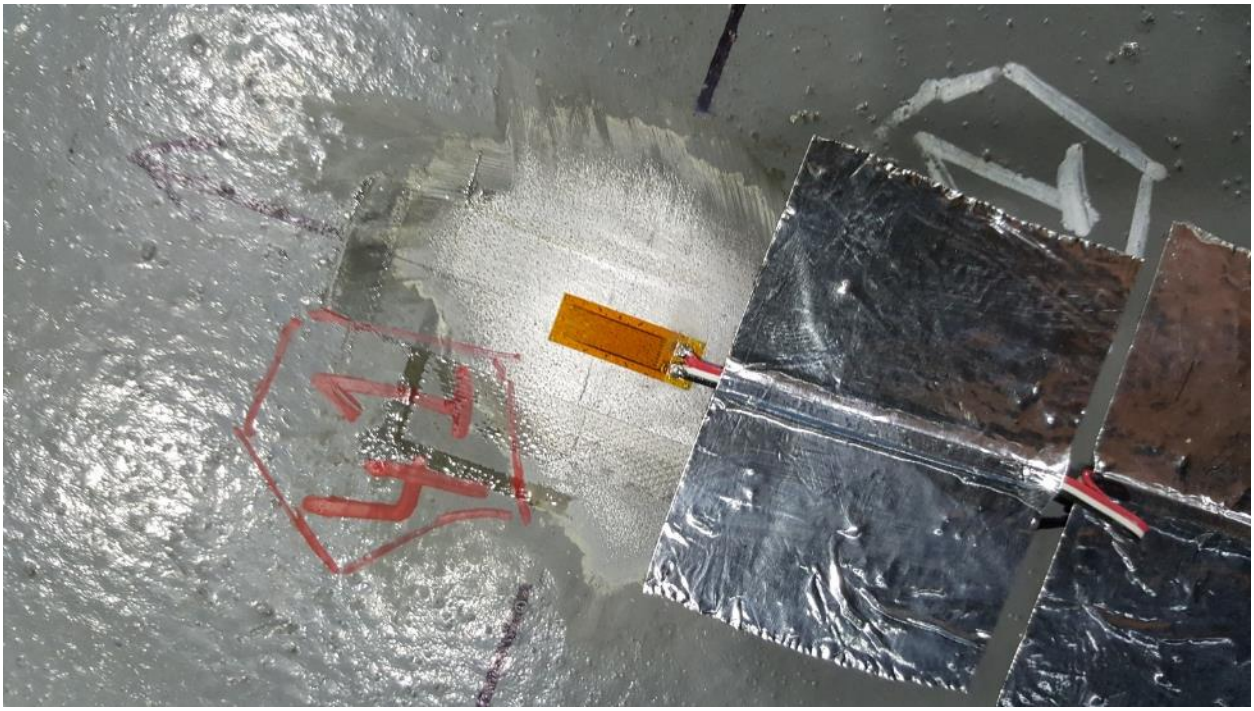


Figure D45. SGBF41 Top Deck Plate, above LH Side Sill Web, at Longitudinal Center of Car

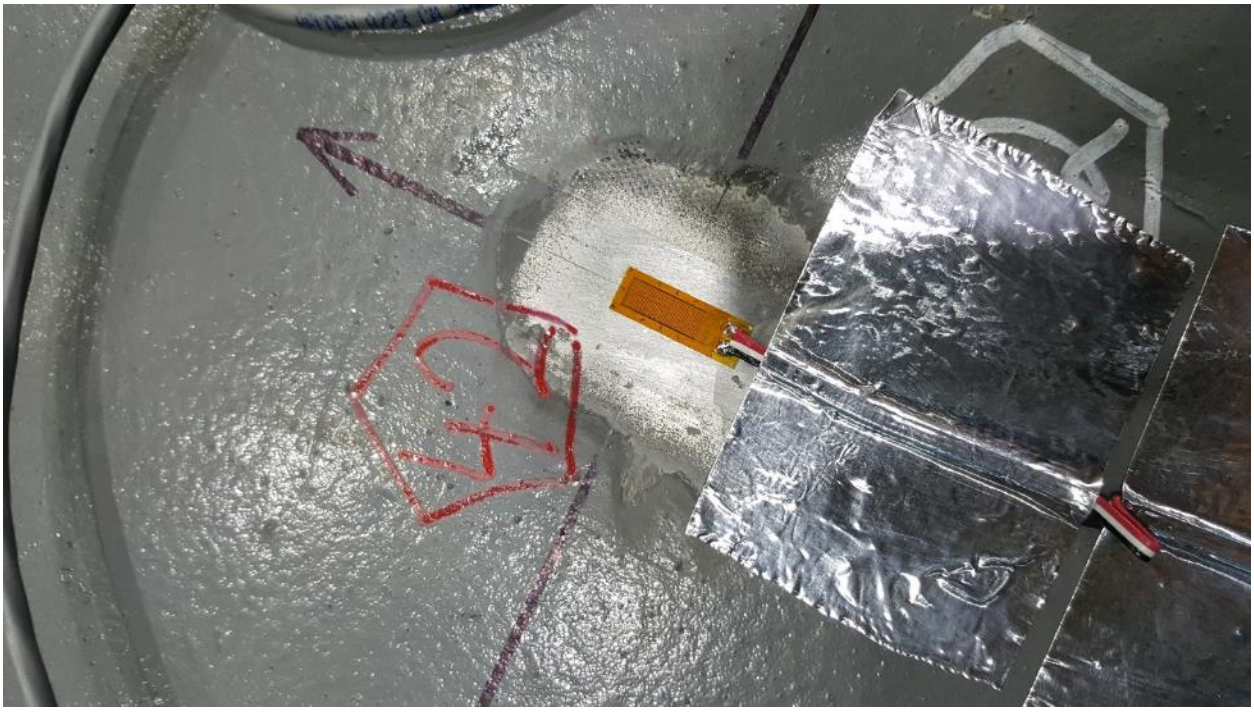


Figure D46. SGBF42 Top Deck Plate, above LH Center Sill Web, at Longitudinal Center of Car

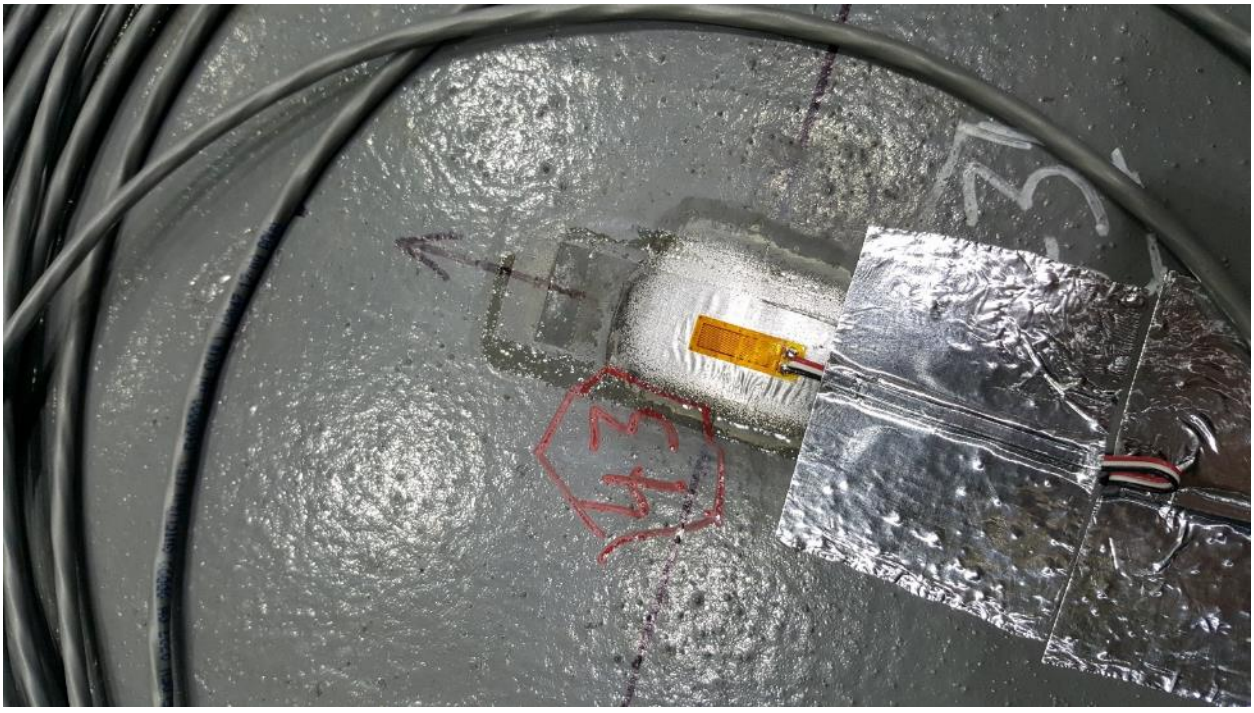


Figure D47. SGBF43 Top of Deck Plate, above RH Center Sill Web, at Longitudinal Center of Car

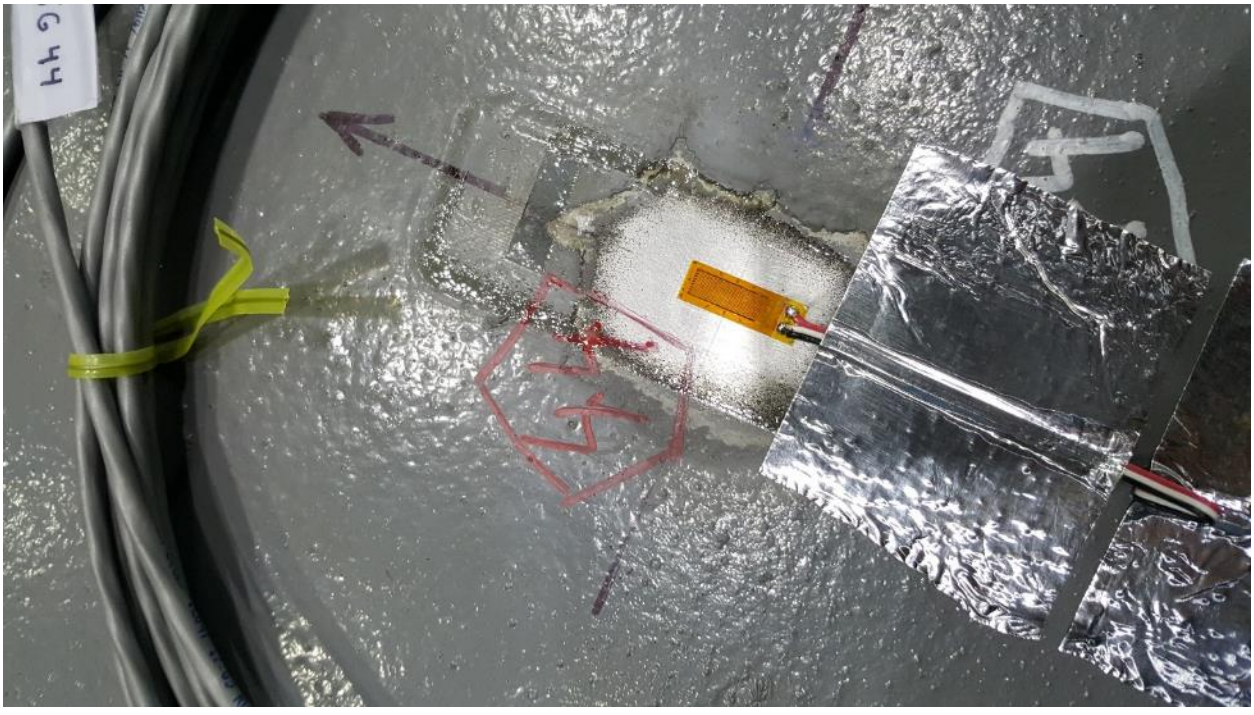


Figure D48. SGBF44 Top of Deck Plate, above RH Side Sill Web, at Longitudinal Center of Car

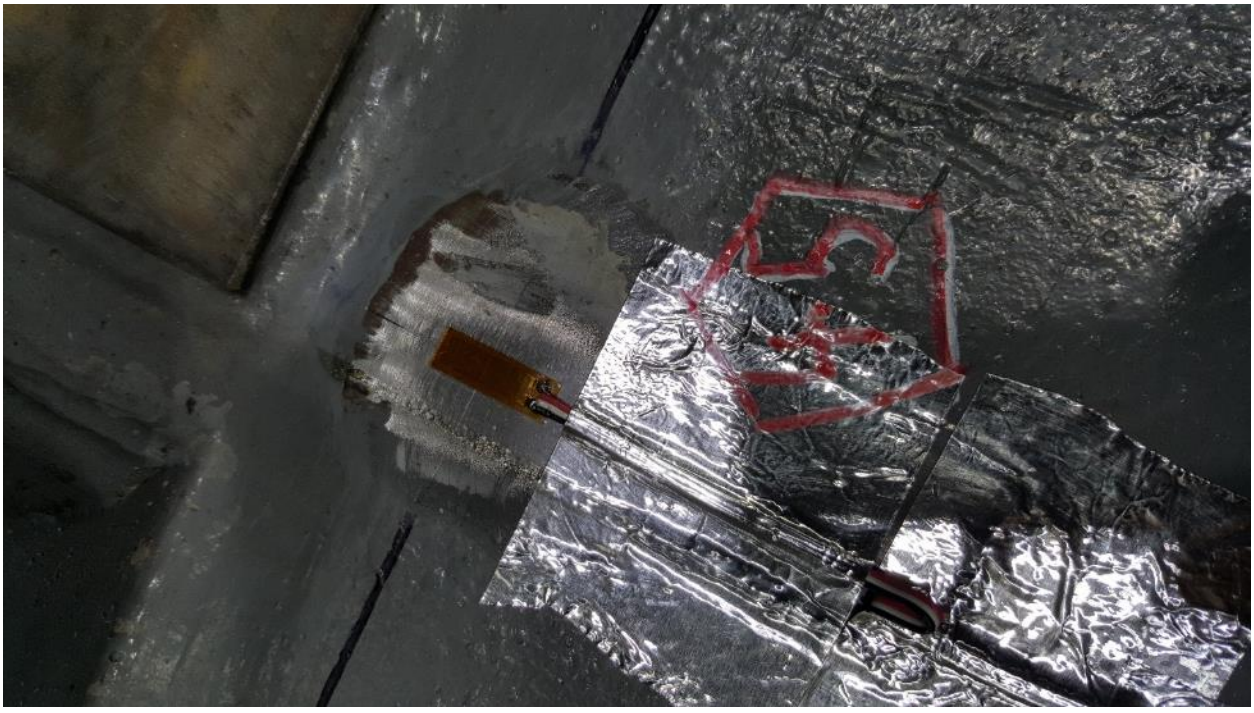


Figure D49. SGBF45 Top of Deck Plate, above LH Side Sill Web, approximately 2" aft of #2 Cross Bearer

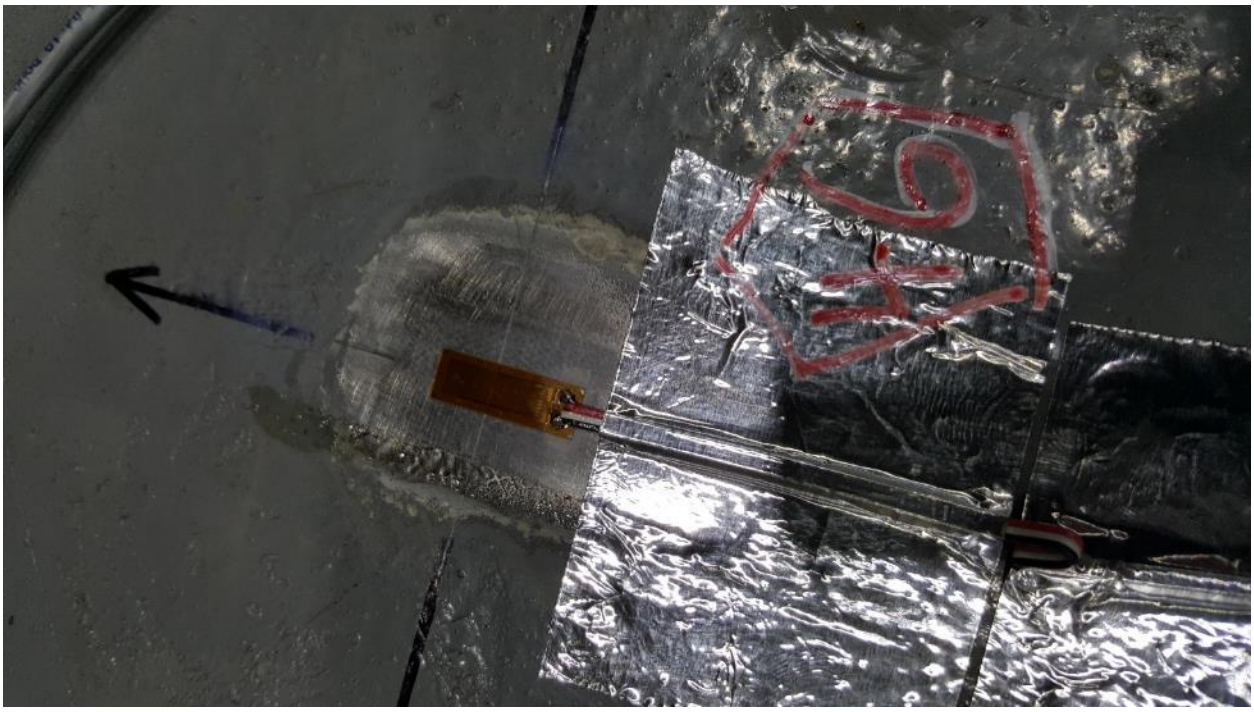


Figure D50. SGBF46 Top of Deck Plate, above LH center Sill Web, approximately 2' aft of #2 Cross Bearer

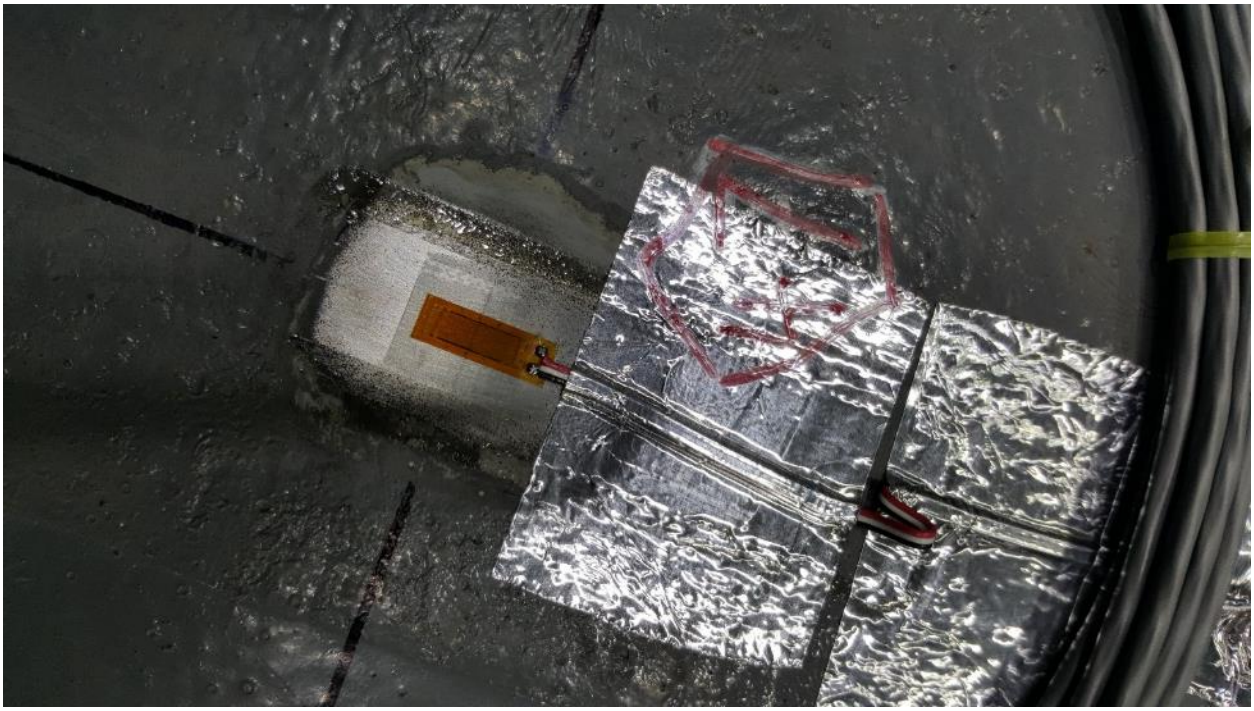


Figure D51. SGBF47 Top of Deck Plate, above RH Center Sill Web, approximately 2” aft of #2 Cross Bearer

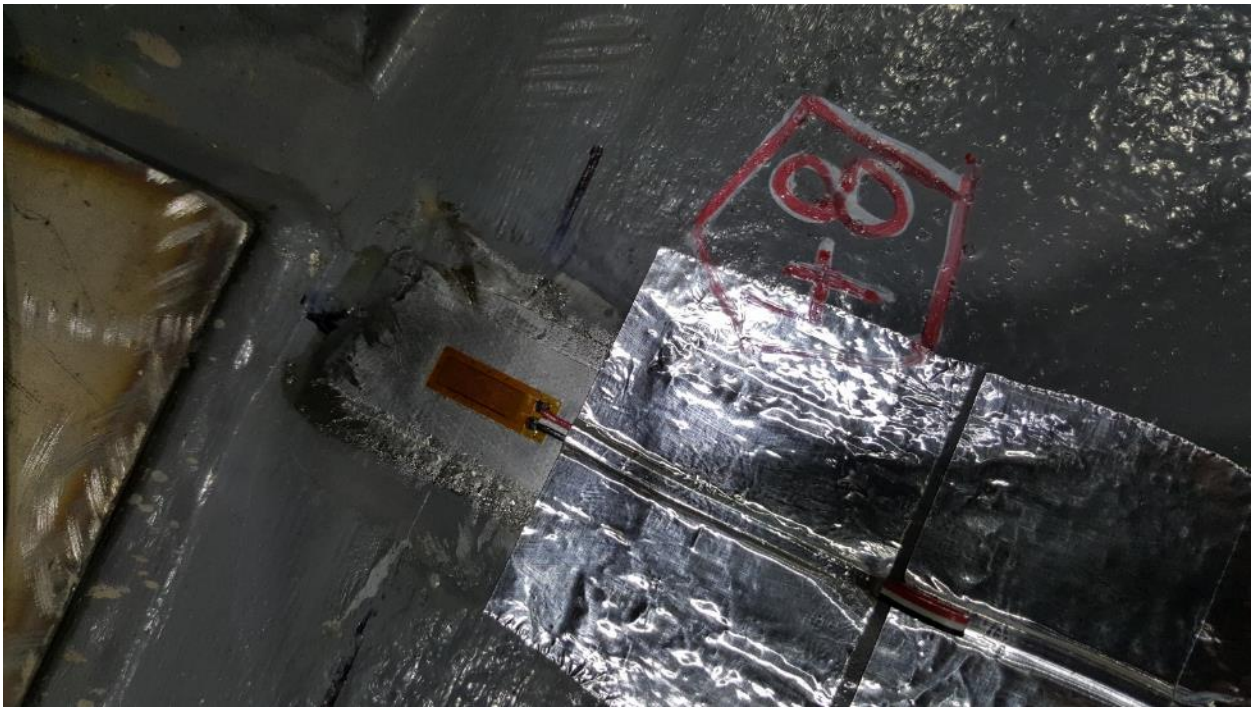


Figure D52. SGBF48 Top of Deck Plate, above LH Center Sill Web, approximately 2” aft of #2 Cross Bearer

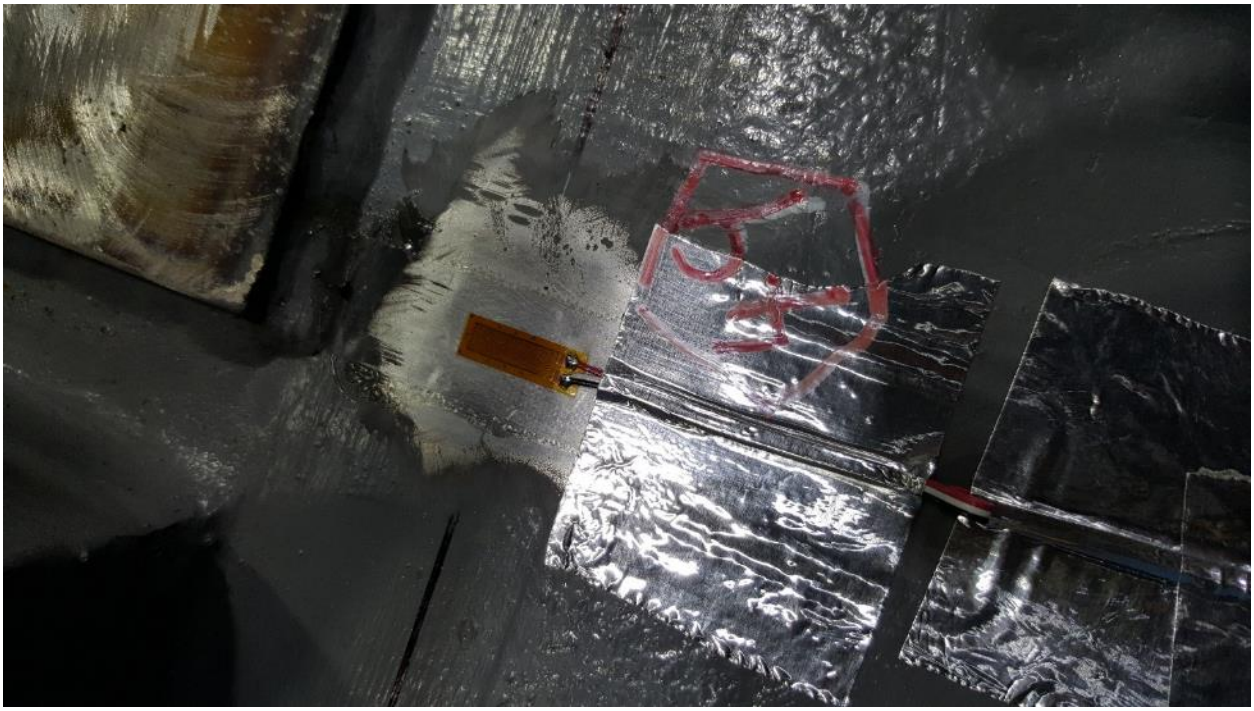


Figure D53. SGBF49 Top of Deck Plate, above RH Side Sill Web, approximately 2' forward of #3 Cross Bearer

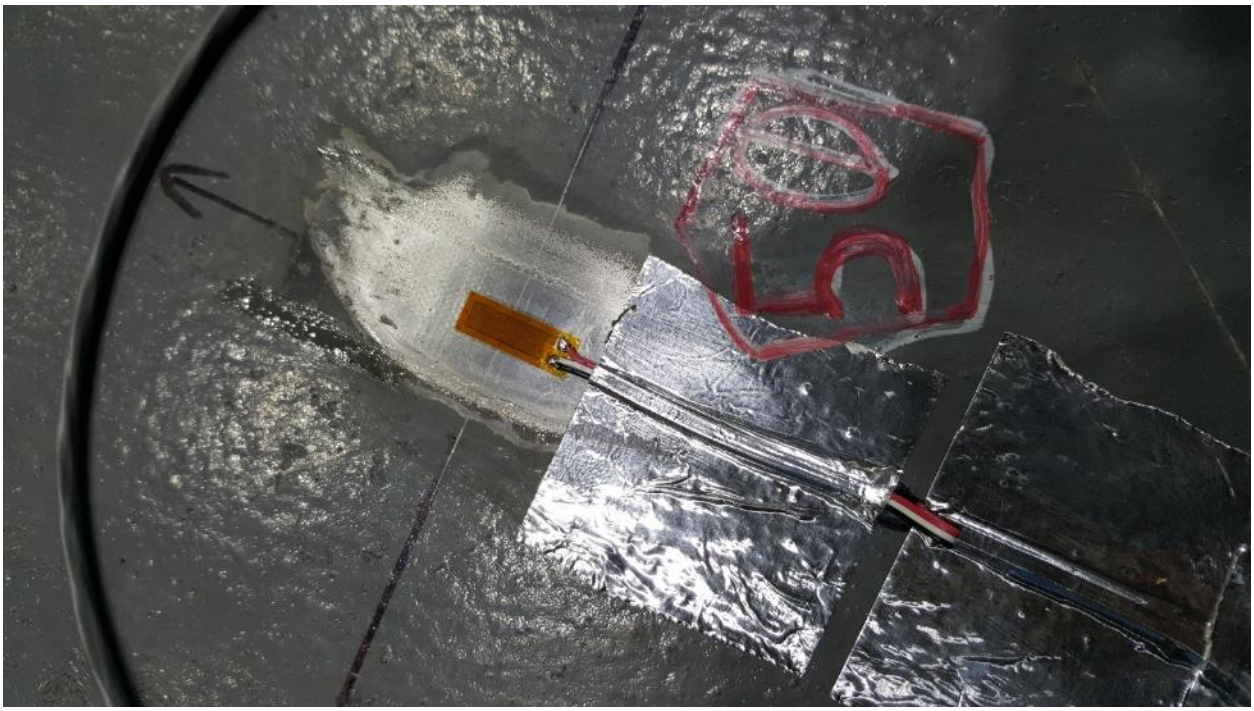


Figure D54. SGBF50 Top of Deck Plate, above LH Center Sill Web, approximately 2' forward of #3 Cross Bearer

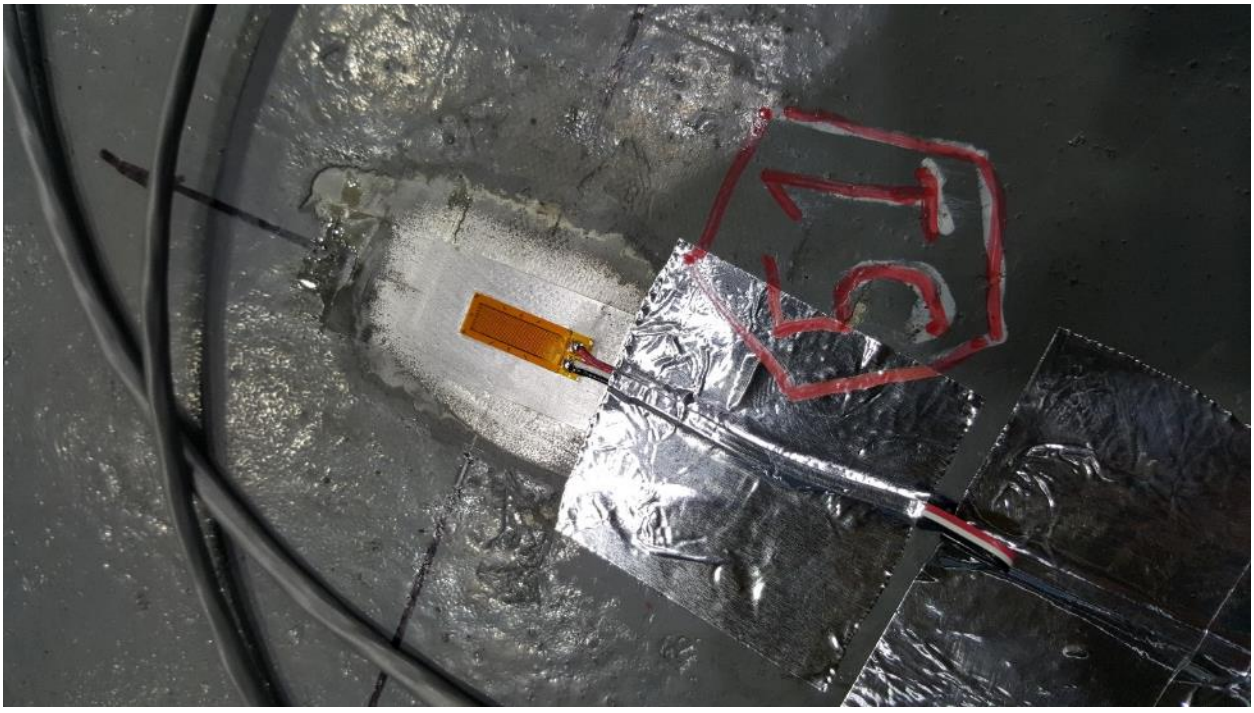


Figure D55. SGBF51 Top of Deck Plate, above RH Center sill Web, approximately 2” forward of #3 Cross Bearer

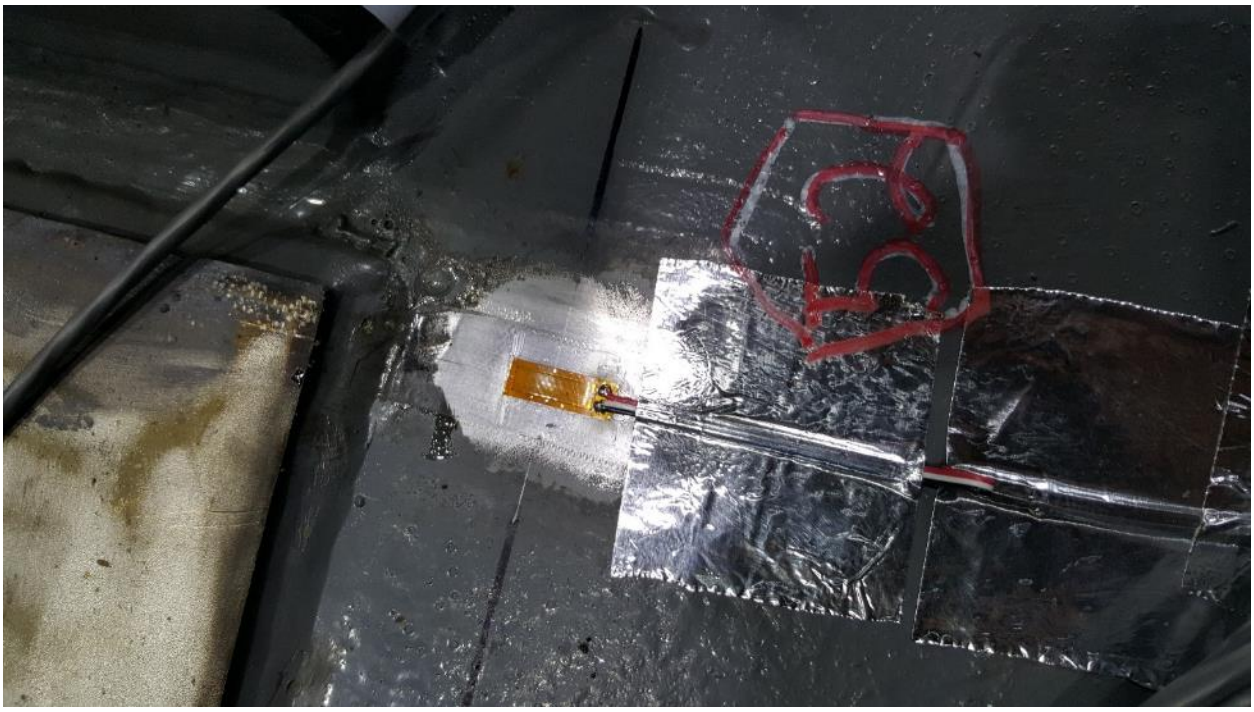


Figure D56. SGBF52 Top of Deck Plate, above LH Center Sill Web, approximately 2” forward of #3 Cross Bearer



Figure D57. SGBF53 Center of Bottom Flange of Cross Bearer #3, centered in open space between RH Side Sill Bottom Flange and Center Sill Bottom Flange



Figure D58. SGBF54 Center of Bottom Flange of Cross Bearer #3, centered in open space between LH Side Sill Bottom Flange and Center Sill Bottom Flange



Figure D59. SGBF55 Center of Bottom Flange of Cross Bearer #2, centered in open space between LH Side Sill Bottom Flange and Center Sill Bottom Flange



Figure D60. SGBF56 Center of Bottom Flange of Cross Bearer #2 centered in open space between RH Side Sill Bottom Flange and Center Sill Bottom Flange



Figure D61. TC57 Center Sill Bottom Flange, Centered in Open Space between Front Body Bolster and Cross Bearer #4

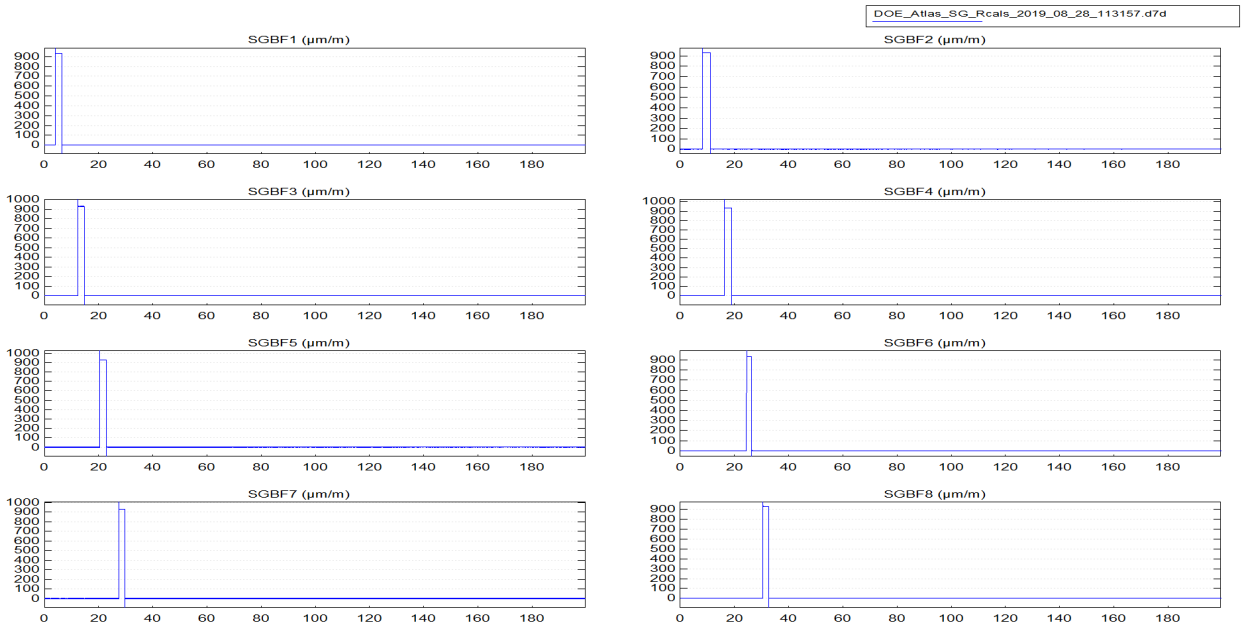


Figure D62. Shunt Calibration of Gages 1-8 with a High Precision 174.650 kΩ Resistor

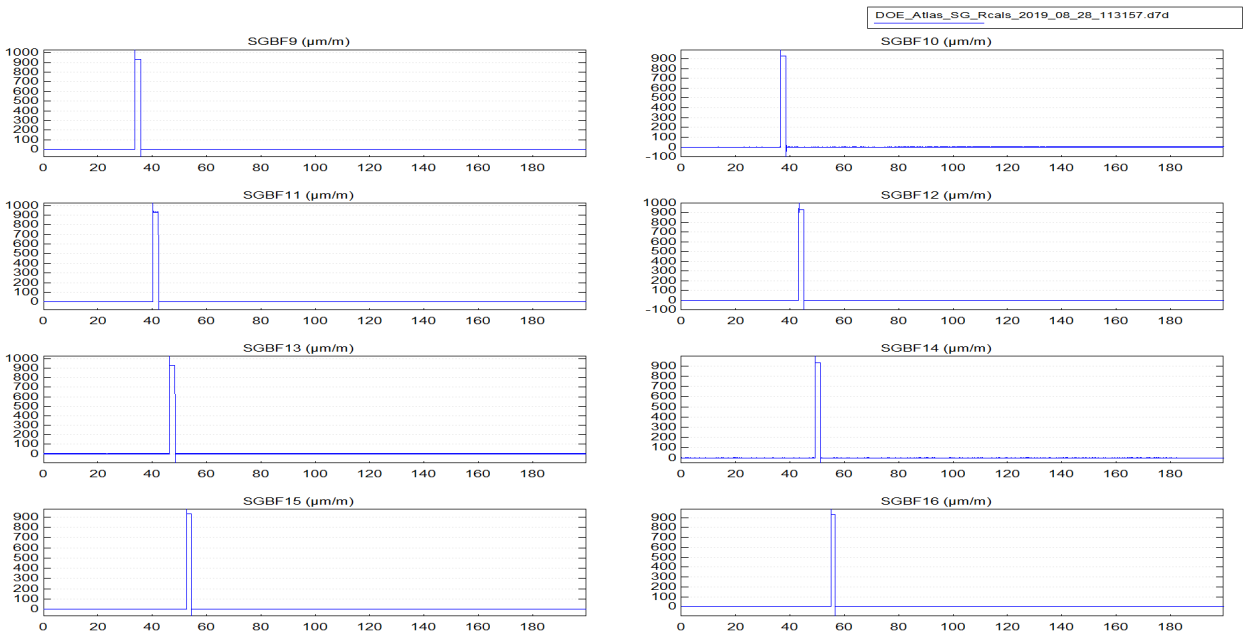


Figure D63. Shunt Calibration of Gages 9-16 with a High Precision 174.650 kΩ Resistor

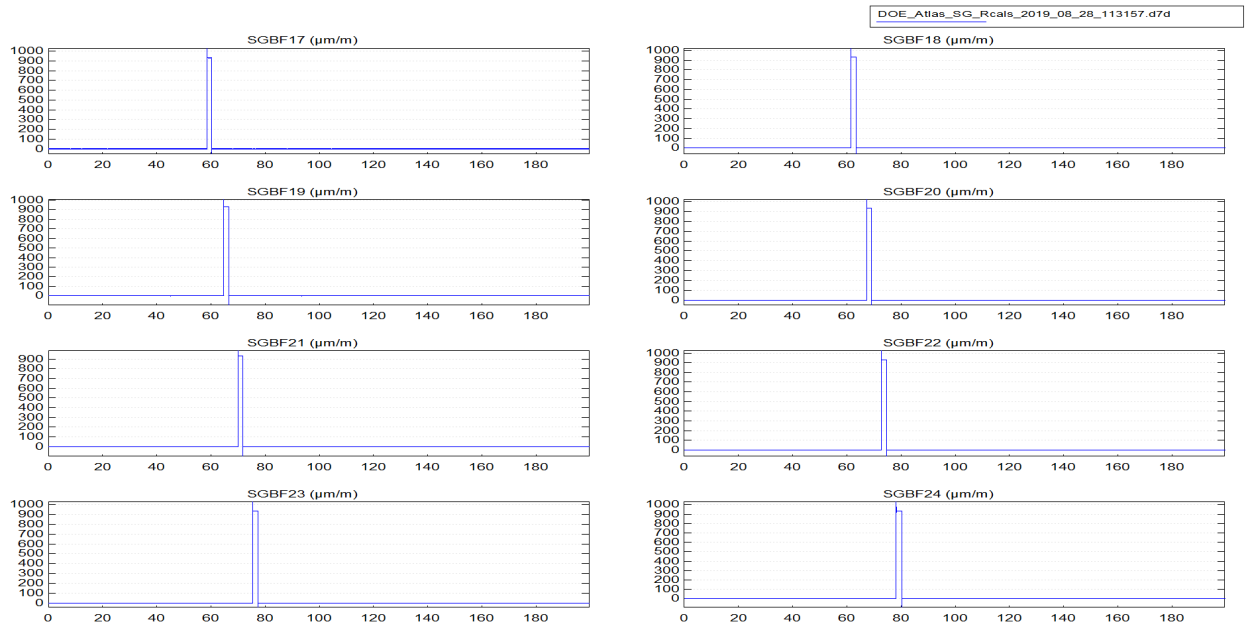


Figure D64. Shunt Calibration of Gages 17-24 with a High Precision 174.650 kΩ Resistor

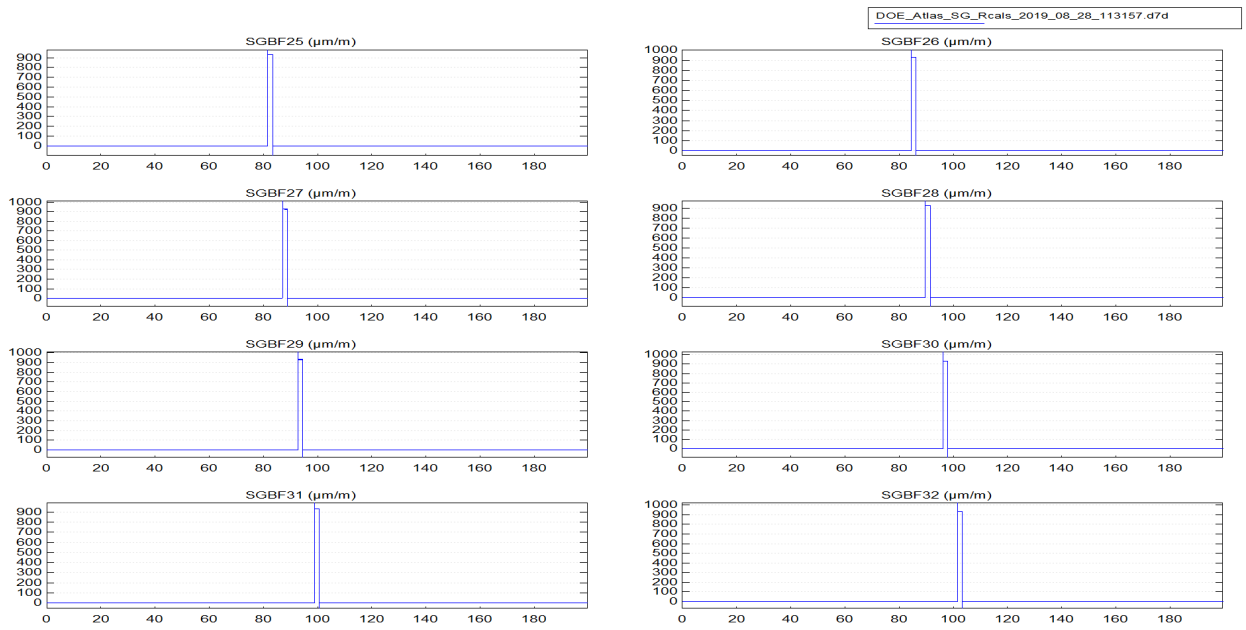


Figure D65. Shunt Calibration of Gages 25-32 with a High Precision 174.650 kΩ Resistor

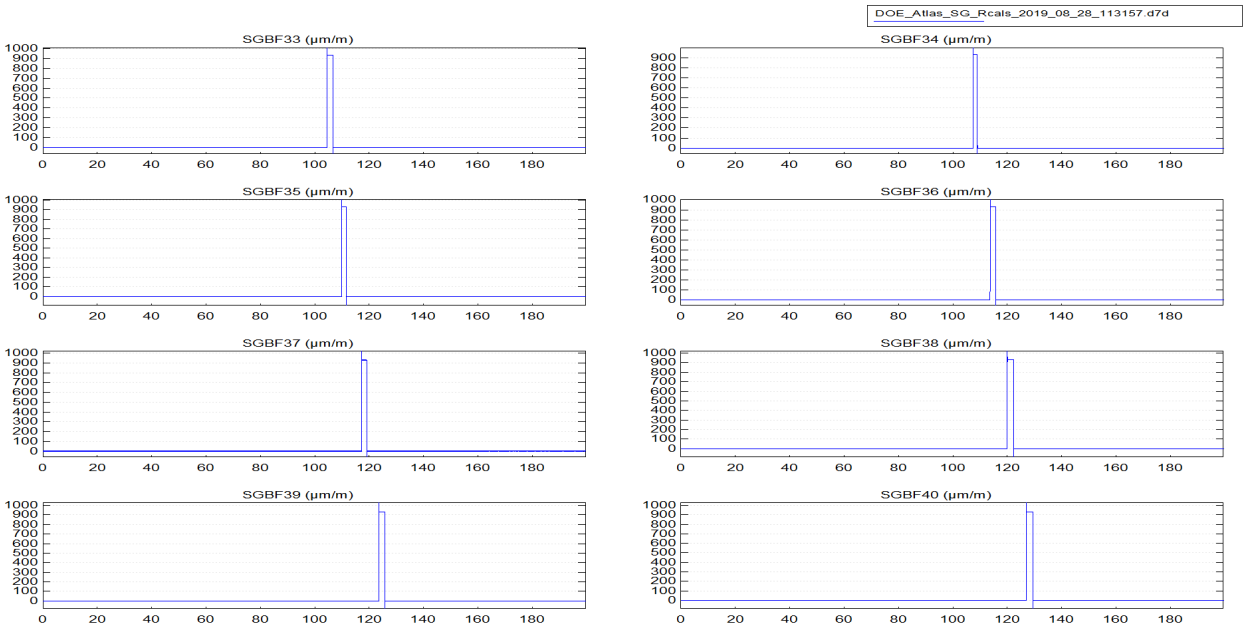


Figure D66. Shunt Calibration of Gages 33-40 with a High Precision 174.650 kΩ Resistor

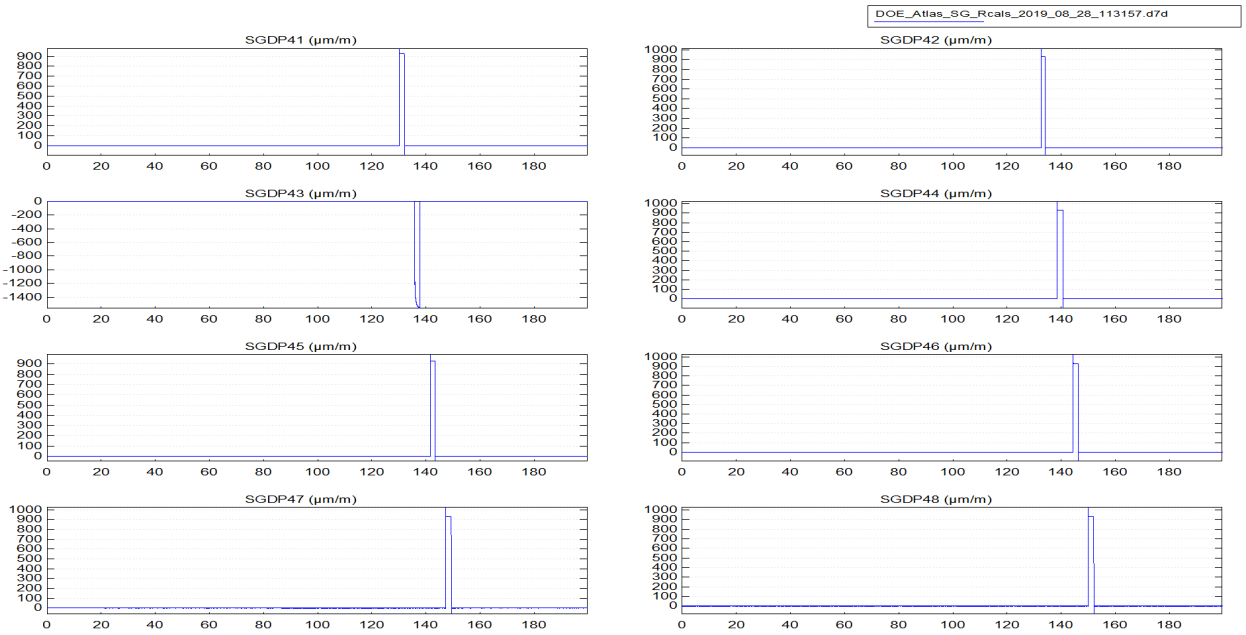


Figure D67. Shunt Calibration of Gages 41-48 with a High Precision 174.650 kΩ Resistor

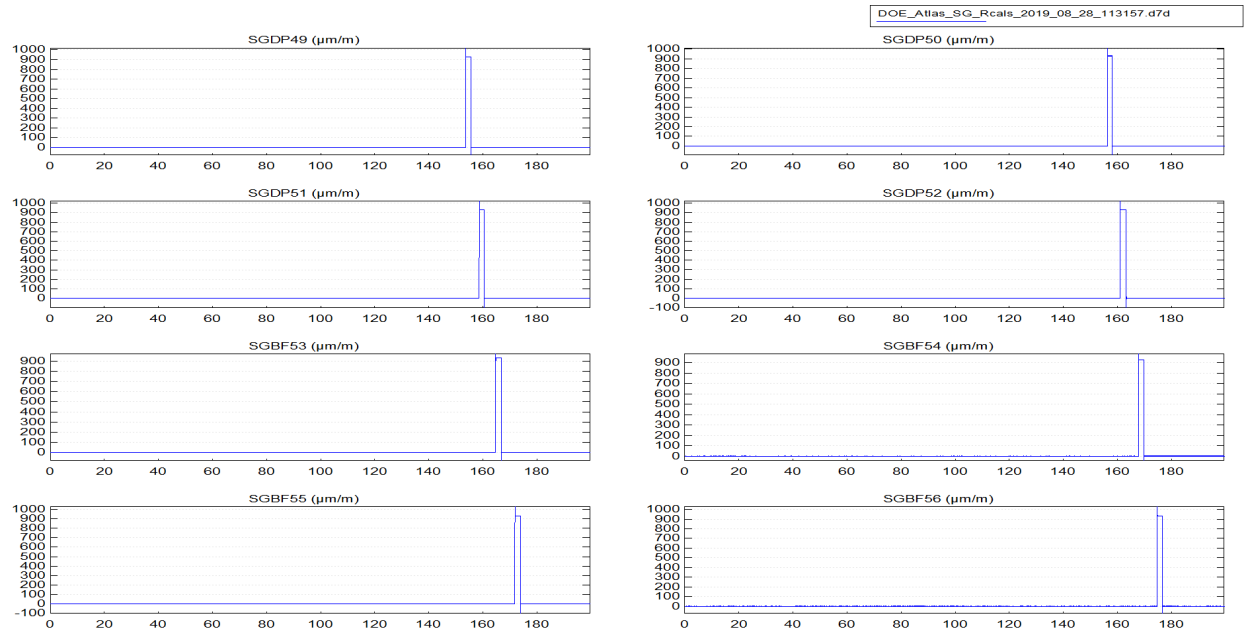


Figure D68. Shunt Calibration of Gages 49-56 with a High Precision 174.650 kΩ Resistor

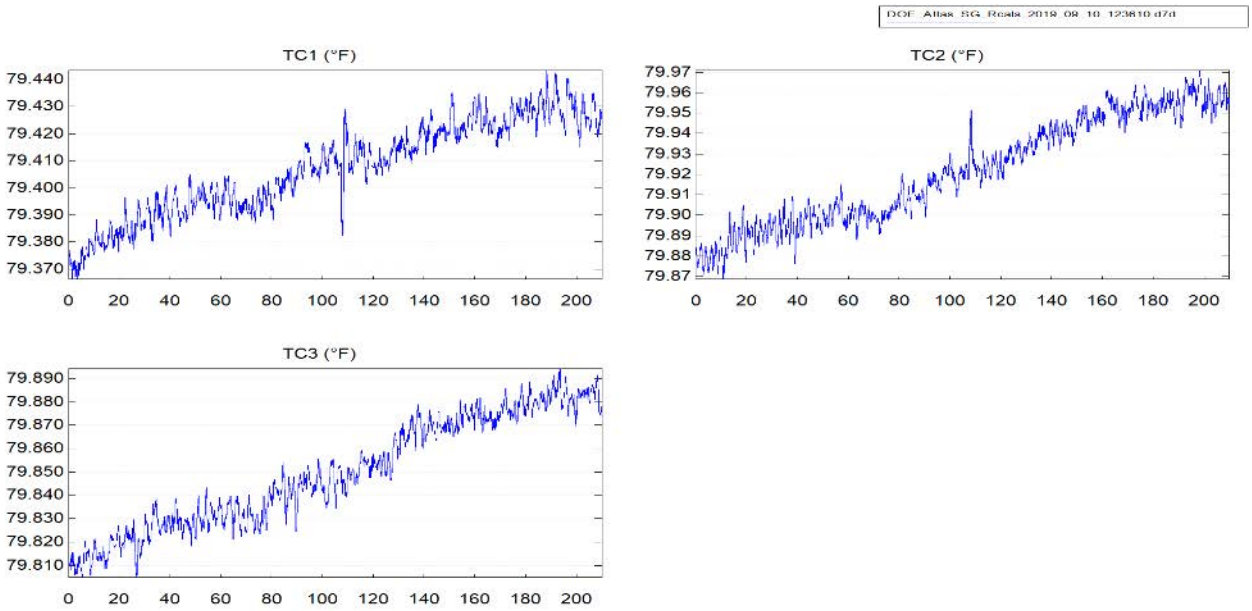


Figure D69. Plot of Three Thermocouples showing Ambient Temperature on September 10, 2019, at 12:30PM

Appendix E. Critical Buckling Load

KASGRO RAIL

S-2043 Critical Buckling Analysis

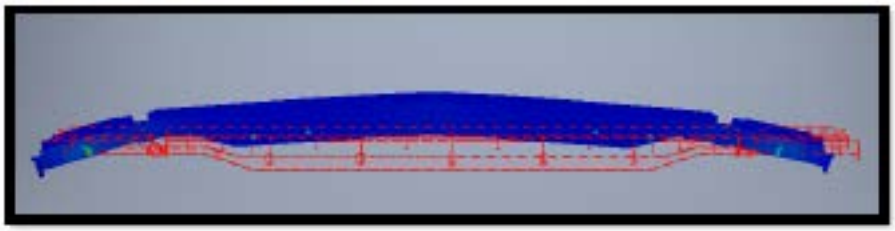
March 2021

Prepared by: Kasgro Engineering

At the request of the TTCI reviewer, Kasgro was asked to look for the critical buckling stress of the structure. Although this is a requirement in the S-2043 specification, when building railcars to AAR specification M1001, Chapter 11, we have not had to consider critical buckling stress except in compression members of Schnabel cars and Schnabel carload fixtures that contained long compression elements. These compression members have a continuous cross section which a theoretical buckling stress could be defined. Unlike the Schnabel compression members, the Atlas car bodies do not have continuous cross sections. Both cars have multiple cross sections and will not behave like a continuous column with a constant cross section. The following analysis is an approximation.

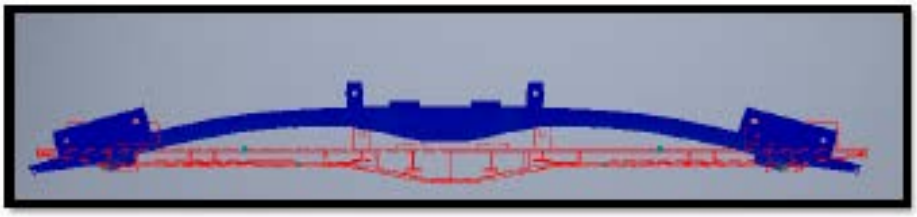
The critical buckling conditions have been re-evaluated to apply a C value of 1.0 (M-1001 4.2.2.11) to represent simple supports on both ends of the car. This is believed to be the most accurate way to represent the critical buckling condition. The linear buckling analysis now shows an EIGV value of 2.13E+7 before a member of the Buffer Car, Figure A, were to buckle. The linear buckling analysis also now shows an EIGV value of 1.03E+7 before a member of the Cask Car, Figure B, were to buckle. The EIGV values well exceed the designed squeeze load for both cars. In other words, it would take EIGV times a (1 lbf.) Squeeze load for the first buckling failure to occur. Since this would be the start of any buckling, the minimum margin of safety against buckling is something greater than one. The figures below show the deformations of the cars under the buckling load. Local buckling at the applied loads can occur prior to a primary structural member.

Figure A (side view of Buffer Car):



Atlas Project 1

Figure B (side view of Cask Car):



Appendix F. Compression Test

Data Acquisition System

A Dewesoft Data Acquisition unit capable of storing a maximum of 60 channels of data was used to monitor and record data on the test car. All data was recorded at 200 samples per second to maximize data storage space. Filtering of all data was accomplished with 30Hz low pass filters.

Test Setup

The following steps were followed before the beginning of the test:

- Compression fixture height and length adjustment
- Cask Car put into the compression fixture
- Alignment of the Cask Car

Figure F1 and Figure F2 show part of the process



Figure F1. Atlas Car set-up in Squeeze Frame



Figure F2. Atlas Car Ready for the Compression Test

Pre-Test (applies to both maximum and minimum load conditions)

Before the beginning of the tests, the car structure was pre-tested up to 750 kips under loaded condition. During the pre-test, the longitudinal load was applied in increments of 20, 40, 60, 80, and 100 percent of the pre-test load. The load was reduced to not more than two (2) percent of the load after each step. The general procedure for the pre-test was as follows:

- With the car on the fixture, each one of the actuators was extended manually until they made contact with the test car.
- The Enerpac hydraulic control system zeroed out the actuators displacements.
- The software parameter for the maximum total force was set to the load limit of 750 kips
- Load cells, strain gages, and displacement sensors were zeroed

The load application followed the sequence shown in Table F1.

Table F1. Pre-Test Loading Sequence

Step	Horizontal Load (lb)	Zero/Record	Comments
1	0	YES/YES	Inspect the car
2	20,000	NO/YES	Hold for 30 sec
3	150,000	NO/YES	Hold for 1 min
4	20,000	NO/YES	Inspect the car
5	300,000	NO/YES	Hold for 1 min
6	20,000	NO/YES	Inspect the car
7	450,000	NO/YES	Hold for 1 min
8	20,000	NO/YES	Inspect the car
9	600,000	NO/YES	Hold for 1 min
10	20,000	NO/YES	Inspect the car
13	750,000	NO/YES	Hold for 1 min
14	0	NO/YES	Inspect the car

This procedure was repeated two more times according to Table F2.

Table F2. Pre-Test Loading Sequence 2 and 3

Step	Horizontal Load (lb)	Zero/Record	Comments
1	0	YES/YES	Inspect the car
2	750,000	NO/YES	Hold for 1 min
3	0	NO/YES	Inspect the car

One-Million Pound Compression Load Test (Max and Min Load)

The longitudinal load was applied in increments of 20, 40, 60, 80, 90, and 100 percent of the full load. The load was reduced to not more than two (2) percent of full load after each step. The general procedure for the test was as follows:

- With the car on the fixture, each one of the actuators was extended manually until they made contact with the test car.
- The Enerpac hydraulic control system zeroed out the actuator displacements.

- The software parameter for the maximum total force was set to the load limit of 1 million pounds
- Load cells, strain gages, and displacement sensors were zeroed

The load application followed the sequence shown in Table F3.

Table F3. One Million Pounds Compression Test

Step	Horizontal Load (lb)	Zero/Record	Comments
1	0	YES/YES	Inspect the car
2	20,000	NO/YES	Hold for 30 sec
3	200,000	NO/YES	Hold for 1 min
4	20,000	NO/YES	Inspect the car
5	400,000	NO/YES	Hold for 1 min
6	20,000	NO/YES	Inspect the car
7	600,000	NO/YES	Hold for 1 min
8	20,000	NO/YES	Inspect the car
9	800,000	NO/YES	Hold for 1 min
10	20,000	NO/YES	Inspect the car
13	900,000	NO/YES	Hold for 1 min
14	20,000	NO/YES	Inspect the car
15	1,000,000	NO/YES	Hold for 1 min
16	0	NO/YES	Inspect the car

All strain gage locations were monitored and recorded during both the pre-test and the test.

Test Results

The test results are presented as follows:

- With the car on the fixture, each one of the actuators was extended manually until they made contact with the test car.
- Maximum Load Condition Results
    - Initial strains and stresses due to the vertical load
    - strains and stresses due solely to the compression load
    - Resulting strains and stresses due to the combined effect of the vertical and longitudinal compressive forces
    - Maximum stresses versus compressive load for the most stressed locations
- Minimum Load Condition Results
    - Initial strains and stresses due to the vertical load
    - strains and stresses due solely to the compression load
    - Resulting strains and stresses due to the combined effect of the vertical and longitudinal compressive forces
    - Maximum stresses versus compressive load for the most stressed locations

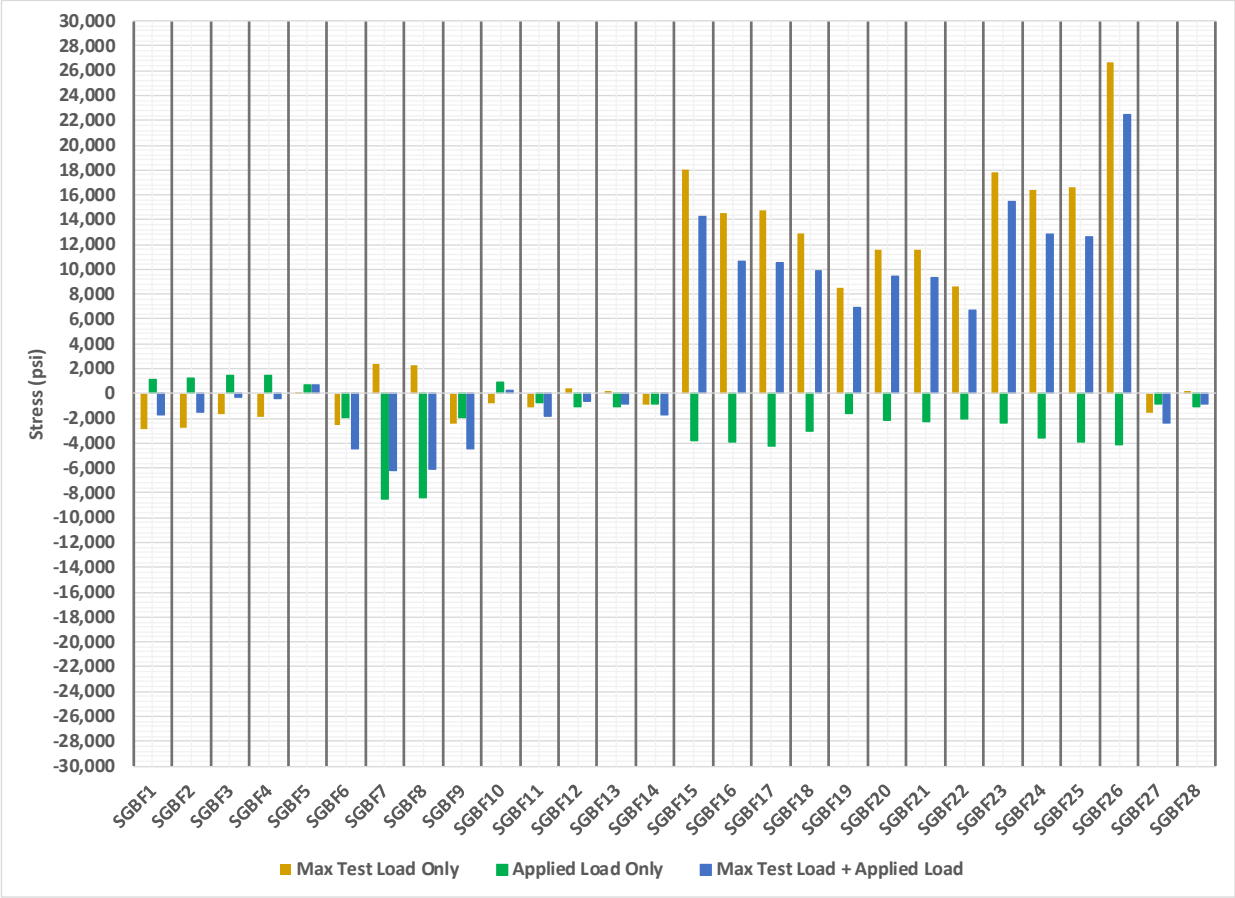


Figure F3. Maximum Load Strain Results (1 of 2)

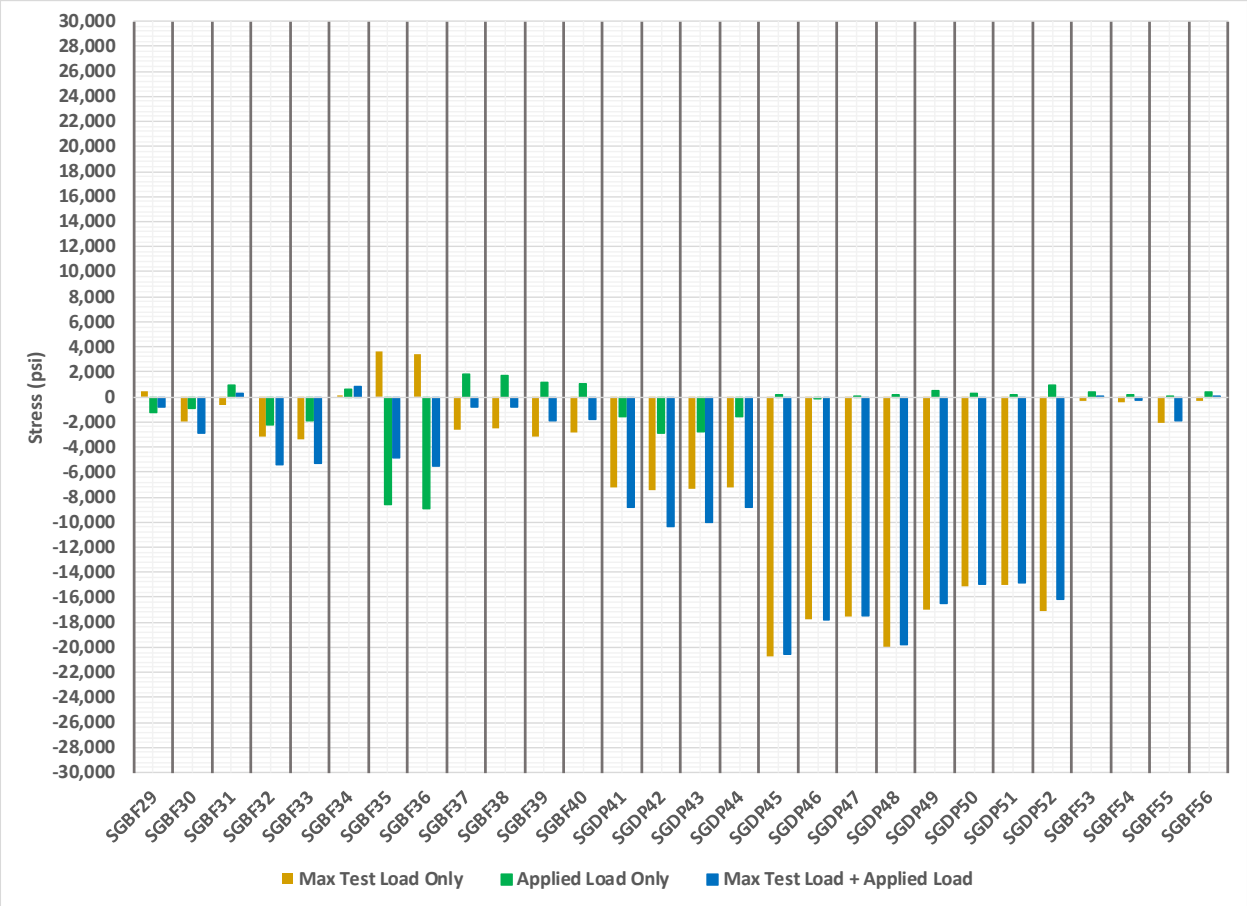


Figure F4. Stress from Squeeze Test with Maximum Test Load (2 of 2)

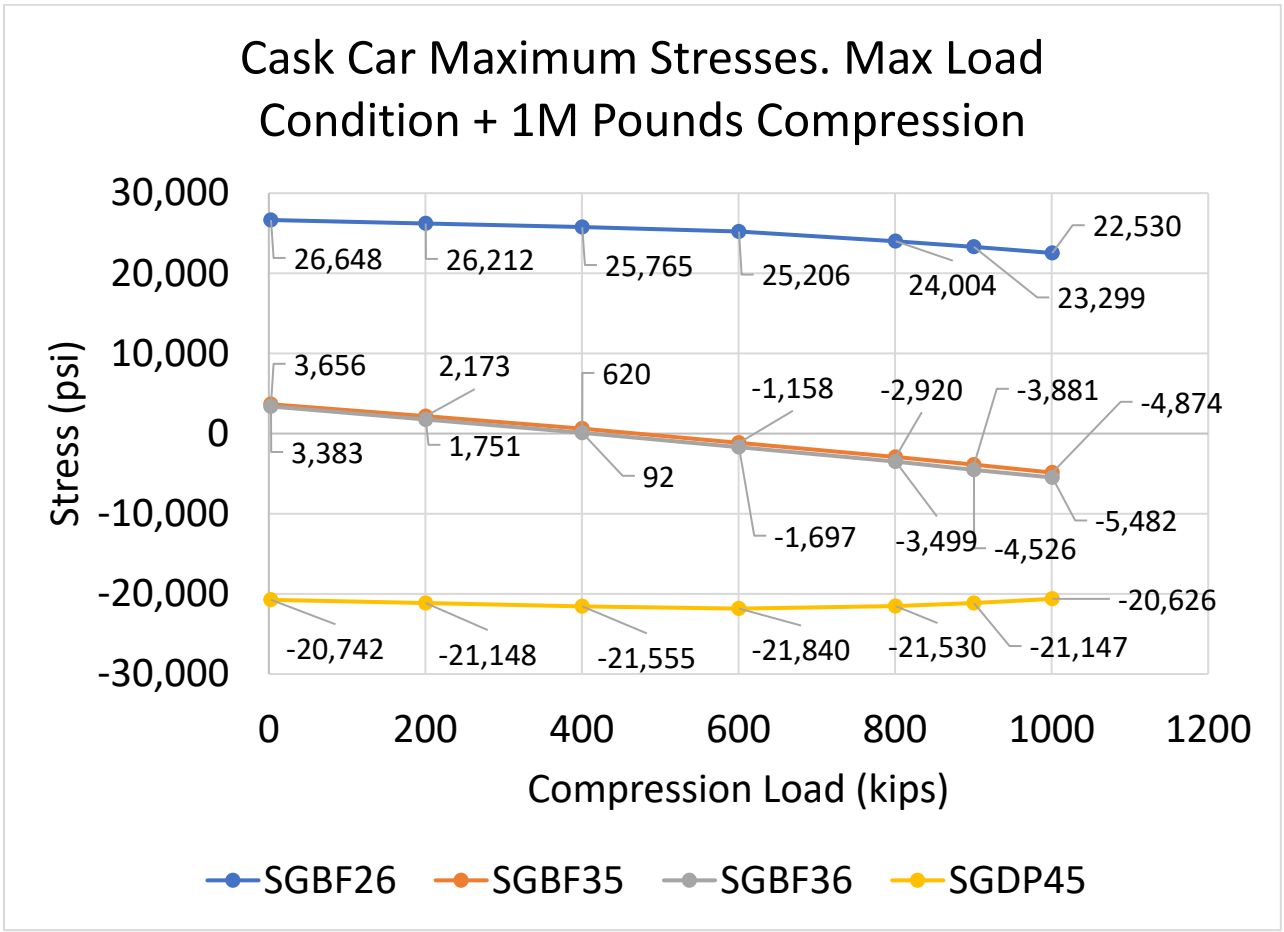


Figure F5. Maximum Stress Values at the Most Stressed Locations (Maximum Load)

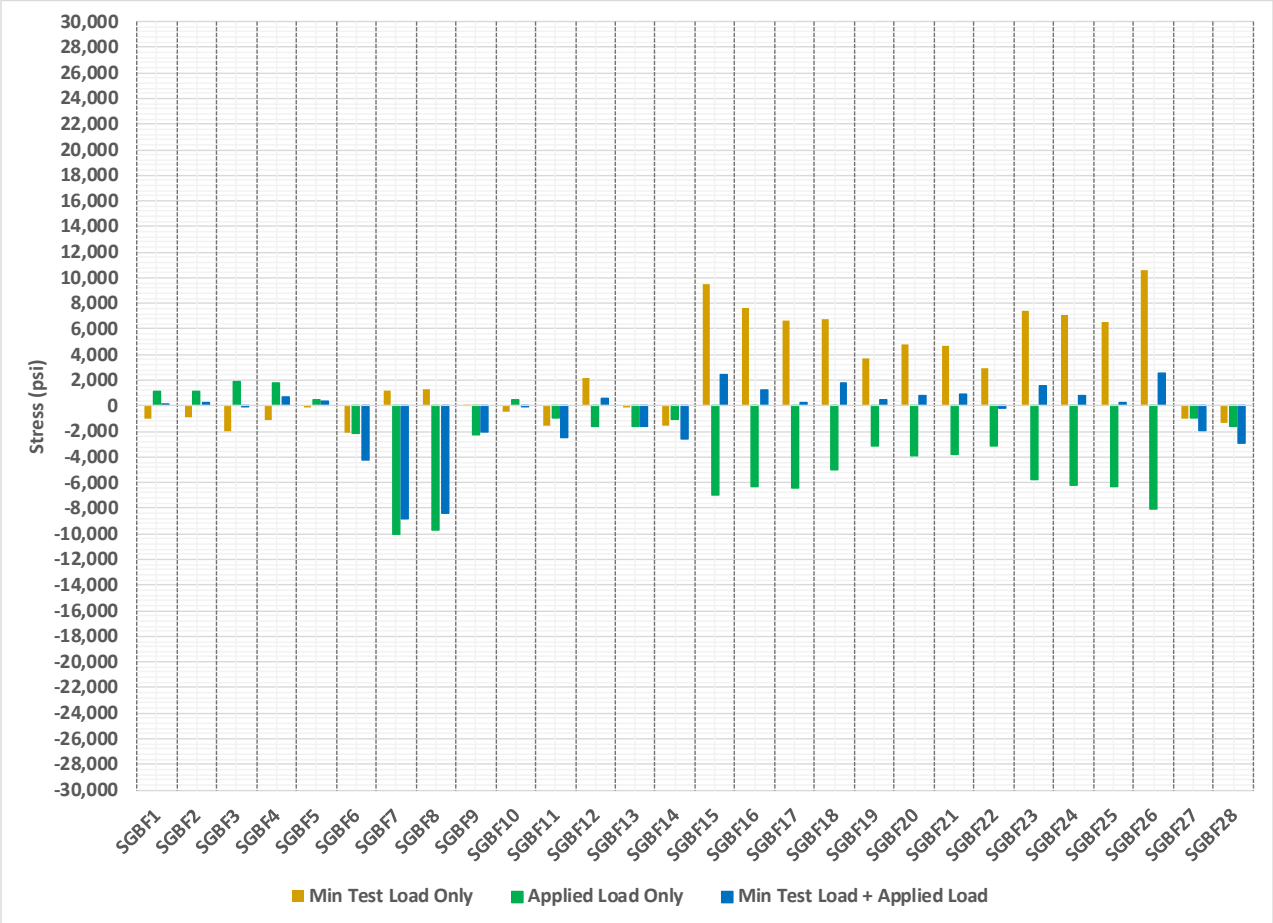


Figure F6. Stress from Squeeze Test with Minimum Test Load (1 of 2)

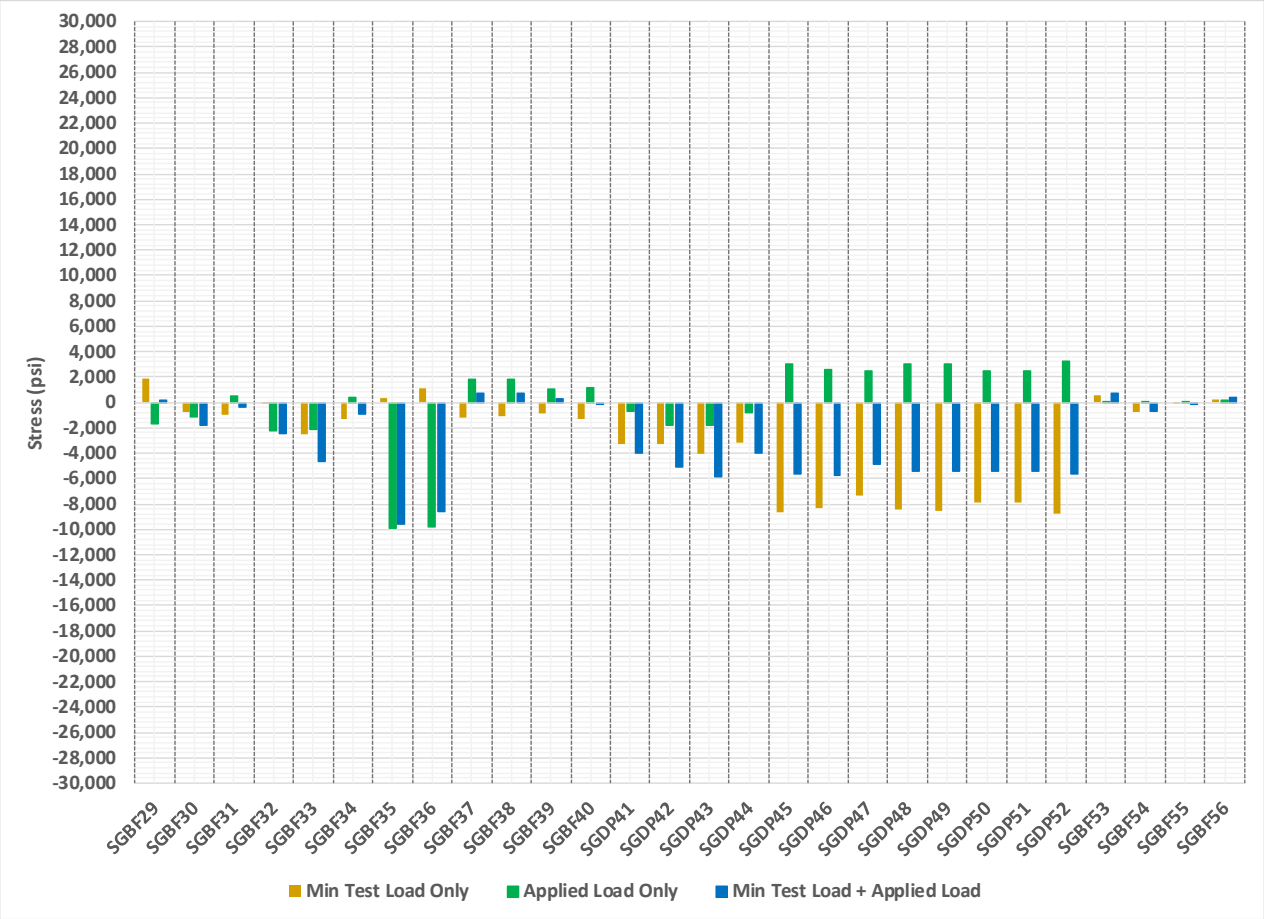


Figure F7. Stress from Squeeze Test with Minimum Test Load (2 of 2)

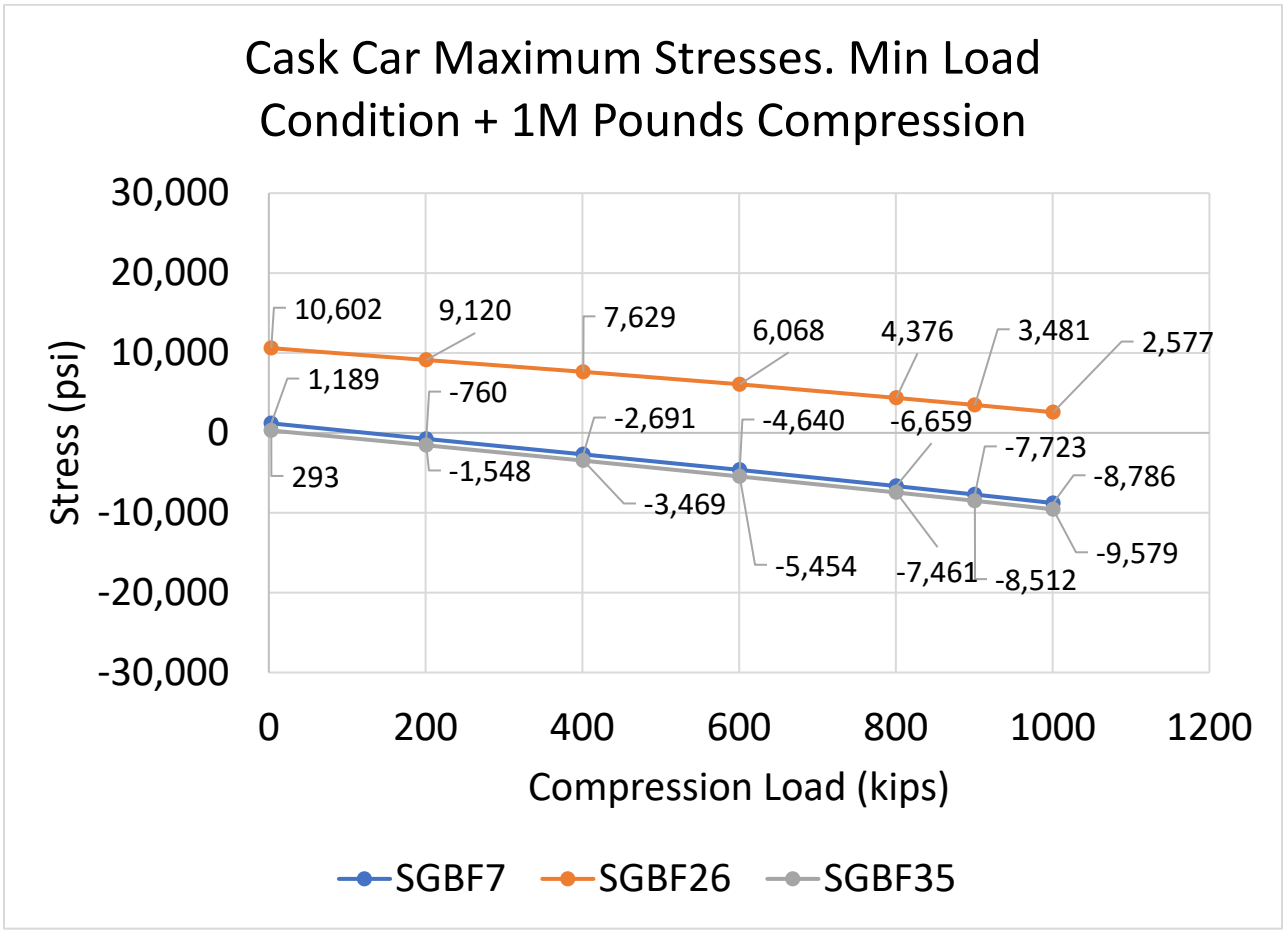


Figure F8. Maximum Stresses in the Minimum Load Condition

Appendix G. Vertical Coupler Force Test Results

The results will be presented as follows:

- Strains and stresses when pushing upwards
- Strains and stresses when pushing downwards
- Results summary

All the results are presented as a series of bar plots showing the maximum and minimum readings for each strain gage.

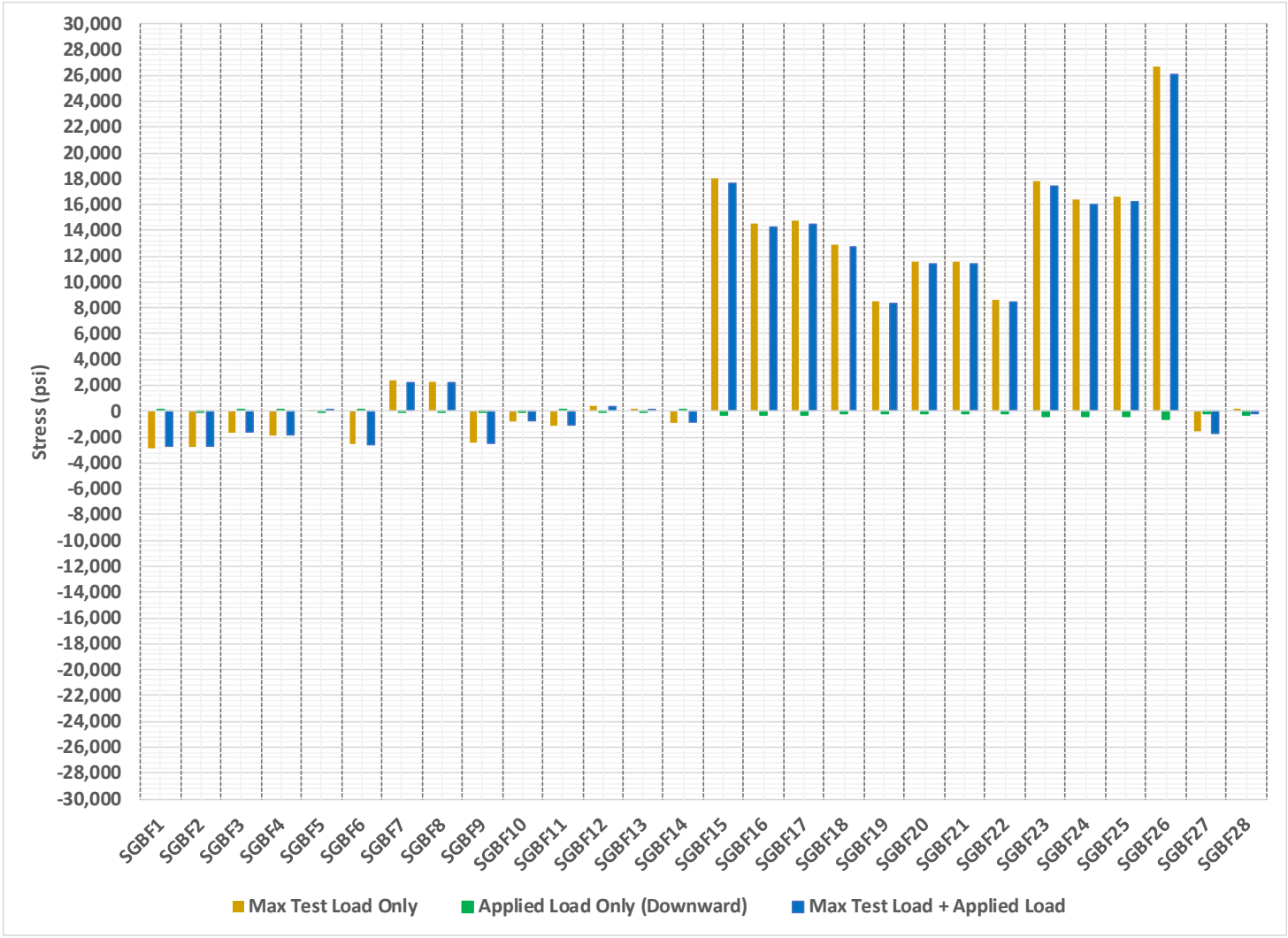


Figure G1. Stress from Downward Coupler Vertical Load Test (1 of 2)

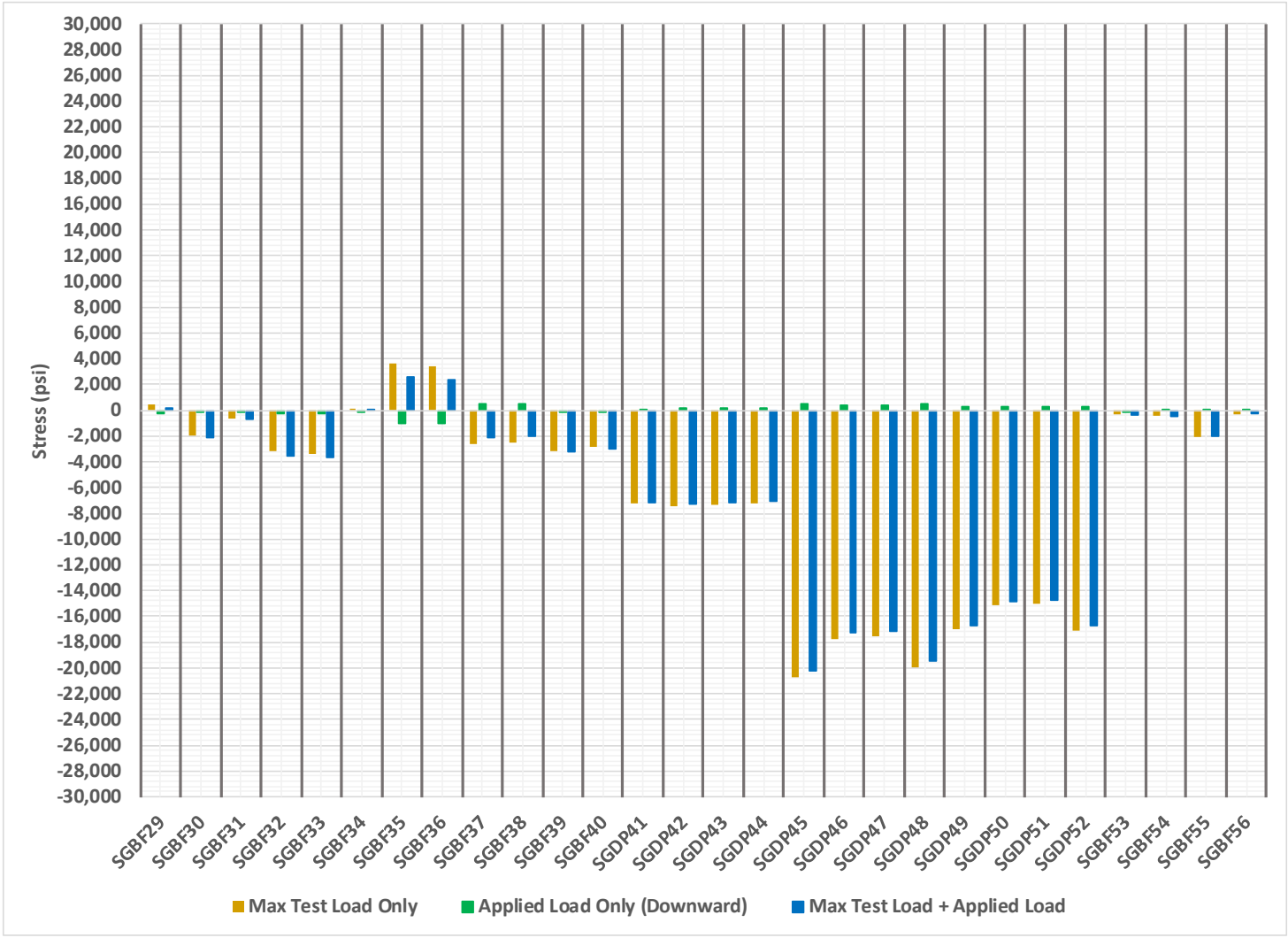


Figure G2. Stress from Downward Coupler Vertical Load Test (2 of 2)

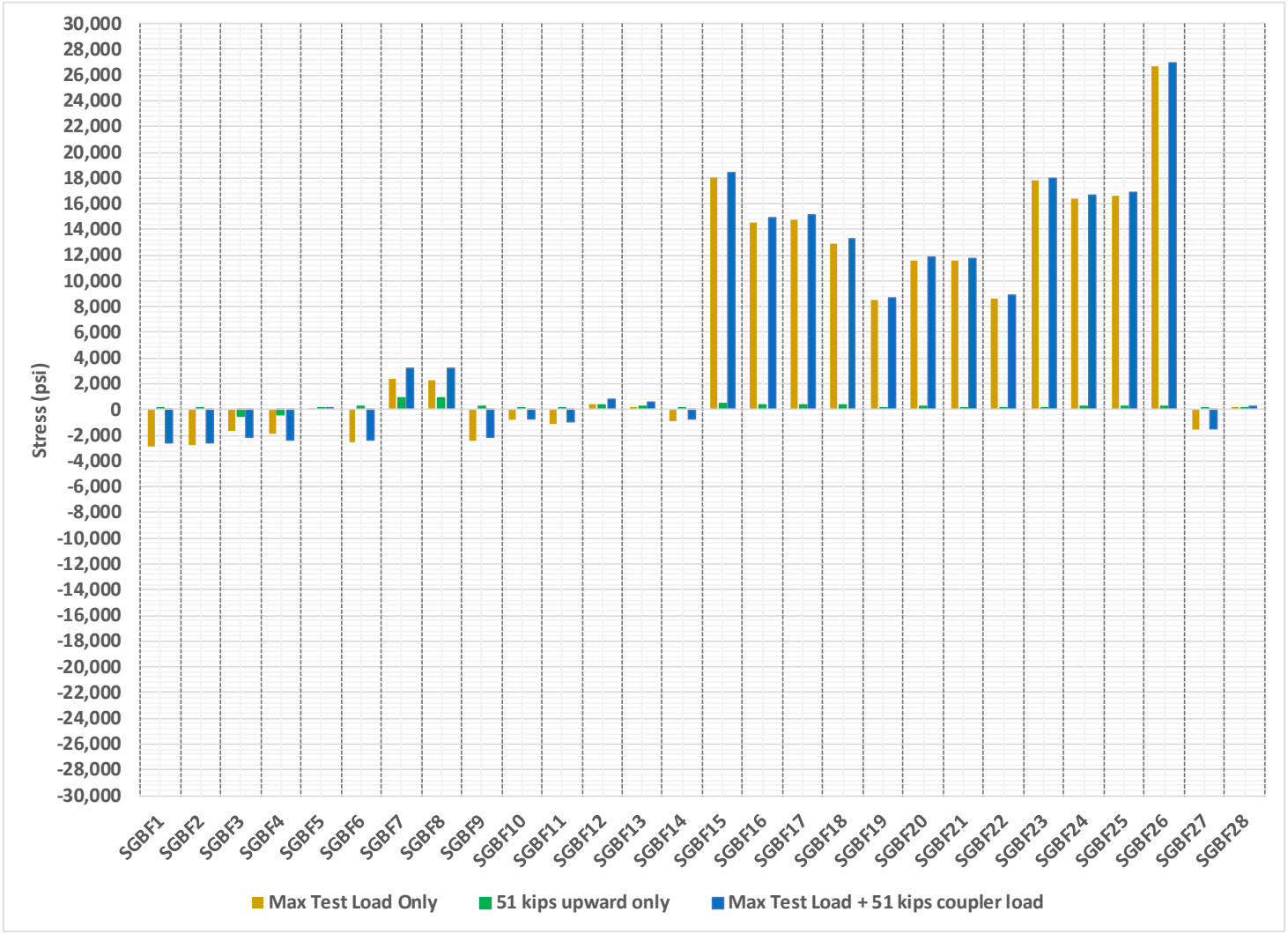


Figure G3. Stress from Upward Coupler Vertical Load Test (1 of 2)

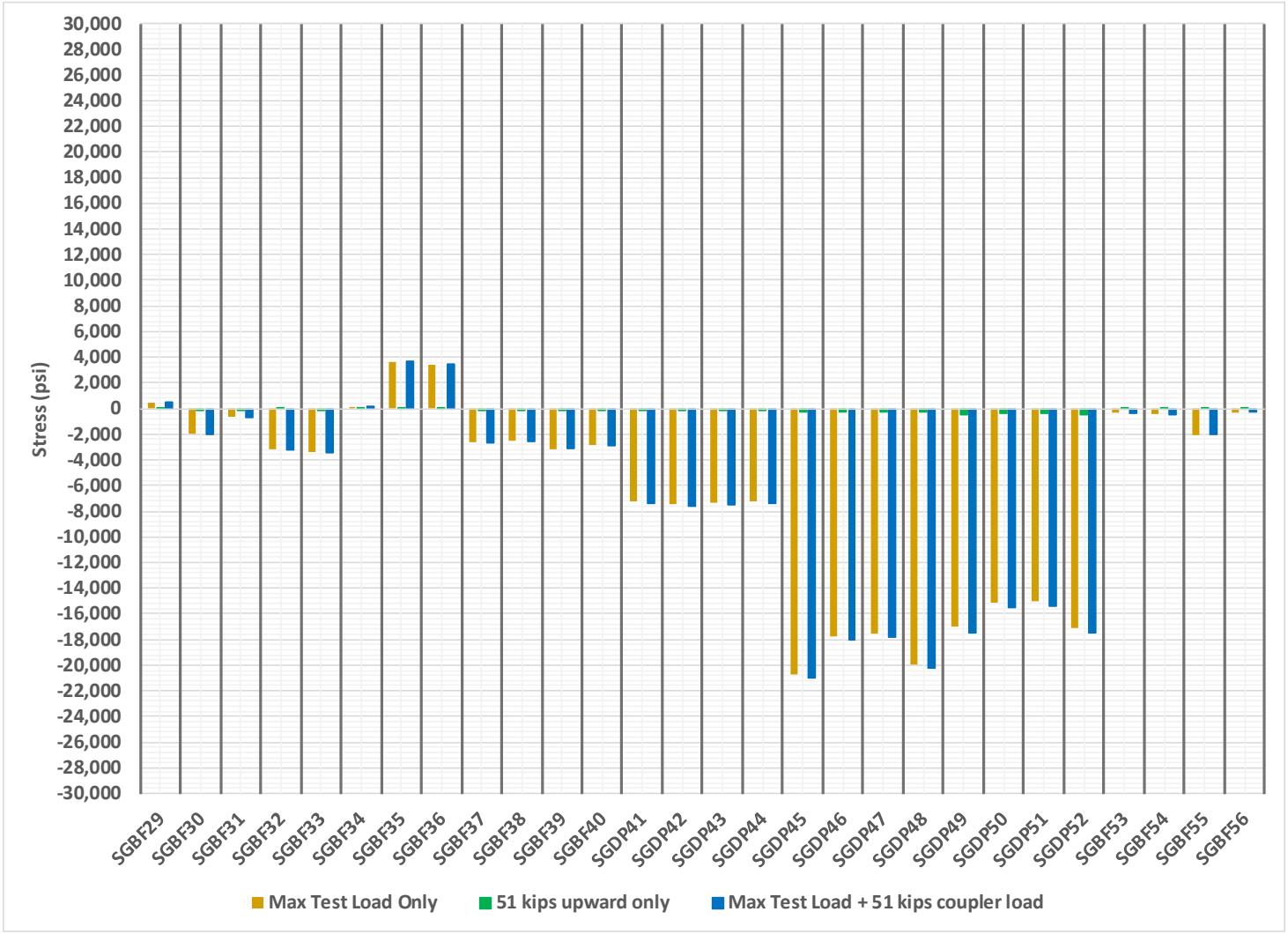


Figure 4. Stress from Upward Coupler Vertical Load Test (2 of 2)

Appendix H. Jacking Results

The results for the jacking test will be presented as follows:

- Strains and stresses for all the strain gages
- Strain time history signal for gages SGBF37, SGBF38, SGBF39, and SGBF40
- Stress time history signal for gages SGBF37, SGBF38, SGBF39, and SGBF40

Figure H1 through Figure H6 show the results for this test.

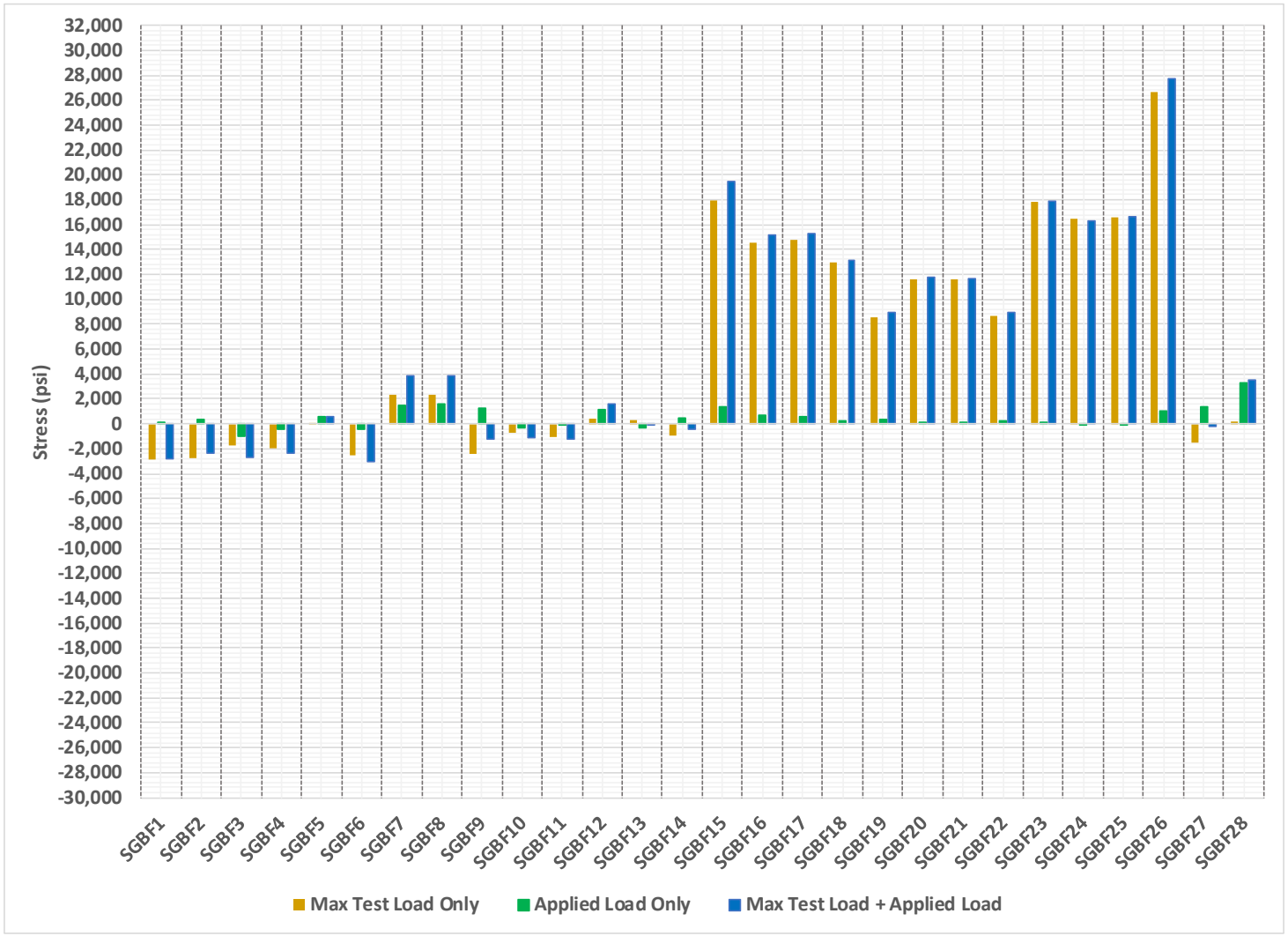


Figure H1. Jacking Test Stresses Maximum Test Load (1 of 2)

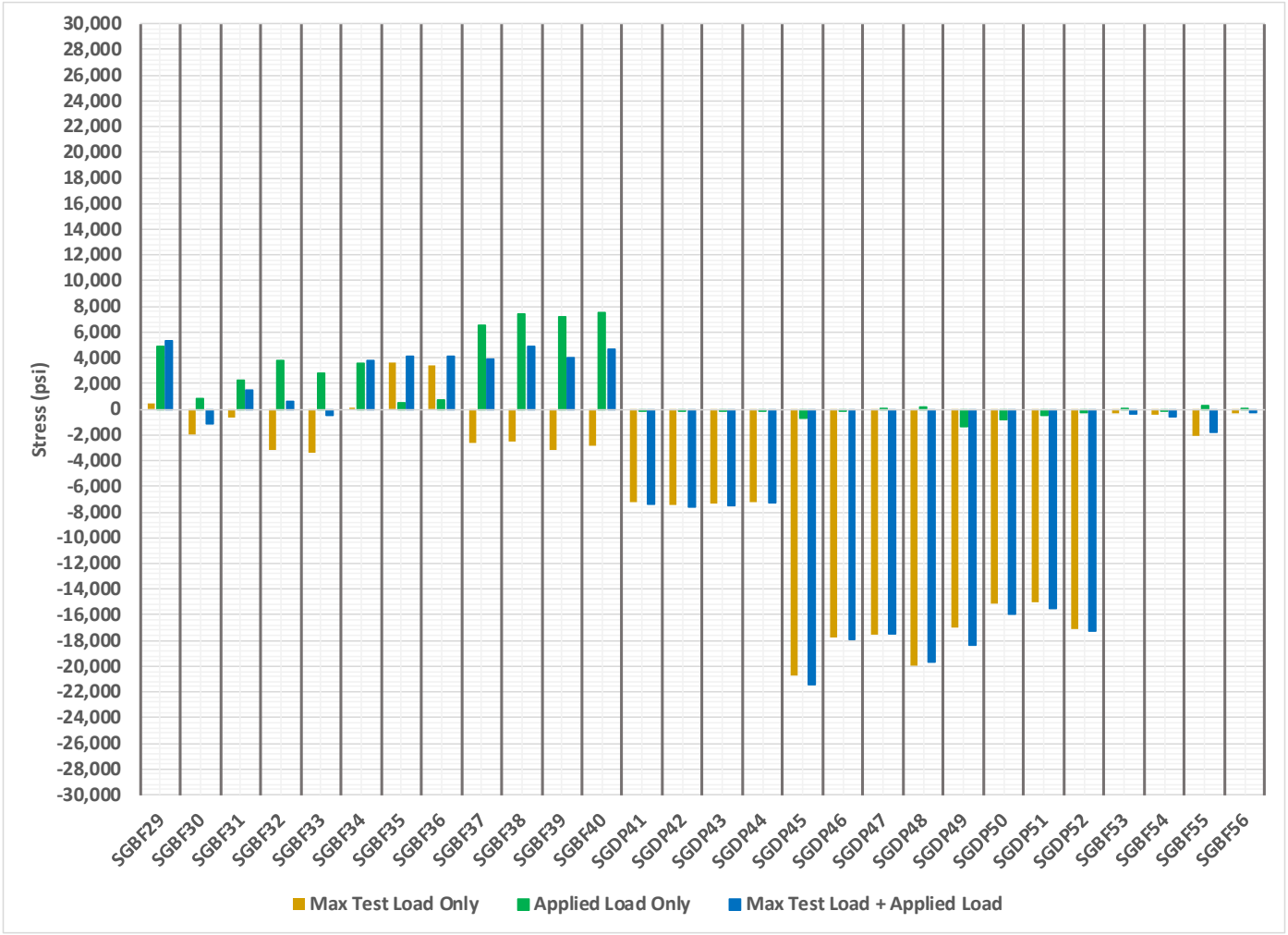


Figure H2. Jacking Test Stresses Maximum Test Load (2 of 2)

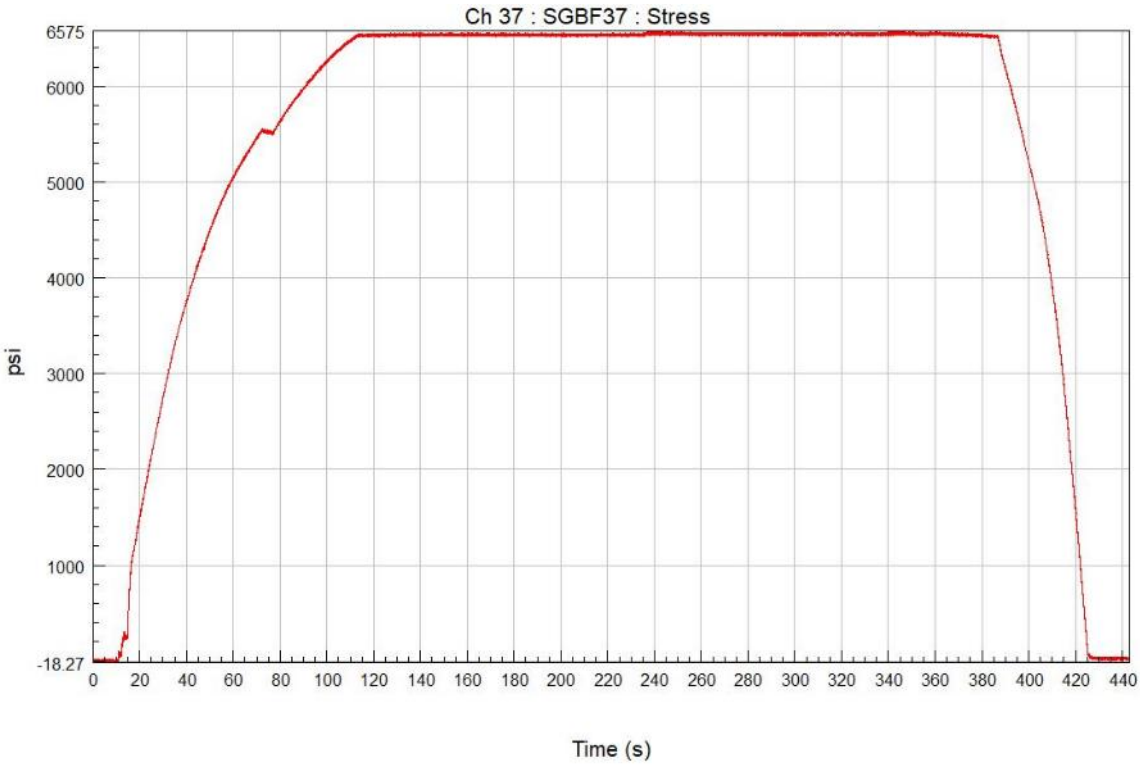


Figure H3. Jacking Test Stress Time History. SGBF37



Figure H4. Jacking Test Stress Time History. SGBF38

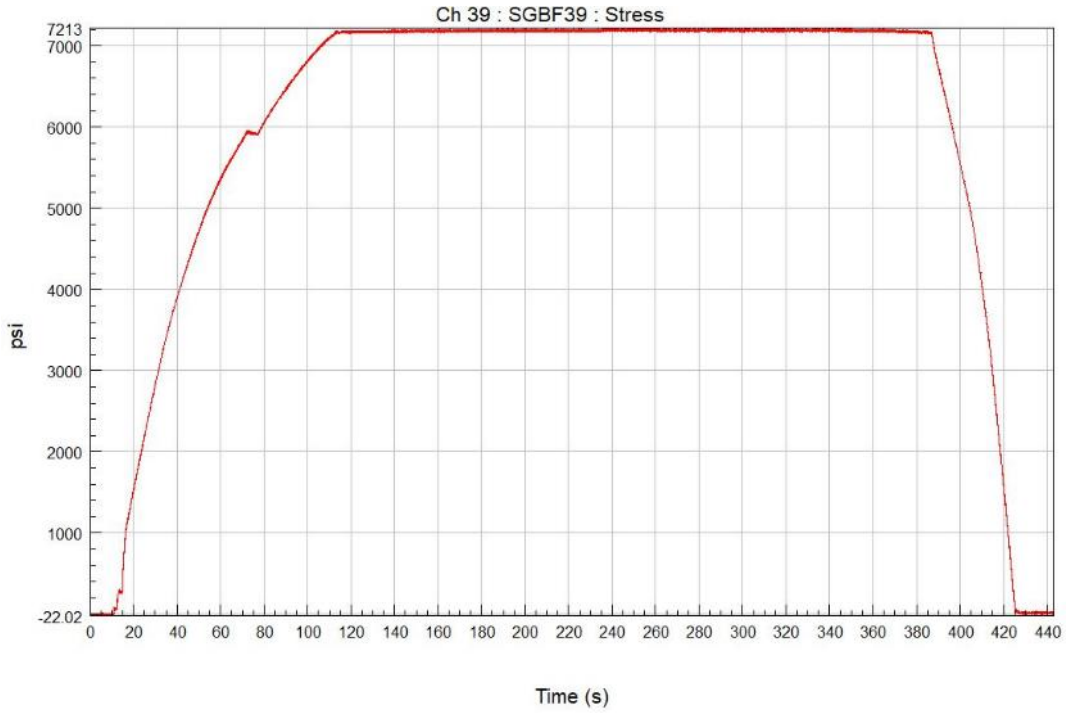


Figure H5. Jacking Test Stress Time History. SGBF39

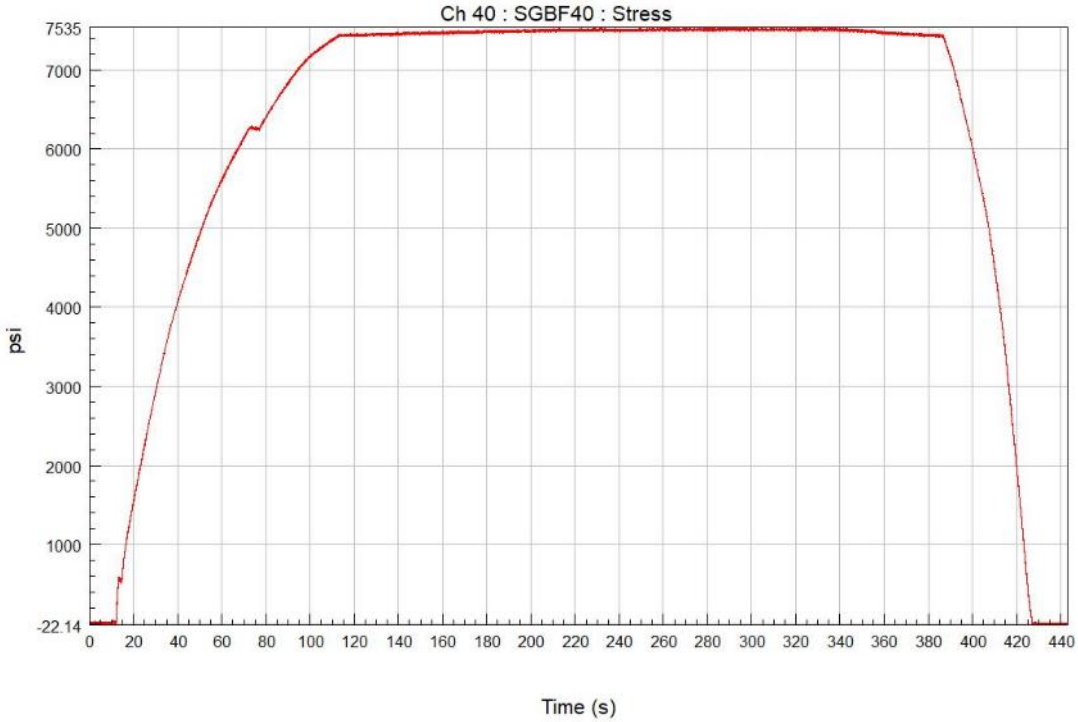


Figure H6. Jacking Test Stress Time History. SGBF40

Appendix I. Twist Test

Results for the Suspension Twist Test in the maximum test load condition are presented below.

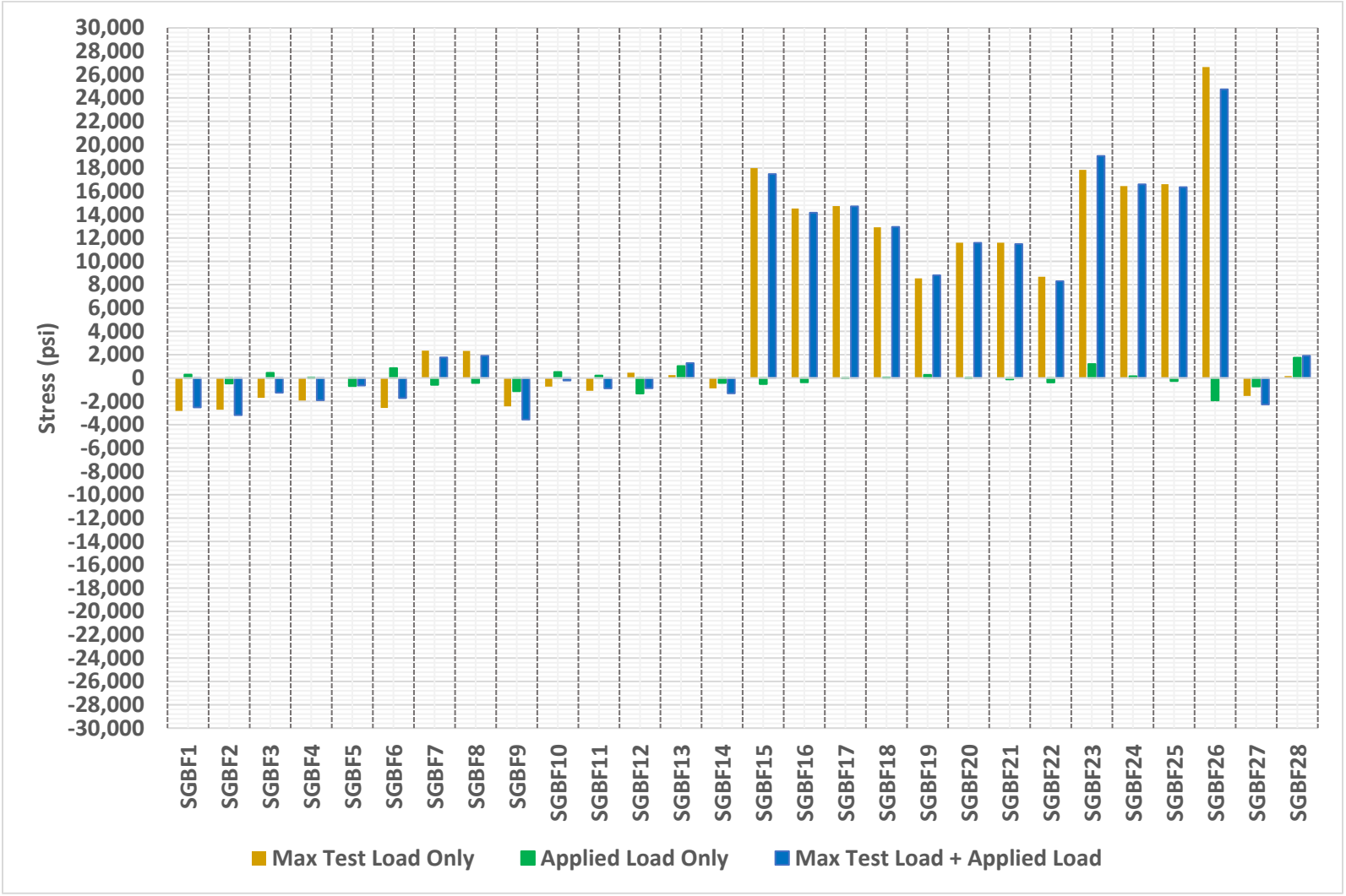


Figure I1. Stress from Suspension Twist Test, A-End LH Side (1 of 2)

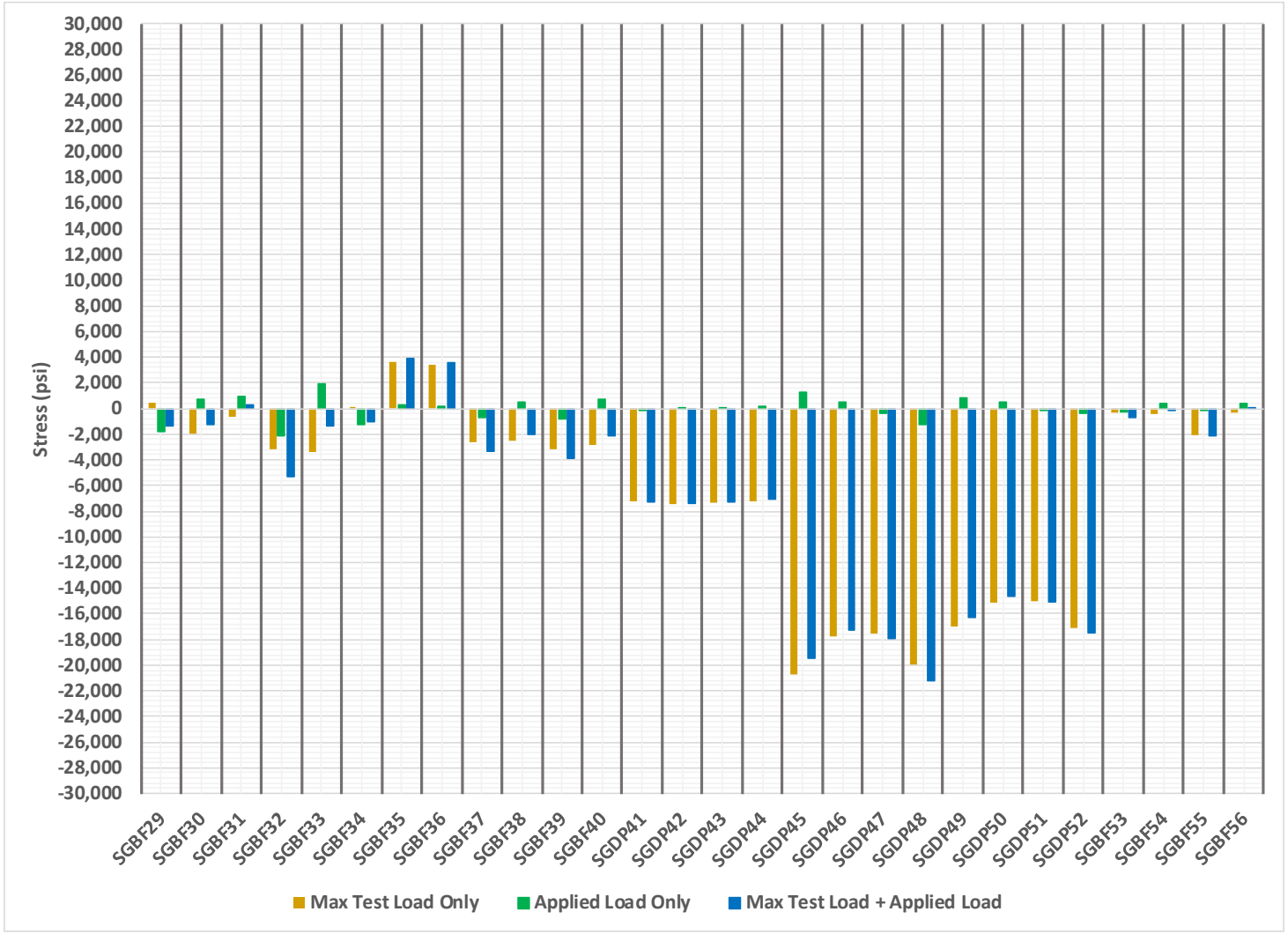


Figure I2. Stress from Suspension Twist Test, A-End LH Side (2 of 2)

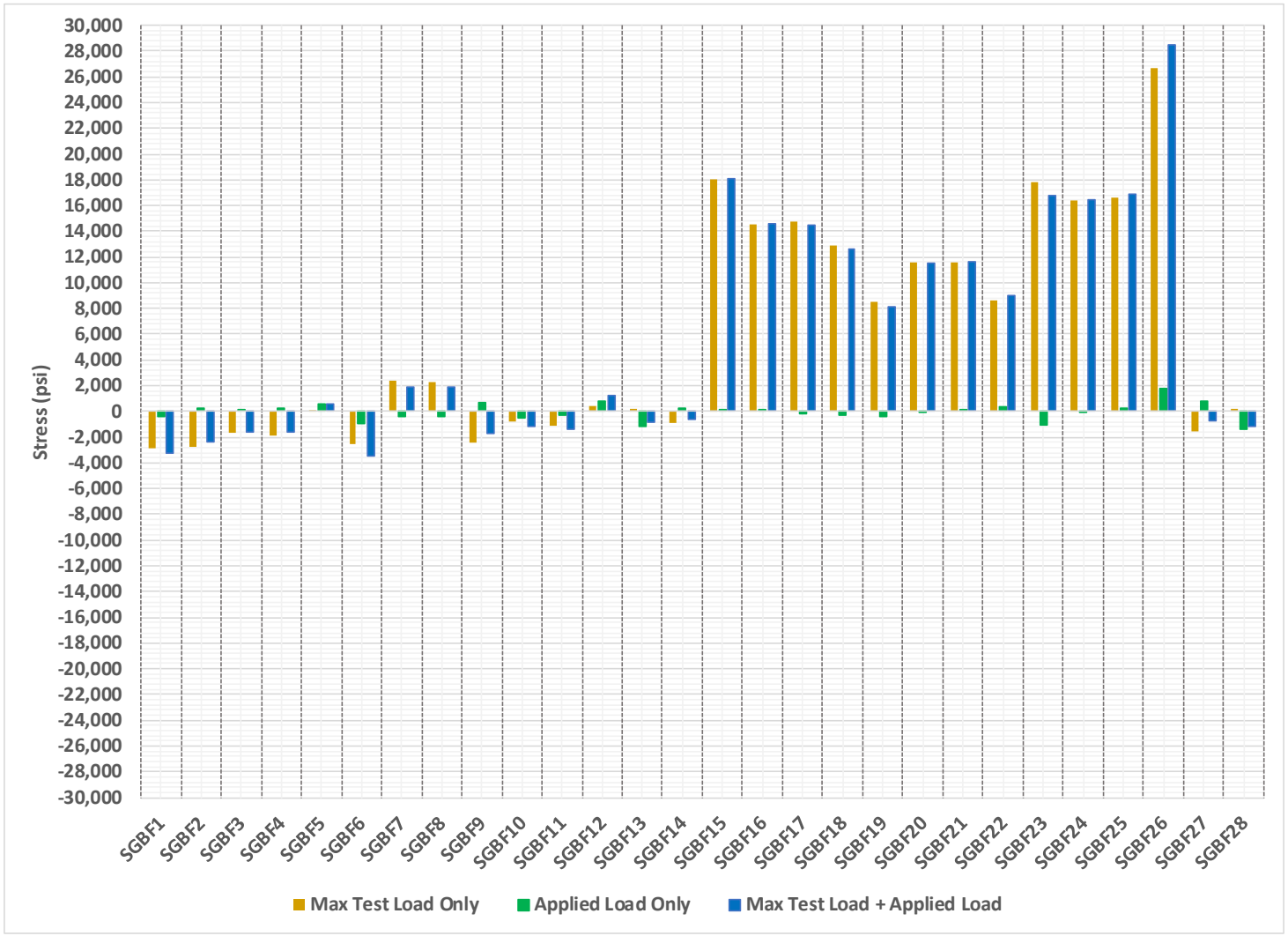


Figure I3. Stress from Suspension Twist Test, A-End RH Side (1 of 2)

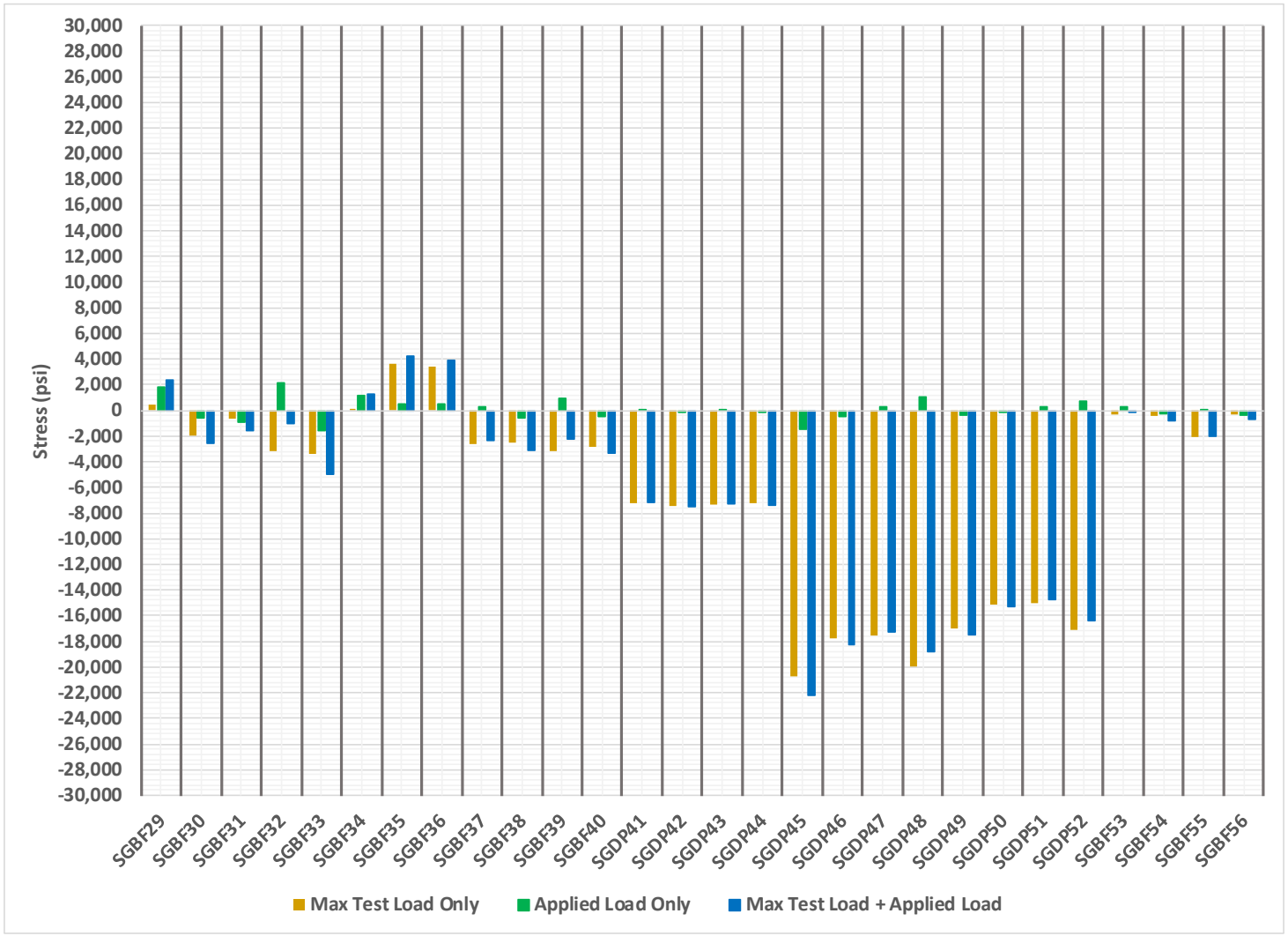


Figure I4. Stress from Suspension Twist Test, A-End RH Side (2 of 2)

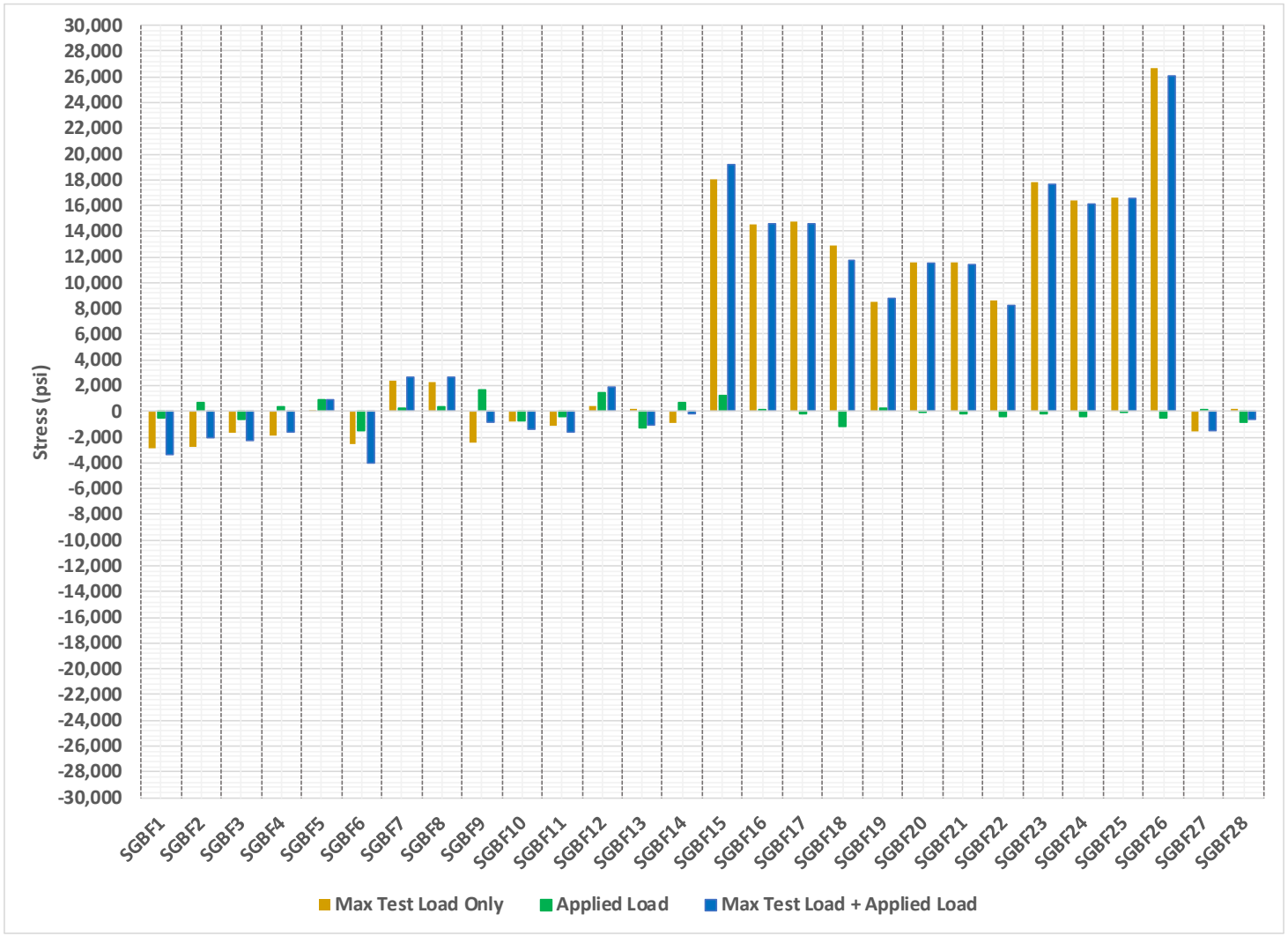


Figure I5. Stress from Suspension Twist Test, B-End LH Side (1 of 2)

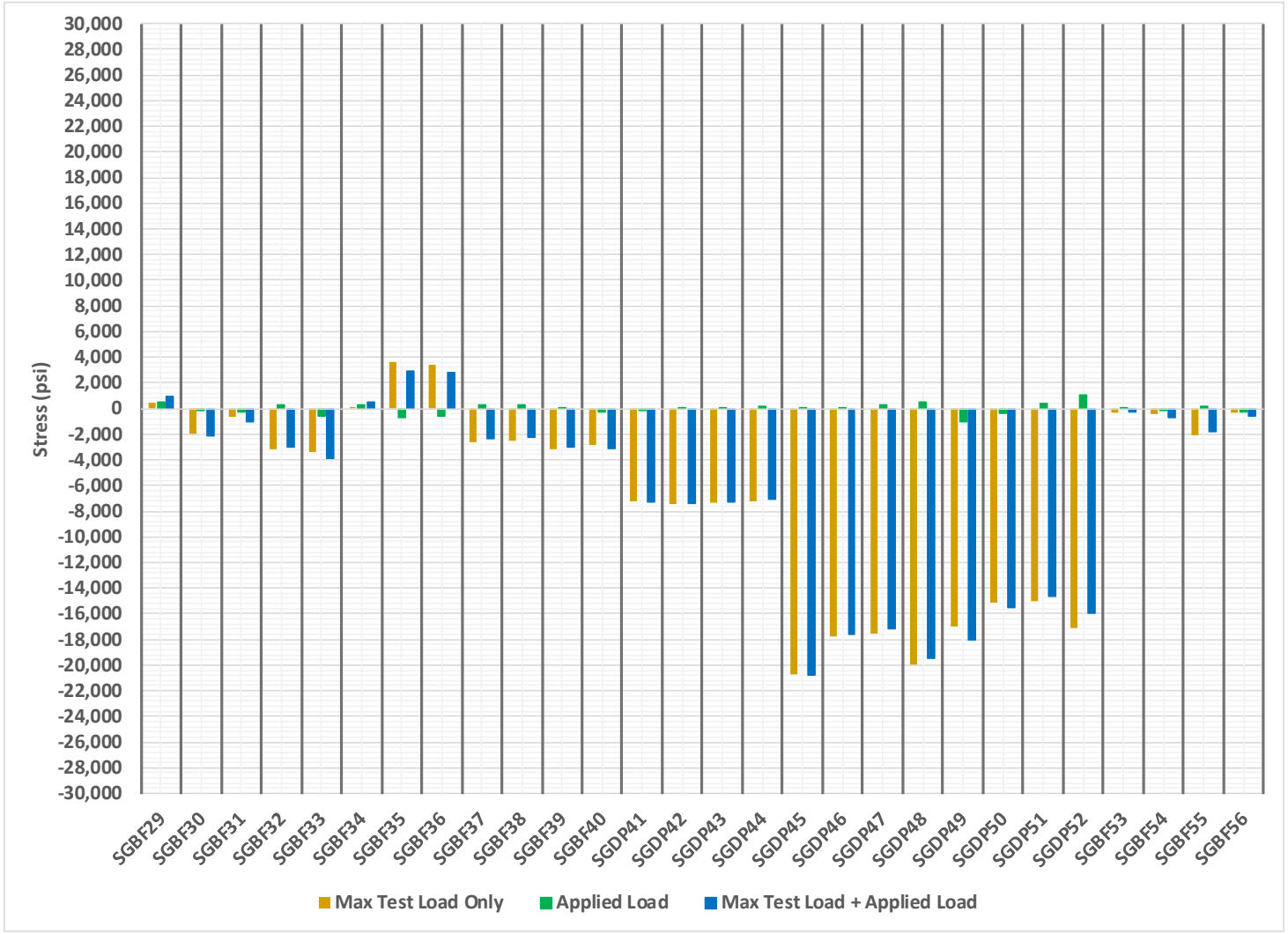


Figure I6. Stress from Suspension Twist Test, B-End LH Side (2 of 2)

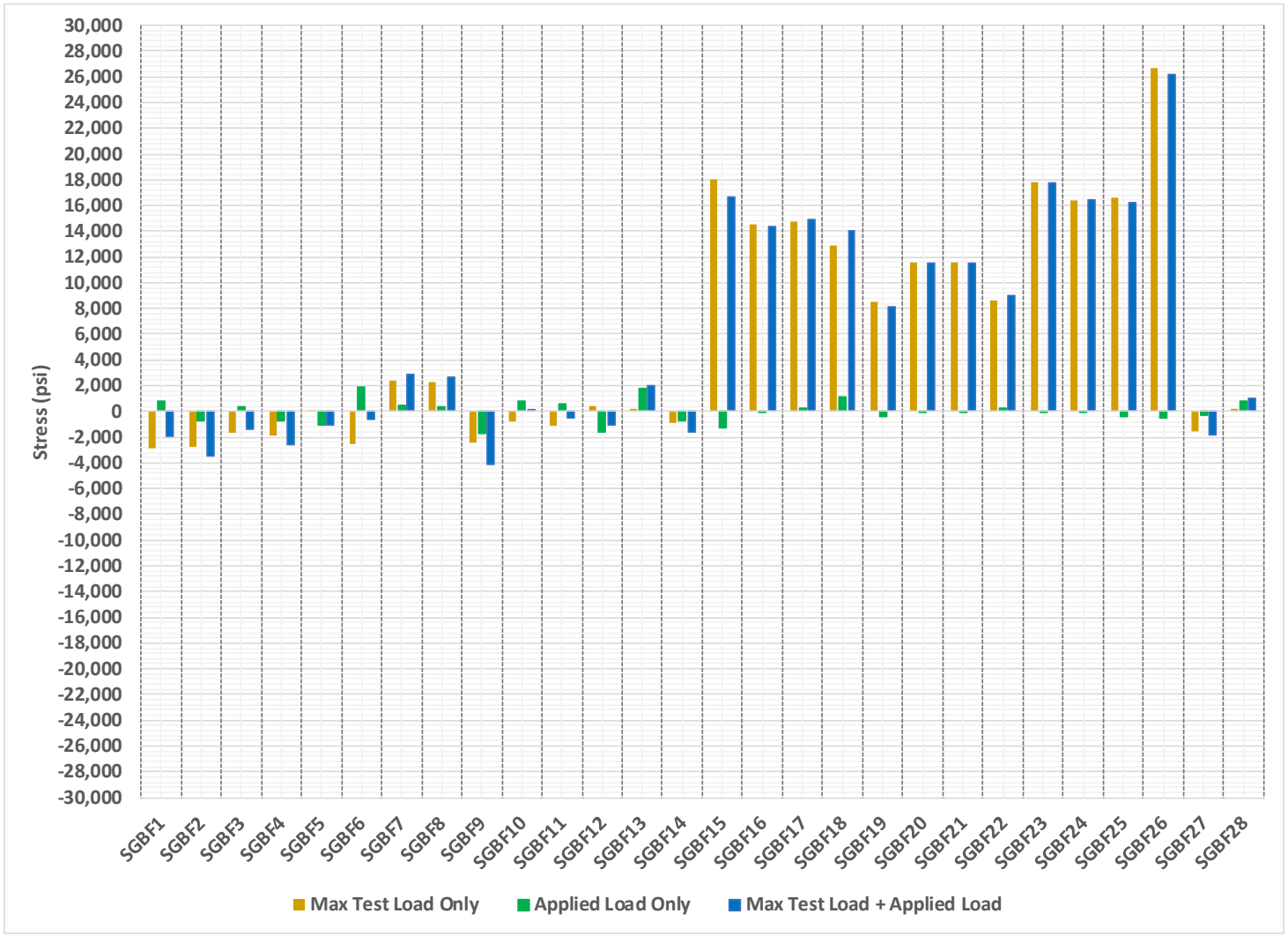


Figure I7. Stress from Suspension Twist Test, B-End RH Side (1 of 2)

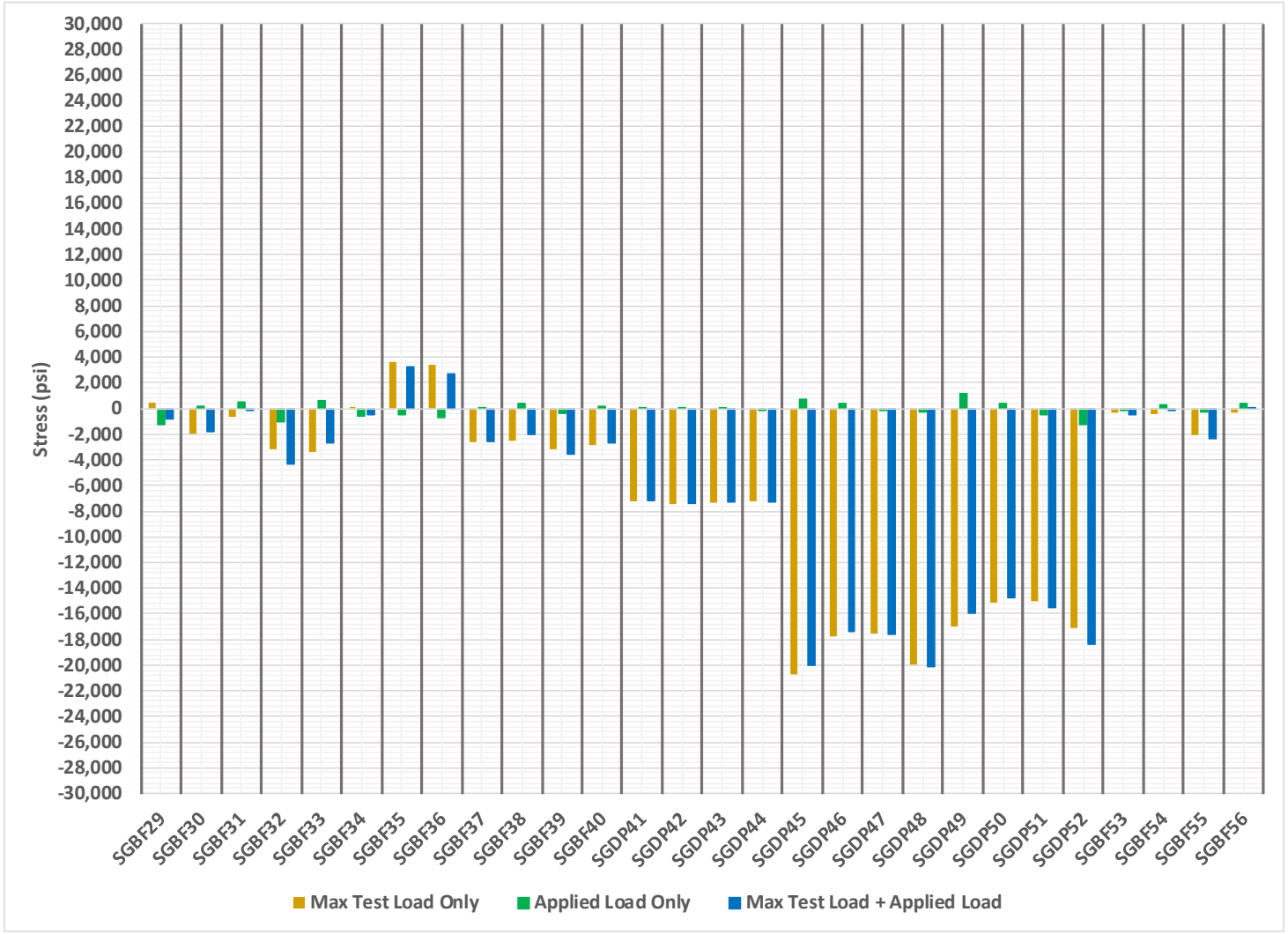


Figure I8. Stress from Suspension Twist Test, B-End RH Side (2 of 2)

E.2. Carbody Twist Test

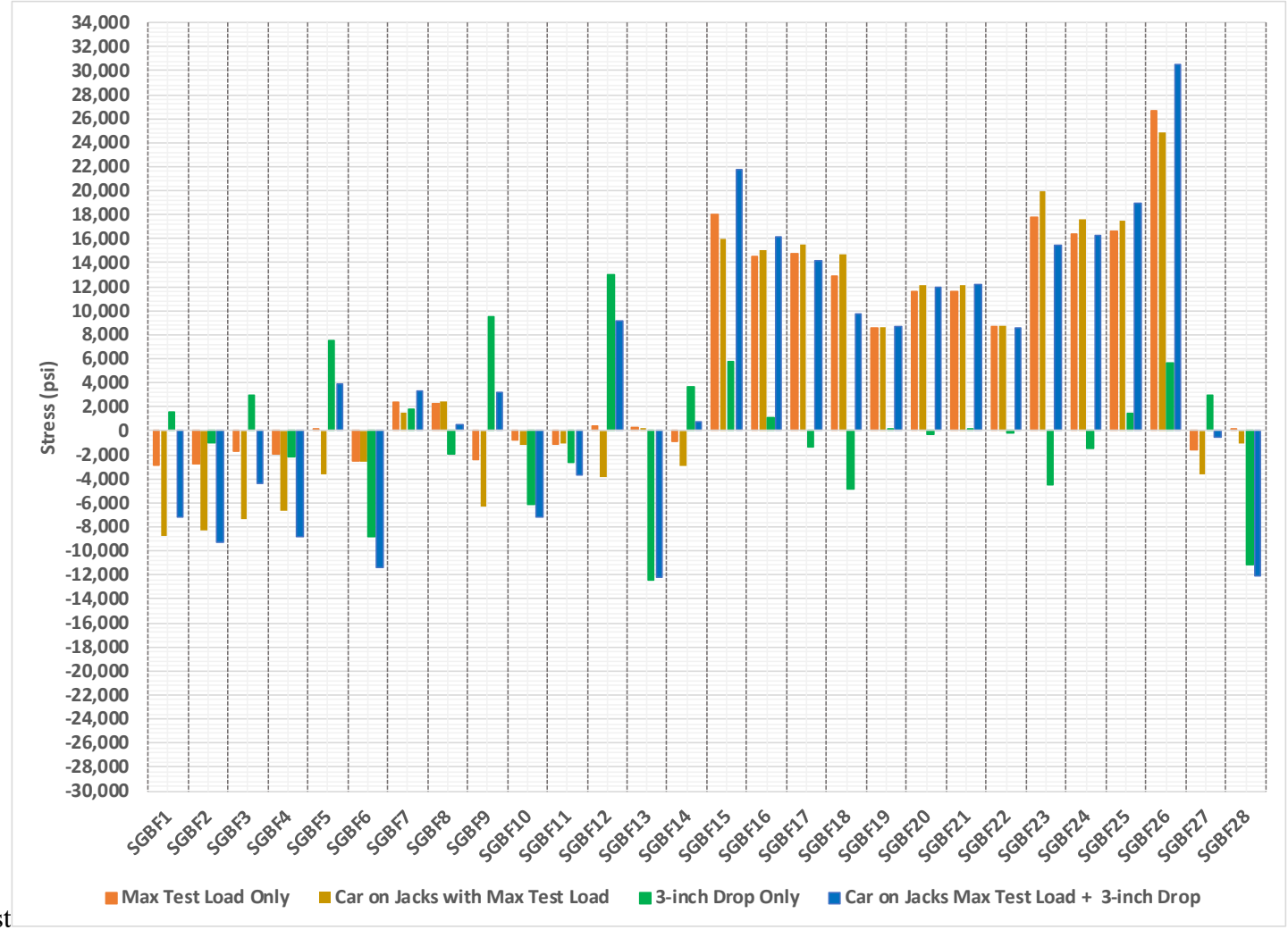


Figure I9. Stress from Carbody Twist Test, B-End RH Side (1 of 2)

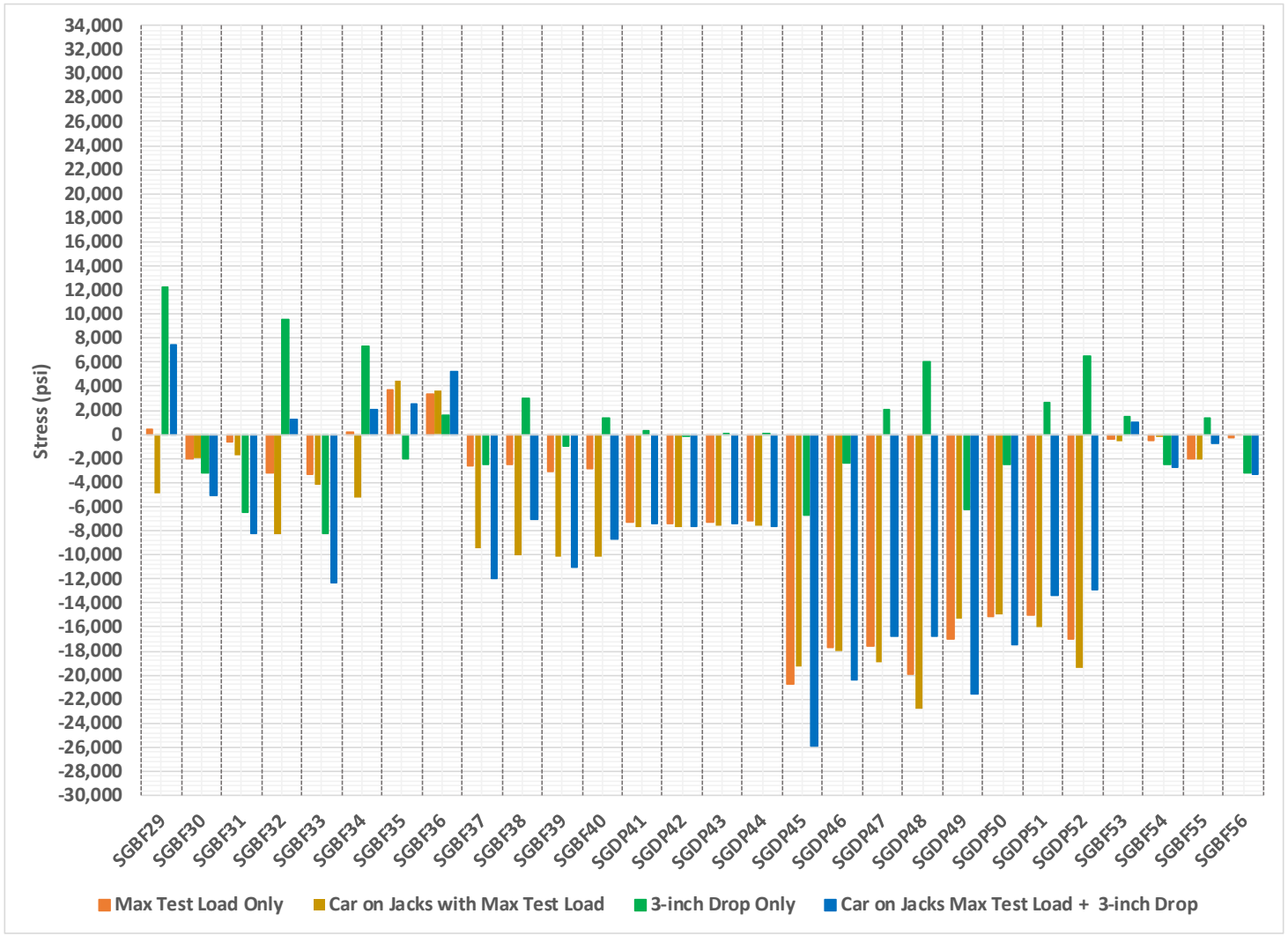


Figure I10. Stress from Carbody Twist Test, B-End RH Side (2 of 2)

Appendix J. Impact Test

The results for these tests are presented as follows:

For each tested speed:

- Strains and stresses
- Time signal of the highest stressed locations in both positive or negative stress

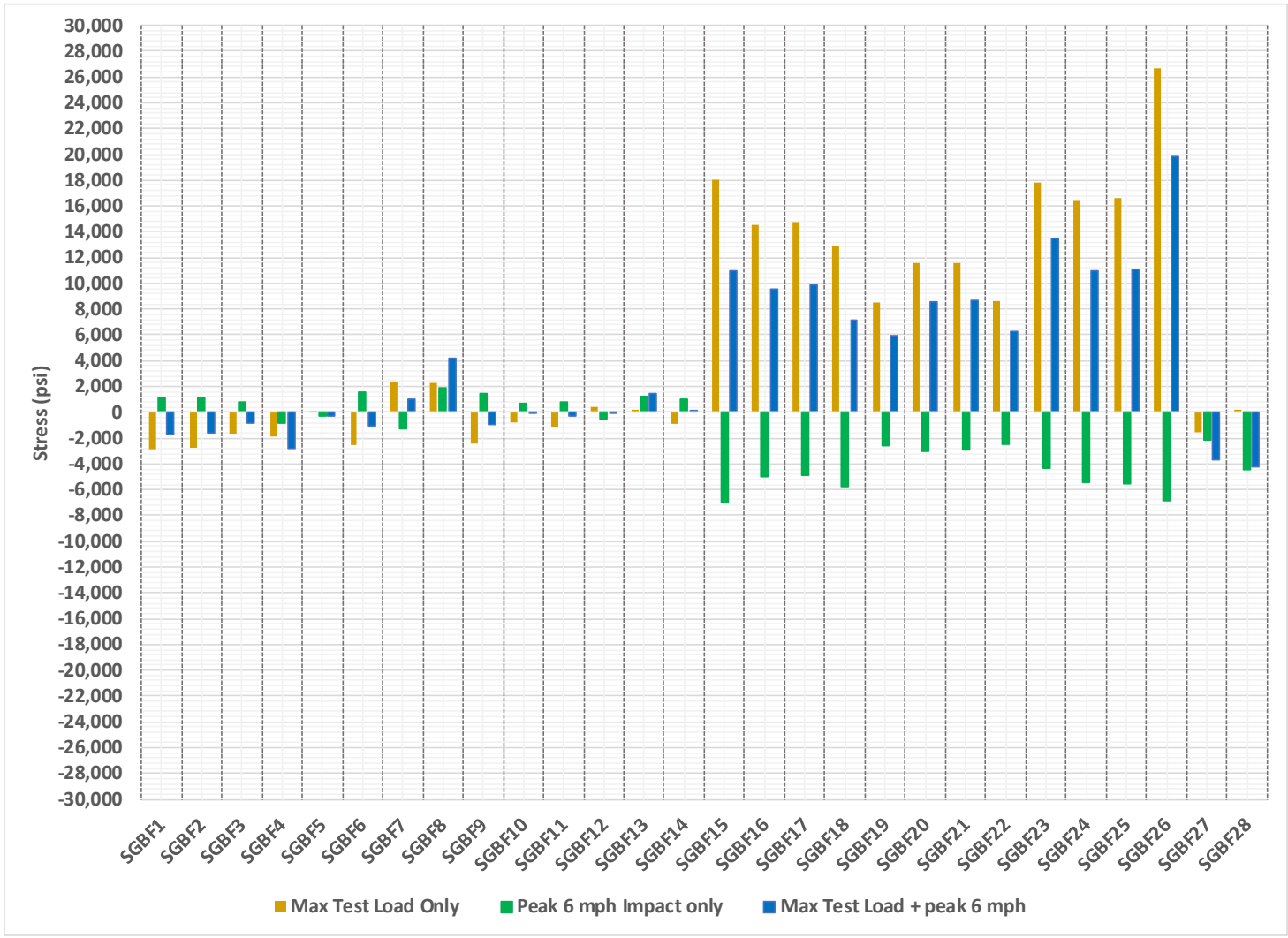


Figure J1. Stresses at 6 mph Impact (1 of 2)

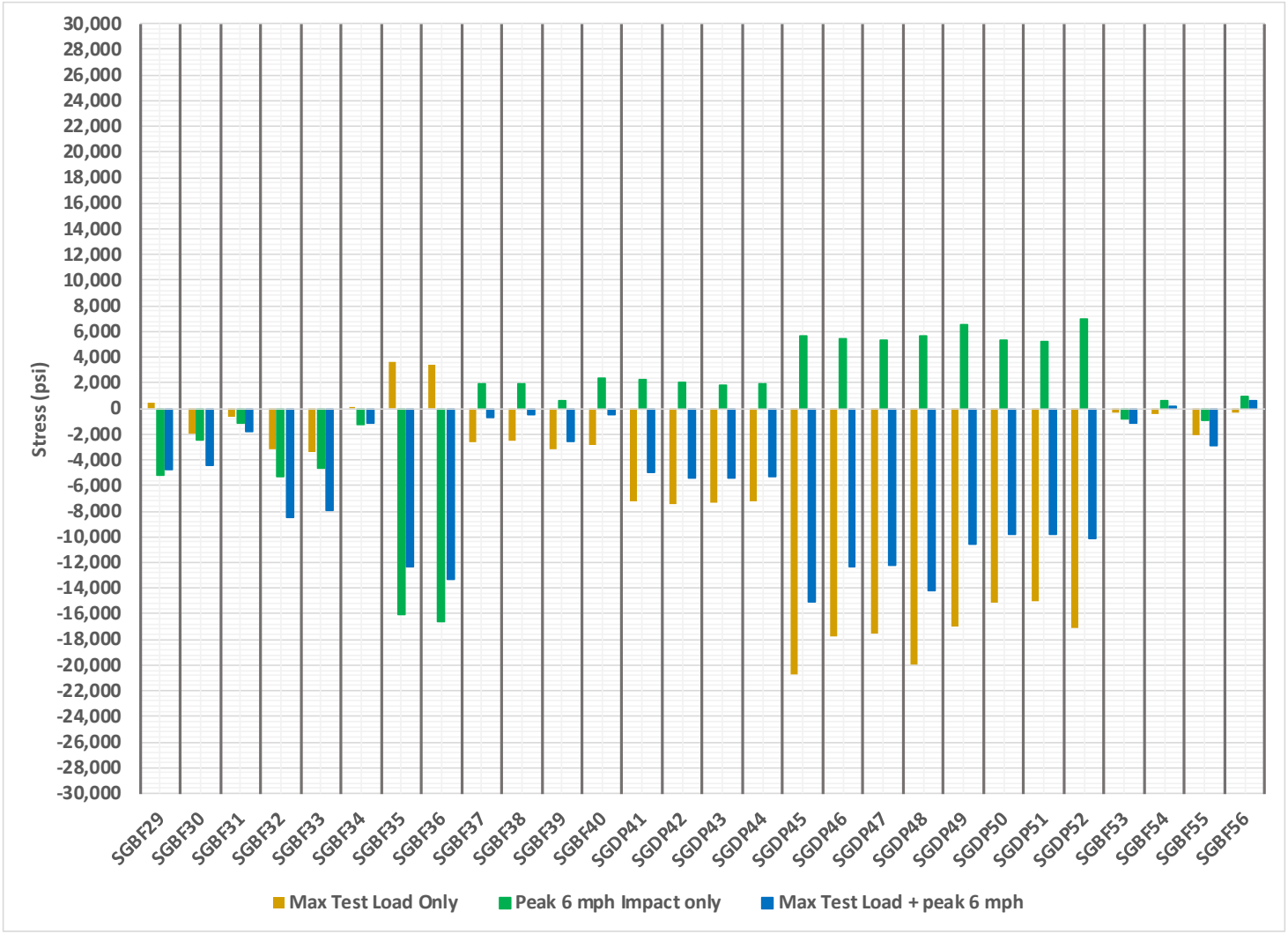


Figure J2. Stresses at 6 mph Impact (2 of 2)

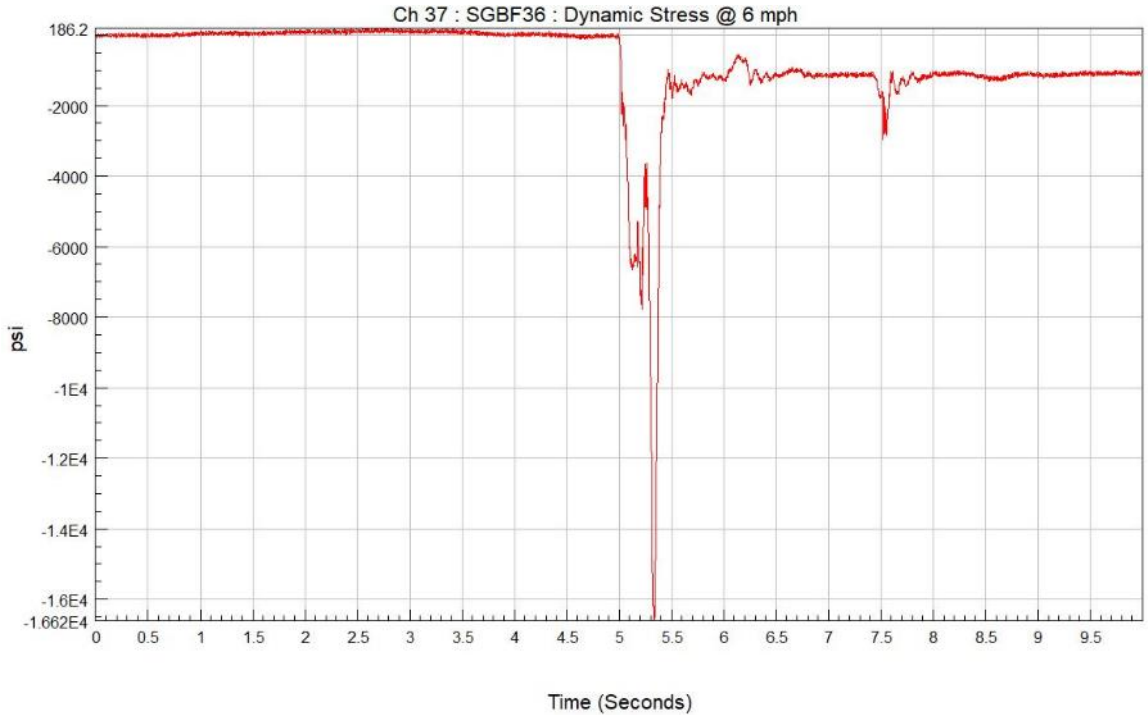


Figure J3. Stress at 6 mph Impact (SGBF36)

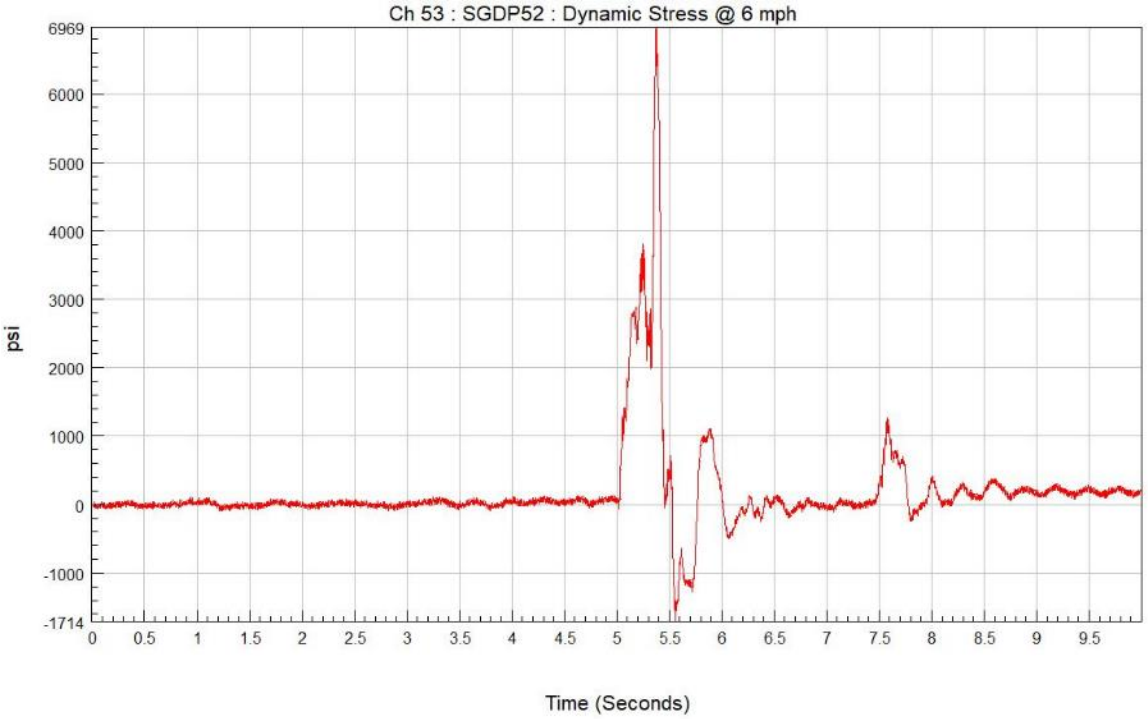


Figure J4. Stress at 6 mph Impact (SGDP52)

Appendix K. ATLAS 12 AXLE FLAT CAR ATTACHMENT TO DECK WELDMENT

ATLAS 12 AXLE FLAT CAR

Attachment to Deck Weldment

HLRM Service

January 2020

Prepared by:

Nicholas Hinsch

Checked by:

Jon Odden

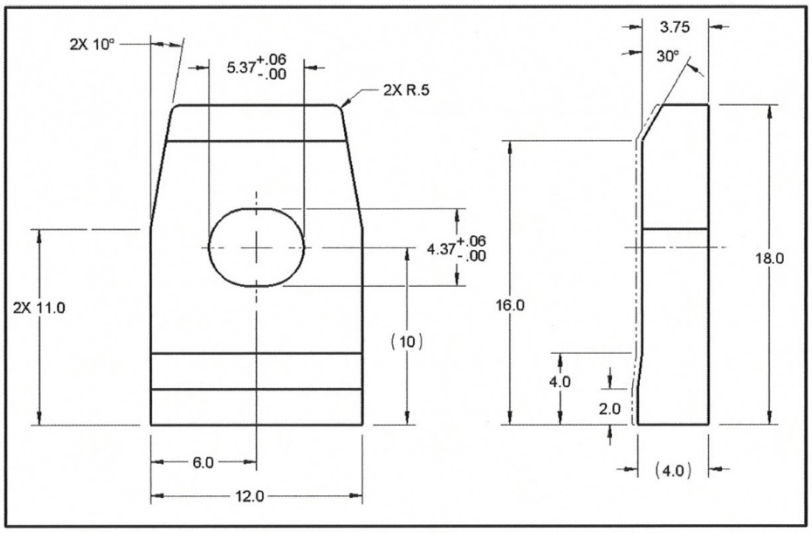


Figure 5-1: Center Pin Attachment Block

S-2043 (4.1.8.1) Loads provided from Areva.

Vertical Load Weld Calculations on Pin Attachments:

All attachments are to be welded to the deck plate.

Assuming 100 % Weld Lateral Load = 611kip Vertical Load = 312 kip
Stress from Doc. /Rev.: Calc-3015276-002 (Rule 88 A.15.c)

Tensile = 3.50 ksi

Shear = 13.2 ksi

Bending = 26.3 ksi

Combined = 37.6 ksi < 50 ksi

Stress from Doc. /Rev.: Calc-3015276-002 (10 CFR 71.45)

Tensile = 3.50 ksi

Shear = 13.2 (5/2) = 33 ksi

Bending = 26.3 (5/2) = 65.75 ksi

Combined = 89.8 ksi > 65 ksi

From the stress results listed above, 100% penetration weld will be required on all attachments to the railcar deck plate.

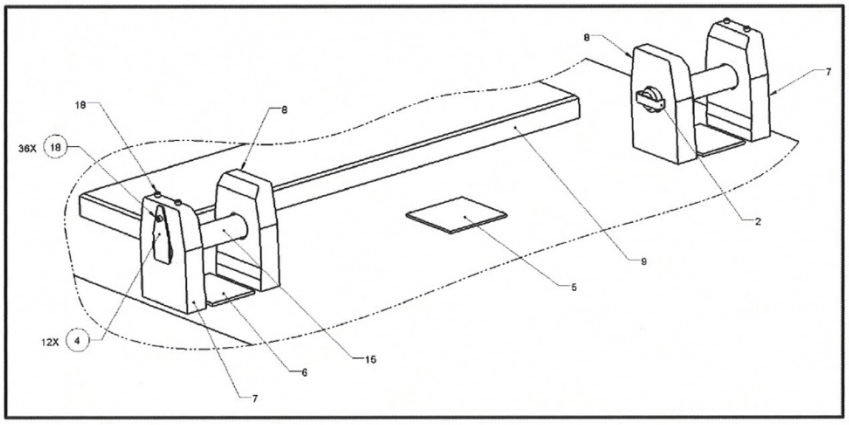


Figure 5-2: Shear Blocks

Shear Block Weld Calculations:

All attachments are to be welded to the deck plate.

Longitudinal Load 2,921 kips

Length of shear block = (21in + 90 in) 2 = 222 inches

q = P/L = 2921 kip / 222 inches = 13.2 k/in (Rule 88 A.15.c)

q = P (10/7.5)/L = 2921 kip (10/7.5) / 222 inches = 17.5 k/in (10 CFR 71.45)

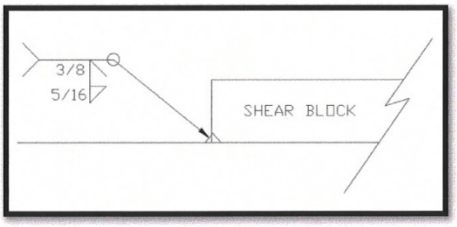
Throat size for bevel and fillet weld shown below:

Throat = $((5/16)^2 + (3/8)^2)^{1/2} = 0.49$

(0.49) (33.06) =16.2 k/in

16.2 k/in > 13.2 k/in (Rule 88 A.15.c)

16.2 k/in < 17.5 k/in (10 CFR 71.45)



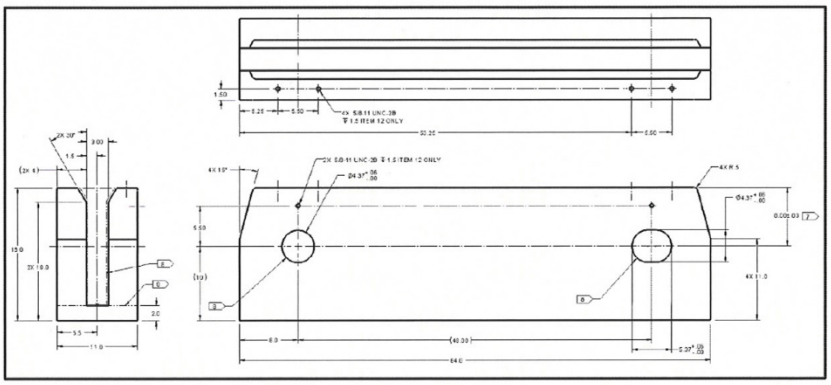


Figure 5-9: Outer Pin Attachment Block

Outer Pin Block Attachment Weld Calculations: (10 CFR 71.45)

All attachments are to be welded to the deck plate.

Longitudinal Load 944 (10/7.5) =1258.7 kip

Vertical Loads 1077 kip

The moment was taken about the CG of the weld.

t = thickness of weld

Moment = 1258.7 kip (10 in) + 2 1077 kip (24 in) = 64,283 in-k

A= (128 + 22) t = 150 t

I_{yy} = 1/12 (2) $(64in)^3$ t + 2 (11 in) t $(32 in)^2$

I = 43690t + 22528t = 66218t

S = (t) 66218/ 32 = 2069.3t

F' = 1258.7/150t = 8.4/t

F" = M/S = 64,283/2069.3=31.07/t

F = $((8.4/t)^2 + (31.07/t)^2)^{1/2}$ = 32.2/t

32.2/33.06 = t = 0.97 which is required

7/8" bevel with 3/8" fillet = t = $((7/8)^2 + (3/8)^2)^{1/2}$ = 0.95 in < 0.97 required to fail. (10 CFR 71.45)

Outer Pin Block Attachment Weld Calculations: (Rule 88 A.15.c)

All attachments are to be welded to the deck plate.

Longitudinal Load 944 kip

Vertical Loads 1077 kip

The moment was taken about the CG of the weld.

t = thickness of weld

Moment = 944 kip (10 in) + 2 (1077 kip) (24 in) = 61,136 in-k

A= (128 + 22) t = 150 t

I_{yy} =1/12 (2) $(64in)^3$ t + 2 (11 in) t $(32 in)^2$

I = 43690t + 22528t = 66218t

S = (t)66218/ 32 = 2069.3t

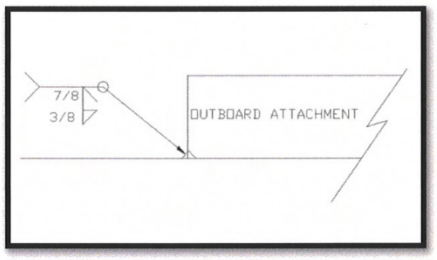
F' = 944/150t = 6.3/t

F" = M/S = 61,136/2069.3t = 29.54/t

$F = ((6.3/t)^2 + (29.54/t)^2)^{1/2} = 30.2/t$

30.2/33.06 = t = 0.91 which is required

7/8" bevel with 3/8" fillet = $t = ((7/8)^2 + (3/8)^2)^{1/2} = 0.95$ in > 0.91 which is required (Rule 88 A.15.c)



IMPLEMENTED 11/2017

4.3.4.1.3 Allowable Design Stresses in Welds

Table 4.3 Allowable design stresses in welds

Kind of Stress	Allowable Design Stress	Metal and Filler Requirements
Tension and compression parallel to the axis of any complete-penetration groove weld	Same as for base metal	Per AWS D15.1, Table 8.1
Tension normal to the axis of complete-penetration groove weld	Same as allowable tensile stress for base metal	
Compression normal to the axis of complete- or partial-penetration groove weld	Same as allowable compressive stress for base metal	
Shear on effective throat of complete-penetration groove weld and partial-penetration groove weld	Same as allowable shear stress for base metal	
Shear stress on effective[a/] throat of fillet weld regardless of direction of application of load; tension normal[b/] to the axis on the effective throat of a partial-penetration groove weld; and shear stress on the effective area of a plug or slot weld. The given stresses shall also apply to such welds made with the specified electrode on steel having a yield stress greater than that of the "matching" base metal. The allowable stress, regardless of electrode classification used, shall not exceed that given in the table for the weaker "matching" base metal being joined.	29.0 ksi	Per AWS D15.1, Table 8.1 Class I
	33.06 ksi	AWS D15.1, Table 8.1 Class II
	38.86 ksi	AWS D15.1, Table 8.1 Class III
	50.46 ksi	AWS D15.1, Table 8.1 Class IV
	56.84 ksi	AWS D15.1, Table 8.1 Class V

a/ For definition of effective throat of fillet welds and partial-penetration groove welds, see paragraph 4.3.4.1.

b/ Fillet welds and partial-penetration groove welds joining the component elements of built-up members, such as flange-to-web connections, may be designed without regard to the tension or compression stress in these elements parallel to the axis of these welds.

Table 8.1 (Continued)
Prequalified Base Metal—Filler Metal Combinations for Matching Strength

Steel Specification Requirements						Filler Metal Requirements[j]		
		Minimum Yield Point/Strength		Tensile Range				
Steel Specification[a,b,c]		ksi	MPa	ksi	MPa	Process	AWS Electrode Specification	Electrode Classification[f,h,k]
Class I (Continued)								
	HSLAS Grade 45 Class 2	45	310	55	380			
	HSLAS Grade 50 Class 2	50	345	60	414			
	HSLAS-F Grade 50	50	345	60	414			
API 5L	Grade B	35	241	60 min.	414 min.			
	Grade X42	42	290	60 min.	414 min.			
AAR M201	Grade A	30	207	60 min.	414 min.			
	Hot rolled, annealed, or normalized weldable steel grades purchased to max. limits of C 0.28, Mn 1.00, P 0.04, S 0.05	(Note g)		(Note g)				
ABS	Grades A, B, CS, D, DS, and E	---		58/71	400/490			
Class II								
ASTM A27	Grade 65-35	35	241	65 min.	448 min.	SMAW	A5.1/A5.1M	E7015
	Grade 70-36	36	248	70 min.	483 min.			E7016
	Grade 70-40	40	276	70 min.	483 min.			E7018
ASTM A131	Grades AH32, DH32, EH32	45.5	314	68/85	469/586			E7028
	Grades AH36, DH36, EH36	51	352	71/90	490/621		A5.5/A5.5M	E7015-XX
	EH36							E7016-XX
ASTM A216	Grade WCB	36	248	70 min.	483 min.			E7018-XX
	Grade WCC	40	276	70 min.	483 min.	SAW	A5.17/A5.17M	F7AX-EXXX
ASTM A242[e]	Type 1	42/50	290/345	63/70	434/483		A5.23/A5.23M	F7AX-EXX-XX
ASTM A441		42/50	290/345	63/70	434/483	GMAW	A5.18/A5.18M	ER70S-X
ASTM A500	Grade C	46	317	62 min.	427 min.			E70C-3X
ASTM A515	Grade 65	35	241	64/85	441/586			E70C-6X
	Grade 70	38	262	70/90	482/621		A5.36/A5.36M	E7XTX-XXX-X
ASTM A516	Grade 65	35	241	65/77	448/531			E8XTX-XXX-X
	Grade 70	38	262	70/85	483/586	FCAW	A5.20/A5.20M	E7XT-X
ASTM A537	Class 1	50	345	70/90	483/621			(Except -2, -3, -10, -GS)
ASTM A572	Grade 42	42	290	60 min.	414 min.		A5.29/A5.29M	E7XTX-XX
	Grade 50	50	345	65 min.	448 min.		A5.36/A5.36M	E7XTX-XXX-X
ASTM A588[e]	(4 in (100 mm) and under)	50	345	70 min.	483 min.			E8XTX-XXX-X
ASTM A595	Grade A	55	379	65 min.	448 min.			

(Continued)

Table 8.1 (Continued)
Prequalified Base Metal—Filler Metal Combinations for Matching Strength

Steel Specification Requirements						Filler Metal Requirements[j]		
		Minimum Yield Point/Strength		Tensile Range				
	Steel Specification[a,b,c]	ksi	MPa	ksi	MPa	Process	AWS Electrode Specification	Electrode Classification[c,h,i]
				Class H (Continued)				
	Grades B and C	60	414	70 min.	483 min.			
ASTM A606		45	310	65 min.	448 min.			
ASTM A607	Grade 45	45	310	60 min.	414 min.			
	Grade 50	50	345	65 min.	448 min.			
	Grade 55	55	379	70 min.	483 min.			
ASTM A618		50	345	70 min.	483 min.			
ASTM A633	Grades A, B[e]	42	290	63/83	434/572			
	Grades C, D (2-1/2 in [64 mm] and under)	50	345	70/90	483/621			
ASTM A656	Grade 60	60	414	70 min.	483 min.			
ASTM A709	Grade 50	50	345	65 min.	448 min.			
	Grade 50W	50	345	70 min.	483 min.			
ASTM A1008	SS Grade 50	50	340	65	410			
	HSLAS Grade 50 Class 1	50	340	65	450			
	HSLAS Grade 55 Class 1	55	380	70	480			
	HSLAS Grade 55 Class 2	55	380	65	448			
	HSLAS Grade 60 Class 2	60	410	70	480			
	HSLAS-F Grade 60	60	410	70	480			
ASTM A1011	SS Grade 50	50	345	65	448			
	HSLAS Grade 50 Class 1	50	345	65	448			
	SS Grade 55	55	379	70	483			
	HSLAS Grade 55 Class 1	55	379	70	483			
	HSLAS Grade 55 Class 2	55	379	65	448			
	HSLAS Grade 60 Class 2	60	414	70	483			
	HSLAS-F Grade 60	60	414	70	483			
ASTM A1018	HSLAS Grade 50 Class 1	50	340	65	448			
	HSLAS Grade 55 Class 1	55	379	70	483			
	HSLAS Grade 55 Class 2	55	379	65	448			
	HSLAS Grade 60 Class 2	60	414	70	483			
	HSLAS-F Grade 60	60	414	70	483			
API 2N(5)		42	290	62/80	427/552			

(Continued)

Table 8.1 (Continued)
Prequalified Base Metal—Filler Metal Combinations for Matching Strength

Steel Specification Requirements						Filler Metal Requirements[j]		
		Minimum Yield Point/Strength		Tensile Range				
	Steel Specification[a,b,c]	ksi	MPa	ksi	MPa	Process	AWS Electrode Specification	Electrode Classification[f,h,i]
				Class II (Continued)				
API 5LX	Grade X52	52	359	66/72	455/496			
ABS	Grades AH32, DH32, EH32	45.5	313	71/90	490/621			
	Grades AH32, DH32, EH36(5)	51	352	71/90	490/620			
AAR M201	Grade B	38	262	70 min.	483 min.			
	Hot rolled, annealed, or normalized weldable grades of carbon steel purchased to max. limits of C 0.34, Mn 1.00, P 0.04, S 0.05	(Note g)		(Note g)				
				Class III				
ASTM A537	Class 2(5)	60	414	80/100	552/689	SMAW	A5.5/A5.5M	E8015-XX
ASTM A572	Grade 60	60	414	75 min.	517 min.			E8016-XX
	Grade 65	65	448	80 min.	552 min.			E8018-XX
ASTM A633	Grade E(5)	60	414	80/100	552/689	SAW	A5.23/A5.23M	F8AX-EXX-XX
ASTM A1008	SS Grade 60	60	414	75	517	GMAW	A5.28/A5.28M	ER80S-XX
	HSLAS Grade 60 Class 1	60	414	75	517			E80C-XX
	HSLAS Grade 65 Class 1	65	448	80	552		A5.36/A5.36M	E8XTX-XXX-X
	HSLAS Grade 65 Class 2	65	448	75	517	FCAW	A5.29/A5.29M	E8XTX-XX
	HSLAS Grade 70 Class 2	70	483	80	552		A5.36/A5.36M	E8XTX-XXX-X
	HSLAS-F Grade 70	70	483	80	552			
ASTM A1011	SS Grade 60	60	414	75	517			
	HSLAS Grade 60 Class 1	60	414	75	517			
	HSLAS Grade 65 Class 1	65	448	80	552			
	HSLAS Grade 65 Class 2	65	448	75	517			
	HSLAS Grade 70 Class 2	70	483	80	552			
	HSLAS-F Grade 70	70	483	80	552			
ASTM A1018	HSALS Grade 60 Class 1	60	414	75	517			
	HSLAS Grade 65 Class 1	65	448	80	552			
	HSLAS Grade 65 Class 2	65	448	75	517			
	HSLAS Grade 70 Class 2	70	483	80	552			
	HSLAS-F Grade 70	70	483	80	552			
AAR TC128	Grade B	50	345	81/101	558/696			
AAR M201	Grade B+	50	345	80 min.	552 min.			

(Continued)

TÜVRheinland®
Industrial Solutions

MAGNETIC PARTICLE INSPECTION REPORT

Mr. Mark Zeigler
Kasgro Rail Corporation
121 Rundle Road
New Castle, PA 16102

Report #: 23 Page 1 of 2
P.O. #: K180079
Work Order #: 473037
Project: Atlas Cask Car

Date: March 4, 2019
Description: Perform Magnetic Particle Inspections of Deck Attachments for Cask car #1

TRIS Procedure: WI-08-002 Rev. 5

Surface Condition: As Welded

Test Method Standard: ASTM E709

Acceptance Standard: AWS D15.1

Type of Material: Carbon Steel

Production Stage:
X In Progress
____ Final
____ Other

For Welds:
X Root Pass
____ Intermediate
____ Final

Equipment Identification:
Model #: Parker DA400
Gage #/Serial #: P135/17999
Cal. Date Due: 6-18-19

Product / Weld Identification Car Body Assembly	Accept	Reject	Linear	Rounded	Cracks	Undercut	Other	Defect Location or Remarks
Item #7 (4)								Outside Lugs
Root								See report #15
Final								See report #17
Item #8 (4)								Inside Lugs
Root								See report #15
Final								See report #17
Item #11 to 3-10								
"A" End								
Final	/							
"B" End								
Final	/							
Item #10 to 3-10								
"A" End (2)								
Final	/							
"B" End (2)								
Final	/							

Technique

Technique #: N/A
Method: Wet ____ Dry X
Fluorescent ____ Visible X

Consumable Batch #: 08A078
Coil N/A FWDC N/A
Head Shot N/A Prods N/A
Amperage: N/A

Yoke Current: AC X DC ____
UV Meter #: N/A
UV Intensity verified at prescribed intervals?
Yes ____ No ____ N/A X
Quantity Tested 100%: X
Random: N/A %

SIGNED: Kasgro Rail

Technician: Daniel S. Gjurich Level: II

Reviewed By: _____ Date: 3/5/19

Testing was performed in accordance with accepted industry practice as well as the test methods referenced TUV Rheinland Industrial Solutions, Inc. has no direct knowledge of the origin, sampling procedure, nor condition of the samples, and makes no claims as to the suitability nor final use of the material. This test report applies only to those items tested. This report shall not be reproduced except in full without the written consent of TUV Rheinland Industrial Solutions, Inc.

TÜVRheinland®
Industrial Solutions

MAGNETIC PARTICLE INSPECTION REPORT

Mr. Mark Zeigler
Kasgro Rail Corporation
121 Rundle Road
New Castle, PA 16102

Report #: 23 Page 2 of 2
P.O. #: K180079
Work Order #: 473037
Project: Atlas Cask Car

Date: March 4, 2019
Description: Perform Magnetic Particle Inspections of Deck Attachments for Cask car #1

TRIS Procedure: WI-08-002 Rev. 5

Surface Condition: As Welded

Test Method Standard: ASTM E709

Acceptance Standard: AWS D15.1

Type of Material: Carbon Steel

Production Stage:
X In Progress
____ Final
____ Other

For Welds:
X Root Pass
____ Intermediate
____ Final

Equipment Identification:
Model #: Parker DA400
Gage #/Serial #: P135/17999
Cal. Date Due: 6-18-19

Product / Weld Identification Car Body Assembly	Accept	Reject	Linear	Rounded	Cracks	Undercut	Other	Defect Location or Remarks
Item #12 to 3-10								
"A" End								
Final	/							
"B" End								
Final	/							
Item #9 to 3-10								
"A" Side of Center	/							
"B" Side of Center	/							

Technique

Technique #: N/A
Method: Wet ____ Dry X
Fluorescent ____ Visible X

Consumable Batch #: 08A078
Coil N/A FWDC N/A
Head Shot N/A Prods N/A
Amperage: N/A

Yoke Current: AC X DC ____
UV Meter #: N/A
UV Intensity verified at prescribed intervals?
Yes ____ No ____ N/A X
Quantity Tested 100%: X
Random: N/A %

SIGNED: Kasgro Rail

Technician: Daniel S. Gjurich Level: II

Reviewed By: _____ Date: 3/5/19

Testing was performed in accordance with accepted industry practice as well as the test methods referenced TUV Rheinland Industrial Solutions, Inc. has no direct knowledge of the origin, sampling procedure, nor condition of the samples, and makes no claims as to the suitability nor final use of the material. This test report applies only to those items tested. This report shall not be reproduced except in full without the written consent of TUV Rheinland Industrial Solutions, Inc.

TÜVRheinland®
Industrial Solutions

VISUAL INSPECTION REPORT

Mr. Mark Zeigler
Kasgro Rail Corporation
121 Rundle Road
New Castle, PA 16102

Report #: 22 Page 1 of 3
P.O. #: K180079
Work Order #: 473037
Project: Atlas

Date: March 4, 2019
Description: Perform Visual Inspections of Deck Attachments for Cask car #1

TRIS Procedure:	Surface Condition:	Production Stage:		VT Gauge Identification:	
NDE-VT-1	As Welded	X	In Progress	Mfg.	G.A.L.
Test Method Standard:	Percent of Inspection:		Final	Weld Gauge	¼",3/8" and ½" Fillet
AWS D15.1	X 100%		Other	Model	#269-465-5750
Acceptance Standard:	%	For Welds:		Serial #	Cert #F4858
AWS D15.1		X	Root Pass	Other	Cam Type Gage
Product Form:			Intermediate		
N/A		X	Final		
Type of Material: Carbon Steel					

Product / Weld Identification	Accept	Reject	Linear	Rounded	Cracks	Undercut	Lack Fusion	Incomplete Pen	Exceed Reinforcement	Weld Undersized	Defect Location, Length
Item #7 to 3-10 (4)											
Root											See Report #16
Final											See Report #16
Item #8 to 3-10 (4)											
Root											See Report #16
Final											See Report #16
Item #11 to 3-10											
"A" End											
Root											See Report #16
Final											See Report #16
"B" End											
Root											See Report #16
Final											See Report #16
SIGNED:											

Daniel S Gjurich
CWI 93041171
QC1 EXP. 4/1/2020

Technician: Daniel S. Gjurich Level: CWI #93041171

Reviewed By: Date: 3/5/19

Testing was performed in accordance with accepted industry practice as well as the test methods referenced TUV Rheinland Industrial Solutions, Inc. has no direct knowledge of the origin, sampling procedure, nor condition of the samples, and makes no claims as to the suitability nor final use of the material. This test report applies only to those items tested. This report shall not be reproduced except in full without the written consent of TUV Rheinland Industrial Solutions, Inc.

VISUAL INSPECTION REPORT

Mr. Mark Zeigler
Kasgro Rail Corporation
121 Rundle Road
New Castle, PA 16102

Report #: 22 Page 2 of 3
P.O. #: K180079
Work Order #: 473037
Project: Atlas

Date: March 4, 2019
Description: Perform Visual Inspections of Deck Attachments for Cask car #1

TRIS Procedure:	**Surface Condition:**	**Production Stage:**	**VT Gauge Identification:**
NDE-VT-1	As Welded	X In Progress	Mfg. G.A.L.
Test Method Standard:	**Percent of Inspection:**	Final	Weld Gauge ¼",⅜" and ½" Fillet
AWS D15.1	X 100%	Other	Model #269-465-5750
Acceptance Standard:	%	**For Welds:**	Serial # Cert #F4858
AWS D15.1		X Root Pass	Other Cam Type Gage
Product Form:		Intermediate	
N/A		X Final	
Type of Material: Carbon Steel			

Product / Weld Identification	Accept	Reject	Linear	Rounded	Cracks	Undercut	Lack Fusion	Incomplete Pen	Exceed Reinforcement	Weld Undersized	Defect Location, Length
Item #10 to 3-10											
"A" End (2)											
Root											See Report #16
Final											See Report #16
"B" End (2)											
Root											See Report #16
Final											See Report #16
Item #12 to 3-10											
"A" End											
Root											See Report #16
Final											See Report #16
"B" End											
Root											See Report #16
Final											See Report #16
SIGNED:											

AWS® Daniel S Gjurich
CWI 93041171
QC1 EXP. 4/1/2020

Technician: Daniel S. Gjurich Daniel S Gjurich Level: CWI #93041171

Reviewed By: _____ Date: 3/5/19

Testing was performed in accordance with accepted industry practice as well as the test methods referenced TUV Rheinland Industrial Solutions, Inc. has no direct knowledge of the origin, sampling procedure, nor condition of the samples, and makes no claims as to the suitability nor final use of the material. This test report applies only to those items tested. This report shall not be reproduced except in full without the written consent of TUV Rheinland Industrial Solutions, Inc.

NDTQ-0100
March 19, 2004
ddk

TÜVRheinland®
Industrial Solutions

VISUAL INSPECTION REPORT

Mr. Mark Zeigler
Kasgro Rail Corporation
121 Rundle Road
New Castle, PA 16102

Report #: 22 Page 3 of 3
P.O. #: K180079
Work Order #: 473037
Project: Atlas

Date: March 4, 2019
Description: Perform Visual Inspections of Deck Attachments for Cask car #1

TRIS Procedure: NDE-VT-1	**Surface Condition:** As Welded	**Production Stage:**	**VT Gauge Identification:**
Test Method Standard: AWS D15.1	**Percent of Inspection:** X 100%	___ In Progress	Mfg. G.A.L.
Acceptance Standard: AWS D15.1	___ %	X Final	Weld Gauge ¼",3/8" and ½" Fillet
Product Form: N/A		___ Other	Model #269-465-5750
Type of Material: Carbon Steel		**For Welds:**	Serial # Cert #F4858
		___ Root Pass	Other Cam Type Gage
		___ Intermediate	
		X Final	

Product / Weld Identification Car Body Assembly	Accept	Reject	Linear	Rounded	Cracks	Undercut	Lack Fusion	Incomplete Pen	Exceed Reinforcement	Weld Undersized	Defect Location, Length
Item #5 to 3-10											
"A" Side of Center											See Report #18
"B" Side of Center											See Report #18
Item #6 to 3-10 (4)											
"A" Side of Center (Left)											See Report #18
"A" Side of Center (Right)											See Report #18
"B" Side of Center (Left)											See Report #18
"B" Side of Center (Right)											See Report #18
Item #9 to 3-10											
"A" Side of Center	/										
"B" Side of Center	/										

Daniel S Gjurich
CWI 93041171
QC1 EXP. 4/1/2020

SIGNED: Kasgro Rail

Technician: Daniel S. Gjurich Daniel S Gjurich Level: CWI #93041171

Reviewed By: C A Date: 3/5/19

Testing was performed in accordance with accepted industry practice as well as the test methods referenced TUV Rheinland Industrial Solutions, Inc. /as no direct knowledge of the origin, sampling procedure, nor condition of the samples, and makes no claims as to the suitability nor final use of the material. This test report applies only to those items tested. This report shall not be reproduced except in full without the written consent of TUV Rheinland Industrial Solutions, Inc.

NDTG-0100
March 19, 2004
dfk

Appendix L. Test Zone Compliance for Dynamic Test Regimes

TTCI performs measurement of Chapter 11 test zones at a minimum annually or at the discretion of clients entering official testing. TTCI's policy establishes test zone measurements be considered valid for 6 months from the last measurement that meets specifications. Table K-1 details the Atlas car test dates for each Chapter 11 and S-2043 special test zones along with the associated measurement date that the test zone was found to comply with the AAR specifications for specified test zones.

Table K1. Atlas Car Test Dates and Test Zone Measurement Compliance Date

Test Zone	Atlas Load Condition	Date Tested	Measurement Date Demonstrating Compliance after Engineering Review
Hunting with KR Profiles	Minimum Test Load	11/14/2019	9/10/2019
Hunting with IWS		10/7/2020	6/20/2020
Twist and Roll		9/14/2020	6/10/2020
Dynamic Curving		6/25/2021, 6/28/2021	3/31/2021
Single Bump		10/5/2020	9/16/2020
Curve Entry/Exit		6/25/2021, 6/28/2021	4/19/2021
Curving with Single Rail Perturbation		10/5/2020, 12/9/2020	8/20/2020
Constant Curving		6/25/2021, 6/28/2021	4/19/2021
Special Trackwork		10/8/2020	7/7/2020, 7/10/2020

Test Zone	Atlas Load Condition	Date Tested	Measurement Date Demonstrating Compliance after Engineering Review
Hunting with KR Profiles	Maximum Test Load	12/11/2019	11/18/2019
Hunting with IWS		7/6/2020	6/20/2020
Twist and Roll		6/30/2020, 7/1/2020	6/10/2020
Yaw and Sway		9/2/2020, 9/3/2020	6/8/2020
Dynamic Curving		6/25/2020, 6/29/2020, 6/30/2020	3/26/2020
Pitch and Bounce (Chapter 11)		6/30/2020, 7/1/2020	4/15/2020
Single Bump		7/6/2020	5/18/2020
Curve Entry/Exit		6/25/2020, 6/30/2020	3/26/2020
Curving with Single Rail Perturbation		8/26/2020	8/20/2020
Constant Curving		6/25/2020, 6/30/2020	3/26/2020
Special Trackwork		8/27/2020, 8/31/2020	7/7/2020, 7/10/2020

TRANSPORTATION TECHNOLOGY CENTER, INC.
A wholly owned subsidiary of the Association of American Railroads

55500 DOT Road • Pueblo, CO 81001
www.aar.com

APPENDIX E
P-21-049 ATLAS CAR POST TEST ANALYSIS REPORT (FORMERLY P-21-042)

ATLAS CAR POST TEST ANALYSIS REPORT

P-21-049

(formerly P-21-042)

Prepared for United States Department of Energy

October 26, 2022
Revised December 6, 2022

PROPRIETARY REPORT

TTCI®
TRANSPORTATION TECHNOLOGY CENTER, INC.

ATLAS CAR POST TEST ANALYSIS REPORT

Prepared for United States Department of Energy

P-21-049
(formerly P-21-042)

Prepared by
Russell Walker
Michael Craft
MaryClara Jones
Matt DeGeorge

Transportation Technology Center, Inc.
A subsidiary of the Association of American Railroads
Pueblo, Colorado USA

October 26, 2022
Revised December 6, 2022

ERRATA STATEMENT

Report: P-21-049

Errata refer to the correction of errors introduced to the article by the publisher. The following errors have been found and corrected since this report was originally submitted.

In MxV Rail report, P-21-042, "Cask Car Post-Test Analysis (S-2043 Section 8.0) and Final Report," two inadvertent typographical errors were present. The corrected text is as follows.

- **Cover and inside cover:** As listed in the committee approved letter dated April 29, 2022 (File 209.240), the report number was erroneously listed as P-21-042. The corrected report number is P-21-049.
- **Executive Summary**, p. ii, fourth column of table, information corrected: "Wheel load at 43% during 3" drop condition." Corrected to "Wheel load at 24% during 3" drop condition."

Standard S-2043 Section	Met/Not Met		
	Preliminary Simulations CSM 58 pads	Revised Simulations CSM 58 pads	Test Result and Details if Not Met
5.2 Nonstructural Static Tests			
4.2.1/5.2.1 Truck Twist Equalization	Met	Not Simulated	Not Met with CSM 58 pads **Minimum Test Load:** Wheel load at 50% during 2″ drop condition. Wheel load at 24% during 3″ drop condition. **Maximum Test Load:** Wheel load at 43% during 2″ drop condition. Wheel load at 29% during 3″ drop condition.

- Section 8.0 Conclusions, Table 65, p. 90, information corrected. Sentence "Wheel load at 43% during 3" drop condition." Corrected to "Wheel load at 24% during 3" drop condition."

Standard S-2043 Section	Met/Not Met		
	Preliminary Simulations	Revised Simulations CSM 58 pads	Test Result and Details if Not Met
5.2 Nonstructural Static Tests			
4.2.1/5.2.1 Truck Twist Equalization	Met	Not Simulated	Not Met with CSM 58 pads – **Minimum Test Load:** Wheel load at 50% during 2" drop condition. Wheel load at 24% during 3" drop condition. **Maximum Test Load:** Wheel load at 43% during 2" drop condition. Wheel load at 29% during 3" drop condition.

For questions or comments on this document, contact **Russell_Walker@aar.com.**

Disclaimer: This report was prepared for the United States Department of Energy (DOE) by Transportation Technology Center, Inc. (TTCI), a subsidiary of the Association of American Railroads, Pueblo, Colorado. It is based on investigations and tests conducted by TTCI with the direct participation of DOE to criteria approved by them. The contents of this report imply no endorsements whatsoever by TTCI of products, services, or procedures, nor are they intended to suggest the applicability of the test results under circumstances other than those described in this report. The results and findings contained in this report are the sole property of DOE. They may not be released by anyone to any party other than DOE without the written permission of DOE. TTCI is not a source of information with respect to these tests, nor is it a source of copies of this report. TTCI makes no representations or warranties, either expressed or implied, with respect to this report or its contents. TTCI assumes no liability to anyone for special, collateral, exemplary, indirect, incidental, consequential, or any other kind of damages resulting from the use or application of this report or its contents.

Executive Summary

Transportation Technology Center, Inc., (TTCI) a subsidiary of the Association of American Railroads (AAR), performed certification testing and modeling on the United States Department of Energy's (DOE) 12-axle cask car (Atlas car). The Atlas car has been developed as part of the DOE's Atlas railcar Design Project that is intended to meet the need for future large-scale transport of spent nuclear fuel and high-level radioactive waste. Tests and modeling were performed according to the AAR's *Manual of Standards and Recommended Practices* (MSRP), Standard S-2043, "Performance Specification for Trains Used to Carry High-Level Radioactive Material," revised 2017.[1]

The objective of this report is to demonstrate acceptable railcar performance. This objective was accomplished by comparing the test results to the modeling predictions as part of the structural and dynamic analysis of the DOE Atlas car. Where necessary, the revised simulation predictions are presented.

The preliminary simulations were performed according to Standard S-2043, Paragraph 4.3 as part of the railcar design phase before the prototype car was built. The results of the preliminary simulation were submitted to the AAR as part of the preliminary design review package. The test results have been compared to the preliminary dynamic analysis predictions and revised model predictions in this report to verify that the model accurately represents the vehicle as required in Standard S-2043, Paragraph 8.

As originally equipped with chlorosulfonated polyethylene (CSM) 58 primary pads, the Atlas railcar with a minimum test load did not meet the Standard S-2043 single-car dynamic test requirement for hunting (Standard S-2043, Paragraph 5.5.7). The hunting tests were the first tests to be performed, and the testing process was paused to solve this problem. During troubleshooting tests the railcar met the hunting requirements with stiffer CSM 70 primary suspension pads, and all the remaining dynamic tests were completed with these pads. With the stiffer pads, the performance met the hunting requirements but not all the curving requirements. After reviewing the available data with the AAR Equipment Engineering Committee (EEC), TTCI performed additional troubleshooting and found that the CSM 58 pads provided the best balance between the curving and the hunting performance results.

The testing data was used to revise the preliminary multi-body vehicle dynamics models that had used CSM 58 pads and to modify this revised model into one that used the CSM 70 primary pads. Both revised models showed good alignment with most relevant testing data, such as wheel loads, although some variation between the predicted behavior and the tested behavior was observed. Regimes with existing CSM 70 pad test data were re-modeled using CSM 70 pads to demonstrate the model was validated. These regimes were also modeled with CSM 58 pads to show the change in performance with the final pad. Numerous other simulations, (in addition to creating and solving models to replicate the conducted tests), were performed to estimate the car's behavior in conditions that are not easily tested, such as buff and draft curving, rail lubrication, and the effect of worn components.

Like the earliest tests, the revised model of the car equipped with CSM 58 pads did not meet the criterion for the standard deviation of lateral carbody acceleration in the hunting regime. In addition, the model revealed other simulation-only regimes, including curving with single rail perturbation simulation regimes with 3-inch amplitude and curving with various lubrication conditions, where the requirements were not met. However, in most circumstances, the model was more conservative than the test results and is indicative of the actual performance.

The following table shows a summary of the test results and the model predictions for the Atlas railcar:

Standard S-2043 Section	Met/Not Met		
	Preliminary Simulations CSM 58 pads	**Revised Simulations CSM 58 pads**	**Test Result and Details if Not Met**
5.2 Nonstructural Static Tests			
4.2.1/5.2.1 Truck Twist Equalization	Met	Not Simulated	Not Met with CSM 58 pads **Minimum Test Load:** Wheel load at 50% during 2″ drop condition. Wheel load at 24% during 3″ drop condition. **Maximum Test Load:** Wheel load at 43% during 2″ drop condition. Wheel load at 29% during 3″ drop condition.
4.2.2/5.2.2 Carbody Twist Equalization	Met	Not Simulated	Met with CSM 58 pads
4.2.3/5.2.3 Static Curve Stability	Met	Not Simulated	Met with CSM 58 pads
4.2.4/5.2.4 Horizontal Curve Negotiation	Met	Not Simulated	Met with CSM 58 pads
5.4 Structural Tests			
5.4.2 Squeeze (Compressive End) Load	Met	Not Simulated	Met with CSM 58 pads
5.4.3 Coupler Vertical Loads	Met	Not Simulated	Met with CSM 58 pads
5.4.4 Jacking	Met	Not Simulated	Met with CSM 58 pads
5.4.5 Twist	Met	Not Simulated	Met with CSM 58 pads
5.4.6 Impact	Met	Not Simulated	Met with CSM 58 pads
5.5 Dynamic Tests			
4.3.11.3/5.5.7 Hunting	Met	Not Met At Minimum Test Load: Car unstable at speeds greater than 65 mph with KR wheel profiles Meets with Maximum Test Load	Not Met with CSM 58 pads At Minimum Test Load: Car unstable at speeds greater than 65 mph with KR wheel profiles Meets with Maximum Test Load

Standard S-2043 Section	Met/Not Met		
	Preliminary Simulations CSM 58 pads	**Revised Simulations CSM 58 pads**	**Test Result and Details if Not Met**
4.3.9.6/5.5.8 Twist and Roll	Met	Met	Not tested with CSM 58 pads – Met with CSM 70 pads
5.5.9 Yaw and Sway	Met	Met	Not tested with CSM 58 pads – Met with CSM 70 pads
5.5.10 Dynamic Curving	Not Met Max. Test Load Wheel L/V 0.88, Limit=0.8, A-end and B-end lead, 39-ft. input	Met	Met with CSM 58 pads – Not met with CSM 70 pads (0.81 Wheel L/V)
4.3.9.7/5.5.11 Pitch and Bounce (Chapter 11)	Met	Met	Not tested with CSM 58 pads – Met with CSM 70 pads
4.3.9.7/5.5.12 Pitch and Bounce (Special)	Met	Not Simulated	Not tested
		Truck center spacing close to Chapter 11 wavelength	
4.3.10.1/5.5.13 Single Bump Test	Met	Met	Not tested with CSM 58 pads – Met with CSM 70 pads
4.3.11.6/5.5.14 Curve Entry/Exit	Met	Met	Not tested with CSM 58 pads – Met with CSM 70 pads
4.3.10.25.5.15 Curving with Single Rail Perturbation	Not met **Empty with Ballast Load:** Wheel L/V 0.96, Limit=0.8 Truck Side L/V 0.52, Limit=0.5 **Loaded** 5.0-degree roll angle, Limit=4.0	Not met **Minimum Test Load** Carbody roll angle =4.2, limit=4.0 **Maximum Test Load** Carbody roll angle =4.7, limit=4.0	Minimum Test Load: Not met with CSM 70 pads (Wheel L/V = 0.88, Truck L/V = 0.50), not tested with CSM 58 pads
4.3.11.4/5.5.16 Standard Chapter 11 Constant Curving	Met	Met	Not tested with CSM 58 pads – Not Met with CSM 70 pads: **Minimum Test Load:** Wheel L/V ratio = 0.86 95% Wheel L/V ratio = 0.66 **Maximum Test Load:** 95% Wheel L/V ratio = 0.63
4.3.11.7/5.5.17 Special Trackwork, No 7 Crossovers	Not Met **Loaded:** Truck side L/V Ratio=0.52, Limit=0.5	Met	Not tested with CSM 58 pads – Met with CSM 70 pads on a No 10 crossover

Standard S-2043 Section	Met/Not Met		
	Preliminary Simulations CSM 58 pads	**Revised Simulations CSM 58 pads**	**Test Result and Details if Not Met**
4.3.11.5 Curving with Various Lubrication Conditions	Not Met **Min Test Load with new profiles:** 95% Wheel L/V = 0.62 (Case 2), Limit=0.6 95% Wheel L/V = 0.66 (Case 4), Limit=0.6 **Min Test Load with worn profiles:** Truck Side L/V = 0.56 (Case 1), 0.62 (Case 2), 0.61 (Case 4), Limit=0.5 95% Wheel L/V = 0.68 (Case 2), 0.61 (Case 4), Limit=0.6 **Max Test Load with worn profiles:** Truck Side L/V = 0.56 (Case 1), 0.62 (Case 2), 0.61 (Case 4), Limit=0.5 95% Wheel L/V = 0.68 (Case 2), 0.61 (Case 4), Limit=0.6	Not Met in following cases **Min Test Load with new profiles:** 95% Wheel L/V = 0.62 (Case 4), Limit=0.6 **Min Test Load with worn profiles:** Truck Side L/V = 0.53 (Case 1), 0.61 (Case 2), 0.58 (Case 4), Limit=0.5 95% Wheel L/V = 0.64 (Case 2), Limit=0.6 **Max Test Load with worn profiles:** Truck Side L/V = 0.52 (Case 1), 0.60 (Case 2), 0.58 (Case 4), Limit=0.5 95% Wheel L/V = 0.66 (Case 2), 0.61 (Case 4), Limit=0.6	Not required
4.3.12 Ride Quality	Met	Not Simulated	Not required
4.3.13 Buff and Draft Curving	Not Met When coupled between other Atlas cars under buff load Truck side L/V Ratio=0.51, Limit=0.50	Met	Not required
4.3.14 Braking Effects on Steering	Met	Not Simulated	Not required
4.3.15 Worn Component Simulations	Not Met Numerous criteria not met in dynamic curving and hunting regimes with several worn components. See reference 2 for details	Not Met in following cases: **Hunting stability, maximum lateral acceleration standard deviation:** Worn CCSB low preload: 0.17 Worn primary pads, soft: 0.19 Worn primary pads, stiff: 0.20	Not required

Table of Contents

1.0 Introduction 1
2.0 Atlas Railcar Description 1
2.1 Variations in Components During Testing 4
3.0 Objective 5
4.0 Refining the FEA 5
4.1 Loading Conditions for Structural Tests 6
4.1.1 Test Loads 6
4.1.2 Measured Stresses from Test Loads 6
4.2 Squeeze (Compressive End) Load 9
4.3 Coupler Vertical Loads 12
4.4 Jacking 14
4.5 Twist 16
4.5.1 Suspension Twist 16
4.5.2 Carbody Twist 19
4.6 Impact 21
5.0 New FEA Predictions 23
6.0 Refining the Dynamic Model 23
7.0 New Dynamic Predictions 27
7.1 Twist and Roll 29
7.1.1 Minimum Test Load 29
7.1.2 Maximum Test Load 30
7.2 Pitch and Bounce (Chapter 11) 32
7.2.1 Minimum Test Load 32
7.2.2 Maximum Test Load 33
7.3 Yaw and Sway 35
7.4 Dynamic Curving 37
7.4.1 Minimum Test Load 37
7.4.2 Maximum Test Load 40
7.4.3 Other Various Load Conditions 41
7.5 Single Bump Test 43
7.5.1 Minimum Test Load 44
7.5.2 Maximum Test Load 45
7.6 Curving with Single Rail Perturbation 47
7.6.1 Minimum Test Load 47
7.6.2 Maximum Test Load 50
7.7 Hunting 53
7.7.1 Minimum Test Load 53
7.7.2 Maximum Test Load 55
7.8 Constant Curving 57
7.8.1 Minimum Test Load 58
7.8.2 Maximum Test Load 59
7.9 Curving with Various Lubrication Conditions 61
7.9.1 Minimum Test Load 62
(1) New Profiles 62

(2) Worn Profiles 62
7.9.2 Maximum Test Load 66
(1) New Profiles 66
(2) Worn Profiles 67
7.10 Limiting Spiral Negotiation 71
7.10.1 Minimum Test Load 71
7.10.2 Maximum Test Load 73
7.11 Special Trackwork: Turnouts and Crossovers (S-2043, Paragraph 4.3.11.7) 74
7.11.1 Minimum Test Load – Turnouts and Crossovers 75
7.11.2 Maximum Test Load – Turnouts and Crossovers 76
7.12 Buff and Draft Curving 77
7.13 Worn Component Simulations 79
7.13.1 Worn Constant Contact Side Bearings 80
7.13.2 Centerplate 82
7.13.3 Primary Pad 84
7.13.4 Friction Wedges 86
7.13.5 Broken Spring 88
8.0 Conclusions 89
References 94

List of Figures

Figure 1. IDOX 010001 during Testing with Minimum Test Load 2
Figure 2. Exploded view of Swing Motion® truck 3
Figure 3. Roller Bearing Adapter Pad 3
Figure 4. Axle and side naming convention 4
Figure 5. Measurement locations reported in Table 4 and Table 5 8
Figure 6. Measurement locations reported in Table 6, and Table 7 12
Figure 7. Measurement locations reported in Table 8 12
Figure 8. Measurement locations with highest stresses during jacking test 14
Figure 9. Suspension twist locations 19
Figure 10. Measurement locations with highest stresses during carbody twist test 21
Figure 11. Measurement locations with highest stresses during impact test 23
Figure 12. Results of the second interaxle stiffness test with CSM 58 and CSM 70 primary pads 27
Figure 13. Twist-and-roll test results and simulation predictions of maximum peak-to-peak carbody roll angle with minimum test load 30
Figure 14. Twist-and-roll test results and simulation predictions of maximum peak-to-peak carbody roll angle with maximum test load using CSM 70 pads 31
Figure 15. Twist-and-roll pre-test and refined model simulation predictions of maximum peak-to-peak carbody roll angle with maximum test load using CSM 70 pads 32
Figure 16. Simulation predictions of maximum vertical carbody acceleration in the pitch and bounce regime with minimum test load 33
Figure 17. Pitch and bounce test results and simulation predictions of maximum vertical acceleration with CSM 70 Pads at maximum test load 34
Figure 18. Pitch and bounce simulation predictions of maximum vertical acceleration with CSM 58 Pads at maximum test load 35
Figure 19. Simulation predictions and test results of maximum truck side L/V ratio in the yaw-and-sway regime with CSM 70 pads and the maximum test load 36
Figure 20. Simulation predictions of maximum truck side L/V ratio in the yaw-and-sway regime with CSM 58 pads and the maximum test load 37
Figure 21. Simulation prediction and test results of maximum wheel L/V ratio in the dynamic curving regime with minimum test load and CSM 70 pads 38
Figure 22. Simulation prediction and test results of maximum wheel L/V ratio in the dynamic curving regime with minimum test load and CSM 58 pads 39

Figure 23. Distance plot of axle 5 lead left wheel L/V ratio during 12 mph run counterclockwise (CCW) through dynamic curve with B-End leading using CSM 70 primary pads 39
Figure 24. Simulation prediction and test results of maximum wheel L/V ratio in the dynamic curving regime with maximum test load using CSM 70 pads 41
Figure 25. Simulation predictions of maximum wheel L/V ratio in the dynamic curving regime with maximum test load using CSM 70 and CSM 58 pads 41
Figure 26. Simulation prediction and test results of minimum vertical wheel load in the single bump regime with minimum test load 45
Figure 27. Simulation prediction and test results of maximum vertical carbody acceleration in the single bump test regime with maximum test load using CSM 70 pads..... 46
Figure 28. Original (2017) and revised simulation predictions of maximum vertical carbody acceleration in the single bump test regime with maximum test load using CSM 58 pads 47
Figure 29. Simulation predictions and test results using CSM 70 primary pads of maximum wheel L/V ratio in the curve with single dip regime with minimum test load..... 48
Figure 30. Simulation predictions using CSM 70 and CSM 58 primary pads of maximum wheel L/V ratio in the curve with single dip regime with minimum test load 49
Figure 31. Simulation prediction and test results of maximum wheel L/V ratio in the curving with single rail perturbation dip regime with maximum test load using CSM 70 and CSM 58 pads 51
Figure 32. Simulation prediction and test results of the standard deviation of carbody lateral acceleration over 2,000 feet with minimum test load using CSM 70 pads and KR profile wheels 54
Figure 33. Simulation prediction and test results of the standard deviation of carbody lateral acceleration over 2,000 feet with minimum test load using CSM 58 pads and KR profile wheels 55
Figure 34. Simulation prediction and test results of maximum wheel L/V ratio in the dynamic curving regime with maximum test load using CSM 70 pads 57
Figure 35. Simulation predictions of maximum wheel L/V ratio in the dynamic curving regime with maximum test load using CSM 70 and CSM 58 pads 57
Figure 36. Test Results and Simulation Predictions of the 95 Percentile Wheel L/V Ratio in the 12-degree Constant Curve with CSM 70 and CSM 58 Primary Pads for Minimum Test Load 59
Figure 37. Test Results and Simulation Predictions of the 95 Percentile Wheel L/V Ratio in the 12-degree Constant Curve with CSM 70 Primary Pads for Maximum Test Load 60

Figure 38. Original (20170 and Revised Simulation Predictions of the 95 Percentile Wheel L/V Ratio in the 12-degree Constant Curve with CSM 58 Primary Pads for Maximum Test Load 61
Figure 39. Worn Wheel Profiles on the Ground Rail Profiles (The Wheelset is Shifted to the High Rail in the Position it Would be in a Left-Hand Curve) 62
Figure 40. Plot of Wheel L/V Ratio versus distance for Case 2 friction with worn profiles, CCW, A-leading. Plot shows data for the lead axle of the trailing span bolster. 64
Figure 41. Plot of Truck Side L/V Ratio versus distance for Case 2 friction with worn profiles, CCW, B-leading. Plot shows data for the high rail of the middle truck on the lead span bolster. 64
Figure 42. Atlas car with minimum test load 95-Percent Wheel L/V Ratio for curving with Case 2 lubrication and worn wheel and rail profiles 65
Figure 43. Minimum Test Load Truck Side L/V Ratio for curving with Case 2 lubrication and worn wheel and rail profiles 65
Figure 44. Predictions of Wheel L/V Ratio for multiple lubrication cases with new wheel and rail profiles (most severe results shown) 66
Figure 45. Predictions of Truck Side L/V Ratio for Case 2 lubrication with worn wheel and rail profiles for both directions of travel, with most severe results shown, at maximum and minimum test load 68
Figure 46. Predictions of 95% Wheel L/V Ratio for Case 2 lubrication with worn wheel and rail profiles for both directions of travel, with most severe results shown, at maximum and minimum test loads 68
Figure 47. Predictions of Truck Side L/V Ratio for Case 4 lubrication with worn wheel and rail profiles for both directions of travel, with most severe results shown, at maximum and minimum test loads 69
Figure 48. Plot of Truck Side L/V Ratio versus distance for Case 2 friction with worn wheel and rail profiles. The plot shows data for the high rail of the middle truck on the lead span bolster 69
Figure 49. Worst-case predictions for Truck Side L/V Ratio at all lubrication cases of worn wheel and rail profiles, at maximum test load 70
Figure 50. Worst-case predictions for 95 percentile Wheel L/V Ratio at all lubrication cases of worn wheel and rail profiles, at maximum test load 70
Figure 51. Simulation prediction and test results of maximum wheel L/V ratio in the limiting spiral regime with minimum test load using CSM 70 pads 72

Figure 52. Simulation prediction and test results of maximum wheel L/V ratio in the limiting spiral regime with minimum test load using CSM 58 pads 72
Figure 53. Simulation prediction and test results of maximum wheel L/V ratio in the dynamic curving regime with maximum test load using CSM 70 pads 74
Figure 54. Simulation predictions of maximum wheel L/V ratio in the dynamic curving regime with maximum test load using CSM 70 and CSM 58 pads 74
Figure 55. Simulation Predictions of Truck side L/V Ratio on No. 7 Crossovers for Original Simulations of Atlas Car with Minimum Test Load 76
Figure 56. Simulation Predictions of Truck Side L/V Ratio on No. 7 Crossover. Original Simulations (a) and revised simulations (b) at maximum load 77
Figure 57. Truck Side L/V Ratio for Curving Simulations Under 250,000 Pounds Draft Force for Revised Simulations with the Minimum Test Load 78
Figure 58. Truck Side L/V Ratio for Curving Simulations Under 250,000 Pounds Buff Force for Revised Simulations with the Minimum Test Load 79
Figure 59. Single Wheel L/V Ratio for Worn CCSB Cases 81
Figure 60. Maximum Carbody Lateral Acceleration for CCSB Wear Cases Plotted Against Speed 82
Figure 61. Hunting stability, considering centerplate wear 84
Figure 62. Hunting stability, considering primary pad deterioration 86

List of Tables

Table 1. Car Dimensions 2
Table 2. Car Configuration 4
Table 3. Summary of structural tests and load condition 6
Table 4. Comparison of highest measured stresses with predicted stresses for Atlas car loaded to the maximum test load condition with no additional applied forces 7
Table 5. Comparison of highest measured stresses with predicted stresses for Atlas car loaded to the minimum test load condition with no additional applied forces 8
Table 6. Comparison of highest total stresses with predicted stresses for squeeze (compressive end) load test in the maximum test load condition 10
Table 7. Comparison of total stresses and stresses from applied load with predicted stresses for squeeze (compressive end) load test in the minimum test load condition 11
Table 8. Comparison of highest measured stresses with predicted stresses for coupler vertical load test 13
Table 9. Comparison of selected measured stresses with predicted stresses for jacking test 15
Table 10. Comparison of selected measured stresses with predicted stresses for suspension twist test with the A-end LH corner lifted 3 inches 17
Table 11. Comparison of selected measured stresses with predicted stresses for suspension twist test with the A-end RH corner lifted 3 inches 17
Table 12. Comparison of selected measured stresses with predicted stresses for suspension twist test with the B-end LH corner lifted 3 inches 18
Table 13. Comparison of selected measured stresses with predicted stresses for suspension twist test with the B-end RH corner lifted 3 inches 18
Table 14. Comparison of selected measured stresses with predicted stresses for carbody twist test 20
Table 15. Comparison of selected measured stresses with predicted stresses for impact test 22
Table 16. Comparison of values used in preliminary modeling and values measured during characterization 24
Table 17. Twist-and-roll test results and simulation predictions using minimum test load 29
Table 18. Twist-and-roll test results and simulation predictions with maximum test load 31
Table 19. Pitch and bounce test results and simulation predictions 33
Table 20. Test results and simulations predictions for Pitch and Bounce with maximum test load 34
Table 21. Yaw-and-sway test results and simulation predictions 36

Table 22. Dynamic curving test results and simulation predictions 38
Table 23. Dynamic curving test results and simulation predictions with maximum test load 40
Table 24. Dynamic Curving with Various Loads (Part 1 of 3) 42
Table 25. Dynamic Curving with Various Loads (Part 2 of 3) 43
Table 26. Dynamic Curving with Various Loads (Part 3 of 3) 43
Table 27. Single bump test results and simulation predictions with minimum test load 44
Table 28. Single bump test results and simulation predictions with maximum test load 46
Table 29. Curving with 2-inch rail dip test results and simulation predictions using measured track inputs with minimum test load 48
Table 30. Simulation prediction for curve with single rail perturbation bump section at varying amplitudes with minimum test load 49
Table 31. Simulation prediction for curve with single rail perturbation dip section at varying amplitudes with minimum test load 50
Table 32. Curving with 2-inch rail dip test results and simulation predictions using measured track inputs with maximum test load 51
Table 33. Simulation prediction for curve with single rail perturbation bump section at varying amplitudes with maximum test load 52
Table 34. Simulation prediction for curve with single rail perturbation dip section at varying amplitudes with maximum test load 53
Table 35. Hunting test results and simulation predictions with minimum test load 54
Table 36. Hunting test results and simulation predictions with maximum test load 56
Table 37. Constant curving test results and simulation predictions with minimum test load 58
Table 38. Constant curving test results and simulation predictions with maximum test load 60
Table 39. Wheel/rail Coefficients of Friction for the Curving with Various Lubrication Conditions Regime 61
Table 40. Simulation Results for Curving with Rail Lubrication Cases 1-4 and New Wheels and Rails, with Minimum Test Load 62
Table 41. Simulation Predictions for Curving with Rail Lubrication Cases 1-4 and Hollow Worn Wheels and Ground Rails, with Minimum Test Load 63
Table 42. Simulation predictions for Curving with Rail Lubrication Cases 1–4 and New Wheels and Rails, Car Loaded with the Maximum Test Load 66
Table 43. Simulation predictions for Curving with Rail Lubrication Cases 1–4 and Hollow Worn Wheels and Ground Rails, Car Loaded with the Maximum Test Load 67
Table 44. Limiting spiral test results and simulation predictions with minimum test load 71
Table 45. Dynamic curving test results and simulation predictions with maximum test load 73

Table 46. Crossover Simulation Predictions with Minimum Test Load 75
Table 47. Crossover Simulation Predictions, Car Loaded at Maximum Load 76
Table 48. Revised Simulation Predictions for 250,000 Draft Force, Minimum Test Load 78
Table 49. Revised Simulation Predictions for 250,000 Buff Force, Minimum Test Load 79
Table 50. Simulation Predictions of the Atlas Cask Car with Worn CCSB in Dynamic Curving..... 80
Table 51. Simulation Predictions of the Atlas Cask Car with Worn CCSB in Hunting..... 81
Table 52. Simulation Predictions of the Atlas Cask Car with Worn CCSB in Twist and Roll 82
Table 53. Simulation Predictions of the Atlas Cask Car with Worn Centerplate in Constant Curving 83
Table 54. Simulation Predictions of the Atlas Cask Car with Worn Centerplate in Dynamic Curving..... 83
Table 55. Simulation Predictions of the Atlas Cask Car with Worn Centerplate in Hunting 84
Table 56. Simulation Predictions of the Atlas Cask Car with Worn Primary Pads in Constant Curving 85
Table 57. Simulation Predictions of the Atlas Cask Car with Worn Primary Pads in Dynamic Curving..... 85
Table 58. Simulation Predictions of the Atlas Cask Car with Worn Primary Pads in Hunting 86
Table 59. Simulation Predictions of the Atlas Cask Car with Worn Friction Wedges in Dynamic Curving..... 87
Table 60. Simulation Predictions of the Atlas Cask Car with Worn Friction Wedges in Pitch and Bounce..... 87
Table 61. Simulation Predictions of the Atlas Cask Car with Worn Friction Wedges in Twist and Roll..... 88
Table 62. Simulation Predictions of the Atlas Cask Car with a Broken Spring in Dynamic Curving..... 88
Table 63. Simulation Predictions of the Atlas Cask Car with a Broken Spring in Pitch and Bounce..... 89
Table 64. Simulation Predictions of the Atlas Cask car with a Broken Spring in Twist and Roll..... 89
Table 65. Summary of Dynamic Modeling and Test Results 90

1.0 INTRODUCTION

The United States Department of Energy (DOE) contracted with the Transportation Technology Center, Inc. (TTCI) to perform dynamic modeling and certification testing on its Atlas railcar. The Atlas railcar has been developed as part of the DOE's Atlas Railcar Design Project that is intended to meet the need for future large-scale transport of high-level radioactive material (HLRM) as defined in AAR Standard S-2043 that includes spent nuclear fuel and high-level waste.

All tests and analyses were performed according to the Association of American Railroads' (AAR) *Manual of Standards and Recommended Practices* (MSRP), Standard S-2043, "Performance Specification for Trains used to carry High-level Radioactive Material," Section 5.0 – Single Car Tests.[1] Single-car testing of the Atlas railcar was conducted at the United States Department of Transportation's Transportation Technology Center (TTC) near Pueblo, Colorado between April 2019 and August 2021. Static brake testing was conducted per relevant requirements of AAR Standards S-401 and S-486 at the manufacturer's facility prior to delivery.

Standard S-2043 requires that both a structural and a dynamic analysis be performed during the car design process. Kasgro Rail Corporation (Kasgro) designed the car and performed the structural analysis, and TTCI performed the dynamic analysis. In this report, the predictions from these analyses are compared to the single car test results. The single-car tests were described in TTCI report P-21-037.[2] The pretest dynamic analysis was described in TTCI report P-17-021.[3]

2.0 ATLAS RAILCAR DESCRIPTION

The Atlas railcar is a 12-axle span bolster car with fittings to accommodate various cradles and end stops designed so the car can carry various casks used for transportation of spent nuclear fuel and/or high-level waste. The car deck is supported on two span bolsters. Each span bolster rested on three 2-axle trucks. Figure 1 shows the car with a test load installed. Table 1 shows the car dimensions.

Kasgro manufactured the Atlas railcar along with two prototype buffer railcars in 2018. The car delivered for testing was numbered IDOX 010001.



Figure 1. IDOX 010001 during Testing with Minimum Test Load

Table 1. Car Dimensions

Dimension	Value
Length over pulling faces	78 feet 1 1/4 inches
Length over strikers	73 feet 5 1/4 inches
Span bolster spacing	38 feet 6 inches
Axle spacing on trucks	72 inches
Distance between adjacent trucks	10 feet 6 inches

The car uses six Swing Motion® trucks (Figure 2). Each truck uses two wheelsets having AAR Class K-axles and AAR1B narrow flange wheels. Narrow flange wheels are specified for this car because the increased gage clearance allows more lateral movement for better performance. The trucks are designed to use a polymer element between the bearing adapter and side frame. This gives the truck a passive steering capability. Figure 3 shows the bearing adapter pad. Table 2 shows the truck configuration used for testing. The secondary suspension is made up of non-AAR-standard springs.

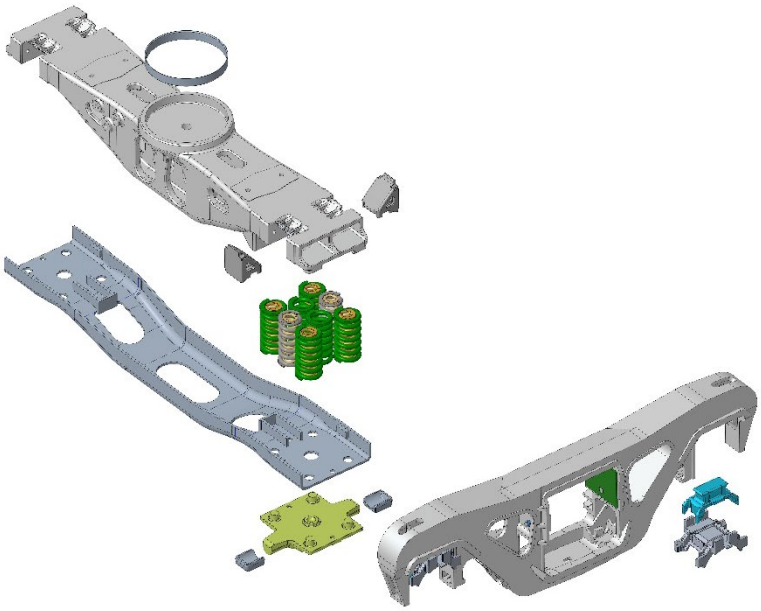


Figure 2. Exploded view of Swing Motion® truck



Figure 3. Roller Bearing Adapter Pad

Table 2. Car Configuration

Component	Description	
Secondary Suspension Springs at End Trucks (A,B,D,E)	(2) 1-94, (2) 1-95, (2) 1-96, (4) 1-97, (4) 1-92, (4) 1-99	
Secondary Suspension Springs at Middle Trucks (C,F)	(2) 1-88, (2) 1-89, (2) 1-90, (4) 1-91, (4) 1-92, (2) 1-93, (4) 1-99	
Primary suspension	12A Adapter Plus pads, ASF-Keystone part number 10522A	
Side Frames	F9N-10FH-UB	
Bolsters	B9N-71 EJFZ on A, F, and C-trucks B9N-71 HN-FX on B, D, and E-trucks	
Side Bearings	Miner TCC-III 60LT	
Friction Wedge, composition faced (four per truck)	ASF-Keystone Part number 48446	
Bearings and Adapters	AAR Class K 6 1/2 × 9 bearings with 6 1/2 × 9 Special Adapter ASF-Keystone Part number 10523A	
Center Bowl Plate	Metal Horizontal Liner	
	End Truck Average	Middle Truck Average
Minimum Test Load Spring Nest Height	8.97 inches	9.13 inches
Maximum Test Load Spring Nest Height	8.20 inches	8.17 inches

The convention for wheel and truck identification is shown in Figure 4. The B-end of a railroad freight car is normally the end with the handbrake, but because the Atlas car has two handbrakes, the car manufacturer designated and stenciled the B-end. The right and left sides of the car are designated when standing at the B-end of the car and looking toward the A-end of the car. Axles are numbered starting from the B-end. For axle numbers greater than nine, the locations are stenciled with letters descending from Z.

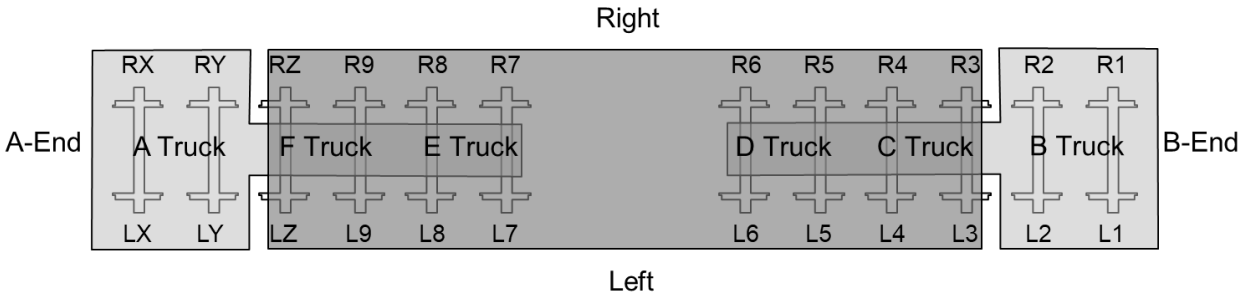


Figure 4. Axle and side naming convention

2.1 Variations in Components During Testing

During initial tests the Atlas car, loaded with the minimum test load, showed some hunting instability at speeds above 65 mph. The Atlas car was stable to 75 mph when loaded with the maximum test load. TTCI tested different side bearings, centerplate liners, and primary pads to address the hunting instability with the minimum test load. The stiffer primary pads (prototype

chlorosulfonated polyethylene or CSM 70 pads) were the only change that improved the hunting performance. After the change to stiffer pads resulted in improved hunting stability performance, all Standard S-2043 prescribed dynamic test regimes were completed with the CSM 70 pads. However, using these stiffer pads, car performance did not meet Standard S-2043 criteria in Dynamic Curving or Curve with Single Rail Perturbation regimes.

On October 15, 2020, TTCI reviewed the results with the AAR Equipment Engineering Committee (EEC). The EEC directed TTCI to re-test the car with softer primary pads with minimum test load in the Dynamic Curving regime. Because the car would be limited to less than 50 mph by AAR Operating Transportation (OT) circular OT-55 when in high-level radioactive material (HLRM) service, the EEC noted that curving performance was more important than high speed stability performance.

During the testing program, TTCI tested the car with a total of four primary suspension pad models. The pads are made from CSM and are categorized by the Shore D durometer hardness value. The production pads the car arrived with were CSM 58 pads. TTCI also tested the car with prototype pad types CSM 70, CSM 68, and CSM 65. The 58 in the model name "CSM 58" pads indicates the minimum hardness value, while the numbers in the names of other pads indicate the target hardness value.

The hunting regime was tested with CSM 58 pads in both the minimum and maximum test load conditions. The dynamic curving regime was tested with CSM 58 pads in the minimum test load condition. All other dynamic tests were completed with CSM 70 pads. Considering the results of curving and hunting tests, the production CSM 58 pads provide the best performance overall, when compared to the alternative pad materials that were tested.

After updating Nucars models with characterization data, the regimes with recorded test data using CSM 70 pads were again simulated with CSM 70 pads to demonstrate the model was validated. These regimes were modeled again with CSM 58 pads to show the change in performance with the final pad as directed by EEC.

3.0 OBJECTIVE

The objective of this report is to demonstrate acceptable railcar performance and it was accomplished by comparing the test results to the modeling predictions as part of the structural and dynamic analysis of the DOE Atlas car. Revised simulation predictions are presented where necessary.

4.0 REFINING THE FINITE ELEMENT ANALYSIS (FEA)

Structural test results are compared to FEA predictions in this section. The FEA results were examined to determine the normal stress in the active direction at the location of the strain gages for comparison to test results. Paragraph 8.1 of Standard S-2043 requires the following:

> *"If any measured stress exceeding 75% of allowable varies from its predicted value by more than 15%, then the model must be refined to provide more accurate predictions. If the designer feels that unique or unforeseen test conditions caused the discrepancy, then adequate*

explanation must be provided so that useful conclusions can be made about the model predictions and the test results."

The results presented in this report show that none of the measured stresses exceed 75 percent of the allowable stress.

4.1 Loading Conditions for Structural Tests

4.1.1 Test Loads

The physical test loads (masses) from Orano Federal Services were designed and fabricated to simulate both the weight and the center of gravity (CG) of the lightest and heaviest payloads the DOE Atlas railcar is designed to transport. The minimum condition test load assembly was designed to simulate the empty MP-197 cask, and the maximum condition test load assembly was designed to simulate the heaviest package (HI-STAR 190XL).[4] Based on actual weights from measurements conducted prior to shipment to TTCI, the maximum test load along with the associated cradle and end stops weighed 479,827 pounds, and the minimum test load and cradle weighed 196,107 pounds.[5]

Table 3 shows the structural tests conducted and the associated load condition(s).

Table 3. Summary of structural tests and load condition

Test Name	Maximum	Minimum
Squeeze (compressive end) load	x	x
Coupler vertical loads	x	
Jacking	x	
Twist	x	
Impact	x	

4.1.2 Measured Stresses Due to Test Loads only

Table 4 shows a summary of stresses from static measurements of the Atlas car, after loading the maximum test load (but without any additional applied force), for the locations with highest measured stress. The maximum measured stress was 38 percent of yield. Table 5 shows summary of stresses from static measurements, after loading the minimum test load (but without any additional applied force), for the locations with highest measured stress. The maximum measured stress was 15 percent of yield. The locations for both the minimum and maximum test loads are highlighted in Figure 5.

Table 4. Comparison of highest measured stresses with predicted stresses for Atlas car loaded to the maximum test load condition with no additional applied forces

Channel Name	Approximate Location	Normal Stress in the Active Direction of the Strain Gage				
		Measured Stress (ksi)	Yield Stress (ksi)	Measured Stress as percent of Yield	Predicted Stress (ksi)	Percent Difference Test vs Predicted
SGBF26	Center of LH side sill bottom flange, 74 1/8 inches from B end body bolster toward center of car	27	72	38%	26	NA*
SGDP45	Top of deck plate, above LH side sill web, 66 3/8 inches from line across centermost edges of B-end end stop pin blocks toward center of car	-21	60	35%	-18	NA*
SGDP48	Top of deck plate, above RH side sill web, 66 3/8 inches from line across centermost edges of B-end end stop pin blocks toward center of car	-20	60	33%	-18	NA*
SGBF15	Center of RH side sill bottom flange, 74 1/8 inches from B end body bolster toward center of car	18	72	25%	26	NA*

*Not required because measured stress does not exceed 75% of allowable

Table 5. Comparison of highest measured stresses with predicted stresses for Atlas car loaded to the minimum test load condition with no additional applied forces

Channel Name	Approximate Location	Normal Stress in the Active Direction of the Strain Gage				
		Measured Stress (ksi)	Yield Stress (ksi)	Measured Stress as percent of Yield	Measured Stress (ksi)	Percent Difference Test vs Predicted
SGBF26	Center of LH side sill bottom flange, 74 1/8 inches from B end body bolster toward center of car.	11	72	15%	10	NA*
SGBF15	Center of RH side sill bottom flange, 74 1/8 inches from B end body bolster toward center of car	9.4	72	13%	10	NA*
SGDP52	Top of deck plate, above LH center sill web, 66 3/8 inches from line across centermost edges of A-end stop pin blocks toward center of car	-8.8	60	15%	-8	NA*
SGDP45	Top of deck plate, above LH side sill web, 66 3/8 inches from across centermost edges of B-end end stop pin blocks toward center of car	-8.7	60	15%	-8	NA*

*Not required because measured stress does not exceed 75% of allowable

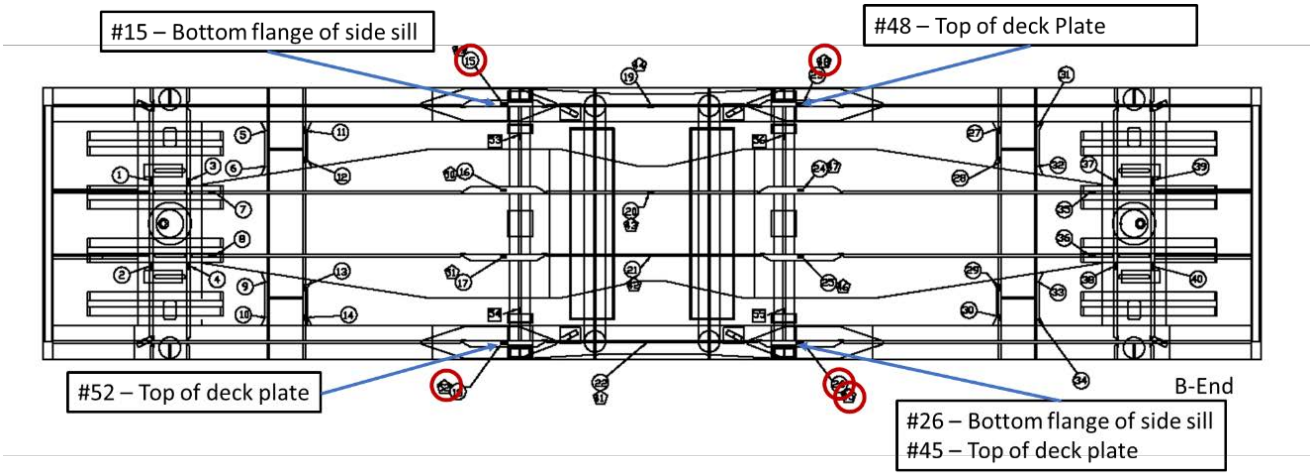


Figure 5. Measurement locations reported in Table 4 and Table 5

4.2 Squeeze (Compressive End) Load

The compressive end-load test was conducted in both the minimum and maximum test load conditions. In both cases, the strain gauges were zeroed before application of the one-million-pound compressive force. The stresses measured from the applied force were then combined with the stresses measured from the applicable test load to calculate the total stress.

Table 6 shows the summary results from the compressive end load test with the maximum test load for the locations with highest total stress. The stress from the applied force is small compared to the tension stress (in the bottom fibers of the car's sills) from the bending imparted by the maximum test load. In these cases, the applied compressive force opposed the tension force and reduced the total stress. The maximum total stress was 35 percent of the material yield.

Table 7 shows the summary results from the compressive end load test using the minimum test load for the locations with the highest stress from the applied force. The maximum total stress was 16 percent of the material yield. The locations are highlighted in Figure 6.

Table 6. Comparison of highest total stresses with predicted stresses for squeeze (compressive end) load test in the maximum test load condition

Channel Name	Approximate Location	Normal Stress in the Active Direction of the Strain Gage						
		Measured Stress from Max Test Load (ksi)	Measured Stress from Applied Force (ksi)	Total Stress (ksi)	Yield Stress (ksi)	Total Stress as percent of Yield	Predicted Total Stress (ksi)	Percent Difference Test vs Predicted
Highest total stress								
SGBF26	Center of LH side sill bottom flange, approx. 74 1/8 inches from B end body bolster toward center of car.	27	-4.1	23	72	32%	19	NA*
SGDP45	Top of deck plate, above LH side sill web, 66 3/8 inches from line across centermost edges of pin blocks toward center of car (directly above SBGF 26)	-21	0.12	-21	60	35%	-18	NA*
Highest stress from applied load								
SGBF36	LH side of bottom flange of center sill 5 3/16 inches from B-end body bolster toward center of car - aligns with center sill web	3.4	-8.9	-5.5	60	9%	-6	NA*
SGBF35	RH side of bottom flange of center sill – 5 3/16 inches from B-end body bolster toward center of car - aligns with center sill web	3.6	-8.5	-4.9	60	8%	-6	NA*

* Not required because measured stress does not exceed 75% of allowable

Table 7. Comparison of total stresses and stresses from applied load with predicted stresses for squeeze (compressive end) load test in the minimum test load condition

Channel Name	Approximate Location	Normal Stress in the Active Direction of the Strain Gage						
		Measured Stress from Min Test Load (ksi)	Measured Stress from Applied Force (ksi)	Total Stress (ksi)	Yield Stress (ksi)	Total Stress as percent of Yield	Predicted Stress (ksi)	Percent Difference Test vs Predicted
Highest total stress (also highest stresses from applied load)								
SGBF35	RH side of bottom flange of center sill – 5 3/16 inches from B-end body bolster toward center of car - aligns with center sill web	0.29	-9.9	-9.6	60	16%	-10	NA*
SGBF7	RH side of bottom flange of center sill - 5 3/16 inches from A-end body bolster toward center of car - aligns with center sill web	1.2	-10	-8.8	60	15%	-10	NA*
SGBF36	LH side of bottom flange of center sill – 5 3/16 inches from B-end body bolster toward center of car - aligns with center sill web	1.1	-9.8	-8.6	60	14%	-10	NA*
SGBF8	LH side of bottom flange of center sill - 5 3/16 inches from A-end body bolster toward center of car - aligns with center sill web	1.3	-9.7	-8.4	60	14%	-10	NA*

* Not required because measured stress does not exceed 75% of allowable

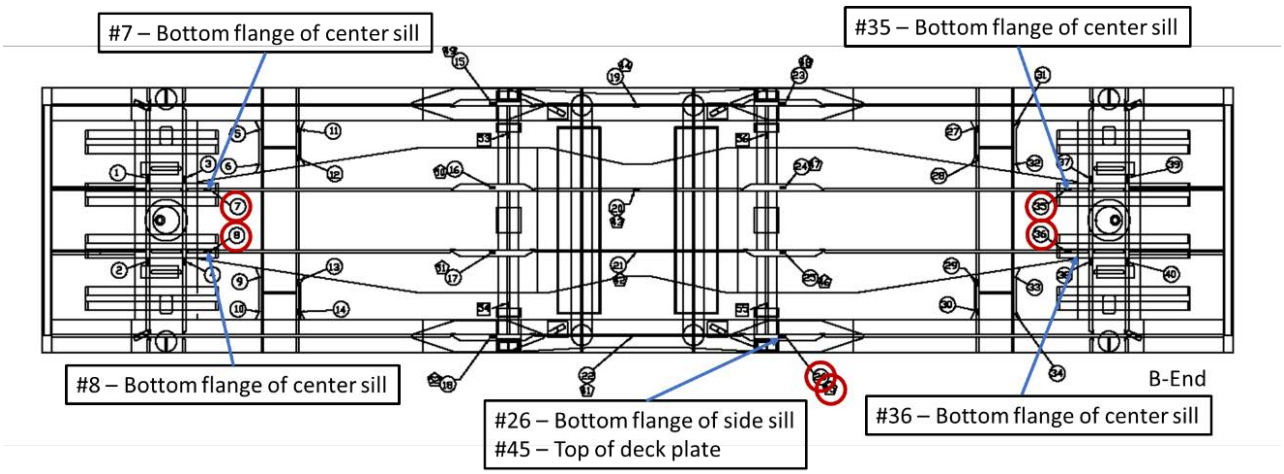


Figure 6. Measurement locations reported in Table 6, and Table 7

4.3 Coupler Vertical Loads

Table 8 shows the summary results from the coupler vertical load test for the locations with highest measured stress. These locations are highlighted in Figure 7. Measurement locations reported in Table 8. The maximum measured stress was 5 percent of the material yield.

The Atlas car couplers are connected to the span bolsters. All the strain gages are applied to the carbody. The forces applied to the couplers may be reacted either from the span bolster into the ground via the trucks or from the span bolster into the carbody via the carbody centerplate. The FEA model used by the car builder to predict stresses in the car body was not capable of modeling the complex contact conditions necessary to simulate this test.

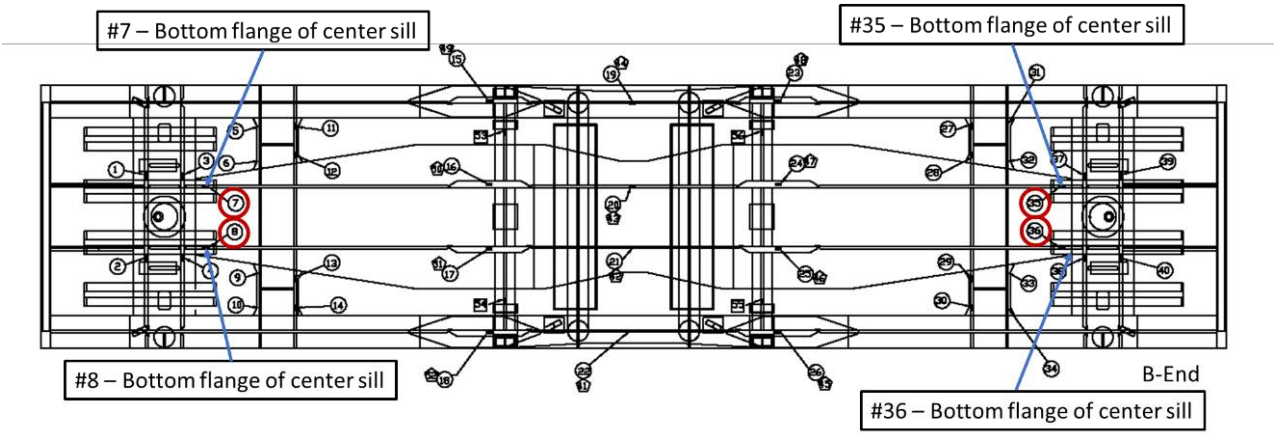


Figure 7. Measurement locations reported in Table 8

Table 8. Comparison of highest measured stresses with predicted stresses for coupler vertical load test

Channel Name	Approximate Location	Normal Stress in the Active Direction of the Strain Gage						
		Measured Stress from Min Test Load (ksi)	Measured Stress from Applied Force (ksi)	Total Stress (ksi)	Yield Stress (ksi)	Total Stress as percent of Yield	Predicted Stress (ksi)	Percent Difference Test vs Predicted
Downward Direction								
SGBF35	RH side of bottom flange of center sill – 5 3/16 inches from B-end body bolster toward center of car - aligns with center sill web	3.7	-1.0	2.6	60	4%	NP**	NA*
SGBF36	LH side of bottom flange of center sill – 5 3/16 inches from B-end body bolster toward center of car - aligns with center sill web	3.4	-.98	2.4	60	4%	NP**	NA*
Upward Direction								
SGBF7	RH side of bottom flange of center sill - 5 3/16 inches from A-end body bolster toward center of car - aligns with center sill web	2.3	.89	3.2	60	5%	NP**	NA*
SGBF8	LH side of bottom flange of center sill - 5 3/16 inches from A-end body bolster toward center of car - aligns with center sill web	2.3	.86	3.2	60	5%	NP**	NA*

*Not required because measured stress does not exceed 75% of allowable

**FEA prediction could not be completed for this test due to the coupler being connected to the span bolster and not the carbody

4.4 Jacking

Table 9 shows the summary results from the jacking test for the locations with the highest measured stress. These locations are highlighted in Figure 8. The maximum measured stress was 8 percent of the material yield.

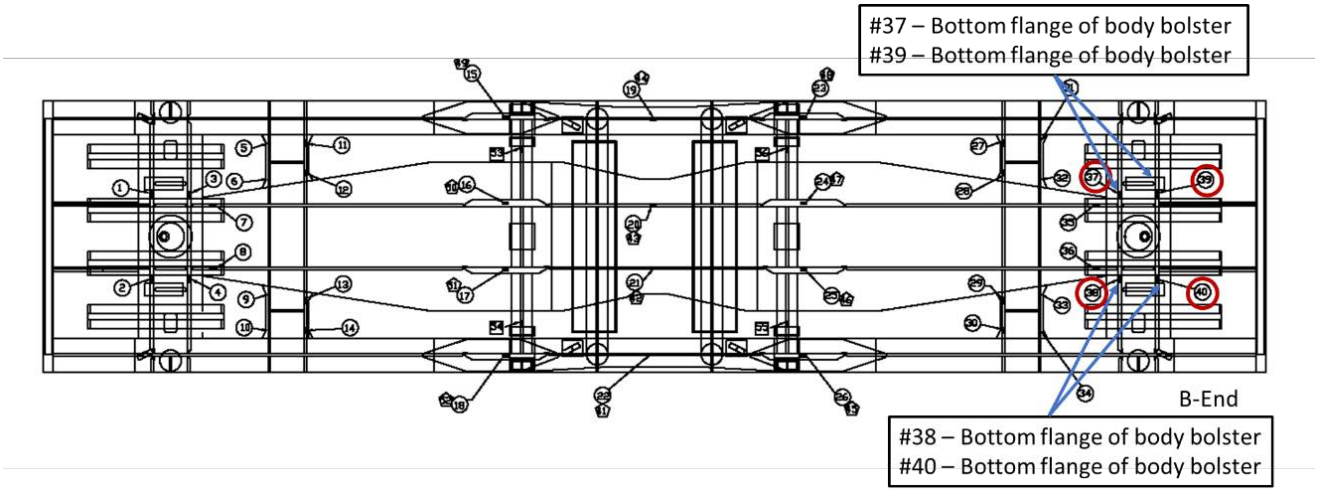


Figure 8. Measurement locations with highest stresses during jacking test

Table 9. Comparison of selected measured stresses with predicted stresses for jacking test

Channel Name	Approximate Location	Normal Stress in the Active Direction of the Strain Gage						
		Measured Stress from Max Test Load (ksi)	Measured Stress from Applied Force (ksi)	Total Stress (ksi)	Yield Stress (ksi)	Total Stress as percent of Yield	Predicted Stress (ksi)	Percent Difference Test vs Predicted
SGBF40	Bottom flange of B-end body bolster. On edge nearest B-end. 2 1/4 inches outboard of center sill bottom flange toward LH side of car.	-2.9	7.5	4.6	60	8%	4.3	NA*
SGBF38	Bottom flange of B-end body bolster. On edge nearest center of car. 2 1/4 inches outboard of center sill bottom flange toward LH side of car.	-2.5	7.4	4.9	60	8%	4.3	NA*
SGBF39	Bottom flange of B-end body bolster. On edge nearest B-end. 2 1/4 inches outboard of center sill bottom flange toward RH side of car.	-3.1	7.2	4.1	60	7%	4.3	NA*
SGBF37	Bottom flange of B-end body bolster. On edge nearest center of car. 2 1/4 inches outboard of center sill bottom flange toward RH side of car.	-2.6	6.5	3.9	60	7%	4.3	NA*

*Not required because measured stress does not exceed 75% of allowable

4.5 Twist

TTCI performed two twist tests as part of the structural tests. The first test, described in Standard S-2043, Paragraph 5.4.5.1, is reported in Section 4.5.1 of this report, "Suspension Twist." This test followed the requirements of MSRP Section C, Part II, Specification M-1001, Paragraph 11.3.3.5. The test was performed in conjunction with the carbody twist equalization test (Standard S-2043, Paragraph 5.2.2). For this test, six wheels on one side of one span bolster were raised 3 inches. This test process was repeated for all four corners of the car.

The second twist test, described in Standard S-2043, Paragraph 5.4.5.2, is detailed in Section 4.5.2 of this report, "Carbody Twist." For this test, the railcar was supported at all four jacking pads, and then one corner was allowed to drop 3 inches.

4.5.1 Suspension Twist

Table 10 through Table 13 show the summary results from the suspension twist test for the locations with the highest measured stress. These locations are highlighted in Figure 9. Standard S-2043, Paragraph 4.1.1.5 says that the allowable design stress for twist load shall be 56 percent of the yield stress. For the grade 80 material this corresponds to 44.8 ksi and for the grade 60 material it corresponds to 33.6 ksi. The maximum measured stress was 40 percent of the material yield.

The Atlas car trucks are connected to the span bolsters. All the strain gages are applied to the carbody. The displacements introduced at the wheels produce forces that are reacted from the ground into the span bolster on the carbody via the trucks, then from the span bolster into the carbody via the carbody centerplate. The FEA model used by the car builder to predict stresses in the carbody was not capable of modeling the complexity of the truck suspension and the centerplate connections.

Table 10. Comparison of selected measured stresses with predicted stresses for suspension twist test with the A-end LH corner lifted 3 inches

Channel Name	Approximate Location	Normal Stress in the Active Direction of the Strain Gage						
		Measured Stress from Max Test Load (ksi)	Measured Stress from Applied Force (ksi)	Total Stress (ksi)	Yield Stress (ksi)	Total Stress as percent of Allowable	Predicted Stress	Percent Difference Test vs Predicted
SGBF26 (highest total stress)	Center of LH side sill bottom flange, approx. 74 1/8 inches from B end body bolster toward center of car.	27	-1.9	25	44.8	56%	NP**	NA*
SGBF32 (highest stress from applied load)	Rear of bottom flange of cross bearer, 18 1/2 inches from B-end body bolster from center of car. 5 3/4 inches outboard of center sill, toward RH side.	-3.2	-2.1	-5.3	33.6	16%	NP**	NA*

* Not required because measured stress does not exceed 75% of allowable

** FEA prediction could not be completed for this test as the wheels are connected to the span bolster and not the carbody

Table 11. Comparison of selected measured stresses with predicted stresses for suspension twist test with the A-end RH corner lifted 3 inches

Channel Name	Approximate Location	Normal Stress in the Active Direction of the Strain Gage						
		Measured Stress from Max Test Load (ksi)	Measured Stress from Applied Force (ksi)	Total Stress (ksi)	Yield Stress (ksi)	Total Stress as percent of Allowable	Predicted Stress	Percent Difference Test vs Predicted
SGBF26 (highest total stress)	Center of LH side sill bottom flange, approx. 74 1/8 inches from B end body bolster toward center of car.	27	1.8	29	44.8	65%	NP**	NA*
SGBF32 (highest stress from applied load)	Rear of bottom flange of cross bearer, 18 1/2 inches from B-end body bolster from center of car. 5 3/4 inches outboard of center sill, toward RH side.	-3.2	2.1	-1.1	33.6	3%	NP**	NA*

* Not required because measured stress does not exceed 75% of allowable

** FEA prediction could not be completed for this test as the wheels are connected to the span bolster and not the carbody.

Table 12. Comparison of selected measured stresses with predicted stresses for suspension twist test with the B-end LH corner lifted 3 inches

Channel Name	Approximate Location	Normal Stress in the Active Direction of the Strain Gage						
		Measured Stress from Max Test Load (ksi)	Measured Stress from Applied Force (ksi)	Total Stress (ksi)	Yield Stress (ksi)	Total Stress as percent of Allowable	Predicted Stress	Percent Difference Test vs Predicted
SGBF26 (highest total stress)	Center of LH side sill bottom flange, approx. 74 1/8 inches from B end body bolster toward center of car.	27	-0.5	26	44.8	58%	NP**	NA*
SGBF9 (highest stress from applied load)	Rear of bottom flange of cross bearer, 18 1/2 inches from A-end body bolster from center of car. 5 3/4 inches outboard of center sill, toward LH side.	-2.4	1.6	-0.8	33.6	2%	NP**	NA*

* Not required because measured stress does not exceed 75% of allowable

** FEA prediction could not be completed for this test as the wheels are connected to the span bolster and not the carbody.

Table 13. Comparison of selected measured stresses with predicted stresses for suspension twist test with the B-end RH corner lifted 3 inches

Channel Name	Approximate Location	Normal Stress in the Active Direction of the Strain Gage						
		Measured Stress from Max Test Load (ksi)	Measured Stress from Applied Force (ksi)	Total Stress (ksi)	Yield Stress (ksi)	Total Stress as percent of Allowable	Predicted Stress	Percent Difference Test vs Predicted
SGBF26 (highest total stress)	Center of LH side sill bottom flange, approx. 74 1/8 inches from B end body bolster toward center of car.	27	-0.5	26	44.8	58%	NP**	NA*
SGBF6 (highest stress from applied load	Rear of bottom flange of cross bearer, 18 1/2 inches from A-end body bolster from center of car. 5 3/4 inches outboard of center sill, toward RH side.	-2.6	1.9	-0.6	33.6	2%	NP**	NA*

* Not required because measured stress does not exceed 75% of allowable

** FEA prediction could not be completed for this test as the wheels are connected to the span bolster and not the carbody.

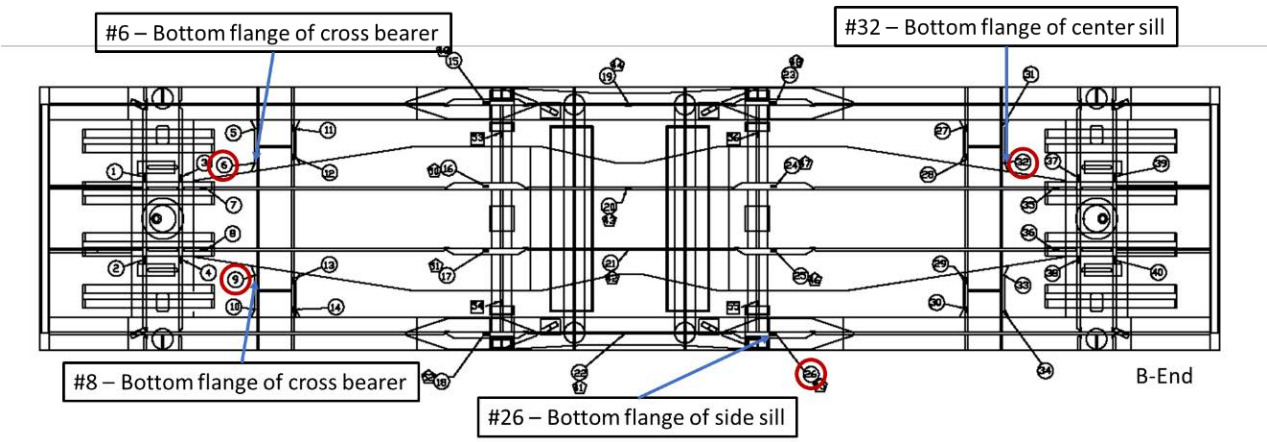


Figure 9. Suspension twist locations

4.5.2 Carbody Twist

Table 14 shows the summary results from the carbody twist test for the locations with the highest measured stress. These locations are highlighted in Figure 10. The maximum measured stress was 43 percent of the material yield.

Table 14. Comparison of selected measured stresses with predicted stresses for carbody twist test

Channel Name	Approximate Location	Normal Stress in the Active Direction of the Strain Gage						
		Measured Stress from Max Test Load (ksi)	Measured Stress with car on Jacks (ksi)	Measured Stress from 3-inch drop (ksi)	Total Stress (ksi)	Yield Stress (ksi)	Total Stress as percent of Yield	Percent Difference Test vs Predicted
SGDP45 (highest total compression stress)	Top of deck plate, above LH side sill web, 66 3/8 inches from line across centermost edges of pin blocks toward center of car (directly above SBGF 26)	-21	-19	-6.7	-26	60	43%	NA*
SGDP45 FEA predictions		NA*	NA*	NA*	NA*			
SGBF26 (Highest total tension stress)	Center of LH side sill bottom flange, approx. 74 1/8 inches from B end body bolster toward center of car.	27	25	5.7	31	72	43%	NA*
SGBF26 FEA predictions		NA*	NA*	NA*	NA*			
SGBF12 (highest stress from applied load)	Rear of bottom flange of #4 cross bearer, RH side between center sill and side sill, near center sill	0.46	-3.8	13	9.2	60	15%	NA*
SGBF12 FEA predictions		NA*	NA*	NA*	NA*			
SGBF29 (#2 ranked stress from applied load)	Front of bottom flange of #1 cross bearer, LH side between center sill and side sill, near center sill	0.46	-4.8	12	7.4	60	12%	NA*
SGBF29 FEA predictions		NA*	NA*	NA*	NA*			

* Not required because measured stress does not exceed 75% of allowable

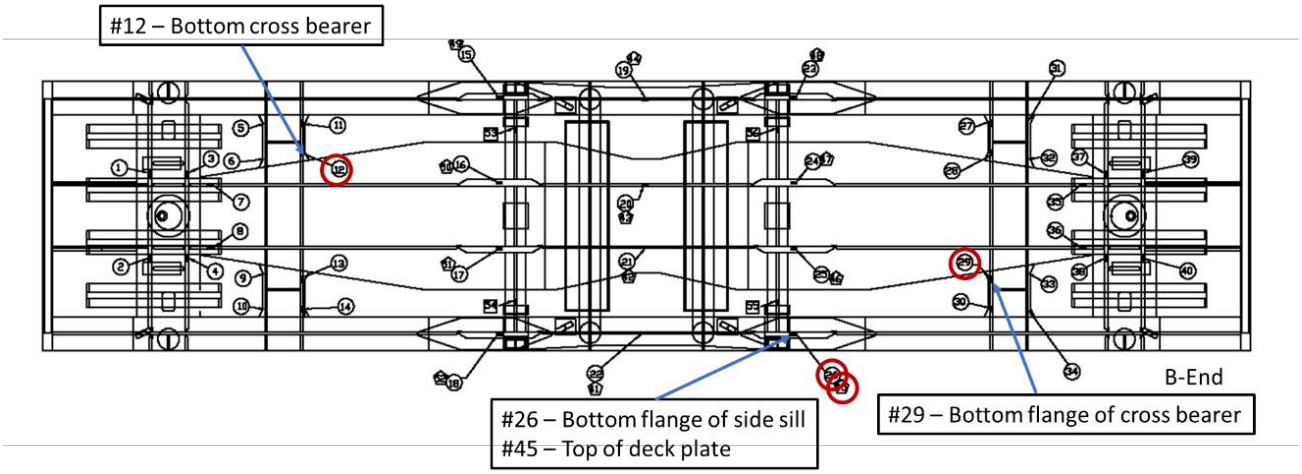


Figure 10. Measurement locations with highest stresses during carbody twist test

4.6 Impact

Table 15 shows the summary results from the impact test for the locations with the highest measured stress. These locations are highlighted in Figure 11.

Standard S-2043, paragraph 4.1.5.9 Allowable Stresses states "All conditions resulting from live and dead loads in combination with impact loads shall follow the guidelines in MSRP Section C Part II, Specification M-1001, paragraph 4.2.2.6." Paragraph 4.2.2.6 states that "such loading may develop the ultimate load carrying capacity of the member being investigated." TTCI used the ultimate stress as the allowable stress for impact tests to comply with the Allowable Stresses statement found in paragraph 4.1.5.9.

The highest stresses were measured at the highest impact speed of 9.6 mph. The coupler load measured on this run was 612 kips. The maximum measured stress was 28 percent of the material yield.

Table 15. Comparison of selected measured stresses with predicted stresses for impact test

Channel Name	Approximate Location	Normal Stress in the Active Direction of the Strain Gage					
		Measured Stress from Max Test Load (ksi)	Measured Stress from Impact Force (ksi)	Total Stress (ksi)	Ultimate Stress (ksi)	Total Stress as percent of Ultimate	Percent Difference Test vs Predicted
SGBF26 (highest total stress)	Center of LH side sill bottom flange, approx. 74 1/8 inches from B end body bolster toward center of car.	27	-6.8	20	90	22%	NA*
SGBF26 FEA predictions		26	-4.1	21.9			
SGBF36 (highest stress from applied load	LH side of bottom flange of center sill – 5 3/16 inches from B-end body bolster toward center of car - aligns with center sill web	3.4	-17	-13	75	17%	NA*
SGBF36 FEA predictions		3	-4	-1			
SGBF35 (#2 rank stress from applied load	RH side of bottom flange of center sill – 5 3/16 inches from B-end body bolster toward center of car - aligns with center sill web	3.4	-17	-13	75	17%	NA*
SGBF35 FEA predictions		3	-4	-1			
SGDP52 (#3 rank stress from applied load	Top of deck plate, above RH center sill web, approx. 2 inches forward of #3 cross bearer	-17	7	-10	75	13%	NA*
SGDP52 FEA predictions		-18	2	-16			

* Not required because measured stress does not exceed 75% of allowable

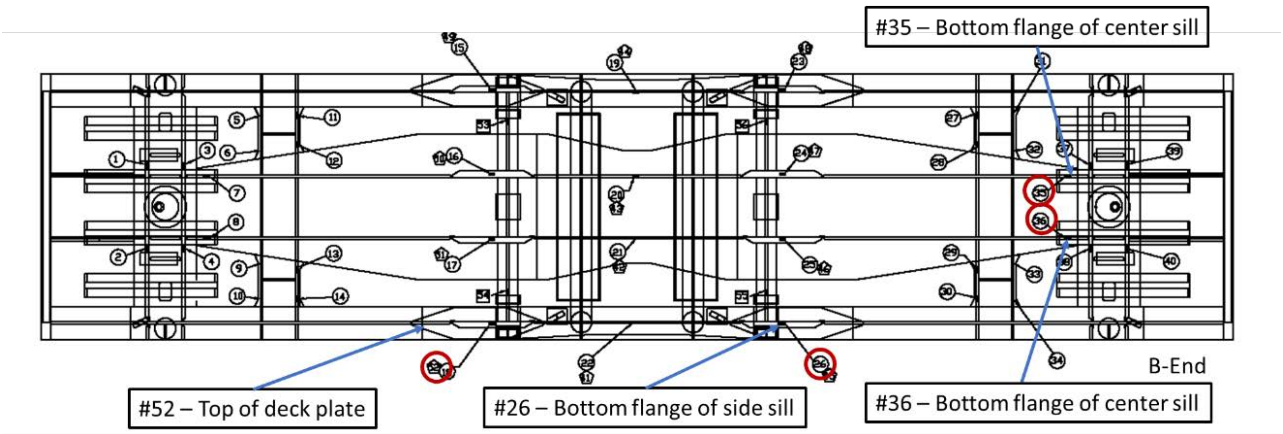


Figure 11. Measurement locations with highest stresses during impact test

5.0 NEW FEA PREDICTIONS

Because none of the measured stresses corresponded with stresses greater than 75 percent of the allowable stress, the tolerance on FEA prediction accuracy does not apply. No new FEA predictions are required.

6.0 REFINING THE DYNAMIC MODEL

Standard S-2043 requires:

"The dynamic model must be refined based on vehicle characterization results if suspension values are measurably different than those used in the original model."

Some of the measured characterization results differ from those used in the original dynamic analysis model. Table 16 provides 1) the suspension stiffness and damping values used for the original model, 2) the values measured during the characterization, 3) the percent difference, 4) information on the origin of the characterization value, and 5) an indication of if and how the characterization value was used to update the model.

Table 16. Comparison of values used in preliminary modeling and values measured during characterization

Parameter		Pre-Test Model Value	Characterization Value	Percent Difference	Notes	Change to model
End Truck Spring vertical stiffness (pound/inch/nest)		31,474	32,472	-3%	Built up from spring component stiffness tests	No change made
End Truck Vertical secondary stiffness (pound/inch/nest)		31,474	35,000	-10%	Characterization value from 0.1 Hz case, minimum and maximum load condition	No change made
End Truck Lateral secondary stiffness (pound/inch/nest)	Min Load	16,976	7,500	118%	Maximum test load, transom restrained	Used 38% of calculated value[6]
	Max Load	18,790	11,500	64%	Maximum test load, transom restrained	Used 58% of calculated value[6]
End Truck Vertical secondary hysteresis width (pound/nest)		5,800	6,000	-3%	Maximum test load	No change made
End Truck Lateral secondary hysteresis width (pound/nest)		5,800	7,900	-27%	Maximum test load, transom restrained	No change made
Middle Truck Spring vertical stiffness (pound/inch/nest)		30,252	31,516	-4%	Built up from spring component stiffness tests	No change made
Middle Truck Vertical secondary stiffness (pound/inch/nest)		30,252	34,500	-12%	Characterization value from 0.1 Hz case, minimum and maximum load condition	No change made
Middle Truck Lateral secondary stiffness (pound/inch/nest)	Min Load	15,595	4,500	233%	Maximum test load, transom restrained, wedges removed	Used 38% of calculated value*
	Max Load	17,363	9,500	84%	Maximum test load, transom restrained, wedges removed	Used 58% of calculated value*
Middle Truck Vertical secondary hysteresis width (pound/nest)		6,000	6,500	-8%	Characterization value from 0.1 Hz case, minimum and maximum load condition	No change made
Middle Truck Lateral secondary hysteresis width (pound/nest)		6,000	7,700	-22%	Maximum test load, transom restrained, wedges installed	No change made
Side bearing preload (pounds)		5000	5240	-5%		No change made

Parameter	Pre-Test Model Value	Characterization Value	Percent Difference	Notes	Change to model
Span Bolster Center plate friction (nondimensional)	0.15	0.17	-12%	Average on the surface. Median of min and max test load values	The friction coefficient was changed to match the characterization value.
Truck Center plate friction (nondimensional)	0.30	0.21	43%	Average on the surface. Median of min and max test load values for the tree trucks tested	The friction coefficient was changed to match the characterization value.
Vertical primary stiffness (pound/inch/pad)	500,000	236,000 288,000	112% 74%	Characterization values range from 194,000 to 288,000 for minimum test load and 213,000 to 510,000 for maximum test load. The average is shown for each load case.	A stiffness of 236,000 is used for minimum test load model and 291,000 is used for maximum test load model.
Lateral primary stiffness (pound/inch/pad)	48,000	35,000 82,000	37% -41%	Characterization values range from 27,000 to 55,000 for minimum test load and 58,000 to 107,000 for maximum test load. The average shown for each load case.	A stiffness of 35,000 is used for minimum test load model and 82,000 is used for maximum test load model.
Longitudinal primary stiffness at axle centerline (pound/inch/pad)	22,500	12.3 13	83% 73%	Data taken from second interaxle test rather than that reported in test report. Characterization values range from 9,900 to 16,100 for minimum test load and 10,100 to 18,400 for maximum test load. The average shown for each load case.	A stiffness of 12,300 is used for minimum test load model and 13,000 is used for maximum test load model.

The lateral secondary suspension stiffness measured during the characterization test was about 58 percent of the value used in the dynamic analysis model for the maximum test load and about 38 percent of the value used for the minimum test load. The measured stiffness is lower because the formula[6] used to estimate the shear stiffness often predicts a higher stiffness than what is found in practice. To match the values from characterization tests, the shear stiffness in the revised dynamic model calculated using the formula were reduced. When compared to the use of Koffman's formula, these modified stiffnesses were 58 percent lower for maximum test load simulations and 38 percent lower for minimum test load simulations. The results of the characterization tests are believed to be more accurate than Koffman's formula.

The original dynamic analysis model used a coefficient of friction value of 0.3 to model the surface between the carbody center plate and the truck center bowl. The coefficient of friction measured during the characterization test was 0.21. The refined dynamic model used a coefficient of friction of 0.21 for this surface. This model used the following:

- A vertical primary pad stiffness of 500,000 pounds per inch per pad for all load conditions.
- A lateral primary pad stiffness of 48,000 pounds per inch per pad for all load conditions.
- A longitudinal primary pad stiffness of 22,500 pounds per inch per pad for all load conditions.

The vertical stiffnesses were measured using CSM 58 primary pads during the characterization tests were about 236,000 pounds per inch and 288,000 pounds per inch per pad for the minimum and maximum test load, respectively. The revised model used these stiffness values for the two test load conditions. Based on the manufacturer's recommendation, a factor of 4X was applied to these values for simulations using CSM 70 primary pads.

The lateral stiffnesses measured with CSM 58 primary pads during the characterization tests were about 35,000 pounds per inch per pad and 82,000 pounds per inch per pad for the minimum and maximum test load, respectively. The revised model used these stiffness values for the two test load conditions. Based on the manufacturer's recommendation, a factor of 1.35X was applied to these values for simulations using CSM 70 primary pads.

While troubleshooting the curving performance in November 2020, TTCI performed a second interaxle longitudinal stiffness test to measure the stiffness of the CSM 70 pads and remeasure the stiffness of the CSM 58 pads. These tests were separate from those presented in the Atlas car single car test report. Figure 12 shows the results of these tests. The longitudinal pad stiffnesses measured during the second interaxle stiffness tests using CSM 58 primary pads were about 12,300 pounds per inch per pad and 13,000 pounds per inch per pad for the minimum and maximum test load, respectively. When this test was performed using the CSM 70 pads the stiffnesses measured were about 28,700 and 31,200 pounds per inch per pad for the minimum and maximum test load, respectively. The revised model used these stiffness values for the two test load conditions with the two pad types.

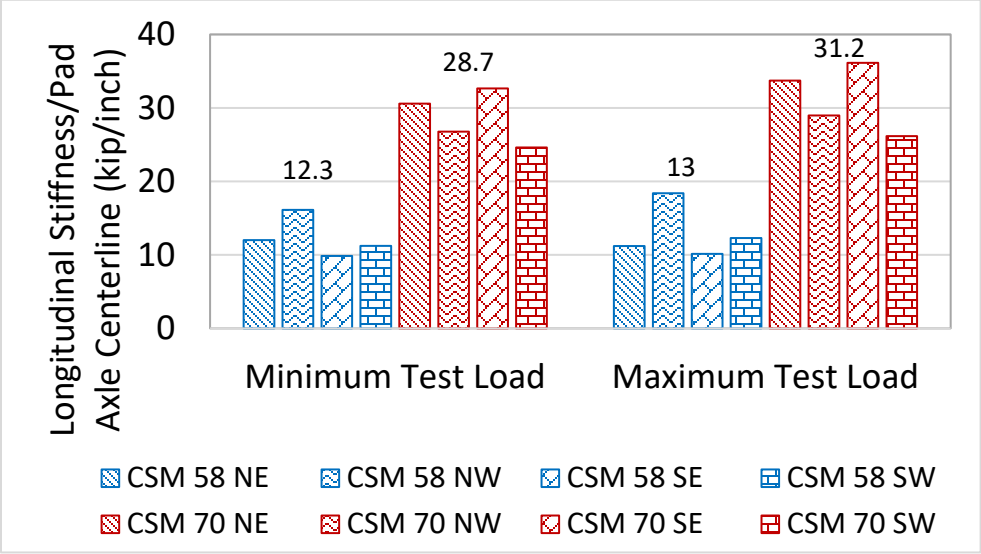


Figure 12. Results of the second interaxle stiffness test with CSM 58 and CSM 70 primary pads

While troubleshooting the hunting performance of Atlas car, TTCI found that the method used to model the connection between the side frame and the primary pad could be altered to better replicate the roll characteristics between the side frame and axle. The original modeling method for this this connection used only a single vertical connection centered at the primary pad located between the side frame and axle. When comparing the predicted lateral suspension displacement with test results, TTCI found that the results matched better when the two connections, separated laterally by the width of the primary pad, were used to model this connection. This new method was implemented in the refined dynamic analysis model.

7.0 NEW DYNAMIC PREDICTIONS

Standard S-2043 states the following:

> *"Test results must be compared to design predictions to verify that the model accurately represents the vehicle. If substantial modifications have been made to the dynamic model, a revised analysis must be performed. The designer may choose to repeat the entire analysis or reanalyze limited cases based on how critically they would be affected by the changes to the model and how large existing margins of safety are. The designer's decisions must be justified through adequate explanation."*

TTCI compared the original and refined dynamic analysis model predictions with the test data to show that the model accurately represented the vehicle. The characterization test results prompted several changes to the dynamic analysis model. As a result, TTCI repeated several portions of the dynamic analysis. The simulation predictions are shown for the original and revised models in Sections 7.1 to 7.10.

Several regimes were simulated using CSM 70 primary pads for comparison with test data to demonstrate model validation and CSM 58 primary pads to demonstrate the expected performance with the primary pad to be used in service. The simulation predictions made using CSM 58 primary

pads were compared to the test data for the hunting and minimum test load dynamic curving where the test data was available. TTCI repeated the following portions of the dynamic analysis because they served to demonstrate the model performance as compared to the test data:

- Twist and roll
- Pitch and bounce
- Yaw and sway
- Dynamic curving
- Single bump test
- Curving with single rail perturbation
- Hunting
- Standard Chapter 11 constant curving
- Limiting spiral negotiation

TTCI repeated the following portions of the dynamic analysis because the original dynamic analysis predictions showed that some metrics were close to or did not meet the criteria.

- Curving with various lubrication conditions
- Turnouts and crossovers
- Buff and draft curving
- Worn component simulation

Because the original dynamic analysis showed a relatively large margin of safety with respect to the criteria for these regimes, the regimes below were not simulated with the revised model:

- Ride quality
- Braking effects on steering

The lightest load modeled during the original dynamic analysis for the Atlas car in 2017 is different than what was tested and modeled during the post-test analysis simulations described in this report. Because of this difference, the original simulation predictions for the lightest car condition will not be compared to the revised predictions for the minimum test load. In 2017, the DOE expected to sometimes move an Atlas car in a Standard S-2043 train without a cask loaded on the car. To meet all dynamic requirements, a ballast load was needed, and Orano designed a ballast load for this purpose. Ballast load properties were used for the “empty” car simulations performed in 2017. Since that time, the DOE determined that any empty Atlas car could be moved using non-Standard S-2043 trains. Because of this determination, the minimum simulated load was changed from the ballast load to a load representing the lightest empty cask that would be carried by a Standard S-2043 train, referred to as the minimum test load. The revised predictions for the maximum test load are consistent with the original predictions for the HI-STAR 190 XL cask. The EEC approved the empty Atlas car for use in non-HLRM trains based on its similarities with the empty Navy M-290 HLRM car. This car has been approved under M-1001 (see Section 4 and Appendix A of [2]).

Most simulation predictions were made using inputs created with measured track geometry. TTCI's experience has shown that simulations with measured track geometry produce better predictions of car performance than those that are obtained with analytic track inputs created with mathematical functions. Because the measured track geometry inputs contain short wavelengths that cause spurious peaks in the data, the 50-millisecond and 3-foot analysis windows described in AAR Chapter 11 and S-2043 are used when analyzing data to produce the most realistic results. The exceptions included some curving with single rail perturbation simulations and special track work simulations of number 7 turnouts and number 7 crossovers that used inputs from mathematically generated inputs.

7.1 Twist and Roll

The simulations of the twist-and-roll regime were conducted according to Standard S-2043, Paragraph 4.3.9.6. The twist-and-roll track tests were conducted according to Standard S-2043, Paragraph 5.5.8. The twist-and-roll regime consists of a series of ten 0.75-inch vertical track deviations offset on each rail to input roll motions to the car.

7.1.1 Minimum Test Load

Table 17 shows the worst-case test results and the simulation predictions for the car loaded with the minimum test load. Figure 13 shows the peak-to-peak roll angle for the results from testing done using CSM 70 pads and modeling predictions using both CSM 70 and CSM 58 primary pads plotted against speed to show the trend in performance. As Figure 13 shows, the simulation predictions and the test results for CSM 70 pads have a lower center roll resonance at the same speed and a similar overall trend. The simulation predictions done using CSM 58 pads show slightly higher lateral acceleration values than the values from the simulation predictions done using CSM 70 pads, but results for other metrics are similar. Only post-test simulation predictions are shown because the pre-test predictions were performed for a load case no longer intended for use (as described in Section 7.0). The twist-and-roll test results and revised simulation predictions **meet** Standard S-2043 criteria for the minimum test load.

Table 17. Twist-and-roll test results and simulation predictions using minimum test load

Criterion	Limiting Value	CSM 70 Pads		CSM 58 Pads
		Test Result	Simulation Prediction Revised Model	Simulation Prediction Revised Model
Roll angle (degree)	4.0	1.4	1.9	1.9
Maximum wheel lateral/vertical (L/V)	0.8	0.27	0.29	0.27
Maximum truck side L/V	0.5	0.19	0.15	0.17
Minimum vertical wheel load (%)	25%	54%	57%	58%
Lateral peak-to-peak acceleration (g)	1.3	0.50	0.29	0.47
Maximum lateral acceleration (g)	0.75	0.26	0.15	0.24
Maximum vertical acceleration (g)	0.90	0.36	0.19	0.20
Maximum vertical suspension deflection (%)	95%	16%	22%	21%

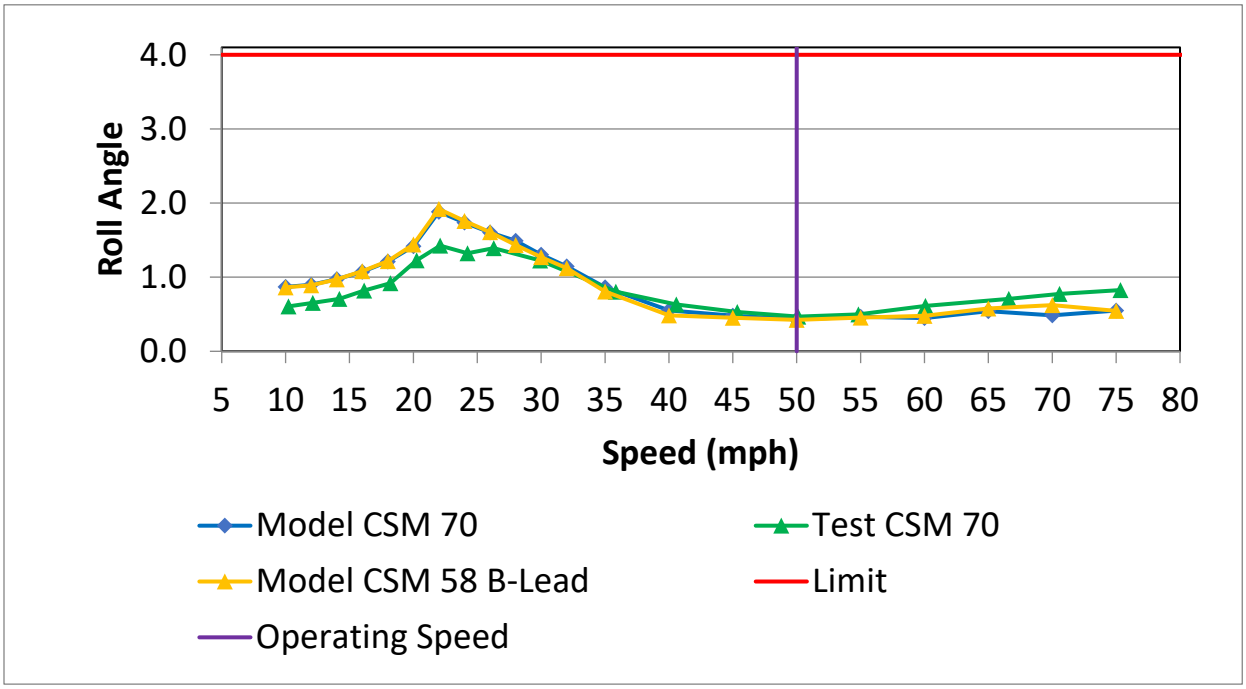


Figure 13. Twist-and-roll test results and simulation predictions of maximum peak-to-peak carbody roll angle with minimum test load

7.1.2 Maximum Test Load

Table 18 shows the worst-case test results and simulation predictions for the car loaded with the maximum test load. Figure 14 shows the peak-to-peak roll angle for test results and modeling predictions done using CSM 70 primary pads plotted against speed to show the trend in performance. Figure 15 shows the peak-to-peak roll angle for the pre-test and refined-models simulation predictions. The test results and simulation predictions (Figure 14) show the lower-center roll resonance at the same speed and similar overall performance trends. The simulation predictions done using CSM 58 pads showed a similar performance to simulation predictions done using CSM 70 pads. The simulation predictions changed very little after changes in model inputs using the characterization results. The revised simulation predictions **meet** Standard S-2043 criteria for the twist and roll tests with maximum test load.

Table 18. Twist-and-roll test results and simulation predictions with maximum test load

Criterion	Limiting Value	CSM 70 Pads		CSM 58 Pads	
		Test Result	Simulation Prediction Revised Model	Simulation Prediction Original Model	Simulation Prediction Revised Model
Roll angle (degree)	4.0	1.3	1.7	2.1	1.8
Maximum wheel lateral/vertical (L/V)	0.8	0.23	0.14	0.14	0.14
Maximum truck side L/V	0.5	0.15	0.08	0.11	0.10
Minimum vertical wheel load (%)	25%	64%	62%	66%	63%
Lateral peak-to-peak acceleration (g)	1.3	0.31	0.34	0.24	0.38
Maximum lateral acceleration (g)	0.75	0.17	0.19	0.13	0.21
Maximum vertical acceleration (g)	0.90	0.20	0.24	0.11	0.25
Maximum vertical suspension deflection (%)	95%	56%	63%	74%	63%

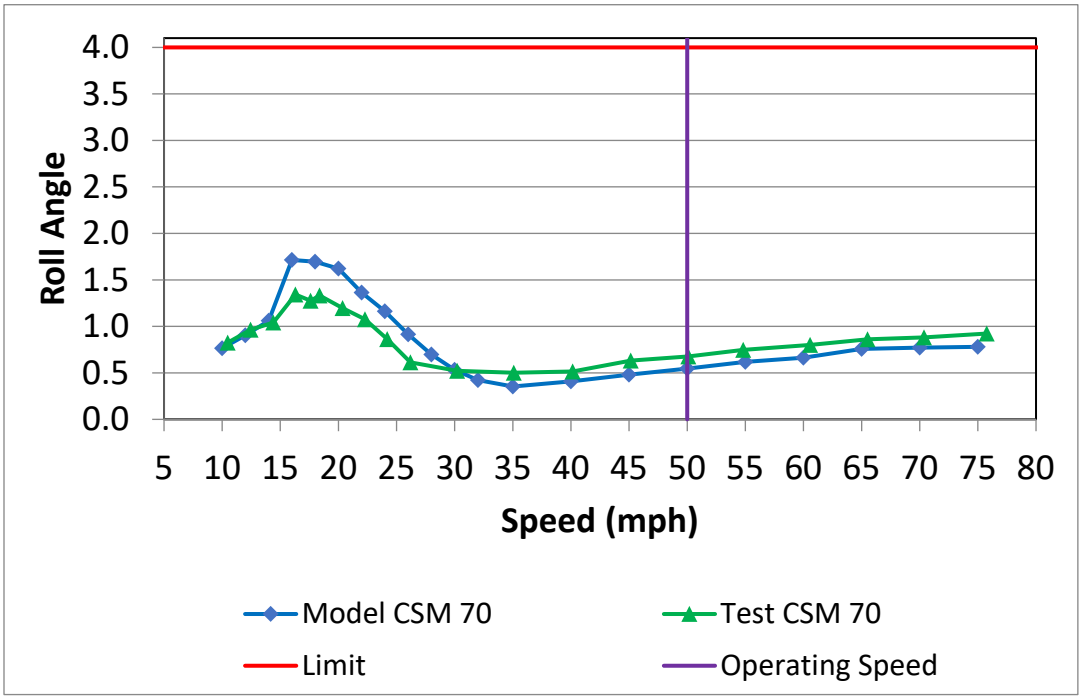


Figure 14. Twist-and-roll test results and simulation predictions of maximum peak-to-peak carbody roll angle with maximum test load using CSM 70 pads

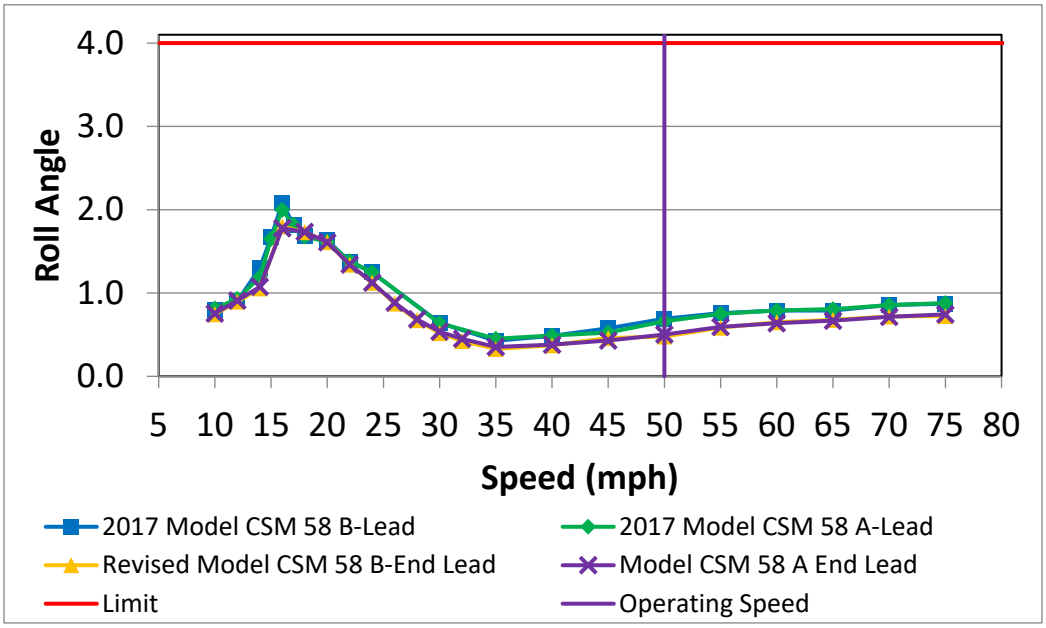


Figure 15. Twist-and-roll pre-test and refined model simulation predictions of maximum peak-to-peak carbody roll angle with maximum test load using CSM 70 pads

7.2 Pitch and Bounce (Chapter 11)

The simulations of the pitch-and-bounce regime were conducted according to Standard S-2043, Paragraph 4.3.9.7. The pitch-and-bounce tests were conducted according to Standard S-2043, Paragraph 5.5.11. The pitch-and-bounce regime consists of a series of ten 0.75-inch vertical track deviations in parallel on each rail to input vertical motions on the car.

Because the truck center spacing of the car (38 feet, 9 inches) is so similar to the wavelength of the perturbations of the standard pitch-and-bounce zone (39 feet), special tests or simulations with inputs at a wavelength equal to the truck center spacing of the car were not performed.

7.2.1 Minimum Test Load

Simulations are required for the minimum test load condition, but testing is not required. Table 19 shows the worst-case simulation predictions for the car loaded with the minimum test load. Figure 16 shows the maximum vertical acceleration for the modeling predictions using CSM 58 primary pads plotted against speed to show the trend in performance. The revised simulation predictions **meet** Standard S-2043 criteria for pitch and bounce done using CSM 58 pads at minimum test load.

Table 19. Pitch and bounce test results and simulation predictions

Criterion	Limiting Value	Simulation Prediction Revised Model
Roll angle (degree)	4.0	0.2
Maximum wheel L/V	0.8	0.18
Maximum truck side L/V	0.5	0.11
Minimum vertical wheel load (%)	25%	61%
Lateral peak-to-peak acceleration (g)	1.3	0.48
Maximum lateral acceleration (g)	0.75	0.26
Maximum vertical acceleration (g)	0.90	0.00
Maximum vertical suspension deflection (%)	95%	0.53

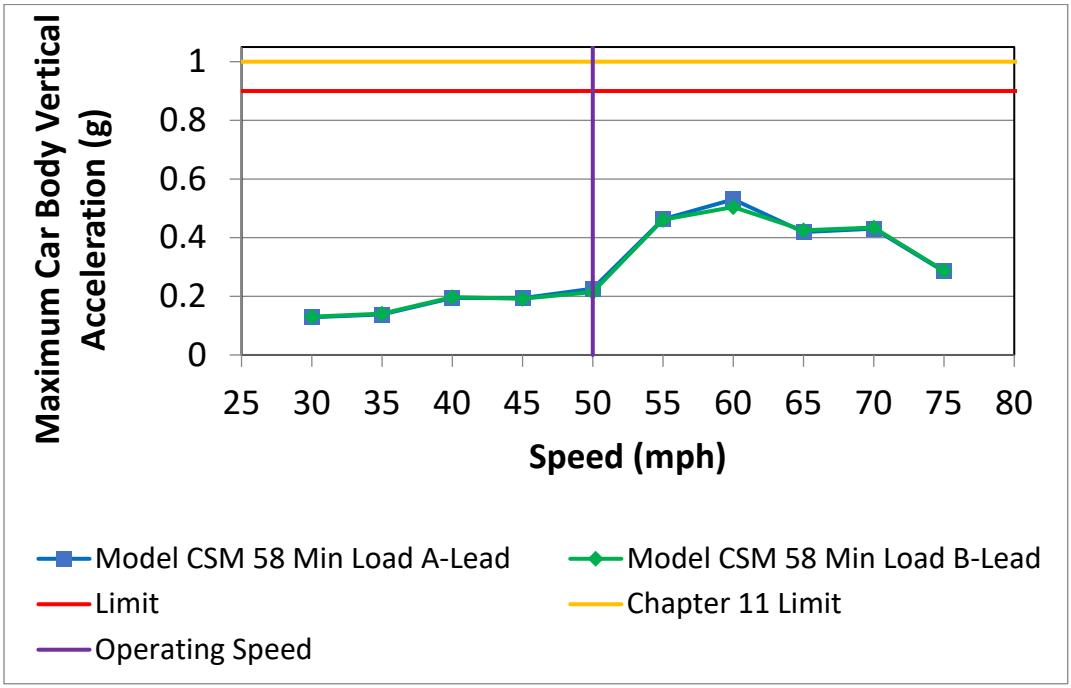


Figure 16. Simulation predictions of maximum vertical carbody acceleration in the pitch and bounce regime with minimum test load

7.2.2 Maximum Test Load

Table 20 shows the worst-case test results and simulation predictions for the car loaded with the maximum test load. Figure 17 shows the test results and modeling predictions of the maximum vertical acceleration using CSM 70 primary pads plotted against speed to show the trend in performance. Figure 18 shows the simulation predictions of maximum vertical acceleration done using CSM 58 primary pads. The maximum vertical acceleration simulation predictions and test results done using CSM 70 primary pads match closely. The simulation predictions done using CSM 58 pads show similar minimum vertical wheel load results, but slightly higher carbody accelerations than the simulation predictions done using CSM 70 pads. The revised simulation predictions showed not only higher lateral/vertical (L/V) ratio and acceleration values but also higher minimum vertical

load values than the original 2017 simulation predictions. The test results and revised simulation predictions **meet** Standard S-2043 criteria for pitch and bounce with maximum test load.

Table 20. Test results and simulations predictions for Pitch and Bounce with maximum test load

Criterion	Limiting Value	CSM 70 Pads		CSM 58 Pads	
		Test Result	Simulation Prediction Revised Model	Simulation Prediction Original Model	Simulation Prediction Revised Model
Roll angle (degree)	4.0	0.2	0.3	0.1	0.3
Maximum wheel lateral/vertical (L/V)	0.8	0.10	0.14	0.06	0.12
Maximum truck side L/V	0.5	0.07	0.09	0.04	0.09
Minimum vertical wheel load (%)	25%	63%	73%	68%	74%
Lateral peak-to-peak acceleration (g)	1.3	0.12	0.25	0.16	0.34
Maximum lateral acceleration (g)	0.75	0.07	0.14	0.08	0.20
Maximum vertical acceleration (g)	0.90	0.25	0.26	0.22	0.38
Maximum vertical suspension deflection (%)	95%	52%	56%	76%	56%

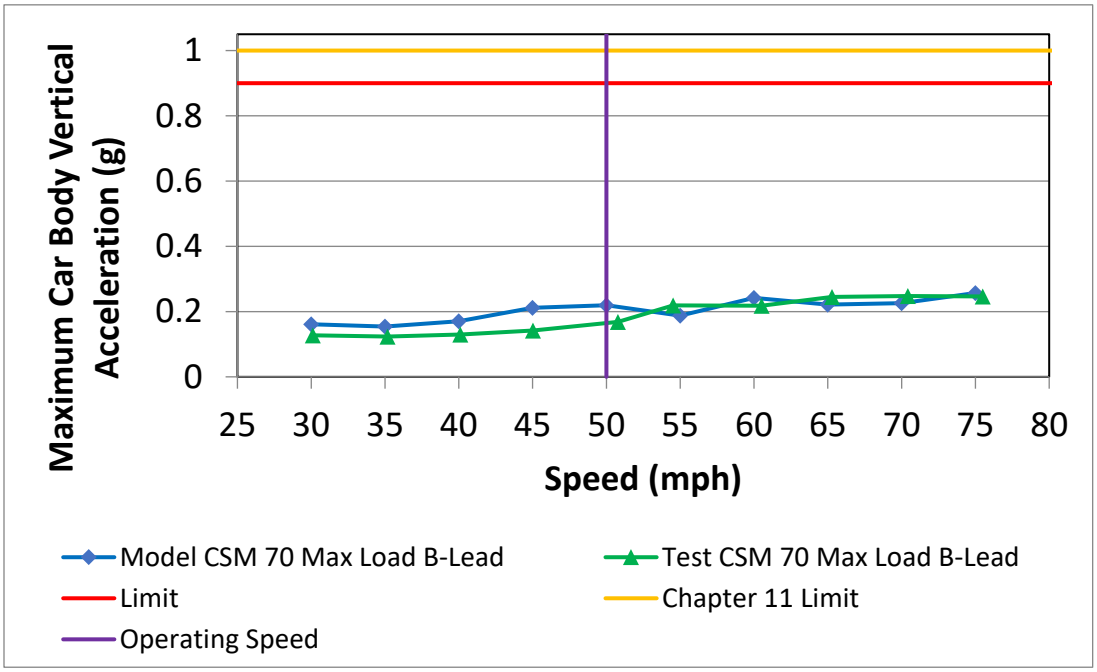


Figure 17. Pitch and bounce test results and simulation predictions of maximum vertical acceleration with CSM 70 Pads at maximum test load

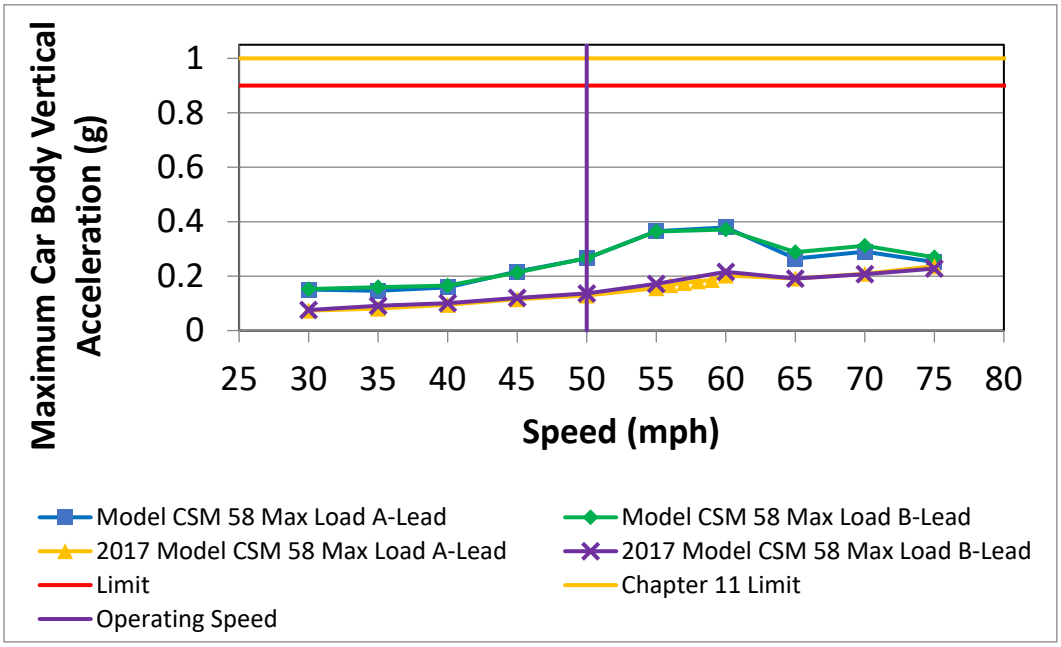


Figure 18. Pitch and bounce simulation predictions of maximum vertical acceleration with CSM 58 Pads at maximum test load

7.3 Yaw and Sway

Simulations of the yaw-and-sway regime were conducted according to Standard S-2043, Paragraph 4.3.9.8. The yaw-and-sway tests were conducted according to Standard S-2043, Paragraph 5.5.9. The yaw-and-sway regime consists of a series of five consecutive 1.25-inch lateral deviations, on a track section with a 1-inch-wide gage, that input lateral and yaw motions on the car.

Table 21 shows the worst-case test results and the simulation predictions for the car loaded with the maximum test load in the yaw-and-sway test regime. Figure 19 shows the test results and modeling predictions of the maximum truck side L/V ratio with CSM 70 primary pads plotted against speed to show the trend in performance. Figure 20 shows the simulation predictions of the maximum truck side L/V ratio with CSM 58 primary pads. The test results and revised simulation predictions **meet** Standard S-2043 criteria for yaw-and-sway with the maximum test load. Using CSM 70 primary pads, the model predicts higher accelerations, higher L/V ratios, and lower vertical wheel loads than those measured in the test. The simulations done using CSM 58 pads showed lower accelerations, lower L/V ratios, and higher vertical wheel loads than simulations done using CSM 70 primary pads. The differences between the original 2017 simulation predictions and the revised simulation predictions were inconsequential relative to Standard S-2043 criteria levels.

Table 21. Yaw-and-sway test results and simulation predictions

Criterion	Limiting Value	CSM 70 Pads		CSM 58 Pads	
		Test Result	Simulation Prediction Revised Model	Simulation Prediction 2017 Model	Simulation Prediction Revised Model
Roll angle (degree)	4.0	0.7	1.2	0.8	1.0
Maximum wheel L/V	0.8	0.53	0.72	0.59	0.55
Maximum truck side L/V	0.5	0.31	0.43	0.30	0.35
Minimum vertical wheel load (%)	25%	68%	55%	56%	66%
Lateral peak-to-peak acceleration (g)	1.3	0.82	1.21	0.67	0.87
Maximum lateral acceleration (g)	0.75	0.44	0.63	0.36	0.47
Maximum vertical acceleration (g)	0.90	0.17	0.28	0.11	0.41
Maximum vertical suspension deflection (%)	95%	58%	61%	70%	59%

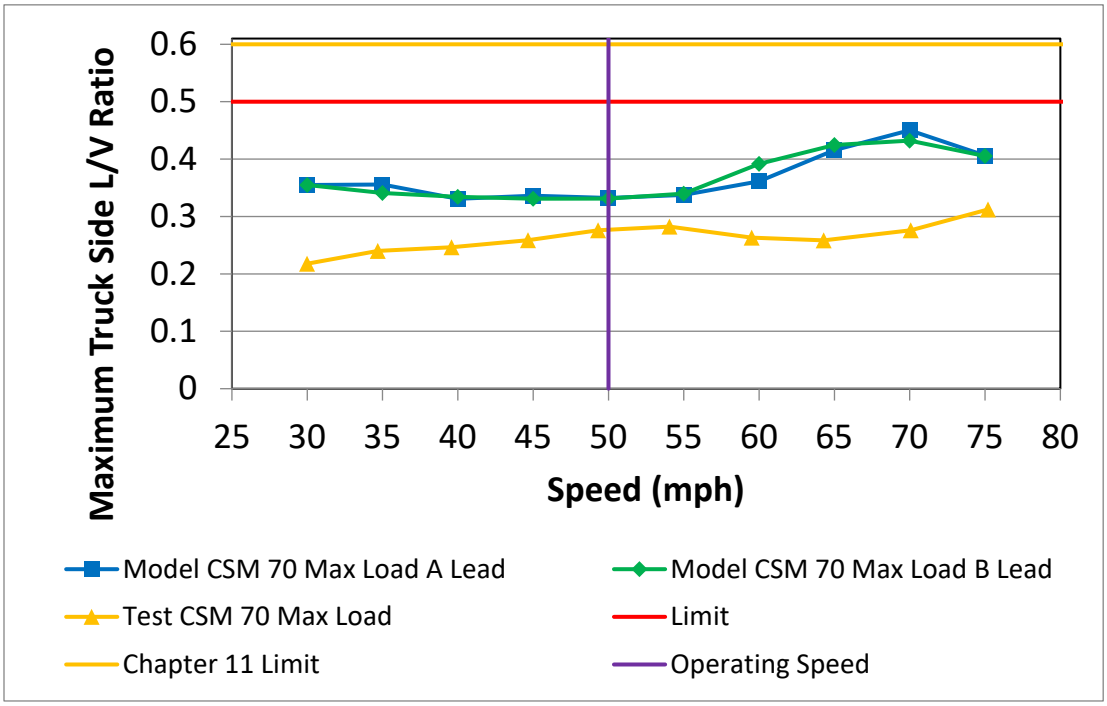


Figure 19. Simulation predictions and test results of maximum truck side L/V ratio in the yaw-and-sway regime with CSM 70 pads and the maximum test load

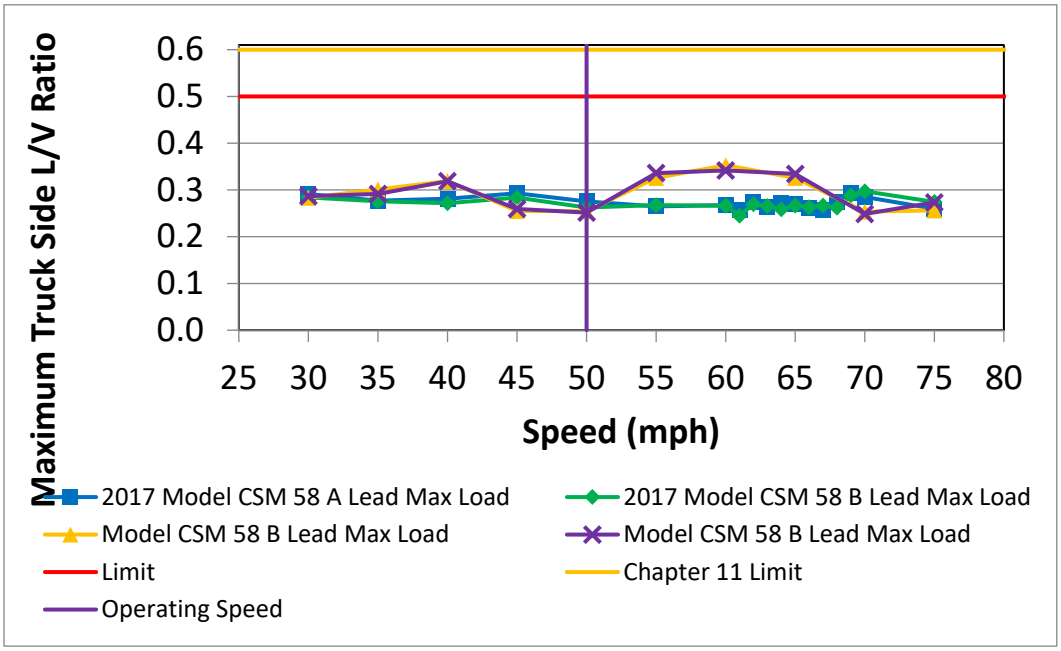


Figure 20. Simulation predictions of maximum truck side L/V ratio in the yaw-and-sway regime with CSM 58 pads and the maximum test load

7.4 Dynamic Curving

Simulations of the dynamic curving regime were conducted according to Standard S-2043, Paragraph 4.3.9.9. The dynamic curving tests were conducted according to Paragraph 5.5.10 of Standard S-2043. The dynamic curve section is on a 10-degree curve with a 4-inch superelevation. The dynamic curving regime consists of a series of 0.5-inch vertical track deviations at a 39-foot wavelength offset on each rail to input roll motions to the car. There are five deviations on the high rail and six deviations on the low rail. At the same time, the track gage changes from 56.5 inches to 57.5 inches to input lateral motions to the car. The simulations and tests were performed at speeds ranging from 10 mph (approximately 3 inches of cant excess) to 32 mph (3 inches of cant deficiency) in increments of 2 mph or less.

7.4.1 Minimum Test Load

Table 22 shows the worst-case test results and the simulation predictions for the car loaded with the minimum test load in the dynamic curving test regime. Figure 21 shows the test results and simulation predictions of the maximum wheel L/V ratio with CSM 70 primary pads plotted against speed to show the trend in performance. Figure 22 shows the test results and simulation predictions of the maximum wheel L/V ratio with CSM 58 primary pads.

The test results did not meet Standard S-2043 criteria for the wheel L/V ratio with CSM 70 pads for dynamic curving with the minimum test load, but all other criteria were met. Figure 23 shows a distance plot of the worst-case test condition. The simulation predictions done using CSM 70 pads did meet Standard S-2043 criteria. Both the test results and revised simulation predictions done using CSM 58 pads **met** Standard S-2043 criteria.

Using CSM 70 primary pads, the model predicts lower wheel L/V ratios and higher minimum vertical wheel loads than those that were measured in the test. The simulations done using CSM 58 pads showed lower L/V ratios than the simulations done using CSM 70 primary pads, but the difference was not as large as what was measured in the test. Only post-test simulation predictions are shown because the pre-test predictions were for a load case no longer intended for use.

Table 22. Dynamic curving test results and simulation predictions

Criterion	Limiting Value	CSM 70 Primary Pad		CSM 58 Primary Pad	
		Test Result	Simulation Prediction Revised Model	Test Result	Simulation Prediction Revised Model
Roll angle (degree)	4.0	0.9	1.0	0.8	1.0
Maximum wheel L/V	0.8	0.90	0.73	0.75	0.71
Maximum truck side L/V	0.5	0.45	0.39	0.39	0.35
Minimum vertical wheel load (%)	25%	31%	54%	40%	53%
Lateral peak-to-peak acceleration (g)	1.3	0.20	0.19	0.19	0.19
Maximum lateral acceleration (g)	0.75	0.16	0.15	0.19	0.16
Maximum vertical acceleration (g)	0.90	0.14	0.12	0.17	0.12
Maximum vertical suspension deflection (%)	95%	26%	23%	22%	23%

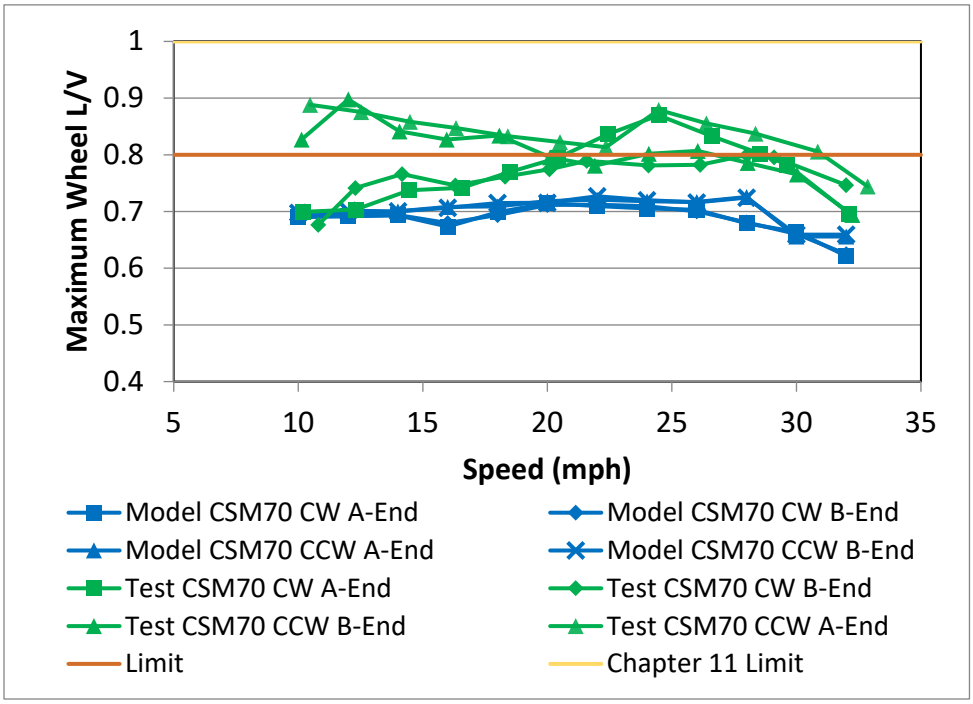


Figure 21. Simulation prediction and test results of maximum wheel L/V ratio in the dynamic curving regime with minimum test load and CSM 70 pads

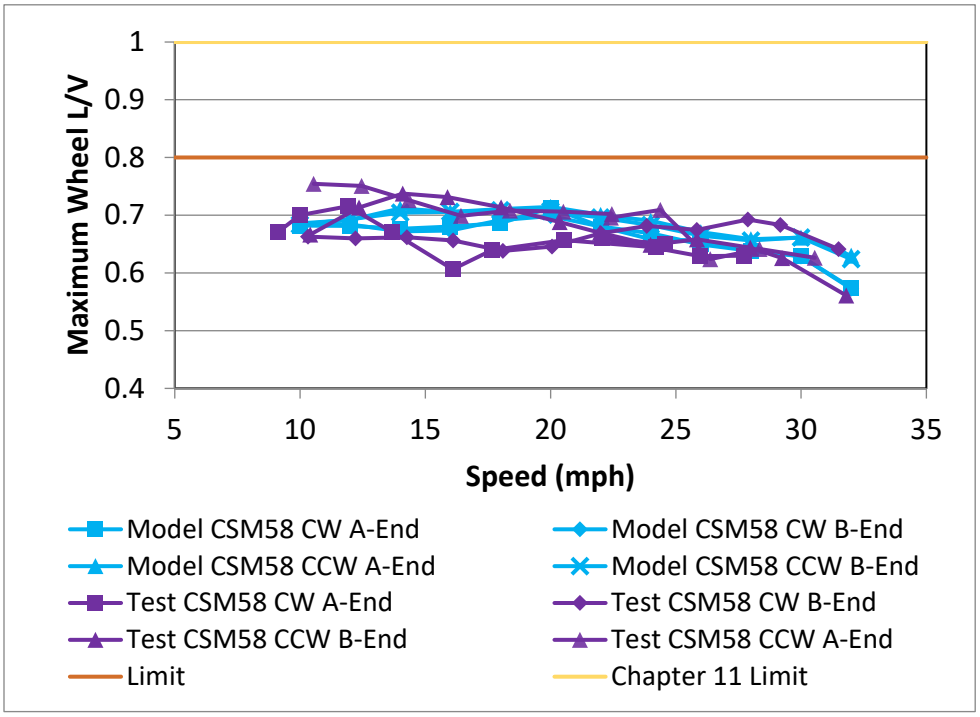


Figure 22. Simulation prediction and test results of maximum wheel L/V ratio in the dynamic curving regime with minimum test load and CSM 58 pads

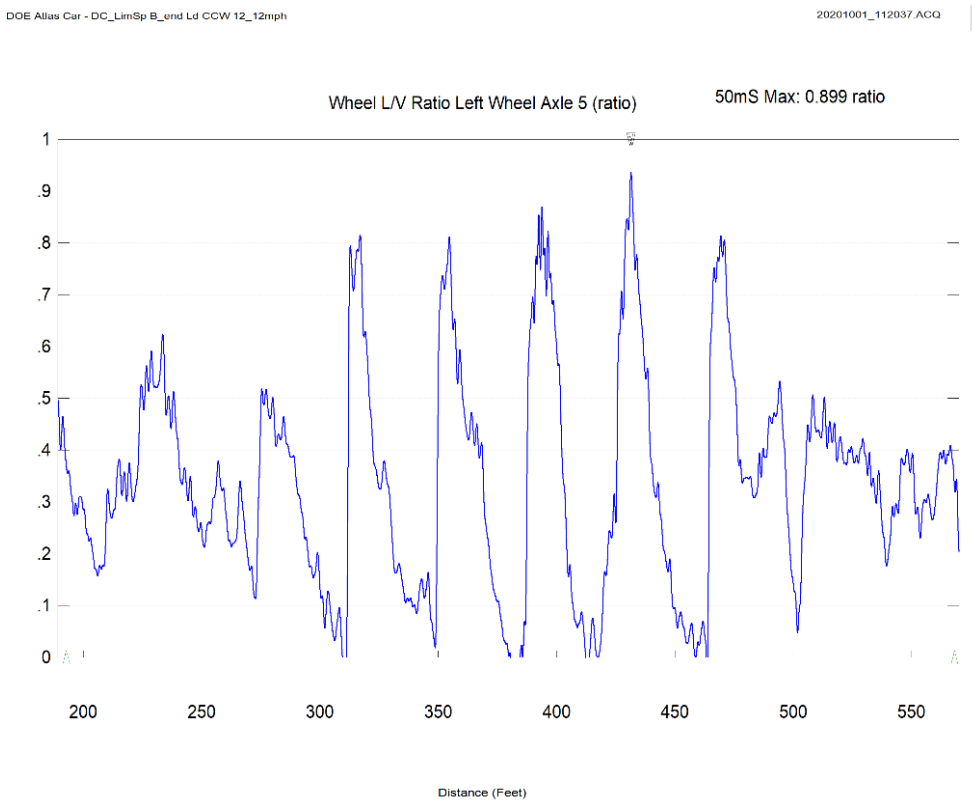


Figure 23. Distance plot of axle 5 lead left wheel L/V ratio during 12 mph run counterclockwise (CCW) through dynamic curve with B-End leading using CSM 70 primary pads

7.4.2 Maximum Test Load

Table 23 shows the worst-case test results and simulation predictions for the car loaded with the maximum test load in the dynamic curving test regime. Figure 24 shows the test results and simulation predictions of the maximum wheel L/V ratio with CSM 70 primary pads plotted against speed to show the trend in performance. Figure 25 shows the original and revised simulation predictions of the maximum wheel L/V ratio with CSM 58 primary pads.

The test results did not meet Standard S-2043 criteria for the wheel L/V ratio with CSM 70 pads for dynamic curving with the maximum test load, but all other criteria were met. The simulation predictions with the revised model using either CSM 70 or CSM 58 pads **met** Standard S-2043 criteria.

Using CSM 70 primary pads, the model predicts lower wheel L/V ratios and higher minimum vertical wheel loads than those that were measured in the test, but the overall trend matches closely, as Figure 24 shows. The simulations done using CSM 58 pads showed lower L/V ratios than the simulations done using CSM 70 primary pads, but the difference was small. The wheel L/V ratios predicted with the original model in 2017 were significantly higher than those predicted with the revised model. This difference is likely explained by the fact that the primary longitudinal stiffness measured in characterization tests and used in the refined model is significantly lower than the original model value.

Table 23. Dynamic curving test results and simulation predictions with maximum test load

Criterion	Limiting Value	CSM 70 Pads		CSM 58 Pads	
		Test Result	Simulation Prediction Revised Model	Simulation Prediction Original Model	Simulation Prediction Revised Model
Roll angle (degree)	4.0	0.8	1.0	1.2	1.0
Maximum wheel lateral/vertical (L/V)	0.8	0.81	0.72	0.88	0.68
Maximum truck side L/V	0.5	0.40	0.37	0.37	0.30
Minimum vertical wheel load (%)	25%	45%	55%	49%	55%
Lateral peak-to-peak acceleration (g)	1.3	0.25	0.12	0.16	0.14
Maximum lateral acceleration (g)	0.75	0.18	0.13	0.13	0.12
Maximum vertical acceleration (g)	0.90	0.11	0.17	0.06	0.25
Maximum vertical suspension deflection (%)	95%	66%	67%	78%	67%

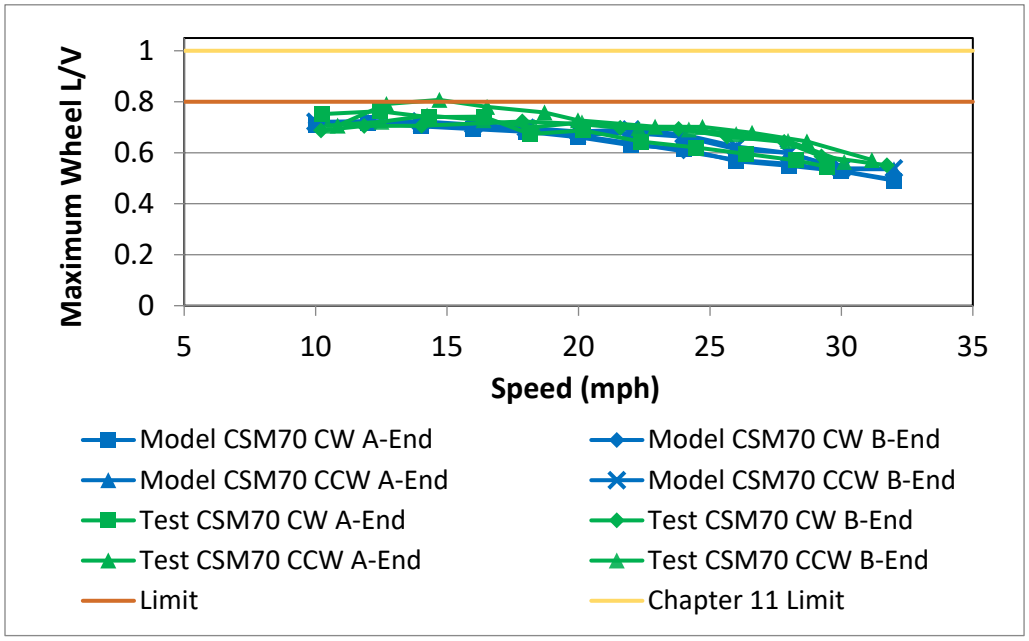


Figure 24. Simulation prediction and test results of maximum wheel L/V ratio in the dynamic curving regime with maximum test load using CSM 70 pads

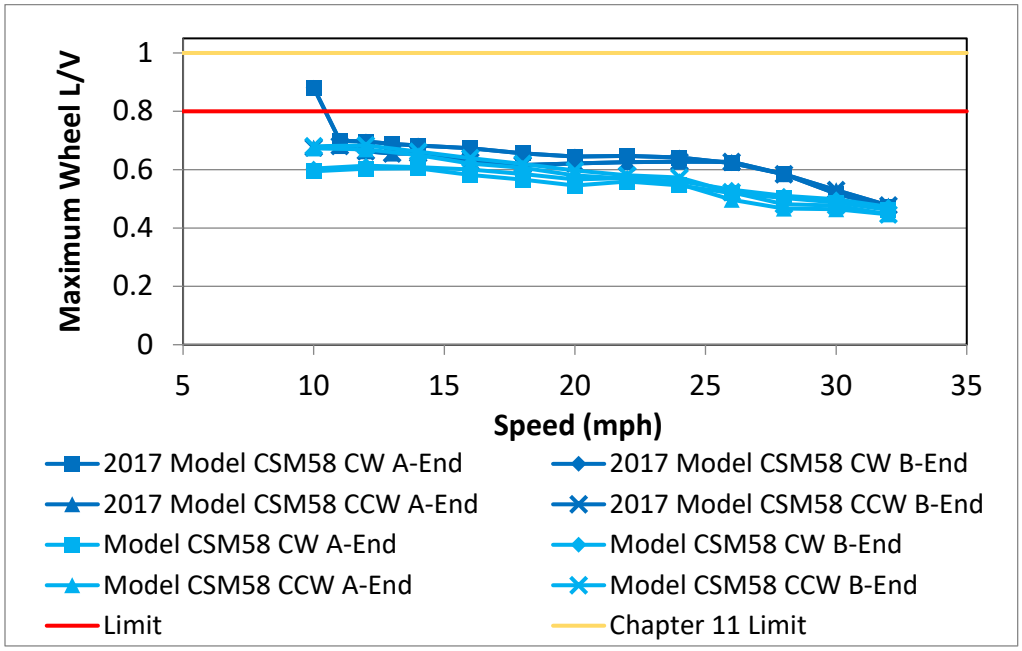


Figure 25. Simulation predictions of maximum wheel L/V ratio in the dynamic curving regime with maximum test load using CSM 70 and CSM 58 pads

7.4.3 Other Various Load Conditions

Table 24 through Table 26 show the worst-case results of simulations of every cask in the dynamic curving regime using the refined model with the different load conditions. The maximum and minimum test load conditions were considered. The simulations for the other casks 16 casks that will be carried on the Atlas car represent those casks in their loaded condition. The maximum wheel L/V

ratio ranged from 0.69 to 0.72, a very narrow window of performance. All simulation predictions for the various load conditions in the dynamic curving regime **met** Standard S-2043 criteria.

Table 24. Dynamic Curving with Various Loads (Part 1 of 3)

Criterion	Limiting Value	Extreme Case		NAC-Intl.			Energy Solutions
		Maximum Test Load	Minimum Test Load	MAGNATRAN	STC	UMS	TS125
Maximum carbody roll angle (degree)	4	0.97	0.97	1.02	1.04	1.04	1.02
Maximum wheel L/V	0.8	0.69	0.71	0.71	0.71	0.71	0.72
Maximum truck side L/V	0.5	0.30	0.35	0.33	0.34	0.34	0.34
Minimum vertical wheel load (%)	25	55.0	52.7	55.5	54.7	54.7	54.6
Peak-to-peak carbody lateral acceleration (g)	1.3	0.12	0.19	0.13	0.15	0.22	0.15
Maximum carbody lateral acceleration (g)	0.75	0.11	0.16	0.13	0.13	0.19	0.15
Maximum carbody vertical acceleration (g)	0.9	0.16	0.12	0.20	0.15	0.16	0.17
Maximum vertical suspension deflection (%)	95	66.8	23.2	46.9	38.0	38.0	40.7

Table 25. Dynamic Curving with Various Loads (Part 2 of 3)

Criterion	Limiting Value	Holtec Intl.		NAC-Intl.		
		HI-STAR-60	HI-STAR-100	HI-STAR-100HB	HI-STAR-180	HI-STAR-190-SL
Maximum carbody roll angle (degree)	4	0.97	1.01	1.02	1.01	0.97
Maximum wheel L/V	0.8	0.71	0.70	0.71	0.70	0.69
Maximum truck side L/V	0.5	0.35	0.32	0.35	0.32	0.31
Minimum vertical wheel load (%)	25	52.2	56.7	53.8	56.7	54.3
Peak-to-peak carbody lateral acceleration (g)	1.3	0.17	0.15	0.16	0.15	0.12
Maximum carbody lateral acceleration (g)	0.75	0.15	0.13	0.13	0.13	0.12
Maximum carbody vertical acceleration (g)	0.9	0.14	0.15	0.12	0.15	0.17
Maximum vertical suspension deflection (%)	95	28.8	44.7	32.6	44.7	61.4

Table 26. Dynamic Curving with Various Loads (Part 3 of 3)

Criterion	Limiting Value	TN Americas LLC						
		AREVA-MP-187	AREVA-MP-197	AREVA-MP197HB	TN-32B	TN-40	TN-40HT	TN-68
Maximum carbody roll angle (degree)	4	1.03	1.04	1.03	1.00	0.99	1.01	1.04
Maximum wheel L/V	0.8	0.70	0.71	0.70	0.70	0.71	0.71	0.72
Maximum truck side L/V	0.5	0.34	0.34	0.33	0.33	0.33	0.34	0.34
Minimum vertical wheel load (%)	25	55.25	54.90	55.63	56.18	55.94	55.80	54.07
Peak-to-peak carbody lateral acceleration (g)	1.3	0.15	0.24	0.20	0.15	0.13	0.14	0.15
Maximum carbody lateral acceleration (g)	0.75	0.14	0.19	0.16	0.14	0.14	0.13	0.14
Maximum carbody vertical acceleration (g)	0.9	0.15	0.15	0.18	0.15	0.15	0.14	0.17
Maximum vertical suspension deflection (%)	95	38.48	36.90	42.38	43.26	44.43	40.41	38.53

7.5 Single Bump Test

Simulations of the single bump regime were conducted according to Standard S-2043, Paragraph 4.3.10.1. The single bump tests were conducted according to Standard S-2043, Paragraph 5.5.13. The single bump test section represents a typical grade crossing with an elevation increase of 1.0 inch over a 7-foot track section, a steady elevation for 20 feet, and then a ramp back down over 7 feet. The simulations and tests were performed at speeds ranging from 30 mph to 75 mph in increments of 5 mph or less.

7.5.1 Minimum Test Load

Table 27 shows the worst-case test results and simulation predictions for the car loaded with the minimum test load in the single bump test regime. Figure 26 shows the test results, the simulation predictions of the minimum vertical wheel load done using CSM 70 primary pads, and simulation predictions done using CSM 58 primary pads plotted against speed to show the trend in performance.

Using CSM 70 primary pads, the model predicts lower minimum vertical wheel loads and higher vertical accelerations than those that were measured in the test, but the overall trend is about the same, as Figure 26 shows. The simulation predictions done using CSM 58 pads were very close to the simulation predictions done using CSM 70 primary pads. Only post-test simulation predictions are shown because the pre-test predictions were for a load case no longer intended for use.

The test results and revised simulation predictions **meet** Standard S-2043 criteria for the single bump test regime with the minimum test load.

Table 27. Single bump test results and simulation predictions with minimum test load

Criterion	Limiting Value	CSM 70 Pads		CSM 58 Pads
		Test Result	Simulation Prediction Revised Model	Simulation Prediction Revised Model
Roll angle (degree)	4.0	0.4	0.2	0.2
Maximum wheel lateral/vertical (L/V)	0.8	0.20	0.10	0.09
Maximum truck side L/V	0.5	0.12	0.07	0.06
Minimum vertical wheel load (%)	25%	66%	59%	61%
Lateral peak-to-peak acceleration (g)	1.3	0.17	0.20	0.18
Maximum lateral acceleration (g)	0.75	0.09	0.10	0.10
Maximum vertical acceleration (g)	0.90	0.37	0.77	0.69
Maximum vertical suspension deflection (%)	95%	18%	36%	34%

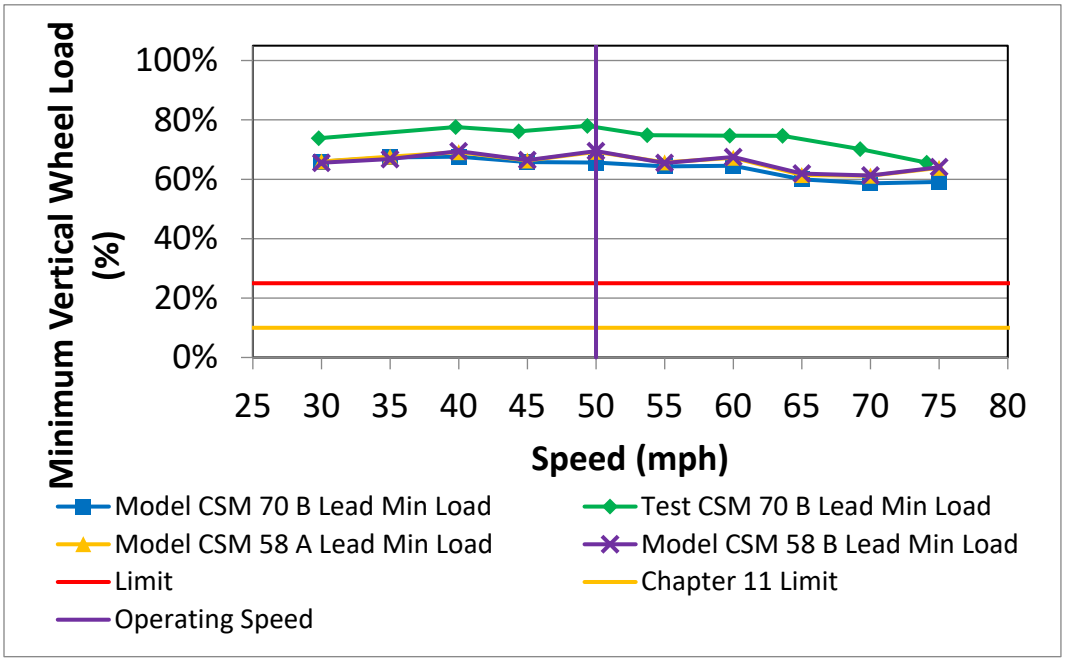


Figure 26. Simulation prediction and test results of minimum vertical wheel load in the single bump regime with minimum test load

7.5.2 Maximum Test Load

Table 28 shows the worst-case test results and simulation predictions for the car loaded with the maximum test load in the single bump test regime. Figure 27 shows test results and simulation predictions of the maximum carbody vertical acceleration done using CSM 70 primary pads plotted against speed to show the trend in performance. Figure 28 shows the original and revised simulation predictions of maximum carbody vertical acceleration done using CSM 58 primary pads.

Using CSM 70 primary pads, the model predicts lower vertical carbody acceleration, 55 mph and below, than what was measured in the test, but, at 60 mph and above, the vertical accelerations match closely, as Figure 27 shows. The simulations done using CSM 58 pads showed a higher carbody vertical acceleration than the simulations done using CSM 70 primary pads. The vertical accelerations predicted by the original model in 2017 were significantly lower than those predicted by the revised model.

The test results and revised simulation predictions **meet** Standard S-2043 criteria for the single bump test regime.

Table 28. Single bump test results and simulation predictions with maximum test load

Criterion	Limiting Value	CSM 70 Pads		CSM 58 Pads	
		Test Result	Simulation Prediction Revised Model	Simulation Prediction Original Model	Simulation Prediction Revised Model
Roll angle (degree)	4.0	0.3	0.3	0.1	0.4
Maximum wheel lateral/vertical (L/V)	0.8	0.13	0.07	0.02	0.06
Maximum truck side L/V	0.5	0.08	0.05	0.02	0.05
Minimum vertical wheel load (%)	25%	71%	67%	71%	69%
Lateral peak-to-peak acceleration (g)	1.3	0.17	0.15	0.05	0.14
Maximum lateral acceleration (g)	0.75	0.09	0.09	0.03	0.09
Maximum vertical acceleration (g)	0.90	0.37	0.39	0.22	0.55
Maximum vertical suspension deflection (%)	95%	52%	62%	72%	62%

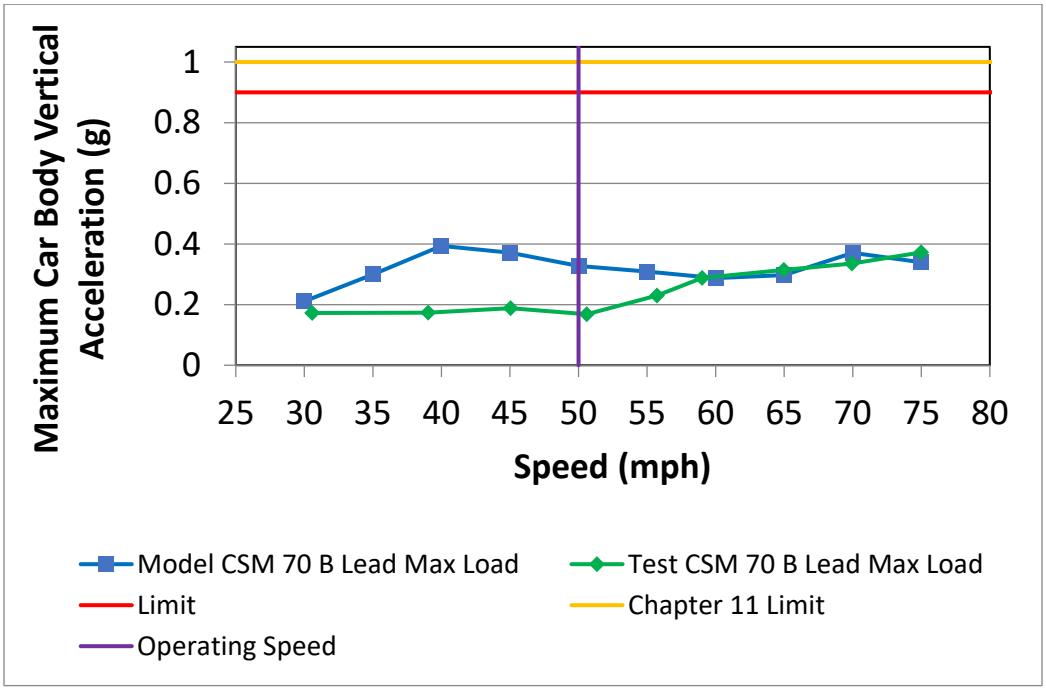


Figure 27. Simulation prediction and test results of maximum vertical carbody acceleration in the single bump test regime with maximum test load using CSM 70 pads

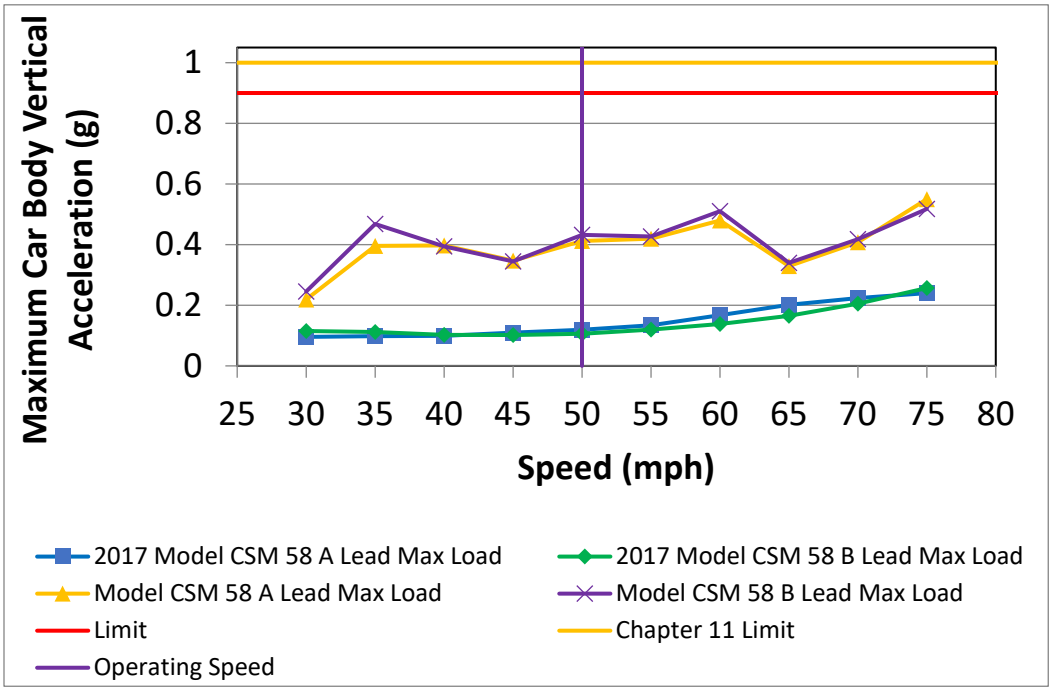


Figure 28. Original (2017) and revised simulation predictions of maximum vertical carbody acceleration in the single bump test regime with maximum test load using CSM 58 pads

7.6 Curving with Single Rail Perturbation

Simulations of the curving with a single-rail perturbation regime were conducted according to Standard S-2043, Paragraph 4.3.10.2. The tests of the curving with single rail perturbation regime were conducted according to Standard S-2043, Paragraph 5.5.15. Simulations were made for 1-, 2-, and 3-inch outside rail dips and 1-, 2-, and 3-inch inside rail bumps in a 12-degree curve with zero superelevation. The inside rail bump was a flat-topped ramp with an elevation change over 6 track feet, a steady elevation over 12 track feet, and then a ramp back down over 6 track feet. The outside rail dip was the reverse.

The tests were performed with 2-inch amplitude perturbations. Simulations were performed using measured track geometry from the test zone for comparison with the test results. Measured inputs were not available for the other bump and dip amplitudes so ideal track inputs were used. The outside rail dip predictions and the test results are presented here because the dip section was the most severe condition for both the simulations and the tests. TTCI used 50-millisecond windows when processing wheel force statistics.

7.6.1 Minimum Test Load

Table 29 shows the worst-case test results and simulation predictions for the car loaded with the minimum test load in the curve with single rail perturbation, 2-inch dip regime. The simulation predictions shown in Table 29 used measured track geometry as input. Figure 29 shows the test results and the simulation predictions of the maximum wheel L/V ratio with CSM 70 primary pads plotted against speed to show the trend in performance. Figure 30 shows the simulations predictions

of the maximum wheel L/V ratio with CSM 70 and CSM 58 primary pads plotted together to show the trend and the difference in performance between the two pads.

Using CSM 70 primary pads, the model predicts higher maximum wheel L/V ratios and higher truck side L/V ratios than those that were measured in the test. The simulation predictions of the wheel L/V ratios were all at a similar level regardless of the simulation direction or speed, whereas the test results were much more variable.

The simulations done using CSM 58 pads predicted lower wheel L/V ratios and lower truck side L/V ratios than the ratios that were predicted using CSM 70 pads. Only post-test simulation predictions are shown because the pre-test predictions were for a load case no longer intended for use.

Table 29. Curving with 2-inch rail dip test results and simulation predictions using measured track inputs with minimum test load

Criterion	Limiting Value	CSM 70		CSM 58
		Test Result	Simulation Prediction Revised Model	Simulation Prediction Revised Model
Roll angle (degree)	4.0	0.8	1.6	1.6
Maximum wheel L/V	0.8	0.88	1.01	0.80
Maximum truck side L/V	0.5	0.50	0.54	0.39
Minimum vertical wheel load (%)	25%	39%	47%	49%
Lateral peak-to-peak acceleration (g)	1.3	0.23	0.14	0.19
Maximum lateral acceleration (g)	0.75	0.17	0.09	0.13
Maximum vertical acceleration (g)	0.90	0.28	0.09	0.09
Maximum vertical suspension deflection (%)	95%	21%	28%	27%

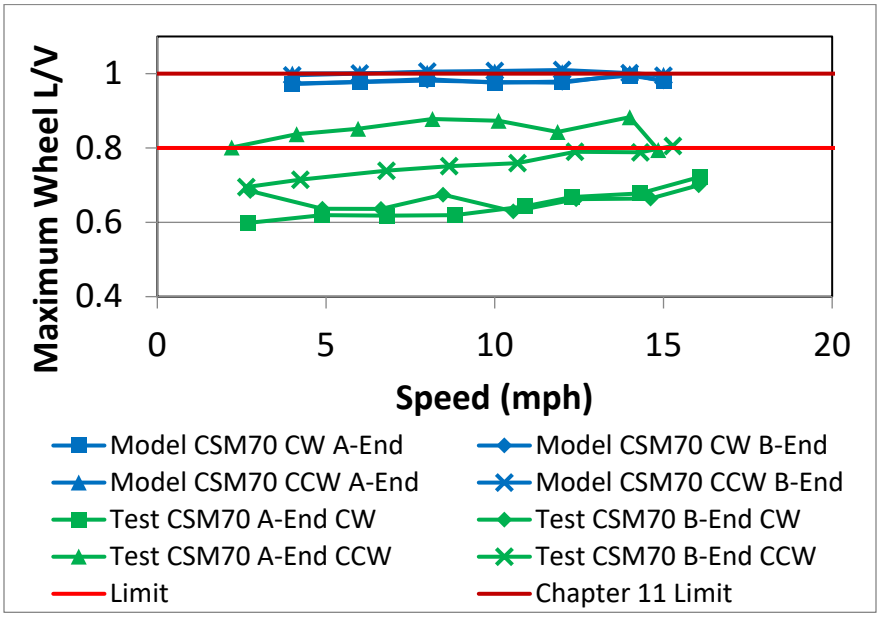


Figure 29. Simulation predictions and test results using CSM 70 primary pads of maximum wheel L/V ratio in the curve with single dip regime with minimum test load

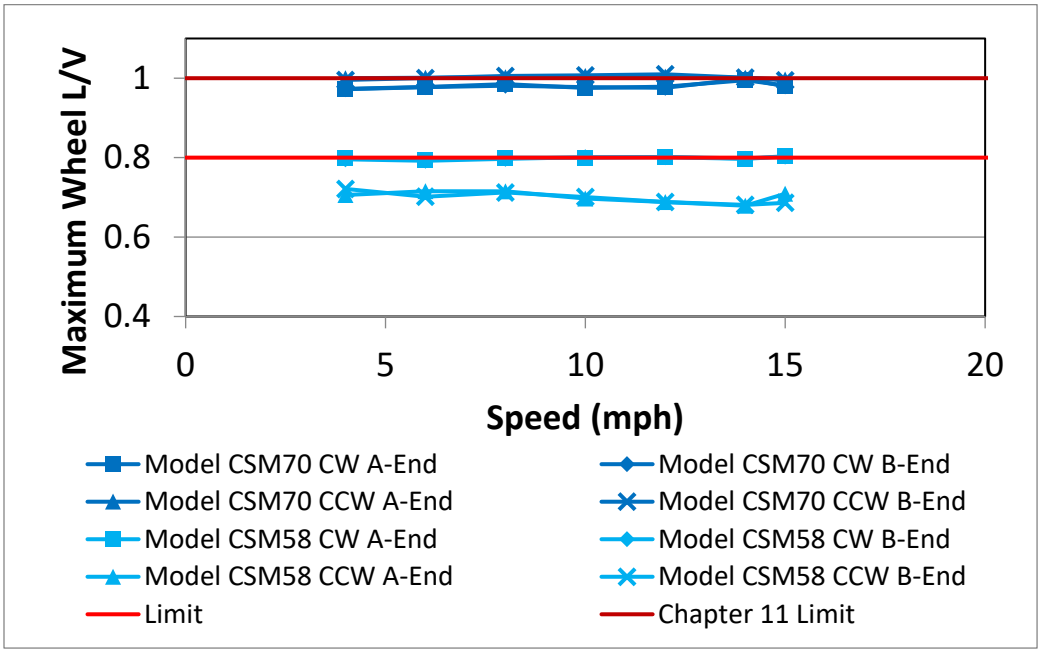


Figure 30. Simulation predictions using CSM 70 and CSM 58 primary pads of maximum wheel L/V ratio in the curve with single dip regime with minimum test load

Table 30 shows the worst-case simulation predictions for the car loaded with the minimum test load in the curve with a single rail perturbation regime with 1-, 2-, and 3-inch bumps using CSM 58 pads. Table 31 shows the worst-case simulation predictions for the car loaded with the minimum test load in the curve with a single rail perturbation regime with 1-, 2-, and 3-inch dips. The simulation predictions shown in Table 30 and Table 31 used ideal track geometry as input.

Table 30. Simulation prediction for curve with single rail perturbation bump section at varying amplitudes with minimum test load

Criterion	Limiting Value	Simulation Predictions Revised Model CSM 58 Pads		
		1-inch	2-inch	3-inch
Roll angle (degree)	4.0	0.4	1.6	4.2
Maximum wheel L/V	0.8	0.49	0.58	0.68
Maximum truck side L/V	0.5	0.27	0.30	0.32
Minimum vertical wheel load (%)	25%	60%	51%	39%
Lateral peak-to-peak acceleration (g)	1.3	0.07	0.16	0.26
Maximum lateral acceleration (g)	0.75	0.04	0.08	0.14
Maximum vertical acceleration (g)	0.90	0.07	0.09	0.14
Maximum vertical suspension deflection (%)	95%	22%	30%	43%

Table 31. Simulation prediction for curve with single rail perturbation dip section at varying amplitudes with minimum test load

Criterion	Limiting Value	Simulation Predictions Revised Model CSM 58 Pads		
		1-inch	2-inch	3-inch
Roll angle (degree)	4.0	0.4	1.1	3.1
Maximum wheel L/V	0.8	0.52	0.63	0.80
Maximum truck side L/V	0.5	0.30	0.33	0.38
Minimum vertical wheel load (%)	25%	53%	44%	36%
Lateral peak-to-peak acceleration (g)	1.3	0.07	0.14	0.23
Maximum lateral acceleration (g)	0.75	0.03	0.06	0.13
Maximum vertical acceleration (g)	0.90	0.06	0.08	0.11
Maximum vertical suspension deflection (%)	95%	21%	28%	34%

The test results and simulation predictions did not meet Standard S-2043 criteria for the maximum wheel L/V ratio or maximum truck side L/V ratio with CSM 70 pads for the curve with a single rail perturbation 2-inch dip regime with minimum test load, but all other criteria were met. The revised simulation predictions done using CSM 58 pads **met** Standard S-2043 criteria for the curve with a single rail perturbation 2-inch dip regime (measured) with minimum test load. The maximum wheel L/V ratio **met (did not exceed)** the limit of 0.8.

Simulation predictions of ideal track input with 1-, 2-, and 3-inch bumps and dips did not meet Standard S-2043 criteria for the maximum peak-to-peak roll angle in the 3-inch bump simulations. By itself, the 3-inch bump and dip regimes roll the track about 3 degrees, so very little suspension deflection is allowed within the 4-degree peak-to-peak Standard S-2043 limit. Therefore, on behalf of the DOE, TTCI is requesting an exception from the AAR EEC. All other criteria were met, although the maximum wheel L/V ratio was at the limit of 0.8 in the 3-inch dip simulations.

7.6.2 Maximum Test Load

Table 32 shows the worst-case test results and simulation predictions for the car loaded with the maximum test load in the curve with a single rail perturbation, 2-inch dip regime. The simulation predictions shown in Table 32 used measured track geometry as input. Figure 31 shows test results and simulation predictions of the maximum wheel L/V ratio using CSM 70 primary pads and simulation results using CSM 58 primary pads plotted against speed to show the trend in performance.

Using CSM 70 primary pads, the model predicts higher maximum wheel L/V ratios and higher truck side L/V ratios than those that were measured in the test. The simulation predictions of wheel L/V ratios were all at a similar level regardless of the simulation direction or speed, whereas the test results were much more variable.

The simulations done using CSM 58 pads predicted lower wheel L/V ratios and lower truck side L/V ratios than those that were predicted with CSM 70 pads. Only the post-test simulation predictions are shown because the pre-test predictions were not made using a measured track input.

The simulation predictions done using CSM 70 pads did not meet Standard S-2043 criteria for the maximum wheel L/V ratio for the curve with a single rail perturbation 2-inch dip regime with a maximum test load, but all other criteria were met. The results from testing done using CSM 70 pads and revised simulation predictions done using CSM 58 pads **met** Standard S-2043 criteria for the curve with a single rail perturbation, 2-inch dip regime with maximum test load.

Table 32. Curving with 2-inch rail dip test results and simulation predictions using measured track inputs with maximum test load

Criterion	Limiting Value	CSM 70 Pads		CSM 58 Pads
		Test Result	Simulation Prediction Revised Model	Simulation Prediction Revised Model
Roll angle (degree)	4.0	1.6	2.2	2.2
Maximum wheel lateral/vertical (L/V)	0.8	0.79	0.90	0.52
Maximum truck side L/V	0.5	0.44	0.45	0.31
Minimum vertical wheel load (%)	25%	45%	49%	51%
Lateral peak-to-peak acceleration (g)	1.3	0.16	0.18	0.19
Maximum lateral acceleration (g)	0.75	0.14	0.12	0.12
Maximum vertical acceleration (g)	0.90	0.15	0.09	0.09
Maximum vertical suspension deflection (%)	95%	81%	74%	73%

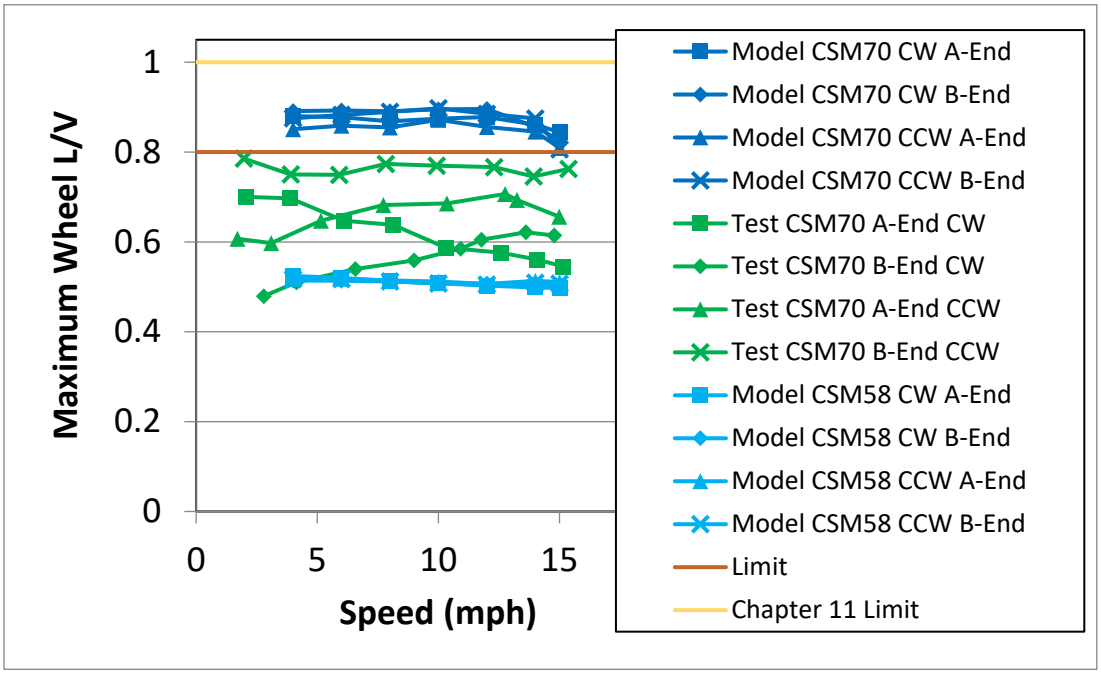


Figure 31. Simulation prediction and test results of maximum wheel L/V ratio in the curving with single rail perturbation dip regime with maximum test load using CSM 70 and CSM 58 pads

Table 33 shows the worst-case simulation predictions for the car loaded with the maximum test load in the curve with single rail perturbation regime with 1-, 2-, and 3-inch bumps. Table 34 shows the worst-case simulation predictions for the car loaded with the maximum test load in the curve with single rail perturbation regime with 1-, 2-, and 3-inch dips. The simulation predictions shown in Table 33 and Table 34 used CSM 58 pads and ideal track geometry as input. The simulation predictions over the 3-inch bump and the 3-inch dip did not meet the maximum peak-to-peak roll angle criteria. All other criteria were met.

The wheel L/V ratios predicted with the revised model were more than 45 percent lower than those predicted with the original model. The difference between wheel L/V ratio predictions is likely because the primary pad stiffness measured in the characterization test was much lower than the value used in the original model. The original and revised predictions for other metrics were closer.

Table 33. Simulation prediction for curve with single rail perturbation bump section at varying amplitudes with maximum test load

Criterion	Limiting Value	Simulation Predictions Revised Model CSM 58 Pads					
		1-inch		2-inch		3-inch	
		Original	Revised	Original	Revised	Original	Revised
Roll angle (degree)	4.0	0.5	0.4	3.0	2.8	5.0	4.7
Maximum wheel L/V	0.8	0.53	0.25	0.59	0.30	0.64	0.33
Maximum truck side L/V	0.5	0.29	0.19	0.33	0.19	0.33	0.23
Minimum vertical wheel load (%)	25%	58	60	53	52	38	40
Lateral peak-to-peak acceleration (g)	1.3	0.05	0.07	0.14	0.12	0.21	0.18
Maximum lateral acceleration (g)	0.75	0.05	0.03	0.08	0.06	0.12	0.11
Maximum vertical acceleration (g)	0.90	0.04	0.07	0.08	0.12	0.07	0.13
Maximum vertical suspension deflection (%)	95%	77	63	86	79	94	92

Table 34. Simulation prediction for curve with single rail perturbation dip section at varying amplitudes with maximum test load

Criterion	Limiting Value	Simulation Predictions Revised Model CSM 58 Pads					
		1-inch		2-inch		3-inch	
		Original	Revised	Original	Revised	Original	Revised
Roll angle (degree)	4.0	0.5	0.5	2.6	2.6	4.5	4.5
Maximum wheel L/V	0.8	0.57	0.28	0.68	0.36	0.79	0.43
Maximum truck side L/V	0.5	0.32	0.20	0.35	0.19	0.38	0.24
Minimum vertical wheel load (%)	25%	64	61	56	49	44	40
Lateral peak-to-peak acceleration (g)	1.3	0.06	0.07	0.11	0.12	0.19	0.19
Maximum lateral acceleration (g)	0.75	0.05	0.03	0.07	0.07	0.10	0.11
Maximum vertical acceleration (g)	0.90	0.04	0.06	0.07	0.10	0.06	0.13
Maximum vertical suspension deflection (%)	95%	73	63	82	75	88	89

7.7 Hunting

Simulations of the hunting regime were conducted according to Standard S-2043, Paragraph 4.3.11.3.1. The hunting tests were conducted according to Standard S-2043, Paragraph 5.5.7. The simulations used inputs from the measured track geometry of the test site, a 5,500-foot section of tangent track on the TTC Railroad Test Track (RTT).

7.7.1 Minimum Test Load

Table 35 shows the worst-case test results and simulation predictions for the car loaded with the minimum test load in the hunting test regime. Figure 32 shows the test results and simulation predictions of the standard deviation of carbody lateral acceleration over 2,000 feet using CSM 70 primary pads plotted against speed to show the trend in performance. Figure 33 shows the test results and simulation predictions of the standard deviation of carbody lateral acceleration over 2,000 feet with CSM 58 primary pads.

Using CSM 70 primary pads, the model predicts higher lateral accelerations than those that were measured in the test, but the overall trend matches closely, as shown in Figure 32. The simulations done using CSM 58 pads predicted higher lateral accelerations at speeds of 65 mph and below, but lower lateral accelerations above 65 mph. Only post-test simulation predictions are shown because the pre-test predictions were for a load case no longer intended for use.

The test results and simulation predictions done using CSM 70 pads met Standard S-2043 criteria. The test results and revised simulation predictions done using CSM 58 pads **did not meet** the Standard S-2043 carbody lateral acceleration standard deviation criteria at speeds above 65 mph, but all other criteria were met.

Table 35. Hunting test results and simulation predictions with minimum test load

Criterion	Limiting Value	CSM 70 Pads		CSM 58 Pads	
		Test Result	Simulation Prediction Revised Model	Test Result	Simulation Prediction Revised Model
Roll angle (degree)	4.0	0.5	0.2	0.7	0.2
Maximum wheel lateral/vertical (L/V)	0.8	Not Measured*	0.14	Not Measured*	0.24
Maximum truck side L/V	0.5	Not Measured*	0.09	Not Measured*	0.15
Minimum vertical wheel load (%)	25%	Not Measured*	71%	Not Measured*	69%
Lateral peak-to-peak acceleration (g)	1.3	0.17	0.35	0.80	0.57
Maximum lateral acceleration (g)	0.75	0.10	0.19	0.43	0.31
Lateral Carbody Acceleration Standard Deviation (g)	0.13	0.03	0.05	0.22	0.14
Maximum vertical acceleration (g)	0.90	0.27	0.18	0.28	0.32
Maximum vertical suspension deflection (%)	95%	7%	17%	10%	16%

* L/V and vertical wheel load data is not available for high-speed stability tests with KR wheels (IWS required to obtain those measurements).

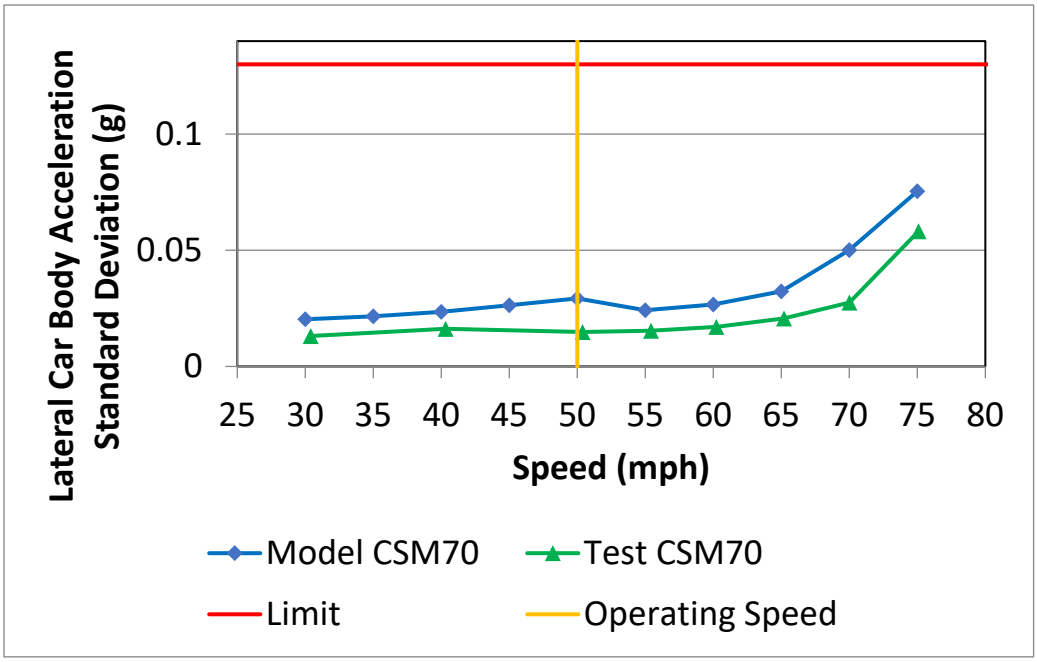


Figure 32. Simulation prediction and test results of the standard deviation of carbody lateral acceleration over 2,000 feet with minimum test load using CSM 70 pads and KR profile wheels

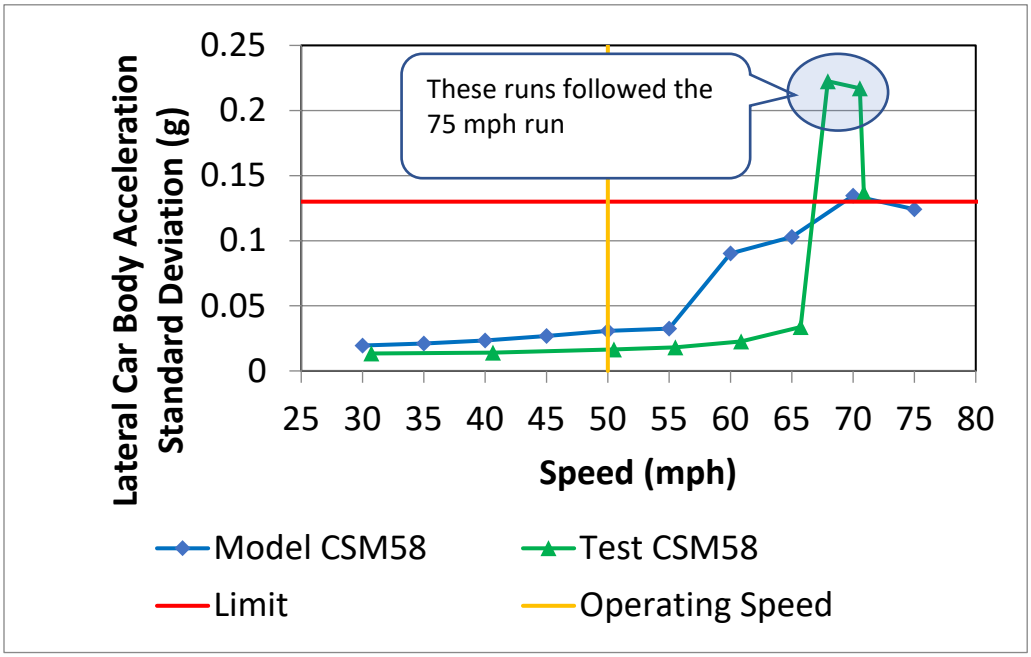


Figure 33. Simulation prediction and test results of the standard deviation of carbody lateral acceleration over 2,000 feet with minimum test load using CSM 58 pads and KR profile wheels

7.7.2 Maximum Test Load

Table 36 shows the worst-case test results and simulation predictions for the car loaded with the maximum test load in the hunting test regime. Figure 34 shows the test results and simulation predictions for the standard deviation of carbody lateral acceleration over 2,000 feet using CSM 70 primary pads plotted against speed to show the trend in performance. Figure 35 shows the test results and simulation predictions of the standard deviation of carbody lateral acceleration over 2,000 feet using CSM 58 primary pads. Using either CSM 70 or CSM 58 primary pads, the model predicts higher lateral accelerations than those that were measured in the test at speeds below 70 mph, and it predicts lower lateral accelerations at speeds above 70 mph, as shown in Figure 34 and Figure 35.

The pre-test (2017) simulations done using CSM 58 primary pads do not match test data as well as the revised model, except at 75 mph. The pre-test simulations show wheel loads much lower than what was predicted in the revised simulations. This difference between the simulations and the predictions is because the data analysis for the pre-test simulation included data from the curve spirals (entry and exit) and a significant portion of the curve at each end of the tangent test zone. By contrast, data from the revised simulations was only processed data in the tangent track portion consistent with the requirements of Standard S-2043. More details on the pre-test simulations are available in Walker and Trevithick [2].

Test results and revised simulation predictions done using both CSM 70 and CSM 58 pads **met** Standard S-2043 criteria for hunting with maximum test load.

Table 36. Hunting test results and simulation predictions with maximum test load

Criterion	Limiting Value	CSM 70 Pads		CSM 58 Pads		
		Test Result	Simulation Prediction Revised Model	Test Result	Simulation Prediction Original Model	Simulation Prediction Revised Model
Roll angle (degree)	4.0	0.6	0.3	0.6	3.7	0.3
Maximum wheel lateral/vertical (L/V)	0.8	Not Measured*	0.09	Not Measured*	0.20	0.09
Maximum truck side L/V	0.5	Not Measured*	0.08	Not Measured*	0.17	0.08
Minimum vertical wheel load (%)	25%	Not Measured*	81%	Not Measured*	25%	81%
Lateral peak-to-peak acceleration (g)	1.3	0.18	0.21	0.34	0.37	0.33
Maximum lateral acceleration (g)	0.75	0.09	0.13	0.24	0.25	0.18
Lateral Carbody Acceleration Standard Deviation (g)	0.13	0.03	0.03	0.04	0.09	0.07
Maximum vertical acceleration (g)	0.90	0.18	0.30	0.25	0.13	0.34
Maximum vertical suspension deflection (%)	95%	47%	53%	63%	86%	87%

* L/V and vertical wheel load data is not available for high-speed stability tests with KR wheels (IWS required).

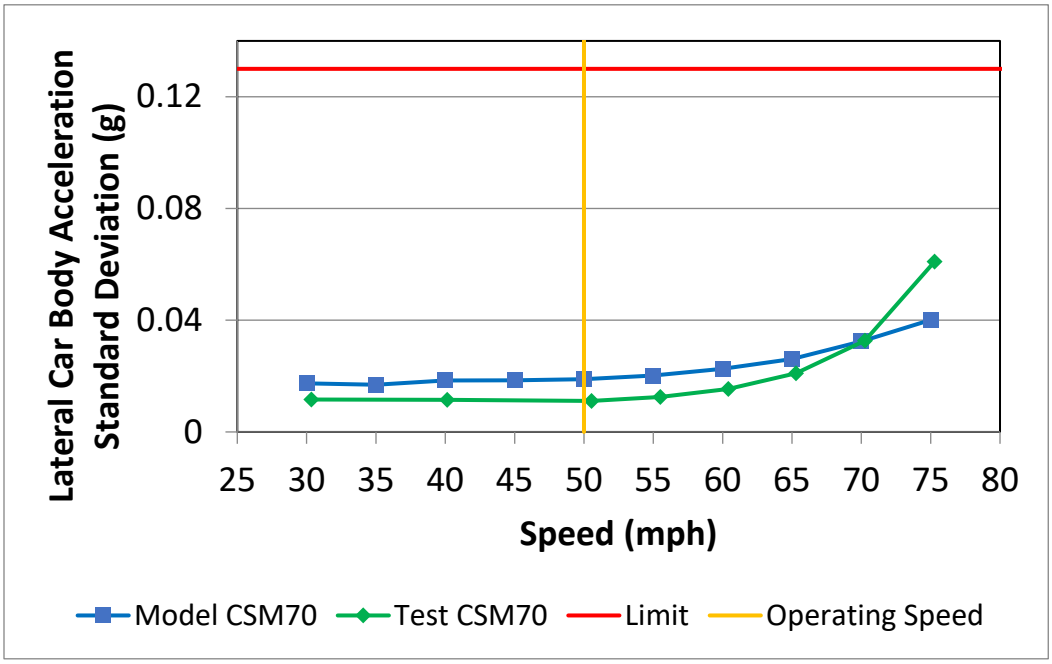


Figure 34. Simulation prediction and test results of maximum wheel L/V ratio in the dynamic curving regime with maximum test load using CSM 70 pads

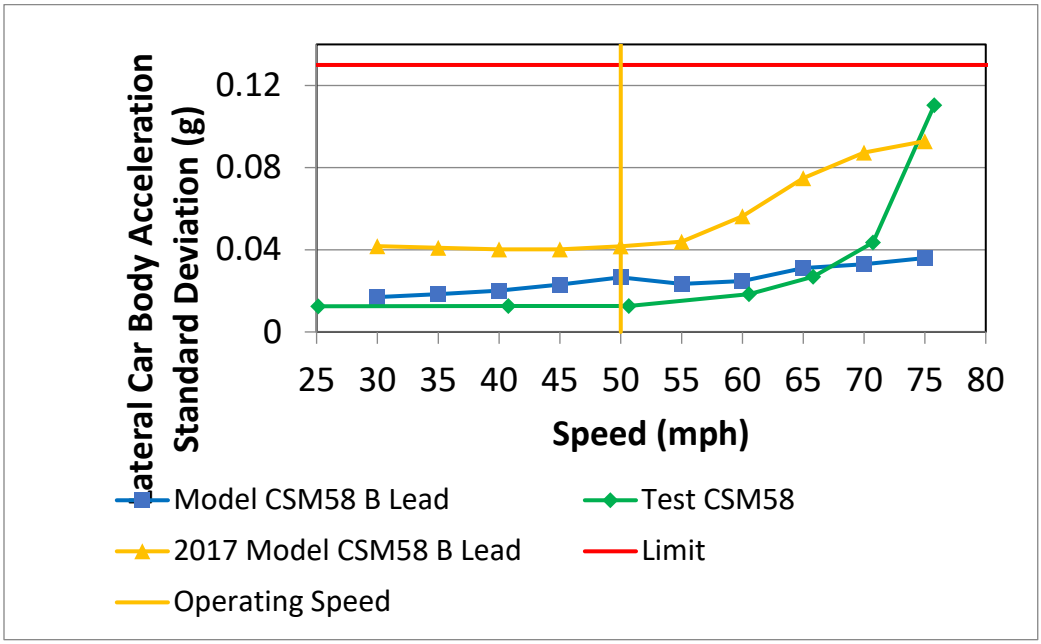


Figure 35. Simulation predictions of maximum wheel L/V ratio in the dynamic curving regime with maximum test load using CSM 70 and CSM 58 pads

7.8 Constant Curving

Simulations of the constant curving regime were conducted according to Standard S-2043, Paragraph 4.3.11.4. The constant curving tests were conducted according to Standard S-2043, Paragraph 5.5.16.

The constant curving regime was modeled using measured track geometry from the 7.5-, 10-, and 12-degree curves of the Wheel-Rail Mechanisms (WRM) loop at the TTC.

Simulation predictions presented for constant curving include the 95th percentile wheel L/V ratio for the steady curve portion of the inputs. This criterion is not listed in Table 4.1 of the Standard S-2043 design paragraph but is listed in Table 5.1 of the Standard S-2043 single car test paragraph. The 95th percentile wheel L/V ratio is relevant to these simulations because the simulations are performed with measured track geometry inputs rather than ideal track geometry.

7.8.1 Minimum Test Load

Table 37 shows the worst-case test results and simulation predictions for the car loaded with the minimum test load in the constant curving test regime. Figure 36 shows the test results and simulation predictions of the maximum wheel L/V ratio plotted against speed to show the trend in performance. The test results are shown for CSM 70 pads and simulation results are shown for both CSM 70 and CSM 58 pads.

Using CSM 70 primary pads, the model predicts lower maximum wheel L/V ratios than those that were measured in the test, but the overall trend matches, and the magnitude was in the same range as the test data, as Figure 36 shows. The simulations done using CSM 58 pads predicted lower wheel L/V ratios than simulations done using CSM 70 pads. Only post-test simulation predictions are shown because the pre-test predictions were for a load case no longer intended for use.

The test results did not meet the criteria for the maximum wheel L/V ratio or the 95th percentile wheel L/V ratio using CSM 70 pads. The final choice of CSM 58 pads over CSM 70 pads was made to improve curving performance. The simulation predictions using both CSM 70 and CSM 58 pads with the revised model **met** Standard S-2043 criteria, although the 95th percentile wheel L/V ratio was at the limit of 0.6 for CSM 70 pads.

Table 37. Constant curving test results and simulation predictions with minimum test load

Criterion	Limiting Value	CSM 70		CSM 58
		Test Result	Simulation Prediction Revised Model	Simulation Prediction Revised Model
Roll angle (degree)	4.0	0.3	0.76	0.77
Maximum wheel L/V	0.8	0.86	0.68	0.52
95% Wheel L/V	0.6	0.66	0.60	0.47
Maximum truck side L/V	0.5	0.47	0.36	0.34
Minimum vertical wheel load (%)	25	54	52.5	52.7
Lateral peak-to-peak acceleration (g)	1.3	0.19	0.23	0.15
Maximum lateral acceleration (g)	0.75	0.17	0.17	0.14
Maximum vertical acceleration (g)	0.90	0.12	0.16	0.15
Maximum vertical suspension deflection (%)	95	18	25.5	25.1

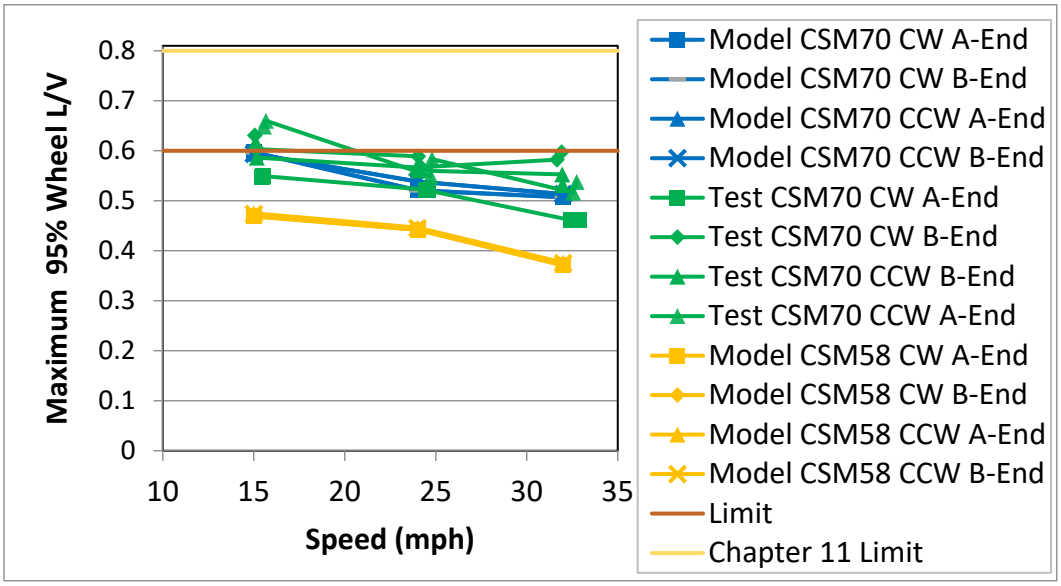


Figure 36. Test Results and Simulation Predictions of the 95 Percentile Wheel L/V Ratio in the 12-degree Constant Curve with CSM 70 and CSM 58 Primary Pads for Minimum Test Load

7.8.2 Maximum Test Load

Table 38 shows the worst-case test results and simulation predictions for the car loaded with the maximum test load in the constant curving test regime. Figure 37 shows the test results and simulation predictions for the maximum wheel L/V ratio plotted against speed to show the trend in performance. The results are shown tests done using CSM 70 pads, and the results are shown for simulations done with both CSM 70 and CSM 58 pads.

Using CSM 70 primary pads, the model predicts lower maximum wheel L/V ratios than were measured in the test, but the overall trend matches, and the magnitude was in the same range as the test data, as Figure 37 shows. The simulations done using CSM 58 pads predicted lower wheel L/V ratios than simulations done with CSM 70 pads. Only post-test simulation predictions are shown because the pre-test predictions were for a load case no longer intended for use.

The test results did not meet the criteria for the maximum wheel L/V ratio or the 95th percentile wheel L/V ratio with CSM 70 pads. The simulation predictions done using both CSM 70 and CSM 58 pads with the revised model **met** Standard S-2043 criteria.

Table 38. Constant curving test results and simulation predictions with maximum test load

Criterion	Limiting Value	CSM 70		CSM 58	
		Test Result	Simulation Prediction Revised Model	Simulation Prediction Original Model	Simulation Prediction Revised Model
Roll angle (degree)	4.0	0.5	0.95	1.7	0.97
Maximum wheel L/V	0.8	0.73	0.65	0.64	0.41
95% Wheel L/V	0.6	0.63	0.57	0.54	0.35
Maximum truck side L/V	0.5	0.38	0.34	0.36	0.28
Minimum vertical wheel load (%)	25	50	56.3	56	55.4
Lateral peak-to-peak acceleration (g)	1.3	0.17	0.15	0.19	0.15
Maximum lateral acceleration (g)	0.75	0.17	0.13	0.16	0.13
Maximum vertical acceleration (g)	0.90	0.09	0.16	0.12	0.15
Maximum vertical suspension deflection (%)	95	50	69.4	76	69.0

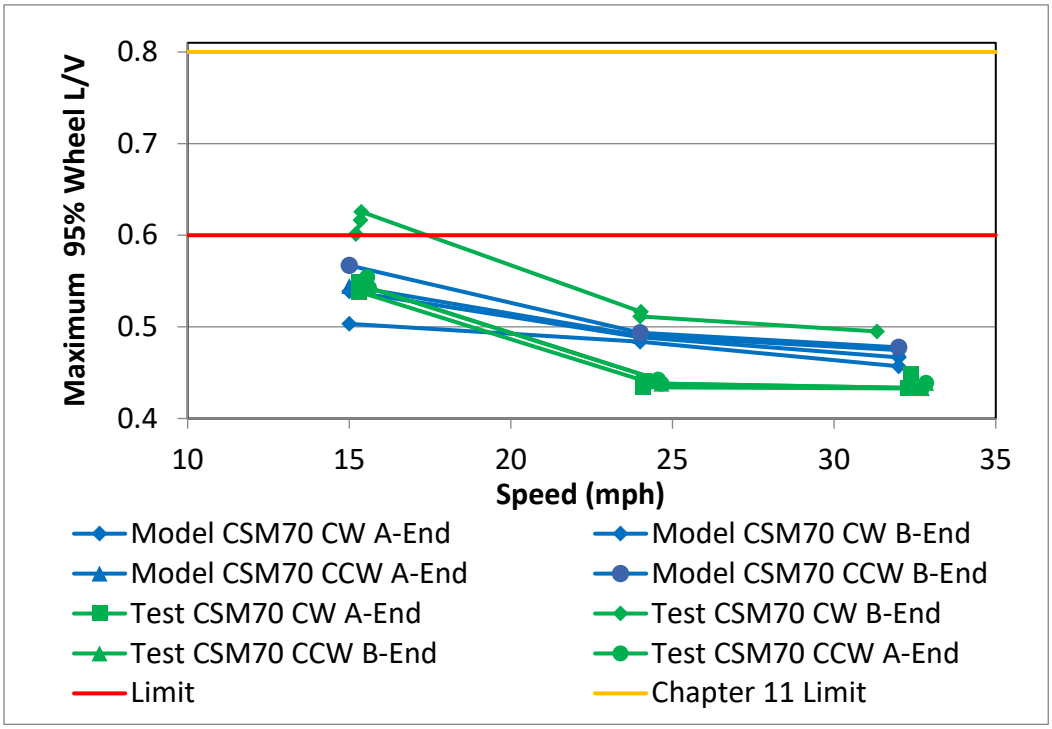


Figure 37. Test Results and Simulation Predictions of the 95 Percentile Wheel L/V Ratio in the 12-degree Constant Curve with CSM 70 Primary Pads for Maximum Test Load

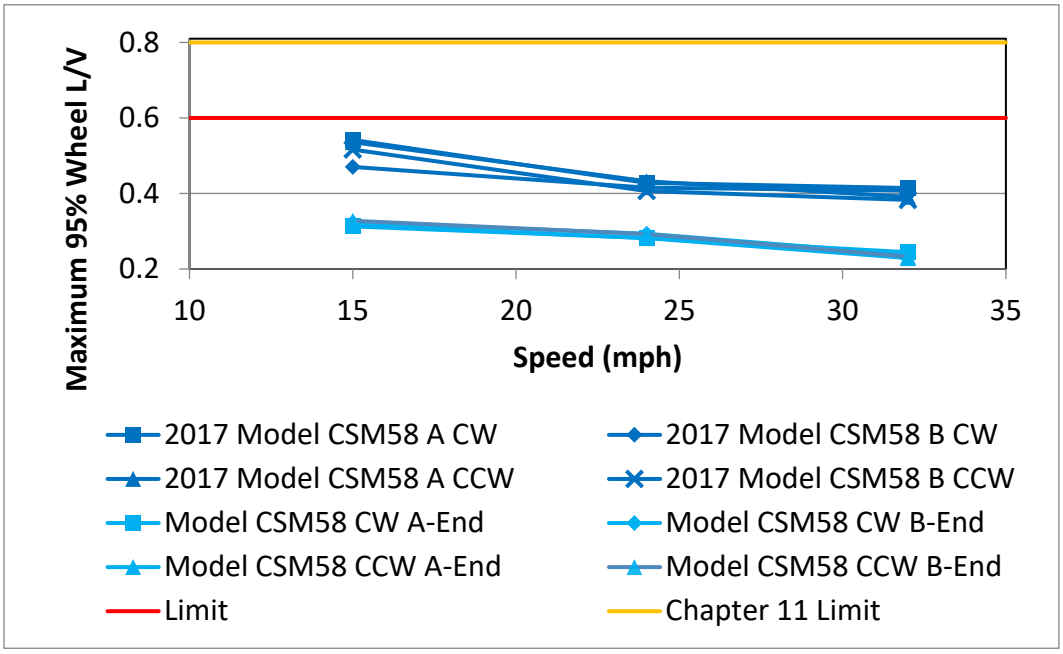


Figure 38. Original (20170 and Revised Simulation Predictions of the 95 Percentile Wheel L/V Ratio in the 12-degree Constant Curve with CSM 58 Primary Pads for Maximum Test Load

7.9 Curving with Various Lubrication Conditions

The simulations of curving with various lubrication conditions were performed according to Standard S-2043, Paragraph 4.3.11.5. The constant curving simulations were repeated in a 10-degree curve with the coefficient of friction conditions shown in Table 39. The simulations were performed using both a new wheel profile on a new rail profile and a hollow-worn wheel profile on a worn rail profile. Figure 39 shows the worn wheel and rail profiles used for the simulations. In this plot, the right side is the high rail (outside rail). The gap between the rail profile (in red) and the wheel profile (in blue) on the gage corner of the rail represents a two-point contact condition. The lubrication and profile conditions are designed to test the performance when the wheelset cannot provide normal steering forces due to the wear.

Table 39. Wheel/rail Coefficients of Friction for the Curving with Various Lubrication Conditions Regime

Friction Coefficient	High Rail Crown	High Rail Gage Face	Low Rail Crown
Case 1	0.5	0.5	0.5
Case 2	0.5	0.2	0.5
Case 3	0.5	0.2	0.2
Case 4	0.2	0.2	0.5

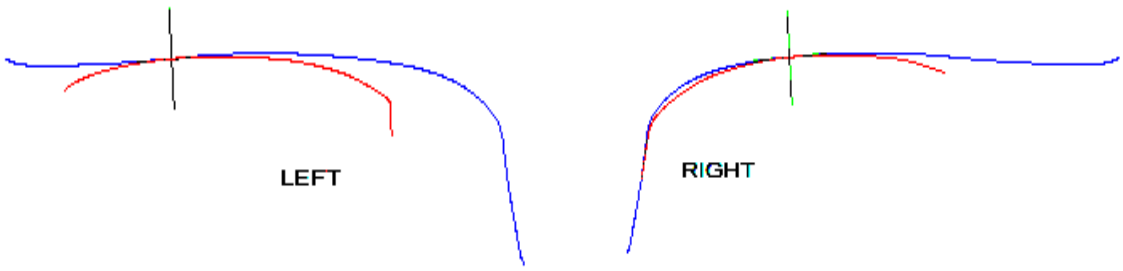


Figure 39. Worn Wheel Profiles on the Ground Rail Profiles
(The Wheelset is Shifted to the High Rail in the Position it Would be in a Left-Hand Curve)

7.9.1 Minimum Test Load

(1) New Profiles

Table 40 shows the simulation predictions for the four friction cases with the new wheel profiles at the minimum test load. The simulations of Cases 1, 2, and 3 meet Standard S-2043 criteria. Although it does meet the corresponding AAR Chapter 11 criterion, the Case 4 simulation does **not meet** the Standard S-2043 Paragraph 5 criterion for 95th percentile wheel L/V ratios. The AAR Chapter 11 criterion is 0.8 for 95th percentile single wheel L/V ratio.

Table 40. Simulation Results for Curving with Rail Lubrication Cases 1-4 and New Wheels and Rails, with Minimum Test Load

Criterion	Limiting Value	Case 1 New	Case 2 New	Case 3 New	Case 4 New
Maximum carbody roll angle (degree)	4.0	0.68	0.67	0.67	0.65
Maximum wheel L/V	0.80	0.63	0.66	0.39	0.72
Maximum truck side L/V	0.50	0.36	0.36	0.25	0.43
Minimum vertical wheel load (%)	25	52	52	52	53
Peak-to-peak carbody lateral acceleration (g)	1.30	0.23	0.23	0.28	0.25
Maximum carbody lateral acceleration (g)	0.75	0.17	0.17	0.20	0.19
Lateral carbody acceleration standard deviation (g)	0.13	0.03	0.03	0.04	0.04
Maximum carbody vertical acceleration (g)	0.90	0.15	0.15	0.14	0.14
Maximum vertical suspension deflection (%)	95	22	22	22	22
95% Wheel L/V Ratio	0.60	0.48	0.50	0.33	0.62

(2) Worn Profiles

Table 41 shows simulation predictions for the four friction cases with hollow-worn wheel profiles and worn rail profiles. The simulations of Case 3 meet all Standard S-2043 criteria. The simulations of Cases 1, 2, and 4 do not meet Standard S-2043 criteria for truck side L/V ratios (0.5 threshold).

Although AAR Chapter 11 limits do not apply to this regime, it may be noted that cases 1 and 4 meet the AAR Chapter 11 criterion for truck side L/V ratios (0.6), but Case 2 does not. The Case 2 simulations also do not meet Standard S-2043 criteria for the 95th percentile wheel L/V ratio (0.6), but they do meet the AAR Chapter 11 criterion of 0.8.

Table 41. Simulation Predictions for Curving with Rail Lubrication Cases 1-4 and Hollow Worn Wheels and Ground Rails, with Minimum Test Load

Criterion	Limiting Value	Case 1 Worn	Case 2 Worn	Case 3 Worn	Case 4 Worn
Maximum carbody roll angle (degree)	4.0	0.63	0.65	0.64	0.65
Maximum wheel L/V	0.80	0.67	0.74	0.43	0.68
Maximum truck side L/V	0.50	**0.53**	**0.61**	0.30	**0.58**
Minimum vertical wheel load (%)	25	52	51	53	52
Peak-to-peak carbody lateral acceleration (g)	1.30	0.30	0.30	0.28	0.30
Maximum carbody lateral acceleration (g)	0.75	0.20	0.20	0.20	0.20
Lateral carbody acceleration standard deviation (g)	0.13	0.04	0.04	0.04	0.04
Maximum carbody vertical acceleration (g)	0.90	0.16	0.17	0.17	0.17
Maximum vertical suspension deflection (%)	95	22	22	22	22
95% Wheel L/V Ratio	0.60	0.56	**0.64**	0.37	0.59

Figure 40 shows a plot of the wheel L/V ratio versus distance for the worst worn-case simulation and the underbalance speed for the Case 2 lubrication condition with worn wheel profiles. Figure 41 shows a plot of the truck side L/V ratio versus distance for the worst-case simulation and the underbalance speed for the Case 4 lubrication with worn wheel profiles. Figure 42 shows a plot of the 95th percentile wheel L/V ratio versus speed for the Case 2 lubrication condition with the worn wheel profile for both directions of travel, with the worst-case result of car orientation shown (either A- or B-end leading). Figure 43 shows a plot of the truck side L/V ratio versus the speed for the Case 2 lubrication condition with the worn wheel profile.

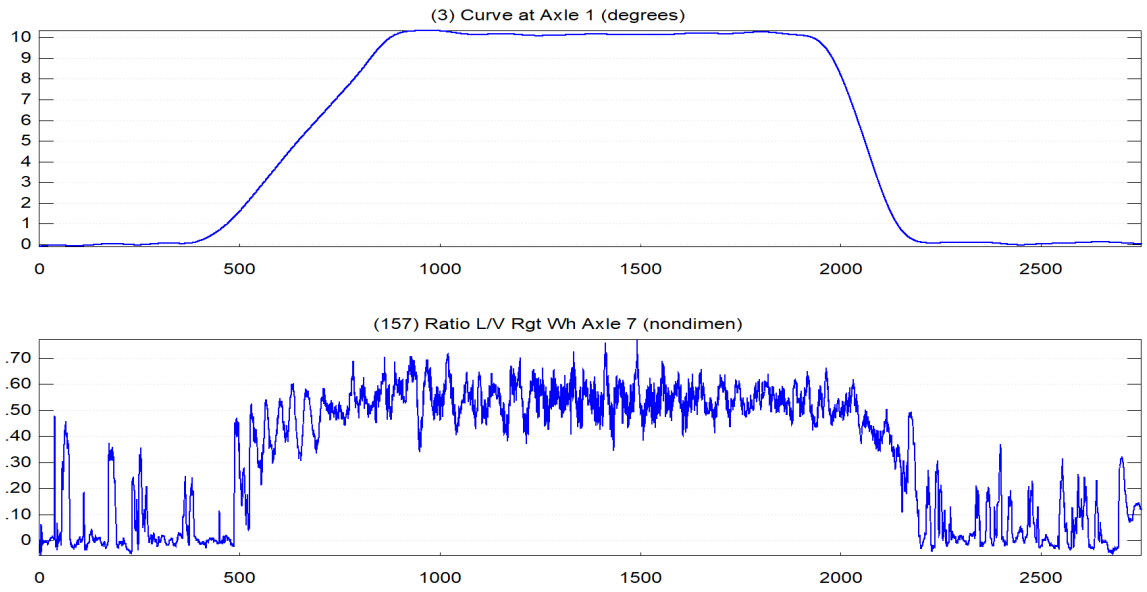


Figure 40. Plot of Wheel L/V Ratio versus distance for Case 2 friction with worn profiles, CCW, A-leading. Plot shows data for the lead axle of the trailing span bolster.

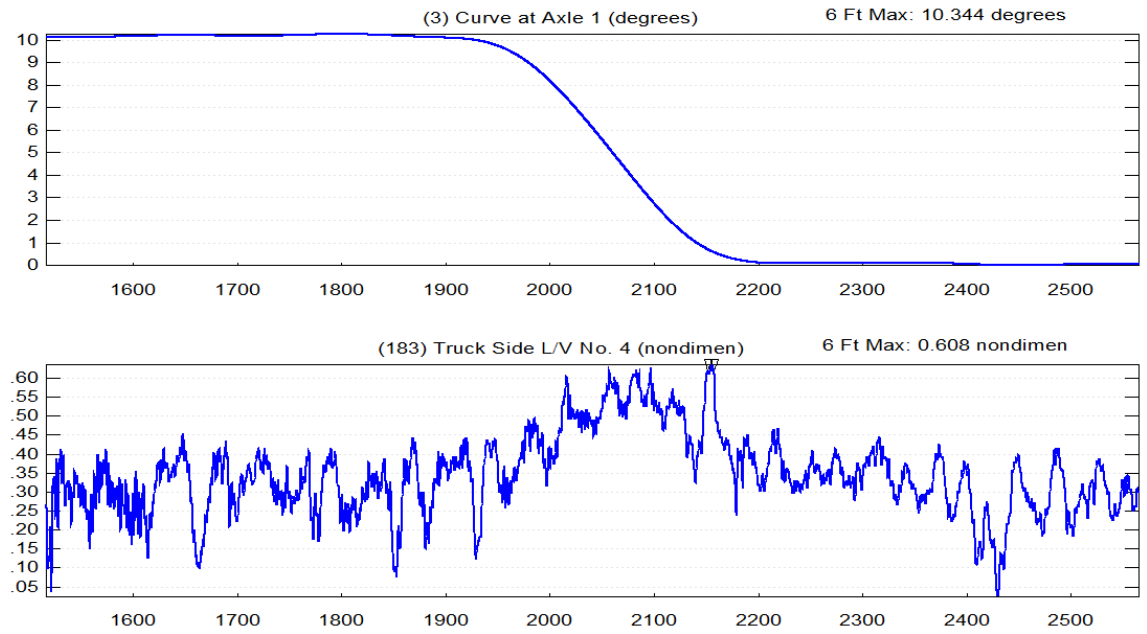


Figure 41. Plot of Truck Side L/V Ratio versus distance for Case 2 friction with worn profiles, CCW, B-leading. Plot shows data for the high rail of the middle truck on the lead span bolster.

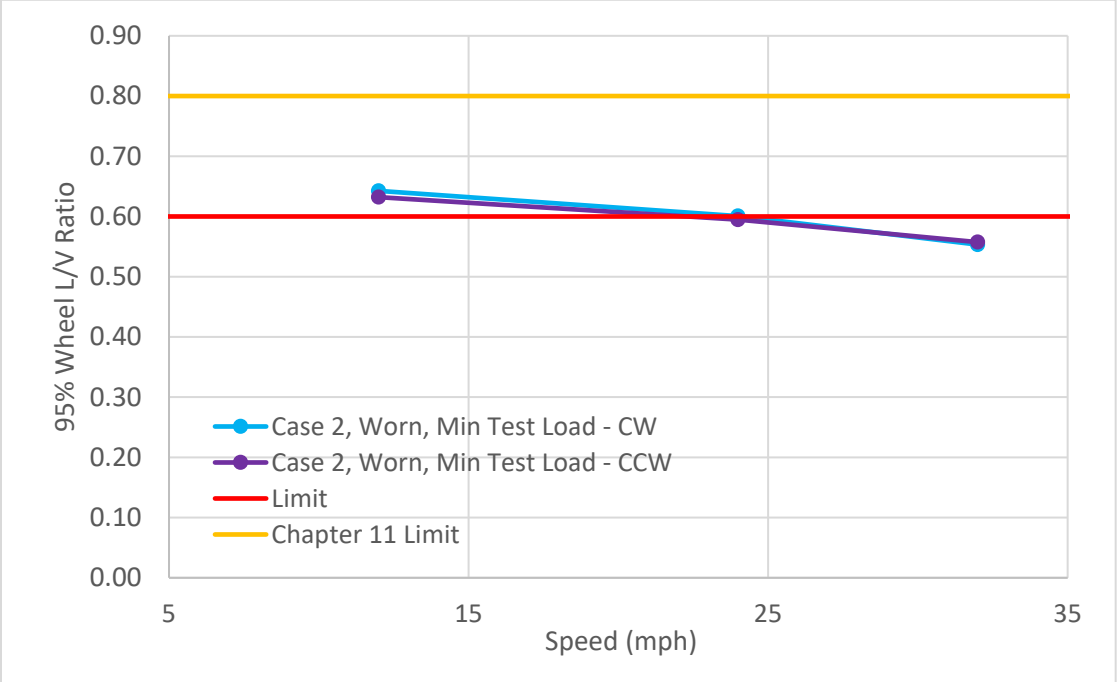


Figure 42. Atlas car with minimum test load 95-Percent Wheel L/V Ratio for curving with Case 2 lubrication and worn wheel and rail profiles

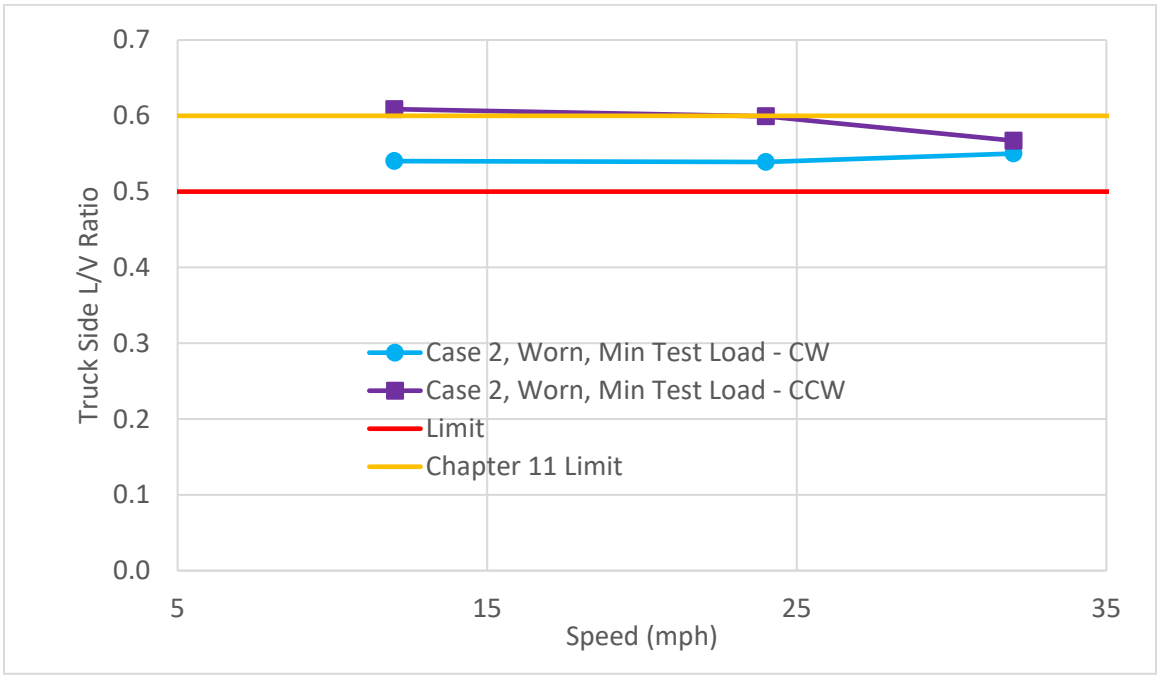


Figure 43. Minimum Test Load Truck Side L/V Ratio for curving with Case 2 lubrication and worn wheel and rail profiles

7.9.2 Maximum Test Load

(1) New Profiles

Table 42 shows the simulation predictions at the maximum test load for the four friction cases with new wheel and rail profiles. The table shows the worst-case results for any simulation, clockwise (CW) or CCW with A-end and B-end leading. The revised simulated performance of the car loaded with the HI-STAR 190 XL cask (maximum test load) **meets** Standard S-2043 criteria for curving under all the lubrication condition cases when considering new wheel and rail profiles. Figure 44 shows the plot of the maximum wheel L/V ratio against speed for Case 4 lubrication conditions with new wheel profiles to demonstrate the trend in performance.

Table 42. Simulation predictions for Curving with Rail Lubrication Cases 1–4 and New Wheels and Rails, Car Loaded with the Maximum Test Load

Criterion	Limiting Value	Case 1 New	Case 2 New	Case 3 New	Case 4 New
Maximum carbody roll angle (degree)	4.0	0.69	0.69	0.68	0.66
Maximum wheel L/V	0.80	0.64	0.67	0.38	0.71
Maximum truck side L/V	0.50	0.30	0.33	0.22	0.43
Minimum vertical wheel load (%)	25	55	55	56	56
Peak-to-peak carbody lateral acceleration (g)	1.30	0.27	0.28	0.22	0.23
Maximum carbody lateral acceleration (g)	0.75	0.20	0.22	0.15	0.17
Lateral carbody acceleration standard deviation (g)	0.13	0.03	0.03	0.03	0.03
Maximum carbody vertical acceleration (g)	0.90	0.21	0.21	0.20	0.20
Maximum vertical suspension deflection (%)	95	67	67	67	67
95% Wheel L/V Ratio	0.60	0.37	0.41	0.27	0.56

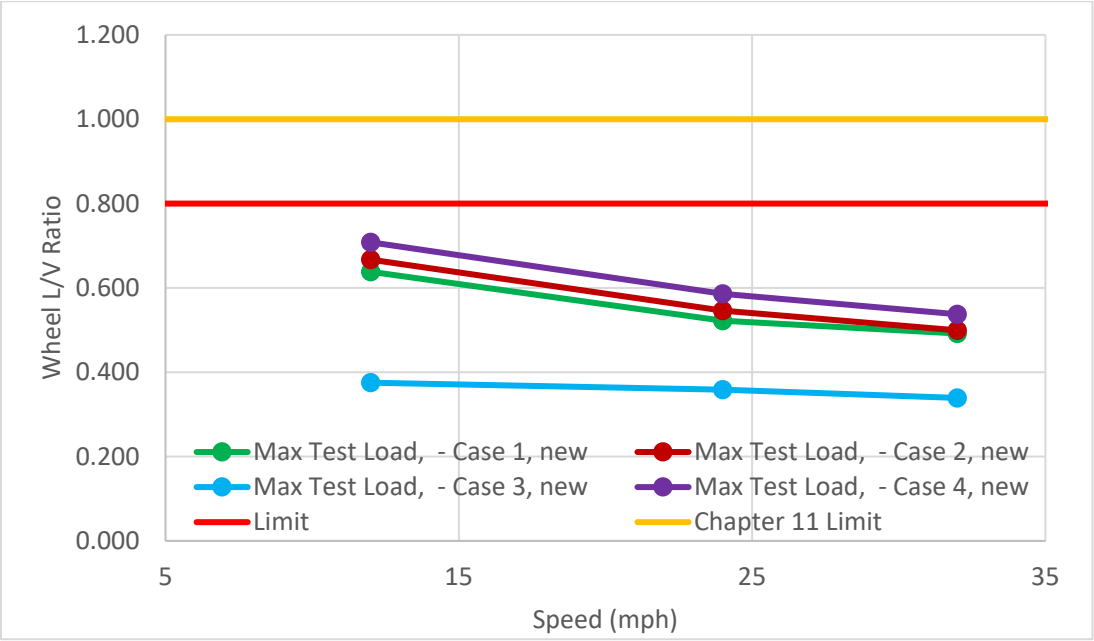


Figure 44. Predictions of Wheel L/V Ratio for multiple lubrication cases with new wheel and rail profiles (most severe results shown)

(2) Worn Profiles

Table 43 shows the simulation predictions of the car loaded with the maximum test load for the four friction cases with hollow worn wheel profiles and ground rail profiles. The table shows the worst-case results for runs in the CW and CCW directions with the A-end and B-end leading. The simulations of Case 3 meet all Standard S-2043 criteria. The simulations of Cases 1, 2, and 4 **do not meet** Standard S-2043 criteria for truck side L/V ratios, although they do meet the corresponding AAR Chapter 11 criteria. The AAR Chapter 11 criterion for truck side L/V ratio is 0.6. The Case 2 and Case 4 simulations predictions **do not meet** the Standard S-2043 limit for the 95 percent wheel L/V ratio although these predictions do meet the corresponding AAR Chapter 11 criteria. Therefore, on behalf of the Department of Energy, TTCI is requesting an exception from the AAR EEC.

Table 43. Simulation predictions for Curving with Rail Lubrication Cases 1–4 and Hollow Worn Wheels and Ground Rails, Car Loaded with the Maximum Test Load

Criterion	Limiting Value	Case 1 Worn	Case 2 Worn	Case 3 Worn	Case 4 Worn
Maximum carbody roll angle (degree)	4.0	0.72	0.74	0.73	0.71
Maximum wheel L/V	0.80	0.66	0.73	0.40	0.68
Maximum truck side L/V	0.50	0.52	0.60	0.25	0.58
Minimum vertical wheel load (%)	25	56	55	56	56
Peak-to-peak carbody lateral acceleration (g)	1.30	0.28	0.28	0.26	0.28
Maximum carbody lateral acceleration (g)	0.75	0.17	0.18	0.17	0.17
Lateral carbody acceleration standard deviation (g)	0.13	0.04	0.04	0.04	0.04
Maximum carbody vertical acceleration (g)	0.90	0.20	0.20	0.20	0.20
Maximum vertical suspension deflection (%)	95	68	67	67	67
95% Wheel L/V Ratio	0.60	0.57	0.66	0.33	0.61

Figure 45 shows a plot of the maximum truck side L/V versus speed for the CW and CCW with the worst-case A- or B-end leading results (Case 2), and both minimum and maximum test load conditions are shown. Figure 46 shows a plot of the maximum 95 percent wheel L/V ratio versus speed for the CW and CCW with the worst-case A- or B-end leading results (Case 2), and both minimum and maximum test load conditions are shown. Figure 47 shows a plot of the maximum truck side L/V ratio versus speed for Case 4, with both the minimum and maximum test load conditions shown for comparison. Figure 48 shows a plot of the truck side L/V ratio versus distance for the 12 mph CCW run with the B-end leading. The plot shows the data for the middle truck of the lead span bolster. The peak value occurs in the exit spiral of the curve.

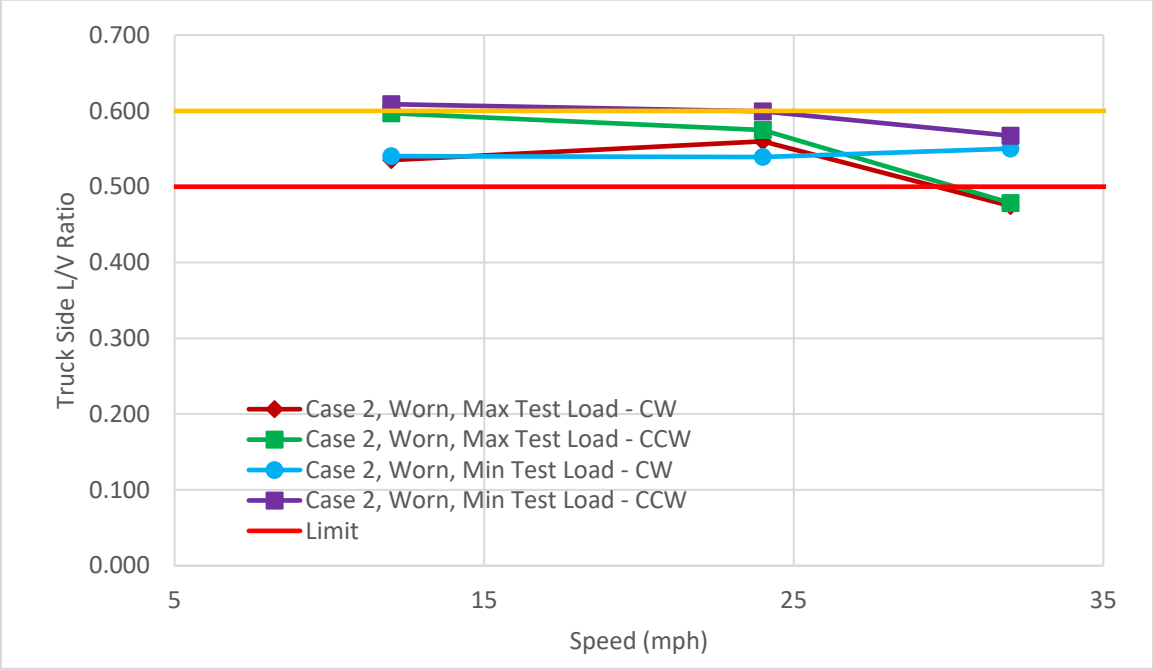


Figure 45. Predictions of Truck Side L/V Ratio for Case 2 lubrication with worn wheel and rail profiles for both directions of travel, with most severe results shown, at maximum and minimum test load.

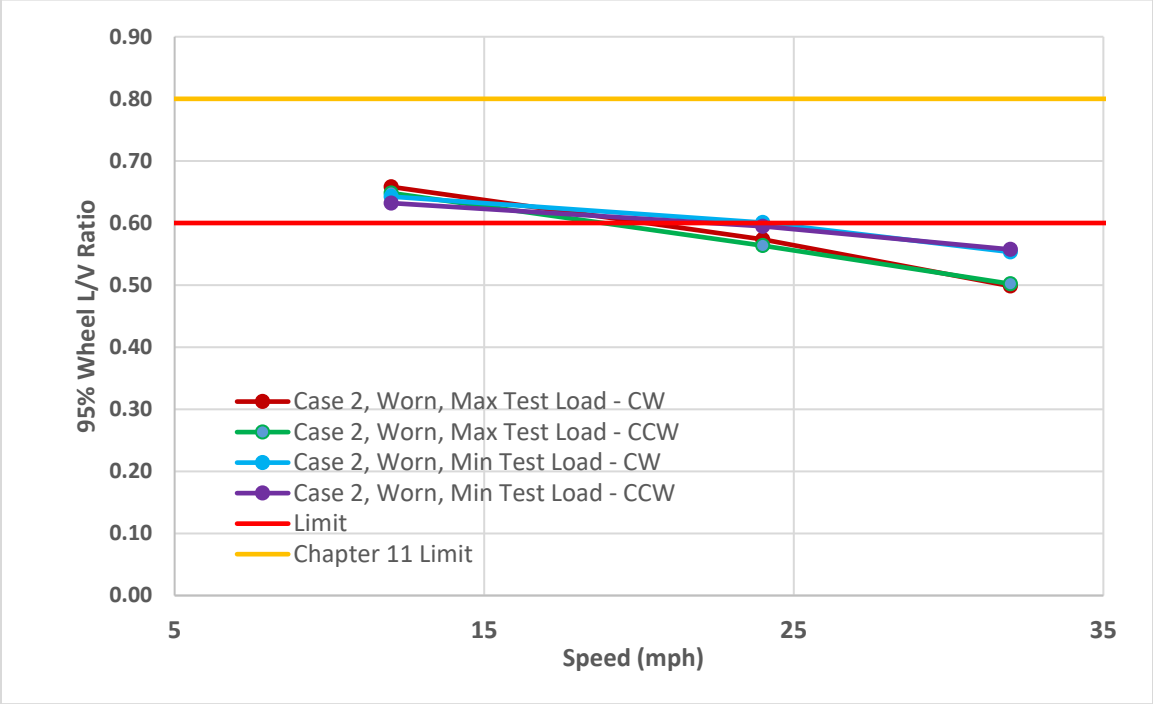


Figure 46. Predictions of 95% Wheel L/V Ratio for Case 2 lubrication with worn wheel and rail profiles for both directions of travel, with most severe results shown, at maximum and minimum test loads

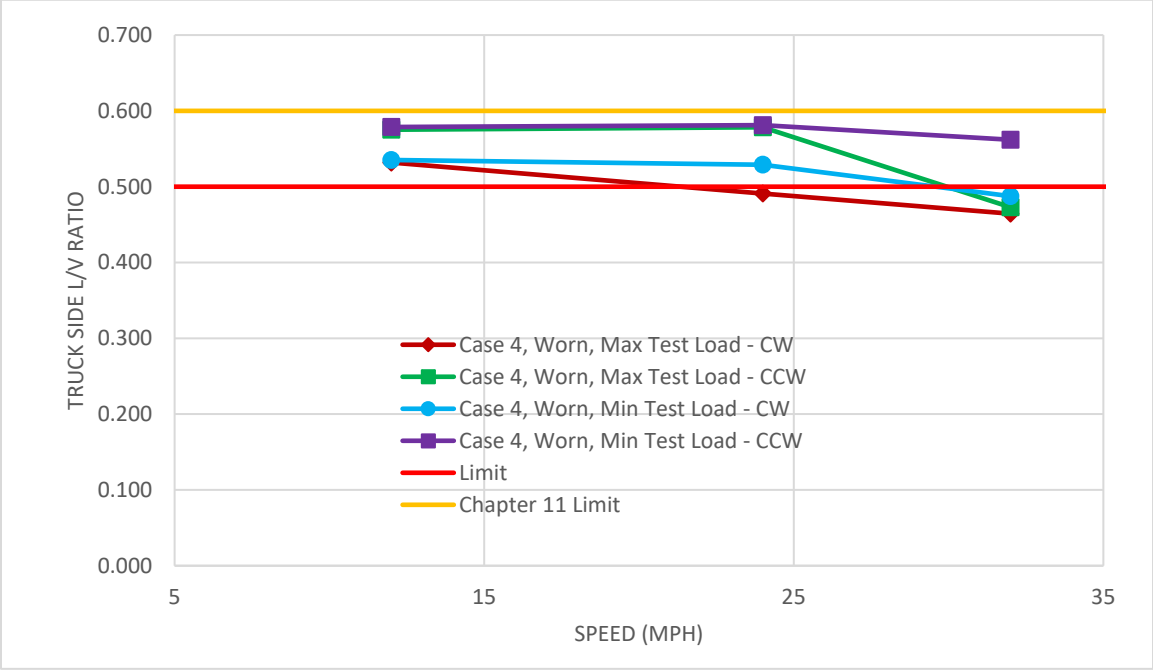


Figure 47. Predictions of Truck Side L/V Ratio for Case 4 lubrication with worn wheel and rail profiles for both directions of travel, with most severe results shown, at maximum and minimum test loads

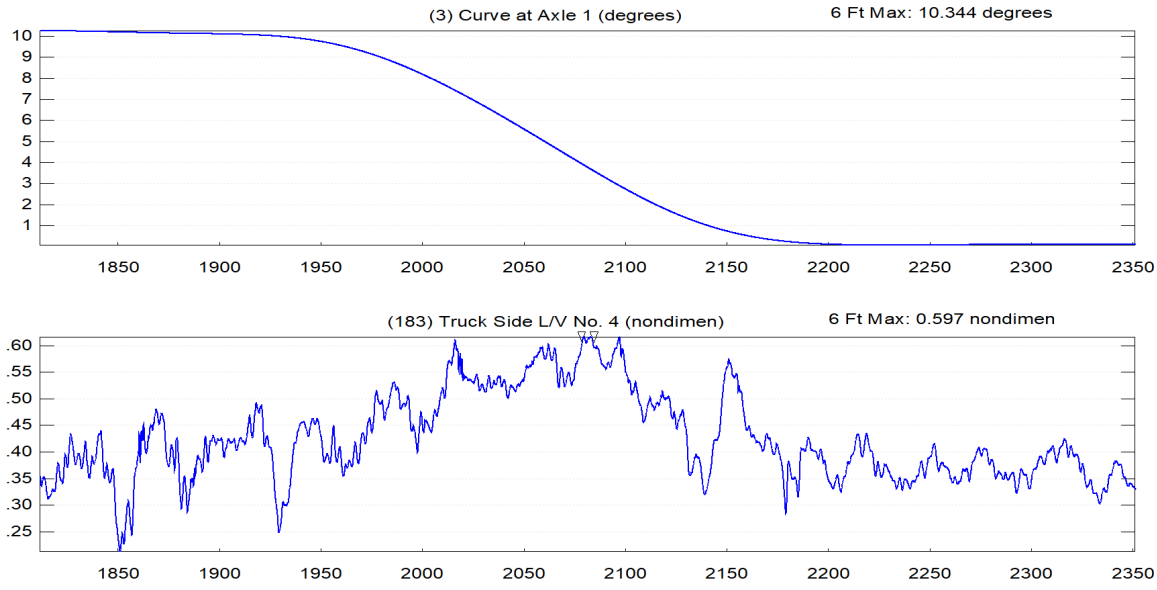


Figure 48. Plot of Truck Side L/V Ratio versus distance for Case 2 friction with worn wheel and rail profiles. The plot shows data for the high rail of the middle truck on the lead span bolster

Figure 49 and Figure 50 show how lubrication impacts the results of the various cases, for both the truck side L/V ratios and the 95th percentile wheel L/V ratios, respectively.

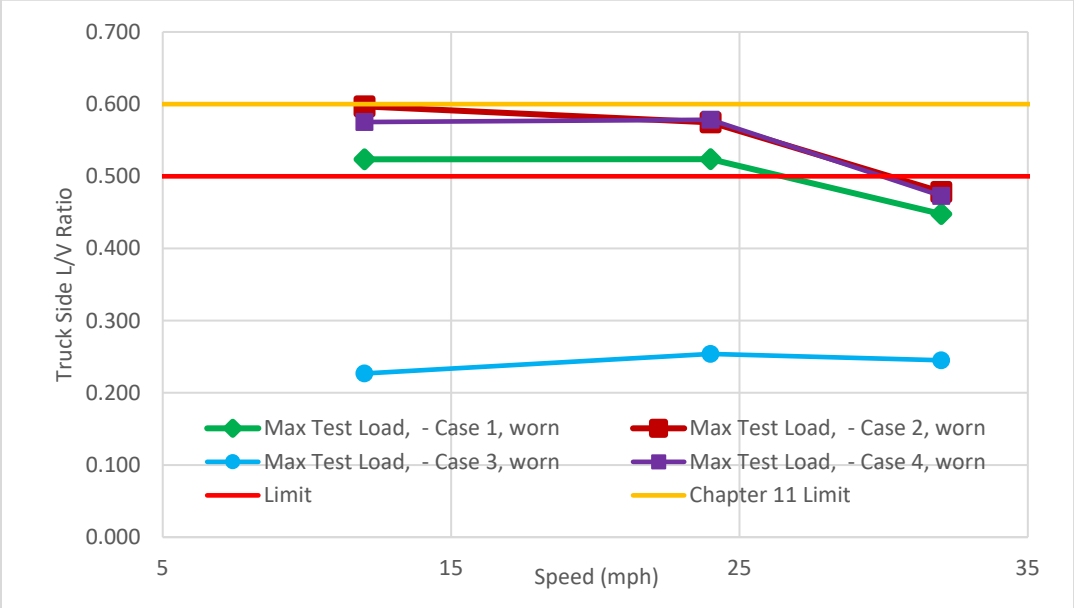


Figure 49. Worst-case predictions for Truck Side L/V Ratio at all lubrication cases of worn wheel and rail profiles, at maximum test load

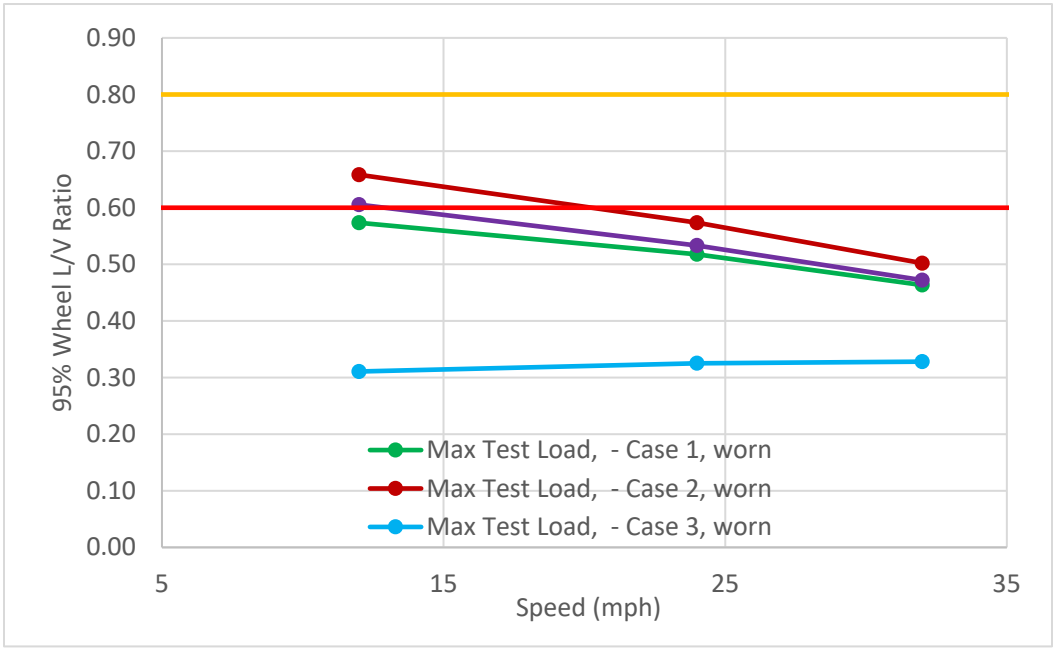


Figure 50. Worst-case predictions for 95 percentile Wheel L/V Ratio at all lubrication cases of worn wheel and rail profiles, at maximum test load

7.10 Limiting Spiral Negotiation

The simulations of the limiting spiral regime were conducted according to Standard S-2043, Paragraph 4.3.11.6. The limiting spiral has a steady curvature change from 0 to 10 degrees and a steady superelevation change from 0 inch to 4 3/8 inches in 89 feet.

7.10.1 Minimum Test Load

Table 44 shows the worst-case test results and the simulation predictions for the car loaded with the minimum test load in the limiting spiral test regime. Figure 51 shows the test results and the simulation predictions of the maximum wheel L/V ratio with CSM 70 primary pads plotted against speed to show the trend in performance. Figure 52 shows test results and simulation predictions of maximum wheel L/V ratio with CSM 58 primary pads.

Using CSM 70 primary pads, the model predicts lower wheel L/V ratios and higher minimum vertical wheel loads than those that were measured in the test, but the overall trend matches closely, as shown in Figure 51. The simulations done using CSM 58 pads showed lower L/V ratios than simulations done using CSM 70 primary pads, but the test results showed higher wheel L/V ratios with CSM 58 primary pads than those with CSM 70 pads. Only post-test simulation predictions are shown because the pre-test predictions were for a load case no longer intended for use.

The test and revised simulation results **meet** Standard S-2043 criteria for the limiting spiral regime at the minimum test load.

Table 44. Limiting spiral test results and simulation predictions with minimum test load

Criterion	Limiting Value	CSM 70 Pads		CSM 58 Pads	
		Test Result	Simulation Prediction Revised Model	Test Result	Simulation Prediction Revised Model
Roll angle (degree)	4.0	1.5	0.7	1.6	0.8
Maximum wheel lateral/vertical (L/V)	0.8	0.67	0.62	0.69	0.50
Maximum truck side L/V	0.5	0.38	0.35	0.42	0.27
Minimum vertical wheel load (%)	25%	42%	55%	56%	54%
Lateral peak-to-peak acceleration (g)	1.3	0.15	0.12	0.18	0.16
Maximum lateral acceleration (g)	0.75	0.13	0.10	0.16	0.11
Maximum vertical acceleration (g)	0.90	0.09	0.13	0.16	0.23
Maximum vertical suspension deflection (%)	95%	29%	24%	16%	24%

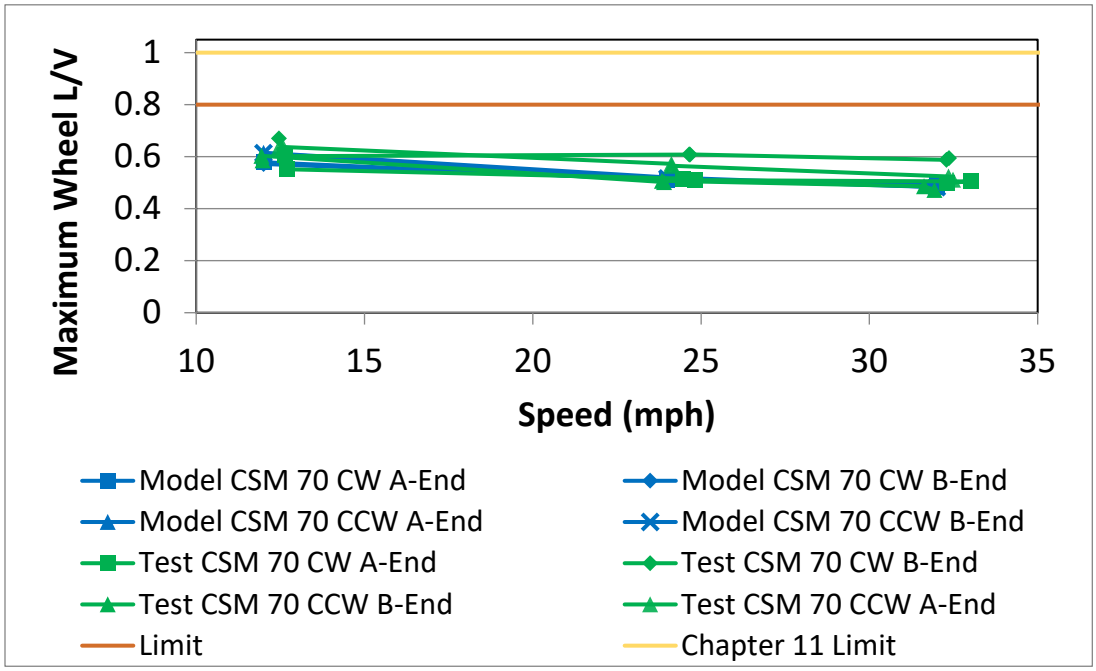


Figure 51. Simulation prediction and test results of maximum wheel L/V ratio in the limiting spiral regime with minimum test load using CSM 70 pads

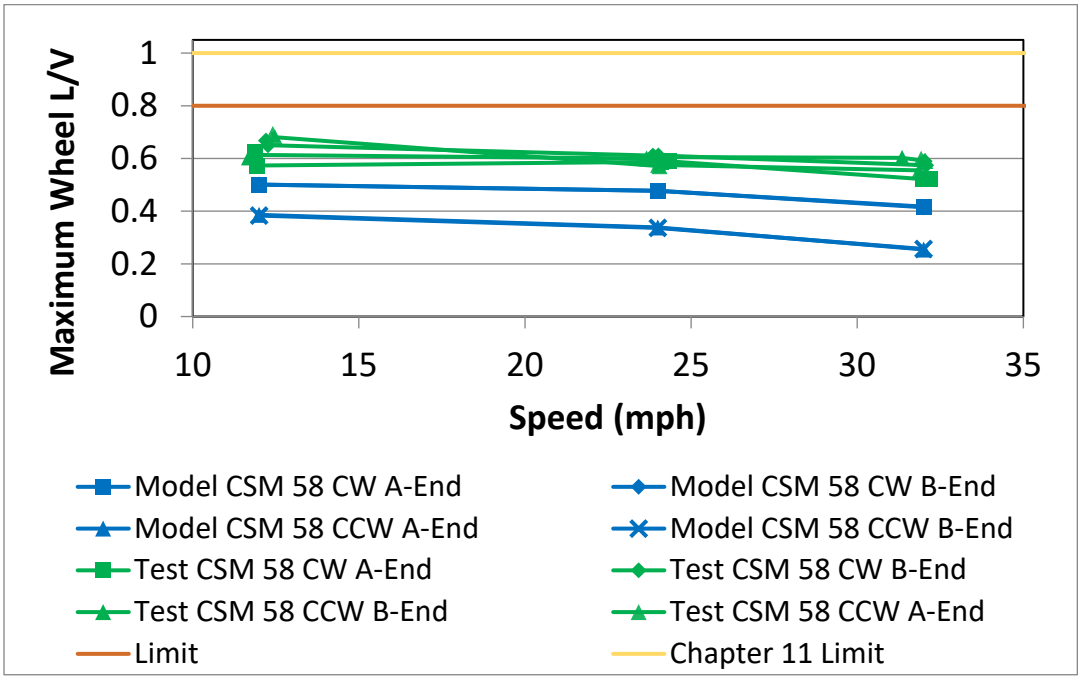


Figure 52. Simulation prediction and test results of maximum wheel L/V ratio in the limiting spiral regime with minimum test load using CSM 58 pads

7.10.2 Maximum Test Load

Table 45 shows the worst-case test results and simulation predictions for the car loaded with the maximum test load in the limiting spiral test regime. Figure 53 shows the test results and simulation predictions of the maximum wheel L/V ratio with CSM 70 primary pads plotted against speed to show the trend in performance. Figure 54 shows the original and revised simulation predictions of maximum wheel L/V ratio with CSM 58 primary pads.

Using CSM 70 primary pads, the model predicts lower wheel L/V ratios and higher minimum vertical wheel loads than those that were measured in the test. The simulations done with CSM 58 pads showed lower L/V ratios than simulations done using CSM 70 primary pads, but the difference was small. The wheel L/V ratios predicted with the original model in 2017 were about 10 percent higher than those predicted with the revised model.

The test and revised simulation results **meet** Standard S-2043 criteria for the limiting spiral regime at maximum test load.

Table 45. Dynamic curving test results and simulation predictions with maximum test load

Criterion	Limiting Value	CSM 70 Pads		CSM 58 Pads	
		Test Result	Simulation Prediction Revised Model	Simulation Prediction Original Model	Simulation Prediction Revised Model
Roll angle (degree)	4.0	1.3	1.0	2.3	1.0
Maximum wheel lateral/vertical (L/V)	0.8	0.74	0.52	0.49	0.44
Maximum truck side L/V	0.5	0.39	0.30	0.31	0.21
Minimum vertical wheel load (%)	25%	52%	60%	54%	59%
Lateral peak-to-peak acceleration (g)	1.3	0.12	0.11	0.13	0.14
Maximum lateral acceleration (g)	0.75	0.13	0.08	0.11	0.11
Maximum vertical acceleration (g)	0.90	0.17	0.17	0.07	0.28
Maximum vertical suspension deflection (%)	95%	68%	69%	78%	69%

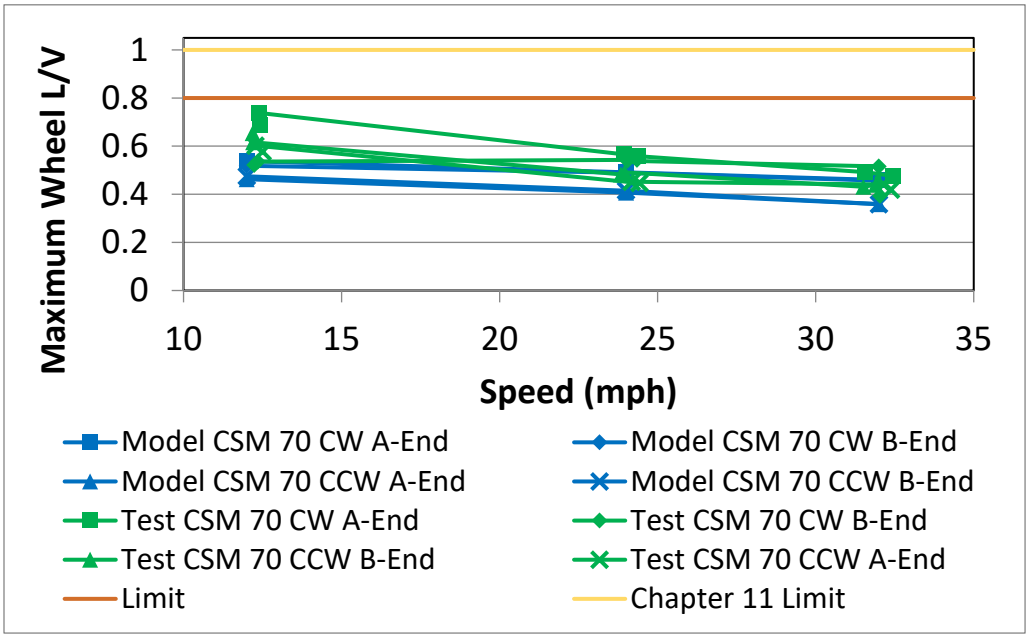


Figure 53. Simulation prediction and test results of maximum wheel L/V ratio in the dynamic curving regime with maximum test load using CSM 70 pads

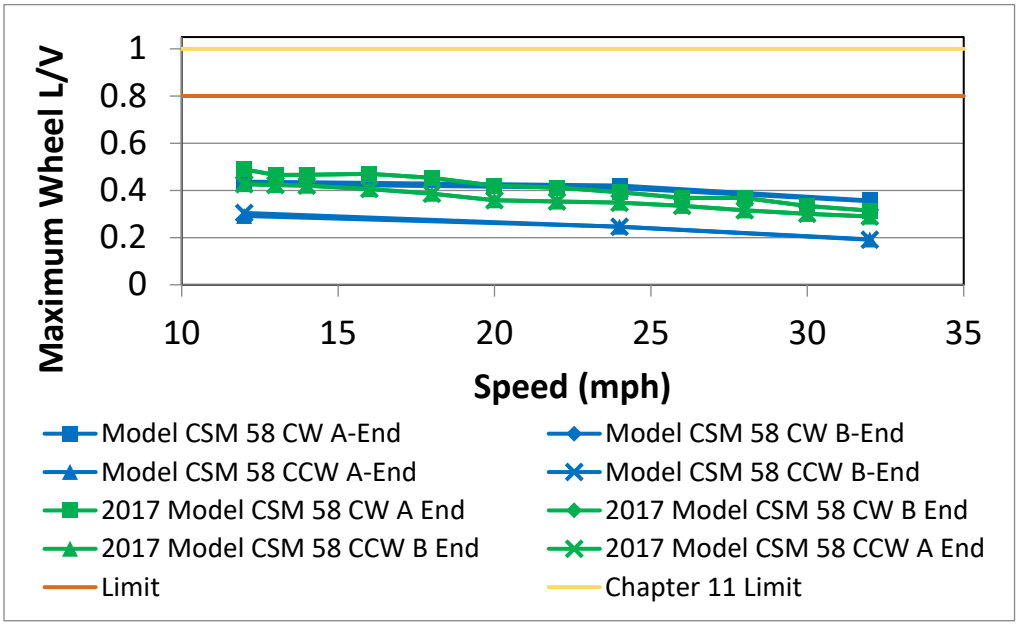


Figure 54. Simulation predictions of maximum wheel L/V ratio in the dynamic curving regime with maximum test load using CSM 70 and CSM 58 pads

7.11 Special Trackwork: Turnouts and Crossovers (Standard S-2043, Paragraph 4.3.11.7)

The simulations of the turnout and crossover regime were conducted according to Standard S-2043, Paragraph 4.3.11.7. The original simulations were performed using a No. 7 AREMA straight point turnout and a No. 7 crossover on 13-foot track centers at speeds up to 15 mph. Additional revised

simulations were performed only for the No. 7 crossover, because, while the preliminary simulation predictions met Standard S-2043 criteria in the turnout, the predictions did not meet all Standard S-2043 criteria in the crossover (the crossover was the most severe case).

Because TTCI does not have measured track geometry available for a No. 7 crossover it used ideal track inputs. These inputs included track geometry deviations due to the switch riser, the turnout entry angles, and the closure curves. The changing rail geometry was modeled based on the unworn shapes of the components. The nominal clearance of the guardrails at the frogs were modeled as well. TTCI used 50-millisecond windows when processing wheel force statistics because the changes in rail profiles along the track introduced extremely short duration, unrealistic spikes in the simulation predictions.

7.11.1 Minimum Test Load – Turnouts and Crossovers

Table 46 shows the worst-case simulation predictions for the crossover regime. The revised simulation predictions **met** Standard S-2043 criteria for the No. 7 crossover at the minimum test load, with the maximum truck side L/V ratio equal to the criterion of 0.5. Figure 55 shows a plot of the truck side L/V ratio in the crossover. Only the post-test simulation predictions are shown because the pre-test predictions were for a load case no longer intended for use.

Table 46. Crossover Simulation Predictions with Minimum Test Load

Criterion	Limiting Value	No. 7 Crossover A-Lead	No. 7 Crossover B-Lead
Maximum carbody roll angle (degree)	4.0	0.1	0.1
Maximum wheel L/V	0.80	0.78	0.78
Maximum truck side L/V	0.50	0.50	0.50
Minimum vertical wheel load (%)	25	57%	56%
Peak-to-peak carbody lateral acceleration (g)	1.30	0.35	0.41
Maximum carbody lateral acceleration (g)	0.75	0.15	0.25
Maximum carbody vertical acceleration (g)	0.90	0.53	0.52
Maximum vertical suspension deflection (%)	95	24%	23%

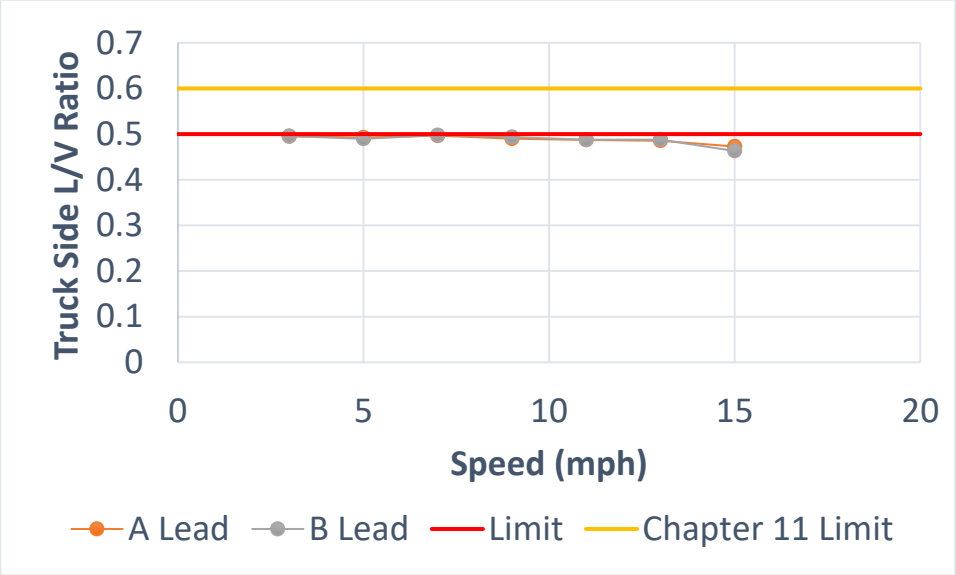


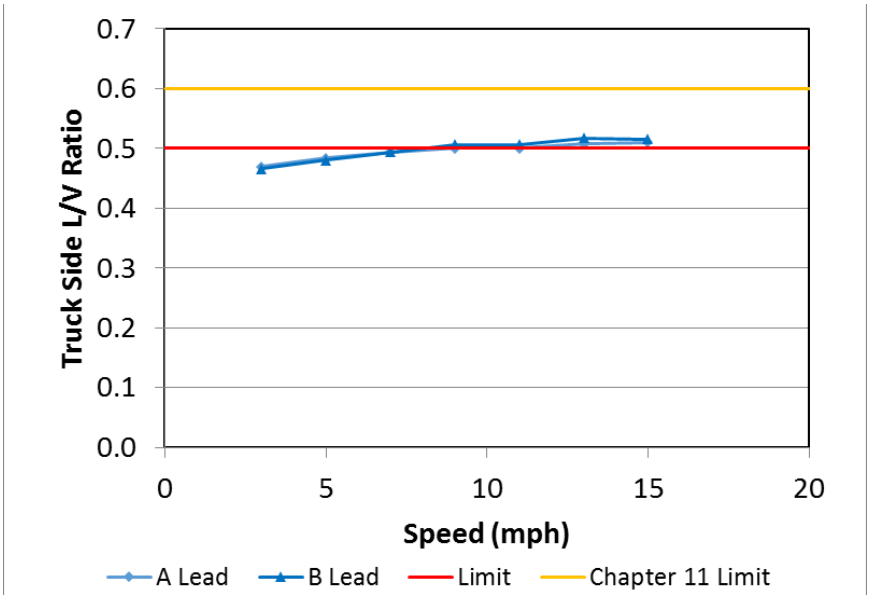
Figure 55. Simulation Predictions of Truck side L/V Ratio on No. 7 Crossovers for Original Simulations of Atlas Car with Minimum Test Load

7.11.2 Maximum Test Load – Turnouts and Crossovers

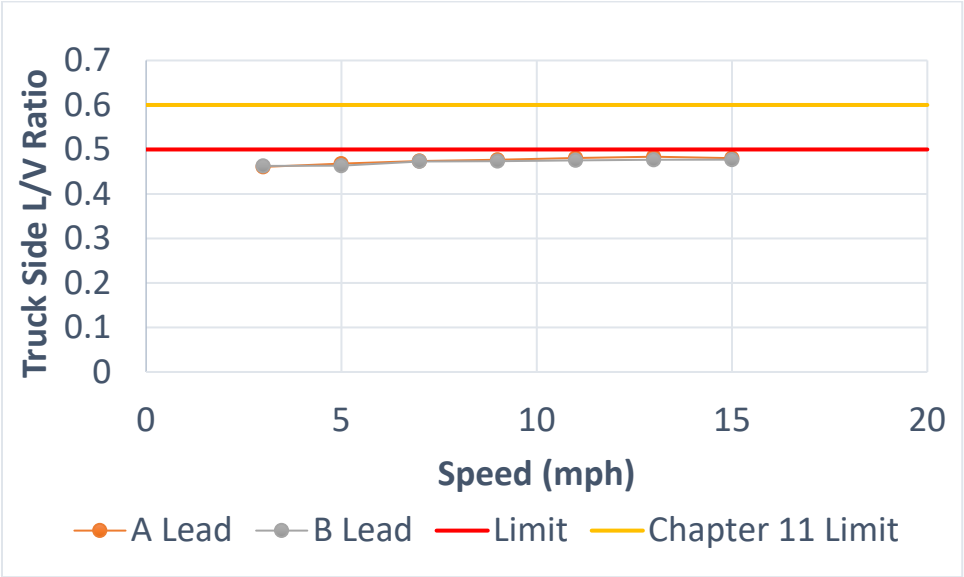
Table 47 shows the worst-case simulation predictions for the crossover regime. Figure 56 shows a plot of the maximum truck side L/V versus speed to show the trend in performance. The original simulation predictions did not meet the Standard S-2043 criterion for the truck side L/V ratio in the No. 7 crossover, but all other criteria were met. The revised simulation predictions **met** all Standard S-2043 criteria because the measured primary longitudinal stiffness used in the revised model was lower and more representative of the actual vehicle than what was used in the original model.

Table 47. Crossover Simulation Predictions, Car Loaded at Maximum Load

		Original		Revised	
Criterion	Limiting Value	No. 7 Crossover A-Lead	No. 7 Crossover B-Lead	No. 7 Crossover A-Lead	No. 7 Crossover B-Lead
Maximum carbody roll angle (degree)	4.0	0.3	0.3	0.3	0.3
Maximum wheel L/V	0.80	0.65	0.67	0.61	0.60
Maximum truck side L/V	0.50	0.51	0.52	0.48	0.48
Minimum vertical wheel load (%)	25	64	65	62	69
Peak-to-peak carbody lateral acceleration (g)	1.30	0.22	0.24	0.30	0.54
Maximum carbody lateral acceleration (g)	0.75	0.13	0.13	0.25	0.23
Maximum carbody vertical acceleration (g)	0.90	0.10	0.09	0.09	0.36
Maximum vertical suspension deflection (%)	95	73	75	64	61



(a)



(b)

Figure 56. Simulation Predictions of Truck Side L/V Ratio on No. 7 Crossover. Original Simulations (a) and revised simulations (b) at maximum load

7.12 Buff and Draft Curving

The simulations of the buff and draft curving regime were conducted according to Standard S-2043, Paragraph 4.3.13. The simulations were performed using measured track geometry of the 12-degree curve of the WRM loop at the TTC. The simulations were designed to simulate the cask car coupled to the following:

- A base car as described in the AAR MSRP Section C-II, Standard M-1001 Chapter 2, Paragraph 2.1.4.2.3.

- A long car with 90-foot-long over strikers, 66-foot-long truck centers, 60-inch-long couplers, and conventional draft gear.
- A like car.
- A buffer car–the car the cask car will be coupled to in HLRM service.

The in-train forces were calculated for a 12-degree curve for each of the coupled car geometries, and the load was applied to the coupler as an external force, made up of two components: one lateral and one longitudinal.

Table 48 shows the worst-case simulation predictions for draft force cases, and Table 49 shows the worst-case simulation predictions for the buff force cases. Figure 57 shows a plot of the maximum truck side L/V ratio for the four draft force cases modeled in both the original and revised simulations. Similarly, Figure 58 shows the plot of the buff maximum truck side L/V ratios. All revised simulation predictions **meet** all Standard S-2043 criteria for all buff and draft curving cases.

Table 48. Revised Simulation Predictions for 250,000 Draft Force, Minimum Test Load

Criterion	Limiting Value	Base	Long	Like	Buffer Car
Maximum carbody roll angle (degree)	4.0	0.8	0.6	0.8	0.7
Maximum wheel L/V	0.80	0.55	0.50	0.55	0.50
Maximum truck side L/V	0.50	0.47	0.34	0.47	0.35
Minimum vertical wheel load (%)	25	46	57	46	56
Peak-to-peak carbody lateral acceleration (g)	1.30	0.18	0.17	0.16	0.16
Maximum carbody lateral acceleration (g)	0.75	0.12	0.12	0.12	0.12
Lateral carbody acceleration standard deviation (g)	0.13	0.00	0.00	0.00	0.00
Maximum carbody vertical acceleration (g)	0.90	0.11	0.12	0.12	0.12
Maximum vertical suspension deflection (%)	95	19	19	20	18

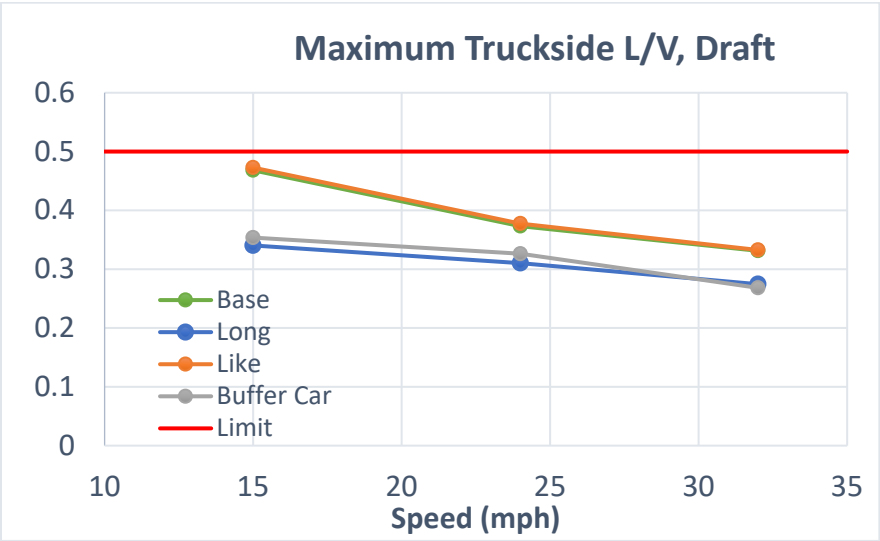


Figure 57. Truck Side L/V Ratio for Curving Simulations Under 250,000 Pounds Draft Force for Revised Simulations with the Minimum Test Load

Table 49. Revised Simulation Predictions for 250,000 Buff Force, Minimum Test Load

Criterion	Limiting Value	Base	Long	Like	Buffer Car
Maximum carbody roll angle (degree)	4.0	0.7	0.8	0.7	0.7
Maximum wheel L/V	0.80	0.52	0.55	0.52	0.52
Maximum truck side L/V	0.50	0.39	0.39	0.40	0.37
Minimum vertical wheel load (%)	25	55	53	55	56
Peak-to-peak carbody lateral acceleration (g)	1.30	0.15	0.15	0.15	0.17
Maximum carbody lateral acceleration (g)	0.75	0.11	0.11	0.11	0.12
Maximum carbody vertical acceleration (g)	0.90	0.12	0.12	0.10	0.13
Maximum vertical suspension deflection (%)	95	35	31	36	32

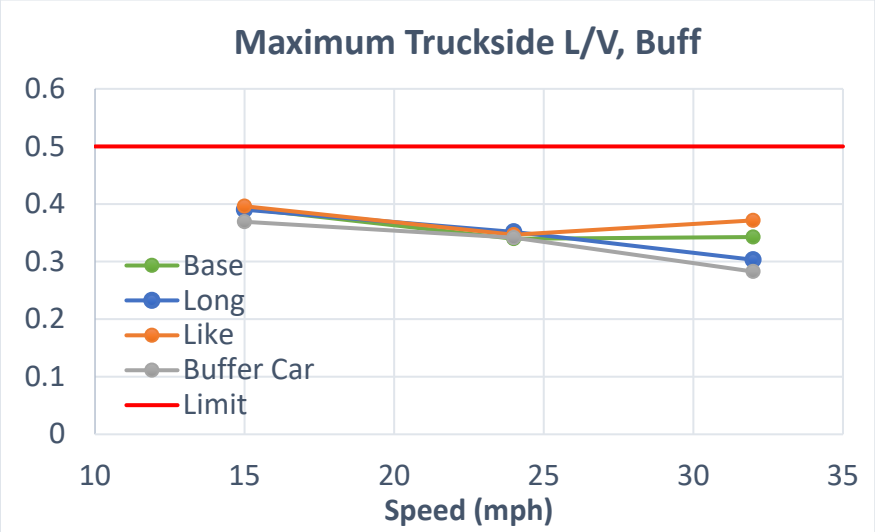


Figure 58. Truck Side L/V Ratio for Curving Simulations Under 250,000 Pounds Buff Force for Revised Simulations with the Minimum Test Load

7.13 Worn Component Simulations

The worn component simulations were conducted according to Standard S-2043, Paragraph 4.3.15. The wear of the following components was simulated:

- Constant Contact Side Bearings (CCSB)
- Center plate
- Primary pad
- Friction wedges
- Broken springs

The hunting, dynamic curving, constant curving, and twist-and-roll worn component simulations were performed with the minimum test load because this configuration generally produced the worst performance. The pitch-and-bounce simulations for the worn wedge and broken spring conditions were performed with the maximum test load condition.

In Sections 7.13.1 to 7.13.5, the worst-case simulation predictions for the worn components are summarized in tables together with the criteria and base line predictions for the new condition car. In cases where the component wear causes the performance to degrade such that the car does not meet criteria, plots are shown to demonstrate the trend in performance. Only simulation predictions with the revised model are shown in Sections 7.13.1 to 7.13.5 because, except for the simulation in the pitch and bounce regime, the load conditions are not comparable.

7.13.1 Worn Constant Contact Side Bearings

The wear in a CCSB may result in a loss of side bearing preload. The wear of the carbody centerplate or the truck center bowl may result in a reduction of the CCSB setup height. To examine the effect of these types of CCSB wear, simulations were performed with the following:

- The CCSB having half the stiffness and half the preload of new CCSB (3,000-pound nominal preload). This condition will reduce the both the turning moment and the the roll stiffness between the truck bolster and the span bolster.
- The setup height of the new CCSB reduced to 4 7/8 inch. This reduction will increase the turning moment between the truck bolster and span bolster. It will also increase the roll stiffness and reduce the roll clearance between the truck bolster and span bolster.

The performance of the car with worn CCSB was checked during dynamic curving, hunting, and twist and roll simulation with the minimum test load.

Table 50 shows the worst-case simulation predictions for the baseline, low preload, and tight clearance conditions. All performance criteria were **met** for the dynamic curving simulations with worn CCSB. Figure 59 shows a plot of the maximum wheel L/V ratio versus speed for the baseline case and the two worn CCSB cases to show the trend in performance.

Table 50. Simulation Predictions of the Atlas Cask Car with Worn CCSB in Dynamic Curving

Criterion	Limiting Value	Revised Models		
		Baseline	CCSB, Low Preload	CCSB, Tight Clearance
Maximum carbody roll angle (degree)	4.0	0.97	0.95	0.99
Maximum wheel L/V	0.80	0.71	0.71	0.71
Maximum truck side L/V	0.50	0.35	0.35	0.35
Minimum vertical wheel load (%)	25	52.69	52.51	53.22
Peak-to-peak carbody lateral acceleration (g)	1.30	0.19	0.18	0.23
Maximum carbody lateral acceleration (g)	0.75	0.16	0.16	0.18
Maximum carbody vertical acceleration (g)	0.90	0.12	0.11	0.12
Maximum vertical suspension deflection (%)	95	23.22	23.19	24.01

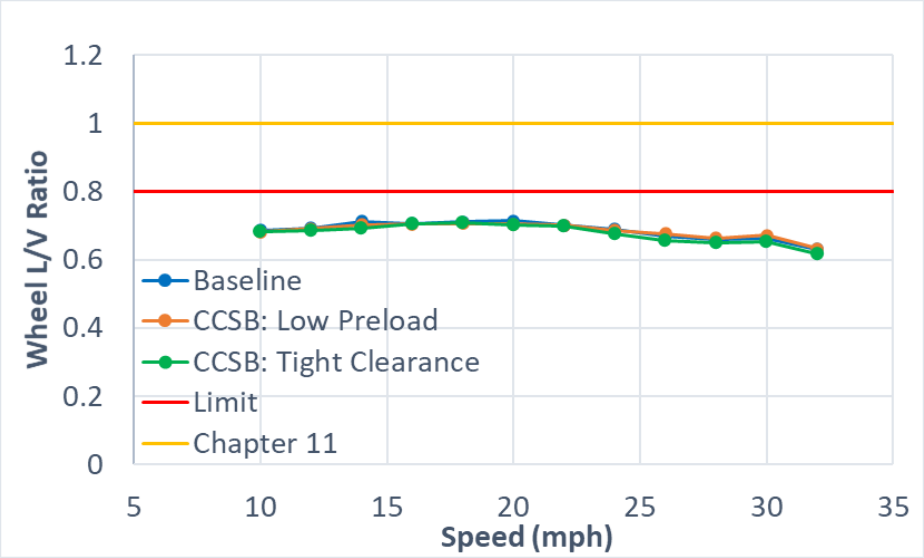


Figure 59. Single Wheel L/V Ratio for Worn CCSB Cases

Table 51 shows a comparison of the hunting simulation predictions for unworn baseline and the worn CCSB simulations. Similar to the test results, the baseline simulations and the "Low Preload" worn CCSB condition did not meet the Standard S-2043 criterion for the maximum standard deviation of carbody lateral acceleration. All other Standard S-2043 criteria were met.

As the CCSB preload is reduced, the hunting performance deteriorates. Figure 60 shows the standard deviation of the carbody lateral acceleration over 2,000 feet, and all configurations show a severely deteriorated performance at speeds above 50 mph, although the tight bearing clearance does not exceed the limit. All worn side bearing performance **meets** Standard S-2043 criteria up to 60 mph. This speed is above the limiting operating speed of the cask car in HLRM service.

Table 51. Simulation Predictions of the Atlas Cask Car with Worn CCSB in Hunting

Criterion	Limiting Value	Revised Models		
		Baseline	CCSB, Low Preload	CCSB, Tight Clearance
Maximum carbody roll angle (degree)	4.0	0.30	0.41	0.27
Maximum wheel L/V	0.80	0.28	0.39	0.21
Maximum truck side L/V	0.50	0.14	0.21	0.15
Minimum vertical wheel load (%)	25	71.1	61.4	70.6
Peak-to-peak carbody lateral acceleration (g)	1.30	0.59	0.64	0.55
Maximum carbody lateral acceleration (g)	0.75	0.31	0.36	0.31
Lateral carbody acceleration standard deviation (g)	0.13	0.14	0.17	0.11
Maximum carbody vertical acceleration (g)	0.90	0.32	0.17	0.17
Maximum vertical suspension deflection (%)	95	16.5	16.1	16.8

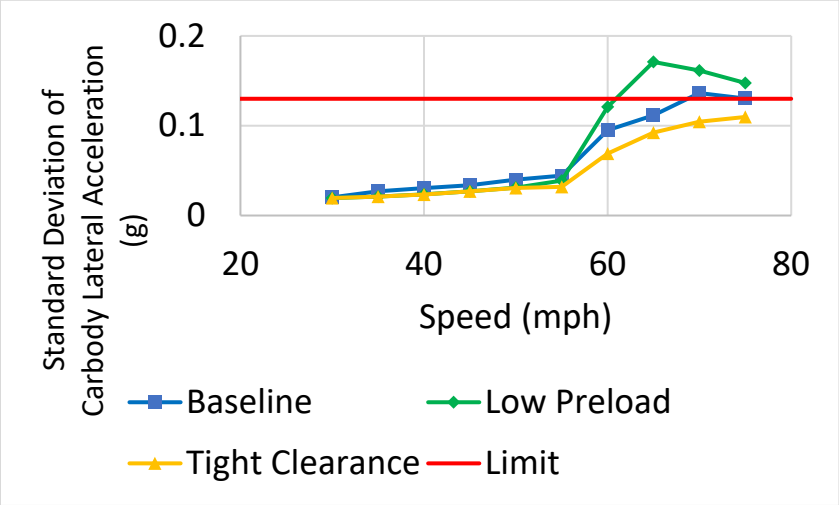


Figure 60. Maximum Carbody Lateral Acceleration for CCSB Wear Cases Plotted Against Speed

Table 52 shows a comparison of twist-and-roll simulation predictions for the baseline and worn CCSB simulations. The simulation predictions for the worn CCSB **meet** Standard S-2043 criteria for twist and roll simulations.

Table 52. Simulation Predictions of the Atlas Cask Car with Worn CCSB in Twist and Roll

Criterion	Limiting Value	Baseline	CCSB, Low Preload	CCSB, Tight Clearance
Maximum carbody roll angle (degree)	4.0	1.9	2.0	1.9
Maximum wheel L/V	0.80	0.27	0.30	0.17
Maximum truck side L/V	0.50	0.17	0.17	0.12
Minimum vertical wheel load (%)	25	58	58	59
Peak-to-peak carbody lateral acceleration (g)	1.30	0.53	0.54	0.46
Maximum carbody lateral acceleration (g)	0.75	0.29	0.27	0.25
Maximum carbody vertical acceleration (g)	0.90	0.24	0.24	0.23
Maximum vertical suspension deflection (%)	95	21	22	21

7.13.2 Centerplate

To examine the effect of centerplate wear, simulations were performed with centerplate friction increased from 0.3 for the baseline case to 0.5 for the worn case. Table 53 shows a comparison of the constant curving simulation predictions for the baseline and worn centerplate simulations. The simulation predictions for worn centerplates **meet** Standard S-2043 criteria for constant curving.

Table 53. Simulation Predictions of the Atlas Cask Car with Worn Centerplate in Constant Curving

Criterion	Limiting Value	Baseline	Worn Centerplate
Maximum carbody roll angle (degree)	4.0	0.77	0.77
Maximum wheel L/V	0.80	0.52	0.52
Maximum truck side L/V	0.50	0.34	0.34
Minimum vertical wheel load (%)	25	52.7	53.4
Peak-to-peak carbody lateral acceleration (g)	1.30	0.15	0.15
Maximum carbody lateral acceleration (g)	0.75	0.14	0.14
Maximum carbody vertical acceleration (g)	0.90	0.15	0.14
Maximum vertical suspension deflection (%)	95	24.8	24.9

Table 54 shows a comparison of the dynamic curving simulation predictions for the baseline and worn centerplate simulations. The simulation predictions for the baseline and worn simulation **meet** the criteria for dynamic curving (the tested car also met this performance specification).

Table 54. Simulation Predictions of the Atlas Cask Car with Worn Centerplate in Dynamic Curving

Criterion	Limiting Value	Baseline	Centerplate Wear
Maximum carbody roll angle (degree)	4.0	0.97	1.01
Maximum wheel L/V	0.80	0.71	0.71
Maximum truck side L/V	0.50	0.35	0.35
Minimum vertical wheel load (%)	25	52.69	53.56
Peak-to-peak carbody lateral acceleration (g)	1.30	0.19	0.19
Maximum carbody lateral acceleration (g)	0.75	0.16	0.17
Maximum carbody vertical acceleration (g)	0.90	0.12	0.11
Maximum vertical suspension deflection (%)	95	23.22	24.05

Table 55 shows a comparison of the hunting simulation predictions for baseline and worn centerplate simulations. The baseline simulation predictions **did not meet** the criteria for a standard deviation of the lateral carbody acceleration over 2,000 feet. All worn centerplate performances meet Standard S-2043 criteria up to 65 mph. This speed is above the limiting operating speed of the cask car in HLRM service. Figure 61 plots the lateral carbody acceleration standard deviation against vehicle speed, and the worn centerplate condition is marginally more favorable than the baseline condition. All other criteria were met for hunting with worn centerplates.

Table 55. Simulation Predictions of the Atlas Cask Car with Worn Centerplate in Hunting

Criterion	Limiting Value	Baseline	Centerplate Wear
Maximum carbody roll angle (degree)	4.0	0.3	0.3
Maximum wheel L/V	0.80	0.28	0.19
Maximum truck side L/V	0.50	0.14	0.13
Minimum vertical wheel load (%)	25	71	70
Peak-to-peak carbody lateral acceleration (g)	1.30	0.59	0.57
Maximum carbody lateral acceleration (g)	0.75	0.31	0.31
Lateral carbody acceleration standard deviation (g)	0.13	0.14	0.13
Maximum carbody vertical acceleration (g)	0.90	0.32	0.17
Maximum vertical suspension deflection (%)	95	16	16

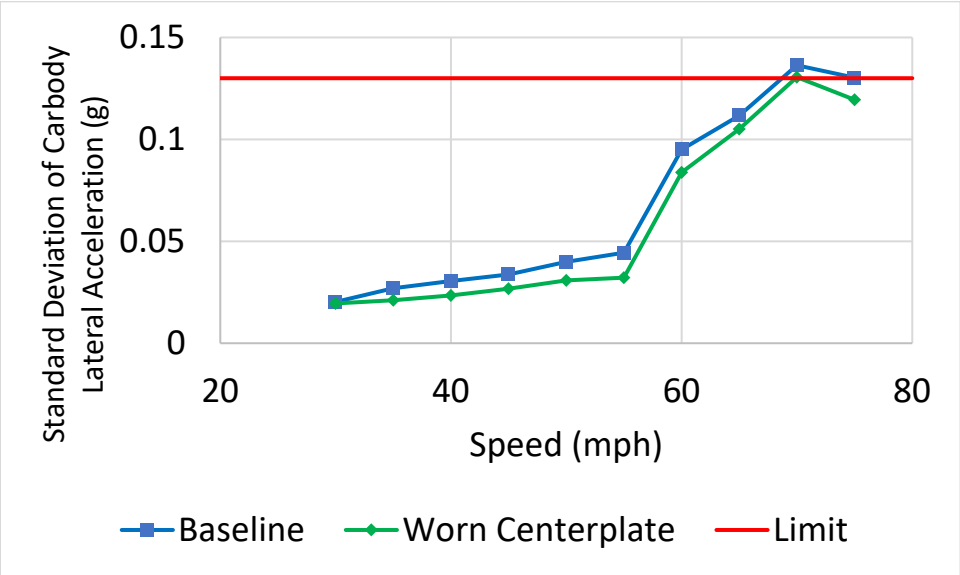


Figure 61. Hunting stability, considering centerplate wear

7.13.3 Primary Pad

It is not clear how the primary pads of the Swing Motion® trucks will wear over time. To examine the possible impact of various changes, the worn primary pads were simulated with both lower and higher longitudinal and lateral stiffness. For the lower stiffness runs, the stiffness was reduced by a factor of 2. For the higher stiffness runs, the stiffness was increased by a factor of 20.

Table 56 shows a comparison of the constant curving simulation predictions for the baseline and worn primary pad simulations. The simulation predictions for the worn primary pads **meet** Standard S-2043 criteria for constant curving.

Table 56. Simulation Predictions of the Atlas Cask Car with Worn Primary Pads in Constant Curving

Criterion	Limiting Value	Baseline	Soft Primary Pad	Stiff Primary Pad
Maximum carbody roll angle (degree)	4.0	0.77	0.77	0.77
Maximum wheel L/V	0.80	0.52	0.43	0.71
Maximum truck side L/V	0.50	0.34	0.29	0.37
Minimum vertical wheel load (%)	25	52.70	52.50	53.60
Peak-to-peak carbody lateral acceleration (g)	1.30	0.15	0.15	0.22
Maximum carbody lateral acceleration (g)	0.75	0.14	0.12	0.19
Maximum carbody vertical acceleration (g)	0.90	0.15	0.15	0.16
Maximum vertical suspension deflection (%)	95	24.80	24.54	25.06

Table 57 shows a comparison of the dynamic curving simulation predictions for the baseline and worn primary pad simulations. The simulation predictions showed that both baseline and worn pad conditions **met** the Standard S-2043 criteria for the wheel L/V ratio for dynamic curving.

Table 57. Simulation Predictions of the Atlas Cask Car with Worn Primary Pads in Dynamic Curving

Criterion	Limiting Value	Baseline	Soft Primary Pad	Stiff Primary Pad
Maximum carbody roll angle (degree)	4.0	0.97	0.91	1.04
Maximum wheel L/V	0.80	0.71	0.66	0.75
Maximum truck side L/V	0.50	0.35	0.33	0.39
Minimum vertical wheel load (%)	25	52.69	52.67	53.61
Peak-to-peak carbody lateral acceleration (g)	1.30	0.19	0.18	0.22
Maximum carbody lateral acceleration (g)	0.75	0.16	0.18	0.19
Maximum carbody vertical acceleration (g)	0.90	0.12	0.12	0.13
Maximum vertical suspension deflection (%)	95	23.22	23.93	24.36

Table 58 shows a comparison of hunting simulation predictions for baseline and worn primary pad simulations. The simulation predictions do not meet the Standard S-2043 criterion for the maximum standard deviation of lateral carbody acceleration over 2,000 feet. The trends of lateral carbody acceleration standard deviation versus speed are shown in Figure 62, where, if the pads deteriorate in a significantly softer condition, then the stable vehicle speed is significantly reduced.

All other criteria, including peak-to-peak carbody lateral acceleration and maximum carbody lateral acceleration, were **met** for hunting with worn primary pads.

Table 58. Simulation Predictions of the Atlas Cask Car with Worn Primary Pads in Hunting

Criterion	Limiting Value	Baseline	Soft Primary Pad	Stiff Primary Pad
Maximum carbody roll angle (degree)	4.0	0.3	0.4	0.5
Maximum wheel L/V	0.80	0.28	0.35	0.43
Maximum truck side L/V	0.50	0.14	0.20	0.26
Minimum vertical wheel load (%)	25	71	62	55
Peak-to-peak carbody lateral acceleration (g)	1.30	0.59	0.74	0.73
Maximum carbody lateral acceleration (g)	0.75	0.31	0.40	0.40
Lateral carbody acceleration standard deviation (g)	0.13	0.14	0.19	0.20
Maximum carbody vertical acceleration (g)	0.90	0.32	0.18	0.23
Maximum vertical suspension deflection (%)	95	17	19	20

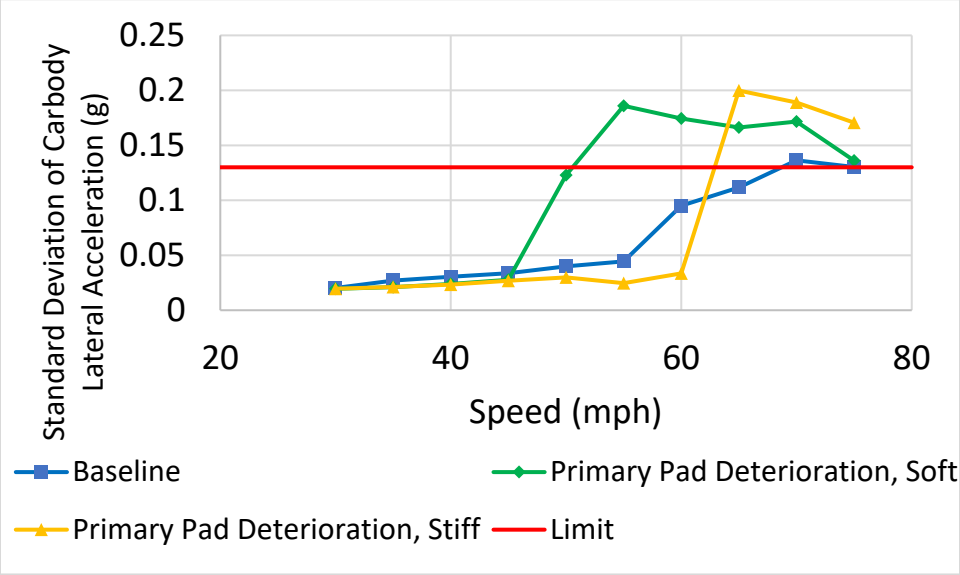


Figure 62. Hunting stability, considering primary pad deterioration

7.13.4 Friction Wedges

The wedge rise limit for the Swing Motion® trucks used in the cask car is 11/16 inch. The worn wedge simulations were performed with the wedges at this state of wear in all locations.

Table 59 shows a comparison of the dynamic curving simulation predictions for baseline and the worn friction wedge simulations. The simulation predictions for dynamic curving with worn wedges **met** Standard S-2043 criteria.

Table 59. Simulation Predictions of the Atlas Cask Car with Worn Friction Wedges in Dynamic Curving

Criterion	Limiting Value	Baseline	Friction Wedge Wear
Maximum carbody roll angle (degree)	4.0	1.0	1.0
Maximum wheel L/V	0.80	0.71	0.70
Maximum truck side L/V	0.50	0.35	0.35
Minimum vertical wheel load (%)	25	53	54
Peak-to-peak carbody lateral acceleration (g)	1.30	0.19	0.17
Maximum carbody lateral acceleration (g)	0.75	0.16	0.14
Maximum carbody vertical acceleration (g)	0.90	0.12	0.17
Maximum vertical suspension deflection (%)	95	23	24

Table 60 shows a comparison of the pitch-and-bounce simulation predictions for the baseline and worn friction wedge simulations. The pitch-and-bounce simulations were performed for the maximum test load condition. The simulation predictions for the **worn** friction wedges met Standard S-2043 pitch-and-bounce criteria.

Table 60. Simulation Predictions of the Atlas Cask Car with Worn Friction Wedges in Pitch and Bounce

Criterion	Limiting Value	Baseline	Friction Wedge Wear
Maximum carbody roll angle (degree)	4.0	0.3	0.3
Maximum wheel L/V	0.80	0.12	0.14
Maximum truck side L/V	0.50	0.09	0.09
Minimum vertical wheel load (%)	25	74	72
Peak-to-peak carbody lateral acceleration (g)	1.30	0.34	0.29
Maximum carbody lateral acceleration (g)	0.75	0.17	0.14
Maximum carbody vertical acceleration (g)	0.90	0.38	0.29
Maximum vertical suspension deflection (%)	95	56	56

Table 61 shows a comparison of the twist-and-roll simulation predictions for the baseline and worn friction wedges. The simulation predictions for the worn friction wedges **meet** Standard S-2043 twist-and-roll criteria.

Table 61. Simulation Predictions of the Atlas Cask Car with Worn Friction Wedges in Twist and Roll

Criterion	Limiting Value	Baseline	Worn Friction Wedges
Maximum carbody roll angle (degree)	4.0	1.9	1.8
Maximum wheel L/V	0.80	0.27	0.18
Maximum truck side L/V	0.50	0.17	0.12
Minimum vertical wheel load (%)	25	58	59
Peak-to-peak carbody lateral acceleration (g)	1.30	0.53	0.42
Maximum carbody lateral acceleration (g)	0.75	0.29	0.21
Maximum carbody vertical acceleration (g)	0.90	0.24	0.36
Maximum vertical suspension deflection (%)	95	21	22

7.13.5 Broken Spring

The cask car uses different springs in the end trucks than those used in the center trucks of a span bolster. Broken spring simulations were done with one 1-96 spring removed from the spring nest of the leading truck of the trailing span bolster to represent a broken or missing spring. This location was chosen because the modeling and testing of the Atlas railcar showed that this location is critical for the dynamic curving regime. The dynamic curving and twist-and-roll simulations were performed for the minimum test load condition, and pitch-and-bounce simulations were performed for the maximum test load condition.

Table 62 shows a comparison of the dynamic curving simulation predictions for the baseline and broken spring simulations. The simulation predictions **met** the Standard S-2043 criteria for dynamic curving with a broken spring.

Table 62. Simulation Predictions of the Atlas Cask Car with a Broken Spring in Dynamic Curving

Criterion	Limiting Value	Baseline	Broken spring
Maximum carbody roll angle (degree)	4.0	1.0	1.0
Maximum wheel L/V	0.80	0.71	0.71
Maximum truck side L/V	0.50	0.35	0.37
Minimum vertical wheel load (%)	25	53	53
Peak-to-peak carbody lateral acceleration (g)	1.30	0.19	0.17
Maximum carbody lateral acceleration (g)	0.75	0.16	0.14
Maximum carbody vertical acceleration (g)	0.90	0.12	0.12
Maximum vertical suspension deflection (%)	95	23	24

Table 63 shows a comparison of the pitch-and-bounce simulation predictions for the baseline and broken spring simulations. All simulation predictions for broken springs **meet** Standard S-2043 criteria in the pitch-and-bounce regime.

Table 63. Simulation Predictions of the Atlas Cask Car with a Broken Spring in Pitch and Bounce

Criterion	Limiting Value	Baseline	Missing Springs
Maximum carbody roll angle (degree)	4.0	0.3	0.3
Maximum wheel L/V	0.80	0.12	0.15
Maximum truck side L/V	0.50	0.09	0.09
Minimum vertical wheel load (%)	25	74	72
Peak-to-peak carbody lateral acceleration (g)	1.30	0.34	0.32
Maximum carbody lateral acceleration (g)	0.75	0.17	0.15
Maximum carbody vertical acceleration (g)	0.90	0.38	0.28
Maximum vertical suspension deflection (%)	95	56	57

Table 64 shows a comparison of the twist-and-roll simulation predictions for the baseline and broken spring simulations. The simulation predictions for the broken springs **meet** Standard S-2043 criteria for the twist-and-roll regime.

Table 64. Simulation Predictions of the Atlas Cask car with a Broken Spring in Twist and Roll

Criterion	Limiting Value	Baseline	Missing Springs
Maximum carbody roll angle (degree)	4.0	1.9	1.9
Maximum wheel L/V	0.80	0.27	0.28
Maximum truck side L/V	0.50	0.17	0.16
Minimum vertical wheel load (%)	25	58	59
Peak-to-peak carbody lateral acceleration (g)	1.30	0.53	0.44
Maximum carbody lateral acceleration (g)	0.75	0.29	0.21
Maximum carbody vertical acceleration (g)	0.90	0.24	0.26
Maximum vertical suspension deflection (%)	95	21	20

8.0 CONCLUSIONS

The FEA simulations and structural test strain measurements both showed that stresses were less than 75 percent of the allowable stress, thereby eliminating the requirement in Standard S-2043, Paragraph 8.1 for the FEA to be refined. When applying the maximum test load, the largest difference between measured and predicted stress was 8.0 ksi on SGBF15. The other measurement at a similar location, SGBF26, was within 4 percent of the predicted stress.

On behalf of the Department of Energy, TTCI is requesting exceptions from the AAR EEC because the post-test simulation predictions of the Atlas car with the production CSM 58 pads did not meet some of the criteria for hunting, curving with single rail perturbation, and curving with various lubrication conditions. The onset of instability in the hunting regime occurred at speeds above 65 mph—beyond the 50-mph limit recommended in AAR circular OT-55 for cars in HLRM service. Although the performance simulated for curving with a single rail perturbation did not meet Standard S-2043 criteria for the carbody roll angle, it did meet the criteria for all other metrics, including those for wheel/rail forces.

Constant curving test results using prototype CSM 70 pads did not meet S-2043 criteria for the maximum wheel L/V ratio or the 95-percent wheel L/V ratio. While constant curving simulation predictions with both the refined model using prototype CSM 70 pads and the production CSM 58 pads met S-2043 criteria, predictions using CSM 58 pads showed a 20 percent reduction in wheel L/V ratios compared to predictions done with CSM 70 pads.

Criteria for all other test regimes were met. Table 65 contains a summary of the simulation predictions for CSM 58 pads and test results.

Table 65. Summary of Dynamic Modeling and Test Results

Standard S-2043 Section	Met/Not Met		
	Preliminary Simulations	Revised Simulations CSM 58 pads	Test Result and Details if Not Met
5.2 Nonstructural Static Tests			
4.2.1/5.2.1 Truck Twist Equalization	Met	Not Simulated	Not Met with CSM 58 pads – **Minimum Test Load:** Wheel load at 50% during 2” drop condition. Wheel load at 24% during 3” drop condition. **Maximum Test Load:** Wheel load at 43% during 2” drop condition. Wheel load at 29% during 3” drop condition.
4.2.2/5.2.2 Carbody Twist Equalization	Met	Not Simulated	Met with CSM 58 pads
4.2.3/5.2.3 Static Curve Stability	Met	Not Simulated	Met with CSM 58 pads
4.2.4/5.2.4 Horizontal Curve Negotiation	Met	Not Simulated	Met with CSM 58 pads
5.4 Structural Tests			
5.4.2 Squeeze (Compressive End) Load	Met	Not Simulated	Met with CSM 58 pads
5.4.3 Coupler Vertical Loads	Met	Not Simulated	Met with CSM 58 pads
5.4.4 Jacking	Met	Not Simulated	Met with CSM 58 pads
5.4.5 Twist	Met	Not Simulated	Met with CSM 58 pads
5.4.6 Impact	Met	Not Simulated	Met with CSM 58 pads

Standard S-2043 Section	Met/Not Met		
	Preliminary Simulations	**Revised Simulations CSM 58 pads**	**Test Result and Details if Not Met**
5.5 Dynamic Tests			
4.3.11.3/5.5.7 Hunting	Met	Not Met At Minimum Test Load: Car unstable at speeds greater than 65 mph with KR wheel profiles Meets with Maximum Test Load	Not Met with CSM 58 pads At Minimum Test Load: Car unstable at speeds greater than 65 mph with KR wheel profiles Meets with Maximum Test Load
4.3.9.6/5.5.8 Twist and Roll	Met	Met	Not tested with CSM 58 pads – Met with CSM 70 pads
5.5.9 Yaw and Sway	Met	Met	Not tested with CSM 58 pads – Met with CSM 70 pads
5.5.10 Dynamic Curving	Not Met Max Test Load Wheel L/V 0.88, Limit=0.8, A-end and B-end lead,	Met	Met with CSM 58 pads – Not met with CSM 70 pads (0.81 Wheel L/V)
4.3.9.7/5.5.11 Pitch and Bounce (Chapter 11)	Met	Met	Not tested with CSM 58 pads – Met with CSM 70 pads
4.3.9.7/5.5.12 Pitch and Bounce (Special)	Met	Not Simulated	Not tested
4.3.10.1/5.5.13 Single Bump Test	Met	Met	Not tested with CSM 58 pads – Met with CSM 70 pads
4.3.11.6/5.5.14 Curve Entry/Exit	Met	Met	Not tested with CSM 58 pads – Met with CSM 70 pads
4.3.10.25.5.15 Curving with Single Rail Perturbation	Not met **Empty with Ballast Load:** Wheel L/V 0.96, Limit=0.8 Truck Side L/V 0.52, Limit=0.5 **Loaded** 5.0-degree roll angle, Limit=4.0	Not met **Minimum Test Load** Carbody roll angle =4.2, limit=4.0 **Maximum Test Load** Carbody roll angle =4.7, limit=4.0	**Minimum Test Load:** Not met with CSM 70 pads (Wheel L/V = 0.88, Truck L/V = 0.50), not tested with CSM 58 pads

Standard S-2043 Section	Met/Not Met		
	Preliminary Simulations	**Revised Simulations CSM 58 pads**	**Test Result and Details if Not Met**
4.3.11.4/5.5.16 Standard Chapter 11 Constant Curving	Met	Met	Not tested with CSM 58 pads – Not Met with CSM 70 pads: **Minimum Test Load:** Wheel L/V ratio = 0.86 95% Wheel L/V ratio = 0.66 **Maximum Test Load:** 95% Wheel L/V ratio = 0.63
4.3.11.7/5.5.17 Special Trackwork, No 7 Crossovers	Not Met **Loaded:** Truck side L/V Ratio=0.52, Limit=0.5	Met	Not tested with CSM 58 pads – Met with CSM 70 pads on a No 10 crossover
4.3.11.5 Curving with Various Lubrication Conditions	Not Met **Min Test Load with new profiles:** 95% Wheel L/V = 0.62 (Case 2), Limit=0.6 95% Wheel L/V = 0.66 (Case 4), Limit=0.6 **Min Test Load with worn profiles:** Truck Side L/V = 0.56 (Case 1), 0.62 (Case 2), 0.61 (Case 4), Limit=0.5 95% Wheel L/V = 0.68 (Case 2), 0.61 (Case 4), Limit=0.6 **Max Test Load with worn profiles:** Truck Side L/V = 0.56 (Case 1), 0.62 (Case 2), 0.61 (Case 4), Limit=0.5 95% Wheel L/V = 0.68 (Case 2), 0.61 (Case 4), Limit=0.6	Not Met in following cases **Min Test Load with new profiles:** 95% Wheel L/V = 0.62 (Case 4), Limit=0.6 **Min Test Load with worn profiles:** Truck Side L/V = 0.53 (Case 1), 0.61 (Case 2), 0.58 (Case 4), Limit=0.5 95% Wheel L/V = 0.64 (Case 2), Limit=0.6 **Max Test Load with worn profiles:** Truck Side L/V = 0.52 (Case 1), 0.60 (Case 2), 0.58 (Case 4), Limit=0.5 95% Wheel L/V = 0.66 (Case 2), 0.61 (Case 4), Limit=0.6	Not required
4.3.12 Ride Quality	Met	Not Simulated	Not required
4.3.13 Buff and Draft Curving	Not Met Like car buff load Truck side L/V Ratio=0.51, Limit=0.50,	Met	Not required

Standard S-2043 Section	Met/Not Met		
	Preliminary Simulations	Revised Simulations CSM 58 pads	Test Result and Details if Not Met
4.3.14 Braking Effects on Steering	Met	Not Simulated	Not required
4.3.15 Worn Component Simulations	Not Met Numerous criteria not met in dynamic curving and hunting regimes with several worn components. See reference 2 for details	Not Met in following cases **Hunting stability, maximum lateral acceleration standard deviation:** Worn CCSB low preload: 0.17 Worn primary pads, soft: 0.19 Worn primary pads, stiff: 0.20	Not required

References

1. AAR *Manual of Standards and Recommended Practices*, Car Construction Fundamentals and Details, Performance Specification for Trains Used to Carry High-Level Radioactive Material, Standard S-2043, Effective: 2003; Last Revised: 2017, Association of American Railroads, Washington, D.C.

2. Walker, R., MC Jones, JC Valades-Salazar, R. Joy, M. Miller, and B. Whitsitt, "S-2043 Certification Tests of United States Department of Energy Atlas Railcar Design Project 12-Axle Cask Car." Report No. P-21-037, Transportation Technology Center, Inc., Pueblo, CO, In press.

3. Walker, R. and S. Trevithick, "S-2043 Certification: Preliminary Simulations of Kasgro-Atlas 12-Axle Cask Car." Report No. P-17-021, Transportation Technology Center, Inc., Pueblo, CO, December 2017.

4. Orano Federal Services, September 2019, "DW-20-001 HLRM Atlas Railcar Test Loads Final Document Package", provided to DOE by Transportation Technology Center, Inc., Pueblo, CO.

5. Orano Federal Services, September 2019, "DW-19-013rev1 "HLRM Railcar TTCI Task Order #1; Transmittal of EIR-3022576-001, Revised Assembly Instructions for the DOE Atlas Railcar Test Loads."

6. Koffman, J. L., "Spring Stresses and Deflections". *The Railway Gazette*, January 30, 1959.

TRANSPORTATION TECHNOLOGY CENTER, INC.
A wholly owned subsidiary of the Association of American Railroads

55500 DOT Road • Pueblo, CO 81001
www.aar.com

APPENDIX F
P-20-032 AAR STANDARD S-2043 SINGLE-CAR CERTIFICATION TESTS OF U.S. DEPARTMENT OF ENERGY BUFFER RAILCAR

AAR STANDARD S-2043 SINGLE-CAR CERTIFICATION TESTS OF U.S. DEPARTMENT OF ENERGY ATLAS RAILCAR DESIGN PROJECT BUFFER RAILCAR

Certification Report P-20-032

Prepared for U.S. Department of Energy
by Russell Walker, Juan Carlos Valdes-Salazar, MaryClara Jones,
Brent Whitsitt, and Richard Joy
Transportation Technology Center, Inc

October 26, 2022
Revised December 6, 2022

TRANSPORTATION TECHNOLOGY CENTER, INC.

P.O. Box 11130 | Pueblo, CO 81001
www.ttci.tech

TTCI is a wholly owned subsidiary of the Association of American Railroads.

ERRATA STATEMENT

Report: P-20-032

Errata refer to the correction of errors introduced to the article by the publisher. The following errors have been found and corrected since this report was originally submitted.

In MxV Rail report, P-20-032, "AAR Standard S-2043 Single-Car Certification Tests of U.S. Department of Energy Atlas Railcar Design Project Buffer Railcar," one inadvertent typographical error was present. The corrected text is as follows.

- Section 5.1.4 - The coefficient of friction in the centerplate was estimated using the following equation:

$$\mu = \frac{3\,(Torque - 2SBld \times SBdst \times \mu_{sb})(\mathrm{CPrad}^2 - \mathrm{Hrad}^2)}{2\,(\mathrm{Tld} - 2 \times \mathrm{SBld})(\mathrm{Cprad}^3 - \mathrm{Hrad}^3)}$$

For questions or comments on this document, contact **Russell_Walker@aar.com.**

Disclaimer: This report was prepared by Transportation Technology Center, Inc. (TTCI) of Pueblo, Colorado, a subsidiary of the Association of American Railroads (AAR). Investigations and/or tests reported herein were authorized by the AAR and conducted in accordance with the appropriate AAR standard(s). This report is provided for consideration by the appropriate AAR technical committee and does not constitute in any way approval or disapproval of the product(s) tested. The contents of this report imply no endorsements whatsoever by TTCI or AAR of products, services, or procedures, nor are they intended to suggest the applicability of the test results under circumstances other than those described in this report. TTCI is not a source of information with respect to these tests, nor is it a source of copies of this report. TTCI MAKES NO REPRESENTATION OR WARRANTIES, EITHER EXPRESSED OR IMPLIED, WITH RESPECT TO THIS REPORT OR ITS CONTENTS. TTCI ASSUMES NO LIABILITY FOR SPECIAL, COLLATERAL, EXEMPLARY, INDIRECT, INCIDENTAL, CONSEQUENTIAL, OR ANY OTHER KIND OF DAMAGES RESULTING FROM THE USE OR APPLICATION OF THIS REPORT OR ITS CONTENTS.

EXECUTIVE SUMMARY

Transportation Technology Center, Inc., a subsidiary of the Association of American Railroads (AAR) performed certification testing on the United States Department of Energy's (DOE) buffer railcar. The buffer railcar has been developed as part of DOE's Atlas Railcar Design Project, which is intended to meet the need for future large-scale transport of spent nuclear fuel and high-level radioactive waste. Tests were performed according to AAR *Manual of Standards and Recommended Practices*, Standard S-2043, "Performance Specification for Trains Used to Carry High-Level Radioactive Material," revised 2017.[1] The table below shows the tests performed and the results of the tests. Vehicle characterization tests are not listed because there are no criteria.

S-2043 Section	Critical Data (Criteria) for Conditions Not Met	Met/Not Met
5.2 Nonstructural Static Tests		
5.2.1 Truck Twist Equalization	Not Applicable	Met
5.2.2 Carbody Twist Equalization	Not Applicable	Met
5.2.3 Static Curve Stability	Not Applicable	Met
5.2.4 Horizontal Curve Negotiation	Not Applicable	Met
5.4 Structural Tests		
5.4.2 Squeeze (Compressive End) Load	Not Applicable	Met
5.4.3 Coupler Vertical Loads	Not Applicable	Met
5.4.4 Jacking	Not Applicable	Met
5.4.5 Twist	Not Applicable	Met
5.4.6 Impact	Not Applicable	Met
5.5 Dynamic Tests		
5.5.7 Hunting	Not Applicable	Met
5.5.8 Twist and Roll	Not Applicable	Met
5.5.9 Yaw and Sway	Not Applicable	Met
5.5.10 Dynamic Curving	Not Applicable	Met
5.5.11 Pitch and Bounce (Chapter 11)	Not Applicable	Met
5.5.12 Pitch and Bounce (Special)	Not Applicable	Met
5.5.13 Single Bump Test	Not Applicable	Met
5.5.14 Curve Entry/Exit	Not Applicable	Met
5.5.15 Curving with Single Rail Perturbation	Not Applicable	Met
5.5.16 Standard Chapter 11 Constant Curving	Not Applicable	Met
5.5.17 Special Trackwork	Not Applicable	Met

TABLE OF CONTENTS

1.0 Introduction 1
2.0 Buffer Railcar Description 1
3.0 Test OvervieW 3
4.0 Objective 4
5.0 Results 4
5.1 Vehicle Characterization 4
5.1.1 Component Characterization Tests 4
5.1.2 Vertical Suspension Stiffness and Damping 10
5.1.3 Lateral Suspension Stiffness and Damping 16
5.1.4 Truck Rotation Stiffness and Breakaway Moment 21
5.1.5 Interaxle Longitudinal Stiffness 23
5.1.6 Modal Characterization 25
5.2 Nonstructural Static Tests 28
5.2.1 Truck Twist Equalization 28
5.2.2 Carbody Twist Equalization 29
5.2.3 Static Curve Stability 31
5.2.4 Horizontal Curve Negotiation 31
5.3 Static Brake Tests 32
5.4 Structural Tests 32
5.4.1 Preliminary and Post Test Inspection 35
5.4.2 Squeeze (Compressive End) Load 35
5.4.3 Coupler Vertical Loads 36
5.4.4 Jacking 37
5.4.5 Twist 38
5.4.6 Impact 41
5.4.7 Securement System 41
5.5 Dynamic Tests 42
5.5.1 Hunting 44
5.5.2 Twist and Roll 46
5.5.3 Yaw and Sway 46
5.5.4 Dynamic Curving 47
5.5.5 Pitch and Bounce (Chapter 11) 48
5.5.6 Special Pitch and Bounce 49
5.5.7 Single Bump Test 50
5.5.8 Limiting Spiral Negotiation 51
5.5.9 Normal Spiral Negotiation 52
5.5.10 Curving with Single Rail Perturbation 54
5.5.11 Standard Chapter 11 Constant Curving 56
5.5.12 Special Trackwork 57
5.6 Ride Quality 61
6.0 Additional Tests 61
7.0 Conclusions 62
Appendix A: Test Plan A-1

Appendix B: Static Brake Force Test Documentation B-1
Appendix C: Buffer Car Gage Drawing C-1
Appendix D: Kasgro Buckling Analysis D-1
Appendix E: Compressive End Load Test E-1
Appendix F: Coupler Vertical Loads F-1
Appendix G: Jacking Test Results G-1
Appendix H: Carbody Twist Results H-1
Appendix I: Impact Tests I-1
Appendix J: Kasgro Securement Analysis J-1

LIST OF FIGURES

Figure 1. Buffer Railcar during Static Testing 1
Figure 2. Buffer Railcar Arrangement Drawing 2
Figure 3. Bearing Adapter Pad 3
Figure 4. Buffer Railcar Spring Group 5
Figure 5. Miner TCC-III 60LT CCSB 7
Figure 6. A-truck Left Side CCSB Measured Force-Displacement Data 7
Figure 7. A-truck Right Side CCSB Measured Force-Displacement Data 8
Figure 8. Koni Vertical Damper Mounted in MTS Load Frame (left) and on Buffer Railcar Truck (right) 8
Figure 9. Damper Characterization Data 9
Figure 10. Damper Bushing Characterization Data 10
Figure 11. Brackets for Vertical and Lateral Actuators 10
Figure 12. The Buffer Car Installed in the MSU while Configured for Vertical Suspension Testing 11
Figure 13. String Potentiometer for Measuring Spring Vertical Displacement (Damper Installed) . 12
Figure 14. String Potentiometer with Damper Removed 12
Figure 15. LVDTs for Measuring Pad Vertical Displacements 13
Figure 16. Truck Vertical Wheel Load Plotted against Average Secondary Suspension Displacement, Dampers Removed, 0.5hz 14
Figure 17. Truck Vertical Wheel Load Plotted against Average Primary Suspension Displacement, Dampers Removed, 0.1hz 15
Figure 18. Truck Vertical Wheel Load versus Average Suspension Displacement at 0.1 Hz Input with Wedges and Dampers Installed 15
Figure 19. Buffer Railcar Ready for Lateral Force Test 16
Figure 20. Load Cell for Lateral Force Measurements 17
Figure 21. LVDTs used to Record Pad Lateral Movements 18
Figure 22. Truck Lateral Load Plotted against Lateral Secondary Suspension Displacement, Dampers Removed, 0.1 Hz 19
Figure 23. Truck Lateral Load Plotted against Lateral Primary Suspension Displacement, Dampers Removed, 0.1 Hz. 20
Figure 24. Secondary Suspension with Wedges and Dampers Removed and with the Transom Restrained Showing Displacement to the Lateral Stops 20
Figure 25. Buffer Railcar Positioned on Air Bearing Table 21
Figure 26. Truck Rotation Data for Buffer Railcar A-truck 22
Figure 27. Buffer Railcar Interaxle Test Actuator and Load Cell 23
Figure 28. Example Data for Longitudinal Axle Stiffness Tests 24
Figure 29. Actuators Attached to Buffer Railcar during Modal Testing with Vertical Input 25
Figure 30. Distribution of Accelerometers during the Buffer Railcar Modal Test 26
Figure 31. Time History Plot for Bounce Mode 27

Figure 32. Frequency Analysis for the Bounce Mode 27
Figure 33. L1 Truck Twist Result for All Increments 29
Figure 34. Carbody Twist for L3 and L4 Results for All Wheels 30
Figure 35. Buffer Railcar during the Static Curve Stability Test 31
Figure 36. Checking Clearance during the Static Curve Stability Test 31
Figure 37. Clearance between Brake Cylinder and Center Sill with Buffer Railcar in 150-foot Radius Curve 32
Figure 38. Location of Strain Measurements Monitored during Structural Testing 34
Figure 39. Results of Level Loop around the Buffer Railcar Deck, Zero Inches Longitudinal at A-End of Car 35
Figure 40. Coupler Carrier Plate after the Coupler Vertical Load Test 37
Figure 41. Maximum Stressed Locations SGBF40 and SGBF42 38
Figure 42. The End of the Railcar Supported by Four Pneumatic Jacks during the Twist Test 39
Figure 43. SGBF11 and SGBF40 Locations 40
Figure 44. Location of IWS during Dynamic Tests 44
Figure 45. 2,000-foot Standard Deviation of Lateral Acceleration versus Speed 45
Figure 46. Buffer Railcar Twist and Roll Test, Maximum Carbody Roll versus Speed 46
Figure 47. Buffer Railcar Yaw and Sway Test, Maximum Peak-to-peak Lateral Acceleration versus Speed 47
Figure 48. Buffer Railcar Dynamic Curve Wheel L/V Results versus Speed 48
Figure 49. Maximum Vertical Acceleration versus Speed for Pitch and Bounce 49
Figure 50. Maximum Vertical Acceleration versus Speed for Special Pitch and Bounce 50
Figure 51. Maximum Vertical Acceleration versus Speed for Buffer Railcar Single Bump Test 51
Figure 52. Buffer Railcar Limiting Spiral Wheel L/V Results versus Speed 52
Figure 53. Buffer Railcar Normal Spiral Wheel L/V Results versus Speed for the South Spiral of the 12-Degree Curve 53
Figure 54. Curving with Single Rail Bump Perturbation Single Wheel L/V Ratio versus Speed (September 2020) 55
Figure 55. Curving with Single Rail Dip Perturbation Single Wheel L/V Ratio versus Speed (September 2020) 56
Figure 56. Distance Plot of the Highest Measured Single Wheel L/V ratio during the Curving with Single Dip Perturbation Test (Jan/Feb 2020). Not Applicable to S-2043 qualification.. 56
Figure 57. Buffer Railcar Constant Curving 95th Percentile Wheel L/V Ratio versus Speed in 12-degree Curve 57
Figure 58. Maximum 50-millisecond Wheel L/V Ratio versus Speed for the Turnout Test 58
Figure 59. Maximum 50-millisecond Wheel L/V ratio versus Speed for the Crossover Test 59
Figure 60. Pre-test Survey Alignment Measurements for Turnout Test Zone 60
Figure 61. Pre-test Survey Alignment Measurements for Crossover Test Zone 60

LIST OF TABLES

Table 1. Buffer Railcar Dimensions 2
Table 2. Buffer Railcar Truck Configuration 3
Table 3. Spring Characteristics from the Manufacturer 6
Table 4. Spring Characteristics from Testing* 6
Table 5. Comparison of the Spring Characteristics from Testing to the Manufacturer's Specification 6
Table 6. Vertical Suspension Test (Wedges and Dampers Installed) 13
Table 7. Vertical Suspension Test (Wedges Installed, Dampers Removed) 14
Table 8. Vertical Suspension Test (Wedges and Dampers Removed) 14
Table 9. Lateral Suspension Test (Wedges and Dampers Installed) 18
Table 10. Lateral Suspension Test (Wedges Installed, Dampers Removed) 18

Table 11. Lateral Suspension Test (Wedges Removed) 18
Table 12. Lateral Suspension Test (Dampers and Wedges Removed) 19
Table 13. Truck Rotation Moment and Estimate of the Associated Friction Coefficient 22
Table 14. Side frame to Axle Properties Stiffness Data per Pad 24
Table 15. Modal Characterization Results 26
Table 16. Truck Twist Equalization Results 28
Table 17. Carbody Twist Equalization Results 30
Table 18. Survey Measurements 35
Table 19. Highest Stress Locations from Compressive End Load Test 36
Table 20. Buffer Railcar Vertical Coupler Force Test Results Summary 37
Table 21. Buffer Railcar Jacking Test Results Summary 38
Table 22. Summary of Buffer Railcar Twist Test Part 1 Results 39
Table 23. Height of the Four Corners of the Loaded Carbody 40
Table 24. Summary of Buffer Railcar Twist Part 2 Test Results 40
Table 25. Maximum Stresses Measured during Impact Tests 41
Table 26. AAR Standard S-2043 Dynamic Testing Performance Criteria 43
Table 27. Buffer Railcar Hunting Test Dates and Rail Friction Data 44
Table 28. Buffer Railcar Hunting Test Results 45
Table 29. Buffer Railcar Twist and Roll Test Results 46
Table 30. Yaw and Sway Test Results to 75 mph 47
Table 31. Buffer Railcar Dynamic Curving Test Dates and Rail Friction Data 47
Table 32. Buffer Railcar Dynamic Curving Test Results 48
Table 33. Summary of Pitch and Bounce Results 49
Table 34. Summary of Special Pitch and Bounce Test Results 50
Table 35. Summary of Test Results for the Buffer Railcar Single Bump Test 51
Table 36. Buffer Railcar Dynamic Curving Test Dates and Rail Friction Data 51
Table 37. Buffer Railcar Limiting Spiral Summary of Test Results 52
Table 38. Buffer Railcar Constant Curving/Normal Spiral Negotiation Test Dates and Rail Friction Data 53
Table 39. Buffer Railcar Normal Spiral Summary of Test Results 53
Table 40. Friction Coefficient measured during Curving with Single Rail Perturbation Tests 54
Table 41. Summary of Curving with Single Rail Perturbation Test Results 55
Table 42. Summary of Buffer Railcar Constant Curving Test Results 57
Table 43. Top of Rail Friction Measurements for Special Trackwork Tests 57
Table 44. Summary of Turnout Test Results 58
Table 45. Summary of Crossover Test Results 59
Table 46. Special Track Work Components 61
Table 47. Summary of Test Results 62

1.0 INTRODUCTION

The United States Department of Energy (DOE) contracted with Transportation Technology Center, Inc. (TTCI) to perform certification testing on its buffer railcar developed as part of DOE's Atlas Railcar Design Project. The DOE project is intended to meet the needs for future large-scale transport of high-level radioactive material (HLRM) as defined in AAR Standard S-2043, which includes spent nuclear fuel and high-level waste.

All tests were performed according to Association of American Railroads' (AAR) *Manual of Standards and Recommended Practices* (MSRP), Standard S-2043, "Performance Specification for Trains used to carry High-level Radioactive Material," Section 5.0 – Single Car Tests.[2] Single car testing of the buffer railcar was conducted primarily at the U.S. Department of Transportation's Transportation Technology Center (TTC) near Pueblo, Colorado between April 2019 and February 2020. Static brake testing was conducted at the manufacturer's facility prior to delivery. The curving with single rail perturbation test was repeated on September 11, 2020 (see Paragraph 5.5.10).

2.0 BUFFER RAILCAR DESCRIPTION

The buffer railcar is a four-axle flatcar with a permanently attached ballast load (Figure 1). Kasgro Rail Corporation (Kasgro) manufactured two prototype buffer railcars in 2018. Figure 2 shows the general arrangement drawing of the buffer railcar. Table 1 shows the buffer railcar dimensions. The two prototype buffer railcars delivered to TTC were: IDOX 020001 and IDOX 020002. The tests described in this report were conducted on IDOX 020001.



Figure 1. Buffer Railcar during Static Testing

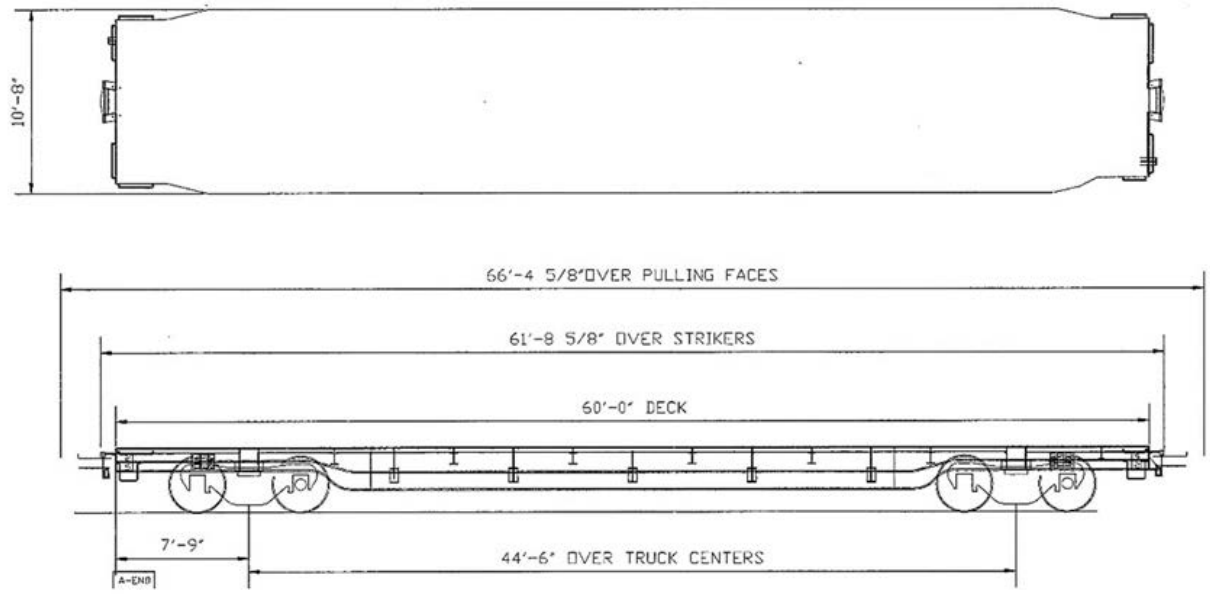


Figure 2. Buffer Railcar Arrangement Drawing

Table 1. Buffer Railcar Dimensions

Dimension	Value
Length over pulling faces	66 feet 4 5/8 inches
Length over strikers	61 feet 8 5/8 inches
Truck center spacing	44 feet 6 inches
Axle spacing on trucks	72 inches

Computer simulations required for AAR Standard S-2043 showed that an empty buffer railcar would not meet S-2043 requirements in the buff and draft curving regime (AAR Standard S-2043 Paragraph 4.3.13). To alleviate this, a ballast weight of 196,000 pounds was added in the model. The added weight was included in the model as permanently installed steel plates. Results of the revised model met buff and draft curving requirements at the resulting gross rail load of 263,000 pounds.[3]

The steel plates were permanently attached to the buffer railcar by welding during the manufacturing process, resulting in a railcar with a permanent gross rail load of 263,000 pounds. Because the railcar is not rated to carry any additional load, this is the only load condition that was tested.

The railcar uses two Swing Motion® trucks. Each truck uses two wheelsets having AAR Class K axles and AAR-1B narrow flange wheels. Narrow flange wheels are specified for this railcar, because the increased gauge clearance allows more lateral movement for better performance. The trucks are specially designed to use a polymer element between the bearing adapter and sideframe. This gives the truck a passive steering capability. Figure 3 shows a bearing adapter pad. Table 2 shows the truck configuration used for testing.



Figure 3. Bearing Adapter Pad

Table 2. Buffer Railcar Truck Configuration

Part	Description	
Secondary suspension (each nest, two per truck)	Five D7 outer coils, five D6 inner coils, five D6A inner inner coils, two 49427-1, two 49427-2 per nest	
Primary suspension (four per truck)	Adapter Plus pads, ASF-Keystone part number 10522A	
Side bearings (two per truck)	Miner TCC-III 60LT	
Friction wedge, composition-faced (four per truck)	ASF-Keystone part number 1-9249	
Bearings and adapters (four per truck)	AAR Class K 6 1/2 x 9 bearings with 6 1/2 x 9 special adapter ASF-Keystone Part number 10523A	
Center bowl plate (one per truck)	Metal horizontal and vertical liners	
Vertical hydraulic dampers (two per truck)	Koni damper 04A 2032	
Side frames (two per truck)	F9N-10FH-UB	
Bolsters (one per truck)	B9N-714N-FS	
	A-end Truck Average	**B-end Truck Average**
Spring nest height	7.75 inches	7.78 inches
Scale weight	131,200 pounds	131,975 pounds

3.0 TEST OVERVIEW

AAR Standard S-2043 requires testing to be conducted in two phases. Each railcar type that will eventually be included in an AAR Standard S-2043 compliant train must first undergo a series of single car tests as described in AAR Standard S-2043 paragraph 5.0. These tests are broken down into several groups: Vehicle Characterization, Nonstructural Static Tests, Static Brake Tests, Structural Tests, and Dynamic Tests. The Static Brake Tests were conducted by Kasgro before the railcars left its facility.

The single car tests are followed by a series of multiple car tests as described in AAR Standard S-2043 Paragraph 6.0. Multiple-car tests are designed to verify that the individual railcars do not adversely affect the performance of adjacent railcars. The multiple-car test train consist must match the anticipated HLRM train as closely as possible, with a minimum of one of each type of railcar to be used.

This report only provides single car test results for the buffer railcar. Single car test results for the other railcar types will be reported separately.

4.0 OBJECTIVE

The objective of the testing reported here was to determine if the DOE's buffer railcar meets the single car test requirements of AAR Standard S-2043, in preparation for inclusion in an AAR Standard S-2043 compliant train. If the AAR Equipment Engineering Committee (EEC) provides conditional approval based on this report (and test reports for additional railcars being prepared in parallel), DOE plans to move forward with multiple car tests. The train consist for multiple car testing is expected to include an Atlas cask car, buffer railcars, and a rail escort vehicle.

5.0 RESULTS

This section provides descriptions and results of each of the tests conducted at TTC under AAR Standard S-2043 as well as the static brake tests conducted at the Kasgro facility. Any variances from the specification will be noted. Each section contains a brief description of the test conducted. The test plan, presented in Appendix A, contains additional details describing the tests.

5.1 Vehicle Characterization

Characterization tests were conducted to verify that the buffer railcar and its components were constructed as designed. The vehicle characterization tests include the following:

- Component characterization
- Vertical suspension stiffness and damping
- Lateral suspension stiffness and damping
- Truck rotation stiffness and breakaway moment
- Interaxle longitudinal stiffness
- Modal characterization

AAR Standard S-2043 requires that measured suspension values be compared to the values used in the original model required by S-4043, Paragraph 4.3, and that the model be adjusted if values are measurably different than those used in the original model. Detailed comparisons of characterization results to model inputs will be provided in the "Post-Test Analysis Report" described in AAR Standard S-2043, Paragraph 8.5. Where possible, preliminary comparisons are provided in the test descriptions below.

Characterization test results are provided in Sections 5.1.1 to 5.1.6.

5.1.1 Component Characterization Tests

TTCI tested the secondary springs, constant contact side bearings (CCSB), and hydraulic vertical dampers to comply with component characterization requirements. Component characterization tests were carried out on a 50,000-pound MTS load frame. TTCI performed component characterization tests in April and May 2019 before any track testing began. Adam Klopp, TTCI

Principal Investigator I, witnessed the component characterization tests as the AAR Observer per S-2043 requirements.

Primary pads were not tested as a separate component because it was determined that a component test could not adequately capture the performance. Instead, the properties of the primary pads were measured during system characterization tests. As described in Sections 5.1.2, 5.1.3, and 5.1.5, the motions between the left and right side frame and the Axle 2 bearing adapters were measured using six Linear Variable Differential Transformers (LVDTs) on each side. The LVDTs were positioned to allow calculation of the relative motion between the side frame and bearing adapter in the longitudinal, lateral, vertical, roll, pitch, and yaw directions. For longitudinal and vertical directions, the individual force on the pad can be determined using the actuator forces and load bar forces, respectively. For the lateral direction the two pads on the same axle act in parallel so the combined or average stiffness may be calculated.

Figure 4 shows the spring configuration for the buffer railcar. Two samples of each spring type were selected from the railcar and characterized in the load frame. The following measurements were recorded:

- Free height
- Stiffness
- Solid height
- Wire diameter

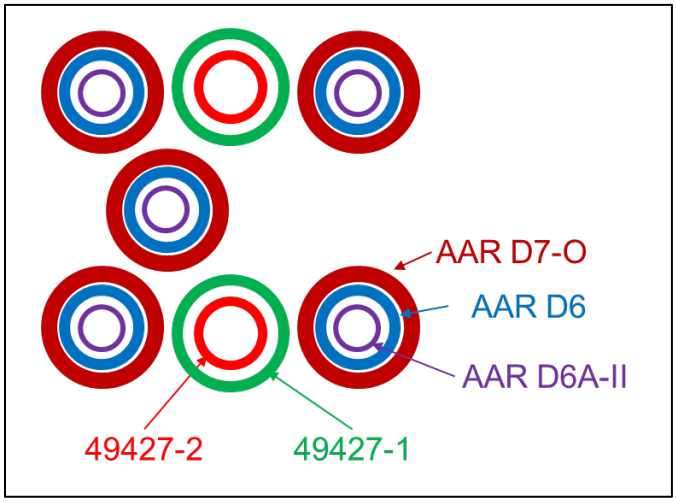


Figure 4. Buffer Railcar Spring Group

Table 3 shows the spring characteristics from either manufacturer or AAR specifications. Table 4 shows the test results of each spring type, and Table 5 shows a comparison of the manufacturer or AAR spring characteristics with the measured characteristics. The springs were within 7 percent or less of the AAR or manufacturer rated stiffness.

Table 3. Spring Characteristics from the Manufacturer

Type	Description	Quantity per Truck	Bar Diameter (in.)	Free HT (in.)	Solid HT (in.)	Spring Rate (lb./in.)
49427-1*	Control coil outer	2	13/16	11 5/16	6 9/16	1,359
49427-2*	Control coil inner	2	9/16	10 13/16	6 9/16	805
D7-O**	Main coil outer	5	15/16	10 13/16	6 9/16	2,033
D6***	Main coil inner	5	21/32	9 15/16	6 9/16	1,395
D6A-II****	Main coil inner inner	5	3/8	9	5 11/16	464

* Manufacturer provided

** Association of American Railroads. Last Revised: 1977. *Manual of Standards and Recommended Practices*. Section D, Trucks and Truck Details. Standard S-338 "Spring-D7, 4 ¼-IN TRAVEL" Washington, DC.

*** Association of American Railroads. Last Revised: 1976. *Manual of Standards and Recommended Practices*. Section D, Trucks and Truck Details. Standard S-336 "Spring-D6, 3 3/8-IN TRAVEL" Washington, DC.

**** Association of American Railroads. Last Revised: 2010. *Manual of Standards and Recommended Practices*. Section D, Trucks and Truck Details. Standard S-337 "Spring-D6A, 3 5/16-IN TRAVEL" Washington, DC.

Table 4. Spring Characteristics from Testing*

Spring Type	Description	Bar Diameter (in.)	Free HT (in.)	Solid HT (in.)	Spring Rate (lb./in.)
49427-1	Control coil outer (R3)	0.813	11.63	6.93	1,367
49427-1	Control coil outer (L4)	0.809	11.25	6.62	1,395
49427-2	Control coil inner (R3)	0.566	10.69	6.32	750
49427-2	Control coil inner (L4)	0.561	10.63	6.26	754
D6	Main coil inner (R3)	0.650	10.19	6.42	1,325
D6	Main coil inner (L4)	0.647	10.19	6.54	1,346
D7-O	Main coil outer (R3)	0.938	11.06	6.79	2,068
D7-O	Main coil outer (L4)	0.937	11.06	6.62	2,078
D6A-II	Main coil inner inner (R3)	0.377	9.13	5.77	449
D6A-II	Main coil inner inner (L4)	0.375	9.13	5.66	449

* Data includes two springs of each type, 10 of the 76 springs in the railcar.

Table 5. Comparison of the Spring Characteristics from Testing to the Manufacturer's Specification

		Percent Differences (%)			
Spring Type	Description	Bar Diameter (in.)	Free HT (in.)	Solid HT (in.)	Spring Rate (lb./in.)
49427-1	Control coil outer (R3)	0.1%	2.8%	5.6%	0.6%
49427-1	Control coil outer (L4)	-0.4%	-0.6%	0.8%	2.6%
49427-2	Control coil inner (R3)	0.6%	-1.2%	-3.6%	-6.8%
49427-2	Control coil inner (L4)	-0.3%	-1.7%	-4.6%	-6.3%
D6	Main coil inner (R3)	-1.0%	2.5%	-2.2%	-5.0%
D6	Main coil inner (L4)	-1.4%	2.5%	-0.4%	-3.5%
D7-O	Main coil outer (R3)	0.1%	2.3%	3.5%	1.7%
D7-O	Main coil outer (L4)	-0.1%	2.3%	0.9%	2.2%
D6A-II	Main coil inner inner (R3)	0.5%	1.4%	1.5%	-3.2%
D6A-II	Main coil inner inner (L4)	0.0%	1.4%	-0.4%	-3.2%

Although the test plan for this work showed the side bearings would be Miner TCC-III 80LT CCSB, the buffer railcar arrived with Miner TCC-III 60LT CCSB. Figure 5 shows the side bearings. The setup height of each CCSB is 5 1/16 inches. Two samples were installed in the load frame to measure the force and displacement characteristics. The side bearings were tested as complete components including the steel cages. The loads were applied using constant velocity inputs at a rate of about 0.37 inches per second. Figure 6 shows the test result from the A-truck left side bearing, and Figure 7 shows the test result from the A-truck right side bearing. The manufacturer's data for this model side bearing shows the force at setup height on the loading side of the curve is 5.8 kips. The measured forces at the corresponding point agree closely at 5.7 kips.



Figure 5. Miner TCC-III 60LT CCSB

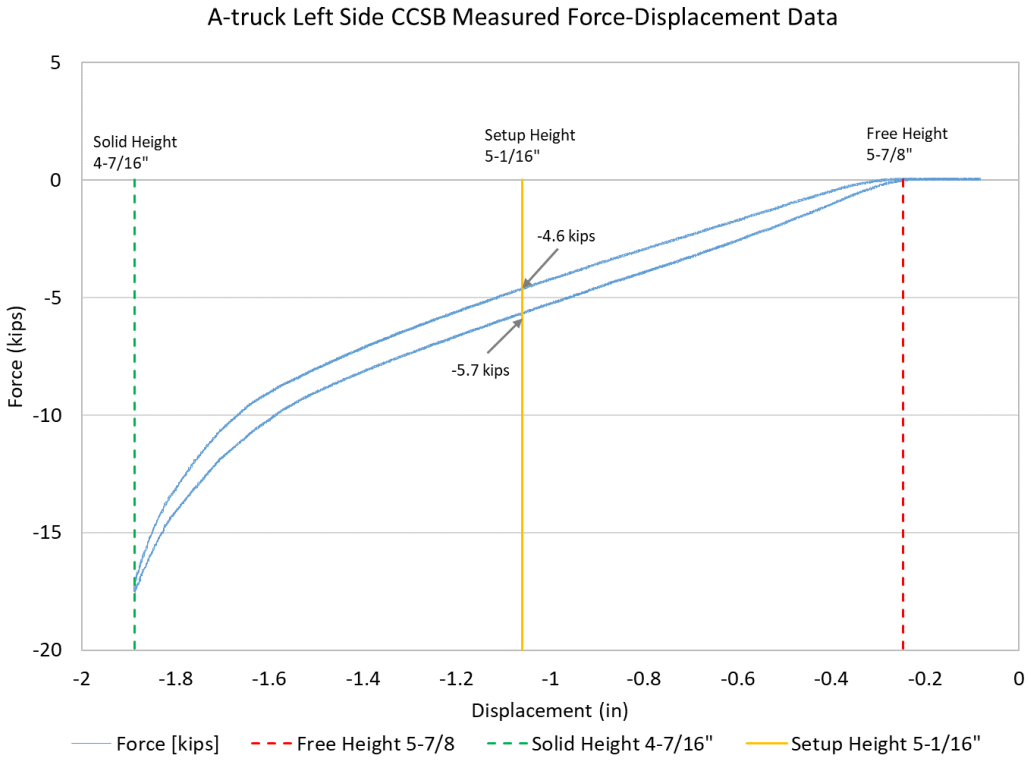


Figure 6. A-truck Left Side CCSB Measured Force-Displacement Data

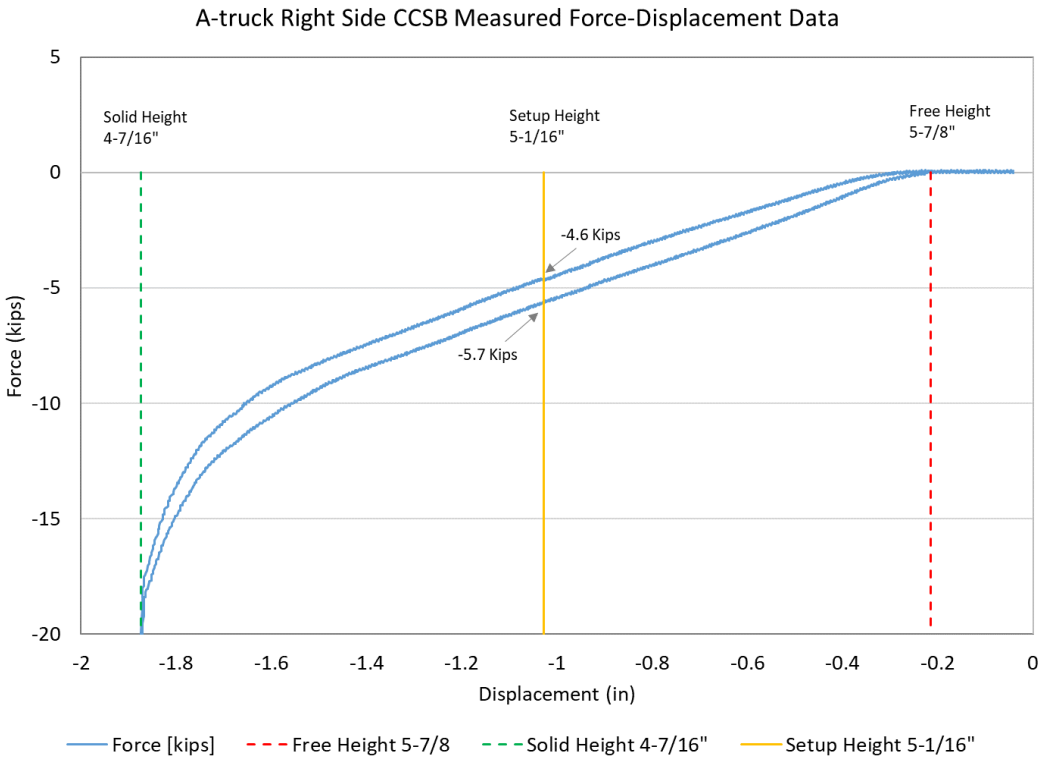


Figure 7. A-truck Right Side CCSB Measured Force-Displacement Data

The buffer railcar is equipped with four Koni 04A 2032 dampers (Figure 8). Technicians removed the dampers in the A-end left hand and A-end right hand positions for characterization. The dampers were tested on the load frame using triangle wave displacements to provide constant velocity inputs. Stroke velocities of 2-, 4-, 8-, 12-, and 14-inch/second were used for input. Koni drawing 0100 27 76 75 shows a 15 percent tolerance on the nominal forces. Figure 9 shows the characterization data for the two dampers together with the minimum and maximum forces from the Koni drawing, demonstrating that the dampers were operating within specification.

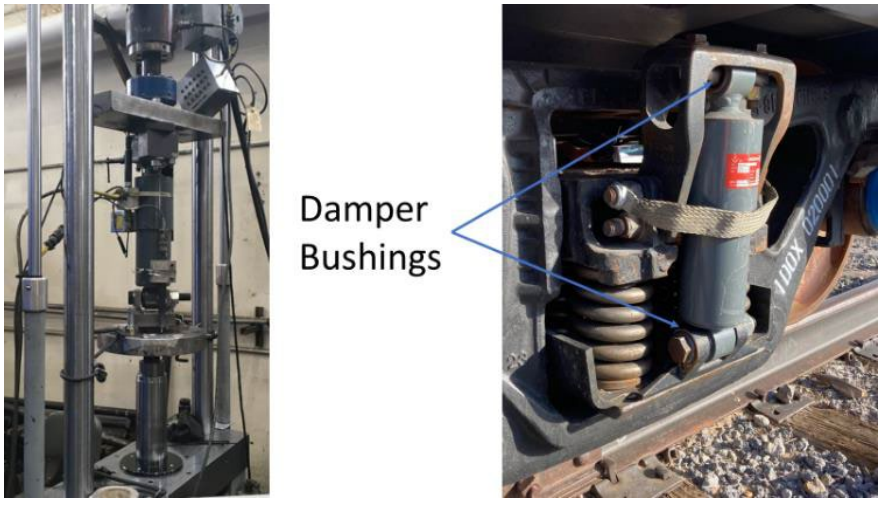


Figure 8. Koni Vertical Damper Mounted in MTS Load Frame (left) and on Buffer Railcar Truck (right)

TTCI also measured bushing displacements during the damper test to determine the stiffness of the damper bushings. Figure 10 shows the force-displacement data for each individual bushing together with the best fit lines and slopes for each. The two bushings of a damper operate in series. The series stiffness of the bushings of the AL and AR dampers is approximately 86,000 and 117,000 pounds per inch, respectively. These values are slightly higher than the 71,377 pounds per inch used in the NUCARS®* model used for pretest predictions.

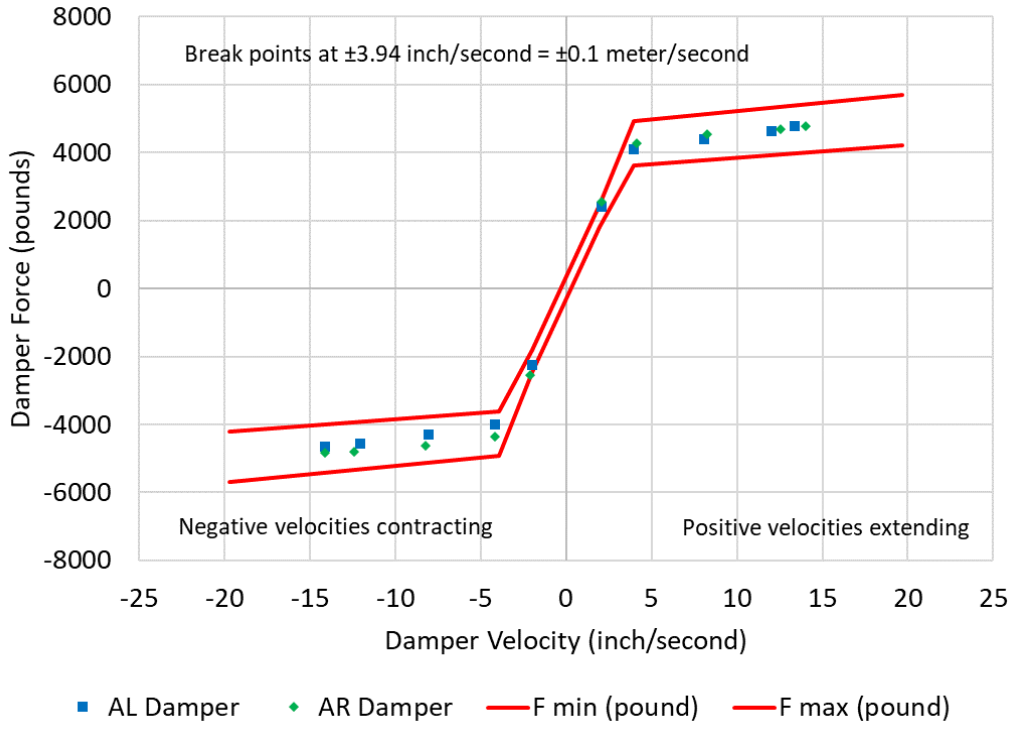


Figure 9. Damper Characterization Data

* NUCARS® is a registered trademark of Transportation Technology Center, Inc., Pueblo, CO.

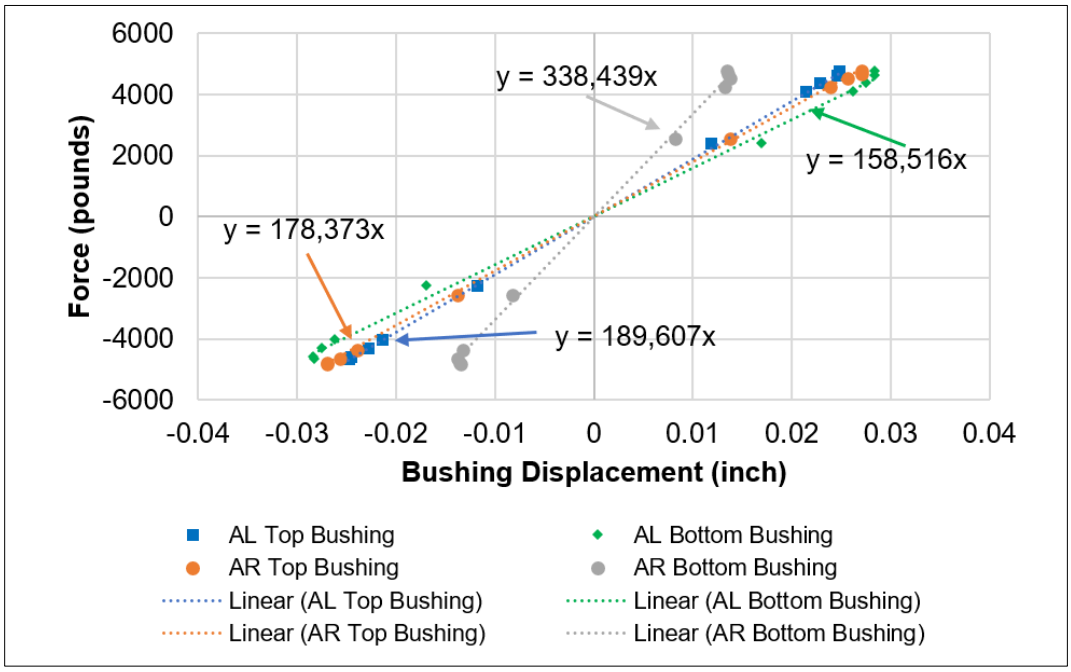


Figure 10. Damper Bushing Characterization Data

5.1.2 Vertical Suspension Stiffness and Damping

The vertical suspension stiffness of the assembled truck was measured on the Mini-Shaker Unit (MSU) in TTC's Rail Dynamics Laboratory. The B-end truck was tested. TTCI fabricated brackets that were welded on the B-end of the buffer railcar to provide connection points for the vertical and lateral actuators (Figure 11). Vertical suspension stiffness and damping tests were performed in October 2019 after most on-track dynamic tests were finished. Although the trucks were broken in, there was no noticeable wear. Abe Meddah, TTCI Principal Investigator II, witnessed the vertical suspension stiffness and damping tests as the AAR Observer per S-2043 requirements.



Figure 11. Brackets for Vertical and Lateral Actuators

The vertical tests were run on the following three configurations:

- Wedges and dampers installed
- Dampers removed
- Wedges and dampers removed

Each configuration was run at 0.1 Hz, 0.5 Hz, and 2 Hz, with the exception of the vertical test with both wedges and dampers removed, which was run at 0.1 Hz only to prevent exciting undamped rigid body modes. Input forces and displacements were adjusted for each run to achieve the desired input range within the capability of the MSU. At low frequencies (0.1 Hz) the suspension was pushed to the stops where possible, but lower amplitude inputs were used at higher frequencies.

The force supplied by the hydraulic actuators was measured by load cells installed between the actuators and the custom brackets where the vertical forces were applied. Forces were also measured on each wheel of the truck using load bars. Displacements across the secondary suspension were recorded using string potentiometers. Figure 12 shows the car installed in the MSU with the actuators configured to apply vertical loads. Examples of the instrumentation are shown in Figure 13 and Figure 14.

The motion between the left and right side frame and the Axle 2 bearing adapters was measured using six LVDTs on each side. The LVDTs were positioned to allow calculation of the relative motion between the side frame and bearing adapter in the longitudinal, lateral, vertical, roll, pitch, and yaw directions (Figure 15).

Data analysis consisted of preparing force versus displacement plots from the measured wheel/rail forces and displacements across the suspension components. These cross-plots were used to obtain suspension stiffness and damping values.

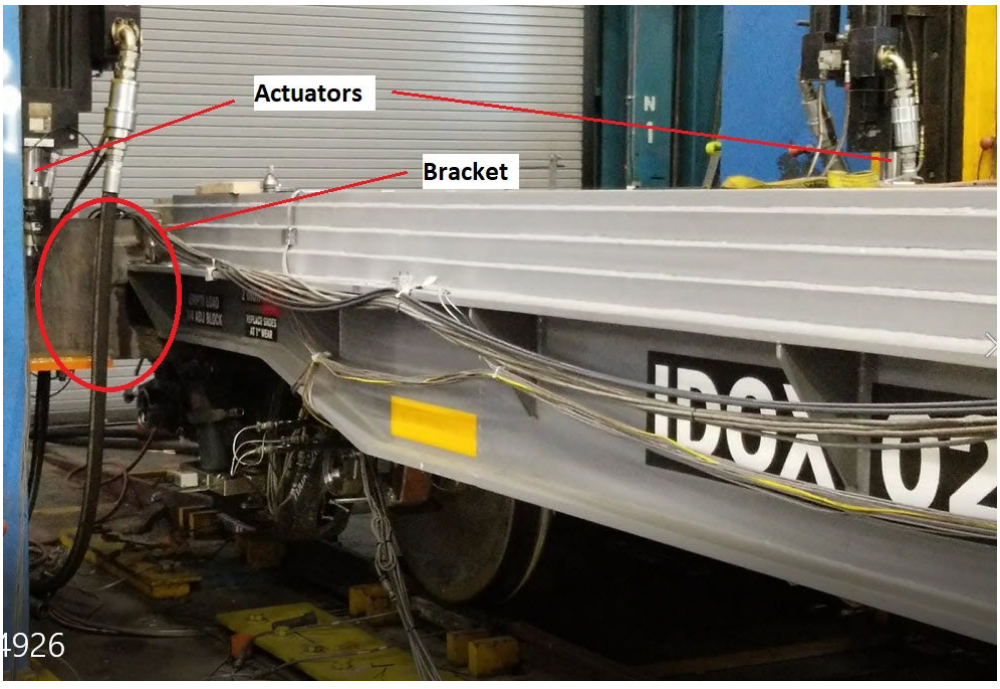


Figure 12. The Buffer Car Installed in the MSU while Configured for Vertical Suspension Testing



Figure 13. String Potentiometer for Measuring Spring Vertical Displacement (Damper Installed)



Figure 14. String Potentiometer with Damper Removed

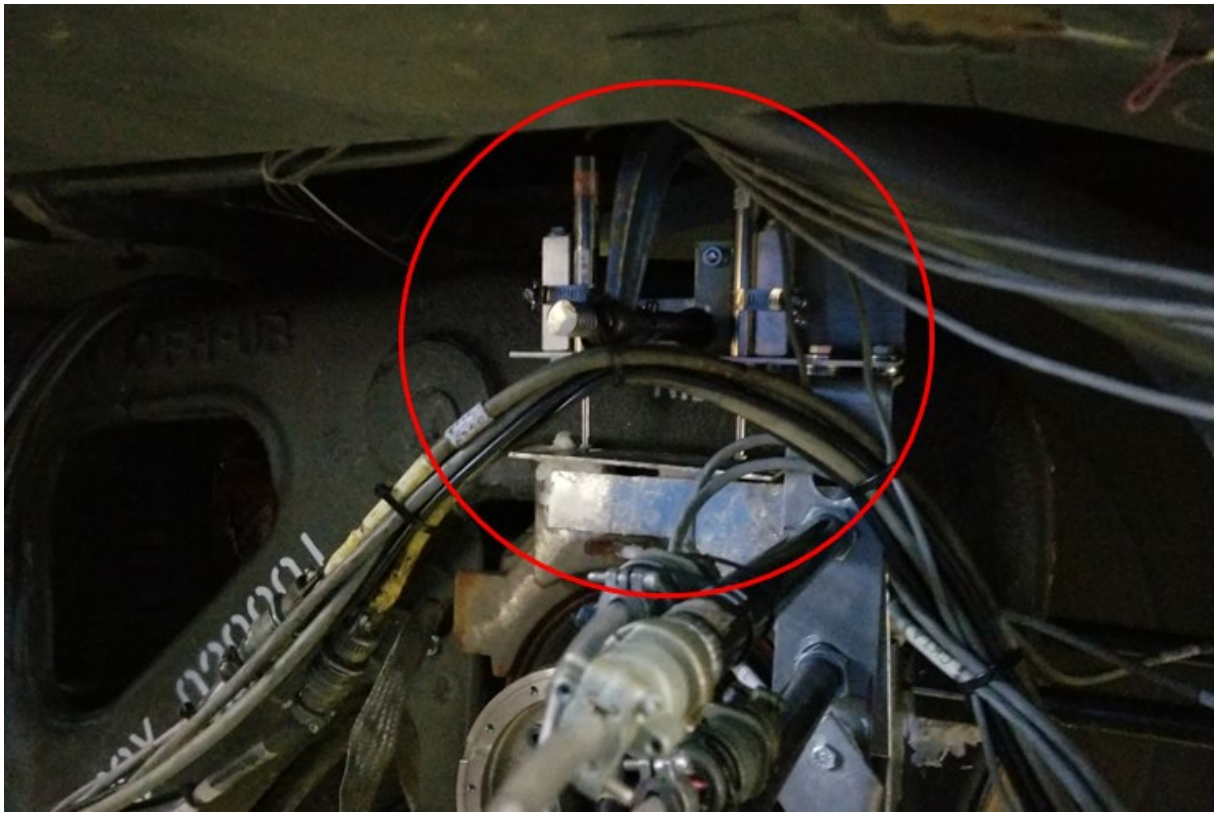


Figure 15. LVDTs for Measuring Pad Vertical Displacements

Tables 6 through 8 show the results for the three conditions tested at the different frequencies. Listed results are the average values per truck set, rather than individual values per spring nest or pad. Figure 16 and Figure 17 show examples of the data for both the springs and the pads. Negative displacements indicate compression, positive displacements indicate extension.

Figure 18 shows a plot of the total truck wheel load versus the average suspension displacement being cycled to the stop at 0.1 Hz. The plot shows that the springs begin to go solid at about -0.9 inch displacement from the static height.

Table 6. Vertical Suspension Test (Wedges and Dampers Installed)

Frequency (Hz)	Secondary Spring Stiffness (kips/inch)	Primary Pad Stiffness (kips/inch)	Secondary Spring Hysterisis Band Width (kips)	Primary Pad Hysterisis Band Width (kips)
0.1	53	3,425	16	16
0.5	55	4,161	28	2
2	75	3,543	47	2

Table 7. Vertical Suspension Test (Wedges Installed, Dampers Removed)

Frequency (Hz)	Secondary Spring Stiffness (kips/inch)	Primary Pad Stiffness (kips/inch)	Secondary Spring Hysterisis Band Width (kips)	Primary Pad Hysterisis Band Width(kips)
0.1	52	3,051	10	19
0.5	53	4,509	17	7
2	53	4,924	24	5

Table 8. Vertical Suspension Test (Wedges and Dampers Removed)

Frequency (Hz)	Secondary Spring Stiffness (kips/inch)	Primary Pad Stiffness (kips/inch)	Secondary Spring Hysterisis Band Width (kips)	Primary Pad Hysterisis Band Width (kips)
0.1	42	3,693	3	12

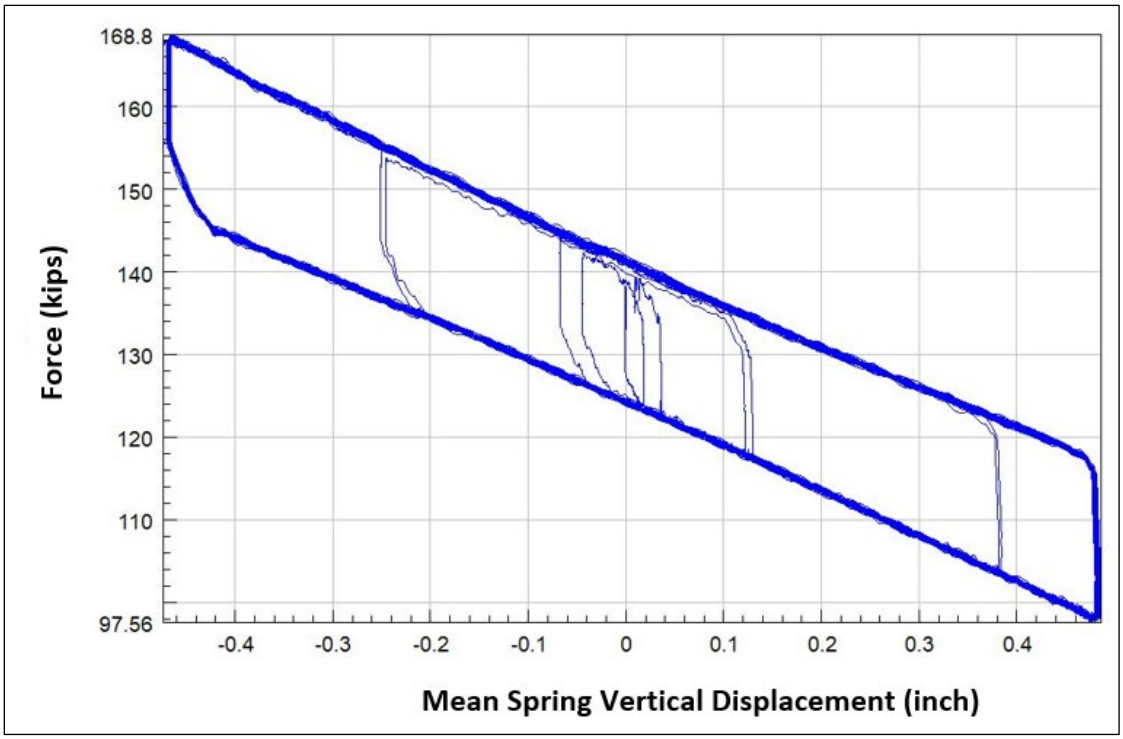


Figure 16. Truck Vertical Wheel Load Plotted against Average Secondary Suspension Displacement, Dampers Removed, 0.5hz

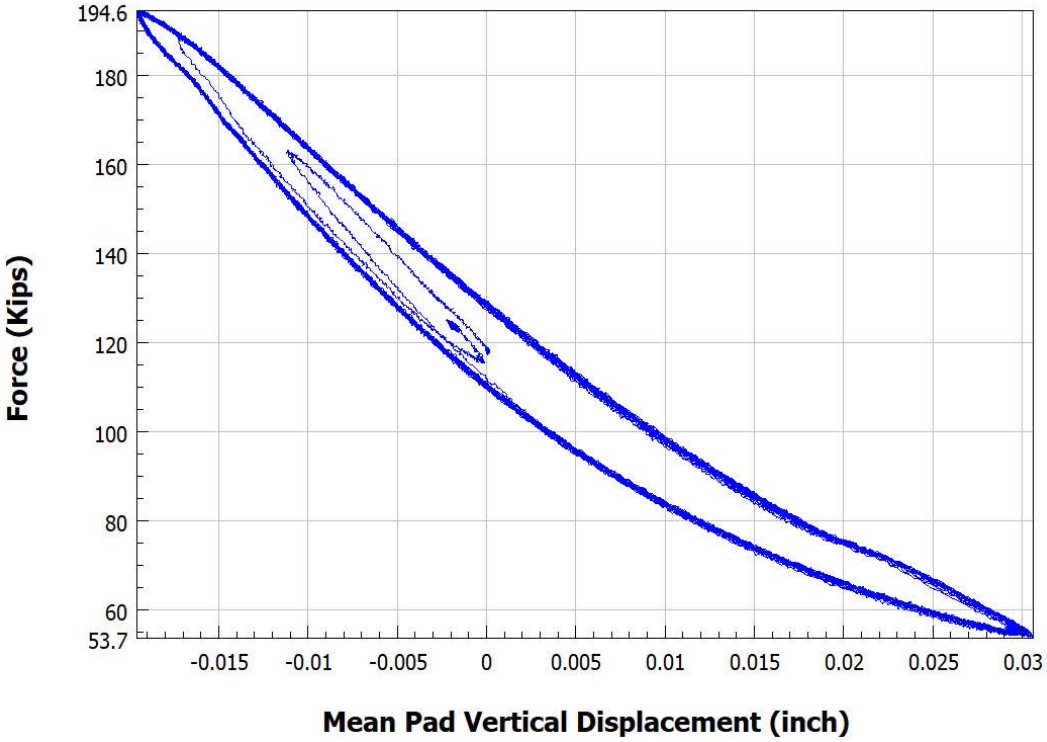


Figure 17. Truck Vertical Wheel Load Plotted against Average Primary Suspension Displacement, Dampers Removed, 0.1hz

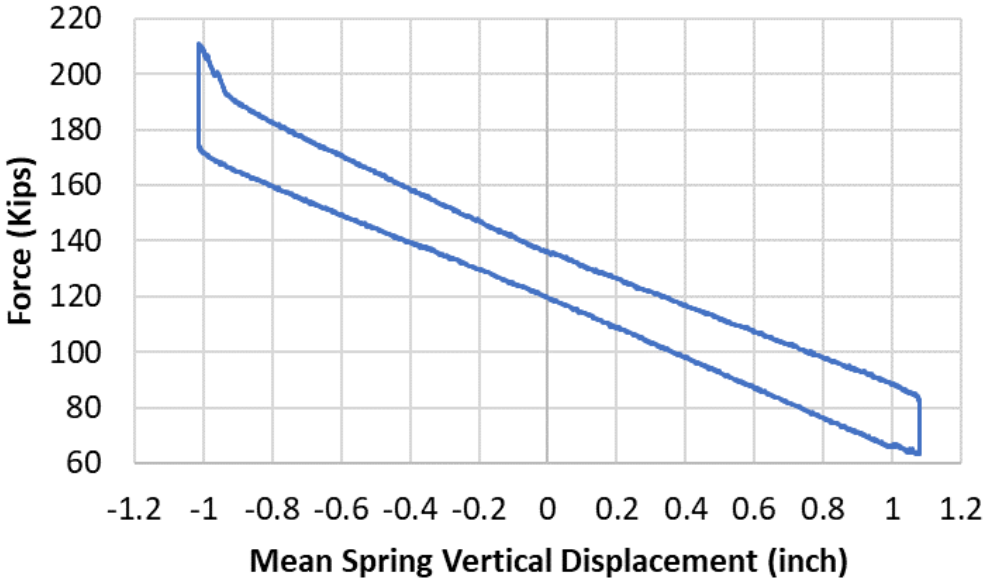


Figure 18. Truck Vertical Wheel Load versus Average Suspension Displacement at 0.1 Hz Input with Wedges and Dampers Installed

5.1.3 Lateral Suspension Stiffness and Damping

Lateral characterization tests were performed by connecting one actuator between the south MSU reaction mass and the carbody. The B-end truck was tested. Loads were applied at several frequencies: 0.1 Hz, 0.5 Hz, and 2.0 Hz, but the most consistent results were found at the lowest frequencies. Input forces and displacements were adjusted for each run to achieve the desired input range within the capability of the MSU. At low frequencies (0.1 Hz) the suspension was pushed to the stops where possible, but lower amplitude inputs were used at higher frequencies. Figure 19 shows a photograph of the MSU configured for lateral characterization testing. TTCI performed lateral suspension stiffness and damping tests in November 2019 after most on-track dynamic tests were finished. Although the trucks were broken in, there was no noticeable wear. Xinggao Shu, TTCI Principal Investigator II, and Adam Klopp, TTCI Principal Investigator I, witnessed the lateral suspension stiffness and damping tests as the AAR Observer per S-2043 requirements.



Figure 19. Buffer Railcar Ready for Lateral Force Test

The Swing Motion® truck design allows the side frames to roll slightly relative to the bolster, transom, and axles. This creates a gravitational stiffness in series with the lateral shear of the spring nest, a complicating factor for lateral characterization tests. The displacement between the bolster and transom was measured to determine the shear stiffness of the spring nests. Additional tests were run while restraining the transom displacement.

The lateral tests were run on the following four configurations at 0.1 Hz, 0.5 Hz, and 2 Hz:

- Wedges and dampers installed
- Dampers removed
- Wedges removed
- Wedges and dampers removed

The runs with the restrained transom were conducted at 0.1 Hz.

The force supplied by the hydraulic actuator was measured by a load cell installed between the actuator and the specially welded bracket where the lateral force was applied. The lateral displacements were measured with laser transducers and a series of LVDTs. Setup and examples of instrumentation are shown in Figure 20.

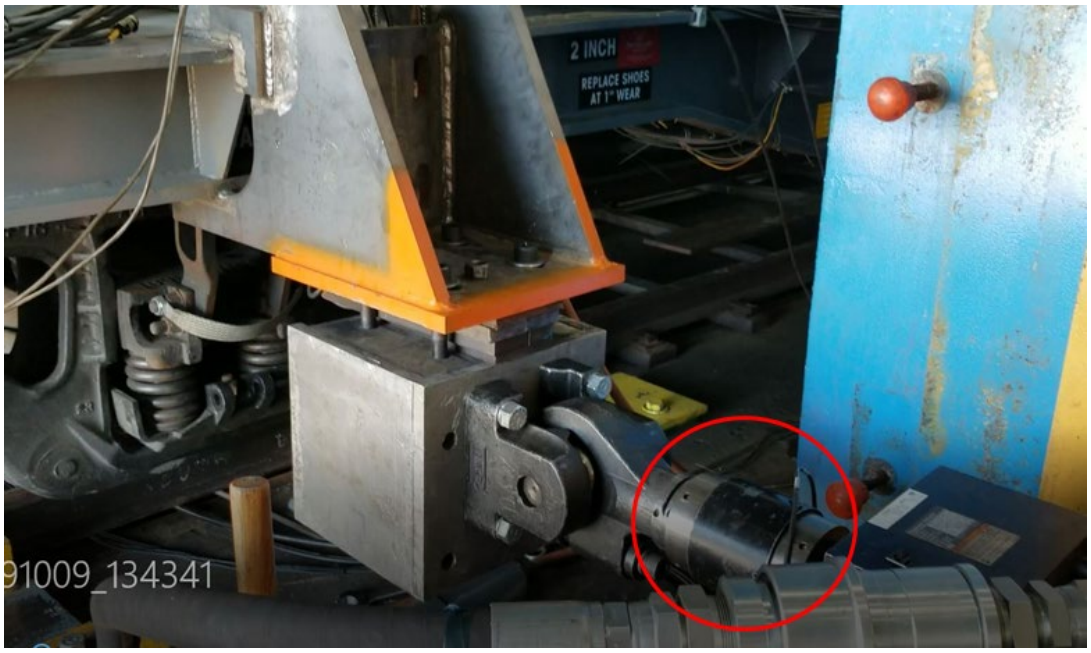


Figure 20. Load Cell for Lateral Force Measurements

The motion between the left and right side frame and the Axle 2 bearing adapters was measured using six LVDTs on each side. The LVDTs were positioned to allow calculation of the relative motion between the side frame and bearing adapter in the longitudinal, lateral, vertical, roll, pitch, and yaw directions (Figure 20). Because the two primary suspension pads work in parallel in the lateral direction, only the combined or average stiffness and damping can be measured. The Swing Motion truck is designed to allow the side frames to roll with relative to the axles, transom, and truck bolster. This action works in series with the secondary suspension lateral spring stiffness to provide a soft lateral suspension compared to other truck designs. For some runs, TTCI isolated the side frame roll motion from the secondary suspension spring shear by connecting the transom to the MSU reaction mass with a stiff bar to prevent it moving laterally due to side frame roll. TTCI then measured the secondary spring lateral displacement without side frame roll motions affecting the measurement. The primary pad stiffness and damping are not reported for transom restrained runs because some of the lateral load is carried by the restraint and is not carried through the pads.

As noted in Section 2.0, these trucks have a primary pad, which allows some lateral movement between the side frames and the axles that works in series with the effect of side frame roll. Lateral displacement was measured in two locations at each pad on one of the axles. The measurements were offset vertically so the roll and lateral shift between the side frame and axle could be determined. The lateral stiffness reported is relative to the lateral movement between the side frame and axle at a vertical position equal to the top of the bearing adapter. Figure 21 shows the instrumentation used to record the lateral movements of the pads.

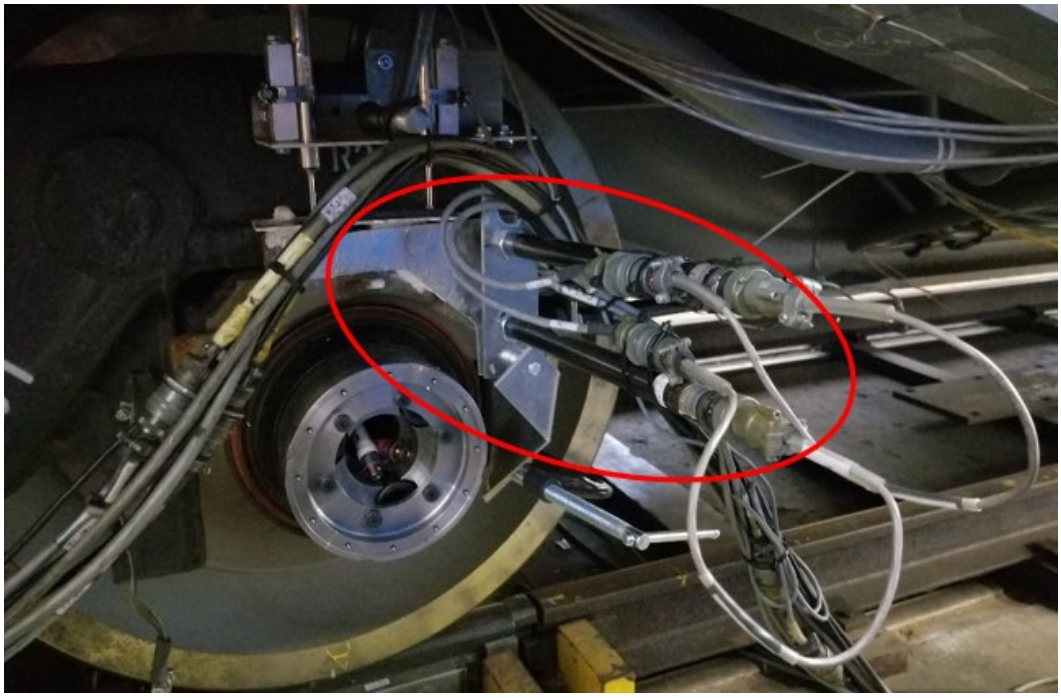


Figure 21. LVDTs used to Record Pad Lateral Movements

Tables 9 through 12 show the results for the lateral suspension and damping tests.

Table 9. Lateral Suspension Test (Wedges and Dampers Installed)

Frequency (Hz)	Spring Stiffness (kips/inch)	Pad Stiffness (kips/inch)	Spring Hysterisis Band Width (kips)	Pad Hysterisis Band Width (kips)
0.1	11	149	12	10
0.5	45	718	6	10
2.0	40	411	20	5
0.1 Transom Restrained	15	NA	13	NA

Table 10. Lateral Suspension Test (Wedges Installed, Dampers Removed)

Frequency (Hz)	Spring Stiffness (kips/inch)	Pad Stiffness (kips/inch)	Spring Hysterisis Band Width (kips)	Pad Hysterisis Band Width (kips)
0.1	12	146	12	9
0.5	13	159	15	14
2.0	37	376	28	12
0.1 Transom Restrained	17	NA	11	NA

Table 11. Lateral Suspension Test (Wedges Removed)

Frequency (Hz)	Spring Stiffness (kips/inch)	Pad Stiffness (kips/inch)	Spring Hysterisis Band Width (kips)	Pad Hysterisis Band Width (kips)
0.1	10	127	2	2
0.1 Transom Restrained	14	NA	3	NA

Table 12. Lateral Suspension Test (Dampers and Wedges Removed)

Frequency (Hz)	Spring Stiffness (kips/inch)	Pad Stiffness (kips/inch)	Spring Hysterisis Band Width (kips)	Pad Hysterisis Band Width (kips)
0.1	10	121	2	2
0.1 Transom Restrained	14	NA	4	NA

Figure 22 and Figure 23 show examples of the Lateral Suspension Stiffness and Damping Test results. Force to the north is positive, and displacement to the south is positive.

Figure 24 shows the lateral suspension with dampers and wedges removed, and the transom restrained, pushed to the left and right lateral stops. The total lateral clearance between the bolster and the transom is about 1.8 inches.

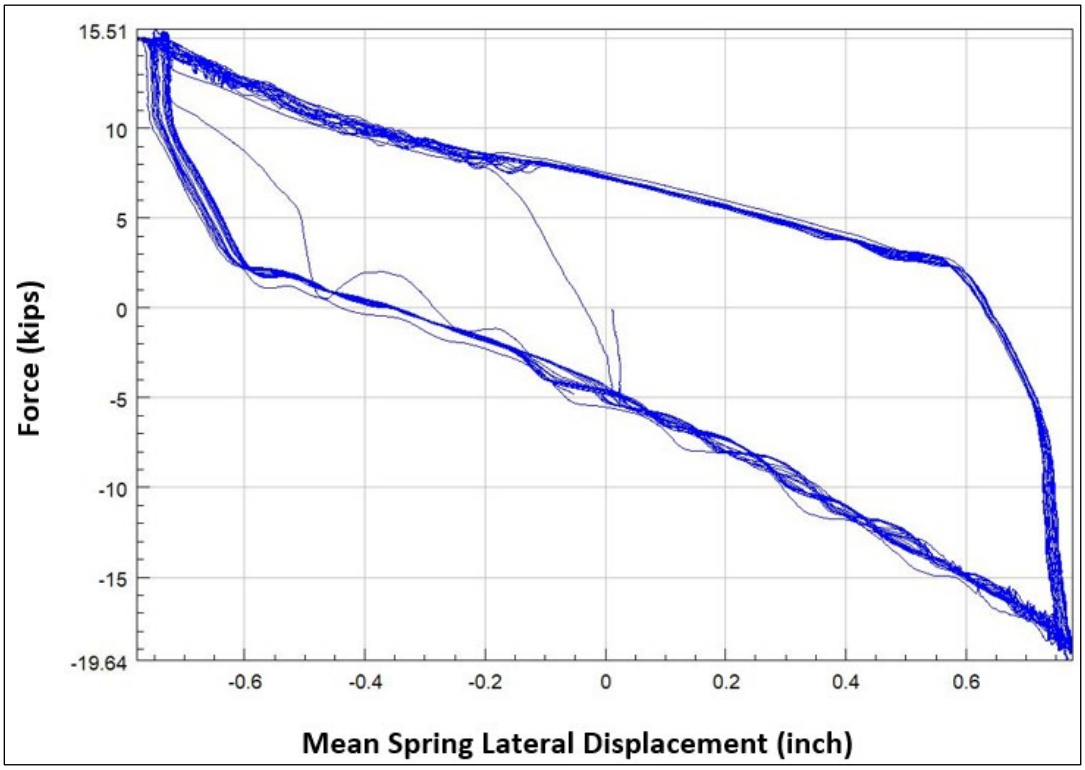


Figure 22. Truck Lateral Load Plotted against Lateral Secondary Suspension Displacement, Dampers Removed, 0.1 Hz

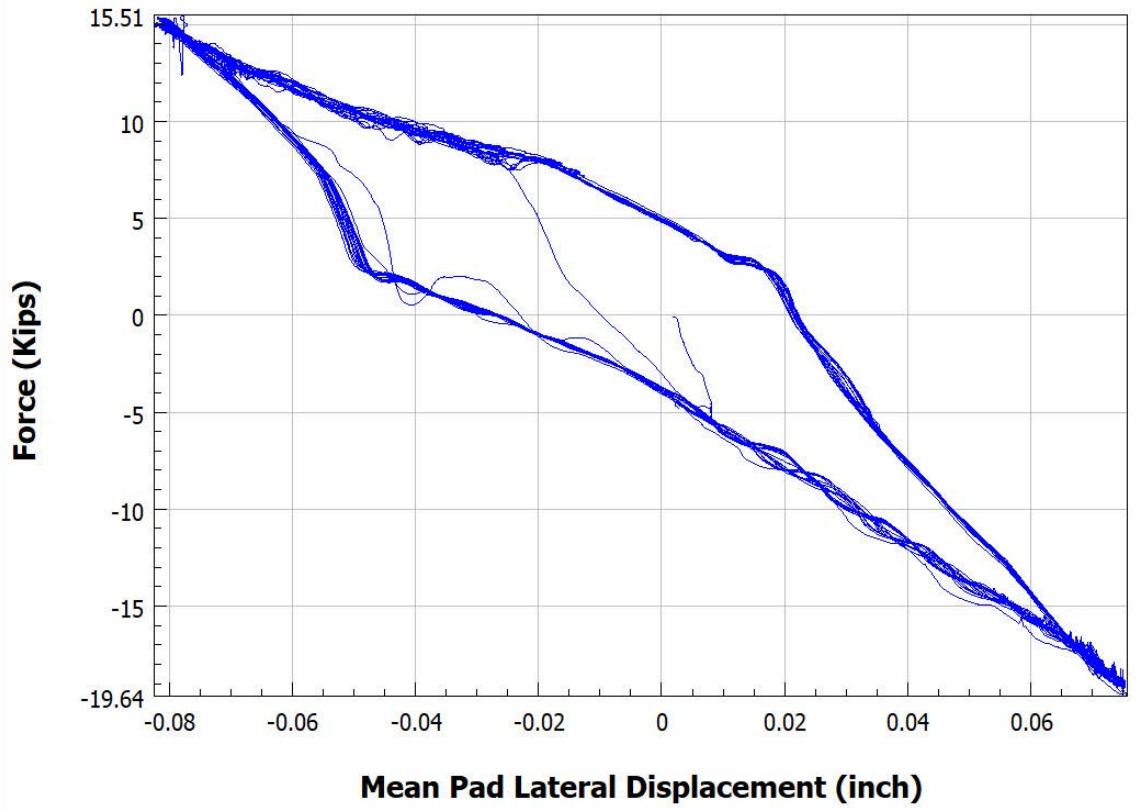


Figure 23. Truck Lateral Load Plotted against Lateral Primary Suspension Displacement, Dampers Removed, 0.1 Hz.

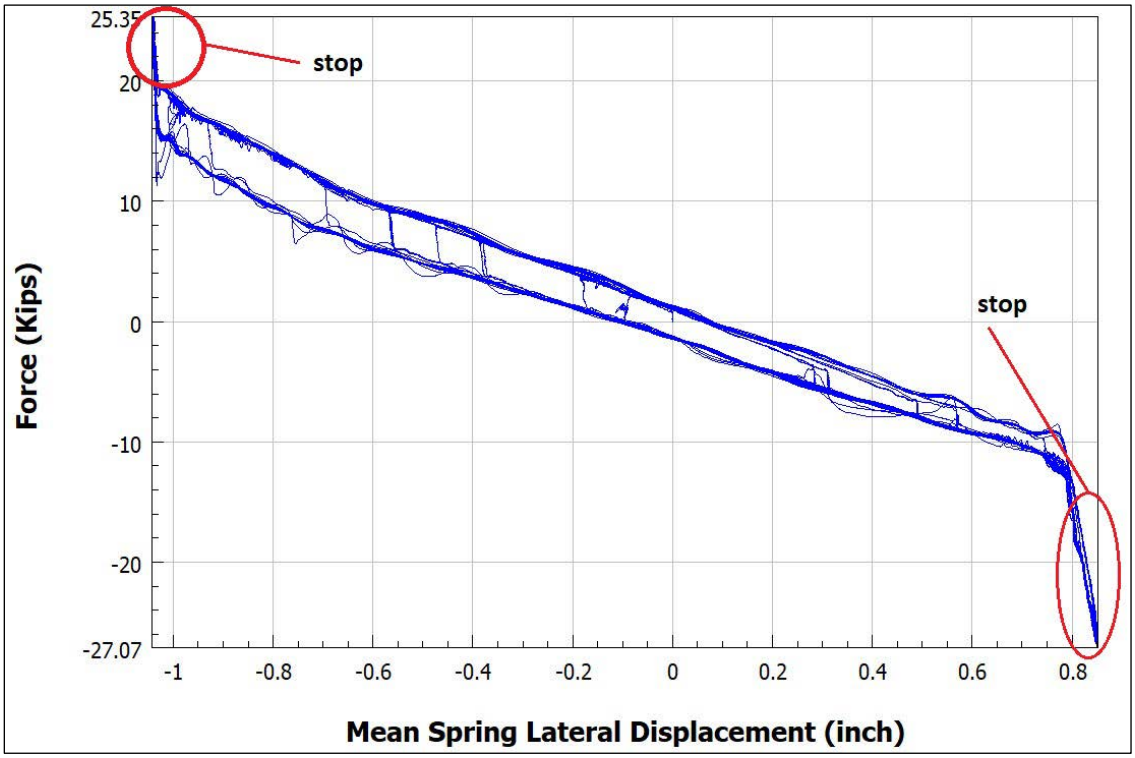


Figure 24. Secondary Suspension with Wedges and Dampers Removed and with the Transom Restrained Showing Displacement to the Lateral Stops

5.1.4 Truck Rotation Stiffness and Breakaway Moment

Truck rotation stiffness and breakaway moment were measured by supporting one end of the buffer railcar on an air bearing table and measuring the force required to rotate the truck relative to the carbody. These tests were performed on the A-end truck. Figure 25 shows the A-end truck of the buffer railcar positioned on the air bearing table. The actuator and load cell are circled in blue, and one of the truck rotation measurements is circled in red. TTCI performed truck rotation tests in May 2019 before any track testing began. The centerplates were lubricated with a lubrication disk. The constant-contact side bearings were installed during the test. Adam Klopp, TTCI Principal Investigator I, witnessed the truck rotation stiffness and breakaway test as the AAR Observer per S-2043 requirements.



Figure 25. Buffer Railcar Positioned on Air Bearing Table

Figure 26 shows the moment versus truck rotation for the buffer railcar. The breakaway moment is the moment just as the truck begins to move from its centered position at zero degree. The plot shows data from several test runs, and all runs were consistent with each other.

The plot appears to have a wider hysteresis for positive rotations (CCW when looking down on the truck). The actuators were installed near the corners of the air bearing table, perpendicular to the table rather than perpendicular to a line that passes through the center of rotation. As a result, the lever arm the actuators act on gets longer for CW rotations and shorter for CCW rotations. The moments and friction values shown are taken as the truck is moving through the zero-rotation position when the length of the lever is as measured.

Table 13 shows the measured friction moment. The typical value is shown. The coefficient of friction in the centerplate was estimated using the following equation:

$$\mu = \frac{3\,(Torque - 2SBld \times SBdst \times \mu_{sb})(\mathrm{CPrad}^2 - \mathrm{Hrad}^2)}{2\,(\mathrm{Tld} - 2 \times \mathrm{SBld})(\mathrm{Cprad}^3 - \mathrm{Hrad}^3)}$$

Where:

- Torque is the average turning torque measured in the test = 232 kip-inch
- SBld is the CCSB preload measured during side bearing component characterization = 5.16 kips
- μ_{sb} is the assumed coefficient of friction between the CCSB and the body = 0.4
- CPrad is the centerplate radius, 8 inches
- Hrad is the centerplate hole radius, 1 inch
- Tld is the A-end truck load, which is the A-end scale weight†: 131 kips – 11 kips truck weight = 120 kips on the side bearings and center plate

Side bearing preload is estimated from the hysteresis loop shown in Figure 6.

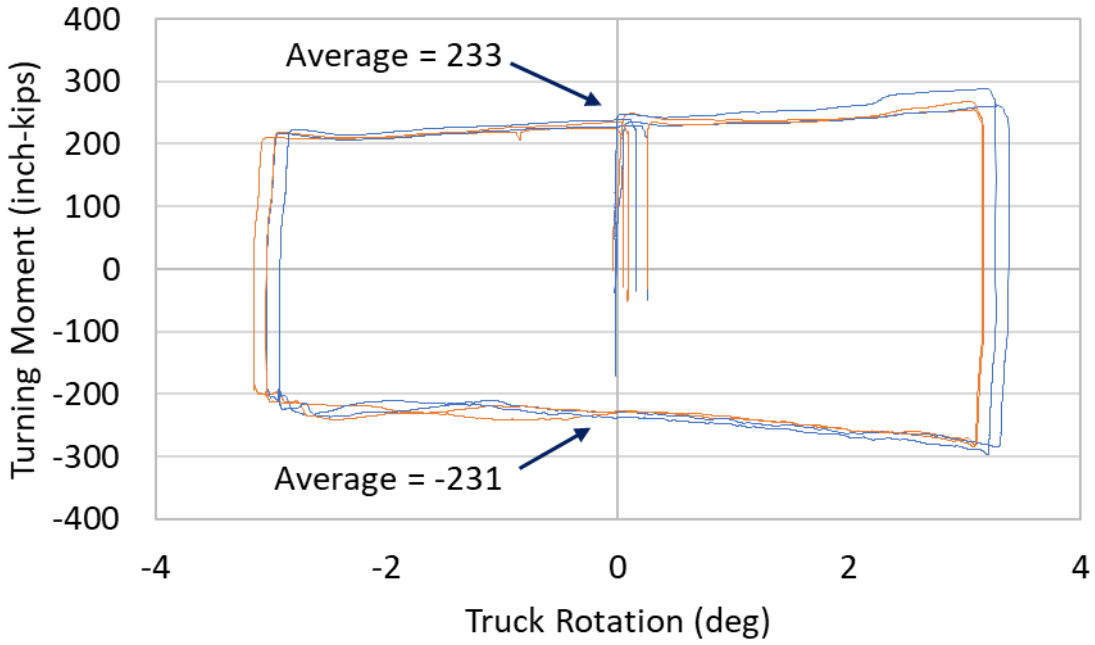


Figure 26. Truck Rotation Data for Buffer Railcar A-truck

Table 13. Truck Rotation Moment and Estimate of the Associated Friction Coefficient

A-Truck	Mean Torque 1,000 inch-pound	Center Plate Friction Coefficient (μ)
	232	0.22

† TTCI measured the A-end weight with a calibrated track scale on May 22, 2019.

5.1.5 Interaxle Longitudinal Stiffness

The longitudinal stiffness of the axle to side frame connection is critical to vehicle performance in curving and high-speed stability regimes. The interaxle longitudinal stiffness is measured by installing independently rotating wheels in the truck with spindles at the bearing endcaps and then forcing the axles apart and pulling them together while measuring the force and displacement (Figure 27). Runs were performed while pushing and pulling in phase on each side of the truck and separately while pushing on one side of the truck and pulling on the other side. TTCI performed the interaxle longitudinal stiffness test in November 2019 after most of the on-track dynamic testing was complete. Adam Klopp, TTCI Principal Investigator I, witnessed the interaxle longitudinal stiffness tests as the AAR Observer per S-2043 requirements.



Figure 27. Buffer Railcar Interaxle Test Actuator and Load Cell

The motion between the left and right side frame and the Axle 2 bearing adapters was measured using six LVDTs on each side. The LVDTs were positioned to allow calculation of the relative motion between the side frame and bearing adapter in the longitudinal, lateral, vertical, roll, pitch, and yaw directions.

The applied force was offset vertically from the level of the axle to side frame connection. This caused the bearing adapters to pitch and shear laterally. The shear stiffness data in Table 14 are based on longitudinal displacements at the level of the top of the bearing adapter. Pitch stiffness data are based on a rotation of the bearing adapter around the bearing. Axle centerline stiffness data are based on the longitudinal motion of the axle at its axis of rotation. Figure 28 shows example data for longitudinal axle stiffness tests.

Axle yaw stiffness data were determined during push-pull runs. Axle yaw stiffness can be expressed as two longitudinal stiffnesses separated by the bearing centerline distance. The effective longitudinal stiffness was calculated from the axle yaw stiffness by this method for comparison to the direct measurements of primary longitudinal stiffness. Given the large variation in the direct measurement of axle centerline longitudinal stiffness, the values derived from axle yaw stiffness

reasonably agree with the average values from the direct measurements. These values were weighted and averaged to establish an effective longitudinal value of 13,000 pounds per inch per pad, which is the key result that will be used in the post-test analysis.

Table 14. Side frame to Axle Properties Stiffness Data per Pad

Shear stiffness (1,000 pounds/inch)	Average	43
	Minimum	26
	Maximum	57
	Standard deviation	13
Pitch stiffness (1,000 inch-pounds/rad)	Average	596
	Minimum	345
	Maximum	750
	Standard deviation	192
Axle centerline stiffness from direct measurement (1,000 pounds/inch)	Average	12
	Minimum	7
	Maximum	15
	Standard deviation	4
Axle yaw stiffness (1,000 inch-pounds/rad)	Average	46,664
	Minimum	41,545
	Maximum	51,782
	Standard deviation	7,239
Axle centerline stiffness derived from axle yaw (1,000 pounds/inch)	Average	14.9

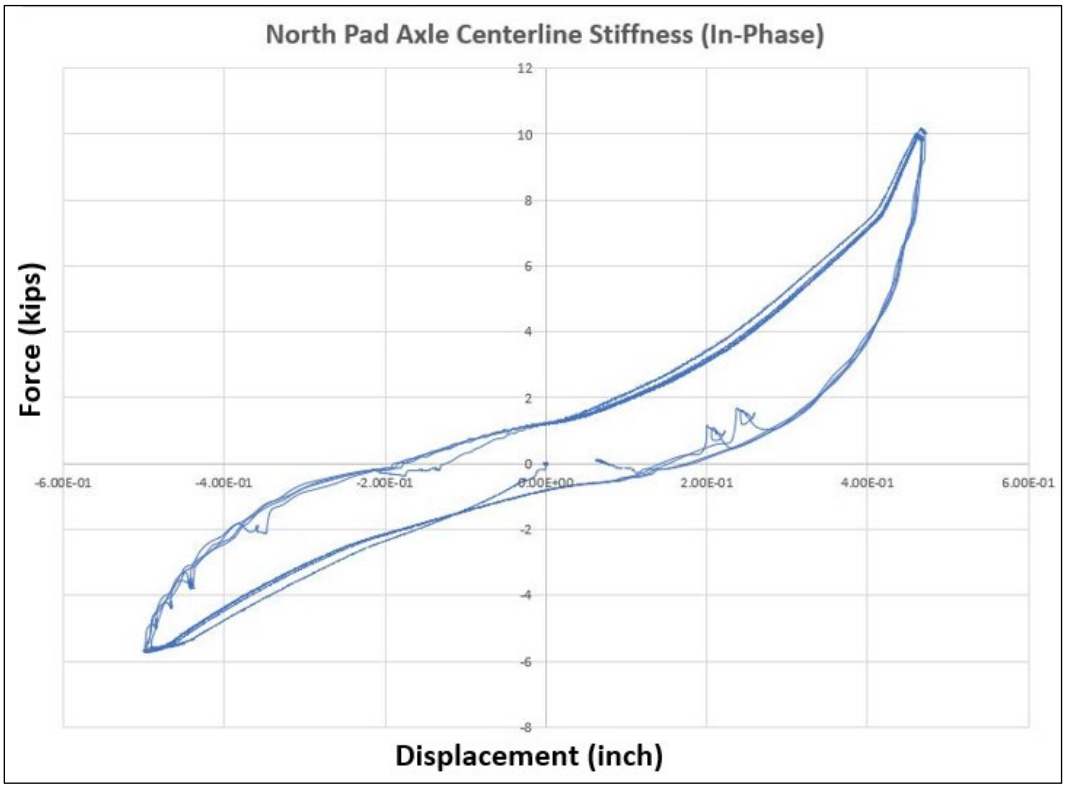


Figure 28. Example Data for Longitudinal Axle Stiffness Tests

5.1.6 Modal Characterization

Modal characterization is performed to identify the rigid and flexible body modes of vibration for the vehicle.

The buffer railcar was excited through actuators attached to the special brackets described in Section 5.1.2. Figure 29 shows the railcar setup for vertical inputs. Dampers and wedges, including the control coils, were removed for all tests because initial testing showed it was not possible to excite the modes with dampers and wedges in place.

Actuators were operated in force control at lower frequencies (0.2 to 10 Hz) and in displacement control input at higher frequencies (3 to 30 Hz). In practice, the displacement control inputs were intended to be constant displacement but were limited by the actuator response and displacement amplitude reduced as frequency increased. Frequency was increased linearly with time for the frequency sweeps, and then the frequency of peak amplitudes were confirmed with dwell runs at discrete frequencies. Inputs included:

- Lateral excitation with one actuator.
- Vertical excitation with two actuators operating in phase.
- Vertical excitation with two actuators operating 180 degrees out of phase.

The buffer railcar deck was instrumented with five vertical accelerometers on the right edge, five vertical accelerometers along the left edge, and five lateral accelerometers along the right edge. The input forces and displacements were also recorded. Figure 30 shows the distribution of the accelerometers used during the modal test. Adam Klopp, TTCI Principal Investigator I, and Abe Meddah, TTCI Principal Investigator I, witnessed the modal characterization tests as the AAR Observer per S-2043 requirements.

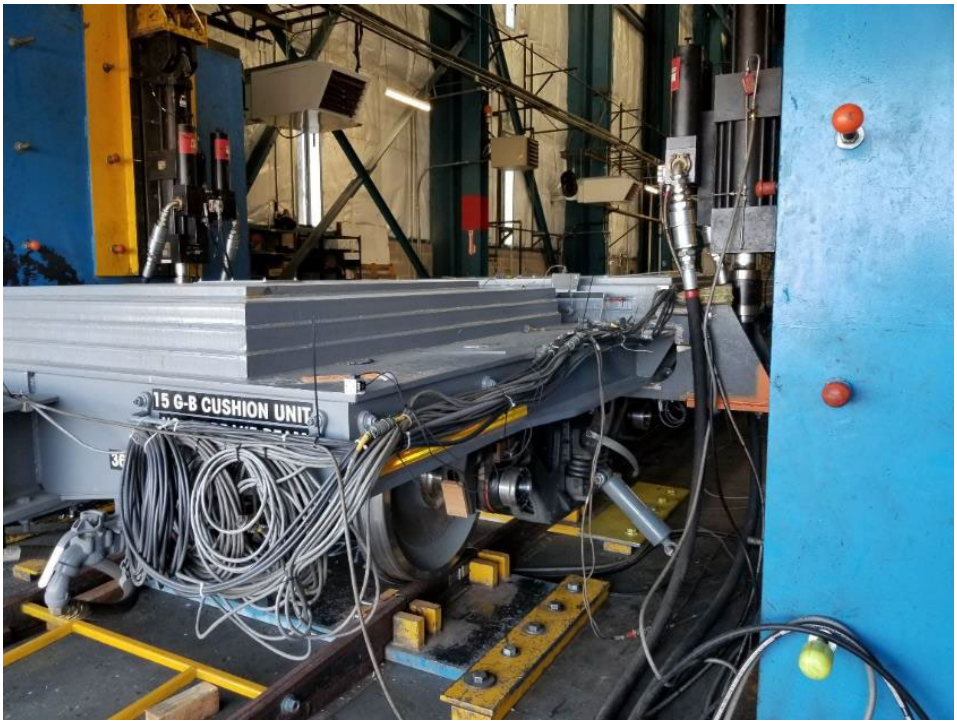


Figure 29. Actuators Attached to Buffer Railcar during Modal Testing with Vertical Input

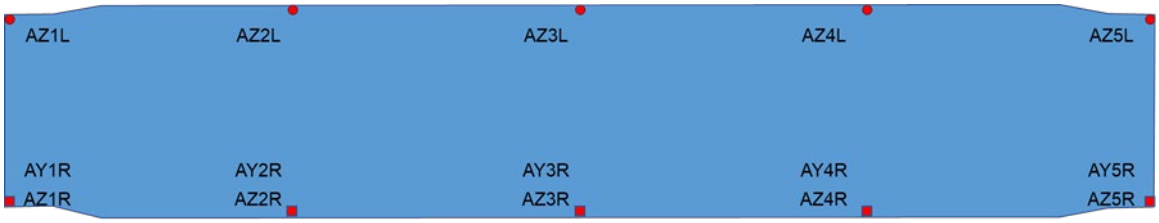


Figure 30. Distribution of Accelerometers during the Buffer Railcar Modal Test

The test was performed according to the following sequence:

1. Vertical rigid body test runs (force control).
2. Roll rigid body test runs (force control).
3. Vertical flexible body test runs (displacement control).
4. Twist flexible body test runs (displacement control).
5. Lateral rigid body test runs (force control).
6. Lateral flexible body test runs (displacement control).

Transfer functions were calculated for each accelerometer with respect to the appropriate input. The transfer functions were examined to identify resonant frequencies. Amplitude and phasing for each accelerometer location were examined at that frequency to identify the mode shape. Table 15 shows results from the modal characterization tests. The rigid body yaw mode could not be excited during these tests because there was a large amount of damping in the system. The flexible body lateral bending mode also could not be excited during these tests. TTCI believes this is because the steel ballast weights welded to the buffer railcar deck increased the stiffness of the railcar, and consequently the lateral flexible body bending frequency was higher than the MSU is able to excite. This frequency is likely higher than would affect vehicle dynamic performance. This case is marked as “Not observed.”

Table 15. Modal Characterization Results

Mode Type	Mode	Frequency (Hz)
Rigid Body	Bounce	1.71
	Pitch	2.44
	Upper center roll	2.19
	Lower center roll	0.98
	Yaw	Not observed
Flexible Body	Twist	16.36
	Lateral bending	Not observed
	Vertical bending	9.00

Figure 31 and Figure 32 show the time history for the identification of the Bounce Mode and its corresponding frequency analysis. The maximum amplitude of the signal is found at 1.71 Hz.

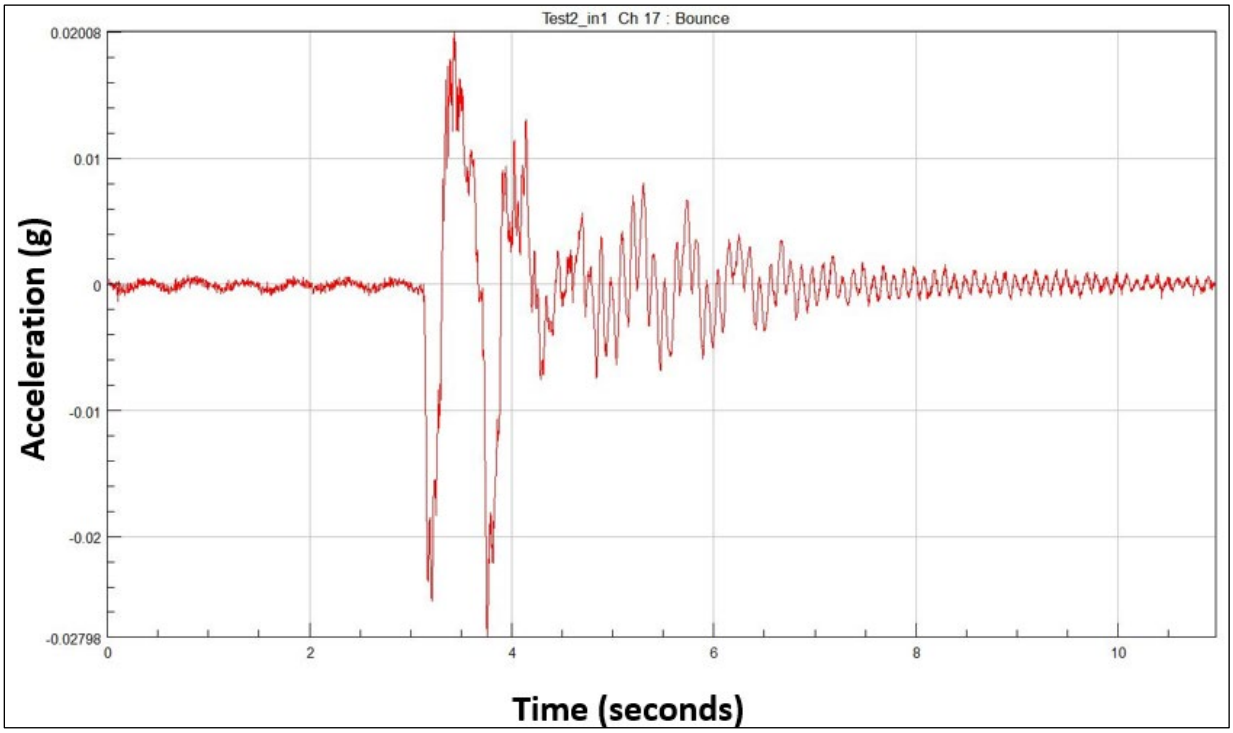


Figure 31. Time History Plot for Bounce Mode

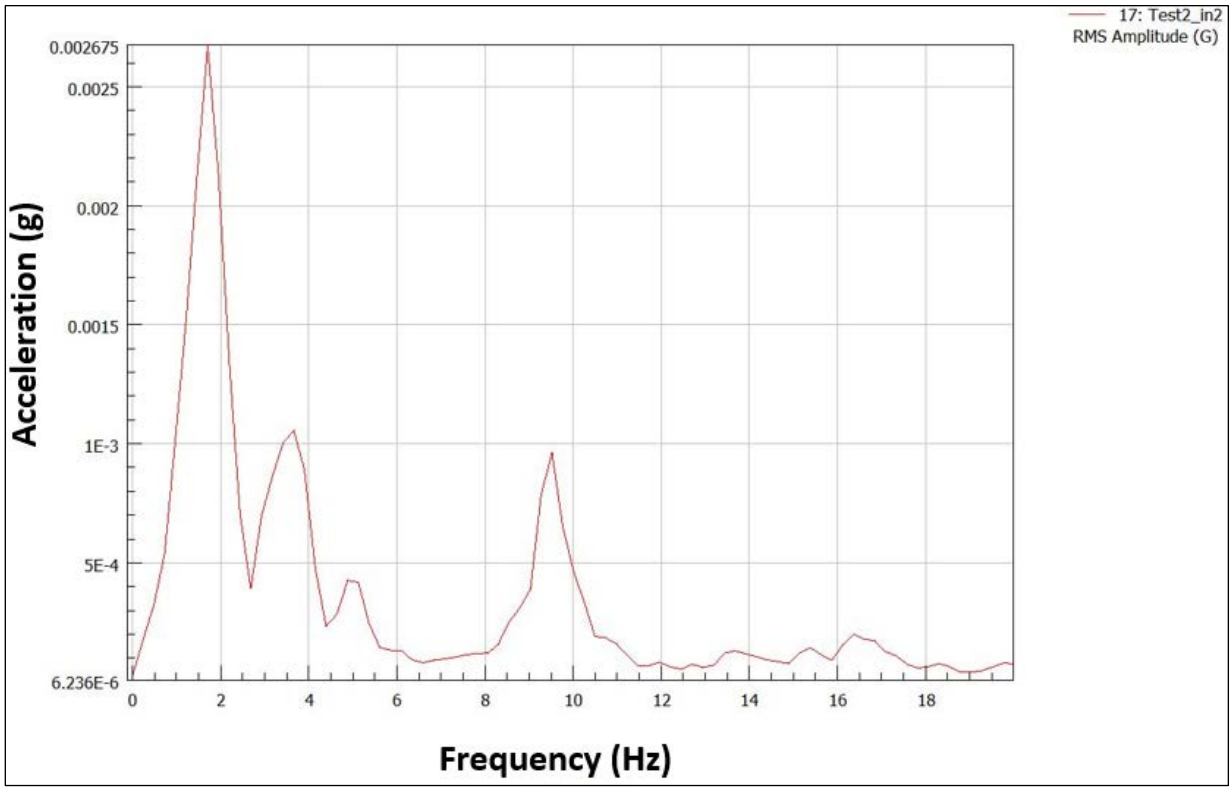


Figure 32. Frequency Analysis for the Bounce Mode

5.2 Nonstructural Static Tests

Nonstructural static tests are performed to verify the vehicle equalizes load properly under common conditions. Test results are provided in Sections 5.2.1 to 5.2.4. The Nonstructural static tests included:

- Truck twist equalization
- Carbody twist equalization
- Static curve stability
- Horizontal curve negotiation

5.2.1 Truck Twist Equalization

The truck twist equalization requirement is to ensure adequate truck load equalization. With the buffer railcar on level track, vertical wheel loads were measured while raising and lowering one wheel from 0.0 inch to 3.0 inches in increments of 0.5 inch. At 2.0 inches of deflection, vertical load at any wheel may not fall below 60 percent of the nominal static load. At 3.0 inches of deflection, vertical load at any wheel may not fall below 40 percent of the nominal static load. Two different wheels were used to monitor truck twist (Left 1 and Right 3).

The truck twist equalization tests were completed on July 26, 2019. Dr. Xinggao Shu, TTCI Principal Investigator II, witnessed the truck twist equalization tests as the AAR Observer per S-2043 requirements. The buffer railcar met the AAR Standard S-2043 requirements. Table 16 shows the worst-case truck twist equalization results. Figure 33 displays the wheel load result for all wheels during the lifting and lowering of the L1 wheel.

Table 16. Truck Twist Equalization Results

Condition	L1 Wheel Location	
	Percent Load	Wheel
2-inch lowering	82	Axle 1 Left
3-inch lowering	77	Axle 1 Left
Condition	**R3 Wheel Location**	
	Percent Load	**Wheel**
2-inch lowering	81	Axle 3 Right
3-inch lowering	77	Axle 3 Right

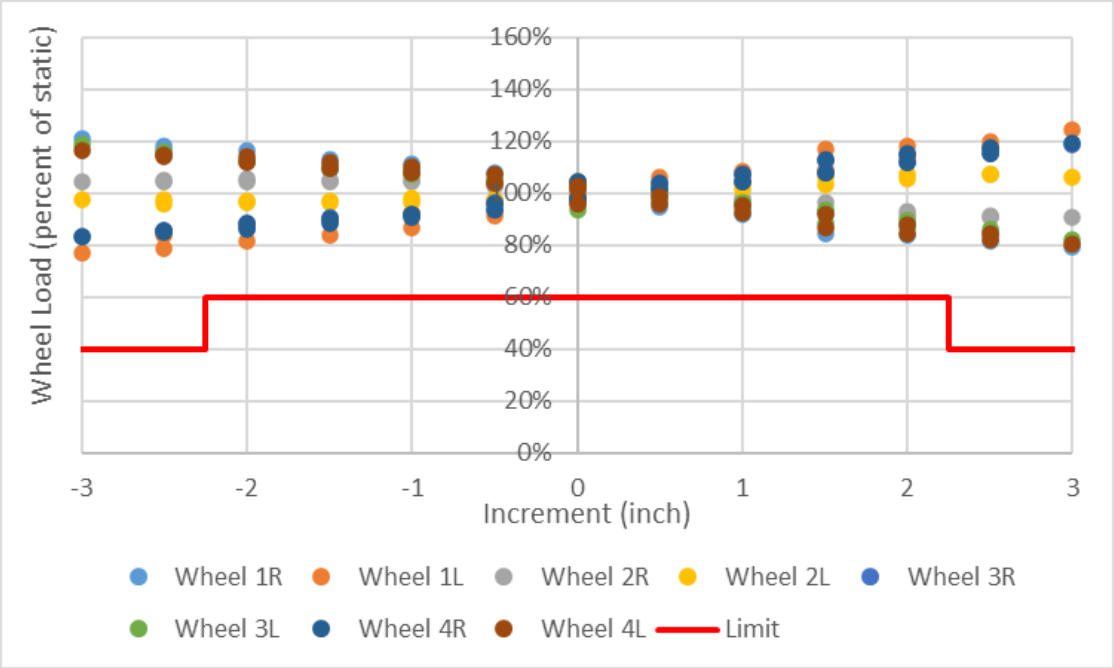


Figure 33. L1 Truck Twist Result for All Increments

5.2.2 Carbody Twist Equalization

The carbody twist equalization requirement is to document wheel unloading under carbody twist, such as during a spiral negotiation.

With the buffer railcar on level track, vertical wheel loads were measured while raising both wheels on one side of a truck. Tests were performed on all four corners of the railcar.

At 2.0 inches of deflection, vertical load at any wheel may not fall below 60 percent of the nominal static load. At 3.0 inches of deflection, no permanent damage should be produced and vertical load at any wheel may not fall below 40 percent of the nominal static load.

Carbody twist tests were completed July 26, 2019. Dr. Xinggao Shu, TTCI Principal Investigator II, witnessed the carbody twist equalization tests as the AAR Observer per S-2043 requirements. The buffer railcar met criteria for carbody twist equalization. No permanent deformation occurred at 3 inches of carbody twist.

Table 17 shows the worst-case test results. Figure 34 displays the percent load for all wheels during the test where L3 and L4 wheels were lifted.

Table 17. Carbody Twist Equalization Results

Condition	B-End Right Truck Side Location	
	Percent Load	Wheel
2-inch raise	88	Axle 4 Right
3-inch raise	81	Axle 3 Right and Axle 4 Right
Condition	**B-End Left Truck Side Location**	
	Percent Load	**Wheel**
2-inch raise	77	Axle 3 Left
3-inch raise	74	Axle 3 Left and Axle 4 Left
Condition	**A-End Right Truck Side Location**	
	Percent Load	**Wheel**
2-inch raise	79	Axle 2 Right
3-inch raise	74	Axle 1 Right and Axle 2 Right
Condition	**A-End Left Truck Side Location**	
	Percent Load	**Wheel**
2-inch raise	75	Axle 2 Left
3-inch raise	74	Axle 1 Left and Axle 2 Left

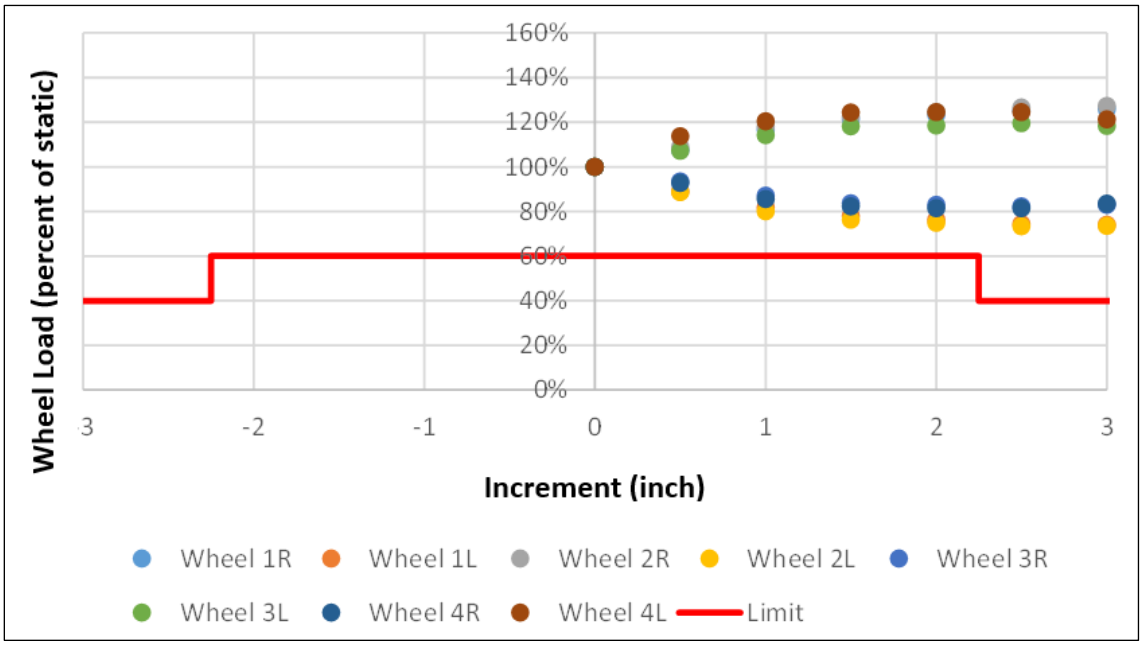


Figure 34. Carbody Twist for L3 and L4 Results for All Wheels

5.2.3 Static Curve Stability

The static curve stability test was performed July 29, 2019. Abe Meddah, TTCI Principal Investigator II, and Adam Klopp, TTCI principal Investigator I, witnessed the static curve stability test as the AAR Observer per S-2043 requirements. The buffer railcar was coupled to a short base car on one end and a long car having 90-foot over strikers, 66-foot truck centers, 60-inch couplers, and conventional draft gear on the other end. The 200,000-pound load was applied and held for more than 20 seconds. The train was chocked in a 10-degree flat curve at the Urban Rail Building at TTC.

The railcar must not experience wheel lift or suspension separation during this test. Wheel lift is defined as 1/8-inch lift when measured 2 5/8 inches from the rim face with a feeler gauge. Figure 35 shows the buffer railcar during the static curve stability test. Figure 36 shows the clearance being checked with a feeler gauge. The buffer railcar met the criteria for the static curve stability test.



Figure 35. Buffer Railcar during the Static Curve Stability Test



Figure 36. Checking Clearance during the Static Curve Stability Test

5.2.4 Horizontal Curve Negotiation

The horizontal curve negotiation test is performed to identify areas of interference between components of buffer railcar suspension, structure, and brake system. The test was performed in a 150-foot radius curve on July 30, 2019. Adam Klopp, TTCI Principal Investigator I, witnessed the horizonal curve negotiation test as the AAR Observer per S-2043 requirements. No interference was

noted; therefore, the buffer railcar met the criteria for this test. Figure 37 displays an area where clearance was closest. Note: an inspector noted that the rubber brake cylinder gasket contacted the center sill; however, it was determined that it was not significant.



Figure 37. Clearance between Brake Cylinder and Center Sill with Buffer Railcar in 150-foot Radius Curve

5.3 Static Brake Tests

AAR Standard S-2043 requires that static brake force measurements be made per AAR MSRP Section E, Standard S-401 and that a single-car air brake test must be performed per the AAR MSRP Section E, Standard S-486. These tests were conducted by Kasgro prior to delivery of the buffer railcar to TTC.

The static brake force measurements were conducted on IDOX 20001 and 20002, at the Kasgro facility in New Castle, Pennsylvania on December 4 and 5, 2019. The single car air brake tests were conducted on IDOX 20001 and 20002, also at the Kasgro facility, Pennsylvania on February 11, 2019.

AAR Standard S-401 testing is documented in a letter from Matt DeGeorge to Jon Hannafious (TTCI) dated August 20, 2020. AAR Standard S-486 testing is documented in a letter from Mike Yon to David Cackovic (TTCI) dated March 12, 2019. Both letters are included in Appendix B.

5.4 Structural Tests

Structural tests were conducted to demonstrate the railcar's ability to withstand the rigorous railroad load environment and to verify the accuracy of the structural analysis. AAR Standard S-2043 refers to AAR MSRP Section C Part II, Specification M-1001, paragraph 11.3 (Reference 1) for structural testing details and criteria.

The AAR Standard S-2043 requirement calls for dimensional measurements at the start and conclusion of the structural tests and strain measurements during testing. In addition, visual inspections for damage are required before and after the individual tests. A key criterion from Reference 1 is that no permanent deformation shall be produced by the testing. This is interpreted as no strain exceeding material yield.

The buffer railcar was instrumented with 51 strain gauges. Gauges were located on the top and bottom of the railcar in key locations specified by Kasgro, the railcar designer. These measurements were used to monitor strain during each of the structural tests and to verify finite element analysis. Figure 35 shows the location of strain measurements. A description of each location is included in Appendix A, and further detail on the locations, placement, and orientation of the gages is found in Appendix C. The gauges were zeroed before each test. Results have been converted from microstrain (με) to stress (σ, ksi) with a positive value indicating tension and a negative value indicating compression using the following formula:

$$\sigma = E\mu\varepsilon/1{,}000{,}000$$

Where:
σ = stress (ksi)
E = Young's modulus (29,000 ksi)
με = microstrain (inch/inch)

The MSRP section C-II, Paragraph 4.2.2.4, states "…the allowable design stress shall be the yield or 80% of ultimate, whichever is lower, or the critical buckling stress." Kasgro's critical buckling analysis (Appendix D) shows that buckling is not limiting for the buffer car. The allowable compressive or tensile stress is yield strength of the material the strain gages were applied to, 50,000 psi for all the buffer car body components, per Kasgro.

The structural tests include the following:

- Preliminary and post-test inspection
- Squeeze (compressive end) load
- Coupler vertical loads
- Jacking
- Twist
- Impact

Structural test results are provided in Sections 5.4.1 to 5.4.6.

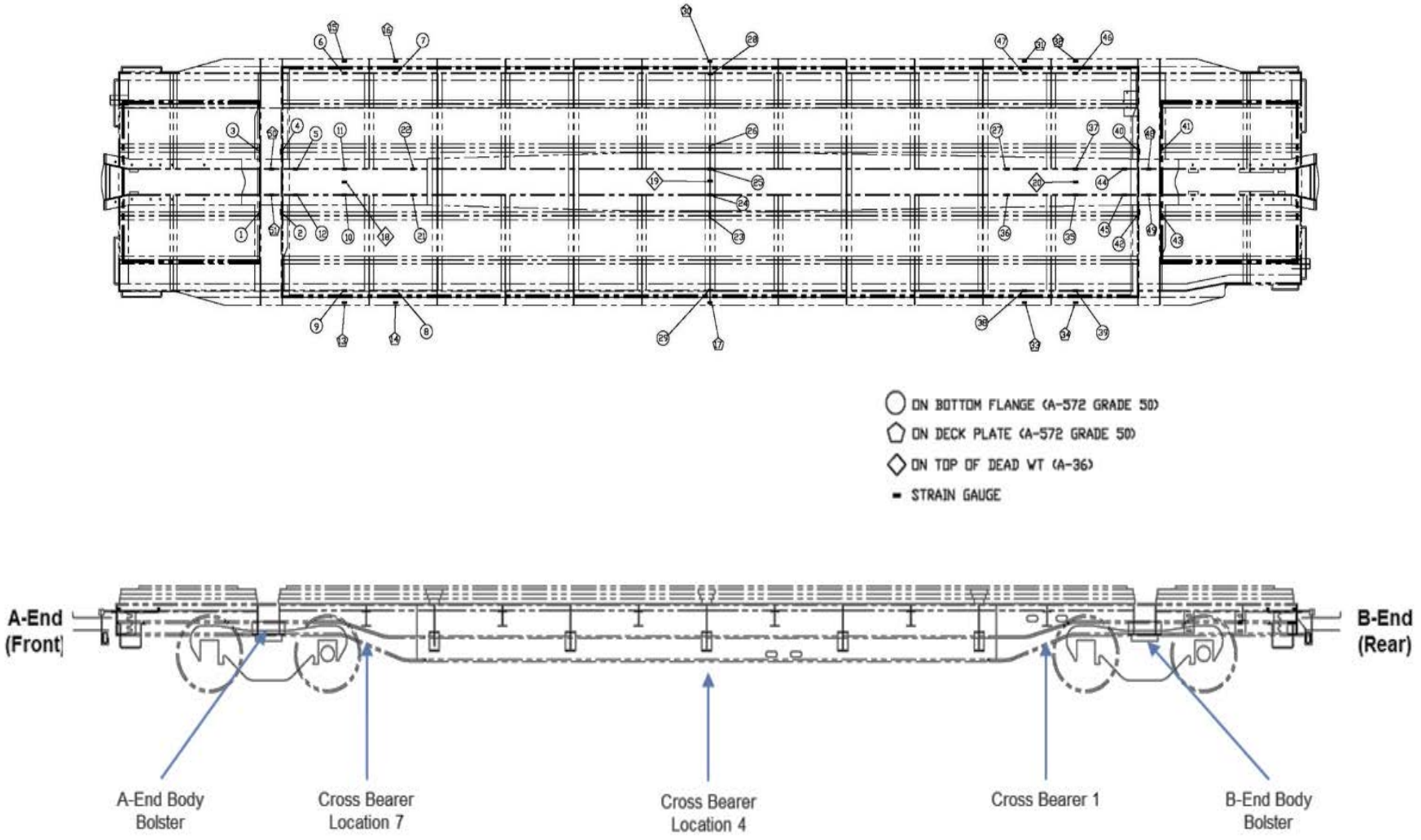


Figure 38. Location of Strain Measurements Monitored during Structural Testing

5.4.1 Preliminary and Post Test Inspection

The buffer railcar length was measured from striker to striker, as well as over the pulling faces. Table 18 shows the results of these measurements before and after tests were performed. The maximum variation in the measurements 9/16 inch, which is considered negligible considering the various clearances in the railcar and the measurement accuracy.

A survey total station was used to measure the shape of the railcar deck before and after testing. The final structural test performed was the 1 million-pound squeeze test. It was considered prudent to document the shape of the deck both before and after this test was conducted so that if any deformation did occur the source of the failure could be more easily identified. Figure 39 shows the results of the level measurements at several points during testing. No change in shape of the deck was noted.

Table 18. Survey Measurements

Condition	Striker to Striker	Length over Pulling Faces
Initial Measurement	61 feet 8 1/16 inches	66 feet 6 5/16 inches
Post Squeeze	61 feet 8 1/2 inches	66 feet 6 1/2 inches

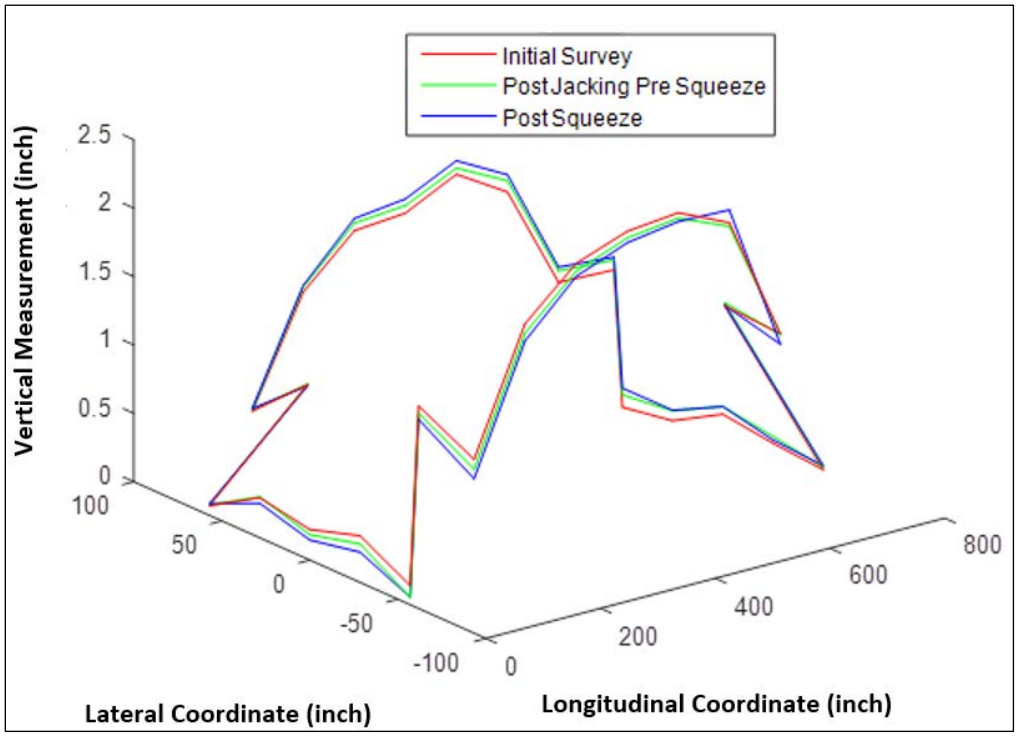


Figure 39. Results of Level Loop around the Buffer Railcar Deck, Zero Inches Longitudinal at A-End of Car

5.4.2 Squeeze (Compressive End) Load

The squeeze (compressive end) load test was performed on November 20, 2019, to verify that the buffer railcar can withstand compressive longitudinal loads. Adam Klopp, TTCI Principal Investigator I, witnessed the squeeze (compressive end) test as the AAR Observer per S-2043 requirements. A horizontal compressive static load was applied at the centerline of the draft system of car interface areas using TTCI's squeeze fixture. The load was cycled up to 750,000 pounds three

times, and then on the fourth cycle the load was increased to 1,000,000 pounds. The applied load was monitored with a load cell. The railcar met criteria for the compressive end load test. No permanent deformation or suspension separation was noted. The maximum measured stress was 60 percent of material yield.

Table 19 shows the summary results from the compressive end load test for the locations with highest measured stress at 1,000,000 pounds of applied load. No evidence of gradual zero-shift (plastic deformation) was noted. A complete set of stress results at maximum compressive load are shown in Appendix E, including a time history plot of the highest stressed areas showing no residual strain.

Table 19. Highest Stress Locations from Compressive End Load Test

Channel Name	Approximate Location	Measured Stress (ksi)	Yield Stress (ksi)	Measured Stress as Percent of Yield
SGBF11	RH edge of bottom flange of center sill, forward of cross bearer 7	-30	50	60%
SGBF10	LH edge of bottom flange of center sill, forward of cross bearer 7	-28	50	56%
SGBF37	RH edge of bottom flange of center sill, aft of cross bearer 1	-26	50	52%
SGDP35	LH edge of bottom flange of center sill, aft of cross bearer 1	-24	50	48%

5.4.3 Coupler Vertical Loads

A 50,000-pound vertical load was applied to the coupler in the upward and downward directions. The test was performed on August 1, 2019, and August 6, 2019. Abe Meddah, TTCI Principal Investigator II, witnessed the test on August 1, 2019, and Dr. Xinggao Shu, TTCI Principal Investigator II, witnessed the coupler vertical loads tests on August 6, 2019, as the AAR Observer per S-2043 requirements. The buffer railcar met criteria for the 50,000-pound coupler vertical load test. No permanent deformation was noted. The maximum measured stress was 26 percent of material yield.

The railcar was inspected before and after the tests with no damage noted. Figure 40 shows no damage to the coupler carrier plate after the coupler vertical load test.

Table 20 shows summary results from the coupler vertical load test for the locations with the highest measured stress. No evidence of gradual zero-shift (plastic deformation) was noted. A complete summary of stress results at the 50,000-pound load is shown in Appendix F.



Figure 40. Coupler Carrier Plate after the Coupler Vertical Load Test

Table 20. Buffer Railcar Vertical Coupler Force Test Results Summary

Channel Name	Approximate Location	Measured Stress (ksi)	Yield Stress (ksi)	Measured Stress as Percent of Yield
Load applied upward				
SGDP35	LH edge of bottom flange of center sill, aft of cross bearer 1	12	50	24%
SGBF37	RH edge of bottom flange of center sill, aft of cross bearer 1	13	50	26%
Load applied downward				
SGDP35	LH edge of bottom flange of center sill, aft of cross bearer 1	-12	50	24%
SGBF37	RH edge of bottom flange of center sill, aft of cross bearer 1	-13	50	26%

5.4.4 Jacking

The jacking test was performed to verify a fully loaded railcar can be lifted free of the trucks when supported at the jacking pads. The test was conducted on July 31, 2019. Dr. Xinggao Shu, TTCI Principal Investigator II, witnessed the jacking test as the AAR Observer per S-2043 requirements. The buffer railcar met criteria for the jacking test. No permanent deformation was noted. The maximum measured stress was 12 percent of material yield.

The test was conducted on the B-end of the buffer railcar. The maximum stress during the test occurred on gauge SGBF40 and gauge SGBF42. Figure 41 shows the location of these gauges. Table 21 presents the summary results. No evidence of gradual zero-shift (plastic deformation) was noted. Plots are provided in Appendix G for all gauges.

Table 21. Buffer Railcar Jacking Test Results Summary

Channel Name	Approximate Location	Measured Stress (ksi)	Yield Stress (ksi)	Measured Stress as Percent of Yield
SGBF42	Front of bottom flange of B-end body bolster near center sill – LH side	6.2	50	12%
SGBF40	Front of bottom flange of B-end body bolster near center sill – RH side	6.1	50	12%

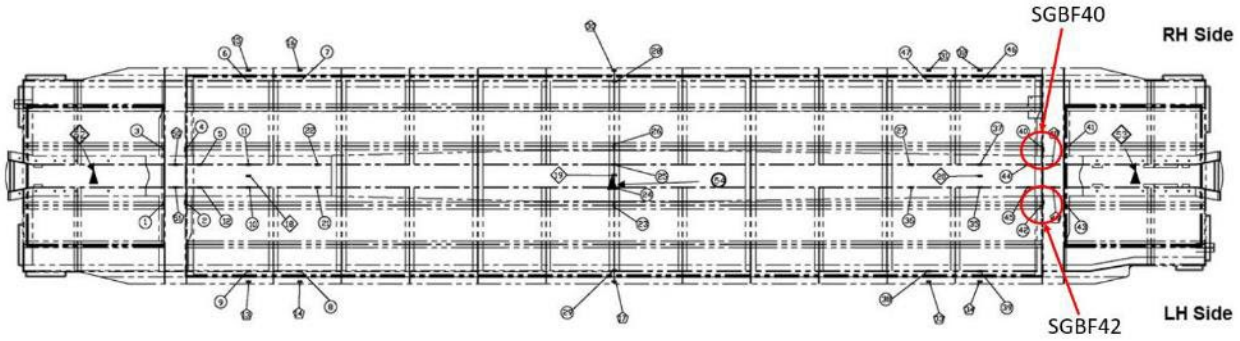


Figure 41. Maximum Stressed Locations SGBF40 and SGBF42

As Figure 42 in the section below shows, the jacking test was conducted while the MSU actuator brackets were installed for other testing. Because of this, the jacks on the B-end could not be placed directly at the jacking pad location and were instead placed approximately 10 inches further away from the railcar centerline. Kasgro simulated the jacking test using FEA assuming the jacks were placed at the jacking pad locations and separately with the jacks placed at the MSU brackets and found that the predicted stress at these gage locations changed from 5.3 ksi when loaded at the jacking pads to 4.4 ksi when loaded at the MSU brackets. The measured and predicted stresses are low with respect to the yield stress for either the jacking pad or MSU bracket loading positions.

5.4.5 Twist

The twist test consists of two parts. The buffer railcar met criteria for both parts of the twist test. No permanent deformation was noted. The maximum measured stress was 18 percent of material yield.

The first part was performed at the same time as the carbody twist equalization test described in Section 5.2.2. As with the carbody twist equalization, vertical wheel loads were measured while raising both wheels on one side of a truck. Tests were performed on all four corners of the buffer railcar. The only additional requirement for the structural test is that strain data be measured. This portion (Part 1) of the twist test was completed on July 26, 2019. Dr. Xinggao Shu, TTCI Principal Investigator II, witnessed the twist (Part 1) test as the AAR Observer per S-2043 requirements.

The largest strain measured during the test corresponds to 1.2 ksi, recorded on strain gauge SGDP48, when the wheels on the A-end, LH side were raised 3 inches. Table 22 presents the results summary for the buffer railcar twist test Part 1.

Table 22. Summary of Buffer Railcar Twist Test Part 1 Results

Channel Name	Corner Raised	Approximate Location	Measured Stress (ksi)	Yield Stress (ksi)	Measured Stress as Percent of Yield
SGDP48	A-LH	Top of deck plate, longitudinally centered over B-end body bolster, above RH edge of center sill	1.2	50	2%
SGDP49	A-RH	Top of deck plate, longitudinally centered over B-end body bolster, above LH edge of center sill	0.82	50	2%
SGDP49	B-LH	Top of deck plate, longitudinally centered over B-end body bolster, above LH edge of center sill	0.84	50	2%
SGDP48	B-RH	Top of deck plate, longitudinally centered over B-end body bolster, above RH edge of center sill	1.1	50	2%

The second portion (Part 2) of the carbody twist test requires that the loaded carbody be supported on the four jacking locations. One corner is then lowered 3 inches. This test was conducted on July 31, 2019. Dr. Xinggao Shu, TTCI Principal Investigator II, witnessed the second portion of the carbody twist test as the AAR Observer per S-2043 requirements. Figure 42 shows the end of the carbody supported on jacks during this test. Table 24 presents the results summary for the buffer railcar twist test Part 2. No evidence of gradual zero-shift (plastic deformation) was noted. Additional plots for all gauges are shown in Appendix H.



Figure 42. The End of the Railcar Supported by Four Pneumatic Jacks during the Twist Test

Table 23 shows the measurements at the four corners during the test, with the planned drop being about 3 inches. However, as the B-end, left hand jack was lowered to 3 inches, the carbody only dropped 2 11/16 inches. No obstructions/supports allowed weight to be carried in another path (CCSBs, etc.); the carbody torsional stiffness limited this deflection. Table 24 shows the maximum measured stress. The carbody strain gauges SGBF40 and SGBF11 showed the maximum (tension) and minimum (compression) stress during the test. Gauge SGBF40 showed a maximum peak value of -3.3 ksi, and gauge SGBF11 showed a minimum peak value of 7.6 ksi. These locations (shown on Figure 43) were inspected after the test and no indication of yielding was found.

Table 23. Height of the Four Corners of the Loaded Carbody

Location	Height Before Test	Height During Test
AL	37 inches	36 7/8 inches
AR	37 1/8 inches	37 1/8 inches
BL	37 1/8 inches	34 7/16 inches
BR	37 inches	37 inches

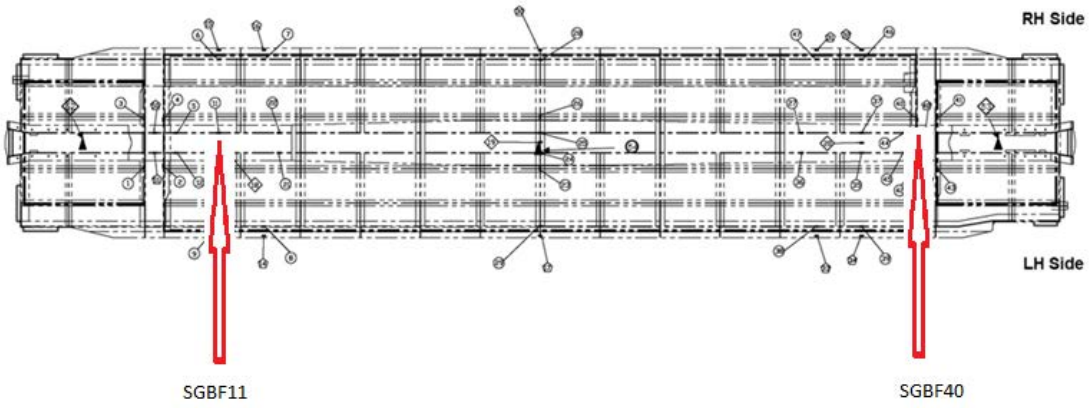


Figure 43. SGBF11 and SGBF40 Locations

Table 24. Summary of Buffer Railcar Twist Part 2 Test Results

Channel Name	Approximate Location	Measured Stress (ksi)	Yield Stress (ksi)	Measured Stress as Percent of Yield
SGBF11	RH edge of bottom flange of center sill, forward of cross bearer 7	-3.3	50	7%
SGBF40	Front of bottom flange of B-end body bolster near center sill – RH side	7.6	50	15%

As Figure 42 shows, the twist test was conducted while the MSU actuator brackets were installed for other testing. Because of this, the jacks on the B-end could not be placed directly at the jacking pad location and were instead placed approximately 10 inches further away from the railcar centerline. Kasgro simulated the twist test with FEA assuming the jacks were placed at the jacking pad locations and separately with the jacks placed at the MSU brackets and found that the predicted stress at SGBF11 changed from -5 ksi when loaded at the jacking pads to -1.9 ksi when loaded at the MSU brackets. The predicted stress at SGBF40 changed from 7.4 ksi when loaded at the jacking

pads to 6.7 ksi when loaded at the MSU brackets. The measured and predicted stresses are low with respect to the yield stress for either the jacking pad or MSU bracket loading positions.

5.4.6 Impact

Impact tests were conducted August 1, 2019. Abe Meddah, TTCI Principal Investigator II, witnessed the impact test as the AAR Observer per S-2043 requirements. The buffer railcar met criteria for the impact tests. The railcar was inspected after the test, and no damage was found. There was no permanent deformation of the railcar. The maximum measured strain was 21 percent of material yield.

The test was conducted by pulling the railcar a specified distance up a constant grade and allowing it to roll into a standing string of three loaded hopper cars equipped with M-901E draft gears. No brakes were applied on the anvil string except for the handbrake on the last railcar. There was no free slack between anvil cars, but the draft gears were not compressed.

The lead hopper car had an instrumented coupler installed to measure the force during coupling. The speed was measured with a speed tach mounted on the railcar. Data was recorded at 1,250 samples per second. Test runs were stopped at 9.6 mph, because at that speed the coupler force was greater than the 600,000-pound design load specified in Section 4.1.10 for a railcar equipped with a 15-inch cushion unit.

The peak magnitude stress was found for each run. In cases where the peak magnitude stress is compressive, it is shown as a negative value. In contrast to most of the other structural tests, the stress value given is dynamic, or relative to the stress just before the test. Table 25 shows the maximum stress for each test run. In each case, the maximum stress is at location SGBF37. No evidence of gradual zero-shift (plastic deformation) was noted. Appendix I provides additional plots of all gauges during the tests.

AAR Standard S-2043 refers to MSRP Section C Part II, Specification M-1001, paragraph 11.3.4.1 (Reference 1) for impact testing details. Successive tests are required at 2-mph increments starting at 6 mph or less. As Table 25 shows, the increment between the first two test runs slightly exceeded the specified 2-mph. This was considered acceptable due to the inherent variation in speed for this type of testing and because the coupler forces remained low.

Table 25. Maximum Stresses Measured during Impact Tests

Speed	Coupler Load (pounds)	Gauge Location	Measured Stress (ksi)	Yield Stress (ksi)	Measured Stress as percent of Yield
4.7	196,081	SGBF37*	-3.6	50	7%
7.2	406,914	SGBF37	-11	50	22%
8.4	492,319	SGBF37	-12	50	24%
9.6	611,648	SGBF37	-16	50	32%
*SGBF 37 is at the right edge of the bottom flange of the center sill, aft of cross bearer 1.					

5.4.7 Securement System

AAR Standard S-2043, Paragraph 5.4.7, requires verification of securement system strength. This paragraph refers to the system of attachment for the HLRM cask to the railcar. It does not apply to the buffer railcar because it is not equipped to carry HLRM. Kasgro analyzed the securement of the ballast weight against the open top loading rules (Appendix J).

5.5 Dynamic Tests

Dynamic tests required by AAR Standard S-2043 include:

- Hunting
- Twist and roll
- Yaw and sway
- Dynamic curving
- Pitch and bounce (Chapter 11)
- Special pitch and bounce
- Single bump test
- Limiting spiral negotiation
- Normal spiral negotiation
- Curving with single rail perturbation
- Standard Chapter 11 constant curving
- Special trackwork

The dynamic tests are conducted to measure compliance with criteria listed in Table 5.1 of AAR Standard S-2043. That table is reproduced here as Table 26. Test results are provided in this report Sections 5.5.1 to 5.5.12.

AAR Standard S-2043 specifies that non-curving tests be performed up to 75 mph where deemed safe by the test engineer. However, the AAR Standard S-2043 limiting criteria do not apply to tests at speeds over 70 mph. These tests are performed only to further quantify performance and establish trends. Test results from tests at speeds over 70 may be included in worst-case performance statistics depending on the following results:

- If the results of tests at speeds over 70 mph meet the test criteria, the results are considered when compiling performance statistics.
- When tests over 70 mph do not meet the criteria, the runs are excluded from consideration for performance statistics, and suitable comments are made in the body of that section.

The buffer railcar was pulled from the B-end during most dynamic tests. Instrumented wheelsets (IWS) for measuring wheel/rail forces were placed in Axles 1 through 4, as Figure 44 shows. Also, AAR Standard S-2043 requires that curving tests and special trackwork tests be performed in the trailing position; therefore, these tests were repeated with the A-end leading as seen at the bottom of Figure 44.

Standard S-2043 and, by reference, MSRP Section C Part II, Specification M-1001 (Reference 1) require a minimum rail coefficient of friction of 0.4 for hunting, twist and roll, dynamic curve, limiting spiral negotiation, and constant curve tests. Rail friction levels were measured for each of the dynamic tests and are reported in the appropriate sections.

Table 26. AAR Standard S-2043 Dynamic Testing Performance Criteria

Criterion	Limiting Value	Notes
Maximum car body roll angle (degree)	4	Peak-to-peak.
Maximum wheel L/V	0.8	Not to exceed indicated value for a period greater than 50 msec. and for a distance greater than 3 feet per instance*.
95th percentile single wheel L/V (constant curving tests only)	0.6	Not to exceed indicated value. Applies only for constant curving tests.
Maximum truck side L/V	0.5	Not to exceed indicated value for a duration equivalent to 6 feet of track per instance.
Minimum vertical wheel load (%)	25	Not to fall below indicated value for a period greater than 50 msec. and for a distance greater than 3 feet per instance*.
Peak-to-peak car body lateral acceleration (G)	1.3 0.60	For non-passenger-carrying railcars For passenger-carrying railcars
Maximum car body lateral acceleration (G)	0.75 0.35	For non-passenger-carrying railcars For passenger-carrying railcars
Car body lateral acceleration standard deviation (G)	0.13	Calculated over a 2,000-foot sliding window every 10 feet over a tangent track section that is a minimum of 4,000 feet long.
Maximum car body vertical acceleration (G)	0.90 0.60	For non-passenger-carrying railcars For passenger-carrying railcars
Maximum vertical suspension deflection (%)	95	Suspension bottoming not allowed. Maximum compressive spring travel shall not exceed 95% of the spring travel from the empty car height of the outer load coils to solid spring height.
Maximum vertical dynamic augment acceleration (g)	0.9	Suspension bottoming not allowed. Vertical dynamic augment accelerations of a loaded car shall not exceed 0.9 G.

AAR Standard S-2043 states that these criteria must be met for all tests performed according to Sections 5.5.7 to 5.5.16. Some exceptions are:

- The notes for carbody lateral acceleration standard deviation require it be computed over a 2,000-foot sliding window in a 4,000-foot tangent track section so that value will only be reported for high-speed stability tests.
- L/V and vertical wheel load data is not available for high-speed stability tests with KR wheels.

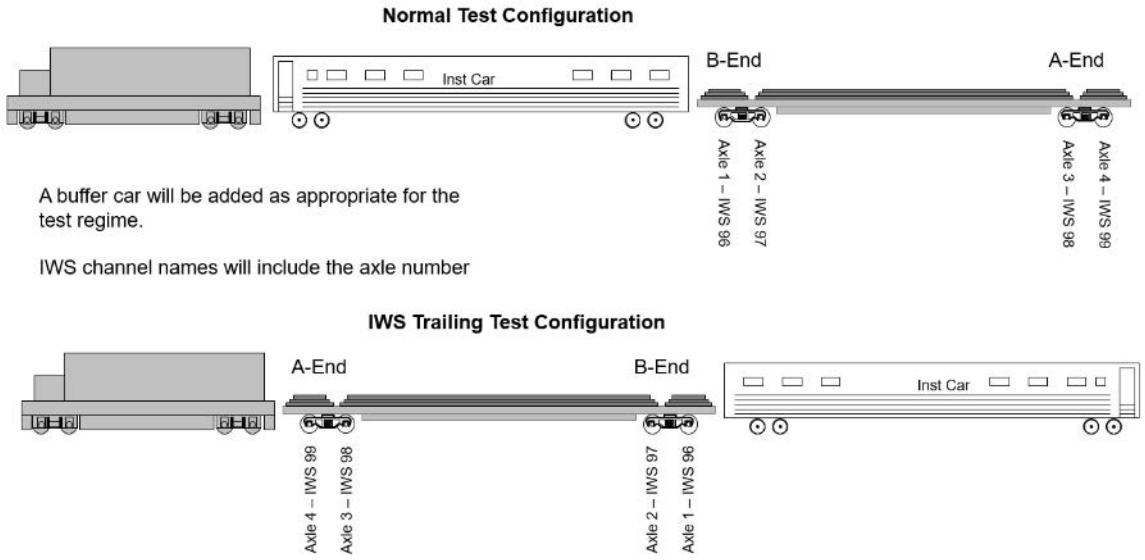


Figure 44. Location of IWS during Dynamic Tests

5.5.1 Hunting

Hunting tests were performed twice, first with wheelsets having KR profiles, and second with IWS having AAR-1B narrow flange profiles. Table 27 shows the date each test was conducted and the measured rail friction. Dr. Xinggao Shu, TTCI Principal Investigator II, witnessed the hunting test with KR profiles on May 22, 2019, and Adam Klopp, TTCI Principal Investigator I, witness the hunting test with IWS on August 15, 2019, as the AAR Observer per S-2043 requirements. The buffer railcar met the criteria for hunting in both conditions.

Table 27. Buffer Railcar Hunting Test Dates and Rail Friction Data

Test Condition	Date	Coefficient of Friction	
		Inside Rail	Outside Rail
Buffer Car with KR profiles	May 22, 2019	0.50	0.50
Buffer Car with IWS AAR-1B narrow flange profiles	August 15, 2019	0.49	0.49

Accelerations above the maximum criteria were observed in the curves adjacent to the test zone with KR profiles. TTCI notified EEC of higher accelerations during their June 2019 monthly meeting. The EEC determined that the criteria do not apply in the curve, and that because the buffer railcar was stable in the tangent test zone, criteria were met. Criteria were met in both tangent and the adjacent curves with AAR-1B narrow flange profiles.

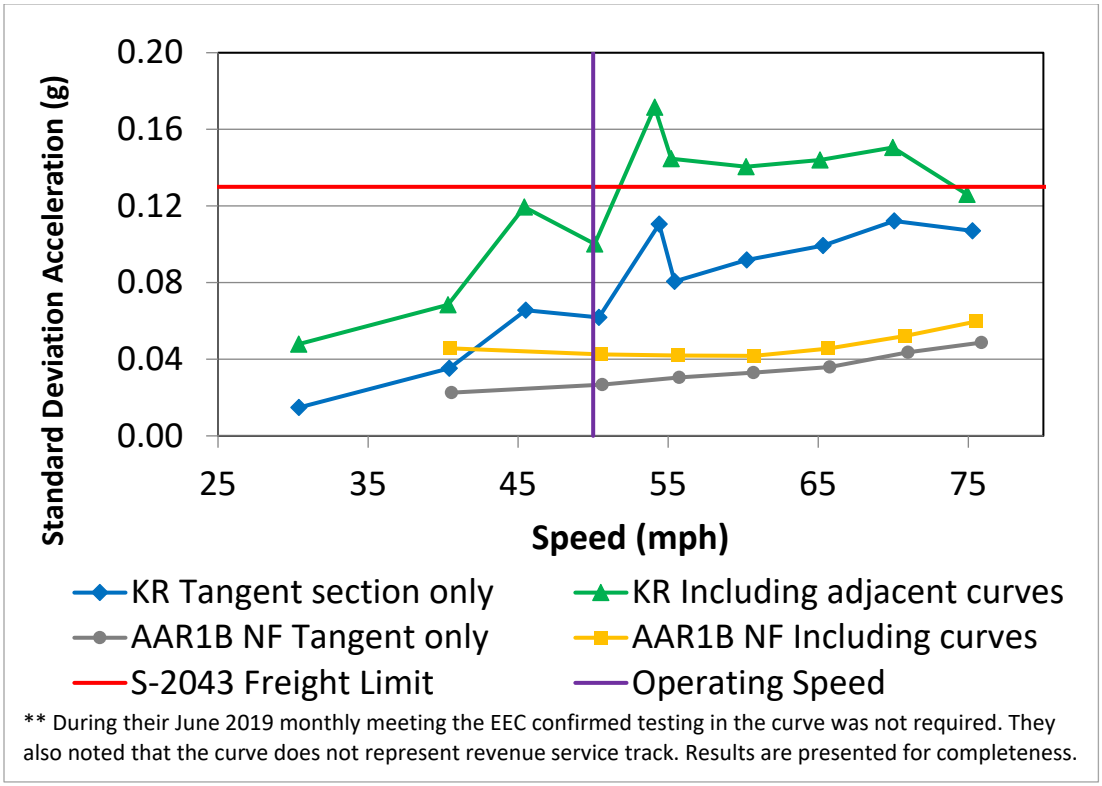
Hunting tests are performed on a tangent section of the Railroad Test Track (RTT) between markers R39 and R33.45. Data is also recorded in the curves adjacent to the test zone to monitor performance. In Table 28, data labeled “including adjacent curves” refers to data collected between R43 and R26, which includes portions of the adjacent curves and spirals. Data labeled “tangent section only” refers to data collected in the tangent section between R39 and R33.45. As noted, the EEC determined that only tangent zone data should be compared to criteria, but the data is included here for reference. Table 28 shows a summary of buffer railcar hunting test results, and Figure 45 shows a plot of 2,000-foot standard deviation of lateral acceleration versus speed for the tangent zone and the zone including adjacent curves. Figure 45 shows a line labeled Operating Speed at 50

mph on the graph. This reflects the recommendation in AAR Circular OT-55-O "Recommended Railroad Operating Practices for Transportation of Hazardous Materials" that trains carrying spent nuclear fuel or HLRM be restricted to a maximum speed of 50 mph.

Table 28. Buffer Railcar Hunting Test Results

Criterion	Limiting Value	KR Wheel Profile	IWS with AAR 1B Narrow Flange Wheel Profile
		Including Adjacent curves/ Tangent Section only	
Maximum carbody roll angle (degree)	4	0.8 / 0.7	0.5 / 0.4
Maximum Wheel L/V Ratio	0.80	Not Measured*	0.26 / 0.12
Maximum Truck Side L/V Ratio	0.50	Not Measured*	0.17 / 0.11
Minimum Vertical Wheel Load (%)	25%	Not Measured*	64% / 77%
Peak-to-peak carbody lateral acceleration (g)	1.3	0.67 / 0.37	0.32 / 0.25
Maximum carbody lateral acceleration (g)	0.75	0.48 / 0.20	0.19 / 0.18
Lateral carbody acceleration standard deviation (g)	0.13	0.17** / 0.11	0.06 / 0.05
Maximum carbody vertical acceleration (g)	0.9	0.29 / 0.28	0.29 / 0.27
Maximum vertical suspension deflection (%)	95	41% / 31%	53% / 53%
Critical Speed	70 mph	50mph** / >75 mph	>75 mph

* L/V and vertical wheel load data is not available for high-speed stability tests with KR wheels (IWS required).
** During their June 2019 monthly meeting the EEC confirmed testing in the curve was not required. They also noted that the curve does not represent revenue service track. Results are presented for completeness.



** During their June 2019 monthly meeting the EEC confirmed testing in the curve was not required. They also noted that the curve does not represent revenue service track. Results are presented for completeness.

Figure 45. 2,000-foot Standard Deviation of Lateral Acceleration versus Speed

5.5.2 Twist and Roll

The twist and roll test was performed on August 20, 2019, and the coefficient of friction was greater than 0.50 on the east rail and greater than 0.50 on the west rail. Adam Klopp, TTCI Principal Investigator I, witnessed the twist and roll test as the AAR Observer per S-2043 requirements. The buffer railcar met the criteria for twist and roll. Table 29 contains a summary of the data from twist and roll tests, and Figure 46 shows a plot of peak-to-peak carbody roll versus speed.

Table 29. Buffer Railcar Twist and Roll Test Results

Criterion	Limiting Value	Test Result
Roll angle (degree)	4.0	1.7
Maximum wheel L/V	0.8	0.2
Maximum truck side L/V	0.5	0.16
Minimum vertical wheel load (%)	25%	66%
Lateral peak-to-peak acceleration (g)	1.3	0.55
Maximum lateral acceleration (g)	0.75	0.31
Maximum vertical acceleration (g)	0.90	0.26
Maximum vertical suspension deflection (%)	95%	48%

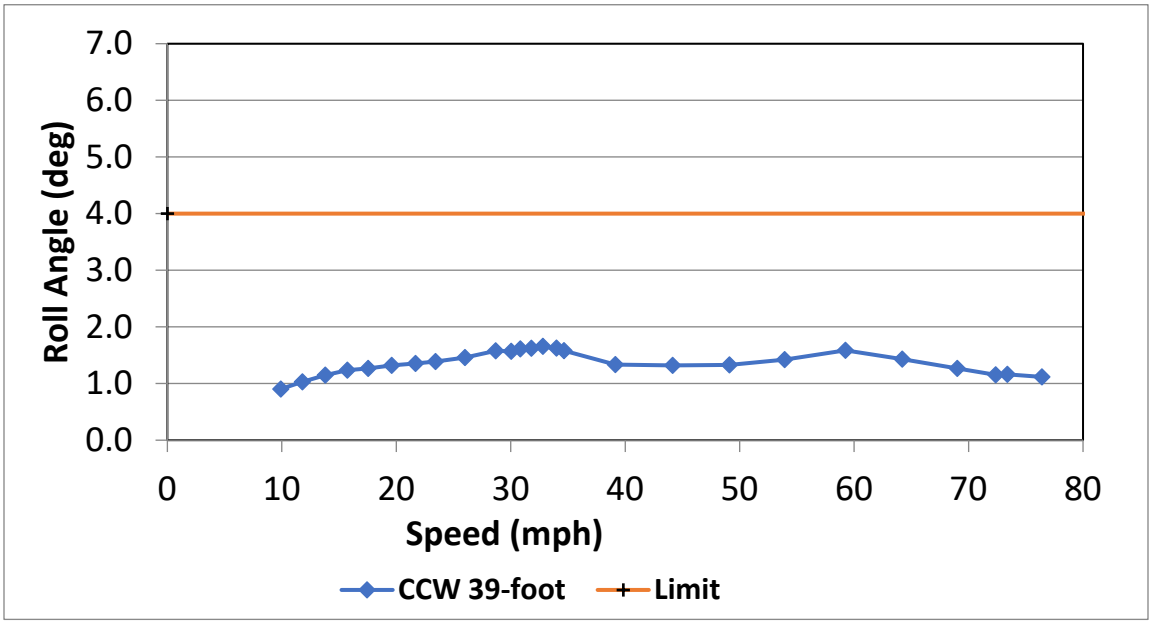


Figure 46. Buffer Railcar Twist and Roll Test, Maximum Carbody Roll versus Speed

5.5.3 Yaw and Sway

Yaw and Sway tests were conducted on August 21, 2019, and the coefficient of friction was 0.49 on the east rail and 0.50 on the west rail. Adam Klopp, TTCI Principal Investigator I, witnessed the yaw and sway test as the AAR Observer per S-2043 requirements. The buffer railcar met the criteria for yaw and sway. Table 30 shows the results of the tests up to 75 mph. Figure 47 shows a plot of the peak-to-peak lateral acceleration versus speed.

Table 30. Yaw and Sway Test Results to 75 mph

Criterion	Limiting Value	Test Result
Roll angle (degree)	4.0	2.0
Maximum wheel L/V	0.8	0.6
Maximum truck side L/V	0.5	0.3
Minimum vertical wheel load (%)	25%	50%
Lateral peak-to-peak acceleration (g)	1.3	0.9
Maximum lateral acceleration (g)	0.75	0.5
Maximum vertical acceleration (g)	0.9	0.3
Maximum vertical suspension deflection (%)	95%	67%

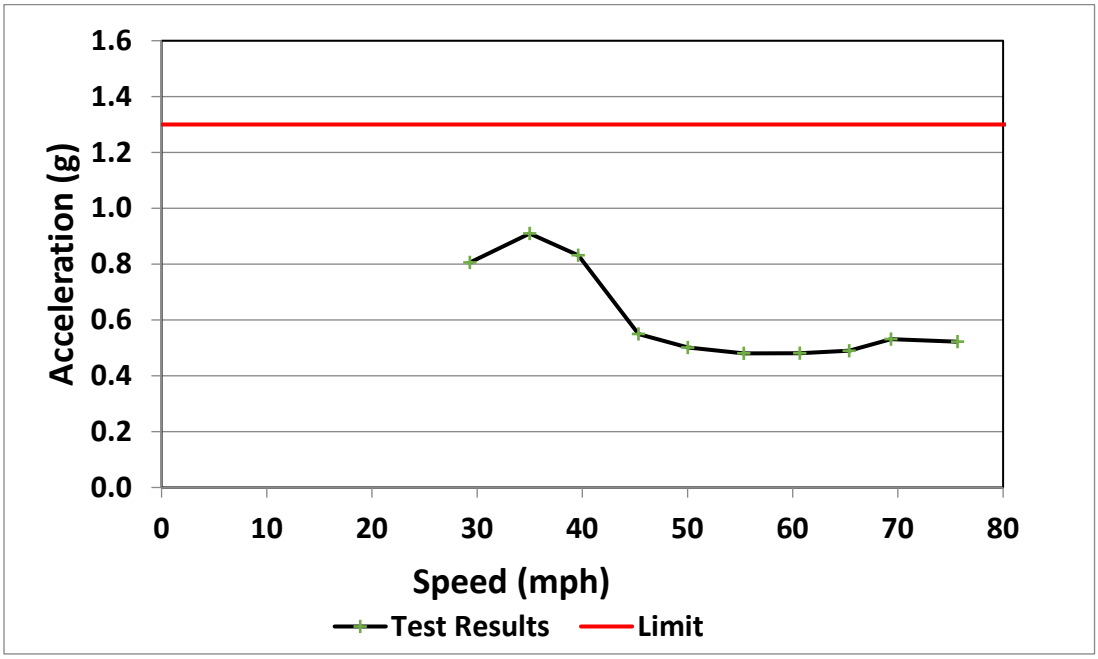


Figure 47. Buffer Railcar Yaw and Sway Test, Maximum Peak-to-peak Lateral Acceleration versus Speed

5.5.4 Dynamic Curving

Dynamic curve testing was conducted in the CW and CCW direction, with A-end leading and with B-end leading. Table 31 lists the test dates and the rail friction data. Adam Klopp, TTCI Principal Investigator I, witnessed the dynamic curving test as the AAR Observer per S-2043 requirements. The buffer railcar met criteria for dynamic curving. Table 32 contains a summary of the buffer railcar dynamic curving test results. Figure 48 shows a plot of maximum wheel L/V versus speed.

Table 31. Buffer Railcar Dynamic Curving Test Dates and Rail Friction Data

Test Condition	Date	Coefficient of Friction	
		Inside Rail	Outside Rail
Buffer car, A-end leading, CW	8-18-2019	0.48	0.46
Buffer car, A-end leading, CCW	8-19-2019	0.47	0.48
Buffer car, B-end leading, CW	8-16-2019	0.42	0.42
Buffer car, B-end leading, CCW	8-18-2019	0.42	0.45

Table 32. Buffer Railcar Dynamic Curving Test Results

Criterion	Limiting Value	Test Result
Roll angle (degree)	4	1.4
Maximum wheel L/V	0.8	0.66
Maximum truck side L/V	0.5	0.45
Minimum vertical wheel load (%)	25%	34%
Lateral peak-to-peak acceleration (g)	1.3	0.96
Maximum lateral acceleration (g)	0.75	0.69
Maximum vertical acceleration (g)	0.90	0.16
Maximum vertical suspension deflection (%)	95%	42%

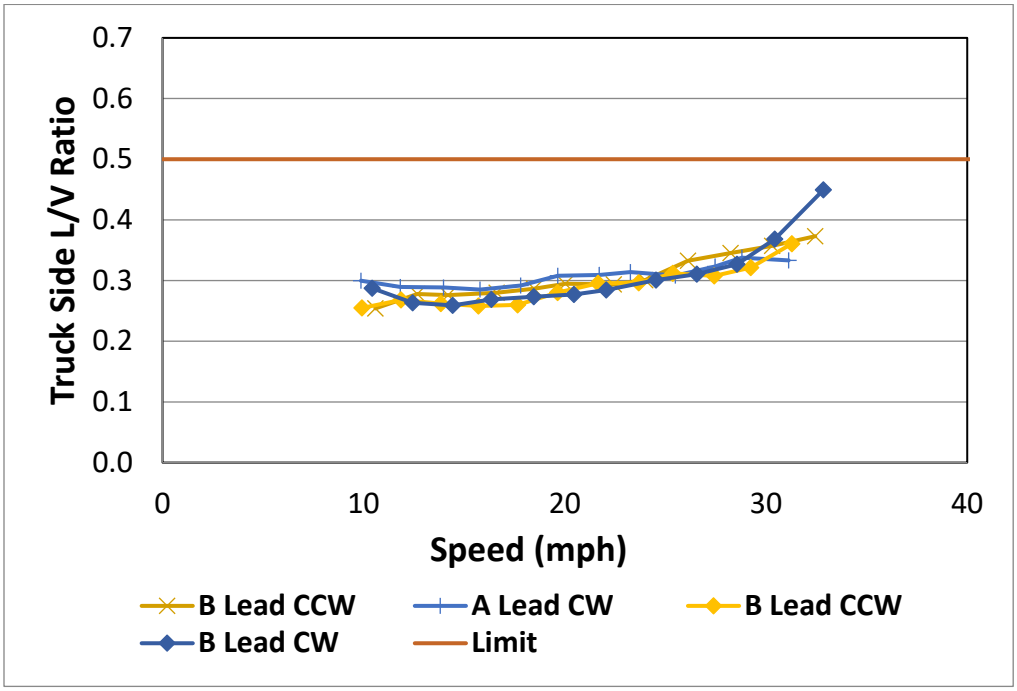


Figure 48. Buffer Railcar Dynamic Curve Wheel L/V Results versus Speed

5.5.5 Pitch and Bounce (Chapter 11)

The pitch and bounce (Chapter 11) test was performed on August 20, 2019. Adam Klopp, TTCI Principal Investigator I, witnessed the pitch and bounce (Chapter 11) test as the AAR Observer per S-2043 requirements. The coefficient of friction was greater than 0.50 on the east rail and greater than 0.50 on the west rail. The buffer railcar met the criteria for pitch and bounce. Note that the results are at the limit for maximum vertical suspension deflection.

Table 33 shows a summary of pitch and bounce test results, and Figure 46 shows a plot of maximum vertical acceleration versus speed.

Table 33. Summary of Pitch and Bounce Results

Criterion	Limiting Value	Test Result
Roll angle (degree)	4	0.4
Maximum wheel L/V	0.8	0.19
Maximum truck side L/V	0.5	0.13
Minimum vertical wheel load (%)	25%	50%
Lateral peak-to-peak acceleration (g)	1.3	0.31
Maximum lateral acceleration (g)	0.75	0.25
Maximum vertical acceleration (g)	0.90	0.80
Maximum vertical suspension deflection (%)	95%	86%

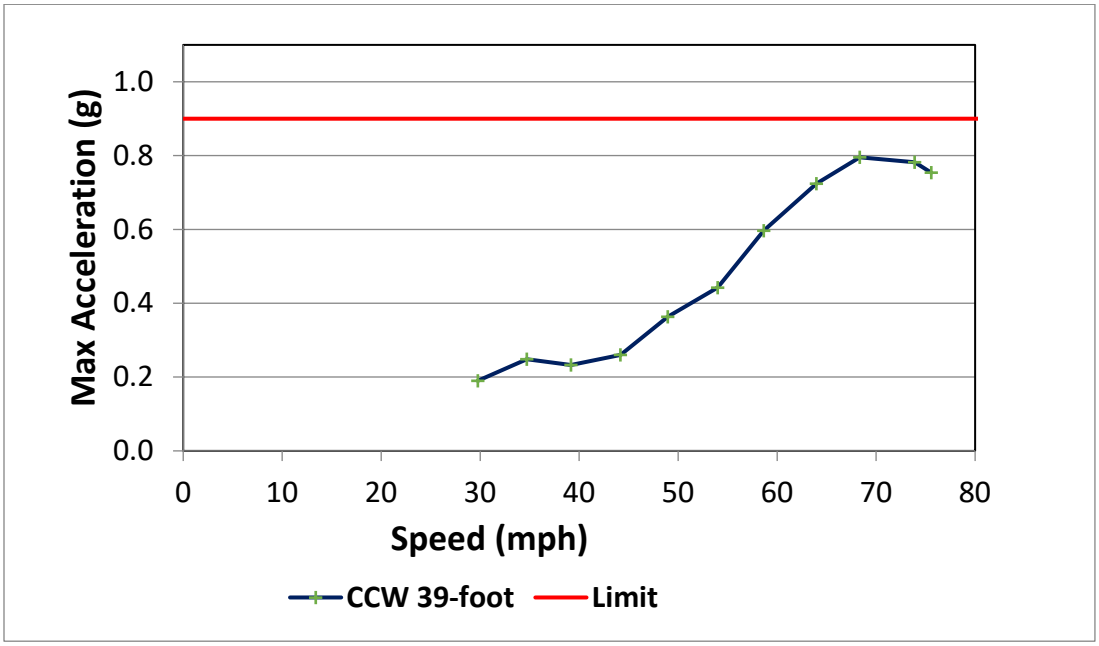


Figure 49. Maximum Vertical Acceleration versus Speed for Pitch and Bounce

5.5.6 Special Pitch and Bounce

AAR Standard S-2043 requires that a special section of track with 3/4-inch bumps at a wavelength equal to the truck center spacing (44.5 foot) be built for the test. TTCI installed ten parallel perturbations of 44.5-foot wavelength and 3/4-inch vertical amplitude on the Transit Test Track (TTT) between TTT-13 and TTT-14.

A special pitch and bounce test was performed on September 5, 2019. Steve Belport, TTCI Principal Investigator II, witnessed the special pitch and bounce test as the AAR Observer per S-2043 requirements. The coefficient of friction was greater than 0.50 on the east rail and greater than 0.50 on the west rail. The buffer railcar met the criteria for the special pitch and bounce test.

Table 34 shows a summary of the special pitch and bounce test results, and Figure 50 shows a plot of maximum vertical acceleration versus speed.

Table 34. Summary of Special Pitch and Bounce Test Results

Criterion	Limiting Value	Test Result
Roll angle (degree)	4	0.4
Maximum wheel L/V	0.8	0.13
Maximum truck side L/V	0.5	0.09
Minimum vertical wheel load (%)	25%	57%
Lateral peak-to-peak acceleration (g)	1.3	0.22
Maximum lateral acceleration (g)	0.75	0.18
Maximum vertical acceleration (g)	0.90	0.5
Maximum vertical suspension deflection (%)	95%	71%

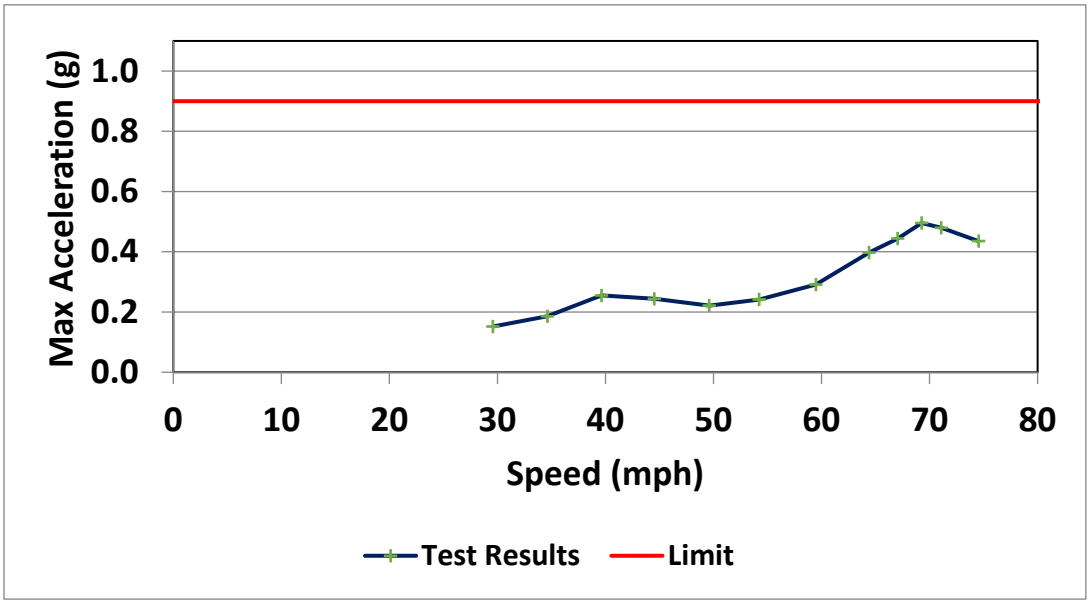


Figure 50. Maximum Vertical Acceleration versus Speed for Special Pitch and Bounce

5.5.7 Single Bump Test

The buffer railcar single bump test was performed on September 5, 2019. Steve Belport, TTCI Principal Investigator II, witnessed the twist and roll test as the AAR Observer per S-2043 requirements. This test is intended to represent a grade crossing and was installed at T15 on the TTT at the TTC. The single bump was a flat-topped ramp with the initial elevation change over 7 feet, a steady elevation over 20 feet, ramping back down over 7 feet. The coefficient of friction on the southeast rail was 0.55 and the coefficient of friction on the northwest rail was 0.55. The buffer railcar met the criteria for the single bump test. Table 35 shows a summary of the test results. Figure 51 shows a plot of maximum vertical acceleration versus speed for the single bump test.

Table 35. Summary of Test Results for the Buffer Railcar Single Bump Test

Criterion	Limiting Value	Test Result
Roll angle (degree)	4	0.5
Maximum wheel L/V	0.8	0.19
Maximum truck side L/V	0.5	0.10
Minimum vertical wheel load (%)	25%	58%
Lateral peak-to-peak acceleration (g)	1.3	0.28
Maximum lateral acceleration (g)	0.75	0.19
Maximum vertical acceleration (g)	0.90	0.56
Maximum vertical suspension deflection (%)	95%	73%

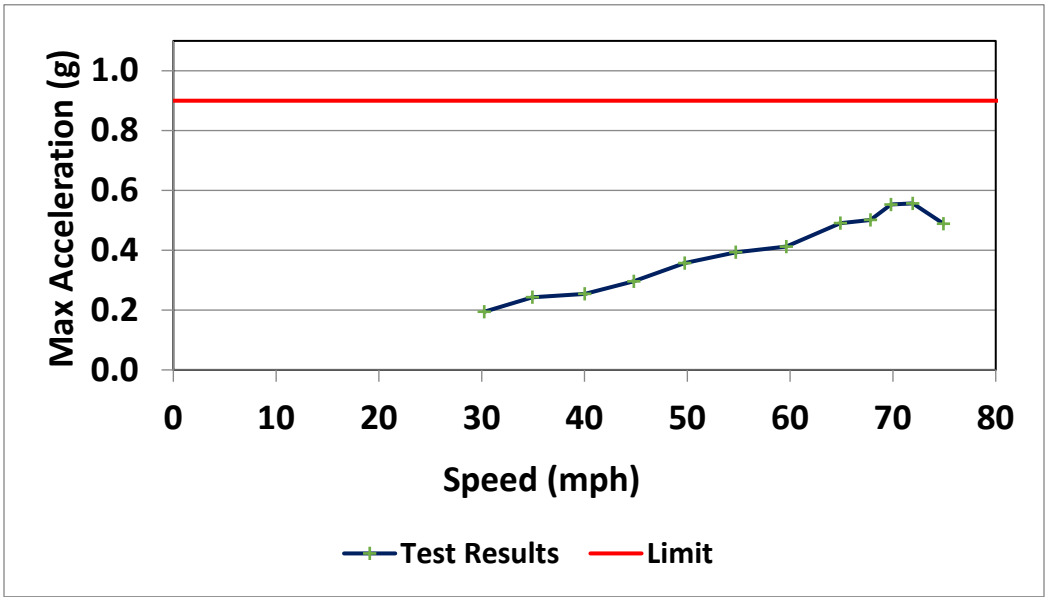


Figure 51. Maximum Vertical Acceleration versus Speed for Buffer Railcar Single Bump Test

5.5.8 Limiting Spiral Negotiation

Limiting spiral testing was conducted in the clockwise (CW) and counterclockwise (CCW) directions and with A-end leading and B-end leading at the same time as dynamic curving tests (see Section 4.5.8). CW tests correspond to spiral entry and CCW tests correspond to spiral exit. Table 36 lists the test dates and the rail friction data. Adam Klopp, TTCI Principal Investigator I, witnessed the limited spiral negotiation test as the AAR Observer per S-2043 requirements. The buffer railcar met the criteria for limiting spiral tests.

Table 36. Buffer Railcar Dynamic Curving Test Dates and Rail Friction Data

Test Condition	Date	Coefficient of Friction	
		Inside Rail	Outside Rail
Buffer car, A-end Leading, CW	8-18-2019	0.48	0.46
Buffer car, A-end Leading, CCW	8-19-2019	0.48	0.48
Buffer car, B-end Leading, CW	8-16-2019	0.5	0.5
Buffer car, B-end Leading, CCW	8-18-2019	0.42	0.45

Table 37 shows a summary of the test results. Figure 52 shows the wheel L/V results versus speed for the limiting spiral test.

Table 37. Buffer Railcar Limiting Spiral Summary of Test Results

Criterion	Limiting Value	Test Result
Roll angle (degree)	4	0.7
Maximum wheel L/V	0.8	0.39
Maximum truck side L/V	0.5	0.28
Minimum vertical wheel load (%)	25%	59%
Lateral peak-to-peak acceleration (g)	1.3	0.17
Maximum lateral acceleration (g)	0.75	0.15
Maximum vertical acceleration (g)	0.90	0.12
Maximum vertical suspension deflection (%)	95%	56%

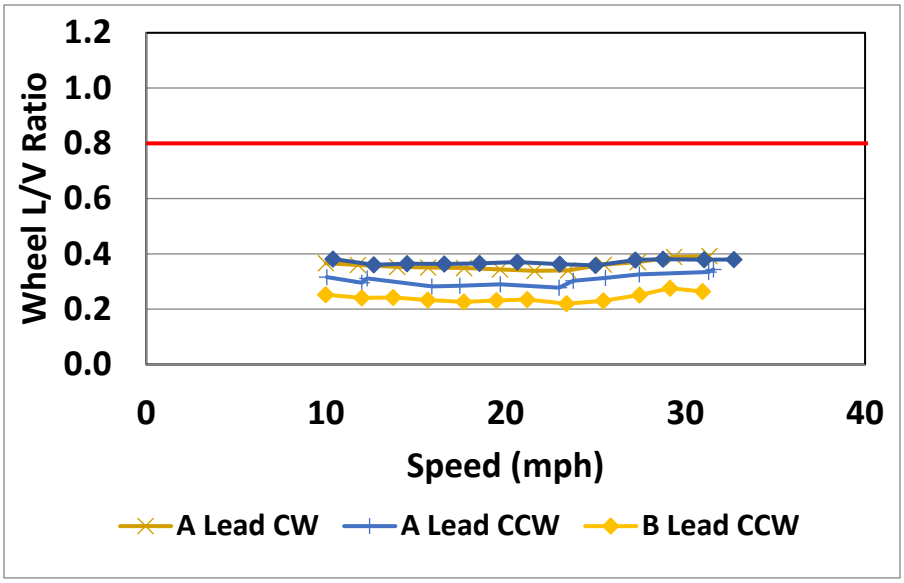


Figure 52. Buffer Railcar Limiting Spiral Wheel L/V Results versus Speed

5.5.9 Normal Spiral Negotiation

Normal spiral negotiation tests were conducted during the constant curving tests. Testing was conducted in the CW and CCW direction and with A-end leading and B-end leading. Test speeds corresponded to -3, 0, and 3 inches of unbalance. Two test runs were recorded at each speed.

Data are summarized from the spirals at each end of each test curve except the 12-degree north spiral. The 12-degree north spiral is not a normal spiral, because although the curvature changes steadily over 200 feet, the superelevation change takes place in the middle 100 feet.

Table 38 shows the test dates and the rail friction data for the different test configurations. When two or more test configurations were done on the same day, rail friction was only measured once. Adam Klopp, TTCI Principal Investigator I, witnessed the twist and roll test as the AAR Observer per S-2043 requirements.

Table 38. Buffer Railcar Constant Curving/Normal Spiral Negotiation Test Dates and Rail Friction Data

Test Condition	Date	Coefficient of Friction					
		7.5-degree		10-degree		12-degree	
		Inside	Outside	Inside	Outside	Inside	Outside
A-end Leading, CW	8-16-2019	0.45	0.44	0.50	0.46	0.50	0.50
A-end Leading, CCW	8-16-2019	0.40	0.44	0.46	0.47	0.50	0.50
B-end Leading, CW	8-16-2019	0.40	0.44	0.46	0.47	0.50	0.50
B-end Leading, CCW	8-18-2019	0.50	0.50	0.44	0.45	0.50	0.49

The buffer railcar met criteria for the normal spiral tests. Table 39 shows a summary of the test results. Figure 53 shows maximum 50-millisecond wheel L/V ratio versus speed for the 12-degree south spiral where the highest values were measured in this regime.

Table 39. Buffer Railcar Normal Spiral Summary of Test Results

Criterion	Limiting Value	Test Result
Roll angle (degree)	4	0.4
Maximum wheel L/V	0.8	0.38
Maximum truck side L/V	0.5	0.23
Minimum vertical wheel load (%)	25%	60%
Lateral peak-to-peak acceleration (g)	1.3	0.29
Maximum lateral acceleration (g)	0.75	0.15
Maximum vertical acceleration (g)	0.90	0.15
Maximum vertical suspension deflection (%)	95%	39%

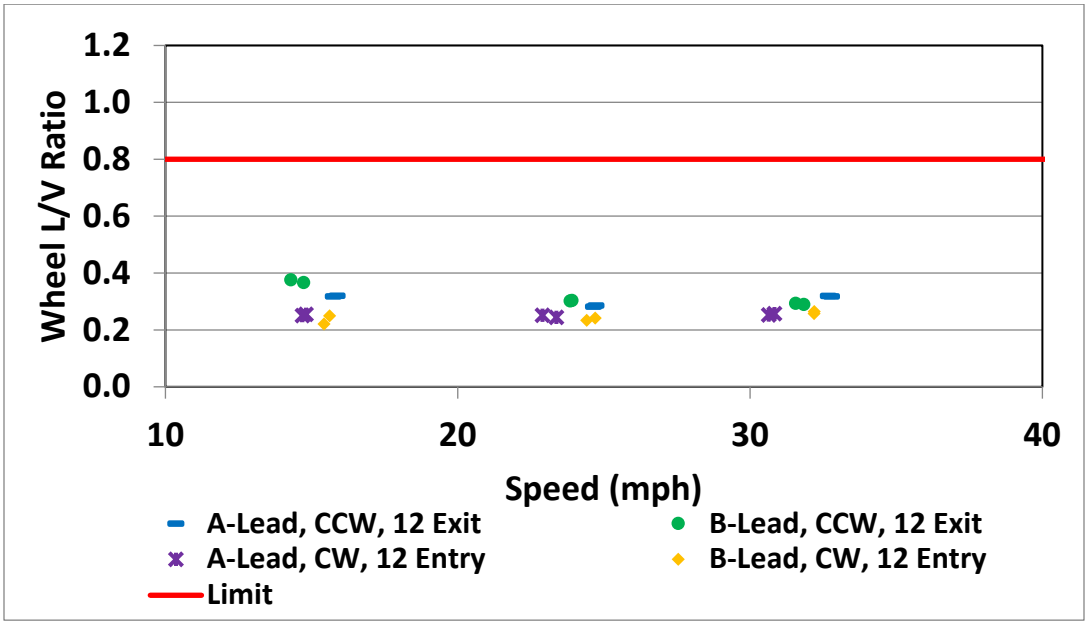


Figure 53. Buffer Railcar Normal Spiral Wheel L/V Results versus Speed for the South Spiral of the 12-Degree Curve

5.5.10 Curving with Single Rail Perturbation

The curving with single rail perturbation tests (bump and dip) were initially conducted on January 30 and February 05, 2020. At that time, the buffer railcar did not meet the single rail L/V criterion for the curving with single rail perturbation tests. However, as part of the subsequent test of the DOE Atlas railcar, it was determined that variations in curvature and alignment existed in the test zone that likely influenced the test results. These variations were corrected as described below. The buffer railcar was retested on September 11, 2020, and the curving with single rail perturbation criteria were met. Adam Klopp, TTCI Principal Investigator I, witnessed both sets of curving with single rail perturbation tests as the AAR Observer per S-2043 requirements.

The curve with single rail perturbation test is intended to represent a low or high joint in a yard or a poorly maintained lead track. Two test scenarios were run, one with a 2-inch outside rail dip and the other with a 2-inch inside rail bump. Both tests were conducted in a 12-degree curve with less than 1/2-inch nominal superelevation (the URB north Y track at TTC). The inside rail bump was a flat-topped ramp with an elevation change over 6 feet, a steady elevation over 12 feet, ramping back down over 6 feet. The outside rail dip was the reverse. The dip and the bump were approximately 300 feet apart on the curve so that performance over one perturbation would not influence performance over the other.

In July 2020, it was found that there were alignment and curvature variations in the curve with the single bump test zone that could potentially influence test results. While AAR Standard S-2043 included detailed specifications for rail surface and cross level in the perturbations, it did not include any specific tolerances for track curvature or alignment.

Because the curvature and alignment variations introduced factors to the test zones that were likely not the intent of AAR Standard S-2043, and that could introduce inconsistency between tests of various vehicles over time, TTCI proposed revisions to AAR Standard S-2043 to include specific tolerances for track curvature and alignment. The proposed revision would leave the existing requirements for the vertical perturbation in place, but limit curvature variation to ±0.5-degree and alignment variations to FRA Class 4 for the length of the railcar being tested before and after the perturbations. EEC approved the proposed revision during its August 20, 2020, webcast meeting.

Testing with the buffer railcar was repeated on the curving with single rail perturbation after the track was adjusted to meet the revised specification. Table 40 shows the coefficient of friction measured in each zone on each day.

Table 40. Friction Coefficient measured during Curving with Single Rail Perturbation Tests

Test Zone	Date	Inside Rail Friction	Outside Rail Friction
Bump	January 30, 2020	0.52	0.54
Bump	February 5, 2020	0.46	0.46
Dip	January 30, 2020	0.54	0.55
Dip	February 5, 2020	0.49	0.49
Bump	September 11, 2020	0.48	0.51
Dip	September 11, 2020	0.42	0.48

Table 41 shows test results from both series of tests. The buffer railcar met the criteria for the curving with single rail perturbation tests with the adjusted track geometry. The initial test exceptions for single wheel L/V ratio criterion for curving occurred in the dip perturbation during two runs of testing in the CCW direction with the A-end leading. The right wheel of axle 2 had the high L/V ratios. The highest value occurred at 6 mph.

Table 41. Summary of Curving with Single Rail Perturbation Test Results

Criterion	Limiting Value	Jan./Feb. 2020 Not Applicable due to S-2043 Qualification		Sept. 2020	
		Test Result Bump	Test Result Dip	Test Result Bump	Test Result Dip
Roll angle (degree)	4	1.7	1.5	1.5	1.4
Maximum wheel L/V	0.8	0.57	**0.81**	0.57	0.70
Maximum truck side L/V	0.5	0.32	0.44	0.37	0.36
Minimum vertical wheel load (%)	25%	57%	59%	58%	60%
Lateral peak-to-peak acceleration (g)	1.3	0.17	0.19	0.15	0.17
Maximum lateral acceleration (g)	0.75	0.18	0.21	0.12	0.13
Maximum vertical acceleration (g)	0.90	0.17	0.17	0.14	0.18
Maximum vertical suspension deflection (%)	95%	77%	80%	63%	68%

Figure 54 and Figure 52 shows results from the September 2020 tests. Figure 51 shows a plot of maximum wheel L/V versus speed for the bump section and Figure 55 shows a plot of maximum wheel L/V versus speed for the dip section. Figure 56 shows a plot of maximum wheel L/V versus speed for the dip section during the initial tests, showing the L/V exceeding the 0.81 limit at 6 mph.

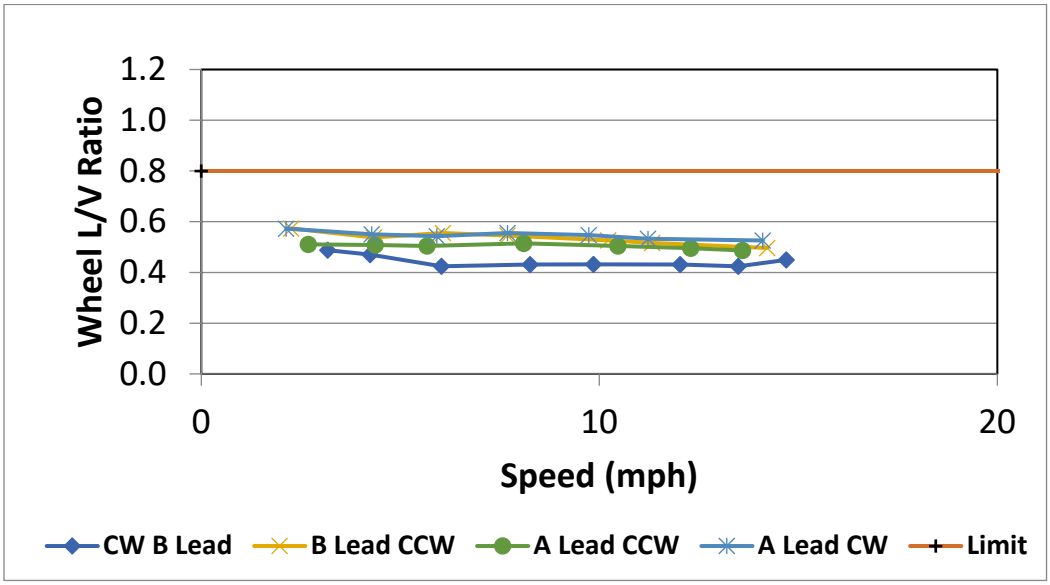


Figure 54. Curving with Single Rail Bump Perturbation Single Wheel L/V Ratio versus Speed (September 2020)

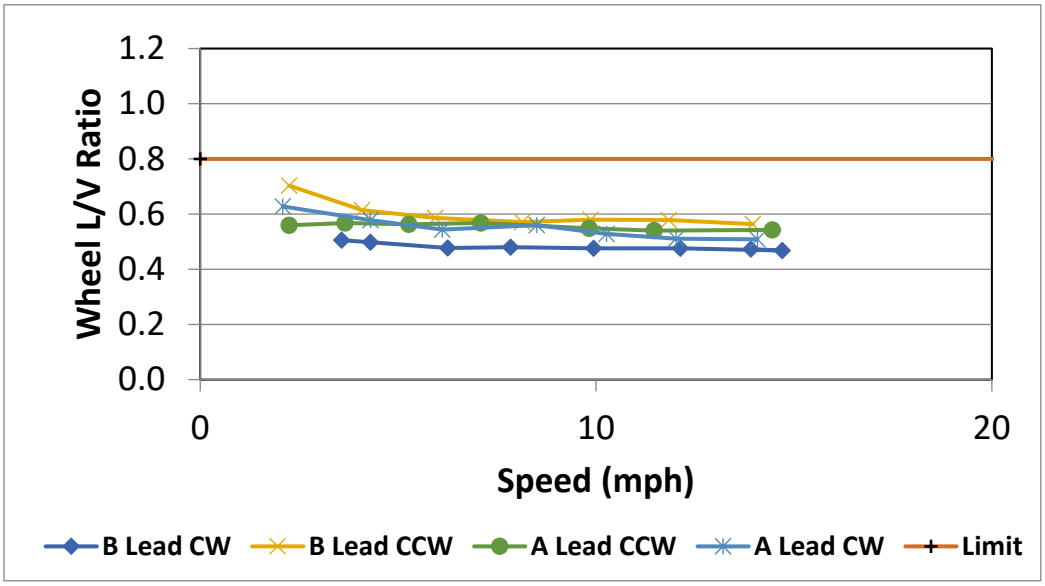


Figure 55. Curving with Single Rail Dip Perturbation
Single Wheel L/V Ratio versus Speed (September 2020)

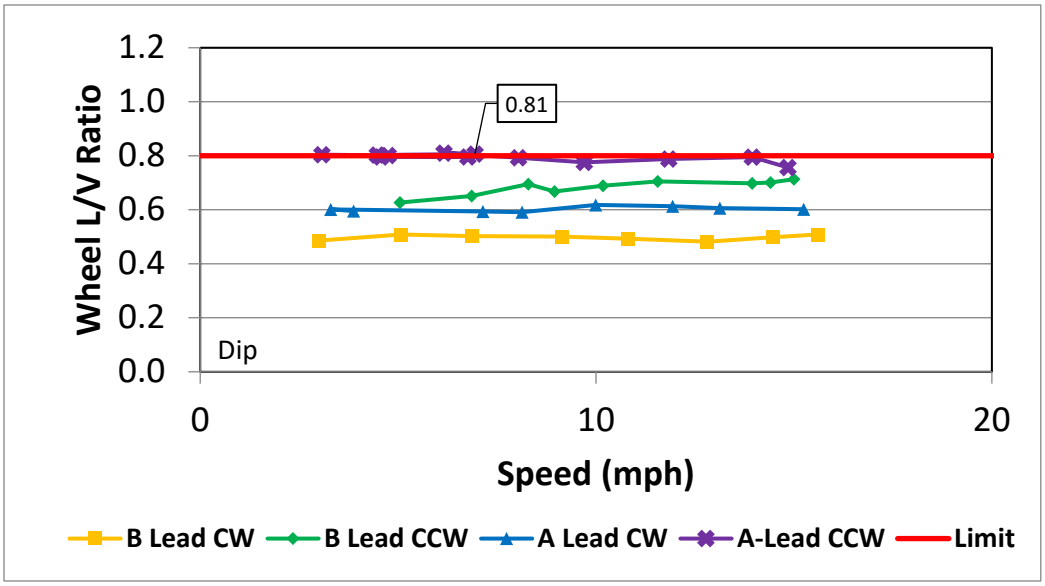


Figure 56. Distance Plot of the Highest Measured Single Wheel L/V ratio during the Curving with Single Dip Perturbation Test (Jan/Feb 2020). Not Applicable to S-2043 qualification.

5.5.11 Standard Chapter 11 Constant Curving

Constant curving tests were conducted with normal spiral negotiation tests (Section 5.5.9). Friction measurements are listed in Section 5.5.9. Constant curve testing was conducted in the CW and CCW directions and with A-end leading and B-end leading. Data are summarized from the 7.5-, 12-, and 10-degree curves on the Wheel Rail Mechanism (WRM) loop for speeds corresponding to 3-inches under balance, balance, and 3-inches over balance speed.

The buffer railcar met the criteria for the constant curving tests. Table 42 shows a summary of the test results. Figure 57 shows the 95th percentile single wheel L/V ratio versus speed in the 12-degree curve.

Table 42. Summary of Buffer Railcar Constant Curving Test Results

Criterion	Limiting Value	Test Result
Roll angle (degree)	4	0.4
Maximum wheel L/V	0.8	0.48
95% Wheel L/V	0.6	0.35
Maximum truck side L/V	0.5	0.28
Minimum vertical wheel load (%)	25%	63%
Lateral peak-to-peak acceleration (g)	1.3	0.21
Maximum lateral acceleration (g)	0.75	0.18
Maximum vertical acceleration (g)	0.90	0.14
Maximum vertical suspension deflection (%)	95%	34%

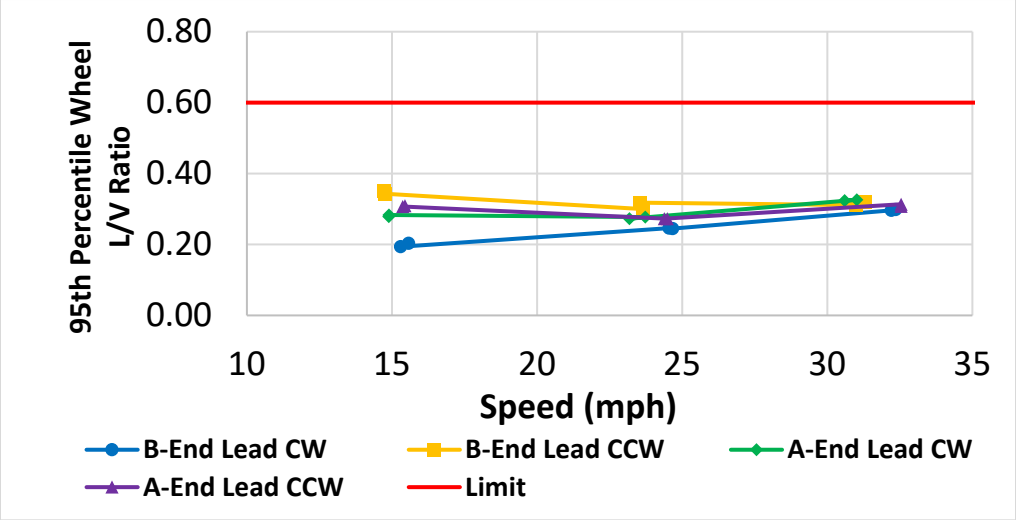


Figure 57. Buffer Railcar Constant Curving 95th Percentile Wheel L/V Ratio versus Speed in 12-degree Curve

5.5.12 Special Trackwork

The buffer railcar turnout tests were conducted on January 30 and February 5, 2020. Adam Klopp, TTCI Principal Investigator I, witnessed the turnout tests as the AAR Observer per S-2043 requirements. Dr. Xinggao Shu, TTCI Principal Investigator II, witnessed the crossover tests as the AAR Observer per S-2043 requirements. The tests were performed with A-end leading and B-end leading. Table 43 shows the top of rail friction measurements for special trackwork tests.

Table 43. Top of Rail Friction Measurements for Special Trackwork Tests

Test	Location	Inside Rail Friction	Inside Rail Friction	Date
Crossover Test	SW 212 A	0.54	0.55	2020-01-29
	Crossover	0.50	0.51	2020-01-29
	SW 212 B	0.55	0.55	2020-01-29
Turnout Test	SW 704	0.50	0.51	2020-01-30
	SW 704	0.47	0.48	2020-02-05

The buffer railcar met AAR Standard S-2043 criteria for the special trackwork tests.

The turnout test was performed at TTC on the 704 switch between the TTT and the north Urban Rail Building (URB) wye. The train was operated through the turnout at walking speed to check clearances, and then speeds were increased to 15 mph in 2 mph increments. Table 44 shows a summary of the turnout test results, and Figure 58 shows a plot of wheel L/V ratio versus speed for the turnout test.

Table 44. Summary of Turnout Test Results

Criterion	Limiting Value	B-End Lead Facing Point	B-End Lead Trailing Point	A-End Lead Facing Point	A-End Lead Trailing Point
Roll angle (degree)	4	0.2	0.2	0.3	0.2
Maximum wheel L/V	0.8	0.54	0.50	0.57	0.54
Maximum truck side L/V	0.5	0.30	0.30	0.29	0.32
Minimum vertical wheel load (%)	25%	79%	81%	79%	78%
Lateral peak-to-peak acceleration (g)	1.3	0.21	0.17	0.19	0.19
Maximum lateral acceleration (g)	0.75	0.18	0.11	0.14	0.16
Maximum vertical acceleration (g)	0.90	0.14	0.13	0.14	0.13
Maximum vertical suspension deflection (%)	95%	46%	43%	24%	29%

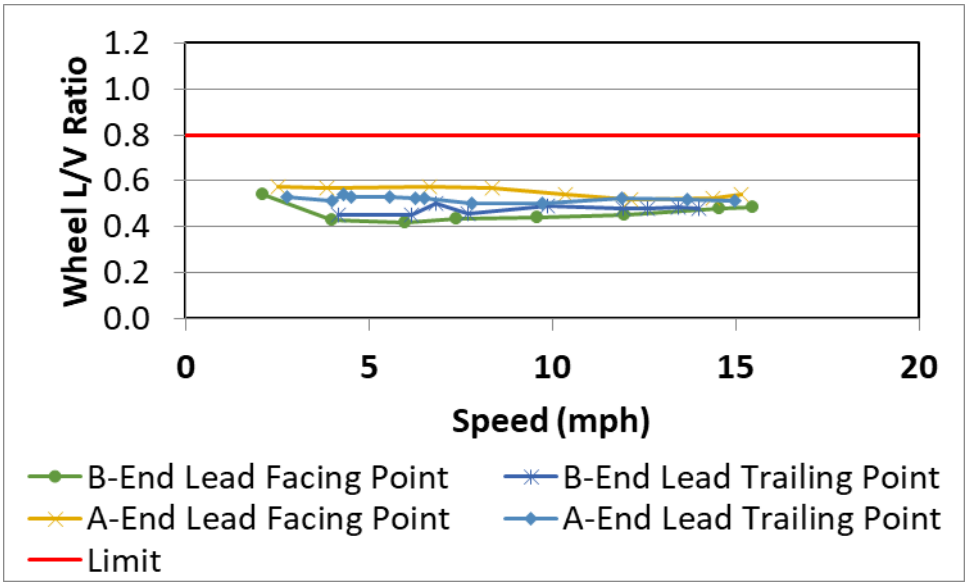


Figure 58. Maximum 50-millisecond Wheel L/V Ratio versus Speed for the Turnout Test

The crossover test was performed on the 212 crossover between the Facility for Accelerated Service Testing (FAST) wye and Impact track. The train was operated through the crossover at walking speed to check clearances, and then speeds were increased to 20 mph in 5 mph increments. Table 45 shows a summary of the crossover test results, and Figure 59 shows a plot of wheel L/V ratio versus speed for the crossover test.

Table 45. Summary of Crossover Test Results

Criterion	Limiting Value	B-End Lead West	B-End Lead East	A-End Lead West	A-End Lead East
Roll angle (degree)	4	0.3	0.2	0.3	0.3
Maximum wheel L/V	0.8	0.54	0.54	0.56	0.58
Maximum truck side L/V	0.5	0.28	0.27	0.30	0.29
Minimum vertical wheel load (%)	25%	75%	77%	65%	72%
Lateral peak-to-peak acceleration (g)	1.3	0.21	0.19	0.30	0.26
Maximum lateral acceleration (g)	0.75	0.14	0.12	0.22	0.19
Maximum vertical acceleration (g)	0.90	0.15	0.15	0.12	0.13
Maximum vertical suspension deflection (%)	95%	38%	31%	31%	35%

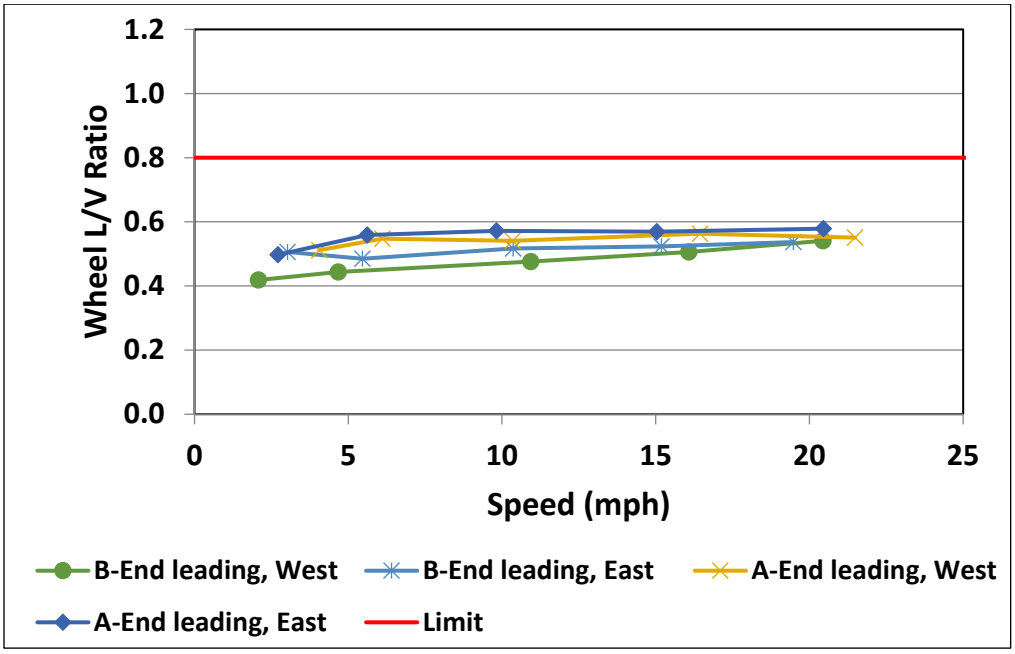


Figure 59. Maximum 50-millisecond Wheel L/V ratio versus Speed for the Crossover Test

AAR Standard S-2043 includes specific requirements for track geometry for the special trackwork tests. However, because of the inherent difficulty in defining turnout alignment specifications, it is acceptable to measure the turnout alignment prior to the commencement of the tests as a baseline and assure that for subsequent tests on that site alignment is maintained within 1/4 inch of the baseline alignment measurement. EEC determined that this was not meant to maintain the same geometry in the long run (the last set of tests at TTC was approximately 10 years prior).

AAR Standard S-2043 also requires that the alignment measurement be included with the test results. Figure 60 and Figure 61 show the X and Y measurements of the track centerline for the turnout and crossover test zones taken prior to the buffer railcar tests. These measurements will be used as a baseline for the 1/4-inch alignment tolerance for subsequent tests through these test zones.

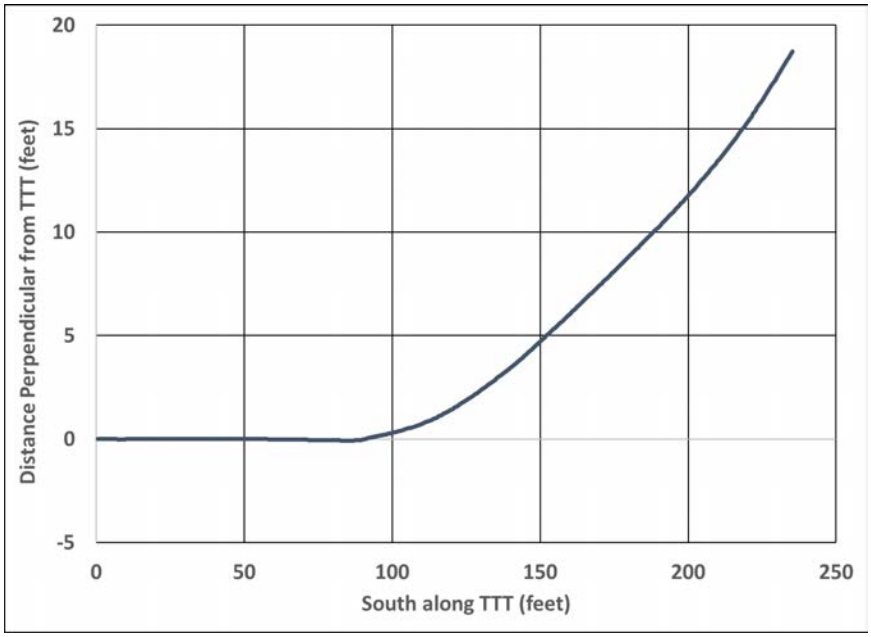


Figure 60. Pre-test Survey Alignment Measurements for Turnout Test Zone

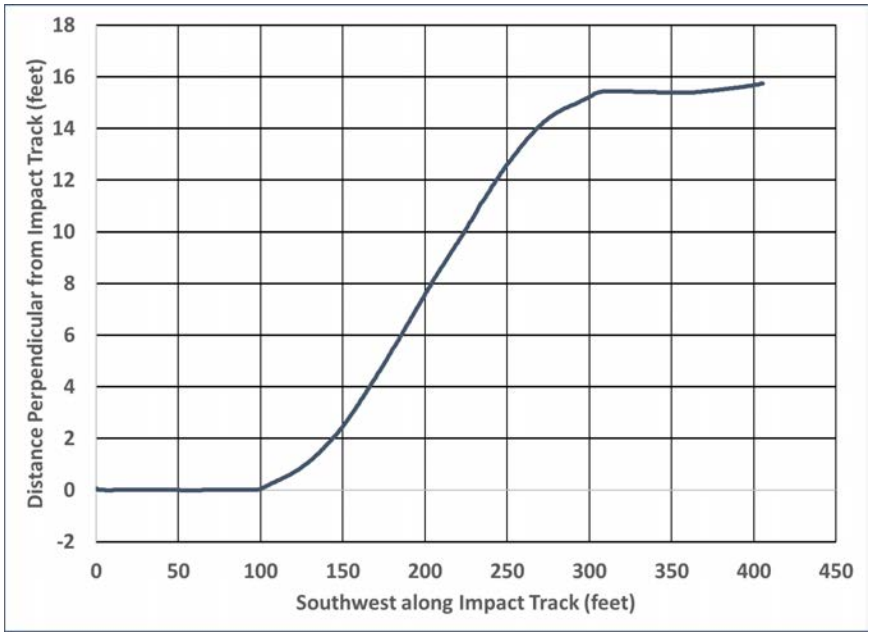


Figure 61. Pre-test Survey Alignment Measurements for Crossover Test Zone

Table 46 shows the description of the track work components contained in the special track work test zones to further document the test conditions.

Table 46. Special Track Work Components

Location	Switch Point		Stock Rail		Frog
	Left	Right	Left	Right	
SW 704	119 pound, 16-foot 6-inch length, standard straight	119 pound, 16-foot 6-inch length, standard straight	119 pound, 39-foot length standard straight	119 pound, 39-foot length standard bent	#8 Rail Bound Manganese
SW 212 A (Impact)	136 pound, 16-foot 6-inch length, samson straight	136 pound, 16-foot 6-inch length, samson straight	136 pound, 39-foot length, samson curved	136 pound, 39-foot length, samson straight	#10 Rail Bound Manganese
SW 212 B (Fast Wye)	136 pound, 16-foot 6-inch length, standard straight	136 pound, 16-foot 6-inch length, standard straight	136 pound, 39-foot length, standard straight	136 pound, 39-foot length, standard bent	#10 Rail Bound Manganese

5.6 Ride Quality

Ride quality testing is not applicable for the buffer railcar because AAR Standard S-2043 requires ride quality testing only for passenger-carrying railcars.

6.0 ADDITIONAL TESTS

Paragraph 5.6 of AAR Standard S-2043 includes a provision for the EEC to require additional testing under special conditions. The EEC has specified no additional for the buffer railcar.

7.0 CONCLUSIONS

Criteria for all AAR Standard S-2034 test regimes were met. Table 46 contains a summary of the test results.

Table 47. Summary of Test Results

S-2043 Section	Critical Data (Criteria) for Conditions Not Met	Met/Not Met
5.2 Nonstructural Static Tests		
5.2.1 Truck Twist Equalization	Not Applicable	Met
5.2.2 Carbody Twist Equalization	Not Applicable	Met
5.2.3 Static Curve Stability	Not Applicable	Met
5.2.4 Horizontal Curve Negotiation	Not Applicable	Met
5.4 Structural Tests		
5.4.2 Squeeze (Compressive End) Load	Not Applicable	Met
5.4.3 Coupler Vertical Loads	Not Applicable	Met
5.4.4 Jacking	Not Applicable	Met
5.4.5 Twist	Not Applicable	Met
5.4.6 Impact	Not Applicable	Met
5.5 Dynamic Tests		
5.5.7 Hunting	Not Applicable	Met
5.5.8 Twist and Roll	Not Applicable	Met
5.5.9 Yaw and Sway	Not Applicable	Met
5.5.10 Dynamic Curving	Not Applicable	Met
5.5.11 Pitch and Bounce (Chapter 11)	Not Applicable	Met
5.5.12 Pitch and Bounce (Special)	Not Applicable	Met
5.5.13 Single Bump Test	Not Applicable	Met
5.5.14 Curve Entry/Exit	Not Applicable	Met
5.5.15 Curving with Single Rail Perturbation	Not Applicable	Met
5.5.16 Standard Chapter 11 Constant Curving	Not Applicable	Met
5.5.17 Special Trackwork	Not Applicable	Met

REFERENCES

1. Association of American Railroads. 2008. *Manual of Standards and Recommended Practices*, Section C, Car Construction, Fundamentals and Details, Washington, D.C.

2. AAR *Manual of Standards and Recommended Practices*, Car Construction Fundamentals and Details, Performance Specification for Trains Used to Carry High-Level Radioactive Material, Standard S-2043, Effective: 2003; Last Revised: 2017, Association of American Railroads, Washington, D.C.

3. Walker, Russell and Shawn Trevithick, Rev. November 20, 2017, "S-2043 Certification: Preliminary Simulations of Kasgro Buffer Railcar," P-17-023, TTCI. Pueblo, CO.

APPENDIX A: TEST PLAN

TEST IMPLEMENTATION PLAN:

SINGLE CAR TEST OF THE BUFFER RAILCAR IN ACCORDANCE WITH ASSOCIATION OF AMERICAN RAILROADS STANDARD S-2043

For the U.S. Department of Energy (DOE)

Prepared by
Transportation Technology Center, Inc.
A subsidiary of the Association of American Railroads
Pueblo, Colorado USA

January 7, 2019

EXECUTIVE SUMMARY

The intent of this Test Implementation Plan (TIP) is to detail the test procedures that will be used to complete single car testing of the U.S. Department of Energy (DOE) Buffer Railcar as required by the Association of American Railroads (AAR) S-2043 standard titled “Performance Specification for Trains used to Carry High-level Radioactive Material,” Section 5.0 – Single Car Tests. This test plan addresses all of the requirements of S-2043 Paragraph 5. A separate test plan will be provided for the Atlas cask cars.

TABLE OF CONTENTS

1.0 Introduction 1
1.1 Purpose 1
1.2 Car Description 1
1.3 Test Tracks 2
2.0 Safety 2
3.0 Test Load 2
4.0 Vehicle Characterization 2
4.1 Component Characterization (S-2043 Paragraph 5.1.3) 4
4.1.1 Secondary Suspension Coil Springs 4
4.1.2 Constant Contact Side Bearings 5
4.1.3 Hydraulic Dampers 5
4.2 Vertical Suspension Stiffness and Damping (S-2043 Paragraph 5.1.4.3) 6
4.3 Lateral Suspension Stiffness and Damping (S-2043 Paragraph 5.1.4.4) 9
4.4 Truck Rotation Stiffness and Break Away Moment (S-2043 Paragraph 5.1.4.5) 10
4.6 Modal Characterization (S-2043 Paragraph 5.1.4.7) 13
4.6.1 Rigid Body Vertical Procedure 17
4.6.2 Rigid Body Roll Procedure 17
4.6.3 Flexible Body Vertical Procedure 17
4.6.4 Flexible Body Twist Procedure 17
4.6.5 Rigid Body Lateral Procedure 17
4.6.6 Flexible Body Lateral Procedure 17
5.0 Non-Structural Static Testing 18
5.1 Instrumentation 18
5.2 Truck Twist Equalization (S-2043, Paragraph 5.2.1) 19
5.3 Carbody Twist Equalization (S-2043, Paragraph 5.2.2) 19
5.4 Static Curve Stability (S-2043, Paragraph 5.2.3) 19
5.5 Horizontal Curve Negotiation (S-2043, Paragraph 5.2.4) 20
6.0 Static Brake Tests 20
6.1 Static Brake Force Measurements 20
6.2 Single-Car Air Brake Test 20
7.0 Structural Tests 20
7.1 Special Measurements (S-2043, Paragraph 5.4.1) 21
7.2 Instrumentation 21
7.3 Squeeze Load (Compressive End Load) (S-2043, Paragraph 5.4.2) 21
7.4 Coupler Vertical Loads (S-2043, Paragraph 5.4.3) 22
7.5 Jacking (S-2043, Paragraph 5.4.4) 23
7.6 Twist (S-2043, Paragraph 5.4.5) 23
7.7 Impact (S-2043, Paragraph 5.4.6) 23
7.8 Securement System (S-2043, Paragraph 5.4.7) 23
8.0 Dynamic Tests 23
8.1 Track geometry (S-2043, Paragraph 5.5.6) 26
8.2 Instrumentation 26
8.2.1 Data Acquisition 28
8.2.2 Functional Checks 28
8.3 Hunting (S-2043, Paragraph 5.5.7) 29
8.3.1 Hunting Test Procedure and Test Conditions 29
8.3.2 Hunting Test Instrumentation and Test Conduct 29
8.4 Twist and Roll (S-2043, Paragraph 5.5.8) 30
8.4.1 Twist and Roll Test Procedure and Test Conditions 30
8.4.2 Twist and Roll Instrumentation and Test Conduct 31

8.5 Yaw and Sway (S-2043, Paragraph 5.5.9) 32
8.5.1 Yaw and Sway Test Procedure and Test Conditions 32
8.5.2 Yaw and Sway Instrumentation and Test Conduct 33
8.6 Dynamic Curving (S-2043, Paragraph 5.5.10) 33
8.6.1 Dynamic Curving Test Procedure and Test Conditions 34
8.6.2 Dynamic Curving Instrumentation and Test Conduct 34
8.7 Pitch and Bounce (S-2043, Paragraph 5.5.11) 36
8.7.1 Pitch and Bounce Test Procedure and Test Conditions 36
8.7.2 Pitch and Bounce Instrumentation and Test Conduct 37
8.8 Pitch and Bounce Special (S-2043, Paragraph 5.5.12) 37
8.9 Single Bump Test (S-2043, Paragraph 5.5.13) 38
8.10 Curve Entry/Exit (S-2043, Paragraph 5.5.14) 38
8.10.1 Limiting Spiral Negotiation 38
8.10.2 Spiral Negotiation Test Procedure and Test Conditions 39
8.10.3 Spiral Negotiation Instrumentation and Test Conduct 39
8.11 Curving with Single Rail Perturbation (S-2043, Paragraph 5.5.15) 40
8.12 Standard Chapter 11 Constant Curving (S-2043, Paragraph 5.5.16) 40
8.12.1 Curving Test Procedure and Test Conditions 41
8.12.2 Curving Instrumentation and Test Conduct 41
8.13 Special Track Work (S-2043, Paragraph 5.5.17) 42
9.0 Test Schedule 44
Attachment A – Test Track Details 47
Attachment B – Strain Gauge Locations For Structural Tests 50

LIST OF FIGURES

Figure 1. Buffer Railcar Arrangement Drawing 1
Figure 2. Truck Characterization Test Set-Up in MSU, Showing TTCI Standard Test Car and Vertical Actuators attached to Reaction Masses 3
Figure 3. Spring Group Arrangement 4
Figure 4. Damping Rate Modeled for the Buffer Car 5
Figure 5. Air Bearing Table Configuration for Truck Rotation Tests 10
Figure 6. Possible Layout of String Pots for Truck Rotation Tests 11
Figure 7. Longitudinal Actuator Installation for Performing Inter-Axle Stiffness Tests 12
Figure 8. Inter-Axle Stiffness Test Setup Showing LVDTs for Measuring Pitching and Yawing of Bearing Adaptor 12
Figure 9. Example of Actuator Attachment Bracket to be Welded to Car 14
Figure 10. Locations of Modal Accelerometers 15
Figure 11. Load Bar Installation Locations 18
Figure 12. 2 1/2 Million-Pound Squeeze Test Fixture with Passenger Car Taken to Structural Failure 22
Figure 13. Applying Coupler Vertical Loads 22
Figure 14. Time and Distance to Climb Limits 25
Figure 15. IWS Configuration 26
Figure 16. Twist and Roll Test Zone 30
Figure 17. Yaw and Sway Test Zone 32
Figure 18. Dynamic Curving Test Zone 34
Figure 19. Pitch and Bounce Test Zone 36
Figure 20. Curving Test Zone 41

Figure 21. Preliminary Test Schedule 45
Figure A1. Strain Gauge/Thermocouple Locations A3

LIST OF TABLES

Table 1. Car Dimensions 1
Table 2. Vehicle Characterization 3
Table 3. Secondary Suspension Spring Types 4
Table 4. Damper Characterization Run List 6
Table 5. Measurements for Damper Characterization Tests 6
Table 6. Measurements for Vertical and Lateral Suspension Characterization 8
Table 7. Run Matrix for Vertical Characterization. 9
Table 8. Run Matrix Lateral Characterization. 10
Table 9. Measurements for Truck Rotation Characterization 11
Table 10. Measurements for Interaxle Yaw Stiffness Measurements 13
Table 11. Measurements for Modal Characterization 15
Table 12. Run List for Modal Testing 16
Table 13. Summary of Non-Structural Static Tests 18
Table 14. Measurements for Non-Structural Static Tests 18
Table 15. Structural Tests 20
Table 16. Measurements for Structural Tests* 21
Table 17. Dynamic Tests 24
Table 18. Dynamic Limiting Criteria 25
Table 19. Measurement List for Instrumented Wheel Set Testing 27
Table 20. Hunting Run List 30
Table 21. Twist and Roll Test Runs. 31
Table 22. Loaded Yaw and Sway Test Runs 33
Table 23. Dynamic Curving Test Runs 35
Table 24. Pitch and Bounce Test Runs 37
Table 25. Special Pitch and Bounce Test 37
Table 26. Single Bump Test Runs 38
Table 27. Limiting Spiral Test Runs. 39
Table 28. Curving with Single Rail Perturbation Test Runs 40
Table 29. Standard Chapter 11 Constant Curving Test Runs 42
Table 30. Special Trackwork Turnout Test 43
Table 31. Special Trackwork Crossover Test 43
Table A1. Strain Gauge and Thermocouple Channels A4

1.0 INTRODUCTION

1.1 Purpose

The intent of this Test Implementation Plan (TIP) is to detail the test procedures that will be used to complete single car testing of the U.S. Department of Energy (DOE) Buffer Railcar as required by the Association of American Railroads (AAR) S-2043 standard titled "Performance Specification for Trains used to Carry High-level Radioactive Material," Section 5.0 – Single Car Tests[1]. S-2043 refers to MSRP Section C-Part II, M-1001, Chapters 2 and 11 for descriptions of several of the tests[2, 3]. A separate test plan will be provided for the Atlas cask cars.

1.2 Car Description

The car to be tested is a 4-axle flat car with a permanently attached ballast load. Some basic car dimensions, used in preparing the test plan are shown in Table 1. The design uses Swing Motion® trucks. AMSTED Rail designed the trucks to use primary pads to improve steering performance and vertical KONI dampers to control carbody motion. Figure 62 shows the buffer car arrangement drawing.

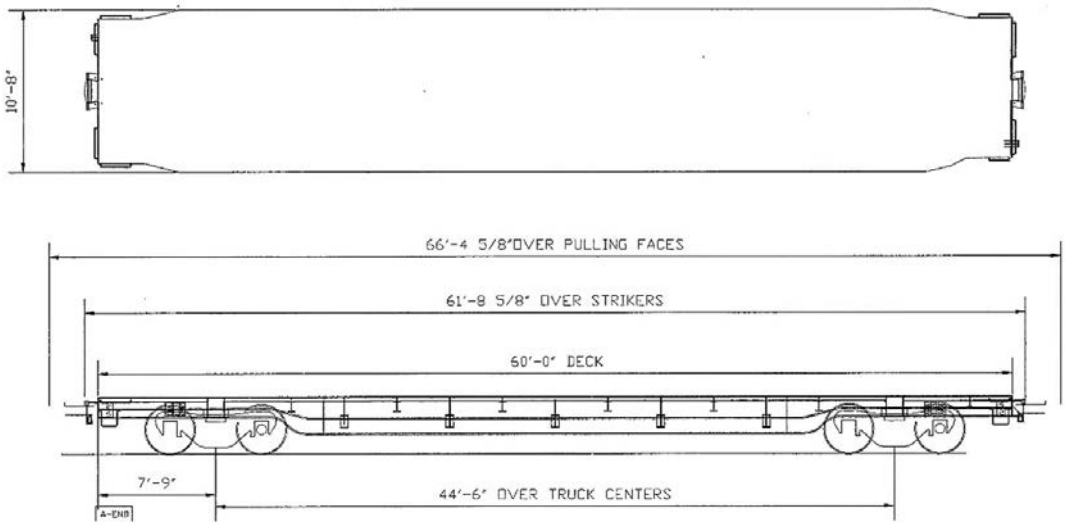


Figure 62. Buffer Railcar Arrangement Drawing

Table 1. Car Dimensions

Dimension	Value
Length over pulling faces	66' 4-5/8"
Length over strikers	61' 8-5/8"
Truck Center Spacing	44' 6"
Axle Spacing on trucks	72"

The requirements for single car tests are described in Section 5.0 of the AAR S-2043 specification. The AAR specification requires that all single car tests and subsequent data analysis be witnessed by a qualified AAR observer. Transportation Technology Center, Inc. (TTCI) will provide the qualified AAR observer to meet this requirement of the specification.

1.3 Test Tracks

Testing is planned on various test tracks at the Transportation Technology Center including the Railroad Test Track (RTT), the Wheel Rail Mechanisms (WRM) Loop, the Precision Test Track (PTT), the URB Wye, the Tight Turn Loop (TTL or Screech Loop), and a crossover between the Impact Track and FAST Wye. These tracks are described in Attachment A.

2.0 SAFETY

Work is to be conducted in accordance with the most current versions of TTCI's Safety Rulebook[4] and Operating Rulebook[5], which are maintained on TTCI's intranet site.

S-2043 requires that maximum test speeds for all non-curving tests be increased to 75 mph from the standard Chapter 11 maximum of 70 mph where deemed safe by the TTCI test team (see Paragraph 8.0 of this document). The applicable test procedures' maximum test speed is listed as 75 mph; however, it is the responsibility of the TTCI test team to determine the maximum safe test speed.

3.0 TEST LOAD

Based on dynamic modeling predictions, the buffer car must be ballasted to a gross rail load of 263,000 pounds to meet the S-2043 Buff-Draft Curving requirements. Because of this, the car was designed with a permanently attached steel ballast weight and only this one load condition will be tested as the car is not rated to carry any additional load.

4.0 VEHICLE CHARACTERIZATION

Vehicle characterization will be performed to verify that the components and vehicle as a whole were built as designed. Tests will be performed to characterize the properties of the carbody and its suspension in the Rail Dynamics Laboratory (RDL) at the Transportation Technology Center (TTC). Results of these tests will be used to verify the component and vehicle characteristics used to perform the multi-body dynamic analysis of the vehicle as described in Section 4.3 of the AAR S-2043 specification.

The Mini-Shaker Unit (MSU), a specialized test facility housed in the Rail Dynamics Laboratory (RDL), will be used extensively to measure vehicle truck suspension system characteristics (see Figure 63). The MSU is comprised of reaction masses and computer controlled hydraulic actuators capable of applying vertical, lateral, or roll input dynamic forces to the vehicle undergoing tests. This unit is especially useful in modal characterization of railcar components and partial rail car systems. The MSU can be configured to perform the rigid and flexible body modal studies of strategic components of the vehicle structure.

The MSU is also used for quantifying the suspension characteristics of assembled suspensions for use in multi-body dynamic models. Measured suspension deflections, reaction forces and wheel/rail forces will be used to determine engineering values for the suspension characteristics.

The MSU is equipped with special instrumented rail sections to measure wheel/rail forces. The use of air bearing tables under the wheels of a vehicle or independently rotating wheels allows for inter-axle shear and yaw stiffness measurements.

Several tests will require trucks to be individually tested in the MSU underneath TTCI's standard truck characterization test flatcar (DOTX 304).

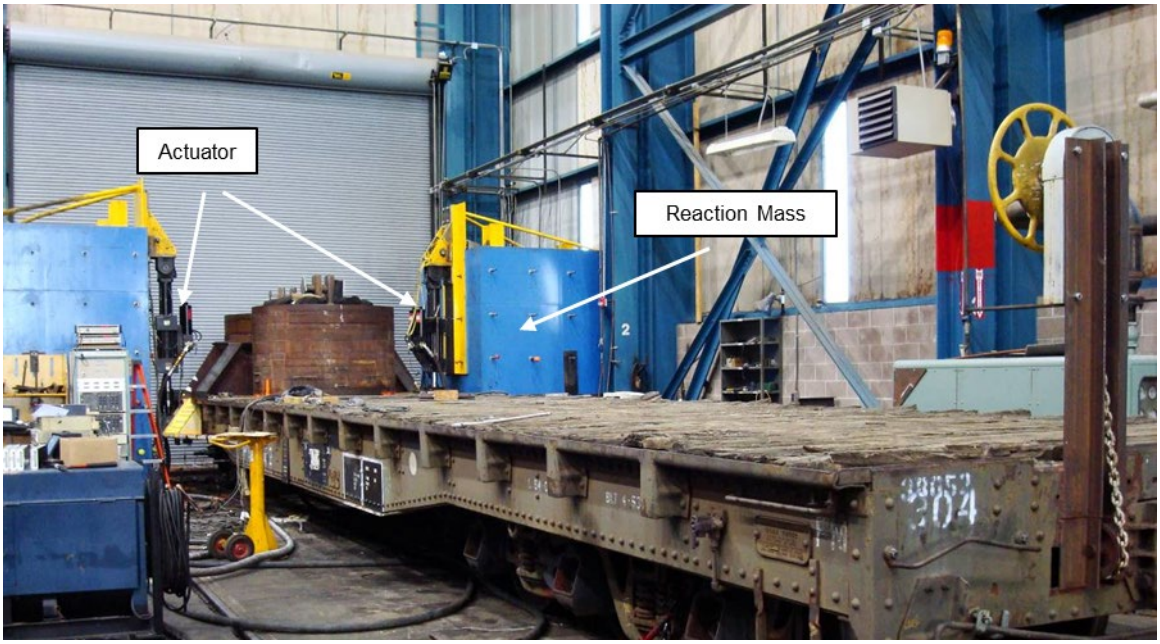


Figure 63. Truck Characterization Test Set-Up in MSU, Showing TTCI Standard Test Car and Vertical Actuators attached to Reaction Masses

Characterization tests are summarized in Table 2. A description of each test is provided in the following subsections. The design of each of these tests is based on the vehicle and suspension arrangement described in the comprehensive report on the multi-body dynamic analyses which TTCI compiled for Kasgro.[6]

Table 2. Vehicle Characterization

Test Name	Comments
5.1.3 Component Characterization	Two samples of each type of spring used will be tested. 2 constant contact side bearings will be tested. 2 hydraulic dampers will be tested.
5.1.4.3 Vertical Suspension Stiffness and Damping	Tests will be performed under DOTX 304. One truck will be tested
5.1.4.4 Lateral Suspension Stiffness and Damping	Tests will be performed under DOTX 304. One truck will be tested
5.1.4.5 Truck Rotation Stiffness and Break Away Moment	Test trucks under each end of the car
5.1.4.6 Inter-Axle Longitudinal Stiffness	Tests will be performed under DOTX 304. One truck will be tested
5.1.4.7 Modal Characterization	Actuators will be attached to the Buffer Carbody. Actuators will be operated in force control at lower frequencies (0.2-10 Hz) and in displacement control for constant acceleration input at higher frequencies (3-30 Hz).

4.1 Component Characterization (S-2043 Paragraph 5.1.3)

Tests will be performed to measure the stiffness and damping characteristics of the following individual suspension components, to meet the requirements of S-2043 section 5.1.3:

- Secondary suspension coil springs
- Constant contact side bearings
- Hydraulic Dampers

4.1.1 Secondary Suspension Coil Springs

The Buffer Railcar uses the spring group arrangement shown in Figure 64. Table 3 shows description for all springs

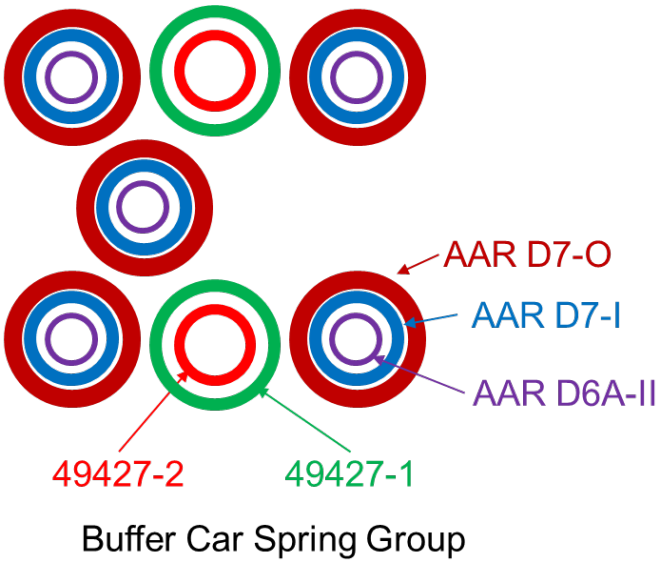


Figure 64. Spring Group Arrangement

Table 3. Secondary Suspension Spring Types

Type	Description	Quantity per Truck	Bar Diameter (inch)	Free HT (inch)	Solid HT (inch)	Spring Rate (pound/inch)
49427-1	Control Coil Outer	2	13/16	11 5/16	6 9/16	1359
49427-2	Control Coil Inner	2	9/16	10 13/16	6 9/16	805
D7-O	Main Coil Outer	5	15/16	10 13/16	6 9/16	2033
D7-I	Main Coil Inner	5	5/8	10 3/4	6 9/16	981
D6A-II	Main Coil Inner Inner	5	3/8	9	5 11/16	464

Two of each spring type will be selected from the car and tested in a load frame to characterize the stiffness of the springs. The force-displacement characteristics will be measured. The following measurements will also be recorded:

- Unloaded free height
- Solid height
- Wire diameter

4.1.2 Constant Contact Side Bearings

The car is equipped with Miner TCC-III 80LT constant contact side bearings (CCSB). The set-up height of each CCSB will be measured and recorded. Two sample CCSB will be installed in a load frame to measure the force–displacement characteristics.

Output results will include a graph of the force - displacement characteristic, including: Unloaded Free Height, Stiffness, and Fully Compressed Height.

4.1.3 Hydraulic Dampers

The car is equipped with four Koni 04A 2032 vertical dampers using the damping rate shown in Figure 65. Two sample dampers will be installed in a load frame to measure the force velocity characteristics of the damper and the force displacement characteristics of the damper's bushings for comparison to the values input to the model.

The length of the dampers as installed on the car and the secondary spring height will be measured and recorded. The average damper length will be used as the zero point for characterization tests. Simulations predict that the highest damper displacements are about ±1 inch. The amplitude (up to ±1 inch) and frequency (up to 3.5 Hz) of the inputs will be adjusted to match the velocities specified in the run list Table 4.

Table 5 shows the measurement list for the damper characterization tests.

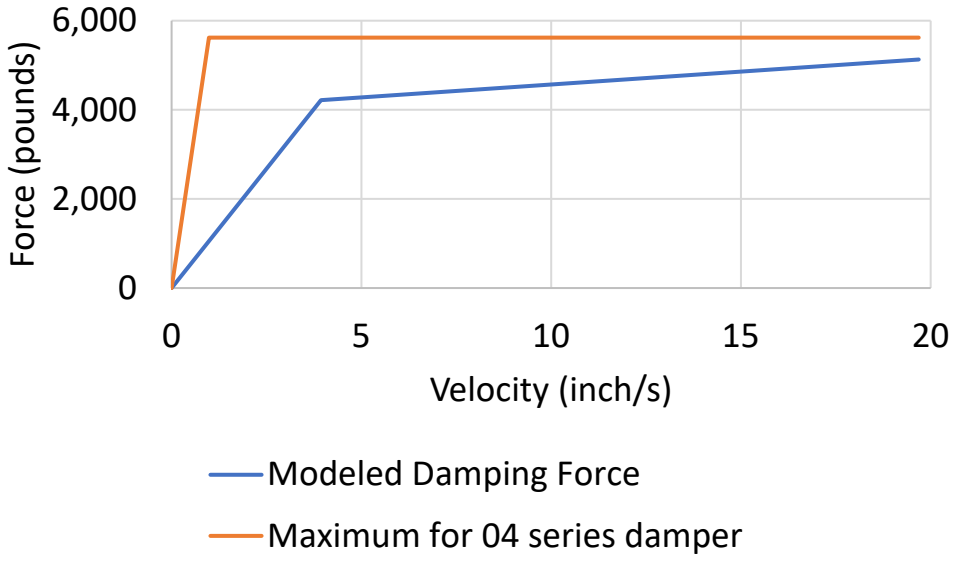


Figure 65. Damping Rate Modeled for the Buffer Car

Table 4. Damper Characterization Run List

Test Run	Stroke Velocity (inch/second)	Comments
1	1	Triangle wave
2	2	Triangle wave
3	4	Triangle wave
4	6	Triangle wave
5	10	Triangle wave
6	15	Triangle wave. Velocity limited by maximum capacity of test machine
7	15	Sine wave. Velocity limited by maximum capacity of test machine

Table 5. Measurements for Damper Characterization Tests

NO.	Channel Name	Measurement Description	Expected Range	Measurement Frequency Response	Digital Sample Rate	Estimated Accuracy	Comments
1	ZFF	Load Frame Force	±6000 pounds	≥15Hz	≥150Hz	better than 1%	From test machine
2	ZDF	Load Frame Displacement	±4 inches	≥15Hz	≥150Hz	better than 1%	From test machine
3	ZDD	Damper Body Displacement	±4 inches	≥15Hz	≥150Hz	better than 1%	
4	ZDB1	Top Damper Bushing Displacement	±0.1 inch	≥15Hz	≥150Hz	better than 1%	
5	ZDB2	Bottom Damper Bushing Displacement	±0.1 inch	≥15Hz	≥150Hz	better than 1%	

4.2 Vertical Suspension Stiffness and Damping (S-2043 Paragraph 5.1.4.3)

Twist and roll and pitch and bounce performance of a railcar are primarily determined by the characteristics of the vertical suspension. The vertical stiffness and damping characteristics will be measured for the secondary coil spring suspension using the MSU.

For this test, equal measured vertical loads will be applied across the spring groups ranging from zero to 1.5 times the static weight, if possible, but at least to the static weight of the buffer car. These tests will be conducted on one truck. The truck will be tested in the MSU underneath the DOTX 304 flatcar. The flatcar will be ballasted to a load equivalent to the weight of the buffer railcar. Vertical hydraulic actuators will be attached to each side of the carbody and the MSU reaction masses, as shown Figure 63. Vertical deflections across the primary and secondary suspensions of each truck will be measured using displacement transducers and force versus displacement plots will be generated based upon the measured data.

Tests of both trucks will be conducted with the friction wedge control coils installed, and then repeated with the friction wedges and wedge control coils removed. Tests will be conducted for

input frequencies of 0.1 Hz, 0.5 Hz and 2.0 Hz. The 0.1 Hz tests will be conducted to move the suspension through its full vertical stroke. The 0.5 and 2.0 Hz tests will be limited in travel due to the limitation of the hydraulic flow rate of the actuators, and to avoid damaging the wear surfaces of the friction wedges.

Tests will be performed with and without dampers installed.

The data channels to be recorded are listed in Table 6. The test runs required are summarized in Table 7.

Table 6. Measurements for Vertical and Lateral Suspension Characterization

Channel Name	Description	Units	Expected Range
VinpActN	Input signal North actuator	V	±10
VinpActS	Input signal South actuator	V	±10
FZActN	North actuator force	1000-lb	-50 to 77
FZActS	South actuator force	1000-lb	-50 to 77
DZActN	North actuator displacement	In	±10
DZActS	South actuator displacement	In	±10
FZRailNE	North East rail vertical force	1000-lb	0 to 100
FZRailNW	North West rail vertical force	1000-lb	0 to 100
FZRailSE	South East rail vertical force	1000-lb	0 to 100
FZRailSW	South West rail vertical force	1000-lb	0 to 100
FYRailNE	North East rail lateral Force	1000-lb	-20 to 50
FYRailNW	North West rail lateral force	1000-lb	-20 to 50
FYRailSE	South East rail lateral force	1000-lb	-20 to 50
FYRailSW	South West rail lateral force	1000-lb	-20 to 50
DZSprN	North Vertical bolster to sideframe disp.	In	10
DZSprS	South Vertical bolster to sideframe disp.	In	10
DYSprST	Lateral bolster to sideframe disp. – top South	In	10
DYSprSB	Lateral bolster to sideframe disp. – bot. South	In	10
DYSprST	Lateral bolster to sideframe disp. – top North	In	10
DYSprSB	Lateral bolster to sideframe disp. – bot. North	In	10
DXPadNE1	Longitudinal displacement, NE pad, outside	In	2
DXPadNE2	Longitudinal displacement, NE pad, inside	In	2
DYPadNE1	Lateral displacement, NE pad, outside	In	2
DYPadNE2	Lateral displacement, NE pad, inside	In	2
DZPadNE1	Vertical displacement, NE pad, outside	In	2
DZPadNE2	Vertical displacement, NE pad, inside	In	2
DXPadSE1	Longitudinal displacement, SE pad, outside	In	2
DXPadSE2	Longitudinal displacement, SE pad, inside	In	2
DYPadSE1	Lateral displacement, SE pad, outside	In	2
DYPadSE2	Lateral displacement, SE pad, inside	In	2
DZPadSE1	Vertical displacement, SE pad, outside	In	2
DZPadSE2	Vertical displacement, SE pad, inside	In	2

Table 7. Run Matrix for Vertical Characterization.

Run	Description
1	Vertical 0.1 Hz (full stroke)
2	Vertical 0.5 Hz (partial stroke)
3	Vertical 2.0 Hz (partial stroke)
4	Vertical 0.1 Hz (full stroke) no dampers
5	Vertical 0.5 Hz (partial stroke) no dampers
6	Vertical 2.0 Hz (partial stroke) no dampers
7	Vertical 0.1 Hz (full stroke) no dampers, no wedges

4.3 Lateral Suspension Stiffness and Damping (S-2043 Paragraph 5.1.4.4)

Twist and roll, yaw and sway, and hunting performance of a railcar are affected by the stiffness and damping characteristics of the lateral suspension. The lateral suspension test will be performed for static vertical loads representing the buffer car weight. The testing method will ensure that static friction does not limit lateral motion during this test.

These tests will be conducted on one truck. The truck will be tested in the MSU underneath the DOTX 304 flatcar. The flatcar will be ballasted to a load equivalent to the load on the truck when installed in the buffer car. Tests will be conducted with the friction wedge control coils installed, and then repeated with the friction wedges and wedge control coils removed.

Vertical deflections across the primary and secondary suspensions of each truck will be measured using displacement transducers and force versus displacement plots will be generated based upon the measured data. A lateral hydraulic actuator will be mounted between the carbody and the MSU reaction mass. Tests will be conducted for lateral input frequencies of 0.1 Hz, 0.5 Hz and 2.0 Hz. The 0.1 Hz tests will be conducted to move the suspension through its full lateral stroke, as determined by the lateral stops between the transoms and the bolsters. The 0.5 and 2.0 Hz tests will probably be limited in travel due to the limitation of the hydraulic flow rate of the actuators, and to avoid damaging the wear surfaces of the friction wedges.

The force will be input at a level above the truck suspension. To minimize carbody roll it may be necessary to use a solid connection (oak blocking or steel shims) between the truck bolster and carbody at the side bearing location.

Lateral deflections across the primary and secondary suspensions of each truck will be measured using displacement transducers. Sufficient displacement transducers will be applied to measure both the lateral and rocking motions of the sideframe and the primary and secondary suspensions.

The channels to be measured are the same as those to be measured during the vertical suspension characterizations as listed in Table 6. The test runs required are summarized in Table 8. Force versus displacement plots will be generated based upon the measured data.

Table 8. Run Matrix Lateral Characterization.

Test Run	Description
1	Lateral 0.1Hz (full Stroke)
2	Lateral 0.5Hz (partial stroke)
3	Lateral 2.0Hz (partial stroke)
4	Lateral 0.1Hz (full Stroke) no wedges
5	Lateral 0.1Hz (full Stroke) no damper
6	Lateral 0.5Hz (partial stroke) no damper
7	Lateral 2.0Hz (partial stroke) no damper
8	Lateral 0.1Hz (full Stroke) no damper, no wedges

4.4 Truck Rotation Stiffness and Break Away Moment (S-2043 Paragraph 5.1.4.5)

Truck rotation stiffnesses and/or break-away moment will also be measured.

For these tests air bearing tables will be used to float the truck at one end of the car to ensure the wheels are unrestrained during the test (Figure 66). The opposite end of the car will be raised up to ensure that the car is level when the air tables are inflated. Hydraulic actuators will be used to rotate the table. To ensure that equal loads are applied on each side of the truck, and to minimize lateral motion and skewing of the air tables the actuators will face in opposite directions during these tests. The air table pit in the Storage Maintenance Building at TTC may be used for these tests.

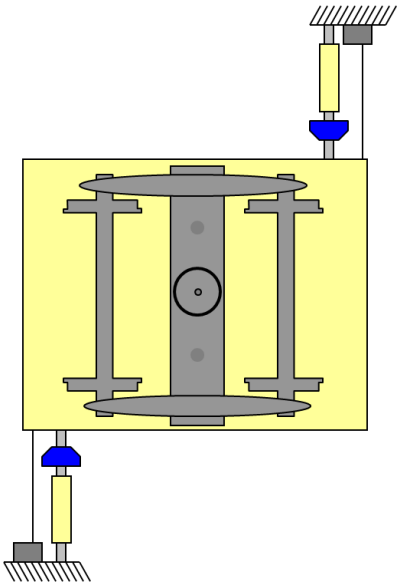


Figure 66. Air Bearing Table Configuration for Truck Rotation Tests

Actuator force and truck bolster rotation relative to the carbody will be measured. This test will be performed at a very low rotational frequency and is considered a static test. Table 9 shows the measurements to be made during truck rotation characterization.

Table 9. Measurements for Truck Rotation Characterization

Channel Name	Description	Units	Expected Range
FYActN	North actuator force	1,000-lb.	±10
FYActS	South actuator force	1,000-lb.	±10
DXTBR	Longitudinal displacement carbody to truck bolster right	In	±5
DXTBL	Longitudinal displacement carbody to truck bolster left	In	±5
DYTBI	Lateral displacement carbody to truck bolster inside	In	±5
DYTBO	Lateral displacement carbody to truck bolster outside	In	±5

Figure 67 shows a sketch of how the string pots might be placed to measure truck rotation. The selection and placement of the string pots must be established so that they are relatively sensitive to translation as well as rotation. The translations of the center plate in the center bowl help the analyst determine if edge contact is occurring, thereby enabling better interpretation of the data. The position of the string pots and load cells relative to the center of rotation must be recorded.

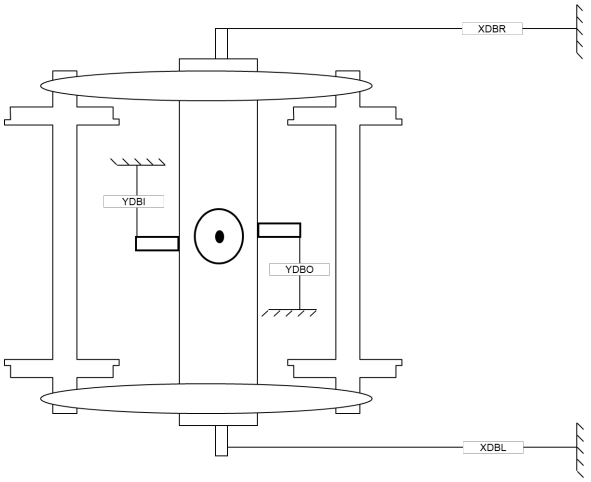


Figure 67. Possible Layout of String Pots for Truck Rotation Tests

4.5 Inter-Axle Longitudinal and Yaw Stiffness (S-2043 Paragraph 5.1.4.6)

The longitudinal stiffness of the primary suspension system will be determined through two tests. These tests will be conducted in the MSU at the same time as the vertical and lateral truck characterization tests (Sections 4.2 and 4.3) with wheelsets with independently rotating wheels (IRWs) installed to eliminate any effects of wheel rolling resistance and slip resistance. Tests will be conducted for the car ballasted to a load equivalent to the buffer car.

The test method uses longitudinal actuators attached between two axles within a truck, at each roller bearing end cap, as shown in Figure 68. The actuators will first be operated in phase in both

directions. Longitudinal stiffness will be determined by plotting force versus displacement. The actuators will then be operated out of phase to determine axle yaw stiffness. These tests will be performed at a very low frequency and are considered static tests.

During these tests, sufficient displacement transducers will be applied to measure both the longitudinal motions of the axles (bearing adaptors) relative to the sideframe, and the pitching motion of the bearing adaptors relative to the sideframes, as shown in Figure 69. The measurements to be recorded are listed in Table 10.

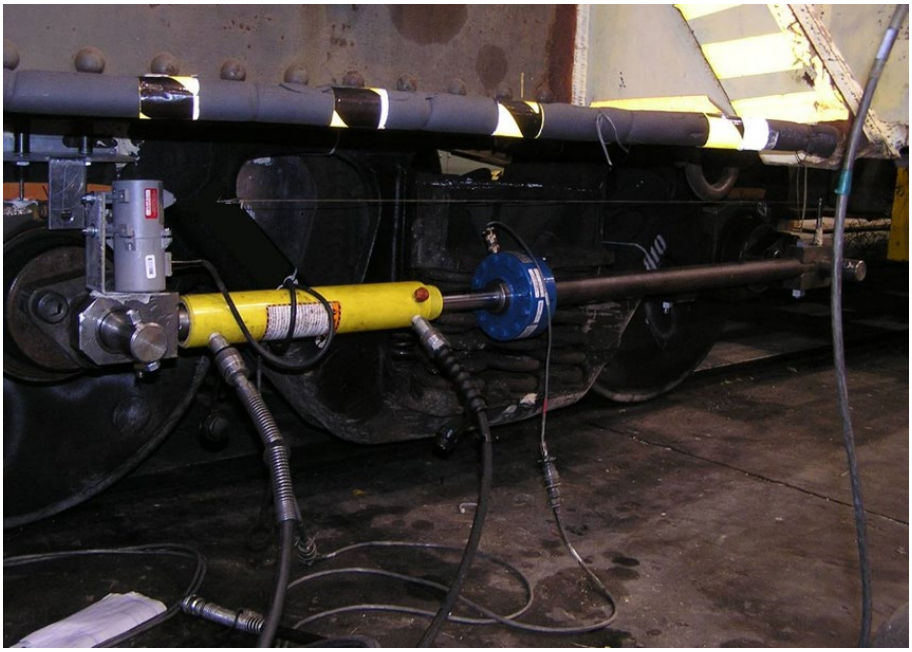


Figure 68. Longitudinal Actuator Installation for Performing Inter-Axle Stiffness Tests

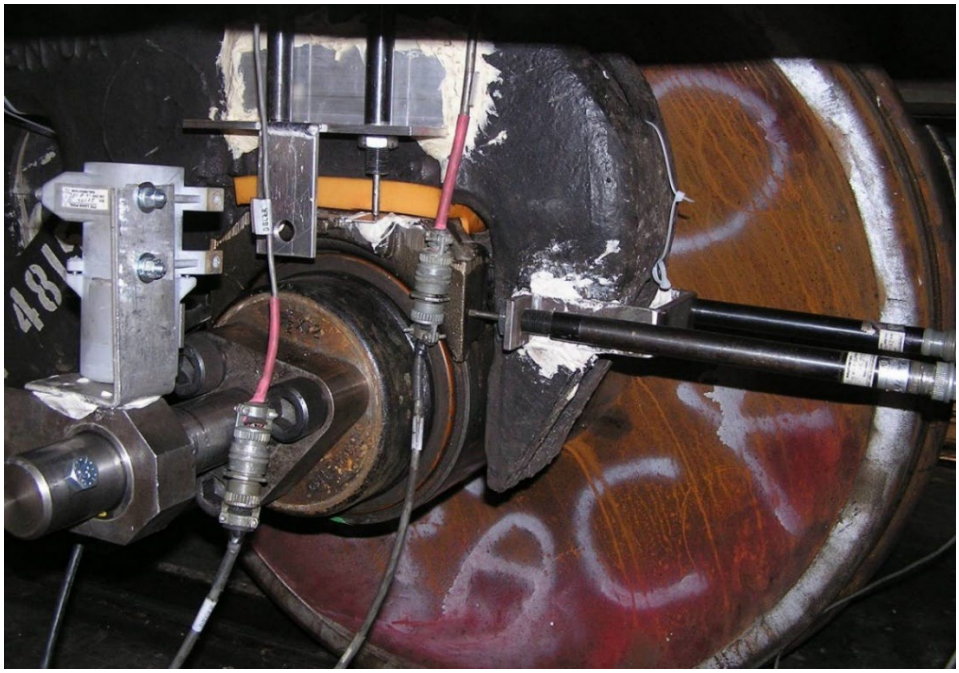


Figure 69. Inter–Axle Stiffness Test Setup Showing LVDTs for Measuring Pitching and Yawing of Bearing Adaptor

Table 10. Measurements for Interaxle Yaw Stiffness Measurements

Channel Name	Description	Units	Expected Range
FXActN	North hydraulic cylinder force	1000-lb	-10 to 20
FXActS	South hydraulic cylinder force	1000-lb	-10 to 20
DXActN	North hydraulic cylinder displacement	In	±10
DXActS	South hydraulic cylinder displacement	In	±10
DXPadNE1	Longitudinal displacement, NE pad, inside	In	2
DXPadNE2	Longitudinal displacement, NE pad, outside	In	2
DYPadNE1	Lateral displacement, NE pad, bottom	In	2
DYPadNE2	Lateral displacement, NE pad, top	In	2
DZPadNE1	Vertical displacement, NE pad, outside	In	2
DZPadNE2	Vertical displacement, NE pad, inside	In	2
DXPadSE1	Longitudinal displacement, SE pad, inside	In	2
DXPadSE2	Longitudinal displacement, SE pad, outside	In	2
DYPadSE1	Lateral displacement, SE pad, bottom	In	2
DYPadSE2	Lateral displacement, SE pad, top	In	2
DZPadSE1	Vertical displacement, SE pad, outside	In	2
DZPadSE2	Vertical displacement, SE pad, inside	In	2

4.6 Modal Characterization (S-2043 Paragraph 5.1.4.7)

The entire railcar will be characterized to identify critical rigid and flexible body modes. The objective of the test is to identify frequencies for the following modes:

Rigid Body

- Bounce
- Pitch
- Yaw
- Lower Center Roll
- Upper Center Roll

Flexible Body

- First mode vertical bending
- First mode twist (torsion)
- First mode lateral bending

The modal tests will be performed on the Buffer railcar in the MSU. Brackets will be welded to the carbody at the carbody bolster on the B-end of the car so the actuators can be attached to the car (Figure 70). TTCI will work with Kasgro to develop a bracket arrangement that does not interfere with the trucks, and to identify allowable areas for welding the brackets to the carbody structure. TTCI will remove the bracket at the conclusion of modal characterization testing.



Figure 70. Example of Actuator Attachment Bracket to be Welded to Car

The carbody will be fitted with enough accelerometers to identify bounce, pitch, roll, yaw, sway, vertical bending, lateral bending, and torsion modes of vibration. The railcar will be excited vertically to induce bounce, pitch, and bending modes. Similarly, the railcar will be excited laterally to identify sway, yaw, and bending, and torsionally to identify lower center roll, upper center roll, and torsion modes. In addition to identifying mode shapes with accelerometers, input force and displacement will be measured to help determine damping rates. The data channels to be recorded during modal tests are listed in Table 11. The approximate measurement locations are shown in Figure 71.

Table 11. Measurements for Modal Characterization

Channel Name	Description	Units	Expected Range
VinpActN	Input signal North actuator	V	±10
VinpActS	Input signal South actuator	V	±10
FZActN	North actuator force	1,000-lb.	-50 to 77
FZActS	South actuator force	1,000-lb.	-50 to 77
DZActN	North actuator displacement	In	±10
DZActS	South actuator displacement	In	±10
AZ1R	Vertical accelerometer, B-end, right side	g	±2
AY1R	Lateral accelerometer, B-end, right side	g	±2
AZ1L	Vertical accelerometer, B-end, left side	g	±2
AZ2R	Vertical accel, ¼ from B-End, right side	g	±2
AY2R	Lateral accel, ¼ from B-End, right side	g	±2
AZ2L	Vertical accel, ¼ from B-End, left side	g	±2
AZ3R	Vertical accelerometer, center, right side	g	±2
AY3R	Lateral accelerometer, center, right side	g	±2
AZ3L	Vertical accelerometer, center, left side	g	±2
AZ4R	Vertical accel, ¼ from A-End, right side	g	±2
AY4R	Lateral accel, ¼ from A-End, right side	g	±2
AZ4L	Vertical accel, ¼ from A-End, left side	g	±2
AZ5R	Vertical accelerometer, A-end, right side	g	±2
AY5R	Lateral accelerometer, A-end, right side	g	±2
AZ5L	Vertical accelerometer, A-end, left side	g	±2

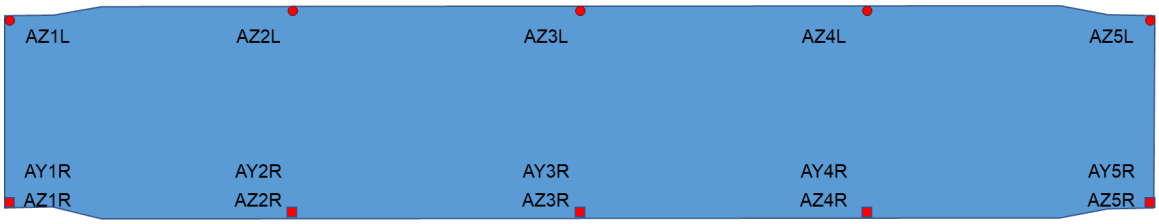


Figure 71. Locations of Modal Accelerometers

Table 12 shows a list of the runs to be performed during modal testing. Rigid body runs will be done using the actuators in force control. Flexible body runs will be done with the actuators in displacement control for constant g runs. The frequency and amplitude values given for each run were based on previous tests[7]. Some changes may be made to frequency and amplitudes used for these runs based on test results.

Table 12. Run List for Modal Testing

Run	Description	Actuator Configuration	Control	Frequency (Hz)	Amplitude
Lateral Rigid Body					
1	Lateral Rigid Body	Lateral	Force	0.2 to 10	5 kips
2	Lateral Rigid Body	Lateral	Force	0.2 to 10	10 kips
3	Lateral Rigid Body	Lateral	Force	0.2 to 10	15 kips
Lateral Flexible Body					
4	Lateral Flexible Body	Lateral	Disp.	3 to 30	0.1 g
5	Optional Lateral Flex Body	Lateral	Disp.	3 to 30	0.2 g
6	Optional Lateral Flex Body	Lateral	Disp.	3 to 30	0.3 g
Vertical Rigid Body					
7	Vertical Rigid Body	Vertical (in phase)	Force	0.2 to 10	5 kips
8	Vertical Rigid Body	Vertical (in phase)	Force	0.2 to 10	10 kips
9	Vertical Rigid Body	Vertical (in phase)	Force	0.2 to 10	15 kips
Vertical Flexible Body					
10	Vertical Flexible Body	Vertical (in phase)	Disp.	3 to 30	0.1 g
11	Optional Vertical Flex Body	Vertical (in phase)	Disp.	3 to 30	0.2 g
12	Optional Vertical Flex Body	Vertical (in phase)	Disp.	3 to 30	0.3 g
Roll Rigid Body					
13	Roll Rigid Body	Vertical (out of phase)	Force	0.2 to 10	5 kips
14	Roll Rigid Body	Vertical (out of phase)	Force	0.2 to 10	10 kips
15	Roll Rigid Body	Vertical (out of phase)	Force	0.2 to 10	15 kips
Twist Flexible Body					
16	Twist Flexible Body	Vertical (out of phase)	Disp.	3 to 30	0.1 g
17	Optional Twist Flex Body	Vertical (out of phase)	Disp.	3 to 30	0.2 g
18	Optional Twist Flex Body	Vertical (out of phase)	Disp.	3 to 30	0.3 g

4.6.1 Rigid Body Vertical Procedure

The actuators will be cycled in phase. Input frequencies will be increased from 0.2 Hz to 10 Hz. The actuators will be operated in force control with 5, 10, and 15 kip sinusoidal inputs. Pitch and Bounce modes will be determined by the phase relationship between the A and B end accelerometers.

4.6.2 Rigid Body Roll Procedure

The actuators will be cycled 180 degrees out of phase. Input frequencies will be increased from 0.2 Hz to 10 Hz. The actuators will be operated in force control with 5, 10, and 15 kip sinusoidal inputs. Roll modes will be determined by the phase relationship between the accelerometers mounted at different positions on the car.

4.6.3 Flexible Body Vertical Procedure

The actuators will be cycled in phase. Input frequencies will be increased from 3 Hz to 30 Hz. The actuators will be operated in displacement control and operated to achieve a constant g input.

4.6.4 Flexible Body Twist Procedure

The actuators will be cycled out of phase. Input frequencies will be increased from 3 Hz to 30 Hz. The actuators will be operated in displacement control and operated to achieve a constant g input.

4.6.5 Rigid Body Lateral Procedure

The actuators will be reconfigured so that one actuator is mounted to excite the car laterally. Input frequencies will be increased from 0.2 Hz to 10 Hz. The actuators will be operated in force control with 5, 10, and 15 kip sinusoidal inputs. The Yaw mode will be determined by the phase relationship between the A and B end accelerometers.

4.6.6 Flexible Body Lateral Procedure

This test will be performed while the actuators are in the lateral configuration. Input frequencies will be increased from 3Hz to 30Hz. The actuators will be operated in displacement control and operated to achieve a constant g input.

5.0 NON-STRUCTURAL STATIC TESTING

Several static tests will be performed to demonstrate the ability of the railcar to maintain adequate vertical wheel loads in extreme load conditions and poor track geometry environments. A summary of the non-structural static tests is presented in Table 13. The data channels to be recorded are presented in Table 14.

Table 13. Summary of Non-Structural Static Tests

Test Name	Instrumentation	Comments
5.2.1 Truck Twist Equalization	This test will be done using 8 load measuring rails. (load bars)	
5.2.2 Carbody Twist Equalization	This test will be done using 8 load measuring rails (load bars)	
5.2.4 Static Curve Stability	Feeler gages	Currently planning to use the AAR short car/long car
5.2.5 Horizontal Curve Negotiation	Visual inspection	Screech loop

5.1 Instrumentation

Figure 72 shows load bar installation locations and Table 14 provides additional details of measurements for the Non-Structural Static Tests.



Figure 72. Load Bar Installation Locations

Table 14. Measurements for Non-Structural Static Tests

Channel Name	Description	Units	Expected Range
1[t	Load bar, axle 1, right wheel	kips	0-60
LB1L	Load bar, axle 1, left wheel	kips	0-60
LB2R	Load bar, axle 2, right wheel	kips	0-60
LB2L	Load bar, axle 2, left wheel	kips	0-60
LB3R	Load bar, axle 3, right wheel	kips	0-60
LB3L	Load bar, axle 3, left wheel	kips	0-60
LB4R	Load bar, axle 4, right wheel	kips	0-60
LB4L	Load bar, axle 4, left wheel	kips	0-60
IC	Instrumented Coupler	kips	±200

5.2 Truck Twist Equalization (S-2043, Paragraph 5.2.1)

This requirement is to ensure adequate truck load equalization. Load bars will be used to measure wheel loads as shown in Figure 72.

- With the car on level track shim each wheel three inches in height. This is the zero condition.
- For one wheel in each truck, measure vertical wheel loads while raising one wheel from 0.0 inch to 3.0 inches, then lowering to -3 inches, then raising back to 0 inches in increments of 0.5 in.
- At 2.0 inches of deflection, vertical load at any wheel may not fall below 60% of the nominal static load.
- At 3.0 inches of deflection, vertical load at any wheel may not fall below 40% of the nominal static load.

Figures 11 and 12 of the dynamic analysis report[6] show that the trucks used in this vehicle are symmetrical front to back and left to right so this test will be performed by raising and lowering just one wheel in every truck.

5.3 Carbody Twist Equalization (S-2043, Paragraph 5.2.2)

This test will be performed in conjunction with the truck twist test. This requirement is to document wheel unloading under carbody twist, such as during a spiral negotiation. Load bars will be used to measure wheel loads as shown in Figure 72. The railcar shall be jacked by 3.0 in. in 0.5-in. increments from underneath the wheels on one side of all trucks at one end of the car. At 2.0 in. of lift, vertical load at any wheel may not fall below 60% of the nominal static load. At 3.0 in., no permanent damage shall be produced and no static wheel load may fall below 40% of the nominal static wheel load.

This test must be performed by raising and lowering each of the four corners of the railcar individually.

5.4 Static Curve Stability (S-2043, Paragraph 5.2.3)

The curve stability test shall follow the requirements of M-1001 paragraph 11.3.3.3. The test consist will undergo a squeeze and draft load of 200,000 pounds without carbody suspension separation or wheel lift. Load application shall simulate a static load condition and shall be of minimum 20 seconds sustained duration.

For the purpose of this test, wheel lift is defined as a separation of wheel and rail exceeding 1/8-in. when measured 2 5/8-in. from the rim face with a feeler gauge.

The car will be subjected to squeeze and draft load on a 10-degree curve located at the Urban Rail Building at TTC. The test car will be coupled to a base car as defined in paragraph 2.1.4.2.3 of the AAR M-1001 specification, and a long car having 90-ft over strikers, 66-ft truck centers, 60-in. couplers, and conventional draft gear.

Coupler forces will be measured during the test.

5.5 Horizontal Curve Negotiation (S-2043, Paragraph 5.2.4)

A horizontal curve negotiation test must be performed per M-1001, paragraph 2.1.4. The specification requires that this car be able to negotiate a curve of 150-foot radius uncoupled. The test will be performed on the screech loop at TTC which has a radius of 150 feet. The test car will be coupled to three short hopper cars so that the test car can be pushed into the curve without the locomotive entering the curve. The car will be pushed into the curve in stages. At each stage personnel will inspect the car paying special attention to:

- Clearance between wheels and carbody
- Clearance between wheels and brake rigging (including brake cylinder)
- Clearance between truck bolster and brake rigging

6.0 STATIC BRAKE TESTS

Static brake shoe force tests are to be conducted by Kasgro at their facility. Kasgro has arranged for the assistance of New York Air Brake and an AAR observer. A TTCI engineer will also be present for testing. The TTCI engineer will confirm that the tests are conducted as described below.

6.1 Static Brake Force Measurements

Static brake force measurements will be conducted per MSRP Section E, Standard S-401 to demonstrate compliance with S-2043 paragraph 4.4. Braking ratios for freight operation must be verified. Brake shoe force variations must also be within the limits provided in Standard S-401.

6.2 Single-Car Air Brake Test

In addition, a single-car air brake test must be performed per the AAR Manual of Standards and Recommended Practices, Section E, Standard S-486, or other applicable standard.

7.0 STRUCTURAL TESTS

Structural tests will be conducted to demonstrate the railcar's ability to withstand the rigorous railroad load environment and to verify the accuracy of the structural analysis. The Chapter 11 requirement of "no permanent deformation" is interpreted as no stress exceeding material yield for the tests described in the following sections. The structural tests are summarized in Table 15.

Table 15. Structural Tests

Test Name	Lead End	Instrumentation	Comments
5.4.2 Squeeze (Compressive End) Load		50-Strain gages, million pound load cell.	
5.4.3 Coupler vertical loads		50-Strain gages, 50K load cell.	Apply 50K pounds up and down at pulling face of coupler.
5.4.4 Jacking		50-Strain gages	
5.4.5 Twist		50-Strain gages, 8 load bars	5.4.5.1 performed in conjunction with 5.2.2. 5.4.5.2 performed separately.
5.4.6 Impact	B	50-Strain gages, Instrumented coupler	

7.1 Special Measurements (S-2043, Paragraph 5.4.1)

A survey of the car will be performed before and after all the structural tests have been conducted. The purpose of this survey is to verify the shape and integrity of the car. In addition, a visual inspection of the car will be made after each structural test. The survey will include:

- Measure the length over strikers
- Measure the length over pulling faces
- Using a theodolite, measure a level loop around the car deck to check for a change in camber or twisting of the carbody

7.2 Instrumentation

Strain measurements are to be taken from gauges installed on the railcar under frame and deck surface for each of the tests described in sections 7.3 - 7.7. Strains will be used for post-test comparison to finite-element analysis (FEA) predictions. The car designer has determined the location for the gauges as required by S-2043 paragraph 5.4.1.2, based on design FEA results. In addition, thermocouples will be installed in 3 locations for temperature compensation of strain measurements.

Table 16 list the measurements for the structural tests. Strain gauge and thermocouple locations, descriptions, material properties at measurement locations, channel names, measurement units, and expected range are included in Attachment B.

Table 16. Measurements for Structural Tests*

Channel Name	Description	Units	Expected Range
LC1	Load cell for compressive end load	kips	0-1,000
LC2	Load cell for coupler test	kips	0-50
IC	Instrumented Coupler for impact test	kips	0-1250
SPD	Speed Tachometer for impact test	mph	0-15

*See Attachment B for details of strain gauge and thermocouple locations on carbody

Most structural tests are static or quasi-static so filter and sample rates are not critical. Data should be filtered at ≥10-Hz and sampled at a minimum of twice the chosen filter frequency. The exception is the impact test regime, where data will be filtered at a rate ≥100-Hz and < (sample rate/2). The minimum sample rate for impact tests is 1000-Hz. Impact test data will be digitally filtered at 100-Hz during data analysis.

7.3 Squeeze Load (Compressive End Load) (S-2043, Paragraph 5.4.2)

The squeeze test shall follow the requirements of M-1001 paragraph 11.3.3.1. A horizontal compressive static load of 1,000,000 pounds will be applied at the centerline of draft to the draft system of car interface areas using TTCI's squeeze fixture (Figure 73) and sustained for a minimum of 60 seconds. The car tested will simulate an axially loaded beam having rotation-free translation-fixed end restraints. No other restraints, except those provided by the suspension system in its normal running condition, will be permissible.

Prior to testing the squeeze load should be cycled to 750,000 pounds three times to stress relieve the railcar, providing a better correlation between FEA predictions and measured stresses.



Figure 73. 2 1/2 Million-Pound Squeeze Test Fixture with Passenger Car Taken to Structural Failure

7.4 Coupler Vertical Loads (S-2043, Paragraph 5.4.3)

The coupler vertical load test shall follow the requirements of M-1001 paragraph 11.3.3.2. A load of 50,000 pounds shall be applied in both directions to the coupler head as near to the pulling face as practicable and held for 60 seconds. This test will utilize a hydraulic cylinder positioned on cribbing to apply the upward force. An A-frame fixture that attaches to the rail and a hydraulic cylinder will be used to apply the downward force (Figure 74).

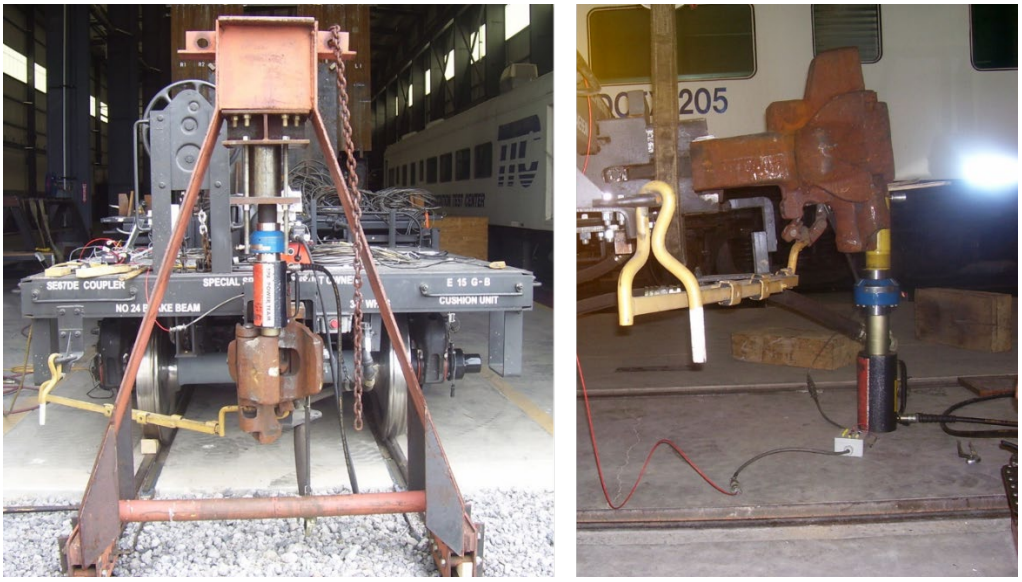


Figure 74. Applying Coupler Vertical Loads

7.5 Jacking (S-2043, Paragraph 5.4.4)

The jacking test shall follow the requirements of M-1001 paragraph 11.3.3.4. Vertical load capable of lifting a fully loaded car will be applied at designated jacking locations sufficient to lift the unit and permit removal of the truck or suspension arrangement nearest to the load application points. M-1001, Chapter 11 requires that the car withstand the test without permanent deformation of car structure. Strain data will be recorded while the carbody is jacked high enough to permit removal of the truck.

7.6 Twist (S-2043, Paragraph 5.4.5)

The twist test shall follow the requirements of M-1001 paragraph 11.3.3.5. The loaded car will be jacked 3 inches from underneath the wheels on one side of one truck at one end of the car. M-1001, Chapter 11 requires that the car withstand the test without permanent deformation of the car structure. This test will be performed in conjunction with the test described in Section 0.

In addition, the carbody will be supported at all four jacking pads and one corner will be allowed to drop 3 in.

Strain data will be recorded during these tests.

7.7 Impact (S-2043, Paragraph 5.4.6)

The impact test shall follow the requirements of M-1001 paragraph 11.3.4.1. The loaded candidate car is to be impacted into a string of three standing, fully loaded cars of at least 70-ton capacity. The impact string will be equipped with M-901E draft gear on the struck end and the hand brake will be fully set on the last car (opposite end).

Free slack between cars will be removed; however, draft gears will not be compressed. No restraint other than the hand brake on the last car will be used.

A series of impacts will be made on tangent track section of the Precision Test Track (PTT) at TTC. Successive impacts will be made in increments of 2 mph or less starting at 4 mph or less until the design coupler force of the car (600,000 pounds) as specified in paragraph 4.1.10 or a speed of 14 mph has been reached, whichever occurs first. The coupler force shall not exceed 1,250,000 pounds during any impact with a speed of 6 mph or less.

Strain data, coupler load, and speed will be measured during these tests.

7.8 Securement System (S-2043, Paragraph 5.4.7)

The buffer car does not include a securement system.

8.0 DYNAMIC TESTS

Dynamic tests include testing as described MSRP Section C Part II, Specification M-1001, Chapter 11, as well as additional requirements. Where Chapter 11 and HLRM criteria differ, the car shall meet both requirements. Table 17 summarizes the required dynamic tests.

M-1001, Chapter 11 specifies a maximum test speed of 70 mph for all non-curving tests. S-2043 requires the maximum speed be increased to 75 mph where deemed safe by the TTCI test team. Tests at speeds over 70 mph shall be used to quantify performance, and limiting criteria will not apply.

Table 18 summarizes S-2043 dynamic limiting criteria. Figure 75 illustrates the application of 50 millisecond and 3 ft. distance limits for L/V ratio and minimum vertical wheel load.

For buffer car tests IWS will be placed in both axles of the B-end truck. The truck with instrumented wheel sets can be placed in either leading or trailing position as required by the particular test.

Table 17. Dynamic Tests

Test Name	Lead End	IWS Position	Comments
5.5.7 Hunting	B	Axles 1-2	Separately with KR wheels
5.5.8 Twist and Roll	B	Axles 1-2	
5.5.9 Yaw and Sway	B	Axles 1-2	
5.5.10 Dynamic Curving	B A	Axles 1-2*	
5.5.11 Pitch and Bounce (Chapter XI)	B	Axles 1-2	
5.5.12 Pitch and Bounce Special	B	Axles 1-2	Create zone with 44-foot 6-inch wavelength
5.5.13 Single bump test	B	Axles 1-2	
5.5.14 Curve Entry/Exit	B A	Axles 1-2*	5.5.13.1 Limiting Spiral tests will be done during Dynamic Curving tests. 5.5.13.2 Spiral Negotiation tests will be done during Constant Curving tests.
5.5.15 Curving with Single Rail Perturbation	B A	Axles 1-2*	Perturbation will be installed on URB north Y. (Two tests, inside bump and outside bump.)
5.5.16 Standard M-1001 Chapter 11 Constant Curving	B A	Axles 1-2*	These tests will be performed on the WRM track in the 7.5-, 10-, and 12-degree curves. Testing will be done clockwise and counterclockwise
5.5.17 Special Track Work	B A	Axles 1-2*	Turnout tests will be carried out on the URB north Y track, possibly in conjunction with 5.5.15 tests. The crossover tests will be conducted on the Impact track to Fast Y crossover.

*This means IWS do not move; for B-end leading tests they are in the leading end, for A-end leading tests they are in the trailing end.

Table 18. Dynamic Limiting Criteria

Criterion	Limiting Value	Notes
Maximum carbody roll angle (degree)	4	Peak-to-peak.
Maximum wheel L/V	0.8	Not to exceed indicated value for a period greater than 50 msec. and for a distance greater than 3 ft. per instance*.
95th percentile single wheel L/V (constant curving tests only)	0.6	Not to exceed indicated value. Applies only for constant curving tests.
Maximum truck side L/V	0.5	Not to exceed indicated value for a duration equivalent to 6 ft. of track per instance.
Minimum vertical wheel load (%)	25	Not to fall below indicated value for a period greater than 50 msec. and for a distance greater than 3 ft. per instance*.
Peak-to-peak carbody lateral acceleration (G)	1.3 0.60	For non-passenger-carrying railcars For passenger-carrying railcars
Maximum carbody lateral acceleration (G)	0.75 0.35	For non-passenger-carrying railcars For passenger-carrying railcars
Carbody lateral acceleration standard deviation (G)	0.13	Calculated over a 2000-ft sliding window every 10 ft. over a tangent track section that is a minimum of 4000 ft. long.
Maximum carbody vertical acceleration (G)	0.90 0.60	For non-passenger-carrying railcars For passenger-carrying railcars
Maximum vertical suspension deflection (%)	95	Suspension bottoming not allowed. Maximum compressive spring travel shall not exceed 95% of the spring travel from the empty car height of the outer load coils to solid spring height.
Maximum vertical dynamic augment acceleration (g)	0.9	Suspension bottoming not allowed. Vertical dynamic augment accelerations of a loaded car shall not exceed 0.9 G.
*Figure 75 illustrates the application of 50 millisecond and 3 ft. distance limits for L/V ratio and minimum vertical wheel load.		

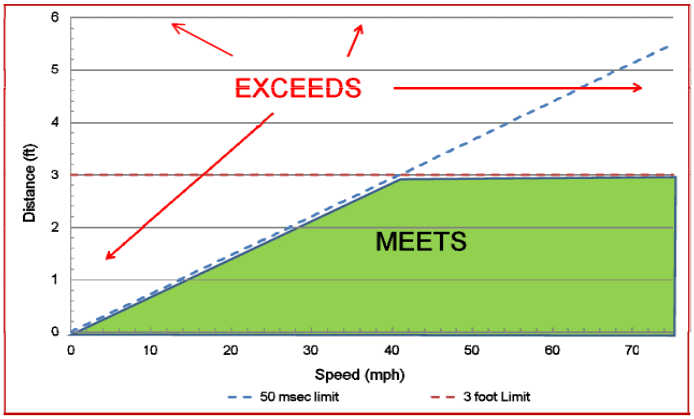


Figure 75. Time and Distance to Climb Limits

8.1 Track geometry (S-2043, Paragraph 5.5.6)

Unless otherwise specified, the track geometry in each test regime must conform to the requirements of MSRP Section C Part II, Specification M-1001, paragraph 11.7.2.5, Table 11.2.

8.2 Instrumentation

The instrumentation / data collection package for these tests will be provided by TTCI and will include all of the necessary transducers for comparison with S-2043 performance measures. Measurements for dynamic tests are listed in Table 19.

To provide precise measurements of wheel/rail forces, two instrumented wheel sets‡ will be installed in both axles of the B-truck, which can be placed in either the leading or trailing position as required by the particular test (see Figure 76).

Carbody lateral acceleration, carbody roll angle measurements, and spring group vertical displacement will be taken on each end of the vehicle.

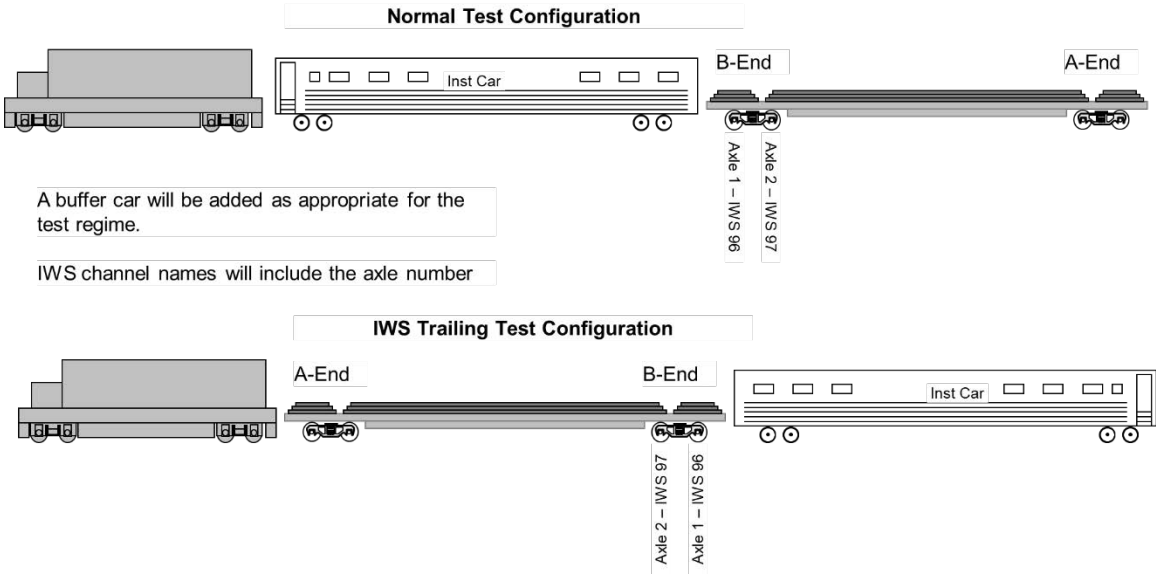


Figure 76. IWS Configuration

Data channels will include:

- Two each – Roll gyroscopes
- Two each – Vertical accelerometers
- Two each – Lateral accelerometers
- Four each – 10-in. string potentiometers
- Two each – Instrumented wheelsets
- One each – Speed tachometer
- One each – Automatic location device

‡ Instrumented wheelsets must meet requirements of M-1001, Appendix C

Table 19. Measurement List for Instrumented Wheel Set Testing

NO.	Channel Name	Measurement Description	Expected Range	Measurement Frequency Response	Digital Sample Rate	Estimated Accuracy
1	Speed	Speed	0-80mph	0-1Hz	≥300Hz	better than 1%
2	ALD	Automatic Location Device	0-5V	≥15Hz	≥300Hz	better than 2%
3	VLX VRX LVLX LVRX TSLVL1 TSLVR1 X=Axle Num.	IWS in Axle 1		≥15Hz	≥300Hz	better than 5%
4		IWS in Axle 2		≥15Hz	≥300Hz	better than 5%
5	ZACBB	Lead carbody vertical acceleration*	between ±2g and ±10g	≥15Hz	≥300Hz	better than 1%
6	ZACBA	Trail carbody vertical acceleration*	between ±2g and ±10g	≥15Hz	≥300Hz	better than 1%
7	YACBB	Lead carbody lateral acceleration*	between ±2g and ±10g	≥15Hz	≥300Hz	better than 1%
8	YACBA	Trail carbody lateral acceleration*	between ±2g and ±10g	≥15Hz	≥300Hz	better than 1%
9	ZDSNBL	Vertical Displacement B truck Left Side	>5 inch	≥15Hz	≥300Hz	better than 1%
10	ZDSNBR	Vertical Displacement B truck Right Side	>5 inch	≥15Hz	≥300Hz	better than 1%
11	ZDSNAL	Vertical Displacement A truck Left Side	>5 inch	≥15Hz	≥300Hz	better than 1%
12	ZDSNAR	Vertical Displacement A truck Right Side	>5 inch	≥15Hz	≥300Hz	better than 1%
13	RDCBB	Carbody roll rotation, B-end	±4deg	≥15Hz	≥300Hz	better than 1%
14	RDCBA	Carbody roll rotation, A-end	±4deg	≥15Hz	≥300Hz	better than 1%
15	GPS	GPS	n/a	≥1Hz	≥1Hz	better than 1%

*Accelerometers to be placed as close as possible to truck centers

8.2.1 Data Acquisition

Data will be filtered at a rate ≥15 Hz and ≤ (sample rate/2). The minimum sample rate is 300 Hz. Data will be post filtered as required (15 Hz) and analyzed in near-real time using the performance criteria for dynamic testing provided in Table 18.

8.2.2 Functional Checks

Functional checks of the instrumentation should be made to verify that all the measurements are working correctly. These functional checks are not a calibration function, but are done to verify the setup.

Common setup errors are faulty transducers, cabling errors, improper gain settings, etc. Perform functional checks to verify that the cables go where they are supposed to and measure about the right value. If a functional check of a transducer shows more than 10% error, look closely at the setup to make sure there are no mistakes.

- Record the functional checks in a data file so you can refer to them later if necessary.
- Perform the functional checks in a specific order and verify that the order matches what you observe in the data file.
- Pay attention to the sign of the output.

The following are typical functional checks for some transducers.

- Roll the accelerometers 90 degrees for a 1g input.
- Pull string pots and verify that extension is positive and that they read 1-inch when pulled one inch.
- Use a block of known size to check LVDTs and bending beams.
- Check speed measurements against GPS speed
- Verify load cells with an R-cal resistor and a breakout box.
- If possible, apply a known force to a load cell. For example, use the car weight and the track grade from your Operating Rule Book to estimate the average expected force on the appropriate channel for a particular piece of track during resistance testing.

Instrumented wheel sets are a special case. The following are suggested for functional tests of IWS. As IWS technology changes the steps might change.

- Verify the cable is connected where you think it is by disconnecting the cable at the wheelset and verifying that the “Disconnected” light comes on at the decoder box where you expect it to.
- Push the R-cal button on the Decoder box and verify that you see the step change in the correct IWS channels.
- Record data on a portion of tangent track.
  - Vertical loads should match the scale weight to within 5%
  - Lateral loads should be small, resulting in L/V ratios of about 0.05. This may vary depending on truck design and condition.
  - Contact position output should be around zero. This may vary depending on truck design and condition.
  - If the wheelset is equipped with a torque bridge its average should be around zero. This may vary depending on truck design and condition.

- If a truck is fully instrumented with IWS, you can compare the net lateral load to a calculated value for a curve.

8.3 Hunting (S-2043, Paragraph 5.5.7)

The high-speed stability (hunting) tests must conform to the requirements of M-1001 paragraph 11.7.2, with the exception of limiting criteria. High-speed stability testing is conducted to confirm that hunting (lateral oscillating instability in the trucks) does not occur within normal operating speeds of the train. Hunting is inherent in typical railroad freight truck designs when components are allowed to wear beyond normal limits.

The car will be equipped with wheel sets having KR wheel profiles (100,000-mile average worn profile), and will be operated at speeds up to 75 mph on tangent track.

8.3.1 Hunting Test Procedure and Test Conditions

The high-speed stability tests shall be conducted under the following conditions:

- The car will be placed at the end of a consist following a stable buffer car (can be the instrumentation car)
- Maximum speed of 70 mph, 75 mph if deemed safe by the TTCI test team
- Track with FRA class 6 or better designation
- Rail profile is AREA 136 lb. or equivalent
- 56 5/16 in. < Track Gauge < 57 in.
- Wheels shall all have KR profile (100,000-mile average worn profile)
- Minimum coefficient of wheel/rail friction of 0.4

Data will be recorded in a short (about 1000-foot) section of the entry and exit spiral at each end of the tangent hunting zone to confirm performance in shallow curves.

8.3.2 Hunting Test Instrumentation and Test Conduct

Because instrumented wheel sets are not available with the KR wheel profile, the hunting tests must be conducted in two configurations:

- Using IWS with the AAR-1B narrow flange profile[7] that is required for all other dynamic tests. During these tests, the wheel sets in positions that are not instrumented must also have the AAR-1B narrow flange wheel profile.
- Using wheel sets (not instrumented) having the KR wheel profile in all positions.

The test car will be instrumented as described in Table 19 with or without instrumented wheel sets as appropriate. Sustained truck hunting shall be determined by measuring the lateral acceleration of the carbody in 2,000-ft windows sliding every 10-ft over a tangent track section that is a minimum of 4,000-ft long. Time histories of the worst-case results that exceed criteria shall be submitted with the report.

Hunting tests will be performed on the RTT track between R39 and R33.5. At a minimum, data will be recorded from R40 to R33 to observe performance in the entry and exit spiral and curve. If hunting is observed during the test it must be reported, even if it occurs in the non-tangent test section. Table 20 shows the run list. Additional speeds may be added by the TTCI test team depending on car performance.

Table 20. Hunting Run List

Filename	Speed (mph)	Comments
	30	Track Conditioning Run
	40	
	50	
	55	
	60	
	65	
	70	
	75	If deemed safe by the TTCI test team

8.4 Twist and Roll (S-2043, Paragraph 5.5.8)

The twist and roll tests must conform to the requirements of M-1001 paragraph 11.8.2, with the exception of limiting criteria. The twist and roll test is conducted to determine the car's ability to negotiate oscillatory cross level perturbations. These perturbations are designed to excite the natural twist and roll motions of the car. The twist and roll test will be conducted on the Precision Test Track (PTT), station 1644+10 to 1651+70. Figure 77 provides a description of the Twist and Roll test zone.

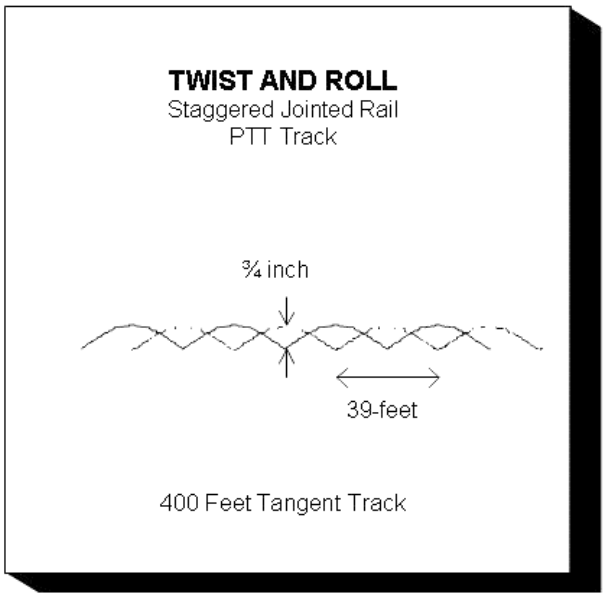


Figure 77. Twist and Roll Test Zone

8.4.1 Twist and Roll Test Procedure and Test Conditions

Twist and roll tests shall be conducted given the following conditions:

- Test car has a stable buffer car at each end (one can be the instrumentation car)
- AAR-1B wheel profiles
- Rail must not have more than 0.25 in. of gauge wear nor have plastic flow on the gauge side greater than 0.25 in.

- Starting test speed is well below predicted resonance and increases in 2 mph increments (or less) until resonance is passed. It is acceptable to approach a resonant condition from a higher speed.
- Minimum coefficient of friction is 0.4
- Tangent track
- Ten staggered perturbations of 39-ft wavelength and 0.75-in. cross-level (see Figure 77)
- Otherwise class 5 or better track

8.4.2 Twist and Roll Instrumentation and Test Conduct

Axles 1 and 2 will be equipped with IWSs as shown in Figure 76. The test shall be conducted with the B end leading (IWS-equipped truck leading). The test car will be instrumented as described in Table 19.

The individual wheel forces and the roll angles at each end if the carbody shall be measured continuously through the test zone. Time histories of the worst-case results that exceed criteria, and the number of exceedances over the various run speeds (as applicable) shall be submitted with the report.

Table 21 shows suggested runs for the twist and roll tests. Runs are performed starting at 10 mph and increasing in 2-mph increments until the lower center roll resonance is passed. Once lower center roll resonance is passed speeds are increased in 5-mph increments until 70 mph is reached. If performance is close to the limits smaller speed increments should be used to assure safety and closely identify the critical speed. If deemed safe by the TTCI test team, a 75-mph run will be performed.

Table 21. Twist and Roll Test Runs.

Filename	Speed	Comments
	10	
	12	
	14	
	16	
	18	
	20	
	22	
	24	
	26	Transition from 2-mph increments to 5-mph increments at the discretion of TTCI test team
	30	
	35	
	40	
	45	
	50	
	55	

	60	
	65	
	70	
	75	If deemed safe by the TTCI test team

8.5 Yaw and Sway (S-2043, Paragraph 5.5.9)

The yaw and sway tests must conform to the requirements of M-1001 paragraph 11.8.4, with the exception of limiting criteria. The yaw and sway test is conducted to determine the ability of the car to negotiate laterally misaligned track, which will excite the car in a yaw and sway motion. The speeds at which the resonant dynamic reactions occur will be found if they occur before 75 mph is reached. Station 1921 to 1927 of the PTT is the test site for the Yaw and Sway Test. Figure 78 provides a description of the Yaw and Sway test zone.

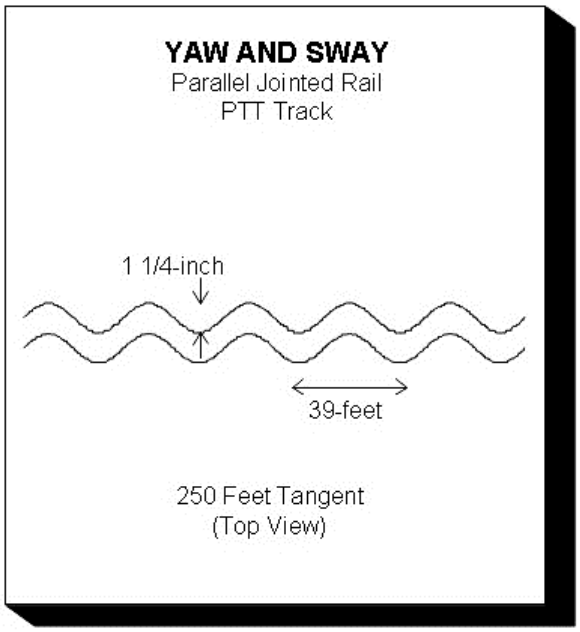


Figure 78. Yaw and Sway Test Zone

8.5.1 Yaw and Sway Test Procedure and Test Conditions

Yaw and sway tests shall be conducted given the following conditions:

- As built (with permanent ballast)
- Test car has a leading stable buffer with a minimum truck center of 45 ft. (can be the instrumentation car)
- No Trailing buffer car
- Minimum coefficient of friction is 0.4
- AAR-1B wheel profiles
- Rail must not have more than 0.25 in. of gauge wear nor have plastic flow on the gauge side greater than 0.25 in.
- Starting test speed is well below predicted resonance and increases in 5 mph increments (or less) until resonance, an unsafe condition, or 75 mph is reached.

- Tangent track
- Constant wide gauge of 57.5 inch
- Five parallel perturbations of 39-ft wavelength and maximum 1.25-in. lateral amplitude (see Figure 78).
- Track is otherwise class 5 or better

8.5.2 Yaw and Sway Instrumentation and Test Conduct

Axles 1-2 will be equipped with IWSs as shown in Figure 76. Dynamic modeling predictions show that the last truck in the car has truck side L/V ratios that are slightly higher than other locations. Because of this the test shall be conducted with the A end leading (IWS-equipped truck trailing). The wheel forces shall be measured continuously through the test zone. Time histories of the worst-case results that exceed criteria shall be submitted with the report.

Table 22 shows suggested runs for the yaw and sway test. Runs are performed starting at 30 mph and increasing in 5 mph increments until 70 mph is reached. If performance is close to the limits smaller speed increments may be used to assure safety and closely identify the critical speed. If deemed safe by the TTCI test team, a 75 mph run will be performed.

Table 22. Loaded Yaw and Sway Test Runs

Filename	Speed	Comments
	30	
	35	
	40	
	45	
	50	
	55	
	60	
	65	
	70	
	75	If deemed safe by the TTCI test team

8.6 Dynamic Curving (S-2043, Paragraph 5.5.10)

The dynamic curving tests must follow the requirements of M-1001 paragraph 11.8.5, with the exception of limiting criteria. The dynamic curving test is designed to determine the ability of the car to negotiate curved track with simultaneous cross level and gage (vertical and lateral) misalignments. The dynamic curving test is conducted on the 10-degree bypass curve of the WRM track. Figure 79 provides a description of the Dynamic Curve Test location.

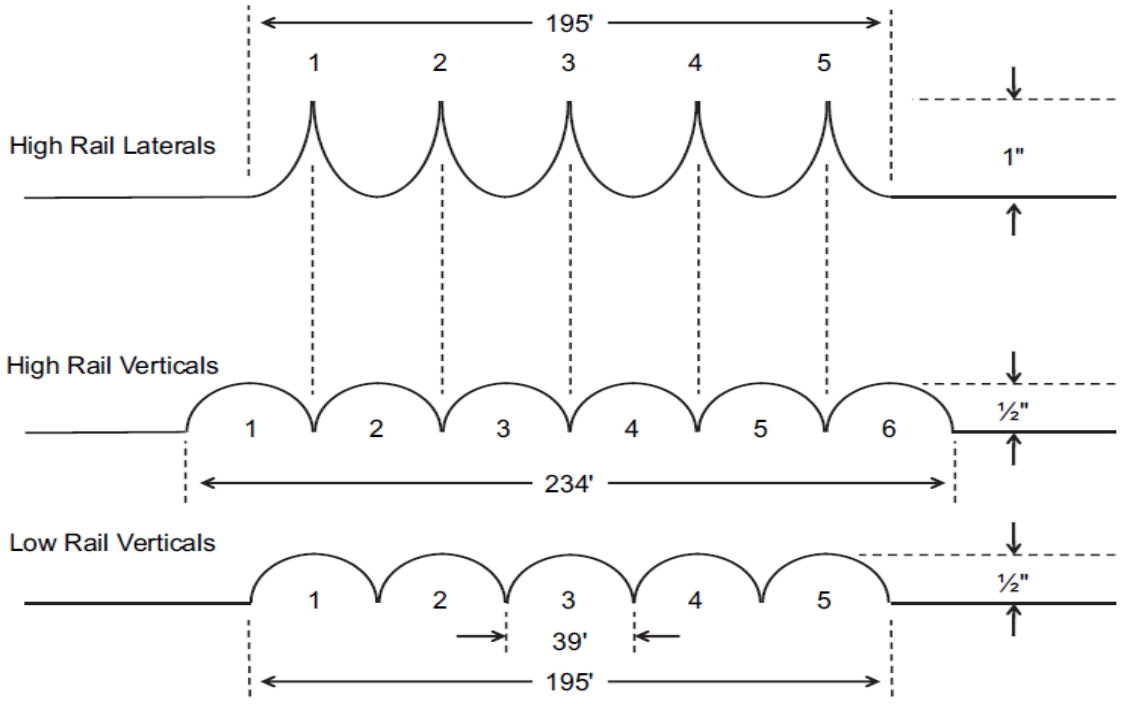


Figure 79. Dynamic Curving Test Zone

8.6.1 Dynamic Curving Test Procedure and Test Conditions

Dynamic curve tests shall be conducted given the following conditions:

- Test car between two stable buffers (one can be the instrumentation car)
- Minimum coefficient of friction is 0.4
- AAR-1B wheel profiles
- Rail must not have more than 0.25 in. of gauge wear nor have plastic flow on the gauge side greater than 0.25 in.
- Curvature is between 10° and 15° with a balance speed between 15 and 25.
- Starting test speed is –3 in. under-balance with (but not limited to) 2 mph increments and a maximum of +3 in. over-balance. The resonance point may be approached from a higher speed.
- Five staggered perturbations of 39-ft wavelength and 0.5-in. cross-level (see Figure 79)
- Five alignment cusps having the maximum gauge of 57.5 in. coincident with low points of the outside rail and the 56.5 in. gauge points associated with the inner rail low points (see Figure 79). There are no alignment variations on the low rail.
- It is recommended that a guard rail be used to prevent unpredicted derailment; however, it must not be in contact with the wheel during normal test running.

8.6.2 Dynamic Curving Instrumentation and Test Conduct

Axles 1 and 2 will be equipped with instrumented wheel sets as shown in Figure 76. IWS Configuration. Testing is required with both B and A ends leading (IWS-equipped truck leading and trailing). The carbody roll angle shall also be measured at one end. The lateral and vertical wheel forces and the roll angle shall be measured continuously through the test zone. Time histories of the

worst-case results that exceed criteria, along with a count of the number of occurrences (as applicable) shall be submitted with the report.

Table 23 shows required runs for the dynamic curving test for each leading end condition. Tests are done CW and CCW.

Table 23. Dynamic Curving Test Runs

Filename	Speed	Direction	Comments
	10	CW	
	12	CW	
	14	CW	
	16	CW	
	18	CW	
	20	CW	
	22	CW	
	24	CW	
	26	CW	
	28	CW	
	30	CW	
	32	CW	
	10	CCW	
	12	CCW	
	14	CCW	
	16	CCW	
	18	CCW	
	20	CCW	
	22	CCW	
	24	CCW	
	26	CCW	
	28	CCW	
	30	CCW	
	32	CCW	

8.7 Pitch and Bounce (S-2043, Paragraph 5.5.11)

The pitch and bounce tests must follow the requirements of M-1001 paragraph 11.8.3, with the exception of limiting criteria. The pitch and bounce test is designed to determine the dynamic pitch and bounce response of the car as it is excited by inputs from the track. The pitch and bounce test is conducted on the PTT track, stations 1710 and 1715. Figure 80 provides a description of the Pitch and Bounce test zone.

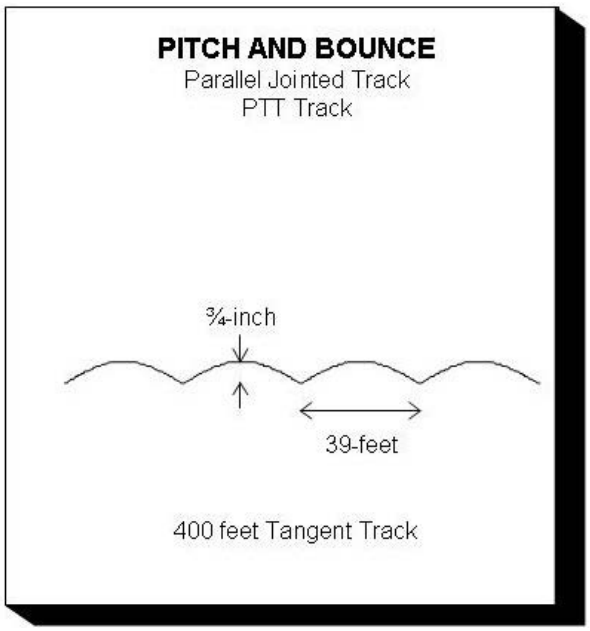


Figure 80. Pitch and Bounce Test Zone

8.7.1 Pitch and Bounce Test Procedure and Test Conditions

Pitch and bounce tests shall be conducted given the following conditions:

- Test car has a stable buffer car at each end with a minimum 45-ft truck center (one can be the instrumentation car)
- AAR-1B wheel profiles
- Rail must not have more than 0.25 in. of gauge wear nor have plastic flow on the gauge side greater than 0.25 in.
- Starting test speed is well below predicted resonance and increases in 5 mph increments (or less) until resonance, an unsafe condition, or 75 mph is reached. It is acceptable to approach a resonant condition from a higher speed.
- Tangent track
- Ten parallel perturbations of 39-ft wavelength and maximum 0.75-in. vertical amplitude (see Figure 80)
- Otherwise class 5 or better track

8.7.2 Pitch and Bounce Instrumentation and Test Conduct

Axles 1 and 2 will be equipped with IWSs as shown in Figure 76. The test shall be conducted with the B end leading (IWS-equipped truck leading). The vertical wheel forces shall be measured continuously through the test zone. Time histories of the worst-case results that exceed criteria, along with a count of the number of occurrences (as applicable) shall be submitted with the report.

Table 24 shows suggested runs for the pitch and bounce test. Runs are performed starting at 30 mph and increasing in 5 mph increments until 70 mph is reached. A 75-mph run will be performed if deemed safe by the TTCI test team. If performance is close to the limits smaller speed increments should be used to assure safety and closely identify the critical speed.

Table 24. Pitch and Bounce Test Runs

Filename	Speed	Comments
	30	
	35	
	40	
	45	
	50	
	55	
	60	
	65	
	70	
	75	If deemed safe by the TTCI test team

8.8 Pitch and Bounce Special (S-2043, Paragraph 5.5.12)

S-2043 requires that a special section of track with 3/4-inch bumps at a wavelength equal to the truck center spacing be built for the car being tested. This distance is 44 feet 6 inches for the buffer car.

TTCI will install 10 parallel perturbations of 44.5-ft wavelength and 0.75-in. vertical amplitude at a location to be determined.

Table 26 shows suggested runs for the special pitch and bounce test. Runs are performed starting at 40 mph and increasing in 5 mph increments until 70 mph is reached. A 75-mph run will be performed if deemed safe by the TTCI test team. If performance is close to the limits smaller speed increments should be used to assure safety and closely identify the critical speed.

Table 25. Special Pitch and Bounce Test

Filename	Speed	Comments
	30	TCR
	40	
	45	
	50	
	55	
	60	
	65	
	70	
	75	If deemed safe by the TTCI test team

8.9 Single Bump Test (S-2043, Paragraph 5.5.13)

This test is intended to represent a grade crossing. Tests will be performed over a 1.0-in. bump on tangent track. The single bump will be a flat-topped ramp with the initial elevation change over 7 ft., a steady elevation over 20 ft., ramping back down over 7 ft. Track geometry for the single bump test must be maintained to the following tolerances:

- ±1/8-inch amplitude for the bump
- ±1/8-inch cross level
- ±1/4-inch gage

The test zone will be installed on the transit test track at T-15 using rail bent specifically for this purpose.

Table 26 shows suggested runs for the single bump test. Runs are performed starting at 40 mph and increasing in 5 mph increments until 70 mph is reached. A 75-mph run will be performed if deemed safe by the TTCI test team. If performance is close to the limits smaller speed increments should be used to assure safety and closely identify the critical speed.

Table 26. Single Bump Test Runs

Filename	Speed	Comments
	40	
	45	
	50	
	55	
	60	
	65	
	70	
	75	If deemed safe by the TTCI test team

8.10 Curve Entry/Exit (S-2043, Paragraph 5.5.14)

8.10.1 Limiting Spiral Negotiation

The spiral negotiation tests must conform to the requirements of M-1001 paragraph 11.7.4, with the exception of limiting criteria. Spiral negotiation, or curve entry and curve exit, tests will be performed in conjunction with the dynamic curving tests. A spiral is the transition from a tangent track to a curve that includes constant rates of change in cross level and curvature with distance. The limiting spiral consists of a steady curvature change from 0 degree to 10 degrees and a steady super elevation change of 4 3/8 inches in 89 feet. The purpose of the exaggerated limiting spiral is to twist the trucks and the carbody.

The limiting spiral test zone is located at the beginning of the 10-degree bypass curve of the Wheel/Rail Mechanisms (WRM) track (see Figure 81) during clockwise operation. Tests are done at the same time as the dynamic curving test and in both the clockwise and counter-clockwise directions, with both B and A ends leading (IWS-equipped truck leading and trailing). Curve entry and exit performance will also be examined for the 7.5-, 12-, and 10-degree curves (see Figure 81).

8.10.2 Spiral Negotiation Test Procedure and Test Conditions

This test will be carried out concurrently with the curving tests conducted on the WRM track. Curving tests will be performed under the following conditions:

- Speed corresponding to 3 in. of cant (superelevation) deficiency, balance speed, and speed corresponding to 3 in. of cant (superelevation) excess (-3 in., 0 in., and +3 in.)
- Use of a leading and trailing buffer car (one of which can be the instrumentation car)
- Test in both directions (turning consist)
- Minimum coefficient of friction is 0.4
- AAR-1B wheel profiles
- Rail must not have more than 0.25 in. of gauge wear nor have plastic flow on the gauge side greater than 0.25 in.
- Minimum curvature is 7° with a balance speed of 20 to 30 mph
- Class 5 track or better
- Spiral geometry shall have a super elevation change rate of 3 in. in 62 ft. and a minimum length of 89 ft.

8.10.3 Spiral Negotiation Instrumentation and Test Conduct

Axles 1-2 will be equipped with instrumented wheel sets as shown in Figure 76. Testing is required with both B and A ends leading (IWS-equipped truck leading and trailing). The lateral and vertical forces and their ratio, L/V, shall be measured continuously through qualified spirals in both directions, and their maxima and minima computed. Time histories of the worst-case results that exceed criteria, along with a count of the number of occurrences (as applicable) shall be submitted with the report.

Table 27 shows required runs for the limiting spiral test. Test speeds correspond to 3-inches under balance, balance, and 3-inches over balance. Tests are done CW and CCW directions. Two runs will be done at each speed.

Table 27. Limiting Spiral Test Runs.

Filename	Speed	Direction	Comments
	12	CW	
	12	CW	
	24	CW	
	24	CW	
	32	CW	
	32	CW	
	12	CCW	
	12	CCW	
	24	CCW	
	24	CCW	
	32	CCW	
	32	CCW	

8.11 Curving with Single Rail Perturbation (S-2043, Paragraph 5.5.15)

This test is intended to represent a low or high joint in a yard or a poorly maintained lead track. Two test scenarios will be run, one with a 2-inch outside rail dip and the other with a 2-inch inside rail bump. Both tests will be conducted on the URB north wye track, a 12-degree curve with less than 1/2-inch nominal superelevation. The inside rail bump shall be a flat-topped ramp with an elevation change over 6-ft, a steady elevation over 12 ft., ramping back down over 6 ft. The outside rail dip shall be the reverse. Two rails have been bent for these perturbations. The two perturbations will be installed in the URB north wye curve about 250 feet apart. Track geometry for the single bump test must be maintained to the following tolerances:

- ±1/8-inch amplitude for the bump
- ±1/8-inch cross level
- ±1/4-inch gage

Table 28 shows required runs for the curving with single rail perturbation test. Tests will be performed in 2-mph increments for 4 mph to 14 mph. Test runs will be performed traveling south on the Transit test track through the diverging route of the turnout onto the north wye track with B-end of the car leading.

Table 28. Curving with Single Rail Perturbation Test Runs

Filename	Speed	Comments
	4	
	6	
	8	
	10	
	12	
	14	

8.12 Standard Chapter 11 Constant Curving (S-2043, Paragraph 5.5.16)

The constant curving tests must follow the requirements of M-1001 paragraph 11.7.3, with the exception of limiting criteria. Constant curving tests were designed to determine the car's ability to negotiate well-maintained track curves. This test is intended to verify that a car will not experience wheel climb or impart large lateral forces to the rails during curving.

As presented in Table 18, maximum wheel L/V ratio shall not exceed 0.8 for more than 50 msec. and the 95th percentile wheel L/V shall not exceed 0.6.

The train will be operated on the 7.5-, 10-, and 12-degree curves of WRM track at speeds corresponding to three inches under balance, balance, and three inches over balance (12, 24, and 32 mph). Tests will be run in both clockwise and counterclockwise directions. Wheel L/V ratios will be monitored to ensure safe test operation. Figure 81 provides a description of the curving test zone.

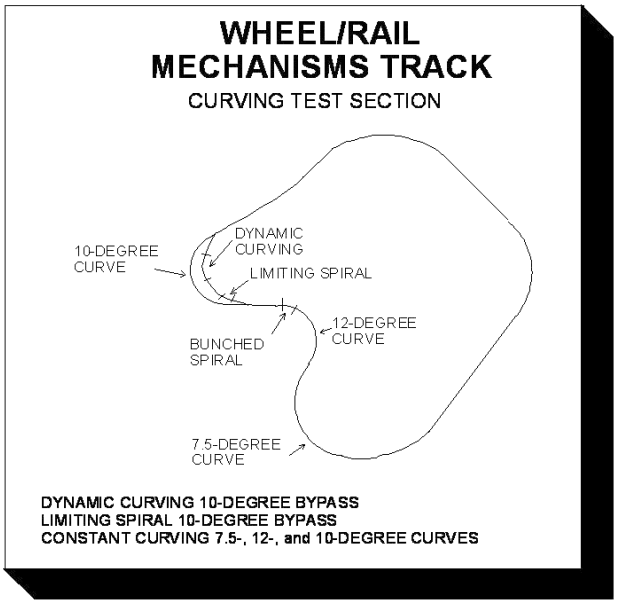


Figure 81. Curving Test Zone

8.12.1 Curving Test Procedure and Test Conditions

Curving tests will be performed under the following conditions:

- Speed corresponding to 3 in. of cant (superelevation) deficiency, balance speed, and speed corresponding to 3 in. of cant (superelevation) excess (-3 in., 0 in., and +3 in.)
- Use of a leading and trailing buffer car (one of which can be the instrumentation car)
- Test in both directions (turning consist)
- Minimum coefficient of friction is 0.4
- AAR-1B wheel profiles
- Rail must not have more than 0.25 in. of gauge wear nor have plastic flow on the gauge side greater than 0.25 in.
- Minimum curvature is 7° with a balance speed of 20 to 30 mph
- Class 5 track or better
- Curve length must be a minimum of 500 ft.

8.12.2 Curving Instrumentation and Test Conduct

Axles 1 and 2 will be equipped with instrumented wheel sets as shown in Figure 76. Testing is required with both B and A ends leading (IWS-equipped truck leading and trailing). The lateral and vertical forces and their ratio, L/V, shall be measured for the length of the body of the curve. A time history of the worst-case results that exceed criteria must be submitted in the report.

Table 29 shows required runs for the steady state curving test. Test speeds correspond to 3-inches under balance, balance, and 3-inches over balance. Tests are done CW and CCW. Repeat each run at least once.

Table 29. Standard Chapter 11 Constant Curving Test Runs

Filename	Speed (mph)	Direction	Comments
	12-15-12	CW	3 in. underbalance speeds for 7.5-, 12-, and 10-degree curves on WRM loop, respectively.
	12-15-12	CW	3 in. underbalance speeds for 7.5-, 12-, and 10-degree curves on WRM loop, respectively.
	24	CW	Approximate balance speed for all curves
	24	CW	Approximate balance speed for all curves
	32	CW	Approximate 3 in. overbalance speed for all curves
	32	CW	Approximate 3 in. overbalance speed for all curves
	12-15-12	CCW	3 in. underbalance speeds for 7.5-, 12-, and 10-degree curves on WRM loop, respectively.
	12-15-12	CCW	3 in. underbalance speeds for 7.5-, 12-, and 10-degree curves on WRM loop, respectively.
	24	CCW	Approximate balance speed for all curves
	24	CCW	Approximate balance speed for all curves
	32	CCW	Approximate 3 in. overbalance speed for all curves
	32	CCW	Approximate 3 in. overbalance speed for all curves

8.13 Special Track Work (S-2043, Paragraph 5.5.17)

The railcar will be run through various switches, turnouts, and crossovers while measuring wheel/rail forces. The railcar must be run through an AREMA straight point turnout with a number 8 or tighter frog angle. The test will be performed in both directions, at speeds from walking speed to the switch speed limit. Similar tests must be performed through a crossover with number 10 or tighter turnouts on 15-ft or narrower track centers.

Switch number 704 between the Transit Test Track and the North URB Wye will be used for the turnout tests. Crossover number 212 between the Impact Track and the FAST Wye will be used for crossover tests.

During the walking speed tests, the railcar will be monitored visually to note any binding or interference between the trucks and carbody.

Axles 1-2 will be equipped with instrumented wheel sets as shown in Figure 76. Testing is required with both B and A ends leading (IWS-equipped truck leading and trailing). The lateral and vertical forces and their ratio, L/V, shall be measured for the length of the body of the curve. A time history of the worst-case results that exceed criteria must be submitted in the report.

Table 30 shows required runs for the special track work turnout test. Test speeds are from walking speed to the turnout speed limit. Tests are done in both directions (switch point leading and trailing) along the diverging route and with B- and A-end leading.

Table 30. Special Track Work Turnout Test

Filename	Speed	Direction	Comments
	Walking	Facing Point	Check Clearances
	4	Facing Point	
	6	Facing Point	
	8	Facing Point	
	10	Facing Point	
	12	Facing Point	
	14	Facing Point	
	15	Facing Point	
	Walking	Trailing Point	Check Clearances
	4	Trailing Point	
	6	Trailing Point	
	8	Trailing Point	
	10	Trailing Point	
	12	Trailing Point	
	14	Trailing Point	
	15	Trailing Point	1

Table 31 shows required runs for the special track work crossover test. Test speeds are from walking speed to the crossover speed limit. Tests are done in both directions and with B- and A-end leading.

Table 31. Special Track Work Crossover Test

Filename	Speed	Direction	Comments
	Walking	Impact-Fast Wye	Check Clearances
	5	Impact-Fast Wye	
	10	Impact-Fast Wye	
	15	Impact-Fast Wye	
	20	Impact-Fast Wye	
	Walking	Fast Wye-Impact	Check Clearances
	5	Fast Wye-Impact	
	10	Fast Wye-Impact	
	15	Fast Wye-Impact	
	20	Fast Wye-Impact	

9.0 TEST SCHEDULE

Figure 82 provides a preliminary test schedule. Detailed scheduling will be based on resource and facility availability. TTCI is evaluating the potential for accelerating the schedule based on anticipated arrival of the railcar in February 2018.

Single Car Testing	Start	Finish	Qtr3 2018	Qtr4 2018	Qtr1 2019	Qtr2 2019	Qtr3 2019	Qtr4 2019	Qtr1 2020	Qtr2 2020	Qtr3 2020	Qtr4 2020
Buffer Car Tests						* *						
Instrumentation Preparation	*Apr-19*	*Apr-19*				■						
Characterization Tests	*May-19*	*Jul-19*				■ ■ ■						
Static Tests	*Jul-19*	*Jul-19*				■						
Structural Tests	*Aug-19*	*Aug-19*				■						
Dynamic Tests	*Aug-19*	*Sep-19*				■ ■						
Contingency	*Oct-19*	*Jan-20*				■ ■ ■ ■						
Cask Car Tests						* *						
Instrumentation Preparation	*Apr-19*	*Apr-19*				■						
Characterization Tests	*May-19*	*Jul-19*				■ ■ ■						
Static Tests	*Aug-19*	*Sep-19*				■ ■						
Structural Tests	*Sep-19*	*Sep-19*				■						
Dynamic Tests	*Oct-19*	*Dec-19*				■ ■ ■						
Contingency	*Jan-20*	*Feb-20*				■ ■						
Reporting / Coordination with EEC						* *						
Data Analysis and Reporting	*Feb-20*	*Aug-20*				■ ■ ■ ■ ■ ■ ■						
Coordination with EEC	*Apr-20*	*Oct-20*				■ ■ ■ ■ ■ ■ ■						
Approval for Multi-Car Test	*Oct-20*					■						

Figure 82. Preliminary Test Schedule

References

1. AAR Manual of Standards and Recommended Practices, Car Construction Fundamentals and Details, Performance Specification for Trains Used to Carry High-Level Radioactive Material, Standard S-2043, Effective: 2003; Last Revised: 2017, Association of American Railroads, Washington, DC

2. AAR Manual of Standards and Recommended Practices, Section C—Part II, Car Construction Fundamentals and Details, Design, Fabrication, and Construction of Freight Cars, Chapter 2, General Data, Implemented 11/2017, Association of American Railroads, Washington, DC

3. AAR Manual of Standards and Recommended Practices, Section C—Part II, Car Construction Fundamentals and Details, Design, Fabrication, and Construction of Freight Cars, Chapter 11, Service-Worthiness Tests and Analyses for New Freight Cars, Implemented 09/2017, Association of American Railroads, Washington, DC

4. Safety Rule Book, TTCI, January 2018 or Latest Revision

5. Operating Rule Book, TTCI, January 2018 or Latest Revision

6. Walker, Russell and Shawn Trevithick. “S-2043 Certification: Preliminary Simulations of Kasgro Buffer Railcar”, Report P-17-023, TTCI, Pueblo, CO, November 2017

7. Walker, Russell and Satima Anankitpaiboon. “S-2043 Certification Tests of Kasgro M-290 12-Axle Flat Car”. Report No. P-09-044, TTCI, Pueblo, CO, December 2009

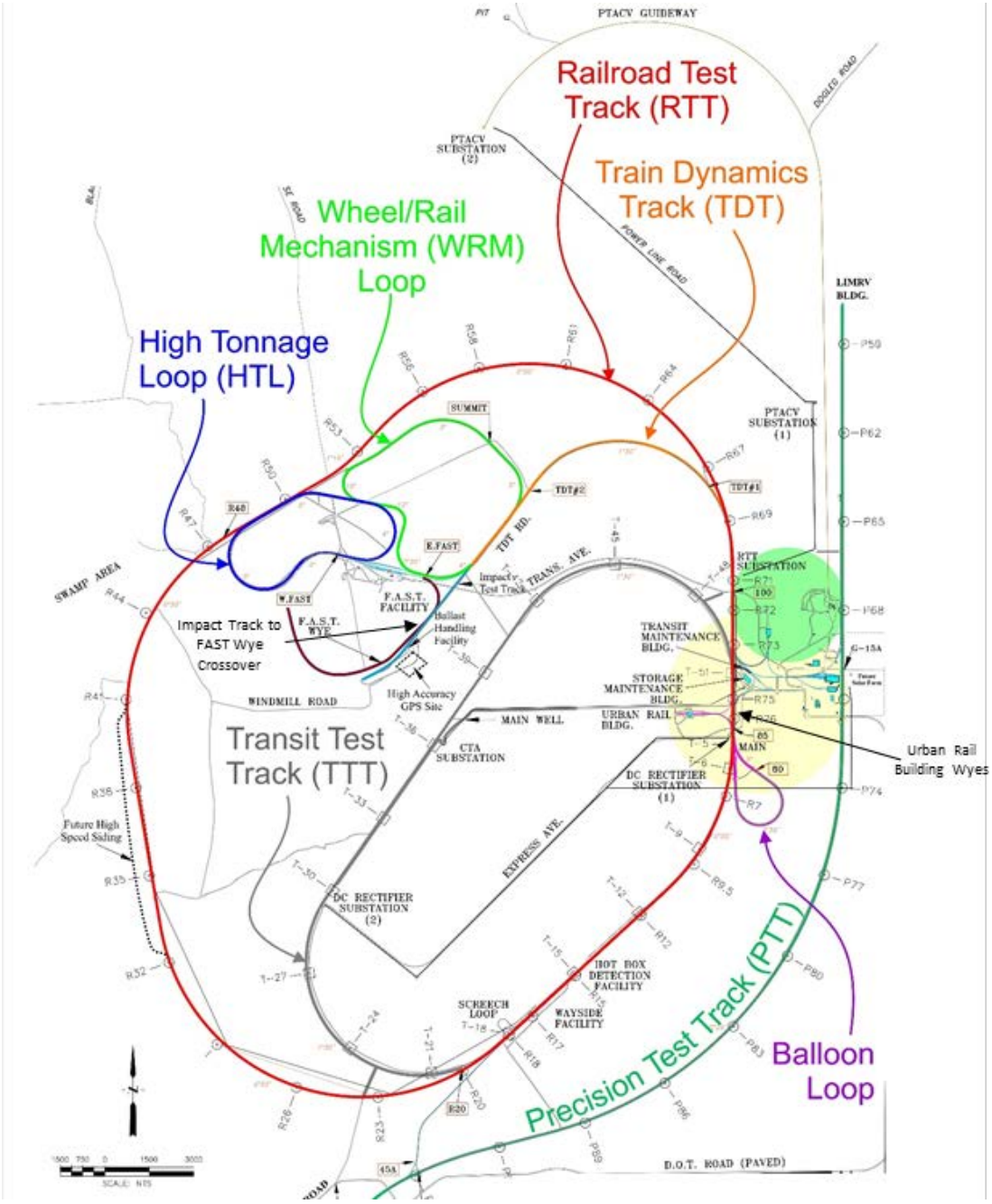
8. Manual of Standards and Recommended Practices Section G Safety and Operations -- Wheels and Axles, Figure B12, Effective September 2016, Association of American Railroads, Washington, DC

9. TTCI network: \DOE Controlled Document Folder\DW - Drawings and Specifications\DW-18-002 Kasgro SG Location Cask and Buffer Car .zip\1155-47 Kasgro SG Location Buffer Car.dwg

ATTACHMENT A – Test Track Details

INTRODUCTION

Testing is planned on various test tracks at the Transportation Technology Center including the Railroad Test Track (RTT), the Wheel Rail Mechanisms (WRM) Loop, the Precision Test Track (PTT), the URB Wye, the Tight Turn Loop (TTL or Screech Loop), and a crossover between the Impact Track and FAST Wye. Figure below shows locations of the various tracks. Sections 2.0 to 6.0 describe the tracks planned to be used for the Atlas and Buffer car testing.



Test Tracks at TTC

RAILROAD TEST TRACK (RTT)

The 13.5-mile Railroad Test Track (RTT) will be used for High Speed Stability (Hunting) testing of the Atlas and buffer cars. The RTT alignment is designed to test passenger vehicles with tilt technology at a maximum running speed of 165 mph. Maximum speed for non-tilting vehicles is typically 124 mph. Freight vehicle testing is limited to 80 mph operating speed, unless qualified for higher speeds.

WHEEL / RAIL MECHANISMS (WRM) LOOP

The Wheel / Rail Mechanisms (WRM) Loop incorporates curve variations constructed to meet the curved track test requirements of AAR Specification M-1001, Chapter 11. These variations are also applicable to S-2043 testing and will be used for several tests of the Atlas and buffer cars. The WRM is maintained as a non-lubricated track for test purposes. Strain gages have been installed in some of the curves for measuring Wheel/Rail interaction forces. The figure below shows details of track in a siding on the inside of the 10-degree curve that is the location of dynamic curve track perturbations.



Adjustable Tie Plates and Perturbations on the WRM

PRECISION TEST TRACK (PTT)

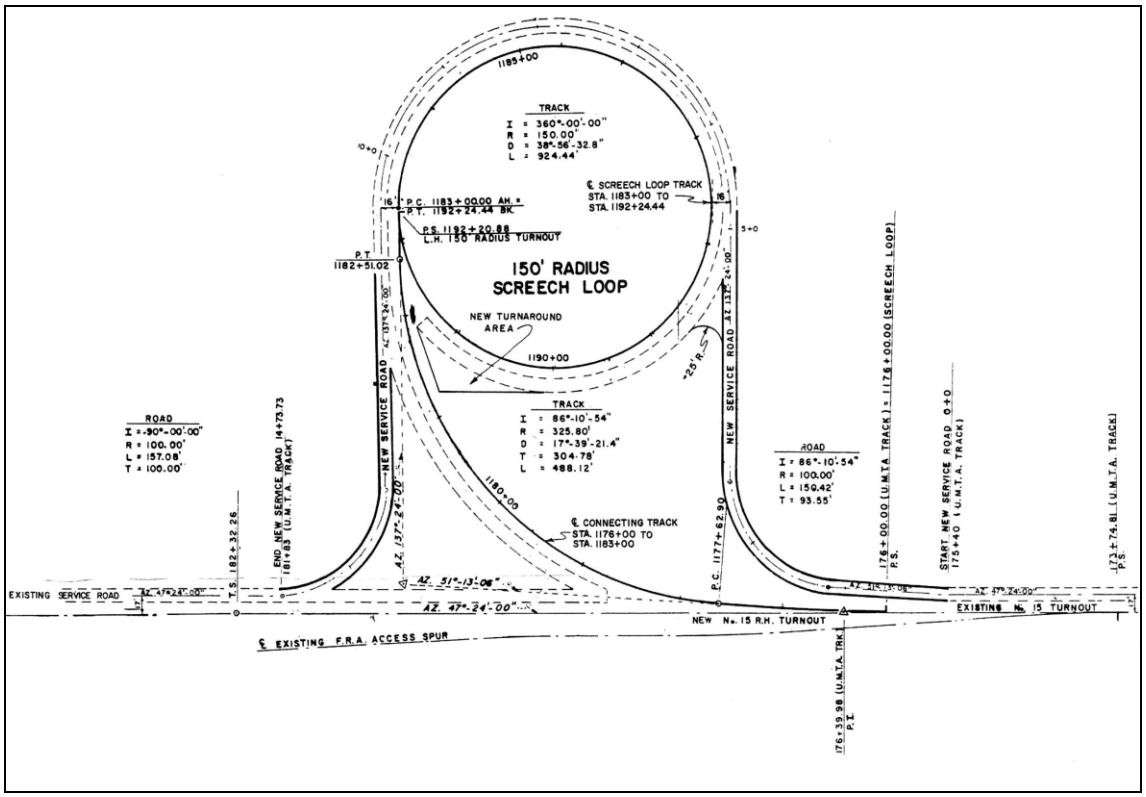
The Precision Test Track (PTT) is a 7.4-mile track section that is used to test for vehicle dynamic response under perturbed track conditions. Three perturbed track test sections have been installed:

- Twist and roll test section in the north tangent section (PTT Stations 1644+10 to 1651+70). Due to the location of these perturbations, and the limited acceleration capability of TTC locomotives, the maximum test speed through this test section is typically about 70 mph, although preparations are being made to achieve 75 mph for this test program.
- Pitch and bounce test section in the south end of the same tangent section (PTT Stations 1710 to 1715).
- Yaw and Sway test section on the south end of the PTT (PTT Approx. Stations 1921 to 1927)

The perturbation sections for twist and roll, and pitch and bounce have been re-built using new ties and adjustable alignment plates with elastic fasteners, screw spikes, and steel shim plates. The adjustable tie plate system is the same that is in place on the WRM Loop.

TIGHT TURN LOOP

The Tight Turn Loop (TTL), also called the screech loop, will be used for the Horizontal Curve Negotiation test. It is located at the lower end of the southeast tangent section of the Transit Test Track. The TTL layout is as shown in the figure below. It consists of a 150' radius loop (38.9-degree curve) constructed as a ballasted track with 119-pound continuous welded rail on wood ties. The loop is connected with a short spur track having a 17 2/3-degree curve. The main purpose of the TTL is to provide a facility for the detailed investigation of wheel noise, truck curving behavior, and rail vehicle stability under extreme curvature conditions.

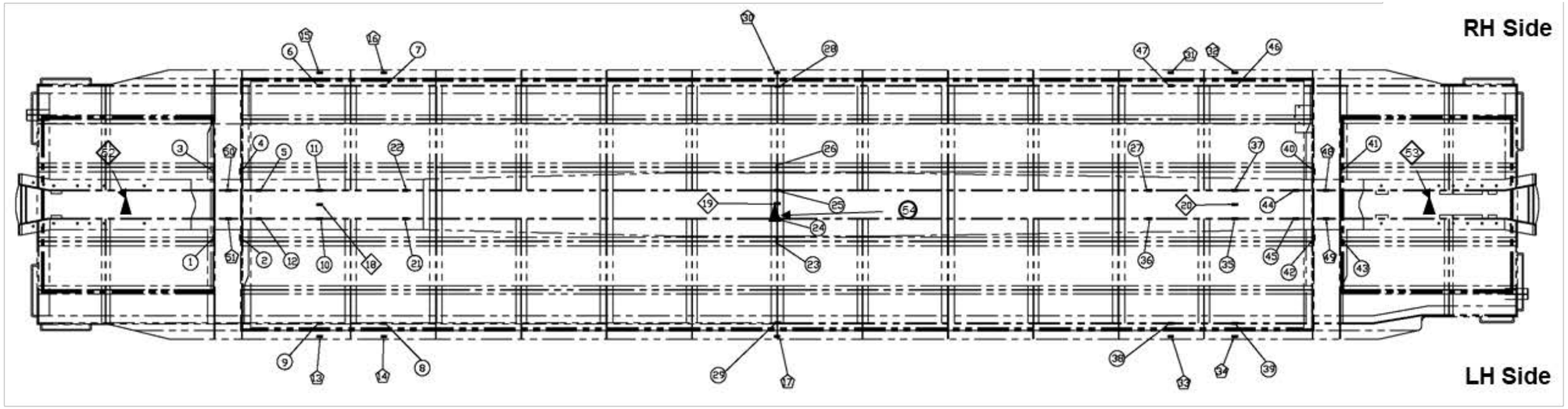


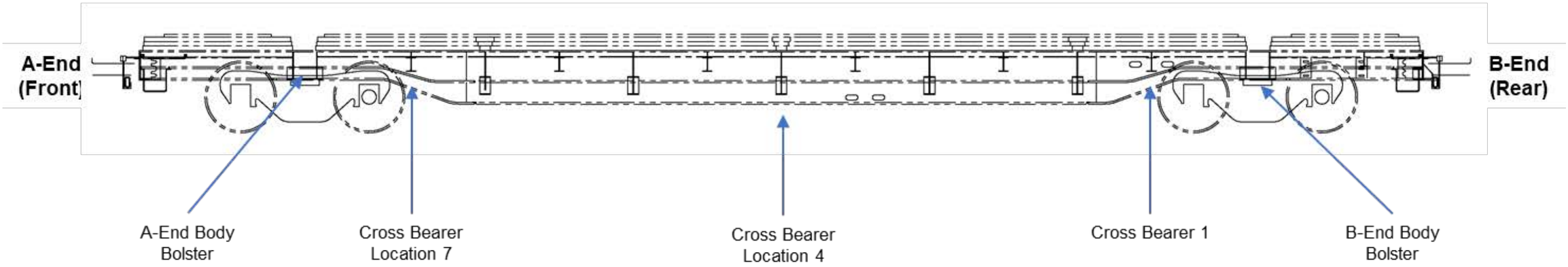
Tight Turn Loop Layout

OTHER LOCATIONS

Testing is also planned on the North URB Wye, which connects the Urban Rail Building access track to the TTT, and on the crossover between the Impact Track and the FAST Wye.

ATTACHMENT B – STRAIN GAUGE LOCATIONS FOR STRUCTURAL TESTS





Strain Gauge/Thermocouple Locations

Strain Gauge and Thermocouple Channel)

Figure B1 Ref	Channel Name	Approximate Locations (confirm based on latest version of Kasgro Drawing 1155-47)[9]	Yield Strain at gauge location (μstr)	Modulus of Elasticity at Gauge Location (10^6 ksi)	Units	Expected Range
1	SGBF1	Front of bottom flange of A-end body bolster near center sill -- LH side	1724	29	μstr	±2,000
2	SGBF2	Rear of bottom flange of A-end body bolster near center sill -- LH side	1724	29	μstr	±2,000
3	SGBF3	Front of bottom flange of A-end body bolster near center sill -- RH side	1724	29	μstr	±2,000
4	SGBF4	Rear of bottom flange of A-end body bolster near center sill -- RH side	1724	29	μstr	±2,000
5	SGBF5	RH edge of bottom flange of center sill, aft of A-end body bolster	1724	29	μstr	±2,000
6	SGBF6	Center of bottom flange of RH side sill, forward of cross bearer 7	1724	29	μstr	±2,000
7	SGBF7	Center of bottom flange of RH side sill, aft of cross bearer 7	1724	29	μstr	±2,000
8	SGBF8	Center of bottom flange of LH side sill, aft of cross bearer 7	1724	29	μstr	±2,000
9	SGBF9	Center of bottom flange of LH side sill, forward of Cross Bearer Location 7	1724	29	μstr	±2,000
10	SGBF10	LH edge of bottom flange of center sill, forward of cross bearer 7	1724	29	μstr	±2,000
11	SGBF11	RH edge of bottom flange of center sill, forward of cross bearer 7	1724	29	μstr	±2,000
12	SGBF12	LH edge of bottom flange of center sill, aft of A-end body bolster	1724	29	μstr	±2,000

Figure B1 Ref	Channel Name	Approximate Locations (confirm based on latest version of Kasgro Drawing 1155-47)[9]	Yield Strain at gauge location (μstr)	Modulus of Elasticity at Gauge Location (10^6 ksi)	Units	Expected Range
13	SGDP13	LH edge of deck plate, forward of cross bearer 7	1724	29	μstr	±2,000
14	SGDP14	LH edge of deck plate, aft of cross bearer 7	1724	29	μstr	±2,000
15	SGDP15	RH edge of deck plate, forward of cross bearer 7	1724	29	μstr	±2,000
16	SGDP16	RH edge of deck plate, aft of cross bearer 7	1724	29	μstr	±2,000
17	SGDP17	LH edge of deck plate, at longitudinal center of car	1724	29	μstr	±2,000
18	SGDW18	Top of dead weight at lateral center of car, forward of cross bearer 7	1241	29	μstr	±1,500
19	SGDW19	Top of dead weight, at lateral and longitudinal center of car	1241	29	μstr	±1,500
20	SGDW20	Top of dead weight at lateral center of car, aft of cross bearer 1	1241	29	μstr	±1,500
21	SGBF21	LH edge of bottom flange of center sill, forward of cross bearer 6	1724	29	μstr	±2,000
22	SGBF22	RH edge of bottom flange of center sill, forward of cross bearer 6	1724	29	μstr	±2,000
23	SGBF23	Bottom flange of cross bearer 4, LH side of center sill, at longitudinal center of car	1724	29	μstr	±2,000
24	SGBF24	LH edge of bottom flange of center sill, at longitudinal center of car	1724	29	μstr	±2,000
25	SGBF25	RH edge of bottom flange of center sill, at longitudinal center of car	1724	29	μstr	±2,000

Figure B1 Ref	Channel Name	Approximate Locations (confirm based on latest version of Kasgro Drawing 1155-47)[9]	Yield Strain at gauge location (μstr)	Modulus of Elasticity at Gauge Location (10^6 ksi)	Units	Expected Range
26	SGBF26	Bottom flange of cross bearer 2, RH side of center sill, at longitudinal center of car	1724	29	μstr	±2,000
27	SGBF27	RH edge of bottom flange of center sill, aft of cross bearer 2	1724	29	μstr	±2,000
28	SGBF28	Center of bottom flange of RH side sill, at longitudinal center of car	1724	29	μstr	±2,000
29	SGBF29	Center of bottom flange of LH side sill, at longitudinal center of car	1724	29	μstr	±2,000
30	SGDP30	RH edge of deck plate, at longitudinal center of car	1724	29	μstr	±2,000
31	SGDP31	RH edge of deck plate, forward of cross bearer 2	1724	29	μstr	±2,000
32	SGDP32	RH edge of deck plate, aft of cross bearer 2	1724	29	μstr	±2,000
33	SGDP33	LH edge of deck plate, forward of cross bearer 2	1724	29	μstr	±2,000
34	SGDP34	LH edge of deck plate, aft of cross bearer 2	1724	29	μstr	±2,000
35	SGBF35	LH edge of bottom flange of center sill, aft of cross bearer 1	1724	29	μstr	±2,000
36	SGBF36	LH edge of bottom flange of center sill, aft of cross bearer 2	1724	29	μstr	±2,000
37	SGBF37	RH edge of bottom flange of center sill, aft of cross bearer 1	1724	29	μstr	±2,000
38	SGBF38	Center of bottom flange of LH side sill, forward of cross bearer 1	1724	29	μstr	±2,000
39	SGBF39	Center of bottom flange of LH side sill, aft of cross bearer 1	1724	29	μstr	±2,000

Figure B1 Ref	Channel Name	Approximate Locations (confirm based on latest version of Kasgro Drawing 1155-47)[9]	Yield Strain at gauge location (μstr)	Modulus of Elasticity at Gauge Location (10^6 ksi)	Units	Expected Range
40	SGBF40	Front of bottom flange of B-end body bolster near center sill – RH side	1724	29	μstr	±2,000
41	SGBF41	Rear of bottom flange of B-end body bolster near center sill -- RH side	1724	29	μstr	±2,000
42	SGBF42	Front of bottom flange of B-end body bolster near center sill – LH side	1724	29	μstr	±2,000
43	SGBF43	Rear of bottom flange of B-end body bolster near center sill -- LH side	1724	29	μstr	±2,000
44	SGBF44	RH edge of bottom flange of center sill, forward of B-end body bolster	1724	29	μstr	±2,000
45	SGBF45	LH edge of bottom flange of center sill, forward of B-end body bolster	1724	29	μstr	±2,000
46	SGBF46	Center of bottom flange of RH side sill, aft of cross bearer 1	1724	29	μstr	±2,000
47	SGBF47	Center of bottom flange of RH side sill, forward of cross bearer 1	1724	29	μstr	±2,000
48	SGDP48	Top of deck plate, longitudinally centered over B-End body bolster, above RH edge of center sill	1,724	29,000	μstr	±2,000
49	SGDP49	Top of deck plate, longitudinally centered over B-End body bolster, above LH edge of center sill	1,724	29,000	μstr	±2,000
50	SGDP50	Top of deck plate, longitudinally centered over A-End body bolster, above RH edge of center sill	1,724	29,000	μstr	±2,000

Figure B1 Ref	Channel Name	Approximate Locations (confirm based on latest version of Kasgro Drawing 1155-47)[9]	Yield Strain at gauge location (μstr)	Modulus of Elasticity at Gauge Location (10^6 ksi)	Units	Expected Range
51	SGDP52	Top of deck plate, longitudinally centered over A-End body bolster, above LH edge of center sill	1,724	29,000	μstr	±2,000
52	TC52	Laterally and longitudinally centered on top of deck plate forward of A-end body bolster	n/a	n/a	°F	-40 to 150
53	TC53	Laterally and longitudinally centered on top of deck plate forward of A-end body bolster	n/a	n/a	°F	-40 to 150
54	TC54	Bottom flange of cross bearer 4 at lateral and longitudinal center of car	n/a	n/a	°F	-40 to 150

APPENDIX B: STATIC BRAKE FORCE TEST DOCUMENTATION

TRANSPORTATION
TECHNOLOGY CENTER, INC.

Matt DeGeorge
Senior Engineer
Phone: 719-584-0724
Email: matt_degeorge@aar.com

August 20, 2020

Subject: Static Brake Force Test Observations Specification Testing of IDOX 020001, 020002, and IDOX 010001 A-End and B-End

Mr. Jon Hannafious
Senior Manager - Equipment Engineering
Transportation Technology Center, Inc.
Pueblo, CO 81001
Email: Jon_Hannafious@aar.com

Dear Mr. Hannafious,

The static brake force specification testing of the buffer cars (IDOX 020001 and 020002) and the Atlas car (IDOX 010001 A-End and B-End) has been completed. Testing was performed at the Kasgro Rail Corporation facility in New Castle, Pennsylvania on December 4, 2018 (buffer cars) and February 12, 2019 (Atlas car) to comply with Specification S-2043 and S-401.

I was present (test witness) for the required Static Brake Force Tests and can conclude that applicable requirements of AAR Specification S-401 have been satisfactorily addressed.

The details and results of this testing is documented in the attached reports. Should you need any additional information, please do not hesitate to get in contact with me.

Sincerely,

Matt DeGeorge

Atlas Buffer Car Static Brake Force Test Report for December 2018

Contract Number: 89243218CNE000004
Author: Matthew DeGeorge
Date: 12/12/2018
Document RP-18-002

TEST OVERVIEW

Brake Shoe Force Test

- Testing designed to comply with AAR Standard S-401 (01/2018 Revision)
- Checklist drafted, reviewed, and finalized by project management
- Prior to testing FRA personnel reviewed the braking system on both buffer cars

Test Personnel

- Tom Sedarski (Amsted Rail; helped perform test)
- Rick Ford (Kasgro Project Manager)
- Mark Zeigler (Kasgro)
- Cory Wagner (Kasgro; performed test)
- Matt DeGeorge (TTCI observer)

Schedule

- 11/14/18 (November Visit)
  - 9:00am: testing began on buffer car IDOX 020002
  - 1:00pm: testing delayed until future date due to equipment
- 12/4/18 (December Visit)
  - 8:30am: testing began on buffer car IDOX 020002
  - 11:30am: testing concluded on buffer car IDOX 020002
  - 12:00pm – 1:00pm: Lunch (buffer cars swapped out)
  - 2:30pm: testing began on buffer car IDOX 020001
  - 4:15pm: testing concluded on buffer car IDOX 020001
- 12/5/18
  - 8:00am: Review of brake force tests on both cars
  - 9:00am – 11:00am: Overview and inspection of Atlas Cask Car

ISSUES / CONCERNS / COMMENTS

- Daily test performed on Single Car Air Brake Test Device each day before testing
- Testing on 11/14/18 was delayed until the December trip due to brake force measurement equipment issues
    - The Bluetooth connection device used to link the force sensors and the recording/readout device was broken resulting in an inability to see measured force outputs
- During the initial testing of buffer car IDOX 020002 a leak was discovered in the brake cylinder pipeline
    - The leak caused a decrease in force at each wheel over time
    - The leak was found using a soapy solution and fixed
- The piston travel on both cars was initially outside the acceptable range and was adjusted during testing
    - After the pistons were readjusted and several brake reductions were performed to stabilize the system, piston travel in both cars met the criteria
- The empty brake ratio testing was not performed due to the fact that the cars are loaded and will never be unloaded or in the empty condition
- The hand brake force measurements were performed first on buffer car IDOX 020002 with a smart hook and a load clevis pin
    - Buffer car IDOX 020001 had the hand brake force tested with the smart hook only

CONCLUSIONS

- Buffer car IDOX 020001 and IDOX 020002 met the criteria put forth in the AAR Standard S-401

Documentation Photographs

Figure B1. Atlas Buffer Railcar Isometric View B-6
Figure B2. Brake Force Measurement System (Control Box and Readout Tablet) B-6
Figure B3. Force Sensor B-7
Figure B4. Brake Force Measurement System (B-end L1, L2 Force Sensors) B-7
Figure B5. Example Force Sensor Location B-8
Figure B6. Brake Force Measurement System (Load Clevis Pin) B-8
Figure B7. Buffer Railcar Instrumentation Setup Diagram (Both Cars had Identical Setup) B-9
Figure B8. Smart Hook B-10
Figure B9. Car Weight B-10
Figure B10. Single Car Air Brake Test Device B-11
Figure B11. Test Device Gauge Calibration Information B-11
Figure B12. Brake Cylinder Gauge Location (B-end, Right Side) B-12
Figure B13. Brake Cylinder Gauge Calibration Information B-12
Figure B14. Rapping Hammer B-13
Figure B15. Piston Travel Setup Information B-13
Figure B16. Brake Force Measurement System Calibration Information B-14
Figure B17. Smart Hook Calibration Information B-15



Figure B1. Atlas Buffer Railcar Isometric View



Figure B2. Brake Force Measurement System (Control Box and Readout Tablet)

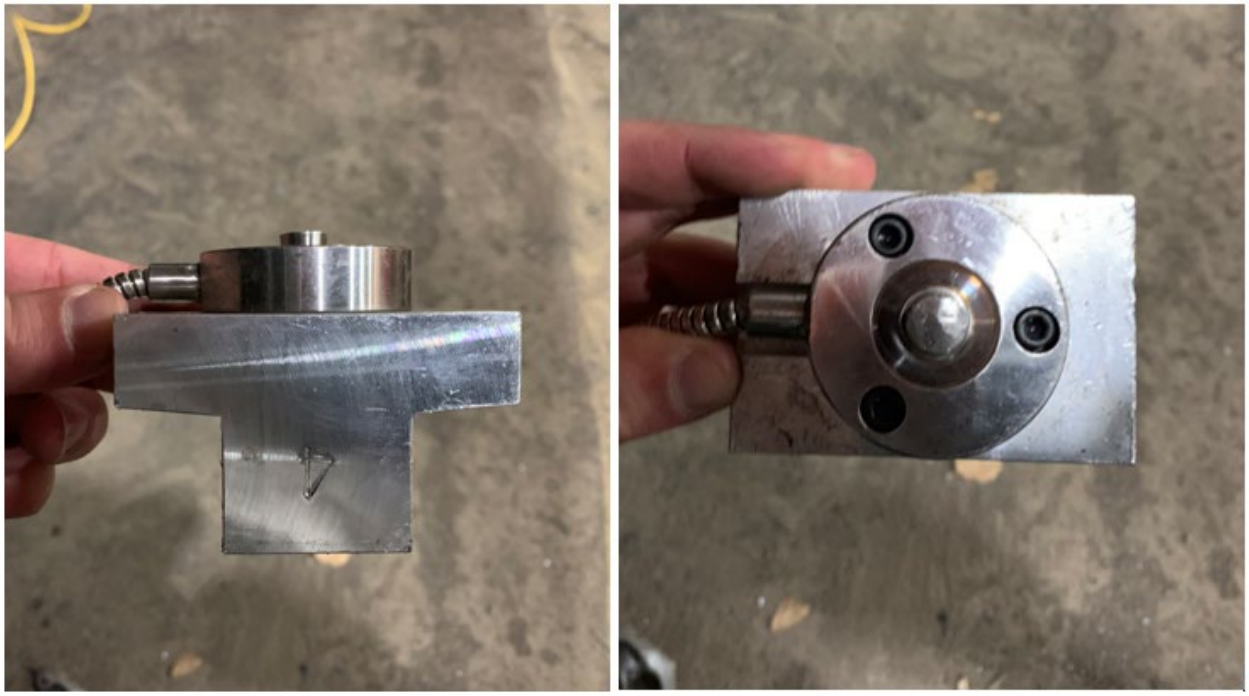


Figure B3. Force Sensor



Figure B4. Brake Force Measurement System (B-end L1, L2 Force Sensors)



Figure B5. Example Force Sensor Location



Figure B6. Brake Force Measurement System (Load Clevis Pin)

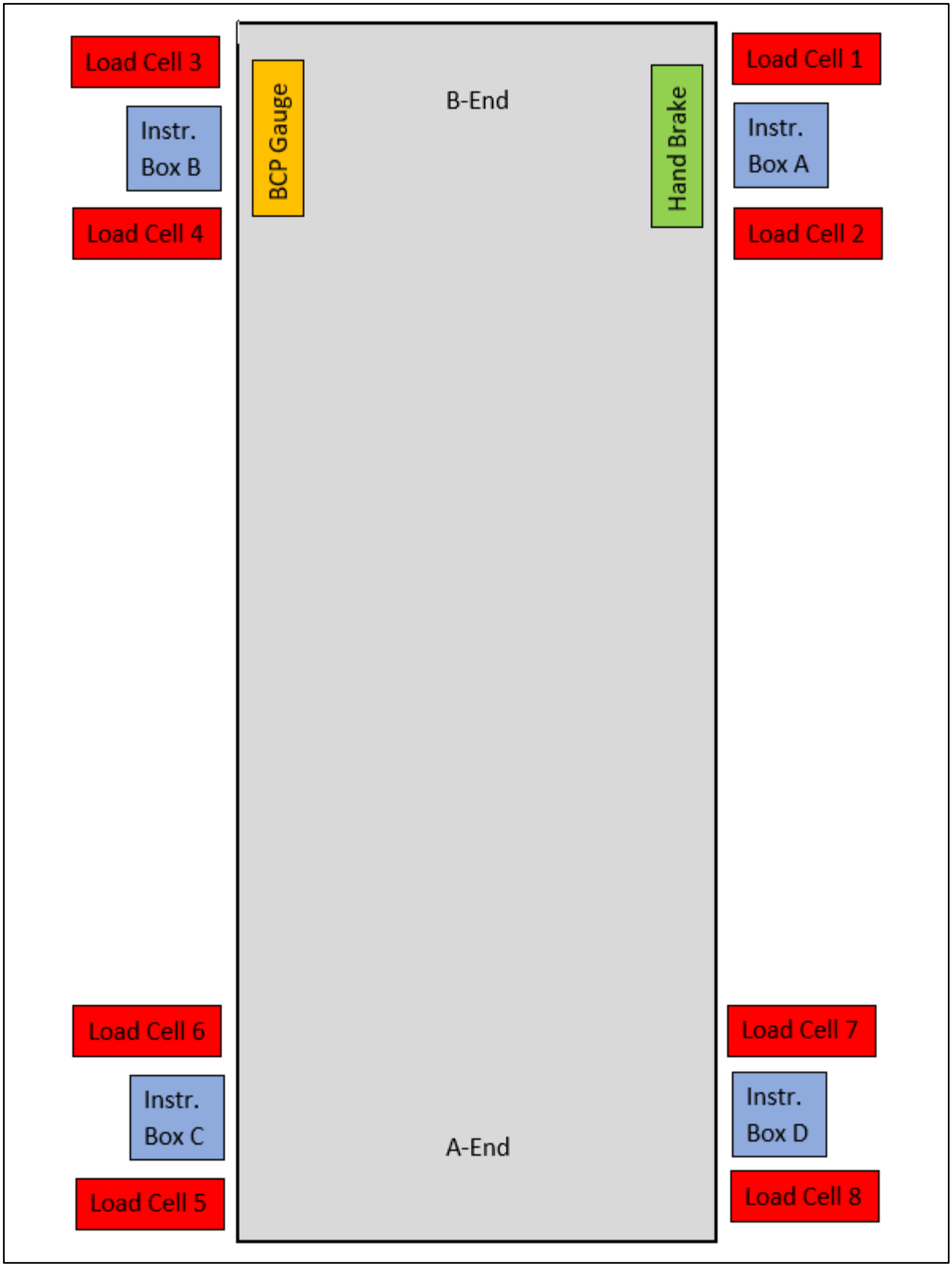


Figure B7. Buffer Railcar Instrumentation Setup Diagram (Both Cars had Identical Setup)

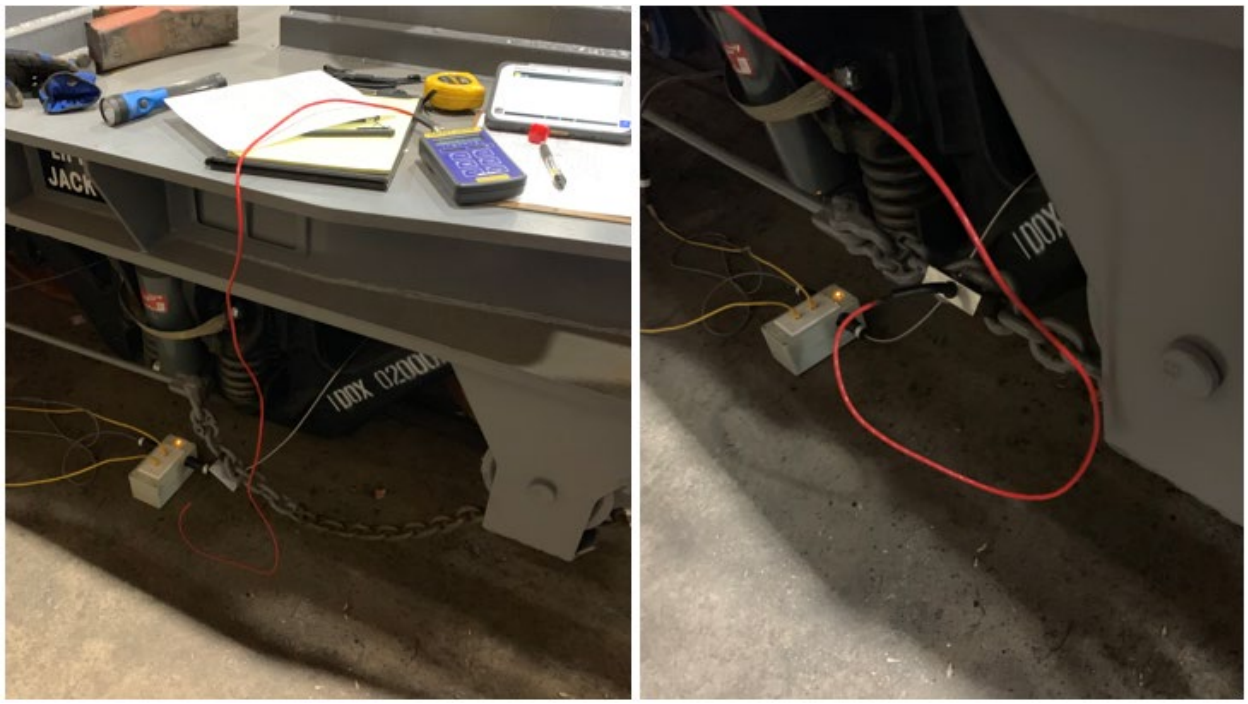


Figure B8. Smart Hook



Figure B9. Car Weight

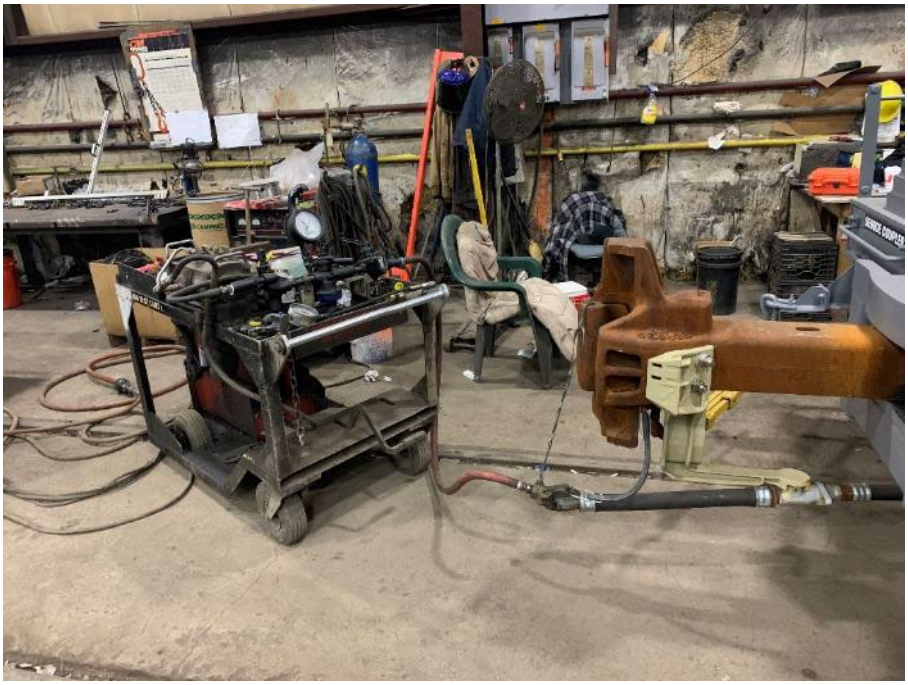


Figure B10. Single Car Air Brake Test Device



Figure B11. Test Device Gauge Calibration Information

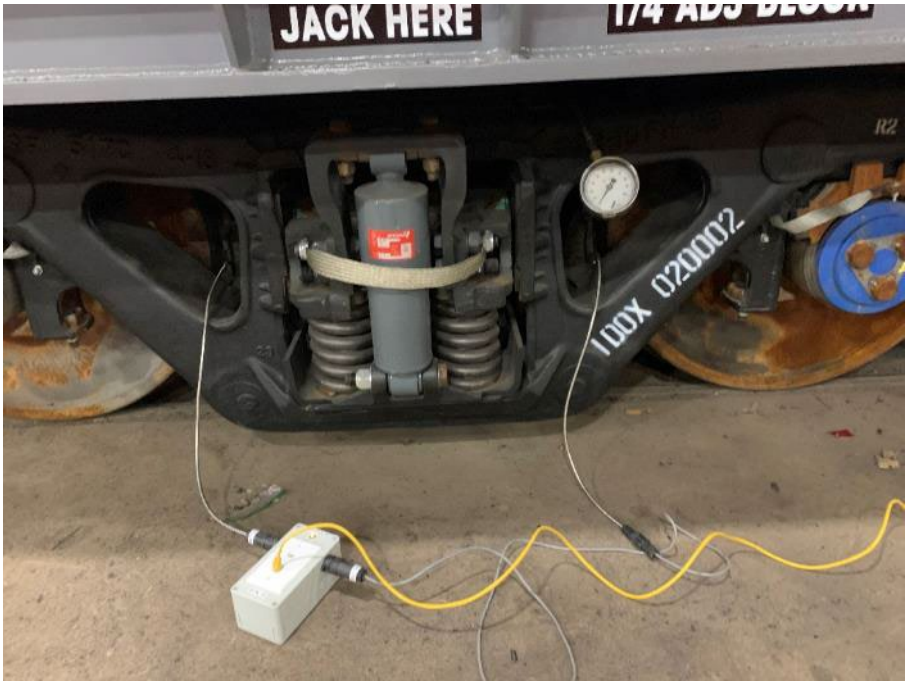


Figure B12. Brake Cylinder Gauge Location (B-end, Right Side)



Figure B13. Brake Cylinder Gauge Calibration Information



Figure B14. Rapping Hammer

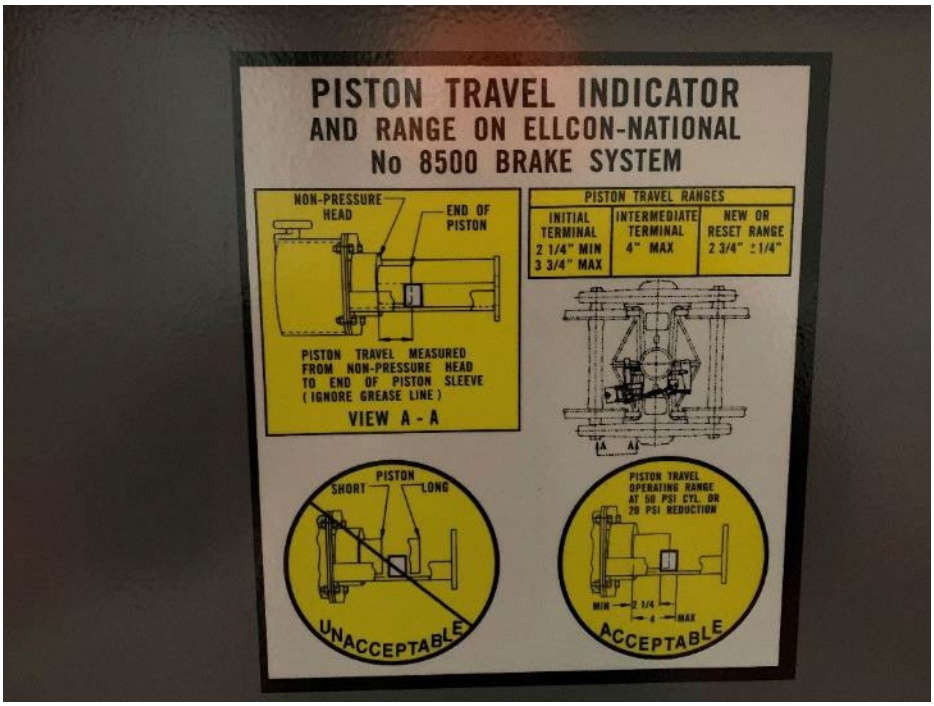
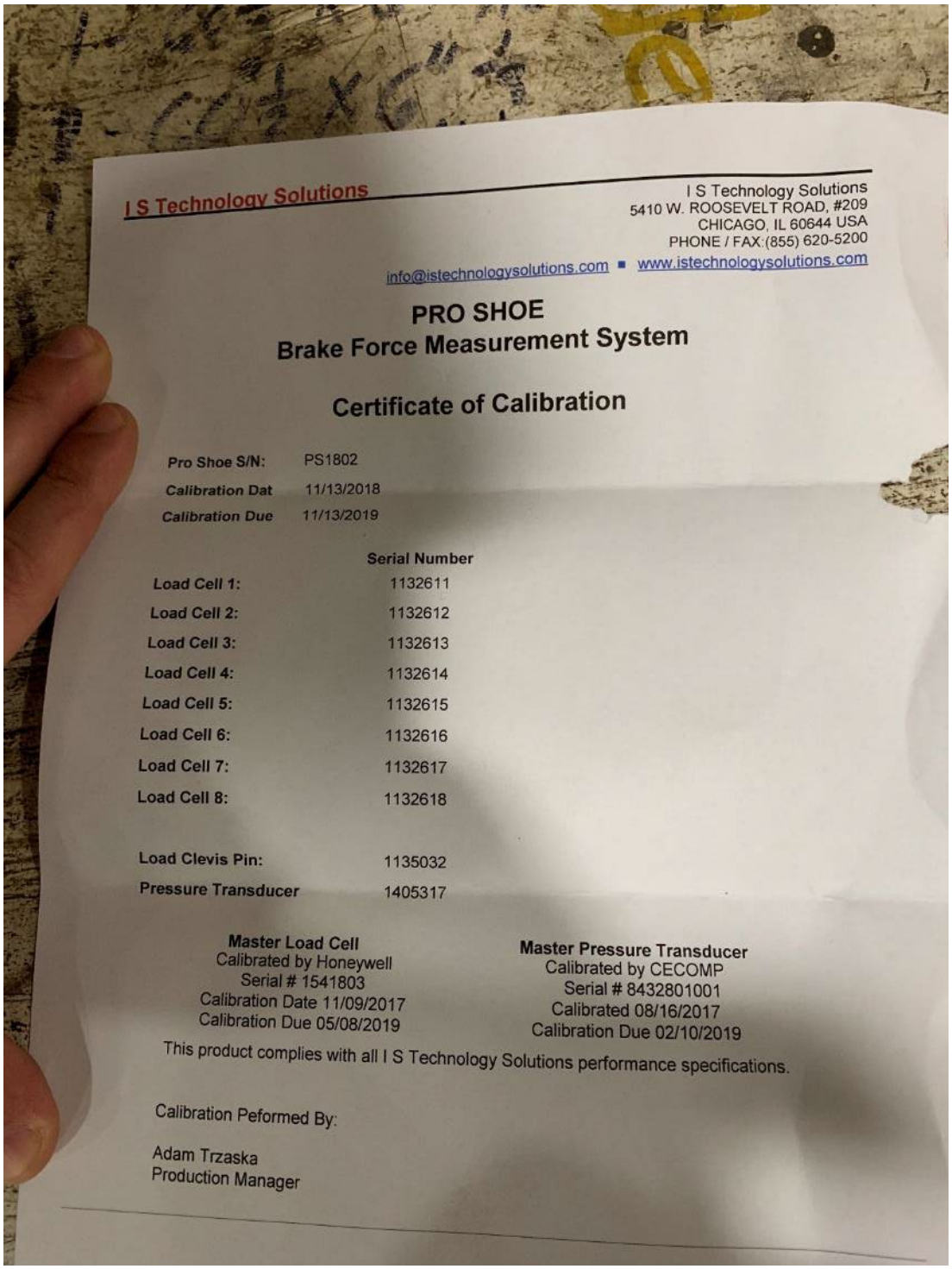


Figure B15. Piston Travel Setup Information



I S Technology Solutions

I S Technology Solutions
5410 W. ROOSEVELT ROAD, #209
CHICAGO, IL 60644 USA
PHONE / FAX:(855) 620-5200

info@istechnologysolutions.com ■ www.istechnologysolutions.com

PRO SHOE
Brake Force Measurement System

Certificate of Calibration

Pro Shoe S/N:	PS1802
Calibration Dat	11/13/2018
Calibration Due	11/13/2019

	Serial Number
Load Cell 1:	1132611
Load Cell 2:	1132612
Load Cell 3:	1132613
Load Cell 4:	1132614
Load Cell 5:	1132615
Load Cell 6:	1132616
Load Cell 7:	1132617
Load Cell 8:	1132618
Load Clevis Pin:	1135032
Pressure Transducer	1405317

Master Load Cell
Calibrated by Honeywell
Serial # 1541803
Calibration Date 11/09/2017
Calibration Due 05/08/2019

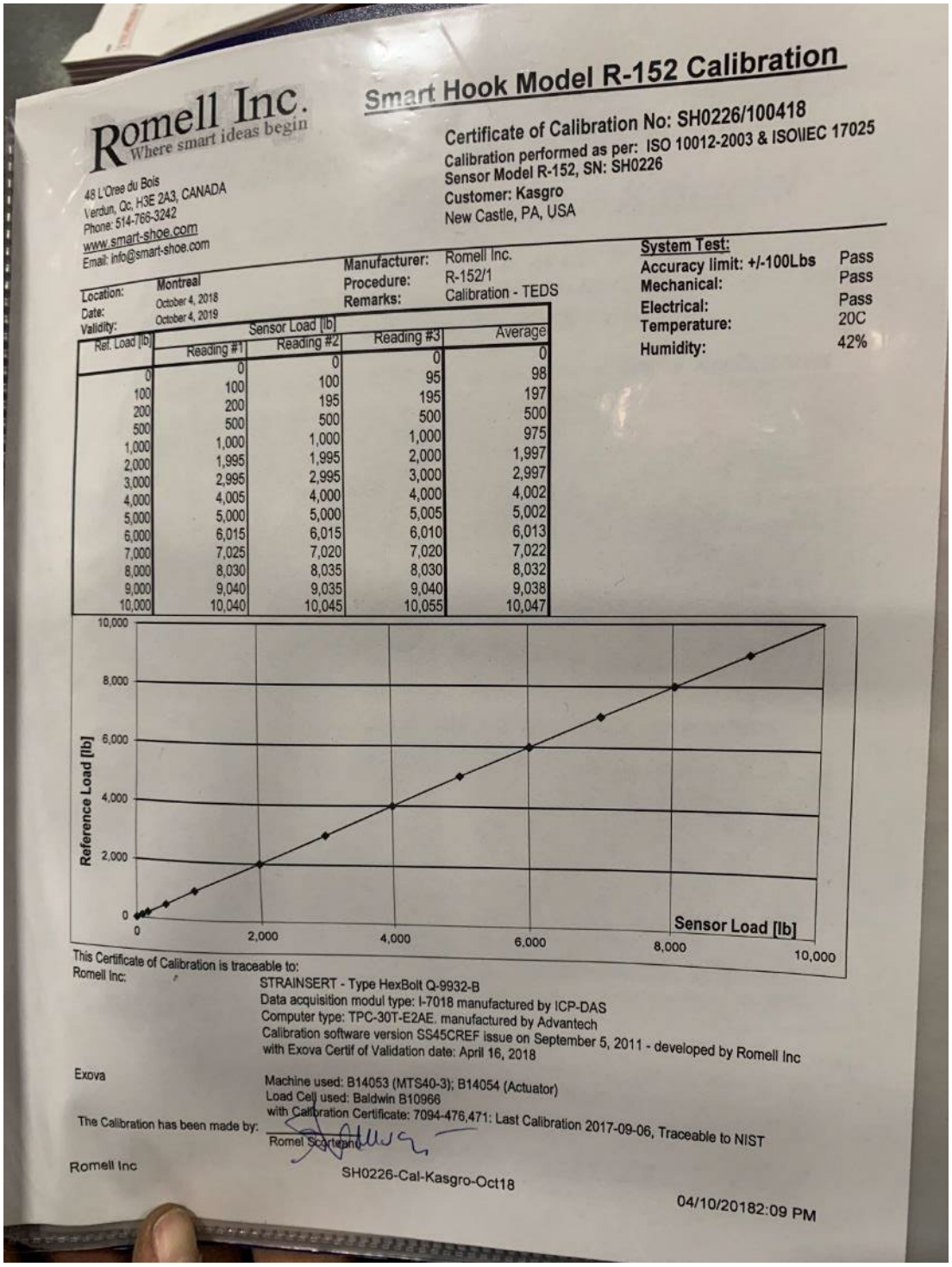
Master Pressure Transducer
Calibrated by CECOMP
Serial # 8432801001
Calibrated 08/16/2017
Calibration Due 02/10/2019

This product complies with all I S Technology Solutions performance specifications.

Calibration Peformed By:

Adam Trzaska
Production Manager

Figure B16. Brake Force Measurement System Calibration Information



Romell Inc.
Where smart ideas begin

48 L'Oree du Bois
Verdun, Qc, H3E 2A3, CANADA
Phone: 514-766-3242
www.smart-shoe.com
Email: info@smart-shoe.com

Smart Hook Model R-152 Calibration

Certificate of Calibration No: SH0226/100418
Calibration performed as per: ISO 10012-2003 & ISO\IEC 17025
Sensor Model R-152, SN: SH0226
Customer: Kasgro
New Castle, PA, USA

Location: Montreal
Date: October 4, 2018
Validity: October 4, 2019

Manufacturer: Romell Inc.
Procedure: R-152/1
Remarks: Calibration - TEDS

System Test:

Accuracy limit: +/-100Lbs	Pass
Mechanical:	Pass
Electrical:	Pass
Temperature:	20C
Humidity:	42%

Ref. Load [lb]	Sensor Load [lb]			
	Reading #1	Reading #2	Reading #3	Average
0	0	0	0	0
100	100	100	95	98
200	200	195	195	197
500	500	500	500	500
1,000	1,000	1,000	1,000	975
2,000	1,995	1,995	2,000	1,997
3,000	2,995	2,995	3,000	2,997
4,000	4,005	4,000	4,000	4,002
5,000	5,000	5,000	5,005	5,002
6,000	6,015	6,015	6,010	6,013
7,000	7,025	7,020	7,020	7,022
8,000	8,030	8,035	8,030	8,032
9,000	9,040	9,035	9,040	9,038
10,000	10,040	10,045	10,055	10,047

This Certificate of Calibration is traceable to:
Romell Inc:
STRAINSERT - Type HexBolt Q-9932-B
Data acquisition modul type: I-7018 manufactured by ICP-DAS
Computer type: TPC-30T-E2AE. manufactured by Advantech
Calibration software version SS45CREF issue on September 5, 2011 - developed by Romell Inc
with Exova Certif of Validation date: April 16, 2018

Exova
Machine used: B14053 (MTS40-3); B14054 (Actuator)
Load Cell used: Baldwin B10966
with Calibration Certificate: 7094-476,471: Last Calibration 2017-09-06, Traceable to NIST

The Calibration has been made by:
Romel Scorteanu

Romell Inc
SH0226-Cal-Kasgro-Oct18
04/10/20182:09 PM

Figure B17. Smart Hook Calibration Information

COMPLETED TEST CHECKLIST

Static Brake Force Test - Atlas Buffer Car

~9:30am Start

Observer Name: Matt DeGeorge Inspection Date: 12/4/18

Names of Test Personnel: Mark Zeigler, Cory Wagner, Tom, Rick Ford
(Performed Test) (Assisted)

Car and Component Identification

Car Number: IDOX 020002 Brake Pipe Length: 93'

Service Portion Type: DB-10 Emergency Portion Type: DB-20

Brake Shoe Force Measurement Device complies with S-4024: (Y) N

Date of Calibration: 11/13/2018

Brake Shoe Force Test

3.2.3: All pins and pin holes free of lubrication (Y) N

3.2.4: Reducing valve is used (if Y must perform Equalization Test) Y (N)
Equalization Test Performed to check Piston Travel

3.2.4: BC Pressure equalizes b/t 63.5 and 66.5 psi with min 30 psi reduction (Y) N
64psi ✓

3.2.5: Rapping done correctly on brake rigging and with acceptable hammer (Y) N

3.2.6: No rapping during hand brake force testing (Y) N

3.2.7: 6.0 to 7.0 psi BP reduction from 90.0 psi BPP results in all brake shoes forced against wheels Yes

Average brake shoe force >= 100 lb per wheel: 376.75 lbs ✓

Wheel	Force (lbs)	Wheel	Force (lbs)
R1	468	L1	346
R2	381	L2	356
R3	380	L3	429
R4	351	L4	304

#3 #4 #6 #5 (R1, R2, R3, R4) — #1 #2 #3 #4 (L1, L2, L3, L4)

Equalization:
Acceptable Range: $2\frac{3}{4} \pm \frac{1}{8}$"
Aend: $2\frac{7}{8}$ inch
Bend: $2\frac{5}{8}$ inch ✓

Net Braking Ratios with 30 psi BP reduction from 90 psi BPP:

): 64psi

Wheel	Force (lbs)	Wheel	Force (lbs)	
#3 R1	4106	L1	3751	#1
#4 R2	4288	L2	4030	#2
#6 R3	4528	L3	4516	#7
#5 R4	3982	L4	3938	#8

(Force (lbs) header: tapped)

untapped
#3: 4130 #1: 3749
#4: 4065 #2: 3963
#6: 4177 #7: 4253
#5: 3965 #8: 3886

Net Brake Ratio is between 11-14%: 12.56% ✓

Handbrake Force/Brake Ratio: 15.35% > 10% ✓

Total Force: 33039 lbs
Avg/Wheel: 4129.88 lbs
Weight of car: 263,000 lbs

4.2: NBR on each wheel is within +/- 12.5% of Average NBR per wheel (Y) N

Max: 4646.11 Min: 3613.65

Additional Comments: -

- Air Brake Testing Device was run through Daily test
- Equalization Performed Several times to set correct piston travel
- multiple brake reductions performed during piston adjustments to allow system to settle
- Slow leak in Brake Cylinder Pipeline (found + repaired + test rerun)
- Empty brake ratio testing not performed (car always loaded)
- Hand brake test done with clevis pin + smart hook (tested independently of each other)

Emergency App Test: BCP: 64psi @ 30 psi red Falls b/t 15 & 20% higher
BCP: 76.5psi @ emergency → 19.53% ✓

Hand Brake Test:
Pin: #2: 11393 #4: 11966 Total Force: 43719 lbs
#1: 9805 #3: 10565 Brake Ratio: 16.62%

Smart Hook: #2: 10332 #4: 10995 Total Force: 40367 lbs
#1: 9071 #3: 9779 Brake Ratio: 15.35%

~11:30am
End of Test

Static Brake Force Test - Atlas Buffer Car

~2:30pm Start

Observer Name: Matt DeGeorge Inspection Date: 12/4/18

Names of Test Personnel: Mark Zeigler, Cory Wagner, Tom, Rick Ford (Performed) (Amsted)

Car and Component Identification

Car Number: IBOX 020001 Brake Pipe Length: 93'

Service Portion Type: DB-10 Emergency Portion Type: DB-20

Brake Shoe Force Measurement Device complies with S-4024:	(Y)	N

Date of Calibration: 11/13/2018

Brake Shoe Force Test

3.2.3: All pins and pin holes free of lubrication	(Y)	N
3.2.4: Reducing valve is used (if Y must perform Equalization Test)	Y	(N)
3.2.4: BC Pressure equalizes b/t 63.5 and 66.5 psi with min 30 psi reduction	(Y)	N
3.2.5: Rapping done correctly on brake rigging and with acceptable hammer (64psi ✓)	(Y)	N
3.2.6: No rapping during hand brake force testing	(Y)	N

3.2.7: 6.0 to 7.0 psi BP reduction from 90.0 psi BPP results in all brake shoes forced against wheels Yes

Average brake shoe force >= 100 lb per wheel: 305 lbs ✓

	Wheel	Force (lbs)	Wheel	Force (lbs)	
#3	R1	307	L1	205	#1
#4	R2	268	L2	292	#2
#6	R3	369	L3	354	#7
#5	R4	364	L4	291	#8

Equalization:
Acceptable Range: 2 3/4 ½
Aend: 2 5/8 inch
Bend: 2 5/8 inch ✓

Net Braking Ratios with 30 psi BP reduction from 90 psi BPP:

BCP: 64psi

	Wheel	Force (lbs)	Wheel	Force (lbs)	
#3	R1	4121	L1	3745	#1
#4	R2	4475	L2	4164	#2
#6	R3	4296	L3	4416	#7
#5	R4	3702	L4	4061	#8

(tapped)

unwrapped
#3: 4006 #1: 3723
#4: 3993 #2: 3903
#6: 4055 #7: 4028
#5: 3584 #8: 3986

Total Force: 32,982 lbs
Avg/wheel: 4122.75
Weight of car: 263,000 lbs

Net Brake Ratio is between 11-14%: 12.54% ✓

Handbrake Force/Brake Ratio: 15.99% >10% ✓

4.2: NBR on each wheel is within +/- 12.5% of Average NBR per wheel (Y) N

Max: 4639.09 Min: 3607.41

Additional Comments: -

- Air Brake Testing Device put through Daily Test
- Equalization Performed several times to set correct piston travel
- multiple brake reductions performed during piston adj. to allow system to settle
- empty brake ratio testing not performed (car always loaded)
- Hand brake test done with just smart hook

Emergency App Test: BCP: 64psi @ 30psi red
BCP: 76.5psi @ emergency
Falls b/t 15 & 20% higher → 19.53%

Hand Brake Test: Smart Hook: #2: 11097 #4: 11630
#1: 9192 #3: 10116

Total Force: 42035 lbs
Brake Ratio: 15.99%

~ 4:15pm
End of Test

Transportation Technology Center, Inc.

Mike Yon
Field Inspector - MID/QA Auditor
Cell: 814-515-3803

Email: Mike_yon@aar.com

March 12, 2019

File:KAS-NEWCPA-MC06-0219-MSY

Subject: Specification testing of (IDOX 20001 and 20002), Heavy Duty Flat Car

Mr. David L. Cackovic
Chief – Technical Standards & Inspections
Transportation Technology Center, Inc.
P.O. Box 11130
Pueblo, CO 81001
E-mail: David_Cackovic@aar.com

Dear Mr. Cackovic,

Specification testing of (IDOX 20001 and 20002), Heavy Duty Flat Car, specifically the Single Car Air Brake Test has been completed. Testing was done at the Kasgro Rail Corporation facility in New Castle, Pennsylvania on February 11, 2019 to comply with S-486.

I was present (test witness) for the required Single Car Air Brake Test and can conclude that applicable requirements of AAR Specification S-486 have been satisfactorily addressed.

Attached information was supplied by the Kasgro Rail Corporation in support of the approval process. Should you need any additional information, please do not hesitate to call.

Sincerely,



Mike Yon

cc: Anna Fox, TTCI
Kasgro, mark@kasgro.com
J. Hannafious, TTCI

Rev.1

Kasgro Rail Corp

FORM 6-A 2/25/2016

Air Brake Test Report
(X=Tested)

CAR NUMBER IDOX 20001

Single Car Test, 1Set	X	Single Car Test, 2 Sets	
Single Car Test (includes B.C. Pressrure Test)	X	Single Car Test (includes B.C. Pressure Test), 2 Sets	
Slack Adjuster Test	X	Retainer Valve Test	X
Empty / Load Valve Test	X	Brake Pipe Leakage Test	X
System Leakage Test	X	Equaillization Pressure	X
Piston Travel (Unit Brakes)		If Equipped With Load Sensor	X
Piston Travel (Trk MTD Brakes)	X	Equaillization Pressure Load Sensor	X
WABCOPAC / NYPOAC Piston Travel Adjustment		Equaillization Pressure Loaded	X
(Truck Mounted Brakes with Slack Adjuster		Equaillization Pressure Empty	X
#1 #2 #3 #4		Slack Adjuster Rack Measurement	X
Lube Handbrake			

SYSTEM REPAIRS- List repairs, parts replaced, Location, and why made.

Piston Travels B 2 5/8 A 2 5/8

EQUALIZATION PRESSURE: SER 63, EM 76 (LOADED CAR NO EMPTY READING)

DB 10C NEW YORK AIR BRAKE ELX 40% LOAD SENSOR
DB-20

Signature of Tester Mike R BL Date 2-11-19

Note: The recording of false, fictitious, or fraudulent statements on this document may be punishable as a felony under federal statues.

Rev.1

Kasgro Rail Corp

FORM 6-A 2/25/2016

Air Brake Test Report
(X=Tested)

CAR NUMBER IDOX 20002

Single Car Test, 1Set	X	Single Car Test, 2 Sets	
Single Car Test (includes B.C. Pressrure Test)	X	Single Car Test (includes B.C. Pressure Test), 2 Sets	
Slack Adjuster Test	X	Retainer Valve Test	X
Empty / Load Valve Test	X	Brake Pipe Leakage Test	X
System Leakage Test	X	Equaillization Pressure	X
Piston Travel (Unit Brakes)		If Equipped With Load Sensor	X
Piston Travel (Trk MTD Brakes)	X	Equaillization Pressure Load Sensor	X
WABCOPAC / NYPOAC Piston Travel Adjustment		Equaillization Pressure Loaded	X
(Truck Mounted Brakes with Slack Adjuster		Equaillization Pressure Empty	X
#1 #2 #3 #4		Slack Adjuster Rack Measurement	X
Lube Handbrake			

SYSTEM REPAIRS- List repairs, parts replaced, Location, and why made.

Piston Travels B 2½, A 2½

EQUAILIZATION PRESSURE SER 63 EM 76 (NO EMPTY LOADED CAR)

DB-10C NEW YORK AIR BRAKE ELX-40% LOAD SENSOR
DB 20

Signature of Tester Mike R BL Date 2-10-19

Note: The recording of false, fictitious, or fraudulent statements on this document may be punishable as a felony under federal statues.

APPENDIX C: BUFFER CAR GAGE DRAWING

This appendix contains details on the location, installation, and shunt calibration of the strain gages used to measure strain on the buffer car.

All the strain gages used on the buffer car are of the same type: CEA-06-500UW-350 with the following characteristics:

- Encapsulated constantan alloy (bondable)
- Grid Length: 0.5 in
- Uniaxial type
- 350 ohm
- Gage Factor: 2.155

Installation procedures are followed from the Vishay standard protocols for bondable strain gages.

Figure C1 to Figure C4 show the locations of the strain gages. These drawing show detailed locations for gages on one quadrant of the car. The gages in the other quadrants are symmetrical.

Figure C5 to Figure C55 show photos of the installed strain gages.

Figure C56 to Figure C58 show photos of the installed thermocouples.

Figure C59 to Figure C65 show data recorded during a shunt calibration check just before the 1 million-pound squeeze test.

List of Figures

Figure C1. Strain Gage Locations C-4
Figure C2. Detailed Strain Gage Locations, on Bottom Flange..... C-5
Figure C3. Detailed Strain Gage Locations, on Deck Plate..... C-6
Figure C4. Detailed Strain Gage Locations, on Top of Dead Weight C-7
Figure C5. SGBF1 Front of Bottom Flange of A-end Body Bolster near Center Sill, LH Side.... C-8
Figure C6. SGBF2 Rear of Bottom Flange of A-end Body Bolster near Center Sill, LH Side C-8
Figure C7. SGBF3 Front of Bottom Flange of A-end Body Bolster near Center Sill, RH Side ... C-9
Figure C8. SGBF4 Rear of Bottom Flange of A-end Body Bolster near Center Sill, RH Side.... C-9
Figure C9. SGBF5 RH Edge of Bottom Flange of Center Sill, Aft of A-end Body Bolster C-10
Figure C10. SGBF6 Center of Bottom Flange of RH Side Sill, Forward of Cross Bearer 7 ..... C-10
Figure C11. SGBF7 Center of Bottom Flange of RH SIDE SILL, Aft of Cross Bearer 7 ..... C-11
Figure C12. SGBF8 Center of Bottom Flange of LH Side Sill, Aft of Cross Bearer 7 ..... C-11
Figure C13. SGBF9 Center of Bottom Flange of LH Side Sill, forward of Cross Bearer Location 7 ..... C-12
Figure C14. SGBF10 LH Edge of Bottom Flange of Center Sill, Forward of Cross Bearer 7 .... C-12
Figure C15. SGBF11 RH Edge of Bottom Flange of Center Sill, Forward of Cross Bearer 7.... C-13
Figure C16. SGBF12 LH Edge of Bottom Flange of Center Sill, Aft of A-end Body Bolster C-13
Figure C17. SGDP13 LH Edge of Deck Plate, Forward of Cross Bearer 7..... C-14
Figure C18. SGDP14 LH Edge of Deck Plate, Aft of Cross Bearer 7 ..... C-14
Figure C19. SGDP15 RH Edge of Deck Plate, Forward of Cross Bearer 7 ..... C-15
Figure C20. SGDP16 RH Edge of Deck Plate, Aft of Cross Bearer 7 ..... C-15
Figure C21. SGDP17 LH Edge of Deck Plate, at Longitudinal Center of Car C-16
Figure C22. SGDW18 Top of Dead Weight at Lateral Center of Car, Forward of Cross Bearer 7 ..... C-16
Figure C23. SGDW19 Top of Dead Weight, at Lateral and Longitudinal Center of Car C-17
Figure C24. SGDW20 Top of Dead Weight at Lateral Center of Car, Aft of Cross Bearer 1 ..... C-17
Figure C25. SGBF21 LH Edge of Bottom Flange of Center Sill, Forward of Cross Bearer 6 .... C-18
Figure C26. SGBF22 RH Edge of Bottom Flange of Center Sill, Forward of Cross Bearer 6.... C-18
Figure C27. SGBF23 Bottom Flange of Cross Bearer 4, LH Side of Center Sill, at Longitudinal Center of Car..... C-19
Figure C28. SGBF24 LH Edge of Bottom Flange of Center Sill, at Longitudinal Center of Car. C-19
Figure C29. SGBF25 RH Edge of Bottom Flange of Center Sill, at Longitudinal Center of Car 20
Figure C30. SGBF26 Bottom Flange of Cross Bearer 2, RH Side of Center Sill, at Longitudinal Center of Car..... C-20
Figure C31. SGBF27 RH Edge of Bottom Flange of Center sill, Aft of Cross Bearer 2 ..... C-21
Figure C32. SGBF28 Center of Bottom Flange of RH Side Sill, at Longitudinal Center of Car.. C-21
Figure C33. SGBF29 Center of Bottom Flange of LH Side Sill, at Longitudinal Center of Car .. C-22
Figure C34. SGDP30 RH Edge of Deck Plate, at Longitudinal Center of Car C-22
Figure C35. SGDP31 RH Edge of Deck Plate, Forward of Cross Bearer 2..... C-23
Figure C36. SGDP32 RH Edge of Deck Plate, Aft of Cross Bearer 2..... C-23
Figure C37. SGDP33 LH Edge of Deck Plate, Forward of Cross Bearer 2..... C-24
Figure C38. SGDP34 LH Edge of Deck Plate, Aft of Cross Bearer 2 ..... C-24

Figure C39. SGBF35 LH Edge of Bottom Flange of Center Sill, Aft of Cross Bearer 1 ..... C-25
Figure C40. SGBF36 LH Edge of Bottom Flange of Center Sill, Aft of Cross Bearer 2 ..... C-25
Figure C41. SGBF37 RH Edge of Bottom Flange of Center Sill, Aft of Cross Bearer 1..... C-26
Figure C42. SGBF38 Center of Bottom Flange of LH Side Sill, Forward of Cross Bearer 1..... C-26
Figure C43. SGBF39 Center of Bottom Flange of LH Side Sill, Aft of Cross Bearer 1 ..... C-27
Figure C44. SGBF40 Front of Bottom Flange of B-end Body Bolster near Center Sil, RH Side C-27
Figure C45. SGBF41 Rear of Bottom Flange of B-end Body Bolster near Center Sill, RH Side C-28
Figure C46. SGBF42 Front of Bottom Flange of B-end Body Bolster Near Center Sill, LH Side C-28
Figure C47. SGBF43 Rear of Bottom Flange of B-end Body Bolster near Center Sill, LH Side C-29
Figure C48. SGBF44 RH Edge of Bottom Flange of Center Sill, Forward of B-end Body Bolster C-29
Figure C49. SGBF45 LH edge of Bottom Flange of Center Sill, Forward of B-end Body Bolster C-30
Figure C50. SGBF46 Center of Bottom Flange of RH Side Sill, Aft of Cross Bearer 1 ..... C-30
Figure C51. SGBF47 Center of Bottom Flange of RH Side Sill, Forward of Cross Bearer 1 ..... C-31
Figure C52. SGDP48 Top of Deck Plate, Longitudinally Centered over B-End Body Bolster, above RH Edge of Center Sill C-31
Figure C53. SGDP49 Top of Deck Plate, Longitudinally Centered over B-end Body Bolster, above LH Edge of Center Sill C-32
Figure C54. SGDP50 Top of Deck Plate, Longitudinally Centered over A-End Body Bolster, above RH Edge of Center Sill C-32
Figure C55. SGDP52 Top of Deck Plate, Longitudinally Centered over A-End Body Bolster, above LH Edge of Center Sill C-33
Figure C56. TC52 Laterally and Longitudinally Centered on Top of Deck Plate Forward of A-end Body Bolster C-33
Figure C57. TC53 Laterally and Longitudinally Centered on top of Deck Plate Forward of A-End Body Bolster C-34
Figure C58. TC54 Bottom Flange of Cross Bearer 4 at Lateral and Longitudinal Center of Car C-34
Figure C59. Shunt Calibration of Gages 1-8 with a High Precision 174.650 kΩ Resistor C-35
Figure C60. Shunt Calibration of gages 9-16 with a High Precision 174.650 kΩ Resistor C-35
Figure C61. Shunt Calibration of Gages 17-24 with a High Precision 174.650 kΩ Resistor C-36
Figure C62. Shunt Calibration of Gages 25-32 with a High Precision 174.650 kΩ Resistor C-36
Figure C63. Shunt Calibration of Gages 33-40 with a High Precision 174.650 kΩ Resistor C-37
Figure C64. Shunt Calibration of Gages 41-48 with a High Precision 174.650 kΩ Resistor C-37
Figure C65. Shunt calibration of Gages 49-51 with a High Precision 174.650 kΩ Resistor, and Plot of the Three Thermocouples. The TTC Weather Station Showed ambient temperature was 63°F on November 18, 2019, at 4:00 PM when this file was Recorded C-38

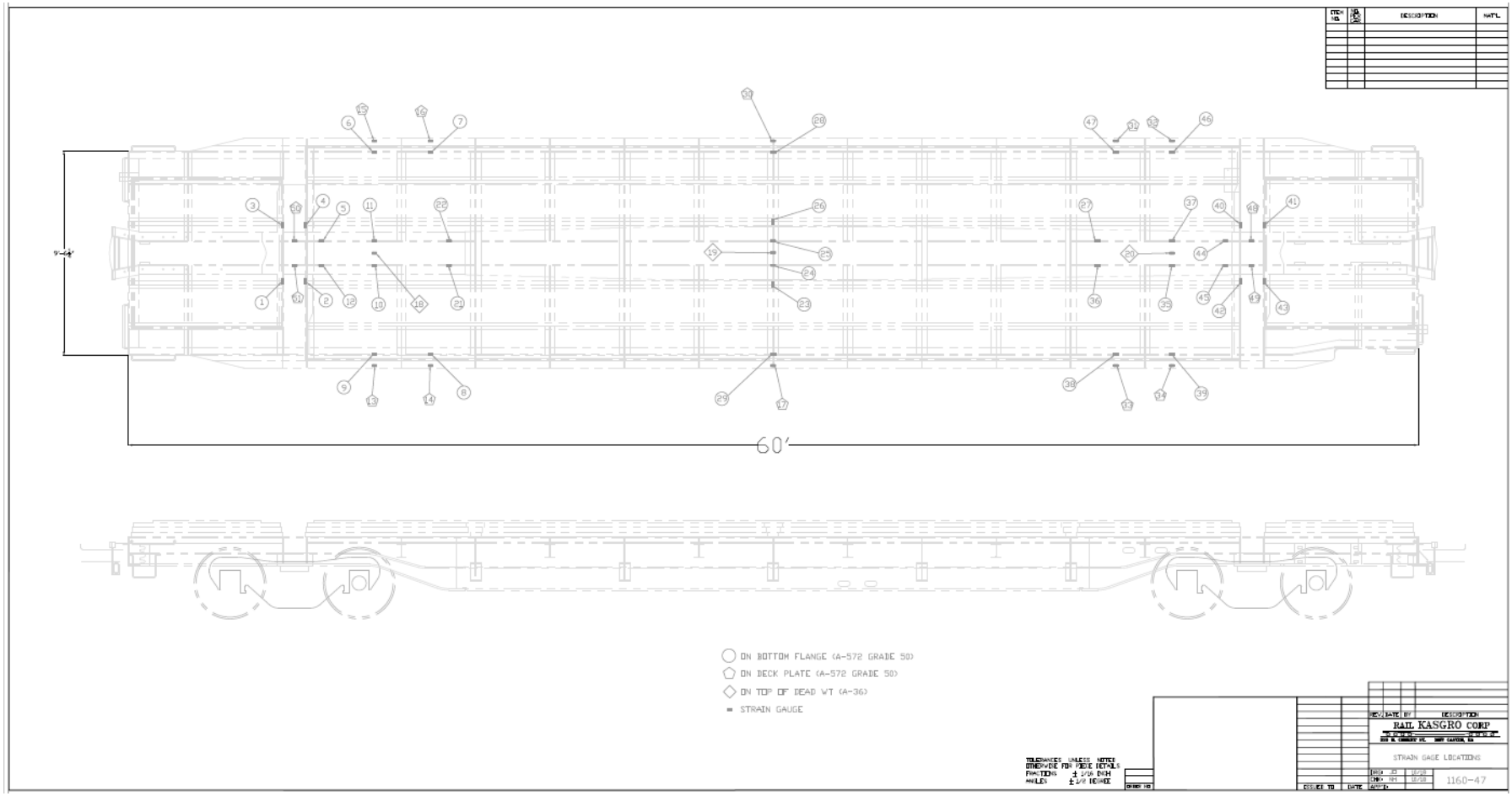


Figure C1. Strain Gage Locations

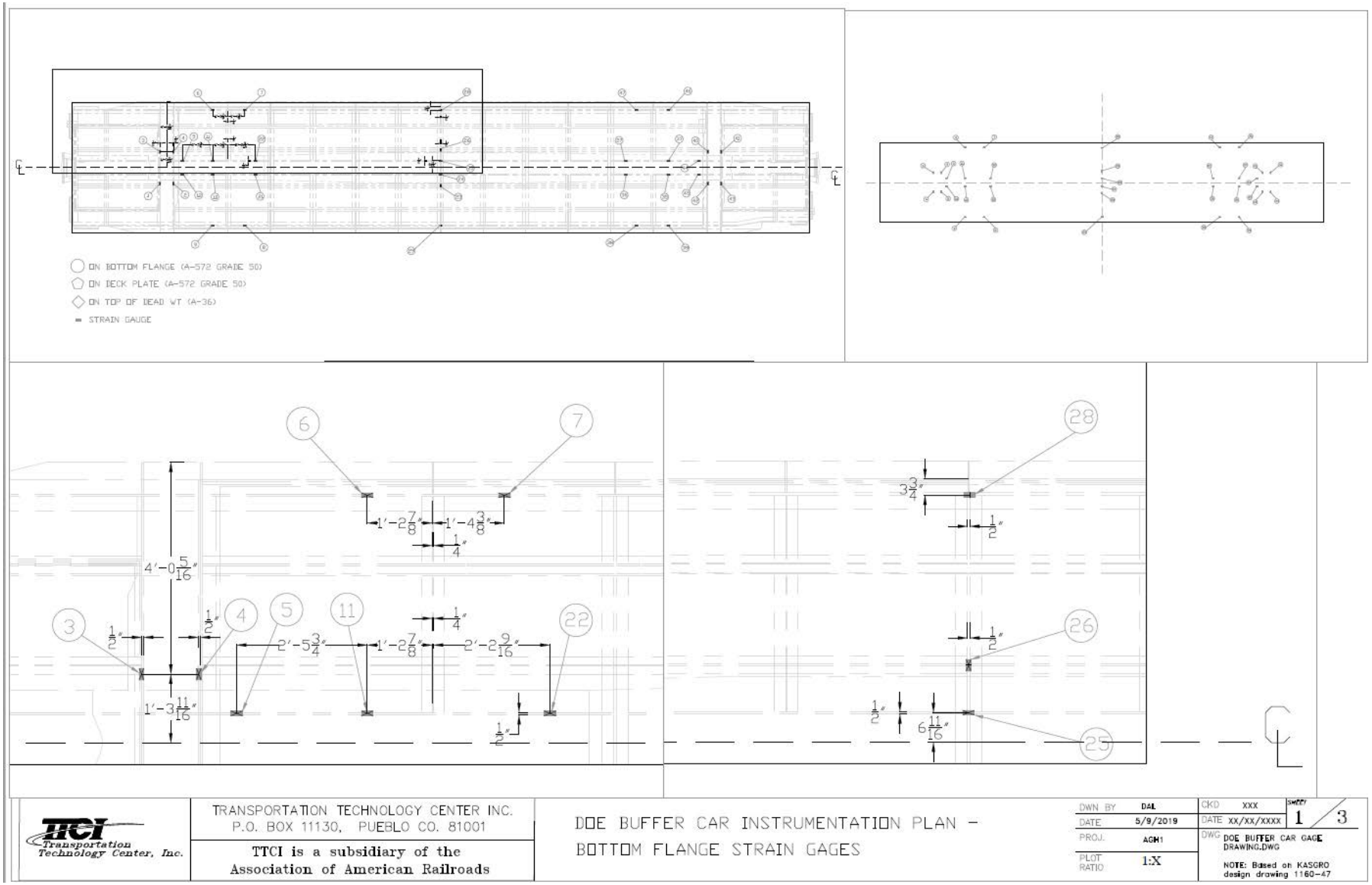


Figure C2. Detailed Strain Gage Locations, on Bottom Flange

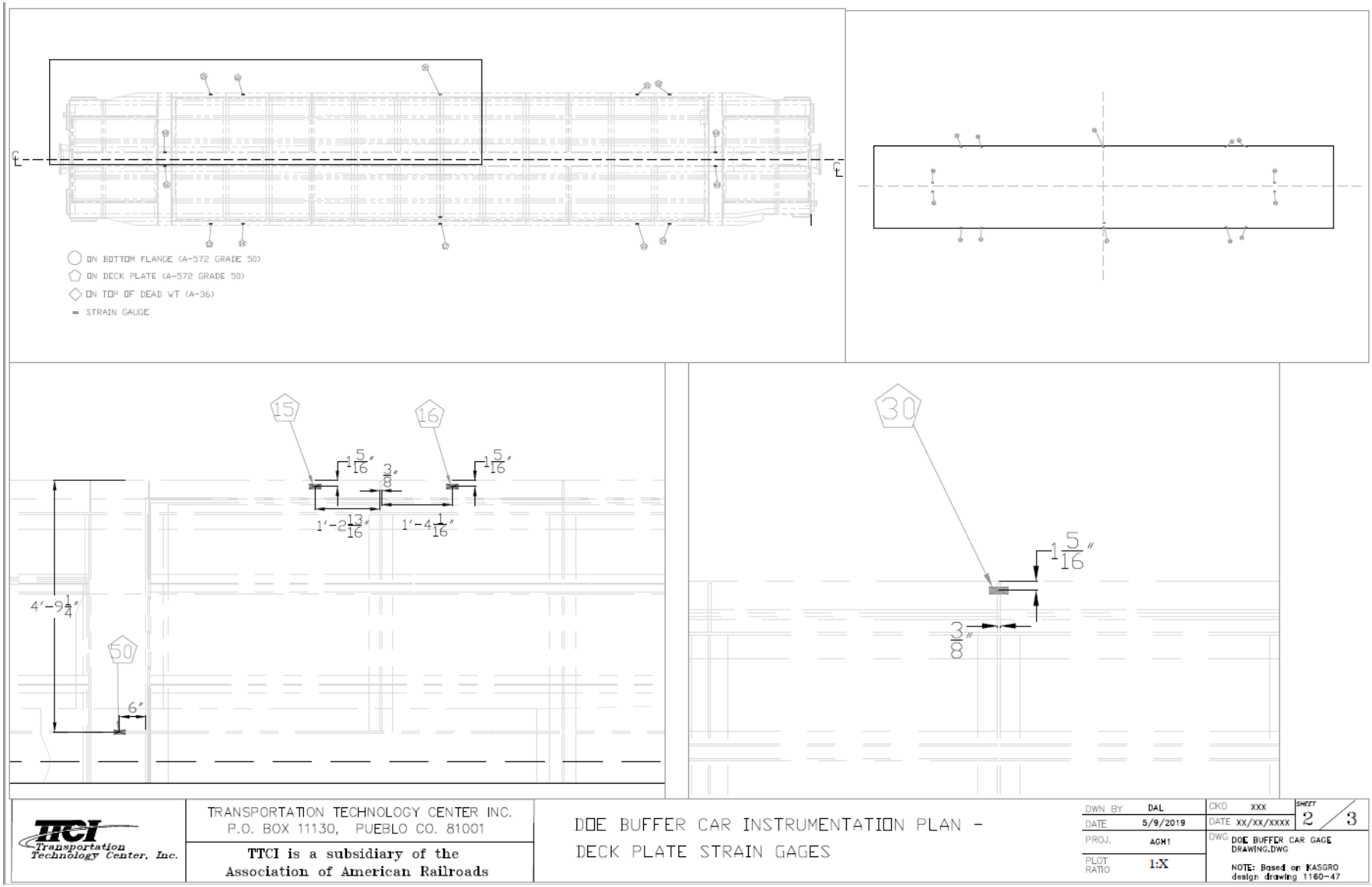


Figure C3. Detailed Strain Gage Locations, on Deck Plate

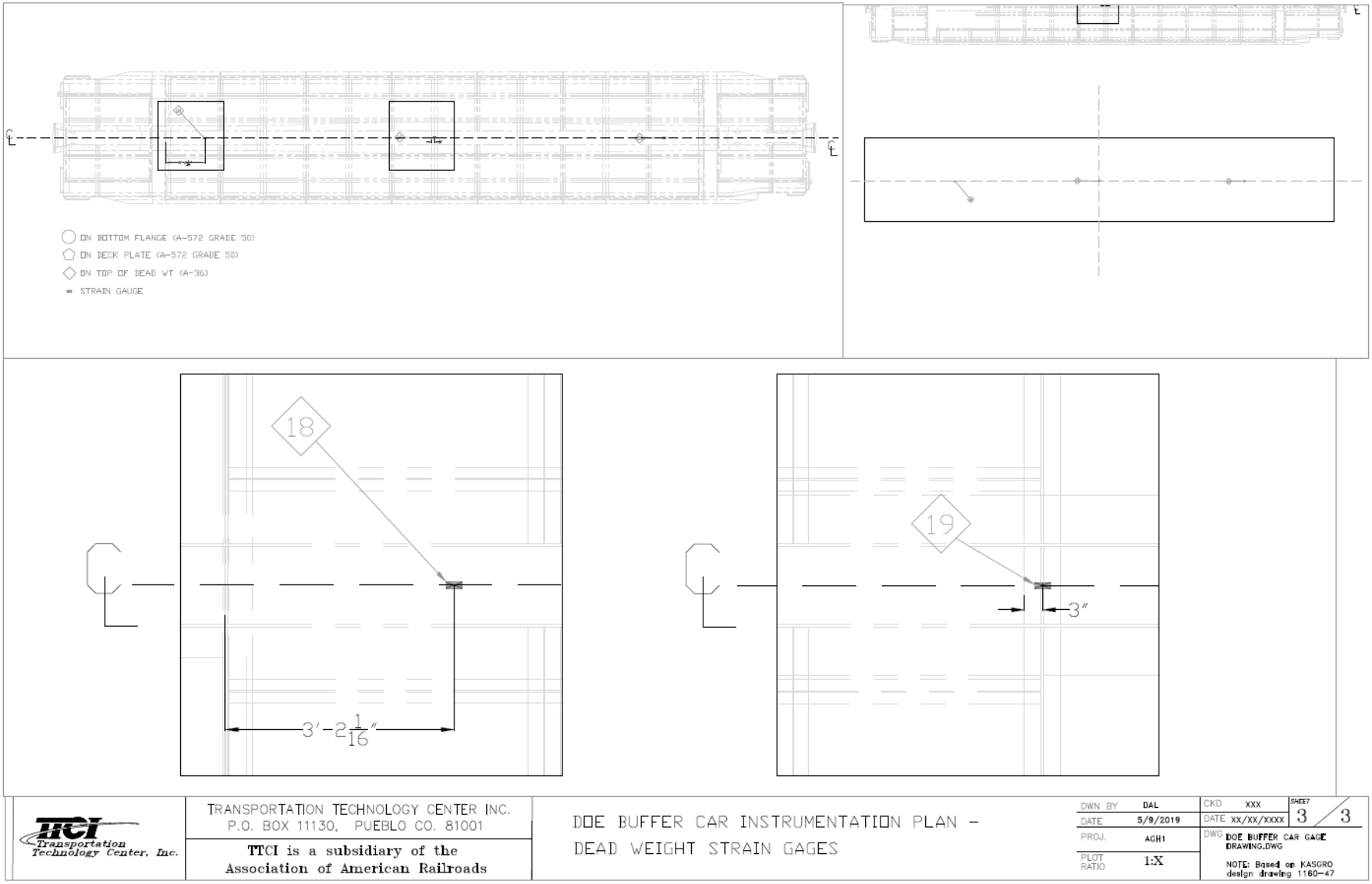


Figure C4. Detailed Strain Gage Locations, on Top of Dead Weight

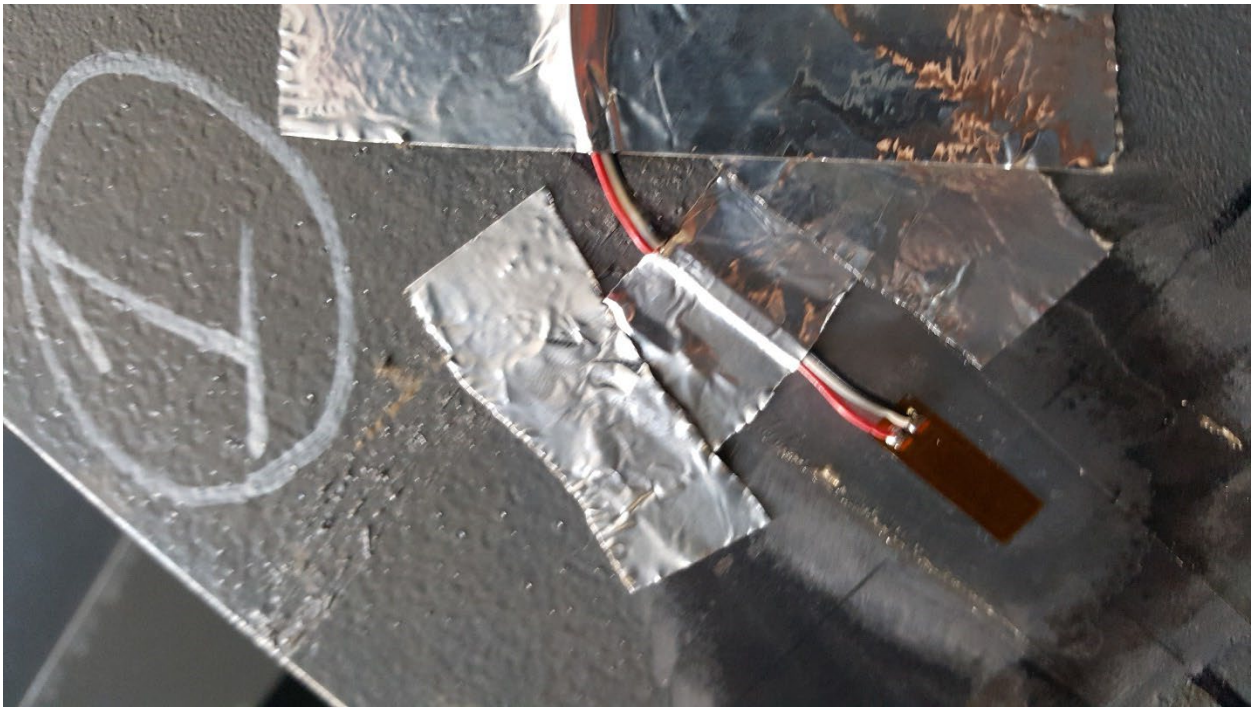


Figure C5. SGBF1 Front of Bottom Flange of A-end Body Bolster near Center Sill, LH Side



Figure C6. SGBF2 Rear of Bottom Flange of A-end Body Bolster near Center Sill, LH Side



Figure C7. SGBF3 Front of Bottom Flange of A-end Body Bolster near Center Sill, RH Side



Figure C8. SGBF4 Rear of Bottom Flange of A-end Body Bolster near Center Sill, RH Side



Figure C9. SGBF5 RH Edge of Bottom Flange of Center Sill, Aft of A-end Body Bolster

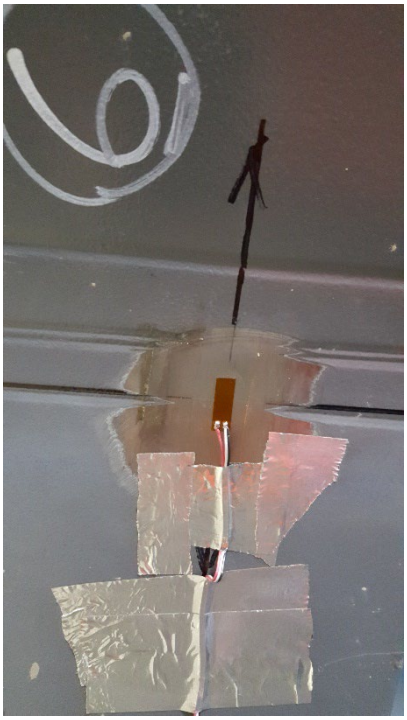


Figure C10. SGBF6 Center of Bottom Flange of RH Side Sill, Forward of Cross Bearer 7

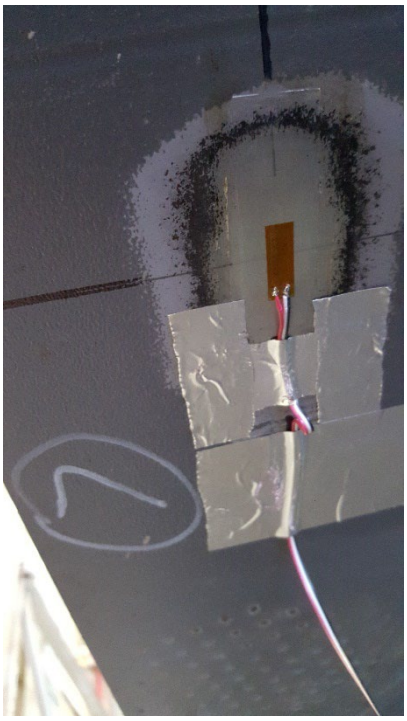


Figure C11. SGBF7 Center of Bottom Flange of RH SIDE SILL, Aft of Cross Bearer 7



Figure C12. SGBF8 Center of Bottom Flange of LH Side Sill, Aft of Cross Bearer 7



Figure C13. SGBF9 Center of Bottom Flange of LH Side Sill, forward of Cross Bearer Location 7



Figure C14. SGBF10 LH Edge of Bottom Flange of Center Sill, Forward of Cross Bearer 7

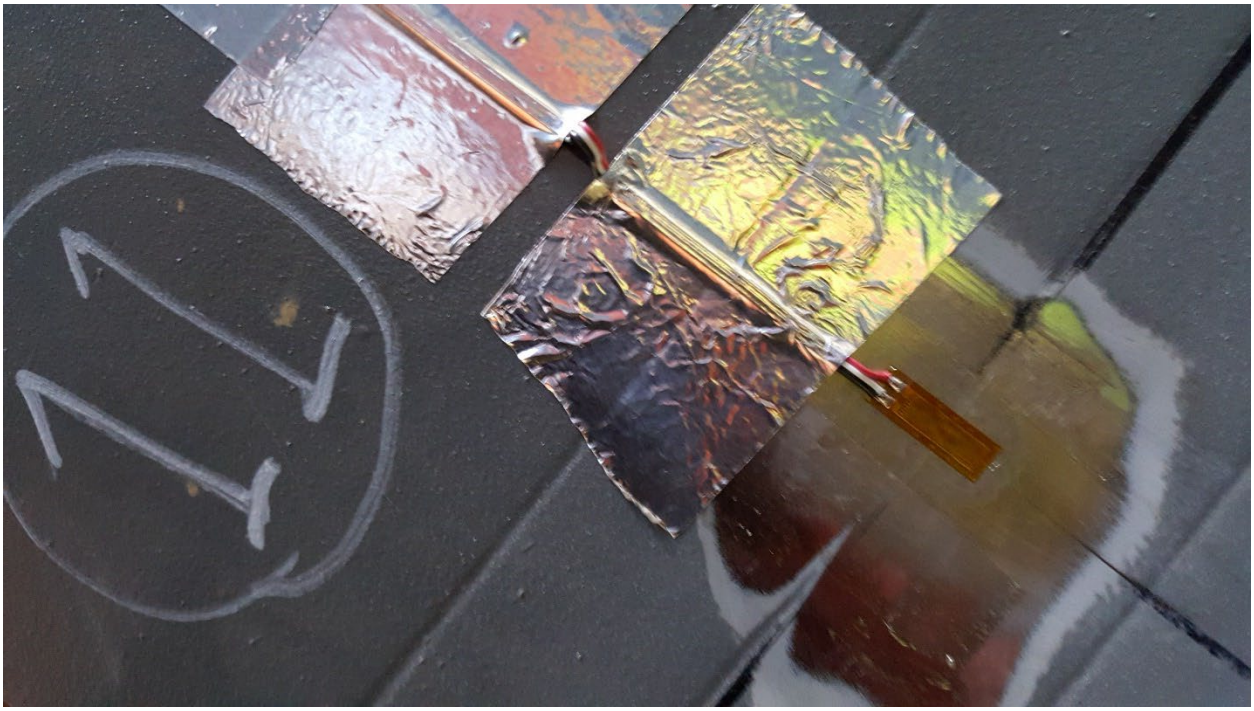


Figure C15. SGBF11 RH Edge of Bottom Flange of Center Sill, Forward of Cross Bearer 7

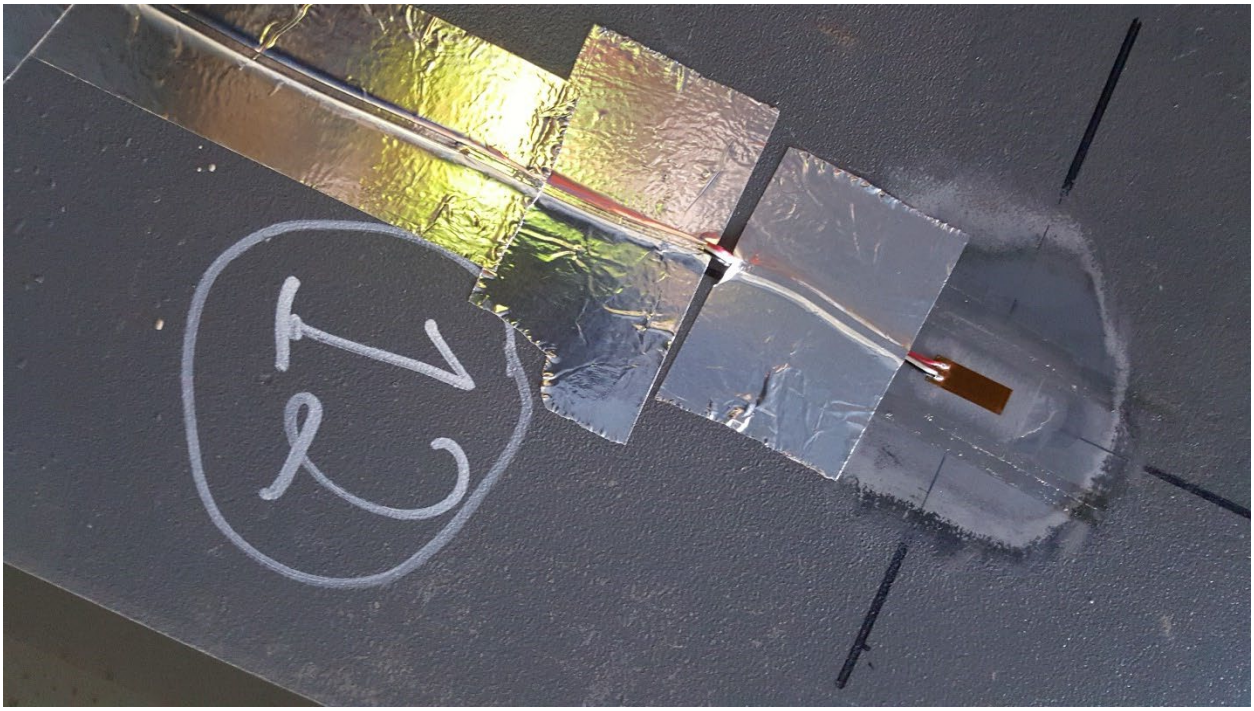


Figure C16. SGBF12 LH Edge of Bottom Flange of Center Sill, Aft of A-end Body Bolster



Figure C17. SGDP13 LH Edge of Deck Plate, Forward of Cross Bearer 7

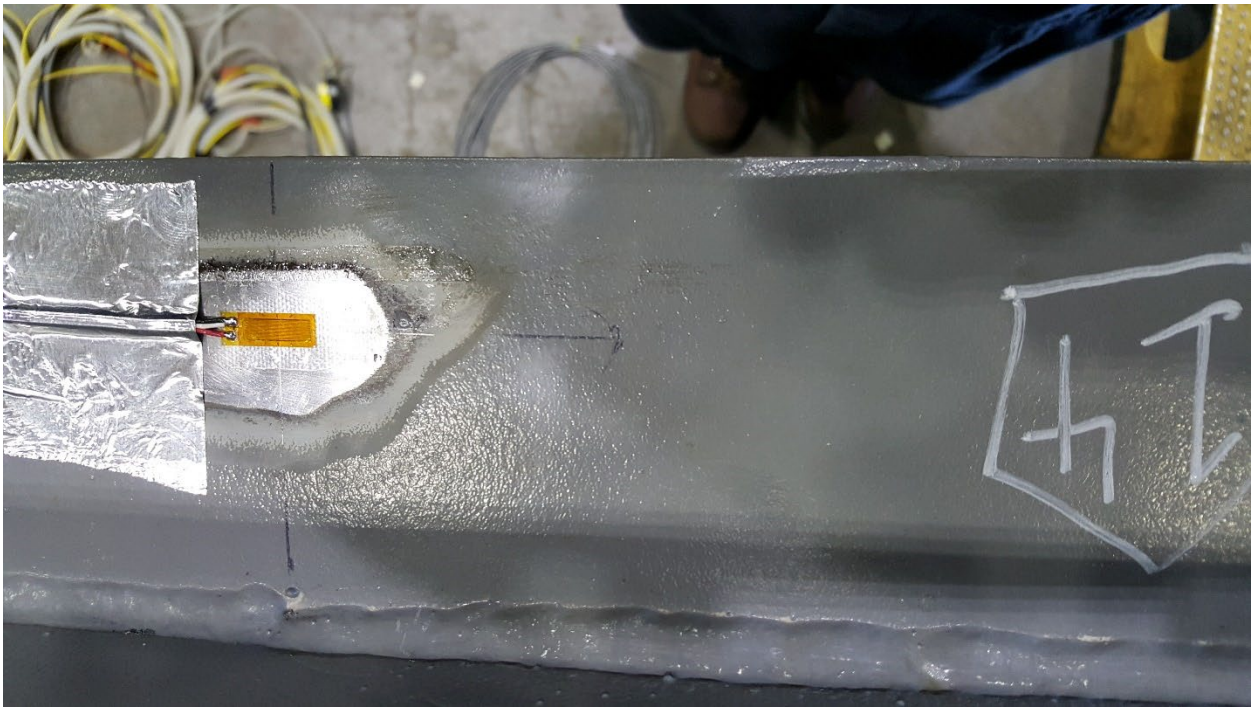


Figure C18. SGDP14 LH Edge of Deck Plate, Aft of Cross Bearer 7



Figure C19. SGDP15 RH Edge of Deck Plate, Forward of Cross Bearer 7

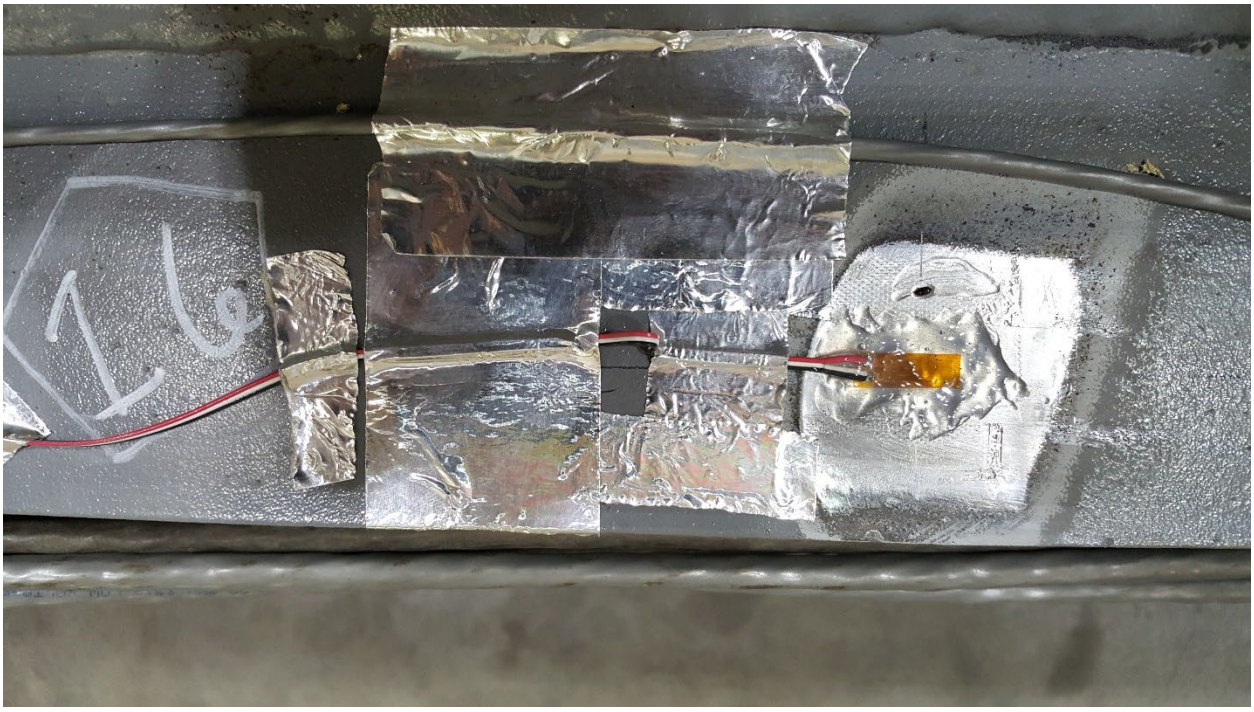


Figure C20. SGDP16 RH Edge of Deck Plate, Aft of Cross Bearer 7

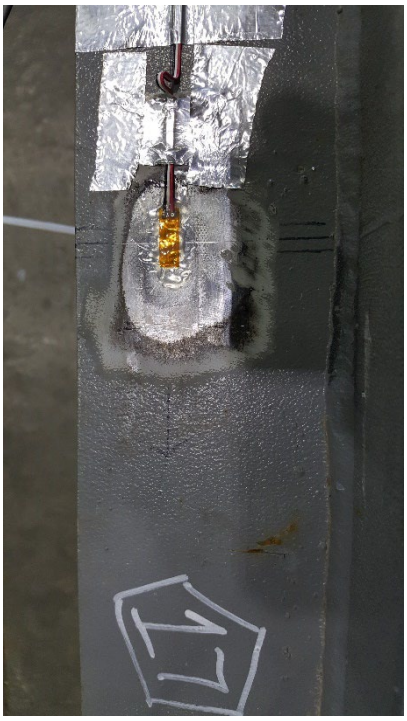


Figure C21. SGDP17 LH Edge of Deck Plate, at Longitudinal Center of Car

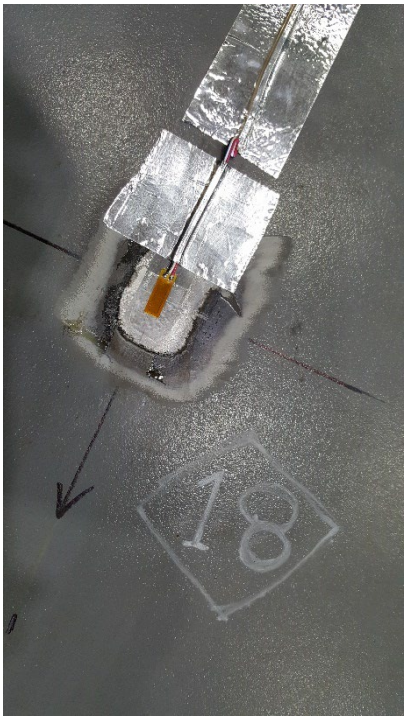


Figure C22. SGDW18 Top of Dead Weight at Lateral Center of Car, Forward of Cross Bearer 7



Figure C23. SGDW19 Top of Dead Weight, at Lateral and Longitudinal Center of Car

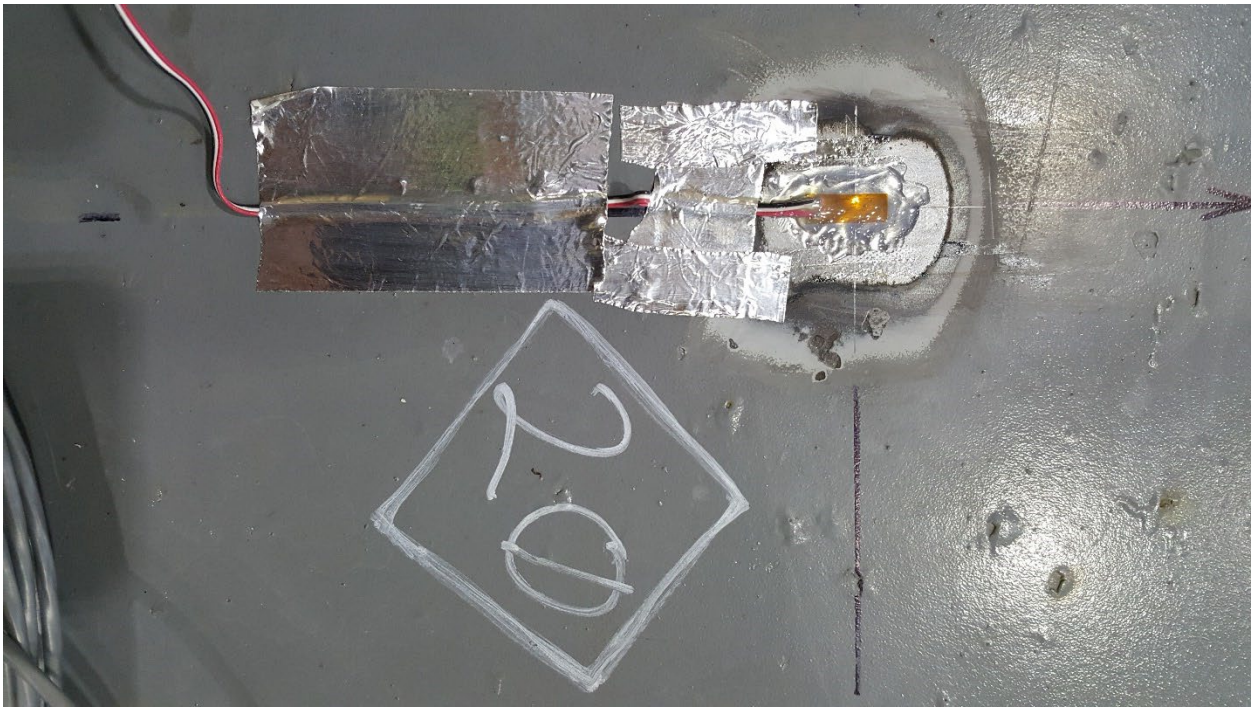


Figure C24. SGDW20 Top of Dead Weight at Lateral Center of Car, Aft of Cross Bearer 1



Figure C25. SGBF21 LH Edge of Bottom Flange of Center Sill, Forward of Cross Bearer 6



Figure C26. SGBF22 RH Edge of Bottom Flange of Center Sill, Forward of Cross Bearer 6



Figure C27. SGBF23 Bottom Flange of Cross Bearer 4, LH Side of Center Sill, at Longitudinal Center of Car

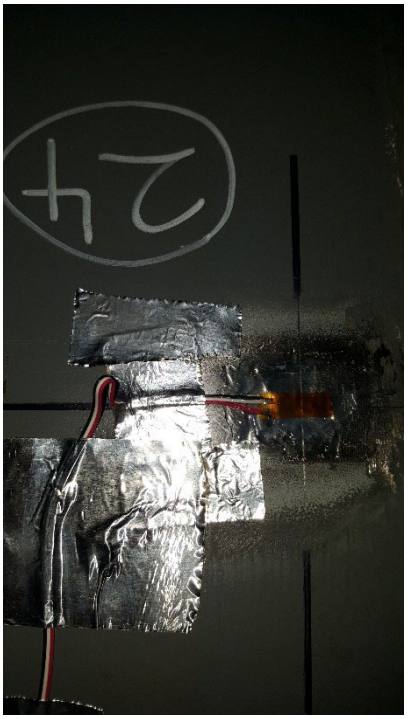


Figure C28. SGBF24 LH Edge of Bottom Flange of Center Sill, at Longitudinal Center of Car



Figure C29. SGBF25 RH Edge of Bottom Flange of Center Sill, at Longitudinal Center of Car

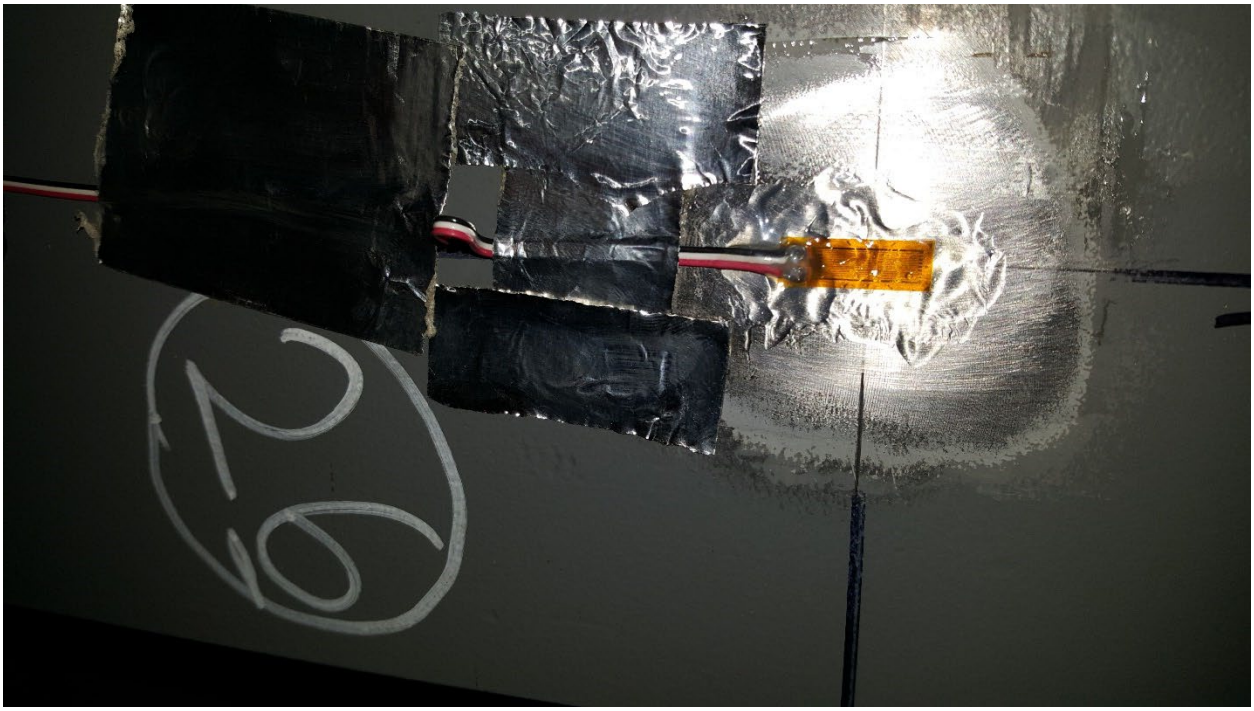


Figure C30. SGBF26 Bottom Flange of Cross Bearer 2, RH Side of Center Sill, at Longitudinal Center of Car



Figure C31. SGBF27 RH Edge of Bottom Flange of Center sill, Aft of Cross Bearer 2

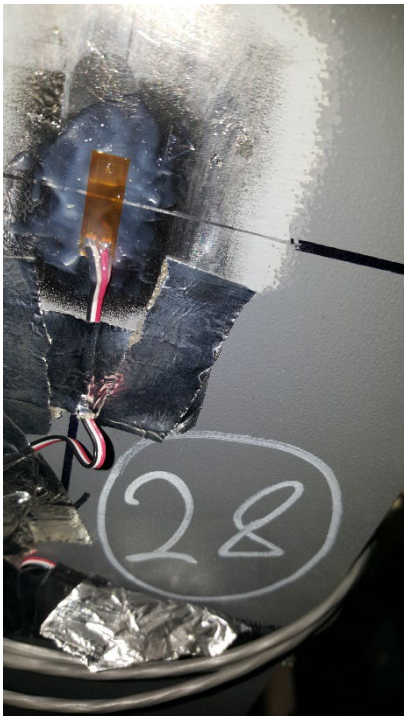


Figure C32. SGBF28 Center of Bottom Flange of RH Side Sill, at Longitudinal Center of Car



Figure C33. SGBF29 Center of Bottom Flange of LH Side Sill, at Longitudinal Center of Car



Figure C34. SGDP30 RH Edge of Deck Plate, at Longitudinal Center of Car



Figure C35. SGDP31 RH Edge of Deck Plate, Forward of Cross Bearer 2

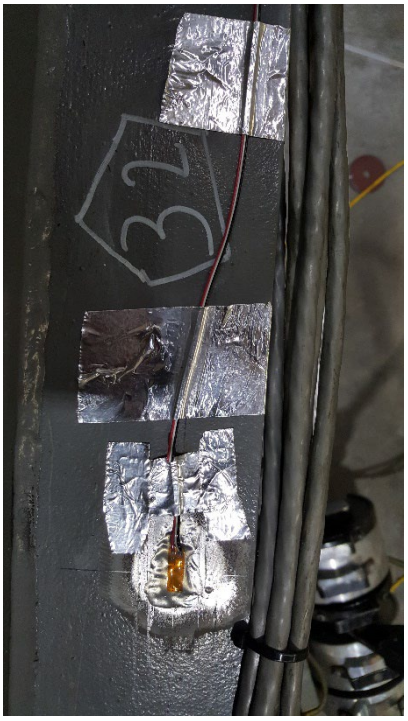


Figure C36. SGDP32 RH Edge of Deck Plate, Aft of Cross Bearer 2

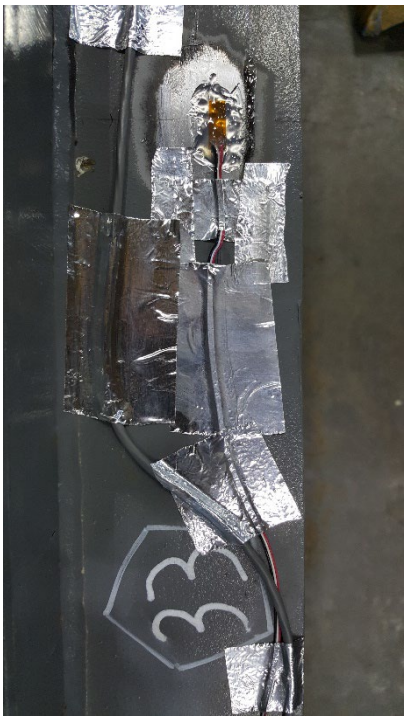


Figure C37. SGDP33 LH Edge of Deck Plate, Forward of Cross Bearer 2

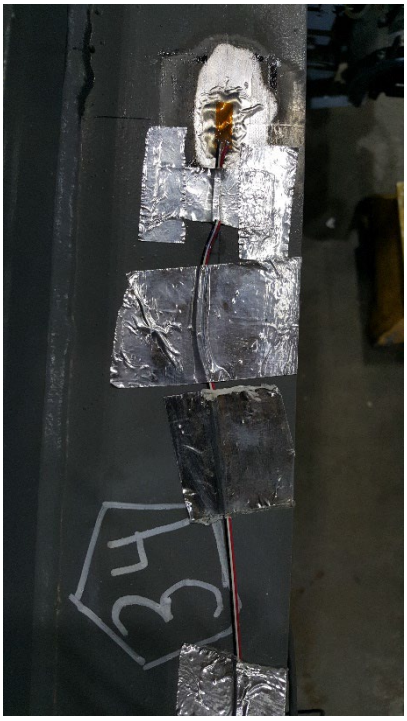


Figure C38. SGDP34 LH Edge of Deck Plate, Aft of Cross Bearer 2



Figure C39. SGBF35 LH Edge of Bottom Flange of Center Sill, Aft of Cross Bearer 1



Figure C40. SGBF36 LH Edge of Bottom Flange of Center Sill, Aft of Cross Bearer 2



Figure C41. SGBF37 RH Edge of Bottom Flange of Center Sill, Aft of Cross Bearer 1

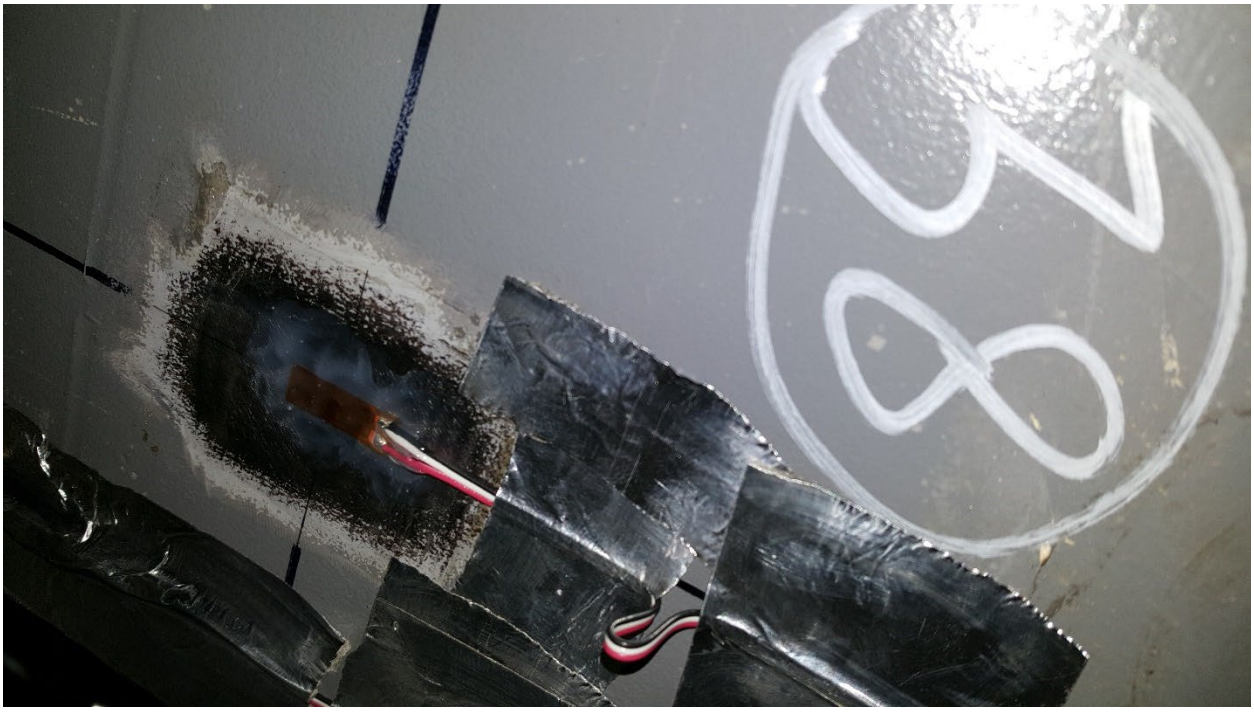


Figure C42. SGBF38 Center of Bottom Flange of LH Side Sill, Forward of Cross Bearer 1



Figure C43. SGBF39 Center of Bottom Flange of LH Side Sill, Aft of Cross Bearer 1



Figure C44. SGBF40 Front of Bottom Flange of B-end Body Bolster near Center Sil, RH Side



Figure C45. SGBF41 Rear of Bottom Flange of B-end Body Bolster near Center Sill, RH Side



Figure C46. SGBF42 Front of Bottom Flange of B-end Body Bolster Near Center Sill, LH Side



Figure C47. SGBF43 Rear of Bottom Flange of B-end Body Bolster near Center Sill, LH Side

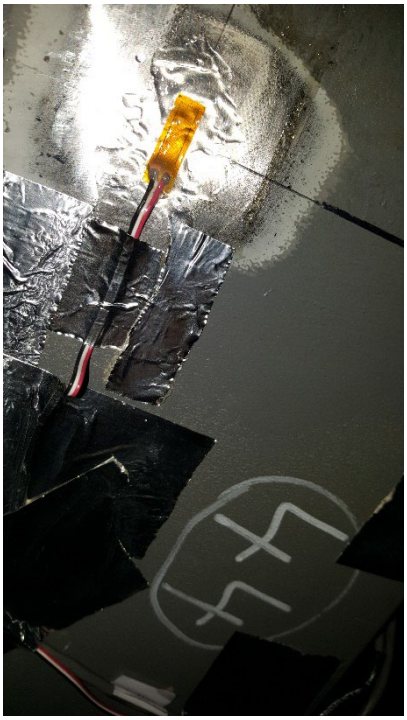


Figure C48. SGBF44 RH Edge of Bottom Flange of Center Sill, Forward of B-end Body Bolster



Figure C49. SGBF45 LH edge of Bottom Flange of Center Sill, Forward of B-end Body Bolster

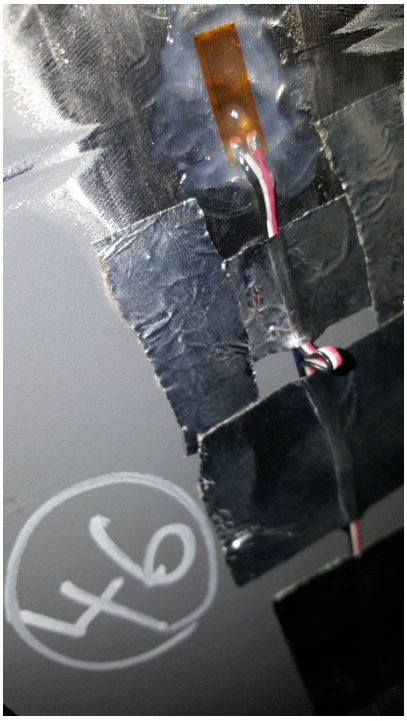


Figure C50. SGBF46 Center of Bottom Flange of RH Side Sill, Aft of Cross Bearer 1



Figure C51. SGBF47 Center of Bottom Flange of RH Side Sill, Forward of Cross Bearer 1



Figure C52. SGDP48 Top of Deck Plate, Longitudinally Centered over B-End Body Bolster, Above RH Edge of Center Sill



Figure C53. SGDP49 Top of Deck Plate, Longitudinally Centered over B-end Body Bolster, above LH Edge of Center Sill



Figure C54. SGDP50 Top of Deck Plate, Longitudinally Centered over A-End Body Bolster, above RH Edge of Center Sill

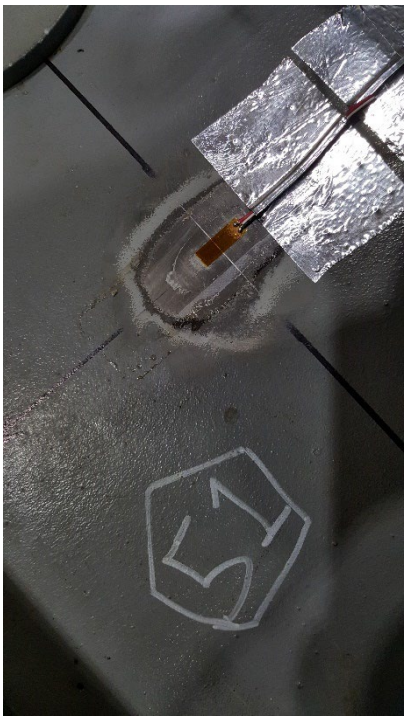


Figure C55. SGDP52 Top of Deck Plate, Longitudinally Centered over A-End Body Bolster, above LH Edge of Center Sill

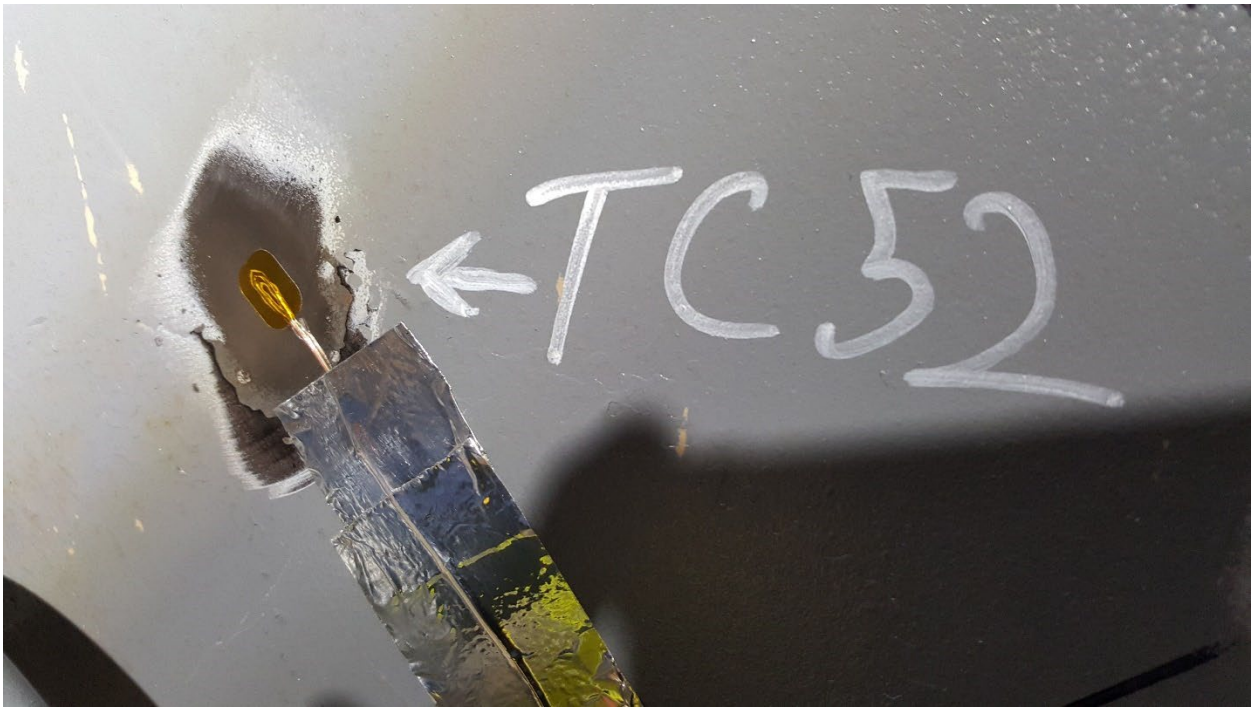


Figure C56. TC52 Laterally and Longitudinally Centered on Top of Deck Plate Forward of A-end Body Bolster



Figure C57. TC53 Laterally and Longitudinally Centered on top of Deck Plate Forward of A-End Body Bolster



Figure C58. TC54 Bottom Flange of Cross Bearer 4 at Lateral and Longitudinal Center of Car

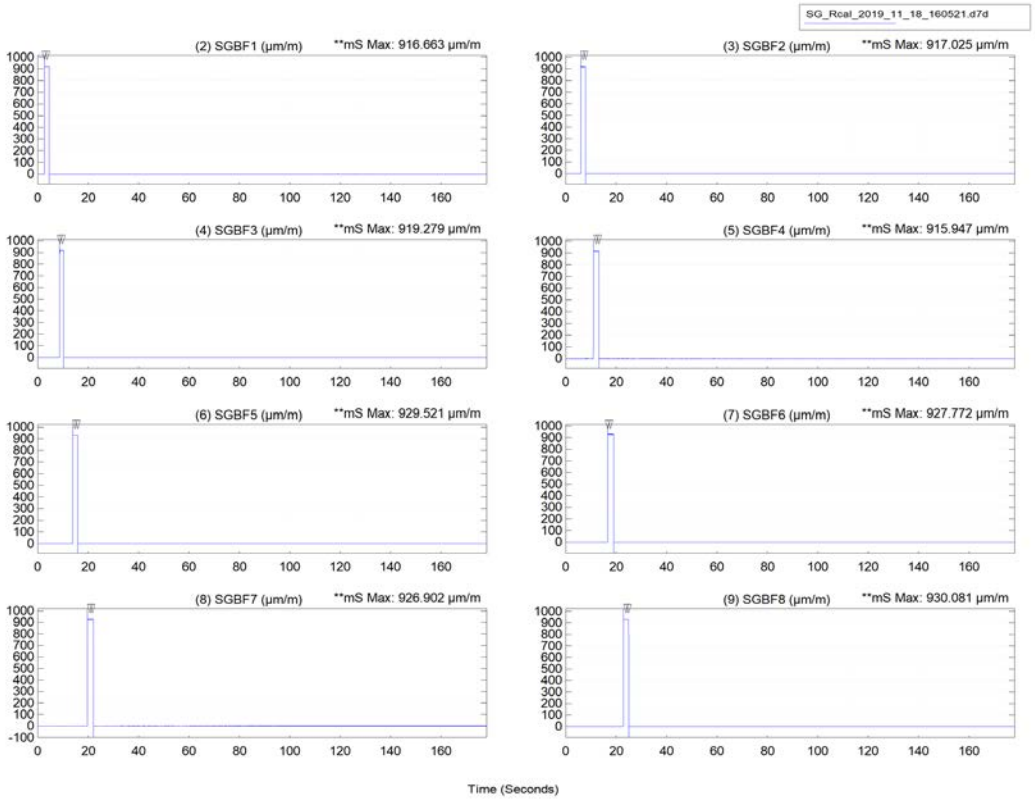


Figure C59. Shunt Calibration of Gages 1-8 with a High Precision 174.650 kΩ Resistor

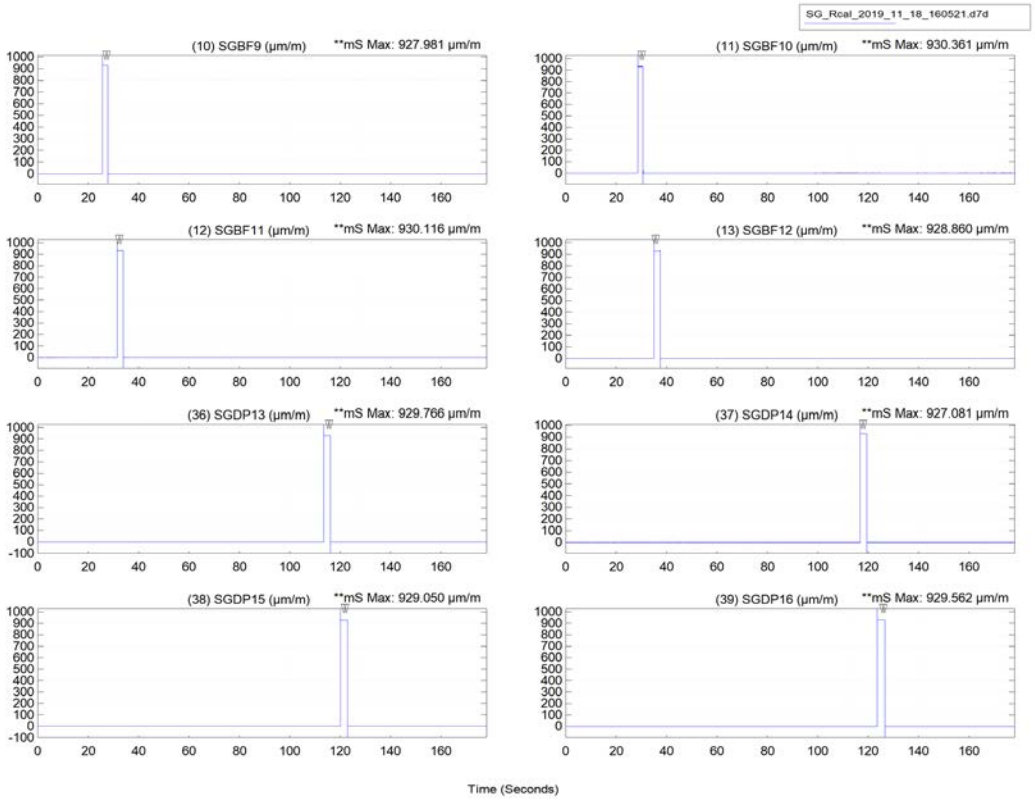


Figure C60. Shunt Calibration of gages 9-16 with a High Precision 174.650 kΩ Resistor

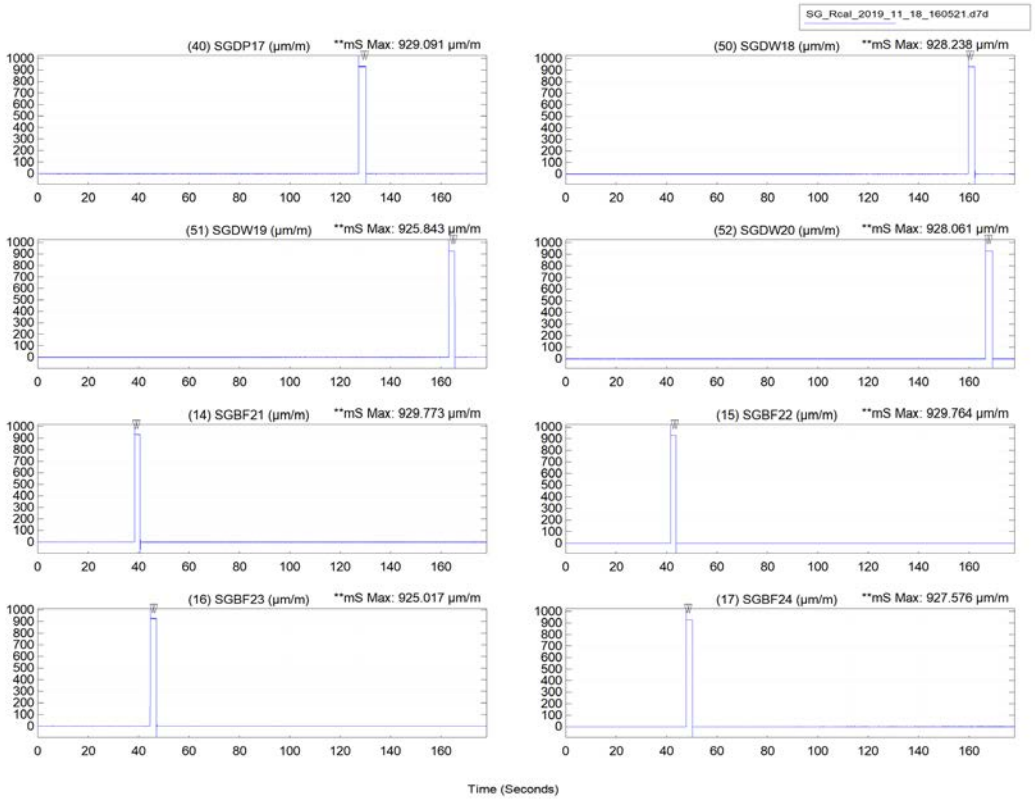


Figure C61. Shunt Calibration of Gages 17-24 with a High Precision 174.650 kΩ Resistor

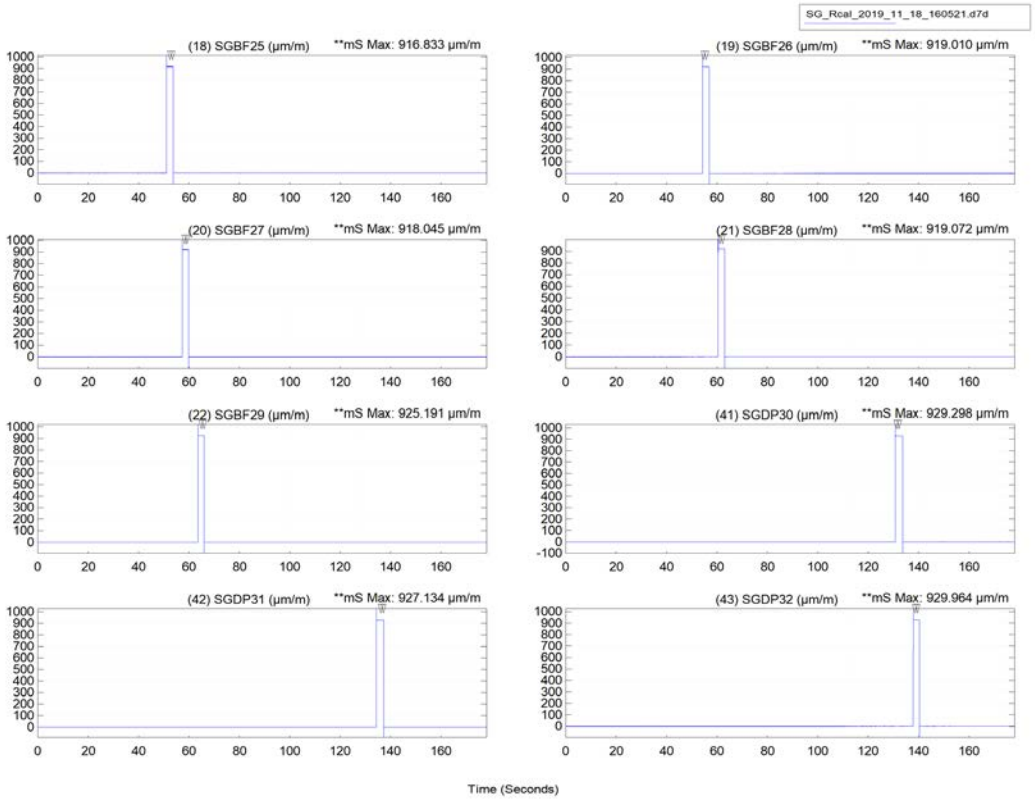


Figure C62. Shunt Calibration of Gages 25-32 with a High Precision 174.650 kΩ Resistor

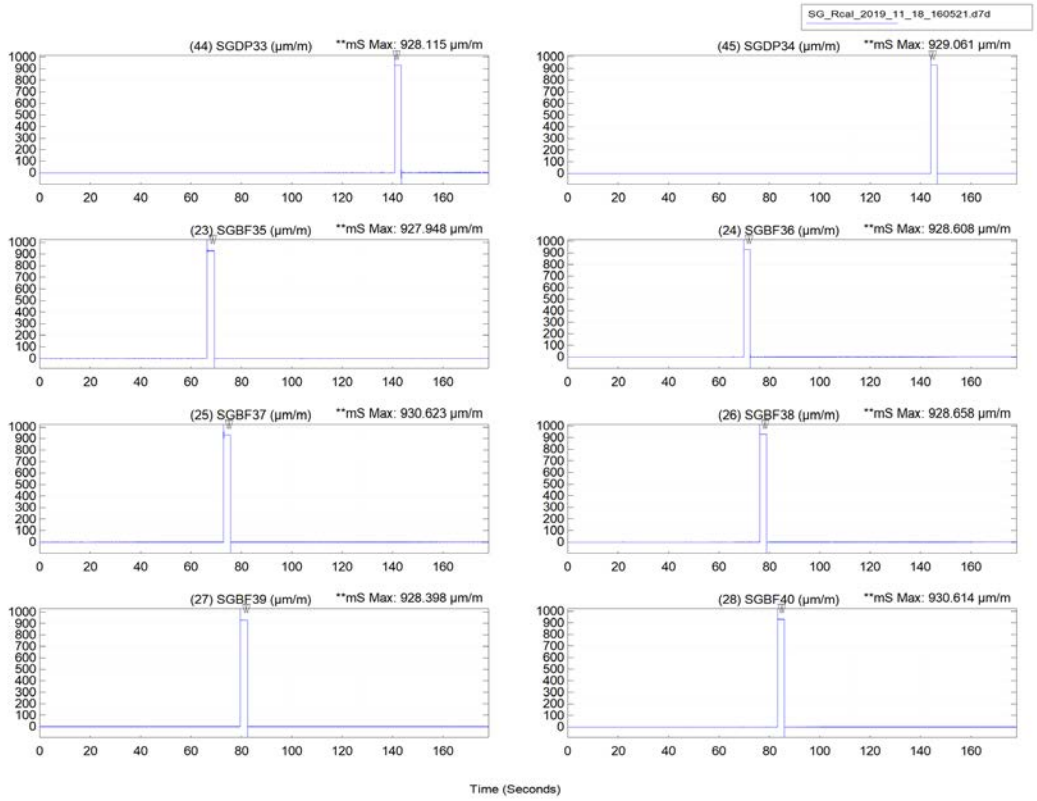


Figure C63. Shunt Calibration of Gages 33-40 with a High Precision 174.650 kΩ Resistor

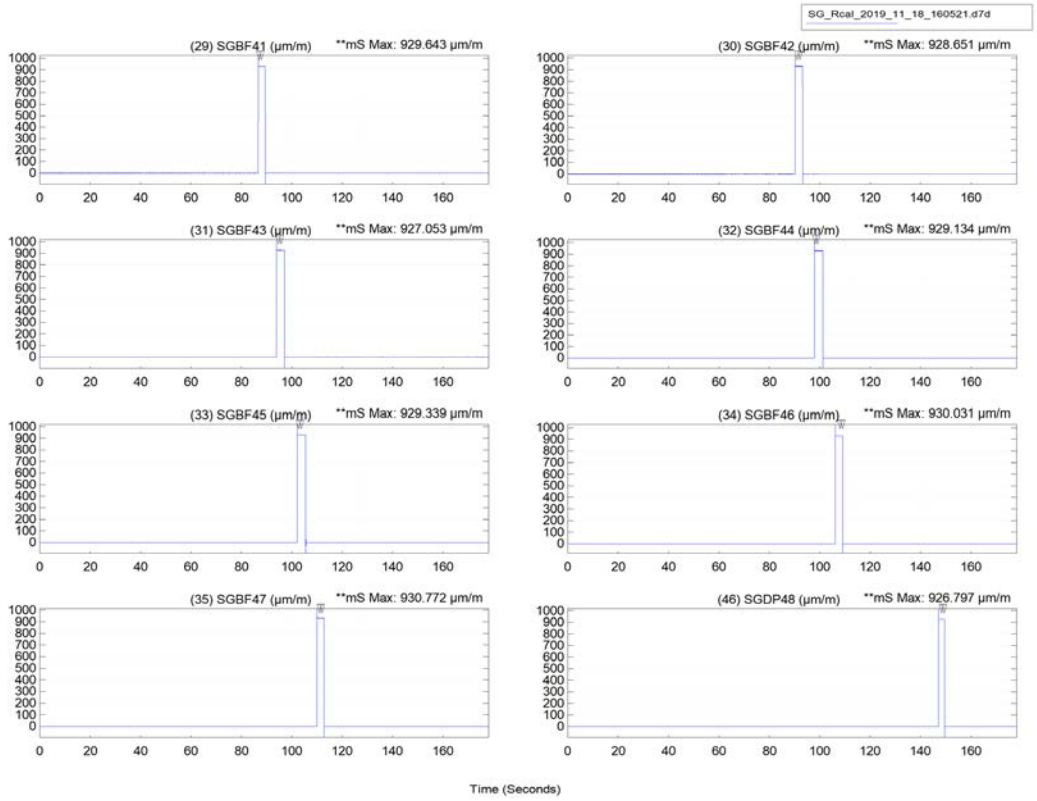


Figure C64. Shunt Calibration of Gages 41-48 with a High Precision 174.650 kΩ Resistor

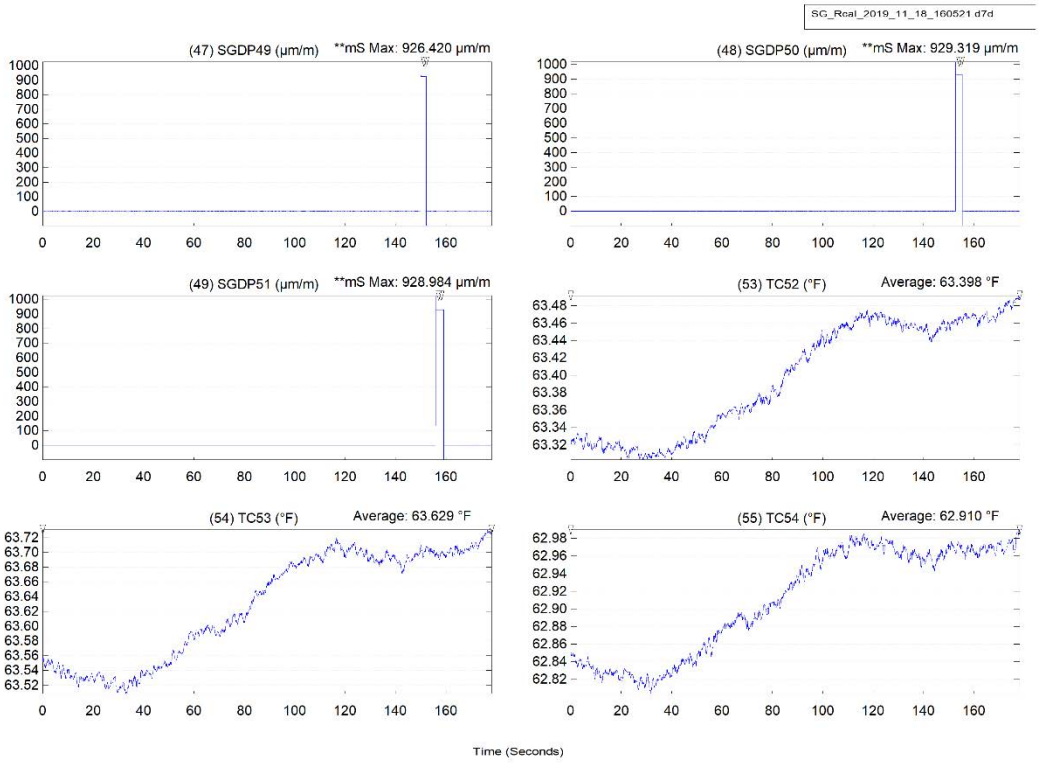


Figure C65. Shunt calibration of Gages 49-51 with a High Precision 174.650 kΩ Resistor, and Plot of the Three Thermocouples. The TTC Weather station showed ambient temperature was 63°F on November 18, 2019, at 4:00 pm when this file was recorded

APPENDIX D: KASGRO BUCKLING ANALYSIS

KASGRO RAIL

S-2043 Critical Buckling Analysis

March 2021

Prepared by: Kasgro Engineering

At the request of the TTCI reviewer, Kasgro was asked to look for the critical buckling stress of the structure. Although this is a requirement in the S-2043 specification, when building railcars to AAR specification M1001, Chapter 11, we have not had to consider critical buckling stress except in compression members of Schnabel cars and Schnabel carload fixtures that contained long compression elements. These compression members have a continuous cross section which a theoretical buckling stress could be defined. Unlike the Schnabel compression members, the Atlas car bodies do not have continuous cross sections. Both cars have multiple cross sections and will not behave like a continuous column with a constant cross section. The following analysis is an approximation.

The critical buckling conditions have been re-evaluated to apply a C value of 1.0 (M-1001 4.2.2.11) to represent simple supports on both ends of the car. This is believed to be the most accurate way to represent the critical buckling condition. The linear buckling analysis now shows an EIGV value of 2.13E+7 before a member of the Buffer Car, Figure A, were to buckle. The linear buckling analysis also now shows an EIGV value of 1.03E+7 before a member of the Cask Car, Figure B, were to buckle. The EIGV values well exceed the designed squeeze load for both cars. In other words, it would take EIGV times a (1 lbf.) Squeeze load for the first buckling failure to occur. Since this would be the start of any buckling, the minimum margin of safety against buckling is something greater than one. The figures below show the deformations of the cars under the buckling load. Local buckling at the applied loads can occur prior to a primary structural member.

Figure A (side view of Buffer Car):

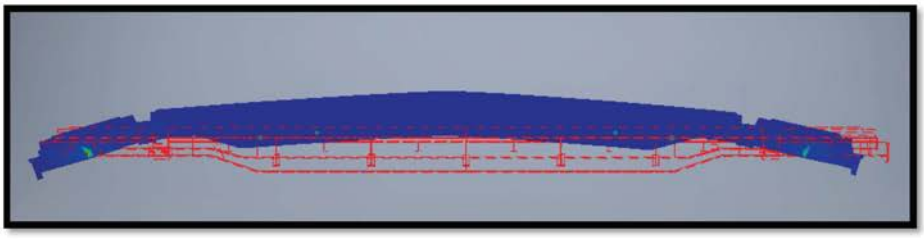
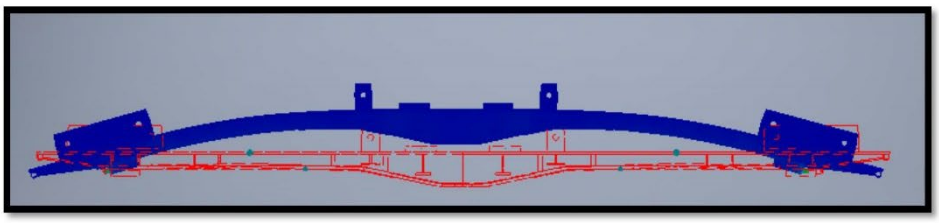


Figure B (side view of Cask Car):



APPENDIX E: COMPRESSIVE END LOAD TEST

Additional results of stresses measured for each strain gauge location during the 1-million-pound compression load test are shown in Figure E1 and Figure E2. Figure E3 shows the maximum stress at the location of highest stress

List of Figures

Figure E1. Stresses Under 1 Million Pounds Compression Load 1 of 2 (first group of gauges) 2
Figure E2. Stresses Under 1 Million Pounds Compression Load 2 of 2 (second group of gauges) . 3
Figure E3. Maximum Stresses at Highest Stress Locations..... 4
Figure E4. Time History of Strain on Four Critical Gages showing that the Strain Returned to Zero at the End of the Test..... 5

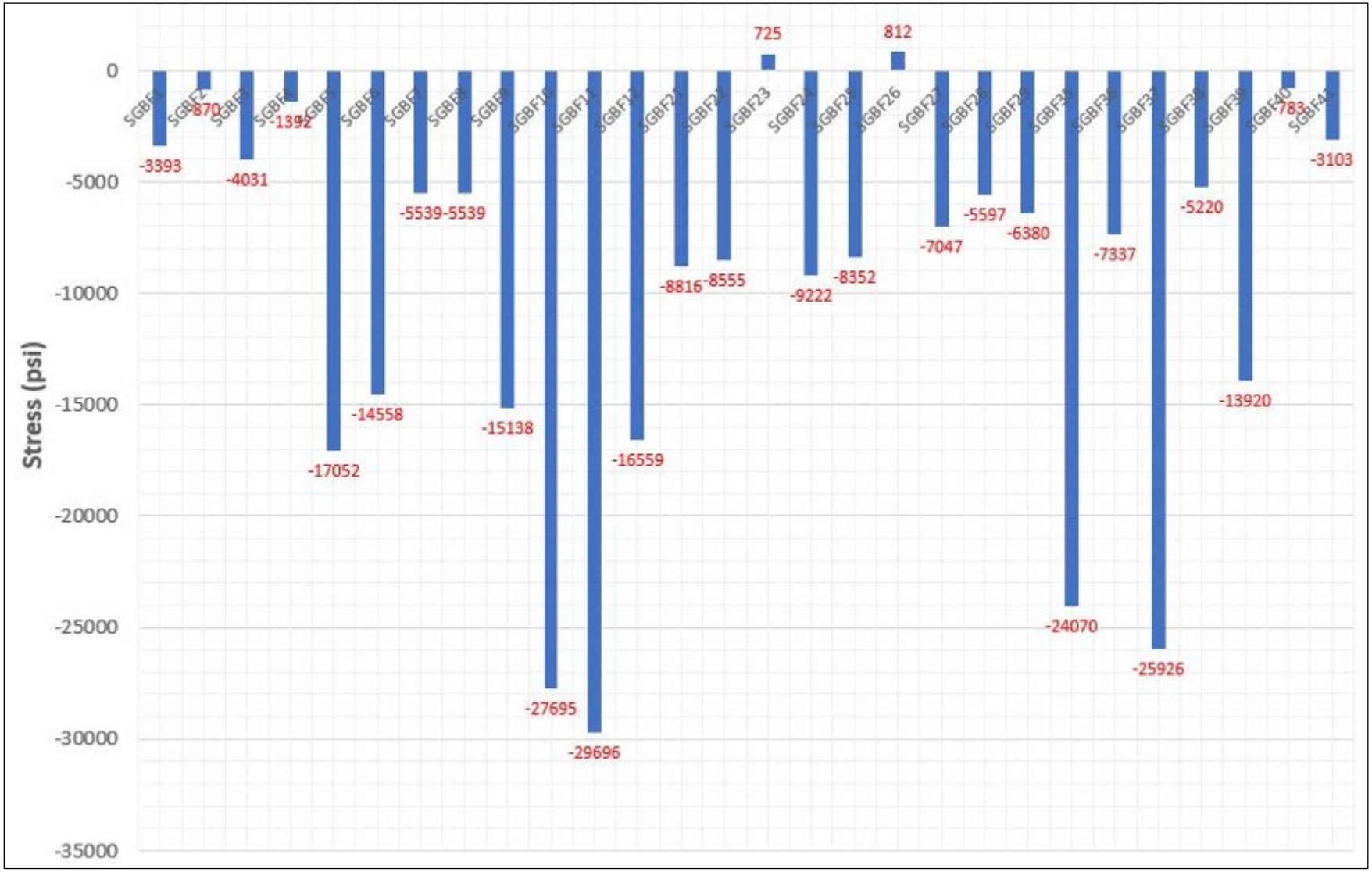


Figure E1. Stresses Under 1 Million Pounds Compression Load 1 of 2 (first group of gauges)

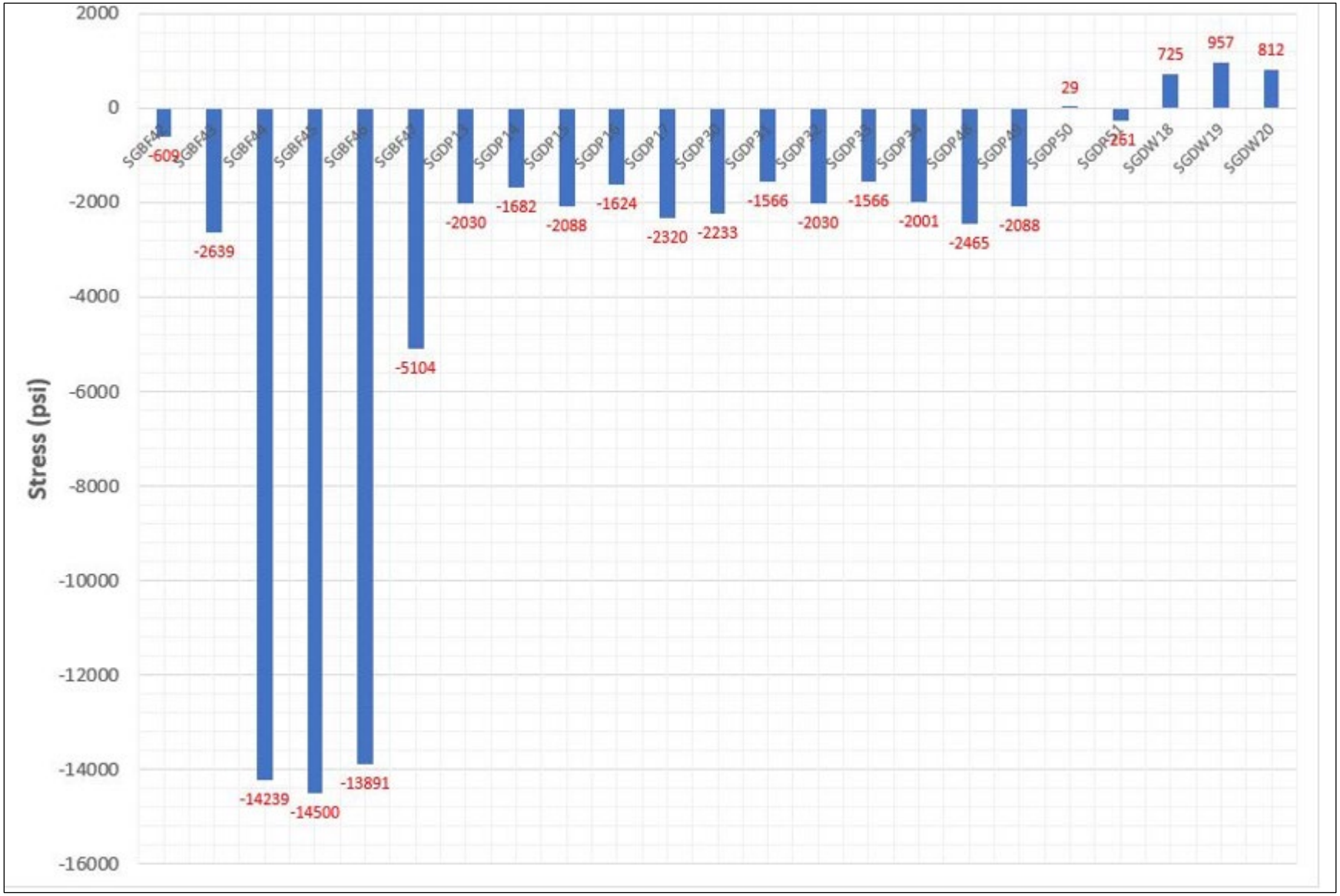


Figure E2. Stresses Under 1 Million Pounds Compression Load 2 of 2 (second group of gauges)

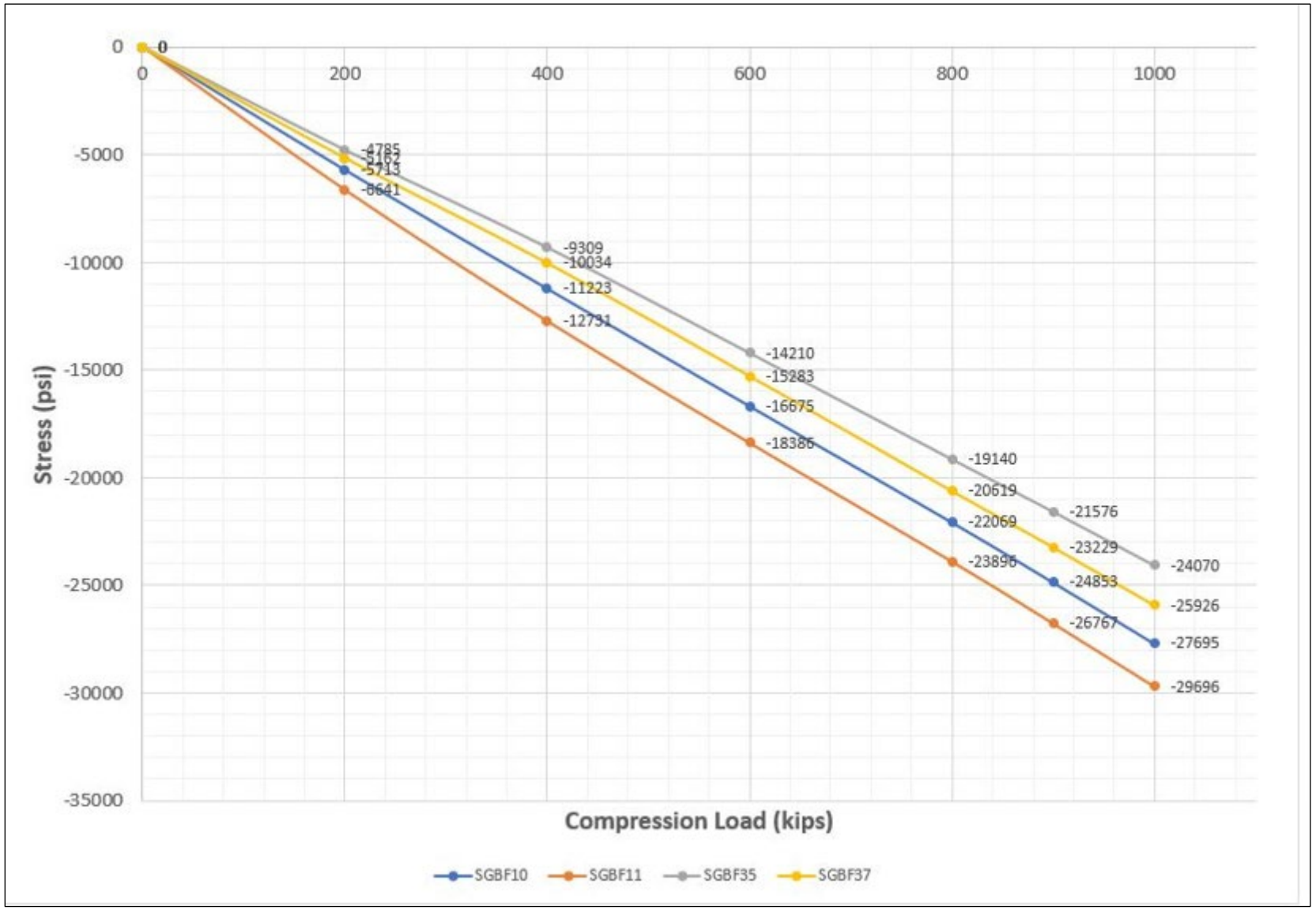


Figure E3. Maximum Stresses at Highest Stress Locations

The following figure shows the full squeeze test up to 1 million pounds for the four highest strained locations. The load was cycled, increasing in 200,000-pound increments until 1 million pounds was reached. After the initial load application, the load was not dropped back to zero until 1 million pounds was reached to prevent shifting of the test fixtures. No re-zero of the gages was done during the whole test after the initial zero before the beginning of the test. It is evident that no permanent deformation was created at these areas.

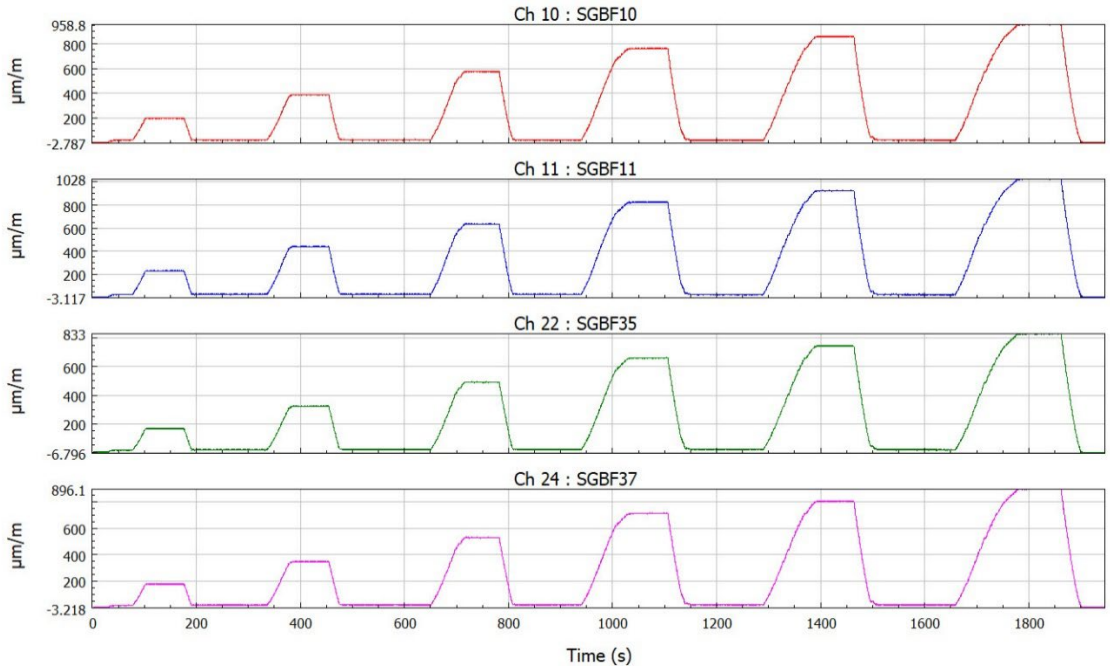


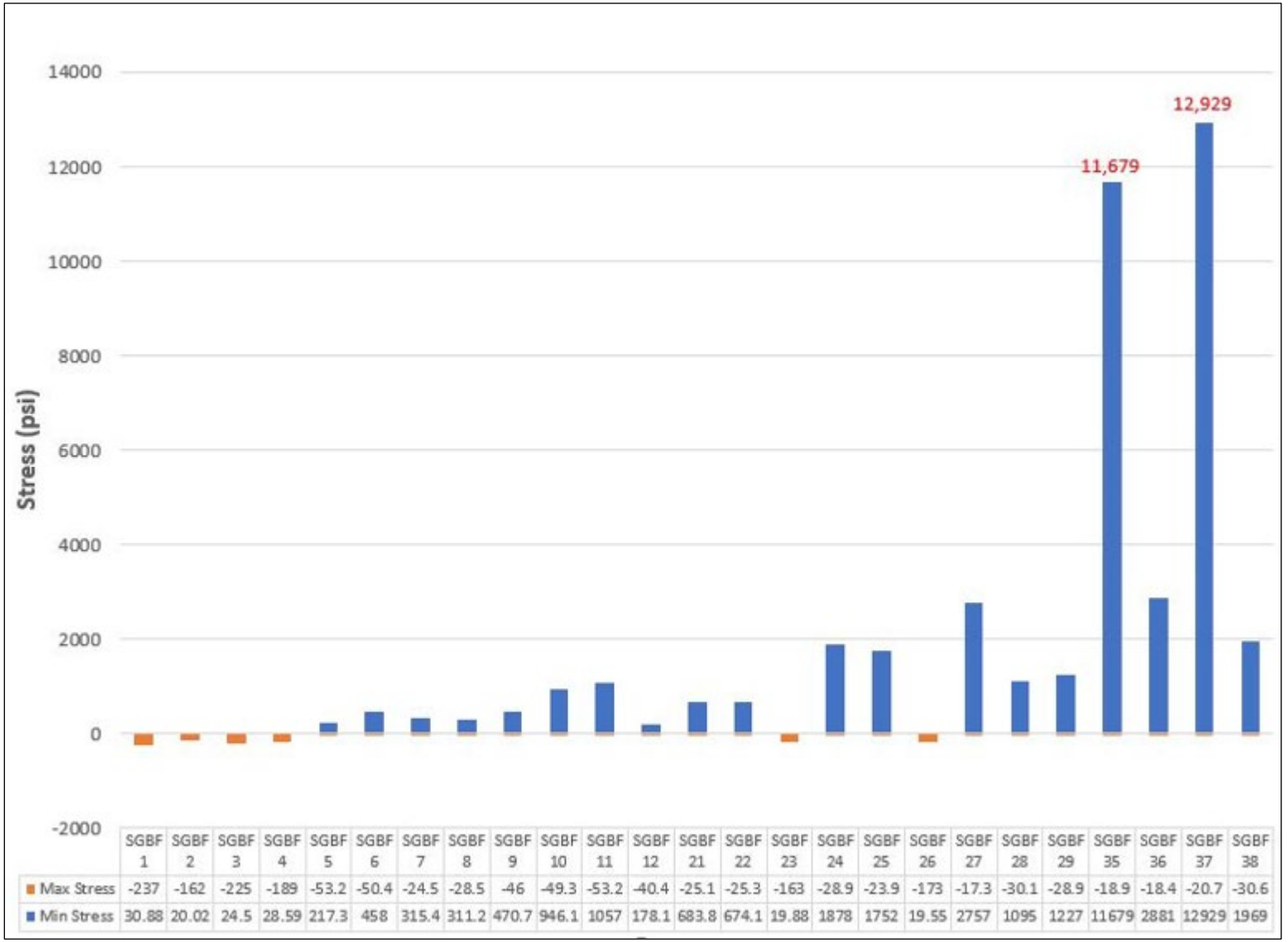
Figure E4. Time History of Strain on Four Critical Gages showing that the Strain Returned to Zero at the End of the Test

APPENDIX F: COUPLER VERTICAL LOADS

Additional results for individual strain gauges during the coupler vertical load test are shown in Figure F1 through Figure F4. The results are presented with stresses under vertical force upward and with stresses under vertical force downward.

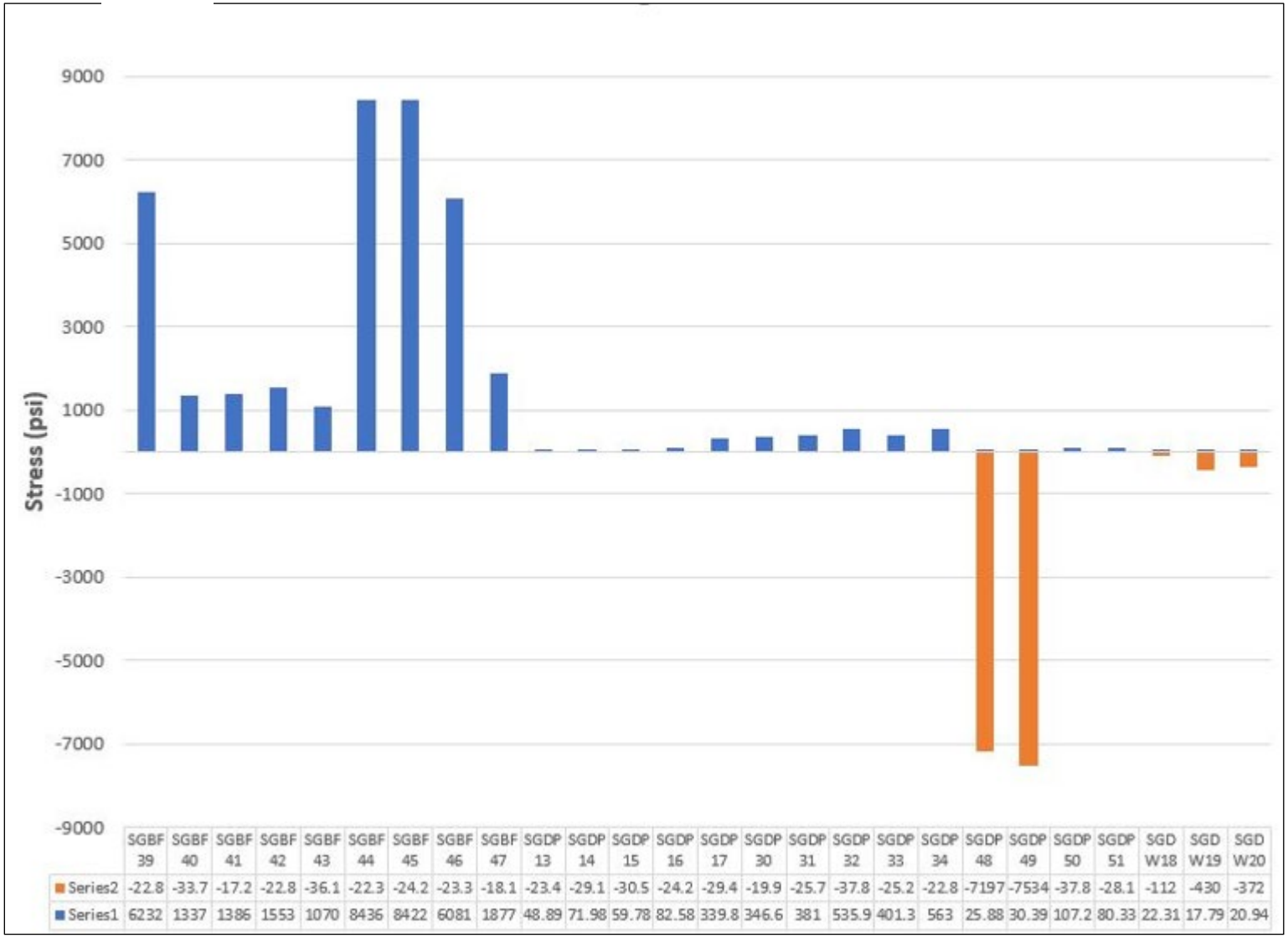
List of Figures

Figure F1. Stresses Under 50 kips Vertical Force (Force Applied Upward) (1 of 2) F-2
Figure F2. Stresses Under 50 kips Vertical Force (Force Applied Upward) (2 of 2) F-3
Figure F3. Stresses Under 50 kips Vertical Force (Force Applied Downward) (1 of 2) F-4
Figure F4. Stresses Under 50 kips Vertical Force (Force Applied Downward) (2 of 2) F-5



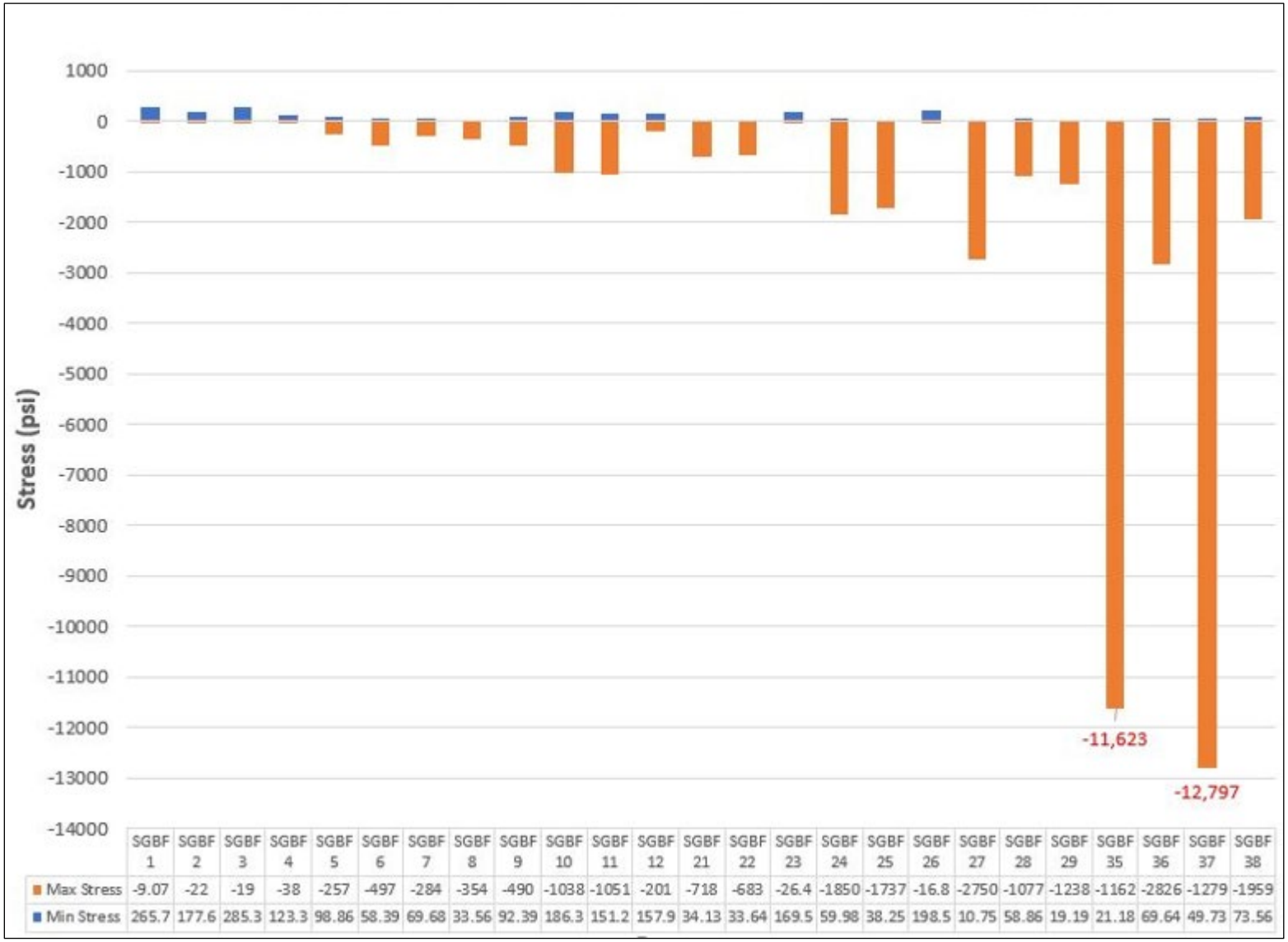
	SGBF 1	SGBF 2	SGBF 3	SGBF 4	SGBF 5	SGBF 6	SGBF 7	SGBF 8	SGBF 9	SGBF 10	SGBF 11	SGBF 12	SGBF 21	SGBF 22	SGBF 23	SGBF 24	SGBF 25	SGBF 26	SGBF 27	SGBF 28	SGBF 29	SGBF 35	SGBF 36	SGBF 37	SGBF 38
Max Stress	-237	-162	-225	-189	-53.2	-50.4	-24.5	-28.5	-46	-49.3	-53.2	-40.4	-25.1	-25.3	-163	-28.9	-23.9	-173	-17.3	-30.1	-28.9	-18.9	-18.4	-20.7	-30.6
Min Stress	30.88	20.02	24.5	28.59	217.3	458	315.4	311.2	470.7	946.1	1057	178.1	683.8	674.1	19.88	1878	1752	19.55	2757	1095	1227	11679	2881	12929	1969

Figure F1. Stresses Under 50 kips Vertical Force (Force Applied Upward) (1 of 2)



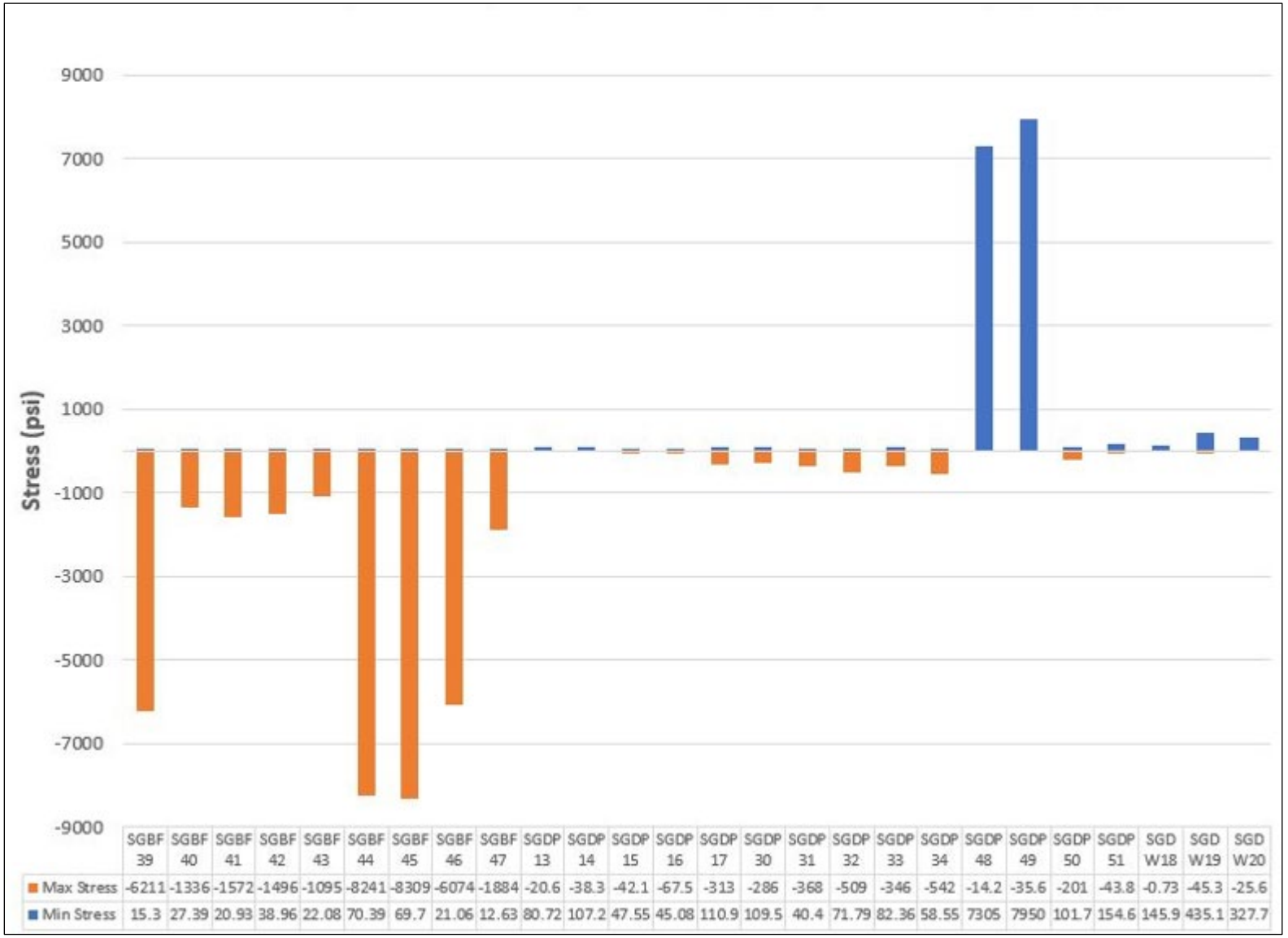
	SGBF 39	SGBF 40	SGBF 41	SGBF 42	SGBF 43	SGBF 44	SGBF 45	SGBF 46	SGBF 47	SGDP 13	SGDP 14	SGDP 15	SGDP 16	SGDP 17	SGDP 30	SGDP 31	SGDP 32	SGDP 33	SGDP 34	SGDP 48	SGDP 49	SGDP 50	SGDP 51	SGD W18	SGD W19	SGD W20
Series2	-22.8	-33.7	-17.2	-22.8	-36.1	-22.3	-24.2	-23.3	-18.1	-23.4	-29.1	-30.5	-24.2	-29.4	-19.9	-25.7	-37.8	-25.2	-22.8	-7197	-7534	-37.8	-28.1	-112	-430	-372
Series1	6232	1337	1386	1553	1070	8436	8422	6081	1877	48.89	71.98	59.78	82.58	339.8	346.6	381	535.9	401.3	563	25.88	30.39	107.2	80.33	22.31	17.79	20.94

Figure F2. Stresses Under 50 kips Vertical Force (Force Applied Upward) (2 of 2)



	SGBF 1	SGBF 2	SGBF 3	SGBF 4	SGBF 5	SGBF 6	SGBF 7	SGBF 8	SGBF 9	SGBF 10	SGBF 11	SGBF 12	SGBF 21	SGBF 22	SGBF 23	SGBF 24	SGBF 25	SGBF 26	SGBF 27	SGBF 28	SGBF 29	SGBF 35	SGBF 36	SGBF 37	SGBF 38
Max Stress	-9.07	-22	-19	-38	-257	-497	-284	-354	-490	-1038	-1051	-201	-718	-683	-26.4	-1850	-1737	-16.8	-2750	-1077	-1238	-1162	-2826	-1279	-1959
Min Stress	265.7	177.6	285.3	123.3	98.86	58.39	69.68	33.56	92.39	186.3	151.2	157.9	34.13	33.64	169.5	59.98	38.25	198.5	10.75	58.86	19.19	21.18	69.64	49.73	73.56

Figure F3. Stresses Under 50 kips Vertical Force (Force Applied Downward) (1 of 2)



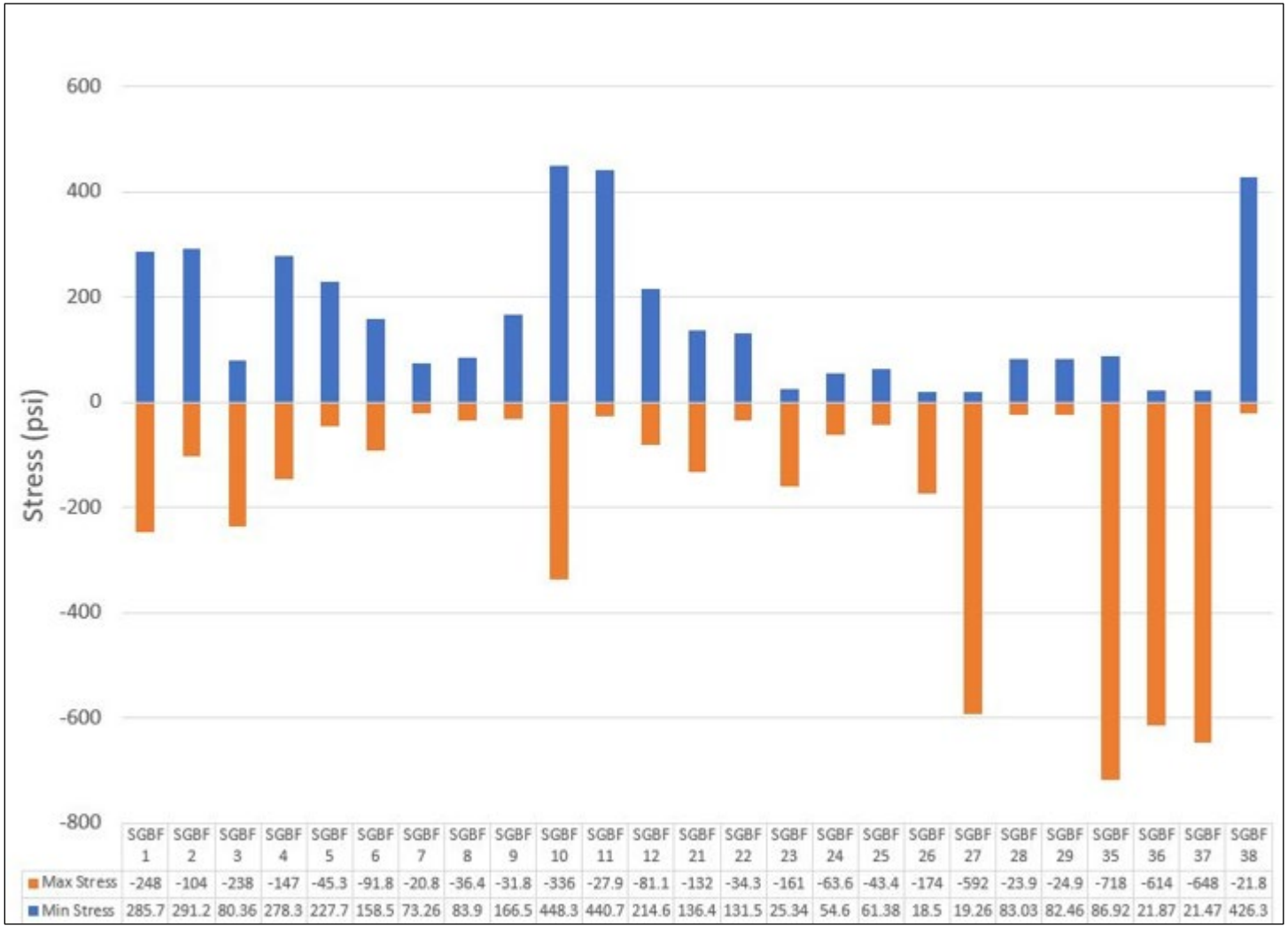
	SGBF 39	SGBF 40	SGBF 41	SGBF 42	SGBF 43	SGBF 44	SGBF 45	SGBF 46	SGBF 47	SGDP 13	SGDP 14	SGDP 15	SGDP 16	SGDP 17	SGDP 30	SGDP 31	SGDP 32	SGDP 33	SGDP 34	SGDP 48	SGDP 49	SGDP 50	SGDP 51	SGD W18	SGD W19	SGD W20
Max Stress	-6211	-1336	-1572	-1496	-1095	-8241	-8309	-6074	-1884	-20.6	-38.3	-42.1	-67.5	-313	-286	-368	-509	-346	-542	-14.2	-35.6	-201	-43.8	-0.73	-45.3	-25.6
Min Stress	15.3	27.39	20.93	38.96	22.08	70.39	69.7	21.06	12.63	80.72	107.2	47.55	45.08	110.9	109.5	40.4	71.79	82.36	58.55	7305	7950	101.7	154.6	145.9	435.1	327.7

Figure F4. Stresses Under 50 kips Vertical Force (Force Applied Downward) (2 of 2)

APPENDIX G: JACKING TEST RESULTS

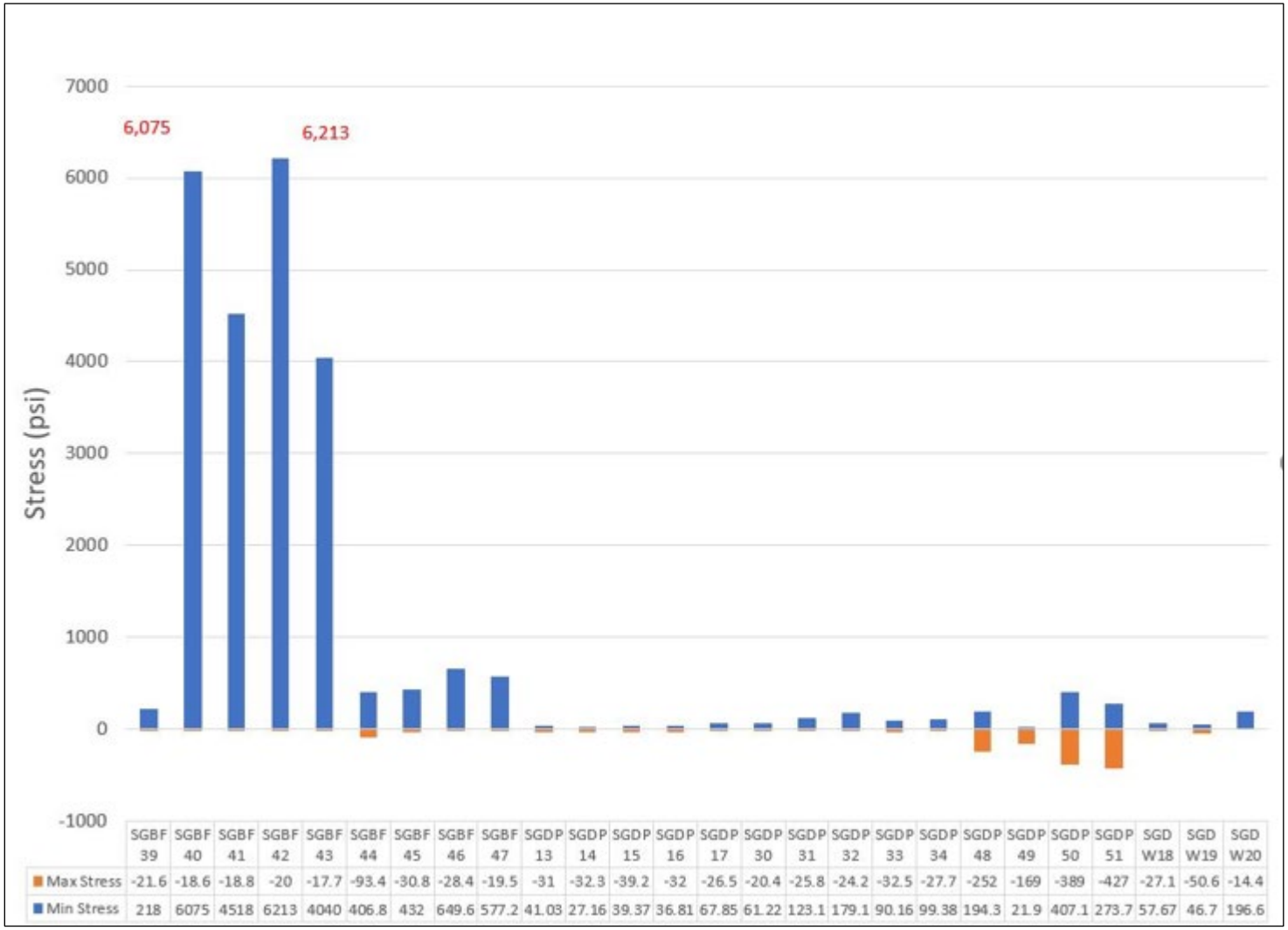
List of Figures

Figure G1. Jacking Test Stresses (1 of 2) G-2
Figure G2. Jacking Test Stresses (2 of 2) G-3



	SGBF 1	SGBF 2	SGBF 3	SGBF 4	SGBF 5	SGBF 6	SGBF 7	SGBF 8	SGBF 9	SGBF 10	SGBF 11	SGBF 12	SGBF 21	SGBF 22	SGBF 23	SGBF 24	SGBF 25	SGBF 26	SGBF 27	SGBF 28	SGBF 29	SGBF 35	SGBF 36	SGBF 37	SGBF 38
Max Stress	-248	-104	-238	-147	-45.3	-91.8	-20.8	-36.4	-31.8	-336	-27.9	-81.1	-132	-34.3	-161	-63.6	-43.4	-174	-592	-23.9	-24.9	-718	-614	-648	-21.8
Min Stress	285.7	291.2	80.36	278.3	227.7	158.5	73.26	83.9	166.5	448.3	440.7	214.6	136.4	131.5	25.34	54.6	61.38	18.5	19.26	83.03	82.46	86.92	21.87	21.47	426.3

Figure G1. Jacking Test Stresses (1 of 2)



	SGBF 39	SGBF 40	SGBF 41	SGBF 42	SGBF 43	SGBF 44	SGBF 45	SGBF 46	SGBF 47	SGDP 13	SGDP 14	SGDP 15	SGDP 16	SGDP 17	SGDP 30	SGDP 31	SGDP 32	SGDP 33	SGDP 34	SGDP 48	SGDP 49	SGDP 50	SGDP 51	SGD W18	SGD W19	SGD W20
Max Stress	-21.6	-18.6	-18.8	-20	-17.7	-93.4	-30.8	-28.4	-19.5	-31	-32.3	-39.2	-32	-26.5	-20.4	-25.8	-24.2	-32.5	-27.7	-252	-169	-389	-427	-27.1	-50.6	-14.4
Min Stress	218	6075	4518	6213	4040	406.8	432	649.6	577.2	41.03	27.16	39.37	36.81	67.85	61.22	123.1	179.1	90.16	99.38	194.3	21.9	407.1	273.7	57.67	46.7	196.6

Figure G2. Jacking Test Stresses (2 of 2)

APPENDIX H: CARBODY TWIST RESULTS

Additional results in the form of stresses from individual strain gauges from the carbody twist test are presented.

List of Figures

Figure H1. Twist Stresses, A-End Left Side (1 of 2) H-2
Figure H2. Twist Stresses, A-End Left Side (2 of 2) H-3
Figure H3. Twist Stresses, A-End Right Side (1 of 2) H-4
Figure H4. Twist Stresses, A-End Right Side (2 of 2) H-5
Figure H5. Twist Stresses, B-End Left Side (1 of 2) H-6
Figure H6. Twist Stresses. B-End Left Side (2 of 2) H-7
Figure H7. Twist Stresses. B-End Right Side (1 of 2) H-8
Figure H8. Twist Stresses. B-End Right Side (2 of 2) H-9
Figure H9. Twist Stresses Part 2 (1 of 2) H-10
Figure H10. Twist Stresses Part 2 (2 of 2) H-11
Figure H11. Twist Stresses Part 2 SGBF11 ..... H-12
Figure H12. Twist Stresses Part 2 SGBF40 ..... H-12

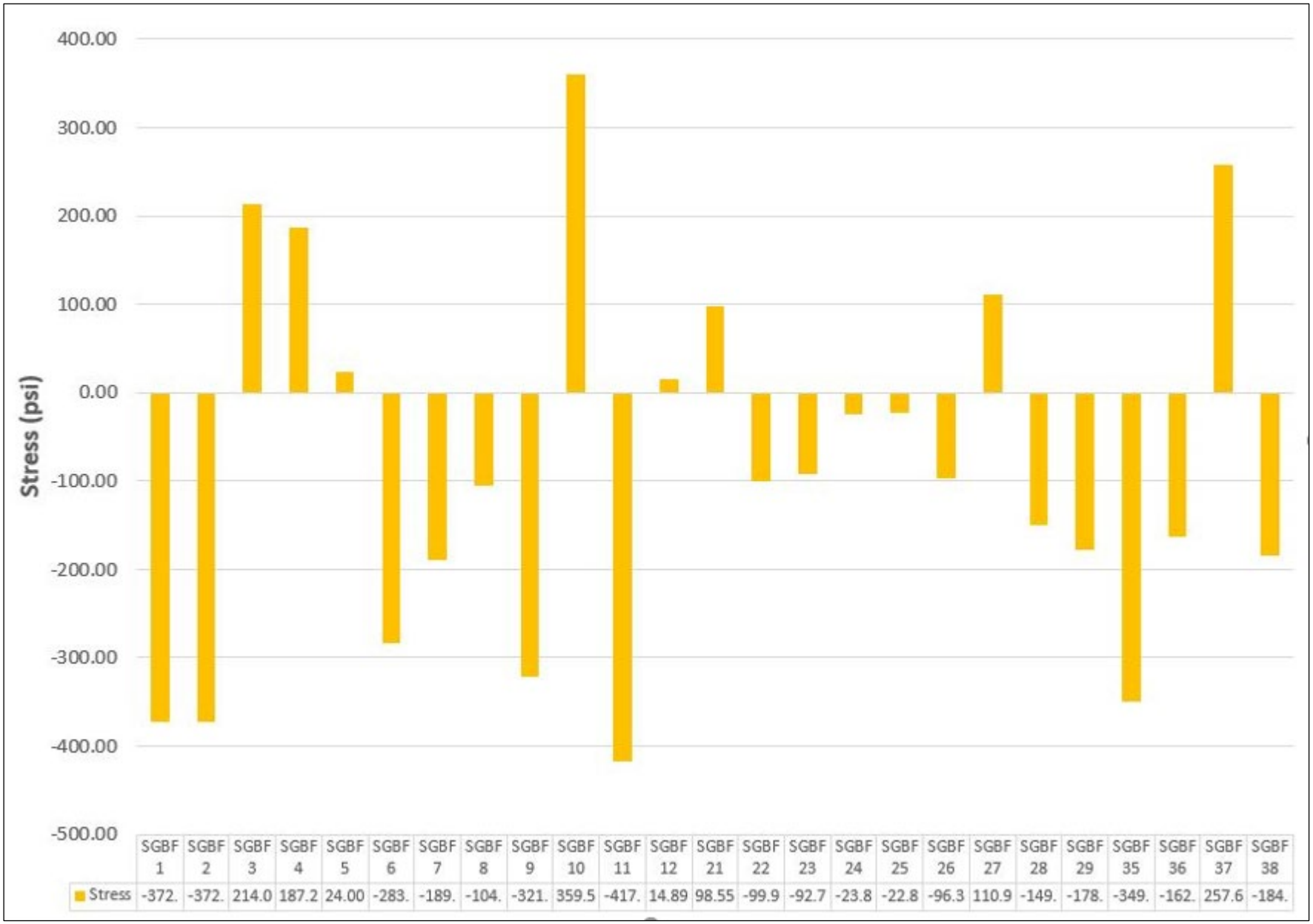


Figure H1. Twist Stresses, A-End Left Side (1 of 2)

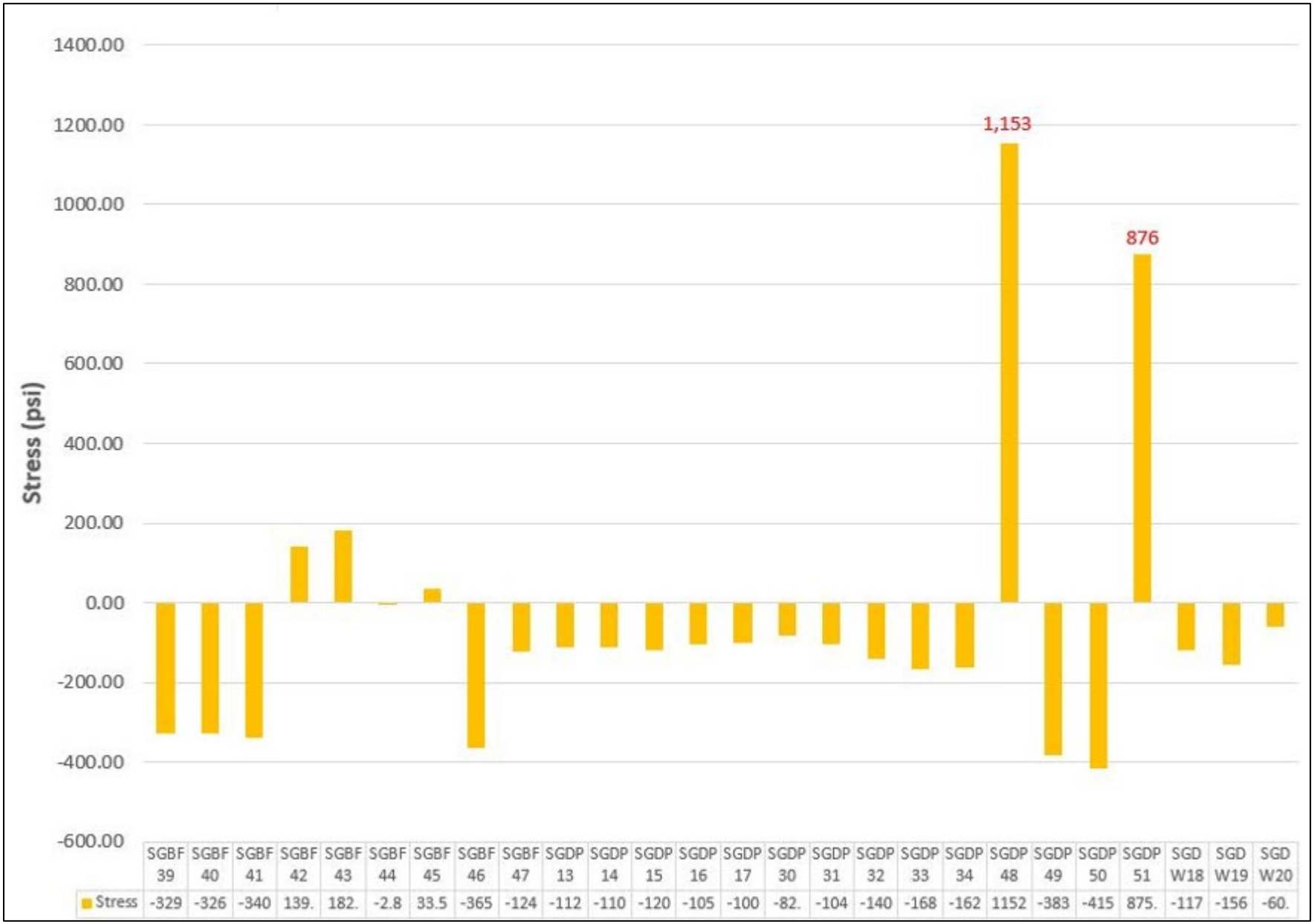


Figure H2. Twist Stresses, A-End Left Side (2 of 2)

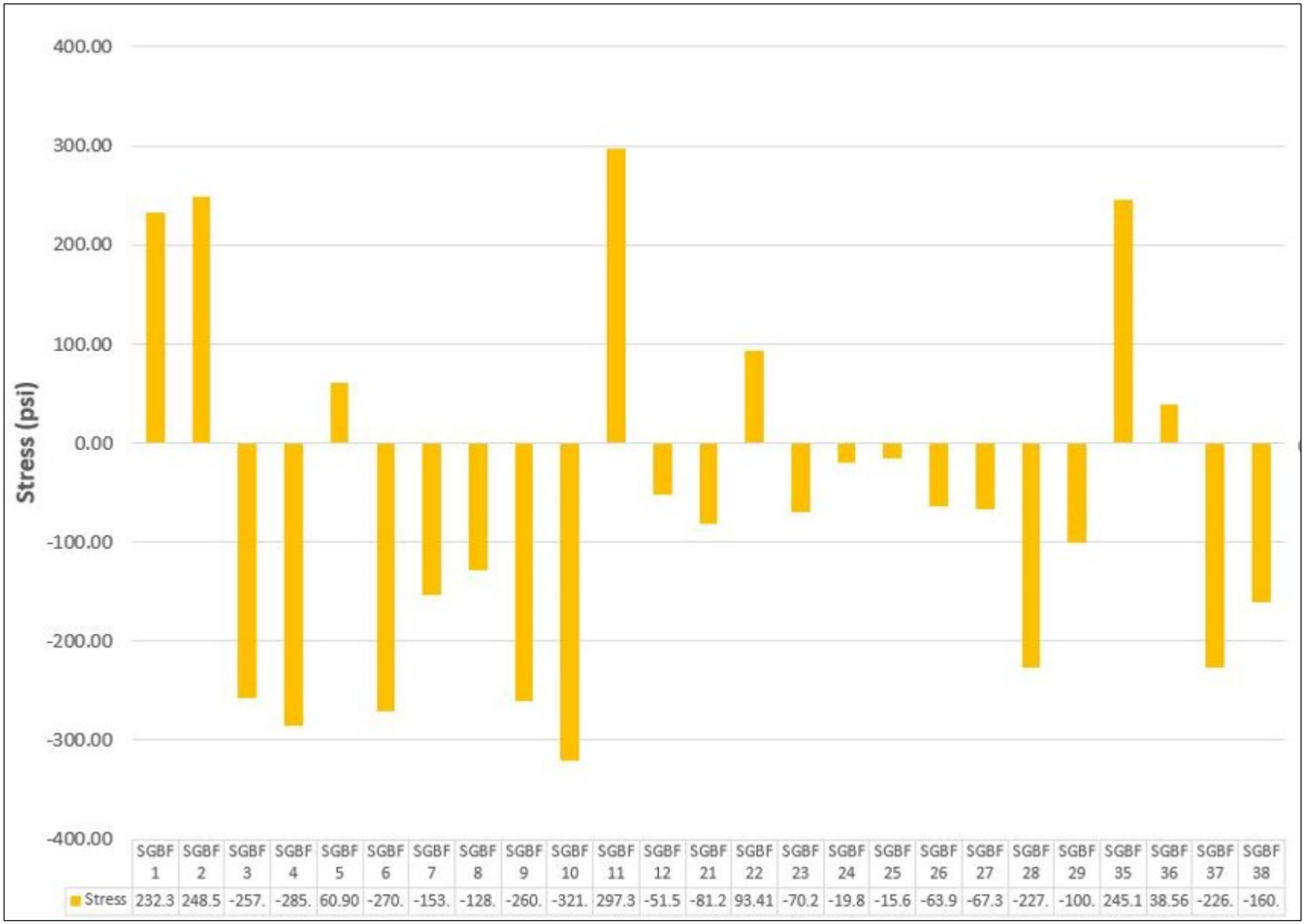
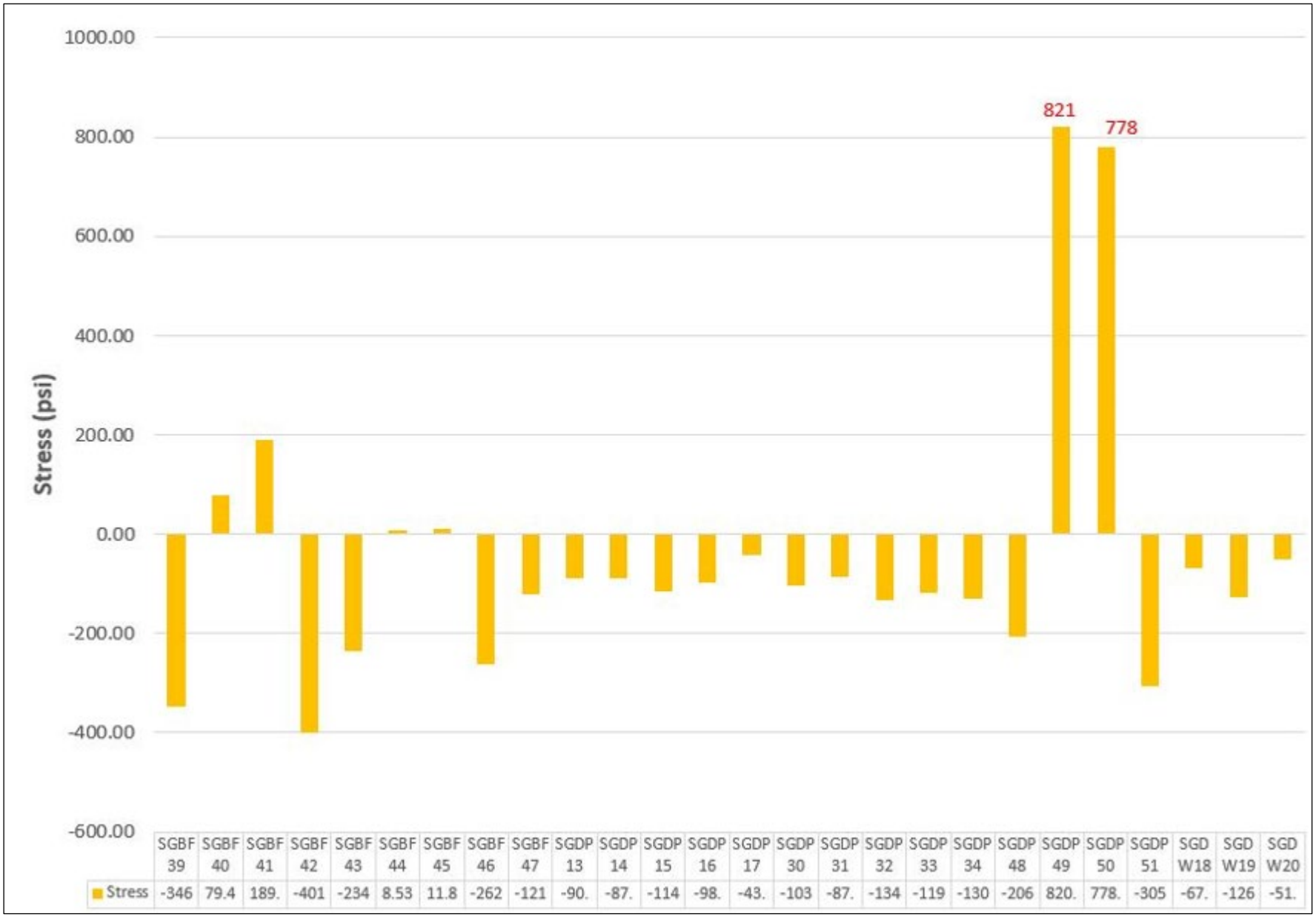
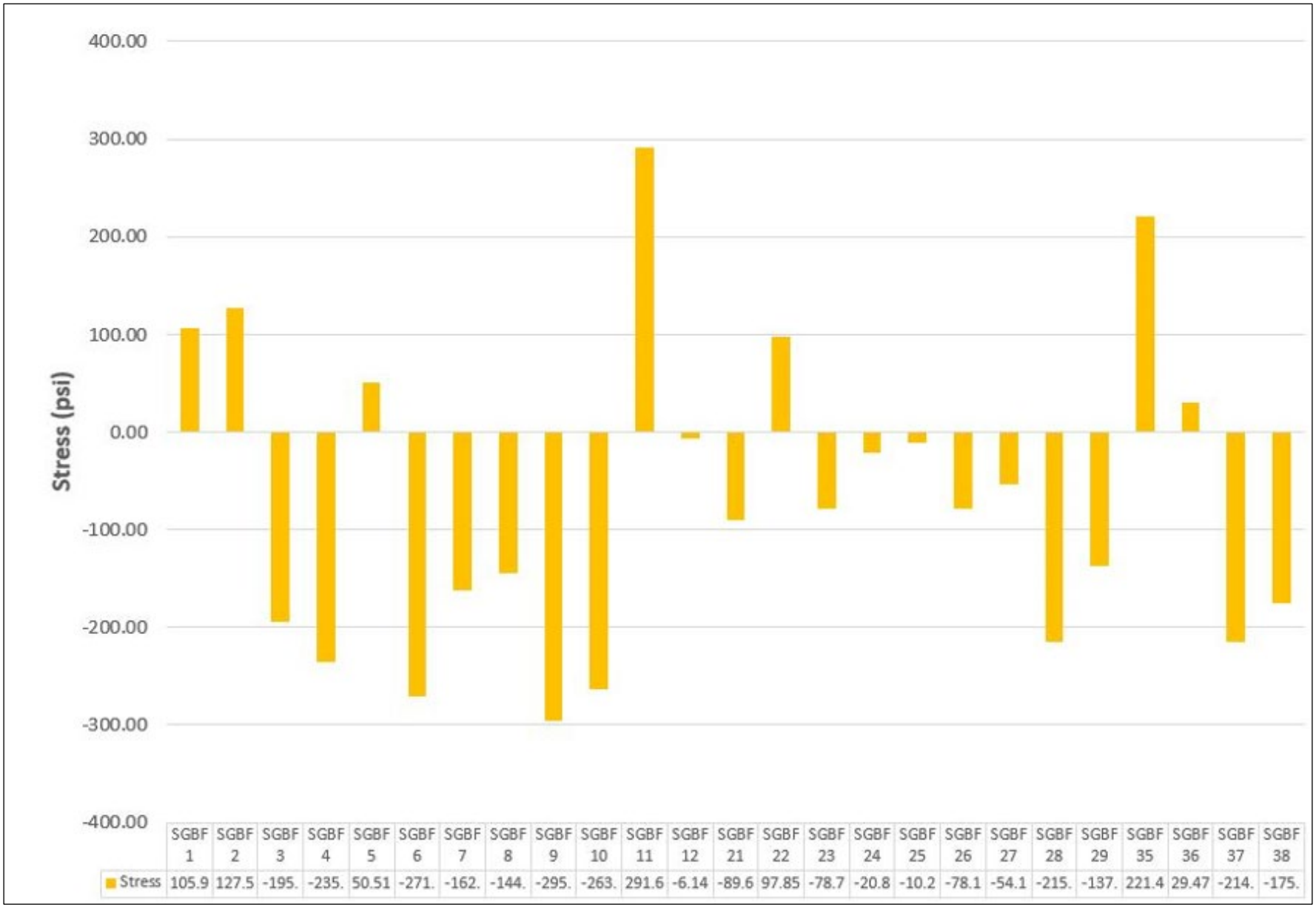


Figure H3. Twist Stresses, A-End Right Side (1 of 2)



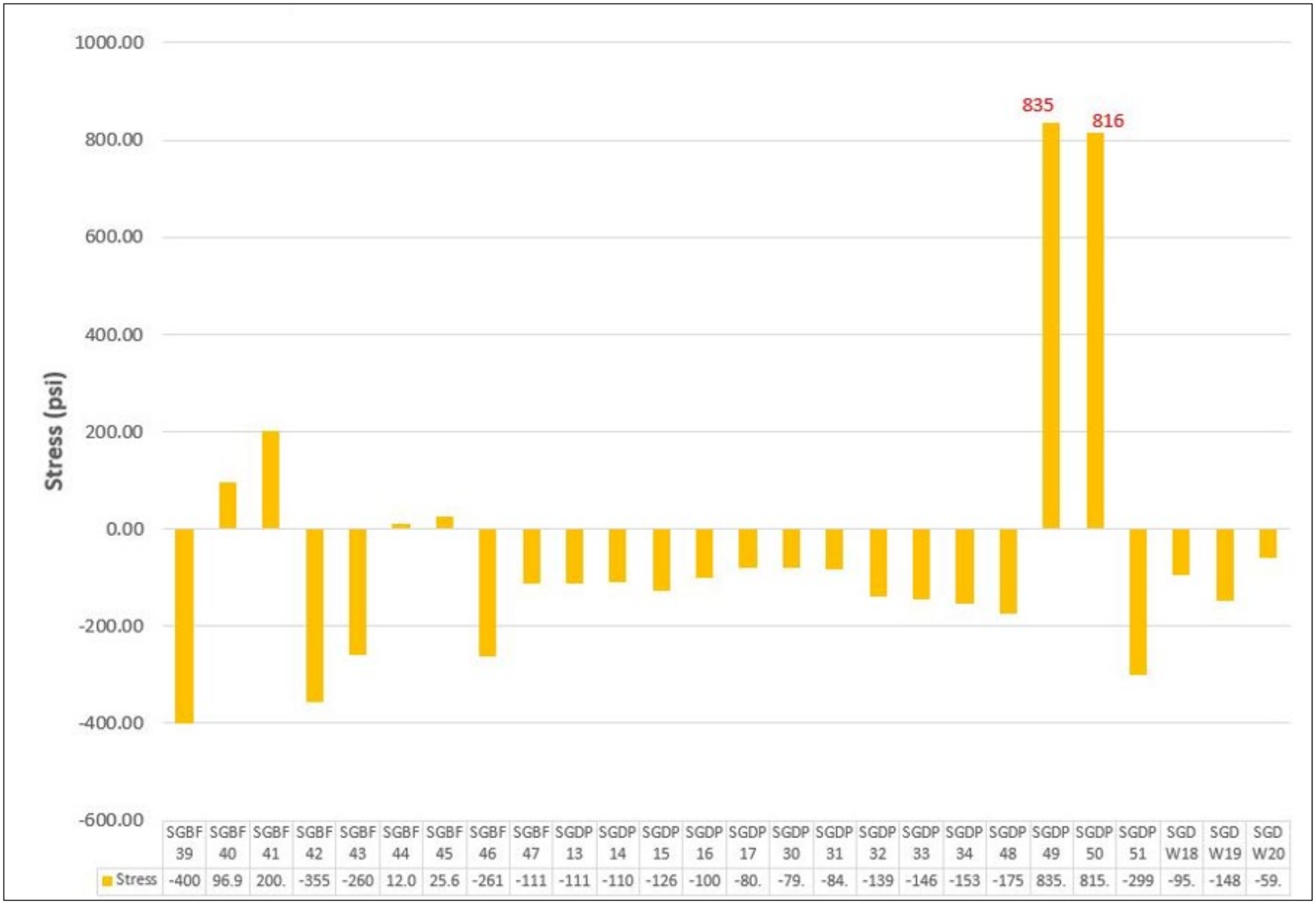
	SGBF 39	SGBF 40	SGBF 41	SGBF 42	SGBF 43	SGBF 44	SGBF 45	SGBF 46	SGBF 47	SGDP 13	SGDP 14	SGDP 15	SGDP 16	SGDP 17	SGDP 30	SGDP 31	SGDP 32	SGDP 33	SGDP 34	SGDP 48	SGDP 49	SGDP 50	SGDP 51	SGD W18	SGD W19	SGD W20
Stress	-346	79.4	189.	-401	-234	8.53	11.8	-262	-121	-90.	-87.	-114	-98.	-43.	-103	-87.	-134	-119	-130	-206	820.	778.	-305	-67.	-126	-51.

Figure H4. Twist Stresses, A-End Right Side (2 of 2)



	SGBF 1	SGBF 2	SGBF 3	SGBF 4	SGBF 5	SGBF 6	SGBF 7	SGBF 8	SGBF 9	SGBF 10	SGBF 11	SGBF 12	SGBF 21	SGBF 22	SGBF 23	SGBF 24	SGBF 25	SGBF 26	SGBF 27	SGBF 28	SGBF 29	SGBF 35	SGBF 36	SGBF 37	SGBF 38
Stress	105.9	127.5	-195.	-235.	50.51	-271.	-162.	-144.	-295.	-263.	291.6	-6.14	-89.6	97.85	-78.7	-20.8	-10.2	-78.1	-54.1	-215.	-137.	221.4	29.47	-214.	-175.

Figure H5. Twist Stresses, B-End Left Side (1 of 2)



	SGBF 39	SGBF 40	SGBF 41	SGBF 42	SGBF 43	SGBF 44	SGBF 45	SGBF 46	SGBF 47	SGDP 13	SGDP 14	SGDP 15	SGDP 16	SGDP 17	SGDP 30	SGDP 31	SGDP 32	SGDP 33	SGDP 34	SGDP 48	SGDP 49	SGDP 50	SGDP 51	SGD W18	SGD W19	SGD W20
Stress	-400	96.9	200.	-355	-260	12.0	25.6	-261	-111	-111	-110	-126	-100	-80.	-79.	-84.	-139	-146	-153	-175	835.	815.	-299	-95.	-148	-59.

Figure H6. Twist Stresses. B-End Left Side (2 of 2)

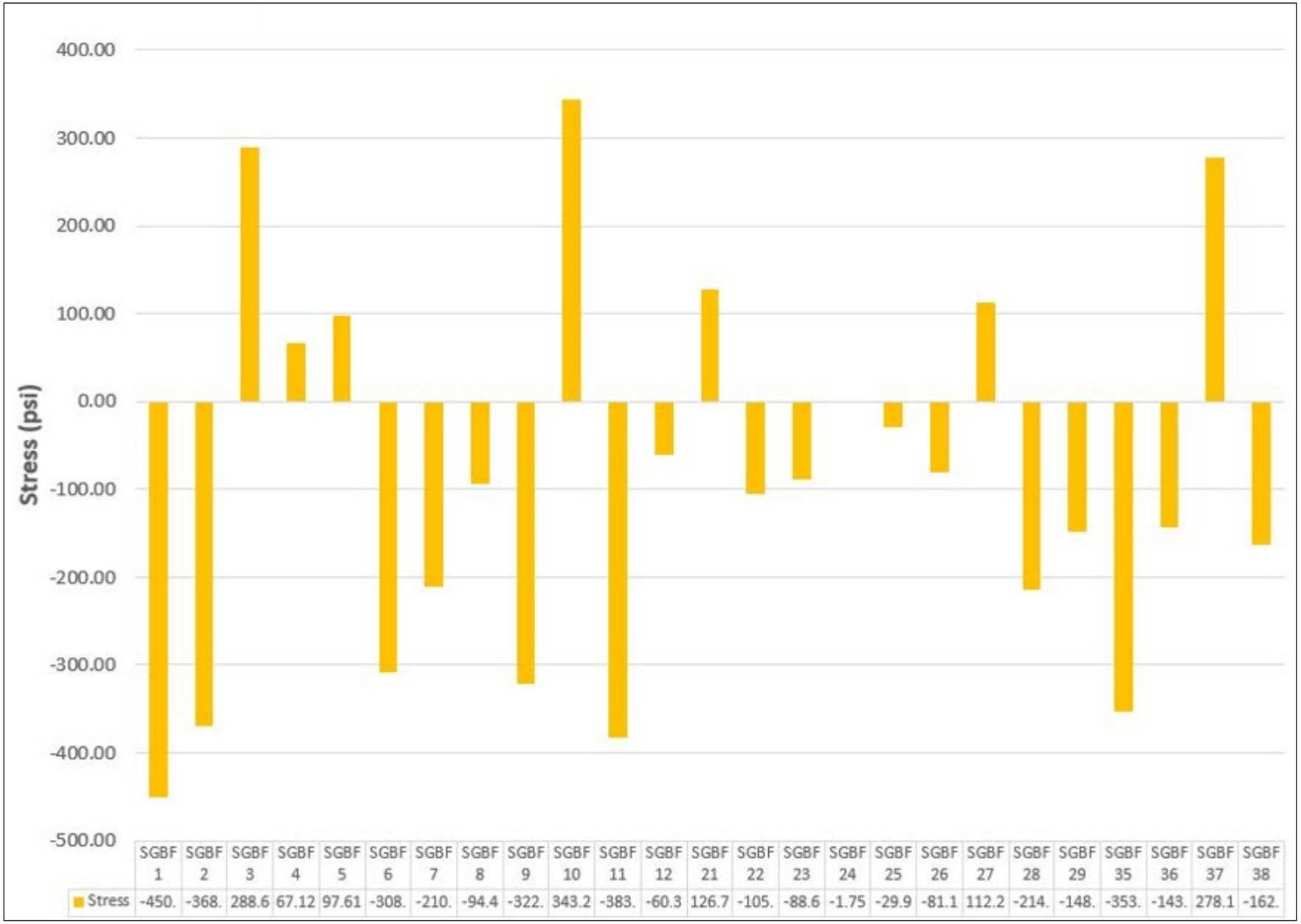
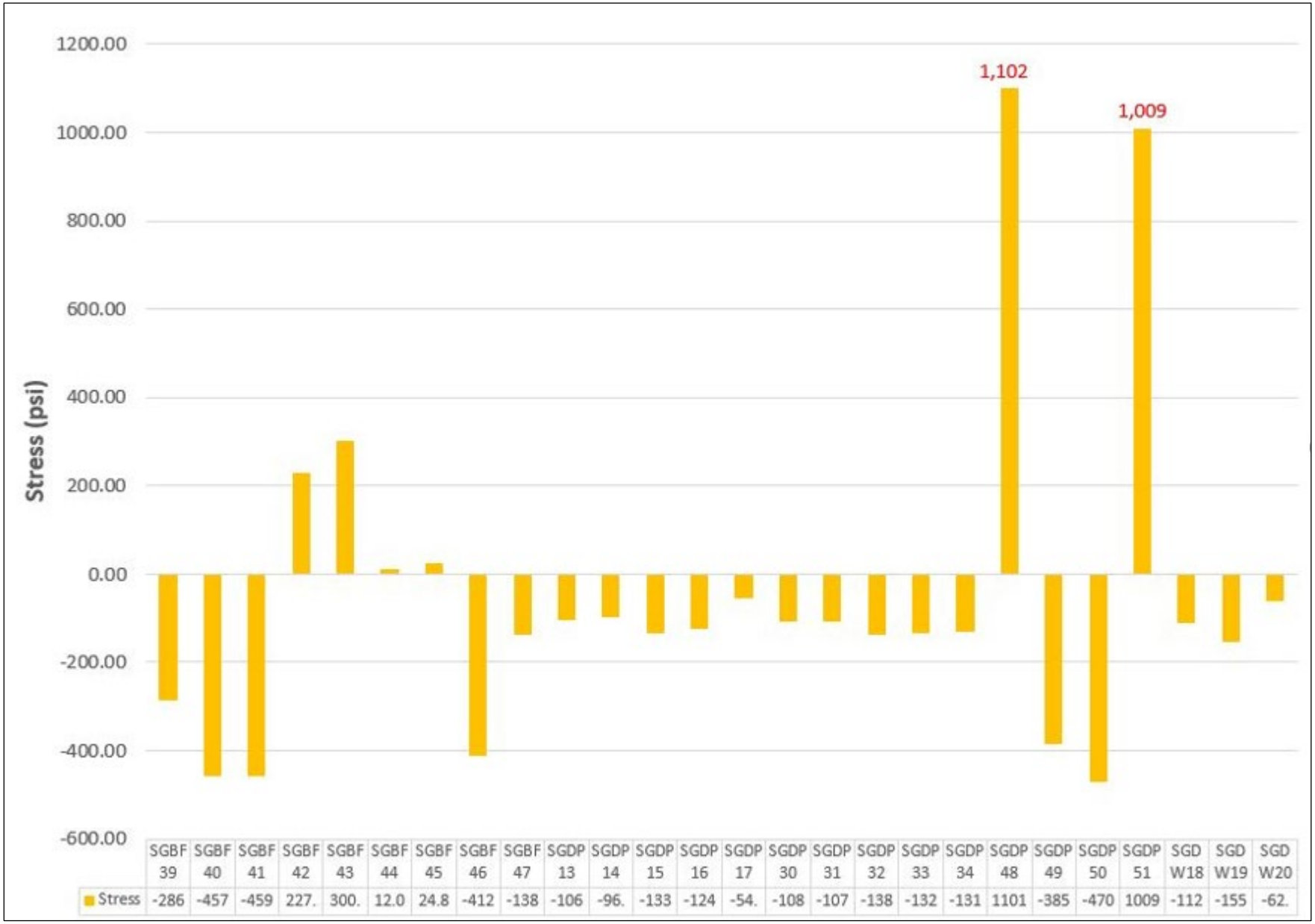
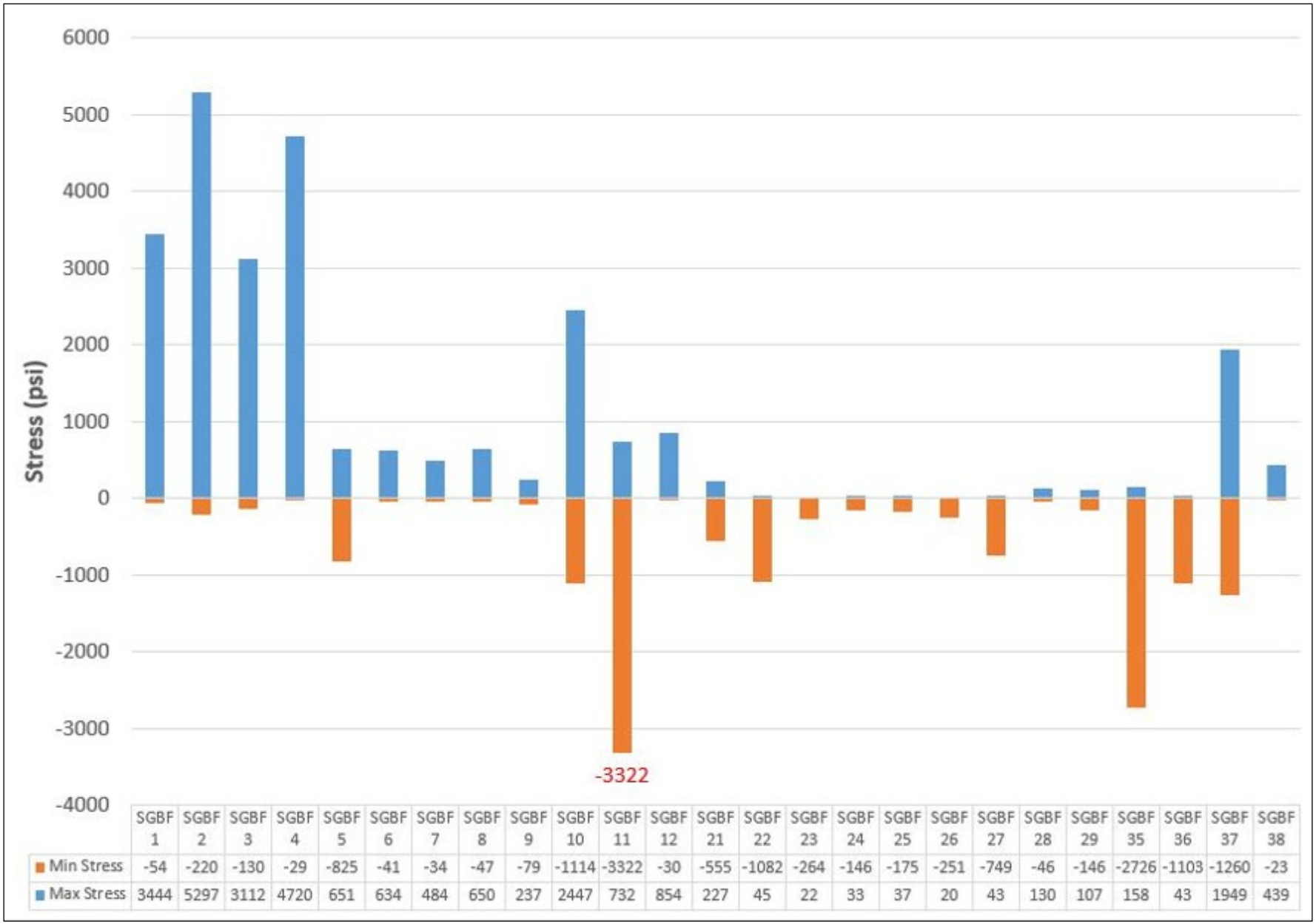


Figure H7. Twist Stresses. B-End Right Side (1 of 2)



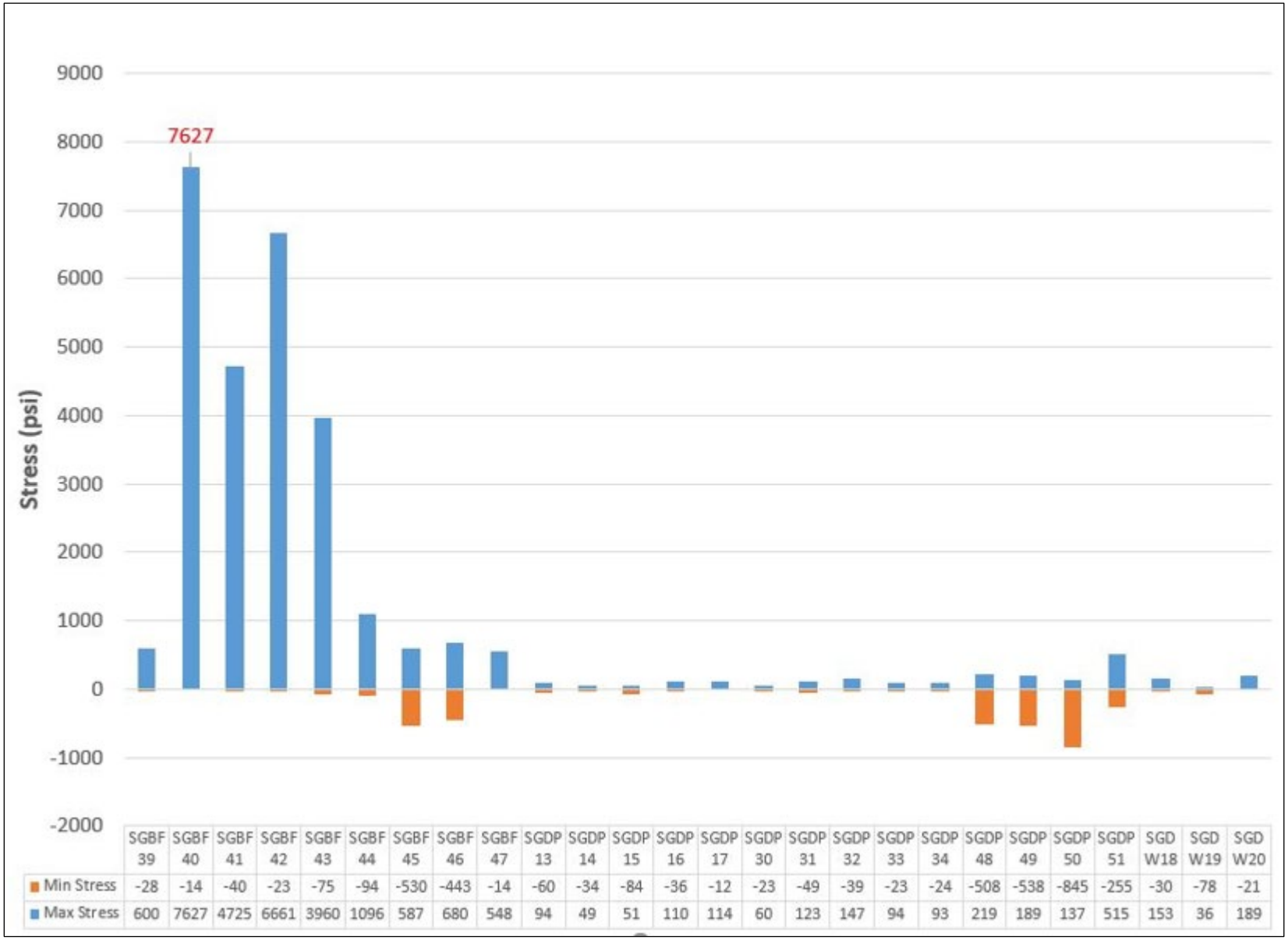
	SGBF 39	SGBF 40	SGBF 41	SGBF 42	SGBF 43	SGBF 44	SGBF 45	SGBF 46	SGBF 47	SGDP 13	SGDP 14	SGDP 15	SGDP 16	SGDP 17	SGDP 30	SGDP 31	SGDP 32	SGDP 33	SGDP 34	SGDP 48	SGDP 49	SGDP 50	SGDP 51	SGD W18	SGD W19	SGD W20
Stress	-286	-457	-459	227.	300.	12.0	24.8	-412	-138	-106	-96.	-133	-124	-54.	-108	-107	-138	-132	-131	1101	-385	-470	1009	-112	-155	-62.

Figure H8. Twist Stresses. B-End Right Side (2 of 2)



	SGBF 1	SGBF 2	SGBF 3	SGBF 4	SGBF 5	SGBF 6	SGBF 7	SGBF 8	SGBF 9	SGBF 10	SGBF 11	SGBF 12	SGBF 21	SGBF 22	SGBF 23	SGBF 24	SGBF 25	SGBF 26	SGBF 27	SGBF 28	SGBF 29	SGBF 35	SGBF 36	SGBF 37	SGBF 38
Min Stress	-54	-220	-130	-29	-825	-41	-34	-47	-79	-1114	-3322	-30	-555	-1082	-264	-146	-175	-251	-749	-46	-146	-2726	-1103	-1260	-23
Max Stress	3444	5297	3112	4720	651	634	484	650	237	2447	732	854	227	45	22	33	37	20	43	130	107	158	43	1949	439

Figure H9. Twist Stresses Part 2 (1 of 2)



	SGBF 39	SGBF 40	SGBF 41	SGBF 42	SGBF 43	SGBF 44	SGBF 45	SGBF 46	SGBF 47	SGDP 13	SGDP 14	SGDP 15	SGDP 16	SGDP 17	SGDP 30	SGDP 31	SGDP 32	SGDP 33	SGDP 34	SGDP 48	SGDP 49	SGDP 50	SGDP 51	SGD W18	SGD W19	SGD W20
Min Stress	-28	-14	-40	-23	-75	-94	-530	-443	-14	-60	-34	-84	-36	-12	-23	-49	-39	-23	-24	-508	-538	-845	-255	-30	-78	-21
Max Stress	600	7627	4725	6661	3960	1096	587	680	548	94	49	51	110	114	60	123	147	94	93	219	189	137	515	153	36	189

Figure H10. Twist Stresses Part 2 (2 of 2)

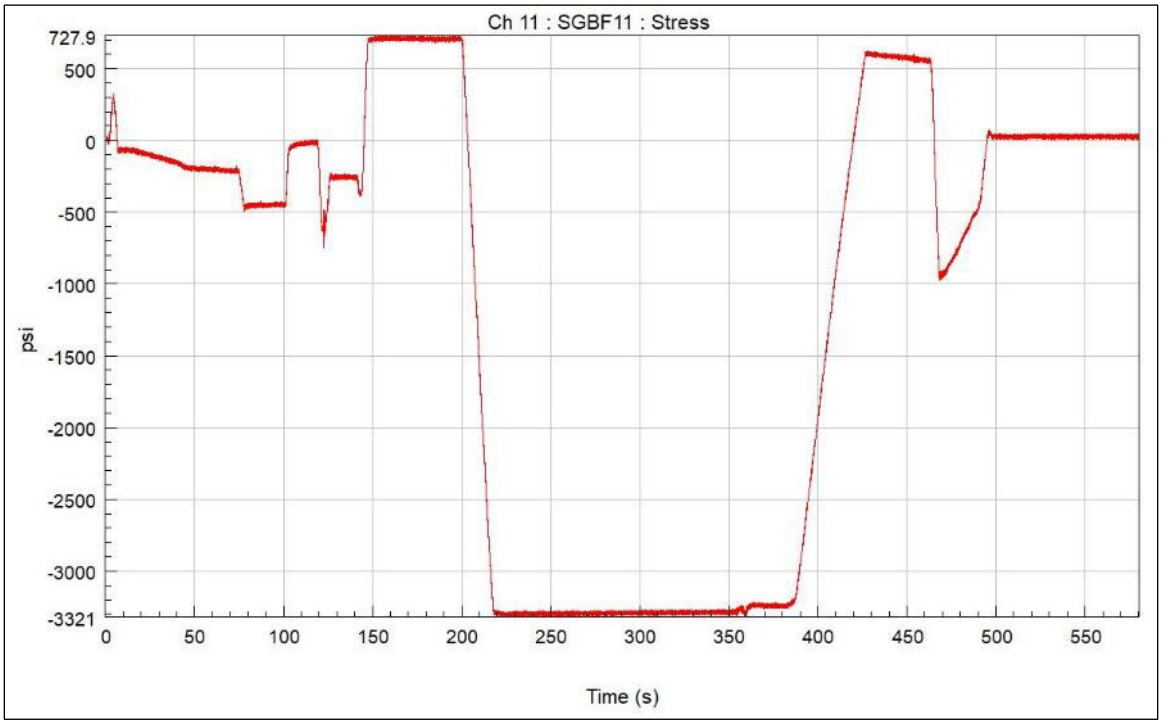


Figure H11. Twist Stresses Part 2 SGBF11

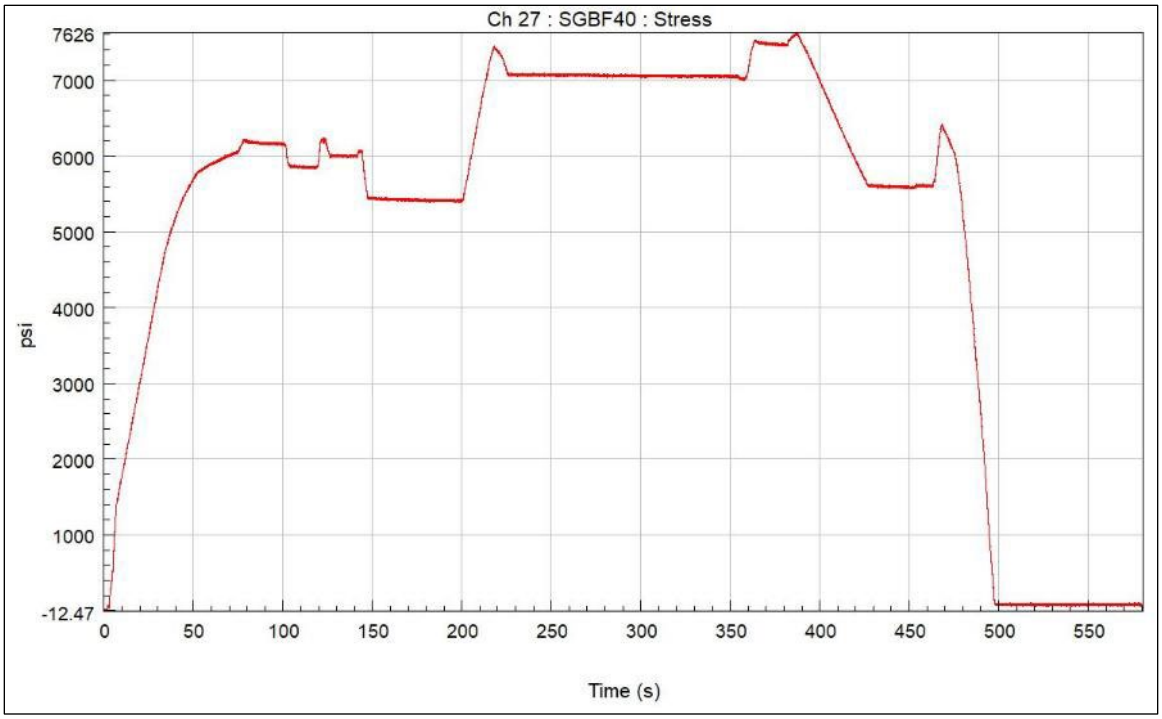


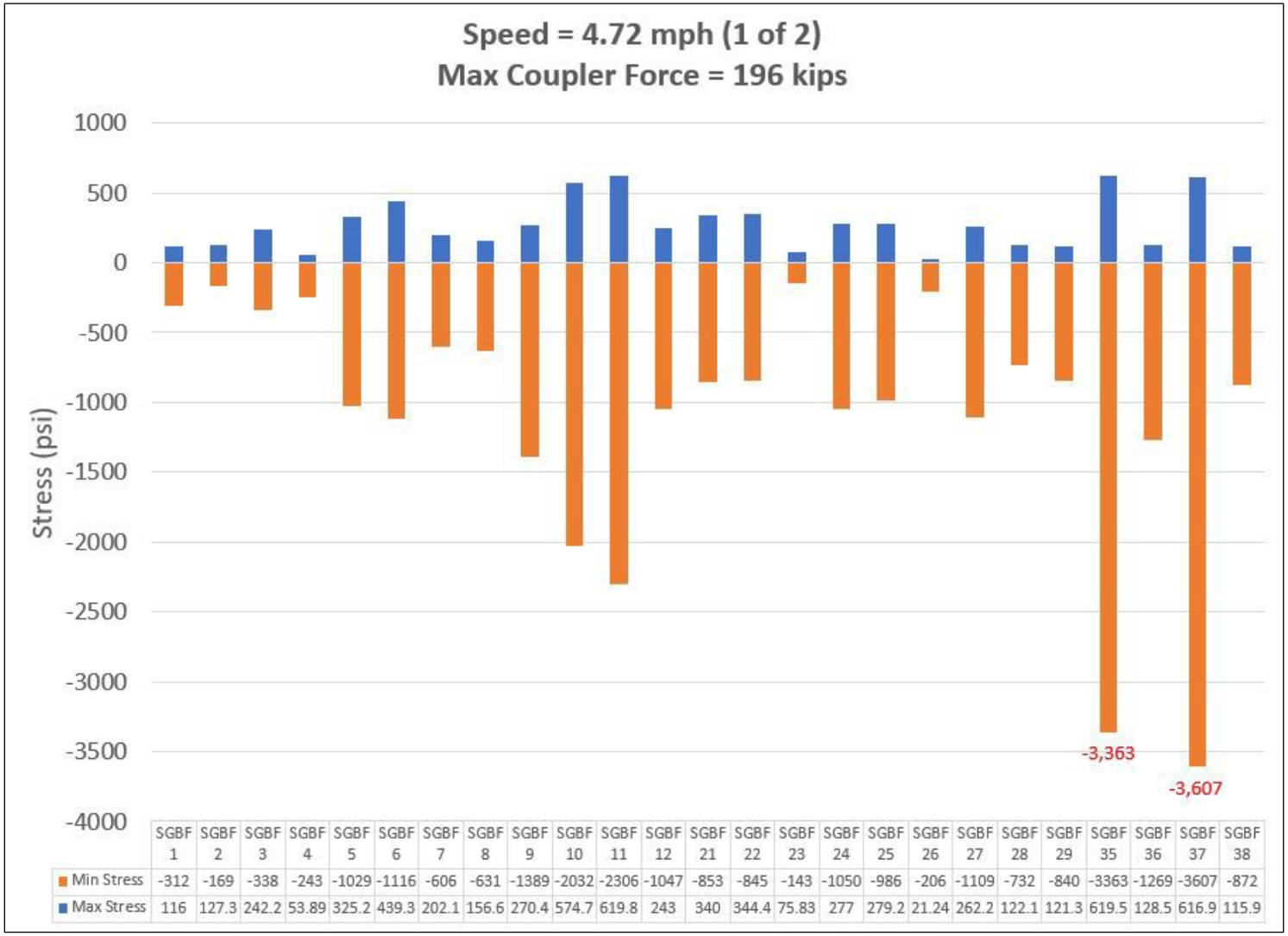
Figure H12. Twist Stresses Part 2 SGBF40

APPENDIX I: IMPACT TESTS

Additional results for individual strain gauges during the impact test are presented in Figures I1 through I16.

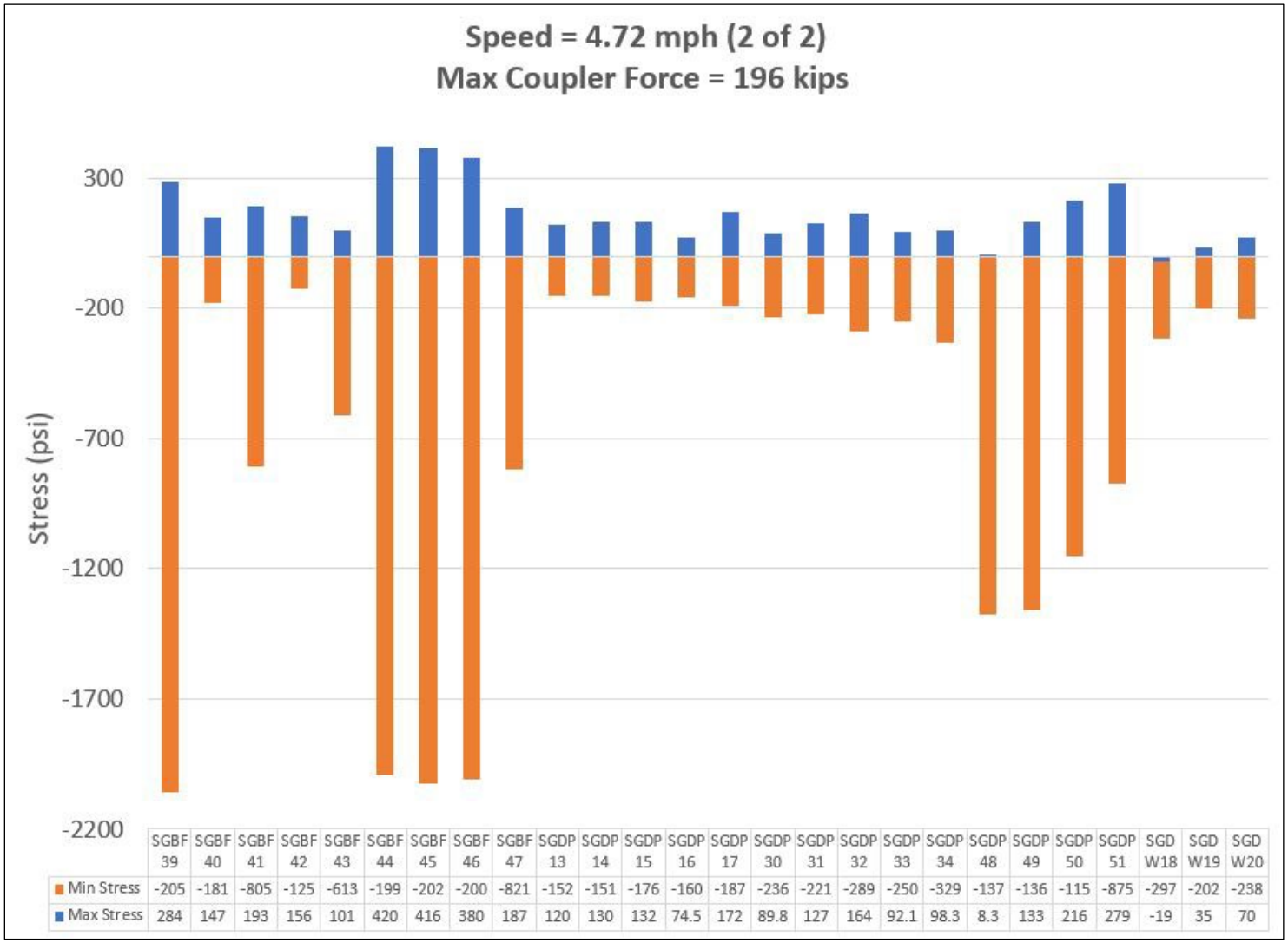
List of Figures

Figure I1. Stresses at 4 mph Nominal Test Speed. (1 of 2) I-2
Figure I2. Stresses at 4 mph Nominal Test Speed. (2 of 2) I-3
Figure I3. Dynamic Stresses, SGBF35, 4mph Nominal Speed I-4
Figure I4. Dynamic Stresses. SGBF37, 4 mph Nominal Speed I-4
Figure I5. Stresses at 6 mph Nominal Test Speed. (1 of 2) I-5
Figure I6. Stresses at 6 mph Nominal Test Speed. (2 of 2) I-6
Figure I7. Dynamic Stresses, SGBF35, 6 mph Nominal Speed I-7
Figure I8. Dynamic Stresses. SGBF37, 6 mph Nominal Speed I-7
Figure I9. Stresses at 8 mph Nominal Test Speed. (1 of 2) I-8
Figure I10. Stresses at 8 mph Nominal Test Speed. (2 of 2) I-9
Figure I11. Dynamic Stresses. SGBF35, 8 mph Nominal Speed I-10
Figure I12. Dynamic Stresses. SGBF37, 8 mph Nominal Speed I-10
Figure I13. Stresses at 9 mph Nominal Test Speed (1 of 2) I-11
Figure I14. Stresses at 9 mph Nominal Test Speed. (2 of 2) I-12
Figure I15. Dynamic Stresses, SGBF35, 9 mph Nominal Speed I-13
Figure I16. Dynamic Stresses, SGBF37, 9 mph Nominal Speed I-13



	SGBF 1	SGBF 2	SGBF 3	SGBF 4	SGBF 5	SGBF 6	SGBF 7	SGBF 8	SGBF 9	SGBF 10	SGBF 11	SGBF 12	SGBF 21	SGBF 22	SGBF 23	SGBF 24	SGBF 25	SGBF 26	SGBF 27	SGBF 28	SGBF 29	SGBF 35	SGBF 36	SGBF 37	SGBF 38
Min Stress	-312	-169	-338	-243	-1029	-1116	-606	-631	-1389	-2032	-2306	-1047	-853	-845	-143	-1050	-986	-206	-1109	-732	-840	-3363	-1269	-3607	-872
Max Stress	116	127.3	242.2	53.89	325.2	439.3	202.1	156.6	270.4	574.7	619.8	243	340	344.4	75.83	277	279.2	21.24	262.2	122.1	121.3	619.5	128.5	616.9	115.9

Figure I1. Stresses at 4 mph Nominal Test Speed. (1 of 2)



	SGBF 39	SGBF 40	SGBF 41	SGBF 42	SGBF 43	SGBF 44	SGBF 45	SGBF 46	SGBF 47	SGDP 13	SGDP 14	SGDP 15	SGDP 16	SGDP 17	SGDP 30	SGDP 31	SGDP 32	SGDP 33	SGDP 34	SGDP 48	SGDP 49	SGDP 50	SGDP 51	SGD W18	SGD W19	SGD W20
Min Stress	-205	-181	-805	-125	-613	-199	-202	-200	-821	-152	-151	-176	-160	-187	-236	-221	-289	-250	-329	-137	-136	-115	-875	-297	-202	-238
Max Stress	284	147	193	156	101	420	416	380	187	120	130	132	74.5	172	89.8	127	164	92.1	98.3	8.3	133	216	279	-19	35	70

Figure I2. Stresses at 4 mph Nominal Test Speed. (2 of 2)

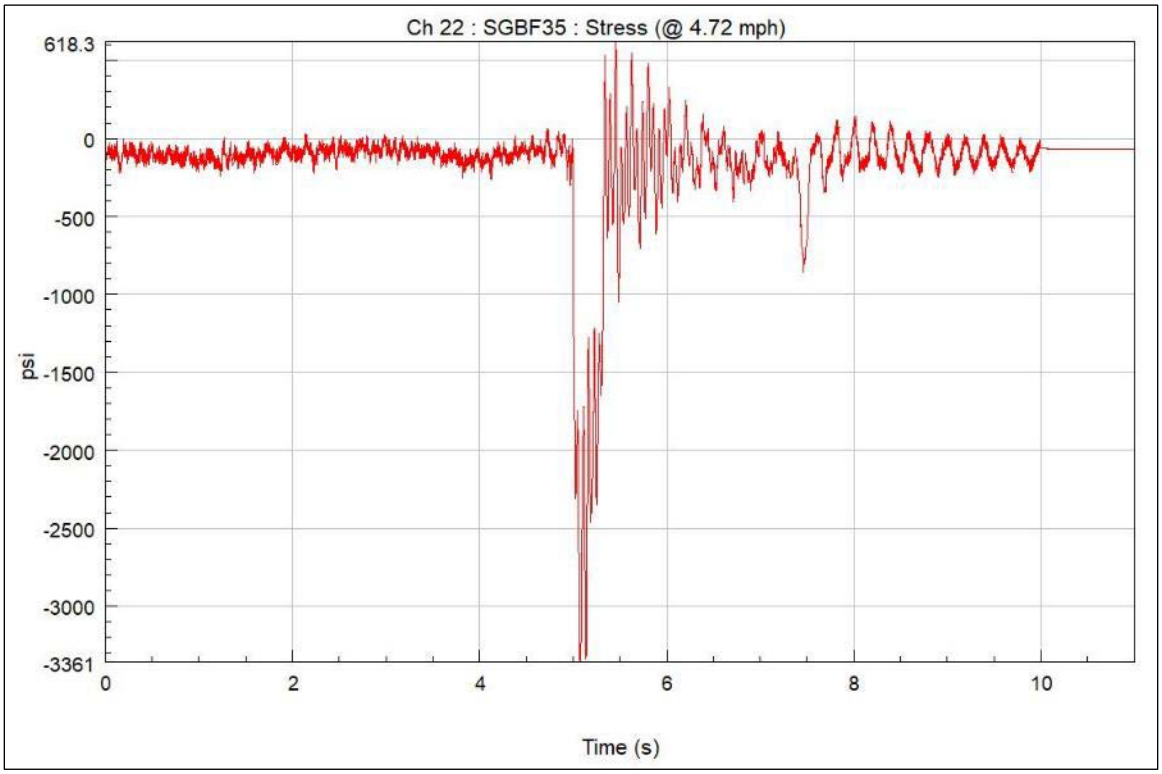


Figure I3. Dynamic Stresses, SGBF35, 4mph Nominal Speed

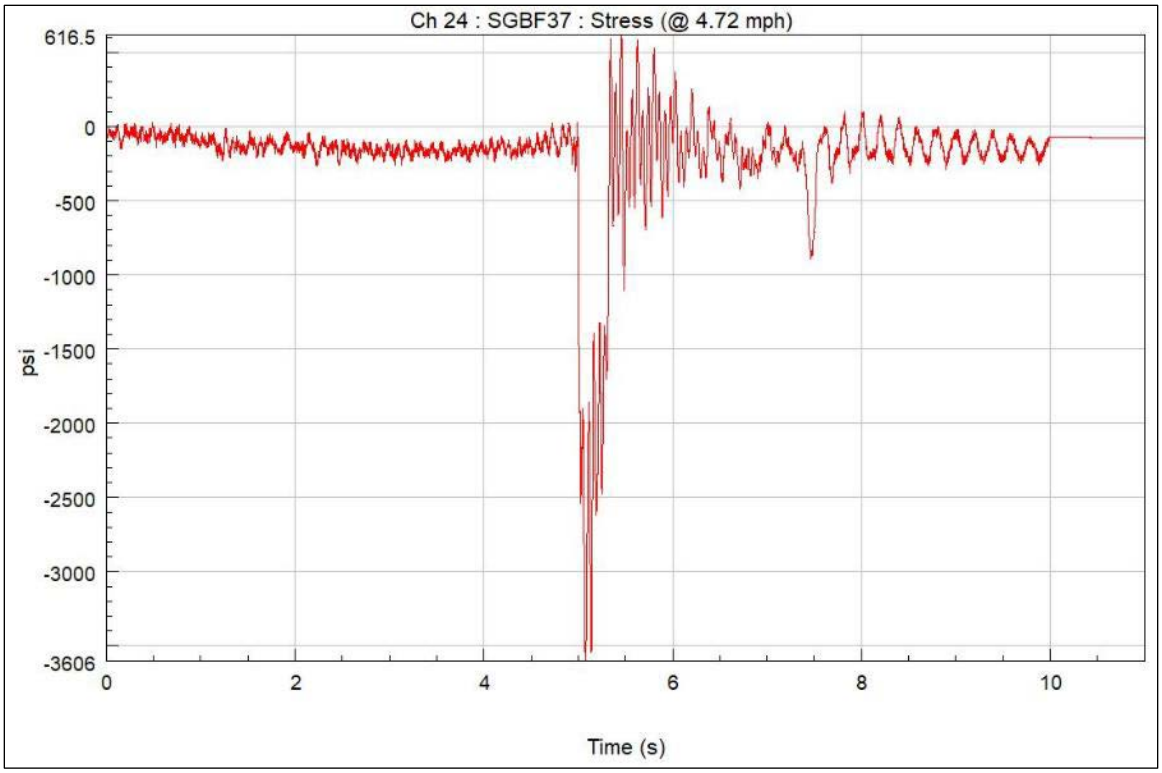
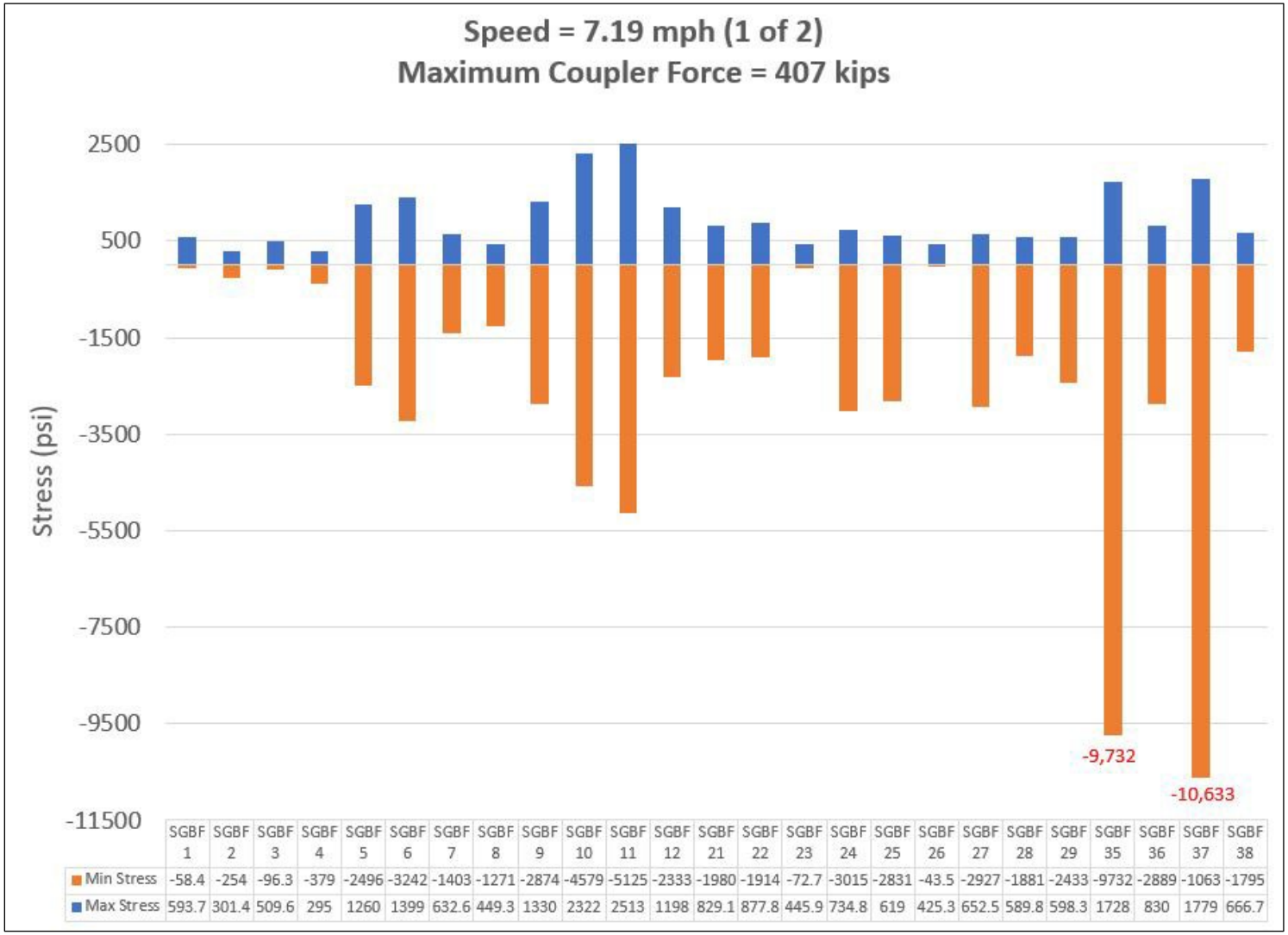
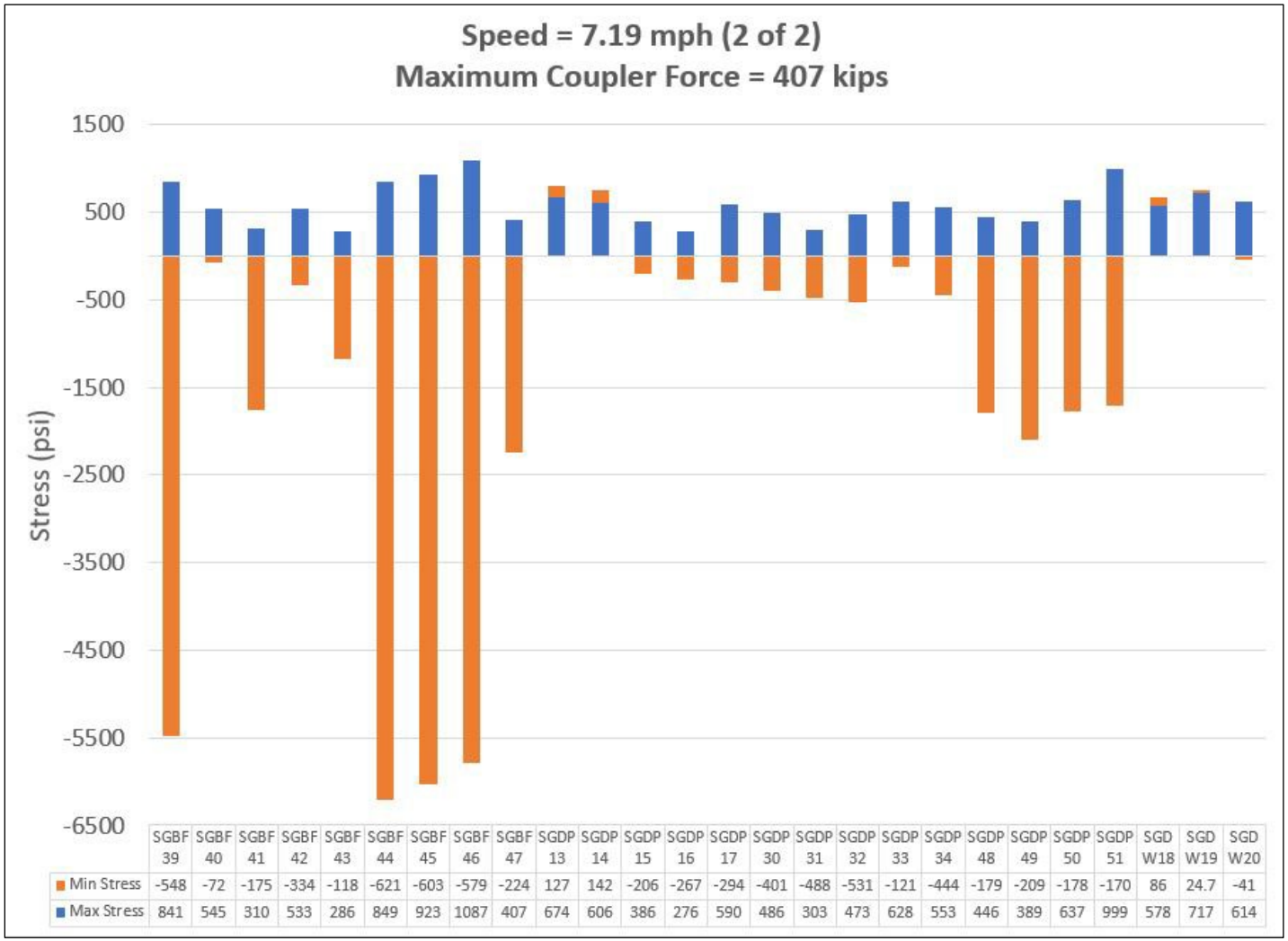


Figure I4. Dynamic Stresses. SGBF37, 4 mph Nominal Speed



	SGBF 1	SGBF 2	SGBF 3	SGBF 4	SGBF 5	SGBF 6	SGBF 7	SGBF 8	SGBF 9	SGBF 10	SGBF 11	SGBF 12	SGBF 21	SGBF 22	SGBF 23	SGBF 24	SGBF 25	SGBF 26	SGBF 27	SGBF 28	SGBF 29	SGBF 35	SGBF 36	SGBF 37	SGBF 38
Min Stress	-58.4	-254	-96.3	-379	-2496	-3242	-1403	-1271	-2874	-4579	-5125	-2333	-1980	-1914	-72.7	-3015	-2831	-43.5	-2927	-1881	-2433	-9732	-2889	-1063	-1795
Max Stress	593.7	301.4	509.6	295	1260	1399	632.6	449.3	1330	2322	2513	1198	829.1	877.8	445.9	734.8	619	425.3	652.5	589.8	598.3	1728	830	1779	666.7

Figure I5. Stresses at 6 mph Nominal Test Speed. (1 of 2)



	SGBF 39	SGBF 40	SGBF 41	SGBF 42	SGBF 43	SGBF 44	SGBF 45	SGBF 46	SGBF 47	SGDP 13	SGDP 14	SGDP 15	SGDP 16	SGDP 17	SGDP 30	SGDP 31	SGDP 32	SGDP 33	SGDP 34	SGDP 48	SGDP 49	SGDP 50	SGDP 51	SGD W18	SGD W19	SGD W20
Min Stress	-548	-72	-175	-334	-118	-621	-603	-579	-224	127	142	-206	-267	-294	-401	-488	-531	-121	-444	-179	-209	-178	-170	86	24.7	-41
Max Stress	841	545	310	533	286	849	923	1087	407	674	606	386	276	590	486	303	473	628	553	446	389	637	999	578	717	614

Figure I6. Stresses at 6 mph Nominal Test Speed. (2 of 2)

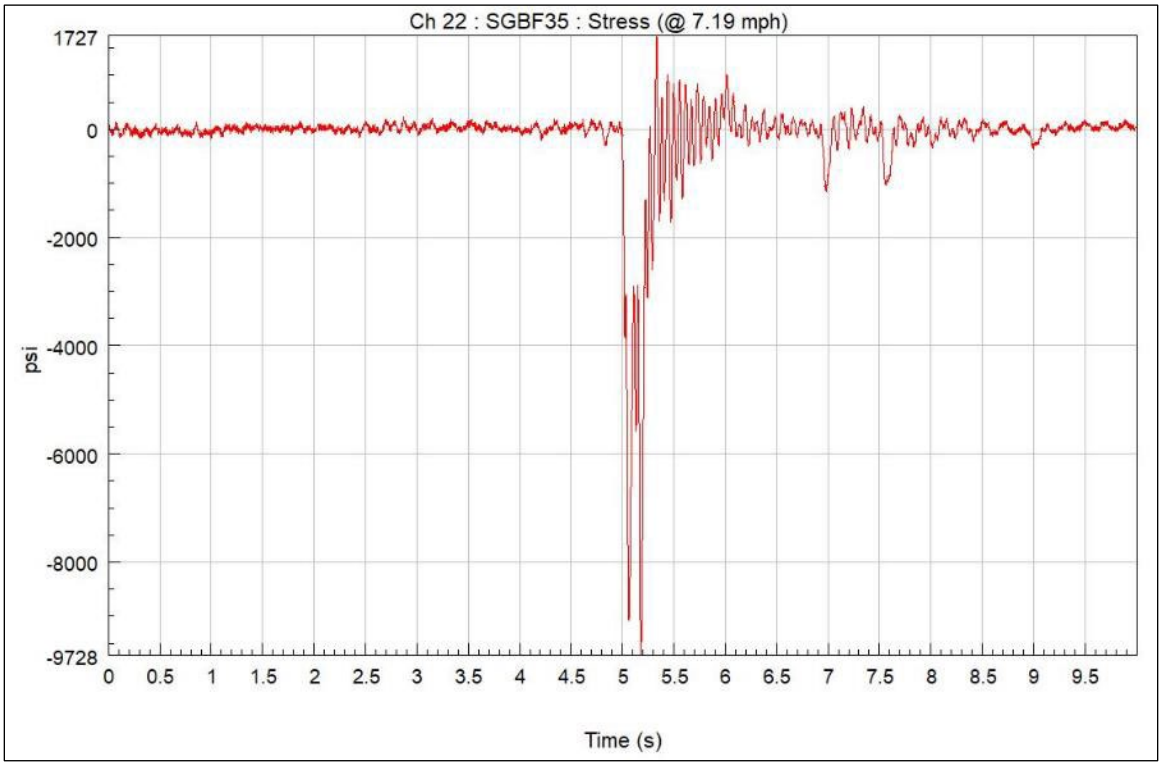


Figure I7. Dynamic Stresses, SGBF35, 6 mph Nominal Speed

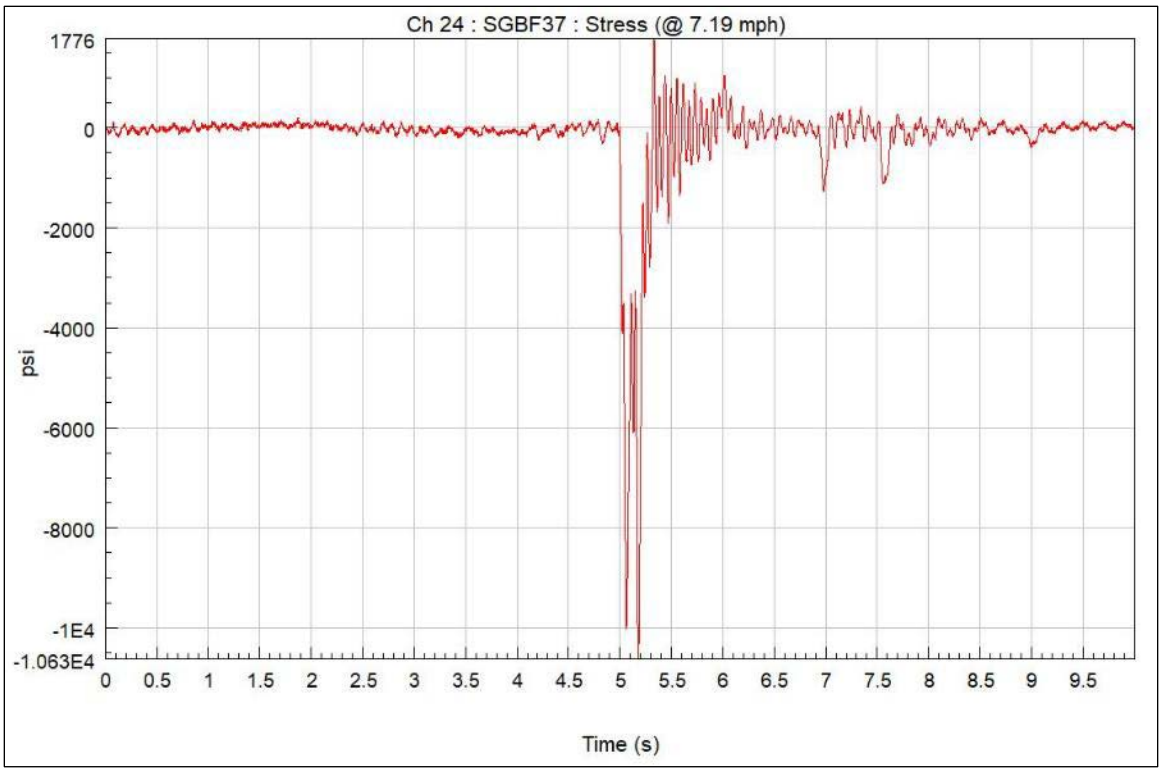
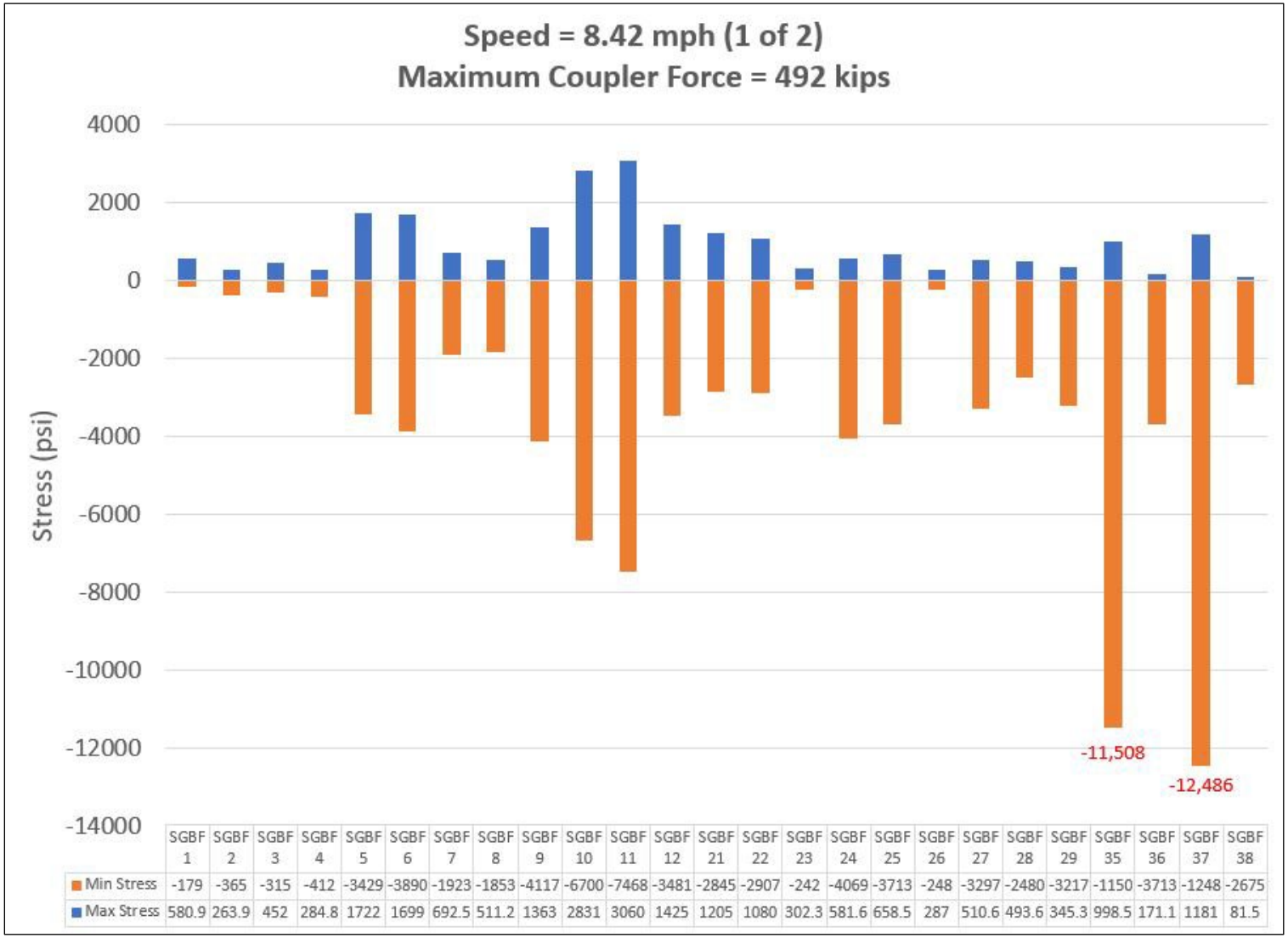
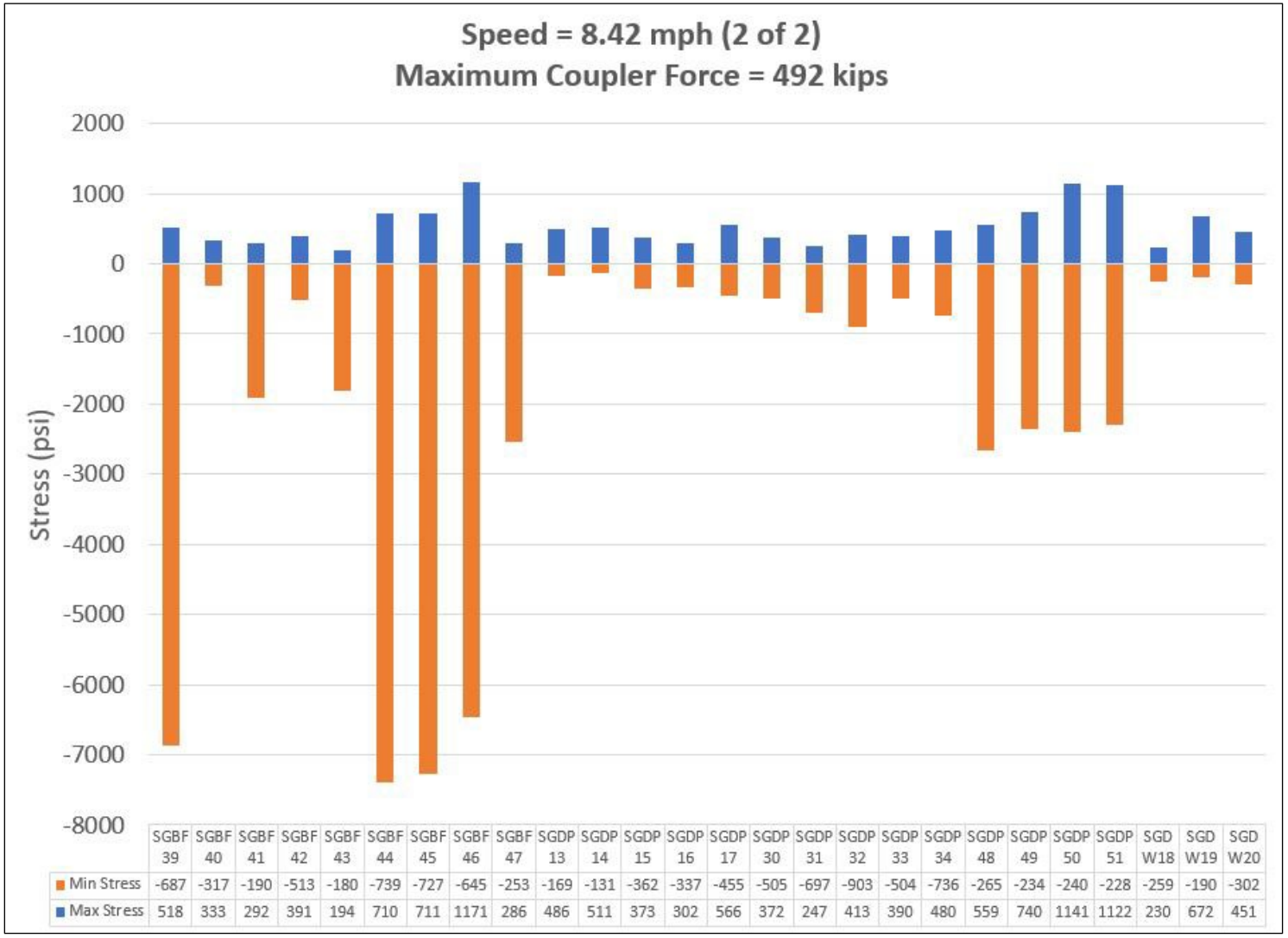


Figure I8. Dynamic Stresses. SGBF37, 6 mph Nominal Speed



	SGBF 1	SGBF 2	SGBF 3	SGBF 4	SGBF 5	SGBF 6	SGBF 7	SGBF 8	SGBF 9	SGBF 10	SGBF 11	SGBF 12	SGBF 21	SGBF 22	SGBF 23	SGBF 24	SGBF 25	SGBF 26	SGBF 27	SGBF 28	SGBF 29	SGBF 35	SGBF 36	SGBF 37	SGBF 38
Min Stress	-179	-365	-315	-412	-3429	-3890	-1923	-1853	-4117	-6700	-7468	-3481	-2845	-2907	-242	-4069	-3713	-248	-3297	-2480	-3217	-1150	-3713	-1248	-2675
Max Stress	580.9	263.9	452	284.8	1722	1699	692.5	511.2	1363	2831	3060	1425	1205	1080	302.3	581.6	658.5	287	510.6	493.6	345.3	998.5	171.1	1181	81.5

Figure I9. Stresses at 8 mph Nominal Test Speed. (1 of 2)



	SGBF 39	SGBF 40	SGBF 41	SGBF 42	SGBF 43	SGBF 44	SGBF 45	SGBF 46	SGBF 47	SGDP 13	SGDP 14	SGDP 15	SGDP 16	SGDP 17	SGDP 30	SGDP 31	SGDP 32	SGDP 33	SGDP 34	SGDP 48	SGDP 49	SGDP 50	SGDP 51	SGD W18	SGD W19	SGD W20
Min Stress	-687	-317	-190	-513	-180	-739	-727	-645	-253	-169	-131	-362	-337	-455	-505	-697	-903	-504	-736	-265	-234	-240	-228	-259	-190	-302
Max Stress	518	333	292	391	194	710	711	1171	286	486	511	373	302	566	372	247	413	390	480	559	740	1141	1122	230	672	451

Figure I10. Stresses at 8 mph Nominal Test Speed. (2 of 2)

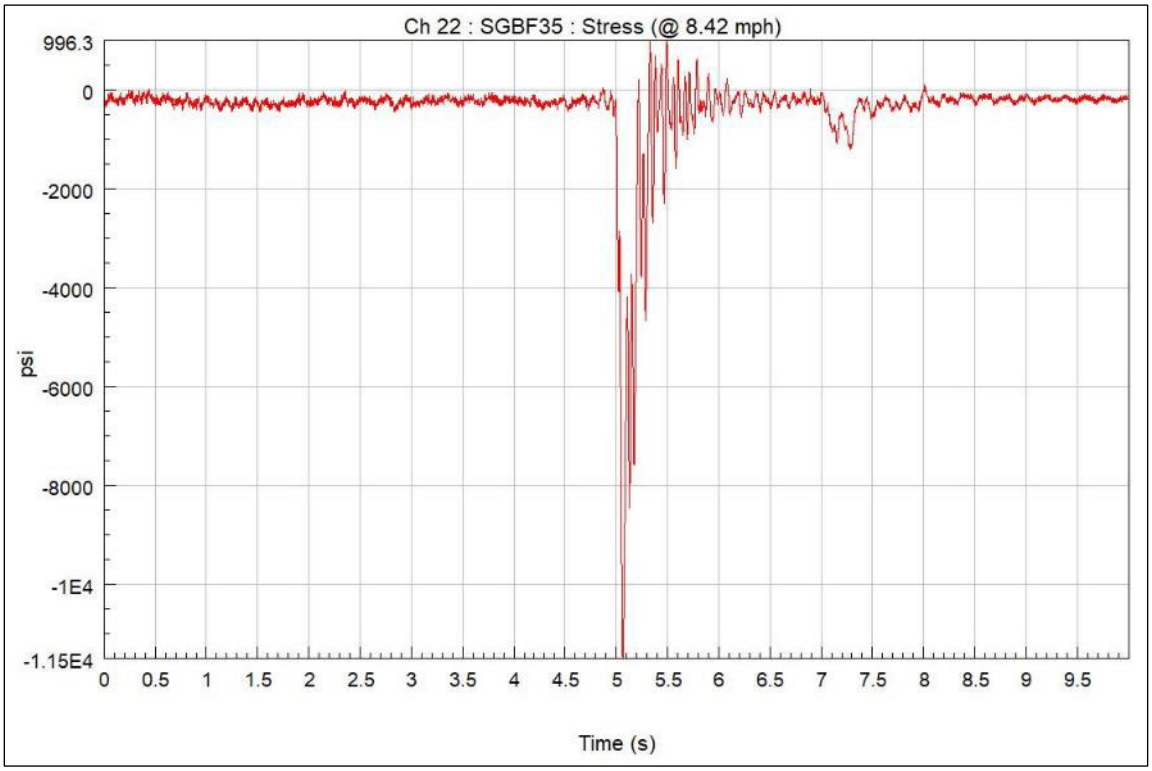


Figure I11. Dynamic Stresses. SGBF35, 8 mph Nominal Speed

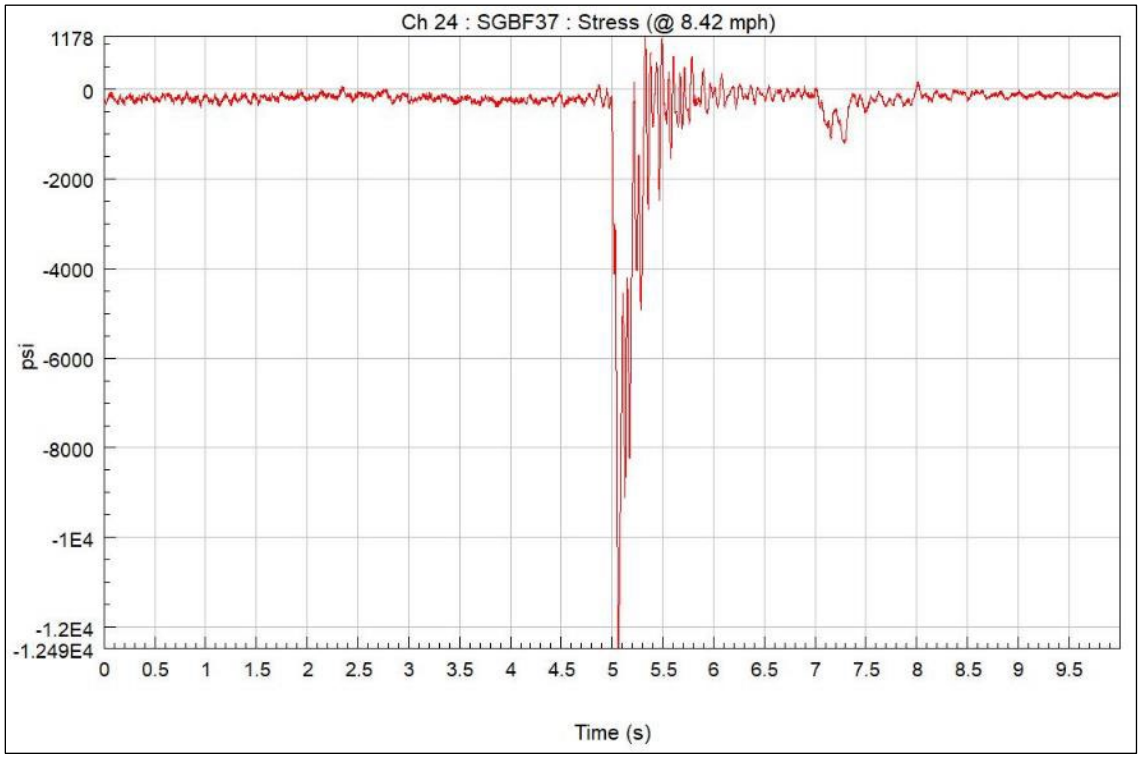
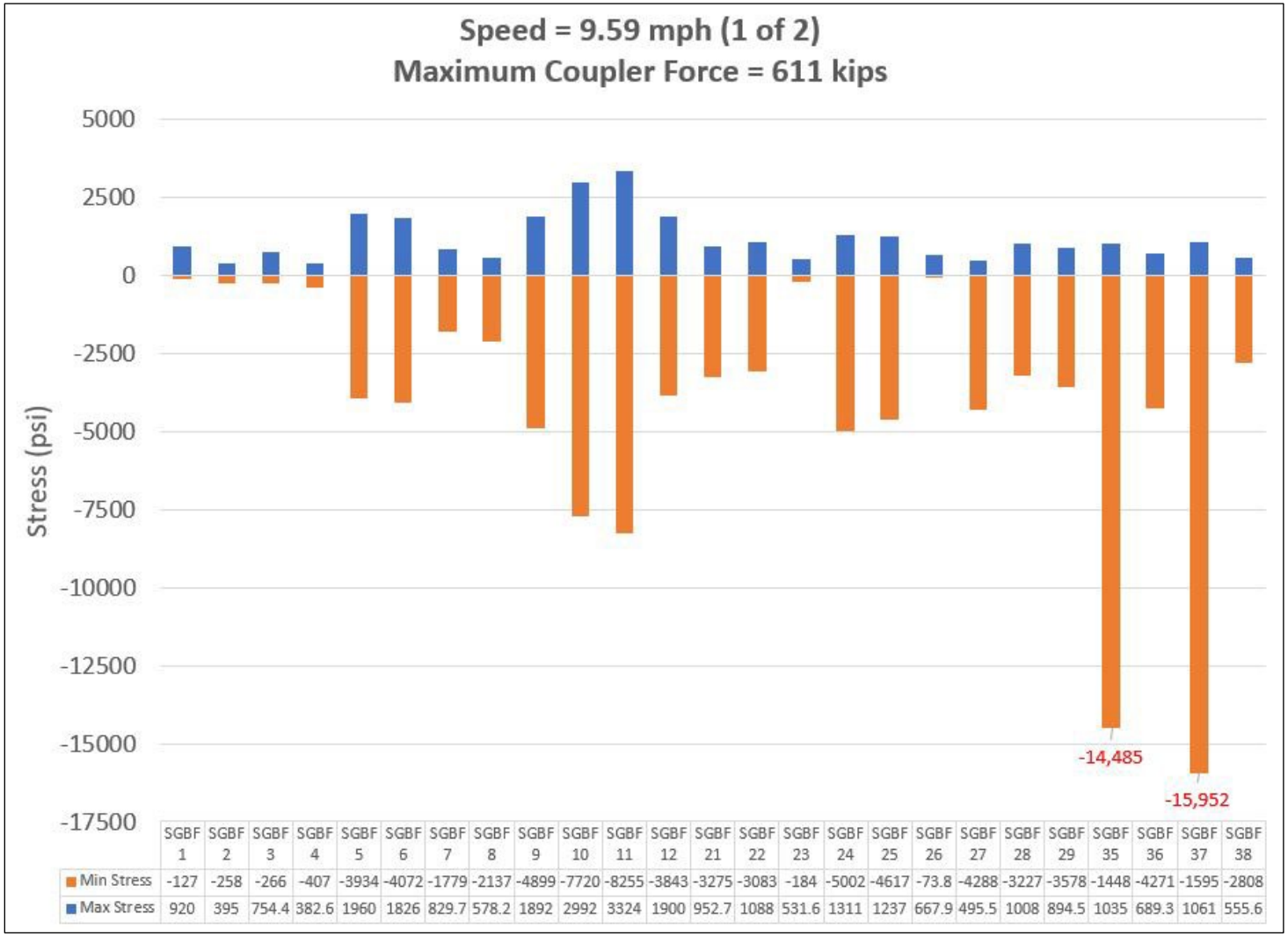
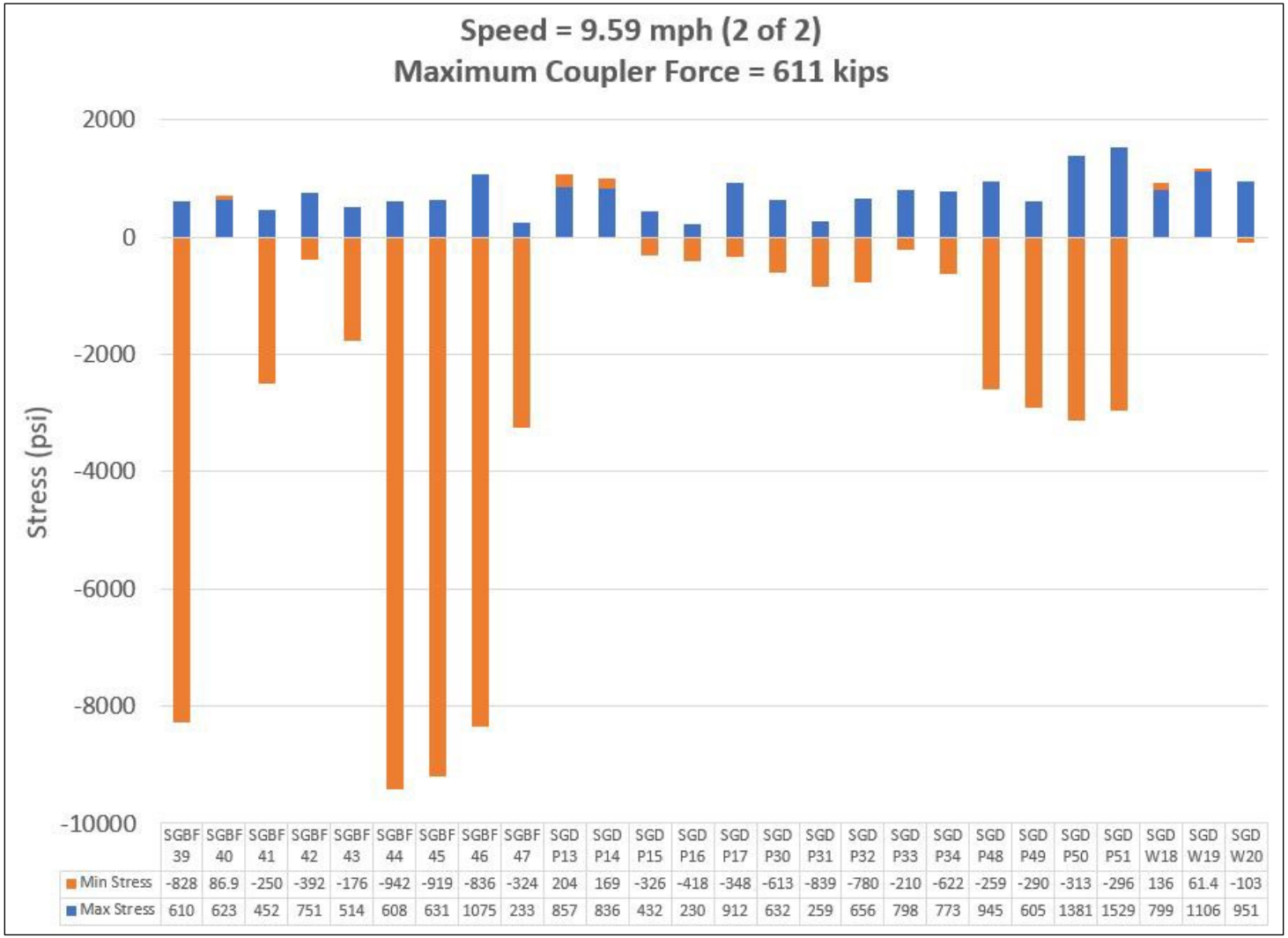


Figure I12. Dynamic Stresses. SGBF37, 8 mph Nominal Speed



	SGBF 1	SGBF 2	SGBF 3	SGBF 4	SGBF 5	SGBF 6	SGBF 7	SGBF 8	SGBF 9	SGBF 10	SGBF 11	SGBF 12	SGBF 21	SGBF 22	SGBF 23	SGBF 24	SGBF 25	SGBF 26	SGBF 27	SGBF 28	SGBF 29	SGBF 35	SGBF 36	SGBF 37	SGBF 38
Min Stress	-127	-258	-266	-407	-3934	-4072	-1779	-2137	-4899	-7720	-8255	-3843	-3275	-3083	-184	-5002	-4617	-73.8	-4288	-3227	-3578	-1448	-4271	-1595	-2808
Max Stress	920	395	754.4	382.6	1960	1826	829.7	578.2	1892	2992	3324	1900	952.7	1088	531.6	1311	1237	667.9	495.5	1008	894.5	1035	689.3	1061	555.6

Figure I13. Stresses at 9 mph Nominal Test Speed (1 of 2)



	SGBF 39	SGBF 40	SGBF 41	SGBF 42	SGBF 43	SGBF 44	SGBF 45	SGBF 46	SGBF 47	SGD P13	SGD P14	SGD P15	SGD P16	SGD P17	SGD P30	SGD P31	SGD P32	SGD P33	SGD P34	SGD P48	SGD P49	SGD P50	SGD P51	SGD W18	SGD W19	SGD W20
Min Stress	-828	86.9	-250	-392	-176	-942	-919	-836	-324	204	169	-326	-418	-348	-613	-839	-780	-210	-622	-259	-290	-313	-296	136	61.4	-103
Max Stress	610	623	452	751	514	608	631	1075	233	857	836	432	230	912	632	259	656	798	773	945	605	1381	1529	799	1106	951

Figure I14. Stresses at 9 mph Nominal Test Speed. (2 of 2)

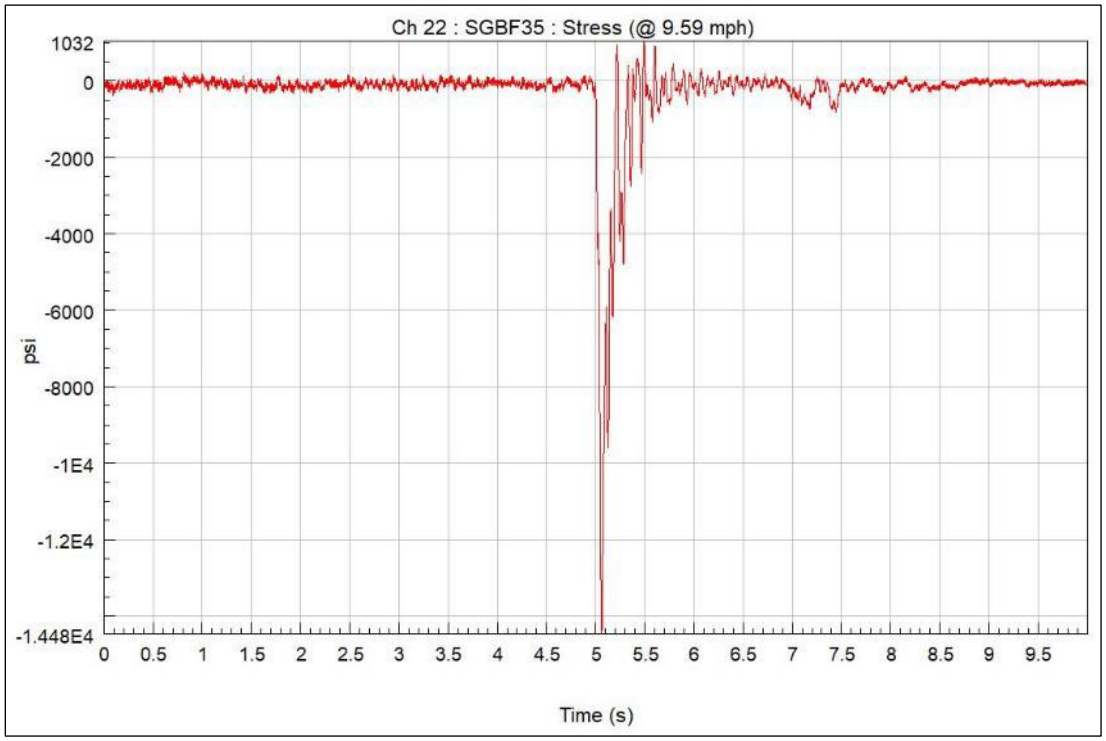


Figure I15. Dynamic Stresses, SGBF35, 9 mph Nominal Speed

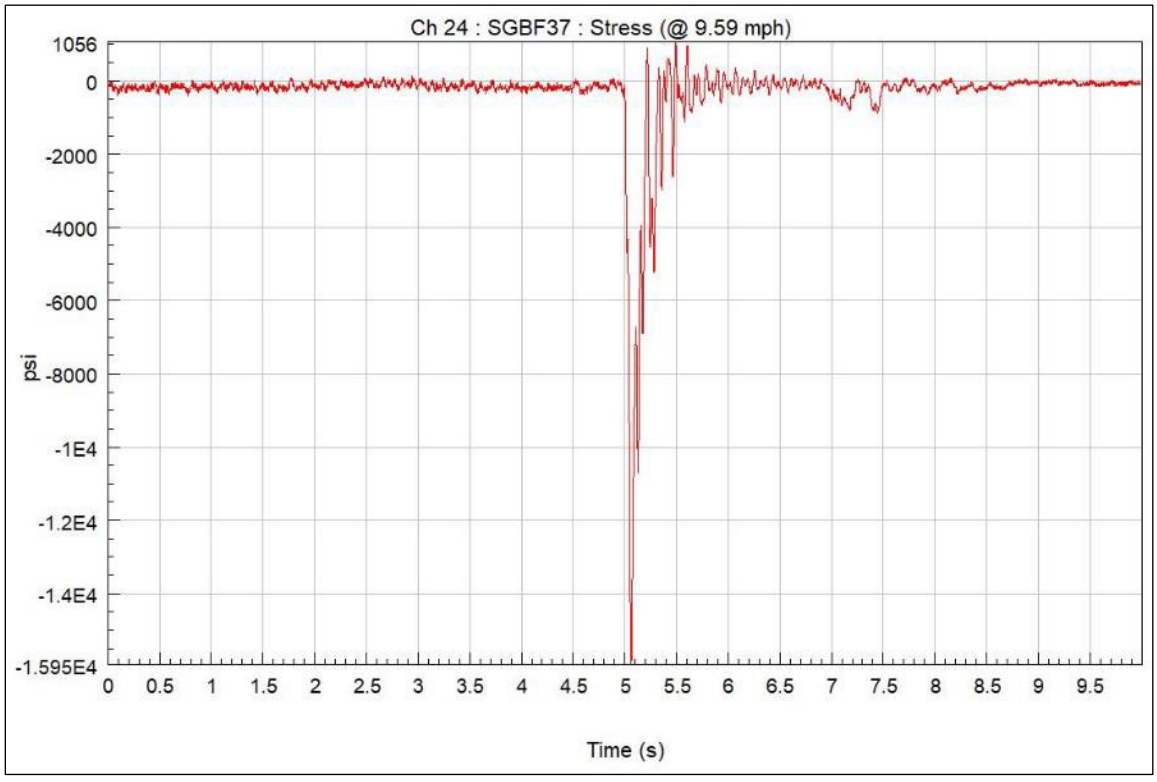
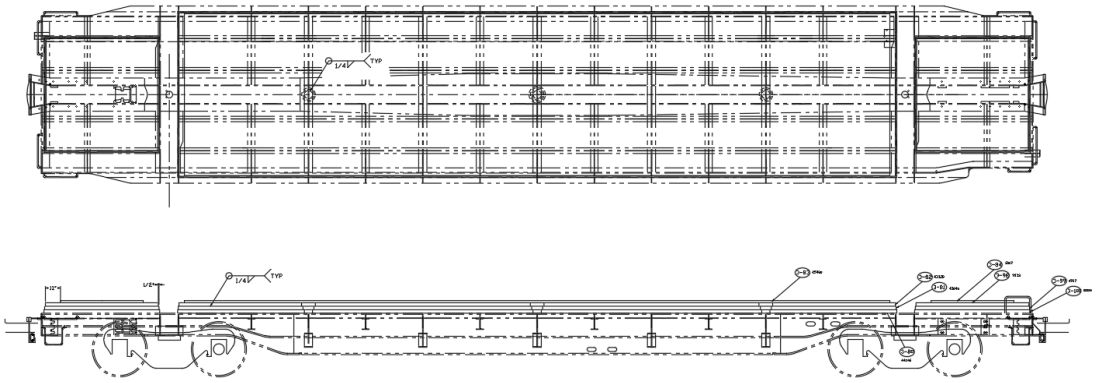


Figure I16. Dynamic Stresses, SGBF37, 9 mph Nominal Speed

APPENDIX J: KASGRO SECUREMENT ANALYSIS

Atlas Buffer Car OTLR

May 26, 2021
Prepared by:
Kasgro Engineering



The loads will be secured on all sides with a single sided 1/4-inch fillet weld. Each load that is attached to the car will be analyzed individually. The car light weight is estimated at 73 k.

- Estimated center load weight: 157,000 lbs.
- Weld size = 0.25 in.
- Effective throat angle = 0.707
- Allowable design stress per AWS D15.1 Table C4 Class 1. = 29 ksi
- (0.25 in) (0.707) (29,000 psi) = 5125.75 lbs./in
- Longitudinal Requirement = (157,000 lbs. (6) / 5125.75 lbs./in) = 183.78 in of weld
- Lateral Requirement = (157,000 lbs. (4) / 5125.75 lbs./in) = 122.52 in of weld
- Vertical Requirement = (73,000 lbs. / 5125.75 lbs./in) = 14.24 in of weld
- Existing securement weld total length = 1,284 in
- Estimated outboard load weight (one per end): 16,500 lbs./weight
- Weld size = 0.25 in.
- Effective Throat Angle = 0.707
- Allowable design stress per AWS D15.1 Table C4 Class 1. = 29 ksi
- (0.25 in) (0.707) (29,000 psi) = 5125.75 lbs./in
- Longitudinal Requirement = (16,500 lbs. (6) / 5125.75 lbs./in) = 19.31 in of weld
- Lateral Requirement = (16,500 lbs. (4) / 5125.75 lbs./in) = 12.88 in of weld
- Vertical Requirement = (73,000 lbs. / 5125.75 lbs./in) = 14.24 in of weld
- Existing securement weld total length = 336 in

Overall, these numbers are conservative considering that all four sides of each load are welded. Each welded connection is reacting to all three directions of force (lateral, longitudinal and vertical.)

APPENDIX G
P-21-013 BUFFER CAR POST TEST ANALYSIS REPORT

BUFFER CAR
POST TEST ANALYSIS REPORT

Prepared for
United States Department of Energy

Report P-21-013

Revised June 23, 2021

TTCI®
TRANSPORTATION
TECHNOLOGY CENTER, INC.

BUFFER CAR
POST TEST ANALYSIS REPORT

Prepared for
United States Department of Energy

Report P-21-013

Russell Walker
Matt DeGeorge
MaryClara Jones
Richard Joy
Nicholas Hinsch (Kasgro Rail)

Transportation Technology Center, Inc.
A subsidiary of the Association of American Railroads
Pueblo, Colorado USA

April 5, 2021
Revised June 23, 2021

Disclaimer: This report was prepared for The United States Department of Energy (DOE) by Transportation Technology Center, Inc. (TTCI), a subsidiary of the Association of American Railroads, Pueblo, Colorado. It is based on investigations and tests conducted by TTCI with the direct participation of DOE to criteria approved by them. The contents of this report imply no endorsements whatsoever by TTCI of products, services or procedures, nor are they intended to suggest the applicability of the test results under circumstances other than those described in this report. The results and findings contained in this report are the sole property of DOE. They may not be released by anyone to any party other than DOE without the written permission of DOE. TTCI is not a source of information with respect to these tests, nor is it a source of copies of this report. TTCI makes no representations or warranties, either expressed or implied, with respect to this report or its contents. TTCI assumes no liability to anyone for special, collateral, exemplary, indirect, incidental, consequential, or any other kind of damages resulting from the use or application of this report or its contents.

EXECUTIVE SUMMARY

The United States Department of Energy (DOE) contracted with Transportation Technology Center, Inc. (TTCI) to perform certification testing on its buffer railcar developed as part of DOE's Atlas Railcar Design Project. The intent of the project is to meet the needs for future large-scale transport of high-level radioactive material (HLRM) as defined in Association of American Railroads' (AAR) *Manual of Standards and Recommended Practices*, Standard S-2043, which includes spent nuclear fuel and high-level waste.

The buffer car met all S-2043 single-car structural and dynamic test requirements.

Finite element analysis (FEA) simulations and structural test strain measurements showed that stresses were less than 75 percent of the allowable stress, eliminating the requirement for FEA to be refined per Paragraph 8.1 of Standard S-2043. The largest difference between measured and predicted stress was 5.7 ksi.

The revised model did not meet the criterion for peak-to-peak carbody lateral acceleration for the 39-foot wavelength inputs (1.38g, limit = 1.3g) or the 44.5-foot wavelength inputs (1.31g, limit = 1.3g) in yaw and sway simulations. In contrast, the buffer car met test requirements for yaw and sway indicating that the model is conservative. The yaw and sway test is only performed with 39-foot wavelength inputs.

The revised modeling predictions did not meet S-2043 criteria for truck side lateral/vertical (L/V) ratio (0.52, limit = 0.5) in the curving with various lubrication conditions regime. This exception occurred for counterclockwise runs with Case 2 lubrication and the worn wheel profile at 12 and 24 mph. The Case 2 lubrication condition is a 0.5 coefficient of friction on the top of both rails and a 0.2 coefficient of friction on the gage face of the high rail. Simulations meet S-2043 criteria for curving with various lubrication conditions during clockwise runs for this lubrication and profile case and for all runs with other lubrication and profile combinations.

Because there were only small changes to the design of the buffer car since original dynamic predictions were performed, only a small subset of the regimes were run with the revised dynamic model. These regimes were chosen because they allowed for comparison with test data, or because the original dynamic predictions for the regime were close to or did not meet the criteria.

The following table shows a summary of test results and model predictions for the buffer car.

S-2043 Section	Met/Not Met		
	Preliminary Simulations	Revised Simulations	Test Result
5.2 Nonstructural Static Tests			
4.2.1/5.2.1 Truck Twist Equalization	Met	Not Simulated	Met
4.2.2/5.2.2 Carbody Twist Equalization	Met	Not Simulated	Met
4.2.3/5.2.3 Static Curve Stability	Met	Not Simulated	Met
4.2.4/5.2.4 Horizontal Curve Negotiation	Met	Not Simulated	Met
5.4 Structural Tests			
5.4.2 Squeeze (Compressive End) Load	Met	Not Required	Met
5.4.3 Coupler Vertical Loads	Met	Not Required	Met
5.4.4 Jacking	Met	Not Required	Met
5.4.5 Twist	Met	Not Required	Met
5.4.6 Impact	Met	Not Required	Met
5.5 Dynamic Tests			
4.3.11.3/5.5.7 Hunting	Met	Met	Met
4.3.9.6/5.5.8 Twist and Roll	Met	Met	Met
5.5.9 Yaw and Sway	Met	Not Met P-P Lat Accel 1.38 Limit=1.3	Met
5.5.10 Dynamic Curving	Met	Met	Met
4.3.9.7/5.5.11 Pitch and Bounce (Chapter 11)	Met	Met	Met
4.3.9.7/5.5.12 Pitch and Bounce (Special)	Met	Met	Met
4.3.10.1/5.5.13 Single Bump Test	Met	Not Simulated	Met
4.3.11.6/5.5.14 Curve Entry/Exit	Met	Not Simulated	Met
4.3.10.25.5.15 Curving with Single Rail Perturbation	Met	Met	Met
4.3.11.4/5.5.16 Standard Chapter 11 Constant Curving	Met	Not Simulated	Met
4.3.11.7/5.5.17 Special Trackwork	Met	Not Simulated	Met
4.3.11.5 Curving with Various Lubrication Conditions	Met	Not Met Truck Side L/V 0.52, Limit=0.50	Not Required
4.3.12 Ride Quality	Met	Not Simulated	Not Required
4.3.13 Buff and Draft Curving	Not Met Truck Side L/V 0.51, Limit=0.50	Met	Not Required
4.3.14 Braking Effects on Steering	Met	Not Simulated	Not Required
4.3.15 Worn Component Simulations	Met	Not Simulated	Not Required

Table of Contents

1.0 Introduction 1
2.0 Buffer Railcar Description 1
3.0 Objective 3
4.0 Refining the Finite Element Analysis (FEA) 4
4.1 Squeeze (Compressive End) Load 4
4.2 Coupler Vertical Loads 5
4.3 Jacking 6
4.4 Twist 7
4.4.1 Suspension Twist 7
4.4.2 Carbody Twist 8
4.5 Impact Test 9
5.0 New Finite Element Analysis Predictions 10
6.0 Refining the Dynamic Model 10
7.0 New Dynamic Predictions 14
7.1 Twist and Roll 15
7.2 Pitch and Bounce 17
7.3 Special Pitch and Bounce (44.5-foot wavelength) 18
7.4 Yaw and Sway 20
7.5 Dynamic Curving 22
7.6 Curving with a Single-rail Perturbation 24
7.7 Hunting 26
7.8 Curving with Various Lubrication Conditions 27
7.9 Turnouts and Crossovers 29
7.10 Buff and Draft Curving 30
8.0 Conclusions 31
References 33

List of Figures

Figure 1. Buffer railcar IDOX 020001 during static testing 1
Figure 2. Buffer railcar IDOX 020001 arrangement drawing 2
Figure 3. Bearing adapter pad 3
Figure 4. Measurement locations with highest stresses during squeeze (compressive end) load test 5
Figure 5. Measurement locations with highest stresses during coupler vertical load test 6
Figure 6. Measurement locations with highest stresses during jacking test 6
Figure 7. Measurement locations with highest stresses during suspension twist test 8
Figure 8. Measurement locations with highest stresses during carbody twist test 8
Figure 9. Measurement locations with highest stresses during impact test 9
Figure 10. Simulation prediction and test results of minimum vertical wheel load in the twist and roll regime 16
Figure 11. Simulation prediction and test results of peak-to-peak roll angle in the twist and roll regime 17
Figure 12. Simulation prediction and test results of maximum vertical carbody acceleration in the pitch and bounce regime 18
Figure 13. Simulation prediction and test results of maximum vertical carbody acceleration in the special pitch and bounce regime 19
Figure 14. Simulation prediction and test results of maximum peak-to-peak lateral carbody acceleration in the 39-foot wavelength yaw and sway regime 21
Figure 15. Simulation prediction of maximum peak-to-peak lateral carbody acceleration in the 44.5-foot wavelength yaw and sway regime 22
Figure 16. Simulation prediction and test results of maximum wheel l/v ratio in the dynamic curving regime 23
Figure 17. Simulation prediction and test results of minimum vertical wheel load in the dynamic curving regime 24
Figure 18. Simulation prediction and test results of maximum wheel L/V ratio in the curving with 2-inch rail dip regime 25
Figure 19. Simulation prediction and test results of maximum 2,000-foot standard deviation of lateral carbody acceleration in the hunting regime 26
Figure 20. Worn wheel profiles on the ground rail profiles. The wheelset is shifted to the high rail in the position it would be in a left-hand curve 27
Figure 21. Simulation predictions of maximum truck side L/V ratio in the curving with various lubrication conditions regime. Case 2 lubrication with worn profiles 28
Figure 22. Simulation predictions of maximum truck side L/V ratio in the turnouts and crossovers regime 29
Figure 23. Simulation predictions of maximum truck side L/V ratio in the buff and draft curving regime 31

List of Tables

Table 1. Car dimensions 2
Table 2. Buffer car truck configuration 3
Table 3. Comparison of highest measured stresses with predicted stresses for squeeze (compressive end) load test 4
Table 4. Comparison of highest measured stresses with predicted stresses for coupler vertical load test 5
Table 5. Comparison of highest measured stresses with predicted stresses for jacking test 6
Table 6. Comparison of highest measured stresses with predicted stresses for suspension twist test. 7
Table 7. Comparison of highest measured stresses with predicted stresses for carbody twist test 8
Table 8. Comparison of highest measured stresses with predicted stresses for the impact test. 9
Table 9. Comparison of values used in preliminary modeling and values measured during characterization 11
Table 10. Characteristics for original and redesigned spring nest 13
Table 11. Twist and roll test results and simulation predictions 16
Table 12. Pitch and bounce test results and simulation predictions 18
Table 13. Special pitch and bounce test results and simulation predictions 19
Table 14. Yaw and sway (39-foot wavelength) test results and simulation predictions 20
Table 15. Yaw and sway (44.5-foot wavelength) simulation predictions 21
Table 16. Dynamic curving test results and simulation predictions 23
Table 17. Curving with 2-inch rail dip test results and simulation predictions 25
Table 18. Hunting test results and simulation predictions 26
Table 19. Wheel/Rail Coefficients of Friction for the Curving with Various Lubrication Conditions Regime 27
Table 20. Simulation predictions for curving with various lubrication conditions 28
Table 21. Turnout and crossover simulation predictions 29
Table 22. Buff and draft curving simulation predictions 30

1.0 INTRODUCTION

The United States Department of Energy (DOE) contracted with Transportation Technology Center, Inc. (TTCI) to perform dynamic modeling and certification testing on a buffer railcar developed as part of DOE's Atlas Railcar Design Project. The DOE project is intended to meet the needs for future large-scale transport of high-level radioactive material (HLRM) as defined in AAR Standard S-2043, which includes spent nuclear fuel and high-level waste.

All tests and analyses were performed according to the Association of American Railroads' (AAR) *Manual of Standards and Recommended Practices* (MSRP), Standard S-2043, "Performance Specification for Trains used to carry High-level Radioactive Material," Section 5.0 – Single Car Tests.[1] Single-car testing of the buffer railcar was conducted primarily at the U.S. Department of Transportation's Transportation Technology Center (TTC) near Pueblo, Colorado between April 2019 and February 2020. The curving with single-rail perturbation test was repeated on September 11, 2020.

Standard S-2043 requires that structural analysis and dynamic analysis be performed during car design. Kasgro Rail Corporation (Kasgro) designed the car and performed the structural analysis, and TTCI performed the dynamic analysis. Predictions from these analyses are compared to single-car test results in this report. The single-car tests are described in TTCI report P-20-032.[2] The pre-test dynamic analysis is described in TTCI report P-17-023.[3]

2.0 BUFFER RAILCAR DESCRIPTION

The buffer railcar is a four-axle flatcar with a permanently attached ballast load (Figure 1). Kasgro manufactured two prototype buffer cars in 2018, IDOX 020001 and IDOX 020002, which were delivered to the TTC. The tests described in this report were conducted on IDOX 020001. Figure 2 shows the general arrangement drawing of the car. Table 1 shows the car dimensions.



Figure 1. Buffer railcar IDOX 020001 during static testing

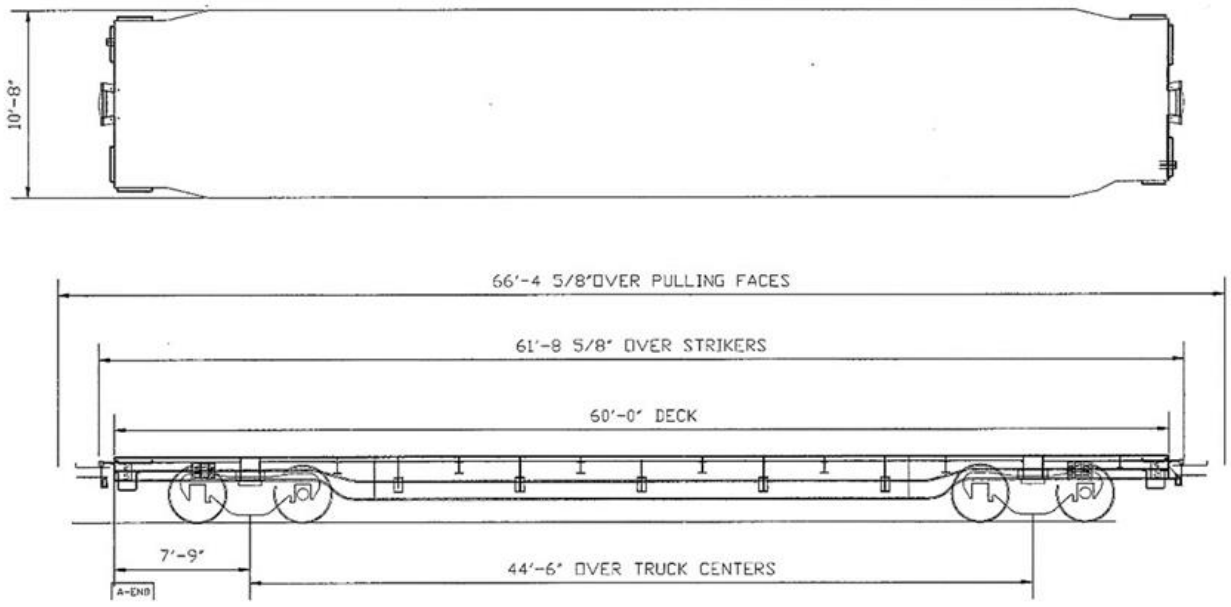


Figure 2. Buffer railcar IDOX 020001 arrangement drawing

Table 1. Car dimensions

Dimension	Value
Length over pulling faces	66 feet, 4 5/8 inches
Length over strikers	61 feet, 8 5/8 inches
Truck center spacing	44 feet 6 inches
Axle spacing on trucks	72 inches

Computer simulations required for Standard S-2043 showed that an empty buffer car would not meet the Standard's requirements in the buff and draft curving regime (S-2043, Paragraph 4.3.13). A ballast weight of 196,000 pounds — included as permanently installed steel plates —was added in the model to resolve this issue.

The steel plates were permanently attached to the car by welding during the manufacturing process, resulting in a car with a permanent gross rail load of 263,000 pounds. Because the car was not rated to carry any additional load, this was the only load condition that was tested.

The car used two Swing Motion® trucks supplied by Amsted Rail. Each truck used two wheelsets having K-axles and AAR1-B narrow flange wheels. Narrow flange wheels were specified for this car because the increased gage clearance allowed more lateral movement for better performance. The trucks were specially designed to use a polymer element between the bearing adapter and side frame. This gave the truck a passive steering capability. Figure 3 shows a bearing adapter pad. Table 2 shows the truck configuration used for testing.



Figure 3. Bearing adapter pad

Table 2. Buffer car truck configuration

Part	Description	
Secondary suspension	Five D7 outer coils, five D6 inner Coils, five D6A inner Coils, two 49427-1, two 49427-2	
Primary suspension	Adapter plus pads, ASF part number 10522A	
Side bearings	Miner TCC-III 60LT	
Friction wedge	Amsted part number 1-9249	
Bearings and adapters	K class 6 1/2 x 9 bearings with 6 1/2 x 9 special adapter ASF Part number 10523A	
Center bowl plate	Metal horizontal liner	
Vertical hydraulic dampers	KONI damper 04a 2032	
Side frames	F9N-10FH-UB	
Bolsters	B9N-714N-FS	
	A-end truck average	B-end truck average
Spring nest height	7.75 inches	7.78 inches
Scale weight	131,200 pounds	131,975 pounds

3.0 OBJECTIVE

The objective of this report is to demonstrate that TTCI compared test results to modeling predictions as part of the structural and dynamic analysis of the DOE buffer car. Where necessary, revised simulation predictions are presented.

4.0 REFINING THE FINITE ELEMENT ANALYSIS (FEA)

Test results are compared to FEA predictions in this section. The FEA results were examined to determine the normal stress in the active direction at the location of the strain gages for comparison to the test results. Paragraph 8.1 of Standard S-2043 requires the following:

> "If any measured stress exceeding 75% of allowable varies from its predicted value by more than 15%, then the model must be refined to provide more accurate predictions."

The results presented in this report show that none of the measured stresses exceed 75 percent of the allowable stress.

4.1 Squeeze (Compressive End) Load

Table 3 provides the summary results from the compressive end load test for the locations with highest measured stress. The locations are highlighted in Figure 4. The maximum measured stress was 60 percent of material yield.

The largest difference between measured and predicted stress for any of the tests was 5.7 ksi (19 percent) on channel SGBF11 during the compressive end load test. Three other measurements in similar locations, (SGBF10, SGBF37, and SGBF35) were closer to the predicted stress.

Table 3. Comparison of highest measured stresses with predicted stresses for squeeze (compressive end) load test

Channel Name	Approximate Location	Measured Stress (ksi)	Yield Stress (ksi)	Measured Stress as percent of Yield	Predicted Stress	Percent Difference Test vs. Predicted
SGBF11	Right edge of bottom flange of center sill, 44.5 inches from A-end body bolster toward car center	-30	50	60%	-24.3	NA*
SGBF10	Left edge of bottom flange of center sill, 44.5 inches from A-end body bolster toward car center	-28	50	56%	-24.3	NA*
SGBF37	Right edge of bottom flange of center sill, 44.5 inches from B-end body bolster toward car center	-26	50	52%	-24.3	NA*
SGDP35	Left edge of bottom flange of center sill, 44.5 inches from B-end body bolster toward car center	-24	50	48%	-24.3	NA*

* Not required because measured stress does not exceed 75% of allowable

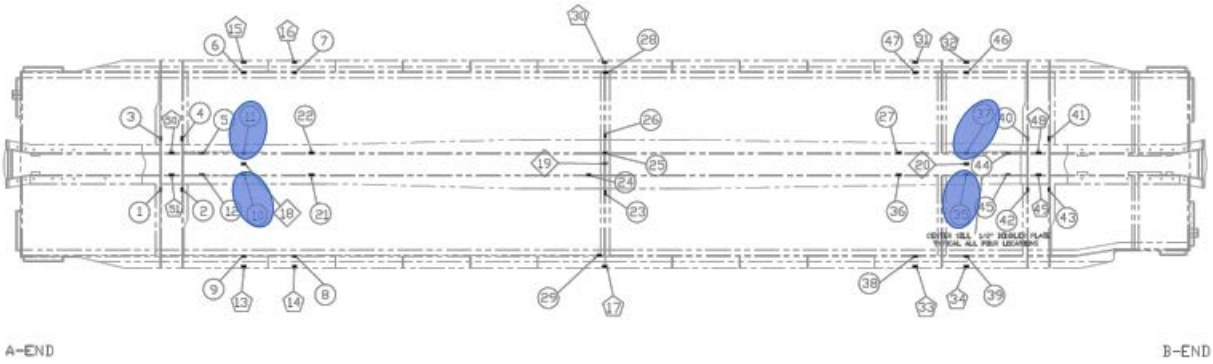


Figure 4. Measurement locations with highest stresses during squeeze (compressive end) load test

4.2 Coupler Vertical Loads

Table 4 shows the summary results from the coupler vertical load test for the locations with highest measured stress. The locations are highlighted in Figure 5. The maximum measured stress was 26% of material yield.

Table 4. Comparison of highest measured stresses with predicted stresses for coupler vertical load test

Channel Name	Approximate Location	Measured Stress (ksi)	Yield Stress (ksi)	Measured Stress as percent of Yield	Predicted Stress	Percent Difference Test vs. Predicted
Load applied upward						
SGBF35	Left edge of bottom flange of center sill, 44.5 inches from B-end body bolster toward car center	12	50	24%	9.3	NA*
SGBF37	Right edge of bottom flange of center sill, 44.5 inches from B-end body bolster toward car center	13	50	26%	9.3	NA*
Load applied downward						
SGBF35	Left edge of bottom flange of center sill, 44.5 inches from B-end body bolster toward car center	-12	50	24%	-8.6	NA*
SGBF37	Right edge of bottom flange of center sill, 44.5 inches from B-end body bolster toward car center	-13	50	26%	-8.6	NA*

* Not required because measured stress does not exceed 75% of allowable

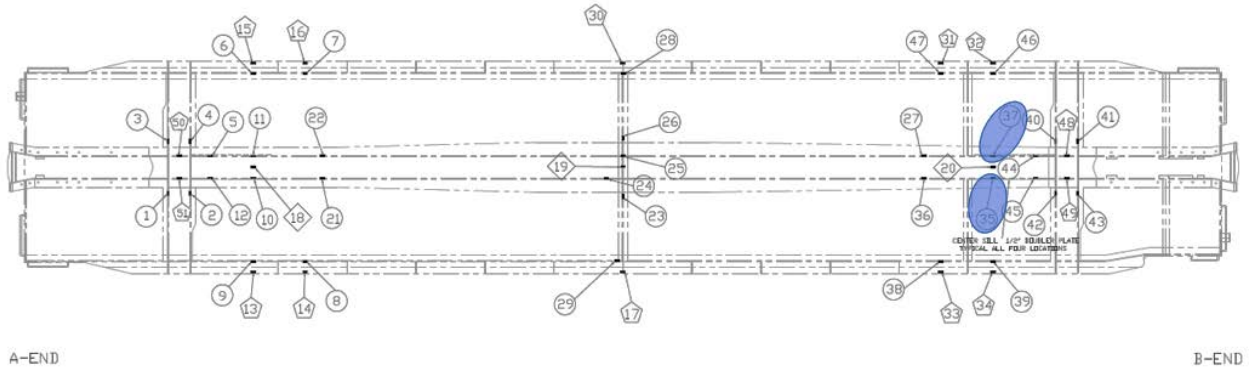


Figure 5. Measurement locations with highest stresses during coupler vertical load test

4.3 Jacking

Table 5 provides the summary results from the jacking test for the locations with highest measured stress. The locations are highlighted in Figure 6. The maximum measured stress was 12 percent of material yield.

Table 5. Comparison of highest measured stresses with predicted stresses for jacking test

Channel Name	Approximate Location	Measured Stress (ksi)	Yield Stress (ksi)	Measured Stress as percent of Yield	Predicted Stress	Percent Difference Test vs. Predicted
SGBF42	Front of bottom flange of B-end body bolster near center sill – left side	6	50	12%	5.3	NA*
SGBF40	Front of bottom flange of B-end body bolster near center sill – right side	6	50	12%	5.3	NA*

* Not required because measured stress does not exceed 75% of allowable

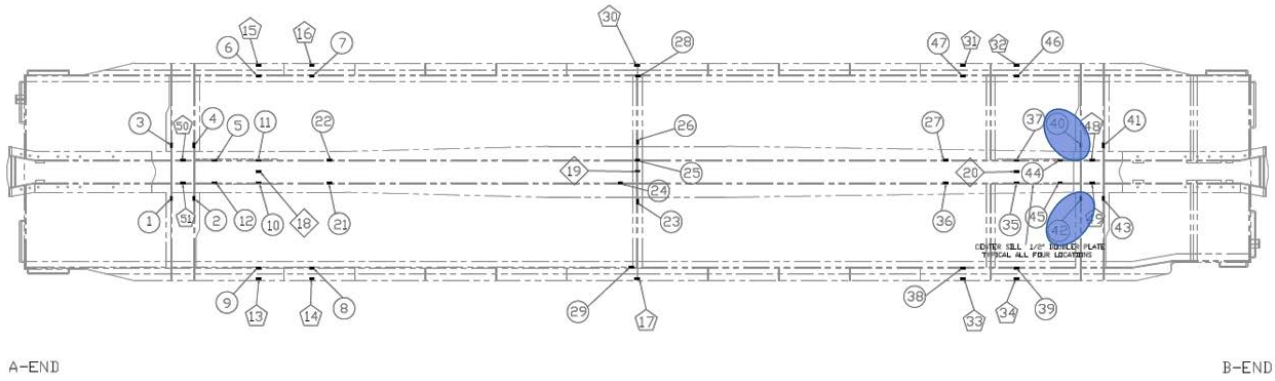


Figure 6. Measurement locations with highest stresses during jacking test

4.4 Twist

TTCI performed two twist tests as part of the structural tests.

The test described in S-2043, Paragraph 5.4.5.1, is reported in Section 4.4.1 of this report, "Suspension Twist." This test followed the requirements of MSRP Section C, Part II, Specification M-1001, Paragraph 11.3.3.5. The test was performed in conjunction with the carbody twist equalization test (S-2043, Paragraph 5.2.2). For this test, two wheels of one side of one truck were raised 3 inches. This was repeated for all four corners of the car.

The test described in S-2043 paragraph 5.4.5.2 is reported in Section 4.4.2 of this report, "Carbody Twist." For this test, the railcar was supported at all four jacking pads and one corner was allowed to drop 3 inches.

4.4.1 Suspension Twist

Table 6 shows the summary results from the suspension twist test for the locations with highest measured stress (locations highlighted in Figure 7). The maximum measured stress was 2 percent of material yield.

Table 6. Comparison of highest measured stresses with predicted stresses for suspension twist test.

Channel Name	Approximate Location	Measured Stress (ksi)	Yield Stress (ksi)	Measured Stress as percent of Yield	Predicted Stress	Percent Difference Test vs. Predicted
Raising wheels A-end left side						
SGDP48	Top of deck plate, longitudinally centered over B-end body bolster, above right edge of center sill	1	50	2%	<1	NA*
Raising wheels A-end right side						
SGDP49	Top of deck plate, longitudinally centered over B-end body bolster, above left edge of center sill	1	50	2%	<1	NA*
Raising wheels B-end left side						
SGDP49	Top of deck plate, longitudinally centered over B-end body bolster, above left edge of center sill	1	50	2%	<1	NA*
Raising wheels B-end right side						
SGDP48	Top of deck plate, longitudinally centered over B-end body bolster, above right edge of center sill	1	50	2%	<1	NA*

* Not required because measured stress does not exceed 75% of allowable

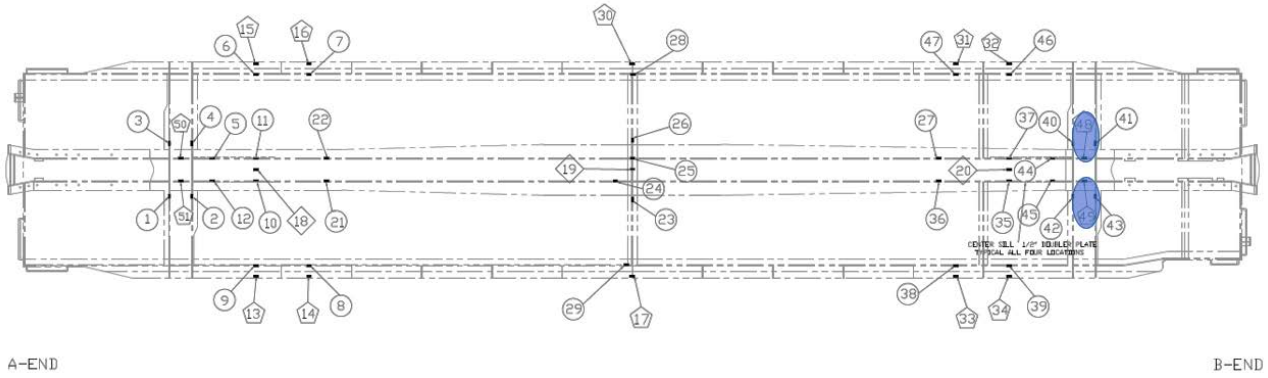


Figure 7. Measurement locations with highest stresses during suspension twist test

4.4.2 Carbody Twist

Table 7 shows the summary results from the carbody twist test for the locations with highest measured stress (locations are highlighted in Figure 8). The maximum measured stress was 18 percent of material yield. The car was supported at three jacking pad locations while the B-end, left-hand jack was lowered to 3 inches. The B-end left jacking pad only dropped 2 11/16 inches, losing contact with the jack.

Table 7. Comparison of highest measured stresses with predicted stresses for carbody twist test

Channel Name	Approximate Location	Measured Stress (ksi)	Yield Stress (ksi)	Measured Stress as percent of Yield	Predicted Stress	Percent Difference Test vs. Predicted
SGBF11	Right edge of bottom flange of center sill, 44.5 inches from A-end body bolster toward car center	-3	50	6%	-5	NA*
SGBF40	Front of bottom flange of B-end body bolster near center sill – right side	8	50	18%	7.4	NA*

* Not required because measured stress does not exceed 75% of allowable

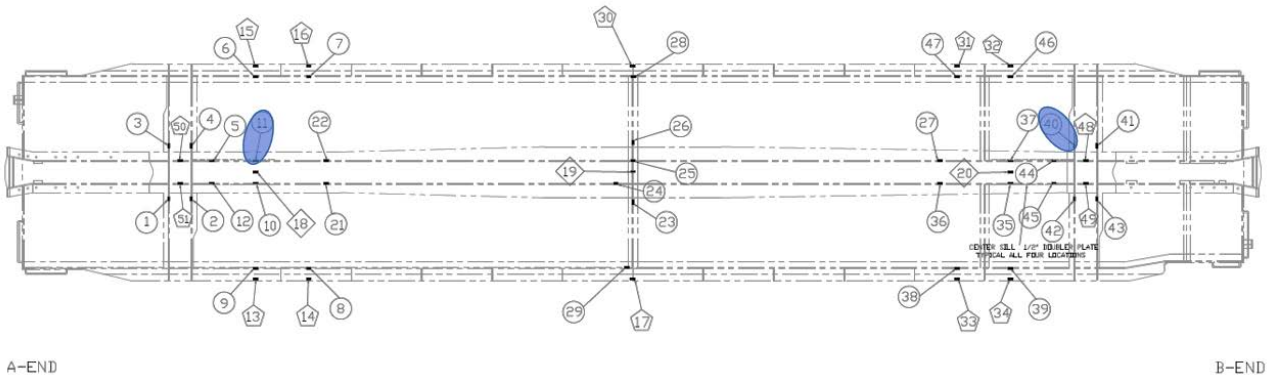


Figure 8. Measurement locations with highest stresses during carbody twist test

4.5 Impact Test

Table 8 shows the summary results from the impact test for the locations with highest measured stress (locations are highlighted in Figure 9). The highest stresses were measured at the highest impact speed of 9.6 mph. The coupler load measured on this run was 612 kips. The maximum measured stress was 32 percent of material yield.

Table 8. Comparison of highest measured stresses with predicted stresses for the impact test.

Channel Name	Approximate Location	Measured Stress (ksi)	Yield Stress (ksi)	Measured Stress as percent of Yield	Predicted Stress	Percent Difference Test vs. Predicted
SGBF37	Right edge of bottom flange of center sill, 44.5 inches from B-end body bolster toward car center	-16	50	32%	-16.5	NA*
SGBF35	Left edge of bottom flange of center sill, 44.5 inches from B-end body bolster toward car center	-14	50	28%	-16.5	NA*
SGBF44	Right edge of bottom flange of center sill, 18.75 inches from B-end body bolster toward car center	-9	50	18%	-9.76	NA*
SGBF45	Left edge of bottom flange of center sill, 18.75 inches from B-end body bolster toward car center	-9	50	18%	-9.76	NA*

* Not required because measured stress does not exceed 75% of allowable

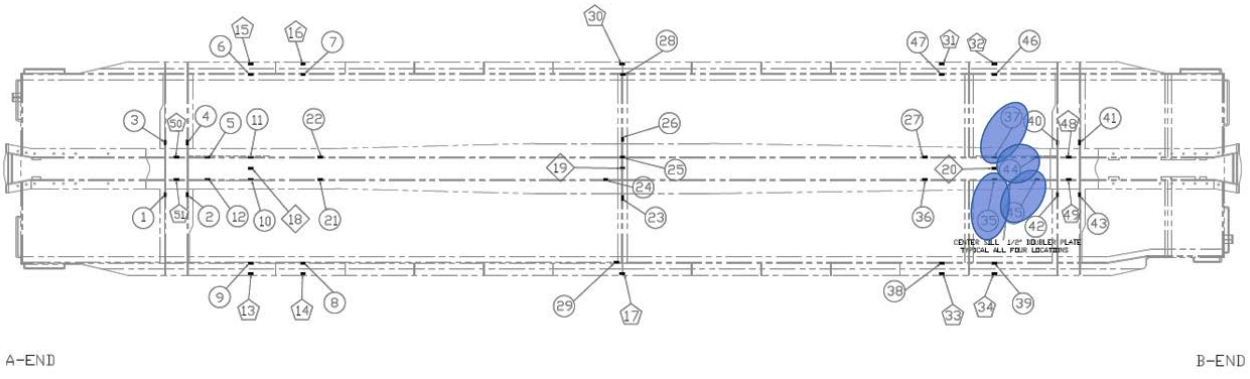


Figure 9. Measurement locations with highest stresses during impact test

5.0 NEW FINITE ELEMENT ANALYSIS PREDICTIONS

Because none of the measured stresses were greater than 75 percent of the allowable stress, the tolerance on FEA prediction accuracy did not apply. No new FEA predictions were required.

6.0 REFINING THE DYNAMIC MODEL

Standard S-2043 requires:

> "The dynamic model must be refined based on vehicle characterization results if suspension values are measurably different than those used in the original model."

Some of the measured characterization results[2] differ from those used in the original dynamic analysis model.[3] Table 9 provides the suspension stiffness and damping values used for the original model, the values measured during the characterization, the percent difference, information on the origin of the characterization value, and an indication if and how the characterization value was used to update the model.

Table 9. Comparison of values used in preliminary modeling and values measured during characterization

Parameter	Model Value	Characterization Value	Percent Difference	Notes	Change to model
Spring vertical stiffness (pound/inch/nest)*	22,400	23,600	5%	Spring nest stiffness compiled using the manufacturer / AAR values compared to values measured during component characterization	Updated for the appropriate spring group
Vertical secondary stiffness (pound/inch/nest)*	22,400	26,000	16%	Manufacturer / AAR values of original nest compared to System Characterizations values measured on the MSU, dampers removed.	Besides changing to the correct spring group, no change was made
Lateral secondary stiffness (pound/inch/nest)*	13,500	8,100	-40%	Average transom restrained; wedges installed runs	Reduced stiffness to 62% of Koffman formula
Vertical secondary damping (pound/nest)	8,000	5,000	-38%	Dampers removed	No change made
Lateral secondary damping (pound/nest)	9,000	6,000	-33%	Average transom restrained; wedges installed runs	No change made
Side bearing preload (pounds)**	7,500	5,700	-24%	Manufacturers static closure compared to average from component characterization	Updated the model to use a Piece Wise Linear (PWL) value based on the characterization data of the side bearing used
Center plate friction (nondimensional)	0.2	0.22	10%		Increased stiffness to characterization value
Damper initial rate (pound/(inch/second))	1070	1054	-1%	Slope of data from -4 inch/second to 4 inch/second	No Change
Damper blowoff velocity (inch/second)	3.94	3.98	1%	Intersection of initial rate line and damper blowoff lines	No Change
Damper blowoff rate(pound/(inch/second)	58	58	0%	Slope of data from -14 to -4 inch/second averaged with slope of data from 4 to 14 inches/second	No Change
Damper bushing series stiffness (pound/inch)	71,377	102,000	43%	Average of series stiffness of AL and AR dampers	Increased the damper bushing series stiffness to the characterization level
Vertical primary stiffness (pound/inch/pad)	500,000	850,000	70%	0.1Hz data. Data varied over a range from 763,000 to 923,000	Increased stiffness to the characterization value
Lateral primary stiffness	48,000	33,500	-30%	0.1Hz data. Data varied over a range	Reduced stiffness to characterization

Parameter	Model Value	Characterization Value	Percent Difference	Notes	Change to model
(pound/inch/pad)				from 30,000-to 37,000	value
Longitudinal primary stiffness at axle centerline (pound/inch/pad)	22,500	13,000	-42%	Average of axle centerline stiffness measured directly and derived from yaw	Reduced stiffness to characterization value

* The original model used 6 D7 OC and 6 D7 IC, during production the truck design was changed to use 5 D7 OC, 5 D6 IC, and 5 D6A IIC as described below

** The model used Miner TCC III 8000 CCSB, during production the car design was changed to use Miner TCC III 6000 CCSB as described below

The original simulation predictions were performed with a spring nest configuration containing six D7 outer coils, six D7 inner coils, two 49427-1 outer control coils, two 49427-2 inner control coils, and a KONI vertical damper. Amsted Rail later determined that this spring nest was not compatible with the KONI Damper because the six-coil nest did not allow enough space to install the damper. To provide space, Amsted Rail redesigned the spring nest to use five D7 outer coils, five D6 inner coils, five D6A inner-inner coils, two 49427-1 outer control coils and two 49427-2 inner control coils. Table 10 shows characteristics for the original and redesigned spring nests.

Table 10. Characteristics for original and redesigned spring nest

Metric	Spring Nest - Original Simulation Predictions	Redesigned Spring Nest
Reserve capacity (percent)	57	54
Load on a single wedge (pound)	6,486	6,870
Total lateral stiffness per nest (pound/inch)	13,509	13,030
Total vertical stiffness per nest (pound/inch)	22,412	23,788
Static free height (inch)	8.13	7.95

A second change to the buffer car equipment was the four constant-contact side bearings mounted between the truck bolsters and carbody bolsters. The dynamic analysis model used characteristics for a Miner TCC-III 80 LT side bearing. The prototype cars arrived with Miner TCC-III 60 LT side bearings installed. The TCC-III 80 LT side bearings have a nominal preload of 8,000 pounds while the TCC-III 60 LT side bearings have a nominal preload of 6,000 pounds. Two of the TCC-III 60 LT side bearings were characterized. The force deflection data from the characterization was used in the refined dynamic model.

The lateral secondary suspension stiffness measured during the characterization test was only about 60 percent of the value used in the dynamic analysis model. Part of this difference was due to the change in the secondary suspension spring group. A larger part of the difference was that the formula used to estimate the shear stiffness often predicts a higher stiffness than is found in practice. The shear stiffness in the revised dynamic model was calculated for the redesigned spring group, and then reduced to 62 percent of the calculated value to match the value from characterization tests.

The original dynamic analysis model used a coefficient of friction value of 0.2 to model the surface between the carbody center plate and the truck center bowl. The coefficient of friction measured during the characterization test was 0.22. The refined dynamic model used a coefficient of friction of 0.22 for this surface.

The characterization data for the KONI vertical damper matched the values used in the dynamic analysis model very closely for the initial rate, blowoff velocity, and the blowoff rate. TTCI made no changes in the refined model for these parameters. The vertical damper bushing stiffness measured during the characterization was about 30 percent higher than the value in the original dynamic analysis model. The bushing stiffness was increased to match the characterization data for the refined dynamic analysis model.

The measured stiffness of the primary suspension pads was different than those used in the original dynamic analysis model. The measured vertical stiffness was 41 percent higher while the

lateral and longitudinal stiffness were 43 and 73 percent lower, respectively. These values of primary suspension pad stiffness were updated to match the characterization values in the refined dynamic analysis model.

While troubleshooting performance of a similar truck design in the time since the original dynamic analysis was performed, TTCI found that the method used to model the connection between the side frame and the primary pad could be altered to better replicate the roll characteristics between the side frame and axle. The original method to model this connection used only a single vertical connection between the side frame and axle centered at the location of the primary pad. When comparing predicted lateral suspension displacement to test results, TTCI found that the results matched better when two connections — separated laterally the width of the primary pad — were used to model this connection. This new method was implemented in the refined dynamic analysis model.

7.0 NEW DYNAMIC PREDICTIONS

Standard S-2043 states the following:

> "Test results must be compared to design predictions to verify that the model accurately represents the vehicle. If substantial modifications have been made to the dynamic model, a revised analysis must be performed. The designer may choose to repeat the entire analysis or reanalyze limited cases based on how critically they would be affected by the changes to the model and how large existing margins of safety are. The designer's decisions must be justified through adequate explanation."

In this section, TTCI compares original and refined dynamic analysis model predictions to test data to show that the model accurately represents the vehicle. Characterization test results prompted several changes to the dynamic analysis model. As a result, TTCI repeated several portions of the dynamic analysis. Simulation predictions are shown for the original and revised models.

TTCI repeated the following portions of the dynamic analysis because they served to demonstrate the model performance compared to test data:

- Twist and roll
- Pitch and bounce
- Yaw and sway
- Dynamic curving
- Curving with single rail perturbation
- Hunting

TTCI repeated the following portions of the dynamic analysis because the original dynamic analysis predictions showed that some metrics were close to or did not meet the criteria.

- Curving with various lubrication conditions
- Turnouts and crossovers
- Buff and draft curving

As will be shown in the following sections, the revised model predictions for the regimes listed above changed very little compared to the original dynamic analysis. Because the revised model showed little change compared to the original model, and because the original dynamic analysis

showed a margin of safety with respect to the criteria for these regimes, the regimes below were not simulated with the revised model:

- Twist and roll – 44.5-foot
- Yaw and sway – 44.5-foot
- Dynamic curve – 44.5-foot
- Single bump
- Constant curving
- Limiting spiral negotiation
- Ride quality
- Braking effects on steering
- Worn component simulations

The proceeding sections show modeling predictions for the original model, the revised model, and test results where available. The buffer car met all the single-car test requirements. The original dynamic analysis predictions met all the requirements except for two of the curving with various lubrication conditions and buff-draft curving requirements.

7.1 Twist and Roll

Simulations of the twist and roll regime were conducted according to Standard S-2043, Paragraph 4.3.9.6. Twist and roll track tests were conducted according to S-2043, Paragraph 5.5.8. The twist and roll regime consists of a series of 10 0.75-inch vertical track deviations offset on each rail to input roll motions to the car. The original simulations were performed with 39- and 44.5-foot wavelengths. Track tests were only performed with 39-foot wavelength. Simulations with a 44.5-foot wavelength were not performed with the revised model because there were no test results for comparison and the original simulations showed a large margin of safety compared to the criteria.

Table 11 shows the worst-case test results and simulation predictions for twist and roll. Figure 10 shows minimum vertical wheel load and Figure 11 shows the maximum peak-to-peak roll angles plotted against speed to show the trend in performance. Test results and simulation predictions met S-2043 criteria (red line) for twist and roll. The Chapter 11 criteria (yellow line) is also shown as reference.

Simulation predictions and test results matched closely for twist and roll. Test results showed lower wheel loads than simulation predictions at speeds above 30 mph, but at the widest point the difference is only about 8 percent of static wheel load. Peak-to-peak carbody roll angle test results showed a mild lower center roll resonance at about 30 mph for the old and new model predictions and at about 33 mph for the test. Peak-to-peak carbody roll angle test results showed a mild upper center roll resonance at about 65 mph for the old model predictions and at about 60 mph for the new model predictions and the test. The upper center roll peak was slightly more pronounced for the revised model predictions than the test data, but it occurred at the same speed and was followed by a similar reduction in amplitude at the higher speeds.

Table 11. Twist and roll test results and simulation predictions

Criterion	Limiting Value	Test Result	Simulation Prediction Original Model	Simulation Prediction Revised Model
Roll angle (degree)	4.0	1.7	1.6	2.1
Maximum wheel lateral/vertical (L/V)	0.8	0.2	0.11	0.19
Maximum truck side L/V	0.5	0.16	0.09	0.13
Minimum vertical wheel load (%)	25%	66%	69%	69%
Lateral peak-to-peak acceleration (g)	1.3	0.55	0.27	0.34
Maximum lateral acceleration (g)	0.75	0.31	0.15	0.20
Maximum vertical acceleration (g)	0.90	0.29	0.16	0.23
Maximum vertical suspension deflection (%)	95%	48%	40%	46%

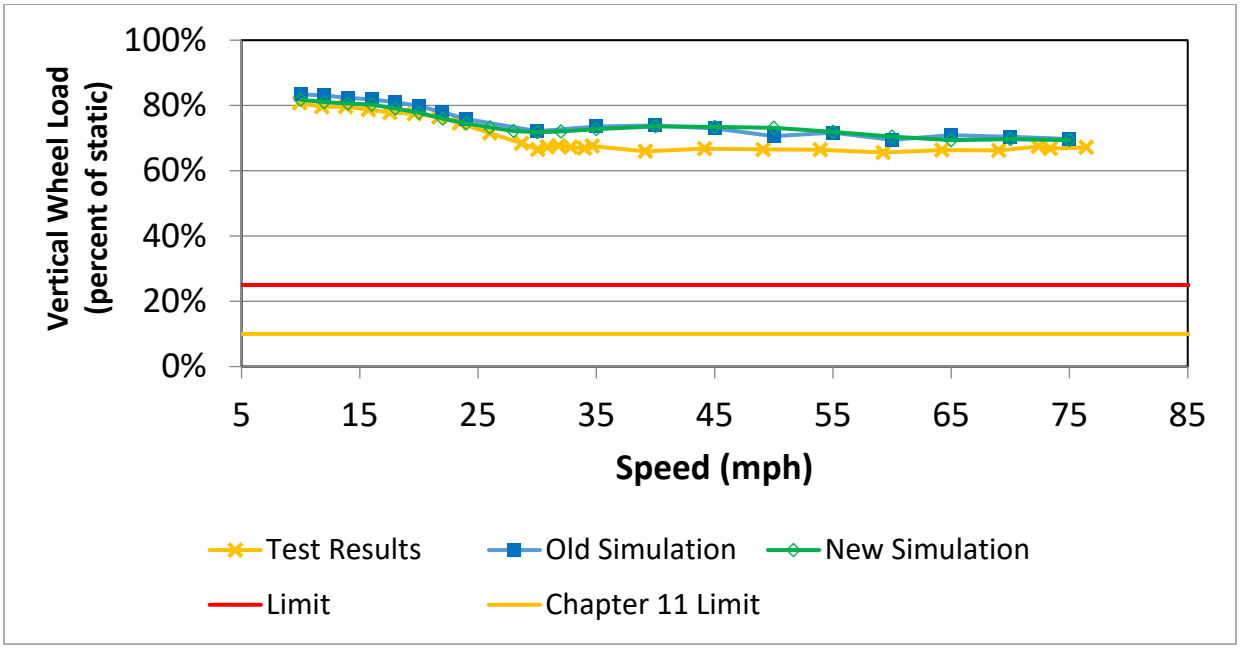


Figure 10. Simulation prediction and test results of minimum vertical wheel load in the twist and roll regime

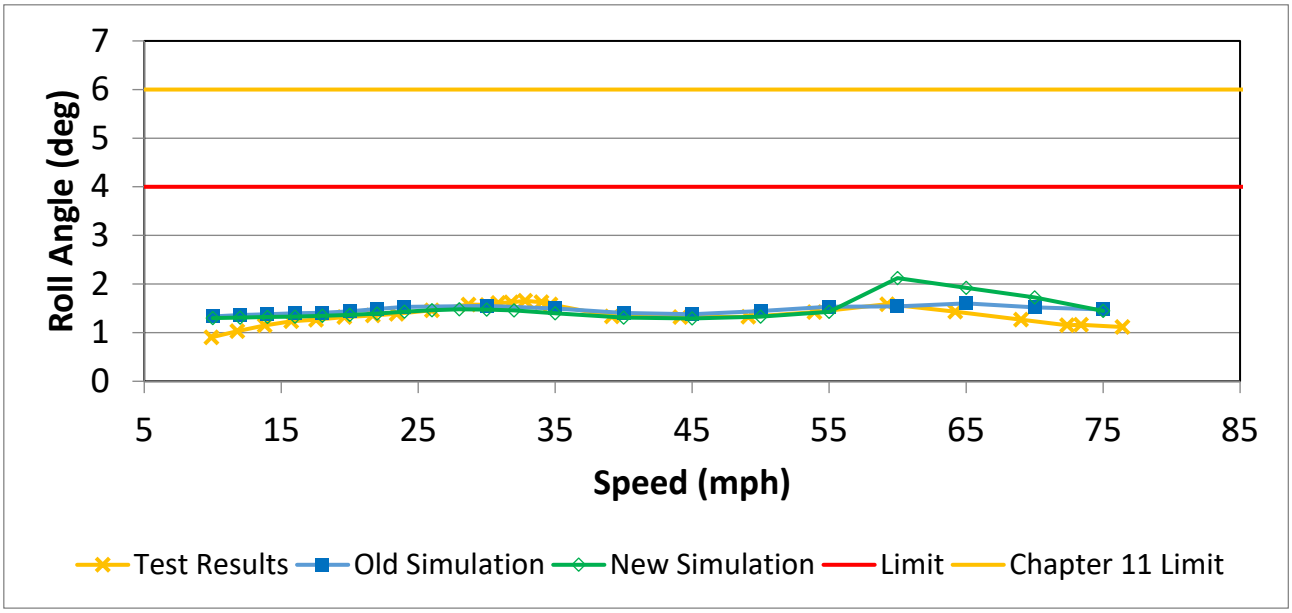


Figure 11. Simulation prediction and test results of peak-to-peak roll angle in the twist and roll regime

7.2 Pitch and Bounce

Simulations of the pitch and bounce regime were conducted according to S-2043, Paragraph 4.3.9.7. Pitch and bounce tests were conducted according to of S-2043, Paragraph 5.5.11. The pitch and bounce regime consisted of a series of 10 0.75-inch vertical track deviations in parallel on each rail to input vertical motions to the car.

Table 12 shows the worst-case test results and simulation predictions for pitch and bounce. Figure 12 shows the maximum carbody vertical acceleration plotted against speed to show the trend in performance. Test results and simulation predictions met S-2043 criteria for pitch and bounce.

Simulation predictions showed lower amplitude resonance at a slightly lower speed than test results for pitch and bounce. For example, the original simulation predicted the maximum carbody vertical acceleration of 0.65 g at about 59 mph; for the refined simulation, the prediction increased to 0.68 g at about 60 mph and the test result showed 0.8 g at 68 mph. The changes to the model that represented the new spring grouping improved the simulation predictions slightly, but there was still a difference when compared to the test results.

Table 12. Pitch and bounce test results and simulation predictions

Criterion	Limiting Value	Test Result	Simulation Prediction Original Model	Simulation Prediction Revised Model
Roll angle (degree)	4.0	0.4	0.2	0.3
Maximum wheel L/V	0.8	0.19	0.06	0.07
Maximum truck side L/V	0.5	0.13	0.05	0.06
Minimum vertical wheel load (%)	25%	50%	60%	59%
Lateral peak-to-peak acceleration (g)	1.3	0.31	0.12	0.15
Maximum lateral acceleration (g)	0.75	0.25	0.06	0.08
Maximum vertical acceleration (g)	0.90	0.80	0.65	0.68
Maximum vertical suspension deflection (%)	95%	86%	74%	75%

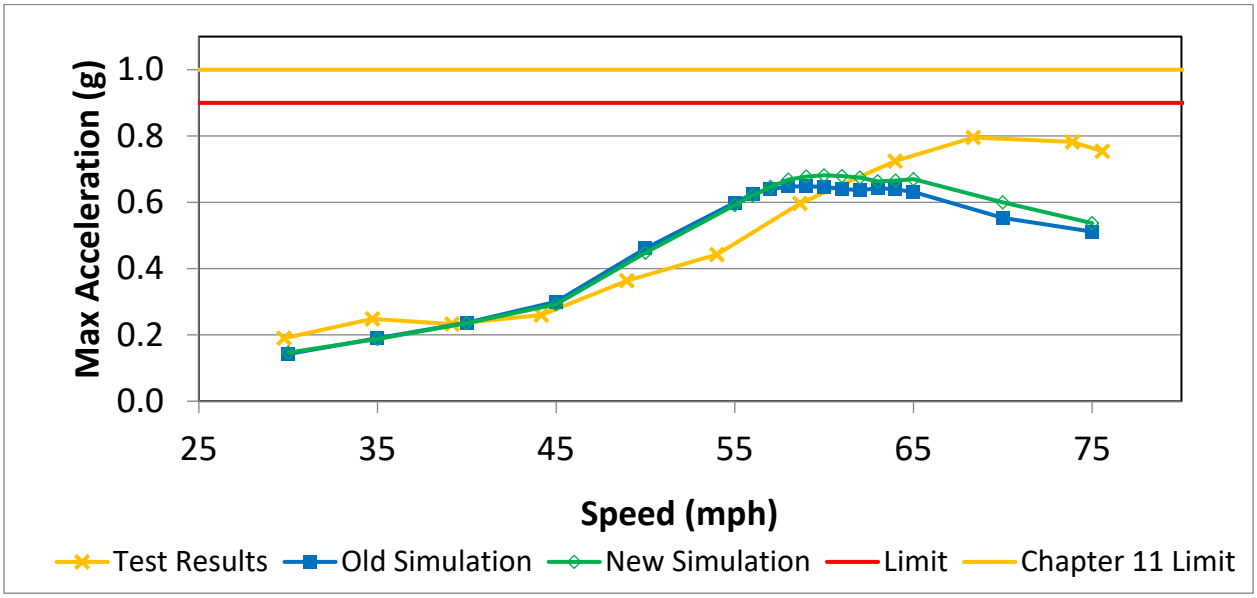


Figure 12. Simulation prediction and test results of maximum vertical carbody acceleration in the pitch and bounce regime

7.3 Special Pitch and Bounce (44.5-foot wavelength)

Simulations of the special pitch and bounce regime (44.5-foot wavelength) were conducted according to S-2043, Paragraph 4.3.9.7. Special pitch and bounce tests were conducted according to S-2043, Paragraph 5.5.12. The special pitch and bounce regime consisted of a series of 10 0.75-inch vertical track deviations in parallel on each rail to input vertical motions to the car. The difference between standard Chapter 11 pitch and bounce and special pitch and bounce is that the standard zone uses track deviations on a 39-foot wavelength while the special zone uses track deviations on a wavelength that matches the truck center spacing of the car being tested — 44.5 feet in this case.

Table 13 shows the worst-case test results and simulation predictions for special pitch and bounce. Figure 13 shows the maximum carbody vertical acceleration plotted against speed to show the trend in performance. Test results and simulation predictions meet S-2043 criteria for special pitch and bounce.

Simulation predictions showed lower amplitude resonance at a slightly lower speed than test results for pitch and bounce. For example, the original simulation predicted the maximum carbody vertical acceleration of 0.47 g at about 60 mph; for the refined simulation, the prediction increased to 0.49 g at about 61 mph, and the test result showed 0.5 g at 69 mph. The changes to the model that represented the new spring grouping improved the simulation predictions slightly, but there was still a difference when compared to the test results.

The simulation predictions did correctly predict the improvement in performance in the special pitch and bounce regime compared to the standard pitch and bounce regime. Minimum vertical wheel loads increased for both the simulation and test in the special pitch and bounce compared to standard pitch and bounce. Maximum carbody acceleration and maximum vertical suspension deflection both decreased for both the simulation and test in the special pitch and bounce compared to standard pitch and bounce.

Table 13. Special pitch and bounce test results and simulation predictions

Criterion	Limiting Value	Test Result	Simulation Prediction Original Model	Simulation Prediction Revised Model
Roll angle (degree)	4.0	0.4	0.2	0.2
Maximum wheel L/V	0.8	0.13	0.08	0.07
Maximum truck side L/V	0.5	0.09	0.06	0.06
Minimum vertical wheel load (%)	25%	57%	65%	64%
Lateral peak-to-peak acceleration (g)	1.3	0.22	0.19	0.17
Maximum lateral acceleration (g)	0.75	0.18	0.12	0.09
Maximum vertical acceleration (g)	0.90	0.5	0.47	0.49
Maximum vertical suspension deflection (%)	95%	71%	61%	61%

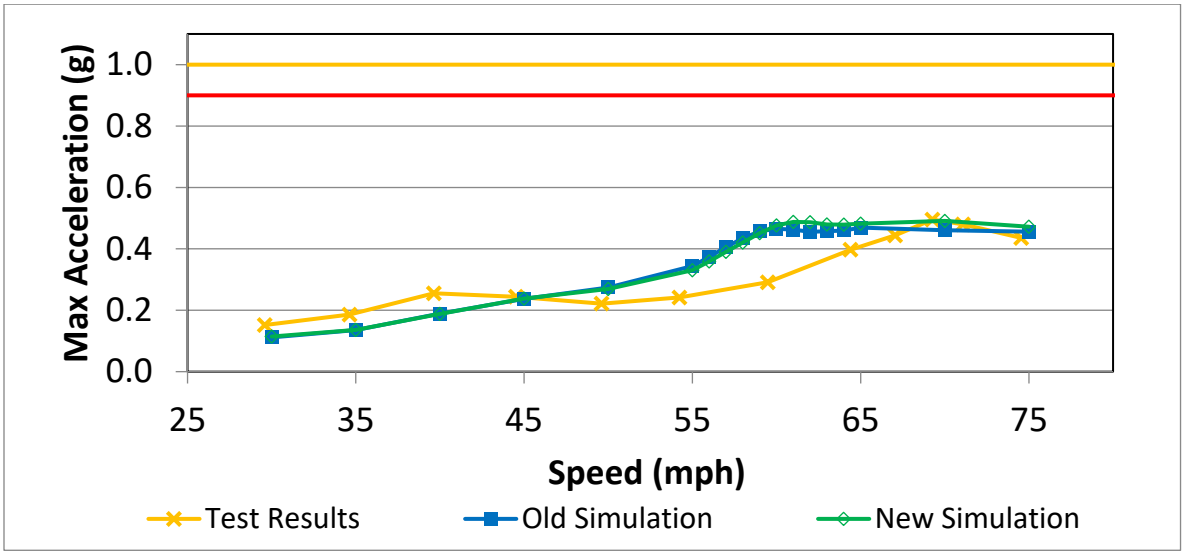


Figure 13. Simulation prediction and test results of maximum vertical carbody acceleration in the special pitch and bounce regime

7.4 Yaw and Sway

Simulations of the yaw and sway regime were conducted according to S-2043, Paragraph 4.3.9.8. Yaw and sway tests were conducted according to S-2043, Paragraph 5.5.9. The yaw and sway regime consisted of a series of five 1.25-inch lateral track deviations on a section with 1-inch wide gage to input lateral and yaw motions to the car. Simulations of 39-foot and 44-foot, 6-inch wavelengths were performed. Testing was carried out with 39-foot wavelength only.

Table 14 shows the worst-case test results and simulation predictions for yaw and sway with 39-foot wavelength. Figure 14 shows the maximum peak-to-peak carbody lateral acceleration plotted against speed to show the trend in performance. Table 15 shows the worst-case simulation predictions for yaw and sway with 44.5-foot wavelength. Figure 15 shows the maximum peak-to-peak carbody lateral acceleration plotted against speed to show the trend in performance. Test results and the original simulation predictions met S-2043 criteria for yaw and sway, but the revised simulation predictions did not meet S-2043 criteria for yaw and sway at speeds between 30 and 35 mph. The revised simulation predictions did meet the slightly less stringent Chapter 11 criteria.

The simulation predictions had a higher amplitude resonance at a lower critical speed that was measured during the test. Unfortunately, the revised model exacerbated this problem by increasing the amplitude of the resonance further, to the point that the simulation predictions no longer met the criteria for yaw and sway.

Table 14. Yaw and sway (39-foot wavelength) test results and simulation predictions

Criterion	Limiting Value	Test Result	Simulation Prediction Original Model	Simulation Prediction Revised Model
Roll angle (degree)	4.0	2.0	1.3	2.3
Maximum wheel L/V	0.8	0.6	0.62	0.62
Maximum truck side L/V	0.5	0.3	0.30	0.29
Minimum vertical wheel load (%)	25%	50%	56%	52%
Lateral peak-to-peak acceleration (g)	1.3	0.9	1.16	**1.38**
Maximum lateral acceleration (g)	0.75	0.5	0.59	0.70
Maximum vertical acceleration (g)	0.90	0.3	0.18	0.18
Maximum vertical suspension deflection (%)	95%	67%	77%	46%

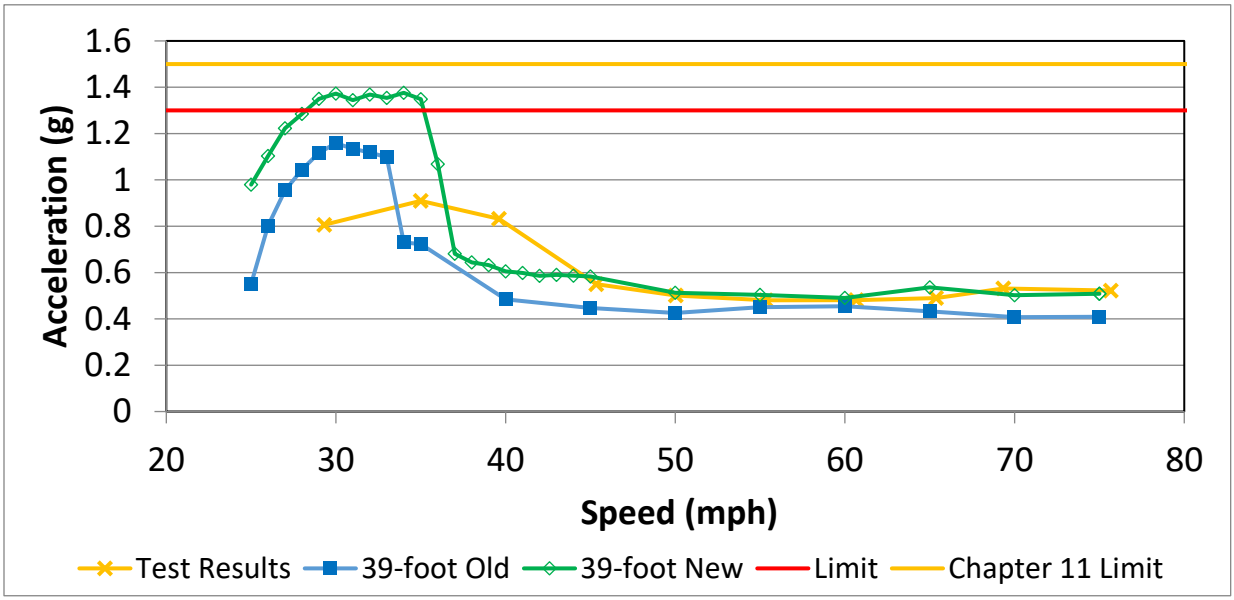


Figure 14. Simulation prediction and test results of maximum peak-to-peak lateral carbody acceleration in the 39-foot wavelength yaw and sway regime

Table 15. Yaw and sway (44.5-foot wavelength) simulation predictions

Criterion	Limiting Value	Simulation Prediction Original Model	Simulation Prediction Revised Model
Roll angle (degree)	4.0	2.0	3.3
Maximum wheel L/V	0.8	0.51	0.47
Maximum truck side L/V	0.5	0.24	0.23
Minimum vertical wheel load (%)	25%	51%	50%
Lateral peak-to-peak acceleration (g)	1.3	1.25	**1.31**
Maximum lateral acceleration (g)	0.75	0.65	0.68
Maximum vertical acceleration (g)	0.90	0.16	0.17
Maximum vertical suspension deflection (%)	95%	79%	49%

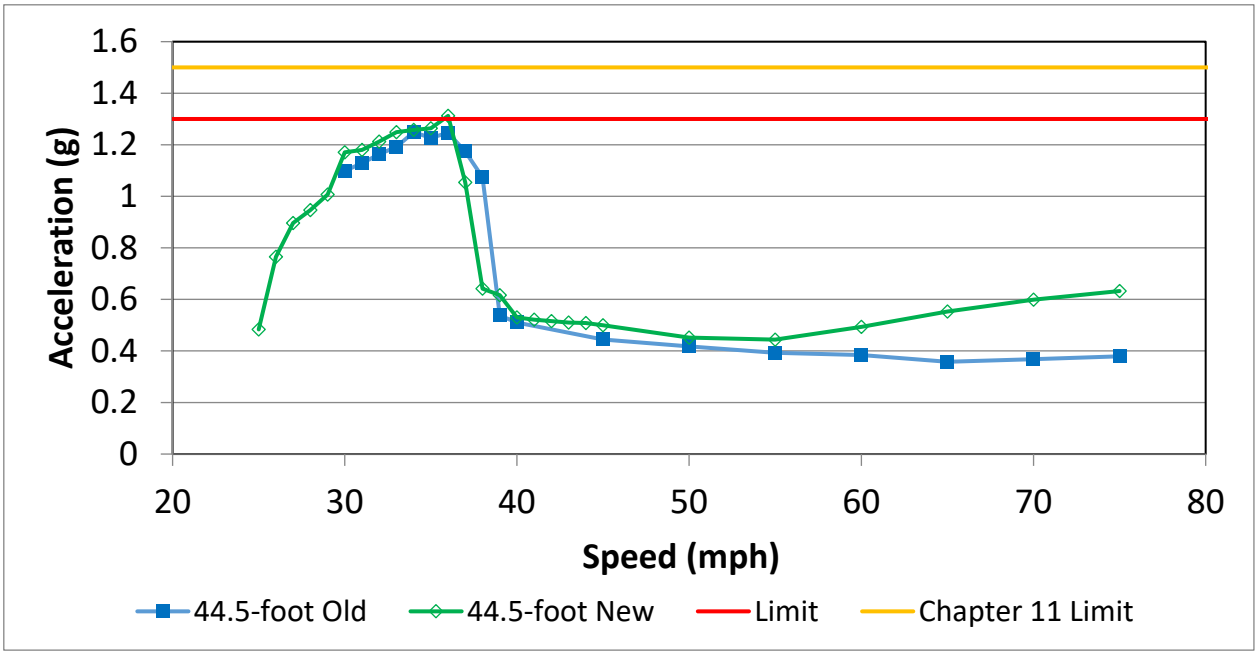


Figure 15. Simulation prediction of maximum peak-to-peak lateral carbody acceleration in the 44.5-foot wavelength yaw and sway regime

7.5 Dynamic Curving

Simulations of the dynamic curving regime were conducted according to Paragraph 4.3.9.9 of S-2043. Dynamic curving tests were conducted according to Paragraph 5.5.10 of S-2043. The dynamic curve section was on a 10-degree curve with 4 inches superelevation. The dynamic curving regime consisted of a series of 0.5-inch vertical track deviations offset on each rail to input roll motions to the car. There were five deviations on the high rail and six deviations on the low rail. At the same time, the gage of the track changed from 56.5 inches to 57.5 inches to input lateral motions to the car. Simulations of 39-foot and 44-foot 6-inch wavelengths were performed at speeds ranging from 10 mph to 32 mph (3 inches of cant deficiency) in increments of 2 mph or less.

Table 16 shows the worst-case test results and simulation predictions for dynamic curving with 39-foot wavelength. Figure 16 shows the maximum wheel L/V ratio and Figure 17 shows minimum vertical wheel load plotted against speed to show the trend in performance. Test results and the simulation predictions met S-2043 criteria for dynamic curving.

Simulations predict slightly lower L/V ratios and slightly higher vertical wheel loads that were measured in the test for dynamic curving. The revised model improved the comparisons slightly for most metrics.

The models show the correct trends with speed compared to test data. Figure 16 shows the maximum wheel L/V ratio is steady across the speed range. Figure 17 shows the minimum vertical wheel holds steady from 10 mph to about 20 mph and then begins to drop off. The test results showed the drop in vertical wheel loads becomes steeper at 30 and 32 mph while the model predicted wheel loads continue to drop at the same rate.

Table 16. Dynamic curving test results and simulation predictions

Criterion	Limiting Value	Test Result	Simulation Prediction Original Model	Simulation Prediction Revised Model
Roll angle (degree)	4.0	1.4	1.0	1.0
Maximum wheel L/V	0.8	0.66	0.53	0.55
Maximum truck side L/V	0.5	0.45	0.25	0.28
Minimum vertical wheel load (%)	25%	34%	62%	58%
Lateral peak-to-peak acceleration (g)	1.3	0.96	0.41	0.67
Maximum lateral acceleration (g)	0.75	0.69	0.28	0.47
Maximum vertical acceleration (g)	0.90	0.16	0.09	0.11
Maximum vertical suspension deflection (%)	95%	42%	33%	34%

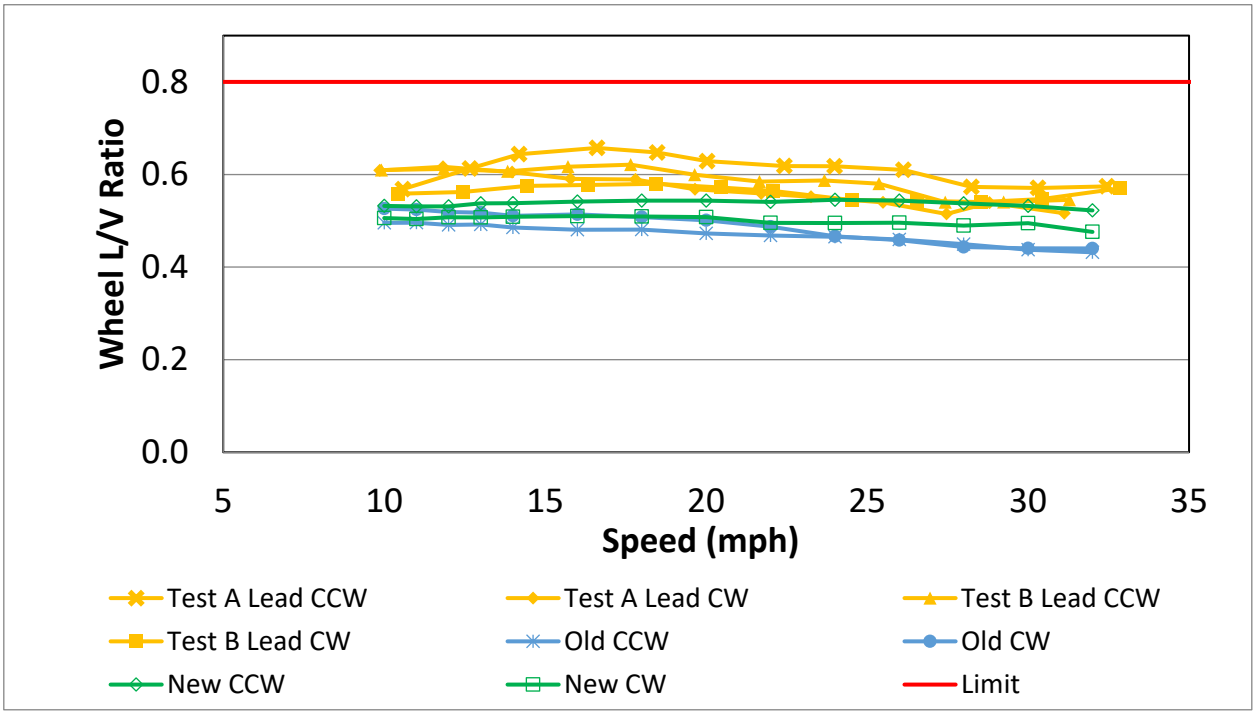


Figure 16. Simulation prediction and test results of maximum wheel l/v ratio in the dynamic curving regime

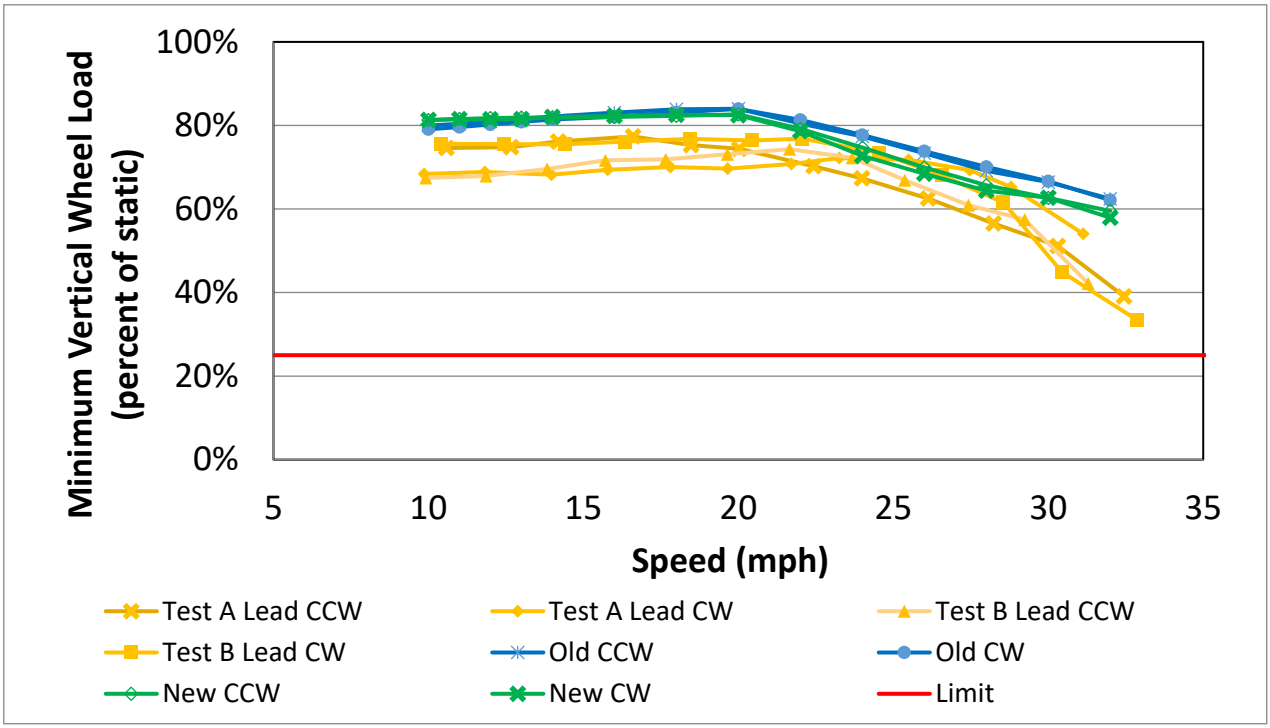


Figure 17. Simulation prediction and test results of minimum vertical wheel load in the dynamic curving regime

7.6 Curving with a Single-rail Perturbation

Simulations of the curving with a single-rail perturbation regime were conducted according to S-2043, Paragraph 4.3.10.2. Curving with single rail perturbation tests were conducted according to S-2043, Paragraph 5.5.15. Simulations were made for 1-, 2-, and 3-inch outside rail dips and 1-, 2-, and 3-inch inside rail bumps in a 12-degree curve with zero superelevation, but only data for the 2-inch dip perturbations are presented here. The inside rail bump was a flat-topped ramp with an elevation change over 6 feet, a steady elevation over 12 feet, ramping back down over 6 feet. The outside rail dip was the reverse. Tests were performed with 2-inch amplitude perturbations. The outside rail dip predictions and test results are presented here because the dip section was the most severe condition for both simulations and tests.

Table 17 shows the worst-case test results and simulation predictions for curving with single rail perturbation with a 2-inch dip. Figure 18 shows the maximum wheel L/V ratio plotted against speed to show the trend in performance. Test results and the simulation predictions met S-2043 criteria for curving with single rail perturbations.

Figure 18 shows that the original simulations predictions matched test results more closely than the revised simulations for test data with A-end lead in the clockwise direction, A-end lead in the counterclockwise direction, and B-end lead in the counterclockwise direction. The revised simulation predictions more closely match the test data with B-end lead in the clockwise direction.

Table 17. Curving with 2-inch rail dip test results and simulation predictions

Criterion	Limiting Value	Test Result	Simulation Prediction Original Model	Simulation Prediction Revised Model
Roll angle (degree)	4.0	1.4	1.7	2.0
Maximum wheel L/V	0.8	0.70	0.57	0.50
Maximum truck side L/V	0.5	0.36	0.29	0.22
Minimum vertical wheel load (%)	25%	60%	67%	65%
Lateral peak-to-peak acceleration (g)	1.3	0.17	0.11	0.13
Maximum lateral acceleration (g)	0.75	0.13	0.07	0.09
Maximum vertical acceleration (g)	0.90	0.18	0.11	0.08
Maximum vertical suspension deflection (%)	95%	68%	35%	37%

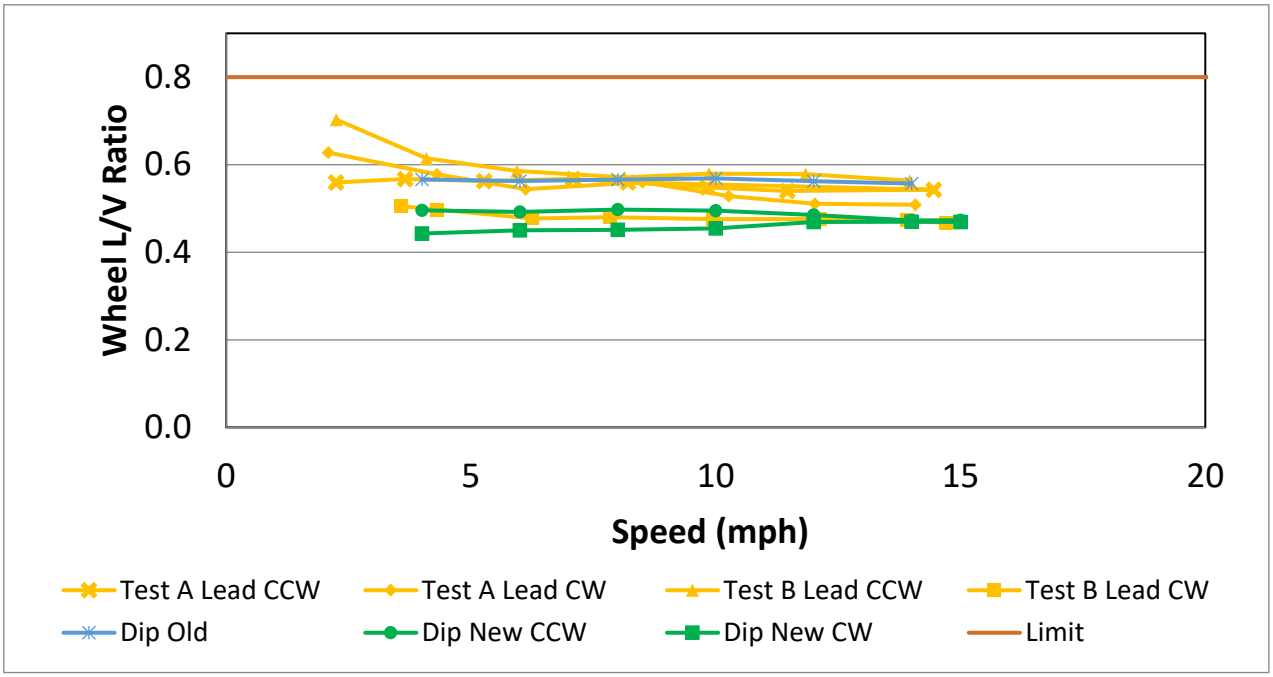


Figure 18. Simulation prediction and test results of maximum wheel L/V ratio in the curving with 2-inch rail dip regime

7.7 Hunting

Simulations of the hunting regime were conducted according to S-2043, Paragraph 4.3.11.3.1. Hunting tests were conducted according to S-2043, Paragraph 5.5.7. Simulations used inputs from measured track geometry of the test site, a 5,500-foot section of tangent track on the TTC Railroad Test Track.

Table 18 shows the worst-case test results and simulation predictions for hunting with a 2-inch dip. Figure 19 shows the 2,000-foot standard deviation of lateral carbody acceleration plotted against speed to show the trend in performance. Test results and the simulation predictions met S-2043 criteria for hunting.

Table 18. Hunting test results and simulation predictions

Criterion	Limiting Value	Test Result	Simulation Prediction Original Model	Simulation Prediction Revised Model
Roll angle (degree)	4.0	0.7	0.4	0.3
Maximum wheel L/V	0.8	*	0.21	0.12
Maximum truck side L/V	0.5	*	0.19	0.10
Minimum vertical wheel load (%)	25%	*	66%	80%
Lateral peak-to-peak acceleration (g)	1.3	0.37	0.41	0.34
Maximum lateral acceleration (g)	0.75	0.20	0.30	0.18
Lateral carbody acceleration standard deviation (g)	0.13	0.11	0.09	0.08
Maximum vertical acceleration (g)	0.90	0.27	0.24	0.22
Maximum vertical suspension deflection (%)	95%	31%	31%	22%

*These tests were performed with non-instrumented wheel sets having a KR tread profile

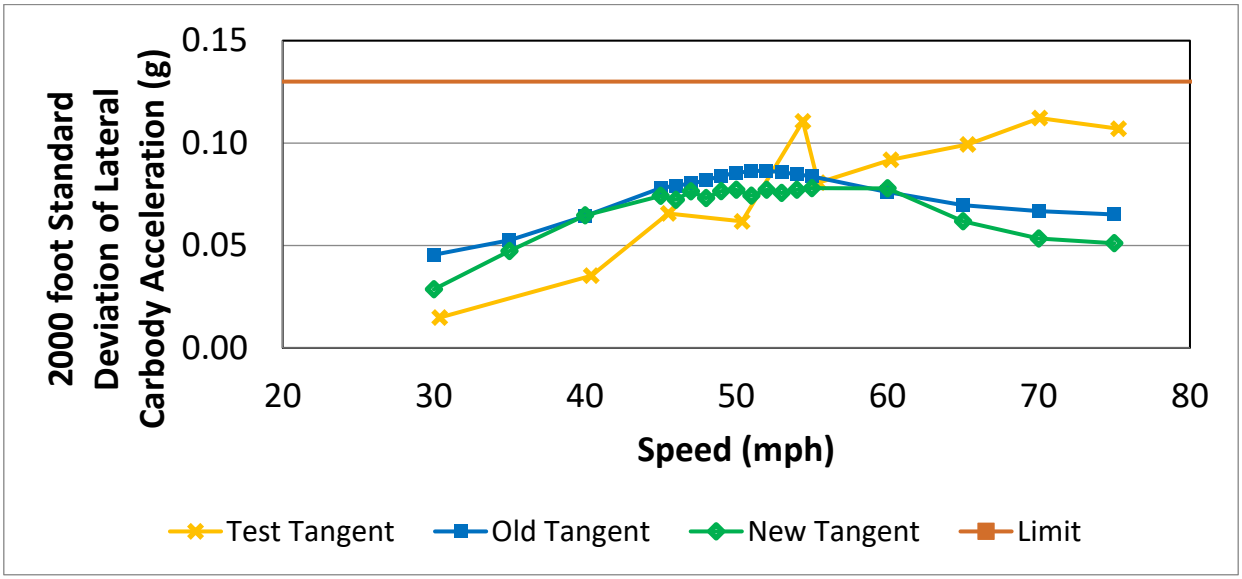


Figure 19. Simulation prediction and test results of maximum 2,000-foot standard deviation of lateral carbody acceleration in the hunting regime

7.8 Curving with Various Lubrication Conditions

Simulations of curving with various lubrication conditions were performed according to S-2043, Paragraph 4.3.11.5. Constant curving simulations were conducted in a 10-degree curve with the coefficient of friction conditions shown in Table 19. Simulations were performed using a new wheel profile on a new rail profile and with a hollow wheel profile on a ground rail profile. Figure 20 shows the worn wheel and rail profiles used for the simulations. The worn wheels were 2 mm hollow and the ground high rail profile had significant gage corner relief. The right side is the high rail in this plot. The gap between the rail profile in red and the wheel profile in blue on the gage corner of the rail represents a distinctive two-point contact condition. The lubrication and profile conditions are designed to show performance when the wheelset cannot provide normal steering forces.

Table 19. Wheel/Rail Coefficients of Friction for the Curving with Various Lubrication Conditions Regime

Friction Coefficient	High Rail Crown	High Rail Gage Face	Low Rail Crown
Case 1	0.5	0.5	0.5
Case 2	0.5	0.2	0.5
Case 3	0.5	0.2	0.2
Case 4	0.2	0.2	0.5



Figure 20. Worn wheel profiles on the ground rail profiles.
The wheelset is shifted to the high rail in the position it would be in a left-hand curve

Table 20 shows the worst-case simulation predictions for curving with various lubrication conditions. Figure 21 shows the maximum truck side L/V ratio plotted against speed to show the trend in performance. Simulation predictions with the revised model did not meet S-2043 criteria for truck side L/V ratio. This exception occurred for counterclockwise runs with Case 2 lubrication and the worn wheel profile at 12 and 24 mph. Simulations met S-2043 criteria for curving with various lubrication conditions during clockwise runs for this lubrication and profile case, and for all runs with other lubrication and profile combinations.

Table 20. Simulation predictions for curving with various lubrication conditions

Criterion	Limiting Value	Simulation Prediction Original Model	Simulation Prediction Revised Model
Roll angle (degree)	4.0	0.5	0.5
Maximum wheel L/V	0.8	0.60	0.59
95th percentile single wheel L/V (constant curving tests only)	0.6	0.57	0.56
Maximum truck side L/V	0.5	0.49	**0.52**
Minimum vertical wheel load (%)	25%	70%	69%
Lateral peak-to-peak acceleration (g)	1.3	0.20	0.23
Maximum lateral acceleration (g)	0.75	0.16	0.17
Maximum vertical acceleration (g)	0.90	0.14	0.15
Maximum vertical suspension deflection (%)	95%	35%	35%

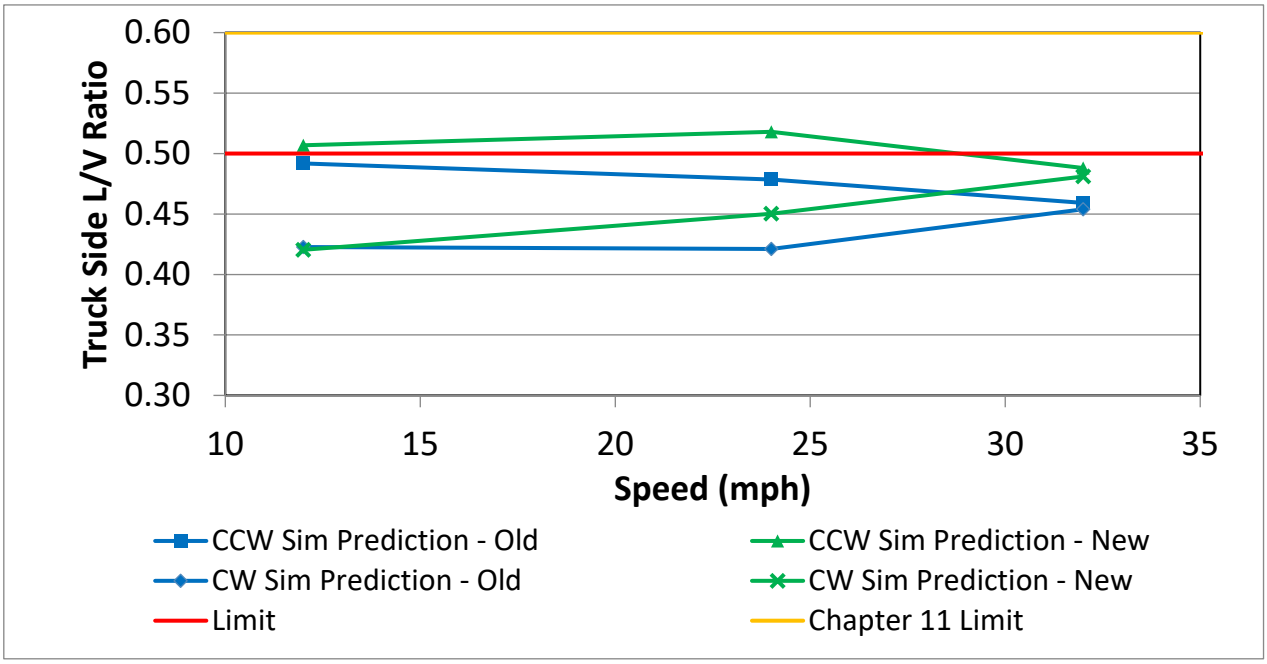


Figure 21. Simulation predictions of maximum truck side L/V ratio in the curving with various lubrication conditions regime. Case 2 lubrication with worn profiles

7.9 Turnouts and Crossovers

Simulations of the turnouts and crossovers regime were conducted according to S-2043, Paragraph 4.3.11.7. Simulations were performed through a No. 7 crossover with straight point turnouts on 13-foot track centers at speeds up to 15 mph. Simulations of the turnouts alone were not repeated with the revised model.

Table 21 shows the worst-case simulation predictions for turnouts and crossovers. Figure 22 shows the maximum truck side L/V ratio plotted against speed to show the trend in performance. Simulation predictions met S-2043 criteria for turnouts and crossovers.

Table 21.Turnout and crossover simulation predictions

Criterion	Limiting Value	Simulation Prediction Original Model	Simulation Prediction Revised Model
Roll angle (degree)	4.0	0.3	0.3
Maximum wheel L/V	0.8	0.68	0.64
Maximum truck side L/V	0.5	0.49	**0.50**
Minimum vertical wheel load (%)	25%	75%	74%
Lateral peak-to-peak acceleration (g)	1.3	0.21	0.19
Maximum lateral acceleration (g)	0.75	0.13	0.13
Maximum vertical acceleration (g)	0.90	0.17	0.16
Maximum vertical suspension deflection (%)	95%	16%	23%

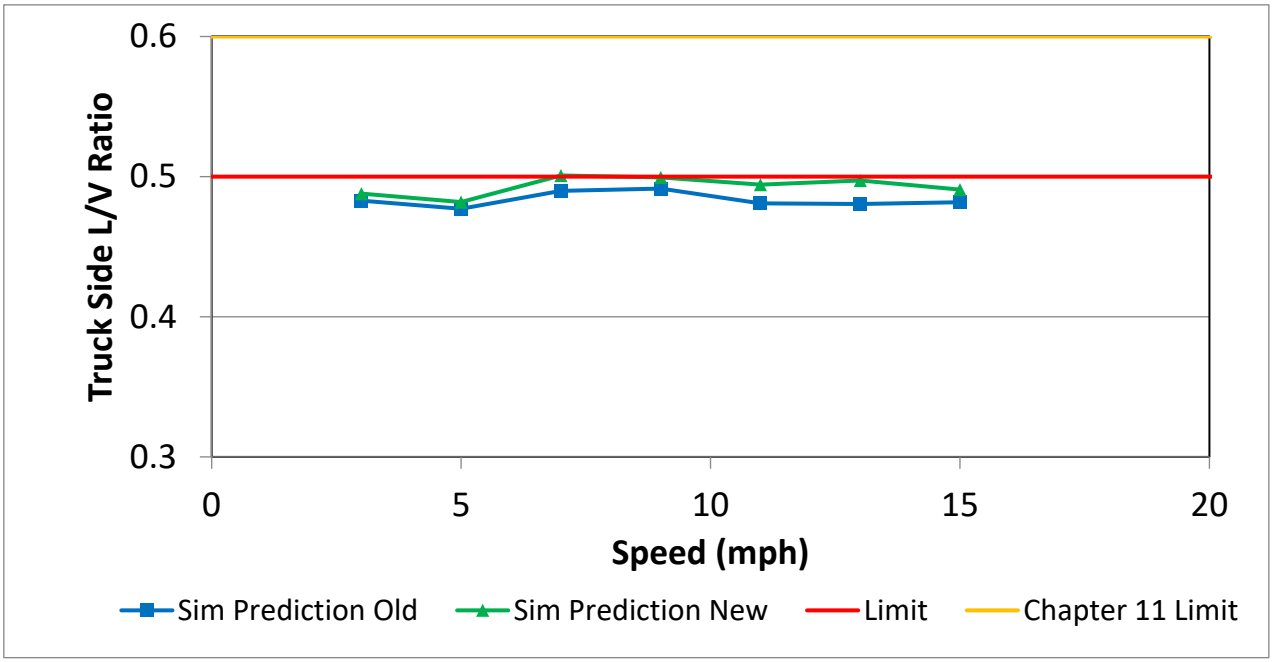


Figure 22. Simulation predictions of maximum truck side L/V ratio in the turnouts and crossovers regime

7.10 Buff and Draft Curving

Simulations of the buff and draft curving regime were conducted according to S-2043, Paragraph 4.3.13. Simulations were performed using measured track geometry of the 12-degree curve of the Wheel/Rail Mechanism Loop at TTC. Simulations were designed to simulate the car coupled to:

- A base car as described in the AAR MSRP Section C-II, Standard M-1001 Chapter 2, Paragraph 2.1.4.2.31.
- A long car having 90-foot over strikers, 66-foot truck centers, 60-inch couplers, and conventional draft gear.
- Like car (coupled to another buffer car).
- Atlas cask car – A car the buffer railcar may be coupled to in HLRM service.
- Rail Escort Vehicle (REV) – A car the buffer railcar may be coupled to in HLRM service.
- Four-axle locomotive – A vehicle the buffer railcar may be coupled to in HLRM service.
- Six-axle locomotive – A vehicle the buffer railcar may be coupled to in HLRM service.

The geometry of the coupled cars was used to calculate the longitudinal and lateral components that would be applied to the car under 250,000 pounds buff and 250,000 pounds draft. These component forces were applied to the carbody in the simulation.

Table 22 shows the worst-case simulation predictions for buff and draft curving. The highest wheel L/V ratios occurred with the buffer car coupled between two base cars and with the buffer car coupled between the REV and the Atlas cask car under draft forces. Figure 23 shows the maximum truck side L/V ratio plotted against speed to show the trend in performance for these two cases. The original simulation predictions did not meet S-2043 truck side L/V ratio criteria for buff and draft curving for cases with the car coupled between two base cars and cases with the car coupled between the Atlas car and the REV. All other S-2043 criteria were met. Simulation predictions with the revised model produced slightly lower truck side L/V ratios that met S-2043 criteria.

Table 22. Buff and draft curving simulation predictions

Criterion	Limiting Value	Simulation Prediction Original Model	Simulation Prediction Revised Model
Roll angle (degree)	4.0	0.7	0.8
Maximum wheel L/V	0.8	0.54	0.54
Maximum truck side L/V	0.5	**0.51**	**0.50**
Minimum vertical wheel load (%)	25%	54%	54%
Lateral peak-to-peak acceleration (g)	1.3	0.15	0.21
Maximum lateral acceleration (g)	0.75	0.15	0.18
Maximum vertical acceleration (g)	0.90	0.13	0.14
Maximum vertical suspension deflection (%)	95%	58%	56%

1 Association of American Railroads. 2011. *Manual of Standards of Recommended Practices*. Section C-II Design, Fabrication, and Construction of Freight Cars, Standard M-1001, Chapter 2. General Data, Paragraph 2.1.4.2.3 “Base Car.” Washington, DC.

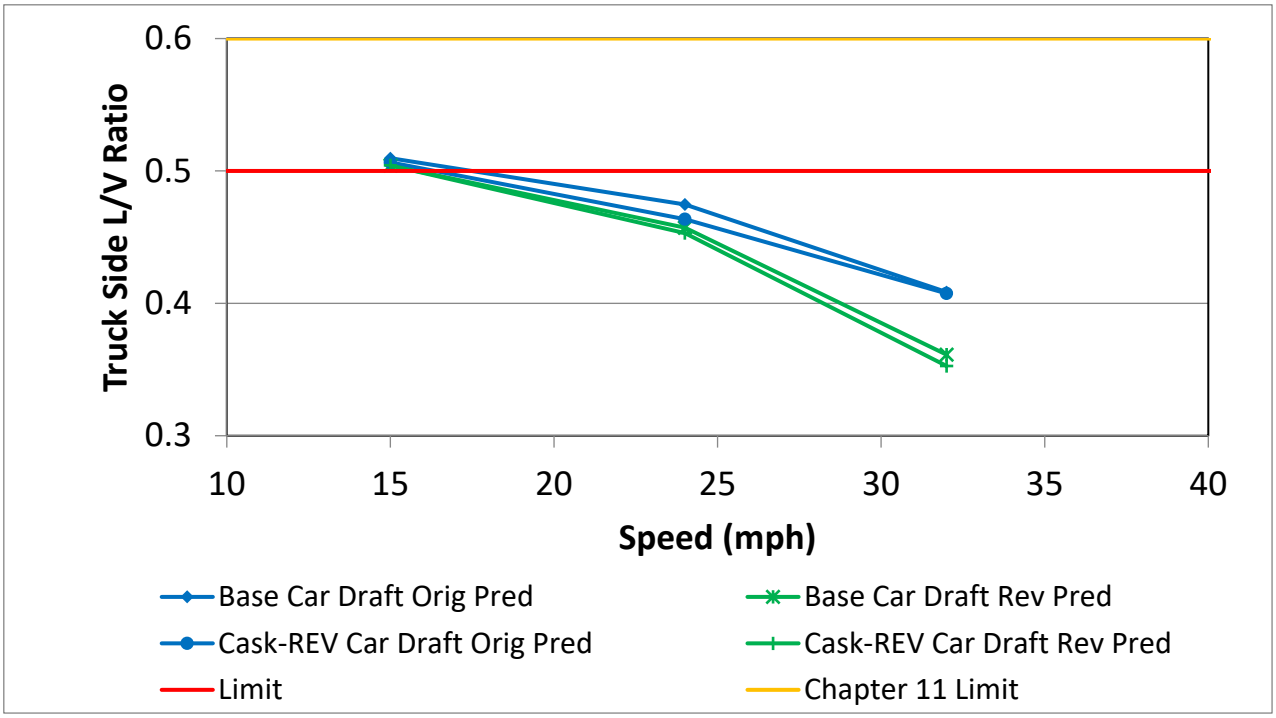


Figure 23. Simulation predictions of maximum truck side L/V ratio in the buff and draft curving regime

8.0 CONCLUSIONS

The buffer car met all S-2043 single-car structural and dynamic test requirements.

FEA simulations and structural test strain measurements both showed that stresses were less than 75 percent of the allowable stress — thus eliminating the requirement in S-2043, Paragraph 8.1 for the FEA to be refined. The largest difference between measured and predicted stress was 5.7 ksi on SGBF11 during the compressive end load test. The other three measurements in similar locations, SGBF10, SGBF37, and SGBF35 were closer to the predicted stress.

The revised model did not meet the criterion for peak-to-peak carbody lateral acceleration for the 39-foot wavelength inputs (1.38g, limit=1.3g) or the 44.5-foot wavelength inputs (1.31g, limit=1.3g) in yaw and sway. In contrast, the buffer car met test requirements for yaw and sway indicating that the model is conservative. The yaw and sway test is only performed with 39-foot wavelength inputs.

The revised modeling predictions did not meet criteria for truck side L/V ratio (0.52, limit=0.5) in the curving with various lubrication conditions regime. This exception occurred for counterclockwise runs with Case 2 lubrication and the worn wheel profile at 12 and 24 mph. The Case 2 lubrication condition is a 0.5 coefficient of friction on the top of both rails and a 0.2 coefficient of friction on the gage face to the high rail. Simulations meet S-2043 criteria for curving with various lubrication conditions during clockwise runs for this lubrication and profile case and for all runs with other lubrication and profile combinations.

Table 23 shows a summary of test results and model predictions for the buffer car.

Table 23. Summary of Simulation Predictions and Test Results

S-2043 Section	Met/Not Met		
	Preliminary Simulations	Revised Simulations	Test Result
5.2 Nonstructural Static Tests			
4.2.1/5.2.1 Truck Twist Equalization	Met	Not Simulated	Met
4.2.2/5.2.2 Carbody Twist Equalization	Met	Not Simulated	Met
4.2.3/5.2.3 Static Curve Stability	Met	Not Simulated	Met
4.2.4/5.2.4 Horizontal Curve Negotiation	Met	Not Simulated	Met
5.4 Structural Tests			
5.4.2 Squeeze (Compressive End) Load	Met	Not Required	Met
5.4.3 Coupler Vertical Loads	Met	Not Required	Met
5.4.4 Jacking	Met	Not Required	Met
5.4.5 Twist	Met	Not Required	Met
5.4.6 Impact	Met	Not Required	Met
5.5 Dynamic Tests			
4.3.11.3/5.5.7 Hunting	Met	Met	Met
4.3.9.6/5.5.8 Twist and Roll	Met	Met	Met
5.5.9 Yaw and Sway	Met	Not Met P-P Lat Accel 1.38 Limit=1.3	Met
5.5.10 Dynamic Curving	Met	Met	Met
4.3.9.7/5.5.11 Pitch and Bounce (Chapter 11)	Met	Met	Met
4.3.9.7/5.5.12 Pitch and Bounce (Special)	Met	Met	Met
4.3.10.1/5.5.13 Single Bump Test	Met	Not Simulated	Met
4.3.11.6/5.5.14 Curve Entry/Exit	Met	Not Simulated	Met
4.3.10.25.5.15 Curving with Single Rail Perturbation	Met	Met	Met
4.3.11.4/5.5.16 Standard Chapter 11 Constant Curving	Met	Not Simulated	Met
4.3.11.7/5.5.17 Special Trackwork	Met	Not Simulated	Met
4.3.11.5 Curving with Various Lubrication Conditions	Met	Not Met Truck Side L/V 0.52, Limit=0.50	Not Required
4.3.12 Ride Quality	Met	Not Simulated	Not Required
4.3.13 Buff and Draft Curving	Not Met Truck Side L/V 0.51, Limit=0.50	Met	Not Required
4.3.14 Braking Effects on Steering	Met	Not Simulated	Not Required
4.3.15 Worn Component Simulations	Met	Not Simulated	Not Required

References

1. AAR *Manual of Standards and Recommended Practices*, Car Construction Fundamentals and Details, Performance Specification for Trains Used to Carry High-Level Radioactive Material, Standard S-2043, Effective: 2003; Last Revised: 2017, Association of American Railroads, Washington, D.C.

2. Walker, Russell, M. Jones, B. Whitsitt, and R. Joy, October 30, 2020, "AAR Standard S-2043 Single-Car Certification Tests of U.S. Department of Energy Atlas Railcar Design Project Buffer Railcar" Report P-20-032, Transportation Technology Center, Inc., Pueblo, CO

3. Walker, Russell and S. Trevithick, Rev. November 20, 2017, "S-2043 Certification: Preliminary Simulations of Kasgro Buffer Railcar," Report P-17-023, Transportation Technology Center, Inc., Pueblo, CO.

TRANSPORTATION TECHNOLOGY CENTER, INC.
A wholly owned subsidiary of the Association of American Railroads

55500 DOT Road • Pueblo, CO 81001
www.aar.com

For questions or comments on this document, contact first_last@aar.com

.

MxV Rail

(formerly TTCI)

350 Keeler Parkway
Pueblo, Colorado USA 81001

A subsidiary of the Association of American Railroads (AAR)

www.mxvrail.com